ANTICANCER AGENTS from NATURAL PRODUCTS

Second Edition

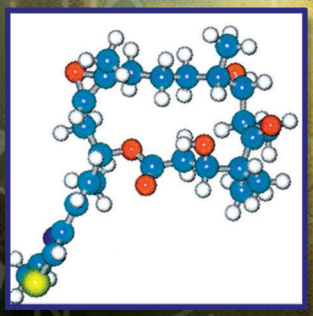

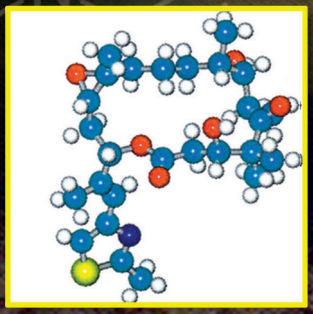

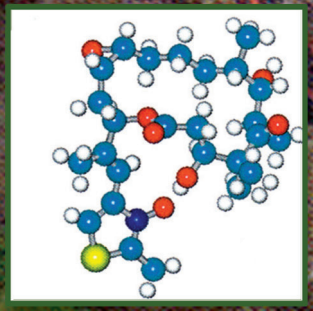

Edited by
Gordon M. Cragg
David G.I. Kingston
David J. Newman

CRC Press
Taylor & Francis Group
an informa business

ANTICANCER AGENTS from NATURAL PRODUCTS

Second Edition

ANTICANCER AGENTS from NATURAL PRODUCTS

Second Edition

Edited by
Gordon M. Cragg
David G.I. Kingston
David J. Newman

CRC Press
Taylor & Francis Group
Boca Raton London New York

CRC Press is an imprint of the
Taylor & Francis Group, an **informa** business

CRC Press
Taylor & Francis Group
6000 Broken Sound Parkway NW, Suite 300
Boca Raton, FL 33487-2742

© 2012 by Taylor & Francis Group, LLC
CRC Press is an imprint of Taylor & Francis Group, an Informa business

No claim to original U.S. Government works
Version Date: 20110427

International Standard Book Number-13: 978-1-4398-1383-6 (eBook - PDF)

This book contains information obtained from authentic and highly regarded sources. Reasonable efforts have been made to publish reliable data and information, but the author and publisher cannot assume responsibility for the validity of all materials or the consequences of their use. The authors and publishers have attempted to trace the copyright holders of all material reproduced in this publication and apologize to copyright holders if permission to publish in this form has not been obtained. If any copyright material has not been acknowledged please write and let us know so we may rectify in any future reprint.

Except as permitted under U.S. Copyright Law, no part of this book may be reprinted, reproduced, transmitted, or utilized in any form by any electronic, mechanical, or other means, now known or hereafter invented, including photocopying, microfilming, and recording, or in any information storage or retrieval system, without written permission from the publishers.

For permission to photocopy or use material electronically from this work, please access www.copyright.com (http://www.copyright.com/) or contact the Copyright Clearance Center, Inc. (CCC), 222 Rosewood Drive, Danvers, MA 01923, 978-750-8400. CCC is a not-for-profit organization that provides licenses and registration for a variety of users. For organizations that have been granted a photocopy license by the CCC, a separate system of payment has been arranged.

Trademark Notice: Product or corporate names may be trademarks or registered trademarks, and are used only for identification and explanation without intent to infringe.

Visit the Taylor & Francis Web site at
http://www.taylorandfrancis.com

and the CRC Press Web site at
http://www.crcpress.com

Contents

Preface ix
Editors xi
Contributors xiii

Chapter 1 Introduction 1
Gordon M. Cragg, David G. I. Kingston, and David J. Newman

Chapter 2 Camptothecin and Its Analogs 5
Nicolas J. Rahier, Craig J. Thomas, and Sidney M. Hecht

Chapter 3 The Discovery and Development of the Combretastatins 27
Kevin G. Pinney, George R. Pettit, Mary Lynn Trawick, Christopher Jelinek, and David J. Chaplin

Chapter 4 Homoharringtonine and Related Compounds 65
Hideji Itokawa, Yukio Hitotsuyanagi, and Kuo-Hsiung Lee

Chapter 5 Podophyllotoxins and Analogs 95
Kuo-Hsiung Lee and Zhiyan Xiao

Chapter 6 Taxol and Its Analogs 123
David G. I. Kingston

Chapter 7 The Vinca Alkaloids 177
Fanny Roussi, Françoise Guéritte, and Jacques Fahy

Chapter 8 The Bryostatins 199
David J. Newman

Chapter 9 The Isolation, Characterization, and Development of a Novel Class of Potent Antimitotic Macrocyclic Depsipeptides: The Cryptophycins 219
Rima S. Al-awar and Chuan Shih

Chapter 10 Chemistry and Biology of the Discodermolides, Potent Mitotic Spindle Poisons 241
Sarath P. Gunasekera and Amy E. Wright

Chapter 11 The Dolastatins: Novel Antitumor Agents from *Dolabella auricularia* 263

Erik Flahive and Jayaram Srirangam

Chapter 12 Ecteinascidin-743 (Yondelis®), Aplidin®, and Irvalec® 291

Carmen Cuevas, Andrés Francesch, Carlos M. Galmarini, Pablo Avilés, and Simon Munt

Chapter 13 Discovery of E7389, A Fully Synthetic Macrocyclic Ketone Analog of Halichondrin B 317

Melvin J. Yu, Yoshito Kishi, and Bruce A. Littlefield

Chapter 14 HTI-286 (Taltobulin), A Synthetic Analog of the Antimitotic Natural Product Hemiasterlin 347

Raymond J. Andersen, David E. Williams, Wendy K. Strangman, and Michel Roberge

Chapter 15 The Actinomycins 363

Anthony B. Mauger and Helmut Lackner

Chapter 16 Anthracyclines 383

Federico-Maria Arcamone

Chapter 17 Ansamitocins (Maytansinoids) 407

Tin-Wein Yu, Heinz G. Floss, Gordon M. Cragg, and David J. Newman

Chapter 18 Benzoquinone Ansamycins 429

Kenneth M. Snader

Chapter 19 Bleomycin Group Antitumor Agents 451

Sidney M. Hecht

Chapter 20 Biochemical and Biological Evaluation of (+)-CC-1065 Analogs and Conjugates with Polyamides 479

Rohtash Kumar and J. William Lown

Chapter 21 Epothilone, A Myxobacterial Metabolite with Promising Antitumor Activity 513

Gerhard Höfle and Hans Reichenbach

Chapter 22 Enediynes 575

Philip R. Hamann, Janis Upeslacis, and Donald B. Borders

Chapter 23 The Mitomycins 623

William A. Remers

Chapter 24 Staurosporines and Structurally Related Indolocarbazoles as Antitumor Agents 647

Michelle Prudhomme

Chapter 25 Combinatorial Biosynthesis of Anticancer Natural Products 671

Steven G. Van Lanen and Ben Shen

Chapter 26 Developments and Future Trends in Anticancer Natural Products Drug Discovery 699

Gordon M. Cragg and David J. Newman

Preface

Natural products continue to make new contributions to cancer chemotherapy since the first edition of this volume was published in 2005. These developments include the clinical introductions of cabazitaxel in June 2010 (the first new taxane drug to enter clinical use since docetaxel was introduced in the 1990s), of ixabepilone (the first epothilone analog to enter clinical use), of the marine natural product analog eribulin (which was approved by the FDA in November 2010 for second line therapy in resistant breast cancer), and of the difluorinated vinca alkaloid vinflunine in 2009. In addition, antibody drug conjugates are showing considerable promise in cancer therapy. While the enediyne calicheamicin γ_1^I was the first antibody-targeted chemotherapeutic agent to be registered for humans, marketed as Mylotarg (gemtuzumab ozogamicin), it has recently been withdrawn from the US market, but SMANCS, a neocarzinostatin conjugate, is approved in Japan for patients with liver cancer metastases. Of particular note are antibody-maytansinoid (DM1 and DM4) conjugates, and a biological licence application (BLA, equivalent to the NDA application for small molecules) has been submitted to the FDA by Genentech for marketing approval of one such conjugate, T-DM1 or trastuzumab emtansine, as a treatment for Her2+ breast cancer.

The chapters in this book have all been substantially revised and updated from those in the first edition. In some instances where the original authors were unable to undertake the revision of their chapters, updates by an editor have been included. The editors hope that this revised volume will continue to provide examples and inspiration to natural product researchers as well having real value for scientists looking for information on the next generation of anticancer drugs.

Gordon M. Cragg, David G. I. Kingston, and David J. Newman

Editors

Gordon M. Cragg obtained his undergraduate training in chemistry at Rhodes University, South Africa, and his DPhil (organic chemistry) from Oxford University. After two years of postdoctoral research at the University of California, Los Angeles, he returned to South Africa to join the Council for Scientific and Industrial Research. In 1966, he joined the Chemistry Department at the University of South Africa and transferred to the University of Cape Town in 1972. In 1979, he returned to the United States to join the Cancer Research Institute at Arizona State University, working with Professor G. R. Pettit. In 1985, he moved to the National Cancer Institute (NCI), National Institutes of Health (NIH) in Bethesda, Maryland, and was appointed Chief of the NCI Natural Products Branch in 1989. He retired in December 2004 and is currently serving as an NIH Special Volunteer. His major interests lie in the discovery of novel natural product agents for the treatment of cancer and AIDS, with an emphasis on multidisciplinary and international collaboration. He has given over 100 invited talks at conferences in many countries worldwide, and he has received NIH Merit Awards for his contributions to the development of the anticancer drug Taxol® (1991), leadership in establishing international collaborative research in biodiversity and natural products drug discovery (2004), and contributions to developing and teaching NIH technology transfer courses (2004). In 1998–1999 he was President of the American Society of Pharmacognosy and was elected to Honorary Membership of the Society in 2003, and he was named as a Fellow of the Society in 2008. In November 2006, he was awarded the William L. Brown Award for Plant Genetic Resources by the Missouri Botanical Garden, which also named a recently discovered Madagascar plant in his honor, *Ludia craggiana*, and in April 2010, he was awarded an Honorary Doctorate of Science by his South African alma mater, Rhodes University. He has established collaborations between the NCI and organizations in many countries promoting drug discovery from their natural resources. He has published over 150 chapters and papers related to these interests.

David G. I. Kingston was born in London, England, and obtained both his undergraduate and graduate training in chemistry at Cambridge University. His graduate supervisors were Lord Todd and Dr. D. W. Cameron, and his PhD research was on the chemistry of aphid pigments; he completed his PhD degree in 1963. He then did three years of postdoctoral research: one in the Division of Biochemistry at MIT under Professor J. M. Buchanan, and two at Cambridge where he was a Research Fellow of Queens' College and worked with Lord Todd, Franz Sondheimer, and Dudley Williams. He moved to the State University of New York at Albany in 1966 and then to Virginia Polytechnic Institute and State University in 1971, where he currently holds the rank of University Distinguished Professor. He served as President of the American Society of Pharmacognosy in 1988–1989. His research interests are on the isolation and structure elucidation of novel natural products, especially those with anticancer and antimalarial activity, and on the chemistry and mechanism of action of tubulin-binding natural anticancer agents such as taxol, epothilone, and discodermolide, and he currently serves as the principal investigator of the Madagascar International Cooperative Biodiversity Group. He received the Research Achievement Award of the American

Society of Pharmacognosy in 1999, was named Virginia Scientist of the Year in 2002, and was the recipient of the American Chemical Society's Ernest Guenther Award in the Chemistry of Natural Products in 2008. He is currently a member of the National Advisory Council for Complementary and Alternative Medicine of the National Institutes of Health. He has published over 350 papers and holds 15 patents. He is also an elder in his church, the Blacksburg Christian Fellowship.

David J. Newman was born in Grays, Essex, UK. He trained initially as an analytical chemist (Grad.RIC), obtained an MSc in synthetic organic chemistry (University of Liverpool), and then after time in the UK chemical industry, he received a DPhil in microbial chemistry from the University of Sussex in 1968. Following two years of postdoctoral studies at the University of Georgia. On electron-transport proteins, he worked for Smith Kline and French (SK&F) in Philadelphia, Pennsylvania, as a biological chemist predominantly in the area of antibiotic discovery and development. In 1977 he received an MSLS in Information Science from Drexel University. Following the termination of the antibiotic program at SK&F in 1985, he then worked for a number of US-based pharmaceutical companies in natural products–based discovery programs and joined the Natural Products Branch of the National Cancer Institute (NCI) in 1991. He is the current chief of the branch, succeeding Gordon Cragg following his retirement.

In 2003, he was awarded the NIH Merit Award for contributions to the development of anticancer agents from marine and microbial sources. His scientific interests are in the discovery and history of novel natural products as drug leads in the anti-infective and cancer areas and in the application of information technologies to drug discovery.

In conjunction with Gordon Cragg, he has established collaborations between the NCI and organizations in many countries promoting drug discovery from their natural resources. He has published over 150 papers, reviews, and book chapters related to these interests, presented over 90 abstracts, holds 21 related patents, is both a UK Chartered Chemist and a UK Chartered Biologist, and held an adjunct full professorship at the Center of Marine Biotechnology, University of Maryland from 2001 to 2005.

Contributors

Rima S. Al-awar
Ontario Institute for Cancer Research
Toronto, Ontario, Canada

Raymond J. Andersen
Department of Chemistry
University of British Columbia
Vancouver, British Columbia, Canada

Federico-Maria Arcamone
Naxospharma
Novate, Milano, Italy

Pablo Avilés
PharmaMar, S.A.
Madrid, Spain

Donald B. Borders
BioSource Pharm, Inc.
Suffern, New York

David J. Chaplin
Oxigene Inc.
South San Francisco, California

Gordon M. Cragg
Division of Cancer Treatment and Diagnosis
National Cancer Institute
Bethesda, Maryland

Carmen Cuevas
PharmaMar
Madrid, Spain

Jacques Fahy
Institut de Recherche Pierre Fabre
Toulouse, France

Erik Flahive
Ardea Biosciences
San Diego, California

Heinz G. Floss
Department of Chemistry
University of Washington
Seattle, Washington

Andrés Francesch
PharmaMar, S.A.
Madrid, Spain

Carlos M. Galmarini
PharmaMar, S.A.
Madrid, Spain

Françoise Guéritte
Centre de Recherche de Gif
Institut de Chimie des Substances Naturelles, CNRS
Gif-sur-Yvette, France

Sarath P. Gunasekera
Smithsoniam Marine Station
Smithsonian Institution
Fort Pierce, Florida

Philip R. Hamann
John Jay College of Criminal Justice
New York, New York

Sidney M. Hecht
Biodesign Institute and Department of Chemistry and Biochemistry
Arizona State University
Tempe, Arizona

Yukio Hitotsuyanagi
School of Pharmacy
Tokyo University of Pharmacy and Life Science
Tokyo, Japan

Gerhard Höfle
HZI, Helmholtz Centre for Infection Research
Braunschweig, Germany

Hideji ltokawa
Department of Medicinal Chemistry and Natural Products
University of North Carolina at Chapel Hill
Chapel Hill, North Carolina

Christopher Jelinek
Department of Chemistry and Biochemistry
Baylor University
Waco, Texas

David G. I. Kingston
Department of Chemistry
Virginia Polytechnic Institute and State University
Blacksburg, Virginia

Yoshito Kishi
Department of Chemistry
Harvard University
Cambridge, Massachusetts

Rohtash Kumar
Global R&D
Sigma-Aldrich Corporation
Miamisburg, Ohio

Helmut Lackner (Deceased)
Institut für Organische Chemie
Universität Göttingen
Göttingen, Germany

Kuo-Hsiung Lee
Department of Medicinal Chemistry and Natural Products
University of North Carolina at Chapel Hill
Chapel Hill, North Carolina

and

China Medical University and Hospital
Taichung, Taiwan

Bruce A. Littlefield
Eisai Research Institute
Andover, Massachusetts

J. William Lown
Department of Chemistry
University of Alberta
Edmonton, Alberta, Canada

Anthony B. Mauger
Division of Cancer Treatment and Diagnosis
U.S. National Cancer Institute
Kensington, Maryland

Simon Munt
PharmaMar, S.A.
Madrid, Spain

David J. Newman
Division of Cancer Treatment and Diagnosis
National Cancer Institute
Frederick, Maryland

George R. Pettit
Department of Chemistry and Biochemistry
Arizona State University
Tempe, Arizona

Kevin G. Pinney
Department of Chemistry and Biochemistry
Baylor University
Waco, Texas

Michelle Prudhomme
Laboratoire de Synthèse et Etude de Systèmes à Intérêt Biologique
Université Blaise Pascal
Aubière, France

Nicolas J. Rahier
Department of Medicinal Chemistry
Pierre Fabre Research Institute
Toulouse, France

Hans Reichenbach
HZI, Helmholtz Centre for Infection Research
Braunschweig, Germany

William A. Remers
AmpliMed Corporation
Tuscon, Arizona

Michel Roberge
Department of Biochemistry and Molecular Biology
University of British Columbia
Vancouver, British Columbia, Canada

Fanny Roussi
Centre de Recherche de Gif
Institut de Chimie des Substances Naturelles, CNRS
Gif-sur-Yvette, France

Ben Shen
Departments of Chemistry and Molecular Therapeutics
The Natural Products Library Initiative at the Scripps Research Institute (TSRI)
Jupiter, Florida

Chuan Shih
Crown Bioscience Inc.
Taicang Economic Development Area
Jiangsu Province, People's Republic of China

Kenneth M. Snader (Retired)
Developmental Therapeutics Program, Division of Cancer Treatment and Diagnosis
U.S. National Cancer Institute
Vero Beach, Florida

Jayaram Srirangam
Research Science and Technology
Pfizer Global R&D—La Jolla Labs
San Diego, California

Wendy K. Strangman
Departments of Chemistry
University of British Columbia
Vancouver, British Columbia, Canada

Craig J. Thomas
National Institutes of Health Chemical Genomics Center
National Human Genome Research Institute
Bethesda, Maryland

Mary Lynn Trawick
Department of Chemistry and Biochemistry
Baylor University
Waco, Texas

Janis Upeslacis (Retired)
Wyeth Research
Pomona, New York

Steven G. Van Lanen
Department of Pharmaceutical Sciences
University of Kentucky
Lexington, Kentucky

David E. Williams
Department of Chemistry
University of British Columbia
Vancouver, British Columbia, Canada

Amy E. Wright
Harbor Branch Oceanographic Institution
Fort Pierce, Florida

Zhiyan Xiao
Ministry of Education and Institute of Materia Medica
Chinese Academy of Medical Sciences and Peking Union Medical College
Beijing, People's Republic of China

Melvin J. Yu
Eisai Research Institute
Andover, Massachusetts

Tin-Wein Yu
Department of Biological Sciences
Louisiana State University
Baton Rouge, Louisiana

1 Introduction

Gordon M. Cragg, David G. I. Kingston, and David J. Newman

CONTENTS

References 3

The search for new lead compounds is a crucial element of modern pharmaceutical research. Natural products provided the only source of pharmaceuticals for thousands of years, and natural products have made enormous contributions to human health through compounds such as quinine, morphine, aspirin (a natural product analog), digitoxin, antibiotics, and many others. The potential of natural products as anticancer agents was recognized in the 1950s by the U.S. National Cancer Institute (NCI) under the leadership of the late Dr. Jonathan Hartwell, and the NCI has since made major contributions to the discovery of new naturally occurring anticancer agents through its contract and grant support, including an important program of plant and marine collections. Many, although not all, of the compound classes described in the following pages owe their origin in whole or in part to NCI support. In spite of the success of the approach of natural products to anticancer drug discovery, as exemplified by the following chapters, in recent years their importance as a source of molecular diversity for drug discovery research and development has been overshadowed by newer chemical approaches currently in favor. These approaches include chemical ones, which make heavy use of combinatorial chemistry, and biological ones such as manipulation of biosynthetic pathways of microbial metabolites through combinatorial biosynthetic techniques. It is thus worthwhile to review briefly the major reasons why natural products are so important.

First, there is a strong biological and ecological rationale for plants and marine invertebrates to produce novel bioactive secondary metabolites. The importance of plants and marine organisms as a source of novel compounds is probably related in large measure to the fact that they are not mobile, and hence must defend themselves by deterring or killing predators, whether insects, fish, microorganisms, or animals. Plants and marine organisms have thus evolved a complex chemical defense system, which can involve the production of a large number of chemically diverse compounds. It has been proposed that all natural products have evolved to bind to specific receptors,[1] and evidence for the advantage that the natural products give an organism over predators has been found in ecological studies in the marine environment related to predator deterrence.[2] As far as microbial species are concerned, secondary metabolites from the prokaryota and also from certain phyla in the eukaryota are actually synthesized in a combinatorial manner.[3] This is the case because the genes that are ultimately responsible for the chemical structures that are obtained from these microbes, plants, and marine invertebrates can frequently be "shuffled" between taxa, and these shuffled genes produce diverse secondary metabolites, some of which are of use to man.

Second, natural products have historically provided many major new drugs. Several recent reviews have provided data to document the importance of natural products as a source of bioactive compounds,[3–8] and the conclusions can be summarized by a review, which states, "In retrospect, the use of natural products has been the single most successful strategy in the discovery of modern medicines."[9]

Third, natural products provide drugs that would be inaccessible by other routes. A large part of the reason for the importance of natural products in drug discovery is that natural products provide drugs that would be inaccessible by other routes. Thus, compounds such as paclitaxel (Taxol™) or halichondrin would never be prepared by standard "medicinal chemistry" approaches to drug discovery, including even the newer methods of combinatorial chemistry. Likewise, the new approach of combinatorial biosynthesis, although an important one, is unlikely in the near future to yield new compounds of the complexity of bryostatin and camptothecin. The claim that synthetic compounds cannot match natural products for their structural diversity is borne out by a statistical study by Henkel and his collaborators, in which over 200,000 compounds from various databases were compared in various ways for their molecular diversity. The authors concluded that "about 40% of the natural products are not represented by synthetic compounds" and that "the potential for new natural products is not exhausted and natural products still represent an important source for the lead-finding process."[10]

Fourth, natural products can provide templates for future drug design. In many cases, the isolated natural product may not be an effective drug for any of several possible reasons, but it may nevertheless have a novel pharmacophore. Certainly natural products, with their complex three-dimensional structures, are well suited as ligands for such targets as protein–protein interactions and for the selectivity needed to differentiate between the various protein kinases, to cite just two examples. Once a novel natural product chemotype has been discovered, it can be developed by medicinal chemistry or combinatorial chemistry into improved agents, as described in several chapters in this book. Examples of this are the drugs etoposide and teniposide derived from the lead compound podophyllotoxin (Chapter 5); numerous analogs derived from taxol (Chapter 6); topotecan, derived from camptothecin (Chapter 2); and the synthetic clinical candidates, E7389 and HTI-286, developed from the marine leads, halichondrin B and hemiasterlin, respectively (Chapters 13 and 14).

Despite the apparent de-emphasis of natural products in the drug discovery process, particularly by the pharmaceutical industry, Danishefsky in a recent viewpoint on the potential of natural products in the discovery of pharmaceutical leads has expressed the following:

> The central proposition advanced herein is that complex target oriented synthesis, enabled by historic advances in methodology, has enormously expanded the scope of the possible. Accordingly, natural products, a proven long-term source of pharma discovery, re-emerge as potentially valuable elements for synthesis-driven pharma exploitation.[11]

In summary, the approach to drug discovery from natural sources has a historical justification (it has yielded many important new pharmaceuticals), a biochemical rationale (the position of marine organisms and plants in the ecosystem demands that they produce defense substances, many of which have a novel phenotype, and microbial species can produce new secondary metabolites by gene shuffling), and a chemical rationale (natural products provide templates for drug design).

This book covers the major classes of clinically used anticancer natural products. The chapters are grouped by the source organism (microbial, marine, or plant), although it is recognized that the distinction is not always clear-cut, and some so-called marine natural products, for example, may in fact be produced by symbiotic microbial species (see the discussion of bryostatin in Chapter 10). Within each chapter, the coverage includes the history of the drug, a discussion of its mechanism of action, its medicinal chemistry, its synthesis, and its clinical applications. The book concludes with a chapter on the increasingly important biosynthetic approaches to "unnatural natural products," and with a final chapter looking ahead to future developments in anticancer natural products drug discovery. Because of the wealth of information available, the coverage in all these chapters is necessarily selective rather than comprehensive, but the authors and editors have attempted to provide the most important recent results in each area.

The editors hope that this book will not only serve as a convenient summary of the current status of research and development of some of the most effective anticancer agents available today, but will also serve as an inspiration and a challenge to a new generation of scientists to engage in developing new and even better drugs from nature's bounty.

REFERENCES

1. Williams, D. H., Stone, M. J., Hauck, P. R., and Rahman, S. K. Why are secondary metabolites (natural products) biosynthesized? *J. Nat. Prod.* 52, 1189, 1989.
2. Paul, V. J. *Ecological Roles of Marine Natural Products*. Cornell University Press, Ithaca, 1992.
3. Kingston, D. G. I. and Newman, D. J. Mother Nature's combinatorial libraries: Their influence on the synthesis of drugs. *Curr. Opin. Drug Disc. Devel.* 5, 304, 2002.
4. Shu, Y. -Z. Recent natural products based drug development: A pharmaceutical industry perspective. *J. Nat. Prod.* 61, 1053, 1998.
5. Newman, D. J. and Cragg, G. M. Natural products as sources of new drugs over the last 25 years. *J. Nat. Prod.* 70, 461, 2007.
6. Butler, M. S. Natural products to drugs: Natural product-derived compounds in clinical trials. *Nat. Prod. Rep.* 25, 475, 2008.
7. Cragg, G. M., Grothaus, P. G., and Newman, D. J. Impact of natural products on developing new anticancer agents. *Chem. Rev.* 109, 3012, 2009.
8. Newman, D. J., Cragg, G. M., and Snader, K. M. The influence of natural products upon drug discovery. *Nat. Prod. Rep.* 17, 215, 2000.
9. Tulp, M. and Bohlin, L. Functional versus chemical diversity: Is biodiversity important for drug discovery? *Trends Pharm. Sci.* 23, 225, 2002.
10. Henkel, T., Brunne, R. M., Müller, H., and Reichel, F. Statistical investigation into the structural complementarity of natural products and synthetic compounds. *Angew. Chem. Int. Ed.* 38, 643, 1999.
11. Danishefsky, S. On the potential of natural products in the discovery of pharma leads: A case for reassessment. *Nat. Prod. Rep.* 27, 1114, 2010.

2 Camptothecin and Its Analogs

Nicolas J. Rahier, Craig J. Thomas, and Sidney M. Hecht

CONTENTS

2.1 Introduction 5
2.2 Mechanism of Action 6
2.2.1 Poisoning of Topo I 6
2.2.2 Other Biochemical Effects of CPT 8
2.3 Synthetic Studies 9
2.3.1 Asymmetric Total Syntheses 9
2.3.2 Semisynthesis of Topotecan 12
2.3.3 Semisynthesis of Irinotecan 12
2.3.4 Semisynthesis of Belotecan 12
2.4 Medicinal Chemistry 13
2.4.1 A/B/C/D Ring Analogs 13
2.4.2 E-Ring Analogs 14
2.5 Development of Clinically Useful CPT Analogs 15
2.5.1 Topotecan, Irinotecan, and Belotecan 15
2.5.2 Water-Soluble CPT Analogs in Clinical Trials 16
2.5.3 Water-Insoluble CPT Analogs in Clinical Trials 17
2.5.4 CPT Conjugates in Clinical Trials 18
2.5.5 Advances in CPT Formulations 20
2.6 Conclusions 20
Acknowledgments 21
References 21

2.1 INTRODUCTION

Camptothecin (CPT) (**1**) (Figure 2.1) is a naturally occurring alkaloid isolated from the bark of *Camptotheca acuminata*, a tree native to central China. The beginning of interest in *C. acuminata* extracts was in the 1950s; the structure of CPT was determined by x-ray crystallography as a pentacyclic alkaloid and was disclosed in 1966.[1] In addition to its structural novelty, CPT received much attention due to its striking activity in *in vivo* L1210 mouse life-prolongation assays and *in vitro* 9KB cytotoxicity assays.[2] Clinical evaluations were pursued with the water-soluble sodium salt (**2**), which unfortunately yielded only modest results and an unmanageable number of side-effects.[3] In 1985, Hsiang et al. reported that topoisomerase I (topo I) was the cellular target of CPT and thereby renewed interest in its study and clinical advancement.[4] At present, CPT remains one of the most widely investigated natural products and three analogs of CPT have been approved for clinical use in selected cancer indications (i.e., topotecan—Hycamtin, **3**; irinotecan—Camptosar, **4**; and CKD-602—belotecan, **5**). This chapter serves as a summary of the mechanism of action, biological scope, synthetic studies and structure–activity relationships (SARs), and developing clinical applications of CPT and is intended to complement our earlier chapter covering this important natural product.

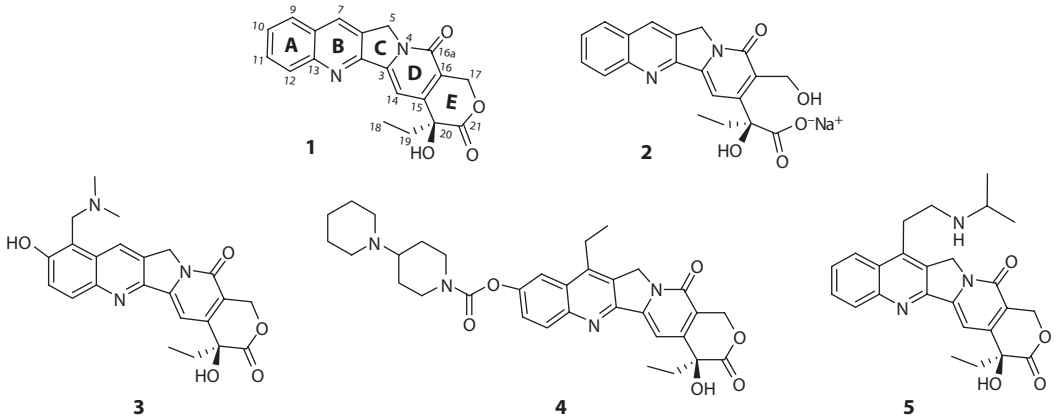

FIGURE 2.1 Structures of CPT (**1**), its water-soluble sodium salt (**2**), topotecan (**3**), irinotecan (**4**), and belotecan (**5**).

2.2 MECHANISM OF ACTION

2.2.1 Poisoning of Topo I

The topoisomerases (types I and II) are essential mammalian enzymes responsible for the relaxation of supercoiled chromosomal DNA.[5] Topo I effects DNA relaxation through an energy-independent single-strand scission, strand passage, and relegation event (Figure 2.2a).[6] X-ray crystallographic analysis shows that topo I fully surrounds the duplex DNA during this process. DNA nicking is accomplished through a nucleophilic attack by a catalytic tyrosine residue (Y723 for human topo I) on the phosphodiester backbone.[7] Topo I is capable of cleaving DNA at numerous sites; however, there is a strong preference for cleavage immediately following selected thymidine residues (–1 position). Numerous poisons of topo I (and topo II) block the religation event between DNA and the DNA–topo covalent binary complex.[8] CPT does not bind to topo I independent of DNA nor is CPT a nonspecific DNA-binding agent,[9] although what is apparently weak binding has been noted for two CPT analogs.[10] Early work by Hertzberg et al. and Pommier et al. demonstrated that CPT analogs with electrophilic halogen substituents were capable of cross-linking topo I and DNA on prolonged exposure to the covalent enzyme–DNA binary complex.[11,12] These studies provided important evidence that CPT interacts directly with the topo I–DNA binary complex. Analyses of CPT-resistant topo I mutants[13,14] offer insight into which amino acids play critical roles in CPT binding and a number of computational models have been presented attempting to define the binding mechanism of CPT to the topo I–DNA binary complex.[15–17] In 2002, Staker et al. reported the structure of a co-crystal of topo I, DNA, and topotecan which demonstrated that CPT binds to the enzyme–DNA complex in proximity to the catalytic tyrosine residue (Figure 2.2b) in a fashion that could readily result in inhibition of religation.[18] The only direct protein-to-drug contact in this crystal structure was found to be a hydrogen bond between Asp533 and the 20-*S* OH group of CPT. Additionally, there was evidence for a hydrogen bond between the CPT A-ring OH moiety and a water molecule. At present, several crystallographic analyses of CPT and other topo I poisons have been published,[19–21] affording insight into the SARs of these agents including a basis for the required stereochemistry of the 20-*S* OH moiety. Moreover, these structural analyses provide rationales for the resistance of selected topo I mutants including the clinically relevant mutations involving Phe361, Arg364, Asp533, and Asn722.[22–24] It is interesting that the last of these topo I mutations also appears in plants that produce CPT.[25]

In parallel with emerging insights into the nature of topo I poisoning by CPT has been a growing understanding of the apoptotic mechanism of CPT. Importantly, CPT-resistant cell lines have

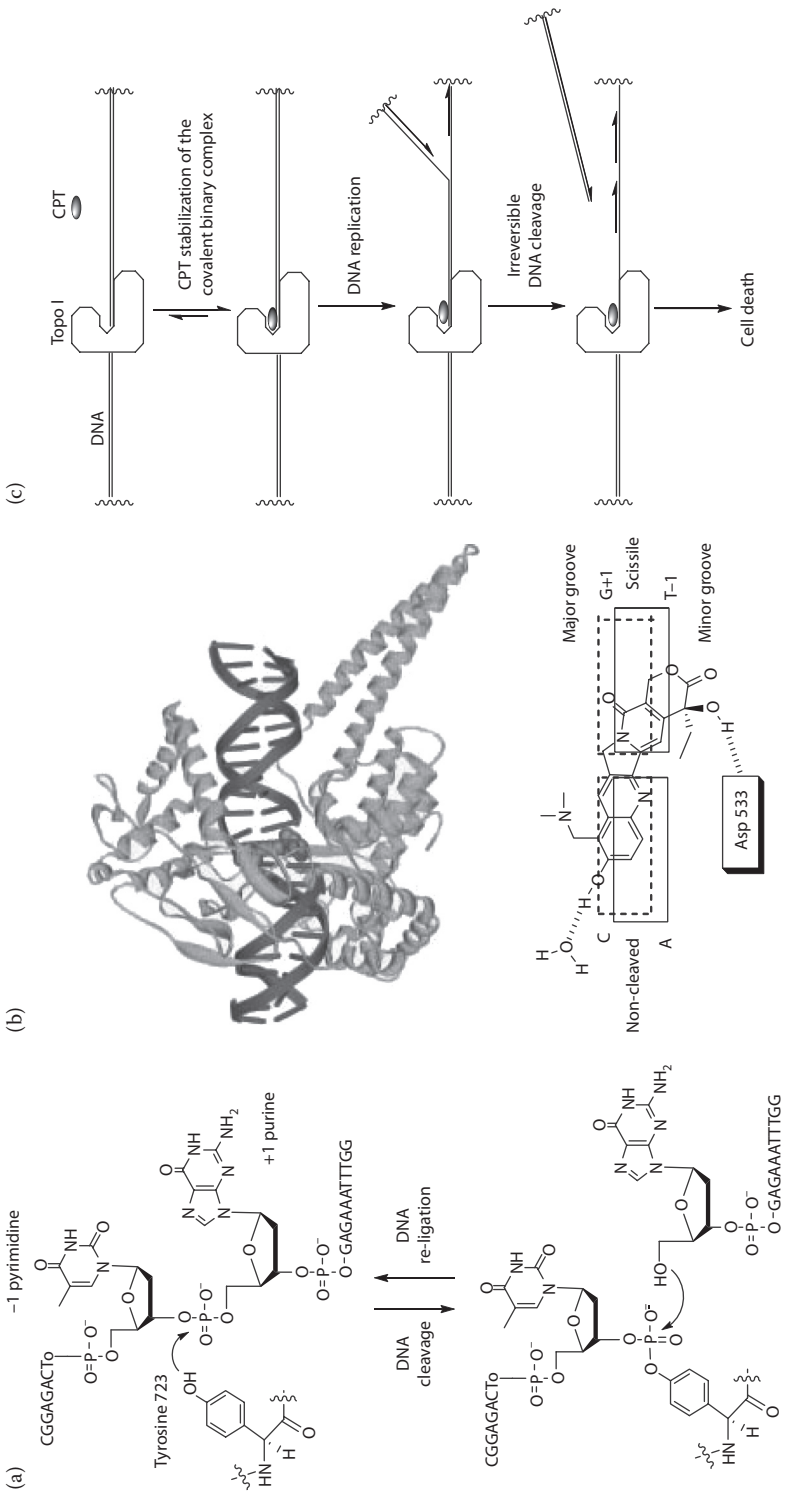

FIGURE 2.2 **(See color insert.)** (a) Mechanism of DNA relaxation by topo I. (b) X-ray crystal structure of the DNA–topo I covalent complex in the presence of topotecan and a two-dimensional representation of the position of topotecan and key interactions with the covalent complex. (c) S-phase-specific cytotoxic mechanism of CPT.

well-characterized topo I mutations[13,14] and deletion of the topo I gene from *Saccharomyces cerevisiae* results in a CPT-resistant but viable organism.[26] Based on these results and several related studies, it is widely believed that topo I is the single locus of CPT-induced cytotoxicity. Gallo et al. reported that CPT disrupted DNA synthesis and induced S-phase-specific cellular cytotoxicity prior to the report that CPT was targeting topo I.[27] At present, it is accepted that irreversible DNA cleavage and S-phase-specific apoptosis is triggered during replication fork collision with the stabilized DNA–topo I covalent complex in the presence of CPT (Figure 2.2c). It is logical to think that the putative requirement for a replication fork collision may impose significant requirements on the way in which CPT (analogs) are used in a clinical setting. Within any cell population (even for highly proliferative cancer cells) only a fraction of cells will be in the S-phase at any specific time. Furthermore, CPT diffuses relatively rapidly from topo I–DNA–CPT binary complexes. These factors argue that transient drug exposure may be clinically less effective than prolonged infusions of CPT-based drug regimens.

Various DNA repair mechanisms that can mitigate the effects of CPT have received considerable attention. The actions of 3′-endonucleases (including *MUS*81/*EME*1 and *MRE*11/*RAD*50) have been implicated as a mechanism for the reversal of the stabilized covalent complex, based largely on the hypersensitivity to CPT of yeast strains bearing mutations within these enzymes.[28–30] The ubiquitination of topo I and subsequent degradation via the proteasome potentially provides another means to resolve the covalent complex.[31] In addition, in 1996, Yang et al. described tyrosyl-DNA phosphodiesterase 1 (Tdp1) as an enzyme that can hydrolyze tyrosine–DNA phosphodiester linkages.[32] At present, ubiquitination and proteolysis of topo I to a DNA–tyrosine product, followed by Tdp1 resolution and release of the free 3′-phosphate, is considered a significant DNA repair mechanism in response to topo I poisons. In a study that focused on a ubiquitin–proteasome pathway for the repair of topo I–DNA complexes, Lin et al. have also recently shown that poly(ADP-ribose) polymerase-1 (PARP-1) plays a key role in the repair of topo I concealed single-stranded DNA breaks following proteomic (and possibly Tdp1) resolution of the covalent complex.[33] The synergistic effects between CPT and pharmacological modulators of the proteasome, PARP-1 and Tdp1 are clearly of interest for more detailed study.

2.2.2 Other Biochemical Effects of CPT

Numerous studies have examined cellular responses to CPT beyond topo I inhibition and S-phase-specific cytotoxicity. In addition to its clinical role, CPT is widely utilized as a tool compound for induction of DNA strand breaks and as a general inducer of apoptosis; unsurprisingly, numerous orthogonal biochemical effects have been described as a consequence of these studies. Several reports have explored the interaction of CPTs with the ATP-binding cassette (ABC) efflux proteins. CPT has been shown to induce expression of breast cancer resistance protein (BCRP or ABCG2).[34] In addition, several studies have demonstrated that CPT and various analogs are substrates of the various ABC transporters that are involved in multidrug-resistant cancers.[14,35,36] Many ongoing SAR studies surround the search for CPT analogs that are not substrates for drug efflux pumps yet retain potent tumor cell cytotoxicity.

Recent studies have implicated additional mechanisms leading to cell death/stasis upon CPT exposure, including autophagy and senescence. Despite these intriguing results, it remains clear that CPT activates numerous pathways associated with apoptosis. CPT is known to induce the expression of p53.[37] Disruption of wild-type p53 function has been shown to increase the cytotoxic nature of CPT in human colon and breast cancer cell lines.[38] CPT-induced DNA damage indirectly inhibits CDK2 resulting in the sustained activity of the transcription factor FOXO1 and the upregulated expression of numerous genes encoding several apoptotic factors.[39] In addition, several reports detail the activation of the transcription factor nuclear factor NFκB in response to CPT and selected analogs. In contrast to the upregulated activity of FOXO1, activation of NFκB stimulates the expression of several antiapoptotic elements and constitutive activation of NFκB has been implicated as a

resistance mechanism to CPT.[40] Another report demonstrates that CPT causes the translocation of the tumor suppressor protein prohibitin from the nucleus to the cytoplasm, from which it localizes to the mitochondria.[41] The relocation of prohibitin is thought to alter p53-mediated transcription as well as trigger apoptosis.

CPT and topo I inhibitors are also of increasing interest as potential antitrypanosome and anti-leishmania agents.[42] Homologs of topo IB have been found within the genome of numerous parasites and RNA interference targeting the topo IB variant of *Trypanosoma brucei* alters DNA synthesis and topo IB gene disruption in *Leishmania major* results in nonviable parasites.[43,44] At least one study has shown that CPT is capable of reducing visceral leishmania burden in a mouse model.[45]

2.3 SYNTHETIC STUDIES

Despite the commercialization of CPT analogs, the raw material for manufacture is still obtained by extraction from the plants *C. acuminata* and *Nothapodytes fetida*. Accordingly, increasing efforts have focused on workable syntheses of CPTs. The following is a summary of some of the strategies for the synthesis of CPT, as well as for the semisyntheses of the clinically approved topotecan, irinotecan, and belotecan.

2.3.1 Asymmetric Total Syntheses

Du has published an excellent review of synthetic approaches to CPT and analogs that appeared prior to 2003.[46] These approaches and newer ones are classified according to the construction of the B, C, or D rings as a key step, and are summarized in Figure 2.3.

A Friedlander reaction of 2-aminobenzaldehyde (**6**) with the assembled CDE-ring framework (**7**) has been used at the beginning of the CPT synthetic work for B-ring annelation of CPT (Figure 2.3a). The asymmetric center of **7** was installed using a few different approaches including resolution procedures, ethylation in the presence of a chiral auxiliary, Sharpless asymmetric dihydroxylation, and asymmetric hydroxylation. The Friedlander condensation has also been used for a large number of analog syntheses because of its reliability. Thus, Pharmacia and Upjohn developed a scaleable total synthesis of irinotecan in 18 steps and 6.4% overall yield using a Friedlander approach.[46]

Curran et al. developed a strategy in which the A fragment (**8**) and the DE fragment (**9**) participate in a [4 + 1] radical annulation reaction leading to the formation of the B and C rings of CPT (Figure 2.3b).[47] According to this methodology, the asymmetric centre of **9** was installed using Sharpless asymmetric dihydroxylation or catalytic asymmetric cyanosilylation reactions. This cascade radical cyclization approach involving isonitrile **8** has been widely used to prepare 7-substituted, A-ring functionalized analogs, including applications in combinatorial chemistry, leading to silatecans and homosilatecans. This methodology is especially well suited for SAR studies.

Another approach for the concomitant formation of two rings of **1** has been developed by Fortunak et al. using an aza Diels–Alder strategy to construct the BC rings of CPT.[48] The key reaction is an intramolecular [4 + 2] cycloaddition of an alkyne and an aryl imidate (**10**) (Figure 2.3c). The asymmetric center was installed using the enolate of **14**. Recently, Zhou et al. dramatically improved the yield of the synthesis of imidate (**10**) using Tf_2O-$2Ph_3PO$ as activator to convert the amide moiety to the corresponding imidate.[49] The asymmetric center was introduced at the end of the synthesis by the classical Sharpless dihydroxylation procedure followed by oxidation. This approach is suitable for the synthesis of A- and B-ring-substituted analogs.

The construction of the C-ring has been used by Comins' and Bennasar's laboratories.[50,51] These approaches feature an *N*-alkylation followed by sp^2–sp^2 C–C bond formation as two key reactions. In the Comins' approach, the quinoline AB-ring fragment (**11**) was coupled to the DE-ring fragment (**12**) by simple alkylation and the C ring was closed using a Heck reaction (Figure 2.3d).[50] The asymmetric center was introduced using a chiral auxiliary. Involving only six steps, the Comins' synthesis represents the shortest total synthesis described for CPT. HomoCPT analogs, diflomotecan

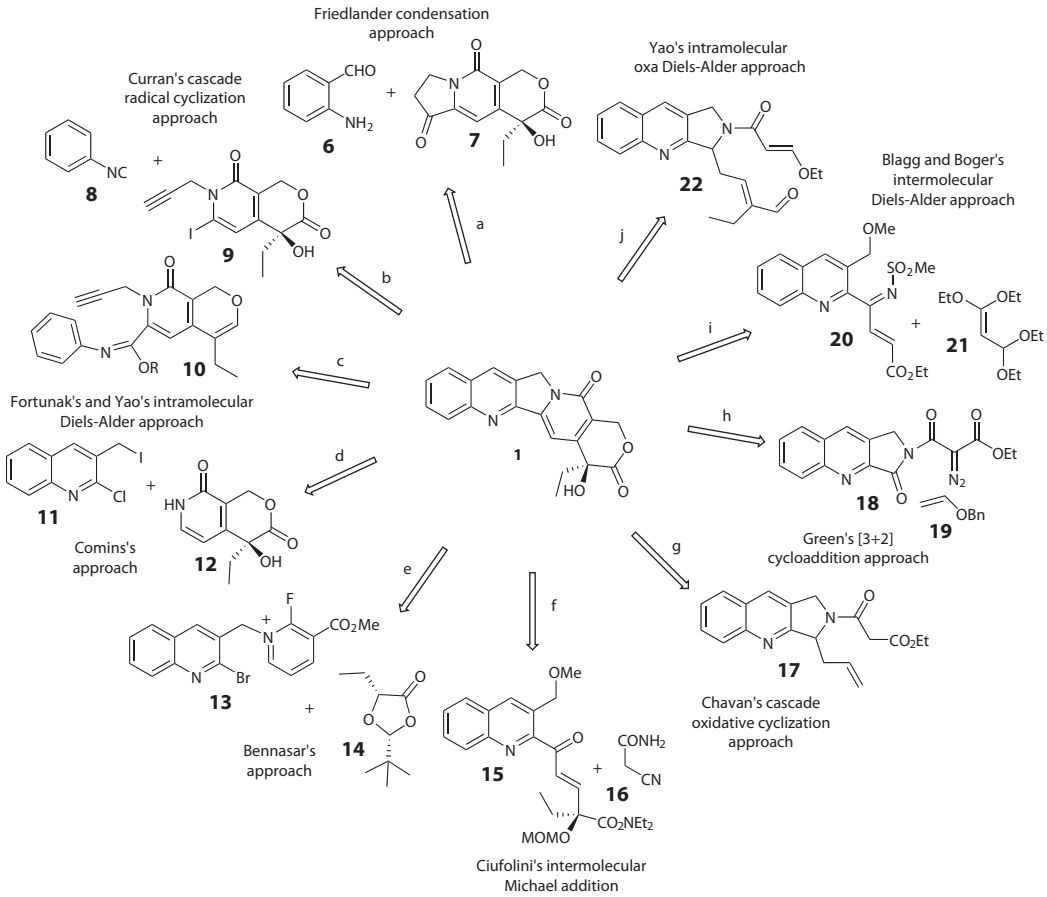

FIGURE 2.3 Different approaches (a–j) for asymmetric total syntheses of CPT.

and elomotecan, were prepared by Lavergne et al.[52] inspired by the Comins' approach. Fang et al. at Glaxo developed a highly efficient synthesis of the DE-ring fragment (**12**) using a Sharpless asymmetric dihydroxylation reaction to introduce the chiral center at C-20, which was then used for the synthesis of lurtotecan.[53]

In Bennasar's approach, the chiral center was introduced by addition of the enolate of **14** to the pyridinium salt (**13**) followed by an intramolecular radical cyclization to form the C ring (Figure 2.3e).[51] For the construction of the pyridone D ring as a key step, Ciufolini and Roschangar used an intermolecular Michael addition reaction (Figure 2.3f).[54] Addition of the potassium enolate of 2-cyanoacetamide (**16**) to α,β-unsaturated ketone **15** gave the intermediate for pyridone formation. The chiral center was introduced earlier in the synthesis by enzymatic desymmetrization using pig liver esterase.

Chavan et al. developed, using Wacker conditions, a one-pot cascade intramolecular Pd-catalyzed oxidative cyclization of **17** followed by aromatization as a key step to construct the D ring (Figure 2.3g).[55] The chiral center was introduced using a Sharpless asymmetric dihydroxylation reaction followed by oxidation. The introduction of asymmetry and the 20-OH group at the end of the synthesis represents a real improvement in addressing the loss of asymmetric intermediates and ameliorating solubility problems.

Kanazwa et al. described a novel approach to CPT by [3 + 2] cycloaddition of the isomünchnone (diazoester) intermediate **18** with benzyl vinyl ether (**19**) in the presence of a catalytic amount of rhodium acetate dimer to construct the D ring (Figure 2.3h).[56] The 20-*S* stereocenter was installed

using Shibasaki's methodology: cyanosilylation in the presence of a Gd complex generated from a glucose derivative.

Blagg and Boger also focused on the construction of the D ring as a key step in their synthesis of CPT (Figure 2.3i).[57] Thus they developed at room temperature, an inverse electron demand Diels–Alder reaction of *N*-methylsulfonyl-1-aza-1,3-butadiene **20** with the electron-rich olefin **21**. The asymmetric center was introduced late in the synthesis using a modified Sharpless asymmetric dihydroxylation reaction.

Liu et al. developed another total synthesis of CPT and 10-OH-CPT involving an intramolecular oxa Diels–Alder reaction for the formation of the D and E rings as a key step (Figure 2.3j).[58] This synthesis is described in more detail next (Scheme 2.1). In the presence of a catalytic amount of pyrrolidine and benzoic acid, 2-aminobenzaldehyde (**23**) reacts with the α,β-unsaturated aldehyde **24**. This Michael addition-aldol condensation cascade was followed by treatment with silica and oxidation with manganese dioxide to afford a 75% yield of the AB rings precursor quinoline **25**. Treatment of **25** with hydroxylamine, followed by deacetylation with potassium carbonate and reduction of the oxime provided the benzylamine derivative **26** in 79% overall yield for the three-step sequence. Acylation of **26** with 3-ethoxyacryloyl chloride (**27**) followed by MnO_2 oxidation of **28** afforded aminal **29** in 71% yield overall for two steps. Acetylation of **29**, followed by treatment with enol silyl ether **30** in the presence of $BF_3 \cdot Et_2O$, led to DE rings precursor **22** in 72% yield. The inverse electron demand oxa Diels–Alder reaction was carried out in mesitylene at 160°C in a sealed tube. Next, addition of 2,3-dichloro-5,6-dicyanobenzoquinone (DDQ) led to aromatization of the D ring, and addition of Et_3SiH led to the reductive removal of the ethoxy group, affording 63% of the pentacyclic derivative **31**. The chiral center at C-20 was introduced by a Sharpless asymmetric dihydroxylation reaction followed by the oxidation of the formed lactol, affording CPT in 83% yield (95% ee). CPT was obtained in 16% overall yield and 95% ee starting from simple, inexpensive, and readily available materials. Furthermore, this synthesis avoids the use of sensitive organometallic reagents. All these factors make this synthesis very efficient and straightforward.

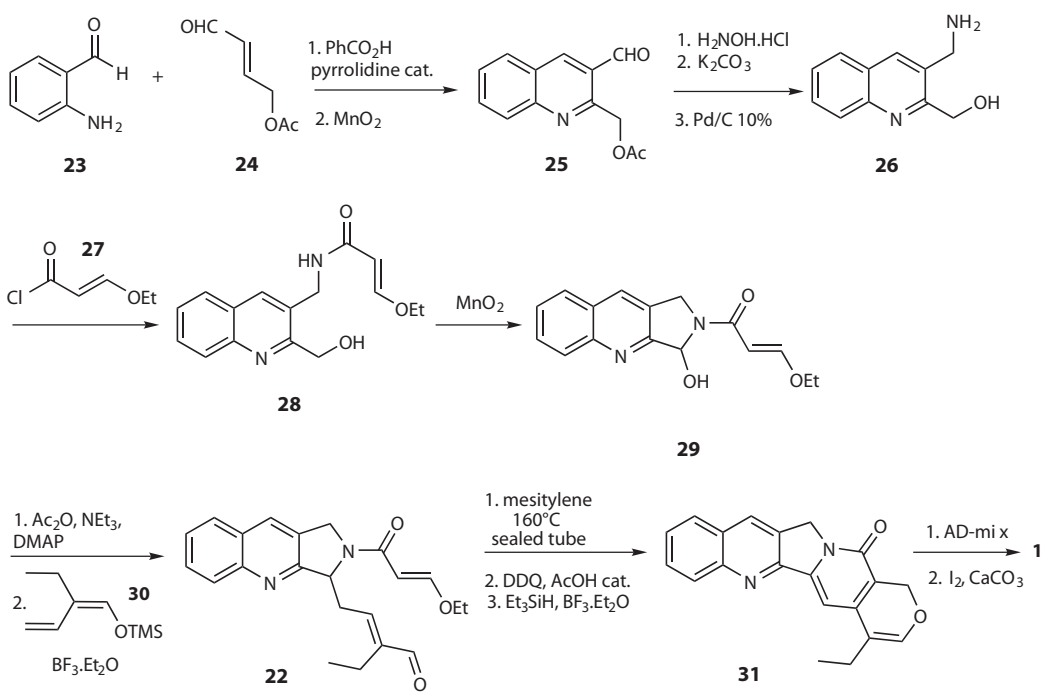

SCHEME 2.1 Yao's total synthesis of CPT.

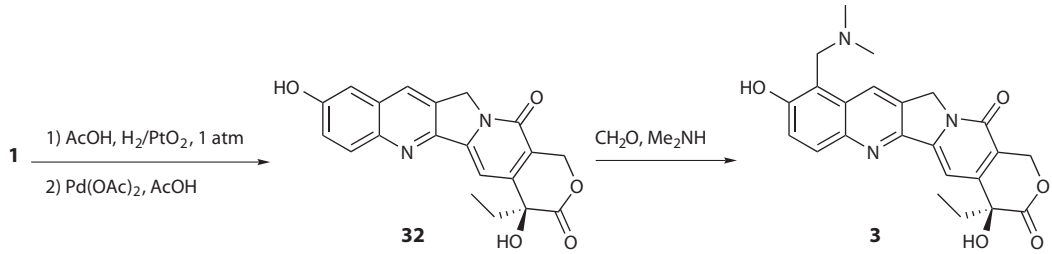

SCHEME 2.2 Semisynthesis of topotecan.

2.3.2 Semisynthesis of Topotecan

The synthesis of the first currently marketed CPT derivative, topotecan, was described in 1991 by Kingsbury et al. in two steps starting from 20(*S*)-CPT (Scheme 2.2).[59] Conversion of 20(*S*)-CPT to 10-hydroxy CPT (**32**) was accomplished through a reduction–oxidation sequence in 71% yield. Treatment of **32** with dimethylamine in aqueous formaldehyde and acetic acid provided topotecan (**3**) in 62% yield.

2.3.3 Semisynthesis of Irinotecan

Sawada et al. first reported the synthesis of irinotecan (**4**) in 1991 (Scheme 2.3).[60] Hydrogen peroxide was added to a solution of 20(*S*)-CPT in aqueous sulfuric acid in the presence of ferrous sulfate and propionaldehyde to afford 7-ethyl CPT (**33**) in 77% yield. 7-Ethyl CPT (**33**) was converted to the corresponding *N*-oxide **34** using hydrogen peroxide in acetic acid. Irradiation of **34** in acidic media furnished the active metabolite of irinotecan (SN-38) (**35**) in 49% yield. Treatment of SN-38 (**35**) with 4-(1-piperidino)-1-(piperidino)-chloroformate then provided irinotecan (**4**) in 80% yield.

2.3.4 Semisynthesis of Belotecan

The synthesis of the most recently approved CPT analog belotecan (**5**) was reported in 2000 by Ahn et al. (Scheme 2.4).[61] 7-Methyl CPT was obtained by a Minisci-type reaction involving CPT, *t*-butyl peroxide, acetic acid, and ferrous sulfate in aqueous sulfuric acid in 86% yield. Then, 7-methyl CPT underwent a Mannich-type reaction when treated with iso-propylamine in DMSO/HCl, providing

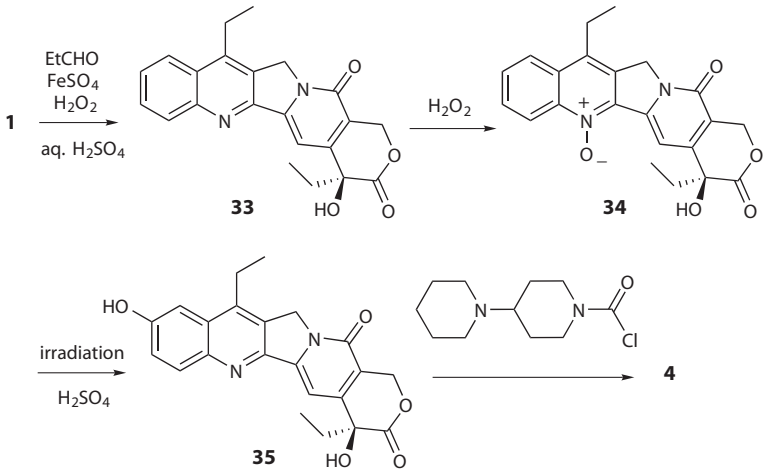

SCHEME 2.3 Semisynthesis of irinotecan.

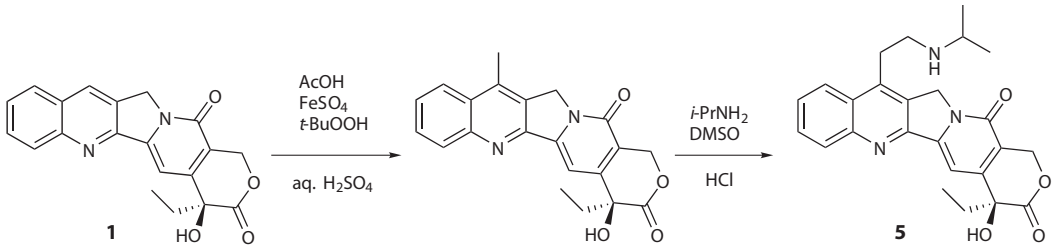

SCHEME 2.4 Semisynthesis of belotecan.

belotecan (**5**) in 47% yield. In this reaction, DMSO was used both as solvent and as the source of one methylene group.

Thus, while the clinically used CPT analogs are still synthesized by semisynthesis, numerous efficient approaches have been developed for the total synthesis of CPTs. Some of these syntheses may well be of utility should naturally derived CPT become insufficient for semisynthesis of **3**–**5**. Furthermore, the total syntheses can be adopted to produce CPT analogs not accessible by semisynthesis.

2.4 MEDICINAL CHEMISTRY

The examination of CPT analogs has been an active area of research since the original discovery of CPT. At present, there is a great deal known regarding the effect of substitutions at each of the accessible carbons of the pentacyclic scaffold, as well as the consequence of the expansion or removal of individual rings. Several reviews have covered the medicinal chemistry of CPT including an examination of the patent literature.[62–64] Akin to our previous chapter on CPT, we will address specific aspects of the medicinal chemistry of CPT via analysis of each ring system.

2.4.1 A/B/C/D Ring Analogs

The A and B rings remain the most critically explored regions of CPT owing to the synthetic accessibility of C7, C9, C10, C11, and C12 and due to early successes realized with analogs modified in this region of CPT. As a result, a great deal is known regarding the SAR at this locus. Alterations at C12 have invariably resulted in a loss of cytotoxicity. Derivatization of C11 is not deleterious to activity, but is generally limited to F, OH, OR, CN, and nitrogen substitutions. Dual substitutions at C10 and C11 typically result in a diminution of activity. Exceptions to this general pattern are fused ring systems such as 10,11-methylenedioxy and 10,11-ethylenedioxy groups [e.g., lurtotecan (**36**) (Figure 2.4)].[65] Electron-donating substituents at C9 and C10 (including halogens) are typically well tolerated, while bulky substituents and electron-withdrawing substituents generally result in a loss in potency. Topotecan (**3**), irinotecan (**4**), and SN-38 (**35**) highlight analogs with favorable biochemical and biological properties having substituents at C10 (Figure 2.4). The planarity of the A/B/C/D ring system is key to its activity; the x-ray crystallographic structure of the ternary complex of topo I, DNA, and topotecan published in 2002 provided a structural basis for this long-standing SAR trend.[18] Beyond the planarity of the ring system, it has been found that bulky substitutions directly attached to either the A or B ring system are detrimental to activity. A good example is the silicon-containing karenitecin (**37**) (Figure 2.4) having a bulky $Si(Me)_3$ moiety on a two-carbon linker attached at C7.[66] However, cyclic substituents connecting C9 and C7 have afforded analogs that retain potent topo I inhibition and cellular activity including exatecan (**38**) (Figure 2.4).[67]

Fewer analogs have been described with C- and D-ring substitutions. In general, substitutions on C5 have resulted in less active analogs. An important exception is DRF-1042 (**39**), a CPT analog that incorporates a 2-hydroxyethoxy moiety on C5; this analog has entered Phase II clinical evaluation

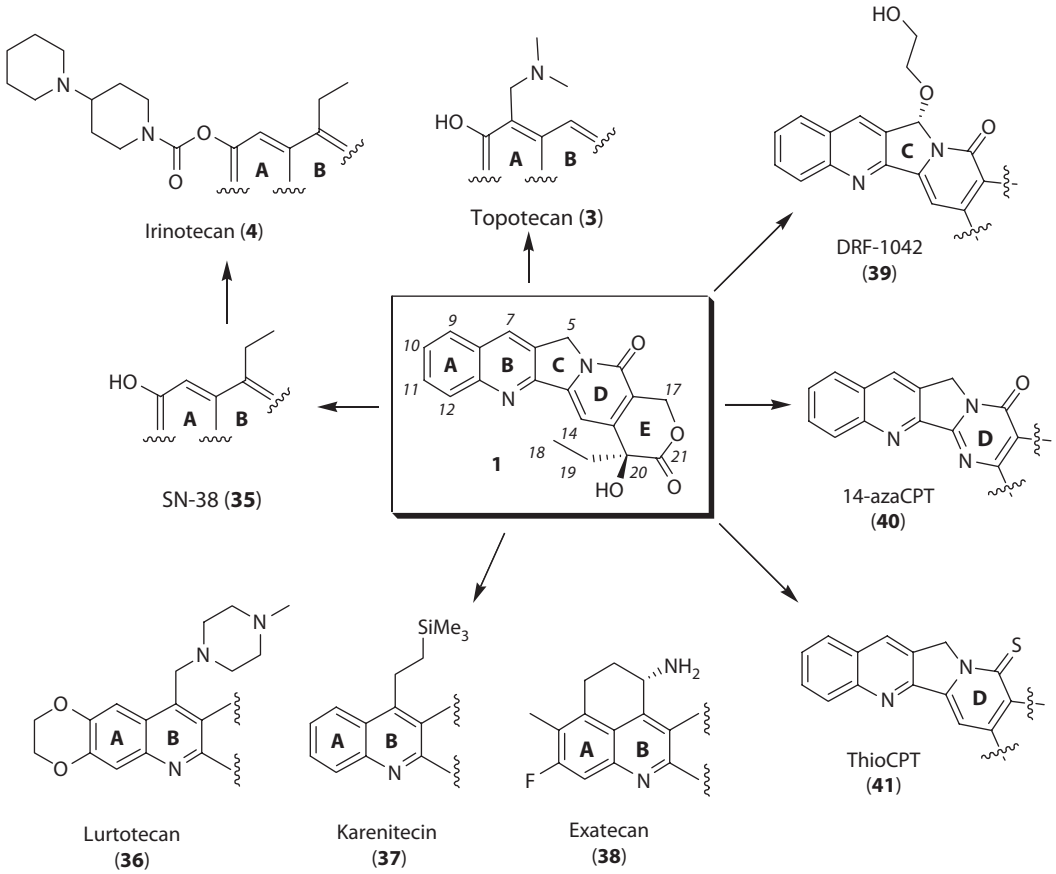

FIGURE 2.4 Structures of selected CPT analogs with substitutions at the A/B/C/D rings.

(Figure 2.4).[68] Prominent successes involving D-ring CPT analogs include 14-azaCPT (**40**) that possesses increased water solubility while retaining its activity as a topo I poison and cytotoxic agent,[69–71] and thioCPT (**41**) which was reported to possess increased cytotoxicity relative to CPT (Figure 2.4).[72] It is interesting that the motivation for the synthesis of 14-aza CPT (**40**) resulted from the discovery that the naturally occurring cytotoxin luotonin A (**44**) functions as a topo I poison.

2.4.2 E-Ring Analogs

Early studies surrounding the E-ring lactone suggested strongly that virtually any modification to this moiety would result in significant loss of activity as a topo I poison and cytotoxic agent. The water-soluble sodium salt (**2**) was the first of numerous attempted alterations to the lactone moiety that had a negative outcome. The lack of activity of the synthetically accessible 20-*R* CPT enantiomer demonstrated the critical nature of the stereochemistry of the 20-OH group.[73,74] This was later validated by the x-ray structure of the topo I–DNA–topotecan complex, which showed a critical hydrogen bond between Asp533 and the 20-*S* hydroxyl group of the CPT analog. Removal or replacement of the 20-*S* hydroxyl group in CPT largely diminished activity, while 20-halogen substituents retained a degree of potency.[74] Conversion of the E-ring lactone to lactam, thiolactone, and imide analogs resulted in CPT analogs with generally better hydrolytic stability, but lacking activity as topo I inhibitors.[73,75]

Given these results, the E-ring lactone was often avoided in SAR explorations of CPT. However, recent studies have overcome some of the issues surrounding this seemingly intractable structural

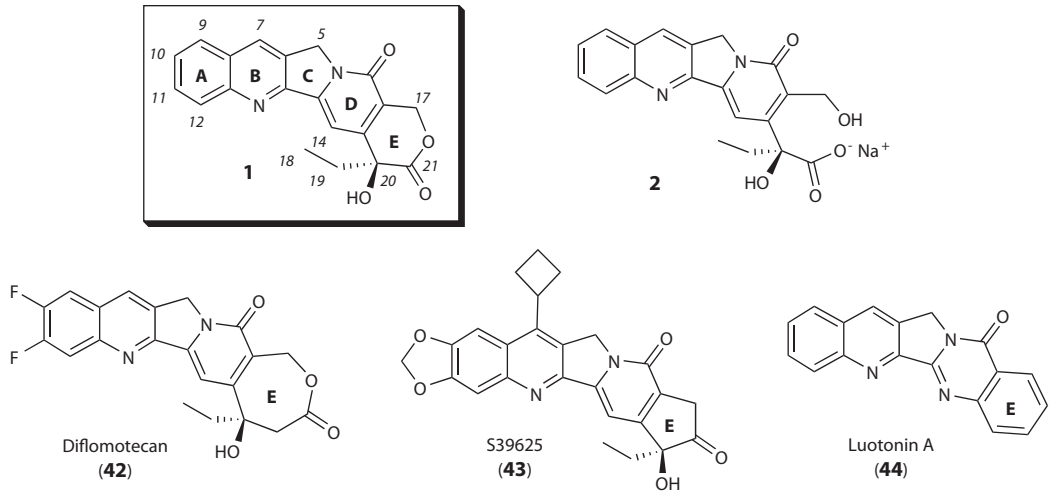

FIGURE 2.5 Structures of selected CPT analogs altered in the E ring.

feature. One major breakthrough involved the identification of β-hydroxylactone ring analogs of CPT that are widely referred to as homo-CPT. In contrast to CPT, homo-CPT analogs are more hydrolytically stable and exhibit potent topo I inhibitory properties. Several homo-CPT analogs have entered clinical trials including diflomotecan (**42**) (Figure 2.5).[76] Another intriguing finding is the success of five-membered α-hydroxyketo ring analogs such as S39625 (**43**) (Figure 2.5).[77] These agents are potent topo I poisons and exhibit favorable activity in colon, prostate, and breast cancer cells. In 2003, Cagir et al. made the surprising finding that the naturally occurring alkaloid luotonin A (**44**) functioned as a topo I poison (Figure 2.5) in spite of the lack of typical functionality appended to its E-ring.[78] This analog retains structural homology with CPT except for the replacement of the E-ring lactone moiety with a benzene ring and the presence of N at the D-ring position analogous to position 14 in CPT. It is interesting that the SAR of the E-ring of luotonin A differs materially from that of CPT.[79,80]

The E-ring lactone, and more specifically the 20-*S* OH group, has widely been utilized as the point of attachment for conjugates. These include conjugation to other cytotoxic agents and carrier molecules such as cyclodextrin and polyethylene glycols. An overview of specific 20-*S* OH conjugates that have entered clinical trials is presented in Section 2.5.4.

2.5 DEVELOPMENT OF CLINICALLY USEFUL CPT ANALOGS[81]

CPT is not used as an anticancer agent owing its poor water solubility and toxicity. In contrast, three CPT derivatives, including topotecan (**3**), irinotecan (**4**), and belotecan (**5**) (Figure 2.1), are currently approved in several countries for the treatment of a variety of tumors. Furthermore, there are a number of CPT analogs in various stages of clinical trials as single agents or in combination regimens.[81] In the past few years, new analogs have entered into clinical trials, others have continued their clinical evaluation, and some have failed. But the most active areas were the development of new drug delivery systems: conjugates (prodrugs) and formulations. The clinical applications of CPT analogs have been discussed in several excellent reviews and a brief summary is provided herein.[82,83]

2.5.1 Topotecan, Irinotecan, and Belotecan

Topotecan (**3**) (Hycamtin™, GlaxoSmithKline) is a semisynthetic derivative of CPT having a basic *N*,*N*-dimethylaminomethyl functional group at C9 that confers improved water solubility to the

molecule. Topotecan was approved by the FDA in 1996 as a second-line treatment for advanced ovarian cancer in patients following unsuccessful treatment with platinum-based therapeutics or paclitaxel-containing chemotherapy regimens. In 2000, topotecan was approved as a second-line treatment for recurrent small cell lung (SCL) cancer, and in 2006 it received approval, in combination with cisplatin, for the treatment of cervical cancer that is not amenable to curative treatment with surgery or radiation therapy. While topotecan is most commonly administered as an intravenous (IV) infusion, it has been recently approved (2007) for oral administration for the treatment of relapsed SCL cancers. Thus, topotecan was the first topo I poison for oral use.[81]

Neutropenia has proven to be the most encountered dose-limiting toxicity; however, a degree of thrombocytopenia is often associated with topotecan treatment as well. In addition, topotecan is currently in development as a single agent against a number of cancers, and also in combination with other drugs and with other treatment modalities, such as radiation therapy.[81,82]

Irinotecan (**4**) (Camptosar™, Pfizer) is a water-soluble prodrug designed to facilitate IV administration of the potent 7-ethyl-10-hydroxycamptothecin analog SN-38 (**35**). It contains a bispiperidine moiety, linked through a carbonyl group to a 10-hydroxy functionality. Enzymatic cleavage of the bispiperidine functionality by carboxylesterases predominantly located in the liver affords SN-38 (**35**), the biologically active compound, which is 1000-fold more potent as a topo I poison *in vitro* as compared with irinotecan. Irinotecan received accelerated approval in 1996 for the treatment of patients with colorectal metastatic carcinoma whose disease has recurred or progressed following initial flurouracil-based therapy. Irinotecan was subsequently approved as a component of first-line therapy in combination with 5-fluorouracil and leucovorin for patients with metastatic colorectal cancers. It has been extended to breast, cervical, lymphoma, ovarian, gastrointestinal, squamous cell, and lung cancers. Irinotecan is most commonly administered as an IV infusion, but an oral form is undergoing clinical trials. The biological half-life of the lactone form of SN-38 exceeds that of topotecan, which represents a potential pharmacological advantage. Indeed, a relatively large percentage of the intact lactone form of both irinotecan and SN-38 persists in the plasma of patients following drug administration, attributable to the preferential binding of irinotecan to serum albumin in its lactone form. The principal dose-limiting toxicity of irinotecan is delayed diarrhea, with or without neutropenia. As for topotecan, irinotecan is currently in development against a number of cancers, both as a single agent and in combination therapy.[81,82]

Belotecan (**5**) (Camtobell™, Chong Kun Dang) is a semisynthetic, water-soluble, CPT analog bearing an isopropylaminoethyl group at position 7 of the B ring. It was launched in South Korea in 2004 for IV treatment of ovarian cancer and SCL cancer. Belotecan has been designed to overcome the poor aqueous solubility and toxicity profile of CPT. Launch in the United States is anticipated.

2.5.2 Water-Soluble CPT Analogs in Clinical Trials

While water-soluble CPT analogs are now employed in clinical practice, the search for new water-soluble derivatives of CPT continues. Exatecan (**38**) (Daiichi Sankyo) is a hexacyclic CPT analog (Figure 2.6), which has been reported to have improved antitumor activity relative to topotecan and irinotecan. It reached Phase III trials as a potential first-line treatment for advanced pancreatic cancer in combination with gemcitabin, but failed to demonstrate improved efficacy in comparison with gemcitabin alone. The same company also discontinued, after Phase I studies, the development of DE-310, a conjugate of exatecan to a 340-kDa carboxymethyldextran carrier.[81]

Lurtotecan (**36**) (GlaxoSmithKline), another hexacyclic analog (Figure 2.6) is, in comparison with topotecan, more potent as topo I poison, more potent in tumor cell cytotoxicity assays, and more water soluble. This compound failed in Phase II clinical trials, but a liposomal formulation (OSI-211, Tigen Pharmaceuticals) is still in Phase II trials for ovarian cancer, SCL cancer, and squamous cell carcinoma. Indeed, this formulation markedly prolongs the systemic duration of lurtotecan.[81]

DRF-1042 (**39**) (Dr Reddy's Foundation) is the lone CPT derivative substituted at C-5 (Figure 2.6), which is in clinical trials. This orally active compound underwent Phase II trials

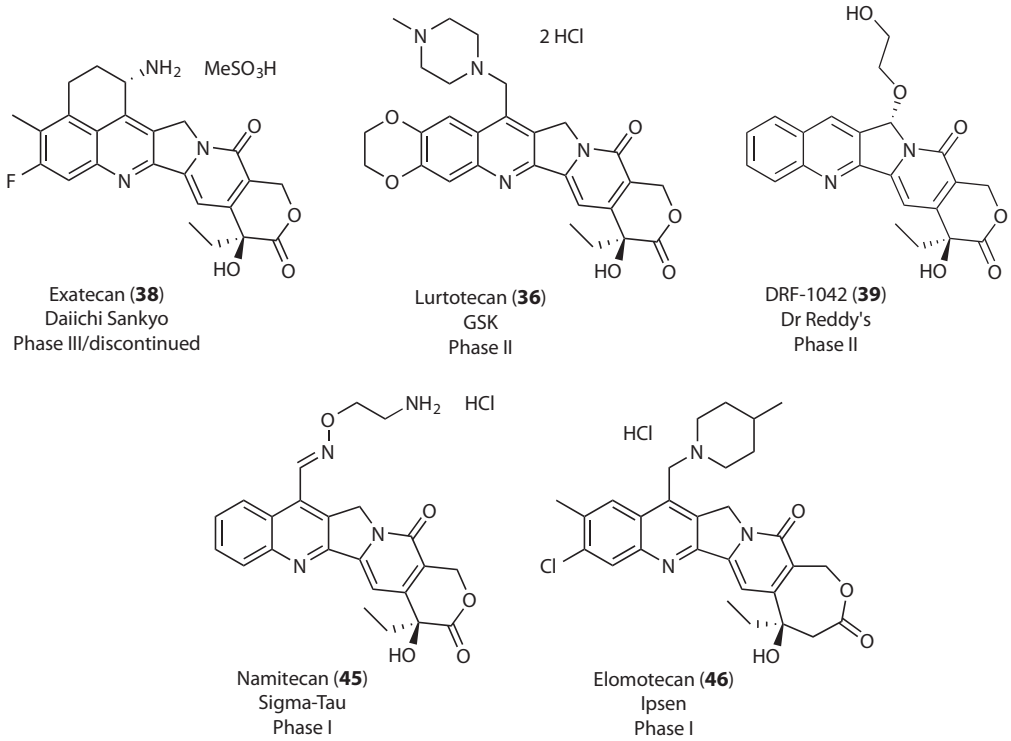

FIGURE 2.6 Water-soluble CPT analogs evaluated in clinical trials.

in India and is planned to enter Phase II trials in the United States against solid tumors. In Phase I, DRF-1042 showed no dose-limiting diarrhea and less neutropenia compared with topotecan and irinotecan.[81]

Namitecan (**45**) (Sigma-Tau) (Figure 2.6) is an imino-CPT derivative undergoing Phase I clinical trials in patients with solid tumors. In preclinical studies, it showed antitumor activity and an improved pharmacological profile compared with irinotecan and topotecan in a range of solid tumors and showed significant activity against tumors expressing different types of resistance.[81]

Elomotecan (**46**) (Ipsen) (Figure 2.6) is a homocamptothecin derivative that inhibits both topo I and topo II. It is in Phase I clinical trials against advanced metastatic cancers. The seven-membered lactone ring demonstrates slow and irreversible hydrolytic ring-opening leading to higher plasma stability and reduced side-effects. Elomotecan, administered both PO and IV, has demonstrated significant activity in all tested models.[81]

2.5.3 Water-Insoluble CPT Analogs in Clinical Trials

Studies have demonstrated that lipophilic CPTs are frequently more potent as topo I poisons than related water-soluble analogs, and have enhanced plasma stability.[84,85] Thus, a number of lipophilic CPTs have been developed for oral administration (Figure 2.7).

Biogen Idec has discontinued the development of 9-amino-CPT (9-AC) (**48**) following a lack of significant results in Phase II trials. Furthermore, 9-nitro-CPT (Rubitecan) (**47**) failed to produce favorable results in Phase III clinical trials for pancreatic cancer. Thus, SuperGen has also halted development of 9-nitro-CPT (**47**), which is the precursor of 9-amino-CPT *in vivo*.[81]

Cositecan (**49**) (BioNumerik) is an orally active, highly lipophilic silylated CPT derivative. Unlike water-soluble CPTs, cositecan is less sensitive to MDR/MRP drug resistance and CPT

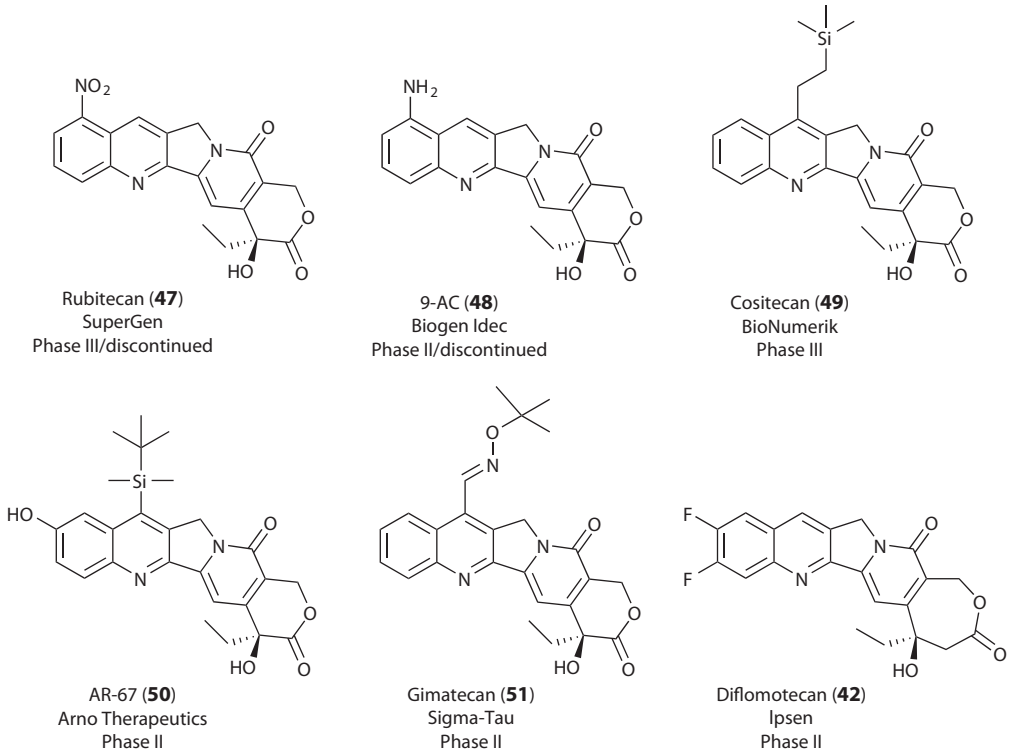

FIGURE 2.7 Structures of clinically studied lipophilic CPT analogs.

resistance-type mechanisms. It is in Phase III clinical trials for advanced ovarian cancer previously treated with platinum and taxane chemotherapy. Five U.S. Phase II trials are also ongoing or completed for different solid tumors.[81]

Arno Therapeutics is developing AR-67 (**50**), a second silylated CPT derivative. In preclinical studies, it demonstrated excellent potency and improved pharmacokinetic properties, with increased stability of the active lactone form in blood samples compared with marketed CPT drugs. Phase II trials against myelodysplastic syndrome have been initiated.[81]

Gimatecan (**51**) (Sigma-Tau) bears an oxyiminomethyl group at position 7 of CPT, which confers improved stabilization of the topo I–DNA covalent binary complex and increased intracellular accumulation. Given orally, gimatecan is in Phase I/II trials for glioma and myelodysplastic syndrome. Phase II trials against breast, colorectal, and epithelial cancers were also conducted.[81]

Diflomotecan (**42**) (Ipsen) was the first homo-CPT analog to enter into development. Phase II trials against SCL cancer have been completed using IV administration, but other Phase II trials in this indication failed PO to achieve their safety and efficacy targets.[81]

2.5.4 CPT Conjugates in Clinical Trials

The conjugation of CPT to small molecules or polymers at the 20-OH position can result in stabilization of the lactone ring, thus delaying its opening and reducing affinity to serum albumin. Moreover, the prodrug approach leads to a slow release of the active drug form, prolonging exposure time, which can dramatically alter the therapeutic index of the CPTs.[86,87]

CZ-48 (**52**) (Christus Stehlin Foundation for Cancer Research) (Figure 2.8), a 20-*O*-alkyl ester of CPT, is presently undergoing Phase I clinical trials with the goal of treating patients having advanced solid tumors.[81] TP-300 (**53**) (Chugai Pharmaceutical) is a water-soluble prodrug of CH-0793076 undergoing Phase I trials in colorectal cancer.[81]

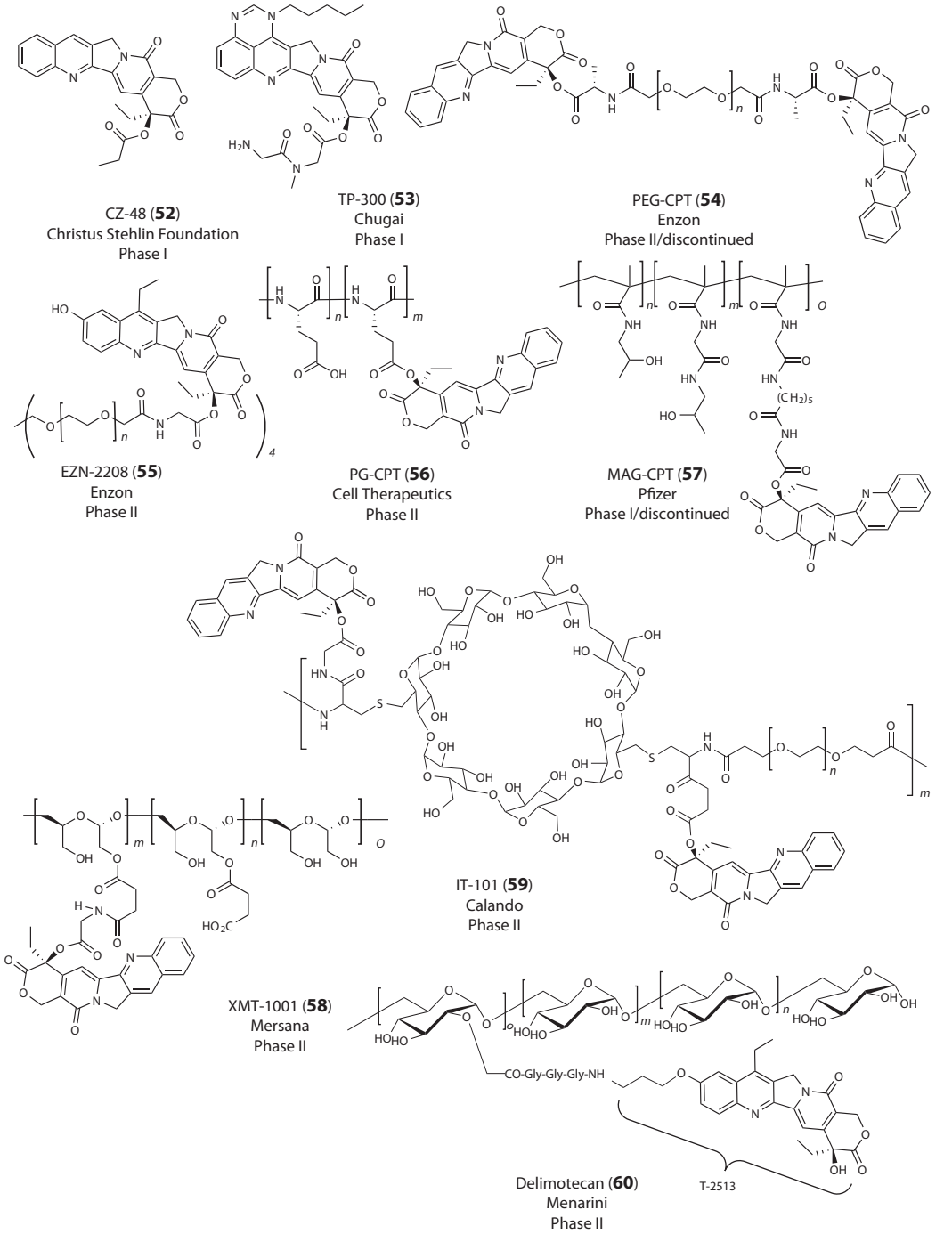

FIGURE 2.8 Structures of clinically studied CPT conjugates.

The conjugation of polymers to the 20-OH position of CPT has been performed as well. Thus, PEG-CPT (Pegamotecan, **54**) (Enzon) is a CPT conjugate with poly(ethylene glycol) that has been assessed clinically. This polymer exhibited excellent water solubility relative to free CPT. The development of PEG-CPT (**54**) was discontinued after analysis of Phase IIb results.[81,86,87] Enzon has also initiated development of EZN-2208 (**55**), a multiarmed PEG conjugated to SN-38 (**35**) via a

glycine linker. EZN-2208 exhibited prolonged circulation compared with SN-38, resulting in higher tumor exposure. Phase II trials with EZN-2208 are planned in colorectal and breast cancer.[81] Nektar Therapeutics is also developing a multiarmed PEG prodrug of irinotecan, NKTR-102, which is undergoing multiple Phase I and II trials.[81]

Another homopolymer, PG-CPT (**56**) (Cell Therapeutics), a polyglutamic acid conjugate of CPT, is in Phase II trials for the treatment of advanced metastatic ovarian cancer and colorectal cancer.[81,86,87]

Copolymers are also used as prodrugs of CPTs. Thus, MAG-CPT (**57**) (Pfizer) is a soluble copolymer linked to CPT through a glycylaminohexanoyl-glycyl spacer. Development was discontinued after Phase I.[81,87] XMT-1001 (**58**) (Mersana) is a polymeric prodrug of CPT in which CPT is attached to a hydrophilic, biodegradable, polyacetal polymer, namely poly(1-hydroxymethylethylene hydroxymethylformal). XMT-1001 releases CPT via two intermediates over an extended time period. Phase II trials in a solid tumor indication are planned.[81,88]

IT-101 (**59**) (Calando Pharmaceuticals) is a cyclodextrin-based polymer conjugate of CPT that self-assembles into nanoparticles. This strategy maintains CPT in its active lactone form and results in accumulation of the drug in tumor tissue. IT-101 (**59**) is in a Phase II clinical trial against ovarian cancer.[81,89]

Finally, delimotecan (**60**) (Menarini), is a carboxymethyldextran polymer prodrug of the active CPT derivative T-2513. This water-soluble polymer is linked to the active drug through the 10-position and not the 20-position. A Phase II trial in advanced metastatic melanoma patients is planned.[81]

2.5.5 Advances in CPT Formulations

In addition, efforts to optimize delivery strategies for CPTs such as nanoparticle encapsulation and liposomal core loading are underway, and some attempts have already reached Phase II.[86] For instance, NeoPharm and PharmaEngine have developed liposome-encapsulated formulations of SN-38 and irinotecan, respectively. They have initiated Phase II trials against various solid tumors such as breast and metastatic colorectal cancers.[81]

In addition, micelle and emulsion delivery systems are being developed. NK-102 (Nippon Kayaku) is a SN-38-releasing polymeric micelle and Tenifatecan (OncoGenex) is an injectable vitamin E emulsion formulation of SN-38. These two formulations of CPTs have recently entered into clinical trials.[81]

Thus, the first generation of CPTs was largely water soluble and the second generation is more lipophilic than CPT itself. These lipophilic compounds were designed for oral administration and to stabilize the lactone E-ring, which remains the Achilles' tendon of these structures. The third generation consists of a few new analogs and several conjugates. The conjugation of CPT analogs to polymers or small molecules is intended to enlarge the therapeutic window of this family. Other strategies to improve the efficiency of CPTs involve the development of new drug delivery systems, new formulations, and different routes of administration.[90] Topotecan and irinotecan were first approved in 1996. They are now approved to treat many other cancer types; thus, CPTs are becoming major chemotherapeutic agents in the treatment of cancer. While this review deals with the CPTs, it may be noted that non-CPT topo I inhibitors have also been under study and some have progressed to clinical trials.[91]

2.6 CONCLUSIONS

Recent studies of the CPTs have uncovered many new facets of the synthesis and mechanism of action of this class of antiumor agent. Of particular note is the level of sophistication of many recent syntheses of the natural product and its analogs, and the success achieved in modifying the E-ring lactone to afford improved stability and simpler pharmacology. The ongoing clinical trials of numerous analogs of CPT reflect a growing consensus regarding the utility of the CPTs, and more generally topo I poisons, as useful agents for cancer chemotherapy.

ACKNOWLEDGMENTS

Nicolas J. Rahier thanks Emilie Routier and Institut de Recherche Pierre Fabre for bibliographical help during the preparation of this chapter. Craig Thomas acknowledges support from the Molecular Libraries Initiative of the National Institutes of Health Roadmap for Medical Research and the Intramural Research Program of the National Human Genome Research Institute, National Institutes of Health.

REFERENCES

1. Wall, M.E., Wani, M.C., Cook, C.E., Palmer, K.H., McPhail, A.T., and Sim, G.A., Plant antitumor agents. I. The isolation and structure of camptothecin, a novel alkaloidal leukemia and tumor inhibitor from *Camptotheca acuminata*, *J. Am. Chem. Soc*., 88, 3888, 1966.
2. Wall, M.E. and Wani, M.C., Camptothecin and taxol: Discovery to clinic, Thirteenth Bruce F. Cain Memorial Award lecture, *Cancer Res*., 55, 753, 1995.
3. Moertel, C.G., Schutt, A.J., Reitemeier, R.J., and Hahn, R.G., Phase II study of camptothecin (NSC-100880) in the treatment of advanced gastrointestinal cancer, *Cancer Chemother. Rep*., 56, 95, 1972.
4. Hsiang, Y.H., Hertzberg, R., Hecht, S.M., and Liu, L.F., Camptothecin induces protein-linked DNA breaks via mammalian DNA topoisomerase I, *J. Biol. Chem*., 260, 14873, 1985.
5. Champoux, J.J., DNA topoisomerases: Structure, function, and mechanism, *Annu. Rev. Biochem*., 70, 369, 2002.
6. Pommier, Y., Pourquier, P., Fan, Y., and Strumberg, D., Mechanism of action of eukaryotic DNA topoisomerase I and drugs targeted to the enzyme, *Biochim. Biophys. Acta*, 1400, 83, 1998.
7. Redinbo, M.R., Stewart, L., Kuhn, P., Champoux, J.J., and Hol, W.G.J., Crystal structures of human topoisomerase I in covalent and noncovalent complexes with DNA, *Science*, 279, 1504, 1998.
8. Pommier, Y., Topoisomerase I inhibitors: Camptothecins and beyond, *Nat. Rev. Cancer*, 6, 789, 2006.
9. Hertzberg, R.P., Caranfa, M.J., and Hecht, S.M., On the mechanism of topoisomerase I inhibition by camptothecin: evidence for binding to an enzyme–DNA complex, *Biochemistry*, 28, 4629, 1989.
10. Yang, D., Strode, J.T., Spielmann, H.P., Wang, A.H.-J., and Burke, T.G., DNA interactions of two clinical camptothecin drugs stabilize their active lactone forms, *J. Am. Chem. Soc*., 120, 2979, 1998.
11. Hertzberg, R.P., Busby, R.W., Caranfa, M.J., Holden, K.G., Johnson, R.K., Hecht, S.M., and Kingsbury, W.D., Irreversible trapping of the DNA–topoisomerase I covalent complex, *J. Biol. Chem*., 265, 19287, 1990.
12. Pommier, Y., Kohlhagen, G.K., Kohn, K.W., Leteurtre, F., Wani, M.C., and Wall, M. E., Interaction of an alkylating camptothecin derivative with a DNA base at topoisomerase I–DNA cleavage sites, *Proc. Natl. Acad. Sci. U.S.A*., 92, 8861, 1995.
13. Pommier, Y., Pourquier, P., Urasaki, Y., Wu, J., and Laco, G.S., Topoisomerase I inhibitors: Selectivity and cellular resistance, *Drug Resist. Updates*, 2, 307, 1999.
14. Beretta, G.L., Perego, P., and Zunino, F., Mechanisms of cellular resistance to camptothecins, *Curr. Med. Chem*., 13, 3291, 2006.
15. Fan, Y., Weinstein, J.N., Kohn, K.W., Shi, L.M., and Pommier, Y., Molecular modeling studies of the DNA–topoisomerase I ternary cleavable complex with camptothecin, *J. Med. Chem.*, 41, 2216, 1998.
16. Kerrigan, J.E. and Pilch, D.S., A structural model for the ternary cleavable complex formed between human topoisomerase I, DNA, and camptothecin, *Biochemistry*, 40, 9792, 2001.
17. Laco, G.S., Collins, J.R., Luke, B.T., Kroth, H., Sayer, J.M., Jerina, D.M., and Pommier, Y., Human topoisomerase I inhibition: Docking camptothecin and derivatives into a structure-based active site model, *Biochemistry*, 41, 1428, 2002.
18. Staker, B.L., Hjerrild, K., Feese, M.D., Behnke, C.A., Burgin, A.B., and Stewart, L., The mechanism of topoisomerase I poisoning by a camptothecin analog, *Proc. Natl. Acad. Sci. U.S.A*., 99, 15387, 2002.
19. Chrencik, J.E., Staker, B.L., Burgin, A.B., Pourquier, P., Pommier, Y., Stewart, L., and Redinbo, M.R., Mechanisms of camptothecin resistance by human topoisomerase I mutations, *J. Mol. Biol*., 339, 773, 2004.
20. Staker, B.L., Feese, M.D., Cushman, M., Pommier, Y., Zembower, D., Stewart, L., and Burgin, A.B., Structures of three classes of anticancer agents bound to the human topoisomerase I–DNA covalent complex, *J. Med. Chem*., 48, 2336, 2005.

21. Marchand, C., Antony, S., Kohn, K.W., Cushman, M., Ioanoviciu, A., Staker, B.L., Burgin, A.B., Stewart, L., and Pommier, Y., A novel norindenoisoquinoline structure reveals a common interfacial inhibitor paradigm for ternary trapping of topoisomerase I–DNA covalent complexes, *Mol. Cancer Ther*., 5, 287, 2006.
22. Urasaki, Y., Laco, G.S., Pourquier, P., Takebayashi, Y., Kohlhagen, G., Gioffre, C., Zhang, H., Chatterjee, D., Pantazis, P., and Pommier, Y., Characterization of a novel topoisomerase I mutation from a camptothecin-resistant human prostate cancer cell line, *Cancer Res*., 61, 1964, 2001.
23. Fujimori, A., Harker, W.G., Kohlhagen, G., Hoki, Y., and Pommier, Y., Mutation at the catalytic site of topoisomerase I in CEM/C2, a human leukemia cell line resistant to camptothecin, *Cancer Res*., 55, 1339, 1995.
24. Jensen, A.D. and Svejstrup, J.Q., Purification and characterization of human topoisomerase I mutants, *Eur. J. Biochem*., 236, 389, 1996.
25. Sirikantaramas, S., Yamazaki, M., and Saito, K., Mutations in topoisomerase I as a self-resistance mechanism coevolved with the production of the anticancer alkaloid camptothecin in plants, *Proc. Natl. Acad. Sci. U.S.A.*, 105, 6782, 2008.
26. Nitiss, J. and Wang, J.C., DNA topoisomerase-targeting antitumor drugs can be studied in yeast, *Proc. Natl. Acad. Sci. U.S.A.*, 85, 7501, 1988.
27. Gallo, R.C., Whang-Peng, J., and Adamson, R.H., Studies on the antitumor activity, mechanism of action, and cell cycle effects of camptothecin, *J. Natl. Cancer Inst*., 46, 789, 1971.
28. Liu, C., Pouliot, J.J., and Nash, H.A., Repair of topoisomerase I covalent complexes in the absence of the tyrosyl–DNA phosphodiesterase Tdp1, *Proc. Natl. Acad. Sci. U.S.A.*, 99, 14970, 2002.
29. Vance, J.R. and Wilson, T.E., Yeast Tdp1 and Rad1-Rad10 function as redundant pathways for repairing Top1 replicative damage, *Proc. Natl. Acad. Sci. U.S.A.*, 99, 13669, 2002.
30. Deng, C., Brown, J.A., You, D., and Brown, J.M., Multiple endonucleases function to repair covalent topoisomerase I complexes in *Saccharomyces cerevisiae*, *Genetics*, 170, 591, 2005.
31. Kanagasabai, R., Liu, S., Salama, S., Yamasaki, E.F., Zhang, L., Greenchurch, K.B., and Snapka, R.M., Ubiquitin-family modifications of topoisomerase I in camptothecin-treated human breast cancer cells, *Biochemistry*, 48, 3176, 2009.
32. Yang, S., Burgin, A.B., Jr., Huizenga, B.N., Robertson, C.A., Yao, K.C., and Nash, H.A., A eukaryotic enzyme that can disjoin dead-end covalent complexes between DNA and type I topoisomerases, *Proc. Natl. Acad. Sci. U.S.A.*, 93, 11534, 1996.
33. Lin, C.-P., Ban, Y., Lyu, Y.L., Desai, S.D., and Liu, L.F., A ubiquitin-proteasome pathway for the repair of topoisomerase I–DNA covalent complexes, *J. Biol. Chem*., 283, 21074, 2008.
34. van Hattum, A.H., Hoogsteen, I.J., Schlueper, H.M.M., Maliepaard, M., Scheffer, G.L., Scheper, R.J., Kohlhagen, G., Pommier, Y., Pinedo, H.M., and Boven, E., Induction of breast cancer resistance protein by the camptothecin derivative DX-8951f is associated with minor reduction of antitumour activity, *Br. J. Cancer*, 87, 665, 2002.
35. Brangi, M., Litman, T., Ciotti, M., Nishiyama, K., Kohlhagen, G., Takimoto, C., Robey, R., Pommier, Y., Fojo, T., and Bates, S.E., Camptothecin resistance: Role of the ATP-binding cassette (ABC), mitoxantrone-resistance half-transporter (MXR), and potential for glucuronidation in MXR-expressing cells, *Cancer Res*., 59, 5938, 1999.
36. Bates, S.E., Medina-Perez, W.Y., Kohlhagen, G., Antony, S., Nadjem, T., Robey, R., and Pommier, Y., ABCG2 mediates differential resistance to SN-38 (7-ethyl-10-hydroxylcamptothecin) and homocamptothecins, *J. Pharmacol. Exp. Ther*., 310, 836, 2004.
37. Houser, S., Koshlatyi, S., Lu, T., Gopen, T., and Bargonetti, J., Camptothecin and zeocin can increase p53 levels during all cell cycle stages, *Biochem. Biophys. Res. Commun*., 289, 998, 2001.
38. Gupta, M., Fan, S., Zhan, Q., Kohn, K.W., O'Connor, P.M., and Pommier, Y., Inactivation of p53 increases the cytotoxicity of camptothecin in human colon HCT116 and breast MCF-7 cancer cells, *Clin. Cancer Res*., 3, 1653, 1997.
39. Huang, H., Regan, K.M., Lou, Z., Chen, J., and Tindall, D.J., CDK2-dependent phosphorylation of FOXO1 as an apoptotic response to DNA damage, *Science*, 314, 294, 2006.
40. Togano, T., Sasaki, M., Watanabe, M., Nakashima, M., Tsuruo, T., Umezawa, K., Higashihara, M., Watanabe, T., and Horie, R., Induction of oncogene addiction shift to NF-κB by camptothecin in solid tumor cells, *Biochem. Biophys. Res. Commun*., 390, 60, 2009.
41. Fusaro, G., Dasgupta, P., Rastogi, S., Joshi, B., and Chellappan, S., Prohibitin induces the transcriptional activity of p53 and is exported from the nucleus upon apoptotic signaling, *J. Biol. Chem*., 48, 47853, 2003.

42. Díaz-González, R., Pérez-Pertejo, Y., Prada, C.F., Fernández-Rubio, C., Balaña-Fouce, R., and Reguera, R.M., Novel findings on trypanosomatid chemotherapy using DNA topoisomerase inhibitors, *Mini-Rev. Med. Chem.*, 9, 674, 2009.
43. Bakshi, R. and Shapiro, T.A., RNA interference of *Trypanosoma brucei* topoisomerase IB: Both subunits are essential, *Mol. Biochem. Parasitol.*, 136, 249, 2004.
44. Balaña-Fouce, R., Garcia-Estrada, C., Perez-Pertejo, Y., and Reguera, R.M., Gene disruption of the DNA topoisomerase IB small subunit induces a non-viable phenotype in the hemoflagellate *Leishmania major*, *BMC Microbiol.*, 8, 113, 2008.
45. Proulx, M.E., Desormeaux, A., Marquis, J.-E., Olivier, M., and Bergeron, M.G., Treatment of visceral leishmaniasis with sterically stabilized liposomes containing camptothecin, *Antimicrob. Agents Chemother.*, 45, 2623, 2001.
46. Du, W., Towards new anticancer drugs: a decade of advances in synthesis of camptothecins and related alkaloids, *Tetrahedron*, 59, 8649, 2003.
47. Curran, D.P., Josien, H., Bom, D., Gabarda, A.E., and Du, W., The cascade radical annulations approach to new analogues of camptothecins. Combinatorial synthesis of silatecans and homosilatecans, *Ann. N. Y. Acad. Sci.*, 922, 112, 2000.
48. Fortunak, J.M.D., Kitteringham, J., Mastrocola, A.R., Mellinger, M., Sisti, N.J., Wood, J.L., and Zhuang, Z.-P., Novel syntheses of camptothecin alkaloids, Part 2, Concise synthesis of (*S*)-camptothecins, *Tetrahedron Lett.*, 37, 5683, 1996.
49. Zhou, H.-B., Liu, G.-S., and Yao, Z.-J., Highly efficient and mild cascade reaction triggered by bis(triphenyl)oxodiphosphonium trifluoromethanesulfonate and a concise total synthesis of camptothecin, *Org. Lett.*, 9, 2003, 2007.
50. Comins, D.L. and Nolan, J.M., A practical six-step synthesis of (*S*)-camptothecin, *Org. Lett.*, 3, 4255, 2001.
51. Bennasar, M.-L., Zulaica, E., Juan, C., Alonso, Y., and Bosch, J., Addition of ester enolates to *N*-alkyl-2-fluoropyridinium salts: Total synthesis of (±)-20-deoxycamptothecin and (+)-camptothecin, *J. Org. Chem.*, 67, 7465, 2002.
52. Lavergne, O., Demarquay, D., Bailly, C., Lanco, C., Rolland, A., Huchet, M., Coulomb, H. et al., Topoisomerase I-mediated antiproliferative activity of enantiomerically pure fluorinated homocamptothecins, *J. Med. Chem.*, 43, 2285, 2000.
53. Fang, F.G., Bankston, D.D., Huie, E.M., Johnson, M.R., Kang, K.-C., LeHoullier, C.S., Lewis, G.C. et al., Convergent catalytic asymmetric synthesis of camptothecin analog GI147211C, *Tetrahedron*, 53, 10953, 1997.
54. Ciufolini, M.A. and Roschangar, F., Practical synthesis of (20 *S*)-(+)-camptothecin: The progenitor of a promising group of anticancer agents, *Targets Heterocycl. Syst.*, 4, 25, 2000.
55. Chavan, S.P., Pathak, A.B., and Kalkote, U.R., Total synthesis of (+)-camptothecin via intramolecular palladium catalyzed cyclization strategy, *Synlett.*, 17, 2635, 2007.
56. Kanazawa, A., Muniz, M.N., Baumlova, B., Ljungdahl, N., and Greene, A.E., New route to natural camptothecin through isomünchnone cycloaddition, *Synlett.*, 15, 2275, 2008.
57. Blagg, B.S.J. and Boger, D.L., Total synthesis of (+)-camptothecin, *Tetrahedron*, 58, 6343, 2002.
58. Liu, G.-S., Dong, Q.-Li, Yao, Y.-S., and Yao, Z.-J., Expeditious total synthesis of camptothecin and 10-hydroxycamptothecin, *Org. Lett.*, 10, 5393, 2008.
59. Kingsbury, W.D., Boehm, J.C., Jakas, D.R., Holden, K.G., Hecht, S.M., Gallagher, G., Caranfa, M.J., McCabe, F.L., Faucette, L.F., Johnson, R.K., and Hertzberg, R.P., Synthesis of water-soluble (aminoalkyl) camptothecin analogs: inhibition of topoisomerase I and antitumor activity, *J. Med. Chem.*, 34, 98, 1991.
60. Sawada, S., Okajima, S., Aiyama, R., Nokata, K., Furuta, T., Yokokura, T., Sugino, E., Yamaguchi, K., and Miyasaka, T., Synthesis and antitumor activity of 20(*S*)-camptothecin derivatives: Carbamate-linked, water-soluble derivatives of 7-ethyl-10-hydroxycamptothecin, *Chem. Pharm. Bull.*, 39, 1446, 1991.
61. Ahn, S.K., Choi, N.S., Jeong, B.S., Kim, K.K., Journ, D.J., Kim, J.K., Lee, S.J., Kim, J.W., Hong, C.I., and Jew, S.-S., Practical synthesis of (*S*)-7-(2-isopropylamino)ethylcamptothecin hydrochloride, potent topoisomerase I inhibitor, *J. Heterocycl. Chem.*, 37, 1141, 2000.
62. Thomas, C.J., Rahier, N.J., and Hecht, S.M., Camptothecin: Current perspectives, *Bioorg. Med. Chem.*, 12, 1585, 2004.
63. Verma, R.P. and Hansch, C., Camptothecins: A SAR/QSAR study, *Chem. Rev.*, 109, 213, 2009.
64. Basili, S. and Moro, S., Novel camptothecin derivatives as topoisomerase I inhibitors, *Expert Opin. Ther. Patents*, 19, 555, 2009.

65. Dark, G.G., Calvert, A.H., Grimshaw, R., Poole, C., Swenerton, K., Kaye, S., Coleman, R. et al., Randomized trial of two intravenous schedules of the topoisomerase inhibitor liposomal lurtotecan in women with relapsed epithelial ovarian cancer: A trial of the National Cancer Institute of Canada Clinical Trials Group, *J. Clin. Oncol*., 23, 1859, 2005.
66. Daud, A., Valkov, N., Centeno, B., Derderian, J., Sullivan, P., Munster, P., Urbas, P. et al., Phase II trial of karenitecin in patients with malignant melanoma: Clinical and translational study, *Clin. Cancer Res*. 11, 3009, 2005.
67. Reichardt, P., Nielsen, O.S., Bauer, S., Hartmann, J.T., Schoeffski, P., Christensen, T.B., Pink, D. et al., Exatecan in pretreated adult patients with advanced soft tissue sarcoma: Results of a phase II—study of the EORTC soft tissue and bone sarcoma group, *Eur. J. Cancer*, 43, 1017, 2007.
68. Chatterjee, A., Digumarti, R., Mamidi, R.N.V.S., Katneni, K., Upreti, V.V., Surath, A., Srinivas, M.L. et al., Safety, tolerability, pharmacokinetics, and pharmacodynamics of an orally active novel camptothecin analog, DRF-1042, in refractory cancer patients in a phase I dose escalation study, *J. Clin. Pharmacol*., 44, 723, 2004.
69. Cheng, K., Rahier, N.J., Eisenhauer, B.M., Gao, R., Thomas, S.J., and Hecht, S.M., 14-Azacamptothecin: a potent water-soluble topoisomerase I poison, *J. Am. Chem. Soc*., 127, 838, 2005.
70. Rahier, N.J., Cheng, K., Gao, R., Eisenhauer, B.M., and Hecht, S.M., Synthesis of 14-azacamptothecin, a water soluble topoisomerase I poison, *Org. Lett*., 7, 835, 2005.
71. Elban, M.A., Sun, W., Eisenhauer, B.M., Gao, R., and Hecht, S.M., Synthesis and biological evaluation of 10,11-methylenedioxy-14-azacamptothecin, *Org. Lett*., 8, 3513, 2006.
72. Samori, C., Guerrini, A., Varchi, G., Zunino, F., Beretta, G.L., Femoni, C., Bombardelli, E., Fontana, G., and Battaglia, A., Thiocamptothecin, *J. Med. Chem*., 51, 3040, 2008.
73. Jaxel, C., Kohn, K.W., Wani, M.C., Wall, M.E., and Pommier, Y., Structure–activity study of the actions of camptothecin derivatives on mammalian topoisomerase I: Evidence for a specific receptor site and a relation to antitumor activity, *Cancer Res*., 49, 1465, 1989.
74. Wang, X., Zhou, X., and Hecht, S.M., Role of the 20-hydroxyl group in camptothecin binding by the topoisomerase I–DNA binary complex, *Biochemistry*, 38, 4374, 1999.
75. Hertzberg, R.P., Caranfa, M.J., Holden, K.G., Jakas, D.R., Gallagher, G., Mattern, M.R., Mong, S.M., Bartus, J.O., Johnson, R.K., and Kingsbury, W.D., Modification of the hydroxy lactone ring of camptothecin: inhibition of mammalian topoisomerase I and biological activity, *J. Med. Chem*., 32, 715, 1989.
76. Kroep, J.R. and Gelderblom, H., Diflomotecan, a promising homocamptothecin for cancer therapy, *Expert Opin. Invest. Drugs*, 18, 69, 2009.
77. Takagi, K., Dexheimer, T.S., Redon, C., Sordet, O., Agama, K., Lavielle, G., Pierre, A., Bates, S.E., and Pommier, Y., Novel E-ring camptothecin keto analogues (S38809 and S39625) are stable, potent, and selective topoisomerase I inhibitors without being substrates of drug efflux transporters, *Mol. Cancer Ther*., 6, 3229, 2007.
78. Cagir, A., Jones, S.H., Gao, R., Eisenhauer, B.M., and Hecht, S.M., Luotonin A: A naturally occurring human DNA topoisomerase I poison, *J. Am. Chem. Soc*., 125, 13628, 2003.
79. Cagir, A., Jones, S.H., Eisenhauer, B.M., Gao, R., and Hecht, S.M., Synthesis and biological properties of E-ring modified luotonin A derivatives, *Bioorg. Med. Chem. Lett*., 14, 2051, 2004.
80. Cagir, A., Eisenhauer, B.M., Gao, R., Thomas, S.J., and Hecht, S.M., Synthesis and topoisomerase I inhibitory properties of luotonin analogues, *Bioorg. Med. Chem*., 12, 6287, 2004.
81. Data obtained from Pharmaprojects—Pharmaceutical Research & Development Pipeline Intelligence, http://www.pharmaprojects.com/, June and September 2009.
82. Garcia-Carbonero, R. and Supko, J.G., Current perspectives on the clinical experience, pharmacology, and continued development of the camptothecins, *Clin. Cancer Res.*, 8, 641, 2002.
83. Kluza, J., Arimondo, P.B., David-Cordonnier, M.-H., and Bailly, C., Camptothecins for drug design, cancer cell death and gene targeting, in *Cancer Drug Design and Discovery*, Neidle, S. Ed., Elsevier Inc., 2008, pp. 173–197.
84. Tanizawa, A., Fujimori, A., Fujimori, Y., and Pommier, Y., Comparison of topoisomerase I inhibition, DNA damage, and cytotoxicity of camptothecin derivatives presently in clinical trials, *J. Natl. Cancer Inst.*, 86, 836, 1994.
85. Burke, T.G., Mishra, A.K., Wani, M.C., and Wall, M.E., Lipid bilayer partitioning and stability of camptothecin drugs, *Biochemistry*, 32, 5352, 1993.
86. Onishi, H. and Machida, Y., Macromolecular and nanotechnological modification of camptothecin and its analogs to improve the efficacy, *Curr. Drug Discov. Technol*., 2, 169, 2005.
87. Kratz, F., Abu Ajaj, K., and Warnecke, A., Anticancer carrier-linked prodrugs in clinical trials, *Expert Opin. Investig. Drugs*, 16, 1037, 2007.

88. Yurkovetskiy, A.V. and Fram, R.J., XMT-1001, a novel polymeric camptothecin pro-drug in clinical development for patients with advanced cancer, *Adv. Drug Deliv. Rev*., 61, 1193, 2009.
89. Davis, M.E., Design and development of IT-101, a cyclodextrin-containing polymer conjugate of camptothecin, *Adv. Drug Deliv. Rev*., 61, 1189, 2009.
90. Glaberman, U., Rabinowitz, I., and Verschraegen, C.F., Alternative administration of camptothecin analogues, *Expert Opin. Drug Deliv.*, 2, 323, 2005.
91. For information concerning current clinical trials, see: http://www.clinicaltrials.gov, Enter "cancer AND topoisomerase I".

3 The Discovery and Development of the Combretastatins

Kevin G. Pinney, George R. Pettit, Mary Lynn Trawick, Christopher Jelinek, and David J. Chaplin

CONTENTS

3.1 Introduction, History, and Structures of Combretastatins 27
3.2 Biochemical and Biological Mechanism of Action 31
3.3 Therapeutic Intervention through Vascular Disruption 32
3.4 Synthesis of Combretastatins 36
3.5 Combretastatin Derivatives and Synthetic Analogs Inspired by the Combretastatins 41
3.6 Preclinical Studies 45
3.6.1 Effects of CA4P on Tumor Blood Flow 45
3.6.2 Tumor Response to CA4P as a Single Agent 46
3.6.3 Treatment Response to CA4P in Combination Therapy 47
3.6.4 Preclinical Studies with CA1P (OXi4503) 48
3.7 Clinical Experience 48
3.7.1 Cancer 48
3.7.2 Ophthalmology 49
3.8 Coda 50
Acknowledgments 51
References 51

3.1 INTRODUCTION, HISTORY, AND STRUCTURES OF COMBRETASTATINS

The Combretaceae plant family (comprising 600 or more species) of shrubs and trees is divided among 20 genera, of which the *Combretum* genus (250 species) of tropical and deciduous trees encompasses the largest number.[1] Some 24 species of *Combretum* are well- known in African folk medicine for applications and problems ranging from heart and worm remedies to wound dressings, treatment for the mentally ill, and scorpion stings.[2] A 2007 report suggests that a number of these traditional medical uses may reside with potent antifungal constituents against dimorphic fungi, molds, and yeasts.[3] The methanol extracts of *Combretum moggii*, *Combretum petrophilum*, and *Combretum nelsonii* proved to be most active against all the pathogens evaluated. An acetone extract of *Combretum caffrum* was found very inhibitory [minimal inhibitory concentration (MIC): 0.02 mg/mL] especially for *Microsporum canis*.

Only the Indian *Combretum latifolium* appears to have been recorded as a folk medical treatment for cancer.[4] However, over 30 years ago, as part of the U.S. National Cancer Institute's (NCI) worldwide exploratory survey of terrestrial plants, both *Combretum molle*[5] and *C. caffrum* (Eckl. and Zeyh.) Kuntze were found to provide extracts significantly active against the murine P-388 lymphocytic leukemia (PS system). *Combretum caffrum* is a deciduous tree (growing to a height of

15 m) in Africa, found principally in the Eastern Cape and Transkei to Natal. This willow-like tree ("bushwillow") is a common sight overhanging stream beds. In autumn, these trees become quite prominent, with displays of reddish-brown fruit and leaves that turn bright red before falling.[6] The powdered root bark has been used by the Zulu of South Africa as a charm to harm an enemy.[2]

In a broader context, the Combretaceae family is well represented in traditional medical practices of, especially, Africa and India.[7] Illustrative is a study of Combretaceae species used in Somalia.[8] These species range from *Combretum hereroense* (young shoots used for respiratory infection) to *Terminalia brevipes* (root bark employed for hepatitis and malaria) to *Commelina forskoolii* (juice for treatment of uterine cancer). Nine other species including *Anogeissus leiocorpus* (fruit and roots as an anthelmintic treatment), *Guiera senegalensis* (fruit and leaves for leprosy and dysentery), and *Quisqualis indica* (leaves for vermifuge) are more widely used in Africa.[9] Other Combretaceae species, such as *Combretum coccineum* and *Combretum constrictum*,[10] are well-known medicinal plants in Indian Ocean Island areas. Even better known is the medicinal herb *Combretum micronthum*, used as an opium antidote for addiction and for other indications from blackwater fever to nausea.[11] Importantly, seven species of the genus *Terminalia*[12] and one *Guiera* species have a long history in African and Asian primitive medical treatments for cancer.[4] In Zimbabwe, *C. molle* and three other *Combretum* species have been summarized along with two *Terminalia* species (250 tropical)[1] as plant extract remedies for diarrhea.[13]

In the classic 1962 compilation and discussion of "Medicinal and Poisonous Plants of Southern and Eastern Africa,"[2] Watt and Breyer-Brandwijk described the root bark of *C. caffrum* (aka *salicifolium* E. Mey.) as the Zulu charm for harming an enemy.

> Some of the powdered material is heated with water in a piece of broken earthenware pot, and the points of two assegais are dipped into the boiling solution. The assegai points are brought near the mouth and the operator licks them and spits in the direction of his enemy whose name is shouted out. This is repeated several times, the weapons being thrust in the same direction and finally into the ground.

Commencing with the discovery of the combretastatins, the question has arisen many times as to whether or not some of the indigenous people of Africa and elsewhere had used extracts of *C. caffrum* for medicinal purposes that included treating cancer. The scientific/medical literature appears to be silent on that issue. In that respect, one of us (G.R.P.) was pleased to be contacted in November 1999 by a South African chemist, Case van Hattem. In the helpful correspondence that ensued, van Hattem provided some interesting information. He reports that, "I have spoken with the chairman of the Transkei Traditional Healers Association, and he confirms that they, 'the Xhosa people,' have been using *C. caffrum* for decades and longer for the treatment of cancer amongst other ailments." The chairman also cautioned that extracts of *C. caffrum* should be used in combination with other plants to be effective, presumably to moderate the toxicity. Another useful contribution made by van Hattem was the observation that, "The tribe in the area of *C. caffrum* are Xhosa and not Zulu. There is a gradual change from *C. caffrum* in the Xhosa area to *C. erythrophyllum* in the Zulu area as one travels northwards from East London through the Transkei." Furthermore, the Xhosa and Zulu do not differentiate between these two botanical species, and in his discussions with Professor A.E. van Wyk, curator of the Herbarium, Department of Botany, University of Pretoria, the conclusion is that *C. caffrum* and *C. erythrophyllum* are nearly identical.

The early events leading to the discovery of the combretastatins began with the first (1973) collection of *C. caffrum* in Africa for the NCI in the former Rhodesia (now Zimbabwe). Several scale-up recollections of *C. caffrum* were completed, and chemical investigations of constituents were pursued by an NCI collaborative research group, but by 1979 that research had led to a dead end with respect to anticancer constituents.

In 1979, one of us (G.R.P.) and colleagues continued with a *C. caffrum* collection in collaboration with the NCI Natural Products Branch. As summarized in the sequel to this introduction, this research subsequently led to the discovery of 20 cancer cell growth inhibitory stilbenes, bibenzyls,

dihydrophenanthrenes, and phenanthrenes from *C. caffrum*. Some of those discoveries led to a number of important advances that range from the first isolation of a cancer cell growth inhibitor, (-)-combretastatin, isolated by using the NCI astrocytoma bioassay (first use for cancer drug discovery), to the first well-established vascular-disrupting anticancer drug, sodium combretastatin A-4 phosphate (CA4P), which has entered human cancer clinical trials.

Several of the natural products isolated from *C. caffrum* are characterized by their remarkable biological activity as inhibitors of tubulin polymerization, potent *in vitro* cytotoxicity against human cancer cell lines, and demonstrated *in vivo* efficacy as vascular-disrupting agents (VDAs; in suitable prodrug formulation) and antiangiogenesis agents. The combretastatins are especially noteworthy for their robust activity in biological systems, while maintaining remarkable simplicity in terms of chemical structure. Combretastatin A-4 (CA4) and combretastatin A-1 (CA1), along with their corresponding phosphate prodrug salts (CA4P and CA1P, respectively), have emerged as compounds of profound therapeutic interest (Figure 3.1). A rapidly growing number of outstanding reviews of the combretastatins and novel analogs inspired by the combretastatins have been published.[14–35] In addition, numerous patents have been issued, or are in the application process, for a wide variety of combretastatins and their analogs.[36–45] The patent literature, in this regard, has recently been reviewed.[46]

The discovery and development of small-molecule (i.e., compounds with molecular weights in the range of 300–800 g/mol) inhibitors of tubulin assembly has been (and continues to be) a challenging and fruitful goal that, to a large degree, began with colchicine (Figure 3.1) in the 1930s and 1940s. Representative, naturally occurring antimitotic ligands,[20,31] in addition to colchicine, include paclitaxel,[47] epothilone A,[48] vinblastine,[49] dolastatin 10,[50–52] and CA4.[53–56] In addition, there are a variety of synthetic compounds that also demonstrate efficient inhibition of tubulin polymerization.[55,56] Because of the poor solubility of CA1 and CA4, sodium phosphate prodrugs CA1P[57] and CA4P[58] were developed in the mid-1990s.

Isolation of the first constituent of *C. caffrum*, (-)-combretastatin (Figure 3.2), as noted before, was achieved in 1982 by Pettit et al.[59] By 1987, the absolute stereochemistry, attributed to the single stereogenic center in the molecule, was determined to be the *R*-configuration.[60] The combretastatins are currently divided into four major groups on the basis of their structural characteristics. These include the A-series (*cis*-stilbenes), B-series (diaryl-ethylenes), C-series (quinone), and D-series (macrocyclic lactones). Representative members of each of these groups are depicted in Figure 3.2.

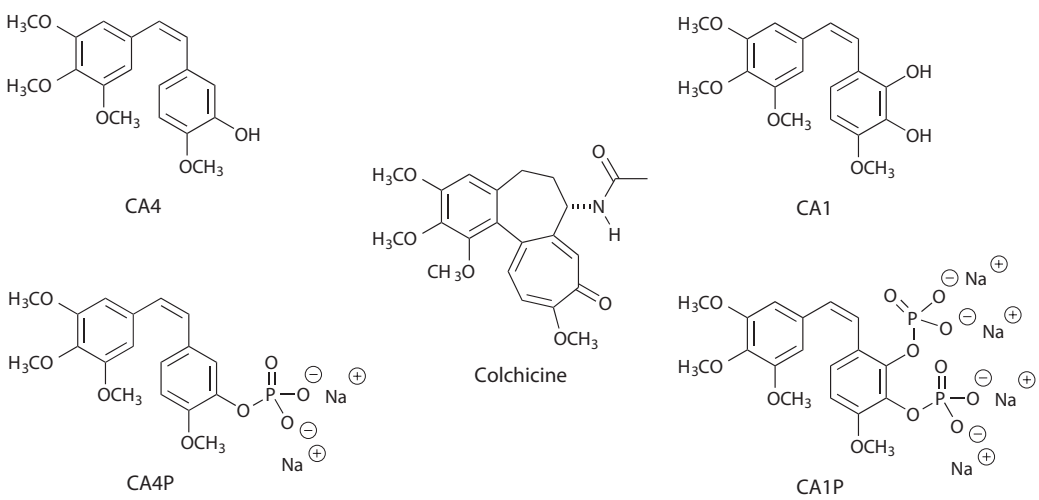

FIGURE 3.1 Structures of CA4, CA4P, CA1, CA1P, and colchicine.

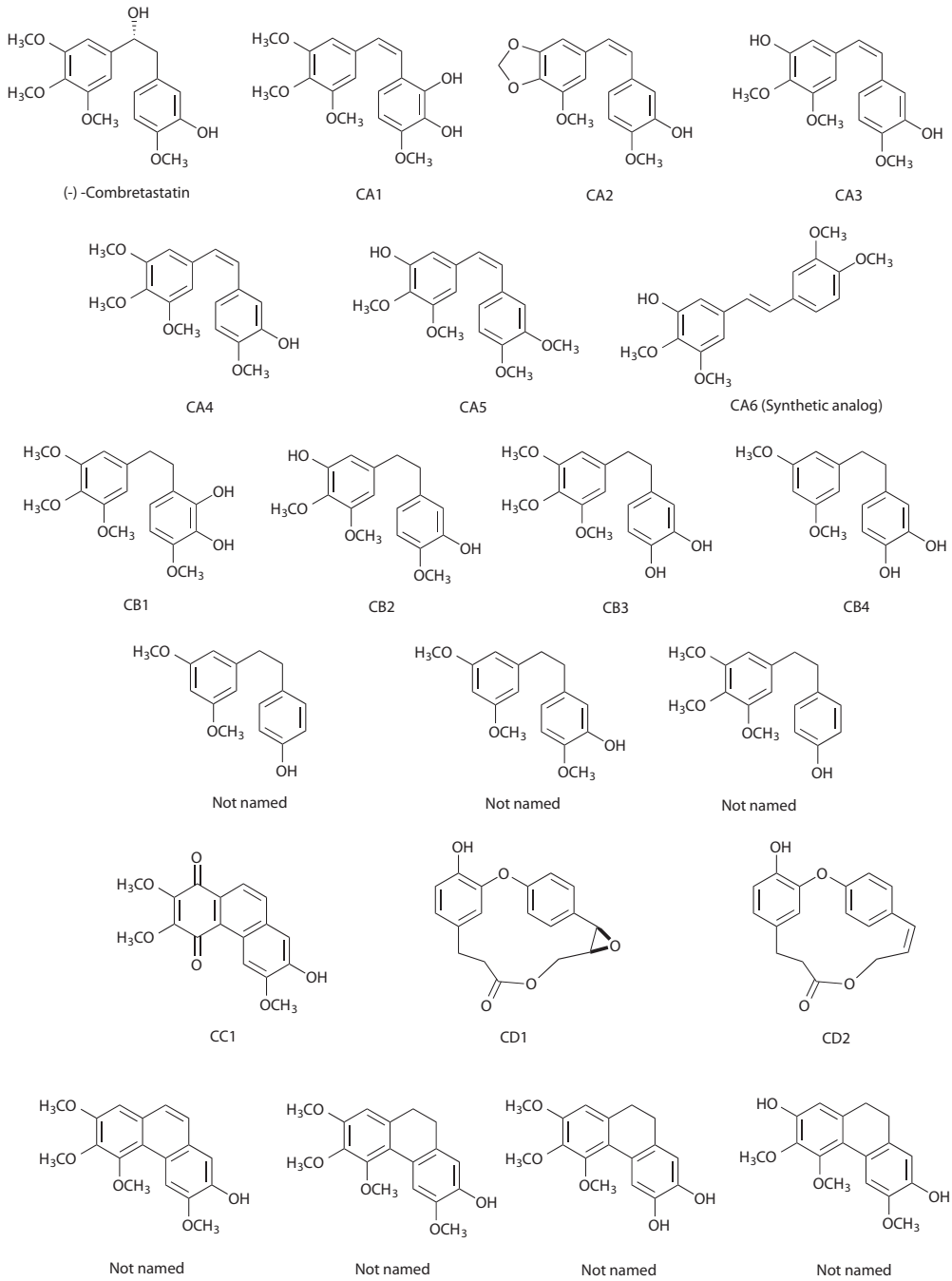

FIGURE 3.2 Natural products isolated from *C. caffrum*.

The combretastatin A- and B-series contain two phenyl rings tilted at 50–60° to each other, and are linked by a two-carbon bridge.[16] The bridge is either unsaturated, as in the case of stilbenes, or saturated. The substituents differ in their respective locations on the phenyl rings, and they usually contain methoxy and hydroxy functionalities. The combretastatin A-series is made up of six constituents, CA1,[61] CA2,[62] CA3,[62] CA4,[63] CA5,[63] and CA6,[63] which retain a *cis*-stilbene moiety. The B-series consists of four compounds—CB1,[61] CB2,[62] CB3,[64] and CB4[64]—with three similar

structures not named according to the prescribed nomenclature.[64] These compounds are similar to the A-series except for a saturated carbon–carbon bridge between the two aryl rings. There is one compound in the C-series, designated combretastatin C1[65] (CC1), which contains a three-ring quinone structure. Two unusual macrocyclic lactones make up the D-series, CD1[66] and CD2.[67] Finally, there are four phenanthrene-like compounds that are currently not named other than by their IUPAC designation.[17]

3.2 BIOCHEMICAL AND BIOLOGICAL MECHANISM OF ACTION

Tubulin-binding, antimitotic, anticancer drugs have long been a major component in the arsenal of "weaponry" available to wage the battle against cancer. The cytoskeletal tubulin–microtubule protein system is a natural target because of its central role in the maintenance of cellular structure, and in essential cellular functions, such as intracellular transport, cell motility, and cell division.[18,20–21] These processes may require either stabilization of microtubule structure or enhanced dynamics for disassembly and reassembly, and are organized and regulated by microtubule isotypes and post-translational modifications, microtubule-associated proteins, and cell signaling pathways.[68–70] During metaphase of the cell cycle, the α,β-tubulin heterodimers undergo linear head to tail polymerization and lateral association to form microtubules, which, collectively, are essential components of the mitotic spindle. This process which organizes chromosomes requires a dynamic microtubule structure. Certain compounds, such as vinblastine,[70] vincristine, colchicine, and podophyllotoxin,[68] exert their biological effect by binding to tubulin heterodimers and inhibiting their assembly into microtubules.[18,20] Other compounds, such as paclitaxel and the epothilones, bind to the microtubule itself and inhibit its disassembly to tubulin dimers thereby stabilizing the microtubule.[18,20] In both cases, cellular division is disrupted by these tubulin-binding compounds through the alteration of tubulin-microtubule dynamics. Although healthy cells are also affected, it is the tumor cells that are more prominently targeted because they are characterized by rapid proliferation, which is dependent on microtubule dynamics.[69]

The structure of the α-tubulin monomer closely resembles that of the β-monomer, and each subunit binds a molecule of guanosine triphosphate (GTP). The GTP bound to the α-subunit is close to the dimer interface, and is not hydrolyzed while the GTP bound to the β-subunit is hydrolyzed to guanosine diphosphate (GDP) and phosphate by the tubulin GTPase activity after incorporation of the tubulin dimer into the growing microtubule.[71,72] A tertiary structure of the α,β-tubulin heterodimer (as contained in the microtubule stabilized by taxol) was reported in 1998 by Downing et al. at a resolution of 3.7 Å, using electron crystallography.[73] This accomplishment marks the culmination of decades of work directed toward the elucidation of this structure and has contributed to the identification of small-molecule-binding sites through techniques such as photoaffinity and chemical affinity labeling.[74–87] Small molecules can bind in at least three known locations on the tubulin-microtubule protein system: the colchicine site,[71,88,89] the vinca-alkaloid site,[70] and the taxoid site.[68,73] These sites are named because of the binding of colchicine, vinblastine, and taxol, respectively, to certain distinct binding pockets on the tubulin dimer itself, or on the microtubule in the case of taxol.[90] Association of the stathmin-like domain (SLD) of the regulatory RB3 protein with tubulin prevents its assembly into microtubules. The x-ray crystal structure of two tubulin dimers in a complex with RB3 SLD (T_2R)[71,88,89] reveals that the overall structure is curved as the result of a shift in the orientation of adjacent tubulin subunits relative to one another as well as within a tubulin dimer. Comparison of the tubulin structure in protofilaments with those of the dimer complex in the presence and absence of a colchicine analog is instructive. For curved tubulin dimers to undergo a conformational change to the straightened form found in linear protofilaments that are able to associate laterally into microtubules, requires a translation of the H7 helix in the β-monomer among other secondary structural changes in the intermediate domain. This is prevented when colchicine and related ligands are bound at the colchicine site. The x-ray crystal structure of T_2R at 3.65 Å resolution bound to the colchicine analog, *N*-deacetyl-*N*-(2-mercaptoacetyl)-colchicine, provides

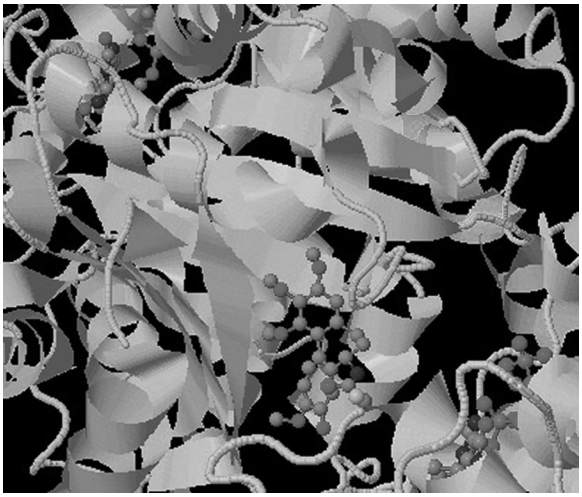

FIGURE 3.3 (**See color insert.**) Colchicine analog (C, gray; O, red; N, blue; S, yellow) bound to the β-subunit (green) of a tubulin complex with the SLD of regulatory protein RB3 (pink). A small region of the α-subunit (blue) binding GTP is shown (C, gray; O, red; N, blue; P, orange). PDB ID: 1SA0.[72,88,89,91,92]

evidence that colchicine does not change the overall shape of the tubulin dimer complex, but exerts more localized effects.[88,89] The ligand is bound in a nonpolar region of the intermediate domain of the β-subunit surrounded by β-strands S8 (β residues 313–320) and S9 (residues 351–356), α-helices H7 (residues 224–243) and H8 (residues 252–260), loop T7 (residues 244–251) of the β-subunit, and loop T5 (residues 173–182) of the α-subunit (Figure 3.3).

This x-ray crystal structure also provides a starting point for docking and molecular modeling of compounds at the colchicine site. The x-ray crystal structure of the tubulin–podophyllotoxin–RB3–SLD complex confirmed that this ligand binds at the colchicine site.[89]

The combretastatin A-series is historically known for its remarkable biological activity in terms of inhibition of tubulin assembly and *in vitro* cytotoxicity against human cancer cell lines. CA1 and CA4 which bind at the colchicine site of β-tubulin[93] are among the most active of the natural products isolated from *C. caffrum* in terms of *in vitro* activity[17] (Tables 3.1 and 3.2).

3.3 THERAPEUTIC INTERVENTION THROUGH VASCULAR DISRUPTION

Although antimitotic agents attack tumor cells directly and disrupt cell division and cell cycle progression, some molecules have been shown to exhibit antivascular and antiangiogenic effects as well. Often, the two classes overlap, as in the case of the combretastatins, where certain compounds that cause direct vascular damage can also prevent angiogenesis.[94,95] VDAs function by destroying existing tumor vasculature through a mechanism that induces morphological changes within endothelial cells, thereby disrupting shape, transport, and motility.[94,96–99] In contrast, antiangiogenic agents inhibit the formation of new blood vessels. In either case, this disruption of vasculature essentially starves the tumor.

Certain tubulin-binding compounds, in prodrug form, demonstrate remarkable selectivity for the destruction of tumor vasculature.[100–103] A model for this process is shown in Figure 3.4. In prodrug form, these VDAs are, for the most part, protected from binding to tubulin. However, once they undergo enzymatic cleavage to their corresponding parent-free phenol (e.g., CA4) or amine analog, the molecules diffuse across the membrane of endothelial cells lining the tumor microvessels where they function as potent inhibitors of tubulin assembly. This results in the net disassembly of microtubules. Microtubules of activated, developing cells in cell culture, exposed to growth factors, undergo depolymerization in response to depolymerization agents much more readily than those of established cells.[104]

TABLE 3.1
Biological Activity of the Naturally Occurring Combretastatins

Name	Structure	Tubulin[a] (μM)	P388[b] (μg/mL)	L1210[c] (μM)	Name	Structure	Tubulin[a] (μM)	P388[b] (μg/mL)	L1210[c] (μM)
(-) Combretastatin	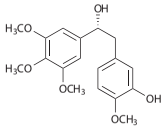	5–7.5	0.011[d]	0.05	CB4	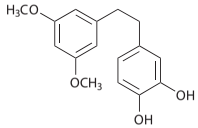	25–30 >100[h]	1.7[h]	1
CA1	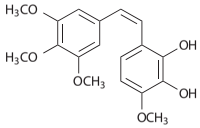	2–3	0.99[e]	0.6	—	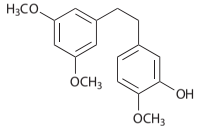	10–15	NA	1
CA2	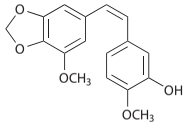	4–5	0.027[f]	0.1	—	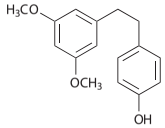	>100	NA	4
CA3	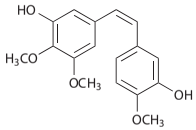	4–5	0.026[f]	0.04	—	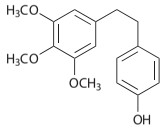	>100	NA	50
CA4	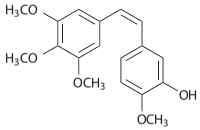	1.9[g] 2–3	0.0034	0.007	CC1	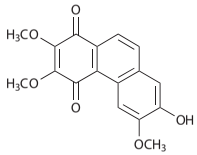	NA	2.2[i]	NA
trans CA4	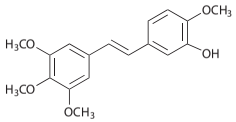	7.5–10	0.050	0.02	CD1	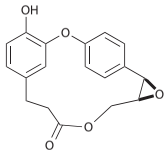	NA	3.3[j]	NA
CA5	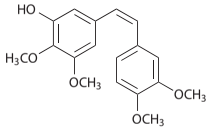	75–100	0.9	2	CD2	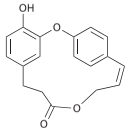	NA	5.2[k]	51[l]

continued

TABLE 3.1 (continued)
Biological Activity of the Naturally Occurring Combretastatins

Name	Structure	Tubulin[a] (μM)	P388[b] (μg/mL)	L1210[c] (μM)	Name	Structure	Tubulin[a] (μM)	P388[b] (μg/mL)	L1210[c] (μM)
CA6	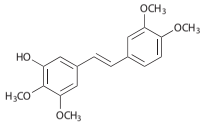	>100	18	30	—	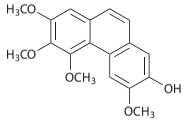	100	NA	1
CB1	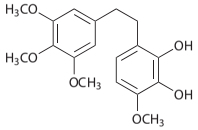	3[e] 4–5	1.7[e]	2	—	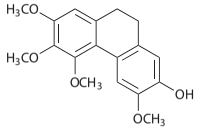	>100	NA	3
CB2	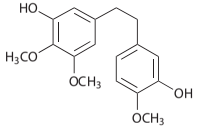	40 >100[h]	0.32[f]	3	—	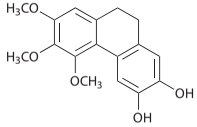	>100	NA	20
CB3	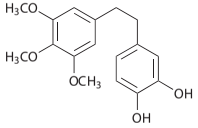	>100	0.4[h]	3	—	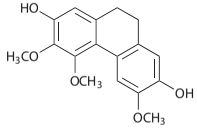	>100	NA	20

[a] Indicates inhibition of tubulin polymerization (IC_{50} micromolar) (data taken from Ref. 17, except as noted).
[b] Indicates cytotoxicity for the PS cell line (P388 leukemia) (ED_{50} in μg/mL); data taken from ref. 63, except as noted.
[c] Indicates cytotoxicity for the L1210 cell line (murine leukemia) (IC_{50} micromolar) (data taken from ref. 17, except as noted).
[d] Data taken from ref. 59.
[e] Data taken from ref. 61.
[f] Data taken from ref. 62.
[g] Data taken from ref. 14.
[h] Data taken from ref. 64.
[i] Data taken from ref. 65.
[j] Data taken from ref. 66.
[k] Data taken from ref. 67.
[l] Data taken from ref. 136.

TABLE 3.2
Cytotoxicity (Sulforhodamine B (SRB) Assay) of CA4, CA1, CA4P, and CA1P against Cancer Cell Lines

	IC_{50} (μM)	GI_{50} (μg/mL) (SRB Assay)					
Compound	Inhibition of Tubulin Polymerization	P388	BXPC-3	SF-295	NCI-H460	KM20L2	DU-145
CA4	1.0	0.0003	0.39	>0.001	0.0006	0.34	0.0008
CA1	1.1	0.3	4.4	ND	0.74	0.061	0.17
CA4P	>40	0.0004	ND	0.036	0.029	0.53	ND
CA1P	ND	<0.01	1.5	0.036	0.038	ND	0.034

Source: Data from Pettit, G.R. et al., *J. Med. Chem.*, 43, 2731, 2000.
Note: Inhibition of tubulin polymerization (IC_{50}) and cytotoxicity (GI_{50}) against murine lymphocytic leukemia (P388) and human cancer cell lines, pancreatic (BXPC-3), CNS (SF-295), nonsmall cell lung (NCI-H460), colon (KM20L2), and prostate (DU-145).

In human endothelial cells *in vitro*, microtubule depolymerization results in the activation of the intracellular RhoA signal transduction pathway.[96] RhoA is a GTPase protein that is activated by binding GTP and deactivated upon its hydrolysis. Activation of this pathway results in the downstream activation of RhoA kinase resulting in reorganization of the actin–myosin cytoskeletal proteins. Treatment of endothelial cells with CA4P disrupts junctional integrity through VE-cadherin resulting in increased cellular permeability.[104] Other rapid morphology changes in the endothelial cells lining the microvessels include rounding up of the cells, and disruption of blood flow which ultimately renders new microvessels nonfunctional for blood delivery, causing hypoxia and necrosis of the tumor.[105–108] The link between microtubule depolymerization and RhoA signal transduction activation has not been

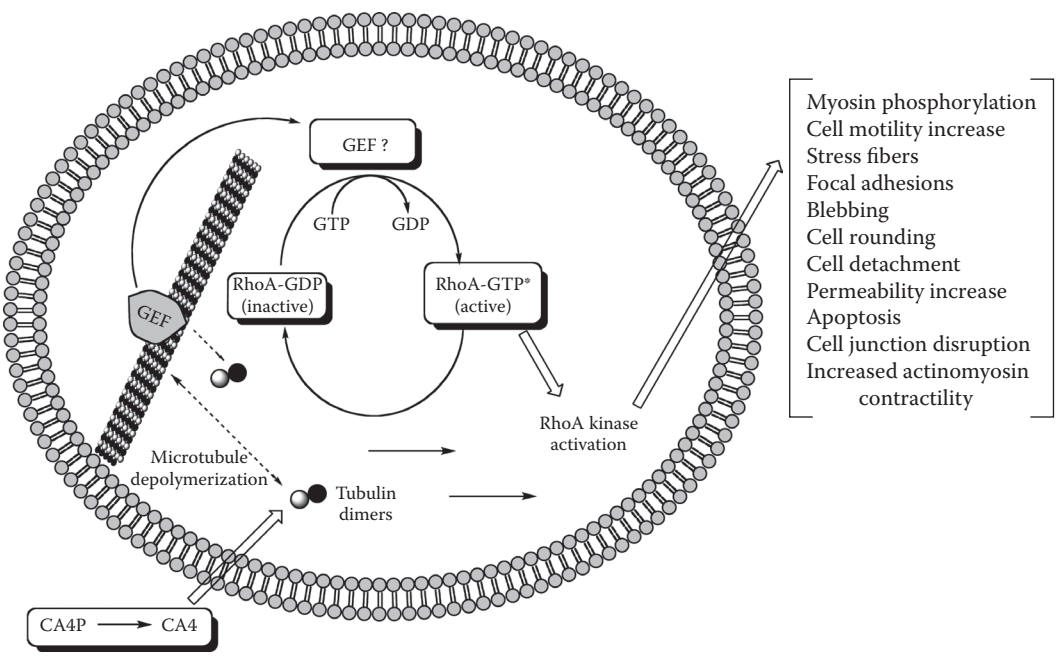

FIGURE 3.4 Model for CA4-induced signal transduction in tumor vasculature endothelial cells.

elucidated, but the release of one or more microtubule-associated proteins such as a guanine nucleotide exchange factor (GEF) would result in the activation of RhoA. Solid tumor survival is dependent on blood, oxygen, and nutrient supply from surrounding vessels.[105] Growing tumors receive their nutrients through existing vasculature in the surrounding area as well as through newly formed neovascularization (angiogenesis). The reason for the selectivity of the VDAs for the microvessels of tumors is largely unproven. However, it may reflect, in part, variability in the cytoskeletal make-up of rapidly proliferating endothelial cells stimulated by growth factors inherent to microvessels feeding tumor cells versus the normal proliferating endothelial cells of microvessels serving healthy cells.[106] Because one single microvessel can feed hundreds or thousands of tumor cells, this method of vascular targeting has the potential to be extremely effective in destroying tumor cells without targeting them directly (as it is the microvessels that are immediately affected).

CA4P and other VDAs are useful as chemotherapeutic agents for cancer treatment as well as for therapeutic intervention in ocular diseases (such as wet, age-related macular degeneration).[109] At present, there are at least three compounds in human clinical development as potential VDAs for cancer chemotherapy that use a tubulin-based biological mechanism. Although none of these compounds has achieved New Drug Application (NDA) approval for marketing by the U.S. Food and Drug Administration, CA4P is the most advanced in clinical trials. In June 2003, CA4P received orphan drug approval by the U.S. Food and Drug Administration for the thyroid cancer group, and a month later it received approval for a "fast-track" phase II clinical trial against the usually quite lethal (median survival time is 4 months) anaplastic thyroid cancer.

3.4 SYNTHESIS OF COMBRETASTATINS

Isolation of CA1 and CA4, as with the other constituents, began with a methylene chloride-methanol extract, initially from the macerated branches, leaves, and fruits, and subsequently from the stem wood of *C. caffrum*.[61,63,110] These extracts were then separated by bioassay (PS system) guided techniques. For example, with respect to CA4, a trace fraction was isolated from 77 kg of dry stem wood. Further separation led to 26.4 mg of a fraction that at first seemed to be a pure compound, but high-field ^{1}H and ^{13}C-NMR (nuclear magnetic resonance) indicated a mixture of three compounds. Conversion to a *t*-butyldimethylsilyl ether derivative and further separation afforded about 9 mg of CA4 silyl ether. Following cleavage of the protecting group from a 1.7-mg sample, a 1.15-mg sample of pure CA4 was obtained. By analogous techniques, CA5 and CA6 were obtained as the other two components of this complex mixture. The structure and configuration of CA4 were established by ^{1}H-NMR spectra,[63] which gave evidence of four methoxy groups and seven protons in the aromatic region. Two of the methoxy groups were equivalent, and three protons were displayed at δ 6.734 (d, $J = 8.4$ Hz), 6.799 (dd, $J = 8.42$, 2.04 Hz), and 6.925 (d, $J = 2.04$ Hz), suggesting ortho–ortho and ortho–meta coupling, and one singlet at δ 6.527 represented the two symmetrical aromatic protons on the A ring of CA4. Two doublets at δ 6.471 and 6.412 ($J = 12.16$ Hz each) were indicative of a *cis*(*Z*)-stilbene. The *trans*(*E*) derivative of CA4 showed a vinyl coupling of $J = 16.30$ Hz. The synthesis of CA4[63] (Scheme 3.1) was achieved through a Wittig reaction between the silyl-protected phosphonium bromide from isovanillin and 3,4,5-trimethoxybenzaldehyde. The *Z*-geometry was confirmed by an x-ray crystal structure determination. The *Z*-isomer was then desilylated with tetrabutylammonium fluoride to afford CA4.

The sodium phosphate salt of CA4[111] and disodium phosphate salt of CA1[57] were both synthesized through an efficient sequence using a dibenzylphosphite-carbon tetrachloride procedure, followed by debenzylation with sodium iodide and chlorotrimethylsilane. Subsequent phosphorylation methods reported include potentially useful procedures based on phosphorous oxychloride[112] or a dialkoxy phosphorous oxychloride[113] using an inverse addition procedure.[112] The corresponding phosphate cation for clinical development has usually been, for CA4P, *tris*(hydroxymethyl)aminomethane (TRIS), and for CA1P, potassium. Other water-soluble derivatives of CA4 have been described and include phosphoryl choline,[114] as well as the CA4 rat metabolites CA4 sulfate and glucuronide.[115] (-)-Combretastatin has also been prepared synthetically.[116]

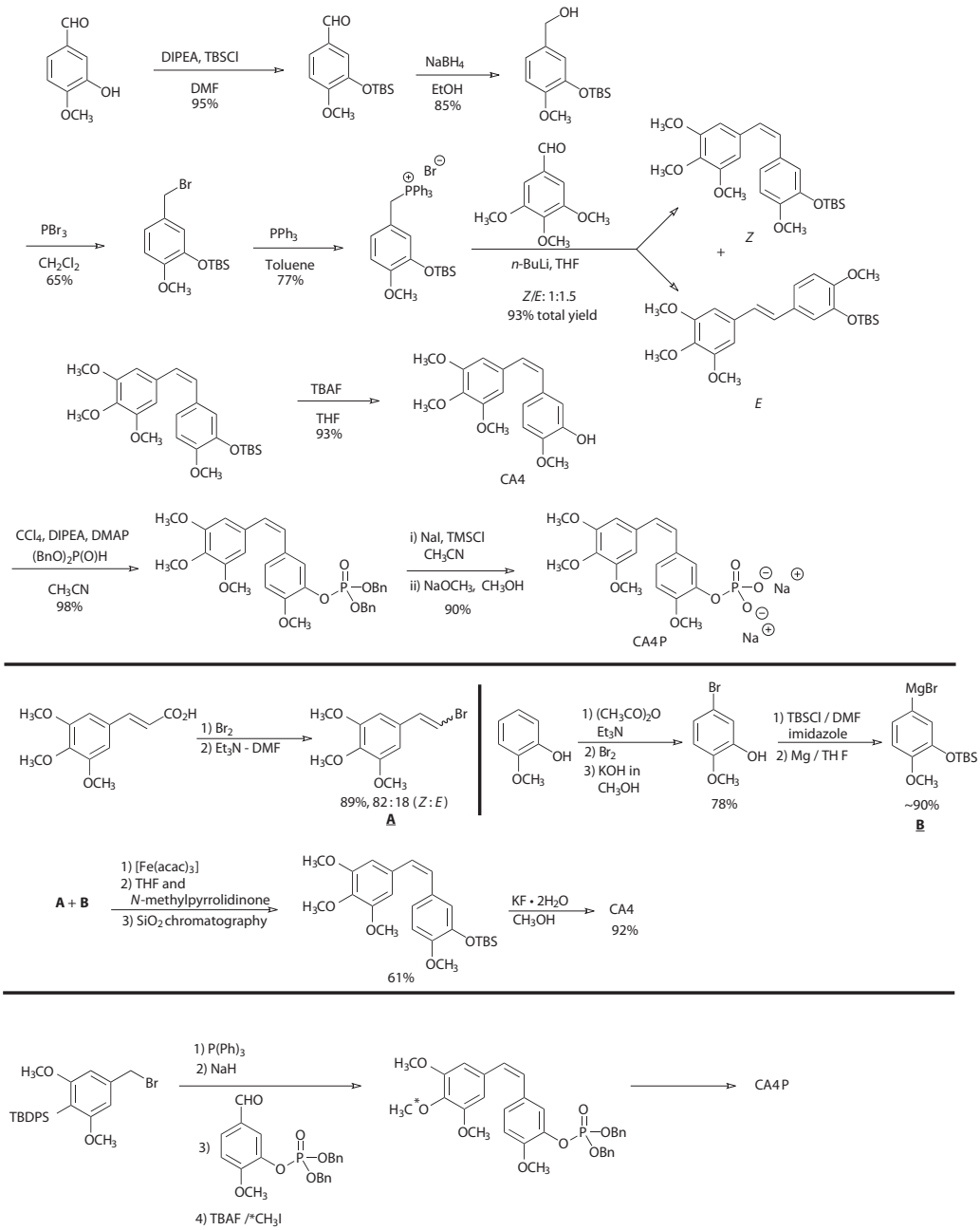

SCHEME 3.1 Synthesis of CA4 and its disodium phosphate prodrug.

In addition to the Wittig reaction used by Pettit et al., other methods have been developed to synthesize CA4 and CA1, including a Perkin condensation of 3,4,5-trimethoxyphenylacetic acid and 3-hydroxy-4-methoxybenzaldehyde,[117] a Suzuki cross-coupling of an ethenyl bromide and 3,4,5-trimethoxyphenyl boronic acid,[117] a biooxidation of arenes to catechols using *Escherichia coli* JM109 followed by a Pd-catalyzed Suzuki coupling,[118] and a modified Suzuki reaction through a hydroboration/protonation of a diaryl-alkyne.[119] A variety of additional synthetic approaches to the combretastatins and related *Z*-stilbenoid molecules have recently been reported,[120–126] thus further expanding

the horizon in terms of methodology available for new analog development. A new synthesis of the increasingly important *E*-stilbene resveratrol, related to *Z*-CA4, employing an aqueous Wittig reaction sequence using trialkyl (benzylidene) ylides and the aldehyde target[127] should prove useful in the future. Another variation in the Wittig approach to CA4 comprises protecting the isovanillin phenol by reaction with poly[4-(chlorodiphenylmethyl)styrene] in THF or dioxane followed by the usual ylide step and deprotection.[128] One of the more attractive new approaches to total synthesis of CA4 makes use of a Kumada–Corrin cross-coupling route (cf. Scheme 3.1, second entry).[122] Because of the facile isomerization of *Z*-CA4P to *E*-CA4P, the development of a synthetic route to CA4P that would allow practical (and very rapid) preparation of, for example, a [^{11}C]-labeled derivative for position emission tomography (PET), while retaining the *Z*-olefin geometry, proved to be unusually challenging for such an otherwise simple synthesis. The successful procedure finally developed and, now in press, is shown in Scheme 3.1 (third entry).[129] Introduction of the phosphate group into B ring prior to the Wittig step avoided the *Z/E* isomerism when introducing the final methyl group into ring A followed by cleavage of the phosphate benzyl esters yielding a selectively constructed CA4P for later labeling.

Similarly, the structure and configuration of CA1[61] was confirmed to be *Z* with an AB system of doublets at δ 6.453 and 6.523 (J = 12.2 Hz) and a two-proton signal at δ 5.438, representing the presence of phenolic groups. The synthesis of CA1[61] (Scheme 3.2) was also achieved through a Wittig reaction; however, availability, at that time, of certain starting materials required that 2,3,4-trihydroxybenzaldehyde be used as a starting substance. After selective methylation at the *para* position and silylation, the benzaldehyde derivative was allowed to react with the phosphonium bromide of 3,4,5-trimethoxybenzyl alcohol to afford the protected *Z*-isomer. After deprotection using tetrabutylammonium fluoride, CA1 was obtained. A new synthesis of CA1 and another of CA1P are especially useful: for CA1 a Sonogashira reaction as a key step (Scheme 3.2, second entry)[130] and a practical synthetic route to [4′–^{14}C] CA1P (Scheme 3.2, third entry).[131,132] Another recent synthesis of CA1P tetrasodium salt has been reported in a patent application.[133]

Soon after the discovery of CA1 by one of us (G.R.P.) and colleagues, as reported in 1987, initial and subsequent chemical observations of the vicinal phenol suggested considerable sensitivity to air and light. Indeed, the rapid degradation of CA1 under oxidative conditions to a number of multicolored products indicated conversion to an unstable *o*-quinone. In turn, that level of reactivity greatly slowed the preclinical development until we were able to complete a practical prodrug synthesis leading to the stable and water-soluble phosphate prodrug CA1P. Our *o*-quinone theory of *in vivo* behaviors ranging from production of many metabolites to distinct differences in mechanisms of action compared with the simple monophenol CA4 has been widely accepted.[134] However, existence of the actual *o*-quinone arising from *in vivo* oxidation, presumably by Fe(III), tyrosine, and/or peroxidases was not confirmed until we were able to trap it as a phenazine derivative in 2004 and publish the chemistry (Scheme 3.3) in 2008.[135] At room temperature in H_2O-CH_2Cl_2 the CA1 *o*-quinone solution turns blue over 10 min and then to black/decomposition!

Further study of *C. caffrum* constituents led to the isolation, characterization, and synthesis of B-, C-, and D-series members. In general, B-series constituents were synthesized by methods analogous to A-series syntheses followed by hydrogenation.[61,62,64] For example, for CB1,[61] a mixture of CA1 in methanol and 5% Pd/C was treated with a positive pressure of H_2 at ambient temperature overnight to afford CB1.

Synthesis of CC1[65] (Scheme 3.4) was achieved through photochemical cyclization of the corresponding stilbene. The improved synthesis of CC1 included selective demethylation of 2,3,4-trimethoxybenzaldehyde with aluminum chloride followed by silylation. Subsequent coupling of the aldehyde with the corresponding ylide and photochemical cyclization, using iodine and a mercury lamp, provided the phenanthrene product. Desilylation using tetrabutylammonium fluoride afforded the phenol, which, on Fremy's salt oxidation, yielded the quinone CC1.

The unusual macrocyclic lactones, CD1 and CD2, have been synthesized by several groups.[136–143] Boger's synthesis using an intramolecular Ullmann macrocyclization[136] to afford CD2 is presented

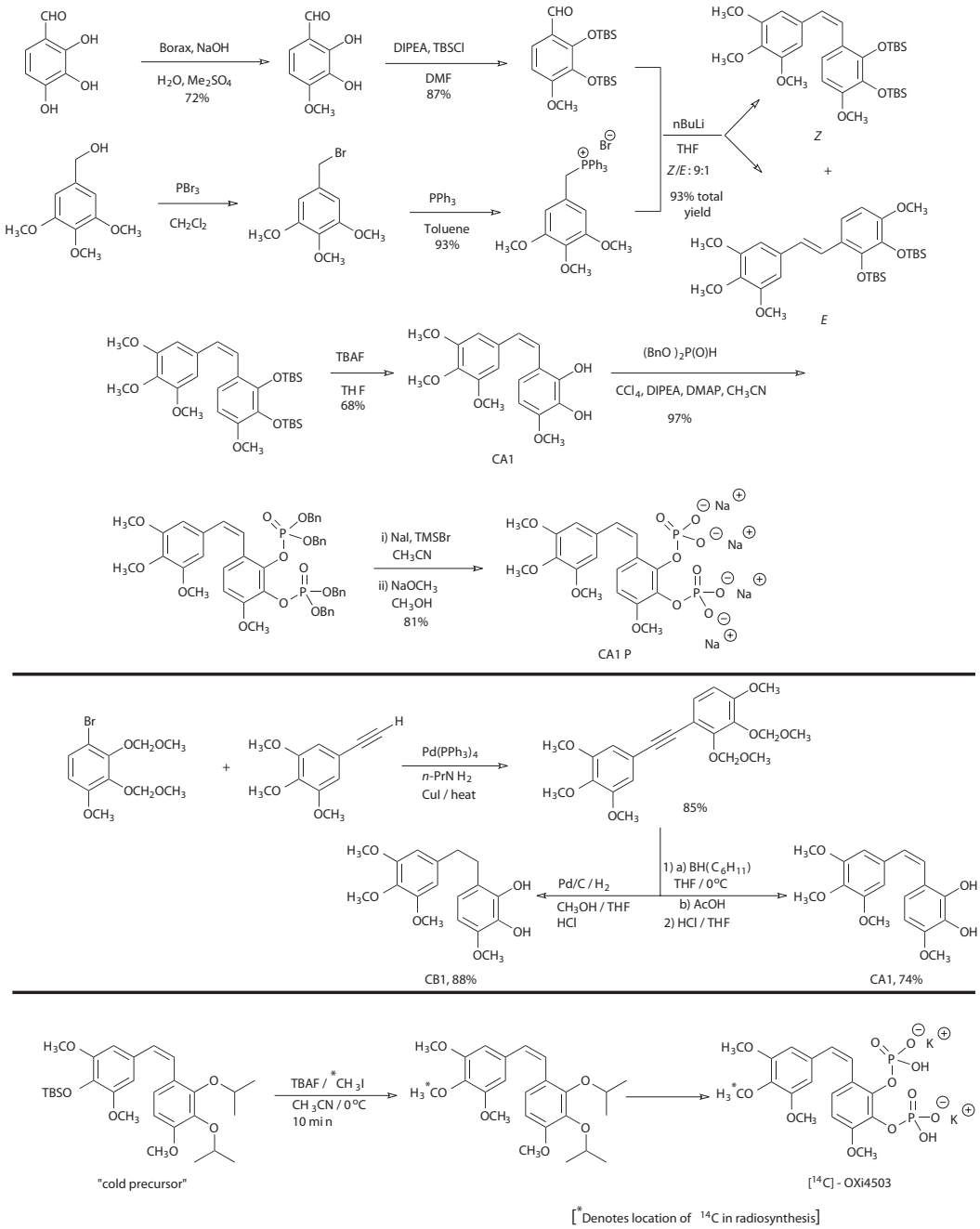

SCHEME 3.2 Synthesis of CA1 and its prodrug CA1P.

here (Scheme 3.5). Esterification of 3-(3-hydroxy-4-methoxyphenyl)propanoic acid with (*Z*)-3-(4-iodophenyl)-2-propenol under Mitsunobu conditions provided the bridged diaryl ester. Upon intramolecular Ullman macrocylization, followed by aryl methyl ether deprotection, CD2 was obtained.

The stereochemical configuration of the epoxide in CD1 was originally postulated to be (3*R*, 4*S*) based on the Cotton effect curve observed in the CD spectrum. More recent synthetic studies by Rychnovsky et al.[141] and independently by Couladouros et al.[142] (Scheme 3.6) have confirmed that the

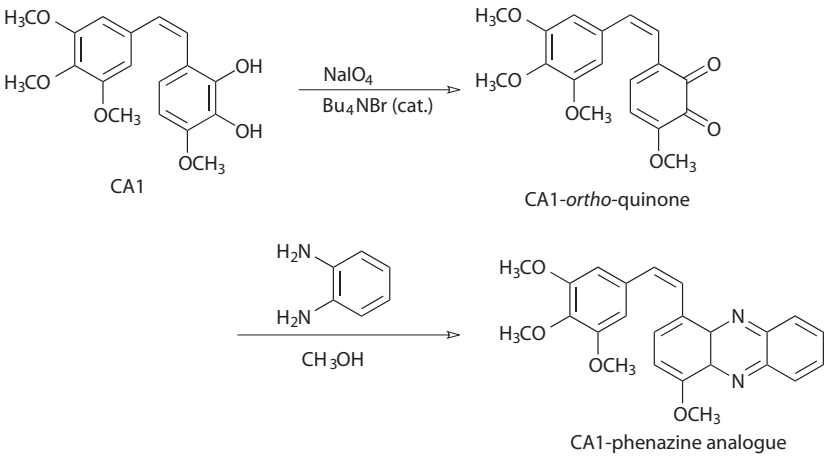

SCHEME 3.3 Chemical trapping of the *o*-quinone generated from CA1.

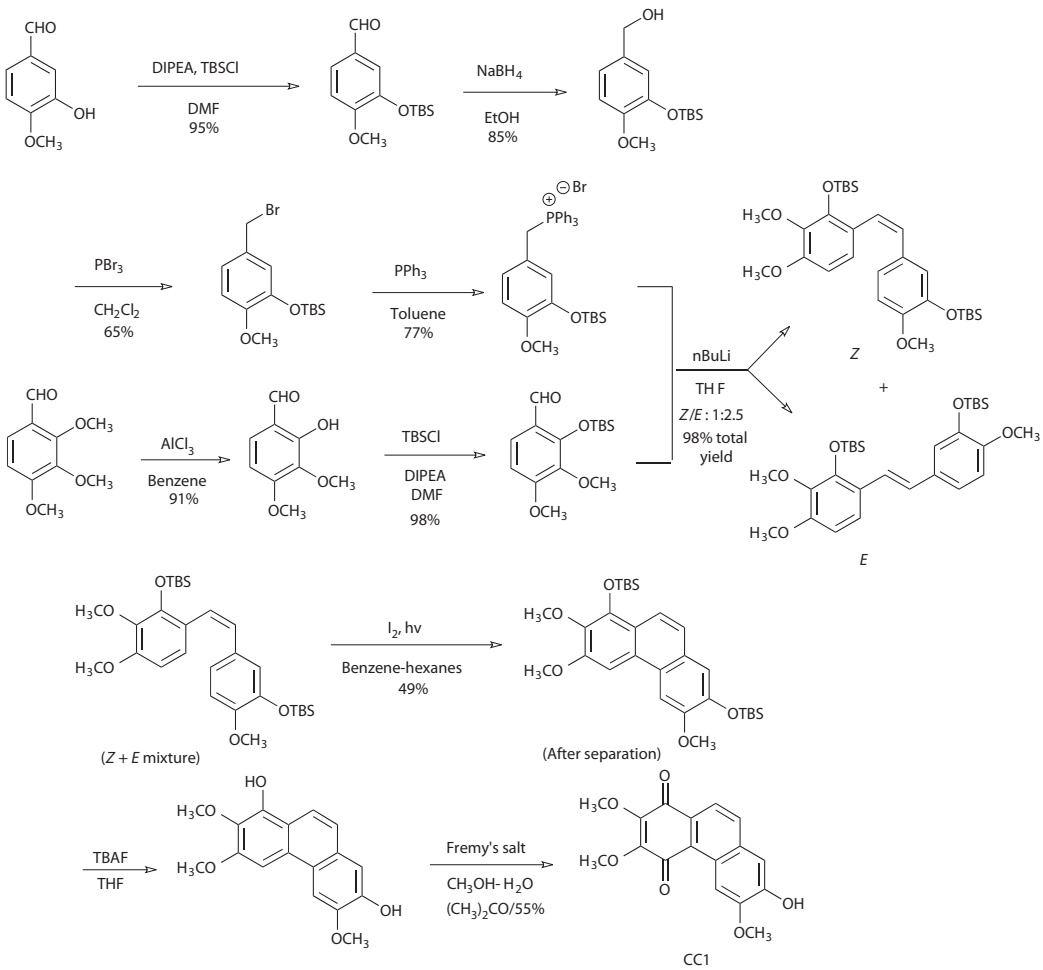

SCHEME 3.4 Synthesis of CC1.

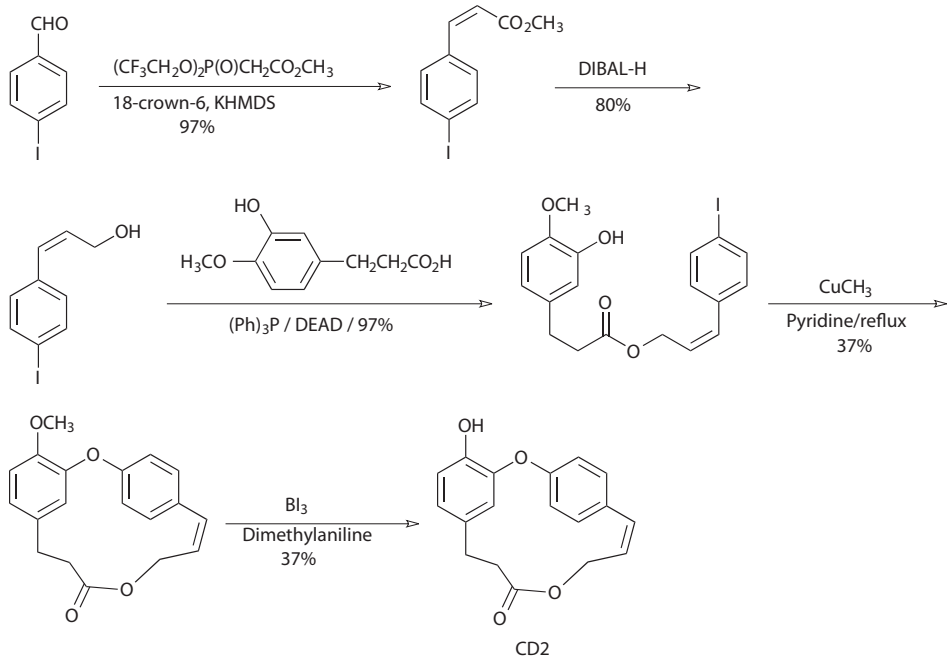

SCHEME 3.5 Synthesis of CD2.

correct stereochemical assignment of the epoxide moiety in CD1 is (3*S*, 4*R*). A phosphate prodrug salt of CD2 and the saturated dihydro-combretastatin D-2 analog have been synthesized by Pettit et al.[143]

3.5 COMBRETASTATIN DERIVATIVES AND SYNTHETIC ANALOGS INSPIRED BY THE COMBRETASTATINS

The relative simplicity of the basic stilbenoid molecular architecture characteristic of CA4 and CA1, along with the ease of synthesis and the versatility afforded by the variety of synthetic routes available for the formation of stilbenoids, has resulted in extensive structure–activity relationship

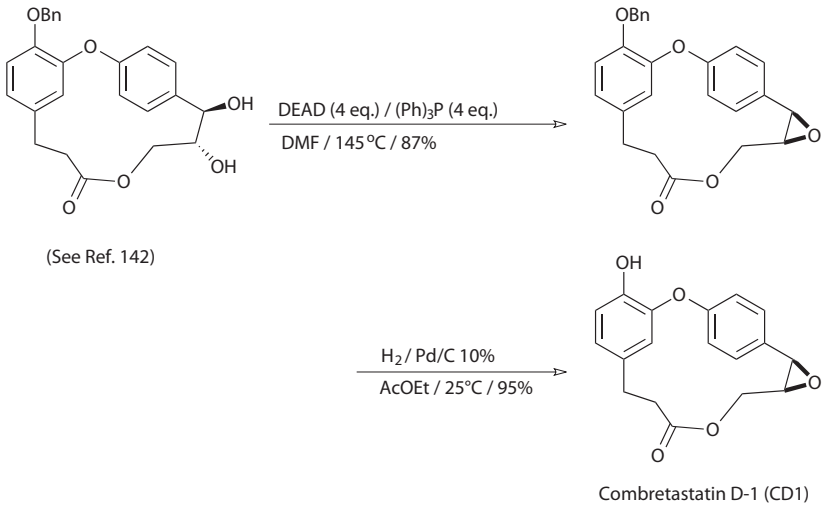

SCHEME 3.6 Synthesis of CD1.

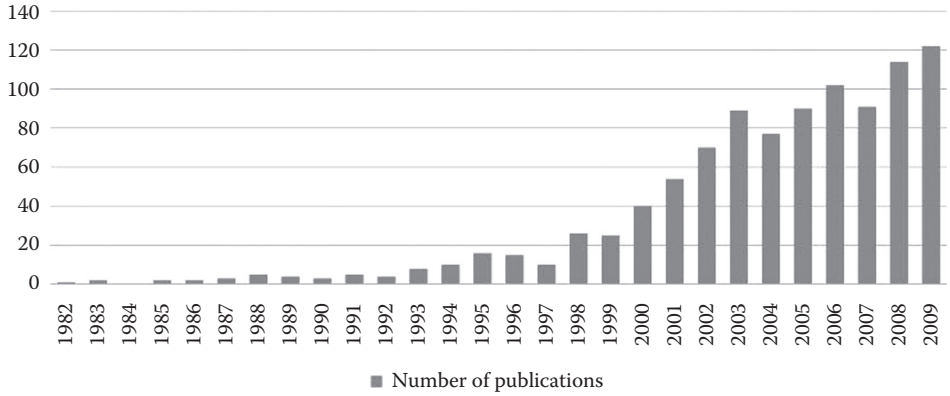

FIGURE 3.5 Combretastatin-related publications, patents, and professional presentations (1982–2009).

studies around the combretastatins. These studies have led to the discovery and development of a large number of structurally distinct combretastatin analogs. In fact, the literature with regard to the combretastatins has exploded in the last 10 years. For example, in 1994, a literature search for CA4 would have produced approximately 30 "hits," while a search today (2010) yields nearly 1000 papers, patents, and professional presentations (Figure 3.5).

A vast array of compounds (Figures 3.6 through 3.8) has been synthesized to mimic the structure and efficacy of the combretastatins, especially CA4 and CA1.[14–35,144] It is instructive to note that many of these combretastatin derivatives are of relatively low molecular weight and have reasonable

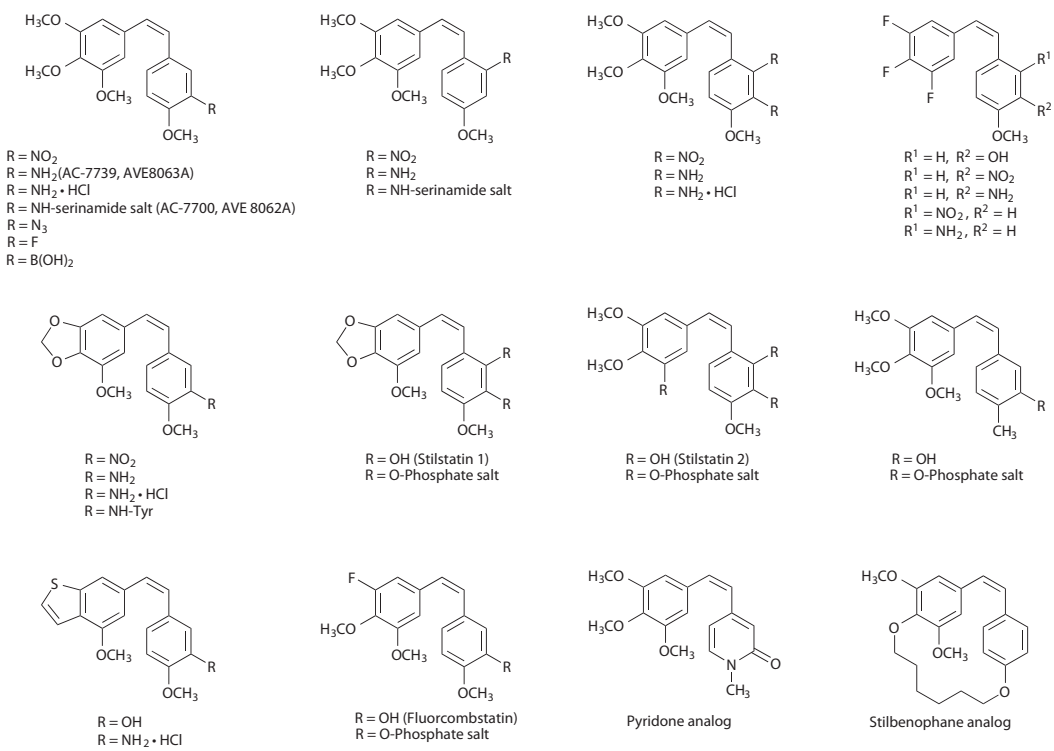

FIGURE 3.6 Combretastatin derivatives containing functional group modifications.

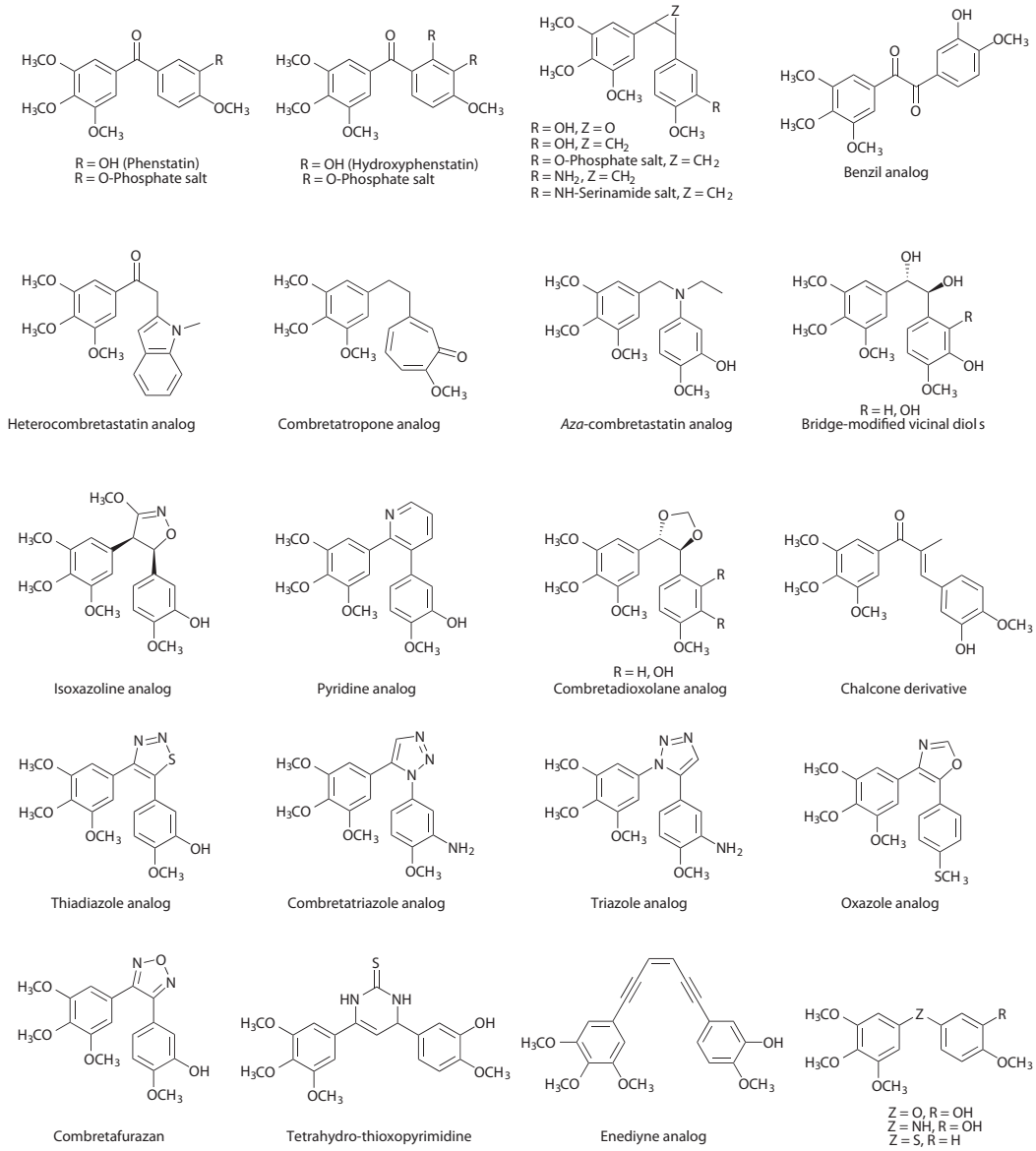

FIGURE 3.7 Combretastatin derivatives containing ethylene bridge modifications.

opportunities for hydrogen-bonding interactions suggesting that they may fall within the general "rules" often observed in the discovery of new drugs that have favorable ADME (adsorption, distribution, metabolism, and excretion) properties. One subpopulation of combretastatin analogs includes compounds that incorporate functional group modifications in which the A and B aryl rings and the ethylene bridge remain essentially intact. A sampling of these compounds (Figure 3.6) selected for their pronounced biological activity and/or their structural uniqueness, includes 3-nitro,[81,145] 3-amino,[81,145] 3-amino acid salts,[145,146] 3-azido,[81] 3-fluoro,[147] and 3-boronic acid analogs.[148] A series of nitro, amine, and amine salts mono-substituted at the 2′-position[149,150] and di-substituted at the 2′,3′-positions[151] have been prepared along with related compounds in which the A ring methoxy groups are replaced with fluorine atoms.[152] Additional combretastatin analogs that fall into this category include 3,4-methylenedioxy-3′-amino acid derivatives,[153] stilstatin 1, stilstatin 2 and their

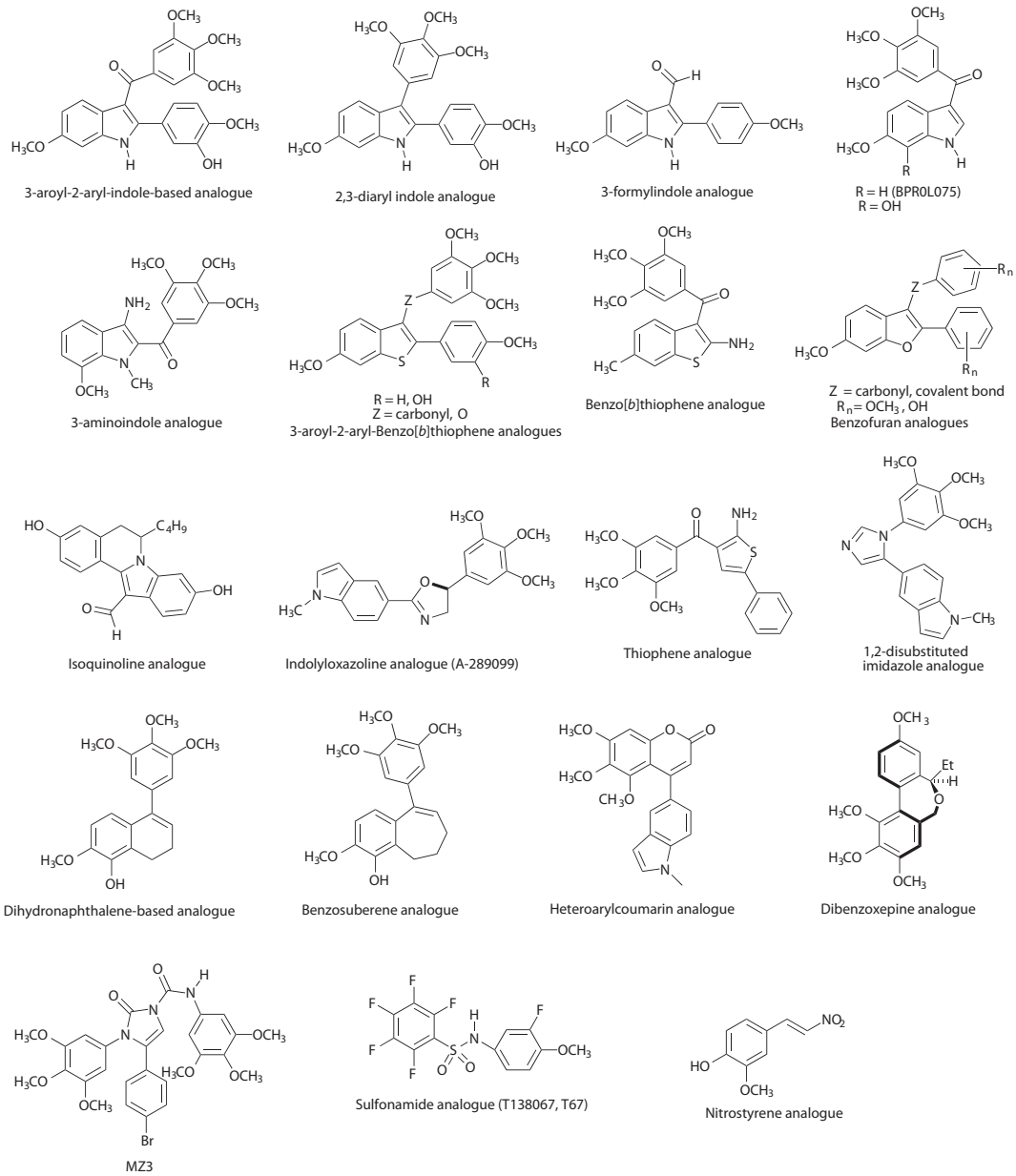

FIGURE 3.8 Synthetic analogs inspired by the combretastatins.

corresponding phosphate prodrug salts[154] 4′-methyl[155] and 3,4,5-trimethyl[156] combretastatin analogs, a benzo[*b*]thiophene deriviative,[157] fluorcombstatin analogs,[158] a pyridone derivative,[159] and stilbenophane analogs[160] (Figure 3.6).

A second grouping of combretastatin analogs is comprised of compounds that deviate from the stilbene functionality primarily through modification of the ethylene bridge located between the two aryl rings (Figure 3.7). A representative group (not intended to be inclusive) includes phenstatin,[161] hydroxyphenstatin,[162] an epoxide analog,[163] cyclopropane derivatives,[164] a benzil analog,[165] heterocombretastatins,[166] combretatropones,[167,168] *aza*-combretastatins,[169] and bridge-modified vicinal diols.[170,171] In addition, ring-constrained combretastatin bridge-modified compounds include

isoxazoline analogs,[172] pyridine derivatives,[172] combretadioxolane analogs,[173–175] and chalcone derivatives,[176] along with thiadiazole,[177] combretatriazole,[178] triazole,[178,179] combretafurazans,[180] oxazole,[181] and tri- and tetra-arylethylene[182] analogs. Additional representative examples include the structurally unique tetrahydro-thioxopyrimidine[183] and enediyne[184] derivatives along with the aryl-aryl ether,[185] amine,[185] and sulfide[186] linked analogs (Figure 3.7).

It is also interesting to note that many combretastatin analogs feature significant structural variation from the basic stilbenoid molecular core structure. These molecules are perhaps best described structurally as being "inspired" by the combretastatins. Many of these compounds have pronounced biological activity against human cancer cell lines (*in vitro*). It is simply impossible to make any reasonable effort to summarize these compounds in an inclusive sense; rather, a very small sampling of combretastatin "inspired" molecules is depicted in Figure 3.8. For example, 3-aroyl-2-aryl indoles,[100,187,188] 2,3-diaryl indoles,[188] 3-formyl indoles,[189] and related indole analogs,[190–193] benzo[*b*] thiophene,[56,194–201] and benzofuran analogs,[188,202,203] have been prepared (Figure 3.8). The evolving story with regard to the combretastatin "inspired" indole analogs (originally prepared by Pinney et al.[100,187] and subsequently expanded through a separate synthetic route by Flynn et al.[188]) is especially noteworthy as these compounds have further "inspired" a wide range of next generation-related indole and aryl-heteroaryl fused ring derivatives.[194,204–209] The [6,6] ring-fused dihydronaphthalenes,[196,210–212] and [6,7] ring-fused benzosuberene derivatives[212] are remarkable in terms of their pronounced *in vitro* cytotoxicity against human cancer cell lines. Additional analogs include dihydroxyindolo[2,1-α]isoquinolines,[213] indolyloxazoline derivatives,[214,215] thiophene-based ligands,[216] disubstituted imidazole analogs,[217] heteroarylcoumarin derivatives,[218] dibenzoxepine analogs,[219] a structurally unique imidazolin-2-one (MZ3) ligand,[220,221] sulfonamide analogs,[222,223] and nitrostyrene analogs that bear structural resemblance to *E*-combretastatin derivatives[224] (Figure 3.8).

A variety of small-molecule VDAs are currently in human clinical development function through a biological mechanism ultimately involving the tubulin–microtubule protein system (Figure 3.9).[32,94] These drugs include CA4P (Zybrestat™, fosbretabulin) and CA1P (OXi4503), which were both discovered by George R. Pettit, Arizona State University, and are sponsored in the clinic by Oxigene, Inc. (see appropriate references throughout), as well as AVE8062[145,146,225,226] [discovered by Ajinomoto, Inc. (AC7700) and sponsored in the clinic by Sanofi-Aventis]. Additional VDAs that demonstrate a tubulin–microtubule protein system component in their mechanism of action include MN-029[227] (sponsored by Medicinova Inc.), NPI-2358[228] (sponsored by Nereus Pharmaceuticals), CYT997[229] (sponsored by Cytopia Research Pty. Ltd.), BNC105[230] (sponsored by Bionomics), ABT-751[231] (sponsored by Abbott Laboratories), and MPC-6827[232] (sponsored by Myriad Pharmaceuticals). Previous clinical studies have also been carried out with ZD-6126[233–236] [licensed from Angiogene Pharmaceuticals, UK, and sponsored in the clinic (previously) by AstraZeneca]. The similarity of CA4P, AVE8062, and CA1P to the natural products CA4 and CA1 is obvious. Likewise, the [6,7,6] ring fusion in ZD-6126 is highly reminiscent of the [6,7,7] (tropolone) ring system of the natural product colchicine.

3.6 PRECLINICAL STUDIES

The recent interest in the anticancer potential of the combretastatins has gained momentum from the observation that CA4P can induce rapid and selective blood flow shutdown within tumor tissue.[105,237,238] As the development and activity of CA4P as a VDA has been the subject of a number of reviews,[16,23,93,94,96,97,99,102,239–241] only a brief summary of the preclinical data will be provided here.

3.6.1 Effects of CA4P on Tumor Blood Flow

A number of studies have demonstrated the rapid and selective effects of CA4P on tumor vascular function.[54,238,242–251] These studies have established that blood flow reductions occur in transplanted and spontaneous rodent tumors and in xenografted human tumors.[104,252–254] Blood flow effects can

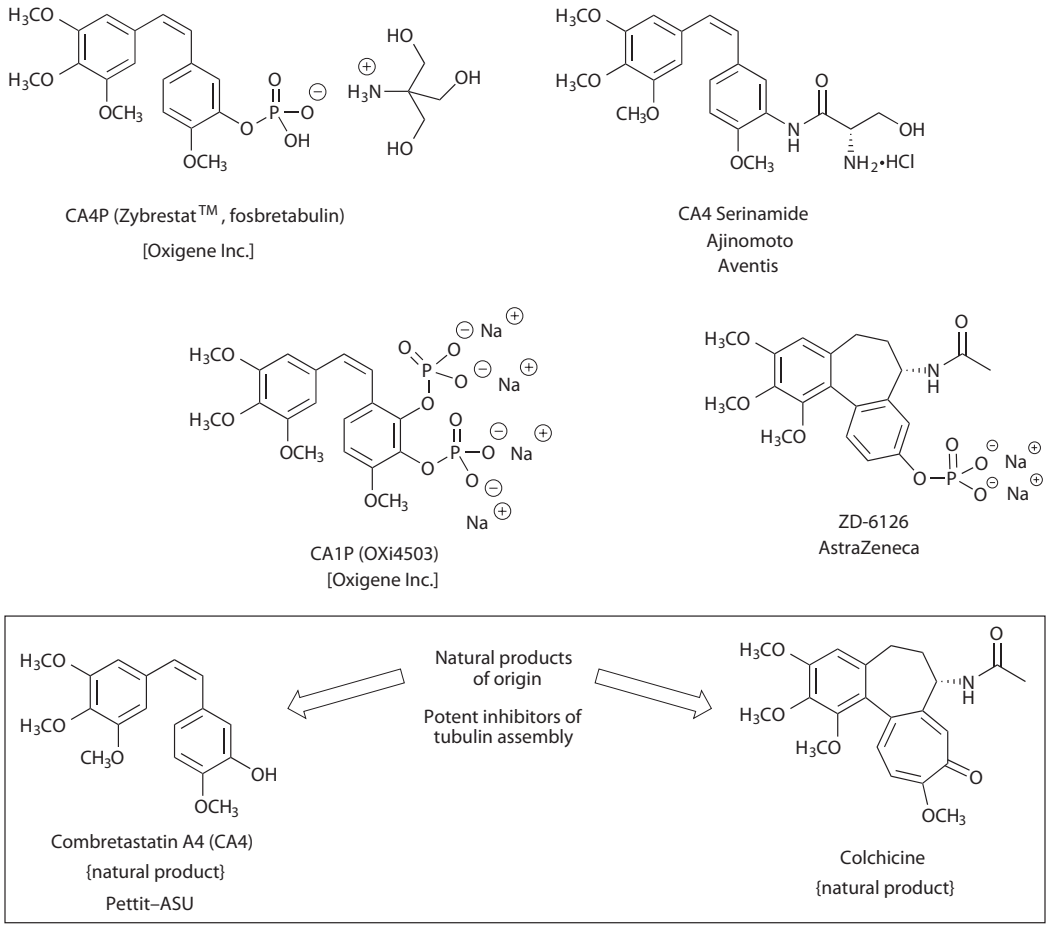

FIGURE 3.9 Small-molecule vascular disrupting agents in clinical development.

be measured within 10–20 min of CA4P administration, a timeframe that closely mimics the *in vitro* effects on endothelial cell shape. These blood flow effects persist for hours, although in some tumors restoration of flow can be observed 24 h following treatment. Because it is known that dramatic tumor cell kill is induced within a few hours of cutting off the blood supply,[255] even short periods of blood flow reduction are expected to induce a significant reduction in tumor cell burden.

3.6.2 Tumor Response to CA4P as a Single Agent

Measurements of clonogenic tumor cell survival in tumors excised following CA4P treatment have shown that extensive tumor cell kill is induced.[54,256] Indeed, these studies show that 24 h after a dose of 100 mg/kg, tumor cell survival is reduced by 90–99% in a number of experimental tumors. Despite the extensive cell kill observed following the vascular shutdown achieved with CA4P, significant growth retardation is very rarely seen. This lack of retardation has been attributed to rapid regrowth from the rim of viable cells surviving at the tumor periphery,[54] and to the recruitment of circulating endothelial progenitor cells which home to this area.[257] Of interest is that treatment with conventional cytotoxic chemotherapy or radiation at doses that induce similar or lower levels of cell kill can cause significant retardation of tumor growth.[102] One possible explanation for this difference

is that the cells in the periphery have access to a more nutritive blood flow than those in the center, which are dependent on the relatively poor and chaotic vascular network present within the tumor mass. This has several consequences, one of which is that the hypoxic and nutrient-deprived cells that are more prevalent in the tumor core will be more resistant to conventional treatments such as radiation and cytotoxic approaches, which are known to be more toxic to well-oxygenated and rapidly proliferating cell populations.[258] Therefore, if this is the case, treatments such as radiation and cisplatin, in contrast to CA4P, will preferentially kill cells in the periphery and spare those in the center of the tumor. Thus, if the cells that have survived treatment are already proliferating and adjacent to a good supply of oxygen and nutrients, they will initiate rapid regrowth, whereas, if the surviving cells are less well supplied, there will be a lag phase before proliferation is initiated. If this hypothesis is correct, CA4P, along with other VDAs, offers great potential to enhance the effectiveness of current treatment approaches by the complementary cell killing of different cell populations. In addition to its ability to target solid tumors, CA4P has recently been shown to elicit significant antitumor activity against orthotopically implanted leukemia.[259] This activity is believed to result from the ability of CA4P to alter the adherence and attachment of leukemic cells which exist in treatment-resistant stromal niches. The ability of CA4P at daily low doses to inhibit neovascularization in a mouse model of oxygen-induced retinopathy indicates that it may also have a role as an antiangiogenic agent.[94,95]

3.6.3 Treatment Response to CA4P in Combination Therapy

Several studies have already indicated the therapeutic potential of combining CA4P with radiation and a variety of chemotherapy agents.[54,245,260] In addition, CA4P has been shown to enhance other therapeutic approaches, such as hyperthermia, antibody-based approaches, and even antiangiogenic agents.[249,261–263]

In a study by Siemann et al., the tumor cell kill induced by cisplatin or cyclophosphamide was enhanced by a factor of 10–500 by post-treatment administration of CA4P.[256] Moreover, no increase in the bone marrow stem-cell toxicity associated with these anticancer drugs was observed, giving rise to a real therapeutic gain. Numerous other studies have shown significant enhancement of the effects of conventional chemotherapeutic agents on tumor response, including cisplatin,[54] fluorouracil,[264] doxorubicin,[265] chlorambucil,[16] melphalan,[16] CPT-11,[266] and Taxol®.[54]

It has been shown that CA4P, when administered shortly following radiation treatment, can significantly enhance tumor response.[106,245,261,262,267] In contrast, no enhancement of radiation damage has been observed in normal tissue.[268]

Combining VDAs with hyperthermia is another potentially useful approach. Clear evidence exists that blood flow to the tumor is important in determining the response to heat.[269] Furthermore, a number of studies have now shown that decreasing tumor blood flow by CA4P treatment can provide an effective means of improving tumor response to hyperthermia.[262,270]

It has also been shown that CA4P can enhance the activity of antibody-based cancer therapeutics.[263] In a study evaluating the efficacy of a radiolabeled anti-CEA antibody against an established human colon cancer in mice, the researchers found that administration of CA4P could improve long-term tumor control from 0% to 85%. Recently, there has been significant interest in combining VDAs such as CA4P with antiangiogenic treatments. Such a strategy was recently investigated by combining CA4P and bevacizumab in the treatment of a model of human clear cell renal cell carcinoma.[271] The results showed that the CA4P–bevacizumab combination led to a significant enhancement of the tumor response beyond that achieved with either vascular targeting therapy alone. A likely explanation for these observations is that while CA4P significantly reduced the viable tumor mass, bevacizumab impaired subsequent tumor regrowth by interfering with the re-establishment of the tumor blood vessel network. From a therapeutic perspective, the enhanced tumor responses resulting from the combination of bevacizumab and CA4P provides an experimental basis for the consideration of such a treatment strategy in the clinic.

3.6.4 Preclinical Studies with CA1P (OXi4503)

The preclinical activity of CA1P has shown that it is a much more potent agent than CA4P, and it can also induce tumor growth delays and regressions when used as a single agent (something not usually observed with CA4P).[272–275] This enhanced activity was unexpected based on the *in vitro* data for tubulin binding and for inhibition of cell proliferation for the active parent drug, CA1. Because regressions are observed, it indicates that CA1P, in addition to the vascular effects, is also directly attacking the remaining viable cells at the rim of the tumor mass. One explanation for this unexpected activity is that it is metabolized *in vivo* to a reactive and cytotoxic *o*-quinone. Evidence that CA1 can be converted to an *o*-quinone by certain oxidative enzymes has recently been published by Folkes et al.[134] Supportive evidence for the *o*-quinone being formed in solid tumors has been provided in a paper by Kirwan et al., who show that CA1 is metabolized by tumor tissue to an agent that covalently binds to the cellular contents of the tumor.[276] Recent studies combining treatment with OXi4503 with antiangiogenic bevacizumab in mouse models of acute myelogenous leukemia demonstrated enhanced activity over that of either monotherapy.[277]

3.7 CLINICAL EXPERIENCE

3.7.1 Cancer

Under the sponsorship of Oxigene, Inc., CA4P and CA1P have moved into clinical trials. To date, there have been 12 clinical trials involving CA4P: 10 completed and 2 ongoing (Table 3.3), and aspects of the clinical experience with CA4P have been reviewed.[109,241]

Ninety-six patients with advanced malignancies were enrolled in three phase I clinical trials, beginning in 1998. These trials explored the safety and pharmacokinetics of three different intravenous administration schedules of CA4P as a single agent [i.e., single dose schedule every 21 days ("1 × /21" study)], weekly for three consecutive weeks every 28 days ("3 × /28" study), and daily for five consecutive days every 21 days ("d × 5" study).[278–282] Doses as high as 114 mg/m^2 (weekly schedule) have been studied. Dose-limiting toxicities have been identified in all three trials, resulting

TABLE 3.3
Completed and Ongoing Clinical Trials with CA4P (Fosbretabulin) in Oncology

Compound	Indication/Use	Clinical Phase	Notes
Combretastatin A-4P	Solid tumors; single agent	Phase I	Three trials completed
Combretastatin A-4P	Solid tumors; combination with carboplatin	Phase Ib	Completed
Combretastatin A-4P	Head and neck/lung/prostate; combination with radiation	Phase I/II	Completed
Combretastatin A-4P	Anaplastic thyroid cancer	Phase II	Completed
Combretastatin A-4P	Anaplastic thyroid cancer in combination with chemotherapy and radiotherapy	Phase I/II	Completed
Combretastatin A-4P	Advanced ovarian cancer; combination with carboplatin and paclitaxel	Phase I/II	Completed
Combretastatin A-4P	Advanced colorectal cancer, combination with iodine-labeled antibody A5B7	Phase I/II	Completed
Combretastatin A-4P	Stage IIIb/IV non small cell lung cancer (NSCLC) combination with carboplatin, paclitaxel and bevacizumab	Phase II (randomized)	Ongoing
Combretastatin A-4P	Anaplastic thyroid cancer (ATC) combination with carboplatin and paclitaxel	Phase II (randomized)	Ongoing

in a maximum tolerated dose in the range of 60–68 mg/m^2. Dose-limiting toxicities have included dyspnea, myocardial ischemia, reversible neurological events, and tumor pain.

A major objective of these studies, in addition to establishing the maximum tolerated dose, was to evaluate the effects on tumor blood flow. Significant reductions in tumor blood flow were seen in all three clinical trials.[278–282] Blood flow reductions were observed at all dose levels evaluated between 52 and 114 mg/m^2, with no clear dose response being discernable. Additional studies have shown blood flow reductions down to 30 mg/m^2 (Oxigene, Inc., unpublished data). Thus, the data on humans confirm the results in animals that tumor blood flow reductions can be seen at doses at or below the maximum tolerated dose. These findings have provided the impetus to move CA4P into later-stage clinical trials.

The preclinical data to date for CA4P indicate that although the compound elicits significant reductions in blood flow, resulting in histologically demonstrable tumor necrosis, it appears to leave a rim of viable tumor cells at the periphery. Replication and growth of these few remaining tumor cells results in an insignificant tumor growth delay in a variety of preclinical models. Because of this phenomenon, the clinical focus was directed at combining CA4P with other treatment therapies and modalities that are more effective at the outer tumor regions. As a result of these findings, a number of phase I/II clinical trials were undertaken which focused on establishing the safety and tolerability of combining CA4P with a number of other treatment strategies including chemotherapy, radiotherapy, and antiangiogenic therapies. These studies showed that CA4P can be safely combined with a number of conventional therapies and has led to the initiation of two randomized phase II studies in non-small-cell lung cancer (NSCLC) and anaplastic thyroid cancer (ATC). The NSCLC study is currently comparing the effects of the approved regimen combining carboplatin and taxol with the antiangiogenic agent bevacizumab to the same combination with the addition of weekly CA4P. The ATC study is comparing the effects of carboplatin and taxol with the same regimen plus weekly CA4P. Results from these studies are expected in late 2010/early 2011.

Combretastatin A-1P (Oxi-4503) has also shown excellent activity in preclinical studies. Oxi-4503 appears to be able to cause tumor regressions with single-agent activity, whereas CA4P's *in vivo* activity is best with combination studies.[275] Two clinical studies are currently underway using Oxi-4503. One is a phase I study evaluating the safety and tolerability in patients with solid tumors. The second study is a phase Ib/II clinical trial focused on assessing the safety/tolerability and efficacy of Oxi-4503 specifically in solid tumors growing in the liver.

3.7.2 Ophthalmology

The retina at the back of the eye is the light-sensing layer of tissue containing the cones, rods, and nerve endings that translate light into neural impulses. Certain types of damage to the retina and/or the choroid, the next posterior tissue layer, can lead to severe vision loss. Typical is age-related macular degeneration (AMD) where abnormal blood vessels develop from the choroid underneath the retina and are known as choroidal neovascularization (CNV). The resulting abnormal vessels leak fluid and blood resulting in scarring and damage to the macular area of the retina necessary for normal central vision. In the dry form (atrophic) of AMD, which rarely leads to blindness, there is no elevated macular scar and no hemorrhage or exudation in the macular region. Whereas in the wet (exudative or neovascular form) AMD, which is less common (<15%), there is a subretinal network of CNV forms and wet AMD causes most of the blindness (over 50 years of age) in industrialized countries.

AMD, myopic macular degeneration (MMD),[283] and polypoidal choroidal vasculopathy (PCV) are among a number of other serious medical problems where the combretastatin VDA/antiangiogenic drugs are expected to provide considerable treatment improvements and current clinical remedies are very encouraging.[284] For example, the first phase II clinical trial of CA4P against MMD achieved the primary endpoint of the trial where all 23 patients obtained stabilization of vision. Parallel phase I/II clinical trials for exudative AMD using CA4P have been in progress at the Johns Hopkins School of Medicine.[283] A phase II ophthalmology clinical trial for PCV has recently been announced.

In addition, results from rabbit to primate preclinical studies have confirmed that two ophthalmological formulations of CA4P have been discovered that when applied topically to the surfaces of the eye are absorbed well and provide therapeutic concentrations to the retina and choroid in the back of the eye. A phase I clinical trial of a topical CA4P formulation for eye diseases involving abnormal vascular growth is planned and if successful should greatly improve the treatment approach for patients and presumably eliminate the current need for multiple (semimonthly to monthly) injections (at $2,000 to $3,000 each) directly into the eye using some of the currently available monoclonal (protein) drugs. A number of topical ophthalmic formulations for reaching out to diseases at the posterior part of the eye have been described in a 2010 Italian patent application.[285] Recurring components of these formulations include xanthan, dexamethasone sodium phosphate, and sodium phosphates.

The potential for treating a variety of other diseases involving abnormal vascular production with the combretastatin VDA drugs appears very encouraging. One of the more obvious is retinoblastoma that occurs once in about some 16,000 live births,[286,287] and is a malignant ocular neoplasm occurring before three years of age. Although multimodality treatments are currently in use leading to over 90% five-year survival rates there is risk of serious morbidity and mortality[287] along with developing osteosarcoma later in life. Based on murine preclinical experiments,[286–288] addition of a combretastatin VDA in a combination drug treatment should prove useful in future retinoblastoma clinical trials. As a single agent against a murine retinoblastoma, subconjunctivally injected CA4P led to a dose-dependent reduction in microvessel density and significant tumor reduction.[288]

Another obvious target for a combretastatin VDA drug is diabetic retinopathy (involves macular edema, microaneurysms, exudates and hemorrhages), which evolves over a number of years with vision loss late in the disease course. Initial experiments against retinal neovascularization in galactose-fed dogs employing intravenous CA4P indicated that successful results would require chronic long-term administration.[289] Given success in the present topical treatments of CA4P to the eye, application to chronic intervention in developing vision loss arising from diabetic retinopathy appears to be attractive.

Clinical successes employing CA4P and CA1P against a number of generally lethal types of cancer are rapidly accelerating. Those very reassuring results, combined with advances now within reach of providing remarkable treatment improvements in diseases of the eye that otherwise lead to partial or complete loss of vision, as always illustrate the depth and extraordinary importance of new drug discovery research focused on naturally occurring substances.

3.8 CODA

Until Mr. Hattem's communications in 1999 (cf. Section 3.1), none of us involved in the sampling of *C. caffrum* 37 years ago, and subsequently, in discovery of the combretastatins, had any knowledge of this plant being used in traditional medical treatments for cancer. From a humanitarian viewpoint, this historical uncertainty is essentially moot. The author (G.R.P.) thinks the real benefit to the people of Zimbabwe and South Africa will be derived from the eventual worldwide success of the CA4 and CA1 prodrugs in treating human cancer and in ocular diseases. These drugs should become two of the least expensive anticancer drugs of all time, greatly benefiting both African countries and their citizens. Indeed, if it were not for the NCI and Arizona State University's Cancer Research Institute, the discovery of CA4, CA1, and their phosphate prodrug developments to the present phases I–III human cancer clinical trials, as well as for the current phase I and phase II human clinical trials in ophthalmology, might have been delayed many more decades or centuries into the future. Hence, there needs to be a worldwide realization that it is in everyone's best interest if the collection of plants and animals for medicinal purposes is facilitated by clear, transparent, and encouraging discovery regulations. Indeed, it is vitally necessary not to impede the discovery of new naturally occurring drugs with legal barriers but instead make every effort to increase the availability. Both the source country and patients worldwide will then benefit from the investment

by governments, universities, and the private sector in the discovery and development of new anticancer and other drugs.

ACKNOWLEDGMENTS

The authors extend their appreciation and special thanks to each of the colleagues named as coauthors on publications involving the discovery and development of the combretastatins. In addition, they express appreciation for helpful communications with Prof. A.E. van Wyk and Mr. Case van Hattem. Furthermore, the authors gratefully acknowledge assistance from the Welch Foundation (K.G.P.; grant no.: AA-1278) and Oxigene Inc. (K.G.P. and M.L.T.) in the area of small-molecule molecular recognition for tubulin, and support provided by 5R01CA090441-07 (G.R.P.) awarded by the Division of Cancer Treatment and Diagnosis, National Cancer Institute, DHHS. Finally, the authors are most appreciative of the valuable editing contributions of Cristin McAnear and Tracy A. Pinney.

REFERENCES

1. Willis, J.C. and Arey Shaw, H.K., *A Dictionary of the Flowering Plants & Ferns*, 8th ed., Cambridge University Press, London, 1973.
2. Watt, J.M. and Breyer-Brandwijk, M.G., *The Medicinal and Poisonous Plants of Southern and Eastern Africa*, 2nd ed., E. and S. Livingston, London, 1962.
3. Masako, P., Picard, J., and Eloff, J.N., The antifungal activity of twenty-four southern African *Combretum* species (Combretaceae), *S. Afr. J. Bot.*, 73, 173, 2007.
4. Hartwell, J.L., *Plants Used Against Cancer*, Quarterman Publications, Laurence, MA, 1982.
5. Wall, M.E., Taylor, H., Ambrosio, L., and Davis, K., Plant antitumor agents. 3. A convenient separation of tannins from other plant constituents, *J. Pharm. Sci.*, 58, 839, 1969.
6. Palmer, E. and Pitman, N., *Trees of Southern Africa*, Vol. 3, A.A. Balkema, Cape Town, 1972.
7. Kokwaro, O., *Medicinal Plants of East Africa*, East African Literature Bureau, Nairobi, 1976.
8. Samuelsson, G., Farah, M.H., Claeson, P., Hagos, M., Thulin, M., Hedberg, O., Warfa, A.M. et al., Inventory of plants used in traditional medicine in Somalia. II. Plants of the families Combretaceae to Labiatae, *J. Ethnopharmacol.*, 37, 47, 1992.
9. Iwu, M.M., *Handbook of African Medicinal Plants*, CRC Press, Boca Raton, FL, 1993.
10. Gurib-Fakim, A. and Brendler, T., *Medicinal and Aromatic Plants of Indian Ocean Islands: Madagascar, Comoros, Seychelles, and Mascarenes*, Medpharm Scientific Publishers, Stuttgart, Germany, 2004, 194.
11. Duke, J., *Medicinal Herbs*, 2nd ed., CRC Press, New York, 2002.
12. Pettit, G.R., Hoard, M.S., Doubek, D.L., Schmidt, J.M., Pettit, R.K., Tackett, L.P., and Chapuis, J.-C., Antineoplastic agents 338. The cancer cell growth inhibitory. Constituents of *Terminalia arjuna* (Combretaceae), *J. Ethnopharmacol.*, 53, 57, 1996.
13. Chinemana, F., Drummond, R.B., Mavi, S., and De Zoys, I., Indigenous plant remedies in Zimbabwe, *J. Ethnopharmacol.*, 14, 159, 1985.
14. Cushman, M., Nagarathnam, D., Gopal, D., Chakraborti, A.K., Lin, C.M., and Hamel, E., Synthesis and evaluation of stilbene and dihydrostilbene derivatives as potential anticancer agents that inhibit tubulin polymerization, *J. Med. Chem.*, 34, 2579, 1991.
15. Sackett, D.L., Podophyllotoxin, steganacin, and combretastatin: Natural products that bind at the colchicine site of tubulin, *Pharm. Ther.*, 59, 163, 1993.
16. Tozer, G.M., Kanthou, C., Parkins, C.S., and Hill, S.A., The biology of the combretastatins as tumour vascular targeting agents, *Int. J. Exp. Pathol.*, 83, 21, 2002.
17. Lin, C.M., Singh, S.B., Chu, P.S., Dempcy, R.O., Schmidt, J.M., Pettit, G.R., and Hamel, E., Interactions of tubulin with potent natural and synthetic analogs of the antimitotic agent combretastatin: A structure–activity study, *Mol. Pharm.*, 34, 200, 1988.
18. Li, Q. and Sham, H.L., Discovery and development of antimitotic agents that inhibit tubulin polymerization for the treatment of cancer, *Expert Opin. Ther. Pat.*, 12, 1663, 2002.
19. Rowinsky, E.K., Siemann, D.W., Remick, S.C., Wood, L.S., and Ziats, N.P., Horizons in cancer therapeutics: From bench to bedside, *Contin. Educ.*, 3, 1, 2002.
20. Hamel, E., Antimitotic natural products and their interactions with tubulin, *Med. Res. Rev.*, 16, 207, 1996.

21. Thorpe, P.E., Vascular targeting agents as cancer therapeutics, *Clin. Cancer Res.*, 10, 415, 2004.
22. Griggs, J., Metcalfe, J.C., and Hesketh, R., Targeting tumour vasculature: The development of combretastatin A4, *Lancet Oncol.*, 2, 82, 2001.
23. Bibby, M.C., Combretastatin anticancer drugs, *Drugs Future*, 27, 475, 2002.
24. Cirla, A. and Mann, J., Combretastatins: From natural products to drug discovery, *Nat. Prod. Rep.*, 20, 558, 2003.
25. Nam, N.-H., Combretastatin A-4 analogues as antimitotic antitumor agents, *Curr. Med. Chem.*, 10, 1697, 2003.
26. Banerjee, S., Wang, Z., Mohammad, M., Sarkar, F.H., and Mohammad, R.M., Efficacy of selected natural products as therapeutic agents against cancer, *J. Nat. Prod.*, 71, 492, 2008.
27. Chaudhary, A., Pandeya, S.N., Kumar, P., Sharma, P.P., Gupta, S., Soni, N., Verma, K.K., and Bhardwaj, G., Combretastatin A-4 analogs as anticancer agents, *Mini-Rev. Med. Chem.*, 7, 1186, 2007.
28. Cragg, G.M. and Newman, D.J., Plants as a source of anti-cancer agents, *J. Ethnopharmacol.*, 100, 72, 2005.
29. Ducki, S., Antimitotic chalcones and related compounds as inhibitors of tubulin assembly, *Anticancer Agent Med. Chem.*, 9, 336, 2009.
30. Hsieh, H.P., Liou, J.P., and Mahindroo, N., Pharmaceutical design of antimitotic agents based on combretastatins, *Curr. Pharm. Design*, 11, 1655, 2005.
31. Kingston, D.G.I., Tubulin-interactive natural products as anticancer agents, *J. Nat. Prod.*, 72, 507, 2009.
32. Lee, R.M. and Gewirtz, D.A., Colchicine site inhibitors of microtubule integrity as vascular disrupting agents, *Drug Dev. Res.*, 69, 352, 2008.
33. Orsini, F. and Sello, G., Natural stilbenes and analogues as antineoplastic agents, *Stud. Nat. Prod. Chem.*, 34, 77, 2008.
34. Singh, R. and Kaur, H., Advances in synthetic approaches for the preparation of combretastatin-based anti-cancer agents, *Synthesis*, 15, 2471, 2009.
35. Tron, G.C., Pirali, T., Sorba, G., Pagliai, F., Busacca, S., and Genazzani, A.A., Medicinal chemistry of combretastatin A4: Present and future directions, *J. Med. Chem.*, 49, 3033, 2006.
36. Pettit, G.R. and Lippert, J.W., Preparation of combretastin A-1 phosphate and combretastin B-1 phosphate prodrugs with increased solubility, PCT Int. Application WO2001081355 A1, 2001.
37. Pettit, G.R. and Minardi, M.D., Preparation of combretastatin A3 diphosphate prodrugs for the treatment of cancer, PCT Int. Application WO2002102766 A2, 2002.
38. Pettit, G.R. and Singh, S.B, Combretastatin A-4, US Patent 4,996,237, 1991.
39. Pettit, G.R. and Singh, S.B., Isolation, structural elucidation and synthesis of novel antineoplastic substances denominated "combretastatins," US Patent 5,569,786, 1996.
40. Pettit, G.R., Combretastatin A-4 prodrug, US Patent 5,561,122, 1996.
41. Pinney, K.G., Pettit, G.R., Mocharla, V.P., Mejia, M.P., and Shirali, A., Description of anti-mitotic agents which inhibit tubulin polymerization, US Patent 6,350,777, 2000.
42. Pettit, G.R. and Grealish, M.P., Synthesis of hydroxyphenstatin and the prodrugs thereof as anticancer and antimicrobial agents, PCT Int. Application WO2001081288 A1, 2001.
43. Pettit, G.R. and Brian, T., Synthesis and formulation of phenstatin and related prodrugs for use as antitumor agents, PCT Int. Application WO9934788 A1, 1999.
44. Pettit, G.R. and Rhodes, M.R., Preparation and formulation of combretastatin A4 prodrugs and their trans-isomers for use as antitumor agents, PCT Int. Application WO9935150 A1, 1999.
45. Pettit, G.R. and Moser, B.R., Preparation of combretastatin A-2 prodrugs as antitumor and antimicrobial agents, PCT Int. Application WO2003059855 A1, 2003.
46. Cai, S.X., Small molecule vascular disrupting agents: Potential new drugs for cancer treatment, *Recent Pat. Anticancer Drug Discov.*, 2, 79, 2007.
47. Kingston, D.G.I., Samaranayake, G., and Ivey, C.A., The chemistry of taxol, a clinically useful anticancer agent, *J. Nat. Prod.*, 53, 1, 1990.
48. Nicolaou, K.C., Winssinger, N., Pastor, J., Ninkovic, S., Sarabia, F., He, Y., Vourloumis, D. et al., Synthesis of epothilones A and B in solid and solution phase, *Nature*, 387, 268, 1997.
49. Owellen, R.J., Hartke, C.A., Dickerson, R.M., and Hains, F.O., Inhibition of tubulin-microtubule polymerization by drugs of the vinca alkaloid class, *Cancer Res.*, 36, 1499, 1976.
50. Pettit, G.R., Kamano, Y., Herald, C.L., Tuinman, A.A., Boettner, F.E., Kizu, H., Schmidt, J.M., Baczynskyj, L., Tomer, K.B., and Bontems, R.J., The isolation and structure of a remarkable marine animal antineoplastic constituent: Dolastatin 10, *J. Am. Chem. Soc.*, 109, 6883, 1987.
51. Pettit, G.R., Srirangam, J., Barkoczy, J., Williams, M., Boyd, M., Hamel, E., Pettit, R. et al., Antineoplastic agents 365. Dolastatin 10 SAR probes, *Anticancer Drug Des.*, 13, 243, 1998.

52. Pettit, G.R., Dolastatin anticancer drugs, in *Marine Anticancer Compounds in the Era of Targeted Therapies*, Chabner, B., Ed., Permanyer Publications, Mallorca, 2009, 19.
53. Lin, C.M., Ho, H.H., Pettit, G.R., and Hamel, E., Antimitotic natural products combretastatin A-4 and combretastatin A-2: Studies on the mechanism of their inhibition of the binding of colchicine to tubulin, *Biochemistry*, 28, 6984, 1989.
54. Chaplin, D.J., Pettit, G.R., and Hill, S.A., Anti-vascular approaches to solid tumor therapy: Evaluation of combretastatin A4 phosphate, *Anticancer Res.*, 19, 189, 1999.
55. Jordon, A., Hadfield, J.A., Lawrence, N.J., and McGown, A.T., Tubulin as a target for anticancer drugs: Agents which interact with the mitotic spindle, *Med. Res. Rev.*, 18, 259, 1998.
56. Pinney, K.G., Bounds, A.D., Dingeman, K.M., Mocharla, V.P., Pettit, G.R., Bai, R., and Hamel, E., A new anti-tubulin agent containing the benzo[b]thiophene ring system, *Bioorg. Med. Chem. Lett.*, 9, 1081, 1999.
57. Pettit, G.R. and Lippert, J.W., Antineoplastic agents 429. Syntheses of the combretastatin A-1 and combretastatin B-1 prodrugs, *Anticancer Drug Des.*, 15, 203, 2000.
58. Pettit, G.R., Temple, C. Jr., Narayanan, V.L., Varma, R., Simpson, M.J., Boyd, M.R., Rener, G.A., and Bansal, N., Antineoplastic agents 322. Synthesis of combretastatin A-4 prodrugs, *Anticancer Drug Des.*, 10, 299, 1995.
59. Pettit, G.R., Cragg, G.M., Herald, D.L., Schmidt, J.M., and Lohavanijaya, P., Isolation and structure of combretastatin, *Can. J. Chem.*, 60, 1374, 1982.
60. Pettit, G.R., Cragg, G.M., and Singh, S.B., Antineoplastic agents, 122. Constituents of *Combretum caffrum*, *J. Nat. Prod.*, 50, 386, 1987.
61. Pettit, G.R., Singh, S.B., Niven, M.L., Hamel, E., and Schmidt, J.M., Isolation, structure, and synthesis of combretastatins A-1 and B-1, potent new inhibitors of microtubule assembly, derived from *Combretum caffrum*, *J. Nat. Prod.*, 50, 119, 1987.
62. Pettit, G.R. and Singh, S.B., Isolation, structure, and synthesis of combretastatin A-2, A-3, and B-2, *Can. J. Chem.*, 65, 2390, 1987.
63. Pettit, G.R., Singh, S.B., Boyd, M.R., Hamel, E., Pettit, R.K., Schmidt, J.M., and Hogan, F., Antineoplastic agents. 291. Isolation and synthesis of combretastatins A-4, A-5, and A-6, *J. Med. Chem.*, 38, 1666, 1995.
64. Pettit, G.R., Singh, S.B., Schmidt, J.M., Niven, M.L., Hamel, E., and Lin, C.M., Isolation, structure, synthesis, and antimitotic properties of combretastatins B-3 and B-4 from *Combretum caffrum, J. Nat. Prod.*, 51, 517, 1988.
65. Singh, S.B. and Pettit, G.R., Isolation, structure, and synthesis of combretastatin C-1, *J. Org. Chem.*, 54, 4105, 1989.
66. Pettit, G.R., Singh, S.B., and Niven, M.L., Isolation and structure of combretastatin D-1: A cell growth inhibitory macrocyclic lactone from *Combretum caffrum*, *J. Am. Chem. Soc.*, 110, 8539, 1988.
67. Singh, S.B. and Pettit, G.R., Antineoplastic agents. 206. Structure of the cytostatic macrocyclic lactone combretastatin D-2, *J. Org. Chem.*, 55, 2797, 1990.
68. Nogales, E., Structural insight into microtubule function, *Annu. Rev. Biochem.*, 69, 277, 2000.
69. Downing, K.H., Structural basis for the interaction of tubulin with proteins and drugs that affect microtubule dynamics, *Annu. Rev. Cell Dev. Biol.*, 16, 89, 2000.
70. Wehbe, H., Kearney, C.M., and Pinney, K.G., Combretastatin A-4 resistance in H460 human lung carcinoma demonstrates distinctive alterations in β-tubulin isotype expression, *Anticancer Res.*, 25, 3865, 2005.
71. Wang, C., Cormier, A., Gigant, B., and Knossow, M., Insight into the GTPase activity of tubulin from complexes with stathmin-like domains, *Biochemistry*, 46, 10595, 2007.
72. Gigant, B., Wang, C., Ravelli, R.B.G., Roussi, F., Steinmetz, M.O., Curmi, P.A., Soel, A., and Knossow, M., Structural basis for the regulation of tubulin by vinblastine, *Nature*, 435, 519, 2005.
73. Nogales, E., Wolf, S.G., and Downing, K.H., Structure of the α,β-tubulin dimer by electron crystallography, *Nature*, 391, 199, 1998.
74. Rao, S., Horwitz, S.B., and Ringel, I., Direct photoaffinity labeling of tubulin with taxol, *J. Natl. Cancer Inst.*, 84, 785, 1992.
75. Staretz, M.E. and Hastie, S.B., Synthesis, photochemical reactions, and tubulin binding of novel photoaffinity labeling derivatives of colchicine, *J. Org. Chem.*, 58, 1589, 1993.
76. Hahn, K.M., Hastie, S.B., and Sundberg, R.J., Synthesis and evaluation of 2-diazo-3,3,3-trifluopropanoyl derivatives of colchicine and podophyllotoxin as photoaffinity labels: Reactivity, photochemistry, and tubulin binding, *Photochem. Photobiol.*, 55, 17, 1992.
77. Wolff, J., Knipling, L., Cahnmann, H.J., and Palumbo, G., Direct photoaffinity labeling of tubulin with colchicine, *Proc. Natl. Acad. Sci. USA*, 88, 2820, 1991.

78. Floyd, L.J., Barnes, L.D., and Williams, R.F., Photoaffinity labeling of tubulin with (2-nitro-4-azidophenyl)deacetylcolchicine: Direct evidence for two colchicine binding sites, *Biochemistry*, 28, 8515, 1989.
79. Bai, R., Pei, X.-F., Boyé, O., Getahun, Z., Grover, S., Bekisz, J., Nguyen, N.Y., Brossi, A., and Hamel, E., Identification of cysteine 354 of beta-tubulin as part of the binding site for the A ring of colchicine, *J. Biol. Chem.*, 271, 12639, 1996.
80. Olszewski, J.D., Marshalla, M., Sabat, M., and Sundberg, R.J., Potential photoaffinity labels for tubulin. Synthesis and evaluation of diazocyclohexadienone and azide analogs of colchicine, combretastatin, and 3,4,5-trimethoxybiphenyl, *J. Org. Chem.*, 59, 4285, 1994.
81. Pinney, K.G., Mejia, M.P., Villalobos, V.M., Rosenquist, B.E., Pettit, G.R., Verdier-Pinard, P., and Hamel, E., Synthesis and biological evaluation of aryl azide derivatives of combretastatin A-4 as molecular probes for tubulin, *Bioorg. Med. Chem.*, 8, 2417, 2000.
82. Sawada, T., Kato, Y., Kobayashi, H., Hashimoto, Y., Watanabe, T., Sugiyama, Y., and Iwasaki, S., A fluorescent probe and a photoaffinity labeling reagent to study the binding site of maytansine and rhizoxin on tubulin, *Bioconjug. Chem.*, 4, 284, 1993.
83. Sawada, T., Kobayashi, H., Hashimoto, Y., and Iwasaki, S., Identification of the fragment photoaffinity-labeled with azidodansyl-rhizoxin as Met-363-Lys-379 on beta-tubulin, *Biochem. Pharm.*, 45, 1387, 1993.
84. Sawada, T., Hashimoto, Y., Li, Y., Kobayashi, H., and Iwasaki, S., Fluorescent and photoaffinity labeling derivatives of rhizoxin, *Biochem. Biophys. Res. Comm.*, 178, 558, 1991.
85. Chavan, A.J., Richardson, S.K., Kim, H., Haley, B.E., and Watt, D.S., Forskolin photoaffinity probes for the evaluation of tubulin binding sites, *Bioconjug. Chem.*, 4, 268, 1993.
86. Safa, A.R., Hamel, E., and Felsted, R.L., Photoaffinity labeling of tubulin subunits with a photoactive analogue of vinblastine, *Biochemistry*, 26, 97, 1987.
87. Williams, R.F., Mumford, C.L., Williams, G.A., Floyd, L.J., Aivaliotis, M.J., Martinez, R.A., Robinson, A.K., and Barnes, L.D., A photoaffinity derivative of colchicine: 6-(4-azido-2-nitrophenylamino) hexanoyldeacetylcolchicine; photolabeling and location of the colchicine-binding site on the alpha-subunit of tubulin, *J. Biol. Chem.*, 260, 13794, 1985.
88. Dorleans, A., Gigant, B., Ravelli, R.B.G., Mailliet, P., Mikol, V., and Knossow, M., Variations in the colchicine-binding domain provide insight into the structural switch of tubulin, *Proc. Natl. Acad. Sci. U.S.A.*, 106, 13775, 2009.
89. Ravelli, R.B.G., Gigant, B., Curmi, P.A., Jourdain, I., Lachkar, S., Sobel, A., and Knossow, M., Insight into tubulin regulation from a complex with colchicine and a stathmin-like domain, *Nature*, 428, 198, 2004.
90. Bhattacharyya, B., Kapoor, S., and Panda, D., Fluorescence spectroscopic methods to analyze drug-tubulin interactions, chap. 17 in *Microtubules, in vitro*, Wilson, L. and Correia, J.J., Eds., Elsevier, *Method. Cell Biol.*, 95, 301, 2010.
91. Berman, H.M., Westbrook, J., Feng, Z., Gilliland, G., Bhat, T.N., Weissig, H., Shindyalov, I.N., and Bourne, P.E., The protein data bank, *Nucleic Acids Res.*, 28, 235, 2000.
92. Research Collaboratory for Structural Bioinformatics, Protein Data Bank Home Page, http://www.pdb.org/ (accessed March 5, 2010).
93. Pinney, K.G., Molecular recognition of the colchicines binding site as a design paradigm for the discovery and development of vascular disrupting agents, chap. 6 in *Vascular-targeted Therapies in Oncology*, Siemann, D.W., Ed., John Wiley & Sons, Ltd., West Sussex, 95–121, 2006.
94. Kanthou, C. and Tozer, G.M., Microtubule depolymerizing vascular disrupting agents: Novel therapeutic agents for oncology and other pathologies, *Int. J. Exp. Pathol.*, 90, 284, 2009.
95. Griggs, J., Skepper, J.N., Smith, G.A., Brindle, K.M., Metcalfe, J.C., and Hesketh, R., Inhibition of proliferative retinopathy by the anti-vascular agent combretastatin-A4, *Am. J. Pathol.*, 160, 1097, 2002.
96. Kanthou, C. and Tozer, G.M., Tumour targeting by microtubule-depolymerising vascular disrupting agents, *Expert Opin. Ther. Targets*, 11, 1443, 2007.
97. Tozer, G.M., Kanthou, C., Lewis, G., Prise, V.E., Vojnovic, B., and Hill, S.A., Tumour vascular disrupting agents: Combating treatment resistance, *Br. J. Radiol.*, 81, S12, 2008.
98. Tozer, G.M., Prise, V.E., Lewis, G., Xie, S., Wilson, I., and Hill, S.A., Nitric oxide synthase inhibition enhances the tumor vascular-damaging effects of combretastatin A-4 3-*O*-phosphate at clinically relevant doses, *Clin. Cancer Res.*, 15, 3781, 2009.
99. Tozer, G.M., Akerman, S., Cross, N.A., Barber, P.R., Bjorndahl, M.A., Greco, O., Harris, S. et al., Blood vessel maturation and response to vascular-disrupting therapy in single vascular endothelial growth factor-A isoform-producing tumors, *Cancer Res.*, 68, 2301, 2008.

100. Hadimani, M., Kessler, R.J., Kautz, J.A., Ghatak, A., Shirali, A.R., O'Dell, H., Garner, C.M., and Pinney, K.G., 2-(3-tert-Butyldimethylsiloxy-4-methoxyphenyl)-6-methoxy-3-(3,4,5-trimethoxybenzoyl)indole, *Acta Crysallogr. C*, C58, 330, 2002.
101. Siemann, D.W., Vascular targeting agents: An introduction, *Int. J. Radiat. Oncol. Biol. Phys.*, 54, 1472, 2002.
102. Chaplin, D.J. and Hill, S.A., The development of combretastatin A4 phosphate as a vascular targeting agent, *Int. J. Radiat. Oncol. Biol. Phys.*, 54, 1491, 2002.
103. Thorpe, P.E., Chaplin, D.J., and Blakeley, D.C., The first international conference on vascular targeting: Meeting overview, *Cancer Res.*, 63, 1144, 2003.
104. Vincent, L., Kermani, P., Young, L.M., Cheng, J., Zhang, F., Shido, K., Lam, G. et al., Combretastatin A4 phosphate induces rapid regression of tumor neovessels and growth through interference with vascular endothelial-cadherin signaling, *J. Clin. Invest.*, 115, 2992, 2005.
105. Chaplin, D.J. and Dougherty, G.J., Tumour vasculature as a target for cancer therapy, *Br. J. Cancer*, 80, 57, 1999.
106. Kanthou, C. and Tozer, G.M., The tumor vascular targeting agent combretastatin A-4-phosphate induces reorganization of the actin cytoskeleton and early membrane blebbing in human endothelial cells, *Blood*, 99, 2060, 2002.
107. Tozer, G.M., Prise, V.E., Wilson, J., Cemazar, M., Shan, S., Dewhirst, M.W., Barber, P.R., Vojnovic, B., and Chaplin, D.J., Mechanisms associated with tumor vascular shut-down induced by combretastatin A-4 phosphate: Intravital microscopy and measurement of vascular permeability, *Cancer Res.*, 61, 6413, 2001.
108. Galbraith, S.M., Chaplin, D.J., Lee, F., Stratford, M.R., Locke, R.J., Vojnovic, B., and Tozer, G.M., Effects of combretastatin A4 phosphate on endothelial cell morphology *in vitro* and relationship to tumor vascular targeting activity *in vivo*, *Anticancer Res.*, 21, 93, 2001.
109. Young, S. and Chaplin, D.J., Combretastin A4 phosphate: Background and current clinical status, *Expert Opin. Investig. Drugs*, 13, 1171, 2004.
110. Pettit, G.R., Singh, S.B., Hamel, E., Lin, C.M., Alberts, D.S., and Garcia-Kendal, D., Isolation and structure of the strong cell growth and tubulin inhibitor combretastatin A-4, *Cell. Mol. Life Sci.*, 45, 209, 1989.
111. Pettit, G.R. and Rhodes, M.R., Antineoplastic agents 389. New syntheses of the combretastatin A-4 prodrug, *Anticancer Drug Des.*, 13, 183, 1998.
112. Gill, G.S., Grobelny, D., and Flynn, B., A practical method for phosphorylation of combretastatin A-4 with phosphorus oxychloride, *Org. Prep. Proc. Int.*, 38, 604, 2006.
113. Li, P., Zeng, Y., Deng, J., Li, H., Zhou, W., and Chen, C., Method for preparing disodium combretastatin A-4 phosphate, Chinese Pat. Appl. CN 2008-10057106, 2008.
114. Yong, Z.Q., Xu, X.P., Chen, Y.C., Bao, X., Weng, L.L., and Zheng, H., Synthesis and cytotoxic activity of novel water-soluble prodrugs of combretastatin A-4, *Chin. Chem. Lett.*, 17, 23, 2006.
115. Aprile, S., Del Grosso, E., and Grosa, G., *In vitro* and *in vivo* phase II metabolism of combretastatin A-4: Evidence for the formation of a sulphate conjugate metabolite, *Xenobiotica*, 39, 148, 2009.
116. Pettit, G.R., Singh, S.B., and Cragg, G.M., Synthesis of natural (-)-combretastatin, *J. Org. Chem.*, 50, 3404, 1985.
117. Gaukroger, K., Hadfield, J.A., Hepworth, L.A., Lawrence, N.J., and McGown, A.T., Novel syntheses of cis and trans isomers of combretastatin A-4, *J. Org. Chem.*, 66, 8135, 2001.
118. Bui, V.P., Hudlicky, T., Hansen, T.V., and Stenstrom, Y., Direct biooxidation of arenes to corresponding catechols with *E. coli* JM109 (PDTG602). Application to synthesis of combretastatins A-1 and B-1, *Tetrahedron Lett.*, 43, 2839, 2002.
119. Lawrence, N.J., Ghani, F.A., Hepworth, L.A., Hadfield, J.A., McGown, A.T., and Pritchard, R.G., The synthesis of (E) and (Z)-combretastatins A-4 and a phenanthrene from *Combretum caffrum*, *Synthesis*, 9, 1656, 1999.
120. Bazin, M.-A., Jouanne, M., El-Khashef, H., and Rault, S., An efficient microwave-promoted route to (*Z*)-stilbenes from *trans*-cinnamic acids: Synthesis of combretastatin A-4 and analogues, *Synlett*, 17, 2789, 2009.
121. Lupattelli, P., D'Auria, M., Di Blasio, N., and Lenti, F., A novel approach to combretastatins: From *trans*-epoxide to CA-4 and its dioxolane derivative, *Eur. J. Org. Chem.*, 1, 141, 2009.
122. Camacho-Davila, A.A., Kumada–Corriu cross coupling route to the anti-cancer agent combretastatin A-4, *Synth. Commun.*, 38, 3823, 2008.
123. Giraud, A., Provot, O., Hamze, A., Brion, J.-D., and Alami, M., One-pot hydrosilylation-protodesilylation of functionalized diarylalkynes: A highly selective access to *Z*-stilbenes. Application to the synthesis of combretastatin A-4, *Tetrahedron Lett.*, 49, 1107, 2008.

124. Lara-Ochoa, F. and Espinosa-Perez, G., A new synthesis of combretastatins A-4 and AVE-8062A, *Tetrahedron Lett.*, 48, 7007, 2007.
125. Arthuis, M., Pontikis, R., and Florent, J.-C., Tandem Heck–Suzuki–Miyaura reaction: Application to the synthesis of constrained analogues of combretastatin A-4, *Tetrahedron Lett.*, 48, 6397, 2007.
126. Robinson, J.E. and Taylor, R.J.K., A Ramberg–Backlund route to the stilbenoid anti-cancer agents combretastatin A-4 and DMU-212, *Chem. Commun.*, 16, 1617, 2007.
127. McNulty, J. and Das, P., Highly stereoselective and general synthesis of (*E*)-stilbenes and alkenes by means of an aqueous Wittig reaction, *Eur. J. Org. Chem.*, 1, 4031, 2009.
128. Shen, W., Diao, Y., Jin, H., Wang, J., and Wang, J., Polymer-supported preparation of combretastatin A4 using poly(4-(chlorodiphenylmethyl)styrene) as solid carrier, Chinese Pat. Appl. CN 2004-10042580, 2004.
129. Pettit, G.R., Minardi, M.D., Hogan, F., and Price, P.M., An efficient synthetic strategy for obtaining 4-methoxy carbon isotope labeled combretastatin A-4 phosphate and other *Z*-combretastatins, *J. Nat. Prod.*, 73, 399, 2010.
130. Odlo, K., Klaveness, J., Rongved, P., and Hansen, T.V., Synthesis of combretastatins A-1 and B-1, *Tetrahedron Lett.*, 47, 1101, 2006.
131. Shirali, A., Sriram, M., Hall, J.J., Nguyen, B.L., Guddneppanavar, R., Hadimani, M.B., Ackley, J.F. et al., Development of synthetic methodology suitable for the radiosynthesis of combretastatin A-1 (CA1) and its corresponding prodrug CA1P, *J. Nat. Prod.*, 72, 414, 2009.
132. Brown, R.T., Murrell, V.L., McMordie, A., Sriram, M., Pinney, K.G., Sharma, S., and Chaplin, D.J., Carbon-14 radiosynthesis of combretastatin A-1 (CA1) and its corresponding phosphate prodrug (CA1P), *J. Labelled Comp. Radiopharm.*, 52, 567, 2009.
133. Gui, Z., Method for preparing combretastatin A-1 phosphate tetrasodium salt, Chinese Pat. Appl. CN 2009-10029897, 2009.
134. Folkes, L.K., Christlieb, M., Madej, E., Stratford, M.R.L., and Wardman, P., Oxidative metabolism of combretastatin A-1 produces quinone intermediates with the potential to bind nucleophiles and to enhance oxidative stress via free radicals, *Chem. Res. Toxicol.*, 20, 1885, 2007.
135. Pettit, G.R., Thornhill, A.J., Moser, B.R., and Hogan, F., Antineoplastic agents. 552. Oxidation of combretastatin A-1: Trapping the *o*-quinone intermediate considered the metabolic product of the corresponding phosphate prodrug, *J. Nat. Prod.*, 71, 1561, 2008.
136. Boger, D.L., Sakya, S.M., and Yohannes, D., Total synthesis of combretastatin D-2: Intramolecular Ullmann macrocyclization reaction, *J. Org. Chem.*, 56, 4204, 1991.
137. Deshpande, V.H. and Gokhale, N.J., Synthesis of combretastatin D-2, *Tetrahedron Lett.*, 33, 4213, 1992.
138. Couladouros, E.A. and Soufli, I.C., Total synthesis of natural (-)-combretastatin D-1, *Tetrahedron Lett.*, 36, 9369, 1995.
139. Couladouros, E.A. and Soufli, I.C., Synthesis of combretastatin D-2. An efficient route to caffrane macrolactones, *Tetrahedron Lett.*, 35, 4409, 1994.
140. Rychnovsky, S.D. and Hwang, K., Synthesis of (±)-combretastatin D-1 and combretastatin D-2, *J. Org. Chem.*, 59, 5414, 1994.
141. Rychnovsky, S.D. and Hwang, K., Synthesis and revised configuration of (+)-combretastatin D-1, *Tetrahedron Lett.*, 35, 8927, 1994.
142. Couladouros, E.A., Soufli, I.C., Moutsos, V.I., and Chadha, R.K., Total synthesis of combretastatin D, *Chem. Eur. J.*, 4, 33, 1998.
143. Pettit, G.R., Quistorf, P.D., Fry, J.A., Herald, D.L., Hamel, E., and Chapuis, J.-C., Antineoplastic agents. 565. Synthesis of combretastatin D-2 phosphate and dihydro-combretastatin D-2, *J. Nat. Prod.*, 72, 876, 2009.
144. Chaplin, D.J., Garner, C.M., Kane, R.R., Pinney, K.G., Prezioso, J.A., and Klaus, E., Functionalized stilbene derivatives as improved vascular targeting agents, US Patent 20030149003 A1, 2003.
145. Ohsumi, K., Nakagawa, R., Fukuda, Y., Hatanaka, T., Morinaga, Y., Nihei, Y., Ohishi, K., Suga, Y., Akiyama, Y., and Tsuji, T., Novel combretastatin analogues effective against murine solid tumors: Design and structure–activity relationships, *J. Med. Chem.*, 41, 3022, 1998.
146. Ohsumi, K., Hatanaka, T., Nakagawa, R., Fukuda, Y., Morinaga, Y., Suga, Y., Nihei, Y., Ohishi, K., Akiyama, Y., and Tsuji, T., Synthesis and antitumor activities of amino acid prodrugs of amino-combretastatins, *Anticancer Drug Des.*, 14, 539, 1999.
147. Lawrence, N.J., Hepworth, L.A., Rennison, D., McGown, A.T., and Hadfield, J.A., Synthesis and anticancer activity of fluorinated analogues of combretastatin A-4, *J. Fluor. Chem.*, 123, 101, 2003.
148. Kong, Y., Grembecka, J., Edler, M.C., Hamel, E., Mooberry, S.L., Sabat, M., Rieger, J., and Brown, M.L., Structure-based discovery of a boronic acid bioisostere of combretastatin A-4, *Chem. Biol.*, 12, 1007, 2005.

149. Monk, K.A., Siles, R., Hadimani, M.B., Mugabe, B.E., Ackley, J.F., Studerus, S.W., Edvardsen, K. et al., Design, synthesis, and biological evaluation of combretastatin nitrogen-containing derivatives as inhibitors of tubulin assembly and vascular targeting agents, *Bioorg. Med. Chem.*, 14, 3231, 2006.
150. Chang, J.-Y., Yang, M.-F., Chang, C.-Y., Chen, C.-M., Kuo, C.-C., and Liou, J.-P., 2-Amino and 2′-aminocombretastatin derivatives as potent antimitotic agents, *J. Med. Chem.*, 49, 6412, 2006.
151. Siles, R., Ackley, J.F., Hadimani, M.B., Hall, J.J., Mugabe, B., Guddneppanavar, R., Monk, K.A. et al., Combretastatin dinitrogen-substituted stilbene analogs as tubulin-binding and vascular-disrupting agents, *J. Nat. Prod.*, 71, 313, 2008.
152. Hall, J.J., Sriram, M., Strecker, T.E., Tidmore, J.K., Jelinek, C.J., Kumar, G.D.K., Hadimani, M.B. et al., Design, synthesis, biochemical, and biological evaluation of nitrogen-containing trifluoro structural modifications of combretastatin A-4, *Bioorg. Med. Chem. Lett.*, 18, 5146, 2008.
153. Pettit, G.R., Anderson, C.R., Herald, D.L., Jung, M.K., Lee, D.J., Hamel, E., and Pettit, R.K., Antineoplastic agents. 487. Synthesis and biological evaluation of the antineoplastic agent 3,4-methylenedioxy-5,4-dimethoxy-3-amino-*Z*-stilbene and derived amino acid amides, *J. Med. Chem.*, 46, 525, 2003.
154. Pettit, G.R., Thornhill, A., Melody, N., and Knight, J.C., Antineoplastic agents. 578. Synthesis of stilstatins 1 and 2 and their water-soluble prodrugs, *J. Nat. Prod.*, 72, 380, 2009.
155. Dougherty, S.T., Walker, S.E., Davis, P.D., and Dougherty, G.J., The novel vascular disrupting agent ANG501 induces cell cycle arrest and enhances endothelial cell sensitivity to radiation, *Cancer Growth Metastasis*, 2, 1, 2009.
156. Gaukroger, K., Structural requirements for the interaction of combretastatins with tubulin: How important is the trimethoxy unit? *Org. Biomol. Chem.*, 1, 3033, 2003.
157. Simoni, D., Romagnoli, R., Baruchello, R., Rondanin, R., Grisolia, G., Eleopra, M., Rizzi, M. et al., Novel A-ring and B-ring modified combretastatin A-4 (CA-4) analogues endowed with interesting cytotoxic activity, *J. Med. Chem.*, 51, 6211, 2008.
158. Pettit, G.R., Minardi, M.D., Rosenberg, H.J., Hamel, E., Bibby, M.C., Martin, S.W., Jung, M.K., Pettit, R.K., Cuthbertson, T.J., and Chapuis, J.-C., Antineoplastic agents. 509. Synthesis of fluorcombstatin phosphate and related 3-halostilbenes, *J. Nat. Prod.*, 68, 1450, 2005.
159. Hatanaka, T., Fujita, K., Ohsumi, K., Nakagawa, R., Fukuda, Y., Nihei, Y., Suga, Y., Akiyama, Y., and Tsuji, T., Novel B ring modified combretastatin analogues: Syntheses and antineoplastic activity, *Bioorg. Med. Chem. Lett.*, 8, 3371, 1998.
160. Mateo, C., Perez-Melero, C., Pelaez, R., and Medarde, M., Stilbenophane analogues of deoxycombretastatin A-4, *J. Org. Chem.*, 70, 6544, 2005.
161. Pettit, G.R., Toki, B., Herald, D.L., Verdier-Pinard, P., Boyd, M.R., Hamel, E., and Pettit, R.K., Antineoplastic agents. 379. Synthesis of phenstatin phosphate, *J. Med. Chem.*, 41, 1688, 1998.
162. Pettit, G.R., Grealish, M.P., Herald, D.L., Boyd, M.R., Hamel, E., and Pettit, R.K., Antineoplastic agents. 443. Synthesis of the cancer cell growth inhibitor hydroxyphenstatin and its sodium diphosphate prodrug, *J. Med. Chem.*, 43, 2731, 2000.
163. Hadfield, J.A., Gaukroger, K., Hirst, N., Weston, A.P., Lawrence, N.J., and McGown, A.T., Synthesis and evaluation of double bond substituted combretastatins, *Eur. J. Med. Chem.*, 40, 529, 2005.
164. Furst, R., Zupko, I., Berenyi, A., Ecker, G.F., and Rinner, U., Synthesis and antitumor-evaluation of cyclopropyl-containing combretastatin analogs, *Bioorg. Med. Chem. Lett.*, 19, 6948, 2009.
165. Mousset, C., Giraud, A., Provot, O., Hamze, A., Bignon, J., Liu, J.-M., Thoret, S., Dubois, J., Brion, J.-D., and Alami, M., Synthesis and antitumor activity of benzils related to combretastatin A-4, *Bioorg. Med. Chem. Lett.*, 18, 3266, 2008.
166. Medarde, M., Ramos, A., Caballero, E., Pélaez-Lamamié de Clairac, R., López, J.L., Grávalos, D.G., and San Feliciano, A., Synthesis and antineoplastic activity of combretastatin analogues: Heterocombretastatins, *Eur. J. Med. Chem.*, 33, 71, 1998.
167. Andres, C.J., Bernardo, J.E., Yan, Q., Hastie, S.B., and Macdonald, T.L., "Combretatropones"—hybrids of combretastatin and colchicine. Synthesis and biochemical evaluation, *Bioorg. Med. Chem. Lett.*, 3, 565, 1993.
168. Janik, M.E. and Bane, S.L., Synthesis and antimicrotubule activity of combretatropone derivatives, *Bioorg. Med. Chem.*, 10, 1895, 2002.
169. Shirai, R., Tokuda, K., Koiso, Y., and Iwasaki, S., Synthesis and anti-tubulin activity of *aza*-combretastatins, *Bioorg. Med. Chem. Lett.*, 4, 699, 1994.
170. Pettit, G.R., Anderson, C.R., Herald, D.L., Jung, M.K., Lee, D.J., Hamel, E., and Pettit, R.K., Antineoplastic agents. 410. Asymmetric hydroxylation of trans-combretastatin A-4, *J. Med. Chem.*, 42, 1459, 1999.

171. Pettit, G.R., Lippert, J.W. III, Herald, D.L., Hamel, E., and Pettit, R.K., Antineoplastic agents 440. Asymmetric synthesis and evaluation of the combretastatin A-1 SAR probes (1S, 2S)- and (1R, 2R)-1,2-dihydroxy-1-(2,3-dihydroxy-4-methoxyphenyl)-2-(3,4,5-trimethoxyphenyl)-ethane, *J. Nat. Prod.*, 63, 969, 2000.
172. Simoni, D., Grisolia, G., Giannini, G., Roberti, M., Randanin, R., Piccagli, L., Baruchello, R. et al., Heterocyclic and phenyl double-bond-locked combretastatin analogues possessing potent apoptosis-inducing activity in HL60 and in MDR cell lines, *J. Med. Chem.*, 48, 723, 2005.
173. Shirai, R., Takayama, H., Nishikawa, A., Koiso, Y., and Hashimoto, Y., Asymmetric synthesis of antimitotic combretadioxolane with potent antitumor activity against multi-drug resistant cells, *Bioorg. Med. Chem. Lett.*, 8, 1997, 1998.
174. Pettit, G.R., Lippert, J., Boyd, M., Verdier-Pinard, P., and Hamel, E., Antineoplastic agents 442. Synthesis and biological activities of dioxostatin, *Anticancer Drug Des.*, 15, 361, 2000.
175. Shirai, R., Okabe, T., and Iwasaki, S., Synthesis of conformationally restricted combretastatins, *Heterocycles*, 46, 145, 1997.
176. Ducki, S., Forrest, R., Hadfield, J.A., Kendall, A., Lawrence, N.J., McGown, A.T., and Rennison, D., Potent antimitotic and cell growth inhibitory properties of substituted chalcones, *Bioorg. Med. Chem. Lett.*, 8, 1051, 1998.
177. Wu, M., Sun, Q., Yang, C., Chen, D., Ding, J., Chen, Y., Lin, L., and Xie, Y., Synthesis and activity of combretastatin A-4 analogues: 1,2,3-thiadiazoles as potent antitumor agents, *Bioorg. Med. Chem. Lett.*, 17, 869, 2007.
178. Cafici, L., Pirali, T., Condorelli, F., Del Grosso, E., Massarotti, A., Sorba, G., Canonico, P.L., Tron, G.C., and Genazzani, A.A., Solution-phase parallel synthesis and biological evaluation of combretatriazoles, *J. Comb. Chem.*, 10, 732, 2008.
179. Odlo, K., Hentzen, J., Fournier dit Chabert, J., Ducki, S., Gani, O.A.B.S.M., Sylte, I., Skrede, M., Florenes, V.A., and Hansen, T.V., 1,5-Disubstituted 1,2,3-triazoles as *cis*-restricted analogues of combretastatin A-4: Synthesis, molecular modeling and evaluation of cytotoxic agents and inhibitors of tubulin, *Bioorg. Med. Chem.*, 16, 4829, 2008.
180. Tron, G.C., Pagliai, F., Del Grosso, E., Genazzani, A.A., and Sorba, G., Synthesis and cytotoxic evaluation of combretafurazans, *J. Med. Chem.*, 48, 3260, 2005.
181. Biersack, B., Effenberger, K., Schobert, R., and Ocker, M., Oxazole-bridged combretastatin A analogues with improved anticancer properties, *ChemMedChem*, 5, 420, 2010.
182. Tanpure, R.P., Harkrider, A.R., Strecker, T.E., Hamel, E., Trawick, M.L., and Pinney, K.G., Application of the McMurry coupling reaction in the synthesis of tri- and tetra-arylethylene analogues as potential cancer chemotherapeutic agents, *Bioorg. Med. Chem.*, 17, 6993, 2009.
183. Lee, L., Davis, R., Vanderham, J., Hills, P., Mackay, H., Brown, T., Mooberry, S.L., and Lee, M., 1,2,3,4-Tetrahydro-2-thioxopyrimidine analogs of combretastatin-A4, *Eur. J. Med. Chem.*, 43, 2011, 2008.
184. Provot, O., Giraud, A., Peyrat, J.-F., Alami, M., and Brion, J.-D., Synthetic approach to enyne and enediyne analogues of anticancer agents, *Tetrahedron Lett.*, 46, 8547, 2005.
185. Lawrence, N.J., Rennison, D., Woo, M., McGown, A.T., and Hadfield, J.A., Antimitotic and cell growth inhibitory properties of combretastatin A-4-like ethers, *Bioorg. Med. Chem. Lett.*, 11, 51, 2001.
186. Barbosa, E.G., Bega, L.A.S., Beatriz, A., Sarkar, T., Hamel, E., do Amaral, M.S., and de Lima, D.P., A diaryl sulfide, sulfoxide, and sulfone bearing structural similarities to combretastatin A-4, *Eur. J. Med. Chem.*, 44, 2685, 2009.
187. Pinney, K.G., Wang, F., and Del Pilar Mejia, M., Preparation of indole-containing and combretastatin-related anti-mitotic and anti-tubulin polymerization agents, PCT WO 2001019794 A2, 2001.
188. Flynn, B.L., Hamel, E., and Jung, M.K., One-pot synthesis of benzo[b]furan and indole inhibitors of tubulin polymerization, *J. Med. Chem.*, 45, 2670, 2002.
189. Gastpar, R., Goldbrunner, M., Marko, D., and von Angerer, E., Methoxy-substituted 3-formyl-2-phenylindoles inhibit tubulin polymerization, *J. Med. Chem.*, 41, 4965, 1998.
190. Ty, N., Dupreye, G., Chabot, G.G., Seguin, J., Tillequin, F., Scherman, D., Michel, S., and Cachet, X., Synthesis and biological evaluation of new disubstituted analogues of 6-methoxy-3-(3′,4′,5′-trimethoxybenzoyl)-1*H*-indole (BPR0L075), as potential antivascular agents, *Bioorg. Med. Chem.*, 16, 7494, 2008.
191. Romagnoli, R., Baraldi, P.G., Sarkar, T., Carrion, M.D., Cara, C.L., Cruz-Lopez, O., Preti, D. et al., Synthesis and biological evaluation of 1-methyl-2-(3′,4′,5′-trimethoxybenzoyl)-3-aminoindoles as a new class of antimitotic agents and tubulin inhibitors, *J. Med. Chem.*, 51, 1464, 2008.
192. Liou, J.P., Chang, Y.L., Kuo, F.M., Chang, C.W., Tseng, H.Y., Wang, C.C., Yang, Y.N., Chang, J.Y., Lee, S.J., and Hsieh, H.P., Concise synthesis and structure—Activity relationships of combretastatin A-4 analogues, 1-aroylindoles and 3-aroylindoles, as novel classes of potent antitubulin agents, *J. Med. Chem.*, 47, 4247, 2004.

193. Dupeyre, G., Chabot, G.G., Thoret, S., Cachet, X., Seguin, J., Guenard, D., Tillequin, F., Scherman, D., Koch, M., and Michel, S., Synthesis and biological evaluation of (3,4,5-trimethoxyphenyl)indol-3-yl-methane derivatives as potential antivascular agents, *Bioorg. Med. Chem.*, 14, 4410, 2006.
194. Putey, A., Popwycz, F., Do, Q.-T., Bernard, P., Talapatra, S.K., Kozielski, F., Galmarini, C.M., and Joseph, B., Indolobenzazepin-7-ones and 6-, 8-, and 9-membered ring derivatives as tubulin polymerization inhibitors: Synthesis and structure–activity relationship studies, *J. Med. Chem.*, 52, 5916, 2009.
195. Chen, Z., Mocharla, V.P., Farmer, J.M., Pettit, G.R., Hamel, E., and Pinney, K.G., Preparation of new anti-tubulin ligands through a dual-mode, addition-elimination reaction to a bromo-substituted, unsaturated sulfoxide, *J. Org. Chem.*, 65, 8811, 2000.
196. Pinney, K.G., Mocharla, V.P., Chen, Z., Garner, C.M., Ghatak, A., Hadimani, M., Kessler, J., and Dorsey, J.M., Preparation of trimethoxyphenyl-containing tubulin binding ligands and corresponding prodrug constructs as inhibitors of tubulin polymerization and antimitotic agents, PCT WO2001068654, 2001.
197. Pinney, K.G., Pettit, G.R., Mocharla, V.P., Mejia, M.P., and Shirali, A., Anti-mitotic agents which inhibit tubulin polymerization, US Patent 6162930, 2000.
198. Pinney, K.G., Pettit, G.R., Mocharla, V.P., Mejia, M.P., and Shirali, A., Anti-mitotic agents which inhibit tubulin polymerization, Australian Patent 732917, 2001.
199. Flynn, B.L., Flynn, G.P., Hamel, E., and Jung, M.K., The synthesis and tubulin binding activity of thiophene-based analogues of combretastatin A-4, *Bioorg. Med. Chem. Lett.*, 11, 2341, 2001.
200. Flynn, B.L., Verdier-Pinard, P., and Hamel, E., A novel palladium-mediated coupling approach to 2,3-disubstituted benzo[b]thiophenes and its application to the synthesis of tubulin binding agents, *Org. Lett.*, 3, 651, 2001.
201. Romagnoli, R., Baraldi, P.G., Carrion, M.D., Cara, C.L., Preti, D., Fruttarolo, F., Pavani, M.G., Tabrizi, M.A., Tolomeo, M., Grimaudo, S., Di Cristina, A., Balzarini, J., Hadfield, J.A., Brancale, A., and Hamel, E., Synthesis and biological evaluation of 2- and 3-aminobenzo[*b*]thiophene derivatives as antimitotic agents and inhibitors of tubulin polymerization, *J. Med. Chem.*, 50, 2273, 2007.
202. Pinney, K.G., Mocharla, V.P., Chen, Z., Garner, C.M., Hadimani, M., Kessler, R., Dorsey, J.M. et al., Preparation of aryl and arylcarbonylbenzothiophenes, -benzofurans, -indenes, and indoles as tubulin binding ligands and corresponding prodrug constructs thereof useful as antitumor agents, US Patent 2004044059, 2004.
203. Flynn, B.L. and Hamel, E., Synthesis of indoles, benzofurans, and related compounds as potential tubulin binding agents, PCT WO2002060872 A1, 2002.
204. Brancale, A. and Silvestri, R., Indole, a core nucleus for potent inhibitors of tubulin polymerization, *Med. Res. Rev.*, 27, 209, 2007.
205. La Regina, G., Sarkar, T., Bai, R., Edler, M.C., Saletti, R., Coluccia, A., Piscitelli, F. et al., New arylthioindoles and related bioisosteres at the sulfur bridging group. 4. Synthesis, tubulin polymerization, cell growth inhibition, and molecular modeling studies, *J. Med. Chem.*, 52, 7512, 2009.
206. Kerr, D.J., Hamel, E., Jung, M.K., and Flynn, B.L., The concise synthesis of chalcone, indanone and indenone analogues of combretastatin A4, *Bioorg. Med. Chem.*, 15, 3290, 2007.
207. De Martino, G., La Regina, G., Coluccia, A., Edler, M.C., Barbera, M.C., Brancale, A., Wilcox, E., Hamel, E., Artico, M., and Silvestri, R., Arylthioindoles, potent inhibitors of tubulin polymerization, *J. Med. Chem.*, 47, 6120, 2004.
208. La Regina, G., Edler, M.C., Brancale, A., Kandil, S., Coluccia, A., Piscitelli, F., Hamel, E. et al., Arylthioindole inhibitors of tubulin polymerization. 3. Biological evaluation, structure–activity relationships and molecular modeling studies, *J. Med. Chem.*, 50, 2865, 2007.
209. Simoni, D., Romagnoli, R., Baruchello, R., Rondanin, R., Rizzi, M., Pavani, M.G., Alloatti, D. et al., Novel combretastatin analogues endowed with antitumor activity, *J. Med. Chem.*, 49, 3143, 2006.
210. Pinney, K.G., Mocharla, V.P., Chen, Z., Garner, C.M., Ghatak, A., and Dorsey, J.M., Tubulin binding ligands and corresponding prodrug constructs, US Patent 6593374, 2003.
211. Ghatak, A., Dorsey, J.M., Garner, C.M., and Pinney, K.G., Synthesis of methoxy and hydroxy containing tetralones: Versatile intermediates for the preparation of biologically relevant molecules, *Tetrahedron Lett.*, 44, 4145, 2003.
212. Sriram, M., Hall, J.J., Grohmann, N.C., Strecker, T.E., Wootton, T., Franken, A., Trawick, M.L., and Pinney, K.G., Design, synthesis, and biological evaluation of dihydronaphthalene and benzosuberene analogs of the combretastatins as inhibitors of tubulin polymerization in cancer chemotherapy, *Bioorg. Med. Chem.*, 16, 8161, 2008.
213. Goldbrunner, M., Loidl, G., Polossek, T., Mannschreck, A., and von Angerer, E., Inhibition of tubulin polymerization by 5,6-dihydroindolo[2,1-α]isoquinoline derivatives, *J. Med. Chem.*, 40, 3524, 1997.

214. Li, Q., Wodds, K.W., Claiborne, A., Gwaltney, S.L. II, Barr, K.J., Liu, G., Gehrke, L. et al., Synthesis and biological evaluation of 2-indolyloxazolines as a new class of tubulin polymerization inhibitors. Discovery of A-289099 as an orally active antitumor agent, *Bioorg. Med. Chem. Lett.*, 12, 465, 2002.
215. Tahir, S.K., Nukkala, M.A., Zielinski Mozny, N.A., Credo, R.B., Warner, R.B., Li, Q., Woods, K.W. et al., Biological activity of A-289099: An orally active tubulin-binding indolyloxazoline derivative, *Mol. Cancer Ther.*, 2, 227, 2003.
216. Romagnoli, R., Baraldi, P.G., Pavani, M.G., Tabrizi, M.A., Preti, D., Fruttarolo, F., Piccagli, L. et al., Synthesis and biological evaluation of 2-amino-3-(3′,4′,5′-trimethoxybenzoyl)-5-aryl thiophenes as a new class of potent antitubulin agents, *J. Med. Chem.*, 49, 3906, 2006.
217. Wang, L., Woods, K.W., Li, Q., Barr, K.J., McCroskey, R.W., Hannick, S.M., Gherke, L. et al., Potent, orally active heterocycle-based combretastatin A-4 analogues: Synthesis, structure–activity relationship, pharmacokinetics, and *in vivo* antitumor activity evaluation, *J. Med. Chem*., 45, 1697, 2002.
218. Ganina, O.G., Daras, E., Bourgarel-Rey, V., Peyrot, V., Andresyuk, A.N., Finet, J.-P., Fedorov, A.Y., Beletskaya, I.P., and Combes, S., Synthesis and biological evaluation of polymethoxylated 4-heteroaryl-coumarins as tubulin assembly inhibitor, *Bioorg. Med. Chem.*, 16, 8806, 2008.
219. Joncour, A., Liu, J.M., Décor, A., Thoret, S., Wdzieczak-Bakala, J., Bignon, J., and Baudoin, O., Synthesis of anti-microtubule biaryls and preliminary evaluation as vascular-disrupting agents, *Chem. Med. Chem.*, 3, 1731, 2008.
220. Fang, L., Shen, L., Fang, Y., Hu, Y., He, Q., and Yang, B., MZ3 can induce G2/M-phase arrest and apoptosis in human leukemia cells, *J. Cancer Res. Clin. Oncol.*, 134, 1337, 2008.
221. Cheng, Y.F., Hu, Y.Z., and He, Q.J., Synthesis and antitumor activity of arylsubstituted imidazolin-2-one derivatives, *Yao Xue Xue Bao*, 40, 711, 2005.
222. Medina, J.C., Clark, D.L., Flygare, J.A., Rosen, T.J., and Shan, B., Pentafluorobenzenesulfonamides and analogs, US Patent 5880151, 1999.
223. Flygare, J.A., Medina, J.C., Shan, B., Clark, D.L., and Rosen, T.J., Pentafluorobenzenesulfonamides and analogs, US Patent 6121304, 2000.
224. Pettit, R.K., Pettit, G.R., Hamel, E., Hogan, F., Moser, B.R., Wolf, S., Pon, S., Chapuis, J.-C., and Schmidt, J.M., *E*-Combretastatin and *E*-resveratrol structural modifications: Antimicrobial and cancer growth inhibitory β-*E*-nitrostyrenes, *Bioorg. Med. Chem.*, 17, 6606, 2009.
225. Hori, K. and Saito, S., Microvascular mechanisms by which the combretastatin A-4 derivative AC7700 (AVE8062) induces tumour blood flow stasis, *Br. J. Cancer*, 89, 1334, 2003.
226. Delmonte, A., AVE8062: A new combretastatin derivative vascular disrupting agent, *Expert Opin. Investig. Drugs*, 18, 1541, 2009.
227. Shi, W. and Siemann, D.W., Preclinical studies of the novel vascular disrupting agent MN-029, *Anticancer Res.*, 25, 3899, 2005.
228. Nicholson, B., Lloyd, G.K., Miller, B.R., Palladino, M.A., Kiso, Y., Hayashi, Y., and Neuteboom, S.T.C., NPI-2358 is a tubulin-depolymerizing agent: In-vitro evidence for activity as a tumor vascular-disrupting agent, *Anticancer Drugs*, 17, 25, 2006.
229. Burns, C.J., Fantino, E., Phillips, I.D., Su, S., Harte, M.F., Bukczynska, P.E., Frazzetto, M. et al., CYT997: A novel orally active tubulin polymerization inhibitor with potent cytotoxic and vascular disrupting activity *in vitro* and *in vivo*, *Mol. Cancer Ther.*, 8, 3036, 2009.
230. Kremmidiotis, G., Beaumont, D.M., Matthews, C.A., Gasic, J., Hall, A., Phillips, R.J., Bibby, D.C., and Leske, A.F., BNC105 is a tubulin targeting agent that is not susceptible to efflux by Pgp transporter expression, and yields additive therapeutic benefit when combined with other anti-cancer agents, in *Proceedings of the 100th Annual Meeting of the American Association for Cancer Research*, Denver, CO, Apr 18–22, 2009, AACR, Philadelphia, Abstract 5564.
231. Luo, Y., Hradil, V.P., Frost, D.J., Rosenberg, S.H., Gordon, G.B., Morgan, S.J., Gagne, G.D., Cox, B.F., Tahir, S.K., and Fox, G.B., ABT-751, a novel tubulin-binding agent, decreases tumor perfusion and disrupts tumor vasculature, *Anticancer Drugs*, 20, 483, 2009.
232. Jones, J.T., Pleiman, C.M., McConville, P., Baranski, J., Roth, B., Baichwal, V., Scholl, J., Mather, G., and Yu, M.K., MPC-6827: A potent tubulin binding and vascular disrupting agent with high brain penetration and anti-tumor activity in a mouse orthotopic glioma model, in *Proceedings of the 100th Annual Meeting of the American Association for Cancer Research*, Denver, CO, Apr 18–22, 2009, AACR, Philadelphia, Abstract 5639.
233. Blakey, D.C., Ashton, S.E., Westwood, F.R., Walker, M., and Ryan, A.J., ZD6126: A novel small molecule vascular targeting agent, *Int. J. Radiat. Oncol. Biol. Phys.*, 54, 1497, 2002.
234. Siemann, D.W. and Rojiani, A.M., Antitumor efficacy of conventional anticancer drugs is enhanced by the vascular targeting agent ZD6126, *Int. J. Radiat. Oncol. Biol. Phys.*, 54, 1512, 2002.

235. Siemann, D.W. and Rojiani, A.M., Enhancement of radiation therapy by the novel vascular targeting agent ZD6126, *Int. J. Radiat. Oncol. Biol. Phys.*, 53, 164, 2002.
236. Micheletti, G., Poli, M., Borsotti, P., Martinelli, M., Imberti, B., Taraboletti, G., and Giavazzi, R., Vascular-targeting activity of ZD6126, a novel tubulin-binding agent, *Cancer Res.*, 63, 1534, 2003.
237. Chaplin, D.J., Pettit, G.R., Parkins, C.S., and Hill, S.A., Antivascular approaches to solid tumour therapy: Evaluation of tubulin binding agents, *Br. J. Cancer*, 74, S86, 1996.
238. Dark, G.G., Hill, S.A., Prise, V.E., Tozer, G.M., Pettit, G.R., and Chaplin, D.J., Combretastatin A-4, an agent that displays potent and selective toxicity toward tumor vasculature, *Cancer Res.*, 57, 1829, 1997.
239. West, C.M.L. and Price, P., Combretastatin A4 phosphate, *Anticancer Drugs*, 15, 179, 2004.
240. Kanthou, C. and Tozer, G.M., Selective destruction of the tumour vasculature by targeting the endothelial cytoskeleton, *Drug Discov. Today: Ther. Strateg.*, 4, 237, 2007.
241. Siemann, D.W., Chaplin, D.J., and Walicke, P.A., A review and update of the current status of the vasculature-disabling agent combretastatin-A4 phosphate (CA4P), *Expert Opin. Investig. Drugs*, 18, 189, 2009.
242. McGown, A.T. and Fox, B.W., Structural and biochemical comparison of the anti-mitotic agents colchicine, combretastatin A4 and amphethinile, *Anticancer Drug Des.*, 3, 249, 1989.
243. Hamel, E. and Lin, C.M., Interactions of combretastatin, a new plant-derived antimitotic agent, with tubulin, *Biochem. Pharm.*, 32, 3864, 1983.
244. Horsman, M.R., Ehrnrooth, E., Ladekarl, M., and Overgaard, J., The effect of combretastatin A-4 disodium phosphate in a C3H mouse mammary carcinoma and a variety of murine spontaneous tumors, *Int. J. Radiat. Oncol. Biol. Phys.*, 42, 895, 1998.
245. Li, L., Rojiani, A., and Siemann, D.W., Targeting the tumor vasculature with combretastatin A-4 disodium phosphate: Effects on radiation therapy, *Int. J. Radiat. Oncol. Biol. Phys.*, 42, 899, 1998.
246. Mason, R.P., Zhao, D., Liu, L., Trawick, M.L., and Pinney, K.G., A perspective on vascular disrupting agents that interact with tubulin: Preclinical tumor imaging and biological assessment, *Integr. Biol.*, 3, 375, 2011.
247. Grosios, K., Holwell, S.E., McGown, A.T., Pettit, G.R., and Bibby, M.C., *In vivo* and *in vitro* evaluation of combretastatin A-4 and its sodium phosphate prodrug, *Br. J. Cancer*, 81, 1318, 1999.
248. Beauregard, D.A., Thelwall, P.E., Chaplin, D.J., Hill, S.A., Adams, G.E., and Brindle, K.M., Magnetic resonance imaging and spectroscopy of combretastatin A4 prodrug-induced disruption of tumour perfusion and energetic status, *Br. J. Cancer*, 77, 1761, 1998.
249. Eikesdal, H.P., Schem, B.-C., Mella, O., and Dahl, O., The new tubulin-inhibitor combretastatin A-4 enhances thermal damage in the BT4An rat glioma, *Int. J. Radiat. Oncol. Biol. Phys.*, 46, 645, 2000.
250. Maxwell, R.J., Pharm, B., Nielsen, F.U., Breidahl, T., Stodkilde-Jorgensen, H., and Horsman, M.R., Effects of combretastatin on murine tumours monitored by ^{31}P MRS, ^{1}H MRS and ^{1}H MRI, *Int. J. Radiat. Oncol. Biol. Phys.*, 42, 891, 1998.
251. Ahmed, B., van Eijk, L.I., Bouma-ter Steege, J.C.A., van der Schaft, D.W.J., van Esch, A.M., Joosten-Achjanie, S.R., Lambin, P., Landuyt, W., and Griffioen, A.W., Vascular targeting effect of combretastatin A-4 phosphate dominates the inherent angiogenesis inhibitory activity, *Int. J. Cancer*, 105, 20, 2003.
252. Galbraith, S.M., Maxwell, R.J., Lodge, M.A., Tozer, G.M., Wilson, J., Taylor, N.J., Stirling, J.J., Sena, L., Padhani, A.R., and Rustin, G.J.S., Combretastatin A4 phosphate has tumor antivascular activity in rat and man as demonstrated by dynamic magnetic resonance imaging, *J. Clin. Oncol.*, 21, 2831, 2003.
253. Zhao, D., Richer, E., Antich, P.P., and Mason R.P., Antivascular effects of combretastatin A4 phosphate in breast cancer xenograft assessed using dynamic bioluminescence imaging (BLI) and confirmed by magnetic resonance imaging (MRI), *FASEB J.*, 22, 2445, 2008.
254. Rustin, G.J., Galbraith, S.M., Anderson, H., Stratford, M., Folkes, L.K., Sena, L., Gumbrell, L., and Price, P.M., Phase I clinical trial of weekly combretastatin A4 phosphate: Clinical and pharmacokinetic results, *J. Clin. Oncol.*, 21, 2815, 2003.
255. Chaplin, D.J. and Horsman, M.R., The influence of tumour temperature on ischemia-induced cell death: Potential implications for the evaluation of vascular mediated therapies, *Radiother. Oncol.*, 30, 59, 1994.
256. Siemann, D.W., Mercer, E., Lepler, S., and Rojiani, A.M., Vascular targeting agents enhance chemotherapeutic agent activities in solid tumor therapy, *Int. J. Cancer*, 99, 1, 2002.
257. Shaked, Y., Tang, T., Woloszynek, J., Daenen, L.G., Man, S., Xu, P., Cai, S.-R. et al., Contribution of granulocyte colony-stimulating factor to the acute mobilization of endothelial precursor cells by vascular disrupting agents, *Cancer Res.*, 69, 7524, 2009.
258. Chaplin, D.J., Horsman, M.R., Trotter, M.J., and Siemann, D.W., Therapeutic significance of microenvironmental factors, in *Medical Radiology, Diagnostic Imaging and Radiation Oncology. Blood Perfusion and Microenvironment of Human Tumors*, Molls, M. and Vaupel, P., Eds., Springer, Berlin, 133, 1998.

259. Petit, I., Karajannis, M.A., Vincent, L., Young, L., Butler, J., Hooper, A.T., Shido, K. et al., The microtubule-targeting agent CA4P regresses leukemic xenografts by disrupting interaction with vascular cells and mitochrondrial-dependent cell death, *Blood*, 111, 1951, 2008.
260. Horsman, M.R., Murata, R., Breidahl, T., Nielsen, F.U., Maxwell, R.J., Stodkiled-Jorgensen, H., and Overgaard, J., Combretastatins: Novel vascular targeting drugs for improving anti-cancer therapy. Combretastatins and conventional therapy, *Adv. Exp. Med. Biol.*, 476, 311, 2000.
261. Landuyt, W., Ahmed, B., Nuyts, S., Theys, J., de Beeck, M.O., Rijnders, A., Anné, J., van Oosterom, A., Van den Bogaert, W., and Lambin, P., *In vivo* antitumor effect of vascular targeting combined with either ionizing radiation or anti-angiogenesis treatment, *Int. J. Radiat. Oncol. Biol. Phys.*, 49, 443, 2001.
262. Horsman, M.R. and Murata, R., Combination of vascular targeting agents with thermal or radiation therapy, *Int. J. Radiat. Oncol. Biol. Phys.*, 54, 1518, 2002.
263. Pedley, R.B., Hill, S.A., Boxer, G.M., Flynn, A.A., Boden, R., Watson, R., Dearling, J., Chaplin, D.J., and Begent, R.H.J., Eradication of colorectal xenografts by combined radioimmunotherapy and combretastatin A-4 3-O-phosphate, *Cancer Res.*, 61, 4716, 2001.
264. Grosios, K., Loadman, P.M., Swaine, D.J., Pettit, G.R., and Bibby, M.C., Combination chemotherapy with combretastatin A-4 phosphate and 5-fluorouracil in an experimental murine colon adenocarcinoma, *Anticancer Res.*, 20, 229, 2000.
265. Nelkin, B.D. and Ball, D.W., Combretastatin A-4 and doxorubicin combination treatment is effective in a preclinical model of human medullary thyroid carcinoma, *Oncol. Rep.*, 8, 157, 2001.
266. Wildiers, H., Ahmed, B., Guetens, G., De Boeck, G., de Bruijn, E.A., Landuyt, W., and van Oosterom, A.T., Combretastatin A-4 phosphate enhances CPT-11 activity independently of the administration sequence, *Eur. J. Cancer*, 40, 284, 2004.
267. Murata, R., Siemann, D.W., Overgaard, J., and Horsmann, M.R., Interaction between combretastatin A-4 disodium phosphate and radiation in murine tumors, *Radiother. Oncol.*, 60, 155, 2001.
268. Murata, R., Overgaard, J., and Horsman, M.R., Combretastatin A-4 disodium phosphate: A vascular targeting agent that improves the anti-tumor effects of hyperthermia, radiation, and mild thermoradiotherapy, *Int. J. Radiat. Oncol. Biol. Phys.*, 51, 1018, 2001.
269. Horsman, M.R., Christensen, K.L., and Overgaard, J., Hydralazine-induced enhancement of hyperthermic damage in a C3H mammary carcinoma *in vivo*, *Int. J. Hyperthermia*, 5, 123, 1989.
270. Eikesdal, H.P., Bjerkvig, R., Mella, O., and Dahl, O., Combretastatin A-4 and hyperthermia: A potent combination for the treatment of solid tumors, *Radiother. Oncol.*, 60, 147, 2001.
271. Siemann, D.W. and Shi, W., Dual targeting of tumor vasculature: Combining antiangiogenic (Avastin) and vascular disrupting (CA4P or OXi4503) agent therapy, *Anticancer Res.*, 28, 2027, 2008.
272. Holwell, S.E., Cooper, P.A., Thompson, M.J., Pettit, G.R., Lippert, L.W., 3rd, Martin, S.W., and Bibby, M.C., Anti-tumor and anti-vascular effects of the novel tubulin-binding agent combretastatin A-1 phosphate, *Anticancer Res.*, 22, 3933, 2002.
273. Hill, S.A., Tozer, G.M., Pettit, G.R., and Chaplin, D.J., Preclinical evaluation of the antitumour activity of the novel vascular targeting agent OXi 4503, *Anticancer Res.*, 22, 1453, 2002.
274. Shnyder, S.D., Cooper, P.A., Pettit, G.R., Lippert, J.W., 3rd, and Bibby, M.C., Combretastatin A-1 phosphate potentiates the antitumour activity of cisplatin in a murine adenocarcinoma model, *Anticancer Res.*, 23, 1619, 2003.
275. Hua, J., Sheng, Y., Pinney, K.G., Garner, C.M., Kane, R.R., Prezioso, J.A., Pettit, G.R., Chaplin, D.J., and Edvardsen, K., Oxi4503, a novel vascular targeting agent: Effects on blood flow and antitumor activity in comparison to combretastatin A-4 phosphate, *Anticancer Res.*, 23, 1433, 2003.
276. Kirwan, I.G., Loadman, P.M., Swaine, D.J., Anthoney, D.A., Pettit, G.R., Lippert, J.W. III, Shnyder, S.D., Cooper, P.A., and Bibby, M.C., Comparative preclinical pharmacokinetic and metabolic studies of the combretastatin prodrugs combretastatin A4 phosphate and A1 phosphate, *Clin. Cancer Res.*, 10, 1446, 2004.
277. Madlambayan, G.J., Meacham, A., Hosaka, K., Mir, S., Jorgensen, M., Scott, E.W., Siemann, D.W., and Cogle, C.R., AML regression by vascular disruption with OXi4503 and anti-angiogenesis with Bevacizumab, *Blood*, 114, A1031, 2009.
278. Dowlati, A., Robertson, K., Cooney, M., Petros, W.P., Stratford, M., Jesberger, J., Rafie, N. et al., A phase 1b pharmacokinetic and translational study of the novel vascular targeting agent combretastatin A-4 phosphate on a single-dose intravenous schedule in patients with advanced cancer, *Cancer Res.*, 62, 3408, 2002.
279. Stevenson, J.P., Rosen, M., Sun, W., Gallagher, M., Haller, D.G., Vaughn, D., Giantonio, B. et al., Phase I trial of the antivascular agent combretastatin A4 phosphate on a 5-day schedule to patients with cancer: Magnetic resonance imaging evidence for altered tumor blood flow, *J. Clin. Oncol.*, 21, 4428, 2003.

280. Rustin, G.J., Galbraith, S.M., Anderson, H., Stratford, M., Folkes, L.K., Sena, L., Gumbrell, L., and Price, P.M., Phase I clinical trial of weekly combretastatin A4 phosphate: Clinical and pharmacokinetic results, *J. Clin. Oncol.*, 21, 2815, 2003.
281. Galbraith, S.M., Maxwell, R.J., Lodge, M.A., Tozer, G.M., Wilson, J., Taylor, N.J., Stirling, J.J., Sena, L., Padhani, A.R., and Rustin, G.J., Combretastatin A4 phosphate has tumor antivascular activity in rat and man as demonstrated by dynamic magnetic resonance imaging, *J. Clin. Oncol.*, 21, 2831, 2003.
282. Anderson, H.L., Yap, J.T., Miller, M.P., Robbins, A., Jones, T., and Price, P.M., Assessment of pharmacodynamic vascular response in a phase I trial of combretastatin A4 phosphate, *J. Clin. Oncol.*, 21, 2823, 2003.
283. Eichler, W., Yafai, Y., Wiedemann, P., and Fengler, D., Antineovascular agents in the treatment of eye diseases, *Curr. Pharm. Des.*, 12, 2645, 2006.
284. Michels, S., Schmidt-Erfurth, U., and Rosenfeld, P.J., Promising new treatments for neovascular age-related macular degeneration, *Expert Opin. Investig. Drugs*, 15, 779, 2006.
285. Mazzone, M.G., Civiale, C., and Cuffari, F., Ophthalmic compositions for treating pathologies of the posterior segment of the eye, PCT Int. Appl. WO 2008-IT456 20080708, 2010.
286. Jockovich, M.-E., Suarez, F., Alegret, A., Piña, Y., Hayden, B., Cebulla, C., Feuer, W., and Murray, T.G., Mechanism of retinoblastoma tumor cell death after focal chemotherapy in a mouse model, *Invest. Ophthalmol. Vis. Sci.*, 48, 5371, 2007.
287. Jockovich, M.-E., Bajenaru, M.L., Piña, Y., Suarez, F., Feuer, W., Fini, M.E., and Murray, T.G., Retinoblastoma tumor vessel maturation impacts efficacy of vessel targeting in the $LH_{BETA}T_{AG}$ mouse model, *Invest. Ophthalmol. Vis. Sci.*, 48, 2476, 2007.
288. Escalona-Benz, E., Jockovich, M.-E., Murray, T.G., Hayden, B., Hernandez, E., Feuer, W., and Windle, J.J., Combretastatin A-4 prodrug in the treatment of a murine model of retinoblastoma, *Invest. Ophthalmol. Vis. Sci.*, 46, 8, 2005.
289. Kador, P.F., Blessing, K., Randazzo, J., Makita, J., and Wyman, M., Evaluation of the vascular targeting agent combretastatin A-4 prodrug on retinal neovascularization in the galactose-fed dog, *J. Ocul. Pharmacol. Ther.*, 23, 132, 2007.

4 Homoharringtonine and Related Compounds*

Hideji Itokawa, Yukio Hitotsuyanagi, and Kuo-Hsiung Lee

CONTENTS

4.1 Introduction 66
4.2 Structures of the Drug and Related Compounds 66
4.3 Synthesis of the Drug 66
4.3.1 Synthesis of Acyl Groups 66
4.3.1.1 Synthesis of the Ester Side-Chain from Chiral Citrates 66
4.3.1.2 Synthesis of Optically Active Monoacid Side-Chains through Chiral Epoxide 68
4.3.1.3 Enantioselective Synthesis of the Ester Side-Chain of HHT 68
4.3.1.4 Synthesis of the Acyl Side-Chain Using "Self-Reproduction of Chirality" Concept 71
4.3.2 Total Synthesis of *Cephalotaxus* Alkaloids 75
4.3.2.1 Dihydro[3]benzazepine Construction via Reductive Neber and Strain-Release Aziridine Rearrangements 76
4.3.2.2 Azomethine Ylide Generation and Cycloaddition via O-Acylation of Vinylogous Amides 77
4.3.2.3 Syntheses of Natural and Non-Natural Cephalotaxus Ester Alkaloids 78
4.3.2.4 Additional Recent Synthetic Studies on the *Cephalotaxus* Alkaloid Skeleton 80
4.4 Biosynthesis of *Cephalotaxus* Alkaloids 82
4.4.1 Biosynthesis of Side-Chain 82
4.4.2 Biosynthesis of Alkaloid Skeleton 83
4.5 Medicinal Chemistry of the Drug 83
4.5.1 Resistance of Vincristine-Sensitive Y79 Retinoblastoma to Cephalotaxus Esters 84
4.6 Development of the Clinical Drug of *Cephalotaxus* Alkaloids 86
4.6.1 Cytotoxity against Myeloma Cell Lines: Effects on Akt Pathway 86
4.6.2 Cytotoxity against Myeloma Cell Lines: Effects on Hypoxia-Inducible Factor-1α 86
4.6.3 Cytotoxity against Myeloma Cell Lines: Effects on MM-Promoting Molecules 86
4.6.4 Cytotoxity against Myeloma Cell Lines—Effects on JAK2-STAT5 Pathway 87
4.6.5 Cytotoxity against Myeloma Cell Lines—Combination Therapy Effects on Residual Leukemic Cells 87
4.6.6 Cytotoxity against Myeloma Cell Lines—Synergistic Effects on Multidrug-Resistant Leukemia Cells 87

* Antitumor Agents 276.

4.7 Clinical Applications 88
4.7.1 Review Articles on Omacetaxine Mepesuccinate (A Derivative of HHT) 88
4.7.2 Phase I Study for AML 88
4.7.3 Phase II Study for CML 89
4.7.4 HHT Action for Adjuvant Arthritis Rats 89
4.8 Conclusion 89
Acknowledgments 90
References 90

4.1 INTRODUCTION

Subsequent to our prior review,[1] we would like to reconsider homoharringtonine (HHT; **1**) and related compounds. As already mentioned in our first article, the genus *Cephalotaxus* contains coniferous evergreen trees and shrubs that are indigenous to Asia. Historically, the bark has long been used in China as a traditional medicine for a variety of indications. Through screening assays and preliminary clinical trials, Chinese investigators discovered that the total alkaloid fraction from *Cephalotaxus fortunei* Hook. F. possessed distinct antitumor activity.[2] HHT (**1**) (cephalotaxine-3,7-dihydroxy-7-methyloctanomethylate-3-carboxylate), one of the most active *Cephalotaxus* alkaloids, was obtained by alcoholic extraction from the Chinese evergreen tree *Cephalotaxus harringtonia* K. Koch var. *harringtonia*.[3] Other *Cephalotaxus* alkaloids have been isolated from various *Cephalotaxus* spp.,[4–6] including the parent compound cephalotaxine (**2**), which was first isolated by Paudler et al.[4] from two *Cephalotaxus* sp. The initial structural proposal was later revised, and Abraham et al.[7] proposed the correct structure and relative stereochemistry of **2** based on x-ray crystallographic analysis of cephalotaxine methiodide. The parent compound and its esters represent a group of alkaloids with a unique ring system.[7–13] Although **2** is devoid of antitumor activity, ester alkaloids derived from **2** are of particular anticancer interest. The most active compounds in this series are **1** and harringtonine (**5**),[9] isolated by Powell et al.[10] In addition to **1** and **5**, the active ester alkaloids isoharringtonine (**6**) and deoxyharringtonine (**8**) have also been isolated from *C. harringtonia*.[9]

HHT (**1**) was investigated in phase II clinical trials as an anticancer agent at the National Cancer Institute, Bethesda, MD. However, its side effects still remain a detrimental issue. Work has thus continued on the study of new components from this plant species and on the development of new analogs on the basis of the structure–activity relationships of these alkaloids. This chapter gives an overview of this work. HHT (**1**) and related cephalotaxine esters have been reviewed previously by Smith et al.[14] and Kantarjian et al.,[15] who selected **1** as the best compound to develop as an anticancer agent.

4.2 STRUCTURES OF THE DRUG AND RELATED COMPOUNDS

In our prior review in 2003,[1] we observed 34 naturally occurring *Cephalotaxus* alkaloids. Subsequently in 2006, 57 alkaloids were listed together with other homoerythrina-type alkaloids in the review by Mei et al.[16] The names and structures of naturally occurring *Cephalotaxus* alkaloids are provided in Table 4.1 and Figures 4.1 through 4.3.[1,16]

4.3 SYNTHESIS OF THE DRUG

4.3.1 Synthesis of Acyl Groups

4.3.1.1 Synthesis of the Ester Side-Chain from Chiral Citrates[35]

The aldehydes **57** and **60**, obtained by selective reduction of one carboxylic acid group in the parent chiral citric acid derivatives under Rosemund conditions, were used in the syntheses of the ester side-chains of *Cephalotaxus* alkaloids (Figures 4.4 through 4.6). As shown in Figure 4.4, after

TABLE 4.1
Naturally Occurring *Cephalotaxus* Alkaloids

No.	Compound	Plant Origin[a]	Reference
1	HHT	Cf, Cha, Cs, Co, Chh	18,21
2	Cephalotaxine	Cf, Cha, Cs, Co, Cw, Chh, Chd	19,21,30
3	Epicephalotaxine	Cf, Cha	17
4	Homodeoxyharringtonine	Chd, Chn	26,30
5	Harringtonine	Cf, Cha, Cs, Chh, Chn	18,30
6	Isoharringtonine	Cf, Cha, Cs, Chh, Chn	19,21,30
7	Bishomodeoxyharringtonine	Chd	26
8	Deoxyharringtonine	Cf, Cha, Chh, Chn	19,30
9	Nordeoxyharringtonine	Chd	26
10	5′-Des-*O*-methylharringtonine	Chd	24
11	5′-Des-*O*-methylharringtonine	Chd	24
12	Deoxyharringtonic acid	Cha	20
13	5′-Des-*O*-methylharringtonine	Chd	24
14	3′S-Hydroxy-5’-des-*O*-methylharringtonine	Chd	24
15	Isoharringtonic acid	Cha, Chd	20,24
16	Neoharringtonine	Cf, Chd	18,29
17	Homoneoharringtonine	Chd	29
18	3′S-Hydroxyneoharringtonine	Chd	29
19	(–)-Acetylcephalotaxine	Cf, Cw, Cfa	17,23
20	(+)-Acetylcephalotaxine	Cf, Cha	18,20
21	Cephalezomine C	Chn	30
22	Cephalezomine D	Chn	30
23	Cephalezomine E	Chn	30
24	Cephalezomine F	Chn	30
25	Anhydroharringtonine	Cf	18
26	Cephalotaxine-α-*N*-oxide	Cf	19
27	Cephalotaxine-β-*N*-oxide	Cf	19
28	11-β-Hydroxycephalotaxine-β-*N*-oxide	Cf	19
29	Isocephalotaxine	Cf	19
30	Desmethylcephalotaxinone	Cf	17
31	Stereoisomer of desmethylcephalotaxinone	Cf, Cha, Cs, Chh, Chn, Cw	19,22,30
32	Demethylcephalotaxine	Cf	17
33	Isocephalotaxinone	Cf	18
34	Cephalezomine J	Chn	31
35	Cephalotaxinone	Cf, Cha, Chh	19,20
36	Cephalotaxinamide	Cha	20
37	Cephalezomine G	Chn	31,34
38	Cephalezomine H	Chn	31
39	11-α-Hydroxyhomodeoxyharringtonine	Chd	27
40	11-β-Hydroxyhomodeoxyharringtonine	Chd	27
41	11-β-Hydroxydeoxyharringtonine	Chd	27
42	11-Hydroxycephalotaxine	Cf, Cs, Chd, Chn	19,21,30
43	4-Hydroxycephalotaxine	Cf	17
44	Drupangtonine	Chd	25
45	Cephalezomine A	Chn	30
46	Cephalezomine B	Chn	30
47	Drupacine	Cf, Cha, Cs, Cw, Chd, Chn	19,21,30

continued

TABLE 4.1 (continued)
Naturally Occurring *Cephalotaxus* Alkaloids

No.	Compound	Plant Origin[a]	References
48	Demethylneodrupacine	Cha	20
49	Cephalotaxidine	Chd, Chn	28,33
50	*Bis*-cephalezomine A	Chn	27
51	*Bis*-cephalezomine B	Chn	33
52	*Bis*-cephalezomine C	Chn	33
53	*Bis*-cephalezomine D	Chn	33
54	*Bis*-cephalezomine E	Chn	33
55	Cephalocyclidin A	Cf, Chn	19,32
56	Hainanensine	Cf, Cha	17

[a] Cf, *Cephalotaxus fortunei*; Cfa, *Cephalotaxus fortunei* var. *alpinia*; Cha, *Cephalotaxus hainanensis*; Chd, *Cephalotaxus harringtonia* var. *drupacea*; Chh, *Cephalotaxus harringtonia* var. *harringtonia*; Chn, *Cephalotaxus harringtonia* var. *nana;* Co, *Cephalotaxus oliveri*; Cs, *Cephalotaxus sinensis*; Cw, *Cephalotaxus wilsoniana.*

Grignard reaction with isopropenylmagnesium bromide, the allylic γ-lactone moiety in **58** set up a palladium-mediated hydrogenolysis of the unwanted carbon–oxygen bond. Subsequent acid-catalyzed cyclization onto the double bond (present as a ca. 20:1 mixture of regio-isomers, favoring the terminal position) afforded (*R*)-**59**, which is the side-chain of anhydroharringtonine (**25**).

In Figure 4.5, Robins' key intermediate (**62**) was prepared by a similar sequence. Thus addition of isopropenylmagnesium bromide at −40°C in Et_2O to **60** afforded a mixture of the desired δ-lactone **61** together with uncyclized material. Treating the crude product with camphorsulfonic acid led to cyclization to **61** in an overall yield of 47%. Hydrogenolysis was carried out by treating **61** with ammonium formate over 10% Pd/C to give a 1:1 mixture of regio-isomeric alkenes, which afforded **62** in 47% yield after brief exposure to refluxing formic acid. Compound (*R*)-**65**, the side-chain of deoxyhomoharringtonine (**4**) was obtained similarly from **57** (Figure 4.6).

4.3.1.2 Synthesis of Optically Active Monoacid Side-Chains through Chiral Epoxide[36]

The main intermediate in this approach is the chiral epoxide (**69**) prepared from the commercially available monomethyl itaconate (**66**) and (+)-(*S*)-methyl mandelate (**67**) via **68** (Figure 4.7). The key step of the strategy was the ring-opening of the epoxide **69** with different organocuprate nucleophiles. Hydrogenolysis as the final step gave the monoacid side-chains (e.g., **65**) of cephalotaxine esters in moderate to good overall yields from epoxide **69**.

4.3.1.3 Enantioselective Synthesis of the Ester Side-Chain of HHT[37]

In the retrosynthetic pathway to (*R*)-**70**, which is the diester side-chain of HHT (**1**), a key goal was to synthesize the cornerstone substituted cyclohexanone (*R*)-**71** (Figure 4.8).

Its synthesis was visualized through an asymmetric Michael addition of the known chiral imine (**72**) to a two-carbon electrophilic alkene (or its equivalent), which would serve as a precursor of the methyl acetate side-chain of **71**. The ultimate strategy employed a Michael condensation between imine **72** and the three-carbon acceptor 2-acetoxyacrylonitrile (**73**) to form adduct **74**. The three-carbon (α-acetoxypropionitrile) side-chain of **74** could subsequently be converted into the two-carbon (methyl acetate) moiety found in **71**.

Transformation of the protected cyanohydrin moiety into a carboxylic acid group is shown in Figure 4.9. Treating ketal **75** with LiOH followed by *in situ* oxidation (NaO_2Cl) of the intermediate aldehyde gave the acid **76**. Methyl ester **77** was obtained by esterification (CH_2N_2) of **76**, or more directly by treating **75** with MnO_2 in MeOH in the presence of NaCN. With the two-carbon side-chain

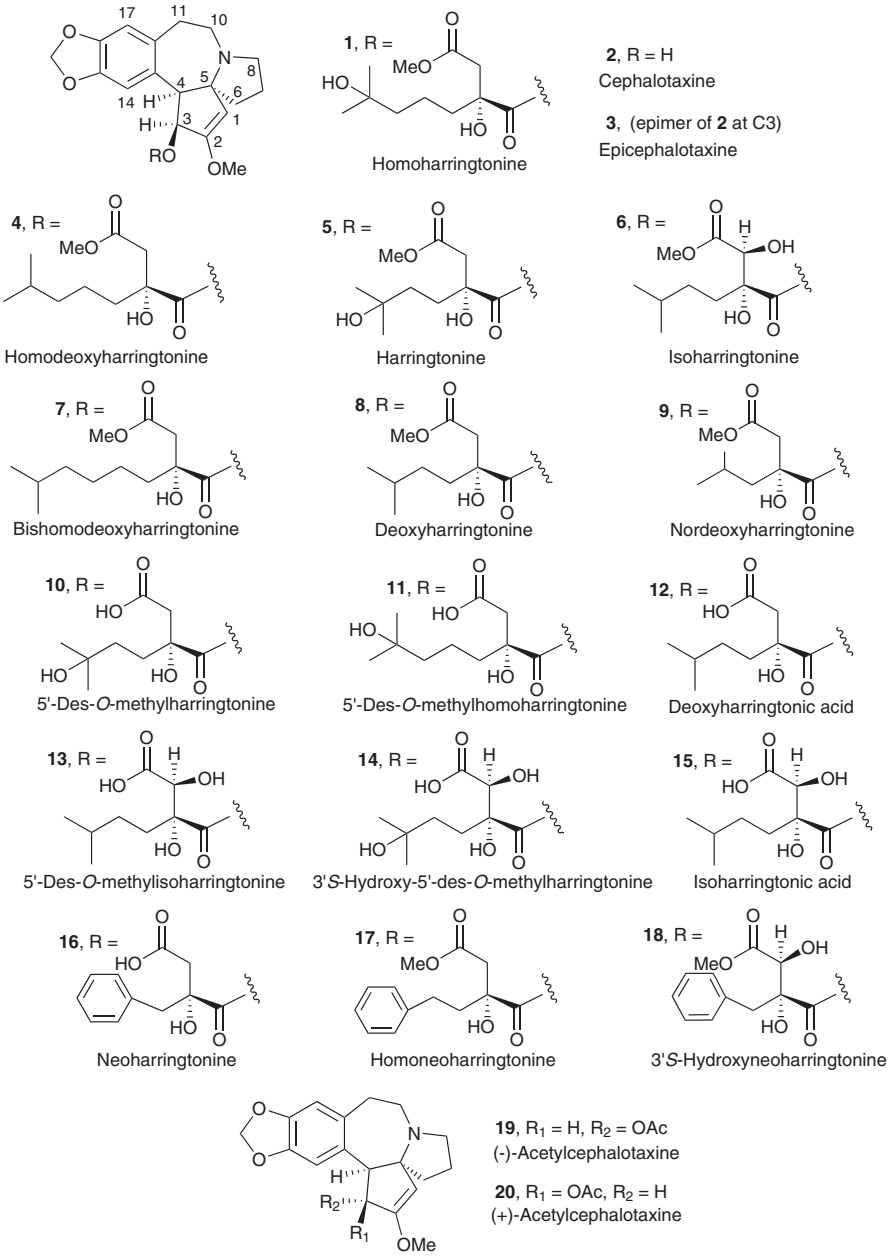

FIGURE 4.1 Naturally occurring *Cephalotaxus* alkaloids.

now in place, the ketal group of **77** could be removed. Mildly, acidic hydrolytic conditions gave ketone **71** with only limited success; however, more drastic conditions resulted in various side-reactions that competed with removal of the ketal group. The best method was to treat ketal **77** with cerium (III) chloride heptahydrate in the presence of NaI in MeCN at reflux to give the cornerstone ketone (*R*)-**71**.

Oxidative cleavage of the cyclohexanone ring of **71** was then explored. For this purpose, the ketone was first converted into the silyl enol ether **78** (TMSCl, Et_3N, NaI), which was ozonized (O_3 then Me_2S) into the sensitive aldehyde **79**. Slow addition of two equivalents of MeMgBr to crude

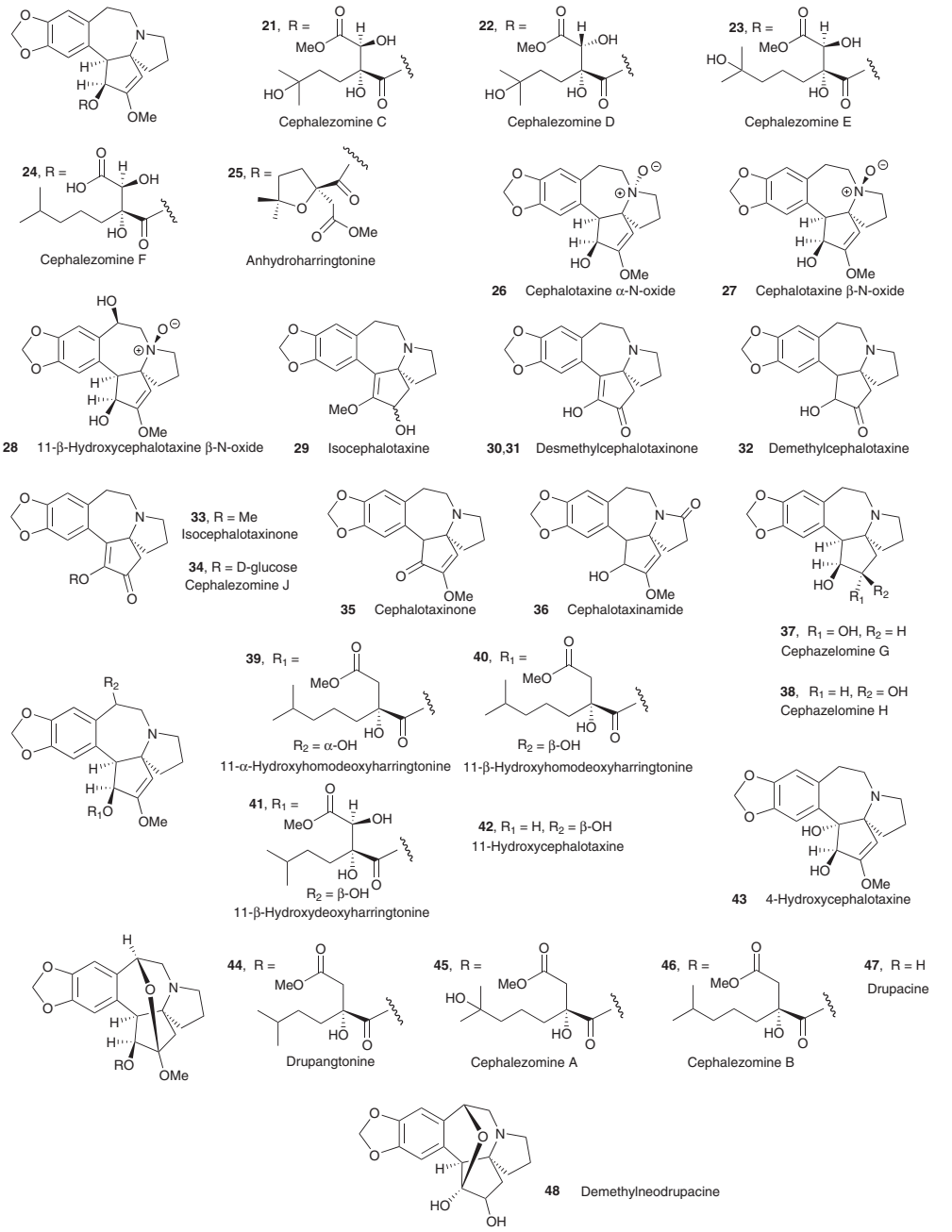

FIGURE 4.2 Structures of naturally occurring *Cephalotaxus* alkaloids.

aldehyde **79** at –40°C and subsequent esterification with CH_2N_2 then afforded an equimolar mixture of epimeric alcohols (**80**) in 35% overall yield, as calculated from ketone **71**. At this point, treating **80** with pyridinium chlorochromate gave ketone (*R*)-**81**. Adding one equivalent of MeMgBr to **81** at –30°C produced carbinol (*R*)-**82** in 42% yield. Hydrogenolysis of the benzyloxy group (H_2, Pd/C, quantitative yield) of **82** gave the target compound, (*R*)-methyl 3,7-dihydroxy-3-methoxycarbonyl-7-methyloctanoate (**70**), identical in all respects with the ester derived from methanolysis of natural HHT (**1**) (Figure 4.9).

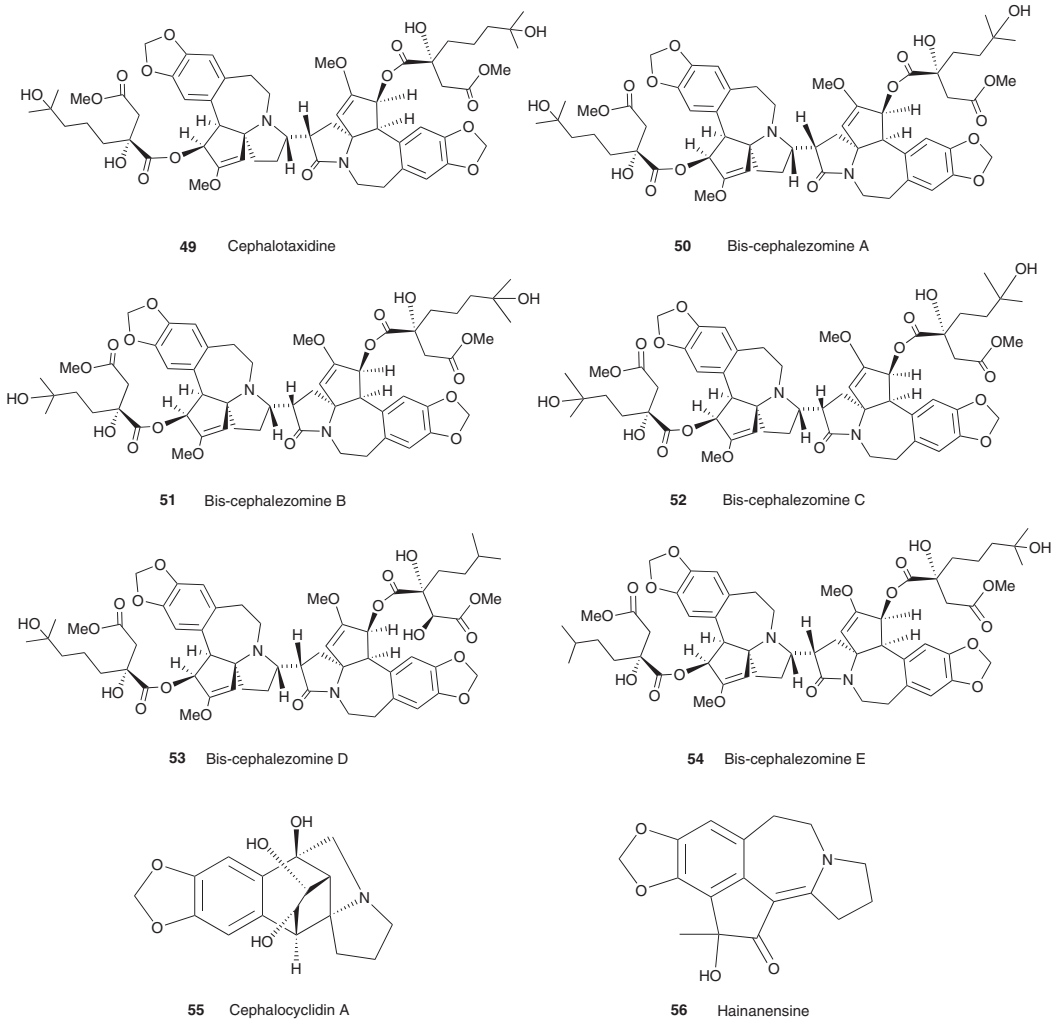

FIGURE 4.3 Structures of naturally occurring *Cephalotaxus* alkaloids.

4.3.1.4 Synthesis of the Acyl Side-Chain Using "Self-Reproduction of Chirality" Concept[40,41]

The initial step in the synthesis of several *Cephalotaxus* acyl chains involved the application of the Seebach concept of "self-reproduction of chirarity." This approach has been used to prepare chiral α-alkylmalates.[38,39] Beginning with readily available chiral starting material (*R*)-malic acid (**83**;

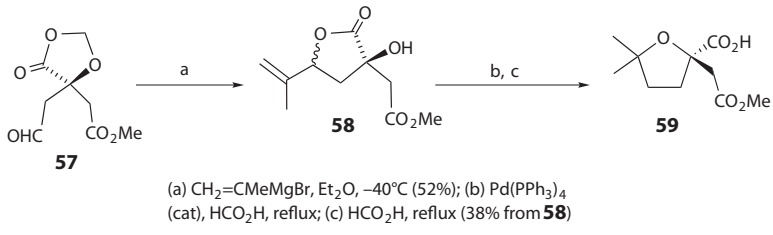

FIGURE 4.4 Synthesis of the anhydroharringtonine side-chain.

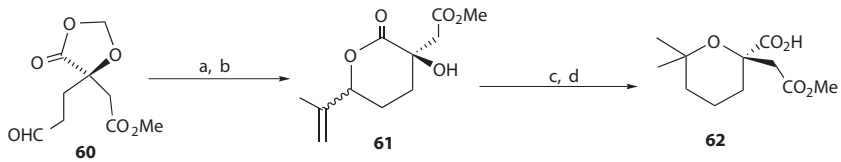

(a) CH_2=CMeMgBr, Et_2O, –40°C; (b) CSA, $CHCl_3$ (47%); (c) 10% Pd/C, HCO_2NH_4, MeOH, rt, 18 h; (d) HCO_2H, 100°C, 30 min (47%)

FIGURE 4.5 Synthesis of Robins' acid.

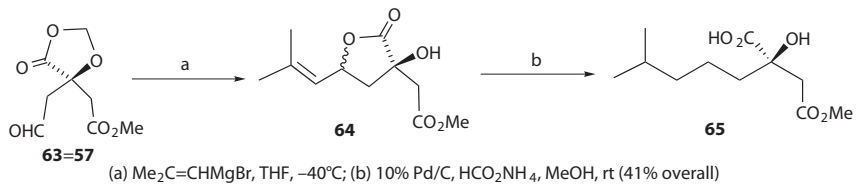

(a) Me_2C=CHMgBr, THF, –40°C; (b) 10% Pd/C, HCO_2NH_4, MeOH, rt (41% overall)

FIGURE 4.6 Synthesis of deoxyharringtonine side-chain.

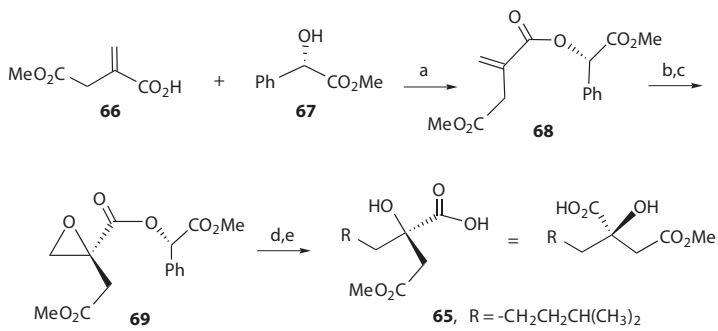

(a) DCC, DMAP, DCM, rt, 5 h (96%); (b) m-CPBA (95% purity), radical inhibitor, DCE, reflux, 16 h (72%); (c) flash chromatography; (d) R_2CuLi, Et_2O, –78 to –60°C, 2 h; (e) H_2, Pd/C, EtOAc, rt, 5 h.

FIGURE 4.7 Synthesis of epoxide **69** and *Cephalotaxus* alkaloid side-chains.

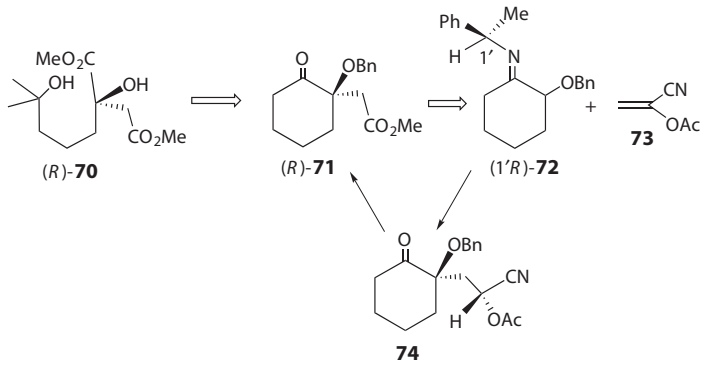

FIGURE 4.8 Retrosynthetic analysis of diester (*R*)-**70**, acyl side-chain of HHT (**1**).

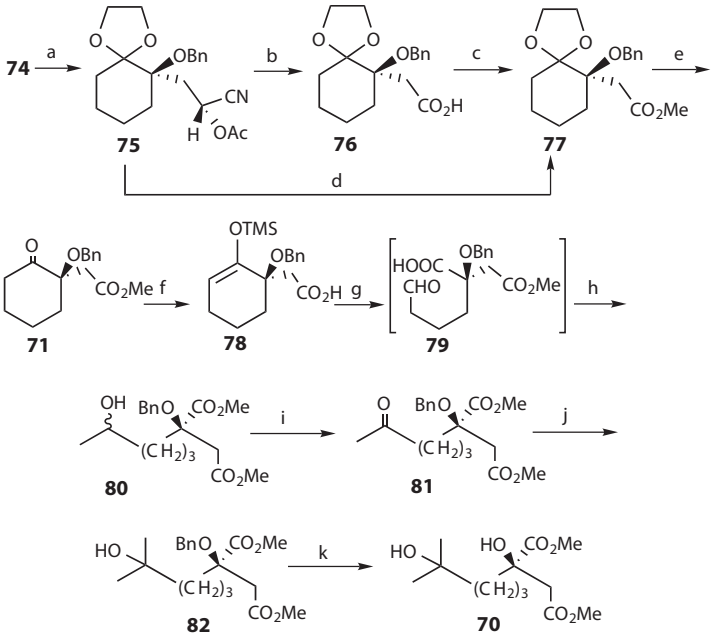

(a) i. $TMSOCH_2CH_2OTMS$, TMSOTf cat., CH_2Cl_2, –78°C to rt, ii. pyridine (80%); (b) i. LiOH, THF, rt, ii. NaO_2Cl, tBuOH, H_2O, NaH_2PO_4, 2-methyl-2-butene, rt (75%, 2 steps); (c) CH_2N_2, 0°C to rt (100%); (d) MnO_2, NaCN, MeOH, rt (61%); (e) $CeCl_3 7H_2O$, NaI cat., CH_3CN, reflux (85%); (f) TMSCl, NaI, Et_3N, CH_3CN, rt; (g) i. O_3/O_2, CH_2Cl_2, MeOH, –78°C, ii. Me_2S, –78°C to rt; (h) i. MeMgBr, THF, –40°C, ii CH_2N_2, 0°C to rt; (35%, 4 steps; (i) PCC, CH_2Cl_2, rt. (80%); MeMgBr, THF, –30°C (42%); (k)H_2, Pd/C, MeOH, rt (100%)

FIGURE 4.9 Synthesis of HHT dimethyl ester side-chain from Michael adduct (**74**).

Figure 4.10), the C1′ carboxylic acid and C2′ hydroxyl group were joined by a *tert*-butyl acetal upon treatment with 2,2-dimethylpropanal and TMSOTf. Only a single diastereoisomer of acetal **84** was observed. Double deprotonation with excess LHMDS formed the dilithium carboxylate-enolate (**85**). Although the C2′ stereocenter was destroyed, its stereochemical information was preserved in the chiral acetal carbon bearing the *tert*-butyl group. Due to the steric demands of this substituent, alkylation of the enolate with prenyl bromide occurred from the distal face, leading to the C2′-R configuration in **86**. Transesterification of **86** with NaOBn removed the acetal to afford benzyl ester **87** as a single enantiomer.

To possibly assist the esterification of cephalotaxine (**2**), the C2′-hydroxy group and the C1′-carboxylic acid in **87** were cyclized into a four-membered β-lactone ring in **88**. The energy strain from endocyclic bond angle compression within β-lactone ring in **87** would necessarily cause exocyclic bond angle expansion, and thereby, relieve local steric congestion at the electrophilic C1′ site. Moreover, the angle strain in a four-membered ring produces higher hybrid orbital s-character in the exocyclic bonds; an effect that could result in increased C1′ electrophilicity through induction. In addition, the increased p-character of the endocyclic bonds within the β-lactone might also help in stabilizing formation of a C′-acylium-like intermediate in activated ester derivatives of **88** through vicinal π-delocalization. Despite these potential advantages, however, the strain associated with the β-lactone moiety of **88** could also be a liability, as C1′-ester activation could lead to undesired ring expansion reactions. In actuality, activation of the lactone acid (**88**) as the Yamaguchi mixed anhydride allowed for efficient acylation of cephalotaxine (**2**) to form the ester **89**, without loss of the β-lactone. Methanolysis of the β-lactone provided (–)-deoxyharringtonine (**8**), with identical spectroscopic data to those of the natural product.[40]

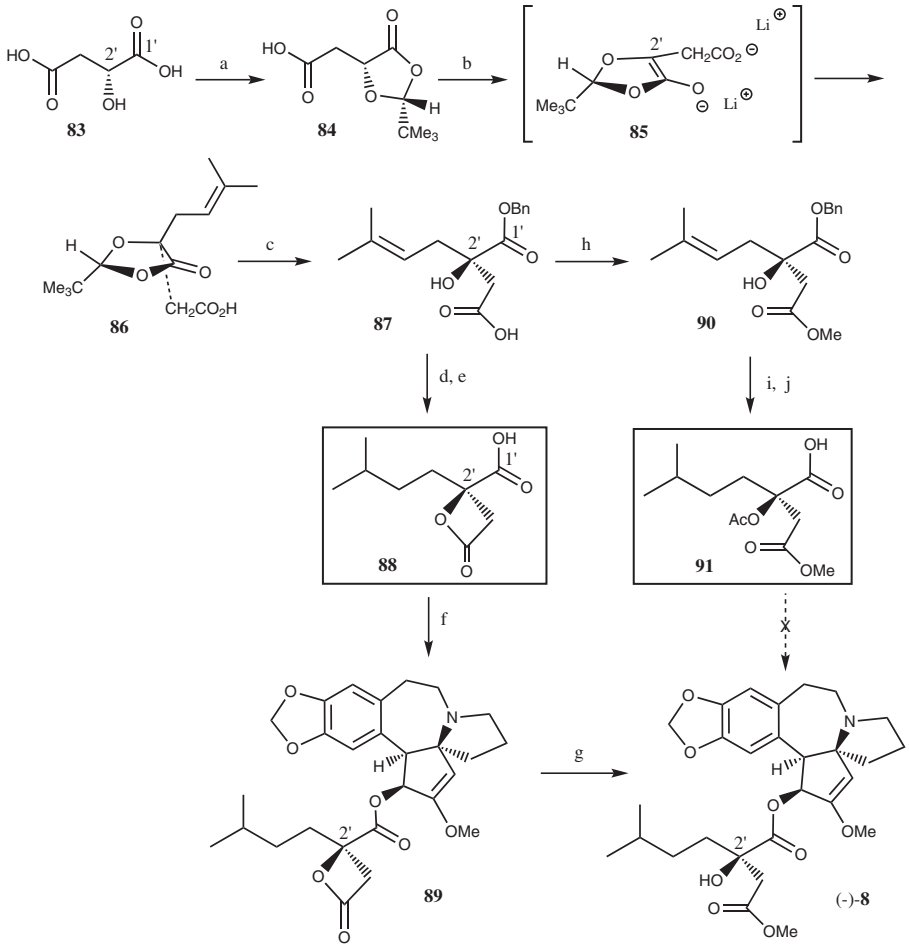

(a) TMSCl, TMS_2NH, CH_2Cl_2, 23 °C; Me_3CCHO, TMSOTf, CH_2Cl_2, -25 °C, 82%; (b) LHMDS, $Me_2C{=}CHCH_2Br$, THF, -78 °C, 66%; (c) NaH, BnOH, THF, 0 °C; (d) 2,4,6-$Cl_3C_6H_2COCl$, DMAP, CH_2Cl_2, 23 °C, 50%; (e) H_2, Pd/C, EtOAc, 23 °C, 99%; (f) 2,4,6-$Cl_3C_6H_2COCl$, DMAP, **2**, CH_2Cl_2, 23 °C, 81%; (g) NaOMe, MeOH, 23 °C, 76%; (h) $TMSCHN_2$, 7:2 PhH/MeOH, 23 °C, 100%; (i) Ac_2O, DMAP, pyr. 23 °C, 74%; (j) Pd/C, H_2, EtOAc, 23 °C, >99%

FIGURE 4.10 Synthesis of *Cephalotaxus* alkaloid (–)-**8** using lactonized side-chain.

To investigate whether the β-lactone moiety did provide favorable effects in the acylation step, an analogous acyclic acyl electrophile (**91**) was prepared in the following manner. Trimethylsilyldiazomethane treatment of carboxylic acid (**87**) afforded the methyl ester **90**. Acetylation of the C2′ hydroxyl group in **90** followed by benzyl ester hydrogenolysis and alkene hydrogenation provided the α-acetoxy carboxylic acid (**91**), which does not have the ring strain elements present in the β-lactone **88**. However, attempts to acylate cephalotaxine (**2**) with **91** under the identical conditions as with **88** led to only trace quantities of protected deoxyharringtonine (**8**). Heating the reaction mixture for several hours was also unsuccessful. This failure reinforced the critical and beneficial effect of the β-lactone moiety of **88** in the synthesis of bioactive *Cephalotaxus* esters.[41]

The successful synthesis of deoxyharringtonine (**8**) also allowed for efficient access to anhydroharringtonine (**25**). Intramolecular alkene alkoxymerculation and reduction (Figure 4.11) of the intermediate chiral hydroxyl diester (**90**) gave the corresponding cyclic tetrahydrofuran.

Subsequent benzyl ester hydrogenolysis provided the acylation precursor **92**. Although the strain imparted by the tetrahydrofuran ring in **92** is significantly less than that of the β-lactone in

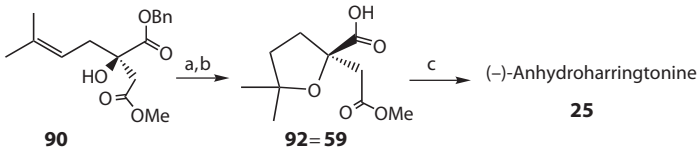

(a) $Hg(OAc)_2$, $NaBH_4$, THF : H_2O 1 : 1 , 23°C, 77%; (b) Pd/C, H_2, EtOAc, 23°C, 99%; (c) 2,4,6-$Cl_3C_6H_2COCl$, DMAP, TEA, **2**, 23°C, 99%

FIGURE 4.11 Preparation of **92**, acyl side-chain of anhydroharringtonine (**25**).

88, acylation of cephalotaxine (**2**) with **92** produced (–)-anhydroharringtonine (**25**) in excellent yield (but with a significantly extended reaction time compared with the synthesis of **8** from **2** and **88**). Thus, this work furnished two natural *Cephalotaxus* esters (**8** and **25**), as well as many non-natural synthetic intermediates for extensive antitumor evaluation.[41]

4.3.2 Total Synthesis of *Cephalotaxus* Alkaloids[41]

Many well-designed syntheses of cephalotaxine (**2**), the basic alkaloid core of the *Cephalotaxus* esters, have been reported in the literature. The racemic approaches have featured several key transformations, including Nazarov cyclization, photostimulated $S_{RN}1$ cyclization,[42] Claisen rearrangement, oxidative ring contraction, acylnitroso Diels-Alder cycloaddition, transannular *N*-conjugate addition, intramolecular alkene hydroamination, and reductive ring expansion of tetrahydroisoquinoline intermediates. Nonracemic routes have featured electrophilic aromatic substitution, Heck arylation, Pummerer-electrophilic aromatic substitution cascade, and acid-catalyzed ring expansion of cyclobutanol derivatives. Moreover, stereospecific reaction was performed via Reformatsky reaction by Hudlicky et al.[43–45] In addition, an important finding in the early synthetic work was that direct esterification of the appropriate acids to cephalotaxine to form the ester side-chains was extremely difficult, most likely due to steric hindrance.[43,44]

However, complete syntheses of the *Cephalotaxus* esters, including **1**, **4**, **8**, and **25**, are even more important, particularly because of their extremely potent antiproliferative effects. Moreover, these complex ester derivatives are quite scarce in the natural plant sources, typically found as only <0.1% of the plant dry weight. Thus, in the work described here, Eckelbarger et al. aimed to establish a synthetic approach to bioactive *Cephalotaxus* esters by a route completely distinct from prior efforts.[40,41]

Important concepts (Figure 4.12) of the synthetic design were to: (a) introduce the nitrogen atom via a Neber rearrangement; (b) assemble the benzazepine core via strain-release rearrangement of *N*-vinyl-2-aryl aziridines; (c) build the spiro-fused pyrrolidine core via 1,3-dipolar cycloaddition of azomethine ylides derived from vinylogous amides; and (d) create strained variants of advanced side-chain intermediates to assist late-stage cephalotaxine acylation (as was discussed in the previous section of this chapter). The latter three strategies had not been used previously in complex natural product synthesis.

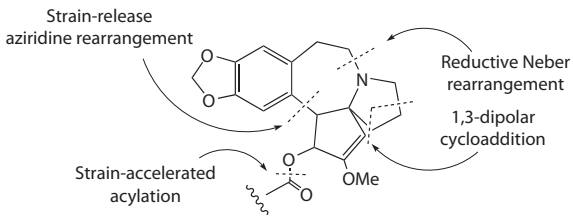

FIGURE 4.12 Key elements in total synthesis.

4.3.2.1 Dihydro[3]benzazepine Construction via Reductive Neber and Strain-Release Aziridine Rearrangements

The first goal was to assemble the seven-membered *N*-heterocycle of the core cephalotaxine (**2**). A widely used synthetic tool for construction of seven-membered rings is a strain-release [3,3]-sigmatropic rearrangement, in which a high-energy three-membered ring is incorporated into a 1,5-diene system. All-carbocyclic divinyl cyclopropane rearrangements are most common, but heterocyclic epoxide-, thiirane-, and aziridine-containing versions have been used. The aziridine-to-azepine transition is not very common, and *N*-aryl-2-vinyl aziridines were generally used to form dihydro[1] benzazepines. However, the synthesis of **2** requires a [3,3]-sigmatropic rearrangement of a *N*-vinyl-2-aryl aziridine to a dihydro[3]benzazepine, as shown in Figure 4.13.

Initial condensation of acetophenone derivatives (**93–95**) with hydroxylamine hydrochloride provided the corresponding oximes (**96–98**), respectively, in high yield (87–95%). Each oxime was reacted with $LiAlH_4$ and iPr_2NH at elevated temperature to give the corresponding aziridines (**99–101**), respectively, in good yields (74–76%), via a reductive Neber rearrangement. *N*-Vinylation of the substituted 2-aryl aziridines was accomplished by addition–elimination with the readily available alkene electrophile 3-chloro-2-cyclopentenone (**102**), prepared in a one-step reaction of 1,3-cyclopentandione with oxalyl chloride. Condensation of **99** and **102** with removal of HCl provided the *N*-vinyl aziridine (**103**) in moderate yield. In comparison, coupling of aziridine (**100** or **101**) with chloroenone (**102**) was significantly less efficient, resulting in only 16% and 26% isolated yields of vinyl aziridines **104** and **105**, respectively.

Although the yields were low in the previous step, the subsequent thermal rearrangement could be optimized using the obtained products. Aziridine (**103**) was then converted to desired dihydro[3]

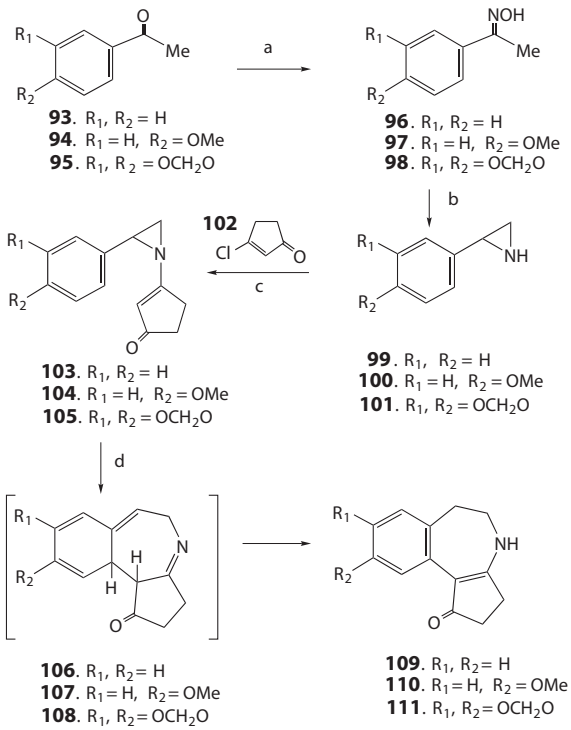

FIGURE 4.13 Synthesis and ring expansion of *N*-vinyl-2-aryl aziridines.

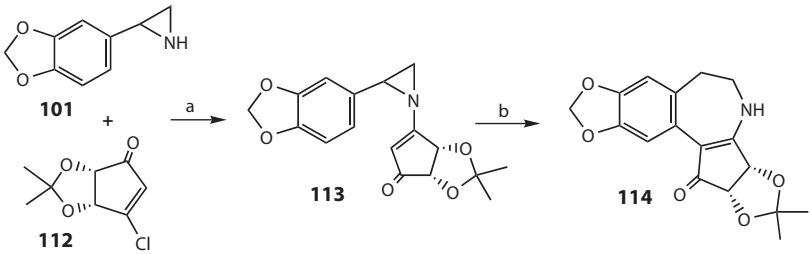

FIGURE 4.14 Synthesis of benzazepine-type compound.

benzazepine (**109**) by heating at 180°C in a dilute solution of 1,4-dioxane, containing Cs_2CO_3. The reaction occurred with complete regioselectivity, but in low yield (30%). However, under the same thermal rearrangement conditions, *p*-methoxyacetophenone-derived aziridine (**104**) was converted to the dihydro[3]benzazepine (**110**) in 52% yield, and rearrangement of aziridine (**105**), which has a 3,4-methylenedioxy-substituted aryl group, resulted in the highest formation of dihydro[3]benzazepine (68% yield of **111**). Thus, electronic-activating groups on the aromatic ring favorably affect the rearrangement (i.e., **104/105** → **110/111**). This result could be rationalized from compression of the HOMO-LUMO gap in a concerted [3,3]-sigmatropic rearrangement, or electronic-activating groups could stabilize a benzylic cation formed by initial aziridine opening in a stepwise ionic mechanism.

Based on this synthetic methodology, the racemic aziridine nucleophile (**101**) was reacted with the isopropylidene-substituted β-chloropentenone (**112**) at ambient temperature to afford a 1:1 diastereomeric mixture of the *N*-vinyl aziridine (**113**; Figure 4.14). The yield (85%) was much better than that of **101** with the unsubstituted β-chloropentenone (**102**). Finally, heating a dilute solution of **113** in 1,4-dioxane as described before led to efficient rearrangement to afford the dihydro[3]benzazepine (**114**).[41] The 1,2-di-*O*-isopropylidene substituent of **114** would serve as a chiral controlling agent in establishing the stereoselectivity of the key azomethine ylide cycloaddition *en route* to cephalotaxine (**2**).

4.3.2.2 Azomethine Ylide Generation and Cycloaddition via *O*-Acylation of Vinylogous Amides

Accordingly, **114** (Figure 4.15) was *N*-alkylated with $TMSCH_2I$ to afford the tertiary vinylogous amide (**115**). The highly reactive acyl electrophile, pivaloyl triflate, was generated *in situ* from pivaloyl chloride and AgOTf, and used for *O*-activation of **115**. Subsequent desilylation with tetrabutylammonium difluorotriphenylsilicate (TBAT) led to the formation of a putative azomethine ylide. Cycloaddition of the ylide with phenyl vinyl sulfone afforded the spiro-fused pyrrolidine (**116**; 77%) as a single stereoisomer. The high level of stereoselectivity in the cycloaddition indicates that the C1–C2 isopropylidene ketal was extremely effective as a stereo-determining element.

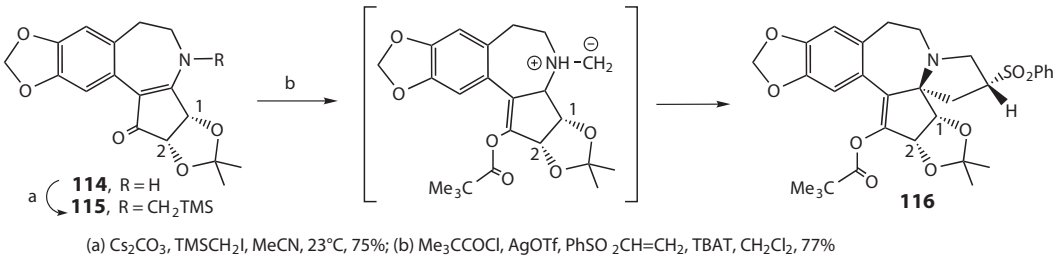

FIGURE 4.15 Generation of spiro-fused ring.

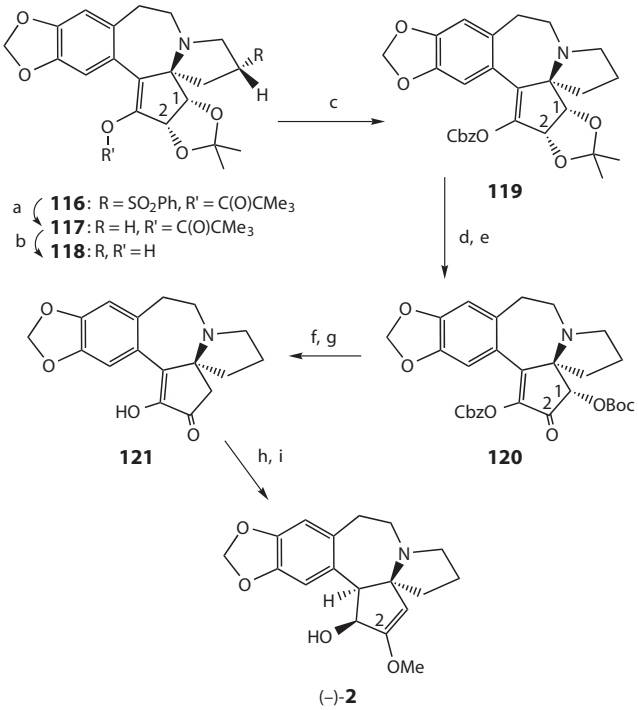

(a) SmI_2, HMPA, tBuOH, THF, –45°C, 74%; (b) Cp_2ZrHCl, THF, 40°C, 99%; (c) KHMDS, CbzCl, THF, 0°C, 86%; (d) 2N HCl, MeOH, 23°C, Boc_2O, $Yb(OTf)_3 \cdot xH_2O$, CH_2Cl_2, 0°C; (e) IBX, DMSO, 23°C, 50% (2 steps); (f) $CrCl_2$, acetone, H_2O, 23°C; (g) H_2, Pd/C, EtOAc, 23°C, 42% (2 steps); (h) $HC(OMe)_3$, *p*-TsOH, CH_2Cl_2, 55°C, 90%; (i) $NaBH_4$, MeOH, –78 to 23°C, 95%

FIGURE 4.16 Synthesis of (–)-cephalotaxine (**2**).

Next, the hexacyclic cycloadduct (**116**) had to be functionalized to provide the correct substituents and stereochemistry in the nonracemic pentacyclic alkaloid (Figure 4.16). To avoid rupture of the pyrrolidine ring via elimination, **116** underwent reductive desulfurization with SmI_2 in the presence of HMPA with 10 equivalents of *t*BuOH as a proton source to produce pyrrolidine (**117**). The pivaloate enol ester moiety in **117** proved to be resistant to both hydrolysis and hydrogenation. Finally, the enol ester in **117** was reductively cleaved with Schwartz reagent to provide the enol **118**, which was then reacylated with benzyl chloroformate and KHMDS to give the enol benzyl carbonate **119**. Although the isopropylidene was easily removed under acidic conditions, regioselective derivatization of the resulting diol proved challenging. Many different attempts at regioselective silylation, acylation, and alkylation with various reagents failed. The only successful protocol was the Lewis acid-catalyzed acylation procedure of Clarke et al. Treating the C1,C2-diol with Boc_2O and $Yb(OTf)_3$, necessarily in its polyhydrated form, gave selective C1-*O*-acylation, while the C2-hydroxyl was converted to a ketone using 2-iodoxybenzoic acid (IBX). Reductive C1-deoxygenation of enone **120** with $CrCl_2$ and hydrogenolysis of the Cbz group provided enol **121**. Sequential methyl enol ether derivatization of the C2 ketone and stereoselective reduction of the C3 enol with $NaBH_4$ finished the synthesis of (–)-cephalotaxine (**2**).[41]

4.3.2.3 Syntheses of Natural and Non-Natural Cephalotaxus Ester Alkaloids

Another *Cephalotaxus* alkaloid synthesis involved a common early sequence (Figure 4.17) beginning with the *R*-malic acid-derived acetal **122**, which underwent double deprotonation and diastereoselective enolate alkylation with allyl bromide.[42] Following NaOBn-mediated transesterification of the

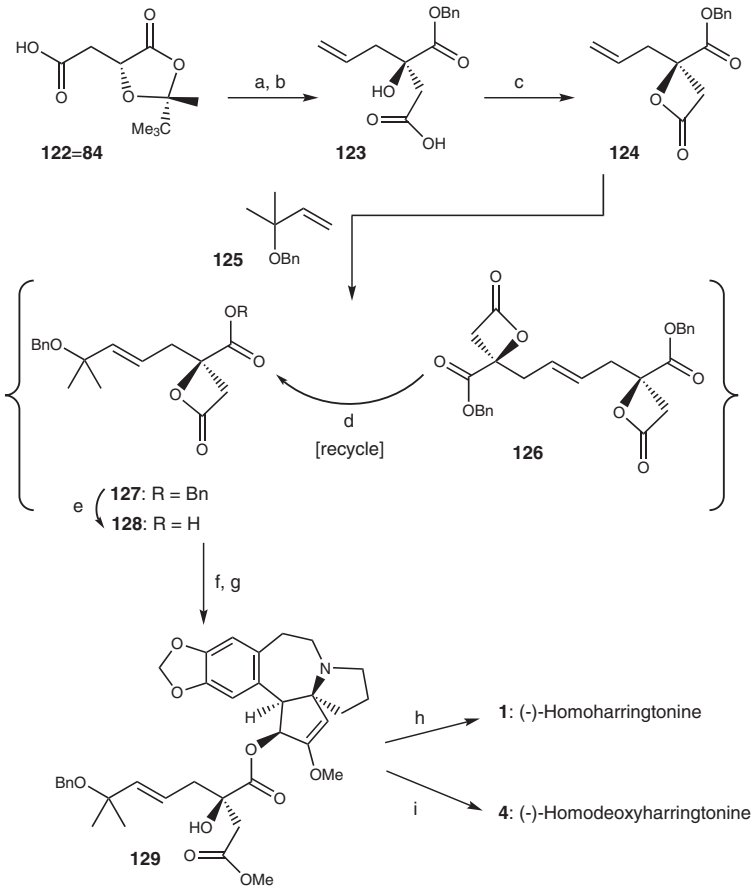

(a) LHMDS, allyl bromide, THF, -78 °C, 59%; (b) BnOH, NaH, THF, 0 → 23 °C, 85%; (c) 2,4,6-trichlorobenzoyl chloride, DMAP, Et_3N, CH_2Cl_2, 23 °C, 67%; (d) Grubbs II, 23 °C, 61%; (e) $Pd(OAc)_2$, Et_3SiH, Et_3N, CH_2Cl_2, 23 °C, 85%; (f) 2,4,6-trichlorobenzoyl chloride, DMAP, Et_3N, **2**, CH_2Cl_2, 23 °C, 97%; (g) NaOMe, MeOH, 0 °C, 79%; (h) Pd/C, H_2, MeOH then 9:1 MeOH/HOAc, 23 °C, 79%; (i) Pd/C, H_2, HOAc, 23 °C, 69%

FIGURE 4.17 Synthesis of (–)-HHT (**1**) and (–)-homodeoxyharringtonine (**4**).

resultant acetal-ester to afford the *R*-α-hydroxy benzyl ester **123**, β-lactone formation was accomplished via a Yamaguchi mixed anhydride to provide the strained intermediate **124**.

Subsequent alkene cross metathesis (Grubbs II) with excess alkene (**125**) provided the desired alkene (**127**) along with the dimeric *bis*-lactone (**126**) as an equilibrium mixture. Although the direct conversion of **124** to **127** was moderate, the recovered dimer (**126**) could be re-equilibrated under olefin metathesis conditions with excess **125** to obtain additional quantities of **127**. Following selective transfer hydrolysis of **127**, the resultant acid **128** was used in a highly efficient cephalotaxine acylation to prepare the corresponding ester, whose β-lactone was then subjected to methanolysis to furnish **129** (79% yield). This intermediate could be converted to both natural products HHT (**1**) and homodeoxyharringtonine (**4**), under different reaction conditions. When the allylic benzyl ether in **129** was subjected to Pd/C-catalyzed hydrogenolysis/hydrogenation in MeOH, followed by the addition of HOAc in the latter stages of the reaction, (–)-HHT (**1**) was isolated (presumably through initial alkene hydrogenation followed by benzyl ester hydrolysis). Alternatively, when the

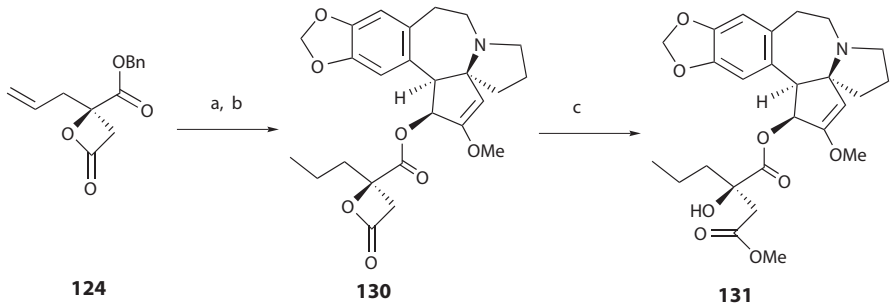

(a) Pd/C, H_2, EtOAC, 23°C, 97%; (b) 2,4,6-trichlorobenzoyl chloride, DMAP, TEA, **2**, CH_2Cl_2, 23°C, 81%; (c) NaOMe, MeOH, 23°C, 93%.

FIGURE 4.18 Synthesis of *bis*(demethyl)deoxyharringtonine analog (**131**).

Pd/C-catalyzed reaction was performed in glacial HOAc as solvent from the beginning, deoxygenation preceded alkene reduction (presumably through E1 elimination of the allylic benzyl ether prior to hydrogenation) to afford (–)-homodeoxyharringtonine (**4**).

The efficient synthesis of the acyl chain precursors in the aforesaid preparation of the natural *Cephalotaxus* esters **1** and **4** also presented the opportunity to prepare a non-natural analog for biological evaluation with only a minor variation in the synthetic sequence. Alkenyl ester **124** was coupled directly (without further chain elongation as shown in Figure 4.16) with cephalotaxine (**2**) to provide the ester–β-lactone (**130**). Methanolysis of the β-lactone in **130** proceeded efficiently to afford the non-natural **131** (Figure 4.18).

The completion of the syntheses of the natural *Cephalotaxus* esters **2**–**4** together with two non-natural synthetic analogs, benzyldehydrohomoharringtonine (**129**) and *bis*(demethyl)deoxyharringtonine (**131**), permitted comparative biological evaluation against "sensitive" and multidrug resistance (MDR) cell lines.[41]

4.3.2.4 Additional Recent Synthetic Studies on the *Cephalotaxus* Alkaloid Skeleton

Hayes et al.[43] accomplished a second generation formal synthesis of (–)-cephalotaxine (**2**), using an alkylidene carbene 1,5-CH insertion reaction to establish a key quaternary stereocenter (Figure 4.19).

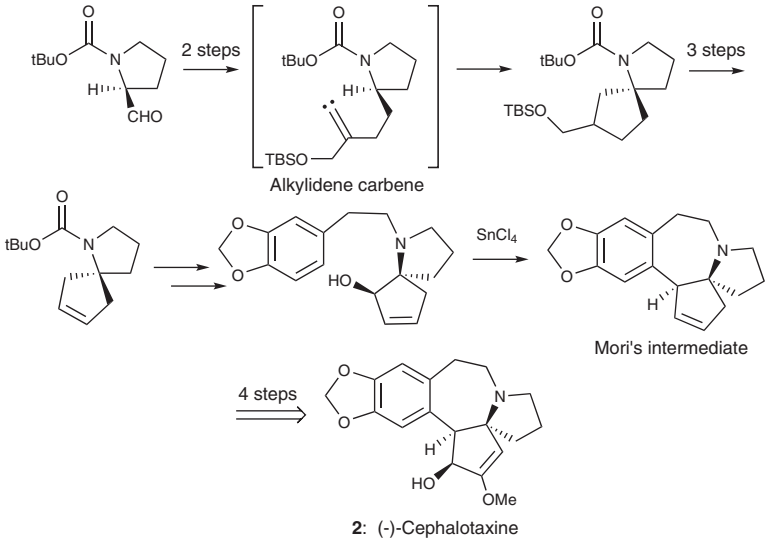

FIGURE 4.19 Second generation formal synthesis of (–)-cephalotaxine (**2**).

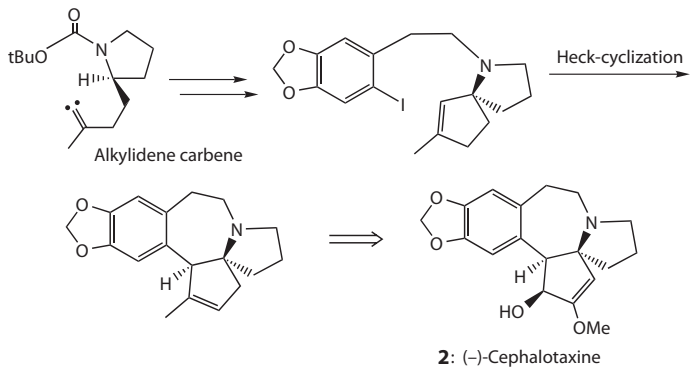

FIGURE 4.20 Formal synthesis of (–)-cephalotaxine (**2**).

Wittig reaction of a L-proline-derived aldehyde with a known ylide gave the carbene precursor, and the 1,5-CH insertion reaction was performed under Ohira's conditions using lithiotrimethylsilyldiazomethane (LTDM). The desired spirocyclic product was converted to *N*-Boc-1-azaspiro[4,4]non-6-ene, by oxidation and decarbonylation of the pendant hydroxymethyl group. Multiple manipulations easily gave the desired Friedel–Crafts cyclization precursor, which upon exposure to $SnCl_4$, provided the desired pentacyclic product, which was identical to "Mori's intermediate." Thus, this protocol represents a formal total synthesis of **2**.[46]

Hayes[46] also reported a second enantioselective formal synthesis of **2**. Again, an alkylidene carbene 1,5-CH insertion reaction was used to construct the spiro[4.4]azanonane core D/E-ring system. However, in this synthetic protocol, a Heck-type cyclization was used to close the tetrahydroazepine C-ring and a selective epoxide rearrangement sequence was used to correctly modify the E-ring of **2**[47] (Figure 4.20).

Figure 4.21 shows a short total synthesis of **2**, in which the pentacyclic core of the alkaloid was constructed by a radical cascade involving 7-endo and 5-endo cyclizations.[48]

Another highly efficient formal synthesis of **2** employed a [2,3]-Stevens rearrangement-acid lactonization sequence as a key transformation from readily available (3,4-dimethoxyphenyl)acetic acid, methyl prolinate, and allyl bromide[49] (Figure 4.22).

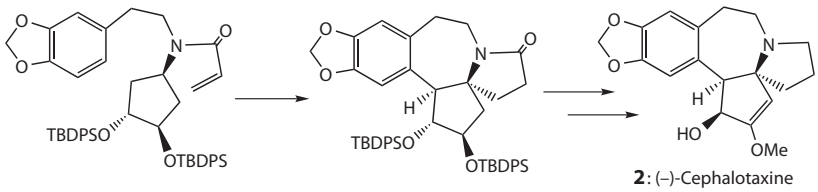

FIGURE 4.21 Short synthesis of (–)-cephalotaxine (**2**).

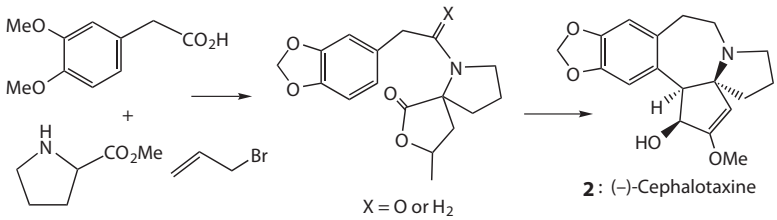

FIGURE 4.22 Highly efficient formal synthesis of (–)-cephalotaxine (**2**).

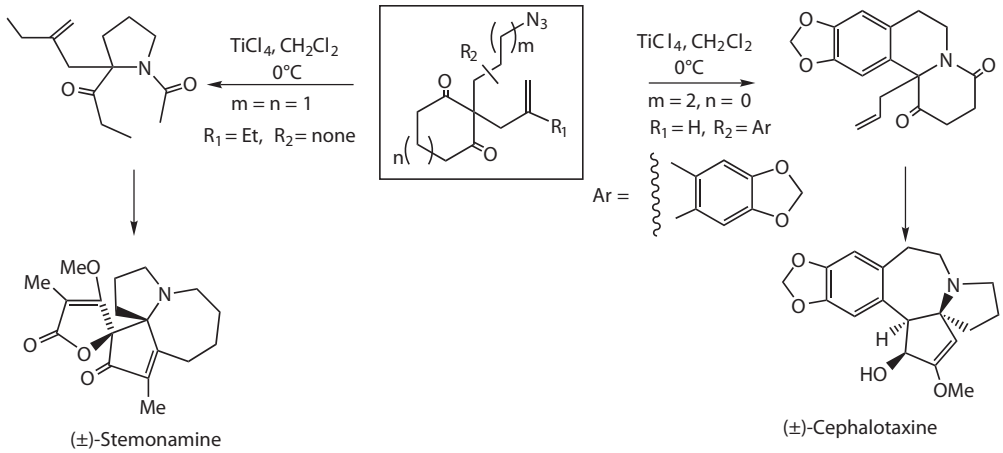

FIGURE 4.23 Formal synthesis of stemonamine and (±)-cephalotaxine (**2**).

An intramolecular Schmidt reaction of appropriately substituted symmetrical azido-diones was also used in the synthesis of natural alkaloids.[50] An aza-quaternary pyrrolo[1,2-a]azepine and aza-quaternary indolizine were important intermediates for syntheses of stemonamine and cephalotaxine (**2**) (Figure 4.23).

4.4 BIOSYNTHESIS OF *CEPHALOTAXUS* ALKALOIDS

4.4.1 Biosynthesis of Side-Chain

The biosyntheses of *Cephalotaxus* alkaloids deoxyharringtonine (**8**), isoharringtonine (**6**), and harringtonine (**5**) were investigated by precursor incorporation experiments, as reported in the recent review on *Cephalotaxus* alkaloids by Guo.[51]

It was established that the acyl portion of **8** is derived from leucine via a pathway that resembles the conversion of valine into leucine in microbial systems. In particular, feeding experiments with *C. harringtonia* showed that 3-carboxy-3-hydroxy-6-methylheptanoic acid, which is linked to **2** in the esterified alkaloid **8**, was biosynthesized from L-leucine via 3-hydroxy-3-carboxy-5-methylhexanoic acid and 3-carboxy-2-hydroxy-5-methylhexanoic acid.[55]

Incorporation experiments with DL-deoxyharringtonic-9-^{14}C acid (**132**) showed that **132** is the precursor of isoharringtonic acid (**133**) and harringtonic acid (**134**) *in vivo* (Figure 4.24). Doubly labeled **8** was synthesized, and its ability to serve as an intact precursor of harringtonine was examined. The results of this experiment indicated, but did not conclusively prove, that **8** is directly converted to harringtonine without prior deacylation.[52,54]

Administration of specifically labeled forms of tyrosine to *C. harringtonia* plants yielded radioactive cephalotaxine (**2**). Degradation of the radioactive alkaloid showed an unusual labeling pattern that was inconsistent with the prevailing hypothesis for cephalotaxine biosynthesis, and a new hypothesis was proposed.[53]

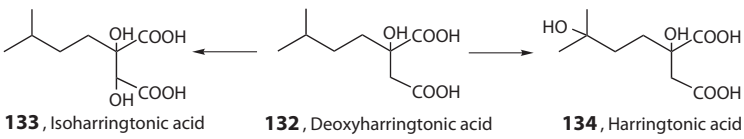

FIGURE 4.24 Biosynthesis of side-chains.

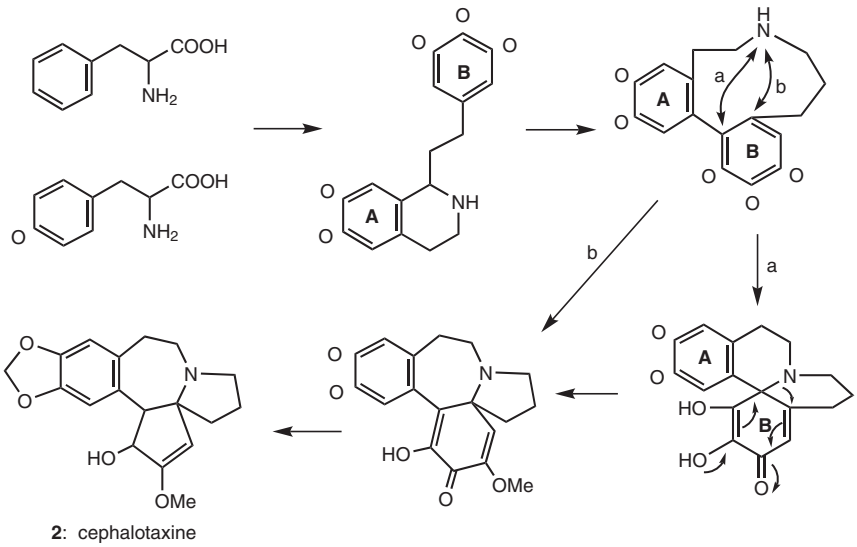

FIGURE 4.25 Biosynthesis of (–)-cephalotaxine (**2**).

4.4.2 Biosynthesis of Alkaloid Skeleton

The biosynthesis of the alkaloid cephalotaxine (**2**) was investigated by precursor incorporation experiments with *C. harringtonia*. Cephalotaxine was biosynthesized from one molecule each of tyrosine and phenylalanine in a manner consistent with the hypothesis that **2** is a modified 1-phenethyltetrahydroisoquinoline alkaloid (Figure 4.25). Incorporation experiments with p-^{14}C- and m-^{14}C-labeled phenylalanine showed that one of the *meta*-carbon atoms of phenylalanine is lost during the conversion of this amino acid into **2**. The remaining *meta*-carbon atom is located at C-2 of **2**. Cephalotaxinone, demethylcephalotaxinone, and demethylcephalotaxine labeled with ^{14}C at C-3 were also synthesized. Incorporation experiments with these labeled alkaloids established that cephalotaxine and cephalotaxinone are irreversibly demethylated *in vivo*.[56]

In another study, feeding experiments with *C. harringtonia* established that **2** is biosynthesized from a molecule of tyrosine and a molecule of phenylalanine. The experiments also suggested that cinnamic acid is not a cephalotaxine precursor, but that some intermediate with α,β-unsaturation probably lies on the pathway between phenylalanine and **2**.[57]

4.5 MEDICINAL CHEMISTRY OF THE DRUG

Figure 4.26 shows the IC_{50} values against parental and drug-resistant HL-60 cancer cell lines, resistance indices (IC_{50} drug-resistant ÷ IC_{50} parental), and calculated lipophilicity values (clog*P*) for the highly potent *Cephalotaxus* esters **1**, **4**, **8**, **129**, and **131**. All compounds except **1** had clog*P* values greater than 1.2 and also low susceptibility to MDR (i.e., resistance indices <19 for **4**, **8**, **129**, and **131**). In contrast, HHT (**1**) had a relatively low clog*P* value (0.95, more polar), but increased susceptibility to MDR (i.e., resistance index is 125). Although these data were obtained on a limited set of analogs, they provide new insights into how acyl chain structure modification could contribute toward overcoming MDR for this compound class.[41] For example, HHT (**1**) and homodeoxyharringtonine (**4**) differ structurally only by a single hydroxyl group on the 6′-position of the acyl side-chain in the former compound (Figure 4.26). This difference drastically affects the lipophilicity of the two molecules: **1** has a polar clog*P* value of 0.95, while **4** has a more hydrophobic clog*P* value of 2.33, and even more importantly, because **4** has a resistance index of only 3, this minor structural variation from **1** to **4** has allowed for effective suppression of MDR in the HL-60 cell line.

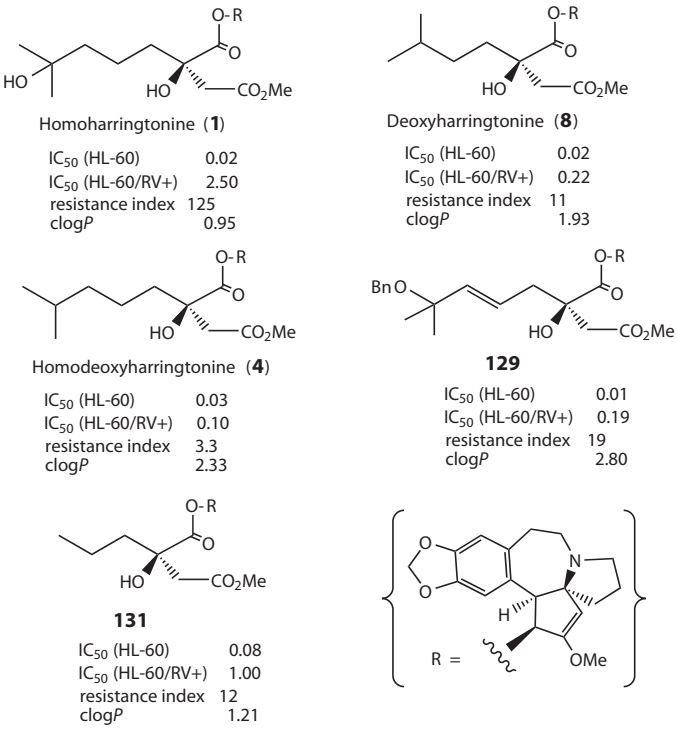

FIGURE 4.26 Comparative antitumor effects of *Cephalotaxus* ester against sensitive and vincristine-resistant HL-60.

It might thus seem surprising that, in view of its MDR liability, **1** has been the favored *Cepahlotaxus* ester for clinical advancement, as reflected by a current phase III clinic prospective trial with **1** for use as a combination therapy for chronic myeloid leukemia.[58] However, **1** is also found in increased natural abundance relative to other *Cephalotaxus* esters. In addition, in the influential work of Kelly, the 6′-oxygen functionality is a prerequisite for efficient acyl chain attachment to cephalotaxine (**2**), and this semisynthetic approach is uniquely suited for **1**. Fortunately, recent synthetic strategies, such as those described earlier, have enabled better access to other, more therapeutically viable *Cephalotaxus* esters, such as **4**, **8**, **129**, and **131**, for the development of additional avenues of chemotherapy against leukemia.[41]

4.5.1 Resistance of Vincristine-Sensitive Y79 Retinoblastoma to *Cephalotaxus* Esters

In an initial cytotoxicity evaluation (Table 4.2), the Y79 retinoblastoma cell line showed significant and unique resistance to both deoxyharringtonine (**8**) and its β-lactone derivative (**89**). After evaluation in comparison with several cytotoxic non-natural synthetic *Cephalotaxus* ester analogs, including benzyldehydrohomoharringtonine (**129**), its β-lactone ester (**130**), and *bis*(demethyl) deoxyharringtonine (**131**; Table 4.3), this selective resistance of Y79 appeared to be a more general phenomenon. All these compounds behaved similarly to deoxyharringtonine (**8**) and its β-lactone derivative (**89**; cf. Table 4.2), and exhibited broad spectrum cytotoxicity against numerous cancer cell lines, with the exception of the Y79 cell line against which the compounds were essentially ineffective.[41]

This specific lack of cytotoxicity against Y79 could be attributed to overexpression of MDR genes; however, Conway et al. have reported that the Y79 cell line is sensitive to vincristine, with an IC_{50} value of approx 0.8 μM. In addition, a comparative microarray analysis of the Y79 cell line

TABLE 4.2
Cytotoxicity of Deoxyharringtonine (8), β-lactone (87), and anhydroharringtonine (25)

	IC_{50} [μM]		
Cell Line	**8**	**87**	**25**
HL-60	0.02	2.68	22.7
HL-60/RV +	0.22	21.8	>100[a]
JURKAT	0.04	5.71	43.0
ALL3	<0.1[b]	1.47	>100[a]
NCEB1	0.07	8.62	>100[a]
JEKO	0.08	10.48	>100[a]
MOLT-3	0.02	2.68	26.8
SKNLP	<0.1[b]	6.46	5.34
Y79	70.59	>100[a]	>100[a]
PC9	0.03	4.23	29.1
H1650	0.04	4.53	—
H1975	0.06	8.42	—
H2030	0.1	7.72	—
H3255	0.08	5.55	—
A431	0.06	—	—
HeLa	0.04	—	—
TC71	0.06	12	>100[a]
HTB-15	0.2	52	>100[a]
WD0082	0.1	5	>100[a]

[a] Lowest compound concentration tested and giving 100% cellular killing.
[b] Highest compound concentration tested.

TABLE 4.3
Cytotoxicity of Compounds 129–131

	IC_{50} [μM]		
Cell Line	**129**	**130**	**131**
HL-60	0.01	5.73	0.08
HL-60/RV+	0.19	40.3	0.8
JURKAT	0.03	12.01	0.19
ALL3	<0.01	4.24	0.16
NCEB1	0.06	39.24	0.5
JEKO	0.08	25.1	0.56
MOLT-3	0.01	6.41	0.06
SKNLP	<0.01	10.04	0.11
Y79	>100	>100	>100
PC9	0.04	11.29	0.13
TC71	0.03	24	0.2
HTB-15	0.1	58	0.5
WD0082	0.05	11	0.2

with normal retinal tissue detected upregulation of several genes typically found to be markers of stem cell-like characteristics, including the mdr gene *ABCG2*.[59] These results suggest that the mechanism of resistance to *Cephalotaxus* esters by Y79 is likely not mediated entirely through the classical ATP-dependent efflux pumps alone but rather through an as yet unknown mechanism involving stem cell-like characteristics. These findings are also consistent with the hypothesis that the appearance of subsequent tumors in leukemias, brain tumors, breast, and lung cancers, as well as many other cancers, is linked to the persistence of cancer stem cells. Rationally designed *Cephalotaxus* esters could potentially serve as small-molecule probes for investigating the genetic basis of this highly resilient retinoblastoma cell line, as well as possibly adding new information on how to overcome resistance in dormant progenitor cancer stem cells.[41]

4.6 DEVELOPMENT OF THE CLINICAL DRUG OF *CEPHALOTAXUS* ALKALOIDS

4.6.1 Cytotoxity against Myeloma Cell Lines: Effects on Akt Pathway[60]

The participation of phosphatidylinositol-3-kinase/Akt-1 in cell survival and proliferation of multiple myeloma (MM) has been well established. Meng et al.[60] demonstrated that HHT (**1**) induced significant cytotoxicity in dexamethasone-sensitive, dexamethasone-resistant, and chemotherapy-sensitive MM cell lines in a time- and dose-dependent manner. HHT also triggered apoptosis in a chemotherapy-resistant patient's myeloma cells. In contrast to dexamethasone, HHT's cytotoxicity against myeloma was not dependent on interleukin (IL)-6, but instead was related to downregulation of Akt phosphorylation/activation and various target genes of Akt, including nuclear factor κB, XIAP, cIAP, and cyclin D1. Moreover, HHT showed *in vivo* antitumor activity in a RPMI8226 myeloma xenograft model. Importantly, an additive antitumor effect was confirmed in myeloma cells treated with HHT and bortezomib, along with inhibition of phosphorylated Akt. Together, these findings with HHT should give useful insights into a novel antimyeloma chemotherapy.

4.6.2 Cytotoxity against Myeloma Cell Lines: Effects on Hypoxia-Inducible Factor-1α[61]

Hypoxia-inducible factor-1α (HIF-1α) is a key transcription factor under anoxic circumstances. Li et al.[61] explored how RNA interference (RNAi) targeting HIF-1α affected the sensitivity of human chronic myelogenous leukemia (CML) K562 cells toward HHT (**1**). HIF-1α short hairpin RNA (shRNA) was constructed using pSilencer 2.1-U6 hygro vector and transfected into K562 cells. Positive clones were screened using hygromycin. After inhibition of HIF-1α, expressions of its target genes, such as vascular endothelial growth factor (VEGF), glucose transporter-1 (Glut-1), phosphoglycerate kinase (PGK), and P-glycoprotein (P-gp) were detected by real-time reverse transcriptase polymerase chain reaction (RT-PCR), and sensitivity of K562 cells to **1** was detected by MTT assay. HIF-1α expression was inhibited at both mRNA and protein levels after transfection of RNAi HIF-1α, which subsequently caused a dramatic decrease in VEGF, Glut-1, PGK, and P-gp under hypoxic conditions. In addition, HIF-1α inhibition increased drug sensitivity of K562 cells to HHT. Thus, HIF-1α inhibition might result in a decrease of genes related to angiogenesis and glycolysis metabolism and an increase of drug sensitivity to HHT in K562 cells.[61]

4.6.3 Cytotoxity against Myeloma Cell Lines: Effects on MM-Promoting Molecules[62]

Because various intrinsic cellular and extrinsic molecular abnormalities cooperatively promote tumor formation in MM, therapeutic approaches that have more than a single molecular target are

increasingly attractive. The antimyeloma effect and mechanism of HHT (**1**), an inhibitor of protein synthesis, were studied. Treatment with HHT significantly reduced Mcl-1, a crucial protein involved in myeloma cell survival in all three myeloma cell lines examined, as well as the levels of c-FLIPL/S, activated caspase-8, and induced active truncated-Bid. In contrast, certain BH3-only proteins, such as Bim, Bik, and Puma, remained unchanged, and their expression levels depended on the cell type. Thus, HHT-induced apoptosis appears to be mediated via both intrinsic and extrinsic apoptosis pathways and the resulting imbalance between BH3-only proteins and Mcl-1 may be pivotal for apoptosis by HHT. In addition, treatment with HHT led to reduced levels of β-catenin and XIAP proteins, which can also contribute to MM progression and resistance to chemotherapy. When used in combination, HHT enhanced the chemotherapeutic effects of three anticancer agents, melphalan, bortezomib, and ABT-737. Thus, HHT could provide an attractive option for MM treatment through its ability to simultaneously target multiple tumor-promoting molecules.[62]

4.6.4 Cytotoxity against Myeloma Cell Lines—Effects on JAK2-STAT5 Pathway[63]

HHT (**1**) is used in China as an efficient therapy in patients with acute myeloid leukemia (AML), but little is known about its mechanism of action. As the abnormal activation of JAK2-associated pathway is important in AML progression, a better understanding of HHT's effect on the JAK2-STAT pathway in AML cells could supply a theoretical basis for wider use of HHT. In the study, cell viability was evaluated by MTT analysis, apoptosis was tested by flow cytometry, and RT-PCR was used to measure the expression of JAK2, STAT5, and the effect gene *Bcl-xL*. Signal proteins such as p-JAK2, p-STAT5, p-AKT, p-ERK activated by abnormally activated JAK2 were tested by Western blotting. HHT inhibited viabilities of primary AML cells and AML cell lines HEL, K562, and HL-60 cells, and AnnexinV-PI double staining confirmed early apoptosis in a dose-dependent manner. When AML cells were treated with **1** for only 6 h (which is much earlier than induction of apoptosis), immunoblotting analyses showed that expressions of p-JAK2, p-STAT5, and p-AKT were downregulated, while the total JAK2, STAT5, and AKT protein levels were stable. With only 6 h of treatment, no changes in p-ERK and BcL-xL proteins were observed, but when extended to 24 h of treatment, Bcl-xL decreased. Similar results were obtained by using AG490, a JAK2-specific inhibitor. In summary, HHT possibly acts as a broad-spectrum PTK inhibitor and inhibits the phosphorylation of the signal proteins caused by oncogenic proteins such as JAK2V617F, BCR/ABL. It thus blocks the survival and proliferative signal pathway of malignant cells.[63]

4.6.5 Cytotoxity against Myeloma Cell Lines—Combination Therapy Effects on Residual Leukemic Cells[64]

In a study of 72 patients with *de novo* AML treated with a regimen of HHT (**1**), cytosine arabinoside, and daunorubicin were separated into two subgroups by a cutoff of 10% bone marrow leukemic cells at the end of first course of induction chemotherapy (T1) or during aplasia (T2). The factors of complete remission (CR) rate, disease-free survival (DFS), and overall survival (OS) were significantly different between the two groups. In addition, it was confirmed that the percentage of residual leukemic cells (RLCs) at T1 or T2 is an independent prognostic factor of AML.[64]

4.6.6 Cytotoxity against Myeloma Cell Lines—Synergistic Effects on Multidrug-Resistant Leukemia Cells[62]

The effects of HHT (**1**) or arsenic trioxide (As_2O_3) in combination with bortezomib on the proliferation capacity and apoptosis of HL-60/ADM cell line and fresh cells from refractory/relapse acute leukemia patients were investigated. HL-60/ADM cells or refractory/relapse leukemia cells were incubated with bortezomib at different doses alone and in combination with HHT or As_2O_3. The

proliferation capacity was observed by MTT assay, and cell apoptosis was evaluated by fluorescence microscopy and flow cytometry. In bortezomib only-treated HL-60/ADM cells, the proliferation inhibition rate and apoptotic cells increased in a time- and dose-dependent manner, with maximum inhibition occurring with 40 nmol/L of bortezomib at 48 h. Doses of 15 μmol/L of As_2O_3 or 752 nmol/L of HHT combined with different doses of bortezomib also inhibited proliferation and induced apoptosis of HL-60/ADM cells. HHT plus bortezomib or As_2O_3 plus bortezomib showed greater anticancer efficacy than either of the drugs alone ($p < 0.01$, $p < 0.05$, respectively).[65]

4.7 CLINICAL APPLICATIONS

4.7.1 Review Articles on Omacetaxine Mepesuccinate (A Derivative of HHT)[66,67]

In two review articles,[63,64] Quintas-Cardama and Cortes examined the most relevant preclinical and clinical studies involving patients with CML receiving therapy with either natural HHT (**1**) or omacetaxine mepesuccinate (Ceflatonin, Myelostat, CGX-653). The latter compound is a semisynthetic subcutaneous bioavailable form of HHT, which ChemGenex Pharmaceuticals Ltd, in collaboration with Stragen Group, is developing as a potential treatment for CML, myelodysplastic syndrome (MDS), and AML. Mechanistically, HHT exerts its antitumor and antiangiogenic activities by inhibiting protein synthesis and promoting apoptosis, and in preclinical studies, omacetaxine mepesuccinate also induced apoptosis in leukemia cell lines.

In phase II studies, omacetaxine mepesuccinate was active in patients with CML resistant to the tyrosine kinase inhibitor (TKI) imatinib mesilate, and who carry the BCR-ABL1T3151 mutation, which is highly insensitive to several TKIs, including imatinib, nilotinib, and dasatinib.[67] Results from the trials also showed that therapy with omacetaxine mepesuccinate was generally well tolerated.[67] Additional phase II and III clinical trials are underway to assess the activity of omacetaxine mepesuccinate, either alone or in combination with TKIs or other cytotoxic drugs, in patients with CML that is resistant to TKI therapy. Phase I and II trials for omacetaxine mepesuccinate in the treatment of AML and MDS are also ongoing, and i.v., s.c., and oral formulations of the drug are being developed. Omacetaxine mepesuccinate looks promising for the treatment of CML, particularly for imatinib-resistant CML. The development of alternative formulations should further expand its potential for success in drug development.[67]

4.7.2 Phase I Study for AML[68,69]

As the response to remission induction in elderly patients with AML remains poor, Wang et al.[68] evaluated the efficacy and toxicity of HHT (**1**), in combination with cytarabine, as an induction therapy for AML. Twenty-three patients (>60 years of age) were treated with a regimen consisting of HHT (2 mg/m^2/day for 7 days) and cytarabine (Ara-C; 100 mg/m^2/day for 7 days; termed HA regimen). The overall response rate was 56.5% with a CR rate of 39.1% and partial remission of 17.4%. No early deaths occurred. The estimated median OS time of all patients was 12.0 (±3.0) months and of only CR patients was 15 months. The estimated 1-year OS rate of all patients treated with HA protocol was 49.3% (±13.5%) and of only CR patients was 62.5% (±17.1%). Therefore, HA regimen is suitable for elderly patients with AML, and has relatively low toxicity and a reasonable response rate.[68]

Xu et al.[69] studied the effectiveness and toxicity of a regimen combining **1**, low-dose cytarabine, and granulocyte colony-stimulating factor (G-CSF) or GM-CSF (termed HAG regimen) in treating patients with relapsed or refractory AML, geriatric AML, and advanced MDS. Forty patients with AML or advanced MDS were treated with HAG regimen for remission induction and consolidation therapy. Twenty patients (50%) achieved CR, including 46.2% patients with relapsed or refractory AML, 60% elderly patients with primary AML who were either untreated or previously treated with only one course of induction therapy, and 66.7% patients with MDS-RAEB. After a follow-up of

6–47 (median 23) months from the date of remission, the median times of relapse-free survival and OS were 7.0 (±1.1) and 28 (±12.3) months, respectively. The most significant toxicity was myelosuppression. Incidences of infection and hemorrhage exceeding grade II were 43.8% and 37.5%, respectively. Nonhematological adverse effects were minimal. The HAG regimen was effective and well tolerated, and appears promising for the treatment of relapsed or refractory AML, geriatric AML, and advanced MDS.[69]

4.7.3 Phase II Study for CML[70,71]

In a phase II clinical trial, previously untreated patients with Ph-chromosome positive chronic phase CML were given HHT (**1**; 2.5 mg/m^2/day) and cytarabine (7.5 mg/m^2/day) together via continuous i.v. infusion for 7 days. If blood counts were adequate, drug cycles were repeated every 28 days, and the primary endpoint was the major cytogenetic response rate after 9 months. Forty of the 44 enrolled patients required reduction in the infusion duration during at least one cycle. Myelosuppression was common; 66% developed neutrophil count < 500/μL, but grade 3 infections occurred in only 7%. Thirty-six of 44 patients (82%) achieved a complete hematologic remission. Only 4 of the 23 patients (17%) having adequate cytogenetic response assessment achieved a major response within nine cycles. Thus, although HHT/cytarabine was generally well tolerated, the cytogenetic response rate did not exceed the level previously seen in patients with interferon-refractory CML and was not nearly as high as that associated with imatinib in newly diagnosed patients.[70]

Sensitization of leukemic cells with G-CSF can enhance the cytotoxicity of chemotherapy in AML; therefore, G-CSF priming was combined with low-dose chemotherapy to evaluate the effect in patients with relapsed and refractory AML. The drug regimen (termed G-HA) combined cytarabine at 7.5 mg/m^2/12 h by s.c. injection, days 1–14, HHT at 1.5 mg/m^2/day by i.v. continuous infusion, days 1–14, and G-CSF at 150 μg/m^2/day by s.c. injection, days 0–14. Thirty-six AML patients were enrolled, 23 refractory and 13 relapsed. Eighteen patients (50%, 95% confidence interval: 33–67%) achieved CR with a median CR duration of 7.2 months, and two elderly patients continued a regimen of maintenance therapy and remained in remission for 26.3 and 14.1 months, respectively, as of the last follow-up. Eight patients (22%) experienced neutropenia (median duration: 6 days; range: 2–22 days). Thirteen of the thirty six (36%) developed severe infections. Grade 1 and 2 nonhematologic toxicities were documented, including nausea and vomiting (20%), liver function abnormality (6%), and heart function abnormality (6%). No central nervous system or kidney toxicity was observed. The G-HA regimen was effective in remission induction for refractory and relapsed AML patients and well tolerated in maintenance therapy in some subgroups of elderly patients. Further studies are necessary to elucidate optimum dose and schedule for this regimen to enhance the treatment efficacy of relapsed or refractory AML patients.[71]

4.7.4 HHT Action for Adjuvant Arthritis Rats[72]

Feng et al.[72] studied the effect of HHT (**1**) on levels of substance P (SP), IL-1β, and tumor necrosis factor (TNF)-α in adjuvant arthritis rats. *Tripterygium wilfordii* polycoside was the positive control. The levels of TNF-α and IL-1β in the serum and synovial membrane decreased and the amounts of SP in the plasma and synovial membrane were suppressed by drug treatment. Thus, HHT exerts anti-inflammatory effects by reducing the levels of TNF-α and IL-1β in the serum and synovial membrane, as well as inhibiting the secretion and release of SP in the plasma and synovial membrane.[72]

4.8 CONCLUSION

Cephalotaxus alkaloids have unique structures and show strong antileukemic activity. Subsequent to our prior review,[1] many alkaloids have been isolated from natural sources and many new synthetic

methodologies developed to prepare both the natural compounds and structurally related analogs for structure–cytotoxicity relationship studies. Notably, HHT (**1**) has been found to be a promising chemotherapeutic agent against myeloid leukemia. Mechanistic studies and combination chemotherapy with other drugs against multidrug-resistant leukemia cells have been investigated.

ACKNOWLEDGMENTS

The authors thank Prof. K. Takeya and Dr. S. Morris-Natschke for their valuable suggestions. Thanks are also due to partial support from National Cancer Institute, NIH Grant No. CA17625-32 awarded to K.H. Lee and also in part to the Taiwan Department of Health, China Medical University Hospital Cancer Research Center of Excellence (DOH100-TD-C-111-005).

REFERENCES

1. This is a revised and updated version of the chapter published in the first edition: Itokawa, H., Wang, X. and Lee, K.H., Homoharringtonine and related compounds, chap. 4, in *Anticancer Agents from Natural Products*, Cragg, G.H., Kingston, D.G.I. and Newman, D.J., Eds., CRC Press, Boca Raton, FL, 2005, 47–70.
2. Huang, C.C., Han, C.S., Yue, X.F., Shen, C.M., Wang, S.W., Wu, F.G. and Xu, B.., Cytotoxicity and sister chromatid exchanges induced in vitro by six anticancer drugs developed in the People's Republic of China, *J. Natl. Cancer Inst*., 71, 841, 1983.
3. Grem, J.L., Cheson, B.D., King, S.A., Leyland-Jones, B. and Suffness, M., *Cephalotaxine* esters: antileukemic advance or therapeutic failure? *J. Natl. Cancer Inst*., 80, 1095, 1988.
4. Paudler, W.W., Kerley, G.I. and McKay, J., The alkaloids of *Cephalotaxus drupacea* and *Cephalotaxus fortunei*, *J. Org. Chem*., 28, 2194, 1963.
5. Delfel, N.E., Alkaloid distribution and catabolism in *Cephalotaxus harringtonia*, *Phytochemistry*, 19, 403, 1980.
6. Spencer, G.F., Plattner, R.D. and Powell, R.G., Quantitative gas chromatography and gas chromatography-mass spectrometry of *Cephalotaxus* alkaloids, *J. Chromatogr*., 120, 335, 1976.
7. Abraham, D.J., Rosenstein, R.D. and McGandy, E.L., Single crystal X-ray structures of chemotherapeutic agents II, the structure of cephalotaxine methiodide, *Tetrahedron Lett.*, 4081, 1969.
8. Powell, R.G., Weisleder, D., Smith, C.R., Jr. and Wolff, I.A., Structure of cephalotaxine and related alkaloids. *Tetrahedron Lett.*, 4081, 1969.
9. Powell, R.G., Weisleder, D. and Smith, C.R., Antitumor alkaloids from *Cephalotaxus harringtonia:* structure and activity, *J. Pharm. Sci*., 61, 1227, 1972.
10. Powell, R.G., Weisleder, D., Smith, C.R., Jr. and Rohwedder, W.K., Structures of harringtonine, isoharringtonine, and homoharringtonine, *Tetrahedron Lett.*, 815, 1970.
11. Mikolajczak, K.L., Powell, R.G. and Smith, C.R., Deoxyharringtonine, a new antitumor alkaloid from *Cephalotaxus*. Structure and synthetic studies, *Tetrahedron*, 28, 1995, 1972.
12. Powell, R.G., Madrigal, R.V., Smith, C.R., Jr. and Mikolajczak, K.L., Alkaloids of *Cephalotaxus harringtonia* var *drupacea* 11-hydroxycephalotaxine and drupacine, *J. Org. Chem.*, 39, 676, 1974.
13. Powell, R.G. and Mikolajczak, K.L., Desmethylcephalotaxinone and its correlation with cephalotaxine, *Phytochemistry*, 12, 2987, 1973.
14. Smith, C.R., Jr., Mikolajczak, K.L. and Powell, R.G., Harringtonine and related cephalotaxine esters, in *Anticancer Agents Based on Natural Product Models, Medicinal Chemistry,* Vol. 16, Cassady, J.M. and Douros, J.D., Eds., Academic Press, New York, NY, 1980, 391.
15. Kantarjian, H.M., Talpaz, M., Santini, V., Murgo, A., Cheson, B. and O'Brien, S.M., Homoharringtonine: history, current research, and future directions, *Cancer*, 92, 1591, 2001.
16. Mei, W., Wu, J. and Dai, H., Advances in studies on chemical constituents in plants of *Cephalotaxus Sieb. et Zucc.* and their pharmacological activities, *Chin. Trad. Herbal Drugs*, 37, 452, 2006.
17. Lin, W., Chen, R.T. and Xue, Z., Studies on the minor alkaloids of *Cephalotaxus fortunei* Hook, *Acta Pharm. Sin.*, 20, 283, 1985.
18. Wang, D.Z., Ma, G.E. and Xu, R.S., Studies on alkaloids of *Cephalotaxus* VII. Studies and semi-synthesis of two anticancer cephalotaxine esters, *Acta Pharm. Sin.*, 27, 173, 1992.
19. Mamadou, B., Akino, J. and Bernard, B., New alkaloids from *Cephalotaxus fortunei*, *J. Nat. Prod.*, 66, 152. 2003.

20. Xue, Z., Xu, L.Z., Chen, D.H. and Huang, L., Studies on the minor alkaloids of *Cephalotaxus hainanensis* Li, *Yao Xue Xue Bao*, 16, 752, 1981.
21. Ren, L.J. and Xue, Z., Studies on the antitumor constituents of *Cephalotaxus sinensis* (Rehd. et Wils.) Li, *Chin. Trad. Herbal Drugs*, 12, 1, 1981.
22. Wang, L.W., Su, H.J., Yang, S.Z., Won, S.J. and Lin, C.N., New alkaloids and a tetraflavonoid from *Cephalotaxus wilsoniana, J. Nat. Prod*., 67, 1182, 2004.
23. Du, J., Qin, M.H. and Nie, R.L., Two new lactones from *Cephalotaxus fortunei* var. *alpinia*, *J. Nat. Prod.*, 62, 1664, 1999.
24. Takano, I., Yasuda, I., Nishijima, M., Hitotsuyanagi, Y., Takeya, K. and Itokawa, H., Alkaloids from *Cephalotaxus harringtonia, Phytochemistry,* 43, 299, 1996.
25. Takano, I., Yasuda, I., Nishijima, M., Hitotsuyanagi, Y., Takeya, K. and Itokawa, H., Drupangtonine, a novel antileukemic alkaloid from *Cephalotaxus harringtonia* var. *drupacea, Bioorg. Med. Chem. Lett.*, 6, 1689, 1996.
26. Takano, I., Yasuda, I., Nishijima, M., Hitotsuyanagi, Y., Takeya, K. and Itokawa, H., New *Cephalotaxus* alkaloids from *Cephalotaxus harringtonia* var. *drupacea, J. Nat. Prod.*, 59, 965,1996.
27. Takano, I., Yasuda, I., Nishijima, M., Hitotsuyanagi, Y., Takeya, K. and Itokawa, H., New oxygenated *Cephalotaxus* alkaloids from *Cephalotaxus harringtonia* var. *drupacea*, *J. Nat. Prod.*, 59, 1192, 1996.
28. Takano, I., Yasuda, I., Nishijima, M., Hitotsuyanagi, Y., Takeya, K. and Itokawa, H., Cephalotaxidine, a novel dimeric alkaloid from *Cephalotaxus harringtonia* var. *drupacea, Tetrahedron Lett.,* 37, 7053, 1996.
29. Takano, I., Yasuda, I., Nishijima, M., Hitotsuyanagi, Y., Takeya, K. and Itokawa, H., Ester-type *Cephalotaxus* alkaloids from *Cephalotaxus harringtonia* var. *drupacea, Phytochemistry,* 44, 735, 1997.
30. Morita, H., Arisaka, M., Yoshida, N. and Kobayashi, J., Cephalezomines A–F, potent cytotoxic alkaloids from *Cephalotaxus harringtonia* var. *nana*, *Tetrahedron*, 56, 2929, 2000.
31. Morita, H., Yoshinaga, M. and Kobayashi, J., Cephalezomines G, H, J, K, L, and M, new alkaloids from *Cephalotaxus harringtonia* var. *nana, Tetrahedron*, 58, 5489, 2002.
32. Kobayashi, J., Yoshinaga, M. and Yoshida, N., Cephalocyclidine A, a novel pentacyclic alkaloid from *Cephalotaxus harringtonia* var. *nana*, *J. Org. Chem.*, 67, 2283, 2002.
33. Yoshinaga, M., Morita, H., Dota, T. and Kobayashi, J., Bis-cephalezomines A–E from *Cephalotaxus harringtonia* var. *nana, Tetrahedron*, 60, 7861, 2004.
34. Taniguchi, T., Yokoyama, S. and Ishibashi, H., Asymmetric total synthesis and revised structure of cephalezomine H, *J. Org. Chem.,* 74, 7592, 2009.
35. Ancliff, R.A., Russell, A.T. and Sanderson, A.J., Synthesis of the ester side chains of some potently antileukemic harringtonia alkaloids from chiral citrate, *Chem. Commun.*, 3243, 2006.
36. Berhal, F., Tardy, S., Perard-Viret, J. and Royer, J., Synthesis of optically active monoacid side-chains of *Cephalotaxus* alkaloids, *Eur. J. Org. Chem.*, 437, 2009.
37. Keller, L., Duma, F. and Angelo, J.D., Enantioselective synthesis of the ester side chain of homoharringtonine, *Eur. J. Org. Chem.*, 2488, 2003.
38. El Bialy, S.A.A., Braun, H. and Tietze, L.F., Enantioselective synthesis of α-alkylmalates as the pharmacophoric group of several natural alkaloids and glycosides, *Eur. J. Org. Chem.*, 2965, 2005.
39. Huang, P.Q. and Li, Z.Y., Asymmetric synthesis of (S)-homocitric acid lactone, *Tetrahedron Asymmetry,* 16, 3367, 2005.
40. Eckelbarger, J.D., Wilmot, J.T. and Gin, D.Y., Strain-release rearrangement of N-vinyl-2-arylaziridines. Total synthesis of the anti-leukemia alkaloid (−)-deoxyharringtonine, *J. Am. Chem. Soc.*, 128, 10370, 2006.
41. Eckelbarger, J.D., Wilmot, J.T., Epperson, M.T., Thakur, C.S., Shum, D., Antczak, C., Tarassishin, L., Djaballah, H. and Gin, D.Y., Synthesis of antiproliferative *Cephalotaxus* esters and their evaluation against several human hepatopoietic and solid tumor cell lines: uncovering differential susceptibilities to multidrug resistance, *Chem. Eur. J.*, 14, 4293, 2008.
42. Schmelhack, M.F., Chong, B.P., Stauffer, R.D., Rogerson, T.D., Chong, A. and Jones, L.D., Total synthesis of the *Cephalotaxus* alkaloids. Problem in nucleophilic aromatic substitution, *J. Am. Chem. Soc.*, 97, 2507, 1975.
43. Hudlicky, T., Kwart, L.D. and Reed, J.W., Synthesis of cephalotaxine alkaloids, chap. 5, in *Alkaloids: Chemical and Biological Perspectives*, Vol. 5, Pelletier, S.W., Ed., John Wiley & Sons, New York, 1987, 639–690.
44. Hudlicky, T. and Reed, J.W., Cephalotaxus alkaloids, in *The Way of Synthesis: Evolution of Design and Methods for Natural Products*, Part 4.5, Wiley-VCH, Weinheim, 2007, 655–687.

45. Hiranuma, S., Shibata, M. and Hudlicky, T. Studies in cephalotaxus alkaloids. Stereospecific total synthesis of homoharringtonine, *J. Org. Chem.*, 48, 5321, 1983.
46. Hameed, A., Blake, A.J. and Hayes, C.J., A second generation formal synthesis of (−)-cephalotaxine, *J. Org. Chem.*, 73, 8045, 2008.
47. Esmieu, W.R., Worden, S.M., Catterick, D., Wilson, C. and Hayes, C.J., A formal synthesis of (−)-cephalotaxine, *Org. Lett.*, 10, 3045, 2008.
48. Taniguchi, T. and Ishibashi, H., Short synthesis of (−)-cephalotaxine using a radical cascade, *Org. Lett.*, 10, 4129, 2008.
49. Sun, M.R., Lu, H.T., Wang, Y.Z., Yang, H. and Liu, H.M., Highly efficient formal synthesis of cephalotaxine, using the Stevens rearrangement-acid lactonization sequence as a key transformation, *J. Org. Chem.*, 74, 2213, 2009.
50. Zhao, Y.M., Gu, P., Zhang, H.J., Zhang, Q.W, Fan, C.A., Tu, Y.Q. and Zhang, F.M., Formal syntheses of (±)-stemonamine and (±)-cephalotaxine, *J. Org. Chem.*, 74, 3211, 2009.
51. Guo, J., Present status of studies on the biosynthesis of *Cephalotaxus* alkaloids, *Zhongcaoyao*, 15, 367, 1984.
52. Gitterman, A., Parry, J., Dufresne, R.F., Sternbach, D.D. and Cabelli, M.D., Biosynthesis of the *Cephalotaxus* alkaloids. Investigations of the biosynthesis of deoxyharringtonine, isoharringtonine, and harringtonine, *J. Am. Chem. Soc.*, 102, 2074, 1980.
53. Parry, R.J. and Schwab, J.M., Biosynthesis of *Cephalotaxus* alkaloids. I. Novel mode of tyrosine incorporation into cephalotaxine, *J. Am. Chem. Soc.*, 97, 2555, 1975.
54. Parry, R.J., Biosynthesis of the *Cephalotaxus* alkaloids, *Recent Adv. Phytochem.*, 13, 55, 1979.
55. Parry, R.J., Sternbach, D.D. and Cabelli, M.D., Biosynthesis of *Cephalotaxus* alkaloids. 2. Biosynthesis of the acyl portion of deoxyharringtonine, *J. Am. Chem. Soc.*, 98, 6380, 1976.
56. Parry, R.J., Chang, M.N.T., Schwab, J.M. and Foxman, B.M., Biosynthesis of the *Cephalotaxus* alkaloids. Investigations of the early and late stages of cephalotaxine biosynthesis, *J. Am. Chem. Soc.*, 102, 1099, 1980.
57. Schwab, J.M., Chang, M.N.T. and Parry, R.J., Biosynthesis of *Cephalotaxus* alkaloids. 3. Specific incorporation of phenylalanine into cephalotaxine, *J. Am. Chem. Soc.*, 99, 2368, 1977.
58. Legros, L., Hayette, S., Nicolini, F.E., Raynaud, S., Chabane, K., Magaud, J.P., Cassuto, J.P. and Michallet, M., BCR-ABLT315I transcript disappearance in an imatinib-resistant CML patient treated with homoharringtonine: a new therapeutic challenge? *Leukemia*, 21, 2204, 2007.
59. Seigel, G.M., Hackam, A.S., Gangly, A., Mandel, L.M. and Gonzalez-Fernandes, F., Human embryonic and neuronal stem cell markers in retinoblastoma, *Mol. Vis.*, 13, 823, 2007.
60. Meng, H., Yang, C., Jin, J., Zhou, Y. and Qian, W., Homoharringtonine inhibits the AKT pathway and induces in vitro and in vivo cytotoxicity in human multiple myeloma cells, *Leuk. Lymphoma*, 49, 1954, 2008.
61. Li, B., Zhuang, W., Chen, P. and Fu, J., Effects of RNA interference targeting hypoxia-inducible factor-1α (HIF-1α) on chemosensitivity of leukemia K562 cells towards homoharringtonine, *Aizheng,* 27, 723, 2008.
62. Kuroda, J., Kamitsuji, Y., Kimura, S., Ashihara, E., Kawata, E., Nakagawa, Y., Takeuichi, M., Murotani, Y., Yokota, A., Tanaka, R., Andreeff, M., Taniwaki, M. and Maekawa, T., Anti-myeloma effect of homoharringtonine with concomitant targeting of the myeloma-promoting molecules, Mcl-1, XIAP, and β-catenin, *Int. J. Hematol.*, 87, 507, 2008.
63. Tong, H., Ren, Y., Zhang, F. and Jin, J., Homoharringtonine affects the JAK2-STAT5 signal pathway through alteration of protein tyrosine kinase phosphorylation in acute myeloid leukemia cells, *Eur. J. Haematol.,* 81, 259, 2008.
64. Xiao, Z., Xue, H., Li, R., Zhang, L., Yu, M. and Hao, Y., The prognostic significance of leukemic cells clearance kinetics evaluation during the initial course of induction therapy with HAD (homoharringtonine, cytosine arabinoside, daunorubicin) in patients with de novo acute myeloid leukemia, *Am. J. Hematol.,* 83, 203, 2008.
65. Cai, Y.X., Meng, F.Y., Sun, Q.X., Fu, Y.B. and Li, L., In vitro effect of bortezomib alone or in combination with harringtonine or arsenic trioxide on proliferation and apoptosis of multidrug resistant leukemia cells, *Zhonghua Xueyexue Zazhi*, 29, 737, 2008.
66. Quintas-Cardama, A. and Cortes, J., Homoharringtonine for the treatment of chronic myelogenous leukemia, *Expert Opin. Pharmacother.,* 9, 1029, 2008.
67. Quintas-Cardama, A. and Cortes, J., Omacetaxine mepesuccinate—a semisynthetic formulation of the natural antitumoral alkaloid homoharringtonine, for chronic myelocytic leukemia and other myeloid malignancies, *IDrugs*, 11, 356, 2008.

68. Wang, J., Lu, S., Yang, J., Song, X., Chen, L., Huang, C., Hou, J. and Zhang, W., A homoharringtonine-based induction regimen for the treatment of elderly patients with acute myeloid leukemia: a single center experience from China, *J. Hematol. Oncol.,* 2, 32, 2009.
69. Xu, J., Xu, C., Liu, T., Xiang, B., Chang, H. and He, C., A clinical trial for homoharringtonine and low-dose cytosine arabinoside combined with G-CSF or GM-CSF to treat the relapsed or refractory acute myeloid leukemia (AML), geriatric AML and advanced myelodysplastic syndromes, *Sichuan Daxue Xuebao, Yixueban*, 40, 129, 2009.
70. Stone, R.M., Donohue, K.A., Stock, W., Hars, V., Linker, C.A., Shea, T., DeAngelo, D.J., Marcucci, G., Bloomfield, C.D., and Larson, R.A., Cancer and Leukemia Group B, A phase II study of continuous infusion homoharringtonine and cytarabine in newly diagnosed patients with chronic myeloid leukemia: CALGB study 19804, *Cancer Chemother. Pharmacol.*, 63, 859, 2009.
71. Zhang, W.G., Wang, F.X., Chen, Y.X., Cao, X.M., He, A.L., Liu, J., Ma, X.R. Zhao, W.H., Liu, S.H., and Wang, J.L., Combination chemotherapy with low-dose cytarabine, homoharringtonine, and granulocyte colony-stimulating factor priming in patients with relapsed or refractory acute myeloid leukemia, *Am. J. Hematol.*, 83, 185, 2008.
72. Feng, H., Kang, H., Song, X., Wu, L., Sun, W. and Dai, Q., Experimental study on effect of homoharringtonine on SP, IL-1β and TNF-α in rats of adjuvant arthritis, *Zhejiang Zhongyiyao Daxue Xuebao*, 32, 726, 2008.

5 Podophyllotoxins and Analogs*

Kuo-Hsiung Lee and Zhiyan Xiao

CONTENTS

5.1 Introduction 95
5.1.1 Discovery of Podophyllotoxins 96
5.1.2 Development of Etoposide and Teniposide 96
5.2 Isolation and Characterization 97
5.3 Biological Activities and Mechanisms of Action 98
5.3.1 Biological Activities 98
5.3.2 Antineoplastic Mechanisms 99
5.3.2.1 Inhibition of Tubulin Polymerization 99
5.3.2.2 Inhibition of DNA Topo II 99
5.3.2.3 Induction of Apoptosis 99
5.4 Biosynthesis 100
5.4.1 Biosynthesis of Podophyllotoxin and Analogs 100
5.4.1.1 Biosynthetic Pathway to Deoxypodophyllotoxin 100
5.4.1.2 Biosynthetic Relationships among Podophyllotoxin Analogs 101
5.4.2 Biotechnological Sources for Podophyllotoxin Analogs 101
5.5 Synthesis and Structure–Activity Studies 102
5.5.1 Synthetic Efforts toward Podophyllotoxin and Analogs 103
5.5.1.1 General Approaches for Total Synthesis 103
5.5.1.2 Chemical Derivatization for Key Analogs 104
5.5.2 Structure–Activity Studies 106
5.5.2.1 General Structure Antineoplastic Activity Relationships 107
5.5.2.2 Molecular Area-Oriented Analog Syntheses 109
5.5.2.3 SAR Models 113
5.6 Preclinical Development 114
5.7 Clinical Development 115
5.8 Conclusions 115
Acknowledgment 116
References 116

5.1 INTRODUCTION

Podophyllotoxins represent an important class of natural products in the armamentarium of antineoplastic agents. Extensive investigations on podophyllotoxins were initialized by the biological assessment of podophyllotoxin (**1**) and the discovery of its mode of action, and culminated in the synthesis and development of the clinically efficacious anticancer drugs, etoposide (**2**) and teniposide (**3**) (Figure 5.1). The long itinerary from podophyllotoxin to etoposide and teniposide exemplifies the

* Antitumor Agents 277.

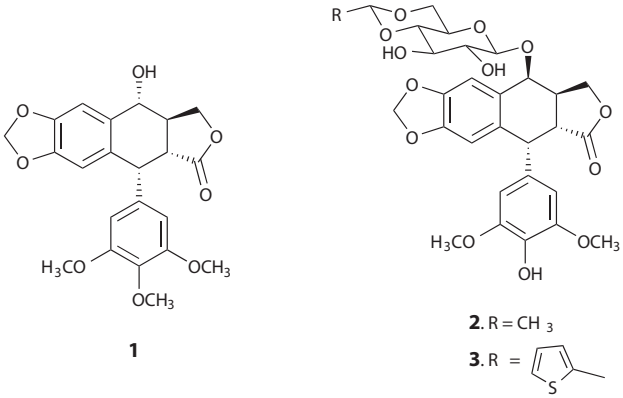

FIGURE 5.1 The structures of podophyllotoxin (**1**), etoposide (**2**), and teniposide (**3**).

fascinating approach to develop clinically useful anticancer drugs from natural product prototypes through chemical modifications. It is particularly distinctive that a radical change in the mechanism of action resulted from the structural modifications of podophyllotoxin. Today several new podophyllotoxin analogs have emerged as potential anticancer drugs, and continue to encourage an enthusiastic pursuit of novel cancer chemotherapeutic agents from podophyllotoxin analogs. Numerous reviews related to these analogs have appeared in the literature. Some recent contributions have provided comprehensive updates on various aspects of this compound class.[1–5] In this chapter, we aim to highlight recent development and accentuate critical features of these analogs.

5.1.1 Discovery of Podophyllotoxins

It has been known for centuries that the genus *Podophyllum* (Podophyllaceae), including American *Podophyllum peltatum* Linnaceus and Indian or Tibetan *Podophyllum emodi* Wall. (syn. *Podophyllum hexandrum* Royle), possesses medicinal properties. *Podophyllum* plants have long been valued for their cathartic and cholagogue properties by the indigenous populations of North America and the Himalayas. Podophyllin, the alcoholic extract of *Podophyllum* rhizome, was listed in the first American Pharmacopeia (1820), and was later introduced into the European Pharmacpeias. However, it was removed from the U.S. Pharmacopeia in 1942 due to its undesirable toxicity.[6]

In the same year, Kaplan demonstrated curative effects of podophyllin on the benign tumor *condylomata acuminata*,[7] which rekindled interest in *Podophyllum* plants and stimulated intensive studies on the action mode and chemical constituents of podophyllin. In 1946, it was first reported that podophyllin showed toxic effects against dividing cells in a manner similar to that of colchicine, the classic antimicrotubule agent.[8] Later, the major constituent podophyllotoxin was observed to inhibit assembly of the mitotic spindle.[9] Other podophyllotoxin compounds were also reported to induce cell cycle arrest at mitosis.[10] Both podophyllin and podophyllotoxin exhibited destructive effects on mice tumors,[11] which raised hopes for their use in the treatment of malignant tumors. However, the zeal in developing podophyllotoxin as cancer chemotherapy was tempered by its unacceptable side-effects, particularly gastrointestinal toxicity.[12] Although podophyllotoxin failed to offer a direct therapeutic application, the pioneer work provided a natural prototype and eventually led to the serendipitous discovery of the hemisynthetic anticancer drugs, etoposide and teniposide.

5.1.2 Development of Etoposide and Teniposide

The tortuous path leading from *Podophyllum* plants to podophyllotoxin and eventually to etoposide and teniposide involves numerous studies conducted over a period of more than a century and

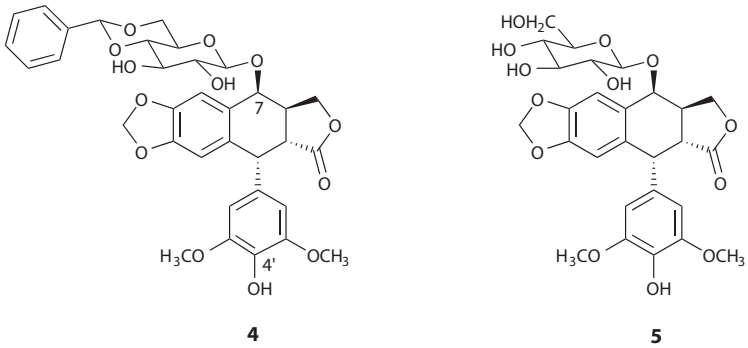

FIGURE 5.2 The structures of epipodophyllotoxin glycosides, DEPBG (**4**), and DEPG (**5**).

represents a successful example of developing clinically useful drugs from natural sources. The story was described retrospectively by the investigators themselves.[13]

In the early 1950s, scientists in Sandoz, Ltd. assumed that, in analogy to cardiac glycosides, podophyllotoxin glycosides might exhibit pharmacological profiles superior to those of the aglycone. This assumption stimulated extensive efforts to acquire both natural and synthetic *Podophyllum* glycosides, and led to the development and commercialization of SP-G, the condensation products of the crude *Podophyllum* glycoside fraction with benzaldehyde in 1963. A highly active "antileukemia factor" was later isolated as a minor component (<0.25%) from SP-G by close chemical and biological collaboration. This component could significantly inhibit cell proliferation *in vitro* and considerably prolong the survival time of leukemic mice at low doses. It was identified as 4′-*O*-demethyl-epipodophyllotoxin benzylidene β-D-glucoside (DEPBG; **4**) with unique structural features of a free phenolic hydroxyl group at C4′ and an epi configuration at C7 (Figure 5.2). Subsequent synthetic efforts to condense 4′-*O*-demethyl-epipodophyllotoxin glucoside (DEPG; **5**) with various aldehydes and ketones led to the discovery of etoposide (**2**) and teniposide (**3**) in the late 1960s.[13] Etoposide was approved for the treatment of testicular cancer by the FDA in 1983, and teniposide was brought into the U.S. market in 1992. These drugs are currently used against a variety of cancers, including small-cell lung cancer, testicular cancer, lymphoma, leukemia, and Kaposi's sarcoma.[14]

5.2 ISOLATION AND CHARACTERIZATION

Podophyllotoxin (**1**), the major constituent of podophyllin, was first isolated in 1880.[15] Not until the 1930s was its empirical formula determined as $C_{22}H_{22}O_8$.[16] The correct structure and configuration of podophyllotoxin were later established by chemical methods,[17,18] and confirmed by total synthesis[19] and resolution of the crystal structure of the 2′-bromo derivative.[20] Structurally, podophyllotoxin belongs to the class of aryltetralinlactone cyclolignans, in which two phenylpropanoid (C_6–C_3) units assemble into a carbocycle through two single carbon–carbon bonds (C2–C7′, C8–C8′) and a lactone is created with oxygen incorporation (Table 5.1). As represented in Table 5.1, the structure of podophyllotoxin is characterized by its unique configurations at the four asymmetric centers (C7, C8, C7′, and C8′), the highly strained *trans*-lactone ring, and the abundance of oxygen atoms. The molecule skeleton contains five rings and is a relatively rigid system in which the methylenedioxy ring A, tetrahydronaphthalene rings B and C, and lactone ring D compose a four-ring pseudoplane, to which the pendent aryl ring E is attached pseudo-axially at C7′.

Besides podophyllotoxin, other structurally related lignans, including deoxypodophyllotoxin, 4′-demethylpodophyllotoxin, 4′-demethylepipodophyllotoxin, α-peltatin, β-peltatin (Table 5.1), and their corresponding glycosides, were also isolated from *Podophyllum* species.[11,18] Podophyllotoxin lignans further extend to D ring stereochemical variants of picro (8R, 8′S),[21] iso (8S, 8′S),[22] and isopicro (8S, 8′R)[23] derivatives (Table 5.1).

TABLE 5.1
Chemical Structures of Main Podophyllotoxin Analogs

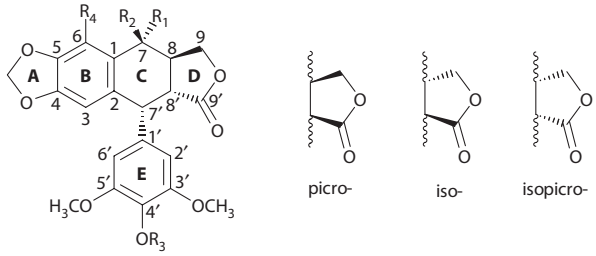

	R_1	R_2	R_3	R_4
Podophyllotoxin	OH	H	CH_3	H
Deoxypodophyllotoxin	H	H	CH_3	H
4′-Demethylpodophyllotoxin	OH	H	H	H
4′-Demethylepipodophyllotoxin	H	OH	H	H
α-Peltatin	H	H	H	OH
β-Peltatin	H	H	CH_3	OH

The podophyllotoxins and analogs are found not only in the Podophyllaceae family, and related lignans have been also isolated from other genera, such as *Jeffersonia*, *Diphylleia,* and *Dysosma* (Berberidaceae), *Catharanthus* (Apocynaceae), *Polygala* (Polygalaceae), *Anthriscus* (Apiaceae), *Linun* (Linaceae), *Hyptis* (Verbenaceae), *Teucrium*, *Nepeta* and *Thymus* (Labiaceae), *Thuja*, *Juniperus*, *Callitris* and *Thujopsis* (Cupressaceae), *Cassia* (Fabaceae), *Haplophyllum* (Rutaceae), *Commiphora* (Burseraceae), and *Hernandia* (Hernandiaceae).[24]

5.3 BIOLOGICAL ACTIVITIES AND MECHANISMS OF ACTION

5.3.1 Biological Activities

Antineoplastic and antiviral properties are undoubtedly the most pronounced pharmacological effects of podophyllotoxin analogs. Although podophyllotoxin was reported to exhibit antimitotic activity and antitumor activity in animals,[11] therapeutic applications of podophyllotoxin analogs as anticancer drugs were not possible until the development of etoposide and teniposide, which not only showed good clinical effects against several types of neoplasms, but also prompted an active pursuit of new anticancer therapies extending for decades.[1–5] Podophyllotoxin is widely used as an antiviral agent for the treatment of *condyloma acuminatum* caused by human papilloma virus (HPV), and is regarded as the most effective cure for venereal, perianal, and other genital warts.[24] Podophyllotoxin analogs were also found to be active against herpes simplex virus type 1/2 (HSV-1, HSV-2), measles virus, Sindbis virus, murine cytomegalovirus, and vesicular stomatitis virus.[1,4] Notably, it has been reported recently that podophyllotoxin analogs act as inhibitors of human immunodeficiency virus (HIV) replication.[25–27]

As an important class of bioactive compounds, podophyllotoxin analogs exhibit a rich variety of biological activities. Besides their therapeutic utility in cancer chemotherapy and viral infection, podophyllotoxin analogs also show anti-inflammatory[28] and immunomodulatory[29] effects, and are potentially useful in the treatment of rheumatoid arthritis, malaria, Alzheimer's disease,[30] and psoriasis vulgaris.[31]

The diverse pharmaceutical effects demonstrated by podophyllotoxin analogs suggest heterogeneous mechanisms of action. However, for most biological activities, the underlying molecular mechanisms are still elusive and scattered evidence often implies divergent mechanisms. For

example, the antiviral effect of podophyllotoxin analogs seems to associate with disparate mechanisms, including disruption of the cellular cytoskeleton,[32] inhibition of reverse transcriptase,[33] and inhibition of integrase.[34] It was also reported recently that podophyllotoxin inhibits E2/E7 interaction of human papillomavirus (HPV) by binding to the hinge domain of E2.[35] Herein, we will focus our discussion on the antineoplastic mechanisms, which are mostly relevant to the theme of this monograph and most extensively studied.

5.3.2 Antineoplastic Mechanisms

Primary molecular mechanisms responsible for the antineoplastic activities of podophyllotoxin analogs include preventing the assembly of tubulin into microtubules, inhibiting the catalytic activity of DNA topoisomerase II (topo II), and inducing apoptosis, although other mechanisms, in some cases still ambiguous, are also involved.

5.3.2.1 Inhibition of Tubulin Polymerization

As early as 1947, it was reported that podophyllotoxin inhibits assembly of the mitotic spindle and induces cell cycle arrest at mitosis.[9] It was later found to bind tubulin, the fundamental monomeric protein subunit of microtubules, at the same binding site as colchicine. Podophyllotoxin and colchicine bind to tubulin with similar affinity, but podophyllotin binds more rapidly and its binding is reversible, while that of colchicine is irreversible.[36]

The microtubule network forms a vital part of the cytoskeleton in eukaryotic cells and plays an important role in mitosis. Microtubules are highly dynamic structures with tubulin monomers constantly added on at one end, and disassociated from the other end. Podophyllotoxin reversibly binds to tubulin, disturbs the dynamic equilibrium between the assembly and disassembly of microtubules, and eventually causes mitotic arrest.[37]

Most *Podophyllum* compounds, including the acetal products of podophyllotoxin glucosides, and peltatins, share this mechanism of action.[38–41] Upon treatment with these compounds, cells can still enter mitosis and undergo a normal pro-phase, but the separation of chromosomes is blocked due to the inhibition of mitotic spindle formation. An accumulation of cells with clumped chromosomes in metaphase characterizes the cytotoxic properties of these compounds.

5.3.2.2 Inhibition of DNA Topo II

Unlike podophyllotoxin, etoposide prevents the entry of cells into mitosis rather than trapping cells in metaphase. Time course analysis with etoposide in tissue culture showed that the disappearance of mitoses begins less than 1 h after drug addition.[42] This observation implies that the compound acts in late S or G_2 phase of the cell cycle, which is the checkpoint for DNA damage or DNA replication, rather than spindle assembly. Indeed, etoposide shows little effects on tubulin polymerization. However, fragmentation of DNA in HeLa cells was observed upon treatment with etoposide.[43–45] It was not recognized until the 1980s that the ability of etoposide to induce DNA breaks was mediated by DNA topo II.[46]

DNA topoisomerases are ubiquitous enzymes that control the topological state of DNA. Topo II catalyzes the cleavage and religation of double-strand DNA.[47] Etoposide stabilizes the covalent DNA–enzyme cleavable complex, inhibits the catalytic activity of topo II, and induces topo II-mediated DNA breakage. These actions convert the essential enzyme into a cellular poison, trigger cascade reactions, and eventually lead to cell death.[48] The topo II inhibition mechanism is shared by etoposide, teniposide, and other therapeutically important 4′-*O*-demethylepipodophyllotoxins (DMEPs).

5.3.2.3 Induction of Apoptosis

Apoptosis is the process of programmed cell death and is well characterized by morphological and biochemical features.[49] Induction of apoptosis appears to be a common mechanism for cancer chemotherapeutic agents, including topo II inhibitors and microtubule damaging agents.

Podophyllotoxin analogs were reported to induce cancer cell death with signs of apoptosis. GL-331, a C7-modified 4′-demethyl epipodophyllotoxin, could increase cellular protein tyrosine phosphatase (PTP) activity significantly and in addition, GL-331-induced internucleosomal cleavage was efficiently prevented by two PTP inhibitors, but not by an inhibitor of serine/theronine phosphatase.[50] Abnormal activation of cyclin B-associated CDC 2 kinase was noted after treatment with etoposide or GL-331 in various cancer cells. GL-331 treatment in NPC-TW01 cells also increased CDC 25A phosphatase activity, and facilitated the association of CDC 25A with Raf-1. Apoptotic DNA fragmentation induced by GL-331 was inhibited by treatment with cyclin B1-specific antisense oligonucleotides.[51]

Podophyllotoxin induced apoptosis in human leukemic (HL-60) cells. It was suggested that the activation of caspases 3, 8, and 9, Bcl-2 hyperphosphorylation, and increased leakage of cytochrome *c* from mitochondria into cytosolic fraction may be responsible for the apoptosis observed. It was further demonstrated by a c-jun *N*-terminal kinase (JNK)-specific antisense oligonucleotide experiment that activation of the JNK signaling pathway may play an important role in the induced Bcl-2 phosphorylation and apoptosis.[52]

Other pathways, such as p53-dependent pathway[53] and Bax-dependent pathway[54] might also be involved in the apoptosis induced by podophyllotoxin analogs.

5.4 BIOSYNTHESIS

Traditionally, podophyllotoxin serves as a starting material for the semisynthesis of etoposide, teniposide, and other podophyllotoxin derivatives/analogs under development as potential anticancer drugs. At present, the commercial source for podophyllotoxin relies on plants of the *Podophyllum* genus; however, these endangered species grow in remote regions and so the natural resource is becoming increasingly scarce. While total synthesis of podophyllotoxin and its analogs has been accomplished, it is not a feasible substitute source because of the tremendous chemical efforts required and the low overall yield produced (cf. Section 5.5). Therefore, a search for an alternative approach is imperative. Biosynthesis is one attractive option and could provide sustainable production of podophyllotoxin in an economical way.

5.4.1 Biosynthesis of Podophyllotoxin and Analogs

Although the biosynthetic pathway to podophyllotoxin and analogs has not been fully elucidated to date, tracer labeling studies in *Podophyllum*, *Linum*, and *Forsythia* species (Oleaceae) have defined some key biochemical steps and precursors in the biosynthesis of podophyllotoxin and analogs, and enzymology studies have revealed the enzymes responsible for individual bioconversions as well as proteins and encoding genes involved. The biosynthetic relationships among several natural podophyllotoxin analogs have also been delineated by feeding experiments.

5.4.1.1 Biosynthetic Pathway to Deoxypodophyllotoxin

The biosynthesis of podophyllotoxin and analogs originates from phenylalanine via the "general phenylpropanoid pathway," where phenylalanine is converted to coniferyl alcohol (**6**) by various enzymes.[55,56] A hypothetical biosynthetic pathway from two molecules of coniferyl alcohol to deoxypodophyllotoxin, a precursor for podophyllotoxin analogs, is illustrated in Figure 5.3. (+)-Pinoresinol (**7**) is obtained exclusively through stereoselective bimolecular phenoxy radical coupling of coniferyl alcohol catalyzed by pinoresinol synthase (PS), which contains both a radical-forming oxidase and a "dirigent protein."[57] (+)-Pinoresinol is then reduced via (+)-lariciresinol (**8**) to (–)-secoisolariciresinol (**9**) by pinoresinol-lariciresinol reductase (PLR),[58,59] and subsequently oxidized to (–)-matairesinol (**10**) by secoisolariciresinol dehydrogenase (SD).[60–62] The biochemical steps leading from (–)-matairesinol to (–)-deoxypodophyllotoxin (**12**) have not yet been well characterized, but probably involve yatein (**11**).[63]

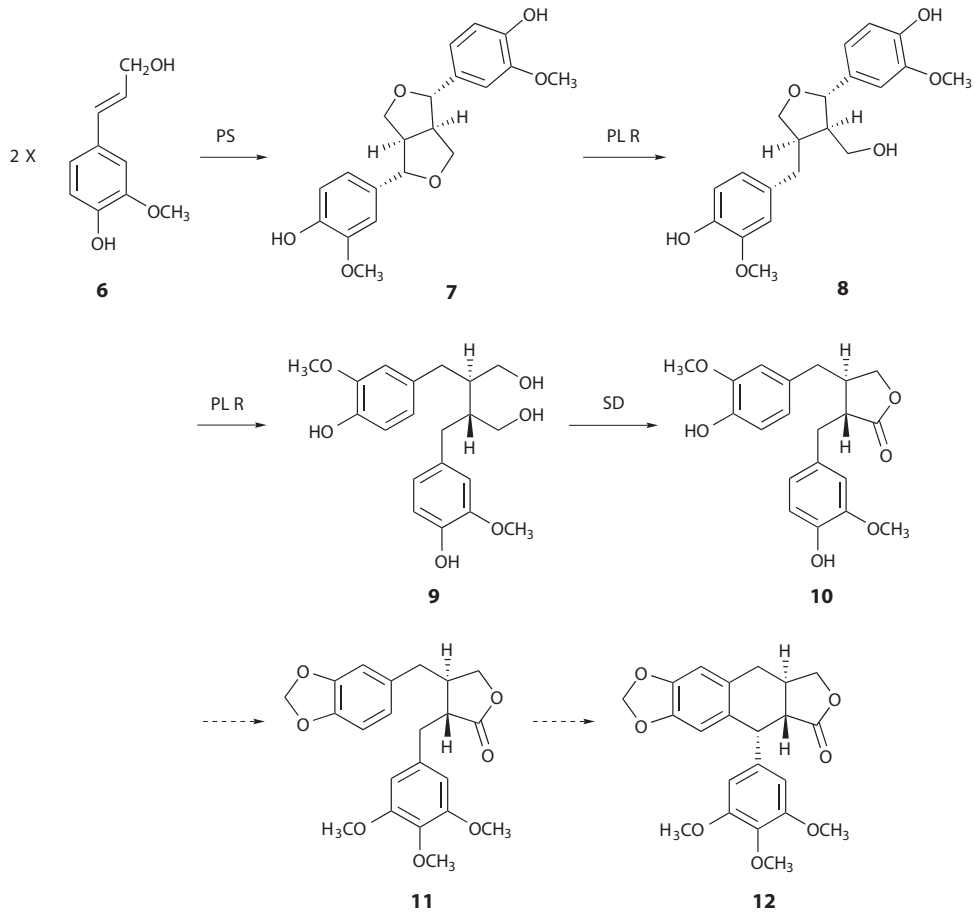

FIGURE 5.3 Hypothetical biosynthetic pathway leading to deoxypodophyllotoxin.

5.4.1.2 Biosynthetic Relationships among Podophyllotoxin Analogs

Several feeding experiments have suggested that deoxypodophyllotoxin is the precursor of key podophyllotoxin analogs, and their interrelationships are summarized in Figure 5.4. In *P. hexandrum* cell cultures, deoxypodophyllotoxin is converted into podophyllotoxin and the corresponding 7-glucoside; whereas in *Linum flavum* cells, 6-methoxypodophyllotoxin and its 7-glucoside are obtained, presumably via β-peltatin and its methyl ether.[64,65] Further enzymatic studies have implicated deoxypodophyllotoxin-7-hydroxylase (D7H), deoxypodophyllotoxin-6-hydroxylase (D6H), sadenosylmethionine:β-peltatin 6-*O*-methyltransferase (SAM: P6M), and β-peltatin-A-methylether-7-hydroxylase (PM7H) as key enzymes responsible for the bioconversions (Figure 5.4).[66]

5.4.2 Biotechnological Sources for Podophyllotoxin Analogs

Biotechnological production is another alternative source for podophyllotoxin and analogs, which could overcome the scarcity of natural sources. Extensive investigations on plant cell, tissue, or organ cultures of various plant species were carried out to identify potential biotechnological sources accumulating podophyllotoxin and analogs.

It has been shown that plant cell cultures of different species, particularly species of *Podophyllum* and *Linum,* can accumulate substantial amounts of cytotoxic lignans, mainly podophyllotoxin and

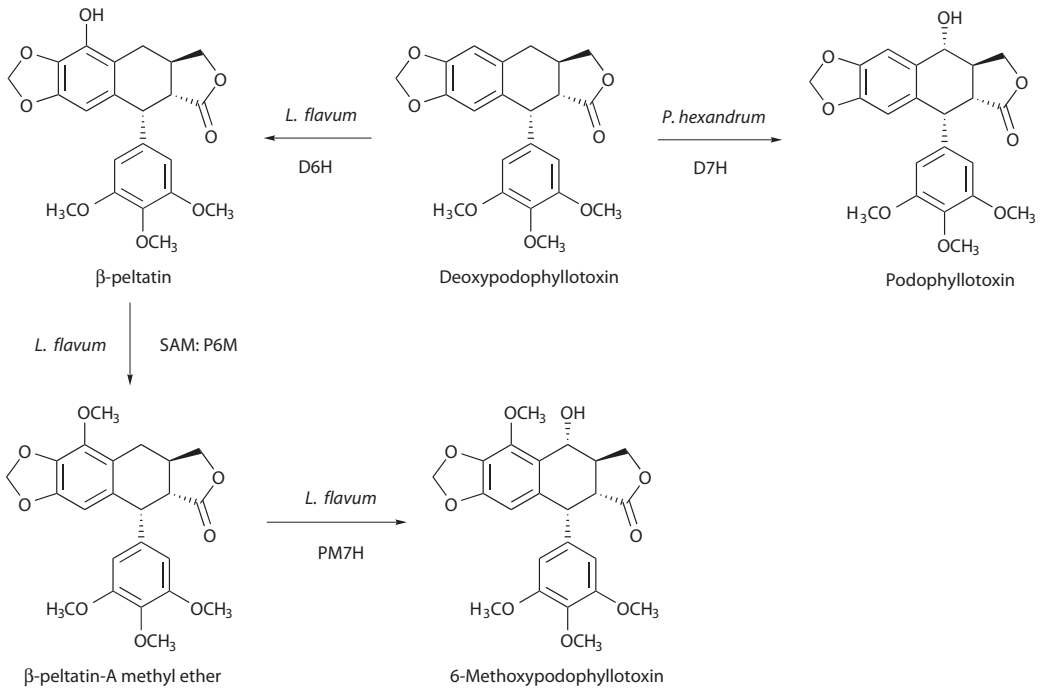

FIGURE 5.4 Biosynthetic relationships among podophyllotoxin analogs.

6-methoxypodophyllotoxin.[67–69] However, biotechnological production using cell culture will only be commercially attractive if high yields can be obtained and sustained. Although different yield improvement strategies have been attempted,[69] the performance of plant cell cultures has not yet been commercially feasible for podophyllotoxin analogs mainly due to low accumulation and slow cell growth.

Callus induction and callus culture were also demonstrated to be viable biotechnological source for podophyllotoxin analogs. The callus culture of *P. peltatum* was first reported to produce podophyllotoxin.[70] Later, accumulation of podophyllotoxin analogs was detected in callus cultures of various species.[67]

Root cultures of *Linum* species section *Syllinum* were found as rich sources for the production of podophyllotoxin and 6-methoxypodophyllotoxin.[5] Hairy root cultures have drawn much attention recently as a promising alternative to cell suspensions for the production of podophyllotoxin analogs. Hairy root cultures of *Linum* species accumulate 6-methoxypodophyllotoxin and its glucoside derivatives.[71,72]

Recently, it was reported that cross-species coculture systems using *P. hexandrum* cell suspensions and *L. flavum* hairy roots can significantly increase podophyllotoxin production.[73]

5.5 SYNTHESIS AND STRUCTURE–ACTIVITY STUDIES

The impressive antitumor potency and clinical efficacy of **2** and **3** have prompted extensive structure–activity studies based on the podophyllotoxin prototype, and numerous podophyllotoxin analogs have been synthesized and evaluated since the 1950s. As highlights of such global efforts, several synthetic analogs (Figure 5.5), NK 611 (**13**; Nippon-Kayaku),[74] GL-331 (**14**; NPRL at UNC),[75] azatoxin (**15**; National Cancer Institute),[76] TOP-53 (**16**; Taiho),[77] Etopophos (**17**; Bristol-Myers),[78] and Tafluposide (**18**; Pierre Fabre),[79] have been produced as either clinical drugs or novel clinical trial candidates for various cancers.

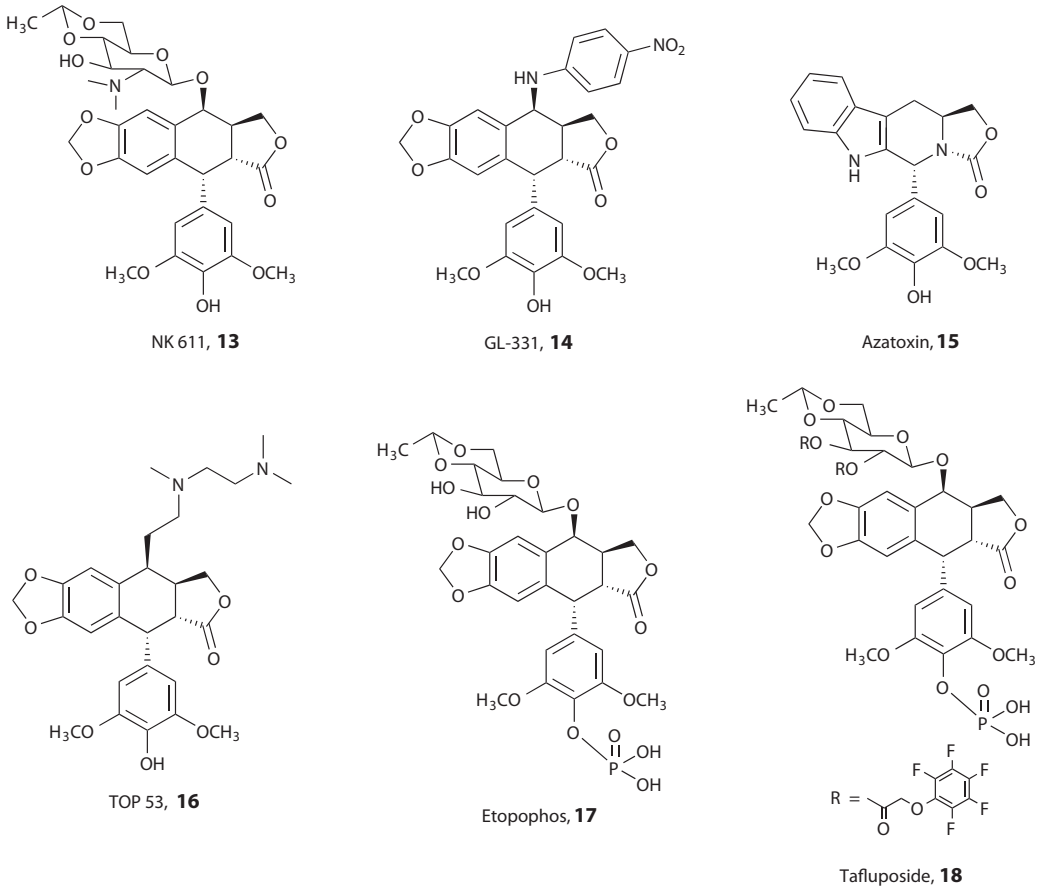

FIGURE 5.5 Podophyllotoxin analogs as clinical candidates.

5.5.1 Synthetic Efforts toward Podophyllotoxin and Analogs

Although several synthetic approaches are available to provide enantiomerically pure podophyllotoxins, the overall low yields disqualify total syntheses as an alternative for naturally produced materials. Therefore, natural (–)-podophyllotoxin remains the major source for the preparation of clinically useful analogs and the starting point for extensive structure–activity studies. Synthetic efforts to obtain podophyllotoxin and analogs, including general approaches to the total synthesis of podophllotoxin and chemical modification to produce key analogs investigated or used clinically, are discussed herein.

5.5.1.1 General Approaches for Total Synthesis

The first total synthesis of podophyllotoxin was accomplished by Gensler et al. in the 1960s.[19] The major challenge in the total synthesis of podophyllotoxin and analogs involves the establishment of four contiguous stereocenters and the construction of the base-sensitive *trans*-lactone ring. To date, four general approaches to the syntheses of podophyllotoxin derivatives have been developed. Key steps in these approaches involve either the elaboration of an χ-oxo ester, the lactonization of a dihydroxy acid, the cyclization of a conjugate addition product, or the utilization of a Diels–Alder reaction to construct the aryltetralin scaffold (Figure 5.6).[12,25,80] In order to achieve the required stereochemistry and improve the overall yield, elegant variations and innovations have been introduced to the aforementioned general routes. Highlights include an addition of an orthoquinonoid pyrone to a furanone, followed by elimination and stereoselective hydrogenation,[81] a synthetic strategy featuring a

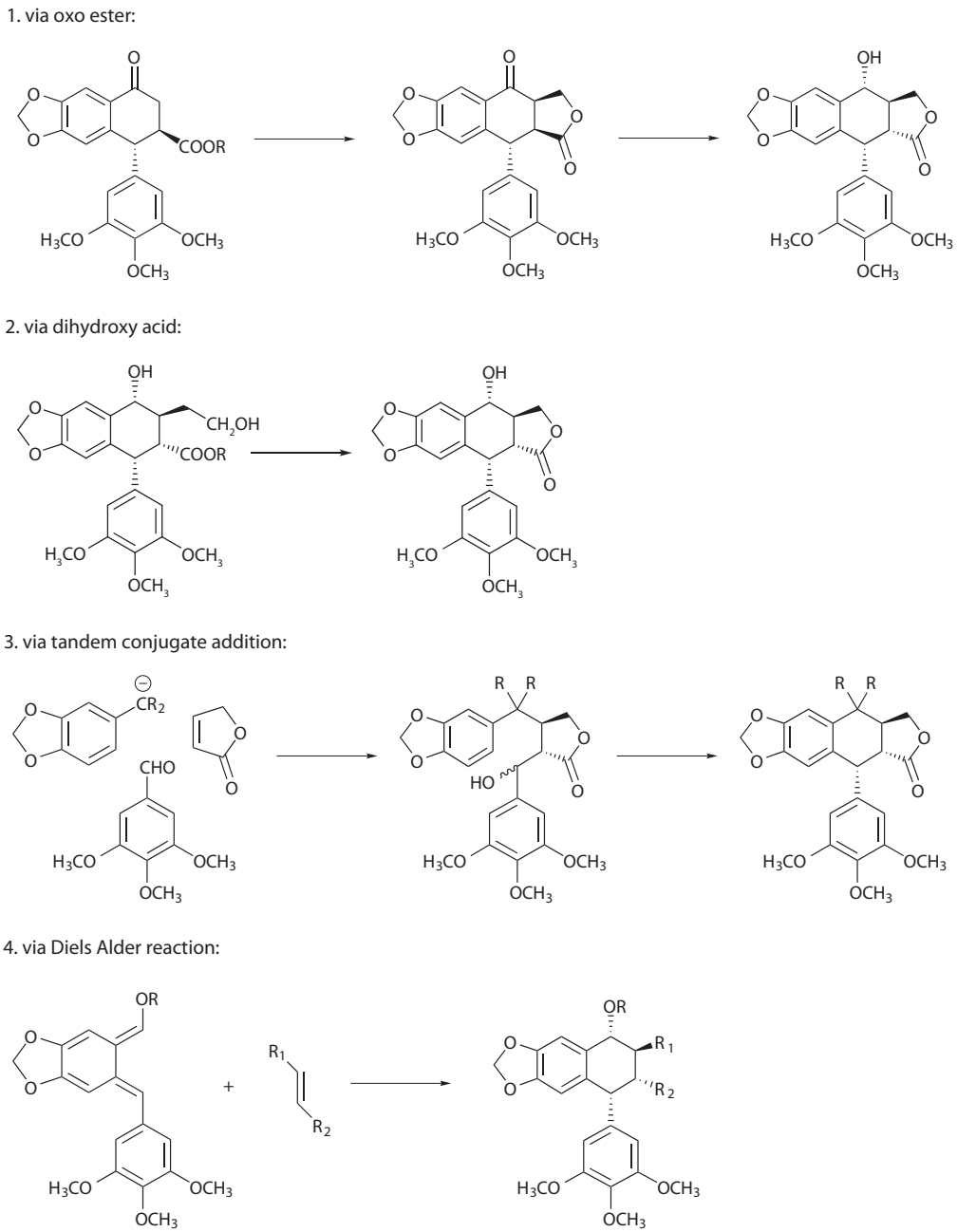

FIGURE 5.6 General synthetic approaches to podophyllotoxin.

tandem Michael addition–alkylation and subsequent aldol reaction,[82,83] and a concise synthesis characterized by a diastereoselective iron(III)-catalyzed intermolecular Friedel–Crafts alkylation.[84]

5.5.1.2 Chemical Derivatization for Key Analogs

DMEP is a key intermediate for the preparation of clinically useful podophyllotoxin derivatives. DMEP was synthesized from podophyllotoxin in the late 1960s via simultaneous 7-epimerization and selective 4′-demethylation using hydrogen bromide.[85] In order to improve stereoselectivity and overall

yield, various synthetic approaches were investigated to realize efficient and facile synthesis of DMEP and its 7β-substituted congeners. In particular, the use of the reagents $Bu_4N^+I^-$ [86] or TMSI[87] and reagent systems of $MeSO_3H/NaI$[88] or $BF_3 \cdot Et_2O/NaI$[89] afforded better stereoselectivity and higher yield.

Etoposide and teniposide were both prepared from DMEP. After 4′-benzyloxycarbonyl protection (**19**), the remaining 7β-hydroxyl is then glycosylated by reaction with tetra-*O*-acetyl-α-D-glucopyranosyl bromide and subsequent $ZnCl_2$-catalyzed methanolysis.[90] The glycosidic derivative (**20**) is treated with aldehydes and ketones in the presence of acid catalysts to yield the corresponding cyclic acetals and ketals, including etoposide and teniposide (Scheme 5.1).[38]

An efficient preparation of Etopophos is shown in Scheme 5.2.[78] Benzyl phosphate protection of the 4′-phenol and glycosylation of C7 with an acetylated sugar characterize this preparation. The overall yield (starting from podophyllotoxin) was over 19%.

The aminosugar intermediate (**21**) was prepared following the procedure used to synthesize etoposide and teniposide (cf. Scheme 5.1). NK 611 was then produced by reductive methylation with aqueous formaldehyde in the presence of $NaBH_3CN$ (Scheme 5.3).[74] Tafluposide is a nonintercalating dual catalytic inhibitor of topo I and topo II derived from etoposide.[79] It was readily prepared with two alternative protocols (Scheme 5.4).[91]

In sharp contrast to the preparation of the other clinically useful derivatives, a two-step one-pot procedure was employed in the manufacture of GL-331 (Scheme 5.5). GL-331 was obtained from podophyllotoxin through simultaneous 7-bromination and 4′-demethylation with hydrogen bromide (HBr, g) and nucleophilic displacement at C7 with the appropriate amine in the presence of $BaCO_3$.[75]

The preparation of 7β-alkyl derivative TOP-53 is shown in Scheme 5.6.[77] The 4′-hydroxyl of DMEP was protected by a benzyloxycarbonyl group before regio- and stereospecific introduction of allyl at the 7β-position using trimethylallylsilane in the presence of boron trifluoride etherate. Oxidation of the 7β-allyl derivative (**22**) with osmic acid and *N*-methylmorpholine-*N*-oxide (NMO), followed by lead tetraacetic acid gave the 7β-formylmethyl derivative (**23**). Reductive amination of **23** gave the 7β-aminoalkyl derivative, and subsequent 4′-deprotection provided the final product TOP-53.

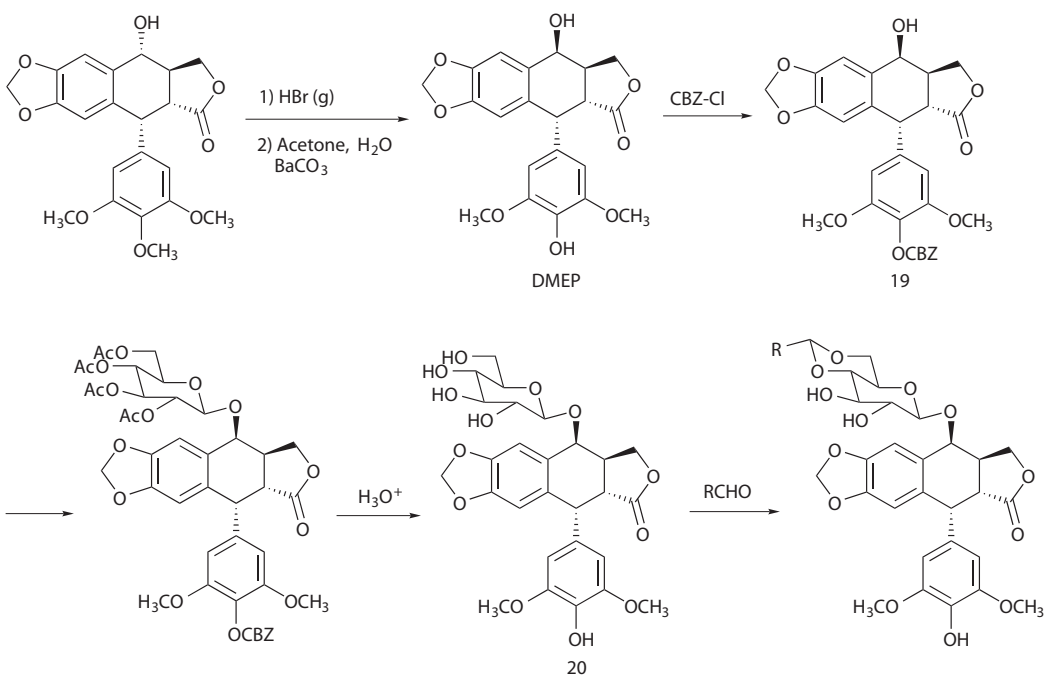

SCHEME 5.1 Synthesis of etoposide and teniposide.

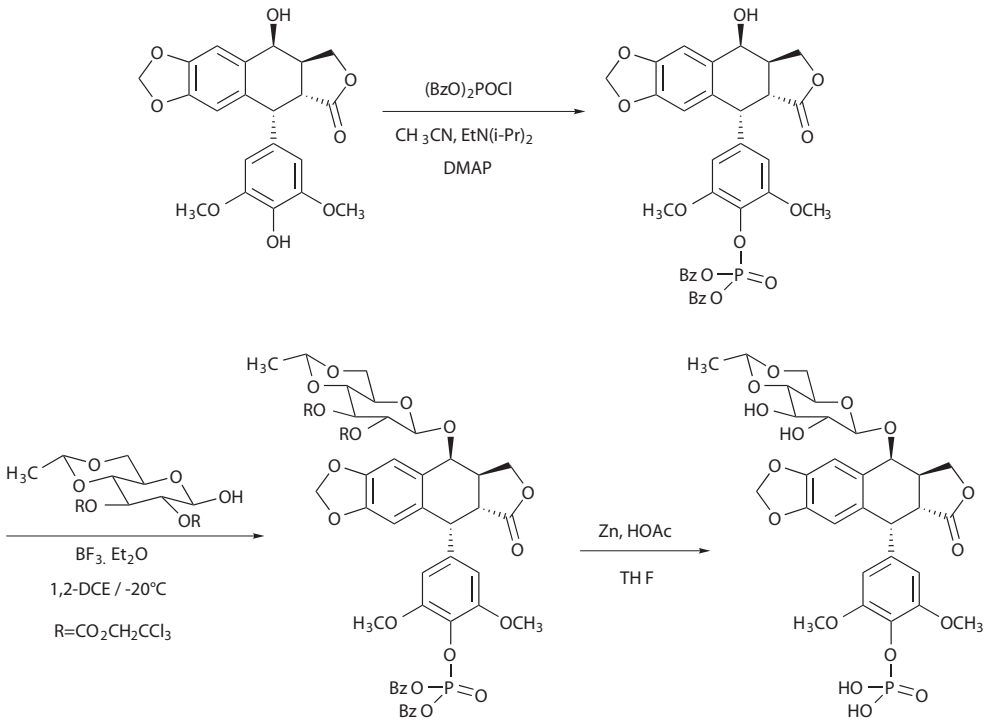

SCHEME 5.2 Preparation of Etopophos.

Azatoxin, a hybrid molecule of etoposide and ellipticine, was rationally designed from a pharmacophore model[92] for topo II inhibitors. It is a potent inhibitor of DNA topo II and tubulin polymerization, and has successfully reached clinical trials. Azatoxin is prepared from L-tryptophanol in two steps.[93] L-Tryptophanol was condensed with diethyl carbonate under treatment with sodium ethoxide to provide oxazolidinone (**24**), and the latter compound was reacted with syringaldehyde dimethyl acetal by catalysis with trifluoroacetic acid to afford azatoxin (Scheme 5.7).

5.5.2 Structure–Activity Studies

Although podophyllotoxin analogs have exhibited numerous biological activities, their antineoplastic activity has been most extensively studied, and we will focus our discussion on structure–antineoplastic activity relationships.

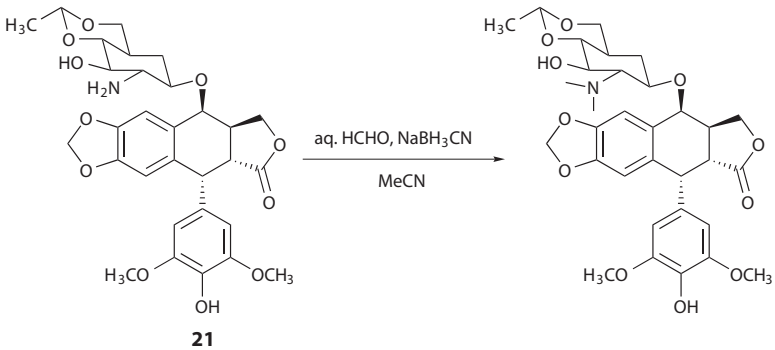

SCHEME 5.3 Preparation of NK 611.

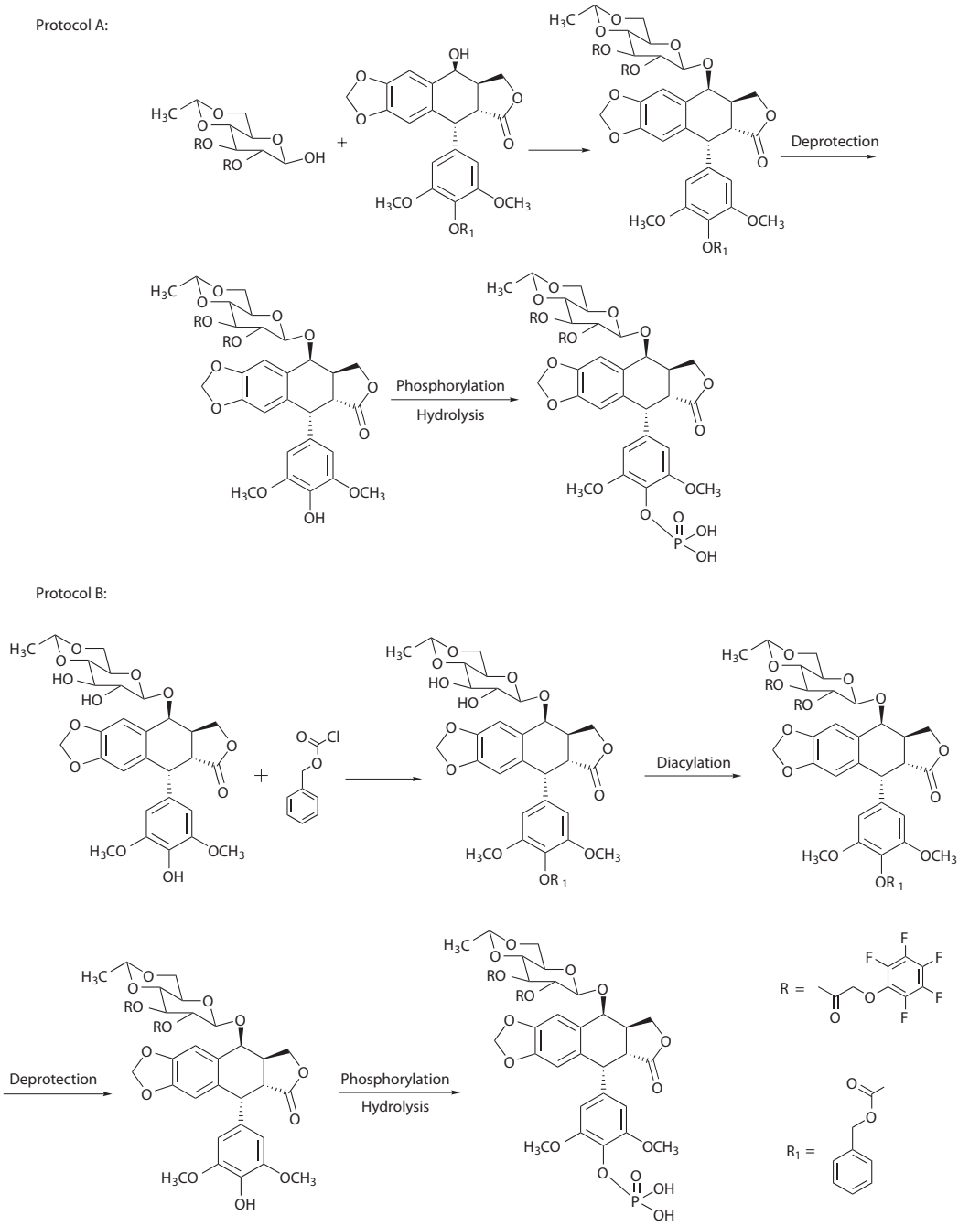

SCHEME 5.4 Preparation of tafluposide.

5.5.2.1 General Structure Antineoplastic Activity Relationships

Structure–activity relationships (SAR) of podophyllotoxin derivatives was first investigated in the 1950s, when Seidlova-Massinova et al. found that a series of compounds related to podophyllotoxin could also induce cell cycle arrest at mitosis.[10] Initial SAR studies of podophyllotoxin analogs were based mainly on the cytotoxic activity derived from antimitotic action. However, as topo II-mediated DNA breakage was recognized as the underlying mechanism for therapeutic efficacy of etoposide

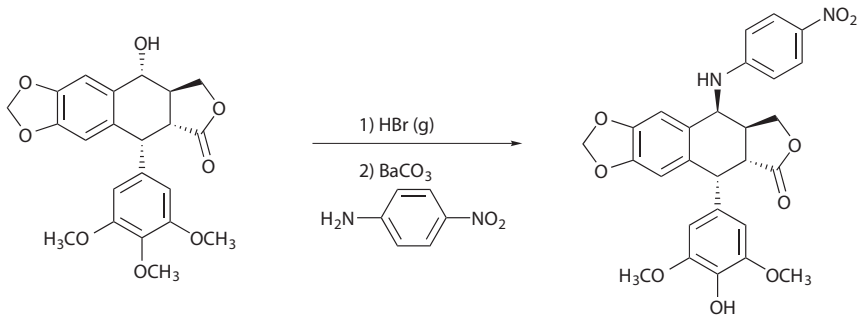

SCHEME 5.5 Preparation of GL-331.

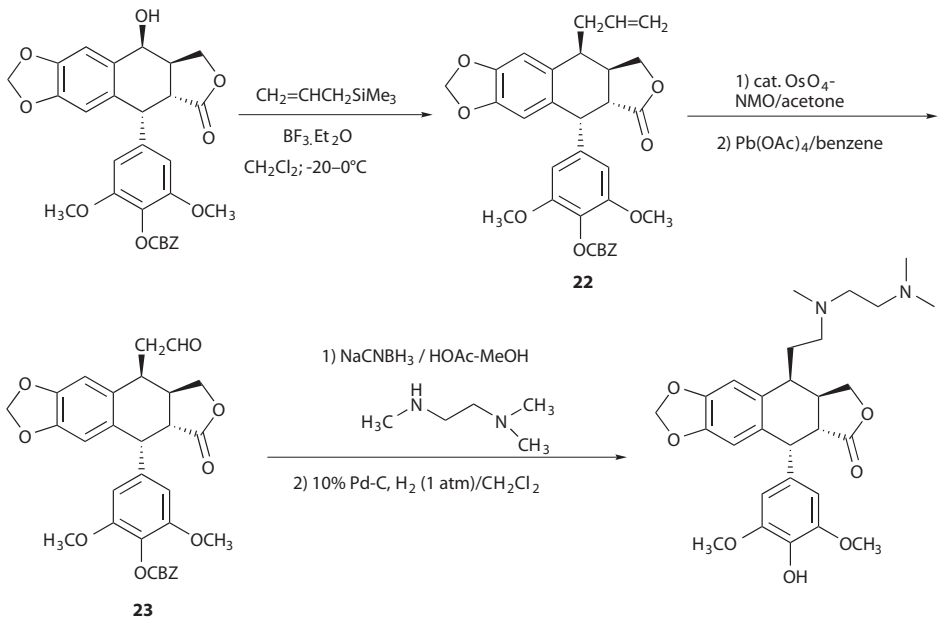

SCHEME 5.6 Preparation of TOP-53.

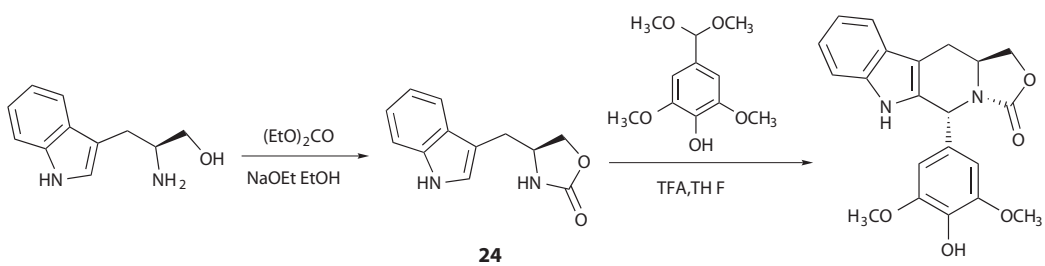

SCHEME 5.7 Preparation of azatoxin.

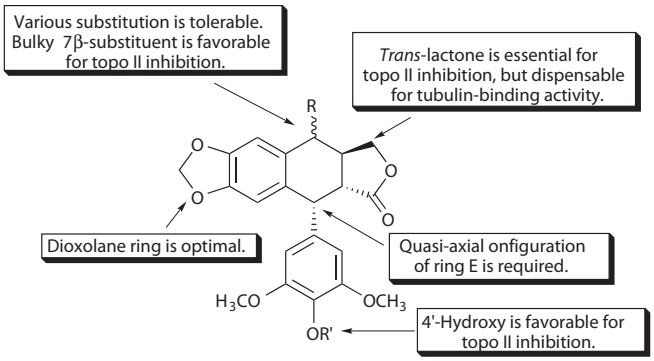

FIGURE 5.7 Key features for podophyllotoxin analogs' antineoplastic activity.

and teniposide in 1980s,[47] structural modifications on podophyllotoxin analogs have been aimed predominantly at enhancing topo II inhibition, which is the primary mechanism of action of therapeutically useful analogs.

The structural features that are critical for the antineoplastic activity of podophyllotoxin analogs are described in Figure 5.7.[2] The structural preferences of topo II inhibitors over antimicrotubule agents have been roughly identified as: (1) 4′-demethylation, (2) 7β-configuration, and (3) 7β-bulky substitution.[6,94]

5.5.2.2 Molecular Area-Oriented Analog Syntheses

Extensive molecular modifications of podophyllotoxin have been thoroughly discussed in previous reviews,[1,95] and are summarized in Table 5.2. We highlight herein only the chemical modifications most relevant to the SAR.

TABLE 5.2
Molecular Modifications of Podophyllotoxin

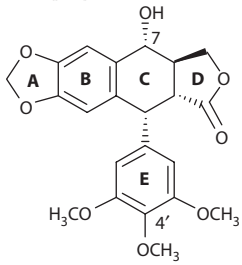

	Modifications
A ring	Removal of the methylenedioxy group to give hydroxy, methoxy, or other oxygenated substituents; replacement of the methylenedioxy ring with heteroaromatic ring systems
B ring	6-Oxygenation to give hydroxy or alkoxy groups
C ring	Extensive C7 modifications, including C7 sugar- and nonsugar- (with *O*-, *S*-, *N*- *C*- and *Se*-linkages) substituents, and 7-aza-derivatives; aromatization of C ring
D ring	Conversion of the γ-lactone to lactam, cyclopeantanone, cyclopentane, sulfide, sulfoxide, sulfone, cyclic ether, and homolactone; substitution of the hydrogen at C8′ to halogen atoms, methyl, or hydroxyl; replacement of C8′ to nitrogen
E ring	Demethylations; oxidation to the *O*-quinotne; esterification of the C4′ hydroxyl

Ring A: The A ring has been modified via two different approaches: (1) opening the methylenedioxy bridge and selectively functionalizing the two phenols,[96] and (2) replacing the methylenedioxy ring with heteroaromatic ring systems.[97] Neither of the approaches provided derivatives with good cytotoxicity or topo II inhibitory activity.

Ring B: Modification on the B ring is mainly related to the two natural products α-peltatin and β-peltatin (Table 5.1). Like podophyllotoxin, these derivatives act as antimitotic agents and interact only weakly with topo II. Many α-peltatin derivatives were synthesized, but all were much less active than etoposide against P388 leukemia.[98,99]

Ring C: The very extensive modification of the C ring has been focused almost exclusively on the C7 position. 7-Epimerization of podophyllotoxin shifts the molecular target from tubulin to topo II, the molecular target of clinical relevance. Therefore, most C7-modified analogs are epipodophyllotoxins.

Etoposide and teniposide were developed through C7 modification in the late 1960s.[38,90] After these first efforts, many other sugar-substituted derivatives were prepared. Some of the clinically useful compounds incorporated nitrogen into the sugar moiety to maintain a favorable activity profile and overcome one of etoposide's main drawbacks, poor water solubility. These compounds increased survival time in mice with L-1210 leukemia (Table 5.3).[74] One of these compounds, NK 611 (**13**), was brought to clinical trials. Tafluposide (**18**) is a lipophilic fluorinated etoposide phosphate, which uniquely inhibits both topo I and topo II. Tafluposide demonstrated high *in vivo* antitumor activity with an unusually broad therapeutic range, and has been advanced to clinical trials.[100]

The preparation of nonglycosidic C7-substituted epipodophyllotoxins began by various modifications of the hydroxy moiety, including esters, carbonates, carbamates, ethers, and thioethers.[95] The introduction of nitrogen at the 7-position provided 7β-alkylamino,[101] -arylamino,[75] -benzylamino,[102] and -halogenated anilino[103] derivatives. Most of them exhibited superior potency in cellular protein–DNA complex formation and topo II inhibitory assays, and showed comparable cytotoxicity to etoposide. Table 5.4 lists some of the most active analogs, among which, GL-331 (**14**) was selected for clinical evaluation. Notably, many 7β-nitrogen-substituted derivatives retained cytotoxicity against **2**-resistant KB variants with decreased cellular uptake of **2**, decreased expression of topo II, or overexpression of multidrug-resistant protein (MDR1).[104] These results implied that different

TABLE 5.3
Nitrogen-Substituted Sugar Derivatives

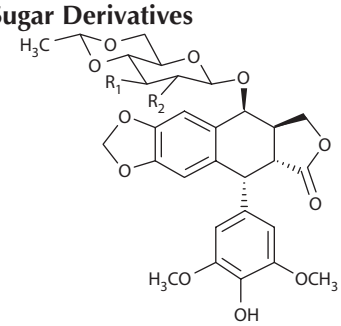

Compound	R_1	R_2	L-1210 (Max. % T/C)
1	—	—	131
2	OH	OH	184
3-1	OH	NH_2	272
3-2	NH_2	OH	361
3-3	OH	NHMe	113
13 (NK 611)	OH	NMe_2	438

TABLE 5.4
4β-Arylamino Derivatives of Podophyllotoxin

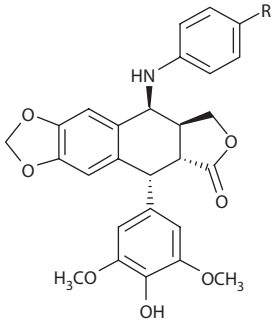

Compound	R	KB Cells (IC_{50} μM)	Topo II (ID_{50} μM)	%Protein–DNA Complex Formation
Etoposide	—	0.2	50	100
14 (GL-331)	NO_2	0.49	10	323
4-1	$NH_2 \cdot HCl$	0.8	5	330
4-2	F	0.24	5	213
4-3	CN	0.64	10	211
4-4	COOEt	0.84	5	207
4-5	3,4-$O(CH_2)_2O$	0.68	10	279

substitutions at the C7 position of epipodophyllotoxins might play a significant role in the biochemical determinants of cellular drug uptake in **2**-resistant cell lines.

Another modification leading to potent compounds was 7β-alkylation. Carbon chains containing hydroxy, amino, or amido groups were introduced at the 7β-position.[77] Many of the derivatives exhibited potent cytotoxicity and topo II inhibition. Selected data for representative 7β-alkylated analogs are shown in Table 5.5. TOP-53 (**16**) has also reached clinical trials.

C ring modification is still a current focus to discover novel podophyllotoxin analogs with better pharmaceutical profiles. Some recent efforts are the incorporation of various bulky substituents,[105–110] the preparation of 7β-[1,2,3-triazol-1-yl]podophyllotoxin congeners with 1,3-dipolar cycloaddition reaction,[111] the introduction of 7β-seleno-substituent,[54] the integration of 7-aza[112] or dihydropyridopyrazole structure by multicomponent synthesis,[113,114] and 7β-conjugation with other antitumor agents.[115,116]

Ring D: The *trans*-fused γ-lactone D ring in etoposide and its derivatives can be converted to the *cis*-fused lactone (*picro* form) under basic conditions, and can also be extensively metabolized *in vivo* to open-ring hydroxy acids. All three metabolic species are inactive.[95]

To overcome the problem of metabolic inactivation, podophyllotoxin derivatives with differently modified D rings, including lactam,[117] cyclopentanone, cyclopentane, sulfide, sulfoxide, sulfone,[118] cyclic ether,[119] 2-aza,[120] homolactone,[121] and C8′-substituted[122,123] derivatives have been prepared. Many of these derivatives showed much less favorable activity as compared with their D ring intact congeners, especially in topo II inhibition assays.

Tetrahydrofuran D ring derivatives were designed to simultaneously eliminate hydrolysis and epimerization of the γ-lactone ring by replacing the lactone carbonyl with a methylene group (Table 5.6). Compounds **6-5** and **6-6** were found to be comparable with **2** in inhibiting topo II and causing DNA breakage, but inferior to their parent compounds with an intact D ring.[117] Recent synthetic efforts following this molecular design strategy replace the lactone ring with cyclosulfite,[124] or 1,5-disubstituted 1,2,3-trazole.[125]

TABLE 5.5
4β-Alkylated Derivatives of Podophyllotoxin

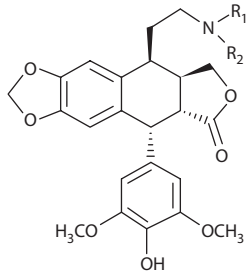

Compound	R_1	R_2	Topo II (IC_{50} μM)	Cytotoxicity (ED_{50} μg/mL)[a] SBC-3	A-549	HLE	G-402	COLO320DM
1	—	—	59.2	1.6	2.9	1.5	4.8	14
5-1	CH_3	$(CH_2)_2N(CH_3)_2$	32.5	0.41	0.82	0.23	0.33	2.0
5-2	CH_3	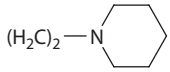	60.9	0.54	1.8	0.36	0.35	3.2
5-3	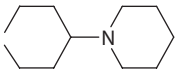	29.8	0.16	1.0	0.31	0.18	2.1	
5-4	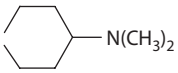	33.6	0.28	0.76	0.13	0.25	0.99	

[a] SBC-3, small-cell lung cancer; A-549, nonsmall-cell lung cancer; HLE, hepatoma; G-402, renal cancer; COLO320DM, colon carcinoma.

TABLE 5.6
Tetrahydrofuran D Ring Derivatives

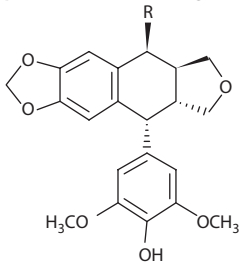

20. R = 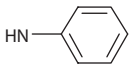

21. R = 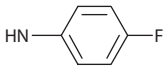

Compound	Topo II Inhibition ID_{50} (μM)	% Protein–DNA Complex Formation
2	50	100
6-5	50	139
6-6	50	125

Although the *trans*-lactone D ring is essential for topo II inhibition, it is not a requisite for tubulin-binding activity.[3] Various C9-oxidized podophyllotoxin analogs, including C9-aldehyde,[126] carboxylic acid, ester, amide, nitrile, anhydride,[127] and imine derivatives,[128] were synthesized and found to be cytotoxic against different tumor cell lines.[129] Notably, some of these derivatives displayed a significant selectivity against human colon carcinoma cells. The C9-oxidized analogs could inhibit microtubule polymerization, arrest cells at the G2/M phase of the cell cycle, and induce a delayed apoptosis.[127]

Ring E: 4′-Demethylation increases the etoposide-like activity (e.g., topo II inhibition) and is considered one of the structural fingerprints for topo II inhibitors in this compound class. The Bristol Myers Company performed extensive E ring modifications, including synthesis of 3′-nitrogen or 3′,4′-dinitrogen-substituted, 4′-acyl, 4′-coupled dimeric, and phosphorous-containing derivatives. Many of these derivatives displayed significant cytotoxicity. The most favorable compound was the 4′-phosphate ester of etoposide (Etopophos).[78] This compound is a water-soluble prodrug of etoposide and currently used in the clinic via intravenous administration.

Introduction of a chlorine atom in the 2′-position was reported to stabilize the resulting compound to C8′ epimerization.[130] However, it significantly decreased the activity in both cytotoxicity and topo II inhibition assays.[131]

5.5.2.3 SAR Models

As the numbers of epipodophyllotoxin derivatives increase, informative SAR must be assembled in a readily usable format. Different approaches have been applied to generate SAR models for this compound class.

The first model is the composite pharmacophore model proposed by MacDonald.[92] This model was derived from superimposition of several topo II inhibitors of the epipodophyllotoxin, anthracycline, and aminoacridine classes. As shown in Figure 5.8, the model defined three pharmacophoric domains: the DNA intercalating moiety, which is a planar, polycyclic molecular surface (**A**), the minor groove-binding site, which is a pendant, *para*-hydroxy- or sulfonylamino-phenyl ring (**B**), and a variable molecular region, which can accommodate considerable structural diversity (**C**). Although later modifications, particularly various C7 modifications and the molecular design of azatoxin, have produced SAR consistent with this model, the preparation and evaluation of podophenazine derivatives[97] failed to support a crucial role for molecular area **A** in topo II inhibition. This generalized SAR model for diverse topo II inhibitors implied a common interaction site on the enzyme; nevertheless, there was no experimental evidence to validate the existence of such a putative site.

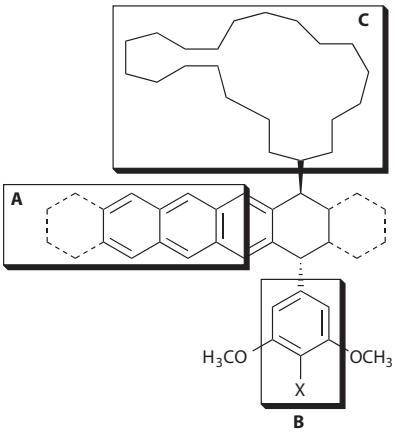

FIGURE 5.8 MacDonald's pharmacophore model.

More recently, the comparative molecular field analysis (CoMFA) technique was applied to 102 epipodophyllotoxin derivatives to generate quantitative SAR (QSAR) models for topo II inhibitory activity.[132] The steric and electrostatic contour plots of the final CoMFA model indicated that diverse and bulky substitutions could be accommodated at C7, which agreed with MacDonald's model. It also suggested that the C7 substituents would interact with the DNA minor groove. Based on this model, several etoposide analogs incorporating minor groove-binding moieties at C7 were synthesized.[133] Some of these compounds were more active than etoposide in both cytotoxicity and topo II inhibition assays.

The application of CoMFA method is often hampered by poor reproducibility due to inconsistent three-dimensional alignment. Therefore, a *k*-nearest neighbor QSAR (*k*NN-QSAR) method using alignment-free two-dimensional topological descriptors was applied to 157 epipodophyllotoxins as topo II inhibitors.[134] The *k*NN-QSAR models afforded higher values of internal leave one out cross-validated R^2 (q^2) and external predictive R^2 as compared with the CoMFA method. The high predictive ability of the QSAR models should guide the rational design of novel derivatives and focused libraries based on the epipodophyllotoxin skeleton, and facilitate the search for bioactive structures from large databases.

A recent computational effort involves the establishment of QSAR between cytotoxicity of podophyllotoxin analogs and their molecular descriptors related to *in silico* tubulin binding, which should afford an efficient tool for rational design of novel podophyllotoxin derivatives as tubulin inhibitors.[135]

5.6 PRECLINICAL DEVELOPMENT

In spite of their impressive clinical efficacy, the therapeutic use of etoposide and teniposide is often hindered by problems, such as poor water solubility, acquired drug resistance, and metabolic inactivation. As discussed previously, research focused on overcoming the aforesaid problems resulted in the discovery and development of several novel podophyllotoxin analogs, including Etopophos, NK 611, GL-331, azatoxin, TOP-53, and tafluposide.

Etopophos (etoposide phosphate), a water-soluble prodrug of etoposide, was developed to overcome the poor water solubility of **2** and **3**. Etopophos is less toxic and more active than etoposide in *in vivo* tumor models. It can be efficiently converted *in vivo* by endogenous phosphatase to the active drug etoposide, and exhibits pharmacological and pharmacokinetic profiles similar to those of etoposide. Notably, the prodrug approach increases the *in vivo* bioavailability from 0.04% to over 50%, and also results in more predictable oral bioavailability.[136]

Another etoposide derivative, NK 611, was also developed to confront the problem of poor water solubility. The introduction of a 2″-dimethylamino group led to a 120-fold increase in water solubility. NK 611 and **2** showed similar antitumor activity against human tumor xenografts, but NK 611 was a more potent topo II inhibitor and more cytotoxic against various human cancer lines including lung, gastrointestinal, ovarian, testicular, breast, head and neck tumor cells, and leukemias.[28]

Compared with **2**, GL-331 causes higher DNA double-strand breakage and G2-phase arrest. It is also more potent against tumor cells both *in vitro* and *in vivo*, and remarkably, overcomes multidrug resistance in many cancer cell lines. Formulated GL-331 shows desirable stability and biocompatability, and has similar pharmacokinetic profiles to those of **2**.[137]

TOP-53 is a more potent topo II inhibitor than **2**. It showed nearly wild-type potency against a mutant yeast type II enzyme highly resistant to **2**, implying therapeutic potential for drug-resistant cancers. TOP-53 exhibited strong activity against a wide variety of tumor cells, with especially high activity to nonsmall-cell lung cancer in both tumor cells and animal tumor models.[138,139]

Azatoxin induces DNA–protein cross-links and protein-linked DNA breaks in HL-60 cells, and also inhibits tubulin polymerization *in vitro*. The latter activity prevails at lower concentration, whereas topo II inhibition becomes prominent at higher concentration. Azatoxin is a potent cytotoxic agent with a mean IC_{50} value of 0.13 μM against a panel of 45 human cell lines.[140]

Tafluposide, a dual inhibitor of topo I and topo II, has shown outstanding antitumor activity *in vivo* against a panel of CAKI-1 (renal), DLD-1 (colon), DU 145 (prostate), and GLC4 (small-cell lung) human tumor xenografts.[141] Tafluposide also demonstrated significant cytotoxicity against cells derived from either hematological or solid tumors.[142]

5.7 CLINICAL DEVELOPMENT

Etoposide is widely used as an antineoplastic agent, especially in combination chemotherapeutic regimens. The combination of etoposide with *cis*-platin is an effective protocol for the treatment of small-cell lung, nonsmall-cell lung, and testicular cancers, and it is also used as salvage therapy for CAV (cyclophosphamide, adriamycin, and vincristine)-resistant or failure small-cell lung cancer. When incorporated into other multidrug treatment protocols, etoposide is also used for the treatment of non-Hodgkin lymphomas resistant to other agents, different types of lymphomas, refractory childhood leukemia, hepatocellular metastasis, refractory acute lymphoblastic leukemia, and other types of cancers. As a water-soluble prodrug of etoposide, Etopophos exhibits pharmacological and pharmacokinetic profiles similar to those of etoposide and is preferable for routine clinical use, especially for intravenous administration. Combination chemotherapy incorporating teniposide has also been applied to various cancers. In various combination therapies, it is used against neuroblastoma (with *cis*-platin), acute lymphoblastic leukemia [with cytarabine (ara-C)], and small-cell lung cancer (with carboplatin).[1,30]

Clinical tests of intravenous and oral formulations of NK 611 suggest that the compound shows better bioavailability than etoposide. When orally administered for 21 days every 35 days, maximum tolerated dose (MTD) was 12.5 mg/day, and the main dose-limiting toxicity was granulocytopenia. When administered as intravenous infusion over 30 min every 28 days, dose-limiting toxicities were granulocytopenia and thrombocytopenia.[143,144]

Formulated GL-331 shows desirable stability and biocompatability, and similar pharmacokinetic profiles to those of **2**. Phase I clinical trials against nonsmall-cell lung and small-cell lung, colon, and head/neck cancers showed marked antitumor efficacy. Side-effects were minimal with cytopenias being the major toxicity. MTD was declared at 300 mg/m^2.[137] However, in a phase II pharmacokinetic study for previously treated Chinese gastric cancer patients, GL-331 failed to give objective responses in spite of adequate blood level of the drug.[145]

5.8 CONCLUSIONS

Etoposide and teniposide have been used as cancer chemotherapy for almost three decades. However, their clinical application is often impeded by problems of acquired drug resistance and poor water solubility. Recent development of anticancer candidates, including NK 611, GL-331 TOP-53, and tafluposide, indicates that molecular modification at position C7 of podophyllotoxin is an effective approach to yield novel analogs with better activity profiles. Chemoinductive manipulation of the *trans*-lactone D ring has also provided novel antitumor agents with selective cytotoxicity. We anticipate continuing chemical modifications of these molecular areas to produce better therapeutic agents with improved pharmacological and pharmacokinetic profiles.

Chemical modification efforts should benefit significantly from achievements in the areas of molecular biology and structural biology, as well as intelligent molecular modeling studies. Reliable, interpretable, and readily usable QSAR models are needed to extract pertinent information from accumulating structural and biological data.

Although antineoplastic activity will undoubtedly continue to be the most clinically relevant property of podophyllotoxin analogs, their antiviral, anti-inflammatory, and immunosuppressive activities are drawing more and more attention. We expect that podophyllotoxin analogs with therapeutic utility other than cancer chemotherapy will be discovered in the future based on extended biological exploration.

ACKNOWLEDGMENT

The investigation on podophyllotoxin analogs performed in the Natural Products Research Laboratories, UNC-Chapel Hill, and the composition of this chapter were supported by NIH grant CA 17625 awarded to K.H. Lee and also in part by the Taiwan Department of Health, China Medical University Hospital Cancer Reserach Center of Excellence (DOH100-TD-C-111-005).

REFERENCES

1. Gordaliza, M., Castro, M.A., Miguel Del Corral, J.M., and San Feliciano, A., Antitumor properties of podophyllotoxin and related compounds, *Curr. Pharm. Des.,* 6, 1811, 2000.
2. Moraes, R.M., Dayan, F.E., and Canel, C., The lignans of *Podophyllum*, *Studies in Natural Products Chemistry*, 26 [Bioactive Natural Products (Part G)], 149, 2002.
3. You, Y., Podophyllotoxin derivatives: current synthetic approaches for new anticancer agents, *Curr. Pharm. Des.,* 11, 1695, 2005.
4. Liu, Y.-Q., Yang, L., and Tian, X., Podophyllotoxin: current perspectives, *Curr. Bioact. Compd.,* 3, 37, 2007.
5. Xu, H., Lv, M., and Tian, X., A review on hemisynthesis, biosynthesis, biological activities, mode of action, and structure–activity relationship of podophyllotoxins: 2003–2007, *Curr. Med. Chem.,* 16, 327, 2009.
6. Imbert, T.F., Discovery of podophyllotoxins, *Biochimie*, 80, 207, 1998.
7. Kaplan I.W., *Condylomata acuminata*, *New Orleans Med. Surg. J.*, 94, 388, 1942.
8. King, L.S. and Sullivan, M., The similarity of the effect of podophyllin and colchicine and their uses in the treatment of *Condylomata acuminata*, *Science*, 104, 244, 1946.
9. Sullivan, B.J. and Weshler, H.I., The cytological effects of podophyllotoxin, *Science*, 105, 433, 1947.
10. Seidlova-Massinova, V., Malinsky, J., and Santavy, F., The biological effect of some podophyllotoxin compounds and their dependence on chemical structure, *J. Natl. Cancer Inst.*, 18, 359, 1957.
11. Hartwell, J.L. and Shear, M.J., Chemotherapy of cancer: classes of compounds under investigation, and active components of podophyllin, *Cancer Res.*, 7, 716, 1947.
12. Canel, C., Moraes, R.M., Dayan, F.E., and Ferreira, D., Podophyllotoxin, *Phytochemistry,* 54, 115, 2000.
13. Stähelin, H. and von Wartburg, A., The chemical and biological route from podophyllotoxin glucoside to etoposide: ninth Cain memorial award lecture, *Cancer Res.*, 51, 5, 1991.
14. O'Dwyer, P.J., Leyland-Jones, B., Alonso, M.T., Marsoni, S., and Wittes, R.E., Etoposide (VP-16-213): current status of an anticancer drug, *N. Engl. J. Med.*, 312, 692, 1985.
15. Podwyssotzki, V., Pharmakologische studien über *Podophyllum peltatum*, *Arch. Exp. Pathol. Pharmacol.*, 13, 29, 1880.
16. Borsche, W. and Niemann, J., Podophyllin, *Justus Liebigs Ann. Chem.*, 494, 126, 1932.
17. Hartwell, J.L. and Schrecker, A.W., Components of podophyllin. V. The constitution of podophyllotoxin, *J. Am. Chem. Soc.*, 73, 2909, 1951.
18. Hartwell, J.L. and Schrecker, A.W., Chemistry of podophyllum, *Fortschr. Chem. Org. Naturst.*, 15, 83, 1958.
19. Gensler, W.J. and Gatsonis C.D., Synthesis of podophyllotoxin, *J. Am. Chem. Soc.*, 84, 1748, 1962.
20. Petcher, T.J., Weber, H.P., Kuhn, M., and von Wartburg, A.J., Crystal structure and absolute configuration of 2'-bromopodophyllotoxin-0.5 ethyl acetate. *J. Chem. Soc. Perkin II*, 3, 288, 1973.
21. Gensler, W.J. and Wang, S.Y., Synthesis of picropodophyllin, *J. Am. Chem. Soc.*, 76, 5890, 1954.
22. Gensler, W.J. and Johnson, F., Compounds related to podophyllotoxin. XIV. Isopodophyllotoxin and epiisopodophyllotoxin, *J. Am. Chem. Soc.*, 85, 3670, 1963.
23. Beard, A.R., Hazell, S.J., Mann, J., and Palmer, C., A practical synthesis of the antitumor agent 2-methyl-4-deoxyisopicropodophyllotoxin and related podophyllin analogs, *J. Chem. Soc. Perkin I*, 11, 1235, 1993.
24. Gordaliza, M., Garcia, P.A., Miguel del Corral, J.M., Castro, M.A., and Gomez-Zurita, M.A., Podophyllotoxin: distribution, sources, applications and new cytotoxic derivatives, *Toxicon*, 44, 441, 2004.
25. Lee, C.T.L., Lin, V.C.K., Zhang, S.X., Zhu, X.K., Vanvliet, D., Hu, H., Beers, S.A. et al., Anti-AIDS agents. 29. Anti-HIV activity of modified podophyllotoxin derivatives, *Bioorg. Med. Chem. Lett.,* 7, 2897, 1997.

26. Zhu, X.-K., Guan, J., Xiao, Z., Cosentino, L.M., and Lee, K.-H., Anti-AIDS agents. Part 61: Anti-HIV activity of new podophyllotoxin derivatives, *Bioorg. Med. Chem.,* 12, 4267, 2004.
27. Chen, S.-W., Wang, Y.-H., Jin, Y., Tian, X., Zheng, Y.-T., Luo, D.-Q., and Tu, Y.-Q., Synthesis and anti-HIV-1 activities of novel podophyllotoxin derivatives, *Bioorg. Med. Chem. Lett.,* 17, 2091, 2007.
28. Bohlin, L. and Rosen, B., Podophyllotoxin derivatives: drug discovery and development, *Drug Discov. Today*, 1, 343, 1996.
29. Pugh, N., Khan, I.A., Moraes, R.M., and Pasco, D.S., Podophyllotoxin lignans enhance IL-1β but suppress TNF-α mRNA expression in LPS-treated monocytes, *Immunopharmacol. Immunotoxicol.,* 23, 83, 2001.
30. Ayres, D.C. and Loike, J.D., *Lignans. Chemical, Biological and Clinical Properties*, Cambridge University Press, Cambridge, 1990.
31. Schwartz, J. and Norton, S.A., Useful plants of dermatology. VI. The mayapple (*Podophyllum*), *J. Am. Acad. Dermatol.*, 47, 774, 2002.
32. Hammonds, T.R., Denyer, S.P., Jackson, D.E., and Irving, W.L., Studies to show that with podophyllotoxin the early replicative stages of herpes simplex virus type 1 depend upon functional cytoplasmic microtubules, *J. Med. Microbiol.*, 45, 167, 1996.
33. Hara, H., Fujihashi, T., Sakata, T., Kaji, A., and Kaji, H., Tetrahydronaphthalene lignan compounds as potent anti-HIV type 1 agents, *AIDS Res. Hum. Retroviruses*, 13, 695, 1997.
34. Eich, E., Pertz, H., Kaloga, M., Schulz, J., Fesen, M.R., Mazumder, A. and Pommier, Y., (−)-Arctigenin as a lead structure for inhibitors of human immunodeficiency virus type-1 integrase, *J. Med. Chem.*, 39, 86, 1996.
35. Saitoh, T., Kuramochi, K., Imai, T., Takata, K.-I., Takehara, M., Kobayashi, S., Sakaguchi, K., and Sugawara, F., Podophyllotoxin directly binds a hinge domain in E2 of HPV and inhibits an E2/E7 interaction in vitro, *Bioorg. Med. Chem.,* 16, 5815, 2008.
36. Cortese, F., Bhattacharyya, B., and Wolf, J., Podophyllotoxin as a probe for the colchicine binding site of tubulin, *J. Biol. Chem.*, 252, 1134, 1977.
37. Shi, Q., Chen, K., Morris-Natschke, S., and Lee, K.H., Recent progress in the development of tubulin inhibitors as antimitotic antitumor agents, *Curr. Pharm. Des.*, 4, 219, 1998.
38. Keller-Juslen, C., Kuhn, M., Stahelin, H., and von Wartburg, A., Synthesis and antimitotic activity of glycosidic lignan derivatives related to podophyllotoxin, *J. Med. Chem.,* 14, 936, 1971.
39. Kelleher, J.K., Tubulin binding affinities of podophyllotoxin and colchicine analogues, *Mol. Pharmacol.,* 13, 232, 1977.
40. Loike, J.D., Brewer, C.F., Sternlicht, H., Gensler, W.J., and Horwitz, S.B., Structure–activity study of the inhibition of microtubule assembly in vitro by podophyllotoxin and its congeners, *Cancer Res.,* 38, 2688, 1978.
41. Brewer, C.F., Loike, J.D., Horwitz, S.B., Sternlicht, H., and Gensler, W.J., Conformational analysis of podophyllotoxin and its congeners. Structure–activity relationship in microtubule assembly, *J. Med. Chem.,* 22, 215, 1979.
42. Stähelin, H.F., 4′-Demethyl-epipodophyllotoxin thenylidene glucoside (VM-26), a podophyllum compound with a new mechanism of action, *Eur. J. Cancer*, 6, 303, 1970.
43. Loike, J.D. and Horwitz, S.B., Effects of podophyllotoxin and VP-16-213 on microtubule assembly in vitro and nucleoside transport in HeLa cells, *Biochemistry*, 15, 5435, 1976.
44. Loike, J.D. and Horwitz, S.B., Effect of VP-16-213 on the intracellular degradation of DNA in HeLa cells, *Biochemistry*, 15, 5443, 1976.
45. Horwitz, S.B. and Loike, J.D., A comparison of the mechanism of action of VP-16-213 and podophyllotoxin, *Lloydia*, 40, 82, 1977.
46. Ross, W., Rowe, T., Glisson, B., Yalowich, J., and Liu, L., Role of topoisomerase II in mediating epipodophyllotoxin-induced DNA cleavage, *Cancer Res.,* 44, 5857, 1984.
47. Zwelling, L.A., DNA topoisomerase II as a target of antineoplastic drug therapy, *Cancer Metastasis Rev.*, 4, 263, 1985.
48. Berger J.M. and Wang J.C., Recent developments in DNA topoisomerase II structure and mechanism, *Curr. Opin. Struct. Biol.*, 6, 84, 1996.
49. Boise, L.H., Gonzalez-Garcia, M., Postema, C.E., Ding, L., Lindsten, T., Turka, L.A., Mao, X., Nunez, G., and Thompson, C.B., bcl-x: a bcl-2-related gene that functions as a dominant regulator of apoptotic cell death, *Cell*, 74, 597, 1993.
50. Huang, T.S., Shu, C.H., Shih, Y.L., Huang, H.C., Su, Y.L., Cao, Y., Yang, W.K., and Whang-Peng, J., Protein tyrosine phosphatase activities are involved in apoptotic cancer cell death induced by GL-331, a new homolog of etoposide, *Cancer Lett.*, 110, 77, 1996.

51. Huang, T.S. Shu, C.H., Yang, W.K., and Whang-Peng, J., Activation of CDC 25 phosphatase and CDC2 kinase involved in GL-331-induced apoptosis, *Cancer Res.*, 57, 2974, 1997.
52. Tseng, C.-J., Wang, Y.-J., Liang, Y.-C., Jeng, J.-H., Lee, W.-S., Lin, J.-K., Chen, C.-H., Liu, I-C., and Ho, Y.-S., Microtubule damaging agents induce apoptosis in HL 60 cells and G2/M cell cycle arrest in HT 29 cells, *Toxicology*, 175, 123, 2002.
53. Zhang, Q.-Y., Jiang, M., Zhao, C.-Q., Yu, M., Zhang, H., Ding, Y.-J., and Zhai, Y.-G., Apoptosis induced by one new podophyllotoxin glucoside in human carcinoma cells, *Toxicology*, 212, 46, 2005.
54. Miao, R., Han, Y., An, L., Yang, J., and Wang, Q., Seleno-podophyllotoxin derivatives induce hepatoma SMMC-7721 cell apoptosis through Bax pathway, *Cell Biol. Inter.*, 32, 217, 2008.
55. Whetten, R. and Sederoff, R., Lignin biosynthesis, *Plant Cell*, 7, 1001, 1995.
56. Dixon, R.A. and Reddy, M.S.S., Biosynthesis of monolignols. Genomic and reverse genetic approaches, *Phytochem. Rev.*, 3, 289, 2003.
57. Davin, L.B., Wang, H.B., Crowell, A.L., Bedgar, D.L., Martin, D.M., Sarkanen, S., and Lewis, N.G., Stereoselective bimolecular phenoxy radical coupling by an auxiliary (dirigent) protein without an active center, *Science*, 275, 362, 1997.
58. Dinkova-Kostova, A.T., Gang, D.R., Davin, L.B., Bedgar, D.L., Chu, A., and Lewis, N.G., (+)-Pinoresinol/(+)-lariciresinol reductase from *Forsythia intermedia*: protein purification, cDNA cloning, heterologous expression and comparison to isoflavone reductase, *J. Biol. Chem.*, 271, 29473, 1996.
59. von Heimendahl, C.B.I., Schäfer, K.M., Eklund, P., Sjöholm, R., Schmidt, T.J., and Fuss, E., Pinoresinol–lariciresinol reductases with different stereospecificity from *Linum album* and *Linum usitatissimum*, *Phytochemistry*, 66, 1254, 2005.
60. Xia, Z.Q., Costa, M.A., Pélissier, H.C., Davin, L.B., and Lewis, N.G., Secoisolariciresinol dehydrogenase purification, cloning and functional expression: implications for human health protection, *J. Biol. Chem.*, 276, 12614, 2001.
61. Okunishi, T., Sakakibara, N., Suzuki, S., Umezawa, T., and Shimada, M., Stereochemistry of matairesinol formation by Daphne secoisolariciresinol dehydrogenase, *J. Wood Sci.*, 50, 77, 2004.
62. Moinuddin, S.G.A., Youn, B., Bedgar, D.L., Costa, M.A., Helms, G.L., Kang, C., Davin, L.B., and Lewis, N.G., Secoisolariciresinol dehydrogenase: mode of catalysis and stereospecificity of hydride transfer in *Podophyllum peltatum*, *Org. Biomol. Chem.*, 4, 808, 2006.
63. Kamil, W.M. and Dewick, P.M., Biosynthetic relationship of aryltetralin lactone lignans to dibenzylbutyrolactone lignans, *Phytochemistry*, 25, 2093, 1986.
64. Van Uden, W., Bouma, A.S., Bracht Walker, J.F., Middel, O., Wichers, H.J., De Waard, P., Woerdenbag, H.J., Kellog, R.M., and Pras, N., The production of podophyllotoxin and its 5-methoxy derivative through bioconversion of cyclodextrin-complexed desoxypodophyllotoxin by plant cell cultures, *Plant Cell Tissue Organ Cult.*, 42, 73, 1995.
65. Van Uden, W., Bos, J.A., Boeke, G.M., Woerdenbag, H.J., and Pras, N., The large-scale isolation of deoxypodophyllotoxin from rhizomes of *Anthriscus sylvestris* followed by its bioconversion into 5-methoxypodophyllotoxin β-D-glucoside by cell cultures of *Linum flavum, J. Nat. Prod.*, 60, 401, 1997.
66. Kuhlmann, S., Kranz, K., Lücking, B., Alfermann, A.W., and Petersen, M., Aspects of cytotoxic lignan biosynthesis in suspension cultures of *Linum nodiflorum*, *Phytochem. Rev.*, 1, 37, 2002.
67. Arroo, R.R.J., Alfermann, A.W., Medarde, M., Petersen, M., Pras, N., and Woolley, J.G., Plant cell factories as a source for anti-cancer lignans, *Phytochem. Rev.*, 1, 27, 2002.
68. Fuss, E., Lignans in plant cell and organ cultures: an overview, *Phytochem. Rev.*, 2, 307, 2003.
69. Farkya, S., Bisaria, V.S., and Srivastava, A.K., Biotechnological aspects of the production of the anticancer drug podophyllotoxin, *Appl. Microbiol. Biotechnol.*, 65, 504, 2004.
70. Kadkade, P.G., Growth and podophyllotoxin production in callus tissues of *Podophyllum peltatum*, *Plant Sci. Lett.*, 25, 107, 1982.
71. Van Uden, W., Homan, B., Woerdenbag, H.J., Pras, N., Malingre, T.M., and Wichers, H.J., Isolation, purification and cytotoxicity of 5-methoxypodophyllotoxin, a lignan from a root culture of *Linum flavum*, *J. Nat. Prod.*, 55, 102, 1992.
72. Oostdam, A., Mol, J.N.M., and van der Plas, L.H.W., Establishment of hairy root cultures of *Linum flavum* producing the lignan 5-methoxypodophyllotoxin, *Plant Cell Rep.*, 12, 474, 1993.
73. Lin, H.W., Kwok, K.H., and Doran, P.M., Production of podophyllotoxin using cross-species coculture of *Linum flavum* hairy roots and *Podophyllum hexandrum* cell suspensions, *Biotechnol. Prog.*, 19, 1417, 2003.
74. Saito, H., Yoshikawa, H., Nishimura, Y., Kondo, S., Takeuchi, T., and Umezawa, H., Studies on lignan lactone antitumour agents. II. Synthesis of *N*-alkylamino- and 2,6-dideoxy-2-aminoglycosidic lignan variants related to podophyllotoxin, *Chem. Pharm. Bull.*, 34, 3741, 1986.

75. Wang, Z.Q., Kuo, Y.H., Schnur, D., Bowen, J.P., Liu, S.Y., Han, F.S., Chang, J.Y., Cheng, Y.C., and Lee, K.H., Antitumour agents. 113. New 4β-arylamino derivatives of 4'-*O*-demethylepipodophyllotoxin and related compounds as potent inhibitors of human DNA topoisomerase II, *J. Med. Chem.*, 33, 2660, 1990.
76. Leteurtre, F., Madalengoitia, J., Orr, A., Guzi, T.J., Lehnert, E., Macdonald, T., Pommier, Y., and Cuzi, T.J., Rational design and molecular effects of a new topoisomerase II inhibitor, azatoxin, *Cancer Res.,* 52, 4478, 1992.
77. Terada, T., Fujimoto, K., Nomura, M., Yamashita, J., Wierzba, K., Yamazaki, R., Shibata, J. et al., Antitumor agents. 3. Synthesis and biological activity of 4 beta-alkyl derivatives containing hydroxy, amino, and amido groups of 4'-*O*-demethyl-4-desoxypodophyllotoxin as antitumor agents, *J. Med. Chem.* 36, 1689, 1993.
78. Saulnier, M.G., Langley, D.R., Kadow, J.F., Senter, P.D., Knipe, J.O., Tun, M.M., Vyas, D.M., and Doyle, T.W., Synthesis of etoposide phosphate, BMY-40481: a water-soluble clinically active prodrug of etoposide, *Bioorg. Med. Chem. Lett.,* 4, 2567, 1994.
79. Perrin, D., van Hille, B., Barret, J.-M., Kruczynski, A., Etiėvant, C., Imbert, T., and Hill, B.T., F11782, a novel epipodophylloid non-intercalating dual catalytic inhibitor of topoisomerases I and II with an original mechanism of action, *Biochem. Pharmacol.,* 59, 807, 2000.
80. Botta, B., Monache, G.D., Misiti, D., Vitali, A., and Zappia, G., Aryltetralin lignans: chemistry, pharmacology and biotransformations, *Curr. Med. Chem.,* 8, 1363, 2001.
81. Bush, E.J. and Jones, E.W., Asymmetric total synthesis of (–)-podophyllotoxin, *J. Chem. Soc. Chem. Commun.*, 15, 1200, 1993.
82. Wu, Y., Zhang, H., Zhao, Y., Zhao, J., Chen, J. and Li, L., A new and efficient strategy for the synthesis of podophyllotoxin and its analogues, *Org. Lett.*, 9, 1199, 2007.
83. Wu, Y., Zhao, J., Chen, J., Pan, C., Li, L. and Zhang, H., Enantioselective sequential conjugate addition-allylation reactions: a concise total synthesis of (+)-podophyllotoxin, *Org. Lett.*, 11, 597, 2009.
84. Stadler, D. and Bach, T., Concise stereoselective synthesis of (-)-podophyllotoxin by an intermolecular iron(III)-catalyzed Friedel–Crafts alkylation, *Angew. Chem. Int. Ed. Engl.*, 47, 7557, 2008.
85. Kuhn, M., Keller-Juslen, C., and von Wartburg, A., Partial syntheses von 4′-demethylepipodophyllotoxins, *Helv. Chem. Acta*, 52, 944, 1969.
86. Kamal, A. and Gayatri, N.L., An effiicient method for 4β-anilino-4′-demethylepi-podophyllotoxins: synthesis of NPF and W-68, *Tetrahedron Lett.*, 37, 3359, 1996.
87. Daley, L., Meresse, P., Bertounesque, E., and Monneret, C., A one-pot, efficient synthesis of the potent cytotoxic podophyllotoxin derivative NPF, *Tetrahedron Lett.*, 28, 2673, 1997.
88. Kamel, A., Laxman, N., and Ramesh. G., Facile and efficient one-pot synthesis 4β-arylamino-podophyllotoxins: synthesis of DNA topoisomerase II inhibitors (NPF and W-68), *Bioorg. Med. Chem. Lett.*, 10, 2059, 2000.
89. Kamal, A., Kumar, B.A., and Arifuddin, M., A one-pot, efficient and facile synthesis of 4β-arylaminopodophyllotoxins: synthesis of NPF and GL-331 as DNA topoisomerase II inhibitors, *Tetrahedron Lett.*, 44, 8457, 2003.
90. Kuhn, M. and von Wartburg, A., On a new glycoside synthesis process II. Glycosides of 4′-demethylepipodophyllotoxins, *Helv. Chem. Acta*, 52, 948, 1969.
91. Imbert, T., Guminski, Y., Monse, B., Hill, B., and Robin, J.-P., Water-soluble derivatives of epipodphyllotoxin, process for their preparation, their use as medicinal products and their intended use in anti-cancer treatments, Pierre Fabre Medicament, Boulogne, France, US6, 107, 284, 2000.
92. MacDonald, T.L., Lehnen, E.K., Loper, J.T., Chow, K-C., and Ross, W.E., On the mechanism of interaction of DNA topoisomerase II with chemotherapeutic agents. In *DNA Topoisomerase in Cancer*, Potmesil, M. and Kohn, K.W., Eds., Oxford University Press: New York, 1991, 199.
93. Tepe, J.J., Madalengoitia, J.S., Slunt, K.M., Werbovetz, K.W., Spoors, P.G., and Macdonald, T.L., Inhibition of DNA topoisomerase II by azaelliptitoxins functionalized in the variable substituent domain, *J. Med. Chem.,* 39, 2188, 1996.
94. Long, B.H., Musial, S.T., and Brattain, M.G., Comparison of cytotoxicity and DNA breakage activity of congeners of podophyllotoxin including VP16-213 and VM26: a quantitative structure–activity relationship, *Biochemistry,* 23, 1183, 1984.
95. Zhang, Y.L. and Lee, K.H., Recent progress in the development of novel antitumor etoposide analogs, *Chin. Pharm. J.*, 46, 319, 1994.
96. Wang, Z.Q., Hu, H., Chen, H.X., Cheng, Y.C., and Lee, K.H., Antitumor agents 124. New 4β-substituted aniline derivatives of 6,7-*O,O*-demethylpodophyllotoxin and related compounds as potent inhibitors of human DNA topoisomerase II, *J. Med. Chem.*, 35, 871, 1992.

97. Cho, S.J., Kashiwada, Y., Bastow, K.F., Cheng, Y.C., and Lee, K.H., Antitumor agents 164. Podophenazine, 2″,3″-dichloropodophenazine, benzopodophenazine, and their 4β-*p*-nitroaniline derivatives as novel DNA topoisomerase II inhibitors, *J. Med. Chem.*, 39, 1396, 1996.
98. Thurston, L.S., Irie, H., Tani, S., Han, F.S., Liu, Z.C., Cheng, Y.C., and Lee, K.H., Antitumor agents 78. Inhibition of human DNA topoisomerase II by podophyllotoxin and α-peltatin analogues, *J. Med. Chem.*, 29, 1547, 1986.
99. Saito, H., Nishimura, Y., Kondo, S., Takeuchi, T., and Umezawa, H., Studies on lignan lactone antitumor agents IV. Synthesis of glycosidic lignan variants related to α-peltatin, *Bull. Chem. Soc. Jpn.*, 61, 1259, 1988.
100. Denny, W.A. and Baguley, B.C., Dual topoisomerase I/II inhibitors in cancer therapy, *Curr. Top. Med. Chem.,* 3, 339, 2003.
101. Lee, K.H., Imakura, Y., Haruna, M., Beers, S.A., Thurston, L.S., Dai, H.J., Chen, C.H., Liu, S.Y., and Cheng, Y.C., Antitumor agents 107. New cytotoxic 4-alkylamino analogues of 4′-demethylepipodophyllotoxin as inhibitors of human DNA topoisomerase II, *J. Nat. Prod.,* 52, 606, 1989.
102. Zhou, X.M., Wang, Z.Q., Chang, J.Y., Chen, H.X., Cheng, Y.C., and Lee, K.H., Antitumor agents 120. New 4-substituted benzylamine and benzyl ether derivatives of 4′-*O*-demethylepipodophyllotoxin as potent inhibitors of human DNA topoisomerase II, *J. Med. Chem.,* 34, 3346, 1991.
103. Lee, K.H., Beers, S.A., Mori, M., Wang, Z.Q., Kuo, Y.H., Li, L., Liu, S.Y., Chang, J.Y., Han, F.S., and Cheng, Y.C., Antitumor agents 111. New 4-hydroxylated and 4-halogenated anilino derivatives of 4′-demethylepipodophyllotoxin as potent inhibitors of human DNA topoisomerase II, *J. Med. Chem.,* 33, 1364, 1990.
104. Chang, J.Y., Han, F.S., Liu, S.Y., Wang, Z.Q., Lee, K.H., and Cheng, Y.C., Effect of 4β-arylamino derivatives of 4′-*O*-demethylpodophyllotoxin on human DNA topoisomerase II, tubulin polymerization, KB Cells, and their resistant variants, *Cancer Res*., 51, 1755, 1991.
105. Xiao, Z., Bastow, K.F., Vance, J.R., and Lee, K.-H., Antitumor agents. Part 227: studies on novel 4'-*O*-demethyl-epipodophyllotoxins as antitumor agents targeting topoisomerase II, *Bioorg. Med. Chem.,* 12, 3339, 2004.
106. Xiao, Z., Bastow, K.F., Vance, J.R., Sidwell, R.S., Wang, H.-K., Chen, M.S., Shi, Q., and Lee, K.-H., Antitumor agents. 234. Design, synthesis, and biological evaluation of novel 4β-[(4″-benzamido)-amino]-4'-*O*-demethyl-epipodophyllotoxin derivatives, *J. Med. Chem.,* 47, 5140, 2004.
107. Guianvarćh, D., Duca, M., Boukarim, C., Kraus-Berthier, L., Leonce, S., Pierre, A., Pfeiffer, B. et al., Synthesis and biological activity of sulfonamide derivatives of epipodophyllotoxin, *J. Med. Chem.,* 47, 2365, 2004.
108. Duca, M., Arimondo, P.B., Leonce, S., Pierre, A., Pfeiffer, B., Monneret, C., and Dauzonne, D., Novel carbamate derivatives of 4-β-amino-4'-*O*-demethyl-4-desoxypodophyllotoxin as inhibitors of topoisomerase II: synthesis and biological evaluation, *Org. Biomol. Chem.,* 3, 1074, 2005.
109. Yu, P.F., Chen, H., Wang, J., He, C.X., Cao, B., Li, M., Yang, N., Lei, Z.Y., and Cheng, M.S., Design, synthesis and cytotoxicity of novel podophyllotoxin derivatives, *Chem. Pharm. Bull. (Tokyo)*, 56, 831, 2008.
110. Hu, C., Xu, D., Du, W., Qian, S., Wang, L., Lou, J., He, Q., Yang, B., and Hu, Y., Novel 4β-anilino-podophyllotoxin derivatives: design synthesis and biological evaluation as potent DNA-topoisomerase II poisons and anti-MDR agents, *Mol. Biosyst.*, 6, 410, 2010.
111. Bhat, B.A., Reddy, P.B., Agrawal, S.K., Saxena, A.K., Kumar, H.M.S., and Qazi, G.N., Studies on novel 4β-[(4-substituted)-1,2,3-triazol-1-yl] podophyllotoxins as potential anticancer agents, *Eur. J. Med. Chem.*, 43, 2067, 2008.
112. Hitotsuyanagi, Y., Fukuyo, M., Tsuda, K., Kobayashi, M., Ozeki, A., Itokawa, H., and Takeya, K., 4-Aza-2,3-dehydro-4-deoxypodophyllotoxins: simple aza-podophyllotoxin analogues possessing potent cytotoxicity, *Bioorg. Med. Chem. Lett.,* 10, 315, 2000.
113. Magedov, I.V., Manpadi, M., Rozhkova, E., Przheval'skii, N.M., Rogelj, S., Shors, S.T., Steelant, W.F.A., Van slambrouck, S., and Kornienkoc, A., Structural simplification of bioactive natural products with multicomponent synthesis: dihydropyridopyrazole analogues of podophyllotoxin, *Bioorg. Med. Chem. Lett.*, 17, 1381, 2007.
114. Magedov, I.V., Manpadi, M., Van slambrouck, S., Steelant, W.F.A., Rozhkova, E., Przheval'skii, N.M., Rogelj, S., and Kornienko, A., Discovery and investigation of antiproliferative and apoptosis-inducing properties of new heterocyclic podophyllotoxin analogues accessible by a one-step multicomponent synthesis, *J. Med. Chem.,* 50, 5183, 2007.
115. Chen, S.W., Xiang, R., Liu, J., and Tian, X., Synthesis and biological evaluation of novel conjugates of podophyllotoxin and 5-FU as antineoplastic agents, *Bioorg. Med. Chem.,* 17, 3111, 2009.

116. Passarella, D., Peretto, B., Blasco y Yepes, R., Cappelletti, G., Cartelli, D., Ronchi, C., Snaith, J., Fontana, G., Danieli, B., and Borlak, J., Synthesis and biological evaluation of novel thiocolchicine-podophyllotoxin conjugates, *Eur. J. Med. Chem.*, 45, 219, 2010.
117. Kadow, J.F., Vyas, D.M., and Doyle, T.W., Synthesis of etoposide lactam via a Mitsunobu reaction sequence, *Tetrahedron Lett.*, 30, 3299, 1989.
118. Gensler, W.J., Murthy, C.D., and Trammell, M.H., Nonenolizable podophyllotoxin derivatives, *J. Med. Chem.*, 20, 635, 1977.
119. Zhou, X.M., Lee, K.J.H., Cheng, J., Wu, S.S., Chen, H.X., Guo, X., Cheng, Y.C., and Lee, K.H., Antitumor agents 144. New γ-lactone ring-modified arylamino etoposide analogs as inhibitors of human DNA topoisomerase II, *J. Med. Chem.*, 37, 287, 1994.
120. Tomioka, K., Kubota, Y., and Koga, K., Synthesis and antitumor activity of podophyllotoxin aza-analogues, *Tetrahedron Lett.*, 30, 2953, 1989.
121. Roulland, E., Bertounesque, E., Huel, C., and Monneret, C., Synthesis of picropodophyllotoxin homolactone, *Tetrahedron Lett.*, 41, 6769, 2000.
122. Glinski-Oomen, M.B., Freed, J.C., and Drust, T., Preparation of 2-substituted podophyllotoxin derivatives, *J. Org. Chem.*, 52, 2749, 1987.
123. VanVliet, D.S. Tachibana, Y., Bastow, K.F., Huang, E.S., and Lee, K.H., Antitumor agents: 207. Design, synthesis, and biological testing of 4β- anilino-2-fluoro-4′-demethylpodophyllotoxin analogues as cytotoxic and antiviral agents, *J. Med. Chem.*, 44, 1422, 2001.
124. Xiao, Z., Han, S.Q., Bastow, K.F., and Lee, K.H., Antitumor Agents. Part 232: Synthesis of cyclosulfite podophyllotoxin analogues as novel prototype antitumor agents, *Bioorg. Med. Chem. Lett.*, 14, 1581, 2004.
125. Imperio, D., Pirali, T., Galli, U., Pagliai, F., Cafici, L., Canonico, P.L., Sorba, G., Genazzani, A.A., and Tron, G.C., Replacement of the lactone moiety on podophyllotoxin and steganacin analogues with a 1,5-disubstituted 1,2,3-triazole via ruthenium-catalyzed click chemistry, *Bioorg. Med. Chem.*, 15, 6748, 2007.
126. Gordaliza, M., Castro, M.A., Miguel del Corral, J.M., López-Vázquez, M.L., García, P.A., San Feliciano, A., García-Grávalos, M.D., and Broughton, H., Preparation and cytotoxicity of podophyllotoxin derivatives lacking the lactone ring. *Tetrahedron,* 53, 15743, 1997.
127. Castro, M.A., del Corral, J.M.M., Gordaliza, M., Garcia, P.A., Gomez-Zurita, M.A., Garcia-Gravalos, M.D., de la Iglesia-Vicente, J., Gajate, C., An, F., Mollinedo, F., and San Feliciano, A., Synthesis and biological evaluation of new selective cytotoxic cyclolignans derived from podophyllotoxin, *J. Med. Chem.,* 47, 1214, 2004.
128. Castro, M.A., Miguel del Corral, J.M., Gordaliza, M., Garcia, P.A., Gomez-Zurita, M.A., and San Feliciano, A., Synthesis and cytotoxic evaluation of C-9 oxidized podophyllotoxin derivatives, *Bioorg. Med. Chem.,* 15, 1670, 2007.
129. Castro, M.A., Miguel Del Corral, J.M., Gordaliza, M., Gomez-Zurita, M.A., Garcia, P.A., and San Feliciano, A., Chemoinduction of cytotoxic selectivity in podophyllotoxin-related lignans, *Phytochem. Rev.,* 2, 219, 2004.
130. Ayres, D.C. and Lim, C.K., Lignans and related phenols. Part XIII. Halogenated derivatives of podophyllotoxin, *J. Chem. Soc., Perkin I*, 111, 1350, 1972.
131. Hu, H., Wang, Z.Q., Liu, S.Y., Cheng, Y.C., and Lee, K.H., Antitumor agents 123. Synthesis and human DNA topoisomerase II inhibitory activity of 2′-chloro derivatives of etoposide and 4β-(arylamino)-4′-*O*-demethylpodophyllotoxins, *J. Med. Chem.*, 35, 866, 1992.
132. Cho, S.J., Tropsha, A., Suffness, M., Cheng, Y.C., and Lee, K.H., Antitumor agents 163. Three-dimensional quantitative structure–activity relationship study of 4'-*O*-demethylepipodophyllotoxin analogs using the modified CoMFA/q^2-GRS approach, *J. Med. Chem.*, 39, 1383, 1996.
133. Ji, Z., Wang, H.K., Bastow, K.F., Zhu, X.K., Cho, S.J., Cheng, Y.C., and Lee, K.H., Antitumor agents 177. Design, syntheses, and biological evaluation of novel etoposide analogs bearing pyrrolecarboxamidino group as DNA topoisomerase II inhibitors, *Bioorg. Med. Chem. Lett.,* 7, 607, 1997.
134. Xiao, Z., Xiao, Y.-D., Feng, J., Golbraikh, A., Tropsha, A., and Lee, K.-H., Antitumor agents. 213. Modeling of epipodophyllotoxin derivatives using variable selection *k* nearest neighbor QSAR method, *J. Med. Chem.,* 45, 2294, 2002.
135. Afroz Alam, M., and Naik, P.K., Molecular modelling evaluation of the cytotoxic activity of podophyllotoxin analogues, *J. Comput. Aided Mol. Des.,* 23, 209, 2009.
136. Hande, K.R., Etoposide: four decades of development of a topoisomerase II inhibitor, *Eur. J. Cancer*, 34, 1514, 1998.
137. Lee, K.H., Novel antitumor agents from higher plants, *Med. Res. Rev.*, 19, 569, 1999.

138. Utsugi, T., Shibata, H., Kumio, S., Aoyagi, K., Wierzba, K., Kobunai, T., Terada, T., Oh-Hara, T., Tsuruo, T., and Yamada, Y., Antitumor activity of a novel podophyllotoxin derivative (TOP-53) against lung cancer and lung metastatic cancer, *Cancer Res.*, 56, 2809, 1996.
139. Byl, J.A., Cline, S.D., Utsugi, T., Kobunai, T., Yamada, Y., and Osheroff, N., DNA topoisomerase II as the target for the anticancer drug TOP-53: mechanistic basis for drug action, *Biochemistry*, 40, 712, 2001.
140. Solary, E., Leteurtre, F., Paull, K.D., Scudiero, D., Hamel, E., and Pommier, Y., Dual inhibition of topoisomerase II and tubulin polymerization by azatoxin, a novel cytotoxic agent, *Biochem. Pharmacol.*, 45, 2449, 1993.
141. Kruczynski, A., Ricome, C., Waud, W.R., and Hill, B.T., *In vivo* antitumor activity of F11782, a non-intercalating dual catalytic inhibitor of topoisomerases I and II, against a panel of human tumor xenografts, *J. Exp. Ther. Oncol.*, 2, 219, 2002.
142. Sargent, J.M., Elgie, A.W., Williamson, C.J., and Hill, B.T., *Ex vivo* effects of the dual topoisomerase inhibitor tafluposide (F 11782) on cells isolated from fresh tumor samples taken from patients with cancer, *Anticancer Drugs*, 14, 467, 2003.
143. Pagani, O., Zucchetti, M., Sessa, C., De Jong, J., D'Incalci, M., De Fusco, M., Kaeser-Froehlich, A., Hanauske, A., and Cavalli, F., Clinical and pharmacokinetic study of oral NK611, a new podophyllotoxin derivative, *Cancer Chemother. Pharmacol.*, 38, 541, 1996.
144. Mross, K., Huettmann, A., Herbst, K., Hanauske, A.-R., Schilling, T., Manegold, C., Burk, K., and Hossfeld, D.K., Pharmacokinetics and pharmacodynamics of the new podophyllotoxin derivative NK 611: a study by the AIO groups PHASE-I and APOH, *Cancer Chemother. Pharmacol.*, 38, 217, 1996.
145. Liu, J.M., Chen, L.T., Chao, Y., Li, A.F.Y., Wu, C.W., Liu, T.-S., Shiah, H.S. et al., Phase II and pharmacokinetic study of GL331 in previously treated Chinese gastric cancer patients, *Cancer Chemother. Pharmacol.*, 49, 425, 2002.

6 Taxol and Its Analogs

David G. I. Kingston

CONTENTS

6.1 Introduction 123
6.2 History 124
6.2.1 Discovery and Preclinical Development 124
6.2.2 Clinical Development 124
6.2.3 Taxol Supply 125
6.2.4 Docetaxel 126
6.3 Biosynthesis of Taxol 127
6.3.1 Diterpenoid Ring System 128
6.3.2 The Side Chain 129
6.4 The Mechanism of Action of Taxol 129
6.5 Medicinal Chemistry of Taxol 130
6.5.1 Ring A Modifications 130
6.5.2 Ring B Modifications 131
6.5.3 Ring C Modifications 135
6.5.4 Ring D Modifications 138
6.5.5 Side Chain Analogs 139
6.5.6 Summary of Taxol's SAR 141
6.6 Prodrugs of Taxol 141
6.6.1 Simple Water-Soluble Derivatives 141
6.6.2 Polymer Conjugates of Taxol 143
6.6.3 Targeted Analogs of Taxol 145
6.6.4 Nanoparticles as Delivery Agents for Taxol 148
6.6.5 Antibody Conjugates of Taxol 150
6.7 Synthetic Studies 151
6.7.1 Semisynthetic Methods 151
6.7.2 Total Synthesis 153
6.8 The Taxol–Tubulin Interaction 154
6.9 Clinical Applications of Taxol, Docetaxel, and Cabazitaxel 157
6.10 Taxol Analogs in Clinical Trials 158
6.11 Conclusion 159
Acknowledgments 160
References 160

6.1 INTRODUCTION

This chapter is a revised and expanded version of the one published in 2005;[1] it has been revised and updated with new material published over the period 2004 to early 2010. Some of the historical background and other material from the previous edition have been condensed to make room for more recent results. Because of the enormous extent of the literature on taxol, with over 48,000 references in SciFinder as of 2010, a short review such as this cannot include all the relevant work.

The selection of work to be included has been guided in part by the author's own interests and by work that illustrates the chemistry and structure–activity relationships (SARs) of this fascinating compound. Several reviews of the chemistry and biology of taxol and related compounds have been published recently, and can be consulted for more details in their respective areas. These include a book chapter on the SARs of taxol,[2] and reviews of structural studies of taxol analogs[3] of the medicinal chemistry of taxol,[4,5] of the development of new generation taxanes,[6,7] and of the clinical development of new taxol analogs.[8]

Arguably no naturally occurring anticancer agent has made a bigger impact on cancer treatment than Taxol™ (**1**), now known as paclitaxel.[9] Although it is now recognized as one of the most important drugs available for the treatment of breast and ovarian cancers, and although it has spawned several analogs that are now in clinical trials, taxol itself almost never became a drug at all. This chapter will briefly cover the early history of the discovery and development of taxol, and will then go on to describe its medicinal chemistry, its synthesis, its interaction with tubulin, and its relationship to compounds such as the epothilones and discodermolide which have similar mechanisms of action.

6.2 HISTORY

6.2.1 Discovery and Preclinical Development

Taxol (**1,** Figure 6.1) was first isolated by Wall and Wani as the antileukemic and cytotoxic constituent of a sample of the bark of *Taxus brevifolia* Nutt., and its structure was published 1971.[10] Although it was clearly an interesting lead compound, its complex structure, low availability from its natural source, and lack of water solubility diminished interest in its development. Fortunately, Dr. Wall and Dr. Matthew Suffness at the National Cancer Institute (NCI) believed in its potential, and so development proceeded with funding from NCI. Modest amounts of taxol were isolated in the early 1970s to allow for additional animal testing, and a turning point was reached when it was found that taxol showed excellent activity against various human solid tumor xenografts in nude mice, including the CX-1 colon and MX-1 breast xenografts. These results were encouraging enough that in 1977 the NCI decided to begin preclinical formulation and toxicity studies of taxol, with a view to eventual clinical trials.

A second major turning point in taxol's development was the discovery by Dr. Susan Horwitz of its unique activity as a promoter of tubulin polymerization (Figure 6.2).[11] Although clinically used drugs such as vinblastine (Velban™) and vincristine (Oncovin™) (Chapter 7) were known to act as inhibitors of tubulin polymerization, taxol was the first compound shown to act in the opposite direction. This discovery demonstrated that taxol was not "just another cytotoxic agent," and awakened a renewed interest in the compound, not least in the biological community.

6.2.2 Clinical Development

Taxol entered Phase 1 clinical trials in 1984, but unfortunately it gave some allergic reactions, most probably related to its formulation as an emulsion with Cremophor EL®, a polyethoxylated castor oil; these reactions were responsible for at least one death.[12] These problems would have spelled the

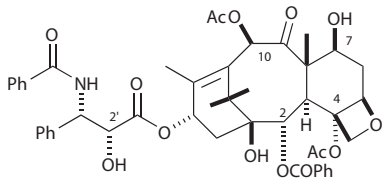

1

FIGURE 6.1 Structure and numbering of taxol (paclitaxel).

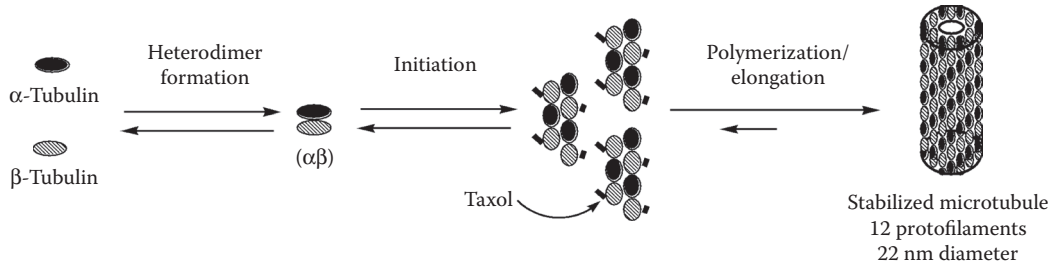

FIGURE 6.2 Tubulin polymerization by taxol.

demise of most drug candidates, but taxol's unique mechanism of action was enough to encourage the clinicians to persevere, and the problems were overcome by lengthening the infusion period and premedicating patients. Ironically, these changes may have contributed to taxol's eventual success, as there is evidence that the cytotoxicity and *in vivo* activity of taxol are increased on prolonged exposure to the drug.[13] In any event, Phase II trials with the lengthened infusion period were initiated in 1985, and these proved to be very successful. The first definitive clinical results were obtained in 1989 against drug-refractory ovarian cancer,[14] and 2 years later excellent clinical results were reported against breast cancer.[15] It was approved by the U.S. Food and Drug Administration (FDA) for the treatment of refractory ovarian cancer in 1992, and for treatment of refractory or anthracycline-resistant breast cancer in 1994.

The discovery and preclinical work as well as the initial clinical studies on taxol were sponsored by the NCI. Once it became clear that the compound had real therapeutic value, but that its further development would require more resources than NCI could allocate, its development was offered to the pharmaceutical industry under a Cooperative Research and Development Agreement (CRADA), and an agreement was signed with Bristol–Myers Squibb (BMS) in 1989. As taxol was never patented, BMS was also granted a 7-year period of exclusivity in return for their development investment.

6.2.3 Taxol Supply

The therapeutic efficacy of taxol became generally known by 1990, but unfortunately the supply of the drug from its natural source of *T. brevifolia* bark was not immediately adequate to the task of supplying a dramatically expanded demand. The situation was further complicated by the fact that *T. brevifolia* was primarily obtained from the old-growth forests of the Pacific Northwest of the United States, and these forests were the natural habitat of the endangered spotted owl. The prospect of large-scale harvesting of *T. brevifolia* for taxol production thus raised serious environmental concerns.[16]

The initial approach to solving this vexing problem was to mount a large-scale collection and extraction program for *T. brevifolia* bark, and this was successfully carried out by Hauser Chemical Research of Boulder, Colorado, under contract from BMS. This approach was then replaced by a semisynthetic process from 10-deacetylbaccatin III (10-DAB, **2,** Figure 6.3), which Potier et al. had

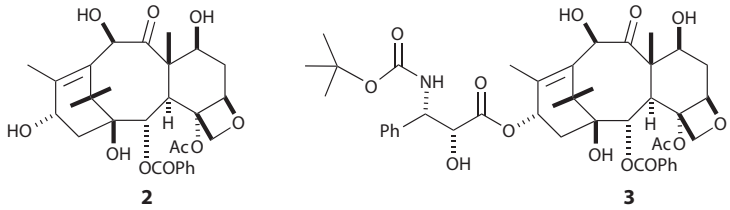

FIGURE 6.3 The structures of 10-DAB (**2**) and docetaxel (**3**).

found to be abundant in the European yew, *Taxus baccata*.[17,18] Several groups developed methods to convert 10-DAB to taxol, including those of Potier[18] and Holton,[19] and the second phase of large-scale production began in 1993 with the adoption by BMS of the Holton semisynthetic process for the synthesis of taxol from 10-DAB. As 10-DAB is available in yew needles in relatively large amounts,[18,20] this approach provided an immediate solution to the supply crisis. The conversion of 10-DAB to taxol involved a coupling reaction with a synthetic β-lactam intermediate; this and other semisynthetic methods will be described later in Section 6.6.1.

A third approach to the production of taxol is that of plant tissue culture. An enormous effort was expended on the development of viable methods of taxol production by plant tissue culture methods, and this subject has been reviewed.[21,22] Production of taxol is enhanced by elicitation with methyl jasmonate and other elicitors, and yields of up to 295 mg/L in 2-week cell cultures of *Taxus media* grown in flasks have been reported.[21] These yields are close to those needed for commercial production, and undoubtedly unpublished proprietary improvements have been made to facilitate large-scale production. The commercial production of taxol by cell culture methods has been reported in 2003 by the Korean company SamYang Genex,[23] who name their product Genexol®. BMS began producing taxol by plant cell culture methods in 2003.[21] The details of this process have not been released, but it is known that production is based on cultures of *Taxus chinensis* in Germany, and that final purification is carried out at the company's plant in Swords, Ireland, based on a method developed in collaboration with Phyton Inc.[24] The method is reported to be much more environmentally friendly than the previous semisynthetic method, requiring only 5 organic solvents instead of the 13 solvents needed for the earlier method.

The production of taxol by the endophytic fungus *Taxomyces andreanae* has also been reported,[25] but the yield was extremely low (approximately 50 ng/L). The fungus *Periconia* sp. was also found to produce taxol at the level of 800 ng/L when stimulated with benzoic acid,[26] and a survey of endophytic fungi from *Taxus chilensis* identified one that produced taxol at a level of almost 1 mg/L.[27] However, at this point the maximum yields of taxol by the fungal route lag behind those of the plant tissue culture route, and no taxol is prepared commercially by this route. Perspectives for biotechnological production of taxol have been reviewed,[28] and it has been suggested that the best prospects for microbial taxol production may require the discovery of endophytes that make large quantities of a precursor taxane that could be converted chemically to taxol.[29]

A final chemical approach is the conversion of mixtures of taxanes differing only in the nature of the *N*-acyl group into *N*-debenzoyltaxol (**18**; Scheme 6.1), which can then be converted into taxol by simple benzoylation; this process has been commercialized by Natural Pharmaceuticals Inc.[30]

The commercial production of taxol is now shared between plant tissue culture methods, semisynthesis from 10-DAB, and direct isolation from *Taxus* sp. The semisynthetic route from 10-DAB or other natural precursors will, however, continue to be an important option for the commercial synthesis of clinical candidates with modified structures.

6.2.4 Docetaxel

This historical section would not be complete without a brief account of the discovery of docetaxel (Taxotere™), until recently the only other taxoid drug (as opposed to formulations of taxol such as Abraxane and Nanoxel) in clinical use. The Potier group at the CNRS in Paris became interested in taxol in the early 1980s, and carried out a series of isolation and semisynthetic studies. Their finding that 10-DAB (**2**) could be obtained in good yield from the needles of *T. baccata*[17,18] led them to develop various approaches to the semisynthesis of taxol from this precursor. One of their first syntheses involved hydroxyamination of a cinnamoyl substituted baccatin III derivative to give a mixture of stereoisomeric and regioisomeric hydroxyamines.[31] As the *t*-butyloxycarbonyl group was being used as an amine protective group, one of these products was a protected version of compound **3**, and so this intermediate was converted to **3** and tested for biological activity. It turned out

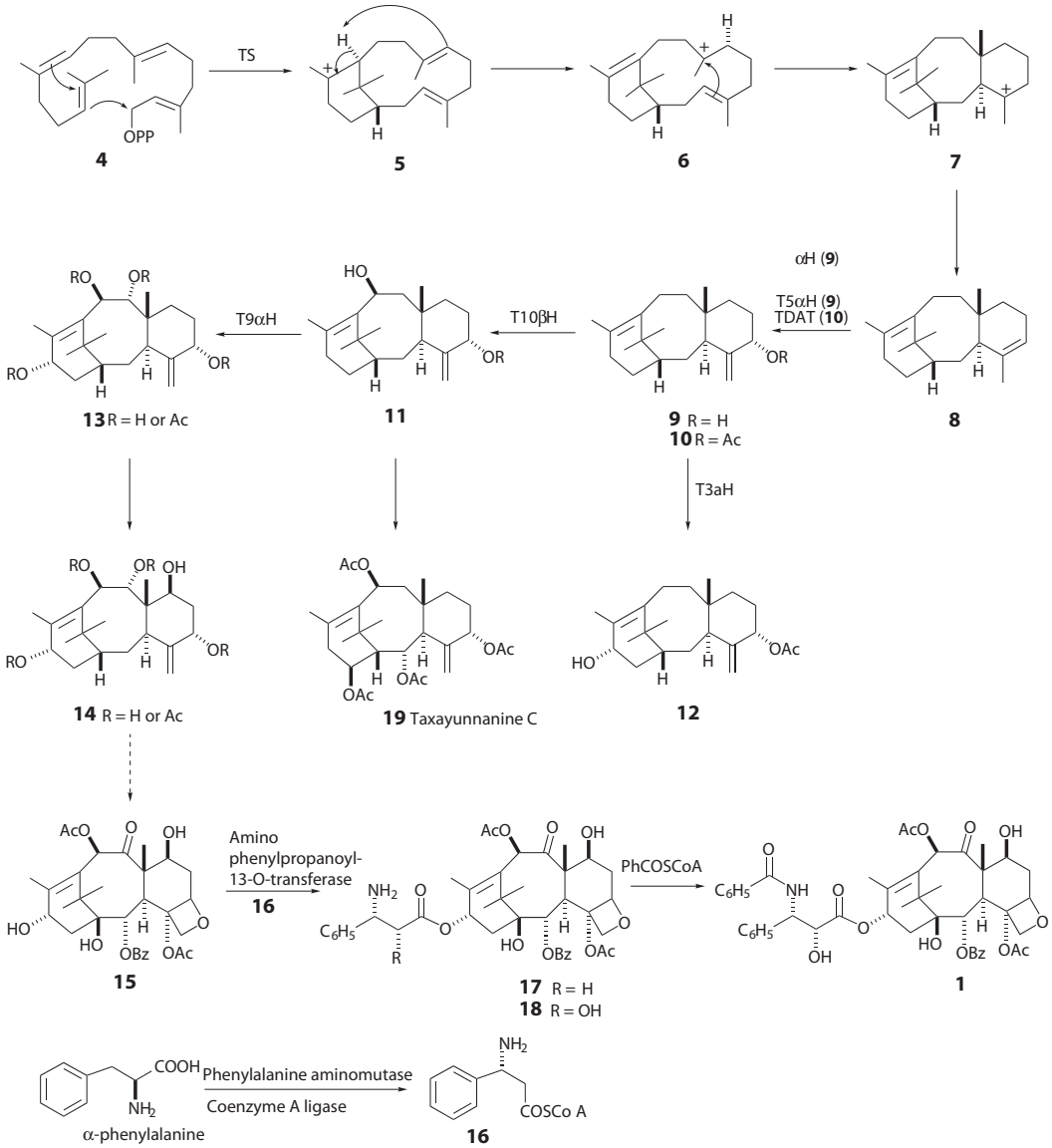

SCHEME 6.1 Biosynthetic pathways to taxol.

to have excellent activity, better than taxol in some assays, and it was thus developed as a parallel drug to taxol. Taxotere™, as the compound was named, entered Phase I clinical trials in 1990,[32] and was approved for treatment of advanced breast cancer in South Africa in 1995 and in the United States in 1996, and for nonsmall-cell lung cancer (NSCLC) in 1999; its generic name is docetaxel.[33]

6.3 BIOSYNTHESIS OF TAXOL

Interest in the biosynthesis of taxol has been driven in part by a need to develop a renewable and environmentally friendly source of this important compound. Significant work has been carried out on the scientific study of the biosynthetic pathways to taxol, but the full complement of taxol biosynthetic genes has not yet been successfully expressed in a heterologous host.

6.3.1 Diterpenoid Ring System

Taxol is a diterpenoid, and until a few years ago all diterpenoids were thought to arise from geranylgeranyl diphosphate which was biosynthesized from mevalonic acid. In recent years, however, a nonmevalonoid pathway to terpenoids has been uncovered [34] and it has been shown that at least some taxane diterpenoids are biosynthesized by this pathway. Thus a feeding experiment with [U-$^{13}C_6$] glucose showed the incorporation of an intact three-carbon precursor, eliminating the acetate-derived mevalonic acid as a precursor.[35]

The first committed step in the biosynthesis of the diterpenoid ring system of taxol is the cyclization of geranylgeranyl diphosphate (**4**) catalyzed by taxadiene synthase (TS) to taxa-4(5),11(12)-diene (**8**)[36] (Scheme 6.1). This step was thought initially to be the slow step, based on the low levels of **8** found in *T. brevifolia* bark and the fact that the cyclization step is slow relative to subsequent oxygenations. Based on the presumed rate determining nature of the cyclization of **4** to **8**, the enzyme responsible for the cyclization, taxadiene synthase, was investigated in detail. The enzyme was purified from *T. brevifolia* bark and characterized as a 79 kDa protein.[37] Genetic studies led to the isolation and expression of a cDNA fragment which was expressed in *Escherichia coli* to produce the same protein.[38] A study of the activity of taxadiene synthase in *Taxus canadensis* cell cultures showed that it was greater than that needed for taxol production *in vivo*, suggesting that the true rate-limiting step of taxol biosynthesis occurs further down the pathway.[39]

The mechanism of the cyclization of **4** to **8** has been shown to involve an intramolecular hydride ion transfer (presumably via an enzyme-bound intermediate) from the putative verticillyl ion **5** to the cation **6**, which then undergoes intramolecular cyclization to the tricyclic cation **7** and finally deprotonation to **8**.[40]

As the taxane ring system is oxygenated at eight positions in taxol, the conversion of **8** to taxol requires a series of oxidation reactions. A survey of the oxygenation patterns of known taxoids[41] suggested the order of the oxygenation to be C5 and C10, then C2, C9, and C13, then C7 and C1, followed finally by epoxidation of the C4–C20 double bond and ring expansion to the oxetane ring. The first oxygenation step was shown to be formation of the C-5 alcohol **9**;[42] the low levels of **9** found in *T. brevifolia* bark suggest that the hydroxylation of **8** to **9** may be slow, but it does not appear to be the rate-limiting step in taxol biosynthesis. Conversion of **9** to the acetate **10** was demonstrated with a soluble enzyme preparation from *T. canadensis*, and this is most probably the next step in the biosynthesis.[43]

It has proved to be difficult to elucidate the order of the hydroxylation reactions downstream of **10**, but a probable sequence is hydroxylation to the 10β-ol (**11**),[44] and the taxoid 10β-hydroxylase (T10βH) enzyme that controls this reaction has been cloned and characterized in yeast.[45] Oxidation to the 13β-ol (**12**) has also been demonstrated.[46] Oxidation of **11** would yield the tetrol **13**; the intermediacy of 2α,10β-diol derivatives has also been proposed.[47] The conversion of taxusin (**13**; R = Ac) to its 7β-hydroxy derivative (**14**) has also been demonstrated.[48] Substrate specificity studies with a set of available P450 hydroxylases suggest that there may well be more than one biosynthetic pathway to taxol in the yew, with the various pathways most probably converging on baccatin III (**15**).[46] cDNAs encoding two new P450 taxane hydroxylases and candidate genes for most of the steps of the taxol biosynthesis pathway have been identified.[49] Some taxanes such as taxayunnanine C (**19**) are oxidized at the 14β position rather than the 13α position of taxol, and studies with labeled taxadiene precursors indicated that the bifurcation between the pathways leading to these two classes of compounds occurs after 10β hydroxylation of the taxane core.[50]

The formation of the oxetane ring has been the subject of much speculation, and interest in it is heightened by the fact that the ring is essential for taxol's mechanism of action.[51–53] The current thinking (Scheme 6.2) is that the exocyclic double bond of a precursor such as **20** is epoxidized to the β-epoxide **21**, which then rearranges to the oxetane **22**.

The rearrangement could either be stepwise[54] or concerted.[55] Studies with baccatin transferases have shown that taxane 10β-*O*-acetyltransferase was able to catalyze the 4-*O*-acetylation of 4-DAB

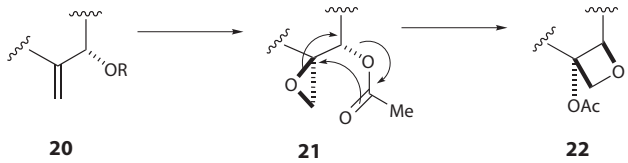

SCHEME 6.2 Proposed mechanism of formation of the oxetane ring of taxol.

to baccatin III, thus suggesting that a separate pathway to the oxetane ring of baccatin III may exist that yields the 4-deacetyl analog as the product.[56] A recent study of various surrogate substrates containing the β-epoxide **21** failed to yield any oxetane-containing products, however, which suggests either that epoxides such as **21** are not on the biosynthetic pathway or (more probably) that oxetane formation only occurs on substrates with different oxygenation patterns than those used.[57]

6.3.2 The Side Chain

The characteristic *N*-benzoylphenyl isoserine side chain of taxol has been shown to arise from phenylalanine, which was efficiently incorporated into taxol.[58,59] The intact side chain was not incorporated into taxol, but the *N*-debenzoyl side chain was incorporated, although not as efficiently as β-phenylalanine.[60] It is thus probable that hydroxylation of the side chain occurs after attachment to baccatin III, and that the major pathway is thus from α-phenylalanine to β-phenylalanine. β-Phenylalanine probably couples to baccatin III via its coenzyme A ester (**16**), followed by *N*-benzoylation, to give *N*-debenzoyl-2′-deoxytaxol (**17**), which finally undergoes hydroxylation to *N*-debenzoyltaxol (**18**) and benzoylation to taxol (**1**).

The overall pathway shown in Scheme 6.1 may be regarded as a plausible pathway to taxol, but the detailed steps and especially the order of the various oxidation steps have not yet been completely established. Steps that have been demonstrated are shown with solid arrows, while those that remain undefined are shown with dotted arrows.

6.4 MECHANISM OF ACTION OF TAXOL

The discovery that taxol was a tubulin polymerization promoter[11] was a key to maintaining interest in it during its lengthy development, since at the time this was an unprecedented mechanism of action for an anticancer drug. Since that time several other natural products, including the epothilones and discodermolide, have been shown to have the same (or very similar) mechanism. Various epothilones are in clinical trials, and the modified epothilone ixabepilone has been approved for clinical use. Discodermolide was in clinical trials as an anticancer agent, but it showed unexpected toxicity and clinical trials have been discontinued. Each of these compounds is described in a separate chapter in this book, and will thus not be discussed here.

The primary mechanism of action of taxol has been investigated extensively. It promotes the polymerization of tubulin heterodimers to microtubules,[11] binding with a stoichiometry of approximately 1 mol of taxol to 1 mol of tubulin dimer. At high concentrations, taxol both stabilizes microtubules and increases the total polymer mass,[61] but these concentrations are higher than those needed to inhibit microtubule functions.[62,63] At clinically relevant concentrations, taxol suppresses dynamic changes in microtubules, leading to mitotic arrest.[64] Taxol interferes with the formation of the mitotic spindle, and this causes the nonsegregation of chromosomes.[65] The actual mechanism by which taxol stabilizes the microtubule is still under investigation, but Xiao et al. speculate that "Taxol induces a loss of flexibility in the involved regions that prevents a 'roll out' of lateral contacts in microtubules that would otherwise open up their wall."[66]

Taxol has been shown to have many biological effects in addition to its ability to stabilize microtubules. Probably the most important activity after its microtubule assembly activity is its

ability to inactivate the antiapoptotic protein Bcl-2. It does this by inducing phosphorylation,[67] which leads to inactivation.[67] The phosphorylation of Bcl-2 may occur through activation of Raf-1 kinase, and it has been proposed that Raf-1 is activated following drug-induced disruptions of microtubules.[68] Taxol also binds directly to Bcl-2.[69]

In spite of taxol's effect on Bcl-2 and other effects such as induction of the production of cytokines,[70] is has been proposed that all the significant effects of taxol are directly traceable to its microtubule-binding activity; as a critical review states: "Unless convincingly proven otherwise, all relevant paclitaxel effects should be assumed to result from its microtubule-binding activity."[71] The actual effects resulting from microtubule binding are however rather complex. As another recent review states:

> Depending on the phase of the cell cycle, taxanes can affect spindle formations, chromosome segregation, or completions of mitosis, thus activating the mitotic or the DNA-damage checkpoints and blocking cell-cycle progression. This complex scenario, with different cell cycle responses related to the specific microtubule function affected in each phase, is reflected in the variety of pathways described to result in apoptosis upon taxane treatment. . .[72]

As the most important biological effects of taxol can be attributed to its microtubule stabilization, the nature of its binding to microtubules becomes of great importance; this subject will be discussed in Section 6.7 of this chapter.

6.5 MEDICINAL CHEMISTRY OF TAXOL

The chemistry and medicinal chemistry of taxol have been extensively investigated, and it is not possible to discuss every aspect of this subject in the space allotted to this chapter. The emphasis of this section will thus be on work that has led to important new understandings or to compounds with improved activity. Readers interested in broader aspects of the subject are referred to any of several reviews.[4,33,73–78]

6.5.1 Ring A Modifications

The C-11(12) double bond in the A-ring of taxol is unreactive to hydrogenation, but the corresponding double bond in baccatin III can be reduced with zinc under acidic conditions. Attempts to prepare docetaxel analogs from dihydrobaccatin III were unsuccessful, as only the inactive 4-deacetyl analog could be obtained.[79] The C-11(12) double bond can, however, be epoxidized if the 10-acetoxyl group is absent, and compound **23** was prepared by epoxidation of 10-deacetoxytaxol; it is more active than taxol in a tubulin assembly assay but less cytotoxic to B16 melanoma cells.[80] A similar result was observed for the derivatives **24** and **25**.[81] The enol **26** is surprisingly stable, and can be converted to the analog **27**, which is slightly more cytotoxic than taxol (Figure 6.4).[82]

The C-18 analog **28** (X = Me, N_3, OAc, CN, or Br) could be prepared by allylic bromination of 7,13-di(triethylsilyl)baccatin III followed by nucleophilic displacement and side chain attachment, but all were less cytotoxic than taxol.[83] A-nortaxol analogs such as **29** were prepared by treatment of taxol with Lewis acids;[84] compounds of this type are much less cytotoxic than taxol, although they do retain some tubulin assembly activity. Similarly, compound **30** with contracted A and C rings is noncytotoxic, but still shows tubulin assembly activity (Figure 6.5).

The hydroxylated baccatin III derivative 14β-hydroxy-10-DAB (**31**) was isolated from *Taxus wallichiana* leaves[85] and has been used as the precursor for a series of 14β-hydroxytaxol analogs.[86] The best of these turned out to be **32**, which is in Phase II clinical trials under the name ortataxel.[87,88] Other compounds prepared from **31** include the A-seco analogs **33** and **34**, which were as active as taxol in the resistant cell line MCF7-R, but were 20–40 times less cytotoxic against several normal cell lines (Figure 6.6).[89]

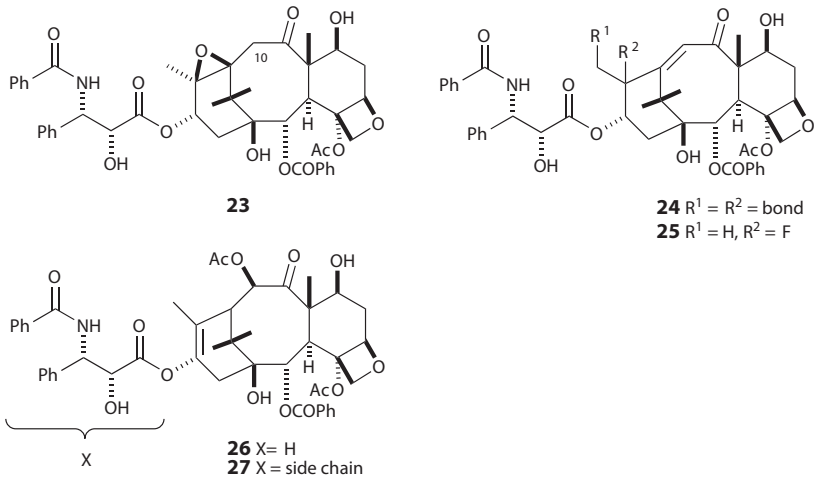

FIGURE 6.4 The structures of A-ring-modified taxanes **23**–**27**.

The importance of the C-1 hydroxyl group was established by the semisynthesis of the 1-deoxytaxol analog **35** from 1-deoxybaccatin VI.[90] Compound **35** was modestly less cytotoxic and less effective at enhancing tubulin polymerization than the comparable C-1 hydroxyl derivative **36**, but it was also somewhat less stable than taxol, and so the C-1 hydroxyl group is an important substituent in all taxane clinical candidates. The similar 1-deoxytaxol analog **37** has also been synthesized from 1-deoxybaccatin VI, and it was found to be as cytotoxic as taxol but fourfold less effective than taxol as a tubulin polymerization agent. These findings were explained by modeling studies showing that **37** can adopt the T-taxol conformation proposed as the tubulin-binding conformation of taxol (Figure 6.7).[91]

6.5.2 Ring B Modifications

Changes at the C-10 position of taxol make relatively small differences to its bioactivity, and in several cases bioactivity can be enhanced by the appropriate substitutions. Taxol itself can be

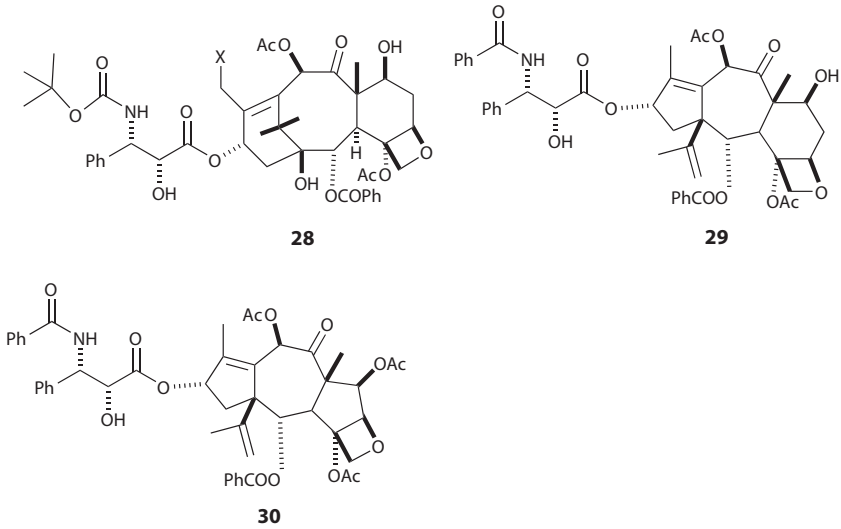

FIGURE 6.5 The structures of A-ring-modified taxanes **28**–**30**.

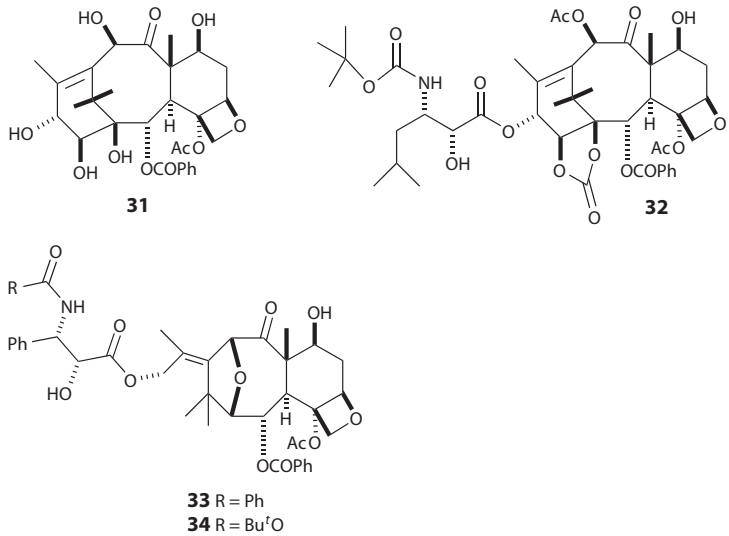

FIGURE 6.6 The structures of A-ring-modified taxanes **31**–**34**.

selectively deacetylated at C-10 by treatment with hydrazine[92] or sodium bicarbonate and hydrogen peroxide to give 10-deacetyltaxol (**38**),[93] which has similar bioactivity to taxol[94] and allowed the preparation of many substituted derivatives. Taxol can also be deoxygenated at C-10 with samarium diiodide to give 10-deacetoxyltaxol (**39**), while similar treatment of docetaxel gives the docetaxel analog **40**;[95,96] 10-Deacetoxytaxol as well as 7-deoxy-10-deacetoxytaxol had comparable cytotoxicity with taxol against NCI/ADR-Res cells.[97] Both 10-deacetyltaxol and its docetaxel analog[96] had similar cytotoxicity to taxol. Acylation of 10-deacetyltaxol has yielded a number of 10-acyl analogs with improved bioactivities, although the best compounds such as **41** also had modified side chains; compound **41** was two orders of magnitude more active than taxol (Figure 6.8).[98]

The C7,C9 dimethoxy analog **42**, known as cabazitaxel or XRP6258 or TXD258, was prepared from 10-DAB.[99] It is more effective against metastatic castration-resistant prostate cancer in combination with prednisone than the combination of mitoxantrone and prednisone,[100] and it was approved by the U.S. FDA in 2009 for use in combination with prednisone for treatment of certain patients

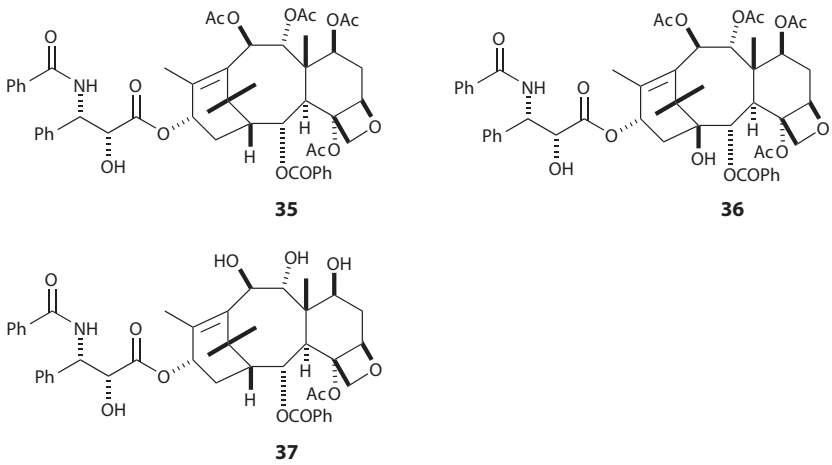

FIGURE 6.7 1-Deoxybaccatin VI (**35**) and structures of 1-deoxytaxanes **36** and **37**.

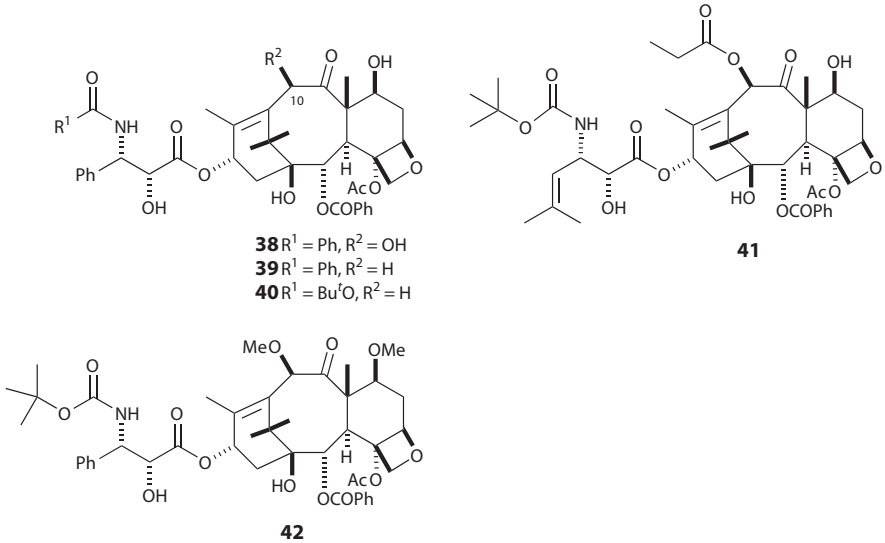

FIGURE 6.8 Taxol analogs **38**–**42** modified at C-10.

with hormone-refractory metastatic prostate cancer.[101] It is in Phase III trials for other cancers, including breast cancer.[102]

Conjugates of taxol with spermine at C-10 and also C-7 were soluble in water and were much less cytotoxic than taxol, leading to the suggestion that they could serve as prodrugs.[103] Various C-10 carbamates were evaluated for permeability, and carbamate **43** had good microtubule assembly activity and low cytotoxicity, suggesting that it might be a useful treatment for Alzheimer's disease and related taupathies.[104] A C-10 thiocolchicine derivative (**44**) and a similar C-7 derivative had reduced cytotoxicity as compared with taxol, and although compound **44** had good affinity for tubulin it was not as effective at promoting tubulin assembly as taxol.[105] Small libraries of taxol substituted at C-10,[106] at C-10 and C-7[107] and at C-10 and C-2[108] have been prepared. It was found that substituent effects were not additive and either reduction of activity or a synergistic effect was frequently observed. A series of C-10 epitaxol derivatives was prepared, and some analogs had reduced interactions with P-glycoprotein (Figure 6.9).[109]

The spiro-epoxide **45** and its 7-methoxymethyl derivative **46** were prepared by the BMS group, and were found to have comparable cytotoxicity and tubulin assembly activity to taxol.[110]

The C-9 position is occupied by a carbonyl group in taxol, but (9*R*)-13-acetyl-9-dihydrobaccatin III was isolated from *T. canadensis* and converted to 9-dihydrotaxol **47**.[111] Various analogs of **47** were also prepared.[112,113] Deoxygenation of (9*R*)-13-acetyl-dihydrobaccatin III via the Barton procedure, followed by side chain attachment, gave the 9-deoxytaxol derivative **48**.[114] The reduction of taxol with SmI_2 yields 9β-hydroxytaxol, and this chemistry was used to prepare the cyclic acetal **49**, which is in clinical trials as tesetaxel.[115,116] The natural taxane 19-hydroxy-10-DAB was used to prepare 19-hydroxydocetaxel (**50**), which had better tubulin assembly activity than taxol and docetaxel (Figure 6.10).[117]

Modifications at the C-2 position have yielded interesting results. The C-2 benzoate group or a similar group is necessary for activity, and 2-debenzoyloxytaxol (**51**),[118] 1-benzoyl-2-debenzoyloxytaxol,[119] and 2-*epi*-taxol[120] are all inactive. 2-*epi*-Taxol is also inactive,[120] as is 1-benzoyl-2-debenzoyloxytaxol.[119] However, 2-debenzoyloxy-2α-benzoylamidotaxol (**52**) retains cytotoxicity against three cell lines, with diminished activity as compared with taxol in two cell lines but slightly increased activity in the third.[121] Taxol analogs with substituted benzoyl groups at C-2 can, however, be more active than taxol, although there is an interesting substituent effect on activity, in that *para*-substituted benzoate analogs are uniformly less active than taxol, while *ortho*- and *meta*-substituted

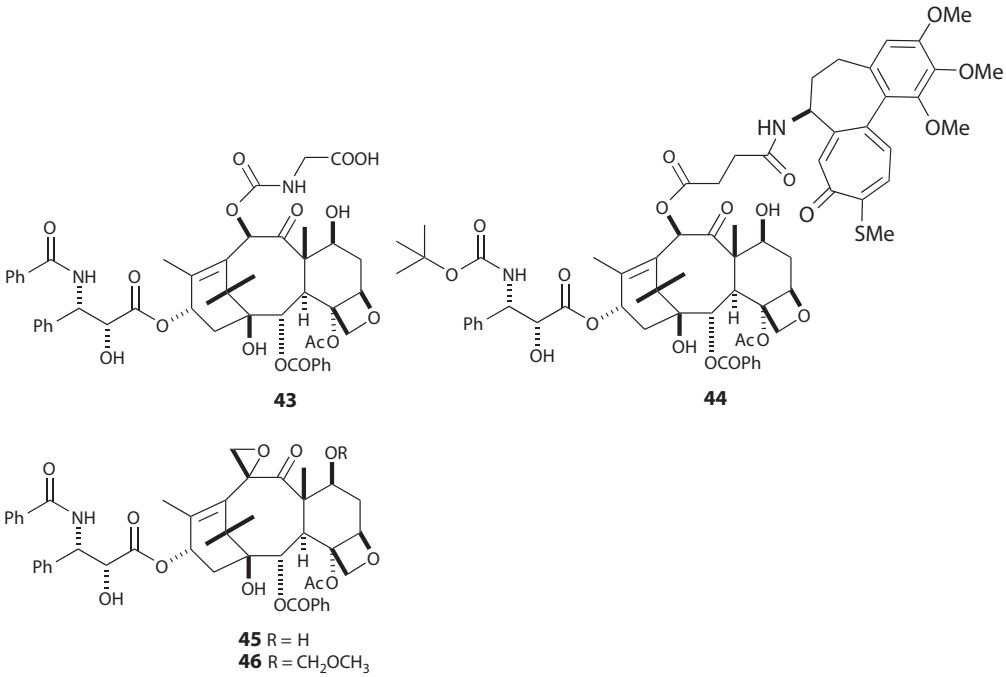

FIGURE 6.9 Taxol analogs **43**–**46** modified at C-10.

analogs can be more active than taxol. Two of the best analogs are the *m*-azidobenzoyl derivative **53** and the *m*-methoxybenzoyl derivative **54**.[122,123] Analogs with 2-heteroaryl groups were also investigated, and thiophene carbonyl and furan carbonyl groups gave comparable activity with taxol.[123–125] Most nonaromatic esters at C-2 gave analogs with lower activity, but a 3,3-dimethylacrylate ester showed better cytotoxicity against several cell lines.[126] Many compounds with a modified C-2 benzoyl group coupled with other modifications have been prepared. One example is compound **55**, or Lx2-

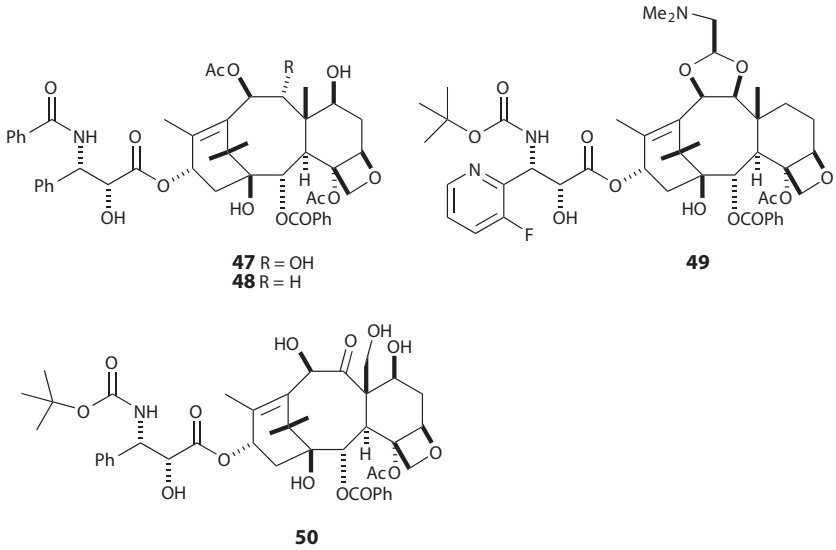

FIGURE 6.10 Taxol analogs **47**–**50** modified at C-10 and C-18.

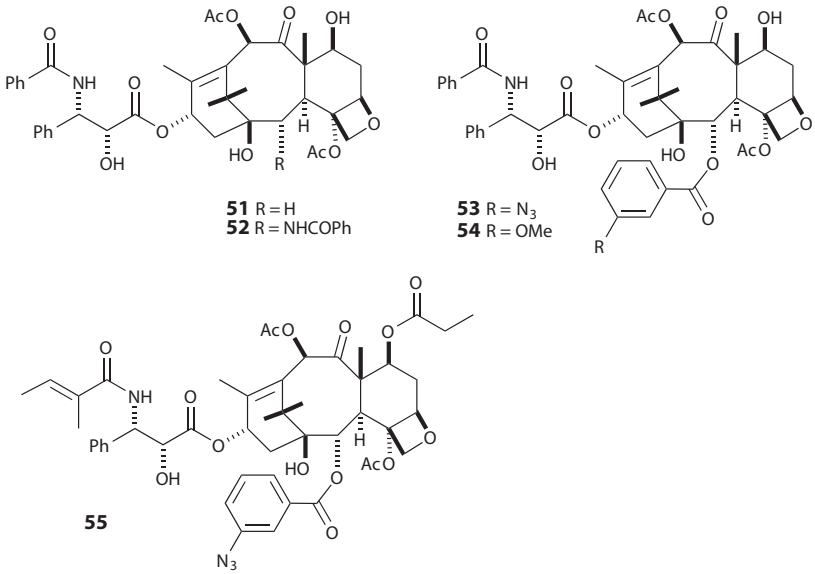

FIGURE 6.11 Taxol analogs **51–55** modified at C-2.

32c, a derivative of the naturally occurring taxol analog cephalomannine; this was reported to have excellent cytotoxicity against both drug-sensitive and drug-resistant cell lines (Figure 6.11).[127]

6.5.3 Ring C Modifications

The C-7 hydroxy group is the most readily modified group in the diterpenoid ring system of taxol, and extensive modifications of it have been made. As the hydroxyl group of a β-hydroxyketone it is readily epimerized,[128] and it can also be readily and selectively derivatized if the C-2′ hydroxyl group on the side chain is suitably protected. Some of the various acyl derivatives which have been prepared have had improved properties as compared with taxol, and 7-hexanoyltaxol (**56**) has been studied as the active component of drug-eluting stents.[129,130] Some simple ether derivatives also have had good activities; thus both thioethers **57** and **58** had improved cytotoxicity and tubulin assembly activity compared with taxol. A series of derivatives of **57** were prepared with different side chain *N*-acyl groups and C-3′ substituents, but compound **57** (BMS-184476) was found to have the best *in vivo* activity,[131] and it was entered into Phase II clinical trials (Figure 6.12).[132,133]

Oxidation of the C-7 hydroxyl group leads to the corresponding ketone, which is unstable in base and undergoes ring-opening to the αβ-unsaturated ketone **59**; this compound is devoid of activity.[134] Deoxygenation at C-7 has been achieved by several groups, and both 7-deoxytaxol **60**,[135,136] 10-acetyl-7-deoxydocetaxel **61**,[137] and 7-deoxy-10-deacetoxytaxol[138] have been prepared; these compounds are slightly less active than taxol in the tubulin assembly assay, but comparably cytotoxic with HCT 116 cells[135,137] or NCI/ADR-RES cells.[138]

Dehydration of taxol was achieved by treatment of the 7-triflate derivative with a non-nucleophilic base to give 6,7-dehydrotaxol (**62**),[139,140] which was comparable with taxol in its tubulin assembly and cytotoxic activity. Compound **62** could be converted to the corresponding diol **63** by osmylation, and this could be epimerized (albeit in low yield) to **64**, the major human metabolite of taxol.[141] An improved synthesis of compound **64** was reported by workers at BMS (Figure 6.13).[142]

Another interesting product was obtained by reaction of **63** with lead tetraacetate to give **65**; this compound was much less active than taxol.[143] Two modifications of the C-ring of taxol have, however, led to compounds which have advanced to clinical trial or clinical candidacy. The first of

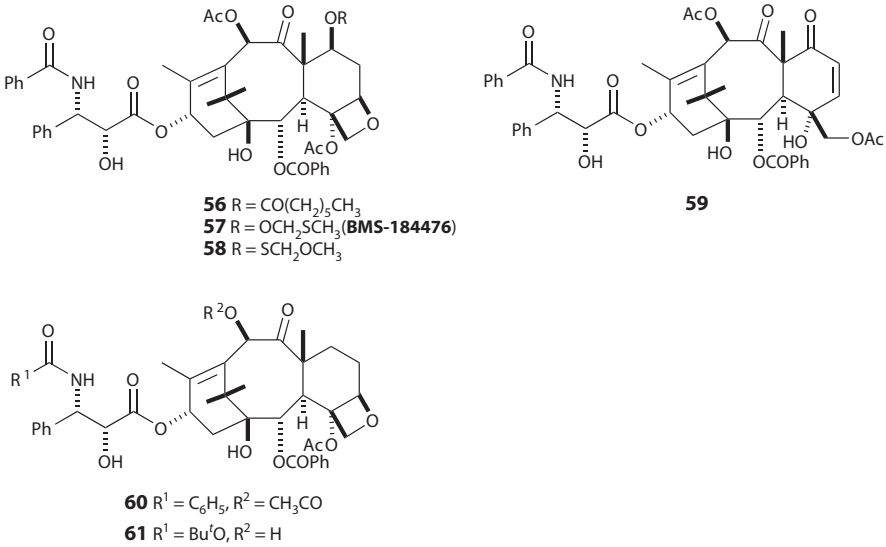

FIGURE 6.12 Taxol analogs **56–61** modified at C-7.

these is the formation of a cyclopropane ring between C-7 and C-18. The cyclopropataxol **66** and its docetaxel analog **67** were discovered independently by workers at BMS[144] and Rhone-Poulenc,[145] and the analog **68** is in Phase III clinical trials against bladder cancer as larotaxel. The C,D-seco analog **69** was prepared by semisynthesis from the naturally occurring taxine, and was found to be inactive both in a cytotoxicity assay and a tubulin assembly assay; this result was explained by a molecular modeling study (Figure 6.14).[146]

The second series of compounds is a surprising one, as it involves cleavage of ring C to give products which no longer maintain the rigid inverted-cup geometry of taxol. The compounds were discovered serendipitously by Appendino,[147] but they showed good activity in the NCl 60-cell line panel and had limited toxicity, and the C-seco norstatin ester **70** (IDN5390) has been selected as an antiangiogenic candidate for extended treatments; the analog of **70** with the normal paclitaxel side chain is much less active.[148] Various acyl derivatives of **70** have been prepared, and these have similar activity to the parent compound, so *in vivo* oxidation and realdolization to the corresponding

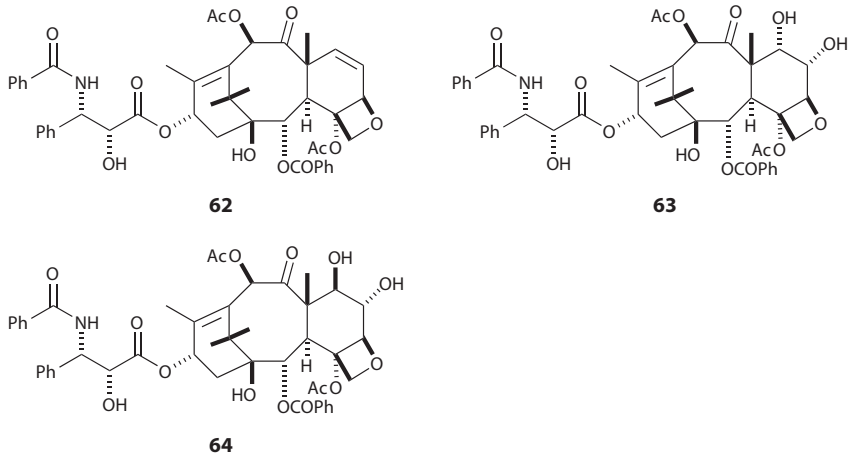

FIGURE 6.13 Taxol analogs **62–64** modified in ring C.

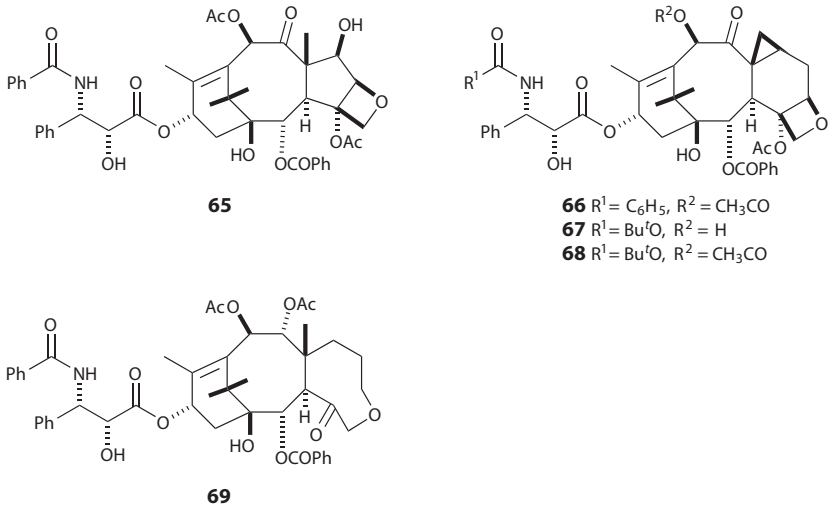

FIGURE 6.14 Taxol analogs **65–69** modified in ring C.

taxane derivative is excluded as the reason for the observed activity.[149] Additional analogs such as the methoxybenzoyl derivative **71** have also been prepared and shown to have comparable cytotoxicity with taxol (Figure 6.15).[150]

Taxol analogs with modifications at C-4 have also been prepared. A C-4 acyl group is important for taxol's activity, as removal of the C-4 acetate leads to an inactive product.[151] Reacylation of C-4 with various acyl groups gave some products with improved activity, and the C-4 carbonate **72** and its *t*-butoxy analog **73**[152] were in Phase I clinical trials as BMS-188797,[153,154] and in Phase II trials as BMS-275183,[155] respectively. Various analogs with C-2 and C-4 acyl modifications have also been made; some of these compounds showed enhanced activity against resistant cell lines.[156]

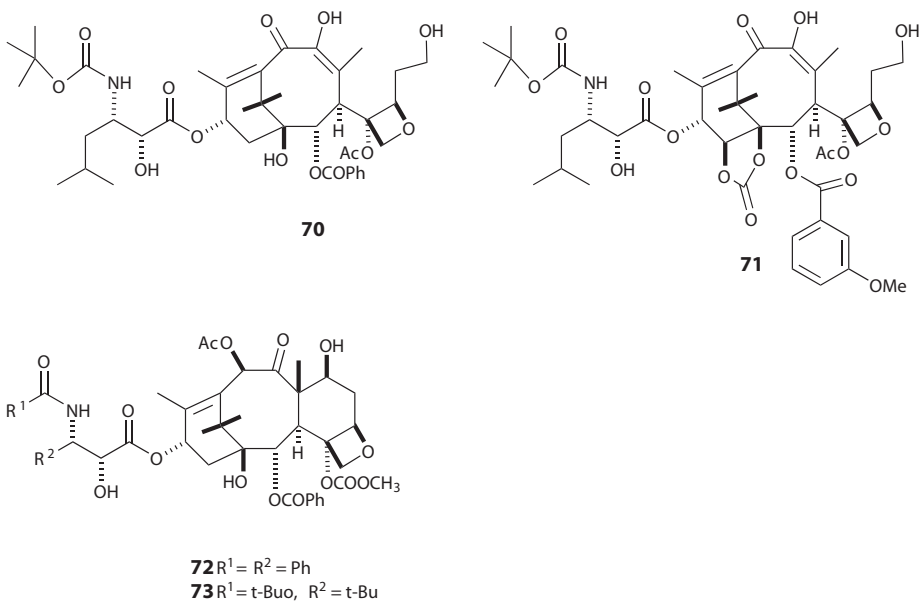

FIGURE 6.15 Taxol analogs **70–73** modified in ring C.

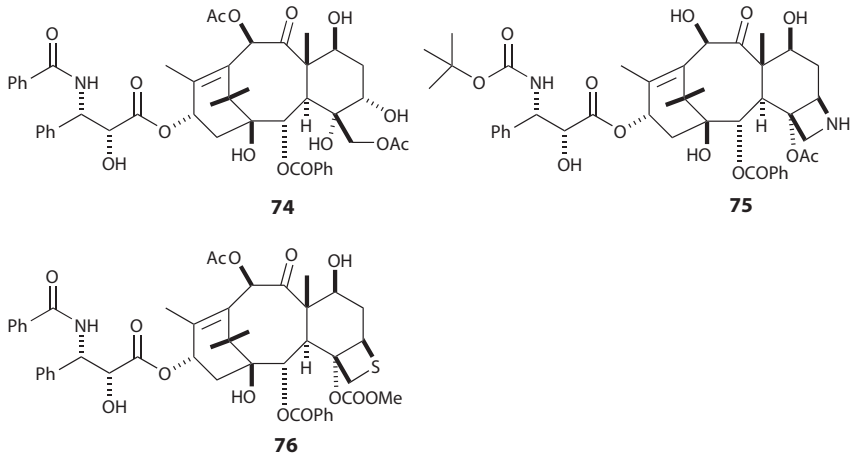

FIGURE 6.16 Taxol analogs **74**–**76** modified in ring D.

6.5.4 Ring D Modifications

The oxetane ring is an unusual feature of the taxol structure, and it plays a significant role in taxol's unique activity. As previously noted, opening of the oxetane ring to a compound such as **59** destroys taxol's activity,[134] as does ring-opening by electrophilic reagents to give compound **74**.[84] Taxol analogs in which the oxetane oxygen atom is replaced with nitrogen (**75**)[157] or sulfur (**76**)[158] are much less active than taxol (Figure 6.16).

The reason for the importance of the oxetane ring cannot be because of its chemical reactivity, as taxol binds noncovalently to tubulin, and because the oxetane ring is stable under normal conditions. It is, thus, probable that it serves as a conformational lock, holding the diterpenoid ring system in its characteristic inverted-cup conformation, and also (in conjunction with the C-4 acetate) as a hydrogen bond acceptor. These conclusions were put on a quantitative basis by Snyder et al.,[159] who predicted that other functional groups would be capable of assisting the binding of taxol to tubulin as effectively as the oxetane ring. This prediction was borne out by the synthesis of the cyclopropane derivative **77** (Figure 6.17), which is almost as active as taxol in a tubulin assembly assay.[160] Compound **77** contains both the necessary C-4 acetate and a rigidifying cyclopropane ring, and

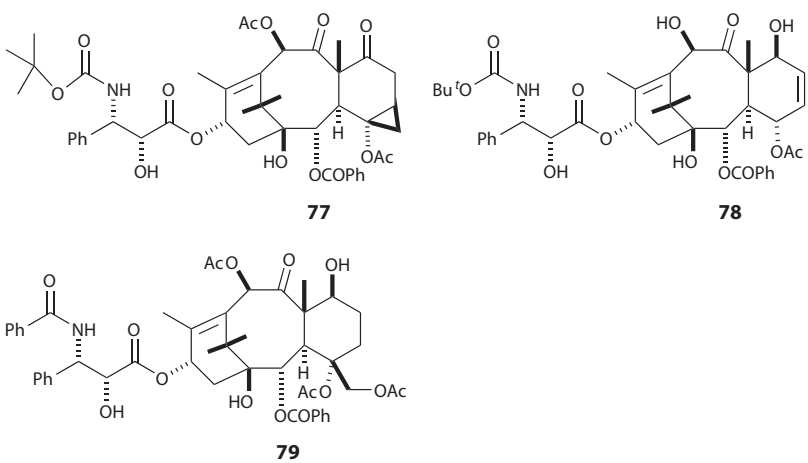

FIGURE 6.17 Taxol analogs **77**–**79** modified in ring D.

both features appear to be necessary for activity. Compound **78** which contains only the C-4 acetate function is much less active than taxol.[161] Similarly, compound **79**, with both C-4 and C-20 acetate functions, but lacking a steric lock, is also inactive as a tubulin assembly agent.[162] The rigid tetracyclic skeleton of taxol is, however, not essential for activity, as evidenced by the activity of the C-seco analogs **70** and **71** discussed before.

6.5.5 Side Chain Analogs

The side chain of taxol is in many ways the most readily modified part of the molecule, as it can be prepared synthetically and linked to baccatin III by one of the various methods described in Section 6.7.1. It has been found that the 3′-phenyl and *N*-benzoyl groups of taxol are not specifically required for activity and several of the taxol analogs in clinical development or in clinical trials have modified side chains.[7,163]

Space does not permit a detailed discussion of all the side chain variations that have been investigated; more complete details can be found in the reviews previously mentioned,[73,74] and a recent review covers the various synthetic methods that have been used for the side chain of taxol.[164]

The side chain itself is necessary for the full activity of taxol, and all the compounds in clinical trial have a substituted isoserine side chain of some nature. However, suitably modified baccatin III derivatives can retain significant activity, as is the case with 2-(*m*-azidobenzoyl) baccatin III (**80**).[165]

Not only is the side chain necessary for full activity, but so also is its regiochemistry and stereochemistry necessary. Analogs with simplified side chains, such as *N*-benzoylisoserine or phenyllactic acid[166] are significantly less active, and analogs with different stereochemistries than the 2′*R*, 3′*S* stereochemistry of taxol are also less active than taxol.[167] Some analogs with conformationally restricted side chains have been prepared, and compound **81** is only moderately less active than taxol.[168] Extension of the side chain by one carbon, as in **82** and **83**, caused a 30-fold loss of tubulin assembly activity,[169] while transposition of the hydroxyl and amino substituents also caused a reduction in activity by a factor of about ten.[167] *N*-methylation to give *N*-methyltaxol reduces the cytotoxic activity against P-388 lymphocytic cells approximately eightfold,[170] and a new synthetic approach to *N*-methyltaxol has been published (Figure 6.18).[171]

Modifications of the 3′-phenyl and *N*-benzoyl substituents have been more fruitful. Replacement of the 3′-phenyl group with various substituted phenyl groups is largely unproductive, but replacement

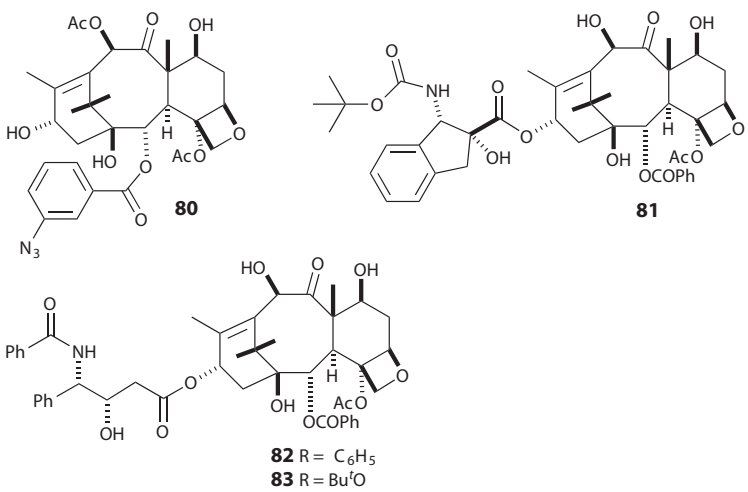

FIGURE 6.18 Baccatin III analog **80** and taxol analogs **81–83** with modified side chains.

with moderately sized alkyl groups such as isobutyl or isobutenyl gives compounds with improved activity;[172] as noted earlier, the analog **32** with this substitution is in clinical trials. Replacement of the 3′-phenyl with a 3′-(2-furyl) group also gives improved activity,[173] and the compound MAC-321 (also designated TL-00139, **84**) is in Phase II clinical trials. The 3′-(fluoropyridyl) group also imparts improved activity, and the analog **85** is in clinical trials as an orally active compound with antitumor activity against NSCLC.[174] A final example is the 3′-(*t*-butyl) analog **86**, which has shown promising activity in several tumor types in a Phase I study, and a Phase II trial in NSCLC has been initiated (Figure 6.19).[175]

Various modifications of the 3′-*N*-substituent have been studied. An acyl substituent at this position is required for activity, and the *t*-butoxycarbonyl group of docetaxel (Taxotere; **3**) has been proven an effective alternative acyl group to the benzoyl group of taxol. Most of the taxol analog clinical candidates surveyed in a recent review[8] have either a benzoyl group or a *t*-butoxycarbonyl group as the 3′-*N*-substituent.

The 2′-hydroxyl group was early on shown to be necessary for activity,[176] and successful modifications (other than acylation to give a prodrug, discussed in the next sections) have been rare. A few cases of compounds with modifications at 2′ and with important activity have been discovered, however. Thus, several 2′-methyl taxol derivatives such as **87** have been prepared and have been found to have improved cytotoxicity as compared with taxol.[177–179] The analog **88** has been found to be more active than taxol in both normal A2780 cells and taxol-resistant A2780 cells.[180] Replacement of the 2′-hydroxyl group with a thiol group gave an inactive compound,[181] but the 2′,2′-difluoro analog **89** is somewhat more active than taxol toward P388 cells (Figure 6.20).[182]

More traditional modifications of the side chain continue to provide potent lead compounds. A publication from the Ojima group describes the synthesis of over 50 taxol analogs modified on the side chain and at C-10 and also in some cases on the C-2 benzoyl group. The most promising compound was analog **90**, which had excellent *in vivo* activity against the drug-resistant CFPAC-1 pancreatic and the DLD-1 human colon tumor xenografts in mice.[183] The same group also found that the C-3′ difluoromethyl analog **91** had strong apoptosis-inducing activity in both multidrug resistant (MDR)-bearing and MDR-negative cancer cells.[184] The *bis*-cyclopropanated analog **92** was over 100-fold more potent than taxol against the drug-resistant human breast cancer cell line LCC6-MDR (Figure 6.21).[185]

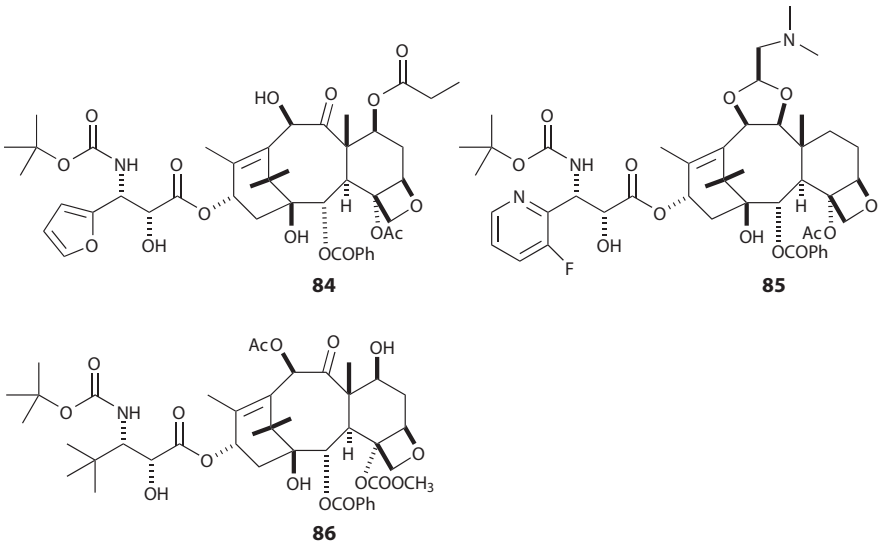

FIGURE 6.19 Taxol analogs **84**–**86** with modified side chains.

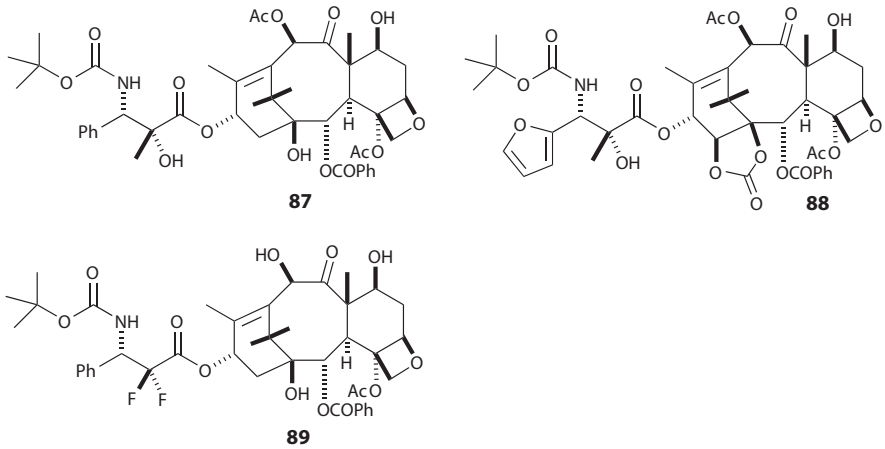

FIGURE 6.20 Taxol analogs **87–89** with modified side chains.

These selected examples indicate that modifications on the side chain of taxol continue to generate interesting lead compounds over 20 years after the first such compounds were made.

6.5.6 Summary of Taxol's SAR

A summary of the SARs of taxol described in the preceding sections is provided in structural form in Figure 6.22.

6.6 PRODRUGS OF TAXOL

6.6.1 Simple Water-Soluble Derivatives

The development of improved delivery methods for taxol continues to receive much attention, and several reviews summarize this work.[186–188] The ultimate goal of much of the recent work has been

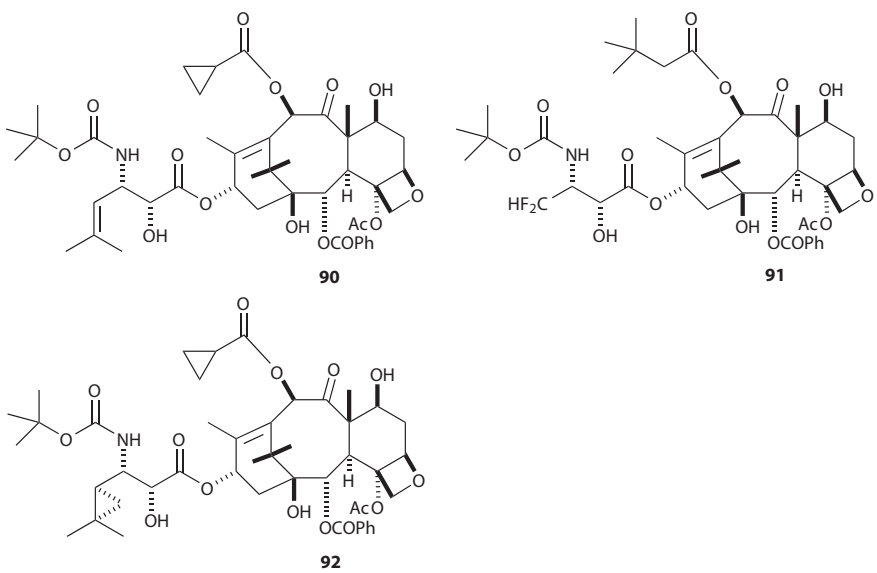

FIGURE 6.21 Taxol analogs **90–92** with modified side chains.

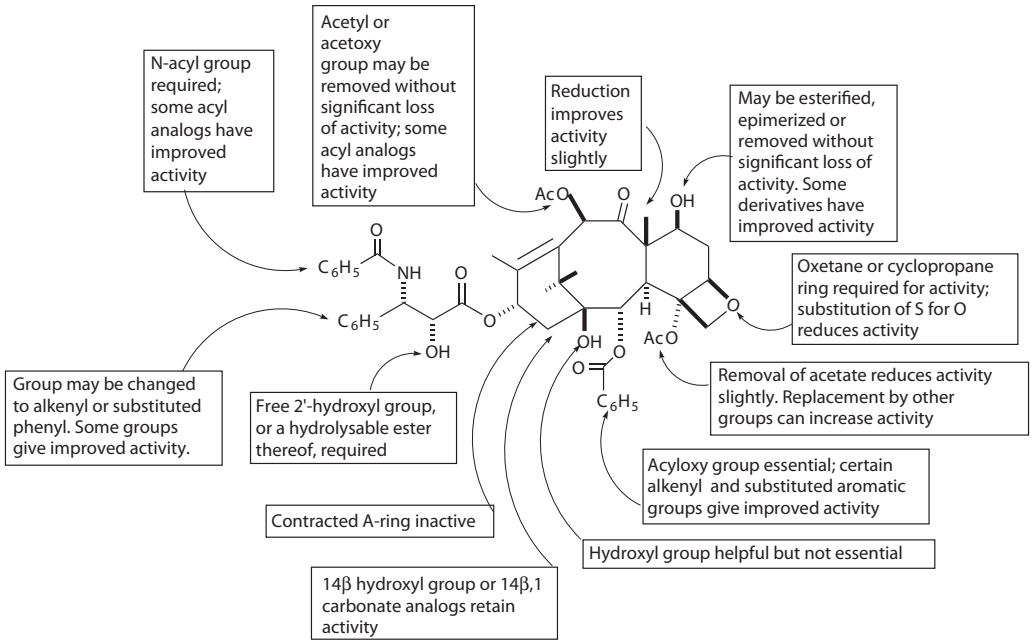

FIGURE 6.22 Summary of the SARs of taxol.

the preparation of taxol analogs which are targeted to tumors, but work on the simpler problem of the preparation of taxol prodrugs with improved water solubility continues.

Conjugation of esters or other groups at the 2′-position has been the most common approach to prodrug creation, as most 2′-esters undergo facile hydrolysis under physiological conditions. Thus, water-soluble docetaxel esters of malic acid such as **93** showed enhanced *in vitro* activity as compared with docetaxel, but somewhat reduced *in vivo* activity.[189] Peptide–taxol conjugates with one or two taxol molecules connected by thioether bonds to cysteine-containing peptides were also prepared, and some compounds were found to have higher *in vitro* potency than taxol.[190] Various 2′-(α-bromoacyl) derivatives of taxol (**94**) were prepared, and found to be more active *in vitro* than simple long-chain esters. Liposome formulations of some of these compounds against the OVCAR-3 xenografted tumor in in SCID mice showed that the longer chain compounds were more efficacious, presumably due to slow hydrolysis of the prodrug to taxol.[191] In a related approach, docetaxels with medium-chain saturated fatty acids esterified at C-2′ have been prepared to enhance their compatibility with nanoemulsion drug-delivery systems.[192] Another solution to the water-solubility problem was developed by noting that the *O*-benzoyl to *N*-benzoyl migration of 2-*O*-benzoyl-3′*N*-debenzoyltaxol (isotaxel; **95a**) is slow at acidic pH values. Compound **95a** is much more water soluble than taxol in acidic solution, and it can thus be used as a prodrug, with conversion to taxol occurring relatively quickly ($t_{1/2}$ = 15 min) under physiological conditions.[193] The same strategy has recently been applied to generate **95b**, a prodrug of canadensol.[194] A refinement of this strategy is provided by the photocleavable prodrug **96**. Irradiation of **96** at 365 nm cleaved the photosensitive coumarin group and allowed isomerization of the initial isotaxel photoproduct to taxol, with essentially complete conversion in 30 min (Figure 6.23).[195]

Simple esters at the 7-position do not convert easily to taxol, but suitable designed derivatives can undergo intramolecular cyclization to release taxol. One example of this approach is the phosphate derivative **97**. This compound is stable in water but releases taxol by internal lactonization after dephosphorylation by phosphatases.[196] Regrettably, **97** was found to bind to plasma proteins and was deemed to be unsuitable for use as a prodrug, although it did show good *in vitro* activity against the murine M109 tumor.[196] Conjugation at the 7-position via a carbonate linker has yielded prodrugs

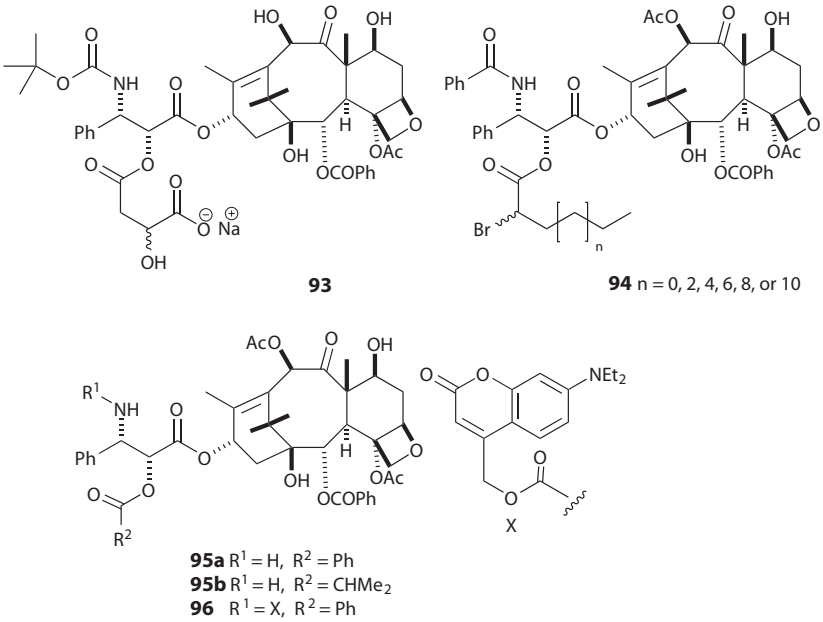

FIGURE 6.23 2′-Acyltaxane prodrugs **93–96**.

which convert to taxol, and the simple glycerol carbonate **98** (Protaxel) is stable at acidic pH but converts to taxol in human serum with a half-life of 10 min.[197] It entered into clinical trials in Europe, but several toxicities were observed and clinical evaluation appears to have been discontinued (Figure 6.24).[198]

6.6.2 Polymer Conjugates of Taxol

Polymer conjugates of taxol offer several advantages compared with small molecule derivatives such as those described before. One important advantage arises because tumor vasculature is more permeable to large molecules than normal vasculature, and so polymer–drug complexes tend to accumulate in extravascular tumor tissues, an effect known as enhanced permeability and retention (EPR) in tumors. A second advantage can arise if the polymer confers enhanced water solubility, and finally some polymers can offer active tumor targeting. This section will focus on conjugates that do not offer any active tumor targeting.

The simple 2′-poly(ethyleneglycol) derivative **99** had good water solubility and *in vitro* activity, but was less active than taxol in an *in vivo* study against P388 leukemia.[199] The 7-poly(ethyleneglycol)

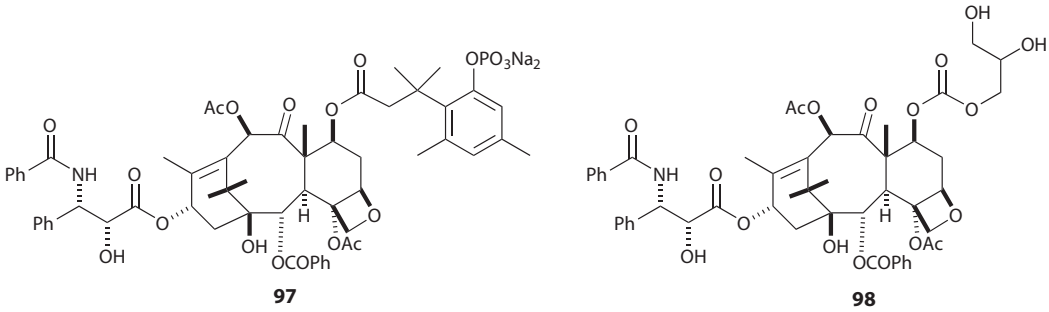

FIGURE 6.24 7-Acyltaxol prodrugs **97** and **98**.

derivative **100** was also found to have excellent water solubility and good *in vivo* activity,[200] and a pyrene derivative of **100** was prepared to allow fluorescence spectroscopic studies of its interaction with tubulin.[201] Paclitaxel poliglumex (**101**), an α-poly-L-glutamic acid conjugate of taxol, has entered Phase III clinical trials in patients with NSCLC [202] and in many other cancers. Other polymer–taxol prodrugs include a poly(vinyl alcohol)–taxol conjugate[203] and a micellar prodrug of taxol conjugated to cyclotriphosphazene (Figure 6.25).[204]

Several studies have been made of polymeric dendrimers as drug delivery vehicles. Dendrimers are well-defined tree-like polymers, and in principle, they can deliver more drug per unit of polymer than can linear polymers. A comparison of dendrimer versus linear architecture was made using a polyamidoamine G4 hydroxyl-terminated dendrimer and a conventional poly(ethyleneglycol) polymer as the drug delivery agents. It was concluded that the polyamidoamine G4 hydroxyl-terminated dendrimer is a promising vehicle for drug delivery of taxol.[205] The "cascade release" dendrimer prodrug **102** was prepared and shown to release taxol on chemical reduction, and the expectation is that larger dendrimer prodrugs of this type will release taxol under bioreductive conditions.[206] Dendrimers can also be used simply as aqueous cosolvents, and polyglycerol dendrimers used in this way gave improved solubility for taxol as compared with polyethylene glycol-400 (PEG-400).[207]

Triazenes are popular dendrimer-forming reagents, and the dendrimer **103** is one of several prepared by Simanek et al.[208,209] Dendrimer **103** was found to be well tolerated *in vivo* and had an IC_{50} of 29 nM against PC-3 cells, compared with 4.5 nM for taxol (Figure 6.26).

Although not a polymer, fullerene has been conjugated to taxol to provide a lipophilic slow-release system suitable for liposome aerosol delivery to the lungs.[210] The selected derivative had a half-life of about 75 min in bovine plasma, formed stable liposomes with dilaurylphosphatidyl choline, and was only slightly less potent than taxol toward cells.

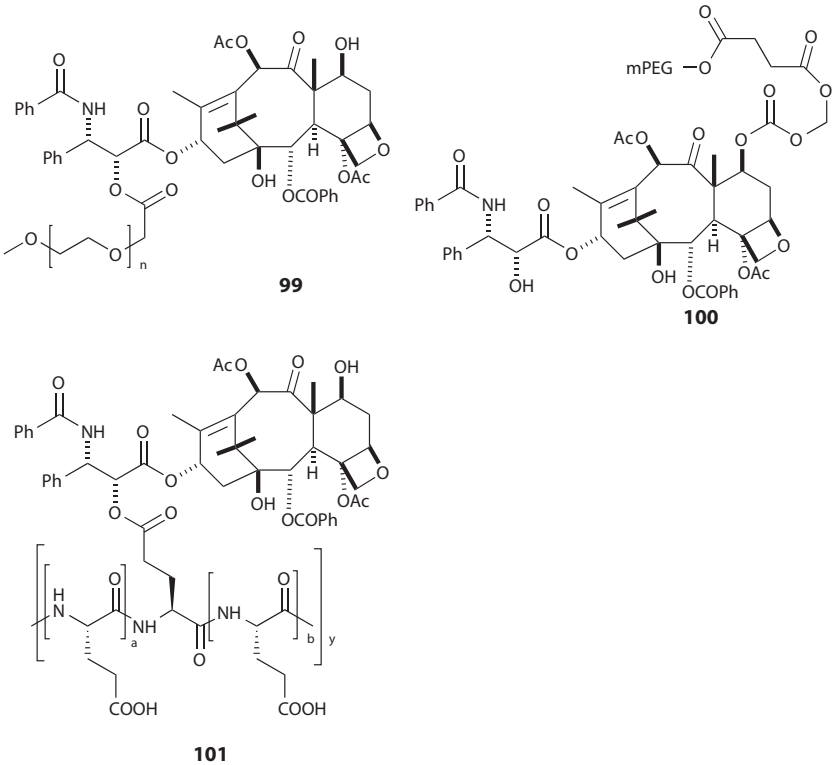

FIGURE 6.25 Polymer–taxol prodrugs **99–101**.

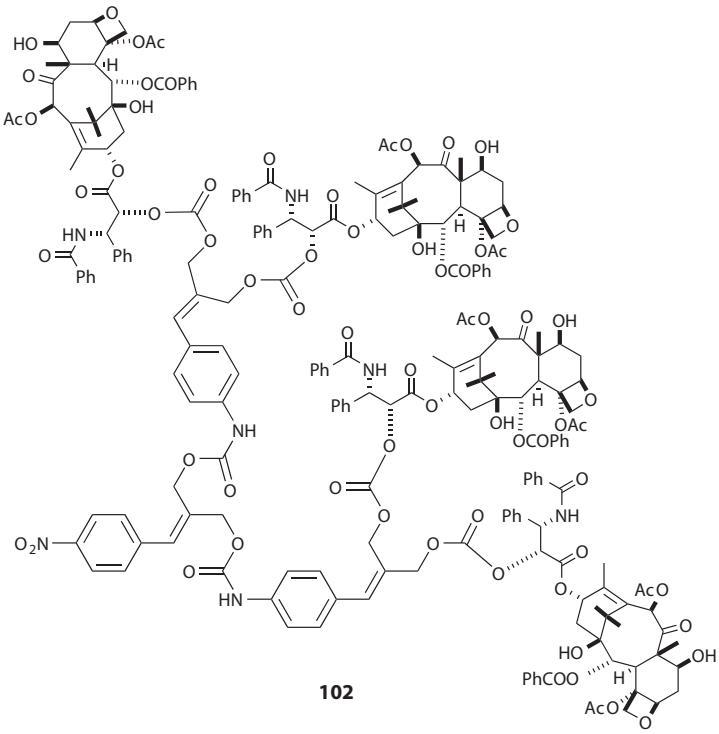

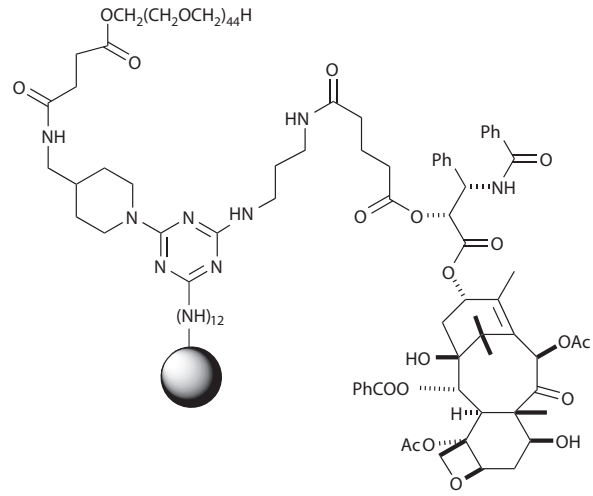

FIGURE 6.26 Dendrimer–taxol prodrugs **102** and **103**.

6.6.3 Targeted Analogs of Taxol

The ability to target taxol specifically to tumors has obvious advantages in reducing toxicity and other undesirable side effects and increasing the efficacy of the drug, and many groups have investigated such targeting. Broadly speaking the approaches are of two types; those using "passive targeting," such as the polymer and dendrimer conjugates described before, and those using "active targeting," where a prodrug group binds specifically to a receptor on the tumor cell. This distinction

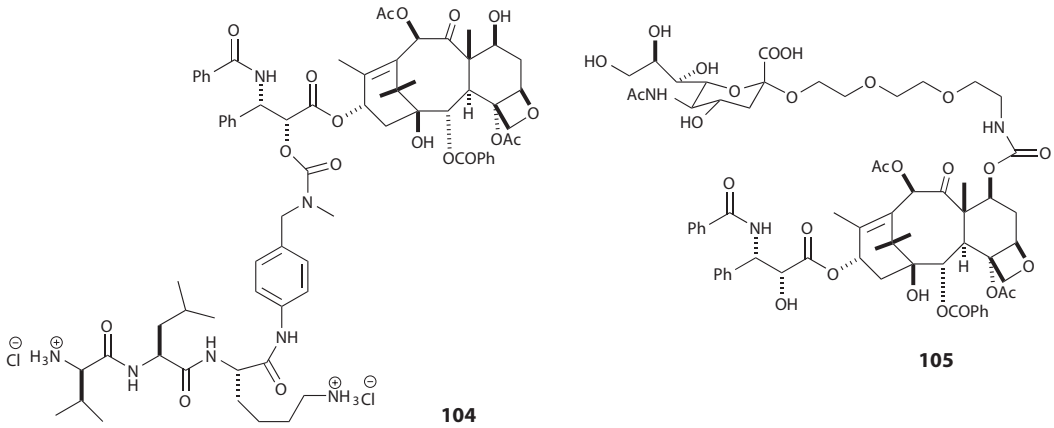

FIGURE 6.27 Enzyme-activated taxol prodrugs **104** and **105**.

is helpful but somewhat arbitrary, and there is significant overlap between the types. This section will, however, focus on actively targeted analogs of taxol.

Targeting can make use of several different biological qualities of tumors, including overexpressed enzymes, hypoxia, and overexpressed receptors. The protease plasmin plays an important role in tumor invasion and metastasis, and is thus present in tumors. Taxol prodrugs were prepared in which substrate peptides for plasmin were linked through a spacer to the 2′-position of taxol. One of the best such compounds is **104**; this compound is one of the least toxic taxol prodrugs reported, and yet it is converted to taxol with a half-life of 42 min by plasmin.[211] The enzyme neuraminidase (sialidase) is also overexpressed in tumor cells, and a water-soluble conjugate of sialic acid and taxol connected by a self-immolative linker at the 7-position (**105**) has been prepared.[212] Compound **105** was somewhat less cytotoxic than taxol, but was much more water soluble. No information on its cleavage by neuraminidase was provided (Figure 6.27).

Most solid tumors exhibit hypoxia, a condition of low oxygen concentration in tissue, and so reductively activated prodrugs have been developed to target it. The nitro compound **106** was cytotoxic to several cell lines and was converted to taxol by chemical reduction.[213] The disulfide bond is easily cleaved under bioreductive conditions, and the combination of taxol with the antiangiogenic compound captopril unit through a disulfide linker gave the prodrug **107**. Compound **107** was 650-fold less toxic than taxol, and was converted to taxol on reduction with dithiothreitol. It also had excellent *in vivo* activity against the L2987 lung carcinoma in nude mice (Figure 6.28).[214]

In the antibody-directed enzyme prodrug therapy (ADEPT) approach,[215] specific enzymes are delivered to tumor sites by monoclonal antibodies (mAbs), and these enzymes are then available to

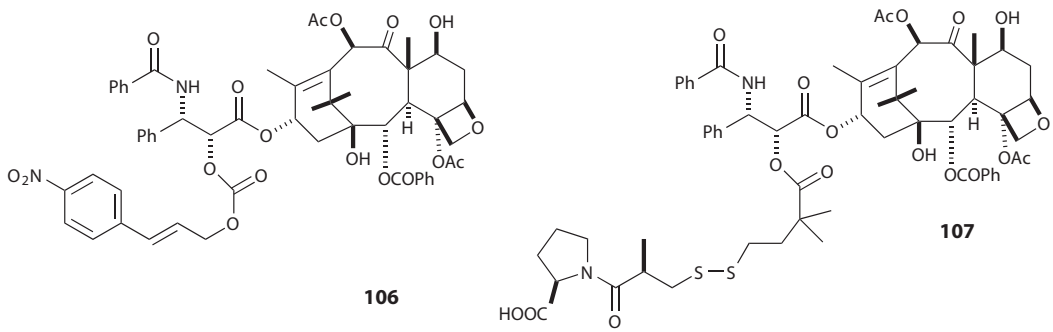

FIGURE 6.28 Hypoxia-activated taxol prodrugs **106** and **107**.

activate a "protected" taxol derivative selectively cleaved by this enzyme, resulting in release of taxol. The taxol analog **108**, for example, can be converted to taxol by hydrolysis of the glucuronide with a glucuronidase, decarboxylation, and internal lactam formation.[216] A *p*-nitrophenol linker has also been used with similar results,[217] and docetaxel has also been targeted by this approach.[218] The β-lactam prodrug **109** is stable in human serum, and taxol is released with a half-life of 50 min on treatment with β-lactamase.[219] One drawback with the use of β-lactamase is that it is a non-human enzyme and may thus create an immunogenic response; this concern is not a problem with the human glucuronidase enzyme used to activate **108** (Figure 6.29).

Cancer cells overexpress various membrane receptors, and these are valuable targets for drug delivery. The natural polysaccharide hyaluronic acid has a strong affinity with cell-specific surface markers such as CD44 and RHAMM, and two groups have prepared hyaluronic acid–taxol conjugates. The Prestwich group prepared a taxol–hyaluronic acid conjugate in which the polymeric hyaluronic acid was linked to taxol through a linker at the 2′-position.[220] The conjugates showed selective toxicities toward breast, colon, and ovarian cancer cell lines that are known to overexpress hyaluronic acid receptors, but were nontoxic to a mouse fibroblast cell line. The Park group also linked hyaluronic acid through the 2′-position of taxol, and found that their conjugates self-assembled to form nanosized micellar aggregates. Taxol was regenerated from the conjugates at acidic pH, and the conjugates were selectively cytotoxic toward hyaluronic acid receptor overexpressing cancer cells than to receptor-deficient cells.[221]

Glucose uptake into cells is mediated by glucose transporters (GLUTs), a family of membrane proteins, and cancer cells express higher levels of GLUTs than normal cells. The glucose ester conjugated prodrug **110** was the most active of several compounds, and could be transported into cells by GLUTs, so glycan-based prodrugs of this type may be good candidates for development.[222]

Peptides also make effective targeting agents. The PEG-peptide derivative **111** binds to the cell surface bombesin/gastrin-releasing peptide receptor, a receptor associated with tumor growth.[223] The prodrug was about twice as potent as taxol to NCI-H1299 human NSCLC cell, suggesting receptor-mediated drug delivery.[224] The α_V integrin receptor is constitutively active and is overexpressed in tumor cells, and an integrin-targeting prodrug has been prepared and found to have improved tumor specificity against the MDA-MB-435 breast cancer in nude mice.[225] Another example of a peptide as a targeting agent is the cyclic peptide EC-1 that binds to extracellular domain of the receptor tyrosine kinase ErbB2. Conjugation of taxol to EC-1 through the usual succinate linker at the 2′-position gave the prodrug **112**, but no biological studies on this compound have yet been reported.[226] The analog taxol-succinic acid-Phe-Phe-Arg-methylketone-factor VIIa has recently been prepared to target tissue factor, which is aberrantly and abundantly expressed on many cancer cells; the construct linked at the 2′-position showed good *in vitro* activity against human KB3-1 cells (Figure 6.30).[227]

Short oligomers of arginine exhibit superior membrane translocation activity, and a series of arginine-based molecular transporters of taxol has been prepared.[228] The general structure of these

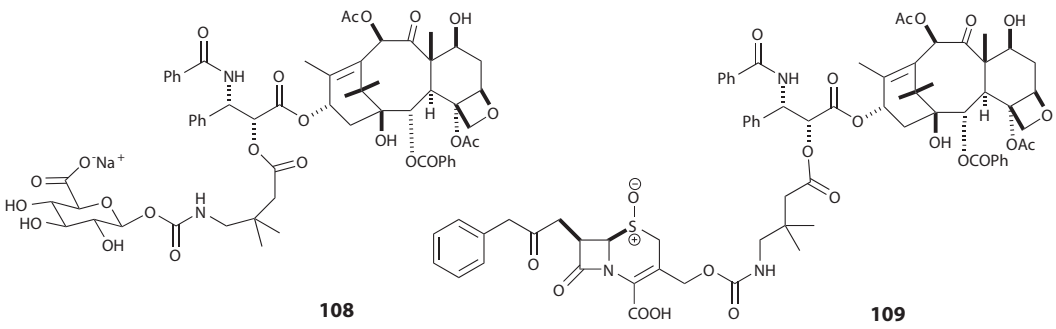

FIGURE 6.29 Taxol prodrugs **108** and **109** for the ADEPT approach.

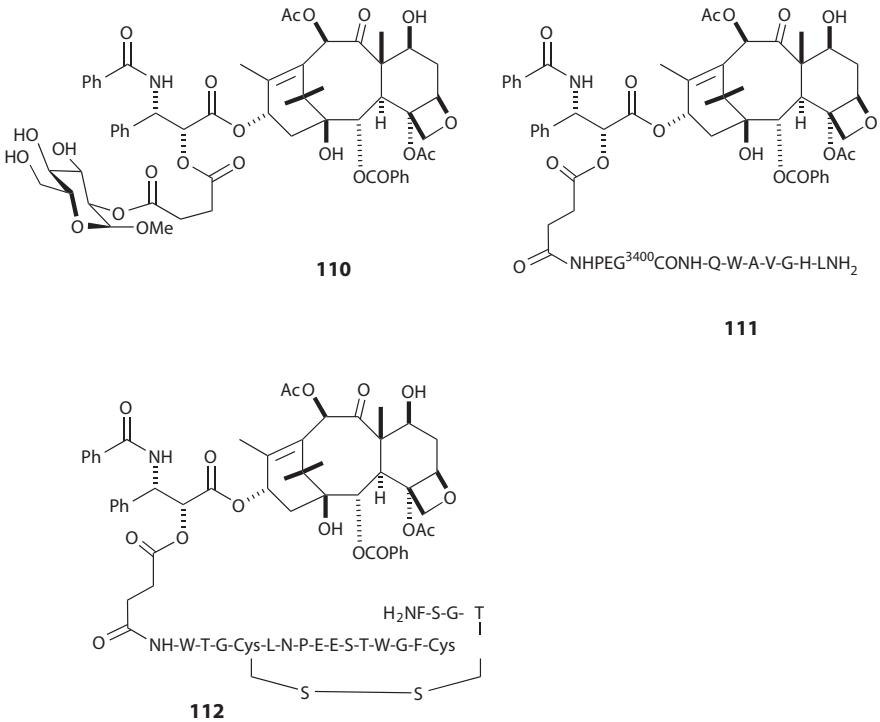

FIGURE 6.30 Carbohydrate- and peptide-targeted taxol prodrugs **110–112**.

compounds is **113**; they are much more water soluble than taxol, and release free taxol with half-lives of minutes to hours, depending on the linker structure and the pH of the medium (Figure 6.31).

The folic acid receptor is known to be overexpressed in human cancers, and it is thus an attractive target for drug delivery.[229] Although several compounds were prepared in an attempt to target it, including **114**, none of them were as active *in vivo* as taxol.[230] In more recent work, however, a folic acid–dendrimer–taxol complex was prepared and found to be selectively active *in vitro* against folic receptor-positive KB cells,[231] so there is still a possibility that this method of targeting will be successful (Figure 6.32).

Biotin has also been used as a targeting agent, as it is a cellular growth promoter, and it is found at higher levels in tumor cells than in normal cells. The biotin-linked taxane **115** and various fluorescent derivatives were prepared and evaluated by Ojima, and it was found that these compounds were incorporated into cells by receptor-mediated endocytosis.[232] A different approach was taken in the synthesis of the docosahexaenoic acid conjugate **116** (DHA–paclitaxel), based on the observation that tumors rapidly take up some fatty acids from arterial blood. Compound **116** proved to be curative for mice with the M109 tumor, in contrast to taxol which was not curative in this system.[233,234] It entered clinical trials, and in a Phase I trial it was found to be well tolerated by patients and to have a favorable toxicity profile.[235] It has reached Phase III clinical trials for advanced NSCLC. Although the precise mechanism of tumor targeting is not clear, it does appear that compound **116** is a promising drug candidate. A docosahexaenoic acid conjugate of a more potent taxol derivative has been prepared by Ojima, and was found to have improved activity as compared with **116**.[232]

6.6.4 Nanoparticles as Delivery Agents for Taxol

Interest in nanoparticle drug delivery methods has increased significantly over the last few years, and several nanoparticle constructs containing taxol as the active constituent have been developed.

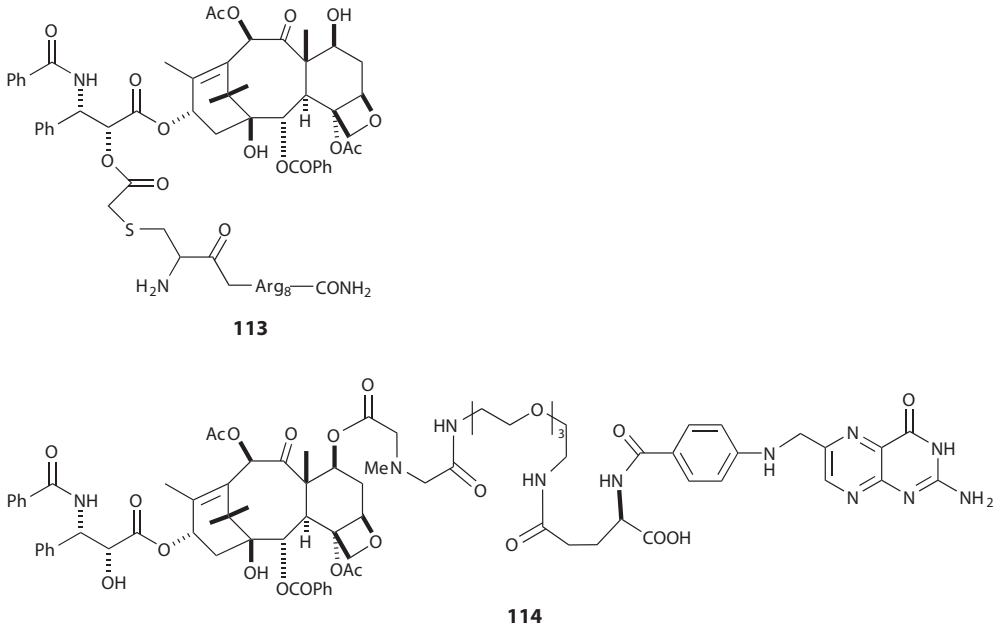

FIGURE 6.31 Arginine- and folic acid-targeted taxol prodrugs **113** and **114**.

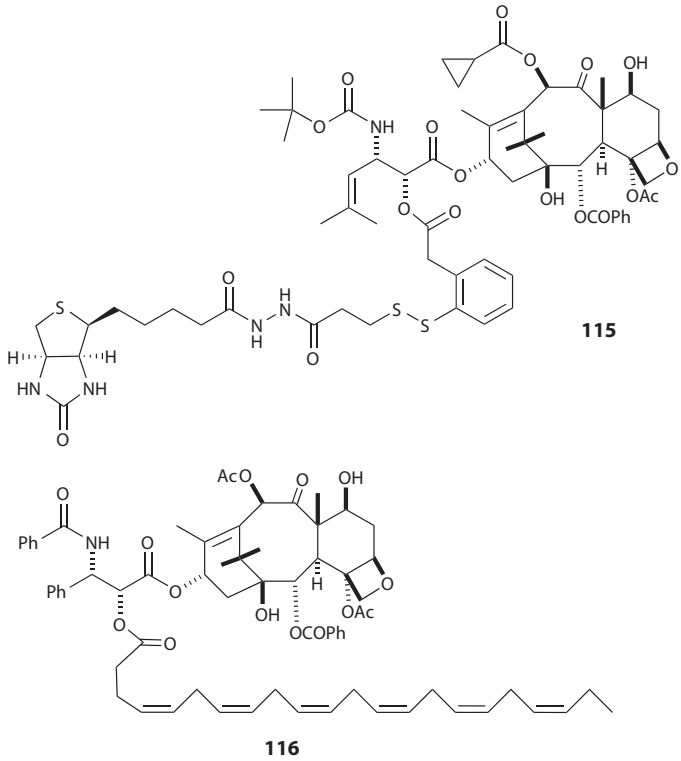

FIGURE 6.32 Biotin- and DHA-targeted taxol prodrugs **115** and **116**.

Two of these have been approved for clinical use. The first of these is the albumin-bound nanoparticle formulation of taxol known as Abraxane® (ABI-007; American Bioscience Inc.). Its infusion time is shorter than for taxol, and it has lower systemic toxicity, so it offers significant clinical benefits. Its development and use have been reviewed.[236–238] A similar formulation has also been introduced in India as Nanoxel.[239] The second of these is the micellar taxol formulation Genexol-PM®, which uses PEG and poly(D,L-lactic acid). It gave high response rates in patients with metastatic breast cancer, and has been approved by the FDA for this indication.[240]

The simplest way of making nanoparticles is by self-assembly, and the preparation of heparin–taxol conjugates illustrates this. Heparin is a natural polysaccharide with a variety of biological activities, and when it is conjugated to taxol the prodrug self-assembles in water to form nanoparticles, and it has better activity against MCF-7 cells than free taxol.[241] PEG is widely used as a conjugation agent for drugs, as noted earlier, and it has been found that conjugation of methyl-PEG with docetaxel at the 2′-position gives a compound that self-assembles to form nanosized micelles which can then solubilize free docetaxel. The concentration of docetaxel in the resulting mixture of docetaxel–PEG and free docetaxel can be as high as 28 mg/mL.[242] The Ansell group has conjugated a series of increasingly hydrophobic lipid anchors to taxol, and then used these to generate nanoparticle formulations by flash precipitation with the well-defined block copolymer poly(ethylene glycol)-*b*-polystyrene. Varying the size of the lipid anchor allowed the control of the half-life of taxol release between 1 and 24 h, and optimum *in vivo* efficacy was achieved in the HT29 colorectal tumor xenograft model with a docosanyldiglycoloyl derivative of taxol.[243]

Self-assembled nanoparticles containing docetaxel were prepared by combining docetaxel with distearoylphosphatidyl-ethanolamine-*N*-poly-(ethylene glycol) 2000 and maleimide-derivatized PEG-distearoylphosphatidylethanolamine. The free maleimide groups around the periphery of the nanoparticle were then reacted with thiol-functionalized epidermal growth factor to form "targeted nanoassemblies," or TNAs. Treatment of *BALB/c* mice with breast tumor xenografts with the TNAs was curative at a dose of 10 mg/kg.[244]

Gold has long been known to form stable nanoparticles, and several groups have used these as the basis for taxol drug delivery systems. The Zubarev group derivatized gold nanoparticles with 4-mercaptophenol, and then coupled the free hydroxyl groups with a C-7 taxol derivative to form the taxol-loaded nanoparticles (**117**). The nanoparticles were well characterized, but no biological data were reported.[245] A direct bonding of the thiolated taxol **118** either to gold nanoparticles or to maleimide-functionalized iron oxide nanoparticles was carried out by Hwu and his group (Figure 6.33). Interestingly, the two different formulations behaved differently toward phosphodiesterase; the loaded iron oxide nanoparticles released taxol with a half-life of about 6 days, but the gold nanoparticles did not release taxol even after 12 days.[246] A third prodrug formulation with gold nanoparticles has been published by Paciotti. In this formulation, a thiolated taxol is coupled with gold nanoparticles that are also derivatized with PEG-thiol and with tumor necrosis factor (TNF), a cytotoxic tumor targeting cytokine which has found limited clinical use in the isolated limb perfusion technique. The resulting construct has promise as a targeted nanoparticle drug delivery system.[247]

6.6.5 Antibody Conjugates of Taxol

The final and most direct strategy is that of linking taxol directly to an mAb. This approach has been adopted by more than one group, but it places stringent demands on the antibody, on the drug, and on the linker between the two. These constraints have been summarized by Safavy, and include the need for a highly potent drug, for a drug–mAb linker with the optimum stability, an internalizing mAb, and the correct ratio of drug to mAb.[248] The method works best for highly potent drugs which are too toxic for direct delivery, such as calicheamicin,[249] and so far no clinical candidates using taxol as the warhead have been developed. Several taxane–antibody immunoconjugates have, however, been developed. Thus, conjugation of taxol to the anti-p75 mAb MC192 was achieved

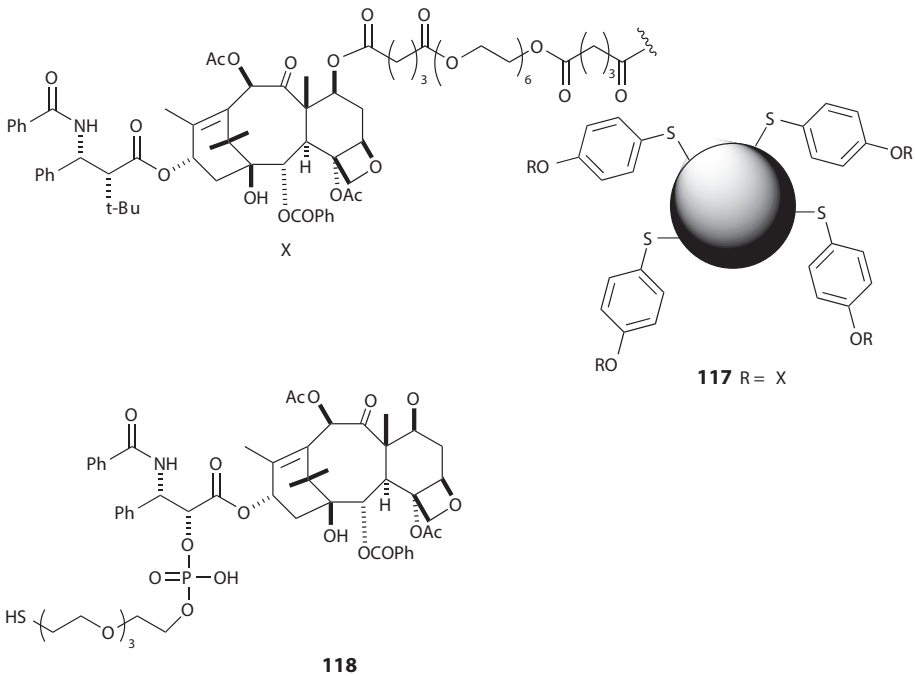

FIGURE 6.33 Gold nanoparticle taxol derivatives **117** and **118**.

through a 2′-glutaric acid linker; the resulting conjugate had improved cytotoxicity and improved selectivity as compared with taxol.[250] Several taxane–antibody immunoconjugates have been prepared by Ojima; as one example, the conjugate **119** was prepared using an antibody that recognized the human epidermal growth factor (EGFR) expressed in human squamous cells. The conjugate was shown to have excellent activity *in vivo* against EGFR-expressing A431 tumor xenografts in SCID mice.[251] Recently, derivative **120** with a branched-chain dPEG linker between an mAb and taxol have been prepared and shown to retain immunogenicity and cytotoxicity (Figure 6.34).[252]

In summary, the targeting of taxol and other taxanes through the approaches described before offers a way to improve therapeutic effect and reduce toxicity. Some analogs are in preclinical development or in clinical trials, and it seems probable that one or more of them will be introduced into clinical use within the next few years.

6.7 SYNTHETIC STUDIES

6.7.1 Semisynthetic Methods

Much of the work described in the preceding sections has only been possible because synthetic methods are available for the attachment of the taxol side chain to baccatin III. In addition, taxol can be manufactured on a large scale by semisynthesis from 10-DAB (**2**), creating a large incentive for the discovery of improved or alternate methods for the synthesis of the side chain and for coupling it to 10-DAB. The semisynthesis of taxol and its analogs thus requires a source of suitably protected 10-DAB, an efficient synthesis of the C-13 side chain, and a good method for coupling the side chain to the C-13 position of protected 10-DAB. This last step is key as the C-13 hydroxyl group of baccatin III is hindered and very unreactive.

As noted earlier, 10-DAB (**2**) can be obtained in good yield from the needles of *T. baccata* and other yew species.[18,20] The natural product must then be protected at C-7 and C-10 before acylation at the C-13 position, but this can be done in a one-pot reaction.[253] The β-phenylisoserine side chain

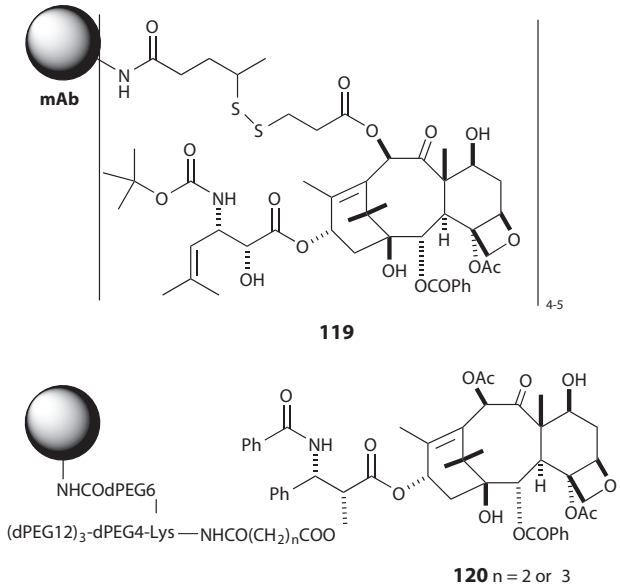

FIGURE 6.34 Antibody-linked taxol derivatives **119** and **120**.

of taxol can be prepared in several ways, and these are discussed in two reviews; [254,255] the interested reader is referred to these reviews for in-depth discussion of the many synthetic approaches that have been utilized.

Many different approaches have been used to couple the side chain to protected baccatin III, and only the most important will be described here. The most important method from a commercial point of view is that based on β-lactam chemistry, as this was the method used by BMS in their semisynthesis of taxol until it was replaced by the plant tissue culture production method. The chemistry was developed independently by Holton[256] and Ojima,[257] and is a simple and efficient route to taxol.

The key nonracemic β-lactam **121** can be prepared by various methods, all of which involve a [2 + 2] cycloaddition reaction. Two different types of approach can be used, depending on whether the chiral auxiliary is associated with the enolate or the imine half of the cycloaddition reaction. Methods that utilize a chiral enolate include the use of a 2-phenylcyclohexanol enolate (**122** + **123**)[258] and of a chiral enolate of Oppolzer's auxiliary.[259] A chiral oxazolidinone enolate has also been used, although this approach requires several steps to remove the chiral auxiliary when it is no longer needed (Figure 6.35).[260,261]

Chiral imines have also yielded diastereoselective 2 + 2 cycloadditions. The imine **124** gave 84% diastereomeric excess of the desired β-lactam, although several steps were required to remove the chiral auxiliary.[262] A better diastereomeric excess was achieved with the imine **125**.[263] The β-lactam can also be prepared selectively from an α-bromoamide precursor; thus, treatment of the intermediate **126** with NaH or TBAF gave β-lactam in good yield without significant loss of optical purity.[264] An alternative and experimentally simpler approach is to prepare the acetate of racemic β-lactam **127** by simple 2 + 2 cycloaddition and then resolve it with a commercially available lipase.[265] Ironically, all this effort to prepare enantiopure β-lactams may be unnecessary, as Ojima has shown that kinetic resolution can be obtained in coupling racemic β-lactams with baccatins.[266]

Coupling of the protected β-lactam, however prepared, with protected baccatin III is an efficient and high-yield reaction. Coupling is normally carried out in the presence of NaH or LiHDMS, and yields greater than 90% are routinely achieved. Thus coupling of β-lactam **121** with the protected baccatin III derivative **128** gives the protected taxol derivative **129**, which can be deprotected to give taxol **1** (Figure 6.36).

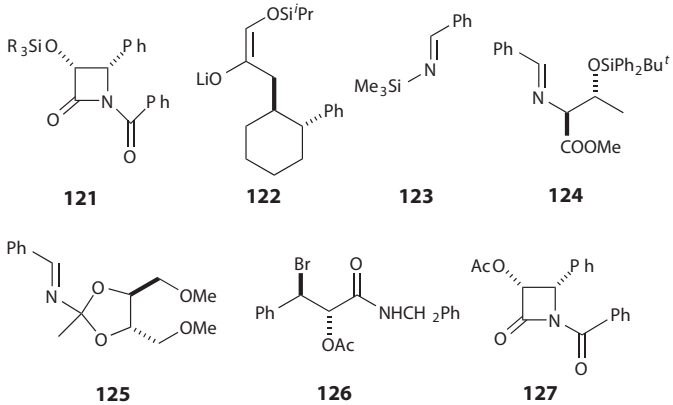

FIGURE 6.35 Synthons **121–127** for the taxol side chain.

Most of the other approaches to taxol from baccatin III also involve cyclic intermediates, as these minimize the steric constraints inherent in acylating the very hindered C-13 hydroxyl group of baccatin III. Groups which have been used successfully include the oxazolidine group, such as **130**, which has been coupled with the protected baccatin III (**131**); the coupled product **132** must then be deprotected by treatment with formic acid and benzoylated to give taxol **1** (Figure 6.37).[267]

Oxazolines such as **133** can also be coupled in high yield; hydrolysis of the intermediate oxazoline **134** gives taxol (**1**). As is also the case with the β-lactam approach, this route is atom economical in that the protecting group is part of the final product (Figure 6.38).[268,269]

Many other methods have been developed for the synthesis of taxol and related compounds from baccatin III. These include coupling of oxazolidine thioesters,[269,270] coupling with *cis*-glycidic acids followed by appropriate manipulations,[271] and coupling with a β-ketoester and subsequent functionalizations.[272]

6.7.2 Total Synthesis

The structure of taxol, with its complex stereochemistry and unique ring structure, represents one of the most challenging natural product synthetic targets. In spite of this complexity, six independent

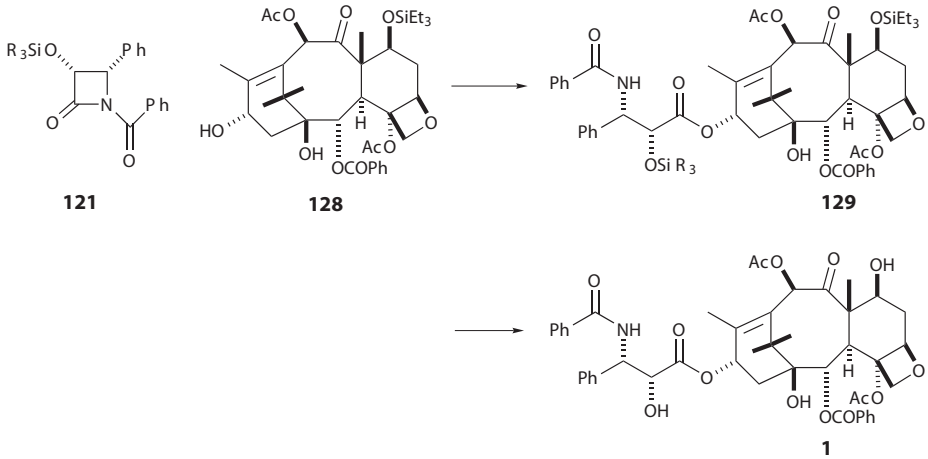

FIGURE 6.36 Synthesis of taxol **1** by the β-lactam approach.

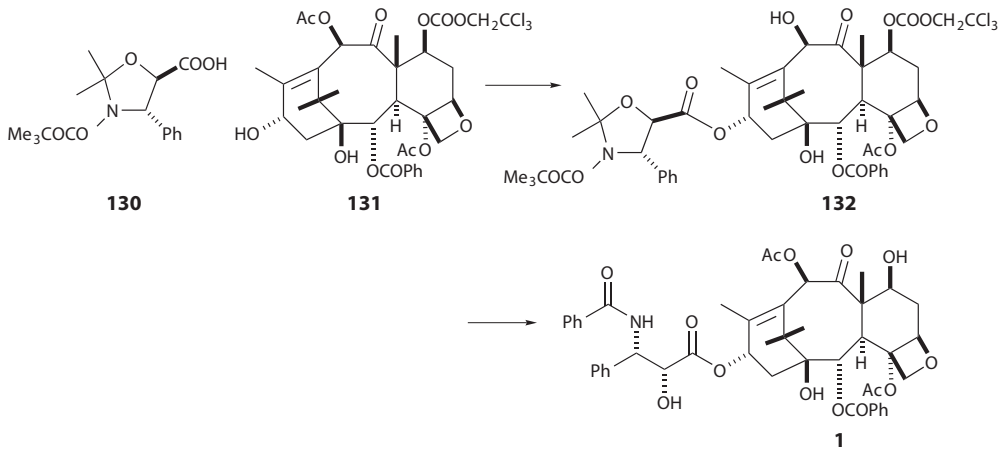

FIGURE 6.37 Synthesis of taxol **1** by the oxazolidine approach.

total syntheses have been achieved, together with numerous partial syntheses and unique synthetic approaches. Because this subject was covered in the previous edition of this book, and because there have not been any new total syntheses of taxol in the last 5 years, this subject will not be discussed again. Readers interested in this aspect of taxol chemistry are referred to any of several reviews of the subject,[74,273] or to the papers describing the six total syntheses that have been published to date. The first two syntheses were published essentially simultaneously by Holton[274,275] and Nicolaou,[276] and were followed by the Danishefsky synthesis,[277] the Wender synthesis,[278,279] the Kuwajima synthesis,[280] and the Mukaiyama synthesis.[281]

Although no new total synthesis of taxol has been published, a promising approach from the Pattenden group has been reported. Sadly a key step of the original synthetic scheme failed, but an alternate approach yielded the tricyclic product **138** in six steps from the cyclohexene derivative **135** and the stannane **136** via the ketoaldehyde **137**.[282] The synthesis was then abandoned because of lack of material, but the authors point out that their advanced intermediate could be converted to the advanced intermediate **139** of the successful Mukaiyama synthesis (Scheme 6.3).[281]

6.8 TAXOL–TUBULIN INTERACTION

As noted earlier in Section 6.4, the primary mechanism of action of taxol is its ability to stabilize microtubules and thus to disturb the equilibrium between tubulin and microtubules that is so essential for normal cellular function. The nature of the interactions between taxol and tubulin has thus been a subject of intense interest, and many different tools have been used to study it.

The location of the taxol-binding site within the tubulin molecule was shown to be on β-tubulin by photoaffinity labeling studies with [^{3}H]-3′-*N*-debenzoyl-3′-*N*-(*p*-azidobenzoyl) taxol, which photolabeled the *N*-terminal proton of β-tubulin.[283] In contrast, 2-debenzoyl-2-(*m*-azidobenzoyl) taxol

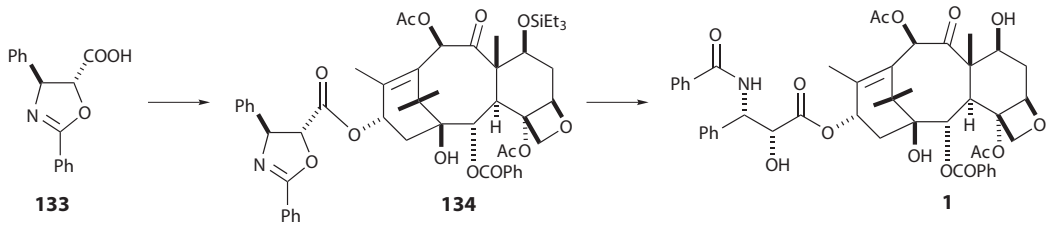

FIGURE 6.38 Synthesis of taxol **1** by the oxazoline approach.

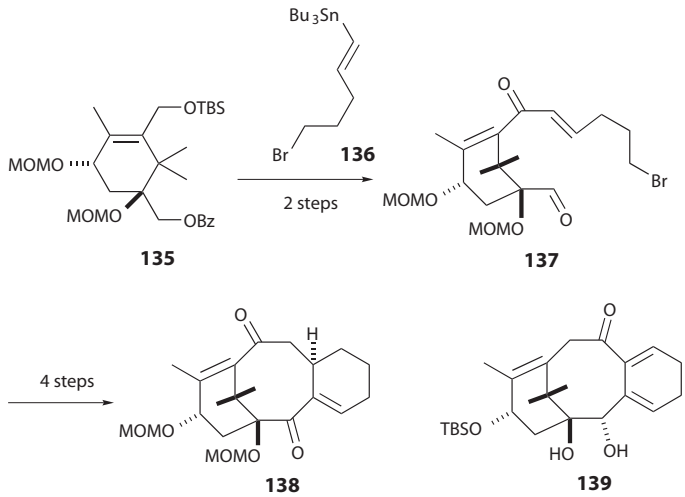

SCHEME 6.3 The Pattenden approach to taxol.

labeled amino acids 217–231 of β-tubulin,[284] and taxol with a photoaffinity label at C-7 bound to Arg[282] in β-tubulin.[285] Although β-tubulin is the tubulin molecule that is labeled most extensively by photoaffinity-labeled taxol, some analogs do label α-tubulin as well as (or instead of) β-tubulin. Thus, [^{3}H]-3′-*N*-debenzoyl-3′-*N*-(*p*-azidobenzoyl) taxol does bind to α-tubulin to a modest extent,[286] and [^{3}H]-2-debenzoyl-2-(*m*-azidobenzoyl) labeled amino acids 281–304 of α-tubulin.[287] These results thus indicate that taxol most probably occupies a binding site located between α- and β-tubulin, but largely on β-tubulin.

In ideal circumstances the binding site of taxol on tubulin would be elucidated by x-ray crystallography, but it has not been proved possible to obtain crystals of the polymeric complex. It has proved possible, however, to obtain electron diffraction data on the αβ-tubulin–taxol complex as zinc-induced sheets, and this has proved enormously important in understanding the taxol–tubulin interaction.[288,289] In this structure, taxol occupies a hydrophobic cleft on β-tubulin, and the binding of taxol in this cleft converts it into a hydrophilic surface.[290] This binding location is consistent with the photoaffinity results reported before showing labeling of β-tubulin by taxol; the labeling of α-tubulin is difficult to explain. The electron crystallographic approach to establishing the tubulin-binding mode of taxol and other tubulin-binding drugs has been reviewed.[291]

Although the electron crystallographic results show the location of taxol on tubulin, the actual binding conformation of taxol cannot be discerned at the resolution obtained, and thus indirect methods must be used to make this determination. A knowledge of the binding conformation of taxol is important in that it would help to explain how compounds as structurally diverse as the epothilones, discodermolide, and eleutherobin could all have the same mechanism of action, and it could also provide a guiding model for the synthesis of simplified compounds which retained tubulin-binding ability.

Studies of the nuclear magnetic resonance (NMR) spectra of taxol in solution indicated the presence of two major conformers, a nonpolar conformer with the C-2 benzoyl group and the C-3′ phenyl side chain exhibiting hydrophobic collapse,[292–294] and a polar form in which the C-2 benzoyl group and C-3′ benzamido side chain are in close proximity.[295–297] However, NMR deconvolution analysis in chloroform also revealed the presence of a third conformer, designated T-taxol, in which the C-2 benzoyl group bisects the angle between the C-3′ phenyl and C-3′ benzamido side chains.[298]

A distinction between these three models for the binding conformation of taxol has been obtained by studies using solid-state NMR to probe the conformation of tubulin-bound taxol. In the first study, an F–F distance of 6.5 Å was determined for the compound **140**,[299] although the full details of this

work have not yet been published. The other two studies used Rotational Echo Double Resonance (REDOR) NMR measurements of labeled taxols on lyophilized microtubules to determine the distances a–e in structure **141**.[300,301] These distances were then compared with the predictions of various models for the conformation of taxol on microtubules. The only model fully consistent with the REDOR data was the T-taxol model.[301] The T-taxol conformation is also consistent with the unexpected activity of 2-*m*-azidobaccatin III,[302] and it docks well into the hydrophobic cleft in β-tubulin described earlier.[290] Strong confirmation of the validity of the T-taxol conformation was provided by the synthesis of the bridged taxol **142**, which closely mapped the T-taxol conformation and was more potent than taxol in a variety of cell- and tubulin-based assays (Figure 6.39).[303,304]

In other work designed to test the limits of the T-taxol model, the known and inactive A-*nor*taxol **143**[84] was converted to the active compound **144** by bridging it to maintain the T-taxol conformation.[305] In contrast, the taxol derivative **145** with a constrained side chain cannot adopt the T-taxol conformation, and it was very much less active than taxol (Figure 6.40).[306]

Although there is strong evidence for the T-taxol structure, a strong argument has been made that a similar structure with a slightly modified side chain conformation know as REDOR-taxol[307] or PTX-NY[301] is a better fit to the experimental data. The debate on the relative merits of T-taxol and REDOR taxol as the best description of the microtubule bound conformation of taxol continues, with arguments for[6,308] and against[309] REDOR taxol being made.

Although most research has focused on the binding of taxol to an internal site in the luminal face of microtubules,[310] recent work has shown that binding also occurs at an external pore site, and this binding has been studied with the use of fluorescent analogs.[311] The docking of taxol analogs to the microtubule-binding site has been used as a way to understand the SAR of taxol,[312] and a QSAR study of the microtubule–taxane interaction has led to the design of 18 analogs, which are suggested as potential synthetic targets.[313]

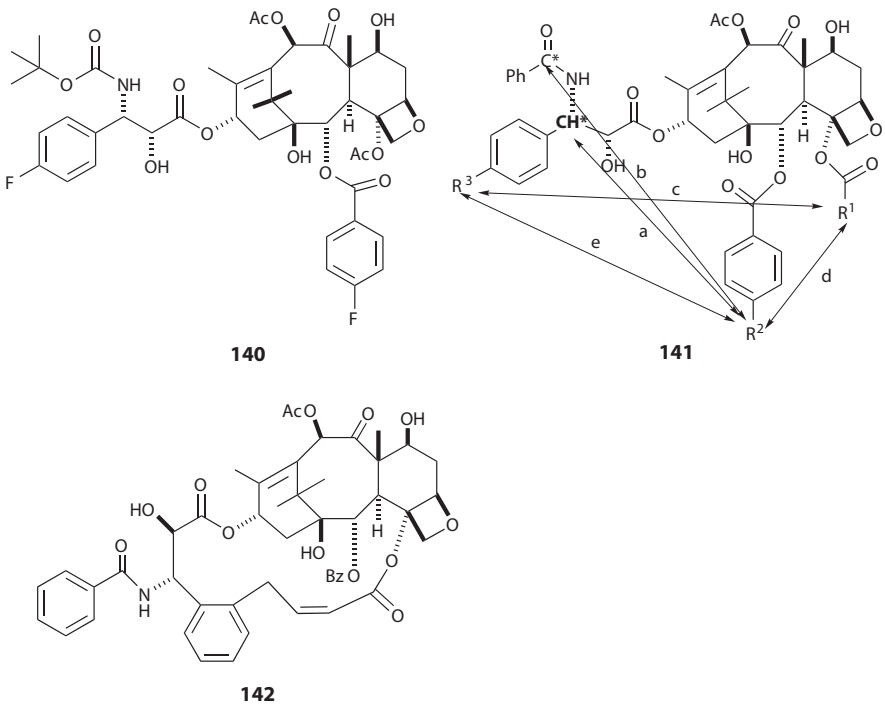

FIGURE 6.39 Labeled taxol, the interatomic distances determined by REDOR, and the most active bridged analog.

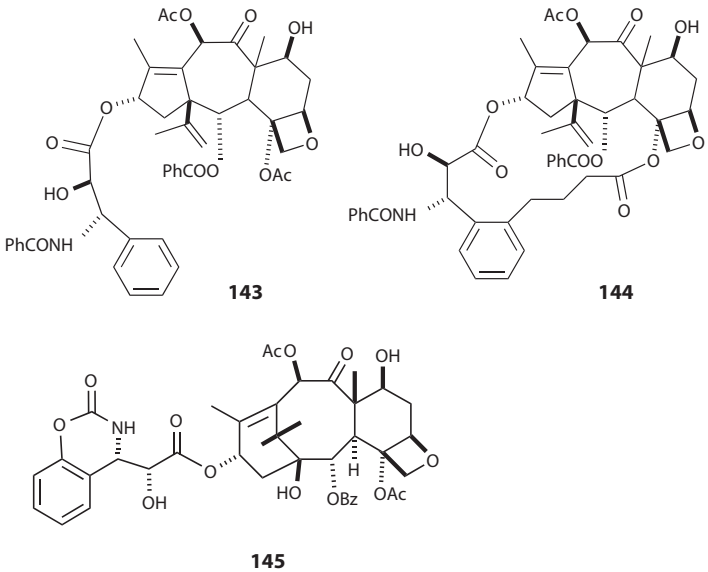

FIGURE 6.40 Validation of the T-taxol conformation by the synthesis of active (**144**) and inactive (**145**) analogs.

6.9 CLINICAL APPLICATIONS OF TAXOL, DOCETAXEL, AND CABAZITAXEL

The preceding discussions have provided a brief and somewhat selective overview of the chemistry and biology of taxol. For most nonscientists, however, the key question is "How well does it work: What are the clinical benefits of taxol and its sister drug docetaxel to the cancer patient?" It is difficult to give an unqualified answer to this question, in part because treatment modalities are continuing to improve. At present the taxane drugs taxol and docetaxel are used for the treatment of breast, lung, and ovarian carcinomas, and also for AIDS-related Kaposi's sarcoma. General reviews covering the use of these drugs in cancer therapy have been written,[314–317] but most reviews cover their use against specific cancers.

The taxanes have proven to be among the most active agents in treating advanced metastatic breast cancer,[318–321] but their benefits in treating early-stage breast cancer have only recently been evaluated. Two reviews have now documented their value, however. One reviewer states "The evidence is now clear that taxanes added to standard adjuvant regimens . . . can improve outcomes for patients with breast cancer,"[322] while a second systematic review of taxane versus nontaxane regimens for treatment of early breast cancer concludes: "The results of this systematic review support the use of taxanes as adjuvant chemotherapy for women with early breast cancer and involved lymph nodes." In the studies summarized in this review, the 5-year relapse-free survival rate was 74% for the control (nontaxane) group versus 79% for the taxane-treated group.[323] Another review of the use of taxanes in breast cancer concluded: "It is now becoming clear that either paclitaxel or docetaxel are inducing substantial benefits . . . This is confirming the capability of the taxanes to impact the natural history of breast cancer."[324]

In the lung cancer area, docetaxel is one of the drugs of choice for the treatment of advanced NSCLC that is refractory to primary chemotherapy.[316,325,326] A study to compare the efficacy of three different treatment regimens (cisplatin and gemcitabine, cisplatin and docetaxel, or carboplatin and taxol) found that the response rates and survival did not differ significantly between the regimens.[314]

The significance of taxol as an anticancer drug was first discovered for ovarian cancer, and this remains an important target.[319] A European–Canadian study confirmed early findings that the

combination of taxol–cisplatin is superior to the previously used regimen of cyclophosphamide–cisplatin,[327] and this is now the standard of care for women with advanced ovarian cancer.

Docetaxel is used as an effective drug against prostate cancer,[328] and its introduction was greeted with enthusiasm.[329] The taxanes have also been investigated for use against and head and neck cancers.[330]

Cabazitaxel (**42**, Figure 6.8) is currently approved for treatment of hormone refactory prostate cancer. It is a poor substrate for P-gp, and is thus less likely to be subject to drug resistance than taxol and docetaxel.[101]

Although the taxanes are certainly not the wonder drugs they were at one time thought to be, they have nevertheless brought significant benefits to many cancer patients. The new analogs referred to in the following section promise real improvements in efficacy over taxol and docetaxel, and improvements in drug delivery will also play a major role in improving treatment. In this connection, the approval of the albumin nanoparticle-based formulation of taxol ABI-007 (Abraxane®)[331] shows that improved formulations can have a dramatic effect. The overall response rate for ABI-007 in patients with metastatic breast cancer was 33%, compared with 19% for taxol, and several reviews have described this formulation in more detail.[332–334]

Although the primary effect of taxol is on the formation of the microtubule spindle, the actual effects *in vivo* are very complex, and the levels of various spindle assembly checkpoint proteins, such as MAD2, BUBR1, Synuclein-gamma, and Aurora A play a role in resistance of tumors to taxol. The importance of these and other factors to chemoresistance to taxol have been reviewed,[335] and the advances achieved by the development of new taxanes that are potentially useful for the treatment of resistant tumors have also been reviewed.[336]

Another major use of taxol is as the drug in drug-eluting stents, to prevent or at least reduce the incidence of restonosis. The use of taxol in the Taxus™ drug-eluting stent has been reviewed,[337] and a comparison of the taxol-eluting stent with other drug-eluting stents has been published.[338] It is thus clear that taxol and its analogs will continue to play an important role in cancer chemotherapy well into the twenty-first century.

6.10 TAXOL ANALOGS IN CLINICAL TRIALS

As described in Section 6.5, numerous taxol analogs have been prepared, and several have entered preclinical development or clinical trial. Listings of taxol analogs in development are contained in several reviews,[163,339,340] and readers are referred to these reviews for further details of taxol analogs in preclinical development.

Four taxol analogs are currently in Phase III clinical trials. The simple C-7 acyl derivatives 7-DHA-taxol (Taxoprexin; **116**) is in Phase III trials for treatment of NSCLC and in Phase II trials for other cancers, and some Phase II results have been reported.[341,342] The interesting cyclopropyl derivative larotaxel (RPR-109881A; **68**) has a broad spectrum of activity and may have the advantage of penetrating into the central nervous system and of bypassing some resistance mechanisms.[343,344] Paclitaxel poliglumex (Xyotax; **101**) is in Phase III trials for the treatment of NSCLC and ovarian cancer.[345,346]

Five taxol analogs and two new formulations of taxol are in Phase II trials. TPI-287 (**146**) is in Phase II trials for treatment of advanced pancreatic cancer and hormone-refractory prostate cancer.[347] Ortataxel (**32**) is in Phase II trials for treatment of NSCLC and taxane-resistant breast cancer.[348] Milataxel (MAC-321, TL-00139; **84**) completed Phase II trials for colorectal cancer in 2009, but a preliminary report concluded: "A syndrome of neutropenic sepsis and diarrhea can be life threatening and close surveillance is needed in patients treated with milataxel at the dose of 35 mg/m^2 every 3 weeks. Clinical activity was not demonstrated in patients with advanced previously treated CRC."[349] As noted earlier, DJ-927 (**85**) is in clinical trials as an orally active compound with antitumor activity against NSCLC.[174] It was withdrawn from development in 2006 because of the lack of a clear advantage over existing drugs,[350] but Phase III trials have restarted under Genta. The simple C-4 carbonate BMS-188797 (**72**)[153] showed objective responses in a Phase I trial for 4 of 16 patients.[351]

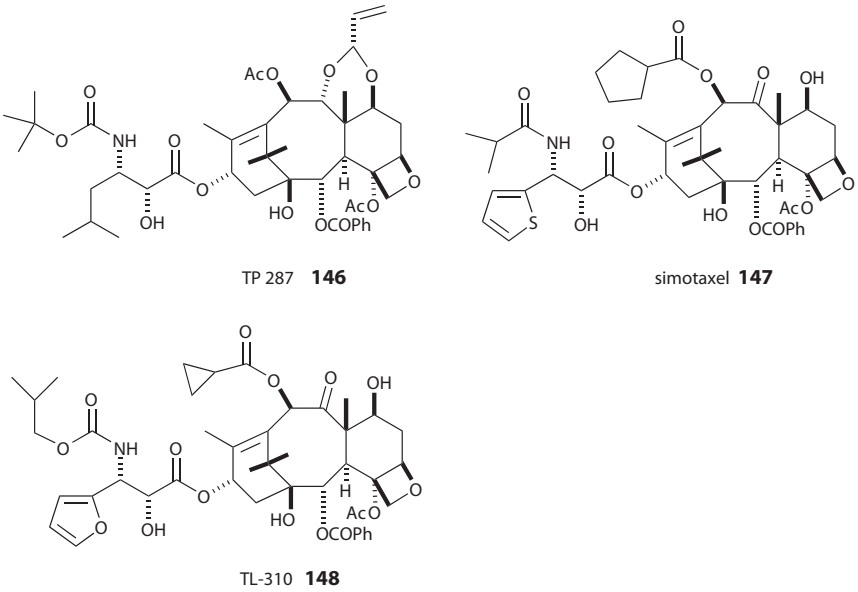

FIGURE 6.41 Clinical candidate TP 287 (**146**) and discontinued compounds simotaxel (**147**) and TL-310 (**148**).

The three new formulations are NK-105, a polymeric micellar macromolecule encapsulated formulation of taxol, EndoTAG-1, a formulation of taxol in a positively charged lipid-based complex, and Nab-docetaxel, an albumin nanoparticle formulation of docetaxel related to Abraxane. NK-105 is in Phase II clinical trials at Nippon Kayaku for the treatment of solid tumors, EndoTAG-1 is in Phase II trials for treatment of advanced pancreatic cancer,[352] and Nab-docetaxel is in Phase II trials for hormone-refractory prostate cancer.[353]

Clinical studies on some analogs have been discontinued over the last few years, and the 4-carbonate derivative BMS-275183 (**73**), the thioether BMS-184476 (**57**),[131] simotaxel (**147**), and TL-310 (**148**) have all been withdrawn from development. These results point to the difficulties of developing improved versions of established drugs such as taxol and docetaxel, and highlight the significant advances that can, in principle, be made by targeting existing drugs to the tumor site (Figure 6.41).

6.11 CONCLUSION

The botanists who collected the bark of *T. brevifolia* in 1962 could not have foreseen the enormous consequences that would flow from that simple act. Providentially, their action initiated a chain of events that has led to the present situation, where the one lead compound of taxol has not only yielded three currently approved clinical agents, but has also led to the development of 33 compounds that are either in clinical trial or advanced preclinical development. It is certain that some of these will advance to clinical use, and taxol will thus be joined by a number of related compounds in providing clinical anticancer agents. In addition, the mechanism of action of taxol, which was unique when it was first discovered, has led to the discovery of several new natural and synthetic compounds with the same mechanism, as described in Section 6.8. In a real sense, taxol can thus be viewed as the progenitor of an even larger number of potential clinical agents. It is almost a certainty that some of them will turn out to have significantly better clinical profiles than taxol itself, with significant life extensions and even cures in some cases. That botanical collection in 1962, coupled with the skill and expertise of numerous scientists, has thus made a huge contribution to cancer treatment, and must surely rank as the most significant such collection ever made!

ACKNOWLEDGMENTS

John Donne wrote that "No man is an island," and this is certainly true of all scientists who have worked on taxol, as we all build on the knowledge and results of others in the area. The author is particularly grateful to his colleagues at the NCI, and especially to the late Matthew Suffness for his early support on the work on taxol when few others believed that it would ever become a clinically used drug. More recently Gordon Cragg and David Newman, the coeditors of this volume, and Yali Hallock have provided continuous support and encouragement, and the former two also provided helpful comments and suggestions on the text of this chapter. The author's work reported herein was supported by grants from BMS and the NCI, most recently under grant CA 69571, and such support is gratefully acknowledged. The author also acknowledges with gratitude the collaboration of his colleagues Susan Bane (SUNY Binghamton), Jake Schaefer (Washington University) and Jim Snyder (Emory University), and of the talented graduate students and research associates whose names are recorded in the publications from his group.

REFERENCES

1. Kingston, D.G.I. Taxol and its analogs, in *Anticancer Agents from Natural Products*, Cragg, G.M., Kingston, D.G.I., Newman, D.J., Eds. CRC Press, Inc., Boca Raton, FL, 2005, 89.
2. Fang, W.-S., Fang, Q.-C., and Liang, X.-T., Structure modifications and their influences on antitumor and other related activities of taxol and its analogs, in *Medicinal Chemistry of Bioactive Natural Products*, Liang, X.-T., Fang, W.-S., Eds. Wiley-Interscience, Hoboken, NJ, 2006, 73.
3. Fang, W.-S. and Wang, S.-R., Structural studies of taxol analogues for drug discovery, *Expert Opin. Drug Discov.* 3, 1109, 2008.
4. Fu, Y., Li, S., Zu, Y., Yang, G., Yang, Z., Luo, M., Jiang, S., Wink, M., and Efferth, T., Medicinal chemistry of paclitaxel and its analogues, *Curr. Med. Chem.* 16, 3966, 2009.
5. Zefirova, O.N., Nurieva, E.V., Ryzhov, A.N., Zyk, N.V., and Zefirov, N.S., Taxol: Synthesis, bioactive conformations, and structure–activity relationships in its analogs, *Russ. J. Org. Chem.* 41, 315, 2005.
6. Ojima, I. and Das, M., Recent advances in the chemistry and biology of new generation taxoids, *J. Nat. Prod.* 72, 554, 2009.
7. Galletti, E., Magnani, M., Renzulli, M.L., and Botta, M., Paclitaxel and docetaxel resistance: Molecular mechanisms and development of new generation taxanes, *ChemMedChem* 2, 920, 2007.
8. Kingston, D.G.I. and Newman, D.J., Taxoids: Cancer-fighting compounds from nature, *Curr. Opin. Drug Discov. Dev.* 10, 130, 2007.
9. Drs. Wall and Wani named the compound they isolated from *Taxus brevifolia* taxol, but unknown to them this name had previously been trademarked by a French company for an unrelated laxative product. This trademark was later acquired by Bristol-Myers Squibb, who then applied it to their formulation of the Wall and Wani compound, and the generic name paclitaxel was assigned to the Wall and Wani compound. Since this review is partly historical in nature, the name taxol will be used to refer to the Wall and Wani compound; no infringement of the Bristol-Myers Squibb trademark is implied.
10. Wani, M.C., Taylor, H.L., Wall, M.E., Coggon, P., and McPhail, A.T., Plant antitumor agents. VI. The isolation and structure of taxol, a novel antileukemic and antitumor agent from *Taxus brevifolia*, *J. Am. Chem. Soc.* 93, 2325, 1971.
11. Schiff, P.B., Fant, J., and Horwitz, S.B., Promotion of microtubule assembly in vitro by taxol, *Nature* 277, 665, 1979.
12. Weiss, R.B., Donehower, R.C., Wiernik, P.H., Ohnuma, T., Gralla, R.J., Trump, D.L., Baker, Jr., J.R., VanEcho, D.A., Von Hoff, D.D., and Leyland-Jones, B., Hypersensitivity reactions from taxol, *J. Clin. Oncol.* 8, 1263, 1990.
13. Rose, W.C., Preclinical antitumor activity of taxanes, in *Taxol, Science and Applications*, Suffness, M. Ed., CRC Press, Inc., Boca Raton, FL, 1995, chap. 8.
14. McGuire, W.P., Rowinsky, E.K., Rosenshein, N.B., Grumbine, F.C., Ettinger, D.S., Armstrong, D.K., and Donehower, R.C., Taxol: A unique antineoplastic agent with significant activity in advanced ovarian epithelial neoplasms, *Ann. Intern. Med.* 111, 273, 1989.
15. Holmes, F.A., Walters, R.S., Theriault, R.L., Forman, A.D., Newton, L.K., Raber, M.N., Buzdar, A.U., Frye, D.K., and Hortobagyi, G.N., Phase II trial of taxol, an active drug in the treatment of metastatic breast cancer, *J. Nat. Cancer Inst.* 83, 1797, 1991.

16. Chase, M., Cancer drug may save many human lives – at cost of rare trees, *Wall Street J.*, 217 (69), A1, A8, 1991.
17. Chauviere, G., Guénard, D., Picot, F., Senilh, V., and Potier, P., Analyse structurale et etude biochimique de produits isoles de l'If: *Taxus baccata* L. (Taxacees). C. R., *Acad. Sc. Paris, Serie II*, 293, 501, 1981.
18. Denis, J.-N., Greene, A.E., Guénard, D., Guéritte-Voegelein, F., Mangatal, L., and Potier, P., A highly efficient, practical approach to natural taxol, *J. Am. Chem. Soc.* 110, 5917, 1988.
19. Holton, R.A., Biediger, R.J., and Boatman, P.D., Semisynthesis of taxol and taxotere, in *Taxol, Science and Applications*, Suffness, M., Ed., CRC Press, Inc., Boca Raton, FL, 1995, chap. 5.
20. Mroczek, T., Glowniak, K., and Hajnos, M., Screening for pharmaceutically important taxoids in *Taxus baccata* var. *Aurea* Corr. with GC/SPE/HPLC-PDA procedure, *Biomed. Chromatogr.* 14, 516, 2000.
21. Tabata, H., Production of paclitaxel and the related taxanes by cell suspension cultures of *Taxus* species, *Curr. Drug Targets* 7, 453, 2006.
22. Exposito, O., Bonfill, M., Moyano, E., Onrubia, M., Mirjalili, M.H., Cusido, R.M., and Palazon, J., Biotechnological production of taxol and related taxoids: Current state and prospects, *Anticancer Agents Med. Chem.* 9, 109, 2009.
23. http://www.genexol.com/eng/app//manufacture/default.asp
24. Wink, M., Alfermann, A.W., Franke, R., Wetterauer, B., Distl, M., Windhövel, J., Krohn, O. et al., Sustainable bioproduction of phytochemicals by plant *in vitro* cultures: Anticancer agents, *Plant Genet. Resour.* 3, 90, 2005.
25. Stierle, A., Strobel, G., and Stierle, D., Taxol and taxane production by *Taxomyces andreanae*, an endophytic fungus of Pacific yew, *Science*, 260, 214, 1993.
26. Li, J.Y., Sidhu, R.S., Ford, E.J., Long, D.M., Hess, W.M., and Strobel, G.A., The induction of taxol production in the endophytic fungus – *Periconia* sp. from *Torreya grandifolia*, *J. Ind. Micro. Biotech.* 20, 259, 1998.
27. Liu, K., Ding, X., Deng, B., and Chen, W., Isolation and characterization of endophytic taxol-producing fungi from *Taxus chilensis*, *J. Ind. Microbiol. Biotechnol.* 36, 1171, 2009.
28. Frense, D., Taxanes: Perspectives for biotechnological production, *Appl. Microbiol. Biotechnol.* 73, 1233, 2007.
29. Strobel, G., Daisy, B., Castillo, U., and Harper, J., Natural products from endophytic microorganisms, *J. Nat. Prod.* 67, 257, 2004.
30. Ganem, B. and Franke, R.R., Paclitaxel from primary taxanes: A perspective on creative invention in organozirconium chemistry, *J. Org. Chem.* 72, 3981, 2007.
31. Guéritte-Voegelein, F., Senilh, V., David, B., Guénard, D., and Potier, P., Chemical studies of 10-deacetyl baccatin III. Hemisynthesis of taxol derivatives, *Tetrahedron* 42, 4451, 1986.
32. Bissery, M.-C., Nohynek, G., Sanderink, G.-J., and Lavelle, F., Docetaxel (taxotere): A review of preclinical and clinical experience. Part I: Preclinical experience, *Anticancer Drugs* 6, 339, 1995.
33. Guéritte, F. General and recent aspects of the chemistry and structure–activity relationships of taxoids. *Curr. Pharm. Des.* 7, 1229, 2001.
34. Rohmer, M., Knani, M., Simonin, P., Sutter, B., and Sahm, H., Isoprenoid biosynthesis in bacteria: A novel pathway for the early steps leading to iospentenyl diphosphate, *Biochem. J.* 295, 517, 1993.
35. Eisenreich, W., Menhard, B., Hylands, P.J., Zenk, M.H., and Bacher, A., Studies on the biosynthesis of taxol: The taxane carbon skeleton is not of mevalonoid origin, *Proc. Natl. Acad. Sci. U.S.A.* 93, 6431, 1996.
36. Koepp, A.E., Hezari, M., Zajicek, J., Vogel, B.S., LaFever, R.E., Lewis, N.G., and Croteau, R., Cyclization of geranylgeranyl diphosphate to taxa-4(5),11(12)-diene is the committed step of taxol biosynthesis in pacific yew, *J. Biol. Chem.* 270, 8686, 1995.
37. Hezari, M., Lewis, N.G., and Croteau, R., Purification and characterization of taxa-4(5),11(12)-diene synthase from Pacific yew (*Taxus brevifolia)* that catalyzes the first committed step of taxol biosynthesis, *Arch. Biochem. Biophys.* 322, 437, 1995.
38. Wildung, M.R. and Croteau, R., A cDNA clone for taxadiene synthase, the diterpene cyclase that catalyzes the committed step of taxol biosynthesis, *J. Biol. Chem.* 271, 9201, 1996.
39. Hezari, M., Ketchun, R.E.B., Gibson, D.M., and Croteau, R., Taxol production and taxadiene synthase activity in *Taxus canadensis* cell suspension cultures, *Arch. Biochem. Biophys.* 337, 185, 1997.
40. Lin, X., Hezari, M., Hoepp, A.E., Gloss, H.G., and Croteau, R., Mechanism of taxadiene synthase, a diterpene cyclase that catalyzes the first step of taxol biosynthesis in Pacific yew, *Biochemistry* 35, 2968, 1996.
41. Floss, H.G. and Mocek, U., Biosynthesis of taxol, in *Taxol: Science and Applications*, Suffness, M., Ed., CRC Press, Inc., Boca Raton, FL, 1995, chap. 7.

42. Hefner, J., Rubenstein, S.M., Ketchum, R.E., Gibson, D.M., Williams, R.M., and Croteau, R., Cytochrome P450-catalyzed hydroxylation of taxa-4(5),11(12)-diene to taxa-4(20),11(12)-dien-5α-ol: The first oxygenation step in taxol biosynthesis, *Chem. Biol.* 3, 479, 1996.
43. Walker, K., Ketchum, R.E.B., Hezari, M., Gatfield, D., Goleniowski, M., Barthol, A., and Croteau, R., Partial purification and characterization of acetyl coenzyme A: Taxa-4(20),11(12)-dien-5α-ol-*O*-acetyl transferase that catalyzes the first acylation step of taxol biosynthesis, *Arch. Biochem. Biophys.* 364, 273, 1999.
44. Wheeler, A.L., Long, R.M., Ketchum, R.E.B., Rithner, C.D., Williams, R.M., and Croteau, R., Taxol biosynthesis: Differential transformations of taxadien-5α-ol and its acetate ester by cytochrome P450 hydroxylases from *Taxus* suspension cells, *Arch. Biochem. Biophys.* 390, 265, 2001.
45. Schoendorf, A., Rithner, C.D., Williams, R.M., and Croteau, R.B., Molecular cloning of a cytochrome P450 taxane 10β-hydroxylase cDNA from *Taxus* and functional expression in yeast, *Proc. Natl. Acad. Sci. U.S.A.* 98, 1501, 2001.
46. Jennewein, S., Rithner, C.D., Williams, R.M., and Croteau, R.B., Taxol biosynthesis: Taxane 13α-hydroxylase is a cytochrome P450-dependent monooxygenase, *Proc. Natl. Acad. Sci. U.S.A.* 98, 13595, 2001.
47. Horiguchi, T., Rithner, C.D., Croteau, R., and Williams, R.M., Studies on taxol biosynthesis. Preparation of 5α-acetoxytaxa-4(200,11-dien-2α,10β-diol) derivatives by deoxygenation of a taxadiene tetra-acetate obtained from Japanese yew, *Tetrahedron* 59, 267, 2003.
48. Chau, M., Jennewein, S., Walker, K., and Croteau, R., Taxol biosynthesis: Molecular cloning and characterization of a cytochrome P450 taxoid 7β-hydroxylase, *Chem. Biol.* 11, 663, 2004.
49. Jennewein, S., Wildung, M.R., Chau, M., Walker, K., and Croteau, R., Random sequencing of an induced *Taxus* cell cDNA library for identification of clones involved in Taxol biosynthesis, *Proc. Natl. Acad. Sci. U.S.A.* 101, 9149, 2004.
50. Ketchum, R.E.B., Horiguchi, T., Qiu, D., Williams, R.M., and Croteau, R.B., Administering cultured *Taxus* cells with early precursors reveals bifurcations in the taxoid biosynthetic pathways, *Phytochemistry* 68, 335, 2007.
51. Walker, K. and Croteau, R., Taxol biosynthesis: A review of some determinant steps, in *Phytochemicals in Human Health Protection, Nutrition, and Plant Defense*, Romeo Kluwer Academic/Plenum Publishers, New York, 1999, p. 31.
52. Pyo, S.-H., Cho, J.-S., Choi, H.-J., and Han, B.-H., Evaluation of paclitaxel rearrangement involving opening of the oxetane ring and migration of acetyl and benzoyl groups, *J. Pharm. Biomed. Anal.* 43, 1141, 2007.
53. Jennewein, S. and Croteau, R., Taxol: Biosynthesis, molecular genetics, and biotechnological applications, *Appl. Microbiol. Biotechnol.* 57, 13, 2001.
54. Giner, J.-L. and Faraldos, J.A., Facile orthoester formation in a model compound of the taxol oxetane: Are biologically active epoxy esters, orthoesters, and oxetanyl esters latent electrophiles?, *Helv. Chim. Acta* 86, 3613, 2003.
55. Croteau, R., Ketchum, R.E.B., Long, R.M., Kaspera, R., and Wildung, M.R., Taxol biosynthesis and molecular genetics, *Phytochem. Rev.* 5, 75, 2006.
56. Ondari, M.E. and Walker, K.D., The taxol pathway 10-*O*-acetyltransferase shows regioselective promiscuity with the oxetane hydroxyl of 4-deacetyltaxanes, *J. Am. Chem. Soc.* 130, 17187, 2008.
57. Kaspera, R., Cape, J.L., Faraldos, J.A., Ketchum, R.E.B., and Croteau, R.B., Synthesis and in vitro evaluation of taxol oxetane ring D precursors, *Tetrahedron Lett.* 51, 2017, 2010.
58. Fleming, P.E., Mocek, U., and Floss, H.G., Biosynthesis of taxoids. Mode of formation of the taxol side chain, *J. Am. Chem. Soc.*, 115, 805, 1993.
59. Fleming, P.E., Floss, H.G., Haertel, M., Knaggs, A.R., Lansing, A., Mocek, U., and Walker, K.D., Biosynthetic studies on taxol, *Pure Appl. Chem.* 66, 2045, 1994.
60. Fleming, P.E., Knaggs, A.R., He, X.-G., Mocek, U., and Floss, H.G., Biosynthesis of taxoids. Mode of attachment of the taxol side chain, *J. Am. Chem. Soc.* 116, 4137, 1994.
61. Schiff, P.B. and Horwitz, S.B., Taxol stabilizes microtubules in mouse fibroblast cells *Proc. Natl. Acad. Sci. U.S.A.* 77, 1561, 1980.
62. Jordan, M.A. and Wilson, L. Microtubules and actin filaments: Dynamic targets for cancer chemotherapy. *Curr. Opin. Cell Biol.* 10, 123, 1998.
63. Jordan, M.A. and Kamath, K., How do microtubule-targeted drugs work? An overview, *Curr. Cancer Drug Targets* 7, 730, 2007.
64. Jordan, M.A., Toso, R.J., Thrower, D., and Wilson, L., Mechanism of mitotic block and inhibition of cell proliferation by taxol at low concentrations, *Proc. Natl. Acad. Sci. U.S.A.* 90, 9552, 1993.

65. Long, B.H. and Fairchild, C.R., Paclitaxel inhibits progression of mitotic cells to G_1 phase by interference with spindle formation without affecting other microtubule functions during anaphase and telephase, *Cancer Res.*, 54, 4355, 1994.
66. Xiao, H., Verdier-Pinard, P., Fernandez-Fuentes, N., Burd, B., Angeletti, R., Fiser, A., Horwitz, S.B., and Orr, G.A., Insights into the mechanism of microtubule stabilization by taxol, *Proc. Natl. Acad. Sci. U.S.A.* 103, 10166, 2006.
67. Haldar, S., Chintapalli, J., and Croce, C. M., Paclitaxel induces *bcl-2* phosphorylation and death of prostate cancer cells, *Cancer Res.*, 56, 1253, 1996.
68. Blagosklonny, M.V., Giannakakou, P., El-Deiry, W.S., Kingston, D.G.I., Higgs, P.I., Neckers, L., and Fojo, T., Raf-1/bcl-2 phosphorylation: A step from microtubule damage to cell death, *Cancer Res.* 57, 130, 1997.
69. Rodi, D.J., Janes, R.W., Sanganee, H.J., Holton, R.A., Wallace, B.A., and Makowski, L., Screening of a library of phage-displayed peptides identifies human Bcl-2 as a taxol-binding protein, *J. Mol. Biol.* 285, 197, 1999.
70. Carboni, J. M., Singh, C., and Tepper, M. A., Taxol and lipopolysaccharide activation of a murine macrophage cell line and induction of similar tyrosine phosphoproteins, *J. Natl. Cancer Inst. Monogr.*, 15, 95, 1993.
71. Blagosklonny, M.V. and Fojo, T., Molecular effects of paclitaxel: Myths and reality (a critical review), *Int. J. Cancer*, 83, 151, 1999.
72. Abal, M., Andreu, J.M., and Barasoain, I., Taxanes: Microtubule and centrosome targets, and cell cycle dependent mechanisms of action, *Curr. Cancer Drug Targets*, 3, 193, 2003.
73. Wang, X., Itokawa, H., and Lee, K.-H., Structure–activity relationships of taxoids, in *Taxus: The Genus Taxus*, Itokawa, H. and Lee, K.-H., Eds. Taylor & Francis, London, 2003, 298.
74. Kingston, D.G.I., Jagtap, P.G., Yuan, H., and Samala, L., The chemistry of taxol and related taxoids, in *Progress in the Chemistry of Organic Natural Products*, Herz, W., Falk, H., and Kirby, G.W., Eds. Springer-Verlag, Vienna, 2002, 53–225.
75. Kingston, D.G.I., Taxol, a molecule for all seasons, *Chem. Commun.*, 867, 2001.
76. Ojima, I., Kuduk, S.D., Chakravarty, S., Lin, S., Wang, T., Geng, X., Miller, M.L. et al., New generation taxoids and hybrids of microtuble-stabilizing anticancer agents, *ACS Symp. Ser.* 796, 59, 2001.
77. Ojima, I., Geney, R., Ungureanu, I.M., and Li, D., Medicinal chemistry and chemical biology of new generation taxane antitumor agents, *IUBMB Life* 53, 269, 2002.
78. Yue, Q.-X., Liu, X., and Guo, D.-A., Microtubule-binding natural products for cancer therapy, *Planta Med.* 76, 1037, 2010.
79. Marder, R., Bricard, L., Dubois, J., Guenard, D., and Guèritte-Voegelein, F., Taxoids: 11,12-dihydro-4-deacetyldocetaxel, *Tetrahedron Lett.* 37, 1777, 1996.
80. Harriman, G.C.B., Jalluri, R.K., Grunewald, G.L., Vander Velde, D.G., and Georg, G.I., The chemistry of the taxane diterpene: Stereoselective synthesis of 10-deacetoxy-11,12-epoxypaclitaxel, *Tetrahedron Lett.* 36, 8909, 1995.
81. Chen, S.-H., Fairchild, C., Mamber, S.W., and Farina, V., Taxol structure–activity relationships: Synthesis and biological evaluation of 10-deoxytaxol, *J. Org. Chem.* 58, 2927, 1993.
82. Kelly, R.C., Wicnienski, N.A., Gebhard, I., Qualls, S.J., Han, F., Dobrowolski, P.J., Nidy, E.G., and Johnson, R.A., 12,13-isobaccatin III. Taxane enol esters (12,13-isotaxanes), *J. Am. Chem. Soc.* 118, 919, 1996.
83. Uoto, K., Mitsui, I., Terasawa, H., and Soga, T., First synthesis and cytotoxic activity of novel docetaxel analogs modified at the C-18-position, *Bioorg. Med. Chem. Lett.* 7, 2991, 1997.
84. Samaranayake, G., Magri, N.F., Jitrangsri, C., and Kingston, D.G.I., Modified taxols. 5. Reaction of taxol with electrophilic reagents, and preparation of a rearranged taxol derivative with tubulin assembly activity, *J. Org. Chem.* 56, 5114, 1991.
85. Appendino, G., Gariboldi, P., Gabetti, B., Pace, P., Bombardelli, E., and Viterbo, D., 14β-hydroxy-10-deacetylbaccatin III, a new taxane from Himalayan yew (*Taxus wallichiana* Zucc.), *J. Chem. Soc., Perkin Trans. 1* 21, 2925, 1992.
86. Ojima, I., Park, Y.H., Sun, C.M., Feneglio, I., Appendino, G., Pera, P., and Bernacki, R.J., Structure–activity relationships of new taxoids derived from 14β-hydroxy-10-deacetylbaccatin III, *J. Med. Chem.* 37, 1408, 1994.
87. Geney, R., Chen, J., and Ojima, I., Recent advances in the new generation taxane anticancer agents, *Med. Chem.* 1, 125, 2005.
88. Beer, M., Lenaz, L., and Amadori, D., Phase II study of ortataxel in taxane-resistant breast cancer, *J. Clin. Oncol.* 26, S1066, 2008.

89. Ojima, I., Lin, S., Chakravarty, S., Fenoglio, I., Park, Y.H., Sun, C.-M., Appendino, G., Pera, P., Veith, J.M., and Bernacki, R.J., Syntheses and structure–activity relationships of novel nor-seco taxoids, *J. Org. Chem.* 63, 1637, 1998.
90. Kingston, D.G.I., Chordia, M.D., Jagtap, P.G., Liang, J., Shen, Y.-C., Long, B.H., Fairchild, C.R., and Johnston, K.A., Synthesis and biological evaluation of 1-deoxypaclitaxel analogues, *J. Org. Chem.* 64, 1814, 1999.
91. Yuan, T.-H., Jiang, Y., Wang, X.-H., Wang, D.-L., Bannerjee, A., Bane, S., Snyder, J.P., and Lin, H.-X., Synthesis, biological activity and tubulin binding poses of 1-deoxy-9-(*R*)-dihydrotaxane analogs, *Bioorg Med. Chem. Lett.* 19, 1148, 2009.
92. Johnson, R.A., Nidy, E.G., Dobrowolski, P.J., Gebhard, I., Qualls, S.J., Wicnienski, N.A., and Kelly, R.C., Taxol chemistry. 7-O-triflates as precursors to olefins and cyclopropanes, *Tetrahedron Lett.* 35, 7893, 1994.
93. Zheng, Q.Y., Darbie, L.G., Cheng, X., and Murray, C.K., Deacetylation of paclitaxel and other taxanes, *Tetrahedron Lett.* 36, 2001, 1995.
94. Chaudhary, A.G. and Kingston, D.G.I., Synthesis of 10-deacetoxytaxol and 10-deoxytaxotere, *Tetrahedron Lett.*, 34, 4921, 1993.
95. Holton, R.A., Somoza, C., and Chai, K.-B., A simple synthesis of 10-deacetoxytaxol derivatives, *Tetrahedron Lett.*, 35, 1665, 1994.
96. Georg, G.I. and Cheruvallath, Z.S., Samarium diiodide-mediated deoxygenation of taxol: A one-step synthesis of 10-deacetoxytaxol, *J. Org. Chem.*, 59, 4015, 1994.
97. Ge, H., Vasandani, V., Huff, J.K., Audus, K.L., Himes, R.H., Seelig, A., and Georg, G.I., Synthesis and interactions of 7-deoxy-, 10-deacetoxy, and 10-deacetoxy-7-deoxypaclitaxel and NCI/ADR-RES cancer cells and bovine brain microvessel endothelial cells, *Bioorg. Med. Chem. Lett.* 16, 433, 2006.
98. Ojima, I., Slater, J.C., Michaud, E., Kuduk, S.C., Bounaud, P.-Y., Vrignaud, P., Bissery, M.-C., Veith, J.M., Pera, P., and Bernacki, R.J., Syntheses and structure–activity relationships of the second-generation anti-tumor taxoids: Exceptional activity against drug-resistant cancer cells, *J. Med. Chem.* 39, 3889, 1996.
99. Attard, G., Greystoke, A., Kaye, S., and De Bono, J., Update on tubulin-binding agents, *Pathol. Biol. (Paris)* 54, 72, 2006.
100. Sartor, A.O., Oudard, S., Ozguroglu, M., Hansen, S., Machiels, J.H., Shen, L., Gupta, S., and De Bono, J.S., Cabazitaxel or mitoxantrone with prednisone in patients with metastatic castration-resistant prostate cancer (mCRPC) previously treated with docetaxel: Final results of a multinational phase III trial (TROPIC) in *ASCO Genitourinary Cancers Symposium*, San Francisco, CA, 2010, Abstract 9.
101. Galsky, M.D., Dritselis, A., Kirkpatrick, P., and Oh, W.K., Cabazitaxel, *Nat. Rev. Drug Discov.* 9, 677, 2010.
102. Pivot, X., Koralewski, P., Hidalgo, J.L., Chan, A., Goncalves, A., Schwartsmann, G., Assadourian, S., and Lotz, J.P., A multicenter phase II study of XRP6258 administered as a 1-h i.v. infusion every 3 weeks in taxane-resistant metastatic breast cancer patients, *Ann. Oncol.* 19, 1547, 2008.
103. Battaglia, A., Guerrini, A., Baldelli, E., Fontana, G., Varchi, G., Samori, C., and Bombardelli, E., Synthesis of 7- and 10-spermine conjugates of paclitaxel and 10-deacetyl-paclitaxel as potential prodrugs, *Tetrahedron Lett.* 47, 2667, 2006.
104. Ballatore, C., Hyde, E., Deiches, R.F., Lee, V.M.-Y., Trojanowski, J.Q., Huryn, D., and Smith III, A.B., Paclitaxel C-10 carbamates: Potential candidates for the treatment of neurodegenerative tauopathies, *Bioorg. Med. Chem. Lett.* 17, 3642, 2007.
105. Danieli, B., Giardini, A., Lesma, G., Passarella, D., Silvani, A., Appendino, G., Noncovich, A., Fontana, G., Bombardelli, E., and Sterner, O., Synthesis and biological evaluation of paclitaxel–thiocolchicine hybrids, *Chem. Biodivers.* 1, 327, 2004.
106. Liu, Y., Ali, S.M., Boge, T.C., Georg, G.I., Victory, S., Zygmunt, J., Marquez, R.T., and Himes, R.H., A systematic SAR study of C10 modified paclitaxel analogues using a combinatorial approach, *Comb. Chem. High Throughput Screen.* 5, 39, 2002.
107. Jagtap, P.G., Baloglu, E., Barron, D.M., Bane, S., and Kingston, D.G.I., Design and synthesis of a combinatorial chemistry library of 10-acyl and 7,10-diacyl analogues of paclitaxel (Taxol™) using solid phase synthesis, *J. Nat. Prod.* 65, 1136, 2002.
108. Baloglu, E., Hoch, J.M., Barron, D.M., Bane, S., and Kingston, D.G.I., Synthesis and biological evaluation of C-3′NH/C-10 and C-2/C-10 modified paclitaxel analogs, *Bioorg. Med. Chem.* 11, 1557, 2003.
109. Spletstoser, J.T., Turunen, B.J., Desino, K., Rice, A., Datta, A., Dutta, D., Huff, J.K. et al., Single-site chemical modification of C10 of the baccatin III core of paclitaxel and taxol C reduces P-glycoprotein interactions in bovine brain microvessel endothelial cells, *Bioorg. Med. Chem. Lett.* 16, 495, 2006.

110. Walker, M.A., Johnson, T.D., Huang, S., Vyas, D.M., and Kadow, J.F., Synthesis of a novel C-10 spiro-epoxide of paclitaxel, *Bioorg. Med. Chem. Lett.* 11, 1683, 2001.
111. Klein, L.L., Synthesis of 9-dihydrotaxol: A novel bioactive taxane, *Tetrahedron Lett.*, 34, 2047, 1993.
112. Li, L., Thomas, S.A., Klein, L.L., Yeung, C.M., Maring, C.J., Grampovnik, D.J., Lartey, P.A., and Plattner, J.J., Synthesis and biological evaluation of C-3′-modified analogs of 9(*R*)-dihydrotaxol, *J. Med. Chem.* 37, 2655, 1994.
113. Klein, L.L., Li, L., Maring, C.J., Yeung, C.M., Thomas, S.A., Grampovnik, D.J., and Plattner, J.J., Antitumor activity of 9(*R*)-dihydrotaxane analogs, *J. Med. Chem.* 38, 1482, 1995.
114. Klein, L.L., Yeung, C.M., Li, L., and Plattner, J.J., Synthesis of 9-deoxotaxane analogs, *Tetrahedron Lett.* 35, 4707, 1994.
115. Roche, M., Kyriakou, H., and Seiden, M., Drug evaluation: Tesetaxel – an oral semisynthetic taxane derivative, *Curr. Opin. Investig. Drugs* 7, 1092, 2006.
116. Novick, S.C., Wu, J., and Ilson, D., Integrated safety findings with tesetaxel, an orally administered taxane, in patients (pts) with gastric, colon, breast, and nonsmall cell lung cancer: Phase II results, *J. Clin. Oncol.* 27S, e13516, 2009.
117. Margraff, R., Bezard, D., Bourzat, J.D., and Commercon, A., Synthesis of 19-hydroxydocetaxel from a novel baccatin, *Bioorg. Med. Chem. Lett.* 4, 233, 1994.
118. Chen, S.-H., Wei, J.-M., and Farina, V., Taxol structure–activity relationships: Synthesis and biological evaluation of 2-deoxytaxol, *Tetrahedron Lett.*, 34, 3205, 1993.
119. Chaudhary, A.G., Chordia, M.D., and Kingston, D.G.I., A novel benzoyl group migration: Synthesis and biological evaluation of 1-benzoyl-2-des(benzoyloxy)paclitaxel, *J. Org. Chem.*, 60, 3260, 1995.
120. Chordia, M.D. and Kingston, D.G.I., Synthesis and biological evaluation of 2-*epi*-paclitaxel, *J. Org. Chem.*, 61, 799, 1996.
121. Fang, W.-S., Fang, Q.-C., and Liang, X.-T., Synthesis of the 2α-benzoylamido analogue of docetaxel, *Tetrahedron Lett.*, 42, 1331, 2001.
122. Chaudhary, A.G., Gharpure, M.M., Rimoldi, J.M., Chordia, M.D., Gunatilaka, A.A.L., Kingston, D.G.I., Grover, S., Lin, C.M., and Hamel, E., Unexpectedly facile hydrolysis of the 2-benzoate group of taxol and synthesis of analogs with increased activities, *J. Am. Chem. Soc.* 116, 4097, 1994.
123. Kingston, D.G.I., Chaudhary, A.G., Chordia, M.D., Gharpure, M., Gunatilaka, A.A.L., Higgs, P.I., Rimoldi, J.M. et al., Synthesis and biological evaluation of 2-acyl analogues of paclitaxel (Taxol), *J. Med. Chem.* 41, 3715, 1998.
124. Nicolaou, K.C., Renaud, J., Nantermet, P.G., Couladouros, E.A., Guy, R.K., and Wrasidlo, W., Chemical synthesis and biological evaluation of C-2 taxoids, *J. Am. Chem. Soc.* 117, 2409, 1995.
125. Georg, G.I., Harriman, G.C.B., Ali, S.M., Datta, A., Hepperle, M., and Himes, R.H., Synthesis of 2-*O*-heteroaroyl taxanes: Evaluation of microtubule assembly promotion and cytotoxicity, *Bioorg. Med. Chem. Lett.* 5, 115, 1995.
126. Ojima, I., Kuduk, S.D., Pera, P., Veith, J.M., and Bernacki, R.J., Syntheses and structure–activity relationships of nonaromatic taxoids: Effects of alkyl and alkenyl ester groups on cytotoxicity, *J. Med. Chem.* 40, 279, 1997.
127. Yang, C.-G., Barasoain, I., Li, X., Matesanz, R., Liu, R., Sharom, F.J., Yin, D.-L., Diaz, J.F., and Fang, W.-S., Overcoming tumor drug resistance with high-affinity taxanes: A SAR study of C2-modified 7-acyl-10-deacetyl cephalomannines, *Chem. Med. Chem.* 2, 691, 2007.
128. Fang, W.-S., Fang, Q.-C., and Liang, X.-T., Reinvestigation to the C-7 epimerization of paclitaxel and related taxoids under basic conditions, *Synth. Commun.* 27, 2305, 1997.
129. Doggrell, S.A., Clinical trials in restenosis with 7-hexanoyltaxol and paclitaxel-eluting stents, *Expert Rev. Cardiovasc. Ther.* 2, 745, 2004.
130. Forrest, M.L., Yanez, J.A., Remsberg, C.M., Ohgami, Y., Kwon, G.S., and Davies, N.M., Paclitaxel prodrugs with sustained release and high solubility in poly(ethylene glycol)-β-poly(ε-caprolactone) micelle nanocarriers: Pharmacokinetic disposition, tolerability, and cytotoxicity, *Pharm. Res.* 25, 194, 2008.
131. Altstadt, T.J., Fairchild, C.R., Golik, J., Johnston, K.A., Kadow, J.F., Lee, F.Y., Long, B.H. et al., Synthesis and antitumor activity of novel C-7 paclitaxel ethers: Discovery of BMS-184476, *J. Med. Chem.* 44, 4577, 2001.
132. Camps, C., Felip, E., Sanchez, J.M., Massuti, B., Artal, A., Paz-Ares, L., Carrato, A. et al., Phase II trial of the novel taxane BMS-184476 as second-line in non-small-cell lung cancer, *Ann. Oncol.* 16, 597, 2005.
133. Plummer, R., Ghielmini, M., Calvert, P., Voi, M., Renard, J., Gallant, G., Gupta, E., Calvert, H., and Sessa, C., Phase I and pharmacokinetic study of the new taxane analog BMS-184476 given weekly in patients with advanced malignancies, *Clin. Cancer Res.* 8, 2788, 2002.

134. Magri, N.F. and Kingston, D.G.I., Modified taxols. 2. Oxidation products of taxol, *J. Org. Chem.*, 51, 797, 1986.
135. Chaudhary, A.G., Rimoldi, J.M., and Kingston, D.G.I., Modified taxols. 10. Preparation of 7-deoxytaxol, a highly bioactive taxol derivative, and interconversions of taxol and 7-*epi*-taxol, *J. Org. Chem.*, 58, 3798, 1993.
136. Chen, S.-H., Huang, S., Kant, J., Fairchild, C., Wei, J., and Farina, V., Synthesis of 7-deoxy- and 7,10-dideoxytaxol via radical intermediates, *J. Org. Chem.* 58, 5028, 1993.
137. Poujol, H., Mourabit, A.A., Ahond, A., Poupat, C., and Potier, P., Taxoides: 7-deshydroxy-10-acetyldocetaxel et nouveaux analogues prepares a partir des alcaloides de l'if, *Tetrahedron* 53, 12575, 1997.
138. Ge, H., Vasandani, V., Huff, J.K., Audus, K.L., Himes, R.H., Seelig, A., and Georg, G.I., Synthesis and interactions of 7-deoxy-, 10-deacetoxy, and 10-deacetoxy-7-deoxypaclitaxel and NCI/ADR-RES cancer cells and bovine brain microvessel endothelial cells, *Bioorg. Med. Chem. Lett.* 16, 433, 2006.
139. Johnson, R.A., Nidy, E.G., Dobrowolski, P.J., Gebhard, I., Qualls, S.J., Wicnienski, N.A., and Kelly, R.C., Taxol chemistry. 7-o-triflates as precursors to olefins and cyclopropanes, *Tetrahedron Lett.* 35, 7893, 1994.
140. Liang, X., Kingston, D.G.I., Lin, C.M., and Hamel, E., Synthesis and biological evaluation of paclitaxel analogs modified in ring C, *Tetrahedron Lett.* 36, 2901, 1995.
141. Yuan, H. and Kingston, D.G.I., Synthesis of 6α-hydroxypaclitaxel, the major human metabolite of paclitaxel, *Tetrahedron Lett.*, 39, 4967, 1998.
142. Wittman, M.D., Kadow, J.F., and Vyas, D.M., Stereospecific synthesis of the major human metabolite of paclitaxel, *Tetrahedron Lett.*, 41, 4729, 2000.
143. Liang, X., Kingston, D.G.I., Long, B.H., Fairchild, C.A., and Johnston, K.A., Paclitaxel analogs modified in ring C: Synthesis and biological evaluation, *Tetrahedron* 53, 3441, 1997.
144. Chen, S.H., Huang, S., Wei, J., and Farina, V., Serendipitous synthesis of a cyclopropane-containing taxol analog via anchimeric participation of an unactivated angular methyl group, *J. Org. Chem.* 58, 4520, 1993.
145. Bouchard, H., Pulicani, J.-P., Vuilhorgne, M., Bourzat, J.-D., and Commerçon, A., Improved access to 19-nor-7β, 8β-methylene-taxoids and formation of a 7-membered C-ring analog of docetaxel by electrochemistry, *Tetrahedron Lett.* 35, 9713, 1994.
146. Ferjancic, Z., Matovic, R., Cekovic, Z., Jiang, Y., Snyder, J.P., Trajkovic, V., and Saicic, R.N., Synthesis, biology, and modeling of a C-4 carbonyl C,D-*seco*-taxoid, *Tetrahedron* 62, 8503, 2006.
147. Appendino, G., Danieli, B., Jakupovic, J., Belloro, E., Scambia, G., and Bombardelli, E., Synthesis and evaluation of C-*seco* paclitaxel analogues, *Tetrahedron Lett.* 38, 4273, 1997.
148. Pratesi, G., Laccabue, D., Lanzi, C., Cassinelli, G., Supino, R., Zucchetti, M., Frapolli, R. et al., IDN 5390: An oral taxane candidate for protracted treatment schedules, *Br. J. Cancer* 88, 965, 2003.
149. Appendino, G., Bettoni, P., Noncovich, A., Sterner, O., Fontana, G., Bombardelli, E., Pera, P., and Bernacki, R.J., Structure–activity relationships of ring C-secotaxoids. 1. Acylative modifications, *J. Nat. Prod.* 67, 184, 2004.
150. Barboni, L., Ballini, R., Giarlo, G., Appendino, G., Fontana, G., and Bombardelli, E., Synthesis and biological evaluation of methoxylated analogs of the newer generation taxoids IDN5109 and IDN5390, *Bioorg. Med. Chem. Lett.* 15, 5182, 2005.
151. Neidigh, K.A., Gharpure, M.M., Rimoldi, J.M., Kingston, D.G.I., Jiang, Y.Q., and Hamel, E., Synthesis and biological evaluation of 4-deacetylpaclitaxel, *Tetrahedron Lett.* 35, 6839, 1994.
152. Mastalerz, H., Cook, D., Fairchild, C.R., Hansel, S., Johnson, W., Kadow, J.F., Long, B.H. et al., The discovery of BMS-275183: An orally efficacious novel taxane, *Bioorg. Med. Chem.* 11, 4315, 2003.
153. Chen, S.-H., Discovery of a novel C-4 modified 2nd generation paclitaxel analog BMS-188797, *Frontiers Biotechnol. Pharmaceut*, 3, 157, 2002.
154. du Bois, A., Jung, B., Loehr, A., Schaller-Kranz, T., Cohen, M., and Frickhofen, N., A phase I and pharmacokinetic study of novel taxane BMS-188797 and cisplatin in patients with advanced solid tumours, *Br. J. Cancer* 94, 79, 2006.
155. Broeker, L.E., de Vos, F.Y.F.L., van Groeningen, C.J., Kuenen, B.C., Gall, H.E., Woo, M.H., Voi, M., Gietema, J.A., de Vries, E.G.E., and Giaccone, G., Phase I trial with BMS-275183, a novel oral taxane with promising antitumor activity, *Clin. Cancer Res.* 12, 1760, 2006.
156. Chordia, M.D., Yuan, H., Jagtap, P.G., Kadow, J.F., Long, B.H., Fairchild, C.R., Johnston, K.A., and Kingston, D.G.I., Synthesis and bioactivity of 2,4-diacyl analogues of paclitaxel, *Biorg. Med. Chem.* 9, 171, 2001.

157. Marder-Karsenti, R., Dubois, J., Bricard, L., Guenard, D., and Gueritte-Voegelein, F., Synthesis and biological evaluation of D-ring-modified taxanes: 5(20)-azadocetaxel analogs, *J. Org. Chem.* 62, 6631, 1997.
158. Gunatilaka, A.A.L., Ramdayal, F.D., Sarragiotto, M.H., Kingston, D.G.I., Sackett, D.L., and Hamel, E., Synthesis and biological evaluation of novel paclitaxel (taxol) D-ring modified analogues, *J. Org. Chem.* 64, 2694, 1999.
159. Wang, M., Cornett, B., Nettles, J., Liotta, D.C., and Snyder, J.P., The oxetane ring in taxol, *J. Org. Chem.* 65, 1059, 2000.
160. Dubois, J., Thoret, S., Gueritte, F., and Guenard, D., Synthesis of 5(20)deoxydocetaxel, a new active docetaxel analogue, *Tetrahedron Lett.* 41, 3331, 2000.
161. Deka, V., Dubois, J., Thoret, S., Gueritte, F., and Guenard, D., Deletion of the oxetane ring in docetaxel analogues: Synthesis and biological evaluation, *Org. Lett.* 5, 5031, 2003.
162. Barboni, L., Datta, A., Dutta, D., Georg, G.I., Vander Velde, D.G., Himes, R.H., Wang, M., and Snyder, J.P., Novel D-seco paclitaxel analogues: Synthesis, biological evaluation, and model testing, *J. Org. Chem.* 66, 3321, 2001.
163. Cragg, G.M. and Newman, D.J., A tale of two tumor targets: Topoisomerase I and tubulin. The Wall and Wani contribution to cancer chemotherapy, *J. Nat. Prod.*, 67, 232, 2004.
164. Borah, J.C., Boruwa, J., and Barua, N.C., Synthesis of the C-13 side-chain of taxol, *Curr. Org. Synth.* 4, 175, 2007.
165. He, L., Jagtap, P.G., Kingston, D.G.I., Shen, H.-J., Orr, G.A., and Horwitz, S.B., A common pharmacophore for taxol and the epothilones based on the biological activity of a taxane molecule lacking a C-13 side chain, *Biochemistry* 39, 3972, 2000.
166. Swindell, C.S., Krauss, N.E., Horwitz, S.B., and Ringel, I., Biologically active taxol analogues with deleted A-ring side chain substituents and variable C-2′ configurations, *J. Med. Chem.* 34, 1176, 1991.
167. Guéritte-Voegelein, F., Guénard, D., Lavelle, F., Le Goff, M.-T., Mangatal, L., and Potier, P., Relationships between the structure of taxol analogues and their antimitotic activity, *J. Med. Chem.* 34, 992, 1991.
168. Barboni, L., Lambertucci, C., Appendino, G., Vander Velde, D.G., Himes, R.H., Bombardelli, E., Wang, M., and Snyder, J.P., Synthesis and NMR-driven conformational analysis of taxol analogues conformationally constrained on the C13 side chain, *J. Med. Chem.* 44, 1576, 2001.
169. Jayasinghe, L.R., Datta, A., Ali, S.M., Zygmunt, J., Vander Velde, D.G., and Georg, G.I., Structure–activity studies of antitumor taxanes: Synthesis of novel C-13 side chain homologated taxol and taxotere analogs, *J. Med. Chem.* 37, 2981, 1994.
170. Morita, H., Gonda, A., Wei, L., Yamamura, Y., Wakabayashi, H., Takeya, K., and Itokawa, H., Taxoids from *Taxus cuspidata* var. *Nana*, *Phytochemistry* 48, 857, 1998.
171. Santhapuram, H.K.R., Datta, A., Hutt, O.E., and Georg, G.I., *N*-methylation of the C-3′ amide of taxanes: Synthesis of *N*-methyltaxol C and *N*-methylpaclitaxel, *J. Org. Chem.* 73, 4705, 2008.
172. Ojima, I., Slater, J.C., Michaud, E., Kuduk, S.C., Bounaud, P.-Y., Vrignaud, P., Bissery, M.-C., Veith, J.M., Pera, P., and Bernacki, R.J., Syntheses and structure–activity relationships of the second-generation antitumor taxoids: Exceptional activity against drug-resistant cancer cells, *J. Med. Chem.* 39, 3889, 1996.
173. Georg, G.I., Harriman, G.C.B., Hepperle, M., Clowers, J.S., Vander Velde, D.G., and Himes, R.H., Synthesis, conformational analysis, and biological evaluation of heteroaromatic taxanes, *J. Org. Chem.* 61, 2664, 1996.
174. Baas, P., Szczesna, A., Albert, I., Milanowski, J., Juhász, E., Sztancsik, Z., von Pawel, J., Oyama, R., and Burgers, S., Phase I/II study of a 3 weekly oral taxane (DJ-927) in patients with recurrent, advanced non-small cell lung cancer, *J. Thorac. Oncol.* 3, 745, 2008.
175. Bröker, L.E., de Vos, F.Y.F.L., van Groeningen, C.J., Kuenen, B.C., Gall, H.E., Woo, M.H., Voi, M., Gietema, J.A., de Vries, E.G.E., and Giaccone, G., Phase I trial with BMS-275183, a novel oral taxane with promising antitumor activity, *Clin. Cancer Res.* 12, 1760, 2006.
176. Magri, N.F. and Kingston, D.G.I., Modified taxols. 4. Synthesis and biological activity of taxols modified in the side chain, *J. Nat. Prod.*, 51, 298, 1988.
177. Denis, J.-N., Fkyerat, A., Gimbert, Y., Coutterez, C., Mantellier, P., Jost, S., and Greene, A.E., Docetaxel (Taxotere) derivatives: Novel $NbCl_3$-based stereoselective approach to 2′-methyldocetaxel, *J. Chem. Soc. Perkin Trans. 1*, 1811, 1995.
178. Kant, J., Schwartz, W.S., Fairchild, C., Gao, Q., Huang, S., Long, B.H., Kadow, J.F., Langley, D.R., Farina, V., and Vyas, D., Diastereoselective addition of grignard reagents to azetidine-2,3-dione: Synthesis of novel taxol analogues, *Tetrahedron Lett.* 37, 6495, 1996.
179. Ojima, I., Wang, T., and Delaloge, F., Extremely stereoselective alkylation of 3-siloxy-β-lactams and its applications to the asymmetric syntheses of novel 2-alkylisoserines, their dipeptides, and taxoids, *Tetrhedron Lett.*, 39, 3663, 1998.

180. Battaglia, A., Bernacki, R.J., Bertucci, C., Bombardelli, E., Cimitan, S., Ferlini, C., Fontana, G., Guerrini, A., and Riva, A., Synthesis and biological evaluation of 2′-methyl taxoids derived from baccatin III and 14β-OH-baccatin III 1,14-carbonate, *J. Med. Chem.* 46, 4822-4825, 2003.
181. Qi, X., Lee, S.-H., Yoon, J., and Lee, Y.-S., Synthesis of novel thiol surrogate of Taxol: 2′-deoxy-2′-mercaptopaclitaxel, *Tetrahedron* 60, 3599, 2004.
182. Uoto, K., Ohsuki, S., Takenoshita, H., Ishiyama, T., Iimura, S., Hirota, Y., Mitsui, I., Terasawa, H., and Soga, T., Synthesis and structure–activity relationships of novel 2′,2′-difluoro analogues of docetaxel, *Chem. Pharm. Bull.* 45, 1793, 1997.
183. Ojima, I., Chen, J., Sun, L., Borella, C.P., Wang, T., Miller, M.L., Lin, S. et al., Design, synthesis, and biological evaluation of new-generation taxoids, *J. Med. Chem.* 51, 3203, 2008.
184. Ojima, I., Lin, S., Slater, J.C., Wang, T., Pera, P., Bernacki, R.J., Ferlini, C., and Scambia, G. Syntheses and biological activity of C-3′-difluoromethyl-taxoids, *Bioorg. Med. Chem.* 8, 1619, 2000.
185. Ojima, I. and Lin, S., Efficient asymmetric syntheses of β-lactams bearing a cyclopropane or an epoxide moiety and their application to the syntheses of novel isoserines and taxoids, *J. Org. Chem.* 63, 224, 1998.
186. Skwarczynski, M., Hayashi, Y., and Kiso, Y., Paclitaxel prodrugs: Toward smarter delivery of anticancer agents, *J. Med. Chem.* 49, 7253, 2006.
187. Safavy, A., Recent developments in taxane drug delivery, *Curr. Drug Deliv.* 5, 42, 2008.
188. Ganesh, T., Improved biochemical strategies for targeted delivery of taxoids, *Bioorg. Med. Chem.* 15, 3597, 2007.
189. Du, W., Hong, L., Yao, T., Yang, X., He, Q., Yang, B., and Hu, Y., Synthesis and evaluation of water-soluble docetaxel prodrugs-docetaxel esters of malic acid, *Bioorg. Med. Chem.* 15, 6323, 2007.
190. Papas, S., Akoumianaki, T., Kalogiros, C., Hadjiarapoglou, L., Theodoropoulos, P.A., and Tsikaris, V., Synthesis and antitumor activity of peptide–paclitaxel conjugates, *J. Peptide Sci.* 13, 662, 2007.
191. Ali, S., Ahmad, I., Peters, A., Masters, G., Minchey, S., Janoff, A., and Mayhew, E., Hydrolyzable hydrophobic taxanes: Synthesis and anti-cancer activities, *Anticancer Drugs* 12, 117, 2001.
192. Huynh, L., Leroux, J.-C., and Allen, C., Enhancement of docetaxel solubility via conjugation of formulation-compatible moieties, *Org. Biomol. Chem.* 7, 3437, 2009.
193. Hayashi, Y., Skwarczynski, M., Hamada, Y., Sohma, Y., Kimura, T., and Kiso, Y., A novel approach of water-soluble paclitaxel prodrug with no auxiliary and no byproduct: Design and synthesis of isotaxel, *J. Med. Chem.* 46, 3782, 2003.
194. Skwarczynski, M., Sohma, Y., Kimura, M., Hayashi, Y., Kimura, T., and Kiso, Y., O–N intramolecular acyl migration strategy in water-soluble prodrugs of taxoids, *Bioorg. Med. Chem.* 13, 4441, 2003.
195. Noguchi, M., Skwarczynski, M., Prakash, H., Hirota, S., Kimura, T., Hayashi, Y., and Kiso, Y., Development of novel water-soluble photocleavable protective group and its application for design of photoresponsive paclitaxel prodrugs, *Bioorg. Med. Chem.* 16, 5389, 2008.
196. Ueda, Y., Mikkilineni, A.B., Knipe, J.O., Rose, W.C., Casazza, A.M., and Vyas, D.M., Novel water soluble phosphate prodrugs of taxol possessing in vivo antitumor activity, *Bioorg. Med. Chem. Lett.* 3, 1761, 1993.
197. Niethammer, A., Gaedicke, G., Lode, H.N., and Wrasidlo, W., Synthesis and preclinical characterization of a paclitaxel prodrug with improved antitumor activity and water solubility, *Bioconjug. Chem.* 12, 414, 2001.
198. Wrasidlo, W., Niethammer, A., Deger, S., Sehouli, J., Kulozik, A., Geilen, W., Henze, G., Gaedicke, G., and Lode, H.N., Pilot study of hydrolytically activated paclitaxel prodrug therapy in patients with progressive malignancies, *Curr. Ther. Res.* 63, 247, 2002.
199. Greenwald, R.B., Pendri, A., Bolikal, D., and Gilbert, C.W., Highly water soluble taxol derivatives: 2′-polyethyleneglycol esters as potential prodrugs, *Biorg. Med. Chem. Lett.* 4, 2465, 1994.
200. Ryu, B.-Y., Sohn, J.-S., Hess, M., Choi, S.-K., Choi, J.-K., and Jo, B.-W., Synthesis and anti-cancer efficacy of rapid hydrolyzed water-soluble paclitaxel pro-drugs, *J. Biomater. Sci. Polym. Ed.* 19, 311, 2008.
201. Sohn, J.-S., Choi, E.-S., Jo, B.-W., Hess, M., and Han, S.-H., Synthesis and characterization of a fluorescent water-soluble paclitaxel prodrug, *J. Nanosci. Nanotech.* 10, 3478, 2010.
202. Singer, J.W., Shaffer, S., Baker, B., Bernareggi, A., Stromatt, S., Nienstedt, D., and Besman, M., Paclitaxel poliglumex (Xyotax; CT-2103): An intracellularly targeted taxane, *Anticancer Drugs* 16, 243, 2005.
203. Kakinoki, A., Kaneo, Y., Tanaka, T., and Hosokawa, Y., Synthesis and evaluation of water-soluble poly(vinyl alcohol)-paclitaxel conjugate as a macromolecular prodrug, *Biol. Pharm. Bull.* 31, 963, 2008.
204. Jun, Y.J., Min, J.H., Ji, D.E., Yoo, J.H., Kim, J.H., Lee, H.J., Jeong, B., and Sohn, Y.S., A micellar prodrug of paclitaxel conjugated to cyclotriphosphazene, *Bioorg. Med. Chem. Lett.* 18, 6410, 2008.

205. Khandare, J., Jayant, S., Singh, A., Chandna, P., Wang, Y., Vorsa, N., and Minko, T., Dendrimer versus linear conjugate: Influence of polymeric architecture on the delivery and anticancer effect of paclitaxel, *Bioconjug. Chem.* 17, 1464, 2006.
206. de Groot, F.M.H., Albrecht, C., Koekkoek, R., Beusker, P.H., and Scheeren, H.W., "Cascade-release dendrimers" liberate all end groups upon a single triggering event in the dendritic core, *Angew Chem. Int. Ed.* 42, 4490, 2003.
207. Ooya, T., Lee, J., and Park, K., Hydrotropic dendrimers of generations 4 and 5: Synthesis, characterization, and hydrotropic solubilization of paclitaxel, *Bioconjug. Chem.* 15, 1221, 2004.
208. Lim, J. and Simanek, E.E., Synthesis of water-soluble dendrimers based on melamine bearing 16 paclitaxel groups, *Org. Lett.* 10, 201, 2008.
209. Lim, J., Chouai, A., Lo, S.-T., Liu, W., Sun, X., and Simanek, E.E., Design, synthesis, characterization, and biological evaluation of triazine dendrimers bearing paclitaxel using ester and ester/disulfide linkages, *Bioconjug. Chem.* 20, 2154, 2009.
210. Zakharian, T.Y., Seryshev, A., Sitharaman, B., Gilbert, B.E., Knight, V., and Wilson, L.J., A fullerene-paclitaxel chemotherapeutic: Synthesis, characterization, and study of biological activity in tissue culture, *J. Am. Chem. Soc.* 127, 12508, 2005.
211. de Groot, F.M.H., van Berkom, L.W.A., and Scheeren, H.W., Synthesis and biological evaluation of 2′-carbamate-linked and 2′-carbonate-linked prodrugs of paclitaxel: Selective activation by the tumor-associated protease plasmin, *J. Med. Chem.* 43, 3093, 2000.
212. Takahashi, T., Tsukamoto, H., and Yamada, H., Design and synthesis of a water-soluble taxol analog: Taxol-sialyl conjugate, *Bioorg. Med. Chem. Lett.*, 8, 113, 1998.
213. Damen, E.W.P., Nevalainen, T.J., van den Bergh, T.J.M., de Groot, F.M.H., and Scheeren, H.W., Synthesis of novel paclitaxel prodrugs designed for bioreductive activation in hypoxic tumour tissue, *Bioorg. Med. Chem.* 10, 71, 2002.
214. Vrudhula, V.M., MacMaster, J.F., Li, Z., Kerr, D.E., and Senter, P.D., Reductively activated disulfide prodrugs of paclitaxel, *Bioorg. Med. Chem. Lett.* 12, 3591, 2002.
215. Leenders, R.G.G., Gerrits, K.A.A., Ruijtenbeek, R., and Scheeren, H.W., β-glucuronyl carbamate based pro-moieties designed for prodrugs in ADEPT, *Tetrahdron Lett.* 36, 1701, 1995.
216. deBont, D.B.A., Leenders, R.G.G., Haisma, H.J., van der Meulen-Muileman, I., and Scheeren, H.W., Synthesis and biological activity of β-glucuronyl carbamate-based prodrugs of paclitaxel as potential candidates for ADEPT, *Bioorg. Med. Chem.* 5, 405, 1997.
217. Schmidt, F., Ungureanu, I., Duval, R., Pompon, A., and Monneret, C., Cancer chemotherapy: A paclitaxel prodrug for ADEPT (Antibody-Directed Enzyme Prodrug Therapy), *Eur. J. Org. Chem.*, 2129, 2001.
218. Bouvier, E., Thirot, S., Schmidt, F., and Monneret, C., First enzymatically activated Taxotere prodrugs designed for ADEPT and PMT, *Bioorg. Med. Chem.* 12, 969, 2004.
219. Vrudhula, V.M., Kerr, D., Siemers, O., Dubowchik, G.M., and Senter, P.D., Cephalosporin prodrugs of paclitaxel for immunologically specific activation by l-49-sfv-β-lactamase fusion protein, *Bioorg. Med. Chem. Lett.* 13, 539, 2003.
220. Luo, Y. and Prestwich, G.D., Synthesis and selective cytotoxicity of a hyaluronic acid-antitumor bioconjugate, *Bioconjug. Chem.*, 10, 755, 1999.
221. Lee, H., Lee, K., and Park, T.G., Hyaluronic acid – paclitaxel conjugate micelles: Synthesis, characterization, and antitumor activity, *Bioconjug. Chem.* 19, 1319, 2008.
222. Lin, Y.-S., Tungpradit, R., Sinchaikul, S., An, F.-M., Liu, D.-Z., Phutrakul, S., and Chen, S.-T., Targeting the delivery of glycan-based paclitaxel prodrugs to cancer cells via glucose transporters, *J. Med. Chem.* 51, 7428, 2008.
223. Safavy, A., Raisch, K.P., Khazaeli, M.B., Buchsbaum, D.J., and Bonner, J.A., Paclitaxel derivatives for targeted therapy of cancer: Toward the development of smart taxanes, *J. Med. Chem.* 42, 4919, 1999.
224. Safavy, A., Raisch, K.P., Matusiak, D., Bhatnagar, S., and Helson, L., Single-drug multiligand conjugates: Synthesis and preliminary cytotoxicity evaluation of a paclitaxel-dipeptide "scorpion" molecule, *Bioconjug. Chem.* 17, 565, 2006.
225. Chen, X., Plasencia, C., Hou, Y., and Neamati, N., Synthesis and biological evaluation of dimeric RDG peptide–paclitaxel conjugate as a model for integrin-targeted drug delivery, *J. Med. Chem.* 48, 1098, 2005.
226. Li, P., Jiang, S., Pero, S.C., Oligino, L., Krag, D.N., Michejda, C.J., and Roller, P.P., Design and synthesis of paclitaxel conjugated with an ErbB2-recognizing peptide, EC-1, *Biopolymers* 87, 225, 2007.
227. Ndungu, J.M., Lu, Y.J., Zhu, S., Yang, C., Wang, X., Chen, G., Shin, D.M., Snyder, J.P., Shoji, M., and Sun, A., Targeted delivery of paclitaxel to tumor cells: Synthesis and in vitro evaluation, *J. Med. Chem.* 53, 3127, 2010.

228. Kirschberg, T.A., VanDeusen, C.L., Rothbard, J.B., Yang, M., and Wender, P.A., Arginine-based molecular transporters: The synthesis and chemical evaluation of releasable taxol-transporter conjugates, *Org. Lett.* 5, 3459, 2003.
229. Gruner, B.A. and Weitman, S.D., The folate receptor as a potential therapeutic anticancer target, *Invest. New Drugs* 16, 205, 1999.
230. Lee, J.W., Lu, J.Y., Low, P.S., and Fuchs, P.L., Synthesis and evaluation of taxol–folic acid conjugates as targeted antineoplastics, *Bioorg. Med. Chem.* 10, 2397, 2002.
231. Majoros, I.J., Myc, A., Thomas, T., Mehta, C.B., and Becker, J.R., Jr., PAMAM dendrimer-based multifunctional conjugate for cancer therapy: Synthesis, characterization, and functionality, *Biomacromolecules* 7, 572, 2006.
232. Ojima, I., Guided molecular missiles for tumor-targeting chemotherapy – case studies using the second-generation taxoids as warheads, *Acc. Chem. Res.* 41, 108, 2007.
233. Bradley, M.O., Swindell, C.S., Anthony, F.H., Witman, P.A., Devanesan, P., Webb, N.L., Baker, S.D., Wolff, A.C., and Donehower, R.C., Tumor targeting by conjugation of DHA to paclitaxel, *J. Control. Release* 74, 233, 2001.
234. Bradley, M.O., Webb, N.L., Anthony, F.H., Devanesan, P., Witman, P.A., Hemamalini, S., Chander, M.C., Baker, S.D., He, L., Horwitz, S.B., and Swindell, C.S., Tumor targeting by covalent conjugation of a natural fatty acid to paclitaxel, *Clin. Cancer Res.* 7, 3229, 2001.
235. Wolff, A.C., Donehower, R.C., Carducci, M.K., Carducci, M.A., Brahmer, J.R., Zabelina, Y., Bradley, M.O. et al., Phase I study of docosahexaenoic acid-paclitaxel: A taxane–fatty acid conjugate with a unique pharmacology and toxicity profile, *Clin. Cancer Res.* 9, 3589, 2003.
236. Green, M.R., Manikhas, G.M., Orlov, S., Afanasyev, B., Makhson, A.M., Bhar, P., and Hawkins, M.J., Abraxane, a novel Cremophor-free, albumin-bound particle form of paclitaxel for the treatment of advanced non-small-cell lung cancer, *Ann. Oncol.* 17, 1263, 2006.
237. Hawkins, M.J., Soon-Shiong, P., and Desai, N., Protein nanoparticles as drug carriers in clinical medicine, *Adv. Drug Deliv. Rev.* 60, 876, 2008.
238. Henderson, I.C. and Bhatia, V., Nab-paclitaxel for breast cancer: A new formulation with an improved safety profile and greater efficacy, *Expert Rev. Anticancer Ther.* 7, 919, 2007.
239. Ron, N., Cordia, J., Yang, A., Ci, S., Nguyen, P., Hughs, M., and Desai, N. Comparison of physicochemical characteristics and stability of three novel formulations of paclitaxel: Abraxane, Nanoxel, and Genexol PM. *Proc. Am. Assoc. Cancer Res. (AACR)* 49, Abstract 5622, 2008.
240. Oerlemans, C., Bult, W., Bos, M, Storm, G., Nijsen, J. F. W., and Hennink, W. E. Polymeric micelles in anticancer therapy: Targeting, imaging and triggered release. *Pharm. Res.*, 27, 2569, 2010.
241. Wang, Y., Xin, D., Liu, K., Zhu, M., and Xiang, J., Heparin-paclitaxel conjugates as drug delivery system: Synthesis, self-assembly property, drug release, and antitumor activity, *Bioconjug. Chem.* 20, 2214, 2009.
242. Liu, J., Zahedi, P., Zeng, F., and Allen, C., Nano-sized assemblies of PEG-docetaxel conjugate as a formulation strategy for docetaxel, *J. Pharm. Sci.* 97, 3274, 2008.
243. Ansell, S.M., Johnstone, S.A., Tardi, P.G., Lo, L., Xie, S., Shu, Y., Harasym, T.O. et al., Modulating the therapeutic activity of nanoparticle delivered paclitaxel by manipulating the hydrophobicity of prodrug conjugates, *J. Med. Chem.* 51, 3288, 2008.
244. Gao, Y., Chen, L., Gu, W., Xi, Y., Lin, L., and Li, Y., Targeted nanoassembly loaded with docetaxel improves intracellular drug delivery and efficacy in murine breast cancer model, *Mol. Pharm.* 5, 1044, 2008.
245. Gibson, J.D., Khanal, B.P., and Zubarev, E.R., Paclitaxel-functionalized gold nanoparticles, *J. Am. Chem. Soc.* 129, 11653, 2007.
246. Hwu, J.R., Lin, Y.S., Josephrajan, T., Hsu, M.-H., Cheng, F.-Y., Yeh, C.-S., Su, W.-C., and Shieh, D.-B., Targeted paclitaxel by conjugation to iron oxide and gold nanoparticles, *J. Am. Chem. Soc.* 131, 66, 2009.
247. Paciotti, G.F., Kingston, D.G.I., and Tamarkin, L., Colloidal gold nanoparticles: A novel nanoparticle platform for developing multifunctional tumor-targeted drug delivery vectors, *Drug Dev. Res.* 67, 47, 2006.
248. Safavy, A., Recent developments in taxane drug delivery, *Curr. Drug Deliv.* 5, 42, 2008.
249. Hamann, P.R., Hinman, L.M., Hollander, I., Beyer, C.F., Lindh, D., Holcomb, R., Hallett, W. et al., Gemtuzumab ozogamicin, a potent and selective anti-CD33 antibody–calicheamicin conjugate for treatment of acute myeloid leukemia, *Bioconjug. Chem.* 13, 47, 2002.
250. Guillemard, V. and Saragovi, H.U., Taxane–antibody conjugates afford potent cytotoxicity, enhanced solubility, and tumor target selectivity, *Cancer Res.*, 61, 694, 2001.

251. Ojima, I., Xudong, G., Xinyuan, W., Chuanxing, Q., Borella, C.P., Hongsheng, X., Willhelm, S.D. et al., Tumor-specific novel taxoid-monoclonal antibody conjugates, *J. Med. Chem.* 45, 5620, 2002.
252. Quiles, S., Raisch, K.P., Sanford, L.L., Bonner, J.A., and Safavy, A., Synthesis and preliminary biological evaluation of high-drug-load paclitaxel–antibody conjugates for tumor-targeted chemotherapy, *J. Med. Chem.* 53, 586, 2010.
253. Baloglu, E., Miller, M.L., Cavanagh, E.E., Marien, T.P., Roller, E.E., and Chari, R.V.J., A facile one-pot synthesis of 7-triethylsilylbaccatin III, *Synlett* 5, 0817, 2005.
254. Wuts, P.G.M., Semisynthesis of taxol, *Curr. Opin. Drug Discov. Dev.* 1, 329, 1998.
255. Borah, J.C., Boruwa, J., and Barua, N.C., Synthesis of the C-13 side-chain of taxol, *Curr. Org. Synth.* 4, 175, 2007.
256. Holton, R.A., Biediger, R.J., and Boatman, P.D., Semisynthesis of taxol and taxotere, in *Taxol: Science and Applications*, Suffness, M., Ed., CRC Press, Inc., Boca Raton, FL, 1995, chap. 5.
257. Ojima, I., Habus, I., Zhao, M., Zucco, M., Park, Y.H., Sun, C.M., and Brigaud, T., New and efficient approaches to the semisynthesis of taxol and its C-13 side chain analogs by means of β-lactam synthon method, *Tetrahedron* 48, 6985–7012, 1992.
258. Ojima, I., Habus, I., Zhao, M., Georg, G.I., and Jayasinghe, L.R., Efficient and practical asymmetric synthesis of the taxol C-13 side chain, *N*-benzoyl-(2*R*,3*S*)-3-phenylisoserine, and its analogues via chiral 3-hydroxy-4-aryl-β-lactams through chiral ester enolate-imine cyclocondensation, *J. Org. Chem.* 56, 1681, 1991.
259. Georg, G.I., Cheruvallath, Z.S., Harriman, G.C.B., Hepperle, M., and Park, H., An efficient semi-synthesis of taxol from (3*R*,4*S*)-*N*-benzoyl-3-[(*t*-butyldimethylsilyl)oxy]-4-phenyl-2-azetidinone and 7-(triethylsilyl)baccatin III, *Bioorg. Med. Chem. Lett.* 3, 2467–2470, 1993.
260. Palomo, C., Aizpurua, J.M., Miranda, J.I., Mielgo, A., and Odriozola, J.M., Asymmetric synthesis of α-keto β-lactams via [2 + 2] cycloaddition reaction – A concise approach to optically active α-hydroxy β-lactams and β-alkyl(aryl)isoserines, *Tetrahedron Lett.* 34, 6325, 1993.
261. Holton, R.A. and Liu, J.H., A novel asymmetric synthesis of cis-3-hydroxy-4-aryl azetidin-2-ones, *Bioorg. Med. Chem. Lett.*, 3, 2475, 1993.
262. Farina, V., Hauck, S.I., and Walker, D.G., A simple chiral synthesis of the taxol side chain, *Synlett*, 1, 761, 1992.
263. Shimizu, M., Ishida, T., and Fujisawa, T., Highly stereocontrolled construction of 3-alkoxyazetidin-2-ones using ester enolate-imine condensation, *Chem. Lett.*, 1403, 1994.
264. Song, C.E., Lee, S.W., Roh, E.J., Lee, S.-G., and Lee, W.-K., A new synthetic route to (3*R*,4*S*)-3-hydroxy-4-phenylazetidin-2-one as a taxol side chain precursor, *Tetrahedron Asymmetry* 9, 983, 1998.
265. Brieva, R., Crich, J.Z., and Sih, C.J., Chemoenzymatic synthesis of the C-13 side chain of taxol: Optically-active 3-hydroxy-4-phenyl β-lactam derivatives, *J. Org. Chem.* 58, 1068, 1993.
266. Lin, S., Geng, X., Qu, C., Tynebor, R., Gallagher, D.J., Pollina, E., Rutter, J., and Ojima, I., Synthesis of highly potent second-generation taxoids through effective kinetic resolution coupling of racemic β-lactams with baccatins, *Chirality* 12, 431, 2000.
267. Commerçon, A., Bezard, D., Bernard, F., and Bourzat, J.D. Improved protection and esterification of a precursor of the taxotere and taxol side chains. *Tetrahedron Lett.* 33, 5185, 1992.
268. Kingston, D.G.I., Chaudhary, A.G., Gunatilaka, A.A.L., and Middleton, M.L., Synthesis of taxol from baccatin III via an oxazoline intermediate, *Tetrahedron Lett.* 35, 4483, 1994.
269. Gennari, C., Carcano, M., Donghi, M., Mongelli, N., Vanotti, E., and Vulpetti, A., Taxol semisynthesis: A highly enantio- and diastereoselective synthesis of the side chain and a new method for ester formation at C-13 using thioesters, *J. Org. Chem.* 62, 4746, 1997.
270. Gennari, C., Vulpetti, A., Donghi, M., Mongelli, N., and Vanotti, E., Semisynthesis of taxol: A highly enantio- and diastereoselective synthesis of the side chain and a new method for ester formation at C13 using thioesters, *Angew. Chem. Int. Ed. Engl.* 35, 1723, 1996.
271. Yamaguchi, T., Harada, N., Ozaki, K., Hayashi, M., Arakawa, H., and Hashiyama, T., Synthesis of taxoids 4. Novel and versatile methods for preparation of new taxoids by employing *cis*- or *trans*-phenyl glycidic acid, *Tetrahedron* 55, 1005, 1999.
272. Mandai, T., Kuroda, A., Okumoto, H., Nakanishi, K., Mikjuni, K., Hara, K.-J., and Hara, K.-Z., A semi-synthesis of paclitaxel via a 10-deacetylbaccatin III derivative bearing a β-keto ester appendage, *Tetrahedron Lett.* 41, 243, 2000.
273. Xiao, Z., Itokawa, H., Lee, and K.-H., Total synthesis of taxoids, in *Taxus: The Genus Taxus*, Itokawa, H. and Lee, K.-H., Eds., Taylor & Francis, London, 2003, chap. 9.
274. Holton, R.A., Somoza, C., Kim, H.-B., Liang, F., Biediger, R.J., Boatman, P.D., Shindo, M. et al., First total synthesis of taxol. 1. Functionalization of the B ring, *J. Am. Chem. Soc.* 116, 1597, 1994.

275. Holton, R.A., Kim, H.-B., Somoza, C., Liang, F., Biediger, R.J., Boatman, P.D., Shindo, M. et al., First total synthesis of taxol. 2. Completion of the C and D rings, *J. Am. Chem. Soc.* 116, 1599, 1994.
276. Nicolaou, K.C., Yang, Z., Liu, J.J., Ueno, H., Nantermet, P.G., Guy, R.K., Claiborne, C.F. et al., Total synthesis of taxol, *Nature* 367, 630, 1994.
277. Danishefsky, S.J., Masters, J.J., Young, W.B., Link, J.T., Snyder, L.B., Magee, T.V., Jung, D.K. et al., Total synthesis of baccatin III and taxol, *J. Am. Chem. Soc.* 118, 2843, 1996.
278. Wender, P.A., Badham, N.F., Conway, S.P., Floreancig, P.E., Glass, T.E., Granicher, C., Houze, J.B. et al., The pinene path to taxanes. 5. Stereocontrolled synthesis of a versatile taxane precursor, *J. Am. Chem. Soc.* 119, 2755, 1997.
279. Wender, P.A., Badham, N.F., Conway, S.P., Floreancig, P.E., Glass, T.E., Houze, J.B., Krauss, N.E. et al., The pinene path to taxanes. 6. A concise stereocontrolled synthesis of taxol, *J. Am. Chem. Soc.* 119, 2757, 1997.
280. Kusama, H., Hara, R., Kawahara, S., Nishimori, T., Kashima, H., Nakamura, N., Morihira, K., and Kuwajima, I., Enantioselective total synthesis of (–)-taxol, *J. Am. Chem. Soc.* 122, 3811–3820, 2000.
281. Mukaiyama, T., Shiina, I., Iwadare, H., Saitoh, M., Nishimura, T., Ohkawa, N., Sakoh, H. et al., Asymmetric total synthesis of taxol, *Chem. Eur. J.* 5, 121, 1999.
282. Goldring, W.P.D., Pattenden, G., and Rimmington, S.L., Synthesis of a tetraoxy-bis-nortaxadiene, en route to taxol, using a cascade radical cyclisation sequence, *Tetrahedron* 65, 6670, 2009.
283. Rao, S., Krauss, N.E., Heerding, J.M., Swindell, C.S., Ringel, I., Orr, G.A., and Horwitz, S.B., 3′-(*p*-azidobenzamido)taxol photolabels the N-terminal 31 amino acids of β-tubulin, *J. Biol. Chem.* 269, 3132, 1994.
284. Rao, S., Orr, G.A., Chaudhary, A.G., Kingston, D.G.I., and Horwitz, S.B., Characterization of the taxol binding site on the microtubule, *J. Biol. Chem.* 270, 20235, 1995.
285. Rao, S., He, L., Chakravarty, S., Ojima, I., Orr, G.A., and Horwitz, S.B., Characterization of the taxol binding site on the microtubule, *J. Biol. Chem.* 274, 37990, 1999.
286. Dasgupta, D., Park, H., Harriman, G.C.B., Georg, G.I., and Himes, R.H., Synthesis of a photoaffinity taxol analogue and its use in labeling tubulin, *J. Med. Chem.* 37, 2976, 1994.
287. Loeb, C., Combeau, C., Ehret-Sabatier, L., Breton-Gilet, A., Faucher, D., Rousseau, B., Commercon, A., and Goeldner, M., [^{3}H](azidophenyl)ureido taxoid photolabels peptide amino acids 281–304 of α-tubulin, *Biochemistry* 36, 3820, 1997.
288. Lowe, J., Li, H., Downing, K.H., and Nogales, E., Refined structure of β-tubulin at 3.5Å resolution, *J. Mol. Biol.* 313, 1045, 2001.
289. Nogales, E., Wolf, S.G., and Downing, K.H., Structure of the αβ-tubulin dimer by electron crystallography, *Nature* 39, 199, 1998.
290. Snyder, J.P., Nettles, J.H., Cornett, B., Downing, K.H., and Nogales, E., The binding conformation of taxol in β-tubulin: A model based on electron crystallographic density, *Proc. Natl. Acad. Sci. U.S.A.* 98, 5312, 2001.
291. Nettles, J.H. and Downing, K.H., The tubulin binding mode of microtubule stabilizing agents studied by electron crystallography, *Top. Med. Chem.* 286, 209, 2009.
292. Dubois, J., Guénard, D., Guéritte-Voeglein, F., Guedira, N., Potier, P., Gillet, B., and Betoeil, J.-C. Conformation of taxotere and analogues determined by NMR spectroscopy and molecular modeling studies, *Tetrahedron*, 49, 6533, 1993.
293. Williams, H.J., Scott, A.I., Dieden, R.A., Swindell, C.S., Chirlian, L.E., Francl, M.M., Heerding, J.M., and Krauss, N.E., NMR and molecular modeling study of the conformations of taxol and of its side chain methylester in aqueous and non-aqueous solution, *Tetrahedron* 49, 6545, 1993.
294. Cachau, R.E., Gussio, R., Beutler, J.A., Chmurny, G.N., Hilton, B.D., Muschik, G.M., and Erickson, J.W., Solution structure of taxol determined using a novel feedback-scaling procedure for NOE-restrained molecular dynamics, *Supercomput. Appl. High Perform. Comput.* 8, 24, 1994.
295. Vander Velde, D.G., Georg, G.I., Grunewald, G.L., Gunn, C.W., and Mitscher, L.A., "Hydrophobic Collapse" of taxol and taxotere solution conformations in mixtures of water and organic solvent, *J. Am. Chem. Soc.* 115, 11650, 1993.
296. Paloma, L.G., Guy, R.K., Wrasidlo, W., and Nicolaou, K.C., Conformation of a water-soluble derivative of taxol in water by 2D-NMR spectroscopy, *Chem. Biol.* 1, 107, 1994.
297. Ojima, I., Kuduk, S.D., Chakravarty, S., Ourevitch, M., and Begue, J.-P., A novel approach to the study of solution structures and dynamic behavior of paclitaxel and docetaxel using fluorine-containing analogs as probes, *J. Am. Chem. Soc.* 119, 5519, 1997.
298. Snyder, J.P., Nevins, N., Cicero, D.O., and Jansen, J., The conformations of taxol in chloroform, *J. Am. Chem. Soc.* 122, 724, 2000.

299. Ojima, I., Inoue, T., and Chakravarty, S., Enantiopure fluorine-containing taxoids: Potent anticancer agents and versatile probes for biomedical problems, *J. Fluorine Chem.*, 97, 3, 1999.
300. Li, Y., Poliks, B., Cegelski, L., Poliks, M., Cryczynski, Z., Piszczek, G., Jagtap, P.G. et al., Conformation of microtubule-bound paclitaxel determined by fluorescence spectroscopy and REDOR NMR, *Biochemistry* 39, 281, 2000.
301. Paik, Y., Yang, C., Metaferia, B., Tang, S., Bane, S., Ravindra, R., Shanker, N. et al., Rotational-echo double-resonance NMR distance measurements for the tubulin-bound paclitaxel conformation, *J. Am. Chem. Soc.* 129, 361, 2007.
302. He, L., Jagtap, P.G., Kingston, D.G.I., Shen, H.-J., Orr, G.A., and Horwitz, S.B., A common pharmacophore for taxol and the epothilones based on the biological activity of a taxane molecule lacking a C-13 side chain, *Biochemistry* 39, 3972, 2000.
303. Ganesh, T., Guza, R.C., Bane, S., Ravindra, R., Shanker, N., Lakdawala, A.S., Snyder, J.P., and Kingston, D.G.I., The bioactive taxol conformation on β-tubulin: Experimental evidence from highly active constrained analogs, *Porc. Natl. Acad. Sci. U.S.A.* 101, 10006, 2004.
304. Ganesh, T., Yang, C., Norris, A., Glass, T., Bane, S., Ravindra, R., Banerjee, A. et al., Evaluation of the tubulin-bound paclitaxel conformation: Synthesis, biology and SAR studies of C-4 to C-3′ bridged paclitaxel analogs, *J. Med. Chem.* 50, 713, 2007.
305. Tang, S., Yang, C., Brodie, P., Bane, S., Ravindra, R., Sharma, S., Jiang, Y., Snyder, J.P., and Kingston, D.G.I., Bridging converts a noncytotoxic *nor*-paclitaxel derivative to a cytotoxic analogue by constraining it to the T-taxol conformation, *Org. Lett.* 8, 3983, 2006.
306. Hodge, M., Chen, Q.-H., Bane, S., Sharma, S., Loew, M., Banerjee, A., Alcaraz, A.A., Snyder, J.P., and Kingston, D.G.I. Synthesis and bioactivity of a side chain bridged paclitaxel: A test of the T-taxol conformation. *Bioorg. Med. Chem. Lett.* 19, 2884, 2009.
307. Geney, R., Sun, L., Pera, P., Bernacki, R.J., Xia, S., Horwitz, S.B., Simmerling, C.L., and Ojima, I., Use of the tubulin bound paclitaxel conformation for structure-based rational drug design, *Chem. Biol.* 12, 339, 2005.
308. Sun, L., Geng, X., Geney, R., Li, Y., Simmerling, C., Li, Z., Lauher, J.W. et al., Design, synthesis, and biological evaluation of novel C14-C3′BzN-linked macrocyclictaxoids, *J. Org. Chem.* 73, 9584, 2008.
309. Yang, Y., Alcaraz, A.A., and Snyder, J.P., The tubulin-bound conformation of paclitaxel: T-taxol vs "PTX-NY", *J. Nat. Prod.* 72, 422, 2009.
310. Nettles, J.H., Li, H., Cornett, B., Krahn, J.M., Snyder, J.P., and Downing, K.H., The binding mode of epothilone A on α,β-tubulin by electron crystallography, *Science* 305, 866, 2004.
311. Barasoain, I., Garcia-Carril, A.M., Matesanz, R., Maccari, G., Trigili, C., Mori, M., Shi, J.-Z. et al., Probing the pore drug binding site of microtubules with fluorescent taxanes: Evidence of two binding poses, *Chem. Biol.* 17, 243, 2010.
312. Xiang, F., Yu, J., Yin, R., Ma, Y., and Yu, L., Structure–activity relationship of taxol inferring from docking taxol analogues to microtubule binding site, *Z. Naturforsch.* 64c, 551, 2009.
313. Hansch, C. and Verma, R.P., Understanding tubulin/microtubule-taxane interactions: A quantitative structure-activity relationship study, *Mol. Pharm.* 5, 151, 2008.
314. Mekhail, T. and Markman, M., Paclitaxel in cancer therapy, *Expert Opin. Pharmacother.* 3, 755, 2002.
315. Hudis, C. and Dang, C. The taxane limbo: How long can we go? *J. Natl. Cancer Inst.* 100, 761, 2008.
316. Rowinsky, E.K. The development and clinical utility of the taxane class of antimicrotubule chemotherapy agents. *Ann. Rev. Med.* 48, 353, 1997.
317. Kuppens, I.E.L.M. Current state of the art of new tubulin inhibitors in the clinic. *Curr. Clin. Pharmacol.* 1, 57, 2006.
318. Saloustros, E., Mavroudis, D., and Georgoulias, V. Paclitaxel and docetaxel in the treatment of breast cancer. *Expert Opin. Pharmacother.* 9, 2603, 2008.
319. Michaud, L.B., Valero, V., and Hortobagyi, G., Risks and benefits of taxanes in breast and ovarian cancer, *Drug Saf.* 23, 401, 2000.
320. Levin, M., The role of taxanes in breast cancer treatment, *Drugs Today* 37, 57, 2001.
321. Crown, J., O'Leary, M., and Ooi, W.-S. Docetaxel and paclitaxel in the treatment of breast cancer: A review of clinical experience. *Oncologist* 9, 24, 2004.
322. Hudis, C., The use of taxanes in early breast cancer, *EJC Supp.* 1, 1, 2003.
323. Nowak, A.K., Wilcken, N.R.C., Stockler, M.R., Hamilton, A., and Ghersi, D., Systematic review of taxane-containing versus non-taxane-containing regimens for adjuvant and neoadjuvant treatment of early breast cancer, *Lancet* 5, 372, 2004.

324. Nabholtz, J.-M. and Gligorov, J., The role of taxanes in the treatment of breast cancer, *Expert Opin. Pharmacother.* 6, 1073, 2005.
325. Kris, M.G. and Manegold, C., Docetaxel (taxotere) in the treatment of non-small cell lung cancer: An international update, *Sem. Oncol.*, 28 (Suppl. 2), 1, 2001.
326. Calderoni, A. and Cerny, T., Taxanes in lung cancer: A review with focus on the European experience, *Crit. Rev. Oncol./Hematol.* 38, 105, 2001.
327. Piccart, M.J., Bertelsen, K., James, K., Cassidy, J., Mangioni, C., Simonsen, E., Stuart, G. et al., Randomized intergroup trial of cisplatin-paclitaxel versus cisplatin-cyclophosphamide in women with advanced epithelial ovarian cancer: Three-year results, *J. Natl. Cancer Inst.* 92, 699, 2000.
328. Beer, T.M., El-Geneidi, M., and Eilers, K.M. Docetaxel (taxotere) in the treatment of prostate cancer. *Exp. Rev. Anticancer Ther.* 3, 261, 2003.
329. Gulley, J. and Dahut, W.L. Chemotherapy for prostate cancer: Finally an advance! *Am. J. Ther.* 11, 288, 2004.
330. Schrijvers, D. and Vermorken, J.B., Taxanes in the treatment of head and neck cancer, *Curr. Opin. Oncol.* 17, 218, 2005.
331. Garber, K., Improved paclitaxel formulation hints at new chemotherapy approach, *J. Natl. Cancer Instit.* 96, 90, 2004.
332. Henderson, I.C. and Bhatia, V., Nab-paclitaxel for breast cancer: A new formulation with an improved safety profile and greater efficacy, *Expert Rev. Anticancer Ther.* 7, 919, 2007.
333. Hawkins, M.J., Soon-Shiong, P., and Desai, N., Protein nanoparticles as drug carriers in clinical medicine, *Adv. Drug Deliv. Rev.* 60, 876, 2008.
334. Harries, M., Ellis, P., and Harper, P., Nanoparticle albumin-bound paclitaxel for metastatic breast cancer, *J. Clin. Oncol.* 23, 7768, 2005.
335. McGrogan, B.T., Gilmartin, B., Carney, D.N., and McCann, A., Taxanes, microtubules and chemoresistant breast cancer, *Biochim. Biophys. Acta* 1785, 96, 2008.
336. Morris, P.G. and Fornier, M.N. Novel anti-tubulin cytotoxic agents for breast cancer. *Expert Rev. Anticancer Ther.* 9, 175, 2009.
337. Kamath, K.R., Barry, J.J., and Miller, K.M. The Taxus™ drug-eluting stent: A new paradigm in controlled drug delivery. *Adv. Drug Deliv. Rev.* 58, 412, 2006.
338. Coolong, A. and Kuntz, R.E., Understanding the drug-eluting stent trials, *Am. J. Cardiol.* 100, 18K, 2007.
339. Kingston, D.G.I. and Newman, D.J., Taxoids: Cancer-fighting compounds from nature, *Curr. Opin. Drug Discov. Dev.* 10, 130, 2007.
340. Dubois, J., Recent progress in the development of docetaxel and paclitaxel analogues, *Expert Opin. Ther. Pat.* 16, 1481, 2006.
341. Jones, R.J., Hawkins, R.E., Eatock, M.M., Ferry, D.R., Eskens, F.A.L.M., Wilke, H., and Evans, T.R.J., A phase II open-label study of DHS-paclitaxel (Taxoprexin) by 2-h intravenous infusion in previously untreated patients with locally advanced or metastatic gastric or oesophageal adenocarcinoma, *Cancer Chemother. Pharmacol.* 61, 435, 2008.
342. Payne, M., Ellis, P., Dunlop, D., Ranson, M., Danson, S., Schacter, L., and Talbot, D., DHA-paclitaxel (Taxoprexin) as first-line treatment in patients with stage IIIb or IV non-small cell lung cancer: Report of a phase II open-label multicenter trial, *J. Thorac. Oncol.* 1, 984, 2006.
343. Metzger-Filho, O., Moulin, C., Azambuja, E.D., and Ahamad, A., Larotaxel: Broadening the road with new taxanes, *Expert Opin.: Drug Eval.* 18, 1183, 2009.
344. Ojima, I. and Geney, R., 109881 (Aventis), *Curr. Opin. Investig. Drugs*, 4, 737, 2003.
345. Bonomi, P., Paclitaxel poliglumex (PPX, CT-2103): Macromolecular medicine for advanced non-small-cell lung cancer, *Expert Rev. Anticancer Ther.* 7, 415, 2007.
346. Boddy, A.V., Paclitaxel poliglumex: Antimitotic drug oncolytic, *Drugs Future* 32, 776, 2007.
347. Hwang, J.J., Marshall, J.L., Malik, S., Chun, H., Ahmed, T., and Pilia, P.A., A Q7D Phase I study of TPI 287, a novel taxane, in advanced malignancies: Imaging studies, pharmacokinetics (PK) and circulating tumor cell (CTC) quantitation., *J. Clin. Oncol.* 24 (18S), 12008, 2006.
348. Beer, M., Lenaz, L., and Amadori, D. Phase II study of ortataxel in taxane-resistant breast cancer. *J. Clin. Oncol.* 26, Abstract 1066, 2008.
349. Ramanathan, R.K., Picus, J., Raftopoulos, H., Bernard, S., Lockhart, A.C., Frenette, G., Macdonald, J. et al., A phase II study of milataxel: A novel taxane analogue in previously treated patients with advanced colorectal cancer, *Cancer Chemother. Pharmacol.* 61, 453, 2008.
350. Roche, M., Kyriakou, H., and Seiden, M. Drug evaluation: Tesetaxel – an oral semisynthetic taxane derivative. *Curr. Opin. Investig. Drugs* 7, 1092, 2006.

351. du Bois, A., Jung, B., Loehr, A., Schaller-Kranz, T., Cohen, M., and Frickhofen, N., A phase I and pharmacokinetic study of novel taxane BMS-188797 and cisplatin in patients with advanced solid tumours, *Br. J. Cancer* 94, 79, 2006.
352. Schuch, G. EndoTAG-1 MediGene. *Curr. Opin. Investig. Drugs* 6, 1259, 2005.
353. Hawkins, M.J., Soon-Shiong, P., and Desai, N. Protein nanoparticles as drug carriers in clinical medicine, *Adv. Drug Deliv. Rev.* 60, 876, 2008.

7 The Vinca Alkaloids*

Fanny Roussi, Françoise Guéritte, and Jacques Fahy

CONTENTS

7.1 Introduction 177
7.2 Discovery of the Antitumor Vinca Alkaloids 177
7.3 Mechanism of Action 179
7.4 Synthesis of Vinca Alkaloids 180
7.5 Structure–Activity Studies 184
7.5.1 Modifications of the Vindoline Moiety 184
7.5.2 Modifications of the Velbanamine Moiety 185
7.6 Clinical Applications 192
7.7 Conclusions 193
References 193

7.1 INTRODUCTION

Vinca alkaloids are a family of indole–indoline dimeric compounds belonging to the family *Apocynaceae*, and represent one of the most important classes of anticancer agents. Vinca alkaloids became clinically useful in cancer chemotherapy after their discovery in the late fifties. More than 40 years latter, the two natural drugs vinblastine (**1**) and vincristine (**2**) are still widely used in cancer chemotherapy, and semisynthetic analogs, such as vindesine (**3**), vinorelbine (**4**), and very recently vinflunine (**5**) have been developed after intensive synthetic and structure–activity relationship studies. Other analogs have emerged as potentially potent drugs, and some of these will perhaps enrich the family of anticancer vinca alkaloids in the near future. This review intends to summarize the current knowledge about the vinca alkaloids, from their discovery to clinical applications with emphasis on the latest analogs that may have an interest in cancer chemotherapy.

7.2 DISCOVERY OF THE ANTITUMOR VINCA ALKALOIDS[1]

Catharanthus roseus (L.) G. DON (formerly named as *Vinca rosea* L.) is known as the Madagascar periwinkle and belongs to the Apocynaceae family. This perennial plant has dark green leaves and pink or white flowers. It is cultivated in most warm countries as an ornamental in parks and gardens, and many varieties have been developed with various colors. Originally, leaves of *C. roseus* were used to treat various diseases. Investigators from different countries of the world have reported hypotensive, hypoglycemic as well as purgative properties.[2] The antitumor properties of *C. roseus* were discovered independently by two teams, one Canadian and one American. In the early fifties, Clark Noble, one of the first members of the University of Toronto insulin team, sent *C. roseus* leaves to his brother Robert Noble in Jamaica to treat diabetes. The challenge for R. Noble, working in Collip's Laboratory at the University of Western Ontario, was to find

* This review is dedicated to the memory of Prof. Pierre Potier whose contribution in the field of vinca alkaloids and other natural products led to the discovery of new antitumor drugs.

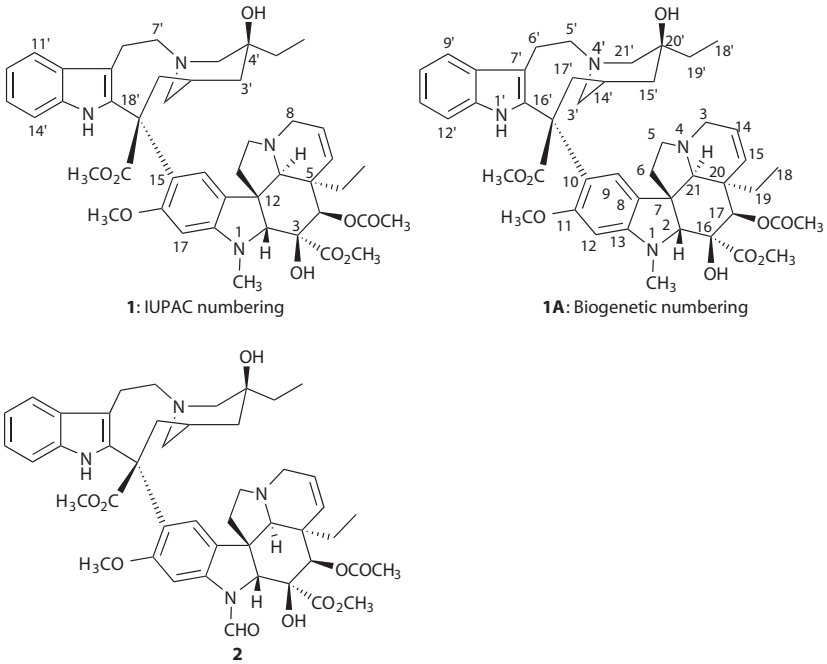

FIGURE 7.1 Vinblastine (**1**) and vincristine (**2**).

substances that could affect blood glucose levels. Instead of these properties, R. Noble found a strong effect on white blood cell counts and bone marrow. Together with the chemist Charles T. Beer, he isolated the active principal formerly named vincaleukoblastine, now known as vinblastine (**1**).[3] Other investigations carried out by Svoboda, Johnson, and collaborators at Lilly Laboratories, also led to the isolation of vinblastine (**1**) when they observed a reproducible antitumor activity of extracts of *C. roseus* leaves.[4] These studies also led to the isolation of other bioactive alkaloids. Thus, leurocristine, also named vincristine (**2**), was isolated from the leaves of the periwinkle (Figure 7.1).[5]

Vinblastine (**1**) and vincristine (**2**) are isolated in minute amounts from the leaves of *C. roseus* (Figure 7.1). For this reason, the semisynthesis and total synthesis of these binary alkaloids has been the subject of a number of studies, as we will see later on. Since the initial clinical trials in the sixties, the so-called vinca alkaloids, vinblastine (Velbe®) and vincristine (Oncovin®) have been widely used in the treatment of different types of cancer.

The complex structure and stereochemistry of vinblastine (**1**) and vincristine (**2**) were elegantly established by Neuss et al.[6] and Moncrief and Lipscomb.[7] Both vinblastine and vincristine are dimeric compounds possessing an indole moiety (the velbanamine "upper" part) and a vindoline dihydroindole nucleus. They only differ by the substituent attached to the nitrogen of the dihydroindole part, vinblastine bearing an *N*-methyl group, whereas vincristine possesses an *N*-formyl function. Two systems have been adopted to number the bisindole-type alkaloids: the biogenetic and the IUPAC numbering.[1] The IUPAC numbering will be used throughout this review. Despite their small structural differences, vinblastine (**1**) and vincristine (**2**) strongly differ in their antitumor properties and clinical toxicities. So far, three other modified natural antitumor vinca alkaloids have been developed as antitumor compounds: vindesine (**3**; Eldesine®),[8] vinorelbine (**4**; Navelbine®),[9] and more recently, a fluorinated structural analog, vinflunine (**5**; Javlor®)[10,11] (Figure 7.2). Thus, the discovery of vinblastine was a milestone in the development of cancer chemotherapy, inducing extensive chemical, biological, and clinical studies that finally led to the discovery of new potent antitumor vinca alkaloids.

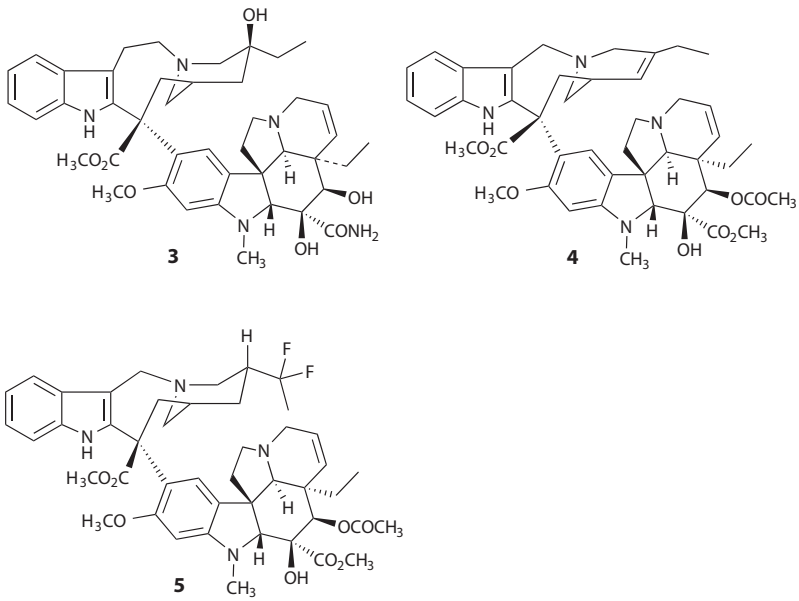

FIGURE 7.2 Vindesine (**3**), vinorelbine (**4**), and vinflunine (**5**).

7.3 MECHANISM OF ACTION

Soon after the discovery of the *in vivo* antitumor properties of the vinca alkaloids, a number of studies focused on their mode of action. Vinblastine was found to be a cell cycle-dependent antimitotic agent that interacts with tubulin,[12] an ubiquitous heterodimeric protein present in all eukaryotic cells. Tubulin and its polymerized form, microtubules, play crucial roles in the maintenance of cellular morphology, intracellular transport, and in the construction of the mitotic spindle during cell division.[13] The formation of microtubules is a dynamic process involving the assembly of tubulin and disassembly of the polymers. The antiproliferative activity of the vinca alkaloids was shown to be due to their interaction with the mitotic spindle.[14] They inhibit the assembly of tubulin into microtubules and, consequently, prevent the cells from undergoing division. They bind to tubulin at different sites from colchicine and antitumor taxoids, but a number of other natural products, such as rhizoxin, maytansine, cryptophycins, or dolastatins, share the same binding site, interacting with the so-called vinca domain of tubulin.[15–17] *In vitro*, the effects of vinca alkaloids on tubulin are concentration dependent. At low concentrations (submicromolar), they inhibit the formation and function of microtubules from tubulin, while spirals are formed at higher concentration.[18,19] Depending on their structure, the effects of vinca alkaloids are different on microtubule dynamics, and these have been associated with the differences observed in their efficacies and toxicities.[20]

Although the cellular target of the vinca alkaloids has been known since the 1970s, the precise location of their binding site remained unknown for a long time until Knossow and collaborators[21] published in 2005 the x-ray structure of vinblastine bound to tubulin in a complex with the RB3 protein stathmin-like domain (RB3-SLD) with a resolution of 4.1 Å. This binding site is at the interface between two tubulin heterodimers ($\alpha 2$–$\beta 1$) in a head-to-tail rearrangement and vinblastine is oriented so that its cleavamine and vindoline moieties each interact with both heterodimers (Figure 7.3). Vinblastine introduces a wedge at the interface of two tubulin molecules and thus interferes with tubulin assembly. Together with electron microscopic and biochemical data, the structure explains vinblastine-induced tubulin self-association into spiral aggregates at the expense of microtubule growth. Besides the direct interaction of vinblastine with tubulin, a previously

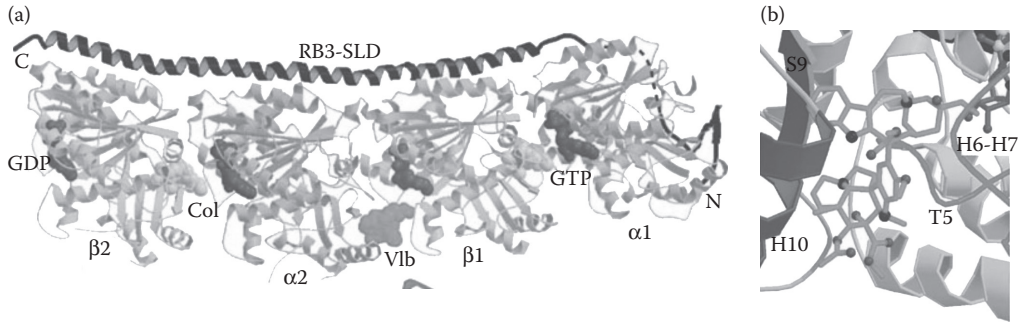

FIGURE 7.3 **(See color insert.)** Vinblastine (Vlb, cyan)-binding site: (a) location of vinblastine in $(Tc)_2R$; (b) precise location of the vinblastine-binding site at the interface between two tubulin heterodimers (α2–β1).[21]

unknown mechanism of action was recently suggested as the depalmitoylation of tubulin in human leukemic lymphocytes.[22]

7.4 SYNTHESIS OF VINCA ALKALOIDS

The availability of bioactive natural substances is often a major problem when they have to be produced on a commercial basis. Vinblastine (**1**) and vincristine (**2**) are isolated in very low yields from the leaves of *C. roseus*. Isolation yields of vincristine (**2**) are on the order of 0.0003% from the dried leaves. Vinblastine (**1**) is obtained in higher yield (0.01%), and has thus been used to produce vincristine, oxidation of the *N*-methyl indoline group of the former leading to the formation of the latter. Vindesine (**3**) is also prepared from vinblastine (**1**) by hydrazinolysis and subsequent hydrogenolysis of the newly formed N–N bond.[8]

For the moment, it is accepted that biotechnological approaches in plant cell culturing may not provide an instant solution to the production of vinca alkaloids. The biosynthesis of vinblastine and vincristine is very complex. It was reviewed by Van der Heijden,[23] O'Connor,[24] and El-Sayed.[25] Starting from tryptophan and geraniol, at least 35 intermediates, 30 enzymes, 2 regulatory genes, and 7 intracellular and intercellular compartments are involved in the production of vinblastine.

Although cultivation of *C. roseus* is a renewable source of vinblastine (**1**), a number of teams have studied the potentiality to obtain antitumor vinca alkaloids by semisynthesis and total synthesis. This was also a synthetic challenge, considering the structural complexity of these molecules. The enantioselective total synthesis of the vindoline moiety has been performed using various strategies[26] but the total synthesis of (+)-catharanthine is less documented.[27]

The successful strategy of the semisynthesis of vinca alkaloids was based on a biogenetic hypothesis involving vindoline (**7**) and catharanthine (**6**) as precursors. These alkaloids are two of the more abundant alkaloids isolated from *C. roseus*, and the idea was that vinblastine (**1**), as well as other binary vinca alkaloids, could result from the union of vindoline (**7**) with an intermediate derived from catharanthine (**6**). After a number of attempts,[1] a vinblastine-type alkaloid possessing the C-18′(*S*) configuration, essential for bioactivity, could be obtained by applying a modification of the Polonovski reaction, also called the Polonovski–Potier reaction, to the N_b-oxide of catharanthine (**8**) and vindoline (**7**). Thus, treatment of catharanthine Nb-oxide (**8**) and vindoline (**7**) with trifluoroacetic anhydride, after reduction by sodium borohydride, led to a new bisindole alkaloid, anhydrovinblastine (**9**) possessing the natural 18′-(*S*) configuration (Scheme 7.1).[28–30]

Semisynthesis of anhydrovinblastine (**9**) was also realized from catharanthine (**6**) and vindoline (**7**) through ferric ion-mediated coupling in acidic aqueous media. The coupling reaction was stereoselective for the formation of the desired 18′-(*S*) isomer and yields were significantly higher (77%).[31] Very recently, an enzyme-catalyzed coupling of catharanthine (**6**) and vindoline (**7**) to anhydrovinblastine

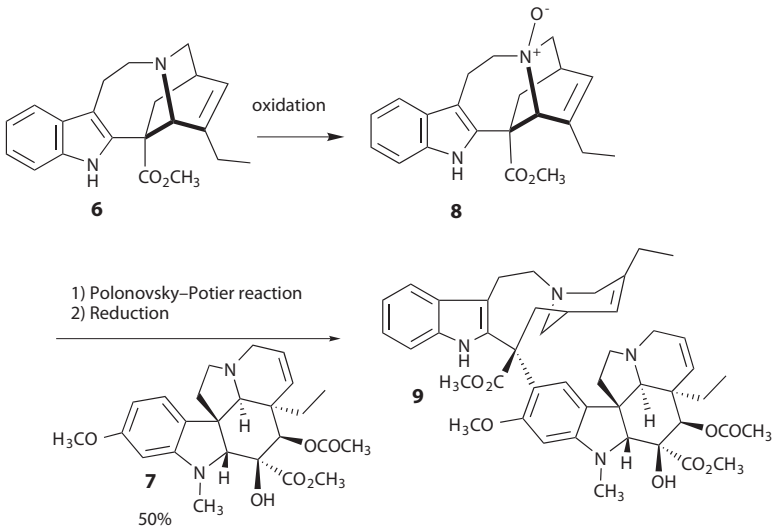

SCHEME 7.1 Semisynthesis of anhydrovinblastine from catharanthine and vindoline.

(**9**) was also carried out using oxidoreductase laccases and atmospheric oxygen followed by a $NaBH_4$ reduction of the enaminium cationic intermediate. Anhydrovinblastine (**9**) was isolated in 56% yield.[32] Because of its facile preparation from catharanthine (**6**) and vindoline (**7**), anhydrovinblastine (**9**) was considered as an attractive key intermediate in the synthesis of other binary alkaloids.[1] Anhydrovinblastine (**9**) was then found to be a natural vinca alkaloid first by feeding experiments of both radioactive catharanthine and vindoline to *C. roseus*,[33] second by its extraction from the plant.[34] More recently, a basic peroxidase with anhydrovinblastine synthase activity was purified from the leaves of *C. roseus*, and shown to produce the dimer from catharanthine and vindoline.[35]

From anhydrovinblastine (**9**), vinblastine (**1**) was first obtained in 30% overall yield through four steps involving hydrogenation to 4′-deoxyleurosidine (**10**), N_b-oxidation and Polonovski reaction leading to enamine (**11**), treatment with thallium triacetate, and reduction with hydrolysis of the C-4′ acetoxy group (Scheme 7.2).[36] Another improved method to provide vinblastine from anhydrovinblastine was to subject enamine (**11**) to $FeCl_3$-promoted oxygenation (40% global yield).[37] As an alternative, anhydrovinblastine was converted into vinblastine (21% conversion) using an antivinblastine monoclonal antibody as a chiral template and $NaBH_3CN$ and oxygen for the oxidation–reduction step.[38]

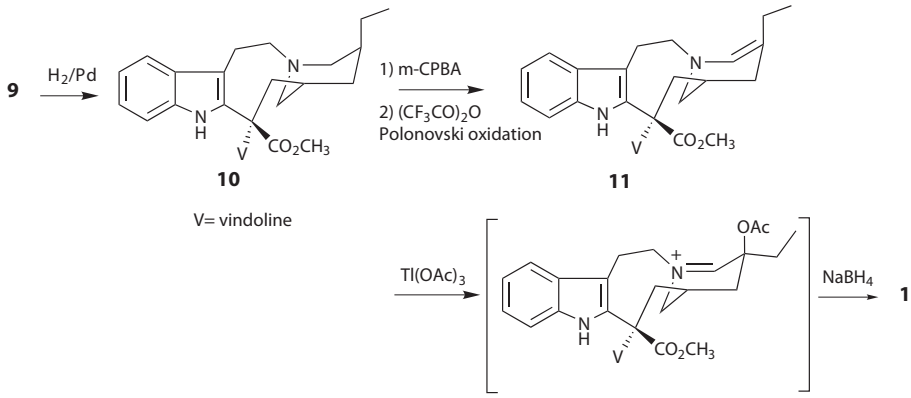

SCHEME 7.2 Conversion of anhydrovinblastine to vinblastine.

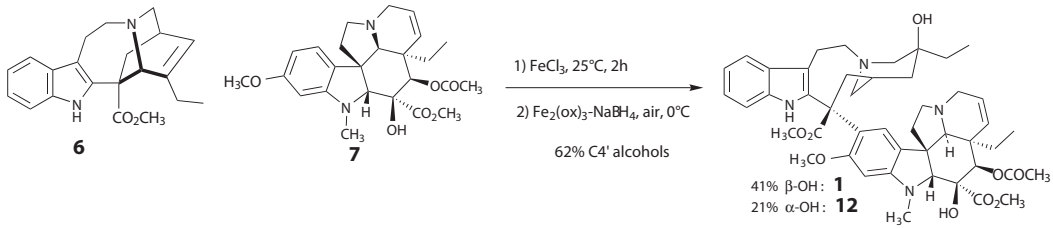

SCHEME 7.3 Direct coupling of catharanthine and vindoline to vinblastine.

Very recently, an impressive direct coupling of catharanthine (**6**) and vindoline (**7**) to provide vinblastine (**1**) [and, in a few more steps, vincristine (**2**) and related natural products] was achieved by Boger's group.[39] This one-pot procedure combined an initial $FeCl_3$-promoted vindoline/catharanthine coupling reaction with a subsequent $Fe_2(ox)_3$–$NaBH_4$/air concomitant oxidation of the C3′=C4′ double bond and reduction of the iminium intermediate. Vinblastine (**1**) (41%) and leurosidine (**12**), its naturally occurring C4′ alcohol isomer (21%), were isolated with a very good yield (combined yield of 62–69%; 2/1 β/α) along with 10% of anhydrovinblastine (**9**) (Scheme 7.3).[39]

Two other strategies have also been used to generate the C-18′*S*/C-15 bond of vinblastine (**1**) from natural vindoline (**7**) and substrates that could lead to the velbanamine part of the binary indole–indoline alkaloids. The first involved reaction of chloroindolenine (**13**) with silver tetrafluoroborate and vindoline (**7**) and led to the intermediate (**14**), which produced vinblastine (**1**) after cyclization and deprotection (Scheme 7.4).[40]

In the second strategy (Scheme 7.5), the coupling methodology was based on a nonoxidative cleavage of the tertiary amine (**16**) that underwent fragmentation after treatment with $ClCO_2CH_2C_6H_4NO_2$ and vindoline (**7**).[41] The indole–indoline dimer (**16**) was then converted into hydroxy aldehyde (**17**) which led to vinblastine (**1**) after hydrogenolysis and reduction of the iminium (**18**).

Finally, a *de novo* synthesis of vinblastine (**1**) was achieved by coupling the chloroindolenine (**19**) with vindoline (**7**) synthesized from 7-mesyloxyquinoline (**20**) (Scheme 7.6).[42] The iminium salt intermediate was first formed after activation of **19** by trifluoroacetic acid, and electrophilic substitution with vindoline (**7**) led to dimer (**21**), which was cyclized into vinblastine after deprotection of the tertiary alcohol and amine groups.

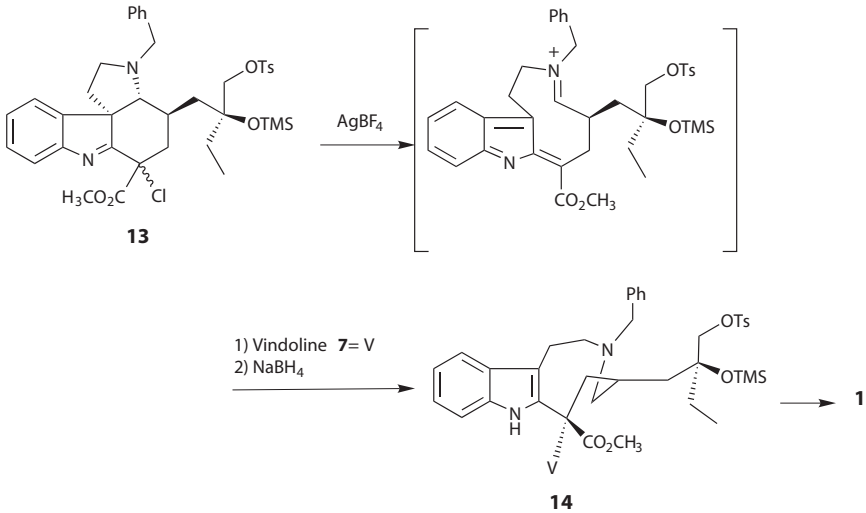

SCHEME 7.4 Conversion of chloroindolenine (**13**) to vinblastine.

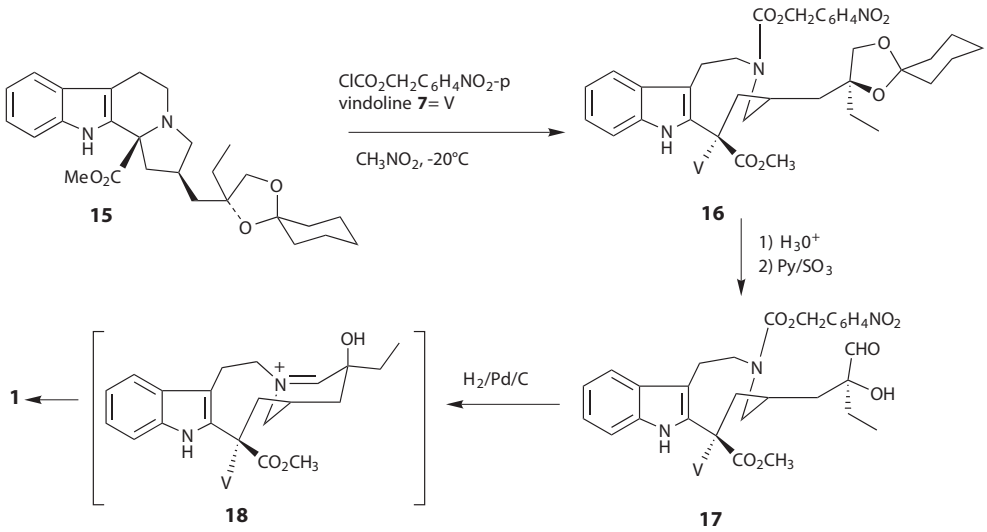

SCHEME 7.5 Conversion of tertiary amine (**15**) to vinblastine.

The same strategy was adopted to synthesize (+)-vincristine (**2**) through a stereoselective coupling of demethylvindoline and carbomethoxyvelbanamine precursor.[43] A versatile route to vinblastine (**1**) which is amenable to the preparation of a range of analogs at C-4′ from intermediate **23** was also developed by Fukuyama et al. through coupling of chloroindolenine (**22**) with vindoline (**7**) (Scheme 7.6).[44]

If anhydrovinblastine (**9**) is an important intermediate in the semisynthesis of a number of natural binary alkaloids, it is also the precursor of unnatural anticancer drugs of the vinca family: vinorelbine (**4**) and vinflunine (**5**). The first synthesis of vinorelbine (**4**) came from the application of the Polonovski–Potier reaction to anhydrovinblastine N_b-oxide (**24**) (Scheme 7.7). Treatment of **24** with trifluoroacetic anhydride led to an unstable quaternary ammonium (**25**), which undergoes fragmentation to a bisiminium salt (**26**). Addition of water and subsequent loss of formaldehyde produces a nucleophilic secondary amine (**27**) that gives rise to vinorelbine (**4**), after intramolecular trapping of the iminium group.[9] Improvement in the synthesis of vinorelbine (**4**) could be obtained by using chloro- or bromo-indolenines of anhydrovinblastine (**28**).[45,46]

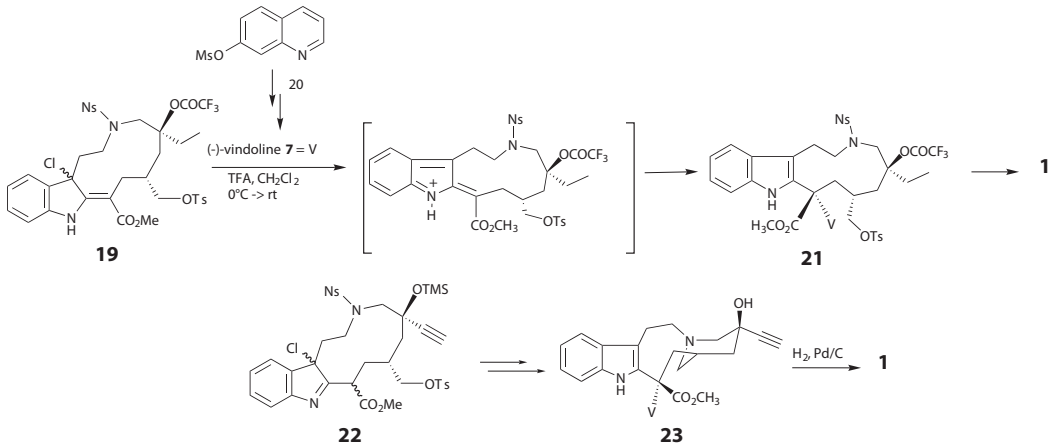

SCHEME 7.6 Conversion of chloroindolenines **19** and **22** to vinblastine.

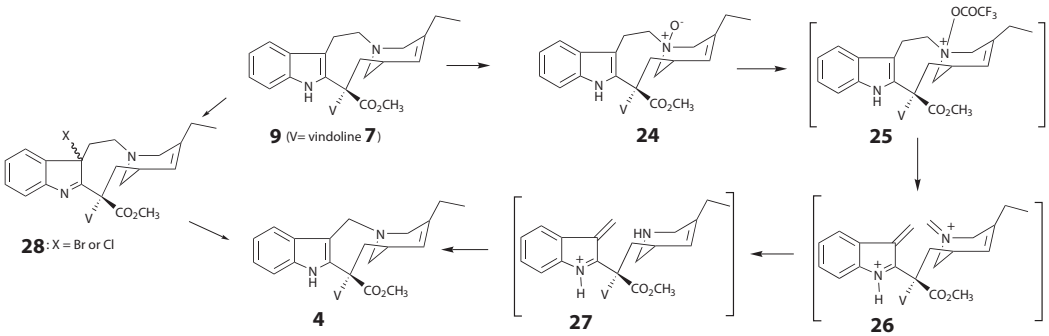

SCHEME 7.7 Conversion of anhydrovinblastine N_b-oxide (**24**) or chloro-indolénine (**28**) to vinorelbine (**4**).

7.5 STRUCTURE–ACTIVITY STUDIES

Structure–activity relationships of vinca alkaloids have been extensively reviewed by Pearce[47] and Borman and Kuehne.[48] Since the discovery of their antitumor properties, many derivatives are said to have been synthesized in the pharmaceutical industry with the aim of improving their pharmacological activities to identify new drugs exhibiting a wider spectrum of clinical efficacy. The natural vinblastine (**1**) extracted from *C. roseus* leaves was used as a starting material as it was for a long time the only compound available in sufficient quantities.

For almost 40 years, several hundred derivatives have been synthesized and evaluated for their potential antitumor properties. Most of these products have been obtained by modifications of the vindoline "lower" part, bearing several reactive functions. Structural changes in the "upper" cleavamine moiety are much less trivial and have shown that even a slight change can dramatically modify biological activities.

7.5.1 Modifications of the Vindoline Moiety

Many such modified derivatives of the vindoline moiety, including vinglycinate (**29**), vindesine (**3**), and vinzolidine (**30**), have been synthesized and evaluated by the Eli Lilly group (Figure 7.4). Vinglycinate (**29**), substituted by a glycine residue at the vindoline C-4 position, was the first vinblastine analog to enter Phase I clinical trials in 1967.[49] Subsequently, modifications at the C-3 position led to the amido-derivative vindesine (**3**),[8] which can be considered as a chemical precursor of vinzolidine (**30**)[47] and vintriptol (**31**).[50] Vinepidine (**32**), corresponding to 4′-*epi*-4′-deoxyvincristine, was also developed by the Lilly group for its increased tubulin affinity relative to vinblastine (**1**).[47] Nevertheless, none of these semisynthetic compounds exerted marked benefits in clinical evaluations relative to vinblastine (**1**) and vincristine (**2**). After 1990, only a few new derivatives have been prepared and evaluated with the aim of discovering novel anticancer drugs with clinical efficacy. These include the aminophosphonate derivative vinfosiltine (**33**) (Figure 7.4), selected for its unusual high potency both *in vitro* and *in vivo* compared with the classical vinblastine and vincristine.[51] Vinfosiltine (**33**) was designed on the basis of the similarity between α-amino phosphonic acids and natural amino acids. However, no evidence of marked benefit in Phase II clinical trials, relative to other vinca alkaloids, has been obtained and development of vinfosiltine was discontinued in 1995.[52] The natural anhydrovinblastine (**9**), biogenetic precursor of the dimeric vinca alkaloid, entered Phase I clinical trials in 1999 for the treatment of advance solid tumors including lung (NSCLC) cancer,[53] but development was discontinued in 2005.[54] Recently, modifications at the C-3 position of anhydrovinblastine were performed with the formation of numerous amide, ester, ether, and carbamate derivatives and their *in vitro* and *in vivo* activities were evaluated, showing that a carbonyl function at that position is important for activity.[55] One of these

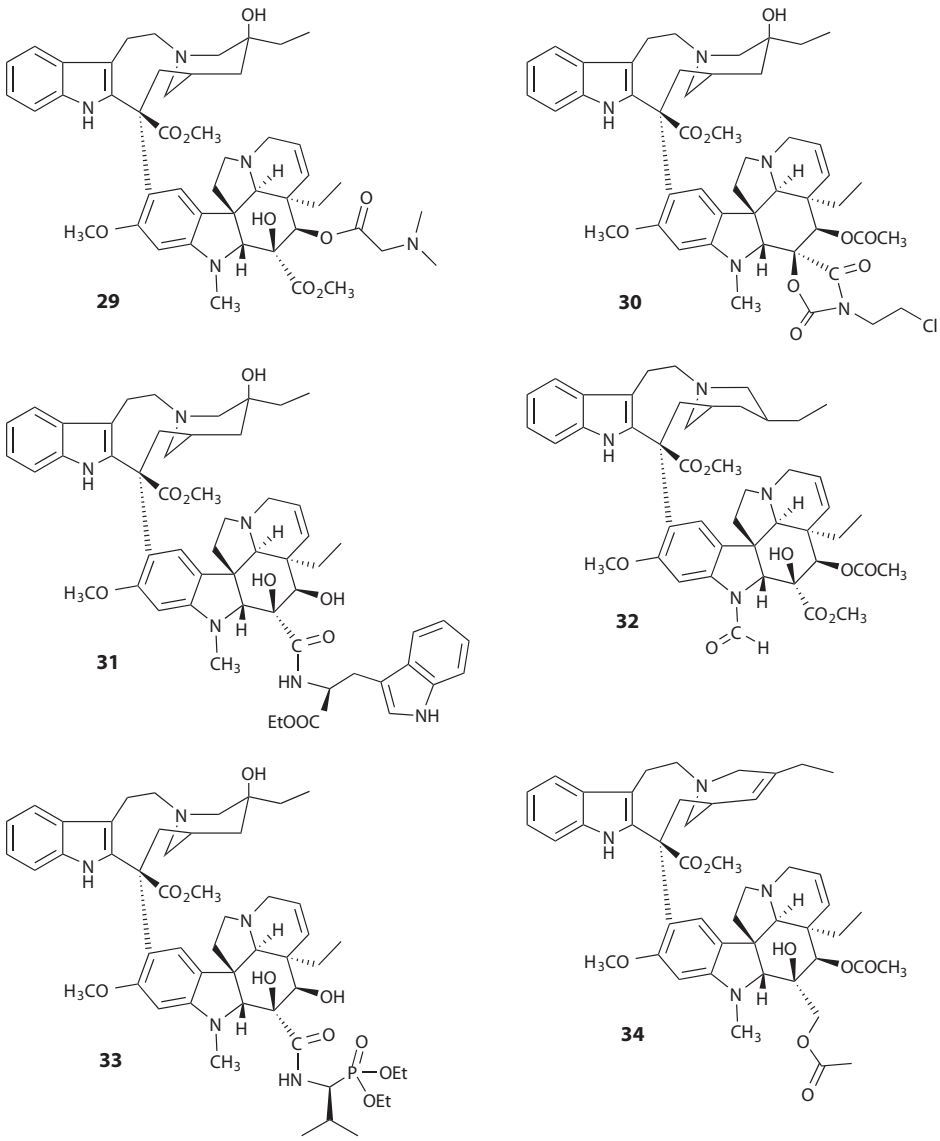

FIGURE 7.4 Analogs modified on the vindoline moiety: vinglycinate (**29**), vinzolidine (**30**), vintriptol (**31**), vinepidine (**32**), vinfosiltine (**33**), and **34**.

compounds (3-decarbomethoxy-acetyloxylmethyl-anhydrovinblastine; **34**) was about tenfold less toxic than classic vinca alkaloids *in vitro* but presented, *in vivo*, superior antitumor activity to vinorelbine against sarcoma 180 in mice as well as a better pharmacokinetic profile (Figure 7.4). Its activity was compared with that of vinflunine (**5**).[56]

7.5.2 Modifications of the Velbanamine Moiety

Two comprehensive reviews have illustrated the consequences of modifications in the velbanamine "upper part" of the vinblastine skeleton.[57,58] So far, only very few substituted derivatives at the A′ ring (mainly at 12′) have been disclosed. None of them exhibited any major improvement in antitumor activity.[56] Nevertheless, the mildness of today's palladium chemistry allowed versatile

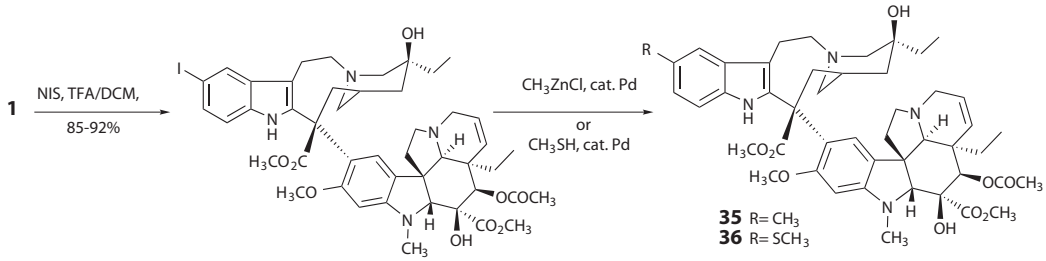

SCHEME 7.8 Conversion of vinblastine to 12′-modified analogs.

functionalization of vinca alkaloids at 12′. New derivatives were elaborated from 12′-iodovinblastine, 12′-iodovincristine, and 12′-iodovinorelbine[59a] using transition metal-based chemistry. Among these compounds, only those with small hydrophobic groups showed cytotoxicity on MCF-7 and HeLa cell lines similar to that of the parent compounds. Compounds **35** and **36** showed *in vivo* antitumor activity in P388 murine leukemia model superior to vinorelbine (Scheme 7.8). In addition, compound **36** showed highly significant reductions in the growth rate of four xenograft tumors.[59b] Based on its promising pharmacological profile, compound **36** entered Phase I clinical trials in 2008 in patients with advanced solid tumors.[60] In the same manner, several C-12′-substituted vinflunine derivatives[61] were shown to exhibit cytotoxicity against A549 cell lines.

In the 1970s, as previously mentioned, the crucial event was the preparation of anhydrovinblastine (**9**) from catharanthine (**8**) and vindoline (**7**) that facilitated access to vinca alkaloid analogs exhibiting antimitotic properties. The major modification of the C′ ring was the transformation of the tryptamine of anhydrovinblastine (**9**) to a gramine via a modified Polonovsky reaction leading to vinorelbine (**4**). Hence, vinorelbine (**4**) represented a new class of bisindole alkaloid, easily accessible in large amount, by semisynthesis. Further chemistry was undertaken on this compound.[57]

Kuehne's group at the University of Vermont, USA, has extensively documented the synthesis of vinblastine derivatives, mainly modified at the piperidine ring (D′) of the velbenamine part.[48,62]As a result, it was clearly shown that subtle modifications at the C-4′ position affect dramatically the interactions with tubulin[62] together with the cytotoxicity potencies.[63] More recently, two series of *homo*-vinblastine derivatives, **37** and **38** (Figure 7.5), have been synthesized by the same group, highlighting the possible isolation of atropoisomers exhibiting *in vitro* activities different from those of the compound bearing the natural conformation.

The authors also mentioned the concept of "thermal pro-drug activation" potentially applicable to these compounds.[64,65] Among them, the 7a′-*homo*-vinblastine **37** including a 10-membered ring C′ was able to inhibit tubulin polymerization at submicromolar concentrations, like vinblastine, but was slightly less cytotoxic than vinblastine when tested against the murine L1210 and S180 cell lines. However, the 18a′-*homo*-derivatives were inactive under the same experimental conditions.[66]

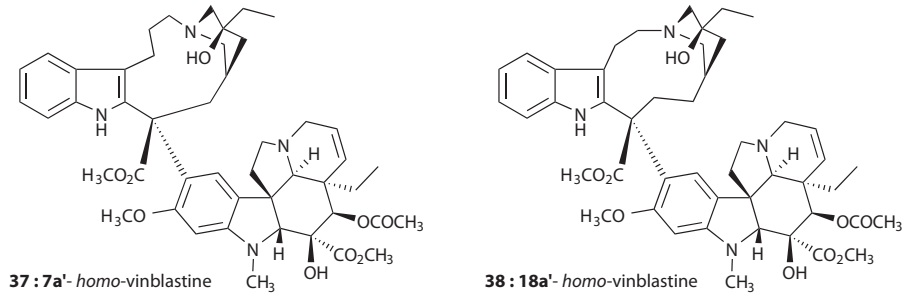

FIGURE 7.5 7a′-*homo*-vinblastine (**37**) and 18a′-*homo*-vinblastine (**38**).

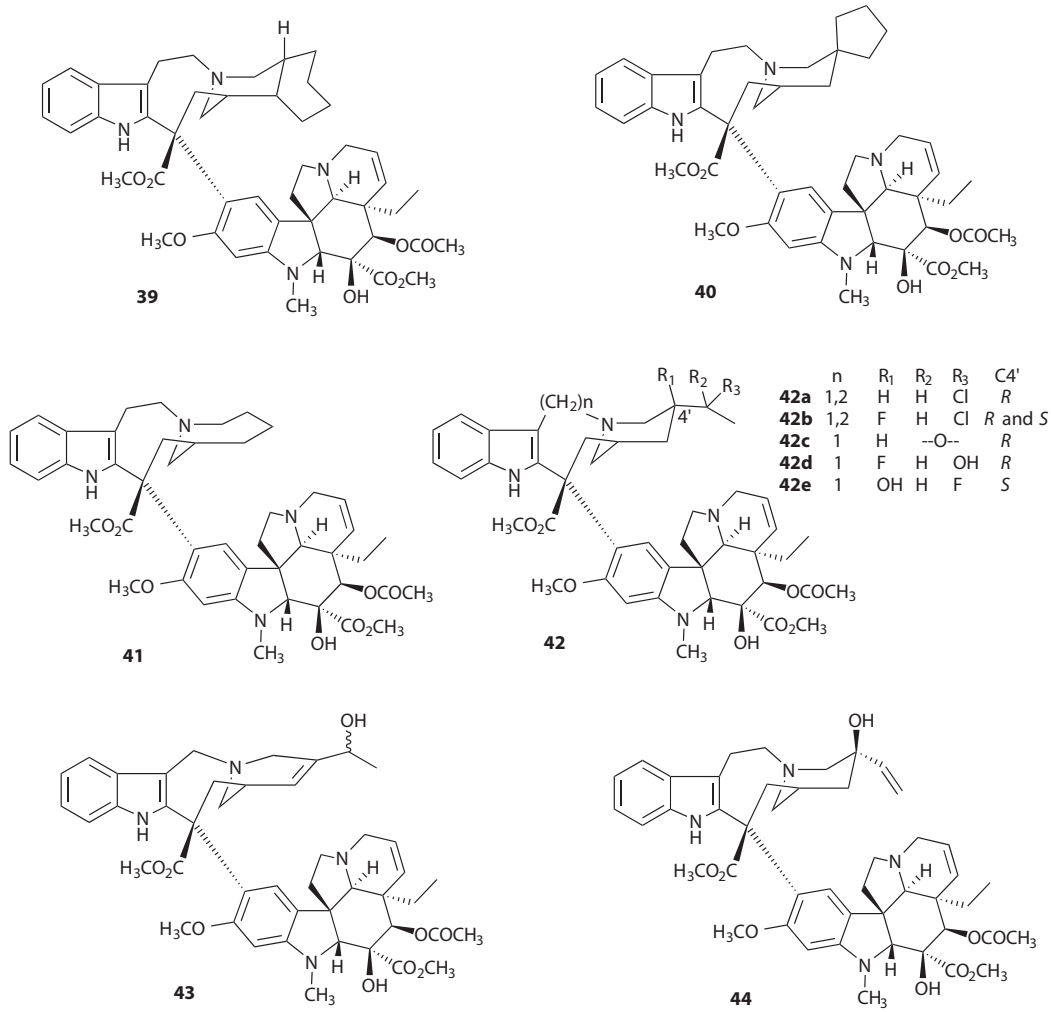

FIGURE 7.6 Analogs modified on the velbanamine moiety (**39**–**44**).

A large series of 62 vinblastine congeners has been prepared and evaluated for their *in vitro* pharmacological properties.[67] As an example derivative, **39** including an additional cyclohexane ring fused at C-3′-4′ (Figure 7.6) induced a very high level of cytotoxicity toward the L1210 murine leukemia cell line ($IC_{50} < 1$ pM compared with 0.4 nM for vinblastine). However, the activity of **39** with RCC-2 cells (rat colon cancer) was slightly lower than that of the parent compound. Similarly, it was further shown that ring D′-modified compounds such as **40** and **41** were as potent as vinblastine in terms of cytotoxicity (Figure 7.6).[67,68]

Almost surprisingly, superacid chemistry applied to vinca alkaloids resulted in the access to newly modified compounds specifically at the C-4′ and C-20′ positions, including vinflunine (**5**).[10] These include compounds **42a** and **42b** substituted by halogen atoms (fluorine and/or chlorine) when the reaction was conducted in the presence of chlorinated solvents, and oxygenated derivatives **42c–e** or **43** (alcohols or ketones) in the presence of hydrogen peroxide (Figure 7.6).[57] A series of such derivatives has been evaluated for their overall pharmacological properties: tubulin polymerization inhibition, cytotoxicity and *in vivo* antitumor activity against the P388 murine leukemia model. However, a lack of correlation between *in vitro* and *in vivo* results has been revealed and no clear structure–activity relationships have been obtained. In the tubulin polymerization inhibition

assay, all the compounds of the study exerted an activity in the micromolar range of IC_{50} close to those of the reference compounds. Clearly, this assay was not discriminatory enough to be included in the selection of such derivatives. More surprisingly, binding of [^{3}H]-vinflunine to tubulin was undetectable using the standard centrifugal gel filtration, unlike the other vinca alkaloids.[69] This observation could appear somewhat paradoxical when considering the overall *in vivo* antitumor activities of vinflunine (**5**). However, cytotoxicity values against the L1210 murine leukemia cells were correlated with the induction of tubulin spirals for a subset of these compounds.[70] Detailed investigations of pharmacokinetic and metabolism properties did not provide results susceptible to help to understand this unusual profile of activities.[71] It should be pointed out that alcohol (**43**), isolated after reaction in superacidic medium in 85% yield, corresponds to a minor metabolite of vinorelbine (**4**).[72] Then, addition of fluorine atoms in vinorelbine [**4**; resulting in vinflunine (**5**), for example] could block a metabolic pathway and modify its pharmacodynamic properties. The data available, however, do not explain the unusual pharmacological profile of **5**: like the other vinca alkaloids, vinorelbine is poorly metabolized and compound **43**, found at very low levels, is not a circulatory metabolite.[73] Should superacids be considered as tools for biomimetic reactions under particular conditions, or on the contrary, should certain cytochromes be able to catalyze superacidic reactions? Further experiments need to be undertaken to validate this hypothesis.

C-4′ analogs of vinblastine (ethynyl, vinyl, and arylacetylene moieties) were also elaborated by Fukuyama's group by total synthesis.[44] Cell growth assay with the K565 cell line showed that only the vinyl analog (**44**) was almost as active as vinblastine on this cell line (Figure 7.6).

Based on the numerous results obtained in the studies mentioned before, it appears clearly that chemical modifications in the piperidine ring D′ and/or at the C-4′ position induce dramatic changes in the pharmacological properties of vinca alkaloids.

An original approach based on the concept of multivalency has been reported: a series of hybrids (**45**) with vinca alkaloids linked to other tubulin-interacting agents (thiocolchicine, podophyllotoxin, and baccatin III) was synthesized (Figure 7.7). Some differences emerged from the length of the spacer between the two pharmacophores, but no clear improvement in the pharmacological properties was observed when compared with the starting vinca derivatives. Surprisingly, however, the vindoline–thiocolchicine hybrid (**46**) retains activity comparable with vinorelbine in terms of G2/M cell cycle arrest and tubulin polymerization inhibition.[74]

In a different domain, targeted delivery of vinca alkaloids has also been investigated. Several experiments have been conducted during the 1980s with conjugates of vinblastine with monoclonal

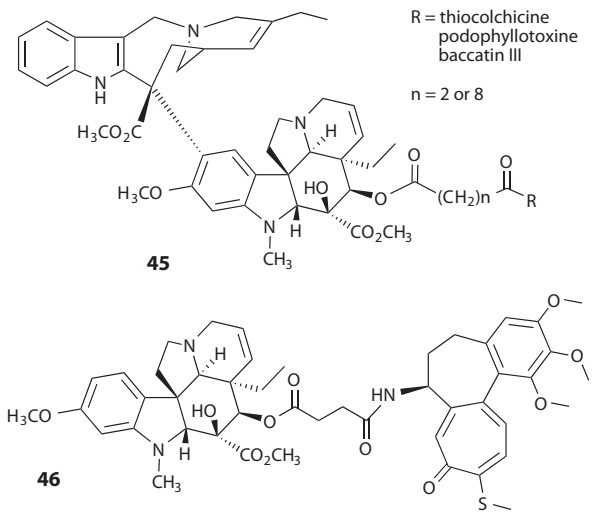

FIGURE 7.7 Hybrids **45** and **46**.

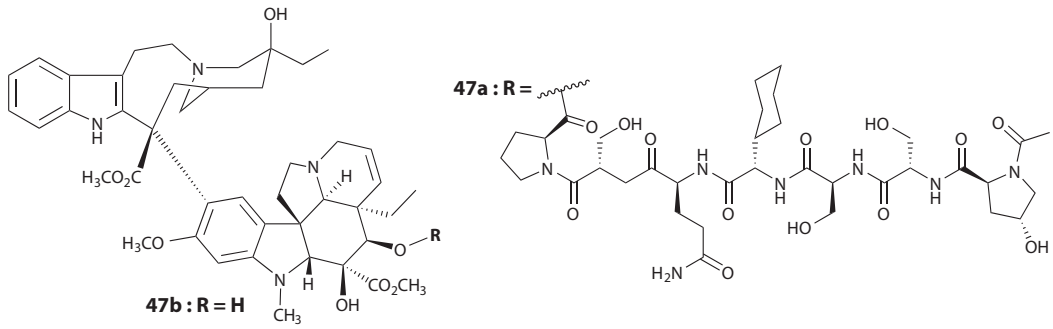

FIGURE 7.8 Vinblastine peptide derivative (**47a**) and deacetylvinblastine (**47b**).

antibodies to deliver the cytotoxic drug to malignant tissues, but no further clinical development has been reported.[75] Later, a peptide-vinblastine derivative (**47a**) targeted at the prostate cancer cells has been reported (Figure 7.8).[76] The proteolytic activity of prostate-specific antigen (PSA) has been exploited to convert the conjugate **47a** to deacetyl-vinblastine (**47b**) at the site of the tumor, as demonstrated by *in vivo* studies using PSA-secreting implanted human prostate cancer cells on nude mice. It should be pointed out that the putative effective drug 4-deacetylvinblastine (**47b**), resulting from the hydrolysis of **47a**, exhibited no *in vivo* activity under the same experimental conditions.

Recently, EC145 (**48**), a folic acid conjugate of deacetylvinblastine monohydrazide was developed successfully (Figure 7.9).[77] Folic acid (vitamin B9) is important in the formation of new cells by participating in the biosynthesis of nucleotide bases. It is transported into cells via folate receptor (FR)-mediated endocytosis. The expression of FR is low in normal tissues but high in several tumors (particularly in ovarian and endometrial cancers). This natural cellular uptake mechanism was exploited for the targeted delivery of deacetylvinblastine monohydrazide (that was found to be completely inactive when administered at nontoxic dose levels). On the contrary, EC145 (**48**) displayed significant antiproliferative activity and tolerability.[78] Three Phase II clinical studies are now conducted with EC145 (against ovarian and endometrial cancers, adenocarcinoma of the lung, and platinum-resistant ovarian cancers).[79]

A more sophisticated application of the FR targeting process is represented by the dual agent EC0225 (**49**) incorporating two anticancer drugs: a vinca alkaloid unit and mitomycin, both of them linked to the peptide-folate residue by two separate disulfide bonds. As a result, synergism between vinblastine and mitomycin was observed and EC0225 (**49**) retain high affinity for FR-positive cells.[80] Based on its impressive preclinical activity, EC0225 started Phase I clinical evaluation in 2007 for the treatment of refractory or metastatic tumors.[81]

As part of their work on tubulin,[21] Knossow's group also published the 4.1 Å and 3.8 Å x-ray structures of phomopsin A and soblidotin (both of which bind in the vinca domain) bound to tubulin in a complex with a SLD. Superimposition of this binding site with that of vinblastine revealed that they significantly overlap: the cleavamine moiety of vinblastine, the cyclic core of phomopsin A, and the first two amino acids of soblidotin occupy the same area and define the core of the vinca domain. However, the vindoline moiety of vinblastine and the lateral chain of phomopsin A and the main part of soblidotin are oriented in opposite directions. In particular, phomopsin A and soblidotin possess extensive contacts with Tyr β224, one of the residues sandwiching the GDP–GTP nucleotide exchange site.[82] To obtain original products that may interfere with both binding sites in tubulin, ten hybrids of vinca alkaloids and phomopsin A have been synthesized by linking the octahydrophomopsin lateral chain to the tertiary amine of the cleavamine moiety of anhydrovinblastine and vinorelbine.[83] Some of these compounds, like **50** and **51**, were very potent inhibitors of tubulin polymerization in spite of their large size (Figure 7.10). Nevertheless, NMR experiments, molecular modeling studies, and the poor effects of these compounds on tubulin nucleotide exchange proved that the added peptide chains of all the synthesized hybrids are far from the GDP–GTP-binding site: the

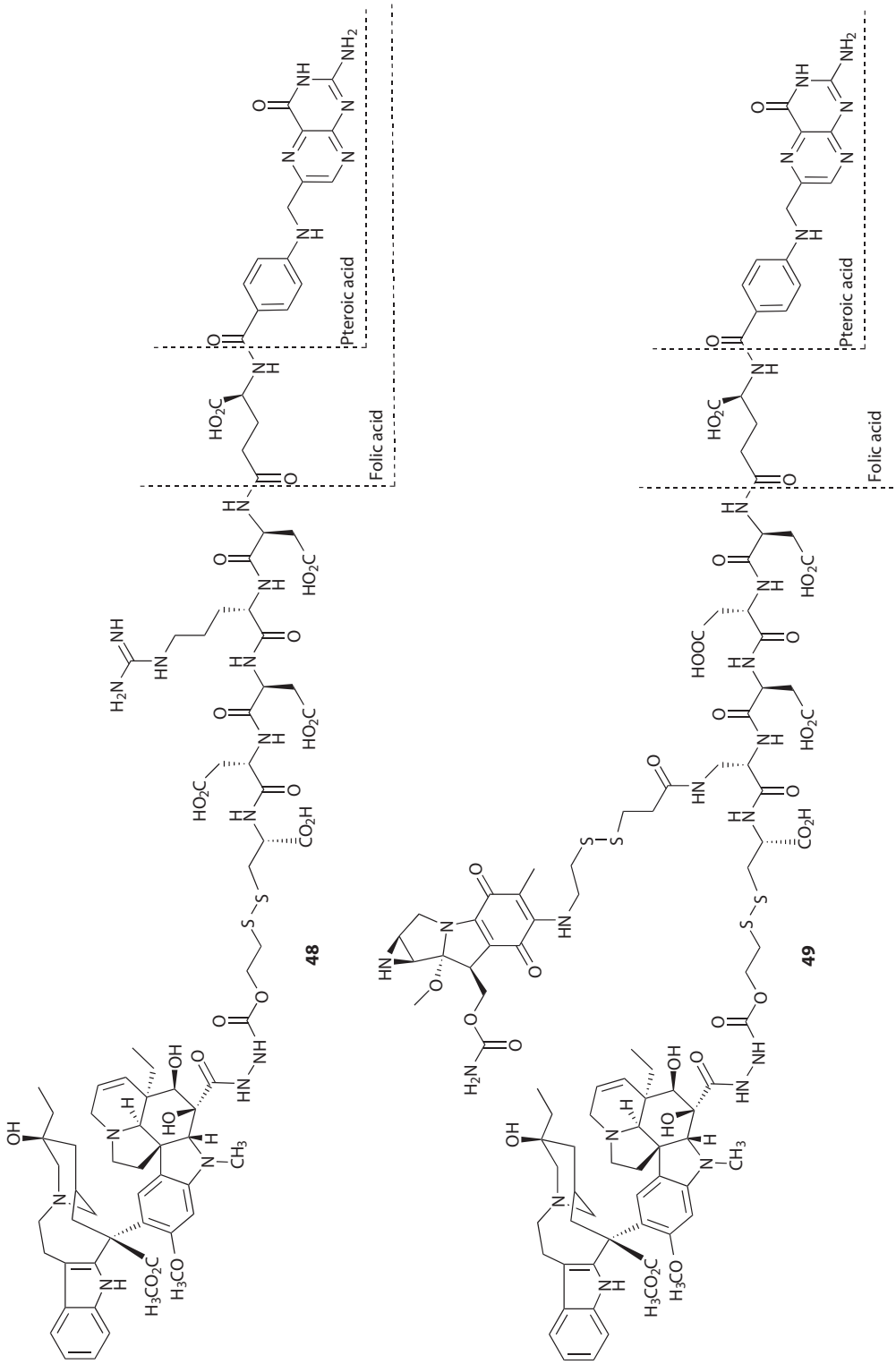

FIGURE 7.9 Folic acid conjugate of deacetylvinblastine hydrazide (**48**) and conjugate (**49**).

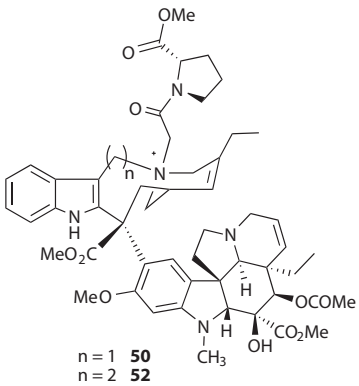

Compound	Microtubule assembly inhibitory activity IC_{50}/IC_{50}VLB	Cytotoxicity (KB) IC_{50}(μM)
1	1	0.001
50	0.9	0.08
51	1.3	0.7
52	2.0	0.1
53	1.8	1.3

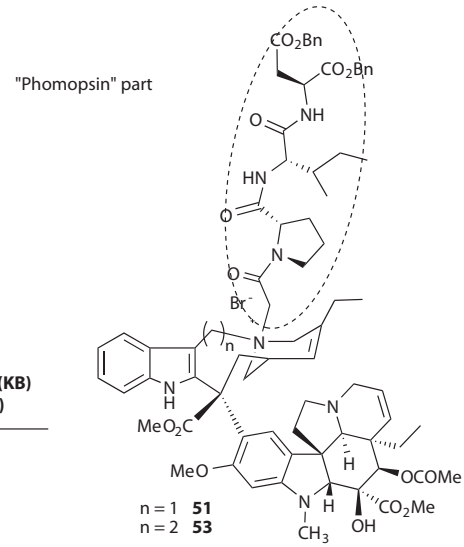

FIGURE 7.10 Vinblastine–phomopsin hybrids.

orientation of these lateral chains is different from those of phomopsin A. These interesting biological activities were explained by the fact that their lateral chain resides in another pocket, at the interface of tubulin β and α.[83] A simplification of the vindoline moiety nevertheless decreased biological activities.[84]

Taken together, all the results available in the literature appear to indicate that the strength of interaction with tubulin is not a sufficient criterion for the selection of a vinblastine derivative for further pharmacological studies. A quantitative comparison permitted to establish the relative binding affinities for tubulin: vincristine > vinblastine > vinorelbine, in parallel to the ability to induce the formation of tubulin spirals, which are considered to be responsible for the neurotoxicity observed as undesirable side-effects in the clinic.[85] Moreover, the cytotoxic activity is not relevant enough: a very potent compound such as vinfosiltine (**33**) may demonstrate a high *in vivo* antitumor activity but within a sharp dose range, resulting in a low therapeutic index. On the contrary, vinflunine (**5**) exhibited markedly lower cytotoxic properties in a panel of several murine and human cell lines compared with the standard vinca alkaloids,[69] but was definitely shown as the most active in a series of *in vivo* experiments including murine models[86] and human xenograft models.[11]

Microtubules are dynamic structures that are continuously shortening and growing. Detailed investigations evaluating microtubule dynamics perturbations have demonstrated that vinorelbine (**4**) and vinflunine (**5**) have a qualitative mode of action different from vinblastine (**1**).[20] Moreover, examinations of the intracellular concentrations of vinorelbine (**4**) and vinflunine (**5**) compared with vinblastine (**1**) suggested the possible presence of sequestered drugs into "intracellular reservoirs."[87] Effects of vinca alkaloids on centromere dynamics has also been studied, leading to the conclusion that suppression of the microtubule dynamics is the primary mechanism of action by which vinca alkaloids block the cell mitosis.[88] Overall, all these observations may contribute, in part, to the original *in vivo* efficacy of these new derivatives, but a correlation between tubulin interactions and antitumor activity remains to be established.

7.6 CLINICAL APPLICATIONS

To date, in addition to the natural vinblastine (**1**) and vincristine (**2**), the semisynthetic compounds that have been approved for clinical use as anticancer drugs are vindesine (**3**), vinorelbine (**4**), and vinflunine (**5**). Vinca alkaloids have been used in both curative and palliative chemotherapy regimens in clinical oncology for approximately 40 years. A comprehensive review of their clinical applications can be found in *Cancer: Principles and Practice of Oncology*.[89] The availability of vinorelbine in human chemotherapy has certainly resulted in renewed interest in this class of compounds.[90,91]

Vincristine (**1**) plays a major role in combination chemotherapy in the treatment of acute lymphoblastic leukemias, and lymphomas and nephroblastoma (Wilms' tumor). Vinblastine (**2**) is commonly used in combination with other anticancer drugs to treat bladder and breast cancers, and is an essential component in the curative regimen for Hodgkin's disease. Vinorelbine (**4**) has been approved worldwide for treating lung cancers (NSCLC) either as a single agent or in combination with cisplatin. It has also been registered for advanced breast cancer in Europe, and an oral formulation is available. Vinflunine (**5**) has been approved in the European Union as a monotherapy in the treatment of metastatic bladder cancer.[92] Several Phase II and Phase III clinical evaluations alone or in combination against breast, ovarian, colon, melanoma, mesothelioma, and renal cancers are ongoing.[93]

Several clinical trials including vinca alkaloids are still under investigation: new formulations, new combinations, or specific targeting. The combination of trastuzumab and vinorelbine in patients with HER2-overexpressing tumors has revived interest in vinorelbine for the management of advanced breast cancer.[94]

In a Phase II clinical evaluation, vinorelbine has been found to be active in sarcoma against pediatric tumors offering potential new applications in the treatment of such cancers.[95]

A carbon-11-labeled vinblastine was synthesized starting from the potassium salt of vinblastine-3-acid and [^{11}C]methyl iodide. It was administrated in a pilot study to two patients with renal carcinoma for application in positron-emission tomography (PET). The authors concluded that individual pharmacokinetic behavior of vinblastine can be considered to be a realistic approach for individualized chemotherapy.[96]

Stable liposomal and immunoliposomal formulations of vinblastine and vincristine have been prepared to target the drugs *in vivo*, particularly against HER2-overexpressing tumors. Using immunoliposomes incorporating vincristine and an anti-HER2 antibody fragment, marked enhancement in cytotoxicity compared with vincristine alone was established. The authors conclude that such active targeting is possible when stable immunoliposomes can be prepared, allowing a potential treatment of solid tumors with vincristine.[97]

Neurotoxic effects are the main side-effects observed with vincristine (**1**) and to a lesser extent with the other vinca alkaloids. These toxic effects have been associated with the affinity for axonal microtubules[98] and with the ability to induce microtubule spirals, as mentioned before.[99] Neutropenia is the principal dose-limiting toxicity of vinca alkaloids, but recovery occurs after treatment.

The emergence of drug-resistant cells is the major limitation in the clinical usefulness of vinca alkaloids, as for many other anticancer drugs.[100] The best described mechanism involves the amplification of the multidrug resistance protein, resulting in an efflux of the drug out of the cells mediated by the Pgp pump. However, studies with vinflunine demonstrated that the level of cross-resistance is much lower than that observed with vinorelbine or vincristine, which has positive implications for its clinical usage.[101] Resistance phenomena are still extensively studied and numerous reviews covering these aspects appear regularly in the literature.[102]

The discovery of antiangiogenic properties of vinca alkaloids in the early 1990s offered new research areas with potential clinical applications.[103] Moreover, other studies highlighted the definite antiangiogenic activity of vinblastine at noncytotoxic doses,[104] as demonstrated both *in vitro* on endothelial cells and *in vivo* using the chick embryo chorioallantoic assay. Moreover, newer data

suggest that vinflunine mediates its antitumor activity at least in part via an antivascular mechanism.[105] Moreover, treatment with vinflunine of mice bearing intrasplenic LS174T xenografts reduced the number of liver metastasis at low doses, supporting a significant antimetastatic effect.[106] These observations will certainly lead to new clinical applications of the vinca alkaloids when used at subtherapeutic doses, such as potentiation of standard cytotoxic compounds or potentiation of specific antiangiogenic derivatives.

Moreover, association of taxanes with vinca alkaloids such as vinorelbine has revealed evidence of potential synergy in preclinical models,[107] supporting promising clinical efficacy particularly in breast cancer.

Finally, "new" targets of vinca alkaloids may be discovered and their participation in the antitumor and anticancer activities will have to be established. As an example, vinorelbine has been described as a potent calmodulin binder, consequently inhibiting the association of calmodulin to its own target proteins.[108] Furthermore, different binding modes to calmodulin has been found for vinflunine and vinblastine, suggesting that vinflunine action on calmodulin can also have an effect on microtubule dynamics.[109]

Treatment of A549 cells with vinorelbine leads to a decrease in the antiapoptotic protein Bcl-2. A novel p53-binding site in the Bcl-2 promoter has been identified and vinorelbine treatment increases that interaction. This mechanism may help to better understand the effectiveness of vinca alkaloids and highlight the possibilities for adapting treatment according to p53 status and Bcl-2 tumor profile expression.[110]

7.7 CONCLUSIONS

Although the anticancer activity linked to clinical efficacy of vinca alkaloids has been recognized for more than four decades, further studies in different domains remain to be undertaken to better understand their mechanism of action. Recent advances in cell biology have identified numerous regulators of cell cycle such as molecular motors or specific kinases involved in the mitotic process. The question might be asked whether a mitotic blocker such as a new generation vinca alkaloid could target certain of these proteins. The recent precise determination of the vinca-binding site will probably permit the design of more selective molecules with the aim of establishing the importance of the strength of interactions with tubulin for the antimitotic activity. A number of new analogs have been prepared recently and a few of them are currently in clinical evaluations: new applications or new indications may be deducted from the corresponding observations. Thus, new drugs belonging to the vinca alkaloids family can still emerge from continuing research.

REFERENCES

1. For the first comprehensive view of the isolation, basic chemistry, structure, biogenesis, synthesis, medicinal chemistry, pharmacology, and medical uses of the vinblastine-like alkaloids, see: *The Alkaloids, Antitumor Bisindole Alkaloids from Catharanthus roseus* (L.) Eds Arnold Brossi, Matthew Suffness, Vol. 37, Academic Press, Inc., 1990.
2. Svoboda, G.H. and Blake, D.A. The phytochemistry and pharmacology of *Catharanthus* roseus (L.) G. DON, in *The Catharanthus Alkaloids*, Taylor, W.I. and Farnsworth, N.R., Eds, Marcel Dekker, Inc., New York, 1975, chap. 2.
3. Noble, R.L., Beer, C.T., and Cutts, J.H., Role of chance observation in chemotherapy: *Vinca rosea, Ann. N. Y. Acad. Sci.*, 76, 882, 1958.
4. Johnson, I.S., Wright, H.F., and Svoboda, G.H., Experimental basis for clinical evaluation of anti-tumor principles from *Vinca rosea* Linn, *J. Lab. Clin. Med*., 54, 830, 1959.
5. Svoboda, G.H., Alkaloids of *Vinca rosea* Linn. (*Catharanthus roseus*). 1X: Extraction and characterization of leurosidine and leurocristine, *Llyodia*, 24, 173, 1961.
6. Neuss, N., Gorman, M., Hargrove, W., Cone, N.J., Biemann, K., Büchi, G., and Manning, R.E., *Vinca* alkaloids, XXI. The structure of the oncolytic alkaloids vinblastine (VLB) and vincristine (VCR), *J. Am. Chem. Soc*., 86, 1440, 1964.

7. Moncrief, J.W. and Lipscomb, W.N., Structure of leurocristine methiodide dihydrate by anomalous scattering methods: relation to leurocristine (vincristine) and vincaleukoblastine (vinblastine), *Acta Cryst.*, 21, 322, 1966.
8. Barnett, C.J., Cullinan, G.J., Gerzon, K., Hoying, R.C., Jones, W.E., Newlon, W.M., Poore, G.A., et al., Structure–activity relationships of dimeric *Catharanthus* alkaloids. 1. Deacetylvinblastine amide (vindesine) sulfate, *J. Med. Chem.*, 21, 88, 1978.
9. Mangeney, P., Andriamialisoa, R.Z., Lallemand, J.Y., Langlois, N., Langlois, Y., and Potier, P., 5′-nor anhydrovinblastine, prototype of a new class of vinblastine derivatives, *Tetrahedron*, 35, 2175, 1979.
10. Fahy, J., Duflos, A., Jacquesy, J.C., Berrier, C., Jouannetaud, M.P., and Zunino, F., *Vinca* alkaloids in superacidic media: a method for creating a new family of antitumor derivatives, *J. Am. Chem. Soc.*, 119, 8576, 1997.
11. Hill, B., Fiebig, H.H., Waud, W.R., Poupon, M.F., Colpaert, F., and Kruczynski, A., Superior in vivo experimental antitumor activity of vinflunine, relative to vinorelbine, in a panel of human tumor xenografts, *Eur. J. Cancer*, 35, 512, 1999.
12. Lee, J.C., Harrison, D., and Timasheff, S.N., Interaction of vinblastine with calf brain microtubule protein, *J. Biol. Chem.*, 24, 9276, 1975.
13. Dustin, P., *Microtubules*, 1st ed., Springer Verlag, Berlin, 1978.
14. Jordan, M.A., Thrower, D., and Wilson, L., Mechanism of inhibition of cell proliferation by *Vinca* alkaloids*, Cancer Res.*, 51, 2212, 1991.
15. Hamel, E., Natural products which interact with tubulin in the vinca domain: maytansine, rhizoxin, phomopsin A, dolastatins 10 and 15 and halichondrin B, *Pharmacol. Ther.*, 55, 31, 1992.
16. Shih, C. and Teicher, B.A., Cryptophycins: a novel class of potent antimitotic antitumor depsipeptides, *Curr. Pharm. Des.*, 7, 1259, 2001.
17. Gupta, S. and Bhattacharyya, B., Antimicrotubular drugs binding to the *Vinca* domain of tubulin, *Mol. Cell. Biochem.*, 253, 41, 2003.
18. Himes, R.H., Kersey, R.N., Heller-Bettinger, I., and Samson, F.E., Action of the vinca alkaloids, vincristine, vinblastine and desacetyl vinblastine amide on microtubules *in vitro, Cancer Res.*, 36, 3798, 1976.
19. Zavala, F., Guénard, D., and Potier, P., Interaction of vinblastine analogues with tubulin, *Experientia*, 34, 1497, 1978.
20. Ngan, V.K., Bellman, K., Panda, D., Hill, B.T., Jordan, M.A., and Wilson, L., Novel actions of the antitumor drugs vinflunine and vinorelbine on microtubules, *Cancer Res.*, 60, 5045, 2000.
21. Gigant, B., Wang, C., Ravelli, R.B.G., Roussi, F., Steinmetz, M.O., Curmi, P.A., Sobel, A., and Knossow, M., Structural basis for the regulation of tubuline by vinblastine, *Nature*, 435, 519, 2005.
22. Caron, J.M. and Herwood, M., Vinblastine, a chemotherapeutic drug, inhibits palmitoylation of tubulin in human leukemic lymphocytes, *Chemotherapy*, 53, 51, 2007.
23. Van der Heijden, R., Jacobs, D.I., Snoeijer, W., Hallared, D., and Verpoorte, R., The *Catharanthus* alkaloids: pharmacognosie and biotechnology, *Curr. Med. Chem.*, 11, 607, 2004.
24. O'Connor, S.E. and Maresh, J., Chemistry and biology of monoterpene indole alkaloids biosynthesis, *Nat. Prod. Rep.*, 23, 532, 2006.
25. El-Sayed, M. and Verpoorte, R., *Catharanthus* terpenoid indole alkaloids: biosynthesis and regulation, *Phytochem. Rev*., 6, 277, 2007.
26. *Racemic total syntheses*: (a) Ando, M., Buechi, G., and Ohnuma, T., Total synthesis of (±)-vindoline, *J. Am. Chem. Soc.*, 97, 6880, 1975; (b) Kutney, J.P., Bunzli-Trepp, U., Chan, K.K., De Souza, J.P., Fujise, Y., Honda, T., Katsube, J., Klein, F.K., and Leutwiler, A., Total synthesis of indole and dihydroindole alkaloids. 14. A total synthesis of vindoline, *J. Am. Chem. Soc.*, 100, 4220, 1978; (c) Andriamialisoa, R.Z., Langlois, N., and Langlois, Y., A new efficient total synthesis of vindorosine and vindoline, *J. Org. Chem.*, 50, 961, 1985; *Enantioselective total syntheses*: (a) Feldman, P.L. and Rapoport, H., Synthesis of (–)-vindoline, *J. Am. Chem. Soc.*, 109, 1603, 1987; (b) Kuehne, M.E., Podhorez, D.E., Mulamba, T. and Bornmann, W.G., Biomimetic alkaloids syntheses. 15. Enantioselective syntheses with epichlorohydrin: total syntheses of (+)-, (–)- and (±)-vindoline and a synthesis of (–)-vindorosine, *J. Org. Chem.*, 52, 347, 1987; (c) Kobayashi, S., Ueda, T., and Fukuyama, T., An efficient total synthesis of (–)-vindoline, *Synlett*, 883, 2000; (d) Ishikawa, H., Elliott, G.I., Velcicky, J., Choi, Y., and Boger, D., Total synthesis of (–)- and ent-(+)-vindoline and related alkaloids, *J. Am. Chem. Soc*., 128, 10596, 2006.
27. Moisan, L., Thuéry, P., Nicolas, M., Doris, E., and Rousseau, B., Formal synthesis of (+)-catharanthine, *Angew. Chem. Int. Ed.*, 45, 5334, 2006 and reference cited.
28. Potier, P., Langlois, N., Langlois, Y., and Gueritte, F., Partial synthesis of vinblastine-type alkaloids, *J. Chem. Soc., Chem. Commun.*, 670, 1975.

29. Langlois, N., Gueritte, F., Langlois, Y., and Potier, P., Application of a modification of the Polonovski reaction to the synthesis of vinblastine-type alkaloids, *J. Am. Chem. Soc.*, 98, 7017, 1976.
30. Kutney, J.-P., Ratcliffe, A.H., Treasurywala, A.M., and Wunderly, S., Studies on the synthesis of bisindole alkaloids II. The synthesis of 3′,4′-dehydrovinblastine, 4′-deoxovinblastine and related analogues. The biogenetic approach. *Heterocycles*, 3, 639, 1975.
31. Vucovic, J., Goodbody, A.E., Kutney, J.P., and Misawa, M., Production of 3′,4′-anhydrovinblastine: a unique chemical synthesis, *Tetrahedron*, 44, 325, 1988.
32. Sagui, F., Chirivi, C., Fontana, G., Nicotra, S., Passarella, D., Riva, S., and Danieli, B., Laccase-catalysed coupling of catharanthine and vindoline: an efficient approach to the bisindole alkaloid anhydrovinblastine, *Tetrahedron*, 65, 312, 2009.
33. Scott, A.I., Guéritte, F., and Lee, S.L., Role of anhydrovinblastine in the biosynthesis of the antitumor dimeric indole alkaloids, *J. Am. Chem. Soc*., 100, 6253, 1978.
34. Goodbody, A.E., Watson, C.D., Chapple, C.C.S., Vukovic, J., and Misawa, M., Extraction of 3′,4′-anhydrovinblastine from *Catharanthus roseus, Phytochemistry*, 27, 1713, 1988.
35. Sottomayor, M., López-Serrano, M., DiCosmo, F., and Ros Barceló, Purification and characterization of a 3′,4′-anhydrovinblastine synthase (peroxidase-like) from *Catharanthus roseus* (L.) G. Don., *FEBS Lett.*, 428, 299, 1998.
36. Mangeney, P., Andriamioliosa, Z.R., Langlois, N., Langlois, Y., and Potier, P., Preparation of vinblastine, vincristine and leurosidine antitumour alkaloids, *J. Am. Chem. Soc.*, 101, 2243, 1979.
37. Kutney, J.-P., Choi, L.S.L., Nakano, J., Tsukamoto, H., McHung, M., and Boulet, C.A., A highly efficient and commercially important synthesis of the antitumor *Catharanthus* alkaloids vinblastine and leurosidine from catharanthine and vindoline, *Heterocycles*, 27, 1845, 1988.
38. Shirahama, T., Kohno, T., Kaijima, T., Nagaoka, Y., Morimoto, D., Hirata, K., and Uesato, S., Stereoselective conversion of anhydrovinblastine into vinblastine utilizing an anti-vinblastine monoclonal antibody as a chiral mould, *Chem. Pharm. Bull.*, 54, 665, 2006.
39. Ishikawa, H., Colby, D.A., Seto, S., Va, P., Tam, A., Kakei, H., Rayl, T.J., Hwang, I., and Boger, D., Total synthesis of vinblastine, vincristine, related natural products, and key structural analogues, *J. Am. Chem. Soc.* 131, 4904, 2009.
40. Kuehne, M.E., Matson, P.A., and Bornmann, W.G., Enantioselective syntheses of vinblastine, leurosidine, vincovaline, and 20′-*epi*-vincovaline, *J. Org. Chem*, 56, 513, 1991.
41. Magnus, P., Mendoza, J.S., Stamford, A., Ladlow, M., and Willis, E., Nonoxidative coupling methodology for the synthesis of the antitumor bisindole alkaloid vinblastine and a lower-half analogue: solvent effect on the stereochemistry of the crucial C-15/C-18′ bond, *J. Am. Chem. Soc*., 114, 10232, 1992.
42. Yokoshima, S., Ueda, T.T., Kobayashi, S., Sato, A., Kuboyama, T., Tokuyama, H., and Fukuyama T., Stereocontrolled total synthesis of (+)-vinblastine, *J. Am. Chem. Soc.*, 124, 2137, 2002.
43. Kuboyama, T., Yokoshima, S., Tokuyama, H., and Fukuyama, T., Stereocontrolled total synthesis of (+)-vincristine, *Proc. Natl. Acad. Sci. U.S.A.*, 101, 11966, 2004.
44. Miyazaki, T., Yokoshima, S., Simizu, S., Osada, H., Tokuyama, H., and Fukuyama T., Synthesis of (+)-vinblastine and its analogues, *Org. Lett*., 9, 4737, 2007.
45. Andriamializoa, R.Z., Langlois, N., Langlois, Y., and Potier, P., Composés antitumoraux du groupe de la vinblastine: nouvelle méthode de préparation, *Tetrahedron*, 36, 3053, 1980.
46. Guéritte, F., Pouilhès, A., Mangeney, P., Andriamialisoa, R. Z., Langlois, N., Langlois, Y., and Potier, P., Composés antitumoraux du groupe de la vinblastine: dérivés de la nor-5′ anhydrovinblastine, *Eur. J. Med. Chem*., 18, 419, 1983.
47. Pearce, H.L., Medicinal chemistry of bisindole alkaloids from *Catharanthus*, in *The Alkaloids*, Vol. 37: *Antitumor Bisindole Alkaloids from Catharanthus roseus* (L.). Brossi, A. and Suffness, M., Eds. Academic Press, Inc., San Diego, CA, 1990, 145.
48. Borman, L.S. and Kuehne, M.E., Functional hot spot at the C-20# position of vinblastine, in *The Alkaloids*, Vol. 37: *Antitumor Bisindole Alkaloids from Catharanthus roseus* (L.). Brossi, A. and Suffness, M., Eds. Academic Press, Inc., San Diego, CA, 1990, 133.
49. Armstrong, J.G., Dyke, R.W., Fouts, P.J., Hawthorne, J.J., Jansen Jr., C.J., and Peabody, A.M., Initial clinical experience with vinglycinate sulfate, a molecular modification of vinblastine, *Cancer Res.*, 27, 221, 1967.
50. Rao, K.S.P.B., Collard, M.P., De Jonghe, J.P.C., Atassi, G., Hannart, J.A., and Trouet, A., Vinblastin-23-oyl amino acid derivatives: chemistry, physicochemical data, toxicity, and antitumor activities against P388 and L1210 leukemias, *J. Med. Chem.*, 28, 1079, 1985.

51. Lavielle, G., Hautefaye, P., Schaeffer, C., Boutin, J.A., Cudennec, C.A., and Pierre, A., New alpha-amino phosphonic acid derivatives of vinblastine: chemistry and antitumor activity, *J. Med. Chem.*, 34, 1998, 1991.
52. Adenis, A., Pion, J.M., Fumoleau, P., Pouillart, P., Marty, M., Giroux, B., and Bonneterre, J., Phase II study of a new *Vinca* alkaloid derivative, S12363, in advanced breast cancer, *Cancer Chemother. Pharmacol.*, 35, 527, 1995.
53. Ramnath, N., Schwartz, G.N., Smith, P., Bong, D., Kanter, P., Berdzik, J., and Creaven, P. J., Phase I and pharmacokinetic study of anhydrovinblastine every 3 weeks in patients with refractory solid tumors, *Cancer Chemother. Pharmacol.*, 51, 227, 2003.
54. Butler, M.S., Natural products to drugs: natural product-derived compounds in clinical trials, *Nat. Prod. Rep.*, 25, 475, 2008.
55. Shao, Y., Zhang, H.-K., Ding, H., Quan, H.-T., Lou L.-G., and Hu, L.-H., Synthesis and structure–activity relationship studies of cytotoxic anhydrovinblastine amide derivatives, *J. Nat. Prod.*, 72, 1170, 2009 and references cited.
56. Li, W., Shao, Y., Hu, L., Zhang, X., Chen, Y., Tong, L., Li, C., Shen, X., and Ding, J., BM6, a new semi-synthetic vinca alkaloid, exhibits its potent in vivo anti-tumor activities *via* its high binding affinity for tubulin and improved pharmacokinetic profiles, *Cancer Biol. Ther.*, 6, 787, 2007.
57. Fahy, J., Modifications in the "upper" or velbenamine part of the *Vinca* alkaloids have major implications for tubulin interacting activities, *Curr. Pharm. Des.*, 7, 1181, 2001.
58. Duflos, A., Kruczynski, A., and Barret, J.-M., Novel aspect of natural and modified *Vinca* alkaloids, *Curr. Med. Chem.-Anticancer Agents*, 2, 55, 2002.
59. (a) Voss, M.E., Ralph, J.M., Xie, D., Manning, D.D., Chen, X., Frank, A.J. Leyhane, A.J., et al., Synthesis and SAR of vinca alkaloid analogues, *Bioorg. Med. Chem. Lett.*, 19, 1245, 2009; (b) Wolf, M.A., Johnson, R.K., Xie, D., Avrutsakaya, A., Mullin, R., Godfrey, B., Mead, M.A. et al., ALB-109564, a novel tubulin inhibitor with improved efficacy over vinorelbine, is better tolerated when dosed iv versus ip, leading to improved activity in human tumor xenograft studies, *Mol. Cancer Ther.*, 8 (12 Suppl), C232, 2009.
60. ClinicalTrials.gov. Web Page, 30 Oct 2008, NCT00724100.
61. Sheng, L.X., Da, Y.X., Long, Y., Hong, L. Z., and Cho, T.P., Synthesis and biological evaluation of C-12′ substituted vinflunine derivatives, *Bioorg. Med. Chem. Lett.*, 18, 4602, 2008.
62. Kuehne, M.E., Zebovitz, T.C., Bornmann, W.G., and Marko, I., Three routes to the critical C16'-C14' part relative stereochemistry of vinblastine. Syntheses of 20′-desethyl-20′-deoxyvinblastine and 20′-desethyl-20′-deoxyvincovaline, *J. Org. Chem.*, 52, 4340, 1987.
63. Borman, L.S., Kuehne, M.E., Matson, P.A., Marko, I., and Zebovitz, T.C., Single site-modified congeners of vinblastine dissociate its various anti-microtubule actions, *J. Biol. Chem.*, 263, 6945, 1988.
64. Borman, L.S. and Kuehne, M.E., Specific alterations in the biological activities of C-20′-modified vinblastine congeners, *Biochem. Pharmacol.*, 38, 715, 1989.
65. Kuehne, M.E., Cowen, S.D., Xu, F., and Borman, L.S., Synthesis of 5a'-homo-vinblastine and congeners designed to establish structural determinants for isolation of atropoisomers, *J. Org. Chem.*, 66, 5303, 2001.
66. Kuehne, M.E., Qin, Y., Huot, A.E, and Bane, S.L., The synthesis of 16a'-homo-leurosidine and 16a'-homo-vinblastine. Generation of atropoisomers, *J. Org. Chem.*, 66, 5317, 2001.
67. Kuehne, M.E., Bornmann, I., Marko, Y., LeBoulluec, K.L., Frasier, D.A., Xu, F., Mulamba, T. et al., Synthesis and biological evaluation of vinblastine congeners, *Org. Biomol. Chem.*, 1, 2120, 2003.
68. Parish, C.A., Dong, J.-G., Bornmann, W.G., Chang, J., Nakanishi, K., and Berova, N., Circular dichroism studies of bisindole *Vinca* alkaloids, *Tetrahedron*, 54, 15739, 1998.
69. Kruczynski, A., Barret, J.M., Etivant, C., Colpaert, F., Fahy, J., and Hill, B.T., Antimitotic and tubulin-interacting properties of vinflunine, a novel fluorinated *Vinca* alkaloid, *Biochem. Pharmacol.*, 55, 635, 1998.
70. Lobert, S., Fahy, J., Hill, B.T., Duflos, A., Etievant, C., and Correia, J.J., *Vinca* alkaloids-induced tubulin spiral formation correlates with cytotoxicity in the leukemic L1210 cell line, *Biochemistry*, 39, 12053, 2000.
71. Bennouna, J., Fumoleau, P., Armand, J.-P., Raymond, E., Campone, M., Delgado, F.-M., Puozzo, C., and Marty, M., Phase I and pharmacokinetic study of the new *Vinca* alkaloid vinflunine administered as a 10-min infusion every 3 weeks in patients with advanced solid tumours, *Ann. Oncol.*, 14, 630, 2003.
72. Yamaguchi, K., Yasuzawa, T., Sakai, T., and Kobayashi, S., Identification of novel metabolites of vinorelbine in rat, *Xenobiotica*, 28, 281, 1998.
73. Van Heugen, J.C., De Graeve, J., Zorza, G., and Puozzo, C., New sensitive liquid chromatography method coupled with tandem mass spectrometric detection for the clinical analysis of vinorelbine and its metabolites in blood, plasma, urine and faeces, *J. Chromatogr. A*, 926, 11, 2001.

74. Passarella, D., Giardini, A., Peretto, B., Fontana, G., Sacchetti, A., Silvani, A., Ronchi, C. et al., Inhibitors of tubulin polymerization: synthesis and biological evaluation of hybrids of vindoline, anhydrovinblastine and vinorelbine with thiocolchicine, podophyllotoxine and baccatin III, *Bioorg. Med. Chem.*, 16, 6269, 2008.
75. Laguzza, B.C., Nichols, C.L., Briggs, S.L., Cullinan, G.J., Johnson, D.A., Starling, J.J., Baker, A.L., Bumol, T.F., and Corvalan, J.R., New antitumor monoclonal antibody–*Vinca* conjugate LY203725 and related compounds, *J. Med. Chem.*, 32, 548, 1989.
76. Brady, S.F., Pawluczyk, J.M., Lumma, P.K., Feng, D.M., Wai, J.M., Jones, R., DeFeo Jones, D. et al., Design and synthesis of a pro-drug of vinblastine targeted at treatment of prostate cancer with enhanced efficacy and reduced systemic toxicity, *J. Med. Chem.*, 45, 4706, 2002.
77. Vlahov, I.R., Santhapuram, H.K.R., Kleindl, P.J., Howard, S.J., Stanford, K.M., and Leamon, C.P., Design and regioselective synthesis of a new generation of targeted chemotherapeutics. Part 1: EC145, a folic acid conjugate of desacetylvinblastine monohydrazide, *Bioorg. Med. Chem. Lett.*, 16, 5093, 2006.
78. Reddy, J.A., Dorton, R., Westrick, E., Dawson, A., Smith, T., Xu, L.-C., Vetzel, M., Kleindl, P., Vlahov I.R., and Leamon C.P., Preclinical evaluation of EC145, a folate–vinca alkaloid conjugate, *Cancer Res.*, 9, 4434, 2007.
79. ClinicalTrials.gov web page, NCT00507741, NCT00511485 and NCT00722592.
80. Leamon, C.P., Reddy, J.A., Vlahov, I.R., Westrick, E., Dawson, A., Dorton, R., Vetzel, M., Santhapuram, H.K., and Wang, Y., Preclinical antitumor activity of a novel folate-targeted dual drug conjugate, *Mol. Pharm.*, 4, 659, 2007.
81. ClinicalTrials.gov web page, NCT00441870.
82. Cormier, A., Marchand, M., Ravelli, R.B.G., Knossow, M., and Gigant, B., Structural insight into the inhibition of tubulin by vinca domain peptide ligands, *EMBO Rep.*, 9, 1101, 2008.
83. Ngo, Q.A., Roussi, F., Cormier, A., Thoret, S., Knossow, M., Guénard, D., and Guéritte, F., Synthesis and biological evaluation of vinca alkaloids and phomopsin hybrids, *J. Med. Chem.*, 52, 134, 2009.
84. Ngo, Q.A., Roussi, F., Thoret, S., and Guéritte, F., Elaboration of simplified vinca alkaloids and phomopsin hybrids, *Chem. Biol. Drug Des.*, 75, 284, 2010.
85. Lobert, S., Vulevic, B., and Correia, J.J., Interaction of vinca alkaloids with tubulin: a comparison of vinblastine, vincristine, and vinorelbine, *Biochemistry*, 35, 6806, 1996.
86. Kruczynski, A., Colpaert, F., Tarayre, J.P., Mouillard, P., Fahy, J., and Hill, B.T., Preclinical in vivo antitumor activity of vinflunine, a novel fluorinated vinca alkaloid, *Cancer Chemother. Pharmacol.*, 41, 437, 1998.
87. Ngan, V.K., Bellman, K., Hill, B.T., Wilson, L., and Jordan, M.A., Mechanism of mitotic block and inhibition of cell proliferation by the semisynthetic vinca alkaloids vinorelbine and its newer derivative vinflunine, *Mol. Pharmacol.*, 60, 225, 2001.
88. Okouneva, T., Hill, B.T., Wilson, L., and Jordan, M.A., The effects of vinflunine, vinorelbine and vinblastine on centromere dynamics, *Mol. Cancer Ther.*, 2, 427, 2003.
89. Lee, J.J. and Harris, L.N. in *Cancer: Principles and Practice of Oncology*, DeVita V.T., Hellman, S. and Rosenberg, S.A., Eds, Lippincott-Raven, Philadelphia, New York, 8th Edition, 2008, 448–456 and references cited.
90. Johnson, S.A., Harper, P., Hortobagyi, G.N., and Pouillart, P., Vinorelbine: an overview, *Cancer Treat. Rev.*, 22, 127, 1996.
91. Gregory, R.K. and Smith, I.E., Vinorelbine—a clinical review, *Br. J. Cancer*, 82, 1907, 2000.
92. EMEA website, 30 Sep 2009.
93. Pharmaprojects Data Base, Acc. No. 22393.
94. Mano, M., Vinorelbine in the management of breast cancer: new perspectives, revived role in the era of targeted therapy, *Cancer Treat. Rev.*, 32, 106, 2006.
95. Kuttesch, J.F. Jr, Krailo, M.D., Madden, T., Johanse, M., and Bleyer, A., Phase II evaluation of intraveinous vinorelbine (Navelbine) in recurrent or refractory pediatric malignacies: a Children's Oncology Group study, *Pediatr. Blood Cancer*, 53, 590, 2009.
96. Solbach, C., Patt, M., Reimold, M., Blocher, A., Dohmen, B.M., Bares, R., Zeller, K.P., and Machulla, H.J., [11C]Vinblastine—syntheses and preliminary imaging in cancer patients, *J. Pharm. Pharmaceut. Sci.*10, 266s, 2007.
97. Noble, C.O., Guo, Z., Hayes, M.E., Marks, J.D., Park, J.W., Benz, C.C., Kirpotin, D.B., and Drummond, D.C., Characterization of highly stable liposomal and immunoliposomal formulations of vincristine and vinblastine, *Cancer Chemother. Pharmacol.*, 64, 741, 2009.
98. Binet, S., Chaineau, E., Fellous, A., Lataste, H., Krikorian, A., Couzinier, J.P., and Meininger, V., Immunofluorescence study of the action of navelbine, vincristine and vinblastine on mitotic and axonal microtubules, *Int. J. Cancer*, 46, 262, 1990.

99. Hill, S.A., Lonergan, S.J., Denekamp, J., and Chaplin, D.J., Vinca alkaloids: anti-vascular effects in murine tumour, *Eur. J. Cancer*, 29, 1320, 1993.
100. Etiévant, C., Kruczynski, A., Barret, J.M., Tait, A.S., Kavallaris, M., and Hill, B.T., Markedly diminished drug-resistance inducing properties of vinflunine (20′,20′-difluoro-3′,4′-dihydrovinorelbine) relative to vinorelbine, identified in murine and human tumour cells *in vivo* and *in vitro*, with clinical implications, *Cancer Chemother. Pharmacol.*, 48, 62, 2001.
101. Dumontet, C. and Sikic, B.I., Mechanisms of action and resistance to antitubulin agents: microtubule dynamics, drug transport, and cell death, *J. Clin. Oncol*., 17, 1061, 1999.
102. Kavallaris, M., Verrills, N.M., and Hill, B.T., Anticancer therapy with novel tubulin-interacting agents, *Drug Resist. Updat.*, 4, 392, 2001.
103. Baguley, B.C., Holdaway, K.M., Thomsen, L.L., Zhuang, L., and Zwi, L.J., Inhibition of growth of colon 38 adenocarcinoma by vinblastine and colchicine. Evidence for a vascular mechanism, *Eur. J. Cancer*, 27, 482, 1991.
104. Vacca, A., Iurlaro, M., Ribatti, D., Minischetti, M., Nico, B., Ria, R., Pellegrino, A., and Dammacco, F., Antiangiogenesis is produced by non-toxic doses of vinblastine, *Blood*, 94, 4143, 1999.
105. Kruczynski, A. and Hill, B.T., Vinflunine, the latest vinca alkaloid in clinical development. A review of its preclinical anticancer properties, *Crit. Rev. Oncol. Hematol.*, 40, 159, 2001.
106. Kruczynski, A., Poli, M., Dossi, R., Chazottes, E., Berrichon, G., Ricôme, C., Giavazzi, R., Hill, B.T., and Taraboletti, G., Anti-angiogenic, vascular-disrupting and anti-metastatic activities of vinflunine, the latest vinca alkaloid in clinical development, *Eur. J. Cancer*, 42, 2821, 2007.
107. Aapro, M.S., Harper, P., Johnson, S.A., and Vermorken, J., Developments in cytotoxic chemotherapy: advances in treatment utilising vinorelbine, *Crit. Rev. Oncol. Hematol*., 40, 251, 2001.
108. Molnar, A., Liliom, K., Orosz, F., Vértessy, B.G., and Ovádi, J., Anti-calmodulin potency of indol alkaloids in *in vitro* systems, *Eur. J. Pharm*., 291, 73, 1995.
109. Makarov, A.A., Tsvetkov, P.O., Villard, C., Esquieu, D., Pourroy, B., Fahy, J., Braguer, D., Peyrot, V., and Lafitte, D., Vinflunine, a novel microtubule inhibitor, suppresses calmodulin interaction with the microtubule-associated protein STOP, *Biochemistry*, 46, 14899, 2007.
110. Bourgareyl-Rey, V., Savry, A., Hua, G., Carre, M., Bressin, C., Chacon, C., Imbert, J., Braguer, D., and Barra, Y., Transcriptional down-regulation of Bcl-2 by vinorelbine: identification of a novel binding site of p53 on Bcl-2 promoter, *Biochem. Pharmacol*., 78, 1148, 2009.

8 The Bryostatins

David J. Newman

CONTENTS

8.1 Introduction 199
8.2 Biological Activities 200
8.3 Chemical Syntheses of Bryostatins 202
8.4 Clinical Trials of Bryostatin 204
8.5 Other Potential Sources of Bryostatin 1 209
8.5.1 Aquaculture 209
8.5.2 Actual Source of the Bryostatins 210
8.5.3 Chemical Analogs 210
8.6 Conclusions 212
References 213

8.1 INTRODUCTION

The bryostatins (Figure 8.1) are a class of highly oxygenated macrolides originally isolated by the Pettit group under the early NCI program (1955–1982) designed to discover novel antitumor agents from natural sources. The initial discovery (of bryostatin 3; Figure 8.1) was indirectly reported in 1970.[1] Subsequent developments leading to the report of the isolation and x-ray structure of bryostatin 1 (Figure 8.1) in 1982,[2] and the multi-year program that culminated in the isolation and purification of (currently) 20 bryostatin structures, have been well documented by a variety of authors over the years.[3–9]

Structurally, all of the molecules possess a 20-membered macrolactone ring. Modifying the description by Hale et al.,[9,10] all bryostatins possess a 20-membered macrolactone in which there are three remotely substituted pyran rings that are linked by a methylene bridge and an (*E*)-disubstituted alkene; all have geminal dimethyls at C_8 and C_{18}, and a four-carbon sidechain (carbons 4 to 1) from the A ring to the lactone oxygen, with another four carbon chain (carbons 24 to 27) on the other side of the lactone oxygen to the C ring. Most have an exocyclic methyl enoate in their B and C rings, though bryostatin 3, in particular, has a butenolide rather than the C-ring methyl enoate, and bryostatins 16 and 17 have glycals in place of the regular C_{19} and C_{20} hydroxyl moieties. In the early reviews by Hale[9] and Mutter,[7] 18 structures (bryostatins 1–18) are listed; and the remaining two structures were thought to be desoxy-bryostatin 4 and desoxy-bryostatin 5 isolated from *Lissodendoryx isodictyalis*.[11] Work reported from Peoples' Republic of China in 1998 (Chinese)[12] and 2004 (English),[13] gave the structure of bryostatin 19 (Figure 8.1) purified from a South China Sea collection of *Bugula neritina*, which was then followed, also in 2004, by the report of bryostatin 20 (Figure 8.1), isolated from an Atlantic-sourced *Bugula neritina* by Lopanik et al.[14] Comparison with the structures of the other 18 bryostatins shows that these are closely related to bryostatin 3 in terms of their basic ring components. There may well be other naturally occurring versions, as at the end of the bryostatin 20 report, the authors mention at least one more isolable from the larvae that has yet to be fully identified.[14]

The levels of all bryostatins so far isolated from natural sources have always been at the minuscule level, with the highest yield being that of bryostatin 10, where 15 mg was isolated from 1.5 kg of wet animal in a sample collected in the Gulf of Aomori.[15] The actual source of these macrolides

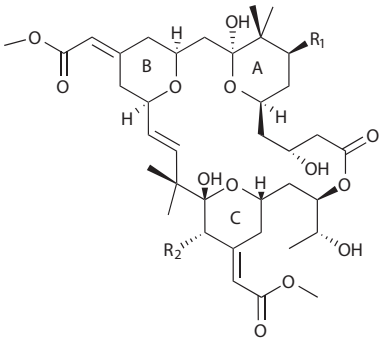

Compound	R_1	R_2
Bryostatin 1	OAc	$OCO(CH)_4n$-Pr
Bryostatin 2	OH	$OCO(CH)_4n$-Pr
Bryostatin 4	$OCOC(CH_3)_3$	OCOn-Pr
Bryostatin 5	$OCOC(CH_3)_3$	OAc
Bryostatin 6	OCOn-Pr	OAc
Bryostatin 7	OAc	OAc
Bryostatin 8	OCOn-Pr	OCOn-Pr
Bryostatin 9	OAc	OCOn-Pr
Bryostatin 10	$OCOC(CH_3)_3$	H
Bryostatin 11	OAc	H
Bryostatin 12	$OCO(CH)_4n$-Pr	OCOn-Pr
Bryostatin 13	OCOn-Pr	H
Bryostatin 14	$OCOC(CH_3)_3$	OH
Bryostatin 15	OAc	$OCO(CH)_4CH(OH)Et$

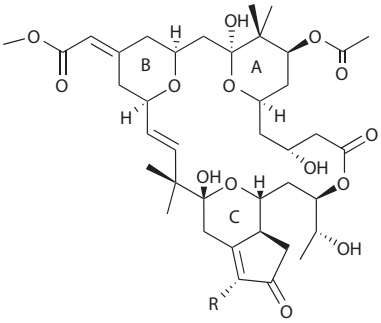

Bryostatin 3 R

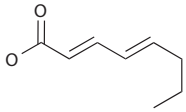

Bryostatin 19

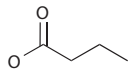

Bryostatin 20 H

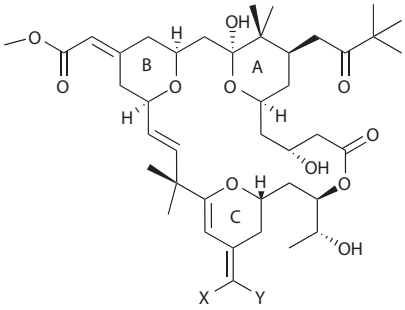

	X	Y
Bryostatin 16	H	$C(O)OCH_3$
Bryostatin 17	$C(O)OCH_3$	H

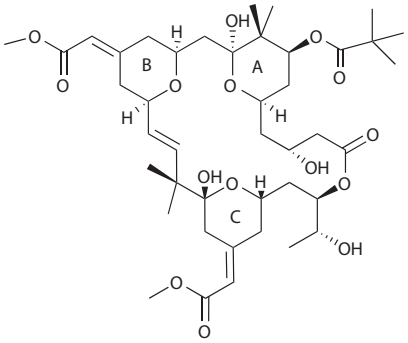

Bryostatin 18

FIGURE 8.1 Structures of the bryostatins.

was debated for a considerable number of years, but there is now significant evidence for microbial involvement and this is discussed in a later section (*vide infra*).

8.2 BIOLOGICAL ACTIVITIES

Almost all the data presented in the following section have been derived from studies with bryostatin 1. However, the basic biology of all the bryostatins is fundamentally the same; they simply differ in potencies in given systems.

Bryostatin 1 exhibited some extremely interesting biological activities from the beginning of testing. Initially, it demonstrated quite variable activities in the then current *in vivo* assays that were used at NCI, which involved the use of the P388 and L1210 murine leukemia lines in normal mice. There was very significant variability in the results from batch to batch but ultimately, using material isolated from *B. neritina* collected in the Gulf of California and from bulked fractions from other collection sites, Pettit et al. were able to publish the structure and some biological activities of bryostatin 1 in 1982.[2] During the initial biological workup of bryostatin fractions by NCI it was realized that the response to P388, L1210, and KB cells mimicked the responses shown by extracts from plants of the families Euphorbiaceae and Thymelaeaceae. The possibility of a phorbol-like structure from *Bugula* seemed remote however, as there had never been reports of either phorbol or daphnane type structures being isolated from marine organisms.[3]

Over the last 20 years, bryostatin 1 has demonstrated a very wide range of biological activities including immune stimulation, differentiation of transformed cells, and enhancement of cytotoxicity of other agents. Initial experiments by Blumberg's group at NCI and their collaborators in subsequent years, demonstrated that bryostatin's anticancer activity was probably based upon its interactions with, and subsequent modulation of protein kinase C isozymes (PKCs) in cells.[16–18] PKCs transfer the terminal phosphate group from ATP following binding of diacylglycerol (DAG) and frequently phosphatidyl serine to the PKC isozyme. As a result of these interactions, PKCs are frequently concentrated at the cytosolic surfaces of cell membranes, and are active at low physiological concentrations of calcium ions, thus modulating the inositol triphosphate (IP_3) cascade within the cell. The recent review by Griner and Kazanietz should also be considered for further information on the interactions between PKC isozymes, phorbol esters (PEs), and other activators.[19]

PKCs can be classified into three major groups; conventional (α, βI/βIII, γ) where Ca^{2+} is required for activation, novel (δ, ϵ, θ, η/L) which are independent of Ca^{2+}, and nontypical (ξ, λ/ι) where no binding by phorbols is known. The first two groups have regulatory and catalytic domains, and the regulatory domain in particular has two cysteine-rich domains known as CRD1 and CRD2. Using binding-displacement studies it was shown that bryostatins, PEs, and DAG all compete for the same binding site(s) on PKC, and by suitable modeling studies, an early pharmacophoric model for DAG and PE was successfully applied to bryostatin binding parameters and also other PKC activators.[20–22] These have subsequently led to the derivation of simpler analogs of the bryostatins and further development of structure–activity relationships by Wender's group at Stanford and later by Keck's group at Utah (see later section).

The main binding sites in the bryostatins included the C_1, C_{19}, and C_{26} oxygen atoms (for convenience, all subsequent comments on chemical analogs will use the bryostatin 1 numeration). This was proven by using chemically modified bryostatins and following their binding affinities with PKC isoforms (see Table 1 in Mutter and Wills[7] for relative binding affinities), but in spite of studies with these agents and other related compounds following cell line responses, no complete explanation as to why the biological response(s) between bryostatin and PE is (are) so different has emerged to date; however, as will be discussed in a later section, by modification of the base structure of bryostatin 1, Keck's group has shown that alteration of the A ring can lead to molecules that give bryostatin-like rather than PE-like results in suitable experimental systems.[23]

When the specific effects of bryostatin 1 on PKC in cell lines were studied in detail, it was found that although bryostatin down-regulated PKC, the expression of PKC was not directly affected. From both x-ray studies of phorbol 13-acetate bound to murine PKC-δ and the nuclear magnetic resonance (NMR) solution structure of a PKC-α CRD2 construct, it was determined that the phorbol esters sit in a polar groove that exists at the tip of the CRD. In addition, binding of such an "activator" does not appear to effect any significant conformational change in the binding domain. Thus the "activator" sits over the inside polar surface of the groove creating a continuous hydrophobic surface covering approximately one-third of the complexed protein. This hydrophobicity increase of the PKC–δ-phorbol ester complex probably promotes its insertion into the plasma membrane, where it can then engage in signaling related to tumorigenesis.[24] It is likely that when bryostatin 1

binds to the CRDs of PKCs, similar changes occur, though specific differences may well occur with different PKCs.

Thus with PKC-δ, where there appears to be a "stabilizing effect" that prevents insertion into the membrane, and then its subsequent degradation via the ubiquitin–proteosome pathway, it is possible that the conformational changes are different than those that occur with PKC-α and PKC-ε where they undergo downregulation via the degradation pathway. For further details as to the potential route of degradation of ubiquitinylated PKCs, scheme 2 in the review by Hale et al.[9] should be referred.

Further evidence for specific binding site/overlaps is given in the 2003 publication from Hale's group where they demonstrated, using solution NMR techniques, that bryostatin 1 (or more precisely, an analog with specific structural features), does overlap its binding site(s) with those of phorbol-13-acetate and phorbol-12,13-dibutyrate in the CRD2 site of human PKC-α.[25] Very recent computational work by Keck's group shows that these are reasonable descriptions of the binding site, and in addition, they demonstrated that the 9-OH group in bryostatin 1, which was thought to be essential for the activity of the bryostatins, is only weakly involved in the differential effects of bryostatins and PEs.[26]

In addition to the interaction with PKCs, a very significant amount of evidence has accumulated that suggests that bryostatin 1, and by inference, other similar compounds, with the possible exception of the 20-deoxy class such as bryostatin 13, can function as very potent immunostimulants. Thus, resting T cells and neutrophils are activated both *in vitro* and *in vivo*,[27–30] and in clinical trials, it has been shown to raise circulating levels of tumor necrosis factor-α (TNF-α) which is normally produced by the body following immunostimulation.[31] In *in vitro* studies with the murine macrophage line, ANA-1, treatment with bryostatin 1 significantly increased TNF-α mRNA expression, and also exhibited synergy with interferon-γ in the production of nitrite and the subsequent expression of the inducible nitric oxide synthetase gene. This gene catalyzes the *in vivo* production of NO from L-arginine, and NO is known to produce strong tumoricidal effects upon murine macrophages, probably via induction of the apoptotic cascade.[32] Thus, bryostatins may well be exerting some of their effects via immunomodulation pathways.[33]

In contrast, bryostatin 13, a 20-deoxy-bryostatin, does not stimulate colony formation in bone marrow progenitor cells whereas bryostatins 1, 3, 8, and 9 do; in addition, bryostatin 13 is claimed to be more potent as an antitumor agent than the other four.[32] Thus, there might be a component of immunostimulation in the antitumor activities of the C_{20}-*O*-acyl bryostatins that is not present in the 20-deoxy class.

In 2003, Battle and Frank suggested that one potential mechanism of bryostatin 1 mediated differentiation in human chronic lymphocytic leukemia (CLL) cells was activation of the signal transducer and activator of transcription (STAT). Thus, in cells taken from clinical trial patients, bryostatin 1 appeared to activate STAT1 in a PKC-dependent manner by induction of an IFN-γ autocrine loop; which led to activation of the JAK–STAT1 signaling pathway and ultimate differentiation of the cells.[34]

There are also reports that imply that bryostatin 1 under certain conditions might have some tumor-inducing capability, though this is an extrapolation from cell line studies. In studies where it was demonstrated that bryostatin 1 can selectively target PKC-βII isozymes in K562 (human erythroleukemia) and HL60 (human promyelocytic) cell lines, such treatment led to membrane translocation and lamin B phosphorylation at specific sites on the lamin proteins. Such translocation/phosphorylation causes breakdown of the nuclear envelope during mitosis, and in these cells such an effect appears to be associated with enhanced proliferation.[35] Thus, care might have to be taken in choosing patients for bryostatin treatment (see later section on clinical trials).

8.3 CHEMICAL SYNTHESES OF BRYOSTATINS

From the initial reports on the structures of the bryostatins, chemists recognized the base molecule as a challenge for their synthetic skills. A significant number of syntheses of parts of the bryostatin 1 molecule have been reported over the years, with an early example being a discussion of routes to

bryostatin 1 by Masamune in 1988.[36] Four total syntheses of various members of the complex have been reported since the initial disclosure of the base structure. The first was the enantiomeric synthesis of bryostatin 7 in 1990 by Masamune's group,[37] being followed a few years later in the 1998–1999 time frame, by papers from the Evans' group giving details of an enantiomeric synthesis of bryostatin 2.[38,39] The third in this initial series was the report by Nishiyama and Yamamura in 2000[40] of the synthesis of bryostatin 3; this was expanded on with respect to the strategies developed by Ohmori in 2004.[41] However, prior to the publication of the 2004 review by Ohmori, these earlier syntheses together with the reported partial syntheses of other bryostatins were reviewed in detail through 2002 by Hale et al.[9]

In 2006, Hale's group reported on their formal total synthesis of bryostatin 7, using a route designed to permit syntheses of other novel analogs that would not have been accessible via the original Masamune route.[42] What was most interesting about this synthetic route was the painstaking operations that the group had to perform on one key intermediate, the AB fragment (Figure 8.2; **1**). They found that although the 500 MHz proton spectrum in deuterochloroform did appear to be congruent with the desired structure, it did not match the 300 MHz proton spectrum, also reported

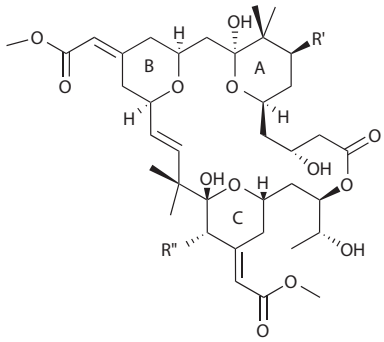

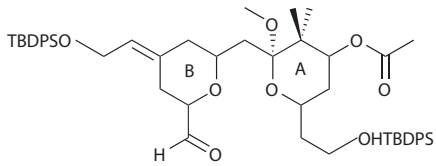

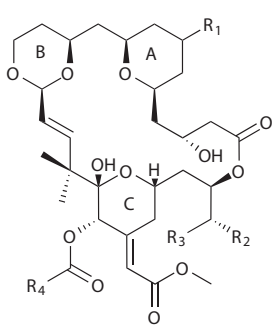

2a, 2b, 2c

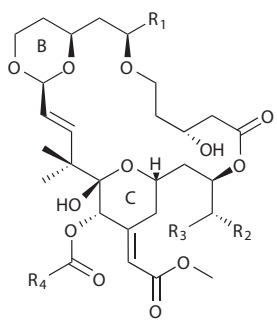

3a, 3b

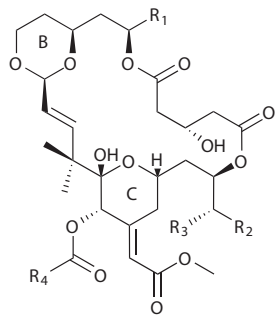

4

Compound	R_1	R_2	R_3	R_4	Ki (nM)
2a	H	OH	CH_3	C_7H_{15}	3.4
2b	H	OH	H	C_7H_{15}	0.25
2c	H	OAc	CH_3	C_7H_{15}	10000.0
3a	t-Bu	OH	CH_3	C_7H_{15}	8.3
3b	H	OH	CH_3	C_7H_{15}	47.0
3c	H	OH	H	C_7H_{15}	8.0
3d	*p*Br-Phenyl	OH	H	C_7H_{15}	1.6
4	$C(CH_3)_2C_2H_5$	OH	CH_3	C_7H_{13}	8.42

FIGURE 8.2 Bryologs and Masamune's intermeditate.

in deuterochloroform by Masamune in 1990. Resolution of these differences took almost 3 years, including use of an authenticated (*S*)-glycidol for the B ring and an authenticated ketone for the synthesis of the A-ring fragment. After 3 years they had confirmed the identities of many previously reported intermediates, but still could not match the spectral characteristics reported by Masamune. Then they happened to notice that some of the intermediate compounds were unstable in deuterochloroform due to the adventitious presence of aqueous HCl in the commercial solvent. On redetermination of the 500 MHz proton NMR in deuterobenzene, all of the resonances matched with the earlier report. Thus it appeared that the original 300 MHz proton spectrum by Masamune's group was in deuterobenzene, not in the deuterochloroform as reported. As a result, in 2006 the Hale group was able to report the formal total synthesis of bryostatin 7 using a route that could be modified to produce novel analogs.

Two years later in 2008, Trost and Dong[43] published their relatively simple and quite elegant synthesis of bryostatin 16 involving use of novel metal-linked catalysis steps[44] that included a ruthenium tandem alkyne–enone coupling, and then a palladium catalyzed alkyne–ynoate macrocyclization to give the cyclized precursor of bryostatin 16.

In spite of all of these elegant methods, to date, no *de novo* synthesis of bryostatin 1 has been published, though in the early days of studying the bryostatins, Pettit et al. demonstrated that bryostatin 2 could be converted to bryostatin 1 and bryostatin 12.[45] Thus, one could argue that a formal synthesis of bryostatin 1 has been achieved by using the bryostatin 2 asymmetric synthesis of Evans et al.[38,39] and then applying the Pettit conversion method.

A truly excellent compendium coupled to a thorough discussion of the chemistry efforts around the synthesis of the bryostatins was recently published by Hale and Manaviazar. It should be read in conjunction with this chapter by any chemists interested in the manifold methods/specific methodological differences that can be, and have been used in both successful and unsuccessful syntheses of these agents.[10]

8.4 CLINICAL TRIALS OF BRYOSTATIN

Although a number of bryostatins have been tested in animals and many have had *in vitro* assessments in many cell lines, only bryostatin 1 entered human clinical trials. Part of the reason is that this compound could be obtained in quantities large enough to be able to produce the compound under cGMP conditions. The history of the initial attempts at large-scale isolations and the methods ultimately used are given in the 1996 review by Newman, and are also covered to some extent in the 1991 and 1996 reviews by Pettit.[4–6] These should be consulted for the details as to sources and methods. As a result of these endeavors, enough cGMP-grade material was produced from wild collections to provide a source for most of the clinical trials shown in Tables 8.1 and 8.2. The trials in the United Kingdom in the early 1990s were not performed using the batches made under NCI's auspices; they were provided by Pettit, but subsequent trials have all used the NCI-sourced materials.

To date, there have been reports in the literature from 8 Phase I (1993–2002) and 16 Phase II (1998–2003) trials where bryostatin 1 was used as monotherapy (Table 8.1). There have also been reports of nine Phase I trials where bryostatin 1 was used in conjunction with vincristine, paclitaxel, cytosine arabinoside (AraC), fludarabine, gemcitabine (GC), temsirolimus, and cisplatin from 1999 to 2009. Commencing in 2002, there have been reports from eight Phase II trials with five combined with paclitaxel, and one each with cisplatin, vincristine, and interleukin (IL)-2 up to mid-2010 (Table 8.2).

Initially, bryostatin 1 demonstrated some partial responses in Phase I trials with myalgia being the predominant dose-limiting toxicity. Subsequent Phase I and Phase II trials with bryostatin as monotherapy, using a variety of treatment regimens in patients with carcinomas ranging from solid tumors (melanomas, renal, and ovarian) to varied leukemias, did not give consistent response patterns whether measured as stable disease (SD), partial (PR), or complete responses (CR). With the Phase II trials, there would be an occasional CR or PR and some SDs, but no consistent responses were observed over the patient population in the trial. However, when one inspects the patient populations from the aspect

TABLE 8.1
Published Data Summary of Bryostatin-1 Monotherapy

Year	Phase	Schedule	Dose Range	Tumor Type(s)	# Pts	CR	PR	SD	Side Effects	Reference
1993	I	1 h infusion; repeated at 14 days for 3 cycles	05–65	Varied	19	0	0	0	Myalgia; phlebitis	Prendiville et al.[46]
1993	I	1 h infusion; 7-, 14-, or 21-day cycle with varied number of cycles	25–50	Varied	35	0	2	0	Myalgia	Philip et al.[31]
1995	I	24 h infusion; repeated at 7-day intervals for a maximum of 8 cycles	25–50	Varied	19	0	4	0	Myalgia; phlebitis	Jayson et al.[47]
1998	I	24–72 h infusions; repeated at 14 days for 4–42 cycles	12–180	NHL, CLL	29	0	0	11	Myalgia	Varterasian et al.[48]
1998	Ib	0.5–24 h infusion; repeated at 8 and 15 days; then repeated at 28 days for a varied number of cycles	12.5–25	Varied	12	0	0	0	Myalgia	Grant et al.[49]
1999	I	No information		Advanced melanoma					None given	Tozer[50]
1999	I	1 h infusion; repeated at 8 and 15 days; then repeated at 28 days for a varied number of cycles	20–57	Varied	22	0	0	4	Myalgia; photophobia	Weitman et al.[51]
2002	I	4–14 days infusions; repeated at 14–21-day intervals; 2–3 cycles	08–24	Varied	37	0	0	6	Myalgia; fatigue	Marshall et al.[52]
1998	II	1 h infusion; repeated at 8 and 15 days; then repeated at 28 days for 1–6 cycles	25	Melanoma	15	0	0	1	Myalgia	Propper et al.[53]
1999	II	1 h infusion; repeated at 8 and 15 days; then repeated at 28 days for 0.67–8 cycles	25	Melanoma	17	0	0	1	Myalgia	Gonzalez et al.[54]
2000	II	72 h infusion; repeated at 14 days for 4–14 cycles.	120	NHL, CLL	25	1	2	2	Myalgia	Varterasian et al.[55]
2000	II	1 h infusion; repeated at 8 and 15 days; then repeated at 28 days for 1–14 cycles	25	RCC	30	1[a]	1[a]	0	Anemia; myalgia	Pagliaro et al.[56]
2001	II	24 h infusion; repeated at 8 and 15 days; then repeated at 28 days for 2–4 cycles	25–35	CRC	28	0	0	0	Myalgia	Zonder et al.[57]
2001	II	24 h infusion; repeated at 8 and 15 days; then repeated at 28 days 72 h infusion; repeated at 15 days; then repeated at 28 days for 2–4 cycles	25–40	Melanoma	49	0	1	14	Myalgia	Bedikian et al.[58]

continued

TABLE 8.1 (continued)
Published Data Summary of Bryostatin-1 Monotherapy

Year	Phase	Schedule	Dose Range	Tumor Type(s)	# Pts	CR	PR	SD	Side Effects	Reference
2001	II	24 h infusion; repeated weekly for 1–9 cycles	25	NHL	14	0	0	1	Myalgia	Blackhall et al.[59]
2001	II	72 h infusion; at 14-day intervals for 2–8 cycles	9	MM	9	0	0	0	Myalgia	Varterasian et al.[60]
2001	II	72 h infusion; at 14-day intervals for 3 cycles.	120	Sarcoma, HNC	24	0	0	6	Myalgia; hyponatremia	Brockstein et al.[61]
2002	II	24 h infusion; repeated at 8 and 15 days; then repeated at 28 days for 1–5 cycles.	25	HNC	14	0	0	1	Myalgia (grade I)	Pfister et al.[62]
2002	II	24 h infusion (low dose); every 7 days 72 h infusion (high dose); every 14 days for 1–31 cycles	25–120	Melanoma	30	0	0	7	Myalgia	Tozer et al.[63]
2003	II	1 h infusion; repeated at 8 and 15 days; then repeated at 28 days for 1–8 cycles.	35–40	RCC	32	0	2	15	Myalgia	Haas et al.[64]
2003	II	24 h infusion (low dose); 1, 8, and 15 days; then repeated every 28 days 72 h infusion (high dose); every 14 days for 1–9 cycles	25–120	Ovarian	54	0	1[a]	19	Myalgia	Armstrong et al.[65]
2003	II	24 h infusion; repeated every 7 days for 1–9 cycles.	19–25	Ovarian	17	0	0	4[a]	Myalgia	Clamp et al.[66]
2003	II	24 h infusion; repeated at 8 and 15 days; then repeated every 28 days for 1–9 cycles	25	RCC	13	0	0	3[a]	Myalgia	Madhusudan et al.[67]
2003	II	24 h infusion (low dose); repeated at 8 and 15 days; then repeated every 28 days 72 h infusion (high dose); every 14 days for varied cycles	25–120	Cervical	65	0	2	20	Myalgia	Armstrong et al.[68]

Note: CLL, chronic lymphocytic leukemia; CR, complete response; CRC, colorectal carcinoma; HNC, head and neck carcinoma; MM, multiple myeloma; NHL, non-Hodgkin's lymphoma; PR, partial response; RCC, renal cell carcinoma; SD, stable disease.

TABLE 8.2
Combination Therapy with Cytotoxic Drugs

Year	Phase	Schedule	Dose Range	Tumor Type(s)	# Pts	CR	PR	SD	Side Effects	Reference
1999	I	No information (abstract only)		Advanced melanoma	17				Tox due to cisplatin	Rosenthal et al.[69]
2001\2003	I	24 h infusion and bolus of vincristine; dose escalation of bryostatin; 1–5 cycles	12.5–62.5 μg M^2 bryostatin; 1.4 mg · M^2V	B-cell cancer	25	1	2	4	Myalgia; neuropathy	Dowalti et al.[70,71]
2002	I	Bryostatin plus paclitaxel; no other information (abstract only)	No information	Esophageal	12				Myalgia	Kortmansky et al.[72]
2002	I	24 h infusion; days 1 and 11; AraC on days 2, 3, 9, and 10; bryostatin dose escalation, fixed AraC; 1–6 cycles	12.5–50 μg M^2 bryostatin; 1–3 g M^2 AraC	Leukemia	23	5	1[a]	0	Myalgia; neutropenia	Cragg et al.[73]
2002 and 2006	I	24 h infusion; FAra for days 2–6; repeat at 28 days; or reverse addition order; 6–9+ cycles	16–50 μg M^2 bryostatin; 12.5–25 mg M^2 FAra	CLL, NHL	59	4	20	?	Neutropenia	Roberts et al.[74–76]
2003 and 2006	I	GC 30 min infusion, bryostatin over 24 h, days 1, 8, and 15 on 28-day cycle	Bryostatin (μg M^2); gemcitabine (mg M^2) at 25/600 to 45/1000	Varied	36	0	2	8	Myalgia	El-Reyes et al.[77,78]
2006	I	Bryostatin plus CCI-779 (temsirolimus); no other information (abstract only)	No information	Varied	9				No information	Hass[79]
2009	I	Bryostatin 1 h or 24 h i.v. plus cisplatin 1 h i.v.; every 2–3 weeks	10–85 μg M^2 bryostatin; 50–75 mg M^2 cisplatin	Varied solid tumors	53	0	4	20	Very low number of G3 tox	Pavlick et al.[80]
2009	I	Bryostatin plus CCI-779 (temsirolimus); no other information (abstract only)	No information	RCC	23					Wong et al.[81]

continued

TABLE 8.2 (continued)
Combination Therapy with Cytotoxic Drugs

Year	Phase	Schedule	Dose Range	Tumor Type(s)	# Pts	CR	PR	SD	Side Effects	Reference
2003	II	1 h infusion of paclitaxel on 1, 8, and 15 days; 24 h infusion of bryostatin on 2, 9, and 16 days; repeated on 28-day cycle; 1–4 cycles	40–50 μg M^2 bryostatin; 90 mg M^2 paclitaxel	NSCLC	11	0	2[a]	5	Myalgia	Winegarden et al.[82]
2003	II	No information (abstract only)	Bryostatin and paclitaxel	Gastric	37				None represented	Chang et al.[83]
2004	II	1 h infusion of bryostatin followed by cisplatin; repeated every 21 days	50–65 μg M^2 bryostatin; 50 mg M^2 cisplatin	Cervical	14	0	0	2	Myalgia; anemia	Nezhat et al.[84]
2006	II	2 h infusion paclitaxel followed by bryostatin over 1 h 24 h later; 3 of 4 weeks.	40 μg M^2 bryostatin; 80 mg M^2 paclitaxel	Gastric	35	1	9	12	Myalgia	Ajani et al.[85]
2006	II	Interleukin-2 (IL-2) on days 1–4, 8–11, and 15–18 of 28-day cycle; bryostatin on days 1, 8, and 15 after first IL-2 cycle over 1 h	11×10^6 IU s.c.; 5–35 μg M^2 bryostatin i.v.	RCC	31	0	1	11	Fatigue; nausea	Peterson et al.[86]
2008	II	Paclitaxel on day 1; then bryostatin on day 2 every week for 3 of 4 weeks	25–50 μg M^2 bryostatin; 80–90 mg M^2 paclitaxel	Gastric	22	0	6	8	Myalgia	Ku et al.[87]
2009	II	Bryostatin 24 h i.v. infusion followed by vincristine i.v. bolus; repeated every 14 days	50 μg M^2 i.v. bryostatin; 1.4–2.0 mg M^2 vincristine i.v.	NHL after autologous stem cell transplant	13	2	2	6	Neutropenia	Barr et al.[88]
2010	II	Paclitaxel over 1 h on days 1, 8, and 15 and bryostatin over 1 h on days 2, 9, and 16 for 28-day cycle (1–10 cycles)	90 mg M^2 paclitaxel; 25 μg M^2 bryostatin	Advanced pancreatic carcinoma	19	0	1	9	Myalgia, leukopenia	Lam et al.[89]

[a] Some question as to the response level.

Note: ? indicates 23 "nondefined" objective response; CLL, chronic lymphocytic leukemia; CR, complete response; NHL, non-Hodgkin's lymphoma; NSCLC, nonsmall-cell lung cancer; PR, partial response; RCC, renal cell carcinoma; SD, stable disease.

of the type(s) of carcinomas, then from the knowledge that is now accruing as to dose-limiting toxicities and methods/timing of administration, there are potential reasons as to why monotherapy with bryostatin is not optimal, except perhaps in a very selective cohort of leukemia patients (see earlier comments on choice of patients because of potential tumorigensis in some carcinoma lines).

However, when bryostatin was combined with another cytotoxin, such as the vinca alkaloids, paclitaxel or nucleosides, and the carcinomas are leukemic in nature, then the response rates, even in Phase I trials began to demonstrate some responses in these mixed treatments. These responses can be seen from inspection of Table 8.2 for those reports where full details are given. At the time of writing of this chapter for the first edition, Kortmansky and Schwartz wrote a prospective review that showed the then current viewpoint that the combination of bryostatin with a cytotoxin may well "indicate a new direction in cancer therapy."[90]

Currently (August 2010), there is one Phase I trial (bryostatin with temsirolimus) that is listed as "still recruiting" (NCT00112476) directed against solid tumors, and one Phase II trial investigating vincristine and bryostatin directed against non-Hodgkin's lymphoma (NHL) underway (NCT00058305) that is listed as "Active but not recruiting" on the NCI clinical trials website (http://clinicaltrials.nci.nih.gov). Results from this latter Phase II trial have been reported recently with the investigators commenting as follows at the end of their article:

> Although assurance of continued clinical development of bryostatin 1 is remote, we are aware that more potent bryostatin analogs (e.g., bryologs) are entering the clinical arena for further testing. Our study further supports the clinical development of this class of potentially interesting and important modulators of protein kinase C.[88]

As noted earlier in this section, some of the early Phase I responses were when the cancers investigated were leukemic in nature. Whether more trials of this nature will be conducted is unknown, but bryostatin itself may well have another therapeutic potential in Alzheimer's disease (see later discussion), so clinical work, though not cancer-directed is still ongoing.

8.5 OTHER POTENTIAL SOURCES OF BRYOSTATIN 1

8.5.1 Aquaculture

All the work reported to date has been with material from wild collections, made predominately in either the Gulf of California or in the Pacific Ocean off Palos Verdes, California. However, it became obvious, even as the initial trials were beginning in the early 1990s, that wild collections would not suffice and production via chemical synthesis would probably not be viable. Thus in the early 1990s, NCI, utilizing the Small Business Innovation Research program (SBIR), established a Phase I and a subsequent Phase II aquaculture program with a small company, CalBioMarine, with the aim of investigating on-land and in-sea aquaculture for production of *Bugula neritina* under conditions that were not affected by the vagaries of Nature. This series of projects was successful, culminating in the proof by CalBioMarine that the organism could be grown under both conditions, and also that bryostatin could be isolated from the aquacultured animal in quantities and at costs less than those incurred in wild collections.[91]

Concomitantly with the Phase II aquaculture experiments, NCI also used the SBIR mechanism to investigate, with the Massachusetts Company Aphios, the potential for super-critical extraction of bryostatins from *B. neritina*, utilizing both wild collections and some of the material from aquaculture. This was successful and a demonstration of the potential for such methods was shown in the review by Newman[6] where a comparison was made of the methods used for the earlier cGMP purification versus the Aphios technique. The earlier method used for cGMP production involved a four-stage extraction–concentration process, and then a six-step process repeated 15 times in order to produce 18 g of bryostatin 1 from 13 metric tonnes of *B. neritina*. The overall process was multi-week in duration and used massive amounts of solvents. In contrast, the super-critical

technique used basically carbon dioxide as the extraction medium on the wet animal mass, followed by supercritical chromatography, and the process was reduced to six simple operations performed within days, yielding material of similar purity.

8.5.2 Actual Source of the Bryostatins

An interesting observation arising from the search for bryostatin sources was that, despite the ubiquitous occurrence of the nominal producing organism, the number of *B. neritina* colonies actually producing detectable bryostatin 1–3 levels was very low and geographically widespread.

One of the discoveries made from the collections made by Calbiomarine of wild *B. neritina* as a source for their aquaculture work, during which time they were collaborating with the Haygood group of ecological microbiologists at the Scripps Institution of Oceanography, was that there appeared to be two potential subspecies, one from deep (below ~10 m) and one from shallow (above ~7 m) waters, which appeared to have different levels of bryostatins associated with them.

Haygood's group proceeded with their investigation of the bacterial flora associated with these bryozoans, and from their initial data, suggested that the actual producer of the bryostatins was a previously unrecognized and as yet, noncultured bacterium.[92] Over the next 10+ years, in conjunction with experts in gene identification and cloning, Haygood and her collaborators have been able to identify and clone, but not yet express in a heterologous host, the putative biosynthetic cluster that should produce a macrolidic structure that they call bryostatin 0, which might then be capable of being further elaborated by as yet unidentified tailoring enzymes to produce the bryostatin molecules isolated to date.

In the multitudinous studies that led to this proposal, Haygood and her collaborators investigated the potential sources of bryostatins both in the adult animal and in the larvae. In a series of excellent initial investigations, they demonstrated that within the larvae of bryostatin-producing animals there were as yet uncultured bacteria given the name of *Candidatus Endobugula sertula* in the first report by Davidson and Haygood in 1999[93] and extended in 2001.[94]

A series of later papers included a review of the possibilities of identification and expression of genes from symbionts,[95] the identification of different symbionts from other *Bugula* species that produced bryostatins and contained similar gene constructs,[96] together with the identification of the putative *bryA* cluster.[97] Further work by Lopanik et al. on Atlantic-sourced, rather than Pacific or Gulf Coast-sourced, *B. neritina*, has confirmed the presence of *bryA*-like fragments from this geographic area's organisms as well.[98]

It should be emphasized that in none of the aforesaid reports does the identification of the *bryA* cluster in these organisms prove the absolute production of bryostatins by the symbiont, but the evidence is highly suggestive. Currently, the complete putative genomic sequence has been identified and sequenced but not yet expressed,[99] but it does include the recognition of an unusual trans acylase,[100] a phenomenon that has also been reported in the genes related to the biosynthesis of the pederin-like marine sourced antitumor agents of the mycalamide group,[101] and which might turn out to be a commonplace finding as the information on marine-microbe clusters develops. Finally, in addition to the genomic work related to bryostatin biosynthesis in a variety of *Bugula* species and locations, recent studies by Haygood and collaborators have demonstrated that bryostatins are important molecules from an ecological as well as a pharmacological perspective, apparently aiding in site recognition for settlement and reproduction.[100,102,103]

8.5.3 Chemical Analogs

Even today, the total synthesis of bryostatin 1 is not a feasible process for the production of this agent in any quantity suitable for clinical development, though as mentioned before, the "formal synthesis of bryostatin 1" could be claimed by combination of the bryostatin 2 synthesis coupled to the Pettit interconversion method. However, the synthesis of a simpler analog with comparable

activity might well be a viable option. In order to have a molecular insight into what were the essential binding sites required for bryostatin activation of PKC, in 1986, Wender et al. commenced this task by analyzing the potential binding site of the phorbol esters on PKC as a guide to the design of simpler analogs of these agents.[20] In 1988, this work was expanded by modeling bryostatin 1 onto the same binding site as a result of the initial results indicating that bryostatin 1 interacted with PKC.[21] Subsequently, the modeling work was refined to produce three analogs that would maintain the putative binding sites at the oxygen atoms at C_1 (ketone), C_{19} (hydroxyl), and C_{26} (hydroxyl) in the original molecule. These binding sites were independently confirmed almost 15 years later in work reported by Hale et al. in 2003.[25]

By utilizing these requirements, Wender's group initially synthesized structures **2a**, **3a**, and **3b** (Figure 8.2), which maintained the recognition features but removed a significant amount of the peripheral substituents. These molecules demonstrated nanomolar binding constants when measured in displacement assays of tritiated phorbol esters, with the figures being in the same general range as bryostatin 1, and **2a** and **3a** had activities in *in vitro* cell line assays close to those demonstrated by bryostatin 1 itself.[104–107] Following on from these examples, modifications were made to the base structure (Figure 8.2) to introduce a second lactone **4** (Figure 8.2) which had 8 nM binding affinity and also inhibited P388 with an ED_{50} of 113 nM.[108] Concomitantly, modifications were made to the base analog **2a** where different fatty acid esters were made (structures not shown). These too, exhibited binding affinities for PKC isozymes in the 7–232 nM range depending upon the fatty acid used.[109]

To show the versatility of the base structure, in 2002, Wender et al. published a simple modification where, by removal of a methyl group in the C_{26} sidechain from compound **2a** to produce **2b** (Figure 8.2), the binding affinity to PKC was increased to the picomolar level,[110] and the compound demonstrated greater potency than bryostatin 1 in *in vitro* cell line assays. This latter work was expanded upon in 2003, when both improved syntheses of the molecule designed to permit further refinements of the model, and proceeding in greater overall yields, were reported.[111,112] It was here that the first edition of this chapter ended.

In the intervening years, the Wender group has continued to provide ever more novel agents, with much fuller details through the middle of 2005 being reported in a 2007 book chapter.[113] They confirmed that deletion of the A ring[114,115] (first reported in the references related to structures **3a** and **3b**) maintained activity. This work subsequently yielded molecules such as **3c** with 8 nM K_i value against PKC and, following addition of a bromophenyl group at position C(9) to give **3d**, comparable in potency with bryostatin 1 against PKC[116] (Figure 8.2). The most recently reported series which maintain the A, B, and C rings, are the two isomeric molecules (Figure 8.3) derived from **5a**, **5b,** and **5c** which have activities in the nM to sub nM range versus the K562 leukemia cell line, with a total synthetic sequence of 38 steps.[117]

Wender's group is not the only one producing synthetic "bryologs." Over the last few years, Keck's group at Utah in conjunction with Peter Blumberg at NIH (the original discoverer of the bryostatin–PKC interaction) have reported quite extensively on a series of compounds exemplified by **6a**–**6c** (Figure 8.3) with PKC binding potencies comparable to bryostatin, having K_is in the range of 0.7–1 nM.[118] In later papers, Keck et al. have reported on activities from these compounds (also known as Merle 21–23; **6a, b,** and **c,** respectively),[119] and those of an "almost bryostatin" (Merle 28; structure **7a** in Figure 8.3)[119] whose synthesis was also described in 2009.[23]

By using information from these compounds together with data from the synthesis and bioassay of Merle 30 (C9-deoxy bryostatin 1; **7b** in Figure 8.3; K_i of 0.38 nM versus PKC), Keck et al. recently reported that bryostatin 1 and Merle 30 (**7b**) behave almost identically in that they do not inhibit the proliferation of the prostate line LNCap, but do antagonize phorbol 12-myristate-13 acetate (PMA) inhibition. On comparison of the response to induction of TNF-α secretion, all three behave differently, with PMA giving a very potent induction, bryostatin having no observable effect and Merle 30 (**7b**) showing a very weak response. The reasonable conclusion that they draw from these results is that the C9-hydroxyl has only a very weak effect on both the binding affinity for bryostatin and the specific biological responses to this agent.[26]

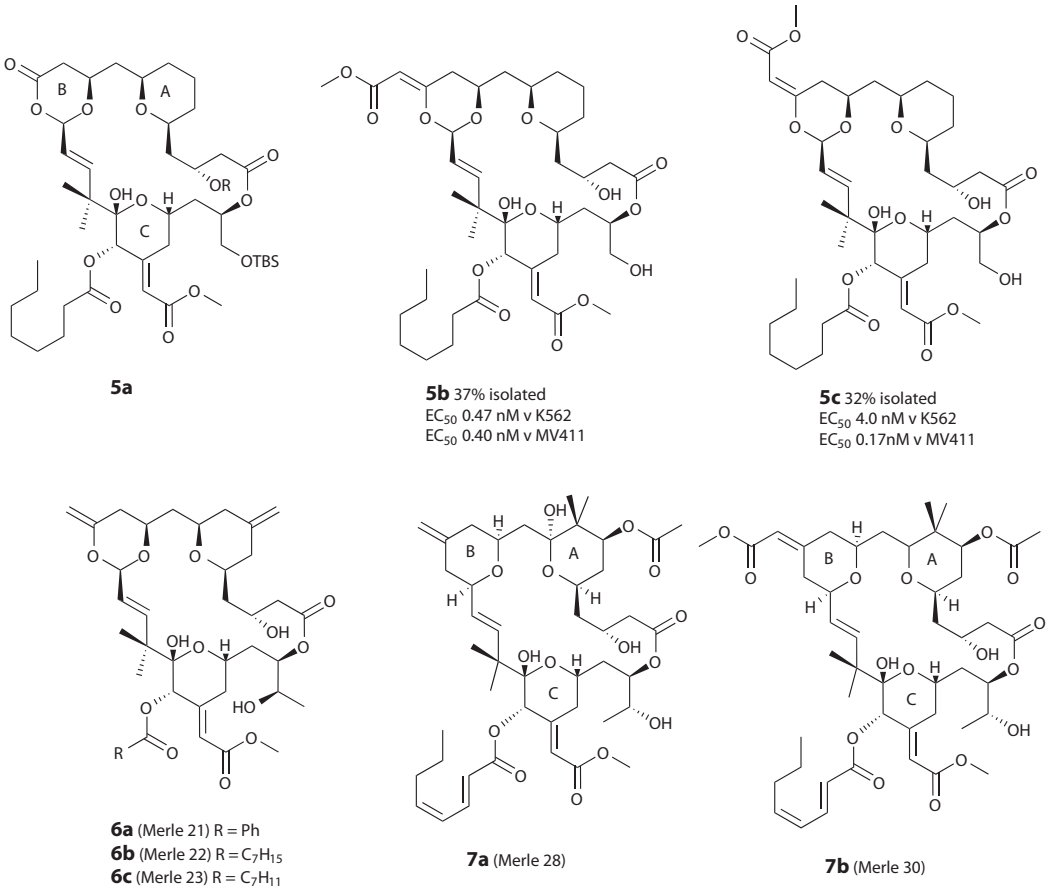

FIGURE 8.3 Wender's later Bryologs and Keck's Merle series.

For this section, and also for the details of bryostatin syntheses, rather than insert the various synthetic schemes that have been used to produce these analogs and their parents, readers who wish to see the specific synthetic details are recommended to peruse the extensive and scholarly review by Hale and Manaviazar[10] who describe the syntheses in exquisite detail through late 2009.

8.6 CONCLUSIONS

One may make the following points from the data given in this chapter:

The unique structural motifs that are part of the bryostatin molecule have now undergone a significant amount of clinical testing. Monotherapy does not appear to be efficacious, and except for the responses reported recently for the Phase II trial of vincristine and bryostatin in NHL[88] the rest of the reported Phase I/II studies do not show consistent patterns of response.

The problems of supply have been addressed both biologically and chemically. Although aquaculture-based production is feasible, the identification of a potential bryostatin 0 gene cluster from the putative microbial symbiont appears to have greater potential, even though it has not as yet been expressed, nor has the "host microbe" been isolated and purified.

The production by total synthesis of simpler "bryologs," exhibiting similar or better levels of biological activity in both cell lines and against PKC isozymes, holds promise for the development of more effective and simpler analogs, as they are enabling the identification of the minimum spatial requirements for significant activity.

Finally, since the first edition was published, bryostatin 1 has been shown to have some potential as a treatment for Alzheimer's disease. This aspect of bryostatin's pharmacology has been identified as a result of work performed by researchers at the University of West Virginia.[120–124] That simpler analogs of bryostatin also may have utility in this disease has been recently demonstrated in a paper published in conjunction with Wender's group[125] indicating that the bryolog known as "picolog" (Figure 8.2; **2b)**[110] could mimic bryostatin in an alpha-secretase cellular model.

This result, coupled to the recent approval by the FDA for a Phase II clinical trial of bryostatin 1 in Alzheimer's patients under the ClinicalTrials.gov identifier number NCT00606164, shows that bryostatin in one version or another may yet have therapeutic potential.

REFERENCES

1. Pettit, G.R., Day, J.F., Hartwell, J.L. and Wood, H.B., Antineoplastic components of marine animals. *Nature*, 227, 962, 1970.
2. Pettit, G.R., Herald, C.L., Doubeck, D.L., Herald, D.L., Arnold, E. and Clardy, J., Isolation and structure of bryostatin 1. *J. Am. Chem. Soc.*, 104, 6846, 1982.
3. Suffness, M., Newman, D.J. and Snader, K.M., Discovery and development of antineoplastic agents from natural sources. In: *Bioorganic Marine Chemistry*. Scheuer P., Ed., Springer-Verlag: Berlin-Heidelberg, 1989; Vol. 3, p. 131.
4. Pettit, G.R., The bryostatins. In: *Progress in the Chemistry of Organic Natural Products*. Hertz W., Kirby G.W., Steglich W. and Tamm C., Eds., Springer-Verlag: New York, 1991; Vol. 57, p. 153.
5. Pettit, G.R., Progress in the discovery of biosynthetic anticancer drugs. *J. Nat. Prod.*, 59, 812, 1996.
6. Newman, D.J., Bryostatin—from bryozan to cancer drug. In: *Bryozoans in Space and Time*. Gordon D.P., Smith A.M. and Grant-Mackie J.A., Eds., NIWA: Wellington, NZ, 1996; p. 9.
7. Mutter, R. and Wills, M., Chemistry and clinical biology of the bryostatins. *Bioorg. Med. Chem.*, 8, 1841, 2000.
8. Pettit, G.R., Herald, C.L. and Hogan, F., Biosynthetic products for anticancer drug design and treatment — the bryostatins. In: *Anticancer Drug Development*. Baguley B.C. and Kerr D.J., Eds., Academic Press: San Diego, 2002; p. 203.
9. Hale, K.J., Hummersone, M.C., Manaviazar, S. and Frigerio, M., The chemistry and biology of the bryostatin antitumour macrolides. *Nat. Prod. Rep.*,19, 413, 2002.
10. Hale, K.J. and Manaviazar, S., New approaches to the total synthesis of the bryostatin antitumor macrolides. *Chem. Asian J.*, 5, 704, 2010.
11. Pettit, G.R., Kamano, Y., Herald, C.L., Schmidt, J.M. and Zubrod, C.G., Relationship of *Bugula neritina* (*Bryozoa*) antineoplastic constituents to the yellow sponge *Lyssodendoryx isodictyalis. Pure Appl. Chem.*, 58, 415, 1986.
12. Lin, H., Yao, X., Yi, Y., Li, X. and Wu, H., Bryostatin 19: A new antineoplastic compound from *Bugula neritina* in South China Sea. *Zhongguo Haiyang Yaowu*, 17, 1, 1998.
13. Lin, H., Liu, G., Yi, Y., Yao, X. and Wu, H., Studies on antineoplastic constituents from marine bryozoan *Bugula neritina* inbiting South China Aea: Isolation and structural elucidaiton of a novel macrolide. *Dier Junyi Daxue Xuebao*, 25, 473, 2004.
14. Lopanik, N., Gustafson, K.R. and Lindquist, N., Structure of Bryostatin 20: A symbiont-produced chemical defense for larvae of the host bryozoan, *Bugula neritina. J. Nat. Prod.*, 67, 1412, 2004.
15. Kamano, Y., Zhang, H.-P., Hino, A., Yoshida, M., Pettit, G.R., Herald, C.L. and Itokawa, H., An inproved source of bryostatin 10, *Bugula neritina* from the Gulf of Aomori, Japan. *J. Nat. Prod.*, 58, 1868, 1995.
16. Hennings, H., Blumberg, P.M., Pettit, G.R., Herald, C.L., Shores, R. and Yuspa, S.H., Bryostatin 1, an activator of protein kinase C, inhibits tumor promotion by phorbol esters in SENCAR mouse skin. *Carcinogenesis*, 8, 1343, 1987.
17. Blumberg, P.M., Pettit, G.R., Warren, B.S., Szallasi, A., Schuman, L.D., Sharkey, N.A., Nakakuma, H., Dell'Aquila, M.L. and de Vries, D.J., The protein kinase C pathway in tumor promotion. *Prog. Clin. Biol. Res.*, 298, 210, 1989.

18. Szallasi, Z., Smith, C.B., Pettit, G.R. and Blumberg, P.M., Differential regulation of protein kinase C isozymes by bryostatin 1 and phorbol 12-myristate 13-acetate in NIH 3T3 fibroblasts. *J. Biol. Chem.*, 269, 2118, 1994.
19. Griner, E.M. and Kazanietz, M.G., Protein kinase C and other diacylglycerol effectors in cancer. *Nat. Revs. Cancer*, 7, 281, 2007.
20. Wender, P.A., Koehler, K.F., Sharkey, N.A., Dell'Aquila, M.L. and Blumberg, P.M., Analysis of the phorbol ester pharmacophore on protein kinase C as a guide to the rational design of new classes of analogs. *Proc. Natl. Acad. Sci., USA* 83, 4214, 1986.
21. Wender, P.A., Cribbs, C.M., Koehler, K.F., Sharkey, N.A., Herald, C.L., Kamano, Y., Pettit, G.R. and Blumberg, P.M., Modeling of the bryostatins to the phorbol ester pharmacophore on protein kinase C. *Proc. Natl. Acad. Sci., USA* 85, 7917, 1988.
22. Lee, J., Kang, J.-H., Lee, S.-Y., Han, K.-C., Torres, C.M., Bhattacharyya, D.K., Blumberg, P.M. and Marquez, V.E., Protein kinase C ligands based on tetrahydrofuran templates containing a new set of phorbol ester pharmacophores. *J. Med. Chem.*, 42, 4129, 1999.
23. Keck, G.E., Poudel, Y.B., Welch, D.S., Kraft, M.B., Truong, A.P., Stephens, J.C., Kedei, N., Lwin, N.E. and Blumberg, P.M., Substitution on the A-ring confers to bryopyran analogues the unique biological activity characteristic of Bryostatins and distinct from that of the phorbol esters. *Org. Lett.*, 11, 593, 2009.
24. Zhang, G.G., Kazanietz, M.G., Blumberg, P.M. and Hurley, J.H., Crystal-structure of the CYS2 activator-binding domain of protein kinase C-delta in complex with phorbol ester. *Cell*, 81, 917, 1995.
25. Hale, K.J., Frigerio, M., Manaviazar, S., Hummersone, M.C., Fillingham, I.J., Barsukov, I.G., Damblon, C.F., Gescher, A. and Roberts, G.C.K., Synthesis of a simplified bryostatin C-ring analogue that binds to the CRD2 of human PKC-alpha and construction of a novel BC-analogue by an unusual Julia olefination process. *Org. Lett.*, 5, 499, 2003.
26. Keck, G.E., Poudel, Y.B., Rudra, A., Stephens, J.C., Kedei, N., Lewin, N.E., Peach, M.L. and Blumberg, P.M., Molecular modeling, total synthesis, and biological evaluation of C9-deoxy Bryostatin 1. *Angew. Chem. Int. Ed.*, 49, 4580, 2010.
27. May, W.S., Sharkis, S.J., Esa, A.H., Gebbia, V., Kraft, A.S., Pettit, G.R. and Sensenbrenner, L.L., Antineoplastic bryostatins are multipotential stimulators of human hematopoietic progenitor cells. *Proc. Natl. Acad. Sci. USA*, 84, 8483–8487, 1987.
28. Hess, A.D., Silanskis, M.K., Esa, A.H., Pettit, G.R. and May, W.S., Activation of human T lymphocytes by bryostatin. *J. Immunol*, 141, 3263, 1988.
29. Berkow, R.L., Schlabach, L., Dodson, R., Benjamin, Jr, W.H., Pettit, G.R., Rustage, P. and Kraft, A.S., *In vivo* administration of the anticancer agent bryostatin 1 activates platelets and neutrophils and modulates protein kinase C activity. *Cancer Res.*, 53, 2810, 1993.
30. Esa, A.H., Warren, J.T., Hess, A.D. and May, W.S., Bryostatins trigger human polymorphonuclear neutrophil and monocyte oxidative metabolism: association with *in vitro* antineoplastic activity. *Res. Immunol.*, 146, 351, 1995.
31. Philip, P.A., Rea, D., Thavasu, P., Carmichael, J., Stuart, N.S., Rockett, H., Talbot, D.C. et al., Phase I study of bryostatin 1: assessment of interleukin 6 and tumor necrosis factor alpha induction *in vivo*. The Cancer Research Campaign Phase I Committee. *J. Natl. Cancer Inst.*, 85, 1812, 1993.
32. Taylor, L.S., Cox, G.W., Melillo, G., Bosco, M.C. and Espinoza-Delgardo, I., Bryostatin and IFN-gamma synergize for the expression of the inducible nitric oxide synthetase gene and for nitric oxide production in murine macrophages. *Cancer Res.*, 57, 2468, 1997.
33. Scheid, C., Prendiville, J., Jayson, G., Crowther, D., Fox, B., Pettit, G.R. and Stern, P.L., Immunomodulation in patients receiving intravenous bryostatin 1 in a phase I clinical study: comparison with effects of bryostatin 1 on lymphocyte function in vitro. *Cancer Immunol. Immunother.*, 39, 223, 1994.
34. Battle, T.E. and Frank, D.A., STAT1 mediates differentiation of chronic lymphocytic leukemia cells in response to bryostatin 1. *Blood*, 102, 3016, 2003.
35. Hocevar, B., Burns, D.J. and Fields, A.P., Indentification of protein kinase C (PKC) phosphorylation sites on human lamin B. *J. Biol. Chem.*, 268, 7545, 1993.
36. Masamune, S., Asymmetric synthesis and its applications: towards the synthesis of bryostatin 1. *Pure Appl. Chem.*, 60, 1587, 1988.
37. Kageyama, M., Tamura, T., Nantz, M.H., Roberts, J.C., Somfai, P., Whritenour, D.C. and Masamune, S., Synthesis of bryostatin 7. *J. Am. Chem. Soc.*, 112, 7407, 1990.
38. Evans, D.A., Carter, P.H., Carreira, E.M., Prunet, J.A., Charette, A.B. and Lautens, M., Asymmetric synthesis of bryostatin 2. *Angew. Chem. Int. Ed.*, 37, 2354, 1998.
39. Evans, D.A., Carter, P.H., Carreira, E.M., Charette, A.B., Prunet, J.A. and Lautens, M., Total synthesis of bryostatin 2. *J. Am. Chem. Soc.*, 121, 7540, 1999.

40. Ohmori, K., Ogawa, Y., Obitsu, T., Ishikawa, Y., Nishiyama, S. and Yamamura, S., Total synthesis of bryostatin 3. *Angew. Chem. Int. Ed.*, 39, 2290, 2000.
41. Ohmori, K., Evolution of synthetic strategies for highly functionalized natural products: A successful route to bryostatin 3. *Bull. Chem. Soc. Japan*, 77, 875, 2004.
42. Manaviazar, S., Frigerio, M., Bhatia, G.S., Hummersone, M.G., Aliev, A.E. and Hale, K.I., Enantioselective formal total synthesis of the antitumor macrolide bryostatin 7. *Org. Lett.*, 8, 4477, 2006.
43. Trost, B.M. and Dong, G., Total synthesis of bryostatin 16 using atom-economical and chemoselective approaches. *Nature*, 456, 485, 2008.
44. Miller, A.K., Catalysis in the total synthesis of bryostatin 16. *Angew. Chem. Int. Ed.*, 48, 3221, 2009.
45. Pettit, G.R., Sengupta, D., Herald, C.L., Sharkey, N.A. and Blumberg, P.M., Synthetic conversion of bryostatin 2 to bryostatin 1 and related bryopyrans. *Can. J. Chem.*, 69, 856, 1991.
46. Prendiville, J., Crowther, D., Thatcher, N., Woll, P.J., Fox, B.W., McGown, A., Testa, N. et al., A phase I study of intravenous bryostatin 1 in patients with advanced cancer. *Br. J. Cancer*, 68, 418, 1993.
47. Jayson, G.C., Crowther, D., Prendiville, J., McGown, A. T., Scheid, C., Stern, P., Young, R. et al., A phase I trial of bryostatin 1 in patients with advanced malignancy using a 24 hour intravenous infusion. *Br. J. Cancer*, 72, 461, 1995.
48. Varterasian, M.L., Mohammad, R.M., Eilender, D.S., Hulburd, K., Rodriguez, D.H., Pemberton, P.A., Pluda, J.M. et al., Phase I study of bryostatin 1 in patients with relapsed non-Hodgkin's lymphoma and chronic lymphocytic leukemia. *J. Clin. Oncol*, 16, 56, 1998.
49. Grant, S., Roberts, J., Poplin, E., Tombes, M.B., Kyle, B., Welch, D., Carr, M. and Bear, H.D., Phase Ib trial of bryostatin 1 in patients with refractory malignancies. *Clin. Cancer Res.*, 4, 611, 1998.
50. Tozer, R.G., NCIC CTG randomized phase II study of two schedules of Bryostatin 1 (NSC339555) in patients with advanced malignant melanoma (IND. 104). *Proc. Am. Soc. Clin. Oncol,*. 18, 2052a, 1999.
51. Weitman, S., Langevin, A.-M., Berkow, R.L., Thomas, P.J., Hurwitz, C.A., Kraft, A.S., Dubowy, R.L., Smith, D.L. and Bernstein, M., A phase I trial of bryostatin-1 in children with refractory solid tumors: A pediatric oncology group study. *Clin. Cancer Res.*, 5, 2344, 1999.
52. Marshall, J.L., Bangalore, N., El-Ashry, D., Fuxman, Y., Johnson, M., Norris, B., Oberst, M. et al., Phase I study of prolonged infusion bryostatin-1 in patients with advanced malignancies. *Cancer Biol. Ther.*, 1, 409, 2002.
53. Propper, D.J., Macaulay, V., O'Byrne, K.J., Braybrooke, J.P., Wilner, S.M., Ganesan, T.S., Talbot, D.C. and Harris, A.L., A phase II study of bryostatin 1 in metastatic malignant melanoma. *Br. J. Cancer*, 78, 1337, 1998.
54. Gonzalez, R., Ebbinghaus, S., Henthorn, T.K., Miller, D. and Kraft, A.S., Treatment of patients with metastatic melanoma with bryostatin-1 – a phase II study. *Melanoma Res.*, 9, 599, 1999.
55. Varterasian, M.L., Mohammad, R.M., Shurafa, M.S., Hulburd, K., Pemberton, P.A., Rodriguez, D.H., Spadoni, V. et al., Phase II trial of bryostatin 1 in patients with relapsed low-grade non-Hodgkin's lymphoma and chronic lymphocytic leukemia. *Clin. Cancer Res.*, 6, 825, 2000.
56. Pagliaro, L., Daliani, D., Amato, R., Tu, S.-M., Johnes, D., Smith, T., Logothetis, C. and Millikan, R., A phase II trial of bryostatin -1 for patients with metastatic renal cell carcinoma. *Cancer*, 89, 615, 2000.
57. Zonder, J.A., Shields, A.F., Zalupski, M., Chaplen, R., Heilbrun, L.K., Arlauskas, P. and Philip, P.A., A phase II trial of bryostatin 1 in the treatment of metastatic colorectal cancer. *Clin. Cancer Res.*, 7, 38, 2001.
58. Bedikian, A.Y., Plager, C., Stewart, J.R., O'Brian, C.A., Herdman, S.K., Ross, M., Papadopoulos, N., Eton, O., Ellerhorst, J. and Smith, T., Phase II evaluation of bryostatin-1 in metastatic melanoma. *Melanoma Res.*, 11, 183, 2001.
59. Blackhall, F.H., Ranson, M., Radford, J.A., Hancock, B.W., Soukop, M., McGown, A.T., Robbins, A., Halbert, G. and Jayson, G.C., A phase II trial of bryostatin 1 in patients with non-Hodgkin's lymphoma. *Br. J. Cancer*, 84, 465, 2001.
60. Varterasian, M.L., Pemberton, P.A., Hulburd, K., Rodriguez, D.H., Murgo, A. and Al-Katib, A.M., Phase II study of bryostatin 1 in patients with relapsed multiple myeloma. *Investig. New Drugs*, 19, 245, 2001.
61. Brockstein, B., Samuels, B., Humerickhouse, R., Arietta, R., Fishkin, P., Wade, J., Sosman, J. and Vokes, E.E., Phase II studies of bryostatin-1 in patients with advanced sarcoma and advanced head and neck cancer. *Investig. New Drugs*, 19, 249, 2001.
62. Pfister, D.G., McCaffrey, J., Zahalsky, A.J., Schwartz, G.K., Lis, E., Gerald, W., Huvos, A. et al., A phase II trial of bryostatin-1 in patients with metastatic or recurrent squamous cell carcinoma of the head and neck. *Investig. New Drugs*, 20, 123, 2002.
63. Tozer, R.G., Burdette-Radoux, S., Berlanger, K., Davis, M.L., Lohmann, R.C., Rusthoven, J.R., Wainman, N., Zee, B. and Seymour, L., A randomized phase II study of two schedules of bryostatin-1 (NSC339555) in patients with advanced malignant melanoma. *Investig. New Drugs*, 20, 407, 2002.

64. Haas, N.B., Smith, M., Lewis, N., Littman, L., Yeslow, G., Joshi, I.D., Murgo, A. et al., Weekly bryostatin-1 in metastatic renal cell carcinoma: A phase II study. *Clin. Cancer Res.*, 9, 109, 2003.
65. Armstrong, D.K., Blessing, J.A., Look, K.Y., Schilder, R. and Nunez, E.V., A randomized phase II evaluation of bryostatin-1 (NSC #339555) in recurrent or persistent platinum-sensitive ovarian cancer: A Gynecologic Oncology Group Study. *Investig. New Drugs*, 21, 373, 2003.
66. Clamp, A.R., Blackhall, F.H., Vasey, P., Soukop, M., Coleman, R., Halbert, G., Robson, L. and Jayson, G.C., A phase II trial of bryostatin-1 administered by weekly 24-hour infusion in recurrent epithelial ovarian carcinoma. *Br. J. Cancer*, 89, 1152, 2003.
67. Madhusudan, S., Protheroe, A., Propper, D., Han, C., Corrie, P., Earl, H., Hancock, B. et al., A multicentre phase II trial of bryostatin-1 in patients with advanced renal cancer. *Br. J. Cancer*, 89, 1418, 2003.
68. Armstrong, D.K., Blessing, J.A., Rader, J. and Sorosky, J.I., A randomized phase II evaluation of bryostatin-1 (NSC #339555) in persistent or recurrent squamous cell carcinoma of the cervix: A Gynecologic Oncology Group Study. *Investig. New Drugs*, 21, 453, 2003.
69. Rosenthal, M.A., Oratz, R., Liebes, L., Chahr, M.H. and Muggia, F.M., Phase I study of bryostatin-1 (NSC 339555) and cisplatinin in advanced malignancies. *Proc. Am. Soc. Clin. Oncol.*, Abs 873, 1999.
70. Dowlati, A., Payne, J., Robertson, P., Ksenich, P., Makkar, V., Overmoyer, B., Jacobberger, J. et al., Phase I trial of combination bryostatin-1 and vincristine in B-cell malignancies: final report. *Clin. Cancer Res.*, 7 (Supplement), 3814s Abs 800, 2001.
71. Dowlati, A., Lazarus, H.M., Hartman, P., Jacobberger, J., W., Whitacre, C., Gerson, S.L., Ksenich, P. et al., Phase I and correlative study of combination Bryostatin 1 and Vincristine in relapsed B-Cell malignancies. *Clin. Cancer Res.*, 9, 5929, 2003.
72. Kortmansky, J., Shah, M.A., Ilson, D., Kaubisch, A., Endres, S., Welch, M., Gonen, M., Kelsen, D.P. and Schwartz, G.K., Reponse to the combination of Bryostatin-1 and paclitaxel is dose-dependent. *Proc. AACR.*, 43, 2737a, 2002.
73. Cragg, L., Andreeff, M., Feldman, E., Roberts, J., Murgo, A., Winning, M., Tombes, M.B., Roboz, G., Kramer, L. and Grant, S., Phase I trial and correlative laboratory studies of bryostatin 1 (NSC 339555) and high-dose 1-B-D-arabinofuranosylcytosine in patients with refractory acute leukemia. *Clin. Cancer Res.*, 8, 2123, 2002.
74. Roberts, J.D., Feldman, E.J., Smith, M.R. and Grant, S., Phase I trial of bryostatin 1 (NSC339555) and fludarabine in patients with chronic lymphocytic leukemia and indolent non-Hodgkins lymphoma. *Blood*, 100, 1495a, 2002.
75. Roberts, J.D., Smith, M.R., Feldman, E.J., Cragg, L. and Grant, S., Phase I study of bryostatin-1 and fludarabine in patients with chronic lymphocytic leukemia and indolent non-Hodgkin's lymphoma. *Clin. Lymphoma*, 3, 184, 2002.
76. Roberts, J.D., Smith, M.R., Feldman, E.J., Cragg, L., Millenson, M.M., Roboz, G.J., Honeycutt, C. et al., Phase I study of bryostatin 1 and fludarabine in patients with chronic lymphocytic leukemia and indolent (Non-Hodgkin's) lymphoma. *Clin. Cancer Res.*, 12, 5809, 2006.
77. Ibrahim, D., El-Rayes, B.F., Gadgeel, S.M., Lorusso, P. and Philip, P.A., A phase I study of the protein kinase C modulator bryostatin-1 and gemcitabine. *Proc. Am. Soc. Clin. Oncol.*, 930a, 2003.
78. El-Rayes, B.F., Gadgeel, S., Shields, A.F., Manza, S., Lorusso, P. and Philip, P.A., Phase I study of bryostatin 1 and gemcitabine. *Clin. Cancer Res.*, 12, 7059, 2006.
79. Haas, N.B., Phase I study of intravenous CCI-779 in combination with bryostatin-1 in solid tumors. *Proc. Am. Soc. Clin. Oncol.*, 3067a, 2006.
80. Pavlick, A.C., Wu, J., Roberts, J., Rosenthal, M.A., Hamilton, A., Wadler, S., Farrell, K. et al., Phase I study of bryostatin 1, a protein kinase C modulator, preceding cisplatin in patients with refractory non-hematologic tumors. *Cancer Chemother. Pharmacol.*, 64, 803, 2009.
81. Wong, Y., Hudes, G.R., Von Mehren, M., Malizzia, L., Roethke, S.K., Litwin, S. and Haas, N.B., Phase I study of temsirolimus (TEM) and bryostatin (BRYO) in patients with metastatic renal cell carcinoma (RCC). *Genitourin. Cancers Symp.*, 313a, 2009.
82. Winegarden, J.D., Mauer, A.M., Gajewski, T.F., Hoffman, P.C., Krauss, S., Rudin, C.M. and Vokes, E.E., A phase II study of bryostatin-1 and paclitaxel in patients with advanced non-small cell lung cancer. *Lung Cancer*, 39, 191, 2003.
83. Chang, B.B., Bleyer, A.W., Faust, J., Yao, J., Craig, C. and Ajani, J.A., Phase II study of Bryostatin-1 (NSC 339555) plus Paclitaxel in patients with metastatic or unresectable locally advanced adenocarcinoma of stomach or gastroesophageal junction. *Proc. Am. Soc. Clin. Oncol.*, 22, 1060a, 2003.
84. Nezhat, F., Wadler, S., Muggia, F., Mandeli, J., Goldberg, G., Rahaman, J., Runowicz, C., Murgo, A.J. and Gardner, G.J., Phase II trial of the combination of bryostatin-1 and cisplatin in advanced or recurrent carcinoma of the cervix: A New York Gynecologic Oncology Group study. *Gynecol. Oncol.*, 93, 144, 2004.

85. Ajani, J.A., Jiang, Y., Faust, J., Chang, B.B., Ho, L., Yao, J.C., Rousey, S. et al., A multi-center phase II study of sequential paclitaxel and bryostatin-1 (NSC 339555) in patients with untreated, advanced gastric or gastroesophageal junction adenocarcinoma. *Investig. New Drugs*, 24, 353, 2006.
86. Peterson, A.C., Harlin, H., Karrison, T., Vogelzang, N.J., Knost, J.A., Kugler, J.W., Lester, E., Vokes, E., Gajewski, T.F. and Stadler, W.M., A randomized phase II trial of interleukin-2 in combination with four different doses of bryostatin-1 in patients with renal cell carcinoma. *Investig. New Drugs*, 24, 141, 2006.
87. Ku, G.Y., Ilson, D.H., Schwartz, L.H., Capanu, M., O'Reilly, E., Shah, M.A., Kelsen, D.P. and Schwartz, G.K., Phase II trial of sequential paclitaxel and 1 h infusion of bryostatin-1 in patients with advanced esophageal cancer. *Cancer Chemother. Pharmacol.*, 62, 875, 2008.
88. Barr, P.M., Lazarus, H.M., Cooper, B.W., Schluchter, M.D., Panneerselvam, A., Jacobberger, J.W., Hsu, J.W. et al., Phase II study of bryostatin 1 and vincristine for aggressive non-Hodgkin lymphoma relapsing after an autologous stem cell transplant. *Am. J. Hematol.*, 84, 484, 2009.
89. Lam, A.P., Sparano, J.A., Vinciguerra, V., Ocean, A.J., Christos, P., Hochster, H., Camacho, F., Goel, S., Mani, S. and Kaubisch, A., Phase II study of paclitaxel plus the protein kinase C inhibitor bryostatin-1 in advanced pancreatic carcinoma. *Am. J. Clin. Oncol.*, 33, 121, 2010.
90. Kortmansky, J. and Schwartz, G.K., Bryostatin-1: A novel PKC inhibitor in clinical development. *Cancer Invest.*, 21, 924, 2003.
91. Mendola, D., Aquaculture of three phyla of marine invertebrates to yield bioactive metabolites: Process development and economics. *Biomol. Engin.*, 20, 441, 2003.
92. Haygood, M.G. and Davidson, S.K., Small-subunit rRNA genes and *in situ* hybridization with oligonucleotides specific for the bacterial symbionts in the larvae of the bryozoan *Bugula neritina* and proposal of '*Candidatus endobugula sertula*'. *Appl. Environ. Microbiol.*, 63, 4612, 1997.
93. Davidson, S.K. and Haygood, M.G., Identification of sibling species of the bryozoan *Bugula neritina* that produce different anticancer bryostatins and harbor distinct strains of the bacterial symbiont "*Candidatus* Endobugula sertula". *Biol. Bull.*, 196, 273, 1999.
94. Davidson, S.K., Allen, S.W., Lim, G.E., Anderson, C.M. and Haygood, M.G., Evidence for the biosynthesis of bryostatins by the bacterial symbiont "*Candidatus* Endobugula sertula" of the bryozoan *Bugula neritina. Appl. Environ. Microbiol.*, 67, 4531, 2001.
95. Hildebrand, M., Waggoner, L.E., Lim, G.E., Sharp, K.H., Ridley, C.P. and Haygood, M.G., Approaches to identify, clone and express symbiont bioactive metabolite genes. *Nat. Prod. Rep.*, 21, 122, 2004.
96. Lim, G.E. and Haygood, M.G., *Candidatus* Endobugula glebosa, a specific bacterial symbiont of the marine bryozoan *Bugula simplex. Appl. Environ. Microbiol.*, 70, 4921, 2004.
97. Hildebrand, M., Waggoner, L.E., Liu, H., Sudek, S., Allen, S., Anderson, C., Sherman, D.H. and Haygood, M., *bryA*: An unusual modular polyketide synthase gene from the uncultivated bacterial symbiont of the marine bryozoan *Bugula neritina. Chem. Biol.*, 11, 1543, 2004.
98. Lopanik, N., Targett, N.M. and Lindquist, N., Isolation of two polyketide synthase gene fragments from the unclutured microbial symbiont of the marine bryozoan *Bugula neritina. Appl. Environ. Microbiol.*, 72, 7941, 2006.
99. Sudek, S., Lopanik, N.B., Waggoner, L.E., Hildebrand, M., Anderson, C., Liu, H., Patel, A., Sherman, D.H. and Haygood, M.G., Identification of the putative bryostatin polyketide synthase gene cluster from "*Candidatus Endobugula sertula*", the uncultivated microbial symbiont of the marine bryozoan *Bugula neritina. J. Nat. Prod.*, 70, 67, 2007.
100. Lopanik, N.B., Shields, J.A., Buchholz, T.J., Rath, C.M., Hothersall, J., Haygood, M.G., Håkansson, K., Thomas, C.M. and Sherman, D.H., *In vivo* and *in vitro trans*-acylation by *bryP*, the putative Bryostatin pathway acyltransferase derived from an uncultured marine symbiont. *Chem. Biol.*, 15, 1175, 2008.
101. Zimmermann, K., Engeser, M., Blunt, J.W., Munro, M.H.G. and Piel, J., Pederin-type pathways of uncultivated bacterial symbionts: Analysis of O-methyltransferases and generation of a biosynthetic hybrid. *J. Am. Chem. Soc.*, 131, 2780, 2009.
102. Paul, V.J., Arthur, K.E., Ritson-Williams, R., Ross, C. and Sharp, K.H., Chemical defenses: From compounds to communities. *Biol. Bull.*, 213, 226, 2007.
103. Lim-Fong, G.E., Regali, L.A. and Haygood, M.G., Evolutionary relationships of "*Candidatus endobugula*" bacterial symbionts and their *Bugula* bryozoan hosts. *Appl. Environ. Microbiol.*, 74, 3605, 2008.
104. Wender, P.A., De Brabander, J., Harran, P.G., Hinkle, K.W., Lippa, B. and Pettit, G.R., Synthesis and biological evaluation of fully synthetic bryostatin analogues. *Tetrahedron Lett.*, 39, 1998.
105. Wender, P.A., De Brabander, J., Harran, P.G., Jimenez, J.-M., Koehler, M.T.F., Lippa, B., Park, C.-M. and Shiozaki, M., Synthesis of the first members of a new class of biologically active bryostatin analogues. *J. Am. Chem. Soc.*, 120, 1998.

106. Wender, P.A., De Brabander, J., Harran, P.G., Jimenez, J.-M., Koehler, M.T.F., Lippa, B., Park, C.-M., Siedenbiedel, C. and Pettit, G.R., The design, computer modeling, solution structure, and biological evaluation of synthetic analogs of bryostatin 1. *Proc. Natl. Acad. Sci. USA*, 95, 6624, 1998.
107. Wender, P.A., Hinkle, K.W., Koehler, M.T.F. and Lippa, B., The rational design of potential chemotherapeutic agents: Synthesis of bryostatin analogues. *Med. Res. Revs.*, 19, 388, 1999.
108. Wender, P.A. and Lippa, B., Synthesis and biological evaluation of bryostatin analogues: the role of the A-ring. *Tetrahedron Lett.*, 41, 1007, 2000.
109. Wender, P.A. and Hinkle, K.W., Synthesis and biological evaluation of a new class of bryostatin analaogues: the role of the C20 substituent in protein kinase C binding. *Tetrahedron Lett.*, 41, 6725, 2000.
110. Wender, P.A., Baryza, J.L., Bennett, C.E., Bi, F.C., Brenner, S.E., Clarke, M.O., Horan, J.C. et al., The practical synthesis of a novel and highly potent analogue of bryostatin. *J. Am. Chem. Soc.*, 124, 13648, 2002.
111. Wender, P.A., Mayweg, A.V.W. and VanDeusen, C.L., A concise, selective synthesis of the polyketide spacer domain of a potent bryostatin analogue. *Org. Lett.*, 5, 277, 2003.
112. Wender, P.A., Koehler, M.T.F. and Sendzik, M., A new synthetic approach to the C ring of known as well as novel bryostatin analogues. *Org. Lett.*, 5, 4549, 2003.
113. Wender, P.A., Baryza, J.L., Hilinski, M.K., Horan, J.C., Kan, C. and Verma, V.A., Beyond natural products: Synthetic analogues of Bryostatin 1. In: *Drug Discovery Research: New Frontiers in the Post-Genomic Era*. Huang Z., Ed., Wiley: New York, 2007; p. 127.
114. Wender, P.A., Baryza, J.L., Brenner, S.E., Clarke, M.O., Craske, M.L., Horan, J.C. and Meyer, T., Function oriented synthesis: The design, synthesis, PKC binding and translocation activity of a new bryostatin analog. *Curr. Drug Discov. Tech.*, 1, 1, 2004.
115. Wender, P.A., Verma, V.A., Paxton, T.J. and Pillow, T.H., Function-oriented synthesis, step economy, and drug design. *Acc. Chem. Res.*, 41, 40, 2008.
116. Wender, P.A. and Horan, J.C., Synthesis and PKC binding of a new class of A-ring diversifiable Bryostatin analogues utilizing a double asymmetric hydrogenation and cross-coupling strategy. *Org. Lett.*, 8, 4581, 2006.
117. Wender, P.A., DeChristopher, B.A. and Schrier, A.J., Efficient synthetic access to a new family of highly potent bryostatin analogues via a prins-driven macrocyclization strategy. *J. Am. Chem. Soc.*, 130, 6658, 2008.
118. Keck, G.E., Kraft, M.B., Truong, A.P., Li, W., Sanchez, C.C., Kedei, N., Lewin, N.E. and Blumberg, P.M., Convergent assembly of highly potent analogues of bryostatin 1 via pyran annulation: Bryostatin look-alikes that mimic phorbol ester function. *J. Am. Chem. Soc.*, 130, 6660, 2008.
119. Keck, G.E., Li, W., Kraft, M.B., Kedei, N., Lewin, N.E. and Blumberg, P.M., The bryostatin 1 A-ring acetate is not the critical determinant for antagonism of phorbol ester-induced biological responses. *Org. Lett.*, 11, 2277, 2009.
120. Etcheberrigaray, R., Tan, M., Dewachtert, I., Kuipéri, C., Van Der Auwera, I., Wera, S., Qiao, L. et al., Therapeutic effects of PKC activators in Alzheimer's disease transgenic mice. *Proc. Natl. Acad. Sci., USA*, 101, 11141, 2004.
121. Sun, M.-K. and Alkon, D.L., Bryostatin-1: Pharmacology and therapeutic potential as a CNS drug. *CNS Drug Rev.*, 12, 1, 2006.
122. Alkon, D.A., Sun, M.-K. and Nelson, T.J., PKC signaling deficits: a mechanistic hypothesis for the origins of Alzheimer's disease. *Trends Pharm. Sci.*, 28, 51, 2006.
123. Montaner, J., Latest advances and research in stroke: Focus on diagnostic and therapeutic targets. *Drug News Perspect.*, 19, 173, 2006.
124. Wang, D., Darwish, D.S., Schreurs, B.G. and Alkon, D.L., Analysis of long-term cognitive-enhancing effects of bryostatin-1 on the rabbit (*Oryctolagus cuniculus*) nictitating membrane response. *Behav. Pharmacol.*, 19, 245, 2008.
125. Khan, T.K., Nelson, T.J., Verma, V.A., Wender, P.A. and Alkon, D.A., A cellular model of Alzheimer's disease therapeutic efficacy: PKC activation reverses A beta-induced biomarker abnormality on cultured fibroblasts. *Neurobiol. Dis.*, 34, 332, 2009.

9 The Isolation, Characterization, and Development of a Novel Class of Potent Antimitotic Macrocyclic Depsipeptides *The Cryptophycins*

Rima S. Al-awar and Chuan Shih

CONTENTS

9.1 Introduction 219
9.2 Isolation and Characterization of the Cryptophycins 220
9.3 Mechanism of Action of the Cryptophycins 221
9.3.1 Cellular Mechanism of Action of Cryptophycin 52 (LY355703) 221
9.3.2 Effects of Cryptophycin 52 (LY355703) on Microtubule Polymerization *In Vitro* .. 223
9.4 Synthesis of Cryptophycin 52 (LY355703) 223
9.4.1 Retrosynthetic Analysis and Final Assembly of the Fragments 223
9.4.2 Preparation of Fragments A–D 224
9.5 SARs of the Cryptophycins 227
9.5.1 SAR of the β-Epoxide Region of Fragment A 227
9.5.2 SAR of the Phenyl Group of Fragment A 228
9.5.3 SAR of the D-Chlorotyrosine of Fragment B 230
9.5.4 SAR of the C/D Ester Bond and the C6, C7 Positions 230
9.6 Comparison of Cryptophycins 52, 55, and 55-Glycinate 232
9.7 Cryptophycin 52 (LY355703) 233
9.7.1 *In Vivo* Antitumor Activity of Cryptophycin 52 (LY355703) 233
9.7.2 Clinical Evaluation of Cryptophycin 52 (LY355703) 233
9.8 Conclusions 234
Acknowledgments 234
Update 235
References 236

9.1 INTRODUCTION

The cryptophycins are potent antitumor depsipeptides first isolated from terrestrial blue–green algae. Initial cellular mechanism of action studies showed them to be associated with the inhibition of mitotic spindle function. This characterization puts the cryptophycins into one of the clinically very important classes of anticancer agents, such as the vinca alkaloids (vincristine, vinblastine, and vinorelbine) and the taxanes (taxol and taxotere) that act primarily on the cellular microtubule structure and function. Extensive preclinical studies have demonstrated that the cryptophycins are highly

active against a broad spectrum of murine solid tumors and human tumor xenografts *in vivo*. One very unique pharmacological property of the cryptophycins is that they do not serve as substrates for either P-glycoprotein (Pgp) or the MRP multidrug-resistant efflux pumps and are highly active against the resistant tumors that express multidrug-resistant phenotypes both *in vitro* and *in vivo*. These results indicate that the cryptophycins may be highly active against human solid tumors that are resistant to the taxanes or the vincas and may offer alternative efficacy or survival advantages over the current therapies. Here we summarize the collaborative structure–activity relationship (SAR) studies conducted among three institutions, Lilly Research Laboratories, University of Hawaii, and Wayne State University, in their identification of cryptophycin 52 (LY355703) as the first-generation cryptophycin to undergo clinical evaluation.

9.2 ISOLATION AND CHARACTERIZATION OF THE CRYPTOPHYCINS

The cryptophycins are peptolides with a 16-membered macrolide ring structure. The macrocyclic ring is composed of two ester linkages (fragments A/D and C/D), two amide linkages (fragments A/B and B/C), and seven asymmetric centers (Figure 9.1). Cryptophycin A or 1 was first isolated from the *Nostoc* sp. ATCC 53798[1] by researchers at Merck in the early 1990s and was found to be very active against strains of *Cryptococcus*. The development of cryptophycin A as a potential antifungal agent was unsuccessful mainly because of the toxicity of the agent. During the same period of time, in an effort to identify novel antitumor agents from blue-green algae (cyanobacteria), researchers at the University of Hawaii led by Richard Moore discovered that the lipophilic extract of *Nostoc* sp. GSV224[2] was highly cytotoxic to human nasopharyngeal carcinoma (KB) and human colorectal adenocarcinoma (LoVo) cells. More important, this lipophylic extract was found to be highly selective toward solid tumor cells versus leukemia cells and normal fibroblasts in the disk diffusion soft agar colony formation assay developed by Corbett at Wayne State University.[3] To follow up on this activity, a total of 26 naturally occurring secondary metabolites were isolated from the *Nostoc* sp. GSV224, with cryptophycin 1 accounting for most of the cytotoxic activity in the crude extract. Through rigorous structure elucidation and determination efforts, the University of Hawaii team established the absolute stereochemistry of all the asymmetric centers of cryptophycin 1 and confirmed that cryptophycin 1 was identical to cryptophycin A, reported on earlier by the Merck group.[4]

The antitumor activity of cryptophycin 1 was then rapidly followed up *in vivo* by the Wayne State University group (Corbett et al.) using various solid-tumor models developed either in syngeneic or severe combined immunodeficiency (SCID) mice. It was quickly determined that cryptophycin 1 was highly active against a number of murine solid tumors and human tumor xenografts when given by intravenous injection. In contrast, the compound was found to be significantly less

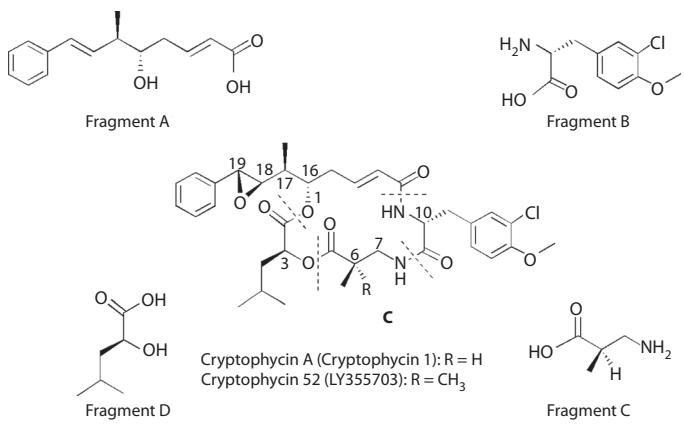

FIGURE 9.1 Chemical structure of crytophycin 1 and its four fragments (A–D).

active when administered by intraperitoneal or oral routes. The lack of activity via these routes was believed mainly to be a result of poorer metabolic stability. Excellent tumor growth inhibition and antitumor activity were observed with cryptophycin 1 in a number of solid tumors, but more important, it was highly active against the murine mammary 16/C tumor that is resistant to paclitaxel because of the overexpression of the multiple-drug-resistant protein Pgp.[5] This renders the cryptophycins some of the very few new antitubulin agents that do not serve as substrates for the multidrug-resistant protein and, hence, may offer significant advantage for the treatment of resistant human solid tumors.

The discovery of the exciting antitumor activity of cryptophycin 1 prompted the Lilly/Hawaii/Wayne State team to develop a unified strategy, not only for producing a large number of analogs for the SAR and the selection of a clinical candidate from the series, but also for developing technologies that can be used for the potential commercial-scale production of the cryptophycin class of compounds. Critical analyses revealed that a large-scale bioproduction of the cryptophycins from cultured blue-green algae was not only technically very challenging but also economically unattractive. For example, cryptophycin 1 can only be obtained in an estimated 0.4% yield from the dry algae mass after an extensive high-performance liquid chromatography purification process. The bioproduction approach also offered limited chemical diversity for the SARs. A total synthetic approach was eventually elected as the major strategy for the chemical investigation of the cryptophycin series of compounds. It offers several advantages over the bioproduction approach, including chemical diversity, synthetic maneuverability, enabling technologies, and last but not least, speed for advancing the project. The majority of the SARs described below were conducted using materials prepared by total synthetic approaches developed jointly between the Lilly Research Laboratories and the University of Hawaii teams. The clinical candidate compound, cryptophycin 52 (LY355703), was prepared via a convergent synthetic approach that was originally developed by the Moore and Tius' groups at the University of Hawaii and was later modified by the Chemical Process Research and Development group at Lilly Research Laboratories, led by Martinelli.[6] The 30-step convergent synthetic sequence of the cryptophycins illustrates both the complexity and the diversity of such an approach for the preparation of this novel chemical series.

9.3 MECHANISM OF ACTION OF THE CRYPTOPHYCINS

The cryptophycins are potent antiproliferative and cytotoxic agents that act against a variety of human tumor cell lines derived from both hematopoietic and solid tumors. The mechanism of action behind the potent cytotoxic effects induced by the cryptophycins appears to be associated with inhibition of mitotic spindle function of the cells.[7] This inhibition of mitosis is accompanied by accumulation of cells at the metaphase–anaphase transition, followed by spindle disorganization and fragmentation and, finally, apoptosis or cell death.[8] Biochemically, it was found that at low concentrations, the cryptophycins interact with microtubules to significantly dampen their dynamic characteristics. At higher concentrations, the process of microtubule polymerization was effectively inhibited by the cryptophycins. Compared with other antitubulin agents such as the vincas and the taxanes, the cryptophycins have a major pharmacological advantage in that they are insensitive to the ABC transporters Pgp and MRP, which are implicated in multidrug resistance.[9] The majority of the cellular and biochemical mechanism of action studies were conducted using the synthetic 6,6-gemdimethyl analog (cryptophycin 52) of the natural product cryptophycin 1.

9.3.1 Cellular Mechanism of Action of Cryptophycin 52 (LY355703)

Flow cytometry studies showed that cryptophycin 52 can potently cause the accumulation of cells (CCRF-CEM cells: from 15% to 60%; HT-29 cells: from 24% to 88%) in the G2/M phase of the cell cycle, and this effect was found to be both time and concentration dependent. Microscopic

examination of cells treated with cryptophycin 52 showed the cells initially accumulating in mitosis and subsequently undergoing apoptosis. Apoptosis was also evaluated by flow cytometry studies by following the end-labeling of fragmented DNA using bromodeoxyuridine (BrdU). It was found that when CCRF-CEM cells were treated with 300 pM of cryptophycin 52, 20% of cells were in interphase, 40% were in the mitotic phase, and 40% were in the apoptotic population (at the 24-h time point), which indicated that the cell death mechanism was mediated through the antimitotic effect induced by the cryptophycins.

Further studies of cryptophycin 52 in HeLa and HT-29 cells using confocal microscopy showed that cryptophycin 52 caused the mitotic spindle to become fragmented, and multiple microtubule foci were found within a ball-like cluster of chromosomes (HeLa cells at 100 pM, approximately equal to the IC_{50}). At 300 pM of cryptophycin 52, only small residual fragments of spindle microtubules are evident in the chromosome cluster of treated HeLa cells (Figure 9.2). Similar effects that caused spindle fragmentation and multiple microtubule foci were also observed when HT-29 cells were treated with cryptophycin 52 at 300 pM and 1 nM. Abnormal spindle structures appeared

The effects of 355703 on HeLa cell mitotic spindle structure

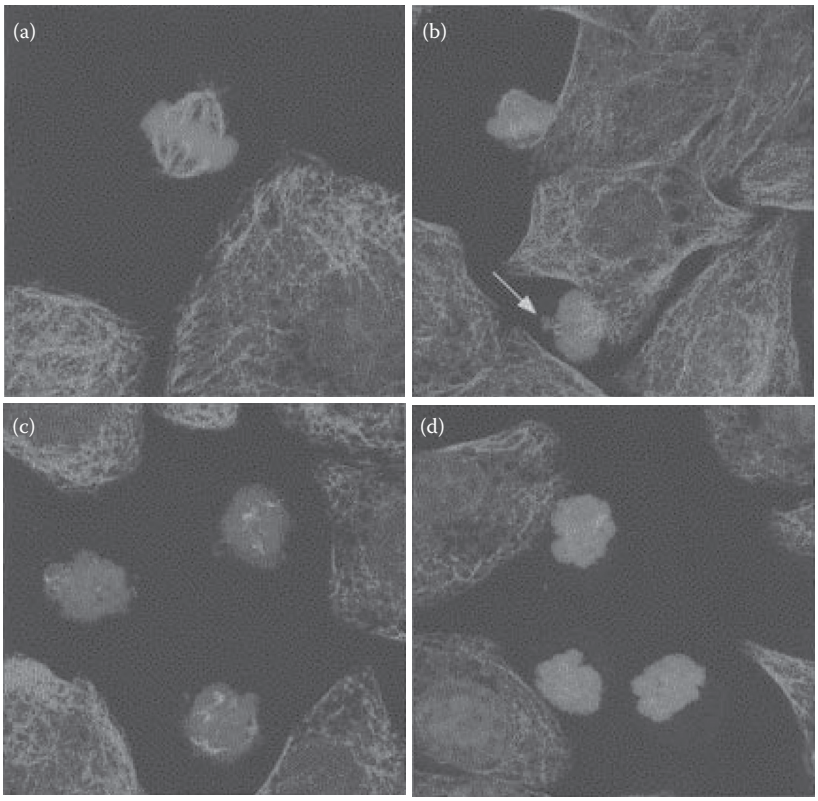

FIGURE 9.2 **(See color insert.)** Fluorescence confocal micrographs of HeLa cells: (a) shows a metaphase mitotic spindle in an untreated control cell. The metaphase spindle is bipolar, with the chromosomes located in a compact metaphase plate at the midpoint between the spindle poles; (b) shows cells treated with 30 pM of LY355703 (approximately IC_{50}) for 8–10 h. The mitotic spindles look relatively normal. The most obvious abnormality involves the displacement of chromosomes from the compact metaphase plate. In the lower spindle, a chromosome (red) can be seen near the spindle pole (arrow); (c) (8–10 h; 100 pM of LY355703), and (d) (8–10 h; 300 pM of LY355703) show increased fragmentation of the spindle microtubules and disorganization of the chromosome mass into ball-like clusters.

within shorter exposure time when a higher concentration (1 nM) of cryptophycin 52 was used. Microtubule bundles were evident in 1-nM compound-treated cells as early as 2 h post-treatment. These bundles are similar to microtubule bundles described in paclitaxel (Taxol®)-treated cells, but not vinblastine- or vincristine-treated cells. The microscopy data clearly supported the notion that microtubules and mitotic spindles are the primary targets of action for cryptophycin 52 and its derivatives. This was further investigated by studying the effect of crytophycin 52 on the dynamics of microtubule polymerization using bovine brain microtubules.[10]

9.3.2 Effects of Cryptophycin 52 (LY355703) on Microtubule Polymerization *In Vitro*

Using a bovine brain microtubule protein preparation that consisted of 70% tubulin and 30% microtubule-associated proteins (MAPs), it was found that cryptophycin 52 potently inhibited the microtubule polymerization (measured by using radiolabeled GTP/GDP bound to tubulin as a sensitive measure of polymerization) with an IC_{50} of 0.49 μM. This effect was comparable with those exerted by vinblastine (0.35 μM) or vincristine (0.34 μM) and was distinct from paclitaxel, which enhanced (or stabilized) the polymerization of tubulin at concentrations >0.3 μM. Microtubules are not simple equilibrium polymers. The hydrolysis of GTP to GDP and inorganic phosphate as tubulin adds to a growing microtubule end creates highly dynamic polymers whose ends grow and shorten stochastically because of the gain and loss of a stabilizing "cap." The dynamics are extremely rapid both *in vitro* and in cells, especially during mitosis. Considerable recent evidence strongly indicates that not just the presence of microtubules but also the dynamics of the microtubules are critical for mitotic progression.[11] Many of the important antimitotic antitumor drugs such as the vinca alkaloids and paclitaxel exert their powerful antiproliferative actions by suppressing the dynamics of spindle microtubules. Importantly, these antimitotic drugs perturb microtubule dynamics by binding to the ends and along the surface of microtubules at concentrations that are far lower than those required to inhibit microtubule polymerization or induce excess microtubule formation.

The effects of cryptophycin 52 on the growing and shortening dynamics of individual microtubules at steady state in real time using video microscopy were thus examined. MAP-free bovine brain tubulin was assembled to polymer mass steady state at the ends of sea urchin flagellar axonemal seeds, and the individual dynamics parameters and the changes in length of the microtubules were recorded for approximately 30–45 min. Through such studies, it was found that cryptophycin 52 powerfully suppressed microtubule dynamics at a concentration of 50 nM and at 500 nM, completely shutting down the dynamics of microtubules (Figure 9.3). The studies also indicate that cryptophycin 52 suppresses microtubule shortening rates considerably more powerfully than microtubule growing rates. This is a sharp contrast to vinblastine, which inhibits both the growing and the shortening of microtubules to similar extents. Overall, the relatively weaker effects of cryptophycin 52 on growing as compared with shortening resemble the action of paclitaxel rather than vinblastine. Thus, cryptophycin 52 has characteristics of both the vinca alkaloids and paclitaxel when it comes to influencing microtubule dynamics.[10]

9.4 SYNTHESIS OF CRYPTOPHYCIN 52 (LY355703)

9.4.1 Retrosynthetic Analysis and Final Assembly of the Fragments

The retrosynthetic analysis of cryptophycin 52 shown in Figure 9.1 represents a straightforward disconnection of the depsipeptide into four corresponding fragments (labeled A–D) through the two ester and two amide linkages. The molecule contains six asymmetric centers, with four contiguous ones present in fragment A, thus making it the most synthetically challenging fragment. For the latter four, the Sharpless asymmetric epoxidation was used as the essential step in controlling two of the four asymmetric centers (*16S* and *17S*), and the final diastereoselective epoxidation of the styrene olefin provided the other two asymmetric centers (*18R* and *19R*) of fragment A. The two distal

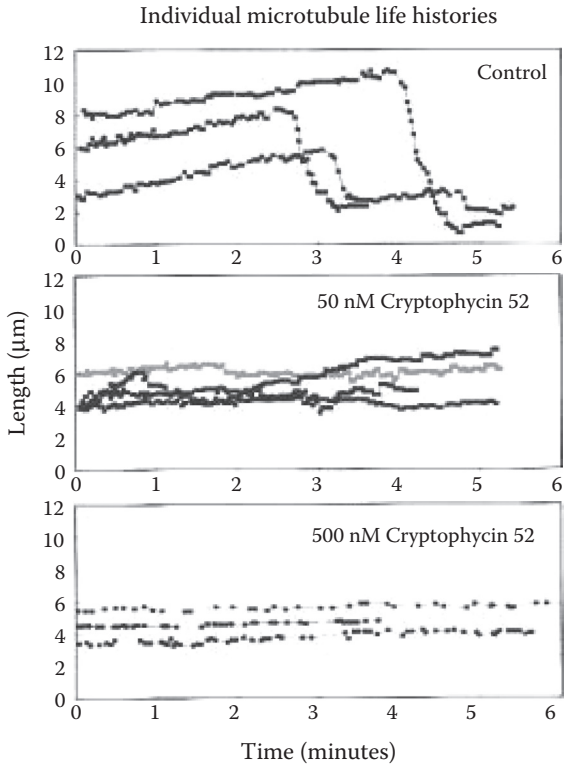

FIGURE 9.3 **(See color insert.)** Microtubule life histories.

asymmetric centers (*3S* and *10R*), in contrast, were obtained from optically pure amino acids (D-tyrosine for fragment B and L-leucine for fragment D, respectively).

In general, the cryptophycin nucleus can be assembled efficiently in a convergent fashion by first combining fragments A and B and fragments C and D to give the protected AB and CD fragments. The TBS group of the AB fragments was then removed (aqueous HF, CH_3CN, 95%) to give the secondary alcohol, which was then coupled with the carboxylic acid of the *N*-BOC C′D fragment (DCC, DMAP, CH_2Cl_2, 95%) to give the fully protected *seco*-ABCD compound (Figure 9.4).[6]

Treatment of the *seco* compound with TFA (removal of the BOC group) followed by 2-hydroxypyridine effectively catalyzed the macrolactamization to give the cyclized 16-membered depsipeptide in 62% yield (Figure 9.5).[12] Diastereoselective epoxidation of the styrylolefin (*m*-CPBA, CH_2Cl_2, 95%) gave a 2:1 ratio of epoxides, with the desirable β-epoxide as the major product. The diastereomeric epoxide mixtures can be separated by reverse-phase high-performance liquid chromatography to provide the more active β-epoxide (cryptophycin 52) for biological evaluation. Alternatively, the 2:1 epoxide mixture can be treated with trimethylsilylchloride to give the corresponding chlorohydrins, which then can be readily separated by flash silica gel chromatography. Treatment of the pure β-chlorohydrin (cryptophycin 55, 355702) with potassium carbonate in acetonitrile converted it back to cryptophycin 52 in high yields.

9.4.2 Preparation of Fragments A–D

Fragment A, the synthetically most challenging fragment, with its four contiguous stereogenic centers, was prepared in 11 total linear steps to give methyl(*5S,6R*)-5-[(*tert*-butyldimethylsilyl) oxy]-6-methyl-8-phenylocta-2(*E*),7(*E*)-dienoate (**1**, 28% overall yield, 95% ee). In this sequence,

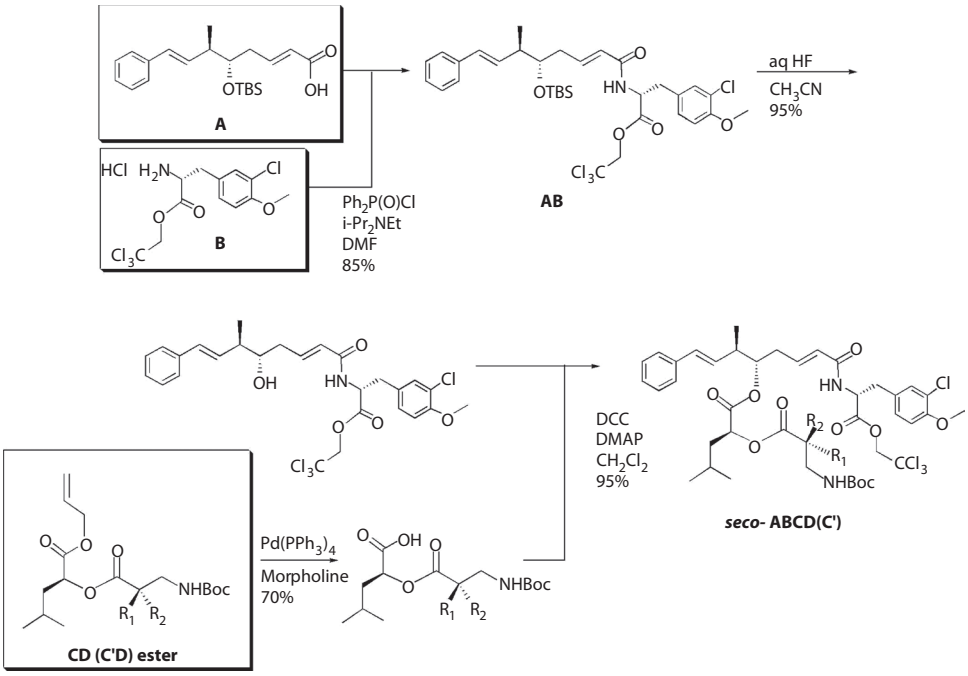

FIGURE 9.4 Convergent synthetic approach to the *seco*-ABCD compound.

the Sharpless asymmetric epoxidation of the allylic alcohol was used as a key reaction to install two of the four asymmetric centers with ~95% ee (Figure 9.6). Regio- and stereoselective opening of the resulting epoxide with trimethylaluminum installed the desired methyl group and resulted in the diols, where the primary one was selectively tosylated in the presence of dibutyl tin oxide and the secondary one was protected as a TBS ether.[13] The styrene moiety was installed via a

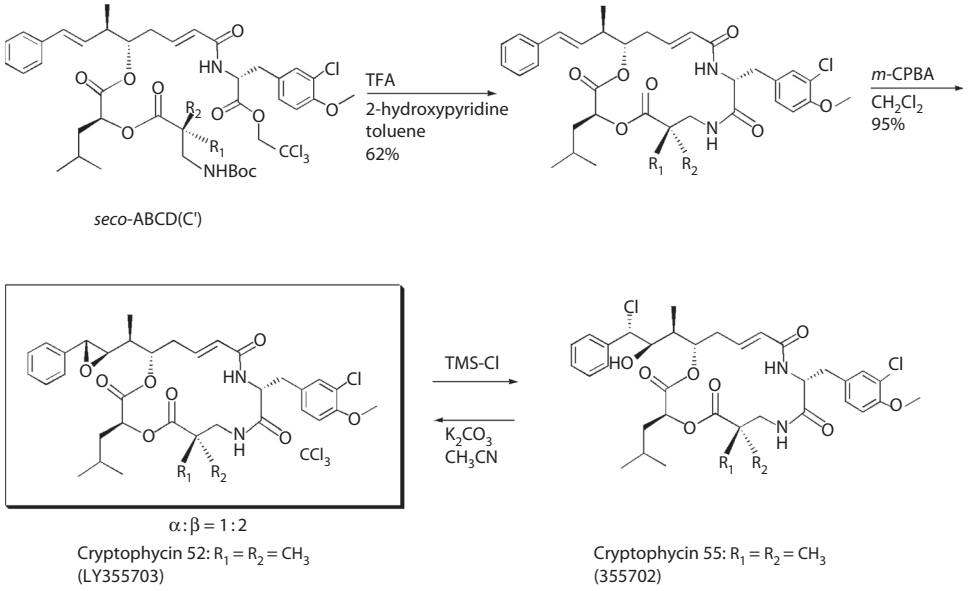

FIGURE 9.5 Macrocyclization and the preparation of cryptophycin 52.

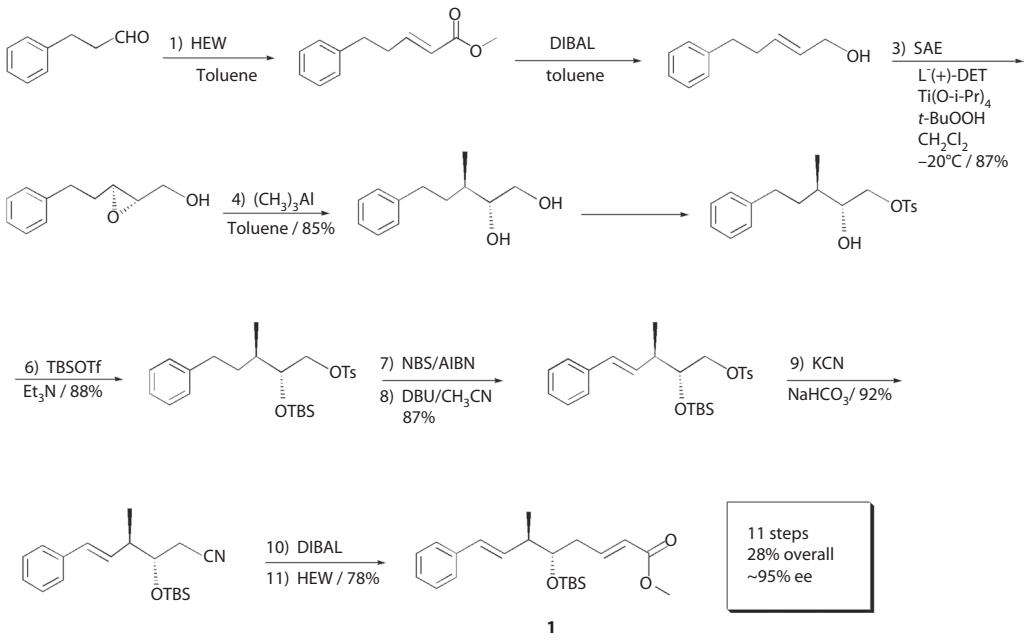

FIGURE 9.6 Sharpless asymmetric epoxidation route to the preparation of fragment A.

dehydrobromination, using DBU as the base. Displacement of the tosylate under buffered conditions afforded the crucial nitrile that was reduced to the aldehyde using DIBAL and subsequent Horner–Emmons–Wadsworth olefination gave the final desired unsaturated ester in good yield.[14]

The other fragments, B, C, and D, were prepared in a more straightforward fashion. Fragment B was obtained in six steps (40% overall yield, 99% ee) from D-tyrosine, as described in Figure 9.7. Fragment C′ (for cryptophycin 52) was obtained in three steps (58% overall) from ethylcyanoacetate,

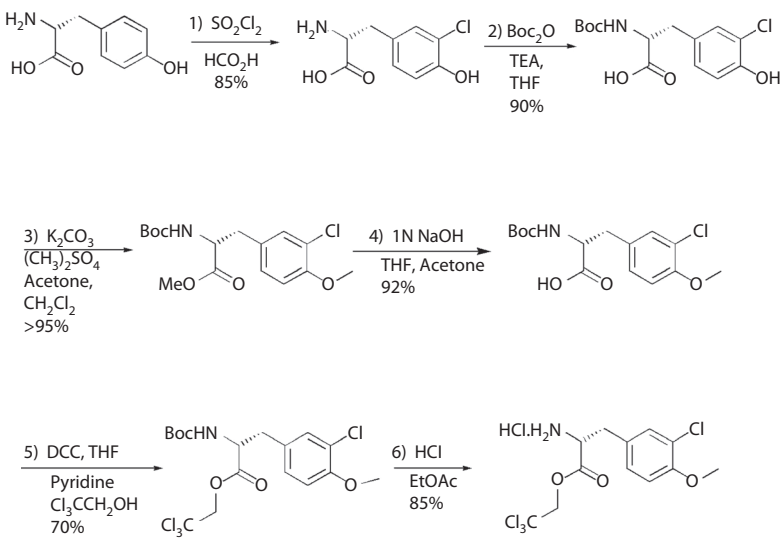

FIGURE 9.7 Preparation of fragment B.

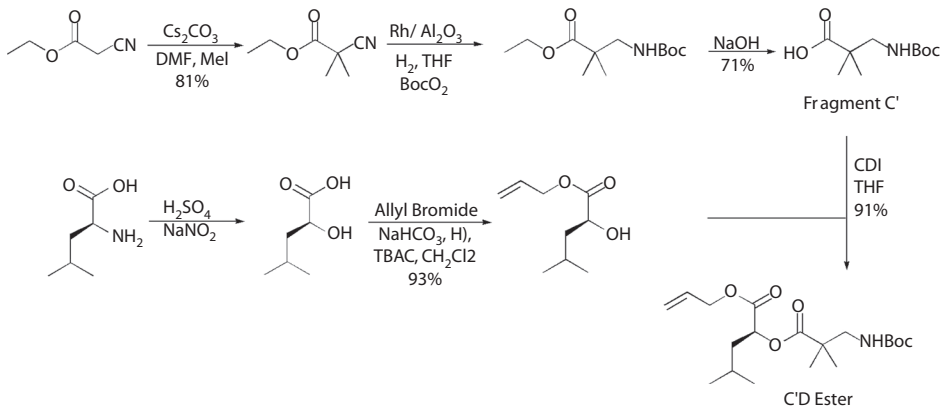

FIGURE 9.8 Preparation of fragment C′–D.

which was then coupled (CDI in THF, 91%) readily with the allyl-L-leucic acid (obtained in two steps from L-leucine) to give the corresponding C′–D fragment (Figure 9.8).

Although the total synthesis of cryptophycin 52 required more than 30 discrete synthetic operations, the convergent nature of the process rendered it quite versatile for creating multiple permeations through the combination of different fragments for SAR purposes. This synthetic sequence was also practical enough for the preparation of reasonably large amounts of material for the phase I and II clinical evaluations.

9.5 SARS OF THE CRYPTOPHYCINS

Over 500 cryptophycin analogs were prepared via either a total synthetic approach or a semisynthetic one, with modifications of the natural cryptophycin 1 or cryptophycin 52, particularly for fragment A analogs. Because the cryptophycins exhibited very potent cytotoxicity toward most of the human malignant carcinoma cell lines tested in culture, a 72-h MTT cell-based assay was used to evaluate the newly synthesized analogs. The IC_{50} for cryptophycins 1 and 52, for example, were in the range of 20–100 pM against several human tumor cell lines (KB, CCRF-CEM, HT-29, SKOV3, LoVo, and GC3). These *in vitro* cell-based assays provided the required sensitivity and broad range (10 pM; approximately >20 μM) of activity essential for differentiating and establishing a firm structure–activity trend for a large number of analogs. In these studies, most of the cytotoxicity data were collected using three cultured human tumor cell lines: KB (Univ. Hawaii) and GC3 human colon carcinoma and CCRF-CEM human leukemia (Lilly Research Labs). The cytotoxicity data cited in the SAR discussion in this section were mostly derived from the GC3 human colon carcinoma cell line unless stated otherwise. The *in vitro* cytotoxicity was then used to prioritize the compounds for the initial *in vivo* antitumor screening, using the Panc 03 (murine pancreatic adenocarcinoma) model, which was then followed by a panel of other murine tumor models and human tumor xenografts (Mam 16C/ADR, Mam 17/ADR, MX-1, GC3, LNCaP, HCT-116, and PC-3).[15]

The SAR described here will be primarily focused on five regions: the epoxide of fragment A and the prodrugs of its corresponding chlorohydrins, the substitution of the phenyl group of fragment A, the modification of the D-chloromethyltyrosine unit of fragment B, the C/D ester bond, and the C6, C7 positions of fragment C.

9.5.1 SAR of the β-Epoxide Region of Fragment A

Early SAR efforts quickly established the importance of the absolute stereochemistry of the four consecutive stereogenic centers of this fragment. One very important structure–activity feature of the

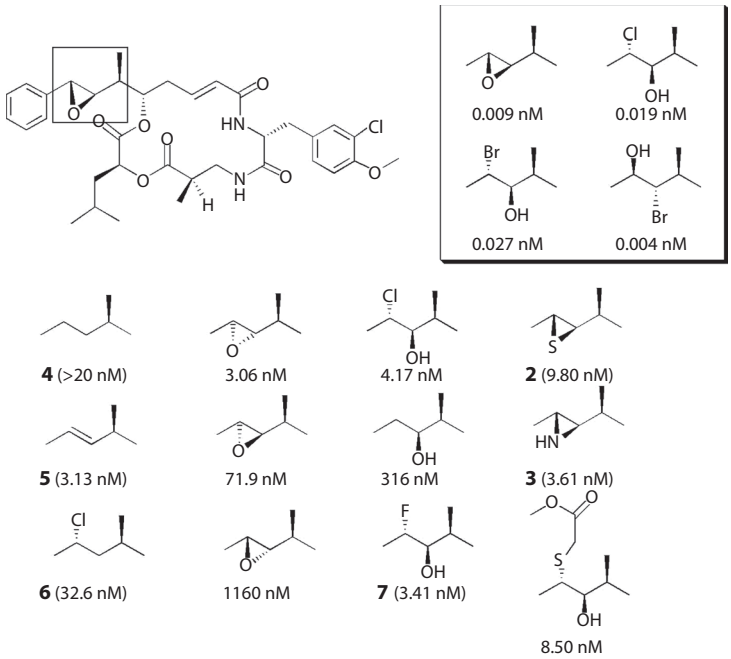

FIGURE 9.9 SAR of β-epoxide region of fragment A.

cryptophycins is centered on the configuration of the styrylepoxide portion of the molecule where only the β-epoxide or its masked equivalents (such as the corresponding β-chlorohydrin, β-bromohydrin, and the reversed β-bromohydrin) possessed potent cytotoxicity ($IC_{50} = 0.004–0.027$ nM) in cell culture assays (Figure 9.9). Epoxides with other configurations (*R/S*, *S/R*, and *S/S)* were much less active. Replacement of the oxygen atom of the epoxide with sulfur (episulfide, **2**) or nitrogen (aziridine, **3**) led to major loss in activity.[16] Removal of the oxygen functionality at C18/C19 also led to inactive phenethyl (**4**), styryl (**5**), and chlorobenzyl (**6**) derivatives of cryptophycin. The corresponding diol and the fluorohydrin (**7**) derivatives of β-epoxide were also much less active in the *in vitro* assays.

Pharmacokinetic data (*vide infra*) clearly suggested that the β-chlorohydrin was rapidly converting to the corresponding β-epoxide *in vivo* in rodents and could account for the majority of the antitumor activity seen in murine tumors and human tumor xenografts. The drawback of the chlorohydrins was their lack of long-term stability in a suitable formulation, which prompted a study to stabilize these derivatives and improve their aqueous solubility by preparing several ester prodrugs. Although several of these derivatives showed weaker *in vitro* activity (CCRF-CEM human leukemia) as compared with cryptophycins 52 and 55, it was necessary to evaluate these derivatives *in vivo* to determine their potential conversion to the active epoxide species (Figure 9.10).[17]

9.5.2 SAR of the Phenyl Group of Fragment A

From this SAR, it was concluded that the activity of the cryptophycins can be modulated by introducing electron-donating or electron-withdrawing groups on the phenyl ring of the styrene oxide region.[18] Introduction of a group larger than a fluorine in the *ortho* position led to loss of activity, whereas the *meta* and *para* positions tolerated many large functional groups. Electron-donating groups such as methyl, hydroxymethyl, and methoxy usually led to highly potent cryptophycin derivatives *in vitro* (*m*-methyl, $IC_{50} = 0.15$ nM; *p*-methoxy, $IC_{50} = 0.28$ nM; *p*-hydroxymethyl, $IC_{50} = 0.004$ nM; compared with $IC_{50} = 0.022$ nM for cryptophycin 52, measured in CCRF-CEM cells). Introduction of *p*-methyl ester also resulted in an active derivative ($IC_{50} = 0.037$ nM;

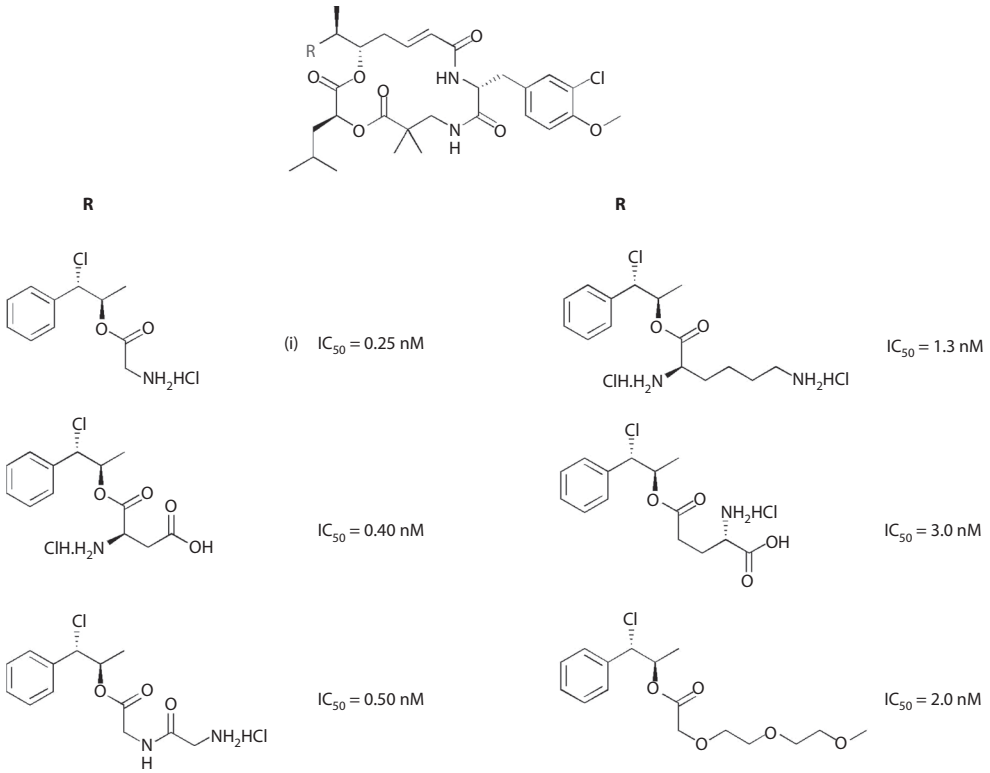

FIGURE 9.10 IC_{50} of prodrugs in CCRF-CEM cells.

cryptophycin 55, IC_{50} = 0.05 nM). Along the same trend, introduction of fluorine at either the *ortho*, *meta*, or *para* positions relative to the oxirane ring of the styrene oxide also led to derivatives with potencies ranging between 0.01 and 0.06 nM.

Taking advantage of the potential substitution at the *para* position to improve the aqueous solubility of the molecule, amines **9–11** were prepared, starting with benzyl chloride **8** (Figure 9.11).[18] Their potency ranged between 0.001 and 0.092 nM, compared with 0.05 nM for cryptophycin 55, which proved that not only are large groups tolerated but these might provide more potent analogs than cryptophycin 52 or 55.

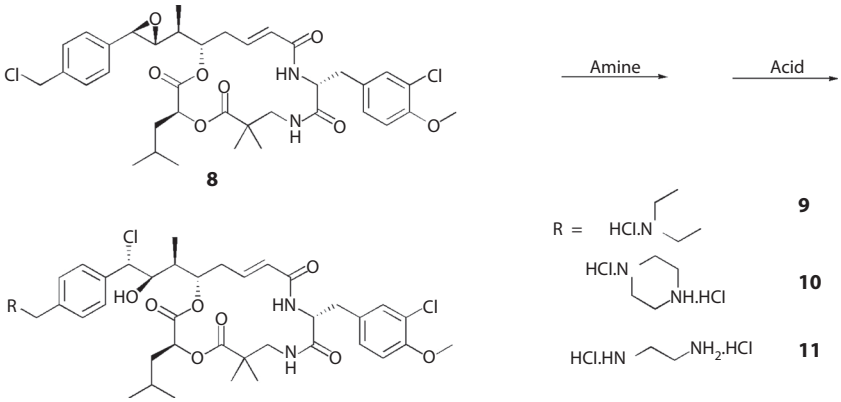

FIGURE 9.11 Preparation of amines **9–11**.

Replacement of the phenyl group of the styrene oxide with other heteroatom-containing aromatics, such as pyridine, thiophene, furan, or thiazole, however, all led to a major loss of cytotoxicity in cell culture. Replacement of the phenyl group with simple alkyl groups (methyl, ethyl, *n*-propyl, methoxy, formyl, and *t*-butyl ester) also led to loss of activity in cell culture studies and to completely inactive analogs in *in vivo* animal studies.

9.5.3 SAR of the D-Chlorotyrosine of Fragment B

SAR studies around fragment B indicated that this is probably the region that is least amenable to structural modification. Various structural modifications of this region of the molecule all led to significant loss of cytotoxicity *in vitro*.[19] These included replacing the chlorine atom with the fluorine, introduction of additional halogen atoms onto the phenyl ring, modification of the methoxy ether, replacing the chloromethoxyphenyl with other aromatic or nonaromatic groups, and replacing chloromethyltyrosine with other simple natural and unnatural amino acids (such as glycine, valine, proline, *p*-aminophenylalanine, *p*-hydroxyphenylglycine, phenylethylglycine, etc.). Methylation of the asymmetric methine carbon at C10 also gave inactive analogs. The only tolerable modification in fragment B was the replacement of the chlorine with a bromine or a methyl group on the phenyl ring of the tyrosine. This led to the corresponding methyl D-tyrosine derivative, which had only a twofold decrease of cytotoxicity *in vitro* ($IC_{50} = 0.04$ nM; cryptophycin 52, $IC_{50} = 0.019$ nM, measured in CCRF-CEM cells).

9.5.4 SAR of the C/D Ester Bond and the C6, C7 Positions

Some of the early studies of cryptophycin 1 indicated that the ester bond between fragments C and D of the macrocyclic ring may be metabolically labile to nucleophilic attack. This is supported by the observation that arenastatin (a closely related natural product isolated from Japanese sponge *Dysidea arenaria*) is completely devoid of activity *in vivo*, although it has potent activity in cell culture.[20] Two approaches were then investigated for the stabilization of the C–D ester bond: (a) geminal substitution—to the carbonyl group and (b) isosteric replacement of the ester bond with other functionalities such as an amide. Both approaches produced very active derivatives—in particular, introduction of a gem-dimethyl group at the C6 position gave an analog (cryptophycin 52, LY355703) with a very much improved *in vivo* antitumor efficacy profile compared with cryptophycin 1. Although geminal disubstitution was effective in protecting the carbonyl group from nucleophilic attack and could be successfully extended to the spirocyclopropyl group (12), however, it was found that potency was rapidly diminished when larger groups (gem-diethyl, gem-di-*n*-propyl, spirocyclopentyl, and spirocyclohexyl) were introduced into the C6 position (Figure 9.12).[21]

The amide isosteric replacement of the C–D ester bond also gave very active analogs 13 and 14, regardless of whether there was a monomethyl or a geminal dimethyl group at the C6 position.[22] Both agents exhibited potent *in vitro* activity ($IC_{50} = 0.015$ nM); however, it was found that the *in vivo* potency for the gem-dimethyl amide analog was significantly lower than that of cryptophycin 52 when compared head-to-head in the Panc 03 model. Replacement of the C–D ester with the corresponding ether linkage (15) causes a major loss of activity in cell culture (240-fold).[22] As part of the SAR studies of Fragment C, it was also found that moving the substituent ($R = CH_3$, 16) from the C6 to the C7 positions retains the activity *in vitro*. However, similar to what was observed for arenastatin, absence of substituents at the C6 position caused the compound to be completely inactive *in vivo* presumably because of the metabolic instability issue with the C–D ester bond. Larger substituents at the C7 position (R = phenyl, 17) did not improve the activity of the compound either *in vitro* or *in vivo*. Excising the C6 carbon atom of the peptolide ring was also attempted, and the result was disappointing. The smaller 15-membered macrocycles 18 and 19 were significantly less active in cell culture (1400-fold) than the natural cryptophycins.[23]

The key findings from the SAR studies conducted around the various regions of the molecule are summarized in Figure 9.13. Overall, it can be concluded, first, that the absolute stereochemistry of

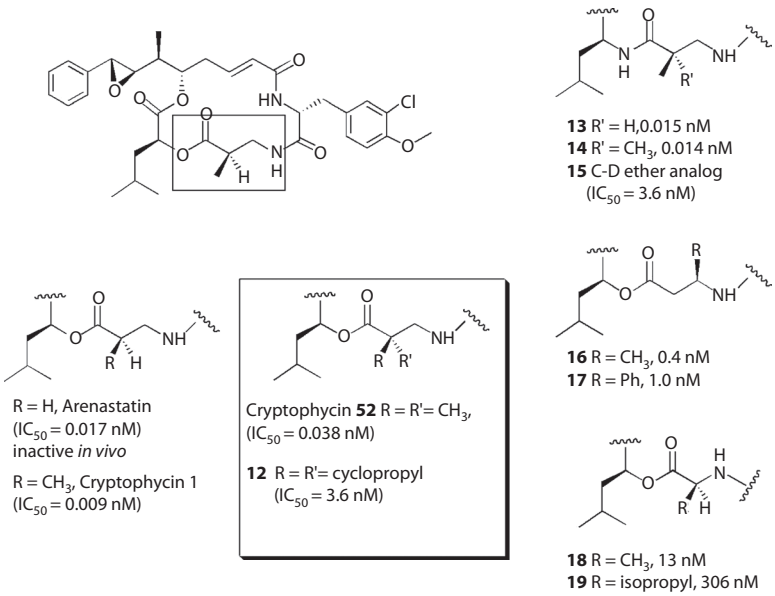

FIGURE 9.12 SAR of CD ester bond and C6, C7 positions.

all seven asymmetric centers is essential for eliciting the biological activity of the cryptophycins, and the opposite configuration at these centers led to major loss of activity. Second, the β-epoxides (*R/R*) at the 18 and 19 positions (fragment A) are consistently much more active than the other isomers (*R/S*, *S/R*, and *S/S*). Third, substitution of the amide nitrogen of the macrocyclic ring led to inactive analogs; x-ray and nuclear magnetic resonance studies indicate that an intrapeptolide hydrogen bond may exist between the NH(8) and CO(12) groups for the macrocyclic ring to adopt certain conformations. Fourth, amide replacement of the ester linkage may be tolerated between the fragment C/D but not between the A/D fragments. Fifth, substituents on the phenyl ring of fragment A are well tolerated; however, substitutions and modifications of the chloromethyl tyrosine unit of Fragment B are limited to a few options.

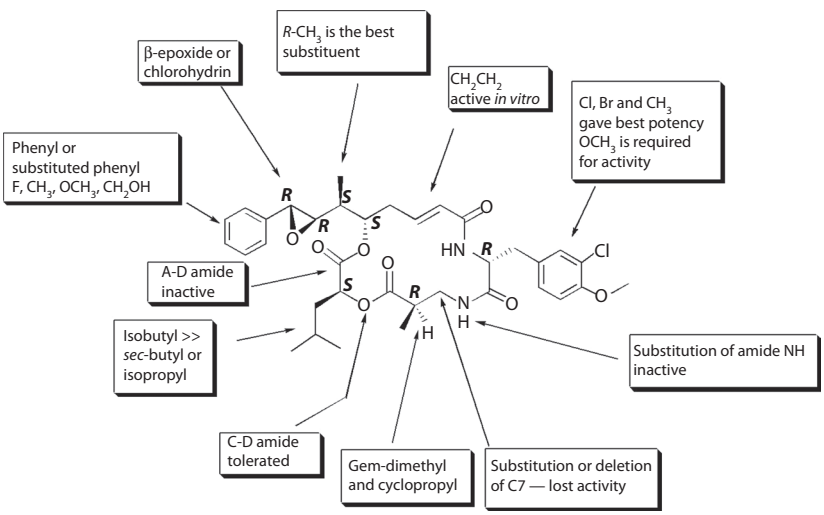

FIGURE 9.13 Key SAR findings of the cryptophycins.

9.6 COMPARISON OF CRYPTOPHYCINS 52, 55, AND 55-GLYCINATE

A comparison of the *in vitro* cytotoxicity and the *in vivo* antitumor activity of cryptophycin 52 (epoxide, LY355703), cryptophycin 55 (chlorohydrins derivative of cryptophycin 52, 355702), and the glycinate derivative of chlorohydrins 55 (analog [i] in Figure 9.10, 368422) are summarized in Table 9.1. All three compounds were found to exert potent cytotoxic activities (200 pM–1 nM) against a number of human tumor cell lines (CCRF-CEM, GC3, HeLa), with the epoxide and chlorohydrins being slightly more potent than the corresponding glycinate derivative. However, it was found that the epoxide compound exhibited the most potent effect *in vivo* when compared on a milligram-by-milligram basis. To achieve similar levels of antitumor activities *in vivo* (maximum tolerated doses), it was usually necessary to dose four- to fivefold more of the chlorohydrins or glycinate as compared to the epoxide. This is primarily because both chlorohydrins and glycinate were found to act as prodrugs (*vide infra*) of the epoxide species *in vivo*. All three cryptophycins (355703, 355702, and 368422) were found to be active against a broad panel of human tumor xenografts including colon, mammary, prostate, pancreatic, and lung. The level of antitumor activity exhibited by the cryptophycins is superior to most of the commonly used anticancer agents such as the vincas, 5-fluorouracil, cisplatin, and doxorubicin. The only other class of compound that demonstrated comparable levels of *in vivo* activity as the cryptophycins in these tumors were the taxanes (such as paclitaxel).

Various studies demonstrated that the chlorohydrin derivative of cryptophycin 52 (355702) can be converted to the more potent epoxide under *in vitro* as well as *in vivo* conditions. It was found that the chlorohydrin derivatives could quite rapidly be transformed into the corresponding epoxide in the formulation (contains 5% ethanol and 5% cremophor) under various storage conditions. This conversion was also found to take place in plasma (*in vitro*) and in animal studies. For example, in mice dosed intravenously with 80 mg/kg of cryptophycin 55, the plasma levels of cryptophycin 52 (converted directly from cryptophycin 55) were almost identical to those found after administration of 20 mg/kg of cryptophycin 52 itself (a dose relationship that was consistent with the findings of the efficacy studies). This observation indicated that the chlorohydrin derivative cryptophycin 55 may act as a prodrug of cryptophycin 52. For the glycinate derivative to convert to the active component epoxide, it requires an enzymatic cleavage step of the ester bond, via the esterases, to generate chlorohydrin 55, which subsequently forms cryptophycin 52. Although the ester hydrolysis of the glycinate (368422) seems quite efficient in mouse plasma, it was discovered that the ester hydrolysis of the glycinate to give the epoxide was significantly reduced in dog and human plasma.

TABLE 9.1
Comparison of the *In Vitro* Cytotoxicity and the *In Vivo* Antitumor Activity of Cryptophycins 52, 55, and 55-Glycinate in Human Tumor Xenografts

	Crypto 52 (355703)	Crypto 55 (355702)	Crypto 55-glycinate (368422)
Cytotoxicity (IC_{50}/nM/GC3 cells)	0.2–0.7	0.2–0.75	1.0
In vivo potency	10–12 mg/kg (CDI/nu/nu)	40–48 mg/kg (CD1/nu/nu)	48–64 mg/kg (CD1/nu/nu)
In vivo antitumor activity[a]			
GC3 colon	+	+	+ + +
LNCap prostate	+ + + +	+ + + +	+ + + +
MX-1 mammary	+ +	+ + +	NT
H116 colon	+ + +	+ + + +	NT

Note: +, 0.7–1.2; + + , 1.3–1.9; + + + , 2.0–2.8; + + + +, >2.8.

[a] All *in vivo* antitumor activities are expressed in log cell kill units: log kill = $T - C/3.2 \times Td$.

9.7 CRYPTOPHYCIN 52 (LY355703)

9.7.1 *In Vivo* Antitumor Activity of Cryptophycin 52 (LY355703)

The antitumor activity of cryptophycin 52 *in vivo*, however, is summarized here to illustrate the broad spectrum of activity of this novel agent against a variety of syngeneic murine solid tumors and human tumor xenografts. Because of the lipophilic nature of the cryptophycins, cryptophycin 52 was formulated in a mixture of 5% cremophor and 5% ethanol in 90% saline, a formulation that is clinically used for paclitaxel. The treatment schedule varied but was generally consistent, with at least five repeated intermittent intravenous injections, usually every other day (q2d), and the doses used in the xenograft studies are usually in the range of 6–10 mg/kg for cryptophycin 52. The maximum tolerated dose for cryptophycin 52 in nude mice is 10 mg/kg per injection, with a total dose of ca. 50–60 mg/kg. Table 9.2 summarizes the antitumor activity (expressed in log kill) of cryptophycin 52 against five human tumor xenografts (HCT-116 colon, H125 lung, LNCaP prostate, TSU prostate, and PC-3 prostate carcinomas). In comparison, the antitumor activity of a group of commonly used oncolytic agents (paclitaxel, doxorubicin, etoposide, vincristine/vinblastine, cytoxan, cisplatin, and 5-fluorouracil) is also included.[24] It is clear from these studies that cryptophycin 52 is a very active anticancer agent with superior antitumor activity compared to many of the commonly used oncolytic drugs. In addition, cryptophycin 52 also exhibited excellent activity against tumors that are resistant to adriamycin (Mamm16C/Adr and Mamm17/Adr—both are syngeneic murine tumors) and vinblastine (UCLA-P3), whereas paclitaxel, doxorubicin, etoposide, and vinblastine are completely inactive in these multidrug-resistant tumors.

9.7.2 Clinical Evaluation of Cryptophycin 52 (LY355703)

Cryptophycin 52, with its broad antitumor activity and potency, was chosen as the first-generation cryptophycin to undergo clinical evaluation, with 25 patients receiving the drug as a 2-h intravenous infusion on days 1 and 8 every 3 weeks. The doses were escalated from 0.1 to 2.22 mg/m^2 where neurological toxicities at or over 1.84 mg/m^2 were found to be dose limiting. An alternative twice-weekly schedule was also investigated with 11 patients in an attempt to reduce the neurotoxicity. Unfortunately, doses over 0.75 mg/m^2 on days 1, 4, 8, and 11 were also not tolerated as a result of nausea and constipation.[25] As a result of phase I studies showing that toxicity was not schedule dependent but most likely associated with cumulative dose, the dose for phase II was set at 1.5 mg/m^2 for days 1 and 8 schedule.

TABLE 9.2
Antitumor Activity (Log Kill[a]) of LY355703 and Other Oncolytics against Human Tumor Xenografts

Agent	HCT-116 Colon	H125 Lung	LNCaP Prostate	TSU Prostate	PC-3 Prostate
Cryptophycin 52	+ + +	+ +	+ + + +	+ +	+
Paclitaxel	+ + +	+	+ + + +	+ + + +	+ +
Doxorubicin	NT	—	—	—	—
Etoposide	—	+	+	—	—
VLB/VCR	+	+ + +	+ + + +	+ + + +	+ +
Cytoxan	—	—	+ + + +	+ + + +	—
Cisplatin	—	—	—	—	—
5-FU	—	—	—	—	—

Note: +, 0.7–1.2; + +, 1.3–1.9; + + +, 2.0–2.8; + + + +, >2.8; NT, not tested.

[a] All *in vivo* antitumor activities are expressed in log cell kill units: log kill = $T - C/3.2 \times Td$.

In phase II clinical trials, LY355703 was used as second-line therapy for metastatic colorectal cancer, for example, or in nonsmall-cell lung cancer patients who had received previous platinum-based chemotherapy. Although partial responses were observed in two patients with platinum-resistant advanced ovarian cancer, no significant activity or stable disease was reported in patients with other tumor types. Toxicities such as arthralgia, constipation, myalgia, and neuropathy were also observed; therefore, these results, along with the lack of efficacy, led to the termination of the clinical trials.

9.8 CONCLUSIONS

The discovery of the cryptophycins as a new class of antimitotic agents has attracted the attention of many synthetic groups to find better routes for their preparation and to investigate the activity of new related analogs.[26] In addition, investigators specializing in antimicrotubule agents have extensively studied their mode of action.[27] The research described in this chapter was the collaborative effort of Eli Lilly, University of Hawaii, and Wayne State University scientists resulting in the identification of cryptophycin 52 as the first generation cryptophycin to undergo clinical evaluation.[28] Extensive SAR studies were conducted and facilitated by the support provided by Lilly's process chemistry group. A convergent and highly efficient synthetic route to cryptophycin 52 was developed and used to both support the SAR and provide the clinical material.

The SAR studies led to a large number of cryptophycins with a broad array of structural diversity and activity. They also revealed some critically important areas for structure–activity optimization. These included the styrene β-oxide region, the C/D ester bond region, and the phenyl region of fragment A. From the assessment of the collective data of *in vitro*/*in vivo* pharmacology, biopharmaceutical properties, ADME/pharmacokinetic evaluation, and toxicological findings, cryptophycin 52 (LY355703) was selected as the first-generation cryptophycin compound for clinical evaluation. The greatest advantage identified during the preclinical investigation of this series was the effectiveness of many of the cryptophycins against tumors that overexpressed the multidrug resistance phenotype. This new class of macrocyclic depsipeptides has proven to be quite novel in its mode of action and in its preclinical antitumor activity.

ACKNOWLEDGMENTS

The authors thank all their colleagues and collaborators who contributed to this work: Andrew H. Fray, Michael J. Martinelli, Eric D. Moher, Bryan H. Norman, Vinod F. Patel, Richard M. Schultz, John E. Toth, David L. Varie, Thomas H. Corbett (Wayne State University), Marc Tius (University of Hawaii), Richard E. Moore (University of Hawaii), Leslie Wilson, and Mary Ann Jordan (University of California at Santa Barbara). Special thanks are also due to Jenniffer Phillips and Susan Koppleman for their help with the references and formatting of the document. They also thank Drs. Gordon Cragg, David Newman (National Cancer Institute), and David Kingston (Virginia Tech University) for giving them an opportunity to summarize the work of the cryptophycin team and for their critical evaluation of this chapter.

UPDATE

D. J. Newman

Since the first edition of this book closed in early 2004, reports covering a significant amount of work on the biosynthesis of the cryptophycin skeleton, syntheses related to cryptophycins and a clinical trial that demonstrated some modest activity in platinum-resistant ovarian cancer have been published through September of 2010.

In the succeeding discussion, reference numbers will continue on from number 29, though they will be formatted as individual citations, rather than the multiple ones frequently used in the First Edition. In addition the conclusions drawn above will not be altered, though some relevant comments are made in the last paragraph of this update.

Clinical Report

In 2006, D'Agostino et al.[29] reported on a multicenter European Phase II trial of cryptophycin 52 (LY355703) covering 26 patients from three Spanish, one Italian and one Slovakian centers. Although the trial was stopped at this number of patients "due to lack of efficacy in other tumor types" (quote from the Discussion section of the report), 24 of the 26 patients were evaluable, with three demonstrating partial remission and seven with stable disease, for an overall response of 41.7%.

Although the initial criterion for trial extension, that of one or more responses was met, due to the lack of efficacy in other tumor trials, the study ceased at this number of patients. The authors did suggest "that this drug may deserve further investigation in this setting" but to date, no further trials have been reported with this particular cryptophycin analog.

Biosynthesis

In 2005, Fortman and Sherman published a review article that demonstrated the potential for microbial genetics to help bridge the gaps between promise and application of marine-sourced natural products.[30] This was rapidly followed by the paper by Beck et al. on the thioesterase domain from the cryptophycin biosynthetic pathway, demonstrating that although it had a considerable tolerance for structural variation within the *seco*-cryptophycin C unit's β-alanine residue, there was a strict spatial requirement at the phenyl group in the unit A δ-hydroxy octadienoate chain elongation intermediate(s).[31]

In the following year 2006, members of the same groups, together with the Hawaii investigators who first discovered the cryptophycins, identified the complete biosynthetic gene cluster by a combination of stable isotope incorporation experiments coupled to the cloning, sequencing, and subsequent gene annotation of the cryptophycin pathway.[32]

Identification of the cryptophycin cluster was facilitated by a careful comparison of the polyketide (PK)/nonribosomal peptide gene clusters from the very closely related but noncyanophycin producer, *Nostoc punctiforme* ATCC 29133. These investigators reported that the producing cluster encoded a collinear set of enzymes that included three distinct modular PK synthases, two modules encoding nonribosomal protein synthetases, and the integrated adenylation/ketoreductase domain that was responsible for the elaboration of the leucic acid subunit. In addition to these activities, the genes that encoded other key biosynthetic steps, including and FAD-linked halogenase (chlorinase) and the putative CYP450 epoxidase were also identified. At the time of the report, a commentary in the same journal by Rohr specifically outlined the potential that this gene cluster had as a potential method for the production of natural and un-natural analogs of the base compound.[33]

The investigators extended the study by demonstrating that the genes could be used to produce a suite of new analogs by altering the available precursor substrates, and the investigation of the

properties of the P450 enabled a chemoenzymatic stereospecific synthesis of cryptophycin 2. That chemoenzymatic synthesis was not an unusual event and could be applied in quite different ways, was amply demonstrated by Seufert et al. the following year when they reported that they could use the thioesterase to release, and cyclize linear cryptophycin substrates that were held by linkage to a PEGA resin. The work extended to an investigation of the tolerance of the thioesterase for a variety of substrates.[34]

Very recently, a thorough discussion of the genetic basis of the transformations involved in the biosynthesis of modular natural products such as the cryptophycins was published in an excellent review by Jones et al.,[35] which should be consulted for the extremely interesting mechanisms involved, in particular those related to enzymatic halogenations.

Synthetic Studies

In the approximately 6 years that have passed since the first edition, a fair number of papers have been published covering synthetic schemes leading to various members of the cryptophycin family of compounds (both natural and semisynthetic variants). The first in this time frame, covering the total synthesis of cryptophycin 3 was reported in 2005 by Danner et al. from the University of Tübingen.[36]

The next group, also from Germany, but this time from Bielefield rather than Tübingen, has published an extensive series of synthetic routes to cryptophycins, including natural, semisynthetic known variants and some novel structures as well. Thus, in 2005, Mast et al. reported on a stereoselective method of synthesizing unit A of cryptophycin that controlled all four stereogenic centers. This permitted them to obtain cryptophycins-1, -52, and a novel epimer of -52, with the potential to develop further.[37] The group then proceeded to expand these methods and up to early 2010, have published a significant number of reports covering improved syntheses of both natural and semisynthetic members of the cryptophycin family.[38–40] The most current report from this group is a 2010 paper demonstrating the facile synthesis using "click chemistry" of a bioactive triazole analog of cryptophycin-52 that they named "clicktophycin."[41]

Other chemistry groups have also published methods of synthesizing various cryotophycins, including Kotoku et al. from Japan, who in 2007 published the stereospecific total synthesis of arenastatin A (cryptophycin 24),[42] and McCubbin et al. from Canada who demonstrated methods of making novel vinyl halide analogs of fragment A via allylation of *in situ* generated β,γ-unsaturated aldehydes.[43] In 2009, a Chinese group also published their syntheses and bioactivities of further novel cryptophycin analogs.[44]

Though it is now close to a decade since cryptophycins were removed from clinical studies, scientists are still interested at all levels in these molecular scaffolds, with a synthetic hybrid of epothilone and cryptophycin, cryptothilone-1 being reported in 2006 by White et al. though in this case, it was not active as a tubulin interactive agent.[45] As further information becomes available on all the scientific fronts, be they cell biology, biosynthesis, and methods of synthesis, it is possible that cryptophycins in one guise or another may yet further aid in drug discovery directed against cancer and other diseases.

REFERENCES

1. Schwartz, R.E., Hirsch, C.F., Sesin, D.F., Flor, J.E., Chartrain, M., Fromtling, R.E., Harris, G.H., Salvatore, M.J., Liesch, J.M., and Yudin, K., Pharmaceuticals from cultured algae. *J. Ind. Microbiol.*, 5, 118–126, 1990.
2. Patterson, G.M.L., Baldwin, C.L., Bolis, C.M., Caplan, F.R., Karuso, H., Larsen, L.K., Levine, I.A. et al., Antineoplastic activity of cultured blue-green-algae (Cyanophyta). *J. Phycol.*, 27, 530–536, 1991.
3. (a) Corbett, T.H., Valeriote, F.A., Polin, L., Panchapor, C., Pugh, S., White, K., Lowinchik, N. et al., Discovery of solid tumor active agents using a soft-agar-colony-formation-disk-diffusion assay, in *Cytoxic anticancer drugs: models and concepts for drug discovery and development*, Valeriote, F.A.,

Corbett, T.H., and Baker, L.H., Eds., Kluwer Academic Publishers, Boston, 35–87, 1992. (b) Valeriote, F.A. et al., Discovery and development of anticancer agents, Valeriote, F. A., Corbett, T. H., and Baker, L. H., Eds., Kluwer Academic Publishers, 67–93, 1997.

4. (a) Golakoti, T., Ohtani, I., Patterson, G.M.L., Moore, R.E., Corbett, T.H., Valeriote, F.A., and Demchik, L., Total structures of cryptophycins, potent antitumor depsipeptides from the blue-green alga Nostoc sp. Strain GSV 224. *J. Am. Chem. Soc.*, 116, 4729–4737, 1994. (b) Golakoti, T., Ogino, J., Heltzel, C.E., Husebo, T.L., Jensen, C.M., Larsen, L.K., Patterson, G.M.L., Moore, R.E., and Mooberry, S.L., Structure determination, conformational analysis, chemical stability studies, and antitumor evaluation of the cryptophycins. Isolation of 18 new analogs from Nostoc sp. strain GSV 224. *J. Am. Chem. Soc.*, 117, 12030–12049, 1995.
5. (a) Corbett, T.H., Valeriote, F., LoRusso, P., Polin, L., Panchapor, C., and Pugh, S., *In vivo* methods for screening and preclinical testing—use of rodent solid tumors for drug discovery, in *Anticancer Drug Development Guide: Preclinical Screening, Clinical Trials, and Approval*, Teicher, B.A., Ed., Humana Press, Totowa, NJ, 75–99, 1997. (b) Corbett, T.H., Valeriote, F.A., Demchik, L., Lowichik, N., Polin, L., Panchapor, C., Pugh, S. et al., Discovery of cryptophycin-1 and BCN-183577: examples of strategies and problems in the detection of antitumor activity in mice. *Invest. New Drugs*, 15, 207–218, 1997.
6. Barrow, R.A., Hemscheidt, T., Liang, J., Paik, S., Moore, R.E., and Tius, M.A., Total synthesis of cryptophycins. Revision of the structures of cryptophycins A and C. *J. Am. Chem. Soc.*, 117, 2479–2490, 1995.
7. (a) Kerksiek, K., Mejillano, M.R., Schwartz, R.E., Georg, G.I., and Himes, R.H., Interaction of cryptophycin 1 with tubulin and microtubules. *FEBS Lett.*, 377, 59–61, 1995. (b) Smith, C.D., and Zhang, X., Mechanism of action of cryptophycin. Interaction with the Vinca alkaloid domain of tubulin. *J. Biol. Chem.*, 271, 6192–6198, 1996. (c) Bai, R., Schwartz, R.E., Kepler, J.A., Pettit, G.R., and Hamel, E., Characterization of the interaction of cryptophycin 1 with tubulin: binding in the Vinca domain, competitive inhibition of dolastatin 10 binding, and an unusual aggregation reaction. *Cancer Res.*, 56, 4398–4406, 1996. (d) Mooberry, S.L., Taoko, C.R., and Busquets, L., Cryptophycin 1 binds to tubulin at a site distinct from the colchicine binding site and at a site that may overlap the vinca binding site. *Cancer Lett.*, 107, 53–57, 1996. (e) Panda, D., Himes, R.H., Moore, R.E., Wilson, L., and Jordan, M.A., Mechanism of action of the unusually potent microtubule inhibitor cryptophycin 1. *Biochemistry*, 36, 12948–12953, 1997.
8. Mooberry, S.L., Busquets, L., and Tien, G., Induction of apoptosis by cryptophycin 1, a new antimicrotubule agent. *Int. J. Cancer*, 73, 440–448, 1997.
9. (a) Smith, C.D. Zhang, X., Mooberry, S.L., Patterson, G.M.L., and Moore, R.E., Cryptophycin: a new antimicrotubule agent active against drug-resistant cells. *Cancer Res.*, 54, 3779–3784, 1994. (b) Wagner, M.M., Paul, D.C., Shih, C., Jordan, M.A., Wilson, L., and Williams, D.C., *In vitro* pharmacology of cryptophycin 52 (LY355703) in human tumor cell lines. *Cancer Chemother. Pharmacol.*, 43, 115–125, 1999.
10. Panda, D., DeLuca, K., Williams, D., Jordan, M.A., and Wilson, L., Antiproliferative mechanism of action of cryptophycin-52: kinetic stabilization of microtubule dynamics by high-affinity binding to microtubule ends. *Proc. Nat. Acad. Sci. USA*, 95, 9313–9318, 1998.
11. (a) Farrell, K.W. and Jordan, M.A., A kinetic analysis of assembly–disassembly at opposite microtubule ends. *J. Biol. Chem.*, 257, 3131–3138, 1982. (b) Farrell, K.W., Jordan, M.A., Miller, H.P., and Wilson, L., Phase dynamics at microtubule ends: the coexistence of microtubule length changes and treadmilling. *J. Cell Biol.*, 104, 1035–1046, 1987. (c) Wilson, L. and Jordan, M.A., Pharmacological probes of microtubule function. *Modern Cell Biol.*, 13, 59–83, 1994. (d) Jordan, M.A. and Wilson, L., Microtubules and actin filaments: dynamic targets for cancer chemotherapy. *Curr. Opin. Cell Biol.*, 10, 123–130, 1998. (e) Yvon, A.-M.C., Wadsworth, P., and Jordan, M.A., Taxol suppresses dynamics of individual microtubules in living human tumor cells. *Mol. Biol. Cell*, 10, 947–959, 1999. (f) Wilson, L., Panda, D., and Jordan, M.A., Modulation of microtubule dynamics by drugs: a paradigm for the actions of cellular regulators. *Cell Struct. Funct.*, 24, 329–335, 1999. (g) Jordan, M.A., Mechanism of action of antitumor drugs that interact with microtubules and tubulin. *Curr. Med. Chem: Anti-cancer Agents*, 2, 1–17, 2002. (h) Jordan, M.A. and Wilson, L., Microtubules as a target for anticancer drugs. *Nat. Rev. Cancer*, 4, 253–265, 2004.
12. Fray, A.H., Intramolecular aminolysis of trichloroethyl esters: a mild macrocyclization protocol for the preparation of cryptophycin derivatives. *Tetrahedron Asymmetry*, 9, 2777–2781, 1998.
13. (a) Martinelli, M.J., Nayyar, N.K., Moher, E.D., Dhokte, U.P., Pawlak, J.M., and Vaidyanathan, R., Dibutyltin oxide catalyzed selective sulfonylation of β-chelatable primary alcohols. *Org. Lett.*, 1, 447–450, 1999. (b) Martinelli, M.J., Vaidyanathan, R., and Khau, V.V., Selective monosulfonylation of internal 1,2-diols catalyzed by di-*n*-butyltin oxide. *Tetrahedron Lett.*, 41, 3773–3776, 2000.
14. For other approaches to Fragment A see: (a) Varie, D.L., Brennan, J., Briggs, B., Cronin, J.S., Hay, D.A., Rieck III, J.A., and Zmijewski, M.J., Bioreduction of (R)-carvone and regioselective Baeyer-Villiger oxidations: application to the asymmetric synthesis of cryptophycin fragment A. *Tet. Lett.*, 39, 8405–8408,

1998. (b) Dhokte, U.P., Khau, V.V., Hutchison, D.R., and Martinelli, M.J., A novel approach for total synthesis of cryptophycins via asymmetric crotylboration protocol. *Tet. Lett.*, 39, 8771–8774, 1998. (c) Furuyama, M. and Shimizu, I., A short enantioselective synthesis of a component of cryptophycin A and arenastatin A. *Tetrahedron Asymmetry*, 9, 1351–1357, 1998. (d) Liang, J., Hoard, D.W., Khau, V.V., Martinelli, M.J., Moher, E.D., Moore, R.E., and Tius, M.A., Synthesis of unit A of cryptophycin via a [2,3]-Wittig rearrangement. *J. Org. Chem.*, 64, 1459–1463, 1999. (e) Liang, J., Moher, E.D., Moore, R.E., and Hoard, D.W., Synthesis of cryptophycin 52 using the Sharpless asymmetric dihydroxylation: diol to epoxide transformation optimized for a base-sensitive substrate. *J. Org. Chem.*, 65, 3143–3147, 2000. (f) Pousset, C., Haddad, M., and Larcheveque, M., Diastereocontrolled synthesis of unit A of cryptophycin. *Tetrahedron*, 57, 7163–7167, 2001. (g) Raghavan, S. and Tony, K.A., Sulfinyl moiety as an internal nucleophile. 1. Efficient stereoselective synthesis of fragment A of cryptophycin 3. *J. Org. Chem.*, 68, 5002–5005, 2003. (h) Phukan, P., Sasmal, S., and Maier, M.E., Flexible routes to the 5-hydroxy acid fragment of the cryptophycins. *Eur. J. Org. Chem.*, 9, 1733–1740, 2003.

15. Moore, R.E., Corbett, T.H., Patterson, G.M.L., and Valeriote, F.A., The search for new antitumor drugs from blue-green algae. *Curr. Pharm. Des.*, 2, 317–330, 1996.
16. Moore, R.E., Cyclic peptides and depsipeptides from cyanobacteria: a review. *J. Ind. Microbiol.*, 16, 134–143, 1996.
17. Al-awar, R.S., Ehlhardt, W.J., Gottumukkala, S.V., Martinelli, M.J., Moher, E.D., Moore, R.E., Munroe, J.E. et al., Preparation of novel cryptophycin pharmaceuticals. PCT Int. Appl., 293 pp. WO 9808505 A1 19980305, 1998.
18. Al-awar, R.S., Ray, J.E., Schultz, R.M., Andis, S.L., Kennedy, J.H., Moore, R.E., Liang, J., Golakoti, T., Subbaraju, G.V., and Corbett, T.H., A convergent approach to cryptophycin 52 analogues: synthesis and biological evaluation of a novel series of fragment a epoxides and chlorohydrins. *J. Med. Chem.*, 46, 2985–3007, 2003.
19. Patel, V.F., Andis, S.L., Kennedy, J.H., Ray, J.E., and Schultz, R.M., Novel cryptophycin antitumor agents: synthesis and cytotoxicity of fragment "B" analogues. *J. Med. Chem.*, 42, 2588–2603, 1999.
20. (a) Kobayashi, M., Aoki, S., Ohyabu, N., Kurosu, M., Wang, W., and Kitagawa, I., Arenastatin A, a potent cytotoxic depsipeptide from the okinawan marine sponge *Dysidea arenaria. Tetrahedron Lett.*, 35, 7969–7972, 1994. (b) Kobayashi, M., Kurosu, M., Ohyabu, N., Wang, W., Fujii, S., and Kitagawa, I., The absolute stereostructure of arenastatin A, a potent cytotoxic depsipeptide from the Okinawan marine sponge *Dysidea arenaria. Chem. Pharm. Bull.*, 42, 2196–2198, 1994.
21. Varie, D.L., Shih, C., Hay, D.A., Andis, S.L., Corbett, T.H., Gossett, L.S., Janisse, S.K. et al., Synthesis and biological evaluation of cryptophycin analogs with substitution at C-6 (fragment C region). *Bioorg. Med. Chem. Lett.*, 9, 369–374, 1999.
22. Norman, B.H., Hemscheidt, T., Schultz, R.M., and Andis, S.L., Total synthesis of cryptophycin analogs. Isosteric replacement of the C-D ester. *J. Org. Chem.*, 63, 5288–5294, 1998.
23. Shih, C., Gossett, L.S., Gruber, J.M., Grossman, C.S., Andis, S.L., Schultz, R.M., Worzalla, J.F., Corbett, T.H., and Metz, J.T., Synthesis and biological evaluation of novel cryptophycin analogs with modification in the β-alanine region. *Bioorg. Med. Chem. Lett.*, 9, 69–74, 1999.
24. (a) Worzalla, J.F., Cao, J., Ehlhardt, W.J., Harrison, S.D., Law, K.L., Martinelli, M.J., Self, T.D. et al., LY355702 and LY355703, new cryptophycin analogues with antitumor activity against human tumor xenografts. *Proc. Am. Assoc. Cancer Res.*, 38, 225, 1997 (Abs. 1516). (b) Polin, L., Valeriote, F. A., Moore, R.E., Tius, M.A., Barrow, R.A., Hemscheidt, T., Liang, J. et al., Preclinical antitumor activity of cryptophycin-52/55 (C-52; C-55) against human tumors in SCID mice. *Proc. Am. Assoc. Cancer Res.*, 38, 225, 1997 (Abs. 1514). (c) Polin, L., Valeriote, F., White, K., Panchapor, C., Pugh, S., Knight, J., LoRusso, P. et al., Treatment of human prostate tumors PC-3 and TSU-PR1 with standard and investigational agents in SCID mice. *Invest. New Drugs*, 15, 99–108, 1997.
25. (a) Sessa, C., Weigang-Kohler, K., Pagani, O., Greim, G., Mora, O., De Pas, T., Burgess, M., Weimer, I., and Johnson, R., Phase I and pharmacological studies of the cryptophycin analogue LY355703 administered on a single intermittent or weekly schedule. *Eur. J. Cancer*, 38, 2388–2396, 2002. (b) Stevenson, J.P., Sun, W., Gallagher, M., Johnson, R., Vaughn, D., Schuchter, L. et al., Phase I trial of the cryptophycin analogue LY355703 administered as an intravenous infusion on a day 1 and 8 schedule every 21 days. *Clin. Cancer Res.*, 8, 2524–2529, 2002.
26. (a) Salamonczyk, G.M., Han, K., Guo, Z.-W., and Sih, C.J., Total synthesis of cryptophycins via a chemoenzymatic approach. *J. Org. Chem.*, 61, 6893–6900, 1996. (b) de Muys, J.-M., Rey, R., Nguyen, D., Go, B., Fortin, S., and Lavallee, J.-F., Synthesis and *in vitro* cytotoxicity of cryptophycins and related analogs. *Bioorg. Med. Chem. Lett.*, 6, 1111–1116, 1996. (c) Rej, R., Nguyen, D., Go, B., Fortin, S., and Lavallee, J.-F., Total synthesis of cryptophycins and their 16-(3-phenylacryloyl) derivatives. *J. Org.*

Chem., 61, 6289–6295, 1996. (d) Gardinier, K.M. and Leahy, J.W., Enantiospecific total synthesis of the potent antitumor macrolides cryptophycins 1 and 8. *J. Org. Chem.*, 62, 7098–7099, 1997. (e) Ali, S.M. and Georg, G.I., Formal syntheses of cryptophycin A and arenastatin A. *Tetrahedron Lett.*, 38, 1703–1706, 1997. (f) Georg, G.I., Ali, S.M., and Stella, V.J., Halohydrin analogues of cryptophycin 1: synthesis and biological activity. *Bioorg. Med. Chem. Lett.*, 8, 1959–1962, 1998. (g) Eggen, M. and Georg, G.I., Enantioselective synthesis of a 3β-dephenylcryptophycin synthon. *Bioorg. Med. Chem. Lett.*, 8, 3177–3180, 1998. (h) White, J.D., Hong, J., and Robarge, L.A., Total synthesis of cryptophycins-1, -3, -4, -24 (arenastatin A), and -29, cytotoxic depsipeptides from cyanobacteria of the Nostocaceae. *J. Org. Chem.*, 64, 6206–6216, 1999. (i) Chakraborty, T.K. and Das, S., Diastereoselective opening of trisubstituted epoxy alcohols: application in the studies directed toward the synthesis of octenoic acid moiety of cryptophycins. *J. Indian Chem. Soc.*, 76, 611–616, 1999. (j) Christopher, J. A., Kocienski, P.J., Kuhl, A., and Bell, R., A synthesis of cryptophycin 4 using a planar chiral molybdenum cationic complex. *Synlett.*, 4, 463–466, 2000. (k) Ghosh, A.K. and Bischoff, A., A convergent synthesis of (+)-cryptophycin B, a potent antitumor macrolide from *Nostoc* sp. cyanobacteria. *Org. Lett.*, 2, 1573–1575, 2000. (l) Barrow, R.A., Moore, R.E., Li, L-H., and Tius, M.A., Synthesis of 1-aza-cryptophycin 1, an unstable cryptophycin. An unusual skeletal rearrangement. *Tetrahedron*, 56, 3339–3351, 2000. (m) Eggen, M., Mossman, C.J., Buck, S.B., Nair, S.K., Bhat, L., Ali, S.M., Reiff, E.A., Boge, T.C., and Georg, G.I., Total synthesis of cryptophycin-24 (Arenastatin A) amenable to structural modifications in the C16 side chain. *J. Org. Chem.*, 65, 7792–7799, 2000. (n) Eggen, M.J., Nair, S.K., and Georg, G.I., Rapid entry into the cryptophycin core via an acyl-β-lactam macrolactonization: total synthesis of cryptophycin-24. *Org. Lett.*, 3, 1813–1815, 2001. (o) Smith, A.B., Cho, Y.S., Zawacki, L.E., Hirschmann, R., and Pettit, G.R., First generation design, synthesis, and evaluation of azepine-based cryptophycin analogues. *Org. Lett.*, 3, 4063–4066, 2001. (p) Martinelli, M.J., Vaidyanathan, R., Khau, V.V., and Staszak, M.A., Reaction of cryptophycin 52 with thiols. *Tetrahedron Lett.*, 43, 3365–3367, 2002. (q) Li, L-H., and Tius, M.A., Stereospecific synthesis of cryptophycin 1. *Org. Lett.*, 4, 1637–1640, 2002. (r) Hoard, D.W., Moher, E.D., Martinelli, M.J., and Norman, B.H., Synthesis of cryptophycin 52 using the Shi epoxidation. *Org. Lett.*, 4, 1813–1815, 2002. (s) Smith, A.B., Cho, Y.S., Pettit, G.R., and Hirschmann, R., Design, synthesis, and evaluation of azepine-based cryptophycin mimetics. *Tetrahedron*, 59, 6991–7009, 2003. (t) Vidya, R., Eggen, M., Nair, S.K., Georg, G.I., and Himes, R.H., Synthesis of cryptophycins via an N-acyl-β-lactam macrolactonization. *J. Org. Chem.*, 68, 9687–9693, 2003. (u) Ghosh, A.K., and Swanson, L., Enantioselective synthesis of (+)-cryptophycin 52 (LY355703), a potent antimitotic antitumor agent. *J. Org. Chem.*, 68, 9823–9826, 2003.

27. (a) Smith, C.D. and Zhang, X., Mechanism of action of cryptophycin. Interaction with the Vinca alkaloid domain of tubulin. *J. Biol. Chem.*, 271, 6192–6198, 1996. (b) Kessel, D. and Luo, Y., Cells in cryptophycin-induced cell-cycle arrest are susceptible to apoptosis. *Cancer Lett.*, 151, 25–29, 2000. (c) Barbier, P., Gregoire, C., Devred, F., Sarrazin, M., and Peyrot, V., *In vitro* effect of cryptophycin 52 on microtubule assembly and tubulin: molecular modeling of the mechanism of action of a new antimitotic drug. *Biochemistry*, 40, 13510–13519, 2001. (d) Watts, N.R., Cheng, N., West, W., Steven, A.C., and Sackett, D.L., The cryptophycin-tubulin ring structure indicates two points of curvature in the tubulin dimer. *Biochemistry*, 41, 12662–12669, 2002. (e) Drew, L., Fine, R.L., Do, T.N., Dourglas, G.P., and Petrylak, D.P., The novel antimicrotubule agent cryptophycin 52 (LY355703) induces apoptosis via multiple pathways in human prostate cancer cells. *Clin. Cancer Res.*, 8, 3922–3932, 2002.
28. For other reviews on the cryptophycins see: (a) Shih, C. and Teicher, B.A., Cryptophycins: a novel class of potent antimitotic antitumor depsipeptides. *Curr. Pharm. Design*, 7, 1259–1276, 2001. (b) Shih, C., Al-Awar, R.S., Fray, A.H., Martinelli, M.J., Moher, E.D., Norman, B.H., Patel, V.F. et al., Synthesis and structure–activity relationship studies of cryptophycins: a novel class of potent antimitotic antitumor depsipeptides. *ACS Symp. Ser.*, 796 (Anticancer Agents), 171–189, 2001. (c) Eggen, M.J. and Georg, G.I., The cryptophycins: their synthesis and anticancer activity. *Med. Res. Rev.*, 22, 85–101, 2002. (d) Tius, M.A., Synthesis of the cryptophycins. *Tetrahedron*, 58, 4343–4367, 2002. (e) Li, T. and Shih, C., Structure activity relationships of cryptophycins, a novel class of antitumor antimitotic agents. *Frontiers Biotech. Pharm.*, 3, 172–192, 2002. (f) Hong, J. and Zhang, Li., Novel approaches to the synthesis of cryptophycin and related depsipeptides. *Frontiers Biotech. Pharm.*, 3, 193–213, 2002. (g) Tius, M.A., Cryptophycin synthesis. *Handbook Environ. Chem.*, 3 (Part P), 265–305, 2003.
29. D'Agostino, G., Del Campo, J., Mellado, B., Izquierdo, M. A., Minarik, T., Cirri, L., Marini, L., Perez-Gracia, J. L., and Scambia, G., A multicenter phase II study of the cryptophycin analog LY355703 in patients with platinum-resistant ovarian cancer. *Int. J. Gynecol. Cancer*, 16, 71–76, 2006.

30. Fortman, J.L. and Sherman, D.H., Utilizing the power of microbial genetics to bridge the gap between the promise and application of marine natural products. *ChemBioChem*, 6 (6), 960–978, 2005.
31. Beck, Z.Q., Aldrich, C.C., Magarvey, N.A., Georg, G.I.., and Sherman, D.H., Chemoenzymatic synthesis of cryptophycin/arenastatin natural products. *Biochemistry*, 44(41), 13457–13466, 2005.
32. Magarvey, N.A., Beck, Z.Q., Golakoti, T., Ding, Y., Huber, U., Hemscheidt, T.K., Abelson, D., Moore, R.E., and Sherman, D.H., Biosynthetic characterization and chemoenzymatic assembly of the cryptophycins. Potent anticancer agents from cyanobionts. *ACS Chem. Biol.*, 1(12), 766–779, 2006.
33. Rohr, J., Cryptophycin anticancer drugs revisited. *ACS Chem. Biol.*, 1(12), 747–750, 2006.
34. Seufert, W., Beck, Z.Q., and Sherman, D.H., Enzymatic release and macrolactonization of cryptophycins from a safety-catch solid support. *Angew. Chem. Int. Ed.*, 46(48), 9298–9300, 2007.
35. Jones, A.C., Monroe, E.A., Eisman, E.B., Gerwick, L., Sherman, D.H., and Gerwick, W.H., The unique mechanistic transformations involved in the biosynthesis of modular natural products from marine cyanobacteria. *Nat. Prod. Rep.*, 27, 1048–1065, 2010.
36. Danner, P., Bauer, M., Phukan, P., and Maier, M.E., Total synthesis of cryptophycin 3. *Eur. J. Org. Chem.*, (2), 317–325, 2005.
37. Mast, C.A., Eißler, S., Stončius, A., Stammler, H.-G., Neumann, B., and Sewald, N., Efficient and versatile stereoselective synthesis of cryptophycins. *Chem. Eur. J.*, 11(16), 4667–4677, 2005.
38. Eißler, S., Stoncius, A., Nahrwold, M., and Sewald, N., The synthesis of cryptophycins. *Synthesis*, 3747, 2006.
39. Nahrwold, M., Eißler, S., and Sewald, N., Cryptophycins. Highly cytotoxic depsipeptides. Highlights, challenges, and recent advances. *Chimica Oggi*, 26 (4 Suppl), 13–16, 2008.
40. Eißler, S., Bogner, T., Nahrwold, M., and Sewald, N., Efficient synthesis of cryptophycin-52 and novel para- alkoxymethyl unit A analogues. *Chem. Eur. J.*, 15(42), 11273–11287, 2009.
41. Nahrwold, M., Bogner, T., Eißler, S., Verma, S., and Sewald, N., Clicktophycin-52: A bioactive cryptophycin-52 triazole analogue. *Org. Lett.*, 12(5), 1064–1067, 2010.
42. Kotoku, N., Narumi, F., Kato, T., Yamaguchi, M., and Kobayashi, M., Stereoselective total synthesis of arenastatin A, a spongean cytotoxic depsipeptide. *Tetrahedron Lett.*, 48(40), 7147–7150, 2007.
43. McCubbin, J.A., Maddess, M.L., and Lautens, M., Total synthesis of cryptophycin analogues via a scaffold approach. *Org. Lett.*, 8(14), 2993–2996, 2006.
44. Liu, W.L., Zhang, J.C., Jiang, F.Q., and Fu, L., Synthesis and cytotoxicity studies of new cryptophycin analogues. *Arch. Pharm. Chem. Life Sci.*, 342, 577–583, 2009.
45. White, J.D., Smits, H., and Hamel, E., Synthesis of cryptothilone 1, the first cryptophycin-epothilone hybrid. *Org. Lett.*, 8(18), 3947–3950, 2006.

10 Chemistry and Biology of the Discodermolides, Potent Mitotic Spindle Poisons

Sarath P. Gunasekera and Amy E. Wright

CONTENTS

10.1 Introduction 241
10.2 Natural Sources 242
10.3 Chemistry 243
10.4 Synthesis 244
10.4.1 Synthesis of Discodermolide 244
10.4.2 Synthesis of Analogs 244
10.5 Biological Activity 246
10.5.1 Immunosuppressive Properties 246
10.5.2 Antitumor Properties 249
10.6 Structure–Activity Studies 253
10.7 Clinical Investigation 259
References 259

10.1 INTRODUCTION

(+)-Discodermolide (**1**) is a highly functionalized, marine sponge-derived polyketide δ-lactone presumably formed by a combination of propionate and acetate units. **1** was first isolated and characterized by Gunasekera et al.[1] at the Harbor Branch Oceanographic Institution (HBOI) from the marine sponge *Discodermia dissoluta*. Crude extracts of the sponge showed strong potency against the murine P388 lymphocytic leukemia cell line, and bioassay-guided fractionation using this assay resulted in the purification of **1**. The structure was defined by spectroscopic methods and was confirmed by x-ray diffraction analysis. The initial reports of (+)-discodermolide's strong *in vitro* antiproliferative and *in vitro* and *in vivo* immunosuppressive activities[2,3] created a wide interest among the synthetic organic chemistry community. The absolute stereochemistry was subsequently defined by total synthesis conducted by the Schreiber group.[4]

(+)-Discodermolide is a member of the group of antimitotic agents known to act by microtubule stabilization, other members of which include Taxol®[5] (**2**), the epothilones A[6] (**3**), B[6] (**4**), and D[7] (**5**), eleutherobin[8] (**6**), laulimalide[9] (**7**), and recently, dictyostatin 1[10] (**8**). Because of its strong microtubule-stabilizing properties and its excellent activity against multidrug-resistant tumors, HBOI licensed (+)-discodermolide (**1**) to Novartis Pharmaceutical Corporation in early 1998 for development as an anticancer drug.

The discovery that discodermolide's mechanism of action is similar to that of Taxol (**2**)[5] (Taxol is a registered trademark of Bristol–Myers Squibb Company, NY), coupled with its limited supply from the natural source, prompted the scientific community to prepare synthetic **1** and its analogs via a number of routes. The unique chemical structure with 13 stereogenic centers posed a major

synthetic challenge for the preparation of sufficient material to allow for the preclinical and clinical studies. Over 15 publications describe the latter work. A major milestone in the development of **1** was the development of a large-scale synthesis of (+)-discodermolide (**1**) by the Smith group.[11] This, coupled with other synthetic schemes, led to a refined process in which over 60 g of synthetic (+)-discodermolide was produced. (+)-Discodermolide was evaluated in Phase I clinical trials for solid tumor malignancies at the Cancer Therapy and Research Center in San Antonio, TX, but the trials were halted due to toxicity issues.[12] Discodermolide has been demonstrated to show synergistic activity with Taxol suggesting that it may have utility in combination therapeutic regimes that would reduce toxicity of the current chemotherapeutic regimes.[13–15] Discodermolide is also unique in the microtubule-stabilizing agents in inducing accelerated cell senescence which may also lead to improved therapeutic options.[16]

10.2 NATURAL SOURCES

The genus *Discodermia* du Bocage belongs to the family Theonellidae. This genus is characterized by the presence of discotriaene spicules in addition to the presence of desmas, which are characteristic of all lithistid sponges. The microsclere compliment of the genus *Discodermia* consists of microxeas and microrhabds.[17] *Discodermia* is represented by at least three valid species, *D. dissoluta* Schmidt, *D. polydiscus* du Bocage, and *D. verrucosa*, in the Caribbean region of the central Atlantic Ocean. Additional as-yet-undescribed species have been collected by HBOI and are in their collection.

(+)-Discodermolide (**1**) was first isolated[1] from a sponge sample collected on March 27, 1987, off Lucaya, Grand Bahamas Island, at a depth of 30 m. Subsequently, sufficient quantity of **1** was isolated from an earlier 1985 collection to allow for the completion of the structure elucidation and preliminary biological evaluations. The 1987 sponge sample was slightly dark in appearance, and the compound responsible for this color coeluted in trace amounts with the first isolate of (+)-discodermolide. This trace impurity gave a pink coloration to the solution of **1**, and further purification attenuated the yield of **1**. The freshly thawed 434 g of sponge sample from the 1987 collection yielded 7 mg of pure (+)-discodermolide. The samples collected in 1985 and most of the subsequent collections did not contain the pink impurity, and the average yield of **1** was 10 mg/kg of the wet sponge sample.

Harbor Branch chemists noted the existence of two chemically distinguishable forms of *D. dissoluta*. Both sponges contained **1** as a minor secondary metabolite and either the tetramic acid-derived alkaloid discodermide (**9**)[18] or a mixture of depsipeptides trivially named polydiscamides as the major metabolites. The major metabolites discodermide (**9**) and polydiscamide A (**10**)[19] occur in gram quantities in 1 kg of the wet sponge sample, but **9** and **10** have not been observed to co-occur in the same sponge sample. The need for larger amounts of discodermolide for preclinical investigation prompted the collection of 20 kg of *Discodermia* spp. in November 1998. From this material, four naturally occurring analogs have been isolated. One sponge sample (wet weight of 1931 g) was collected by submersible on November 23, 1998, at a depth of 147 m, from the Bell Channel Buoy, Grand Bahama Island, and yielded 12.0 mg of **1** and 0.3 mg of 2-*epi*-discodermolide[20] (**11**, yield, 0.00001% of wet weight). The morphology of this sponge is described as a range from a large cup shape to irregular cups forming branches. A second batch of 3570 g of the *Discodermia* sp. collected at a depth of 157 m off Lucaya, Grand Bahama Island, furnished **1** (35 mg), 2-*des*-methyldiscodermolide[20] (**12**, 1.0 mg, yield, 0.00003% wet weight) and 5-hydroxymethyldiscodermolate[20] (**13**, 1.1 mg, yield, 0.00003% wet weight). This sponge sample was tan in color, and the morphology was a cluster of fingers. A third form of *Discodermia* sp. (2480 g) was described as thin, irregular anastomosing branches that are cream in color. It was collected from the same location as the latter sample and yielded **1** (25 mg) and 19-*des*-aminocarbonyldiscodermolide[20] (**14**, 1.1 mg, yield, 0.00006% wet weight). A cyclic analog of **1**, trivially named 9-13-cyclodiscodermolide[20] (**15**), was isolated from a collection of *Discodermia* sp. made in May 1993 off Tartar Bank, south of Cat Island, Bahamas, at a depth of 183–198 m. This specimen was cup shaped and white to yellow in color, and the 2500 g sample furnished only 1.2 mg (yield, 0.00005% wet weight) of 9-13-cyclodiscodermolide (**15**).

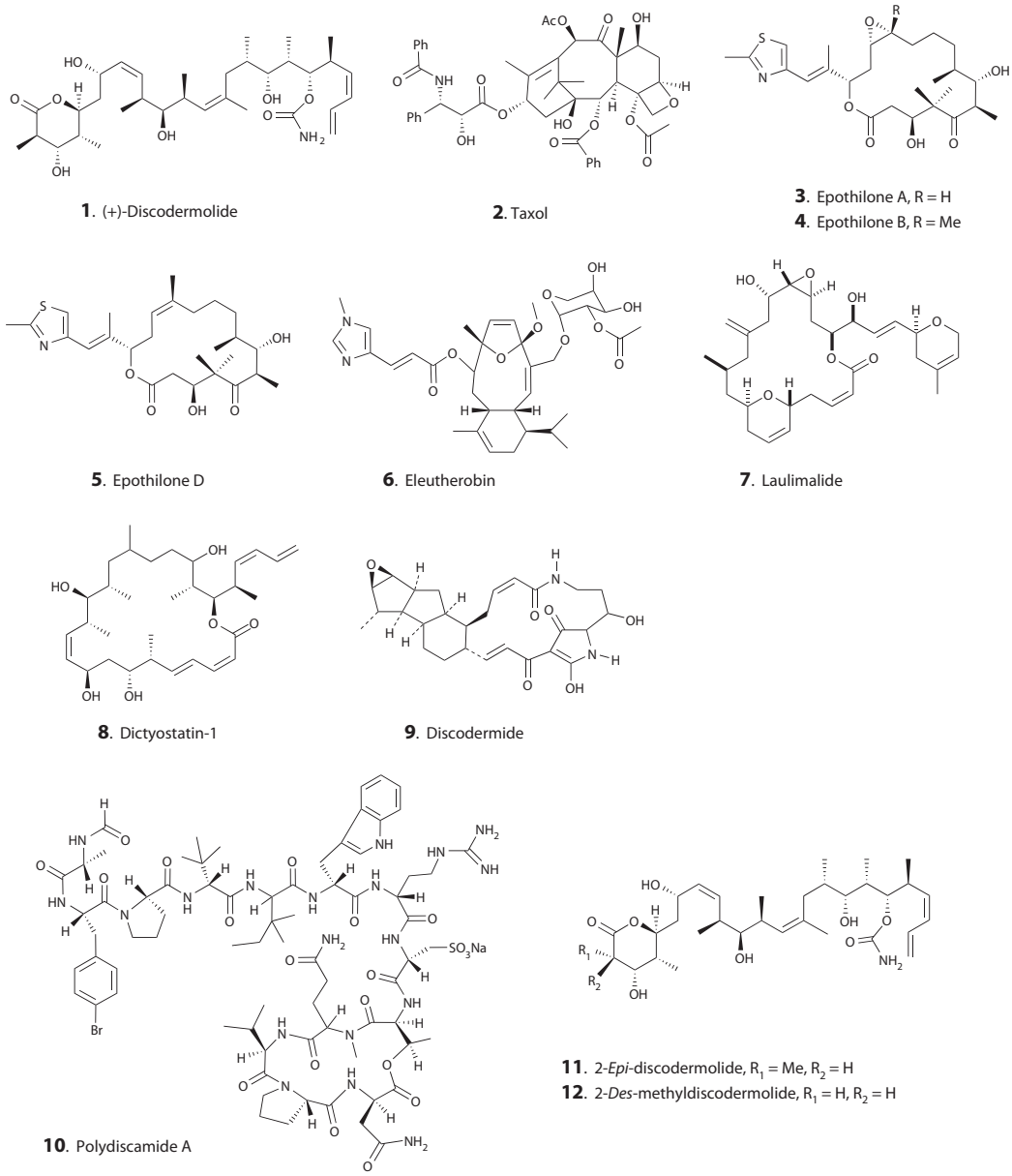

STRUCTURE 10.1 Structures of tubulin hyperstabilizing compounds (**1–8**) and compounds which co-occur with (+)-discodermolide.

10.3 CHEMISTRY

(+)-Discodermolide (**1**) is a polyhydroxy dodecaketide δ-lactone presumably biosynthesized by a combination of four acetate and eight propionate units. Structurally, it bears 13 stereo centers with 15 rotatable σ-bonds. The δ-lactone ring is tetrasubstituted, and the side chain contains one disubstituted (C8) and one trisubstituted (C13) *Z*-double bonds, as well as a terminal *Z*-diene system. Four of the five free secondary hydroxyl groups are located at C3, C7, C11, and C17 positions, and the fifth hydroxyl group is functionalized to a pendant carbamate group. Both in the solid state (as evident from the crystal structure[1]) and in the liquid state (determined by NOE studies in conjunction

with Monte Carlo conformational studies[21]), the structure of **1** exists in a helical conformation, arranging the C1–C19 region into a U-shaped conformation that brings the δ-lactone and the C19 pendant carbamate group in close proximity. The tetrasubstituted δ-lactone preferred a boat-like conformation. This adopted hairpin conformation, in which the two internal (*Z*)-olefins in the side chain act as conformational locks through minimization of (1,3) strain between their respective substituents in concert with the avoidance of *syn*-pentane interactions, results in the restricted mobility of the 19-carbon side chain.

10.4 SYNTHESIS

10.4.1 Synthesis of Discodermolide

The first total synthesis of discodermolide was achieved by the Schreiber group at Harvard University, and their synthesis resulted in the preparation of (–)-discodermolide[22] based on the stereochemistry reported in the first publication.[1] Subsequently, this group, using the identical route to synthesize the natural antipode (+)-discodermolide (**1**), established the absolute configuration.[4,23] Their synthetic plan was adapted on a disconnection of the 24-member carbon chain into three roughly equivalent segments. The δ-lactone-end fragment C1–C7 was coupled to the middle fragment C8–C15, and the carbon skeleton was completed by attachment of a fragment C15–C24 through the use of enolate alkylation chemistry. Since then, Smith et al.[11,24] and Myles et al.[25,26] have prepared both antipodes of discodermolide. Marshall and Jones,[27] Paterson et al.,[28] Arefolov and Panek,[29] and Ardison et al.[30] have synthesized (+)-discodermolide. All these groups used similar triply convergent approaches with different coupling and reaction conditions to achieve the total synthesis. A number of reviews have been published that describe in detail the various approaches used to synthesize small quantities of discodermolide.[31–33] In 1999, in a step that was key to moving discodermolide forward towards clinical evaluation, the Smith group improved on their previously published method[24] and synthesized **1** in 6% overall yield, a procedure that was amenable to gram-scale production.[11,34] They improved the triply convergent approach by synthesizing the three subunits from a common precursor, using a modified Negishi coupling using alkyl zinc species, synthesis of the phosphonium salt via ultrahigh pressure, and finally, using a chemoselective Wittig olefination reaction to give the complete carbon chain.

The Novartis Process Chemistry group, using a combination of methods developed by Smith, Paterson, and their own research group, synthesized 60 g of clinical grade **1,** that was used in the Phase I clinical trials at the Cancer Research Center in San Antonio, TX. This large-scale synthesis of clinical grade **1** involved 39 steps, with the longest linear sequence having 26 steps and 17 large-scale chromatographic purifications. The Novartis group modified the synthesis of the Smith group Weinreb amide[34] that contains the methyl–hydroxy–methyl stereo triad that is repeated in three discodermolide fragments C1–C6, C9–C14, and C15–C21 for pilot plant production.[35] The total synthesis was described in a five-part series.[35–39] The final paper[39] describes the linkage of the methylketone-containing C1–C6 fragment and the C7–C24 aldehyde fragment using a reagent-controlled stereoselective boron enolate aldol coupling procedure developed by Paterson's group.[40] The total synthesis by the Novartis group of 60 g of crystalline (+)-discodermolide using good manufacturing processes represents a significant milestone in both natural product drug development and organic synthesis.

10.4.2 Synthesis of Analogs

The potent and distinct biological properties of discodermolide coupled with the desire to develop compounds with lower toxicity have led to the synthesis of numerous structural analogs. The compounds prepared to date and the synthetic strategies used to prepare them have been recently reviewed by Smith and Freeze.[32] The Schreiber group was the first to prepare discodermolide analogs for structure–activity relationship (SAR) studies.[4,23] They prepared C16 (**16**) and C17 (**17**) epimers,

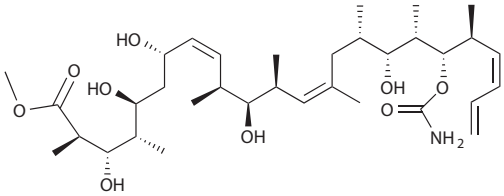

13. 5-Hydroxymethyldiscodermolate

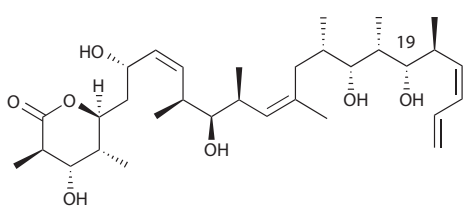

14. 19-*Des*-aminocarbonyldiscodermolide

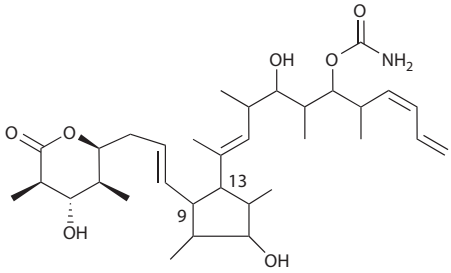

15. 9-13-Cyclodiscodermolide

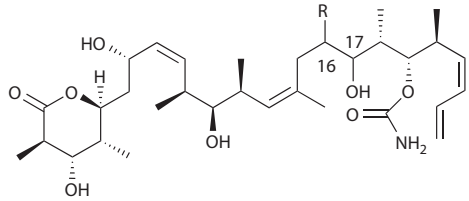

16. R = Me, (C16*R*, C17*R*)
17. R = Me, (C16*S*, C17*S*)
18. R = H, (C17*R*)

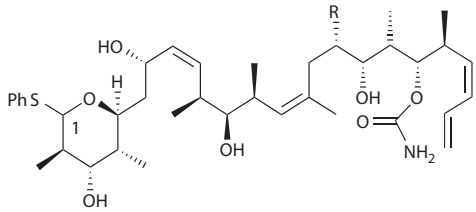

19. β-PhS, R = Me
20. α-PhS, R = Me
21. β-PhS, R = H

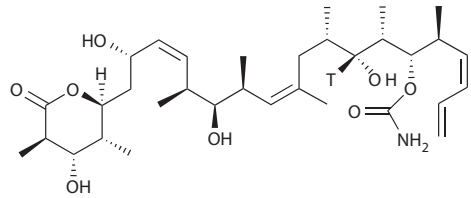

22. ^{3}H-(+)-Discodermolide

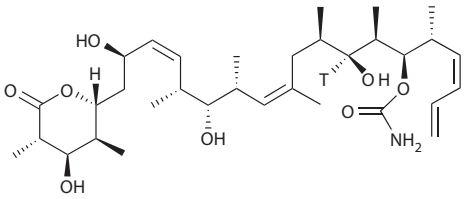

23. ^{3}H-(-)-Discodermolide

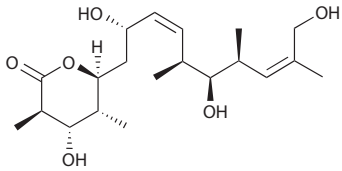

24. Fragment A

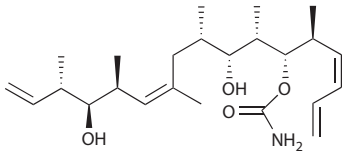

25. Fragment B

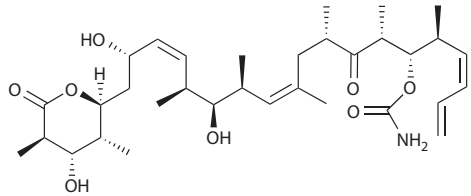

26. (+)-17-Oxo-discodermolide

STRUCTURE 10.2 Structures of naturally occurring and synthetic analogs of (+)-discodermolide.

16-normethyl (**18**), epimers of C1 thiophenyl (**19, 20**), and C1-β thiophenyl 16-normethyldiscodermolide (**21**). Other analogs prepared by the Schreiber group are the C17 tritium-labeled discodermolide enantiomers (**22, 23**), the fragments A (**24**) and B (**25**), C17-keto (**26**), pentyl-NHFmoc ester (**27**), and C24-hydroxybutylester (**28**). The last two analogs and several similar analogs were prepared to study the binding properties of (+)-discodermolide.[23] The Paterson group[28] synthesized 5-*epi*-, 7-*epi*-, and 5,7-*bis*-*epi*-discodermolides (**29–31**) during their aldol-based total synthesis of (+)-discodermolide. They selectively accessed both C7 epimers in the final C6–C7 aldol coupling, which allowed the synthesis of the aforesaid epimers by stereocontrolled reduction of the C5 ketone and subsequent deprotection. The Schreiber group[4] observed that changes in the C17–C20 region of the discodermolide backbone resulted in loss of activity, and therefore Smith's group[41] focused their modifications on the C1–C14 segment of **1** and prepared four analogs including 3-deoxy-discodermolide-2-ene (**32**), 3,7-dideoxy-discodermolide-2-ene (**33**), 8,9-*E*-discodermolide (**34**), and 14-normethyldiscodermolide (**35**) for SAR studies.

Using a small quantity of natural (+)-discodermolide isolated from sponge samples, Gunasekera et al.[42] prepared eight acetylated discodermolide analogs (**36–43**) to study the importance of hydrogen bonding by the hydroxyl groups in the molecule on the cytotoxicity and microtubule stabilizing activity. These analogs were prepared by treating discodermolide with acetic anhydride in pyridine at a controlled temperature and by separating the resulting acetylated mixture by high-performance liquid chromatography methods. Subsequently, the same group has prepared 3-deoxy-discodermolide-2-ene (**32**) and four acetylated analogs of 3-deoxy-discodermolide-2-ene (**44–47**), using acetylated analogs of **1** as the starting material.[43] Temperature- and time-controlled catalytic hydrogenation of **1** resulted in three hydrogenated discodermolide analogs (**48–50**) and one 7-deoxy-hexahydro analog (**51**), which on acetylation, yielded the 7-deoxy-hexahydro-triacetate (**52**). These compounds were used to study the importance of the double bonds in contributing to the activity. In addition, one 6,7-*seco*-analog (**53**) has been generated during the attempted allylic oxidation of the C7 hydroxyl group in **1**, using MnO_2 as an oxidizing agent. This compound **53** on stirring with titanium (IV) isopropoxide in CH_2Cl_2 at room temperature for 2 weeks furnished the 19-hydroxy-6,7-*seco*-analog (**54**). These compounds were used to ascertain the contribution of the C1–C7 unit on the activity.[43]

During the final stages of the 60 g synthesis of **1** conducted by the Novartis group,[39] the three *t*-butyldimethylsilanyl protecting groups in (**55**) were removed by a one-step acid catalyzed procedure. This hydrolysis procedure with concomitant lactonization gave crude **1** in 85% purity and quite a number of various combinations of silyl ether cleavage side products and several cyclized side-products in trace quantities. These minor cyclized side products (**56–61**) have been purified, and their structures were determined by nuclear magnetic resonance (NMR) studies. The formation of five-cyclopentyl (**56–60**) and one-pyrano (**61**) analogs indicated that the hairpin confirmation of **1** in solution brings the two isolated double bonds closer together in correct geometry for the proton catalyzed cyclization.[44]

10.5 BIOLOGICAL ACTIVITY

10.5.1 Immunosuppressive Properties

(+)-Discodermolide (**1**) could be considered a unique compound that exhibits both strong immunosuppressive activity and strong antiproliferative activity.[1] Initial testing of **1** indicated potent immunosuppressive activity in the bidirectional murine mixed lymphocyte assay (MLR) and antiproliferative activity toward P388 murine leukemia cells. Further studies by Longley et al. demonstrated immunosuppressive activity in a number of *in vitro* assays,[2,45] and in an *in vivo* experimental model of graft-versus-host reaction,[3] the Simonsen splenomegaly assay.[46] These studies indicated that **1** suppresses the proliferative responses of splenocytes in the murine two-way mixed lymphocyte reaction, and concavalin A (Con A) stimulated cultures, with IC_{50} values of 0.24 and 0.19 μM, respectively, with no detection of cytotoxicity for murine splenocytes at concentrations of **1** as high as 1.26 μM. In further studies, **1** suppressed the proliferative responses of human peripheral blood

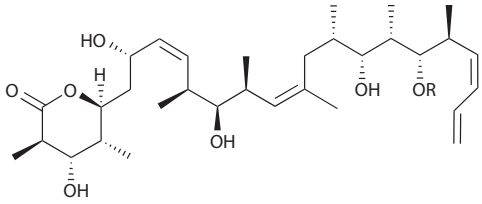

27. R = $CO(CH_2)_5NHFmoc$

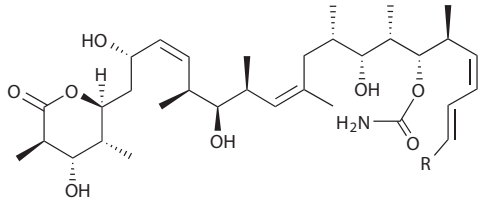

28. R = $-(CH_2)_4OPv$

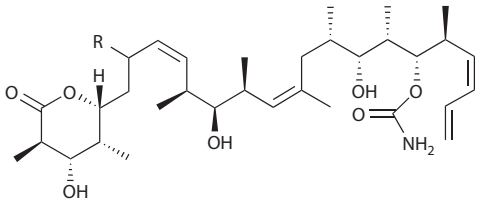

29. 5-*Epi*-discodermolide, R = αOH
31. 5,7-*Bis-epi*-discodermolide, R = βOH

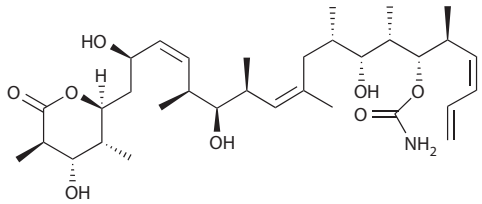

30. 7-*Epi*-discodermolide

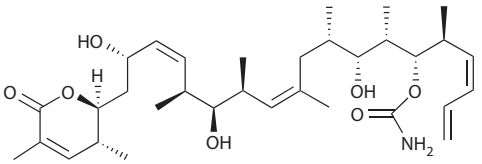

32. 3-Deoxy-discodermolide-2-ene

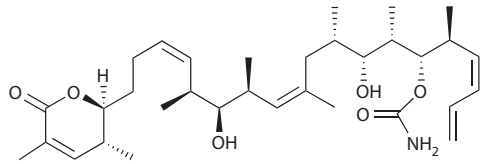

33. 3,7-Dideoxy-discodermolide-2-ene

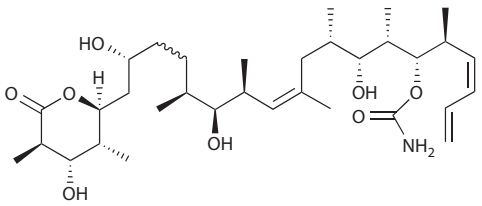

34. 8,9-*E*-Discodermolide

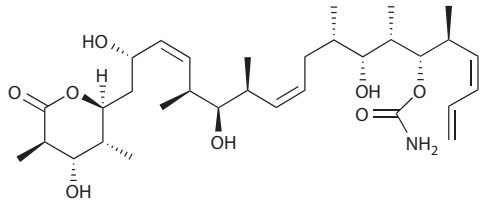

35. 14-Normethyldiscodermolide

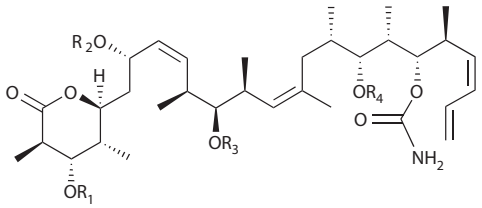

36. Discodermolide-3-acetate, $R_1 = COCH_3$, $R_2 = R_3 = R_4 = H$
37. Discodermolide-7-acetate, $R_2 = COCH_3$, $R_1 = R_3 = R_4 = H$
38. Discodermolide-3,7-diacetate, $R_1 = R_2 = COCH_3$, $R_3 = R_4 = H$
39. Discodermolide-3,11-diacetate, $R_1 = R_3 = COCH_3$, $R_2 = R_4 = H$
40. Discodermolide-3,17-diacetate, $R_1 = R_4 = COCH_3$, $R_2 = R_3 = H$
41. Discodermolide-3,7,11-triacetate, $R_1 = R_2 = R_3 = COCH_3$, $R_4 = H$
42. Discodermolide-3,7,17-triacetate, $R_1 = R_2 = R_4 = COCH_3$, $R_3 = H$
43. Discodermolide- 3,7,11,17-tetraacetate, $R_1 = R_2 = R_3 = R_4 = COCH_3$

STRUCTURE 10.3 Structures of naturally occurring and synthetic analogs of (+)-discodermolide.

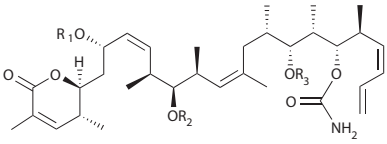

44. 3-Deoxy-discodermolide-2-en-11-acetate, $R_1 = R_2 = H$, $R_3 = COCH_3$
45. 3-Deoxy-discodermolide-2-en-17-acetate, $R_1 = R_2 = H$, $R_3 = COCH_3$
46. 3-Deoxy-discodermolide-2-en-11,17-diacetate, $R_1 = H$, $R_2 = R_3 = COCH_3$
47. 3-Deoxy-discodermolide-2-en-7,11,17-triacetate, $R_1 = R_2 = R_3 = COCH_3$

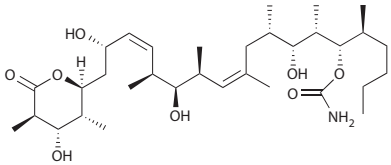

48. 21,23-Tetrahydrodiscodermolide

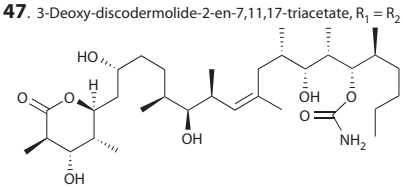

49. 8,21,23-Hexahydrodiscodermolide

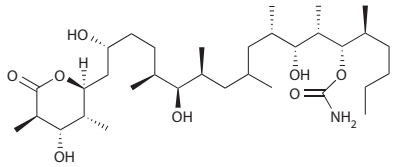

50. 8,13,21,23-Octahydrodiscodermolide

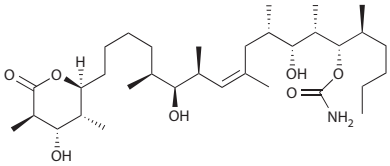

51. 7-Deoxy-8,21,23-hexahydrodiscodermolide

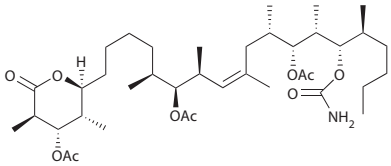

52. 7-Deoxy-8,21,23-hexahydrodiscodermolide-3,11,17-triacetate

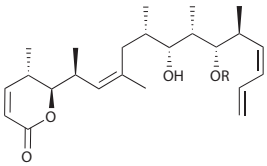

53. 6,7-*Seco*-discodermolide, R = $CONH_2$
54. 19-*Des*-aminocarbonyl-6,7-*seco*-discodermolide

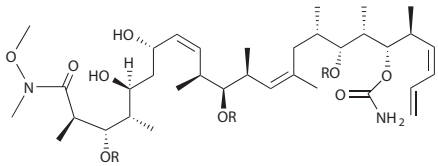

55. R = $Si(CH_3)_2C(CH_3)_3$

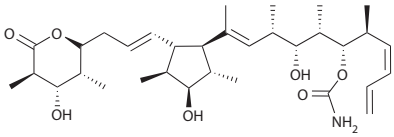

56. 7-Deoxy-7,14-dien-9-13-cyclodiscodermolide

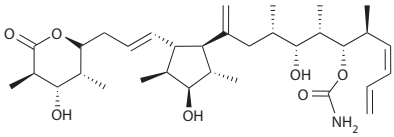

57. 7-Deoxy-7,14(29)-dien-9-13-cyclodiscodermolide

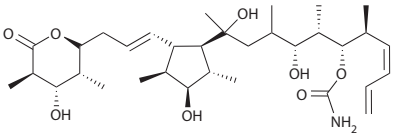

58. 14(*R*)-hydroxy-16(*S*)-9-13-cyclodiscodermolide
59. 14(*S*)-Hydroxy-16(*S*)-9-13-cyclodiscodermolide
60. 14(*S*)-Hydroxy-16(*R*)-9-13-cyclodiscodermolide

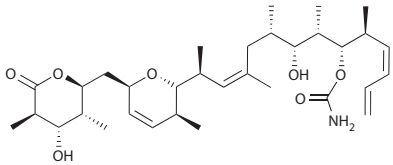

61. 7-(11)-Oxycyclodiscodermolide

STRUCTURE 10.4 Structures of naturally occurring and synthetic analogs of (+)-discodermolide.

leukocytes (PBL) in the two-way mixed lymphocyte reaction, Con-A and phytohemagglutinin mitogenesis assays, with IC_{50} values of 5.65, 28.02, and 30.12 μM, respectively, with no evidence of cytotoxicity toward human PBL at (+)-discodermolide concentrations as high as 80.64 μM.[3]

(+)-Discodermolide was more potent than the clinically used cyclosporin A, a cyclic decapeptide (CsA) isolated from a fungus *Trichoderma inflatum*,[47] in its ability to suppress the PMA–inomycin-induced proliferation of purified murine T-cells. The IC_{50} values observed in this assay were 9.0 and 14.0 μM for **1** and CsA, respectively. **1** had no effect on interleukin-2 (IL-2) production or IL-2 mRNA expression; however, the expression of the low-affinity IL-2 receptor in PMA–ionomycin-stimulated, purified, murine T-lymphocytes, and that of PHA-stimulated human PBL blasts, was affected. *In vivo* studies by Longley et al.[3] reported that **1** is effective in the graft-versus-host splenomegaly response of BALB/c → $CB6F_1$ (BALB/c × C57Bl/6J)F_1 grafted mice. Mice that were administered daily, intraperitoneal injections with dose levels of 1.25, 0.625, and 0.313 mg/kg remained healthy after 7 days on the regimen and continued to demonstrate suppression of splenomegaly with 106%, 72%, and 76% suppression, respectively.

Splenocytes obtained from (+)-discodermolide-treated allogeneic grafted mice were suppressed in their ability to respond *in vitro* to optimal mitogenic concentrations of Con A, and natural killer cell activity directed against YAC-1 tumor cells, compared with vehicle-treated, allogenic grafted control mice. Lower dosages of **1**, however, did not affect the subsequent ability of splenocytes obtained from these mice to produce IL-2 following *in vitro* stimulation with Con A. The unusual *in vivo* immunosuppressive properties of **1** as compared to CsA indicated that **1** has a specific *in vivo* mechanism of action. Using the murine DO11.10 T-hybridoma cell line, Longley et al.[45] reported that the antiproliferative activity of **1** was a result of its ability to block cell proliferation in the G_2/M phase of the cell cycle. Control cultures of DO11.10 cells demonstrated a characteristic pattern of cell cycling. Approximately 68% of the control cells make up the G_1 phase of the cell cycle, and approximately 31% of the cells make up the S phase. Only 1% of these cells are demonstrable in the G_2/M phase in asynchronous cultures at any one time, mainly because of the high proliferative rate of DO11.10 cells. At 24 h postculture initiation, after treatment with 1.0 μg/mL of **1**, the percentage of cells in G_1 phase decreased to 25%, and those in S to 16%. However, the percentage of cells in G_2/M increased to 58%. The results from this study concluded that **1** acts by blocking cells in the G_2/M phase of the cell cycle.[45]

10.5.2 Antitumor Properties

(+)-Discodermolide (**1**) was originally isolated by Gunasekera et al.[1] from the marine sponge *Discodermia dissoluta*, following a cytotoxicity-based bioassay-guided approach. The crude ethanol extracts of the source sponge initially revealed strong antiproliferative activity toward P388 murine leukemia cells in addition to potent immunosuppressive activity in the bidirectional murine mixed lymphocyte assay. (+)-Discodermolide was evaluated for its antiproliferative effects in the National Cancer Institute's (NCI) 60-human tumor cell-line screen.[48] The results of the NCI analyses were reported as growth inhibition 50 (GI_{50}) values, in which the growth of 50% of the cells is inhibited; total growth inhibition (TGI) values, in which the growth of all cells is inhibited (i.e., cytostasis); and lethal concentration 50 (LC_{50}), in which 50% of the cells are killed. **1** demonstrated selective cytotoxicity for 32 cell lines for GI_{50} and 18 cell lines for TGI. According to LC_{50} measurements for the NCI cell lines, **1** was particularly effective against human nonsmall-cell lung cancer (NCI-H23), human colon cancers (COLO 205 and HCC-2998), human melanoma (M14), two of six central nervous system cancer cell lines (SF 295 and SF 539), and two of eight breast cancer cell lines (MDA-MB-435 and MDA-N).

A statistical analysis of this selective toxicity pattern (the COMPARE algorithm)[49] indicated that the cytotoxicity pattern of **1** matched that of several previously tested microtubule interactive agents, including the pattern generated by Taxol (**2**). Computer-assisted structure–activity analysis by Ernest Hamel at NCI predicted antimitotic properties.[50] This finding led to the collaboration of the HBOI group with Billy Day of the University of Pittsburgh and Ernest Hamel of the NCI to begin a study on

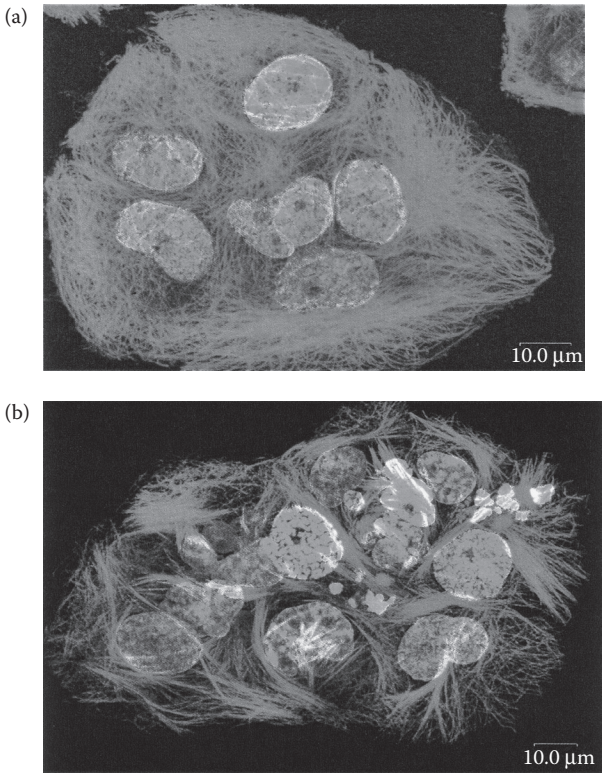

FIGURE 10.1 **(See color insert.)** Immunofluorescence images of A549 cells stained with anti-α-tubulin (green) and propidium iodide (red) and observed by confocal microscopy. Cells were exposed to (a) 0.05% ethanol (vehicle control), or (b) (+)-discodermolide at a concentration of 100 nM.

the antimitotic properties of (+)-discodermolide (**1**). The group found[50] that **1** was equally effective as Taxol (**2**) in inhibiting the growth of two human breast carcinoma cell lines, estrogen receptor-positive MCF-7 cells (IC_{50} = 2.4 nM for **1** and 2.1 nM for **2**), and estrogen receptor-negative MDA-MB-231 cells (the IC_{50} values are not reported). Complete inhibition of growth occurred with 10 nM or greater of each drug and was not reversed by removal. (+)-Discodermolide (**1**) treated cells exhibited highly fragmented condensed nuclei. Flow cytometric studies of cells treated with **1** or **2** at 10 nM showed that both compounds caused cell cycle perturbation and induction of a hypodiploid cell population. **1** caused these effects more extensively at an earlier time point. Immunofluorescence patterns of cells treated with **1** revealed remarkable rearrangement of the microtubule network, demonstrating promotion of microtubule assembly and indicating a Taxol-like effect (Figure 10.1).

1 was also analyzed for its interactions with purified tubulin. It was found that **1** induced the polymerization of tubulin to form microtubules in both the presence and absence of microtubule-associated proteins and guanosine-5′-triphosphate (GTP), and the resulting microtubules induced polymerization at lower temperatures than **2** and were more stable to the cold (4°C) than those formed by **2**. (+)-Discodermolide-induced polymer differed from Taxol-induced polymer in that it was completely stable at 0°C in the presence of high concentrations of Ca^{++} ions. In a quantitative assay designed to select for compounds more potent than Taxol (**2**) in its ability to polymerize tubulin, **1** showed an EC_{50} value of 3.2 µM, versus 23 µM for **2**.[50] Hung et al.[4,51] in the Schreiber group reported similar results using synthetic (+)-discodermolide. Their studies demonstrate similar arrest of MG63 human osteosarcoma cells in the M-phase of the cell cycle, induction of polymerization of purified tubulin, and "bundling" of the microtubule network in Swiss 3T3 cells. They discovered that the binding of microtubules by **1** and **2** were mutually exclusive in competitive binding assays

(i.e., **1** was capable of displacing **2** and vice versa in binding to microtubules). **1** was also found to bind to microtubules with a much higher affinity than **2**.

Longley et al.[48] at HBOI continued further studies on the effect of **1** on cell cycle progression and apoptosis of A549 human lung and GI-101A human breast cells in comparison to Taxol (**2**). The GI-101A cell line used by the Longley group was provided by Josephine Hurst, Goodwin Cancer Center, Plantation, Florida, and is an adherent breast cancer cell line derived from the original parent mammary tumor xenograft cell line, GI-101.[52] The line was originally derived from a local first recurrence of an infiltrating ductal adenocarcinoma (Stage IIIa, T3N2MX) in a 57-year-old female who had previously not received any chemotherapy or radiation therapy. Tumors transplanted into murine hosts are positive for normal human breast tumor markers and for the p53 antigen but are negative for c-erbB-2 oncogene. The A549 human lung and GI-101 human breast cells were incubated at 37°C in 5% CO_2 in the presence or absence of 10 nM of **1** or **2** for 24 h. Cells were harvested, fixed in ethanol, and stained with 0.5 mg/mL of propidium iodide (PI) together with 0.1 mg/mL of RNAse A. Stained preparations were analyzed on a Coulter EPICS ELITE flow cytometer with 488 nM excitation, and the resulting DNA histograms were collected from at least 10,000 PI-stained cells at an emission wavelength of 690 nM. Raw histogram data were further analyzed using a cell cycle analysis program. A549 and GI-101 cells without the drug exhibited a typical pattern of cell cycling, with a large percentage of the cell population comprising the G_1 population, with lesser percentages comprising the S and G_2/M phases of the cell cycle, as shown in Figure 10.2. Cells treated with 10 nM of **1** or **2** for 24 h exhibited decreased percentages of cells comprising the G_1 population, with corresponding increased percentages in both S and G_2/M phases of the cell cycle, indicating the ability of **1** and **2** to induce G_2/M block, as shown in Figure 10.3. Cells undergoing apoptosis are also evident as a peak immediately to the left of the G_1 peak.

(+)-Discodermolide (**1**) indicated strong cytotoxicity in all cancer cell lines tested *in vitro*, and the activity was comparable to that of Taxol. The results are shown in Table 10.1. However, it was interesting to note that **1** was less cytotoxic to the normal kidney epithelial cell line of the African green monkey. These results indicated that **1** selectively targets dividing cancer cells, and suggested that microtubule stabilization is probably the primary mechanism of action of (+)-discodermolide.

Longley's group at HBOI continued studies on the characterization of the molecular basis of apoptosis in (+)-discodermolide-treated tumor cells.[48] This study was designed to detect and characterize the (+)-discodermolide-induced molecular pathways of apoptosis and to evaluate the differences with Taxol-induced apoptosis, by probing Bcl-2, Bcl-Xl, and Raf-1 proteins in JURKAT and MCF-7 cell lines by Western blot analysis, and following the phosphorylation patterns in

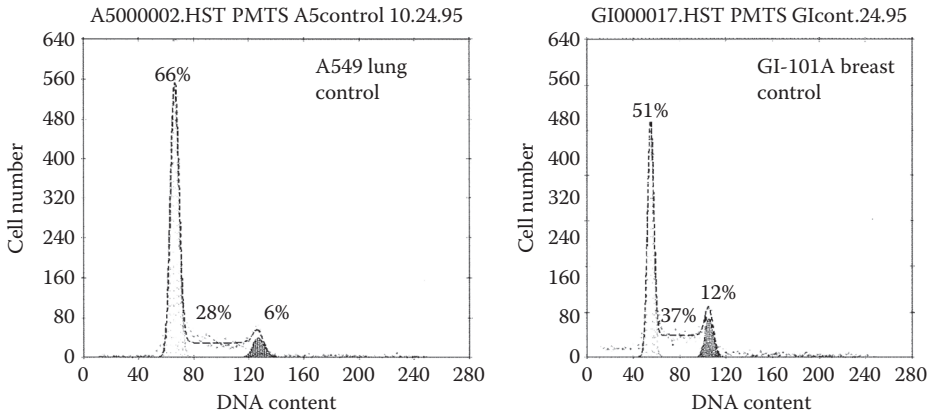

FIGURE 10.2 Cell cycle analysis of A549 and GI-101 control cells.

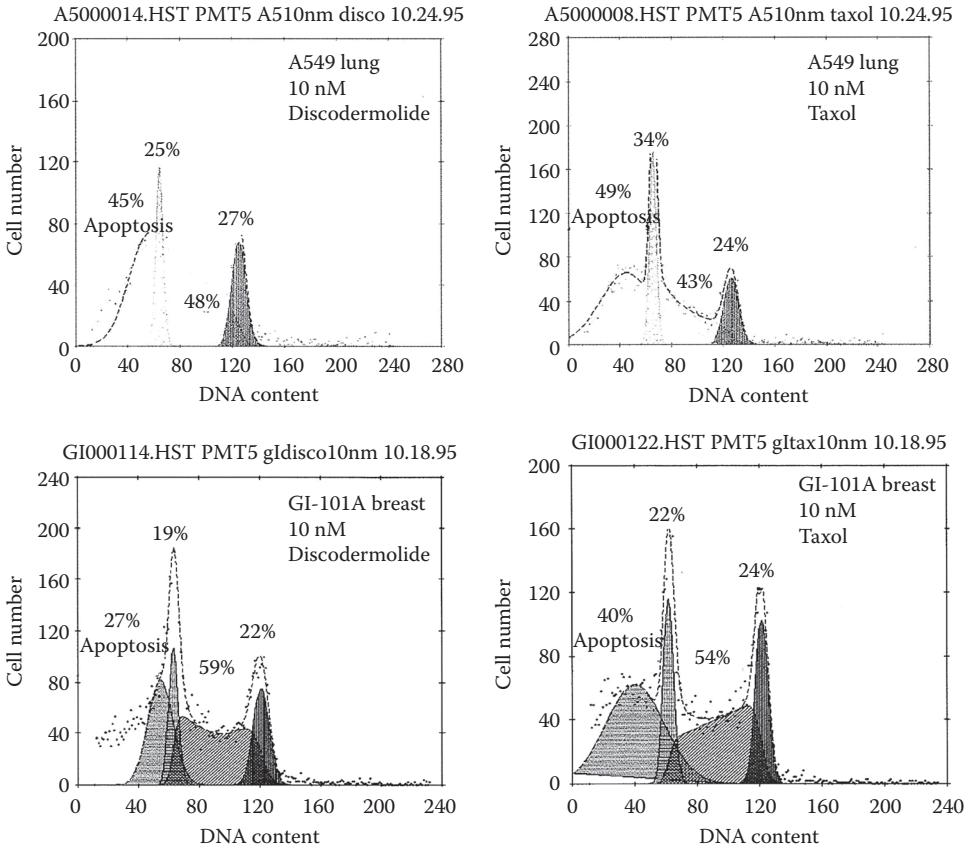

FIGURE 10.3 Cell cycle analysis of A549 and GI-101A treated with (+)-discodermolide (**1**) and Taxol (**2**).

TABLE 10.1
***In Vitro* Cytotoxicity of (+)-Discodermolide (1) in Selected Cancer Cell Lines**

Cell Line	Activity Data (IC_{50} in μM)
Murine P388 leukemia cells	0.033
Human A549 lung cancer cell line	0.015
Human MCF-7 breast cancer cell line	0.0024
Human MDA-MB-231 breast cancer cell line	0.0024
Human NCI/ADR-Res	0.017
PANC-1	0.049
VERO	30
For Taxol	0.0021

Note: A549, human lung adenocarcinoma cell line; P388, cultured murine leukemia cell line; MCF-7, human breast cancer cell line; MDA-MB-231, Breast adenocarcinoma cell line; NCI/ADR-Res, adriamycin drug-resistant cell line; PANC-1, human pancreatic cancer cell line; VERO, normal kidney epithelial cell line of African green monkey.

response to **1** and **2** treatments. The HBOI group detected that both **1** and **2** phosphorylate the Bcl-2 family proteins, and this appears to be accompanied by a loss of Bcl-2 function. They also measured the apoptotic responses by detecting and quantitating DNA fragmentation in various cell populations (MCF-7, DO11.10, and JURKAT) under the treatment of drugs, such as Fas-antigen, dexamethasone, Taxol (**2**), and (+)-discodermolide (**1**), using a time course (6, 12, 24 h) and concentration-dependent (10, 100, and 1000 nM of drug) experiments. The DNA fragmentation analysis, correlated by flow cytometric studies and by microscopy, indicated that **1** induces apoptosis in a dose-dependent manner and appears to do so in the same way as **2**. Also, it appears that the dose range for inducing these apoptotic events is more or less the same depending on the cell line used. In comparative studies of **1**, with the epothilones (**3**, **4**) and eleutherobin (**6**) against a Taxol-dependent human lung carcinoma cell line A549-T12, Martello et al.[13] found that **1** was unable to act as a substitute for **2**, whereas **3**, **4**, and **6** were able to maintain the viability of the cell line suggesting that discodermolide has tubulin-binding properties that set it apart from the other microtubule-stabilizing agents. The presence of low concentrations of **2** amplified the cytotoxicity of **1** 20-fold against this cell line and thus suggested that **1** and **2** may constitute a promising synergistic chemotherapeutic combination.[13] Further investigation of this synergistic effect on cytotoxicity suggests that it is due to the ability of **1** and **2** to synergistically inhibit microtubule dynamic instability and mitosis.[14] This work has been extended to demonstrate that combination treatment of **1** and **2** at doses well below the maximum tolerated dose of either agent in a SKOV-3 xenograft model in nude mice results in tumor regression and suppresses angiogenesis.[15] These studies strongly suggest that a combination therapy of **1** and **2** should be further evaluated for potential use as a cancer therapeutic. Gertsch et al. have shown that the morphology of microtubules induced by treatment with discodermolide is distinctly different than those formed by Taxol or epothilone B.[53] Microtubules induced by discodermolide are susceptible to disassembly when exposed to ultrasound in contrast to those induced by Taxol® or epothilone B which do not disassemble under this treatment. Microtubules induced by combinations of **1** and **2** are also distinctly different morphologically than those formed *in vitro* for **1** alone and appear to be midway in size to those formed by either treatment alone. Another unusual feature of **1** is its ability to induce accelerated cell senescence with potency comparable to the DNA-damaging agent doxorubicin.[16] This activity is unusual for microtubule binding agents and may be in part responsible for the synergistic activity observed between **1** and **2**. It may also lead to discodermolide having some therapeutic advantages over other microtubule-binding agents.

10.6 STRUCTURE–ACTIVITY STUDIES

The Schreiber group was the first to synthesize the unnatural antipode, (–)-discodermolide and a number of structural analogs, thus laying the ground work for SAR analysis.[22,23] Both enantiomers exhibited antiproliferative activity, but at different stages of the cell cycle. The natural (+)-discodermolide (**1**) blocks the cells in the G2/M phase, whereas the (–)-discodermolide inhibits the cell cycle in the S-phase. The two antipodes also showed significantly different potency in cytotoxicity-based assays. In a [^{3}H]-thymidine incorporation assay using NIH3T3 cells, synthetic **1** had an IC_{50} value of 7 nM, compared with 135 nM for the (–)-discodermolide, or a 19-fold loss of activity.[4,23] Removal of the C16S methyl group (e.g., 16-normethyldiscodermolide [**18**]) did not affect the potency. However, epimerization at C16 (e.g., C16R [**16**]) or at C17 (e.g., C16S, C17S [**17**]) showed a significant reduction in activity (IC_{50} = 300 and >300 nM, respectively). Interestingly, the thiophenyl derivatives (**19, 20**), both α and β anomers, as well as the 16-normethyl analog (**18**) were equally active as **1**, suggesting that the carbonyl functionality and C16Me are not essential for the cytotoxicity of **1**. The other analogs prepared by the Schreiber group,[23] the left and right fragments of **1** (**24, 25**), 17-oxo-discodermolide (**26**) and pentyl-NHFmoc ester (**27**) and 24-hydroxybutyl ester (**28**), retain a low level of activity of IC_{50} = 70 nM in the [^{3}H]thymidine incorporation assay using MG63 cells. The three epimeric analogs 5,7-*bis-epi*-, 5-*epi*-, and 7-*epi*-discodermolides (**29–31**) prepared

by the Paterson group[28] are structurally interesting; however, the biological activities of these compounds were not presented in the synthetic publication.

The Smith group[41] prepared four interesting discodermolide analogs, 3-deoxy-discodermolide-2-ene (**32**), 3,7-dideoxy-discodermolide-2-ene (**33**), 8,9-*E*-discodermolide (**34**), and 14-normethyl-discodermolide (**35**)—during their total synthesis of **1**, which used a highly efficient, triply convergent approach. This was the first report that indicated that microtubule stabilization by **1** is extremely sensitive to simple modifications in the molecular structure. The researchers' *in vitro* studies demonstrated that **1** and the structural analogs induced tubulin assembly in the absence of GTP and that the microtubules formed were stable under Ca^{++}-induced depolymerizing conditions. The initial rates of polymerization reflect the nucleation process. It was observed that the rate of tubulin nucleation of the four analogs **32**–**35** was reduced as compared to that of **1**. Analogs **32** and **35** showed similar levels of polymerization to that of **1**, and analogs **33** and **34** demonstrated reduced polymerization, attaining approximately 50% of the level of polymerization observed with (+)-discodermolide (**1**). Electron microscopy examination of the microtubules formed in the *in vitro* assays confirmed that normal microtubules were formed in the presence of the compounds. The microtubules that assembled in the presence of **1** were approximately fivefold shorter than those formed by analogs **32** and **35**; 12-fold shorter than those formed by analogs **33** and **34**, and fourfold shorter than those formed by Taxol (**1**). The same group showed that in a drug-binding competition assay, **1** and analogs **32**, **33**, and **35** are competitive inhibitors of [^{3}H]Taxol binding to preformed microtubules. At 1 μM concentration, Taxol (**2**), (+)-discodermolide (**1**), and analogs **32**, **33**, and **35** exhibited very similar inhibition, whereas analog **34** was essentially inactive in displacing [^{3}H]Taxol binding. At 100 μM, **1** displayed 95% inhibition, **2** displayed 80% inhibition, and analog **32** exhibited >90% inhibition of [^{3}H]Taxol binding to preformed microtubules. Analogs **33–35** demonstrated a range of inhibition between 45% and 65% at 100 μM.

Using natural (+)-discodermolide (**1**) isolated from the sponge *Discodermia*, Gunasekera et al.[43] in the Harbor Branch group prepared eight acetylated analogs (**36–43**) by acetylation of the hydroxyl groups at C3, C7, C11, or C17. These analogs were assayed for biological activity in cultured murine P388 leukemia and human A549 lung adenocarcinoma tumor cell lines to determine the structural requirements for tubulin interaction and cytotoxic effects. The biological data are presented in Table 10.2. The P388 and A549 assay results indicated that acetylation of the hydroxyl groups in the left-hand side of the molecule at C3 and C7 confers a greater cytotoxicity to the discodermolide structure, as seen with analogs **36–38**. Interestingly, the discodermolide acetates **39** and **41** with acetyl groups at C11 showed reduced cytotoxicity as compared to the parent molecule, whereas compounds **40**, **42**, and **43** that include acetylation at C17 caused a dramatic reduction in

TABLE 10.2
Biological Data of Taxol (2), (+)-Discodermolide (1), and Discodermolide Acetates (36–43)

Compound	P388 IC_{50} (nM)	A549 IC_{50} (nM)	G2/M Block (100 nM)	Microtubule Bundling (nM)
Taxol (**2**)	7.7	—	Yes	Yes (100)
(+)-Discodermolide (**1**)	35	34	Yes	Yes (10)
3-Acetate (**36**)	9	9.4	Yes	Yes (10)
7-Acetate (**37**)	2.5	0.5	Yes	Yes (10)
3,7-Diacetate (**38**)	0.7	3.7	Yes	Yes (10)
3,11-Diacetate (**39**)	103	295	No	No (100)
3,17-Diacetate (**40**)	1149	736	No	No (100)
3,7,11-Triacetate (**41**)	166	554	No	No (100)
3,7,17-Triacetate (**42**)	> 6825	> 1307	No	No (100)
3,7,11,17-Tetraacetate (**43**)	837	1307	No	No (100)

cytotoxicity. These results confirmed the previous finding by the Schreiber group[23] that acetylation at C17 reduced the activity by tenfold in the [^{3}H]-thymidine incorporation assay, using MG63 cells. Cell cycle analysis by flow cytometry using A549 cells revealed that the highly cytotoxic analogs caused the accumulation of cells in the G2/M phase. The effect on microtubule bundling follows the cytotoxicity as seen by analogs **33–38**.

The HBOI group isolated and reported three natural discodermolide analogs (**11–13**) that showed modification in the lactone ring system of the molecule. In addition, the group prepared through semisynthesis 3-deoxy-discodermolide-2-ene (**32**) and four 3-deoxy-2-ene acetylated analogs (**44–47**) for SAR studies. The activity data reported in Table 10.3 indicate that the ring-opened methyl ester (**13**) resulted in two- and fivefold reduction in activity in the P388 and A549 assays, respectively. Epimerization at C2 (**11**) results in a fivefold reduction in cytotoxicity and a reduction in the level of tubulin polymerization. Dehydration of the 3-hydroxyl functionality to yield 3-deoxy-discodermolide-2-ene (**32**) results in no loss of biological activity compared to that of the parent (+)-discodermolide (**1**). Interestingly, the 2-des-methyldiscodermolide (**12**) showed greater than fivefold reduction in cytotoxicity, yet the microtubule bundling properties were comparable with **1** and **32.** The analogs **11–13** and **32** showed cell cycle arrest at the G2/M checkpoint and induction of microtubule bundling. These SAR studies confirmed that minor changes in the functional groups on the lactone ring do not significantly affect the antimitotic properties of (+)-discodermolide (**1**). The acetylated analogs of 3-deoxy-discodermolide-2-ene (**44–47**) showed a significant reduction in cytotoxicity and the complete loss of microtubule-stabilizing properties on acetylation of the C11 or C17 hydroxyl groups, indicating the importance of these two hydroxyl groups for the microtubule stabilizing properties of (+)-discodermolide (**1**).

As shown in Table 10.4, both the 21,23-tetrahydrodiscodermolide (**48**) in which the terminal conjugated double bond has been hydrogenated and 8,21,23-hexahydrodiscodermolide (**49**) have similar activity to the parent (+)-discodermolide (**1**), indicating that the C8 double bond and the terminal diene are not essential for the cytotoxicity and tubulin polymerizing action of (+)-discodermolide. The 8,13,21,23-octahydrodiscodermolide (**50**) shows significantly less cytotoxicity

TABLE 10.3
Biological Data of Natural Analogs (11–13) and 3-Deoxy-Discodermolide-2-ene (32) and Analogs (44–47)

Compound	P388 IC_{50} (nM)	A549 IC_{50} (nM)	G2/M Block (100 nM)	Microtubule Bundling (10 nM)[a]
2-*Epi*-discodermolide (**11**)	134	67	Yes	+
2-*Des*-methyldiscodermolide (**12**)	172	120	Yes	+++
5-Hydroxymethyldiscodermolate (**13**)	65	74	Yes	+
3-Deoxy-discodermolide-2-ene (**32**)	34	21	Yes	+++
3-Deoxy-discodermolide-2-en-11-acetate (**44**)	519	519	No	–
3-Deoxy-discodermolide-2-en-17-acetate (**45**)	8103	8103	No	–
3-Deoxy-discodermolide-2-en-11,17-diacetate (**46**)	7587	7587	No	–
3-Deoxy-discodermolide-2-en-7-11-17-triacetate (**47**)	7076	7133	No	–

[a] –, +, ++ and +++ indicate the degree of microtubule bundling observed by immunochemical microscopy, with – having no bundling and +++ having the greatest level.

TABLE 10.4
Biological Data of Hydrogenated Analogs (48–52) and 19-*Des*-Aminocarbonyldiscodermolide (14)

Compound	P388 IC_{50} (nM)	A549 IC_{50} (nM)	G2/M Block (100 nM)	Microtubule Bundling (10 nM)[a]
21,23-Tetrahydrodiscodermolide (**48**)	10	8	Yes	++
8,21,23-Hexahydrodiscodermolide (**49**)	33	68	Yes	++
8,13,21,23-Octahydrodiscodermolide (**50**)	8292	8292	No	–
7-Deoxy-8,21,23-hexahydro-discodermolide (**51**)	309	377	No	++
7-Deoxy-8,21,23-hexahydro-discodermolide-3,11,17- triacetate(**52**)	7052	NT	No	–
19-*Des*-aminocarbonyldiscodermolide (**14**)	128	74	Yes	++

[a] –, +, ++ and +++ indicate the degree of microtubule bundling observed by immunochemical microscopy, with – having no bundling and +++ having the greatest level.

(8.2 μM) and no effect on tubulin polymerization. The retention of the microtubule bundling properties in 21,23-tetrahydrodiscodermolide (**48**) and 19-des-aminocarbonyl-discodermolide (**14**) indicated that the terminal conjugated double bond and the C19-carbamate groups are not essential for the microtubule bundling properties of (+)-discodermolide, but loss of the carbamate does lead to ten fold less potency in the cytotoxicity assays. Further saturation of **48** and **49** showed a fivefold reduction in cytotoxicity in the A549 assay, but comparable activity in the P388 cytotoxicity assay and in the formation of microtubule bundles. These data indicated that the C8 *Z*-double bond is not essential for the biological activity of **1**. Comparison of this finding with the biological activity reported earlier by the Smith group for the C8 E-analog (**34**) indicated that a C8 Z-double bond or C8 σ-bond type flexibility is required to maintain the high activity of (+)-discodermolide. The 7-deoxy-8,21,23-hexahydrodiscodermolide (**51**) showed considerable reduction in cytotoxicity but, interestingly, retained the microtubule stabilizing properties of (+)-discodermolide. A remarkable loss of activity in the P388 and A549 assays on saturation of the C13 *Z*-double bond, as seen in the 8,13,21,23-octahydrodiscodermolide (**50**), indicated that the C13 *Z*-double bond, which partly controls the folding of the molecule, is essential for the cytotoxicity and microtubule stabilizing properties of (+)-discodermolide.

As shown in Table 10.5, the reduction of biological activity in 6,7-*seco*-analogs (**53**, **54**), C9-C13 cyclo-analogs (**56**–**59**) except **57**, and C7–C11-oxycyclo analog (**61**) indicate that the combination of the C7 and C11 hydroxy groups are contributing to the optimum biological activity of (+)-discodermolide (**1**). The C16(R)-analog (**60**) that has the opposite chirality to that of (+)-discodermolide showed the least cytotoxicity among all assayed cyclo-analogs. This observation is significant because of the earlier finding by the Schreiber group[23] that C16(S) is essential for biological activity of (+)-discodermolide (**1**). The significant loss of biological activity in five of the six cyclo-analogs as shown in Table 10.5 that have the rigid ring structure from C6 through C13 could be attributed to the loss of the hairpin folding observed in (+)-discodermolide (**1**), and therefore, these observations confirmed the importance of the hairpin conformation for biological activity in (+)-discodermolide (**1**). These SAR studies confirmed that the C11, and C17 hydroxy groups; the C16(S) stereochemistry; and the C13 Z-double bond that folds the molecule in to the hairpin conformation are essential for the strong microtubule stabilizing properties of (+)-discodermolide (**1**). Two recent reviews by Smith and Frieze[32] and by Shaw[54] detail additional discodermolide analogs and provide an overview of their SARs all of which confirm the findings described before.

One area of very active research relates to defining how (+)-discodermolide binds to microtubules. Early studies indicated that (+)-discodermolide can displace binding of [^{3}H]-Taxol to

TABLE 10.5
Biological Data of 6,7-*Seco*-Discodermolide Analogs (53, 54) and Cyclodiscodermolide Analogs (56–61)

Compound	P388 IC_{50} (nM)	A549 IC_{50} (nM)	G2/M Block (100 nM)	Microtubule Bundling (10 nM)
6,7-*Seco*-Discodermolide (**53**)	3686	6774	No	—
19-*Des*-Aminocarbonyl-6,7-*seco*-discodermolide (**54**)	12,787	12,787	No	—
(7*E*,9*S*,13*S*,14*E*)-7-deoxy-7,14-dien-9-(13)-cyclodiscodermolide (**56**)	2130	6640	No	NT
(7E,9S,13*S*)-7-deoxy-7,14(29)-dien-9-(13)-cyclodiscodermolide (**57**)	190	100	NT	NT
(7*E*,9*S*,13*S*,14*R*)-7-deoxy-14-hydroxy-7-en-9-(13)-cyclodiscodermolide (**58**)	2420	840	NT	NT
(7*E*,9*S*,*13S*,14*S*, 16S)-7-deoxy-14-hydroxy-7-en-9-(13)-cyclodiscodermolide (**59**)	2090	2640	NT	NT
(7*E*,9*S*,13*S*,14*S*,16*R*)-7-deoxy-14-hydroxy-7-en-9-(13)-cyclodiscodermolide (**60**)	7650	>5000	NT	NT
(7*R*,11*S*)-7-(11)-Oxycyclodiscodermolide (**61**)	1000	1460	NT	NT

Note: NT, not tested.

microtubules suggesting that the binding sites are similar or overlap. The synergy observed between (+)-discodermolide and Taxol also lends support to the idea that the sites overlap and provide complementary effects. A number of models have been proposed with a consensus binding model not yet reached. Extensive computational studies, NMR studies and SAR analysis strongly support the idea that (+)-discodermolide adopts a hairpin shape between C-6 and C-16 in solution, bound to β-tubulin or bound to microtubules, that is essential for the biological activity. The lactone and butadiene chains vary slightly in conformation dependent upon the computational analysis conducted but appear to be less important to the overall activity of (+)-discodermolide as witnessed by the variety of modifications that can be made at these sites in the molecule without significant loss of activity.

Carlomagno et al. used transferred NOE (tr-NOE) experiments coupled with computational methods to propose a model of (+)-discodermolide binding to soluble tubulin.[55] They extended this using a technique they developed called INPHARMA which uses protein-mediated interligand NOE signals to define a common pharmacophore model for epothilone A and (+)-discodermolide which supports the model that they bind overlapping sites on tubulin. Published SAR data were used to further support the experimental findings. In their model, the tubulin bound conformation of (+)-discodermolide is similar to the x-ray-derived structure, with a primary difference being the change of the lactone ring from a twist boat conformation with all pseudoequatorial substituents to a flattened chair with the 2-methyl and 3-hydroxyl substituents being in axial positions and the 4-methyl and C-5 main chain being in equatorial positions.

Jiménez-Barbero et al. further explored the solution structure of (+)-discodermolide in D_2O and bound to microtubules using NMR methods and computational methods.[56] Their structure differs

from that of Carlomagno primarily in the lactone ring which adopts both a skew boat and half-chair conformations in D_2O solution with minimal energy (<2 kcal) between them. Their work suggests that the same conformation is found for (+)-discodermolide bound to microtubules. Saturation transfer difference (STD) NMR experiments were conducted with either a 10:1 or 20:1 molar ratio (ligand to protein) and showed strong enhancements for the methyl groups on the periphery of the backbone, the lactone ring (H2–H4), H12, and the C18–C24 portion of the chain. H2 and H22 gave the most significant STD enhancements. Computational analysis using the AUTODOCK program led to a model in which significant STD enhancements. Computational analysis using the AUTODOCK program led (+)-discodermolide binds to the taxane-binding site on β-tubulin involving the α helices 6 and 7 and the β strands 8–10 with their corresponding loops. According to their binding model there are polar contacts of (+)-discodermolide with His 229 (helix 7), several residues at the M loop (Pro274, Thr276, Ser27, and Gln282) and Gly370. His 229 is a key residue in the middle of helix 7. Stabilizing van der Waals interactions are also found, especially with Leu217, Leu275, Pro360, and Leu371. The authors speculate that because in their model (+)-discodermolide directly interacts with the M loop (which is a key element of the lateral interactions between microtubule protofilaments) (+)-discodermolide may stabilize microtubules by stabilizing lateral contacts between protofilaments.

Horwitz, Xiao et al. utilizing hydrogen–deuterium exchange (HDX) in concert with various mass spectrometry methods have defined an alternative model for (+)-discodermolide binding to microtubules.[57] Chicken erythrocyte tubulin was used in the study as it is made up of one α- and one β-tubulin isotype, α1 and βVI, respectively, eliminating ambiguity in the assignment of measured masses and conformational differences between tubulin isotypes. In the HDX methodology the differences in deuterium incorporation is measured between guanosine-5′-[(α,β)-methylene]triphosphate (GMPCPP) induced microtubules and drug-induced microtubules. HDX exchange is achieved by diluting the sample in 0.1 M deuterated MEM buffer and allowing exchange to proceed for 30 min. The samples are then quenched with ammonium phosphate and either analyzed directly by ESI-MS or subjected to pepsin digestion and analyzed by FT-ICR-MS. The overall levels of deuterium incorporation in Taxol or (+)-discodermolide treatments were found to be similar in this study. Detailed analysis of the patterns of protection, deprotection and no change in deuterium incorporation led to a model of binding for both Taxol and (+)-discodermolide to β-tubulin. This model contrasts with that found by Compagno et al. in that Taxol is found to be oriented toward the M-loop while (+)-discodermolide is rotated away from it and towards the *N*-terminal residues Asp26 and Glu22. The largest reduction in labeling for both Taxol and (+)-discodermolide was found in the H6–H7 loop (β212–230) with smaller changes at the core helix βH7 (β231–246). The S9–S10 loop also shows small but significant reduction in labeling with both drugs. In contrast to Taxol, (+)-discodermolide had no effect on labeling of the M-loop of β-tubulin suggesting that it does not interact with the M-loop. Computational docking of (+)-discodermolide using the disk conformation proposed by Carlomagno et al.[55] was not found to be consistent with the observed HDX data. (+)-Discodermolide was then docked in its natural conformation providing a contact map consistent with the HDX data. In this model Taxol and discodermolide have very similar effects on microtubule conformation and stability. Both compounds stabilize the interdimer surface where Taxol has strongest effects on the β-tubulin side while (+)-discodermolide has strongest effects on the α-tubulin side. Both compounds induce stability of the interprotofilament interface between adjacent β-tubulin subunits but do so in opposite fashions, with Taxol interacting with the M-Loop and (+)-discodermolide with the H1–S2 loop. These differences may account for the *in vivo* synergy observed for the drugs. One final outcome of this study is the observation that drug binding varies with tubulin isotype and must be taken into account when designing next generation microtubule stabilizing compounds.

One final report on the tubulin-bound structure of (+)-discodermolide has recently been made by Snyder et al.[58] In this work multiple molecular mechanics conformational searches (AMBER, MMFFs, MM3*, and OPLS 2005, each supplemented with the GBSA/H2O continuum solvent

model) coupled with NMR analysis of molecular flexibility in solution methodology were conducted to define the solution and bound structures of (+)-discodermolide. This work shed additional light on the structural features required to maintain the hairpin structure of (+)-discodermolide. Their work supports the binding pose 1 predicted by Compagno et al. while adding a second binding pose 2 that the authors suggest is a better fit than pose 1 for the SAR data. Pose 2 has three widely spaced hydrogen bonds from O3, N19, and O17 to M-loop residues Pro272, Thr274, and Arg276, respectively. The C4 methyl, C20 methyl, and the C21=C22 double bond form a hydrophobic cluster with Leu361 of the loop connecting B9 and B10. Both poses contrast significantly with the binding model proposed by Horwitz, Xiao et al. described before.

Each of the studies provides significant support for their models of (+)-discodermolide binding to microtubules. Different tubulin isotypes were used in the various studies and this may be the cause for some of the divergence in the conclusions. It seems clear that additional work will be required to provide a consensus model of how (+)-discodermolide binds to microtubules. It also remains to be seen whether the toxicity observed in the clinical trials can be overcome through preparation of suitable analogs that differentially bind to tubulin isotypes.

10.7 CLINICAL INVESTIGATION

Based on preclinical studies in which (+)-discodermolide (**1,** XAA296A) stabilized microtubule polymers more potently than **2** and demonstrated prominent activity against Taxol-refractory xenograft models, **1** was taken into Phase I trial in September 2002 at the Cancer Therapy and Research Center in San Antonio, Texas. Mita et al.[12] report that in the trial, **1** was administered by intravenous infusion at a rate of 0.77 mg/mL/min once every 3 weeks to adult patients with advanced solid malignancies. Twenty-six patients (median age 59.5 years; range 19–79 years, 17 men, 9 women) were treated at the following dose levels (mg/m^2): 0.6 (three patients); 1.2 (three patients); 2.4 (four patients); 4.8 (four patients); 9.6 (four patients); 14.4 (six patients), and 19.2 (two patients). All patients had Karnofsky performance status >70%. The number of patients with G2/G3 adverse events with suspected relationship to (+)-discodermolide are as follows: anemia (5, 1), nausea (6, 0), vomiting (3, 1), fatigue (5, 1), diarrhea (4, 0), mucositis (2, 0), stomatitis (1, 0), pruritis (1, 0), alkaline phosphatase (1, 0), creatinine (1, 0), and myalgias (1, 0). The drug was generally well tolerated with no peripheral neuropathy or neutropenia. One patient with appendix carcinoma had stable disease for four cycles. Pharmacokinetics (PK) was evaluated in 24 patients receiving (+)-discodermolide. (+)-Discodermolide concentrations showed C_{max} at the end of infusion, thereafter rapidly declining in a multiphasic manner. By 24 h postdose, blood concentrations decreased to <10% of C_{max}, but then showed nonlinear PK. This was observed in the majority of concentration–time profiles, suggesting prolonged recycling of drug between tissue and the systemic circulation. The Phase I clinical trials were discontinued in 2004 due to adverse events.

REFERENCES

1. Gunasekera, S.P., Gunasekera, M., Longley, R.E., and Schulte, G.K., Discodermolide: a new bioactive polyhydroxylated lactone from the marine sponge *Discodermia dissoluta*, *J. Org. Chem.*, 55, 4912, 1990 (correction: 56.1346, 1991).
2. Longley, R.E., Caddigan, D., Harmody, D., Gunasekera, M., and Gunasekera, S.P., Discodermolide: a new marine-derived immunosuppressive compound. I. *In vitro* studies, *Transplantation*, 52, 650, 1991.
3. Longley, R.E., Caddigan, D., Harmody, D., Gunasekera, M., and Gunasekera, S.P., Discodermolide: a new marine-derived immunosuppressive compound. II. *In vivo* studies, *Transplantation*, 52, 656, 1991.
4. Hung, D.T., Nerenberg, J.B., and Schreiber, S.L., Distinct binding and cellular properties of synthetic (+)- and (−)-discodermolides, *Chem. Biol.*, 1, 67, 1994.
5. Parness, J. and Horwitz, S.B., Taxol binding to polymerized tubulin *in vitro, J. Cell Biol.*, 91, 479, 1981.
6. Bollag, P.A., McQueney, P.A., Zhu, J., Hensens, O., Koupal, L., Liesch, J., Goetz, M., Lazarides, E., and Woods, C.M., Epothilones, a new class of microtubule-stabilizing agents with a Taxol-like mechanism of action, *Cancer Res.*, 55, 2325, 1995.

7. Hardt, I.H., Steinmetz, H., Gerth, K., Sasse, F., Reichenbach, H., and Höfle, G., New natural epothilones from *Sorangium cellulosum*, strains Soce90/B2 and So ce90/D13: isolation, structure elucidation and SAR studies, *J. Nat. Prod*., 64, 847, 2001.
8. Lindel, T., Jensen, P.R., Fenical, W., Long, B.H., Casazza, A.M., Carboni, J., and Fairchild, C.R., Eleutherobin, a new cytotoxin that mimics Paclitaxel (Taxol) by stabilizing microtubules, *J. Am. Chem. Soc.*, 119, 8744, 1997.
9. Mooberry, S.L., Tien, G., Hernandez, A.H., Plubrukarn, A., and Davidson, B.S., Laulimalide and isolaulimalide, a new paclitaxel-like microtubule-stabilizing agent, *Cancer Res*., 59, 653, 1999.
10. Isbrucker, R.A., Cummins, J., Pomponi, S.A., Longley, R.E., and Wright, A.E., Tubulin polymerizing activity of dictyostatin-1, a polyketide of marine sponge origin, *Biochem. Pharmacol*., 66, 75, 2003.
11. Smith, III, A.B., Kaufman, M.D., Beauchamp, T.J., LaMarche, M.J., and Arimoto, H., Gram-scale synthesis of (+)-discodermolide, *Org. Lett*., 1, 1823, 1999.
12. Mita, C., Lockhart, C., Chen, T.L., Bochinski, K., Curtright, J., Cooper, W., Hammond, L., Rothenberg, M., Rowinsky, E., and Sharma, S., A Phase 1 pharmacokinetic (PK) trial of XAA296A (discodermolide) administered every 3 wks to adult patients with advanced solid malignancies, Abstract *Journal of Clinical Oncology*, 2004 ASCO Annual Meeting Proceedings, Vol 22, No 14S (July 15 Supplement), 2025, 2004.
13. Martello, L.A., McDaid, H.M., Regl, D..L, Yang, C.P., Meng, D., Pettus, T.R., Kaufman, M.D., et al., Taxol and discodermolide represent a synergistic drug combination in human carcinoma cell lines, *Clinical Cancer Research*, 6, 1978, 2000.
14. Honore, S., Kamath, K., Braguer, D., Horwitz. S.B., Wilson, L., Briand, C., and Jordan, M.A., Synergistic suppression of microtubule dynamics by discodermolide and paclitaxel in non-small cell lung carcinoma cells, *Cancer Research*, 64, 4957–4964, 2004.
15. Huang, G.S., Lopez-Barcons, L., Freeze, B.S., Smith, A.B., 3rd, Goldberg, G.L., Horwitz, S.B., and McDaid, H.M., Potentiation of taxol efficacy by discodermolide in ovarian carcinoma xenograft-bearing mice, *Clin. Cancer Res.*, 12, 298–304, 2006.
16. Klein, L.E., Freeze, B.S., Smith, A.B., and Horwitz, S.B. The microtubule stabilizing agent discodermolide is a potent inducer of accelerated cell senescence, *Cell Cycle*, 4, 501–507, 2005.
17. Kelly-Borges, M., Robinson, E.V., Gunasekera, S.P., Gunasekera, M., Nanda, K., Gulavita, N.K., Shirley, A., and Pomponi, S.A., Species differentiation in the marine sponge genus *Discodermia* (Demospongiae: Lithistida): the utility of ethanol extract profiles as species-specific chemotaxonomic markers, *Biochem. Syst. Ecol*., 22, 353, 1994.
18. Gunasekera, S.P., Gunasekera, M., and McCarthy, P., Discodermide: a new bioactive macrocyclic lactam from the marine sponge *Discodermia dissoluta*, *J. Org. Chem*., 56, 4830, 1991.
19. Gulavita, N.K., Gunasekera, S.P., Pomponi, S.A., and Robinson, E.V., Polydiscamide A: a new bioactive depsipeptide from the marine sponge *Discodermia* sp., *J. Org. Chem*., 57, 1767, 1992.
20. Gunasekera, S.P., Paul, G.K., Longley, R.E., Isbrucker, R.A., and Pomponi, S.A., Five new discodermolide analogs from the marine sponge *Discodermia* sp., *J. Nat. Prod*., 65, 1643, 2002.
21. Smith, III, A.B., LaMarche, M.J., and Falcone-Hindley, M., Solution structure of (+)-discodermolide, *Org. Lett*., 3, 695, 2001.
22. Nerenberg, J.B., Hung, D.T., Somers, P.K., and Schreiber, S.L., Total synthesis of the immunosuppressive agent (-)-discodermolide, *J. Am. Chem. Soc*., 115, 12621, 1993.
23. Hung, D.T., Nerenberg, J.B., and Schreiber, S.L., Synthesis of discodermolides useful for investigating microtubule binding and stabilization, *J. Am. Chem. Soc*., 118, 11054, 1996.
24. Smith, III, A.B., Qiu, Y., Jones, D.R., and Kobayashi, K., Total synthesis of (-)-discodermolide, *J. Am. Chem. Soc*., 117, 12011, 1995.
25. Harried, S.S., Yang, G., Strawn, M.A., and Myles, D.C., Total synthesis of (-)-discodermolide: an application of a chelation-controlled alkylation reaction, *J. Org. Chem*., 62, 6098, 1997.
26. Harried, S.S., Lee, C.P., Yang, G., Lee, T.I.H., and Myles, D.C., Total synthesis of (+)-discodermolide, a microtubule-stabilizing agent from the sponge *Discodermia dissoluta*, *J. Org. Chem*., 68, 6646, 2003.
27. Marshall, J.A. and Jones, B.A., Total synthesis of (+)-discodermolide, *J. Org. Chem*., 63, 7885, 1998.
28. Paterson, I., Florence, G.J., Gerlach, K., Scott, J.P., and Sereinig, N., A practical synthesis of (+)-discodermolide and analogs: fragment union by complex aldol reactions, *J. Am. Chem. Soc*., 123, 9535, 2001.
29. Arefolov, A. and Panek J.S., Crotylsilane reagents in the synthesis of complex polyketide natural products: total synthesis of (+)-discodermolide, *J. Am. Chem. Soc*., 127, 5596, 2005.
30. de Lemos E., Porée, F.-H., Bourin, A., Barbion, J., Agouridas, E., Lannou, M.-I., Commerçon, A., Betzer, J.-F., Pancrazi, A., and Ardisson, J., Total synthesis of discodermolide: optimization of the effective synthetic route, *Chemistry*, 14, 11092, 2008.

31. Kalesse, M., The chemistry and biology of discodermolide, *Chem. BioChem.*, 1, 171, 2000.
32. Smith A.B. and Freeze B.S., (+)-Discodermolide: total synthesis, construction of novel analogues, and biological evaluation, *Tetrahedron*, 64, 261, 2008.
33. Paterson, I. and Florence G.J. The chemical synthesis of discodermolide, *Top Curr. Chem.*, 286, 73, 2009.
34. Smith, III, A.B., Beauchamp, T.J., LaMarche, M.J., Kaufman, M.D., Qiu, Y., Arimoto, H., Jones, D.R., and Kobayashi, K., Evolution of a gram-scale synthesis of (+)-discodermolide, *J. Am. Chem. Soc.*, 122, 8654, 2000.
35. Mickel, S.J., Sedelmeier, G.H., Niederer, D., Daeffler, R., Osmani, A., Schreiner, K., Seeger-Weibel, M., et al., Large-scale synthesis of the anti-cancer marine natural product (+)-discodermolide. Part 1: synthetic strategy and preparation of a common precursor, *Org. Process Res. Dev.*, 8, 92, 2004.
36. Mickel, S.J., Sedelmeier, G.H., Niederer, D., Schuerch, F., Grimler, D., Koch, Daeffler, R., et al., Large-scale synthesis of the anti-cancer marine natural product (+)-discodermolide. Part 2: synthesis of fragments C_{1-6} and C_{9-14}, *Org. Process Res. Dev.*, 8, 101, 2004.
37. Mickel, S.J., Sedelmeier, G.H., Niederer, D., Schuerch, F., Koch, G., Kuesters, E., Daeffler, R., et al., W.-C., Wang, R.-M.and Liladhar Waykole, L., Large-scale synthesis of the anti-cancer marine natural product (+)-discodermolide. Part 3: synthesis of fragment C_{15-21}, *Org. Process Res. Dev.*, 8, 107, 2004.
38. Mickel, S.J., Sedelmeier, G.H., Niederer, D., Schuerch, F., Seger, M., Schreiner, K., Daeffler, R., et al., Large-scale synthesis of the anti-cancer marine natural product (+)-discodermolide. Part 4: preparation of fragment C_{7-24}, *Org. Process Res. Dev.*, 8, 113, 2004.
39. Mickel, S.J., Niederer, D., Daeffler, R., Osmani, A., Kuesters, E., Schmid, E., Schaer, K., et al., Large-scale synthesis of the anti-cancer marine natural product (+)-discodermolide. Part 5: linkage of fragments C_{1-6} and C_{7-24} and finale, *Org. Process Res. Dev.*, 8, 122, 2004.
40. Paterson, I., Florence, G.J., Gerlach, K., and Scott, J.P., Total synthesis of the antimicrotubule agent (+)-discodermolide using boron-mediated aldol reactions of chiral ketones, *Angew. Chem. Int. Ed.*, 39, 377, 2000.
41. Martello, L.A., LaMarche, M. J., He, L., Beauchamp, T.J., Smith, A.B., and Horwitz, S.B., The relationship between Taxol and (+)-discodermolide: synthetic analogs and modeling studies, *Chem. Biol.*, 8, 843, 2001.
42. Gunasekera, S.P., Longley, R.E., and Isbrucker, R.A., Acetylated analogs of the microtubule-stabilizing agent discodermolide: preparation and biological activity, *J. Nat. Prod.*, 64, 171, 2001.
43. Gunasekera, S.P., Longley, R.E., and Isbrucker, R.A., Semisynthetic analogs of the microtubule-stabilizing agent discodermolide: preparation and biological activity, *J. Nat. Prod.*, 65, 1830, 2002.
44. Gunasekera, S.P., Mickel, S.J., Daeffler, R., Niederer, D., Wright, A.E., Linley, P., and Pitts T., Synthetic analogs of the microtubule-stabilizing agent (+)-discodermolide: preparation and biological activity, *J. Nat. Prod.*, 67, 749, 2004.
45. Longley, R.E., Gunasekera, S.P., Faherty, D., Mclane, J., and Dumont, F., Immunosuppression by discodermolide, *Ann. N. Y. Acad. Sci.*, 696, 94, 1993.
46. Simonsen, M., Graft versus host reactions: their natural history and applicability as tools of research, *Prog. Allergy*, 6, 349, 1962.
47. Borel, J.F. and Wiesinger, D., Biological effects of cyclosporin A: a new antilymphocytic agent, *Agent Action*, 6, 468, 1977.
48. Longley, R.E., Gunasekera, S.P., and Pomponi, S.A., Discodermolide compounds. U. S. Patent 5,840,750 issued November 24, 1998.
49. Boyd, M.R., The NCI *in vitro* anticancer drug discovery screen, *Cancer Lett.*, 15, 6, 1989.
50. ter Harr, E., Kowalski, R.J., Hamel, E., Lin, C.M., Longley, R.E., Gunasekera, S.P., Rosenkranz, H.S., and Day, B.W., Discodermolide, a cytotoxic marine agent that stabilizes microtubules more potently than taxol, *Biochemistry*, 35, 243, 1996.
51. Hung, D.T., Chen, J., and Schreiber, S.L., (+)-Discodermolide binds to microtubules in stoichiometric ratio to tubulin dimers, blocks taxol binding and results in mitotic arrest, *Chem. Biol.*, 3, 287, 1996.
52. Hurst, J., Maniar, N., Tombarkiewicz, J., Lucas, F., Roberson, C., Steplewski, Z., and Perras, J.W., A novel model of a metastatic breast tumour xenograft line, *Br. J. Cancer*, 68, 274, 1993.
53. Gertsch J., Meier, S., Müller, M., and Altmann, K.H., Differential effects of natural product microtubule stabilizers on microtubule assemby: single agent and combination studies with taxol, epothilone B, and discodermolide, *ChemBioChem.*, 10, 166, 2009.
54. Shaw, S.J. The structure activity relationship of discodermolide analogues. *Mini reviews in Medicinal Chemistry*, 8, 276, 2008.
55. Sánchez-Pedregal, V.M., Kubicek, K., Meiler, J., Lyothier, I., Paterson, I., and Teresa Carlomagno, T., The tubulin-bound conformation of discodermolide derived by NMR studies in solution supports a common pharmacophore model of epothilone and discodermolide, *Angew. Chem. Int. Ed.*, 45, 7388, 2006.

56. Canales A. et al., The bound conformation of microtubule-stabilizing agents: NMR insights in the bioactive 3D structure of discodermolide and dictyostatin, *Chem. Eur. J.*, 14, 7557, 2008.
57. Khrapunovich-Baine, M., Menon, V., Verdier-Pinard, P., Smith, A.B., 3rd, Angletti, R. H., Fiser, A., Horwitz, S.B., and Xiao, H., Distinct pose of discodermolide in Taxol binding pocket drives a complementary mode of microtubule stabilization, *Biochemistry*, 48, 11664, 2009.
58. Jogalekar, A.S., Kriel, F.H., Shi, Q., Cornett, B., Cicero, D., and Snyder, J.P., The discodermolide hairpin structure flows from comformationally stable modular motifs, *J. Med. Chem.*, 53, 155, 2010.

11 The Dolastatins *Novel Antitumor Agents from* Dolabella auricularia*

Erik Flahive and Jayaram Srirangam

CONTENTS

11.1 Introduction and History 263
11.2 Origin, Isolation, and Structure of the Dolastatins 263
11.3 Structure and Synthesis 266
11.4 Bioactivity and Mechanisms of Action 270
11.5 Structural Modifications and SAR 274
11.6 Clinical Update 279
Update 281
References 282

11.1 INTRODUCTION AND HISTORY

Within the field of natural products, marine organisms represent a relatively untapped resource for novel compounds of medicinal interest. The systematic evaluation of biological constituents from marine organisms as potential drug candidates did not begin in earnest until the late 1960s, when the U.S. National Cancer Institute (NCI) initiated a massive screening program directed at the discovery of new anticancer drug leads.[1,2] Over the next 30 years, evaluation of isolates from the marine shell-less mollusk *Dolabella auricularia* (Aplyidae family) has led to the discovery of an impressive number of novel compounds possessing antineoplastic activity. Among the number of substances characterized to date, dolastatins 10 (**1**) and 15 (**2**) and the synthetic compounds derived from them show the most promising antitumor activity and are currently in human clinical trials in the United States, Europe, and Japan. This chapter will provide highlights of this work and will review recent progress in the discovery and development of the dolastatins as potential cancer chemotherapeutic drugs, with particular emphasis on dolastatins 10 and 15.

11.2 ORIGIN, ISOLATION, AND STRUCTURE OF THE DOLASTATINS

Dolabella auricularia (Figure 11.1) and other gastropods of the order Anaspidea (Aplysiomorpha), known as "sea hares" because of the resemblance of the auriculate tentacula of these mollusks to the ears of a hare,[3] typically lack the protection of an external shell. A remarkable feature of *D. auricularia* and other sea hares is their demonstrated ability to sequester and store secondary metabolites from dietary sources in their digestive glands for long periods.[4–6] These accumulated substances, which typically occur in vanishingly small quantities, have long been thought to serve as a chemical defense mechanism against predators, although there is some debate as to their true role.[6–8] Although

* This chapter has been updated by David J. Newman, Natural Products Branch, Developmental Therapeutics Program, Division of Cancer Treatment and Diagnosis, National Cancer Institute, Frederick, MD.

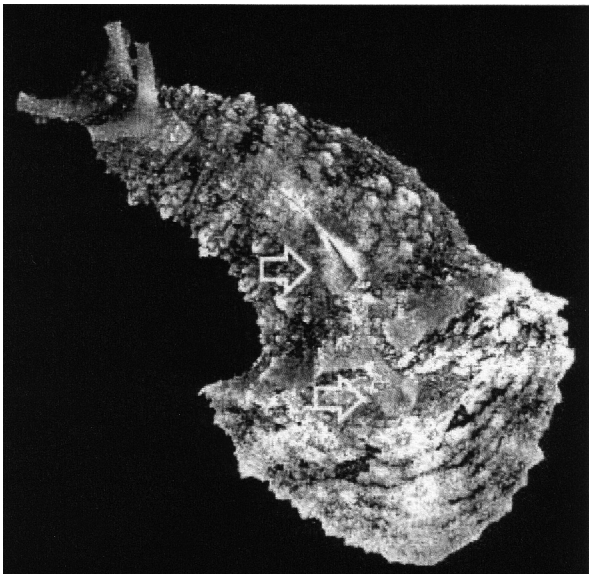

FIGURE 11.1 **(See color insert.)** *Dollabella auricularia.*

the dynamics of sequestration and differentiation processes for this apparent chemical defense mechanism are still unclear, the adaptive strategies of *D. auricularia* and other shell-less mollusks are nonetheless truly remarkable.

Some understanding of both the pharmacological utility as well as the potential dangers of extracts of *D. auricularia* has been known since ancient times.[9–13] However, the potential of *D. auricularia* with respect to modern medical problems was not recognized until the initial report from Pettit et al. at Arizona State University concerning the potent antineoplastic activity of crude extracts of the Indian Ocean variety of this inconspicuous marine animal.[14] Bioassay-guided (murine P388 leukemia cells [PS system]) isolation of the active principles of the crude extracts of *D. auricularia* collected off the coast of the Island of Mauritius in the Western Indian Ocean by Pettit's group eventually led to a considerable number of pure compounds exhibiting an impressive spectrum of antineoplastic and cytostatic activity.

Dolastatins 3–15 (Figure 11.2) were among the first group of compounds discovered and were first described in the chemical literature from 1982 to 1989.[15] Structurally, the dolastatins are a series of novel linear and cyclic peptides that exhibit remarkable potency against neoplastic cells *in vitro* (see Table 11.1). These unique peptide constituents possess many interesting structural features including hitherto unknown, modified amino acid residues and were isolated in very low yield (from 10^{-6}% to 10^{-8}% yield based on crude wet weight), requiring several recollections of the marine animal. The isolation and structure elucidation[16,17] of dolastatins 3–15, which required total synthesis in most cases to verify stereochemistry, has been reviewed.[15,18] Dolastatin 10 (**1**), with an ED_{50} in the subnanomolar range against a number of cancer cell lines, was the most potent antineoplastic substance known at the time of its discovery.[19]

The last of the bioactive peptides isolated by Pettit to date were dolastatins 16–18.[20–22] These compounds, isolated from *D. auricularia* specimens collected in Papua New Guinea, possess unique structural elements typical of peptides in this series including the novel alkynyl β-amino acid of dolastatin 17 (**9**) and β-branched amino acid dolaphenvaline of dolastatin 16 (**8**). Among these, dolastatin 16 was the most potent inhibitor of cell growth against a minipanel of the NCI's human cancer cell lines (mean GI_{50} 2.5×10^{-4} μg/mL, ~18-fold less potent than dolastatin 10). Isolation of a closely related but less bioactive compound, homodolastatin 16, has recently been reported.[23] Yamada et al. of Nagoya University initiated a large-scale collection of *D. auricularia* from Japanese waters (Shima Peninsula)

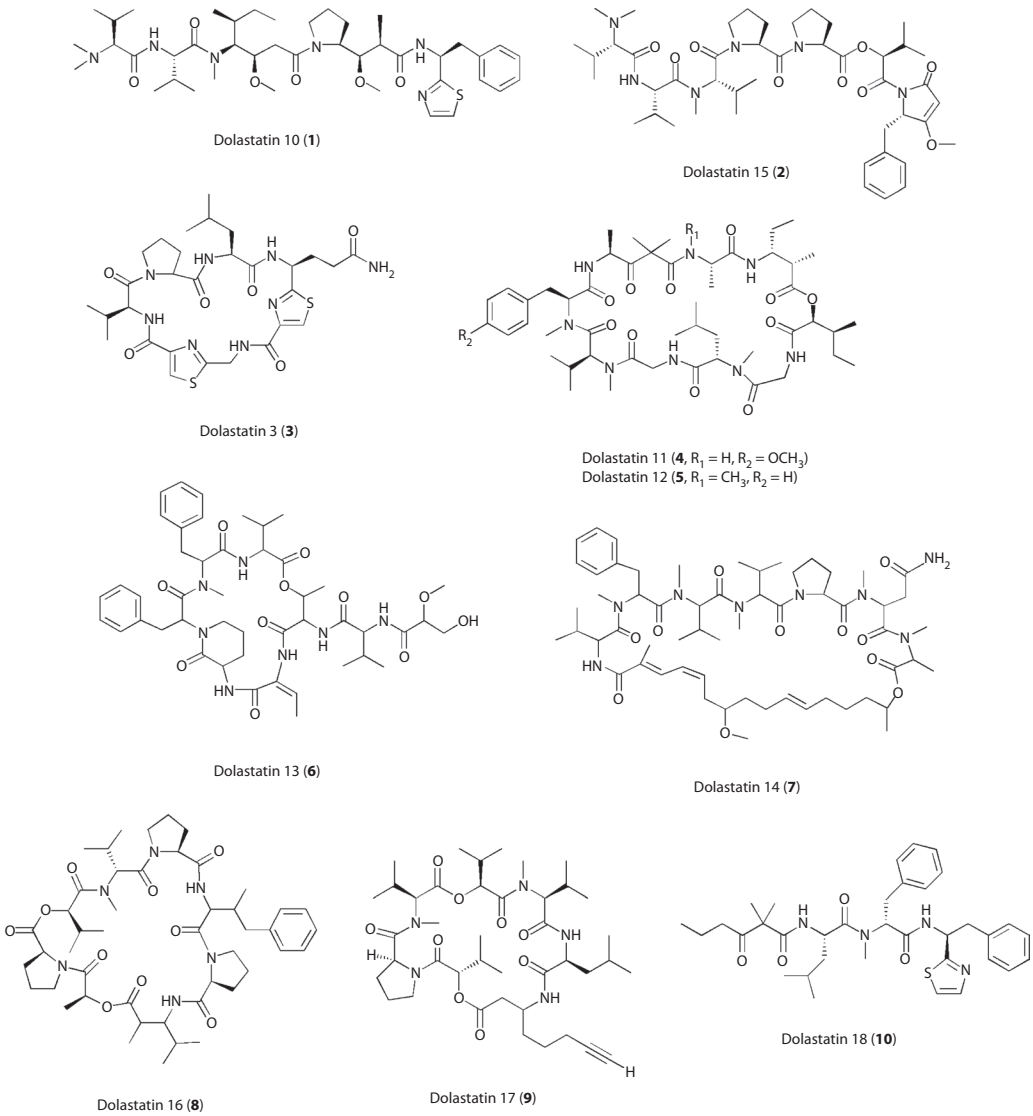

FIGURE 11.2 Dolastatins 1–18.

in the mid-1980s that led to the discovery of yet another series of unique compounds with antitumor activity (Figure 11.3).[24] The majority of these sea hare constituents (Dolastatins C-E,[25–28] dolastatin G/nordolastatin G,[29,30] dolastatin H/isodolastatin H,[31] dolastatin I,[32] aurilide,[33,34] dolabellin,[35] and doliculide[36]) are linear or cyclic pseudopeptides and exhibit potent *in vitro* antitumor activity in some cases. Of these, doliculide (**21**), containing a novel *ortho*-iodo-*N*-methyl-D-tyrosine residue, and dolastatin H (**16**)/isodolastatin H (**17**), which bear close structural resemblance to dolastatin 10, are the most potent inhibitors of antineoplastic growth (see Table 11.1). In addition to the pseudopeptide constituents described by Yamada, a number of sea hare-derived macrolides with antineoplastic activity were reported by these same researchers (dolabellides A and B[24] and doliculols A and B[37]). Despite the structural similarity between the dolastatins discovered by Pettit's and Yamada's groups, it is interesting to note that neither group has yet to isolate an identical compound from *D. auricularia*.

The origin of this impressive array of bioactive secondary metabolites found within sea hares has been the subject of much interest. Although direct biosynthesis or biosynthesis by symbiotic

TABLE 11.1
Summary of Antitumor Agents from the Marine Mollusk *Dollabella auricularia*[79]

Compound	Collection Site	*In Vitro* Activity (μg/mL)
Dolastatin 3 (**3**)	Mauritius	1.6×10^{-1}[a]
Dolastatin 10 (**1**)	Mauritius	3.4×10^{-6}[b]
Dolastatin 11 (**4**)	Mauritius	1.9×10^{-4}[b]
Dolastatin 12 (**5**)	Mauritius	8.8×10^{-2}[b]
Dolastatin 13 (**6**)	Mauritius	3.5[b]
Dolastatin 14 (**7**)	Mauritius	2.7×10^{-3}[b]
Dolastatin 15 (**2**)	Mauritius	2.8×10^{-3}[b]
Dolastatin 16 (**8**)	Mauritius	9.6×10^{-4}[b]
Dolastatin 17 (**9**)	Mauritius	4.5×10^{-1}[b]
Dolastatin 18 (**10**)	Papua New Guinea	3.9×10^{-1}[b]
Dolastatin C (**11**)	Papua New Guinea	17[c]
Dolastatin D (**12**)	Papua New Guinea	2.2[c]
Dolastatin E (**13**)	Shima Peninsula (Japan)	22–40[c]
Dolastatin G (**14**)	Shima Peninsula (Japan)	1[c]
Nordolastatin G (**15**)	Shima Peninsula (Japan)	5.3[c]
Dolastatin H (**16**)	Shima Peninsula (Japan)	2.2×10^{-2}[c]
Isodolastatin H (**17**)	Shima Peninsula (Japan)	1.6×10^{-2}[c]
Dolastatin I (**18**)	Shima Peninsula (Japan)	12[c]
Doliculide (**21**)	Shima Peninsula (Japan)	1.1×10^{-2}[c]
Dolabellin (**20**)	Shima Peninsula (Japan)	6.1[c]
Doliculide (**21**)	Shima Peninsula (Japan)	1×10^{-3}[c]

[a] ED_{50}, P388 (lymphocytic leukemia cells).
[b] GI_{50}, NCI-H460 (nonsmall-cell lung carcinoma).
[c] IC_{50}, HeLa-S_3 (cervical carcinoma cells).

microorganisms has been considered, these theories have slowly given way to strong evidence for exogenous procurement of such metabolites from dietary sources.[38] It is now generally accepted that cyanobacteria consumed by sea hares are the true biosynthetic source of the rich structural diversity represented by the dolastatins. This idea is supported by a number of observations. Collections of the same species from different locations have led to the isolation of similar, but structurally distinct, dolastatins. Furthermore, the incorporation of structurally unique amino acids that is typical of the dolastatins seems to favor a diet-derived origin based on the prevalence of such novel, nonproteinogenic amino acids among marine algae.[39] Moreover, a number of these compounds (dolastatins 3,[40] 10,[41] 12–14,[42,43] and 16[44]) have now been isolated directly from varieties of the blue-green algae *Lyngbya majuscula* and *Symploca hydnoides*, along with new bioactive compounds with closely related structures such as the recently described symplostatins 1–3[45–47] and somamides A and B.[43] This link between the dolastatins and cyanobacteria has important economic and ecological relevance for the future discovery and development of new anticancer drug leads.[48]

11.3 STRUCTURE AND SYNTHESIS

Although structurally complex in many cases, total synthesis of most of the dolastatins has been achieved to date. The importance of these synthetic endeavors should be underscored, as these efforts have allowed further study of this interesting family of compounds in both *in vivo* bioassays and human clinical trials. In this section, an overview of progress made in the synthesis of the

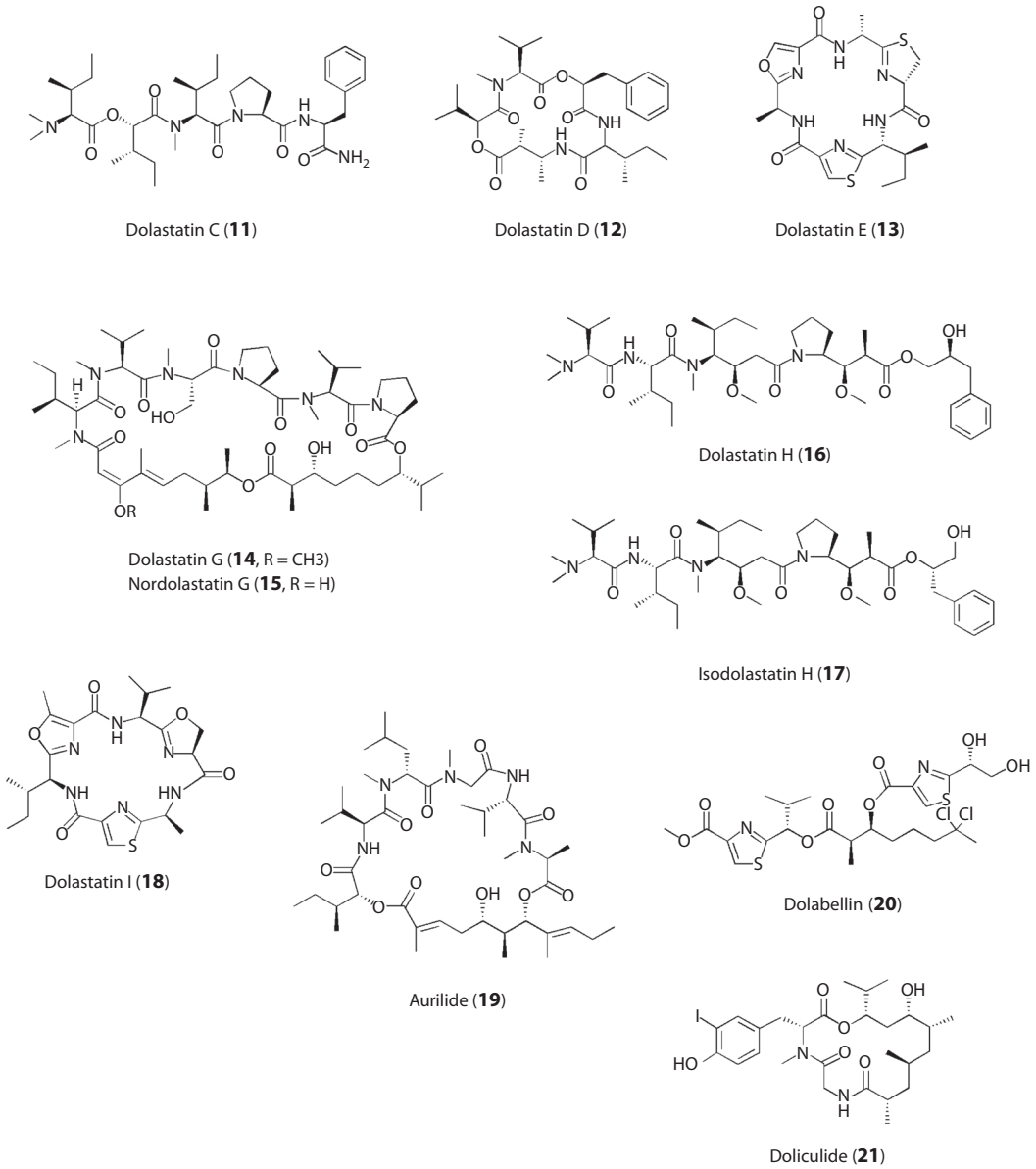

FIGURE 11.3 Dolastatins isolated from Shima Peninsula collection of *Dollabella auricularia*.[24]

various dolastatins and related compounds is presented, with particular attention to the methods devised for preparation of dolastatins 10 and 15 and important derivatives thereof.

Structure determination for dolastatin 3 (**3**), the first in the series to be described, required detailed spectral (nuclear magnetic resonance [NMR] and tandem mass spectrometry [MS] sequencing) and hydrolytic studies, as well as total synthesis.[15] The structurally interesting thiazole-containing amino acids of dolastatin 3 are related to similar cysteine-derived[49] thiazole amino acids found in other biologically active natural products, such as the antineoplastic marine sponge constituents patellamides A–C,[50] the antineoplastic microbial metabolite bleomycin,[51] and the broad-spectrum antibiotic thiostrepton,[52] among others. Several total syntheses of dolastatin 3 have been reported,[49,53–56] highlighted by the synthesis of the thiazole amino acids (Gly)Thz and (Gln)Thz.

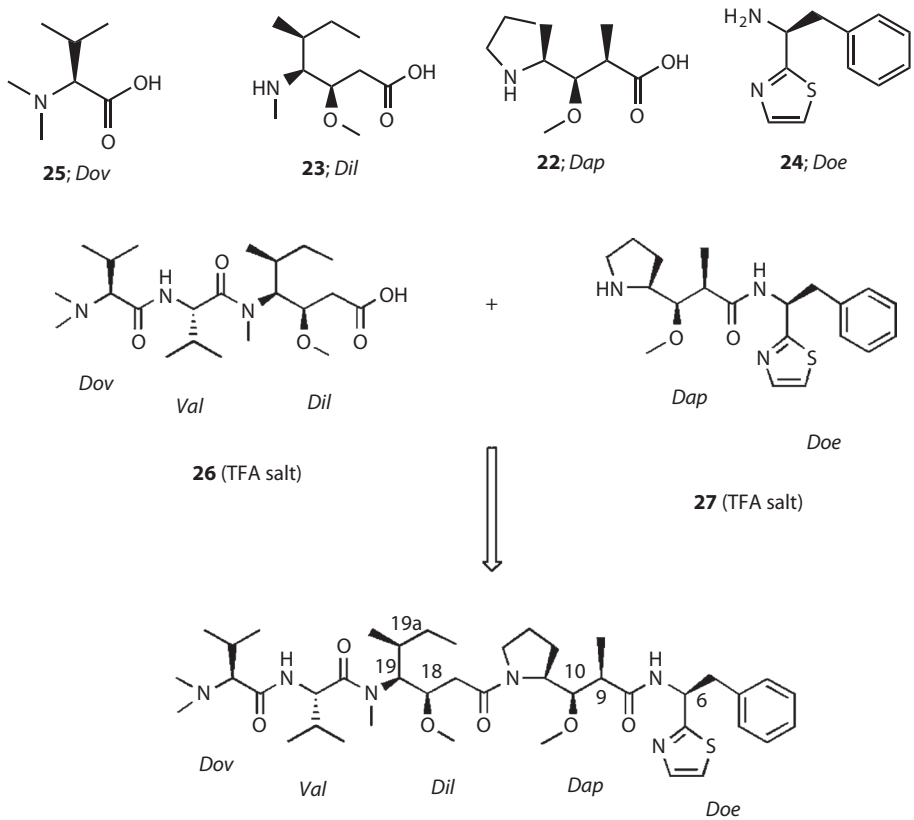

FIGURE 11.4 Dolastatin 10 structural units.

The synthesis of the most bioactive of the dolastatins, dolastatin 10 (**1**), was an extremely challenging undertaking because of the total of nine asymmetric centers of unknown configuration that make up the structure. The most notable structural features of dolastatin 10 are the two novel γ-amino-β-methoxy-acid residues, dolaproine (*Dap*, **22**) and dolaisoleucine (*Dil*, **23**), each containing three chiral centers (Figure 11.4). Similar structural units are also found in the marine tunicate antineoplastic components didemnins A–C[57] and the microbial metabolite bleomycin.[51] Also present is a novel thiazole-containing C-terminal unit dolaphenine (*Doe*, **24**), derived from phenylalanine, which is also found in dolastatin 18 (**10**). The fourth unusual unit is dolavaline (Dov; **25**). Several stereoselective syntheses[58] of the unique *Dap*, *Dil*, and *Doe* subunits have appeared in the chemical literature.

The absolute configuration of dolastatin 10 was confirmed by total synthesis,[59] first reported in 1989 by Pettit's group. Because of the exceptional promise of dolastatin 10 as an anticancer drug, several partial and total syntheses[58] of this peptide have been subsequently reported. Assembly of the amino acid constituents in both stepwise (by Shiori,[60,61] Koga,[62] and Poncet[63]) and convergent fashion has been successfully demonstrated. The general approach followed by Pettit's group for the preparation of initial quantities of dolastatin 10 for preclinical studies was convergent, as shown in Figure 11.4. The absence of a chiral center adjacent to the carboxylic acid of tripeptide *Dov–Val–Dil* (**26**) and the ease of its coupling with a proline derivative made this approach strategically attractive and free of epimerization concerns. In addition, this strategy was particularly amenable to the synthesis of shortened peptide segments and synthetic analogs that were used for elucidation of structure–activity relationships (SARs), as well as to provide insights into the mechanism of action for this drug, as discussed in more detail in Section 11.5. Yamada et al. also found this general [3 + 2]

coupling approach useful for the preparation of the structurally similar compounds dolastatin H (**16**) and isodolastatin H (**17**).[31]

Although the crude structures of dolastatins 11 (**4**) and 12 (**5**) were reported in 1989,[64] the absolute stereochemistry of these cyclopeptides remained undetermined until a total synthesis was reported by Bates et al. in 1997.[65,66] Dolastatins 11 and 12 are closely related cyclodepsipeptides bearing a novel β-amino acid residue, and are structurally very similar to the antifungal natural products majusculamide C[67] and 57-normajusculamide C,[68] components of the marine blue-green alga *Lyngbya majuscula*. This synthetic achievement has allowed for the unique biochemical effects of dolastatin 11 on tubulin and actin to be studied in more detail (see Section 11.4). Dolastatin 13 (**6**)[69] is a structurally complex cyclodepsipeptide containing a novel piperidine unit and a dehydroamino acid residue. Although no total synthesis has appeared to date, it is presumed that the recent discovery of the structurally analogous cyanobacterial metabolites symplostatin 2[46] and somamides A and B[43] will spark interest in construction of this peptide core. Total synthesis of the moderately active dolastatin 14 (**7**), a cyclodepsipeptide containing a polyene hydrocarbon fragment, has not been achieved to date. Several groups have published complementary approaches to the four possible isomers of the polyene subunit (dolatrienoic acid).[70–72] The absolute configurations of both dolastatins 13 and 14 are presently unknown, and their biological effects have not been thoroughly evaluated because of a lack of sufficient material.

The second most potent *D. auricularia* metabolite discovered to date is the linear depsipeptide dolastatin 15 (**2**). This unique peptide component bears many structural similarities to dolastatin 10 (**1**), including the presence of an *N,N*-dimethylvaline (*Dov*) N-terminus (Figure 11.5). The most interesting structural feature of dolastatin 15 is the novel C-terminal dolapyrrolidone unit (*Dpy*), which is presumably derived from biosynthetic modification of *N*-acyl phenylalanine. A total synthesis[73] of **2** was achieved by Pettit's group in 1991, and the absolute configuration was assigned accordingly. A novel synthesis from Poncet's group appeared in 1992[74] and featured reductive *bis*-methylation of the N-terminus as a final step. A second submission from Pettit in 1994 outlined some subtle improvements to the original approach,[75] and recently, a solid-phase synthesis of

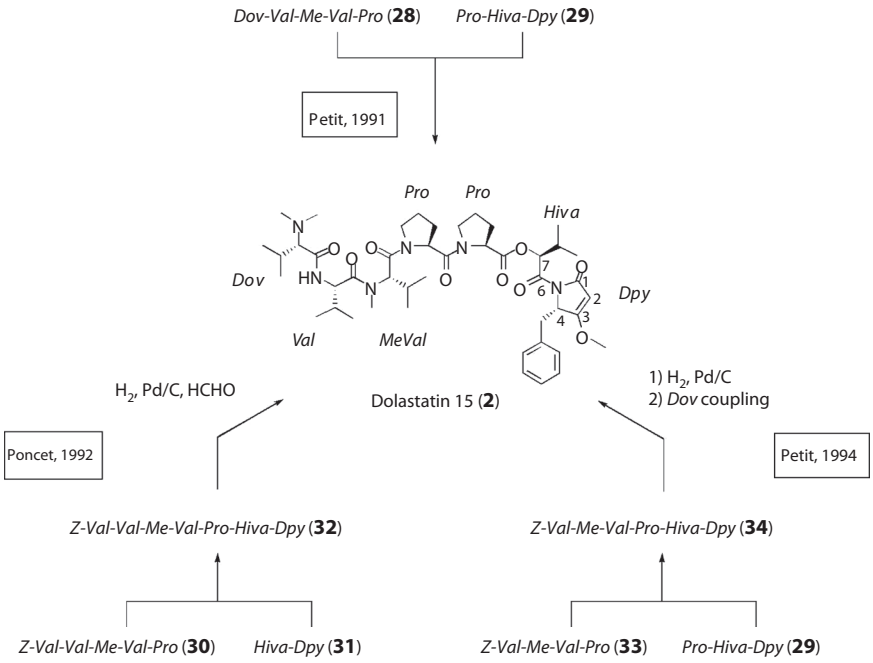

FIGURE 11.5 Synthetic approaches to dolastatin 15.

dolastatin 15 was also reported.[76] All the reported solution–phase syntheses of dolastatin 15 are convergent and take advantage of the reduced tendency of peptide segments coupled at proline to epimerize (see Figure 11.5). More recent approaches incorporate the *Dov* unit in the final step to circumvent purification difficulties associated with early introduction of the *N,N*-dimethylated N-terminus. As mentioned before for dolastatin 10, these complementary, convergent approaches are well suited for rapid preparation of synthetic derivatives useful for uncovering important SARs. The ample supply of synthetic dolastatin 15 has allowed for the biological activity of this unique peptide to be studied in great detail.[77]

Dolastatin 16 (**8**) is a unique cyclodepsipeptide containing novel β-amino acid (dolamethylleucine) and β-branched valine (dolaphenvaline) units reported by Pettit et al. in 1997. The structure and amino acid sequence was determined using high-field NMR and tandem mass spectral interpretations, and the stereochemistry of most of the subunits was determined via chiral high-performance liquid chromatography analysis of the acidic hydrolysate of the natural peptide. This compound exhibits marked antiproliferative effects on cancer cells *in vitro*, but the lack of available synthetic material has prevented further study of its biochemical effects.[20] The structure and partial stereochemistry of dolastatin 17 (**9**) were elucidated in a manner similar to that of dolastatin 16. The absolute stereochemistry of both dolastatins 16 and 17 has not been reported to date. The absolute stereochemistry of the C-terminal dolaphenine unit of dolastatin 18 (**10**) was recently determined via total synthesis and confirmed by x-ray crystal structure.[78]

Among the group of dolastatins (and related compounds) described by Yamada (Figure 11.3),[24] the absolute configuration for each is known, and a synthesis has been described for nearly every compound. This represents a tremendous achievement given the structural complexity of these substances. The various published syntheses of pseudopeptides **11**–**21** have been reviewed in detail by Poncet.[79]

11.4 BIOACTIVITY AND MECHANISMS OF ACTION

The dolastatins are all strong inhibitors of cancer cell growth, and indeed, the discovery of all these substances was guided by bioassay of extracts of the crude animal matter against actual cancer cells *in vitro*. Dolastatin 10 is the most potent antineoplastic agent of the dolastatins, followed by dolastatin 15 (on average, dolastatin 15 appears to be about sevenfold less active than dolastatin 10 in most preclinical models[80]). Dolastatin 10 has been studied most intensively because of its exceptionally potent antiproliferative effect on cancer cells and initial promise as an anticancer drug. Both dolastatins 10 and 15 are currently being pursued as clinical antitumor drug candidates and have reached phase II clinical trials in the United States, Europe, and Japan (see Section 11.6). Dolastatin 10 also exhibits therapeutic potential against other disease indications, as evidenced by its reported antiviral,[81] antibacterial,[82,83] antifungal,[84] and antimalarial[83,84] activities. A comparison of the growth inhibitory effects of dolastatins 10–16 against a selection of human cancer cell lines is presented in Table 11.2.[15]

Both dolastatins 10 and 15 are potent antimitotic agents and, as such, interfere with cell division via disruption of microtubule function.[85] Accumulation of cells trapped in metaphase arrest is observed in cancer cells treated with either of these agents, and at higher concentrations, intracellular microtubules disappear completely.[86] The cytostatic effects of dolastatins 10 and 15 on cells *in vitro* are derived from the binding interaction between these peptides and the β-subunit of the dimeric microtubule protein tubulin.[87] The role that this biochemical interaction plays in the cytotoxic and antitumor effects of these compounds is discussed next. The impressive performance of dolastatins 10 and 15 against cancer cells *in vitro* was followed directly by evaluation of these compounds in several murine tumor models. Both compounds were found to be effective against several human tumor xenografts such as the OVCAR-3 human ovary and LOX human melanoma *in vivo* systems.[15] A number of studies concerning the activity of both compounds against human leukemia[88–92] and lymphoma[93–95] cell lines as well as its efficacy for the treatment of prostate cancer[96]

TABLE 11.2
Comparative Activities (GI_{50}, μg/mL) of Dolastatins 10–16 against a Human Tumor Cell Line Minipanel from the National Cancer Institute Primary Screen

Dolastatin	OVCAR-3[a]	SF-295[b]	A498[c]	NCI-H460[d]	KM20L2[e]	SK-MEL-5[f]
10 (**1**)	9.5×10^{-7}	7.61×10^{-6}	2.6×10^{-5}	3.4×10^{-6}	4.7×10^{-6}	7.4×10^{-6}
11 (**4**)	0.04	0.031	0.023	1.9×10^{-4}	0.037	0.034
12 (**5**)	0.14	0.37	0.78	0.088	0.29	0.32
13 (**6**)	2.5	3.9	4.5	3.5	2.4	2.7
14 (**7**)	4.1×10^{-3}	2.0×10^{-3}	0.038	2.7×10^{-3}	0.020	6.4×10^{-5}
15 (**2**)	1.3×10^{-4}	4.3×10^{-4}	2.7×10^{-4}	2.8×10^{-4}	1.1×10^{-4}	1.7×10^{-4}
16 (**8**)	—	5.2×10^{-3}	—	9.6×10^{-4}	1.2×10^{-3}	3.3×10^{-3}

[a] Ovarian adenocarcinoma.
[b] Brain (glioma).
[c] Renal carcinoma.
[d] Nonsmall-cell lung carcinoma.
[e] Colon carcinoma.
[f] Melanoma.

have been reported. An interesting result to come out of these studies is that both agents are potently cytostatic (log 3 to log 4 more effective than the clinically established drug vincristine), but not cytotoxic at drug concentrations required to achieve maximum growth inhibition. Importantly, the two dolastatin compounds showed low toxicities to resting or proliferating nonleukemic cells. Furthermore, the observed growth inhibition was reversed once treatment was terminated.[90] A summary of results for dolastatins 10 and 15 against human leukemia and lymphoma cells appears in Table 11.3.

The antiproliferative effects of dolastatin 10 on purified tubulin and cellular microtubule assembly generally parallel those of the well-known vinca alkaloids, but its inhibition of cancer cell

TABLE 11.3
Dolastatins 10 and 15 Activity Versus Human Leukemia Cell Lines

	IC_{50} (nM)	
Cell Line	Dolastatin 10 (1)	Dolastatin 15 (2)
BV-173[a]	4.7×10^{-2}	5.9×10^{-1}
KM-3[a]	8.7×10^{-2}	8.9×10^{-1}
K-562[b]	1.2×10^{-1}	1
U-937[c]	1.8×10^{-2}	1.2×10^{-2}
HL-60[d]	5.5×10^{-2}	2.5×10^{-2}
KARPAS-299[e]	9.8×10^{-2}	2.8×10^{-2}
B-cells	1.0	>2.0
T-cells	3.7×10^{-1}	>2.0

[a] Pre-B-cell leukemia.
[b] Erythroleukemia.
[c] Monocytic leukemia.
[d] Myeloid leukemia.
[e] T-cell lymphoma.

growth *in vitro* is much more potent. Both dolastatin 10 and the structurally unrelated mycotoxin phomopsin A are strong noncompetitive inhibitors of the binding of radiolabeled vinca alkaloids. In addition, dolastatin 10 is a potent inhibitor of nucleotide exchange and tubulin-dependent guanine-5-triphosphate (GTP) hydrolysis (Table 11.4). The hydrolysis of GTP bound to the exchangeable nucleotide site on the β-subunit of tubulin is believed to play an important regulatory role in the polymerization of tubulin. Results of extensive competition experiments with dolastatin 10 and other vinca domain drugs[87] have led to a proposed model of the binding sites of this class of antimitotics. Hamel et al. have proposed that dolastatin 10 binds to a "peptide site" near both the vinca site and the exchangeable nucleotide site.[97] According to the model, when dolastatin 10 is bound to its critical active site, the C-terminal end of the peptide effectively blocks access to the vinca alkaloid binding site and the exchangeable nucleotide site. This idea is supported by several structure–activity observations[98] and, in particular, by the fact that a shortened tripeptide segment not containing the latter two C-terminal units (**26**; Figure 11.4) retains tubulin antiproliferative activity, but exhibits reduced inhibition of vinca alkaloid binding and nucleotide exchange.[86]

The effects of dolastatin 15 on the proliferation of cellular microtubules and purified tubulin *in vitro* have also been studied.[97] Similar to dolastatin 10, the structurally similar dolastatin 15 appears to derive its potent antineoplastic effects by interfering with the assembly of microtubules and causing mitotic arrest, though in the case of the latter peptide, the connection is less clear. Dolastatin 15 is roughly one-seventh as active as dolastatin 10, but is nearly seven times more active than vinblastine with respect to cell growth inhibition of L1210 murine leukemia cells.[99] Despite its potent antitumor activity, the activity of dolastatin 15 in the tubulin assembly assay is much weaker than for any of the other drugs that bind in the vinca domain (Table 11.4). In addition, dolastatin 15 does not inhibit the binding of the vinca alkaloids to tubulin and does not affect nucleotide exchange to any degree. Tubulin-dependent GTP hydrolysis is inhibited by dolastatin 15, but to a lesser degree than encountered with dolastatin 10. Hamel et al. have interpreted these results as an indication of a

TABLE 11.4
Relative Inhibitory Effects of Vinca Domain Drugs on [^{3}H]Vincristine Binding, on the Polymerization of Purified Tubulin,[a] on Guanine-5-Triphosphate (GTP) Nucleotide Exchange, and on Tubulin-Dependent GTP Hydrolysis

Drug	Inhibition [^{3}H]Vincristine Binding (Type)	IC_{50}[b] Tubulin Polymerization (μM)	IC_{50} GTP Exchange (μM)	IC_{50} GTP Hydrolysis (μM)
Vinblastine	Competitive	1.5	>80	6
Maytansine	Competitive	3.4	9	4
Rhizoxin	Competitive	6.9	29	13
Phomopsin A	Noncompetitive	1.4	5	3
Dolastatin 10	Noncompetitive	1.2	8	3
Dolastatin 15	NI[c]	23	NI[c]	33
Halichondrin B	Noncompetitive[d]	6.1	17	12
Spongistatin 1	Noncompetitive[d]	5.3	87	—

[a] Standard tubulin assay: preincubation (15 min) of a drug–tubulin mixture (10 μM tubulin) in 1 M monosodium glutamate + 1 mM $MgCl_2$ at 37°C was followed by the addition of GTP, and the polymerization reaction at 37°C was monitored, using a spectrophotometer. The tubulin assay used in the current structure–activity study was a modified method as discussed in Section 10.3 of reference 87.

[b] IC_{50} refers to the drug dosage required for 50% inhibition.

[c] Noninhibitory.

[d] Competition experiments with halichondrin B and spongistatin 1 were carried out using [^{3}H]vinblastine rather than [^{3}H]vincristine.

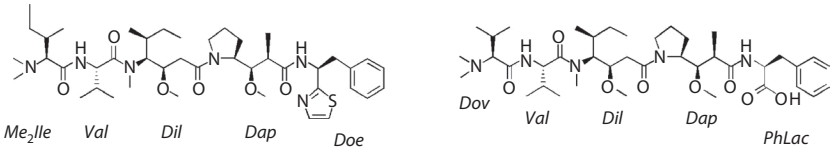

Symplostatin 1 (**35**)

$IC_{50} = 3.0 \times 10^{-4}$ mg/mL
KB cells (epidemoid carcinoma)

Symplostatin 3 (**36**)

$IC_{50} = 3.9 \times 10^{-3}$ mg/mL
KB cells (epidemoid carcinoma)

FIGURE 11.6 **(See color insert.)** Naturally occurring derivatives of dolastatin 10.

relatively weak drug–tubulin interaction for dolastatin 15. More recently, Jordan et al. have shown evidence that the dolastatin 15 derivative cemadotin (**38**; Figure 11.7) may exert its antitumor activity via suppression of dynamic instability of microtubules assembled to steady state.[100] These authors suggest that cemadotin may bind at a novel site in tubulin, distinct from the vinca site. Recent competition studies with radiolabeled dolastatin 15 seem to indicate that the binding sites for antimitotic peptides in the dolastatin family may consist of a series of overlapping domains.[101] Dolastatins 10 and 15 are nevertheless presumed to interact with a similar specific binding site in the vinca domain based on structural homology and GTP hydrolysis considerations,[97] although other targets cannot be ruled out.

With regard to the demonstrated capacity of dolastatins 10 and 15 to disrupt microtubule organization, it is important to note that the exact mechanism by which antimitotic drugs cause cell death remains unclear. Some researchers have suggested that apoptosis induced by phosphorylation of the oncoprotein bcl-2 (an inhibitor of programmed cell death) may play an important role in the mechanism of action of some antitumor agents that are also microtubule poisons,[102,103] and some evidence for this explanation has been shown for dolastatins 10 and 15.[94,104,105]

Some biology of newly discovered, natural analogs of dolastatin 10 was also recently divulged. Cyanobacterial metabolite symplostatin 1 (**35**; Figure 11.6) reportedly exhibited potent microtubule inhibition and was furthermore found to be effective *in vivo* against two drug-insensitive, murine tumor models.[41] A recent study of the molecular pharmacology of symplostatin 1[106] revealed that this closely related substance shares a very similar mechanism of action with dolastatin 10. Symplostatin 3 (**36**; Figure 11.6) is about 10–100-fold less cytotoxic than dolastatin 10 *in vitro*.[47] Soblidotin (**37**, TZT-1027; Figure 11.7), a synthetic derivative of dolastatin now in clinical trials, inhibits microtubule polymerization and interferes with microtubule assembly/disassembly equilibria through interaction with tubulin, as expected from similar work with the parent peptide. Apoptosis by a direct mechanism (cytotoxicity) versus the known antimitotic effect has been observed with soblidotin at higher doses *in vitro*[107] and *in vivo* with murine B16 melanoma xenografts.[108] Of considerable interest is the observation made by Japanese researchers that treatment of

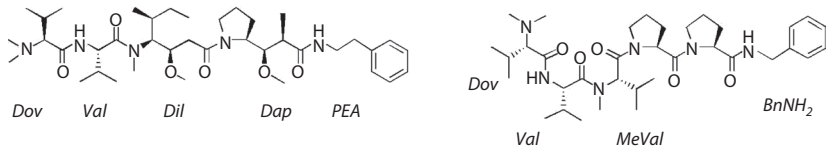

Soblidotin (**37**)
(TZ-1027, Auristatin PE)

$GI_{50} = 3.0 \times 10^{-6}$ mg/mL
NCI-H460 (Lung-NSC)

Cemadotin (**38**)
(LU103793)

$IC_{50} = 7.0 \times 10^{-6}$ mg/mL
HeLa-S_3 (cervical carcinoma)

FIGURE 11.7 **(See color insert.)** Synthetic derivatives of dolastatin 10 (soblidotin) and dolastatin 15 (cematodin) in phase II clinical trials.

an advanced murine tumor model (colon 26 adenocarcinoma) with soblidotin induces tumoral vascular collapse and tumor cell death, necrosis, and tumor regression.[109] This indicates that soblidotin may exert its antitumor activity by both conventional microtubule disruption and by a unique, antitumoral vascular mechanism of action that could prove to be a powerful combination for cancer chemotherapy.

Among other dolastatins whose biology has been studied in detail, dolastatin 11 is particularly interesting because of its unique biochemical effects on tubulin and actin proteins *in vitro*.[110] A recent study concerning the mechanism of action of this peptide showed that dolastatin 11 arrests cells at cytokinesis by causing a rapid and massive rearrangement of the cellular actin filament network.[110] Dolastatin 16 has shown a mean panel GI_{50} value of 2.2×10^1 μg/mL against the NCI's complete panel of 60 cell lines and showed marked inhibitory effects against nonsmall-cell lung carcinoma, colon carcinoma, and melanoma cells in particular.[20] Interestingly, dolastatin 16 shows a relatively low GI_{50}-COMPARE[111] correlation with dolastatins 10 and 15, which may indicate a different mechanism of action for this cyclic peptide relative to the others.

11.5 STRUCTURAL MODIFICATIONS AND SAR

The initial discovery of dolastatin 10 and its potent inhibitory effect on cancer cell growth at unprecedentedly low drug concentrations was soon followed by structure–activity studies on this structurally unique peptide. These efforts were aimed at elucidation of key structural requirements for activity and at reducing structural complexity where possible. The first structural modifications of dolastatin 10 to be prepared and evaluated against tumor cells *in vitro* were 19 of the possible 128 stereoisomers of the natural peptide, which were synthesized in connection with absolute configuration determinations for the nonproteinogenic *Dil, Dap*, and *Doe* residues.[98,112] Among the various stereoisomers tested, only two retained antitumor activity comparable with the natural peptide. Change of chirality at most stereocenters resulted in moderate to substantial decrease in activity against the murine P388 cell line, with the exception of the (6R)-isomer [isodolastatin-(6R), **42**; Table 11.5] and (19aR)-isomer, where reversal of stereochemistry at the *Doe* α-carbon (position 6) and *Dil* side chain (position 19a) was attended by no loss of antitumor activity (Figure 11.8). Moreover, a clear correlation between inhibition of tubulin polymerization and inhibition of L1210 leukemia cell growth was demonstrated for all stereoisomers that retained some antitumor activity. Interestingly, the shortened tripeptide segment *Dov–Val–Dil–OMe* ester is completely inactive against tumor cell growth and yet retains substantial inhibitory effects on tubulin polymerization. Hamel et al. have speculated that the *Dil* subunit may be essential for the interaction of dolastatin 10 with tubulin, although the exact nature of the link between affinity for tubulin binding and antineoplastic activity is not completely clear.[86] This early work set the stage for more fundamental changes to the peptide backbone of dolastatin 10, carried out mainly by the research groups of Pettit,[86,112–114] Poncet,[115–117] and Miyazaki.[118,119]

Most of the attention given to the preparation of dolastatin 10 analogs has centered on modifications of the C-terminus (e.g., *Doe* unit). Modifications at this position allow for structure simplification (e.g., thiazole replacement) without diminution of antineoplastic activity and may furthermore permit fine-tuning of selectivity in some cases. A survey of interesting results from some of these SAR studies is given in Table 11.5. In particular, the phenethylamine core of the

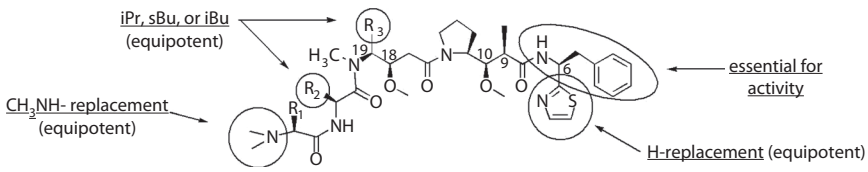

FIGURE 11.8 Effects of structural modifications on dolastatin 10 activity.

TABLE 11.5
Survey of Dolastatin 10 Modifications and Effect on Inhibition of Tumor Cell Proliferation and Tubulin Polymerization

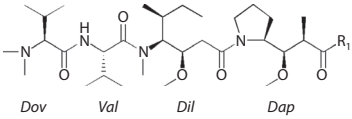

No.	Compound	Mean GI_{50} ($\times 10^8$ M)[a]	Correlation Coefficient[b]	L1210, IC_{50} (nM)[c]	Tubulin, IC_{50} (μg/mL)[d]
1	Dolastatin 10	0.012	1.00	0.5	1.3 ± 0.2
42	Isodolastatin-(6R)	0.1[e]	—	—	—
	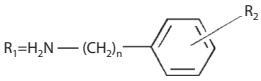				
43	$n = 0$, $R_2 = H$	1.0	0.828	60	1.8 ± 0.2
44	$n = 1$, $R_2 = H$	0.174	0.851	80	1.6 ± 0.2
37	$n = 2$, $R_2 = H$	0.049	0.901	0.6	1.3 ± 0.2
45	$n = 2$, $R_2 =$ *ortho*-Cl	—	—	3	1.2 ± 0.2
46	$n = 2$, $R_2 =$ *meta*-Cl	—	—	2	1.6 ± 0.2
47	$n = 2$, $R_2 =$ *para*-Cl	0.076	0.835	0.4	1.5 ± 0.2
48	$n = 3$, $R_2 = H$	0.182	0.805	20	1.3 ± 0.05
49	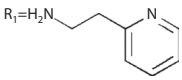	0.085	0.847	5	1.2 ± 0.2
50	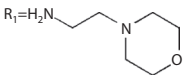	3.8	0.667	500	2.6 ± 0.5
51	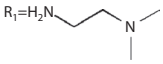	8.2	<0.6	>1000	2.1 ± 0.3
52	R_1 = Phe–OMe	0.020	0.903	5	1.6 ± 0.04
53	R_1 = Phe–NH_2	0.282	0.852	10	1.0 ± 0.2
54	R_1 = Met–OMe	0.040	0.904	6	1.4 ± 0.2
55	R_1 = Ile–OMe	0.016	0.899	7	1.7 ± 0.2
56	R_1 = OMe	—	—	30	1.3 ± 0.1
57	*Dap–Doe* → *Pro–PEA*[f]	3.8	0.667	800	2.9 ± 0.3
58	*Dov–Val–Dil–Doe* (*Dap* omitted)	19.5	0.711	200	2.1 ± 0.1

[a] Mean GI_{50} obtained from quadruplicate screenings of compounds indicated against the National Cancer Institute's full 60-cancer cell line panel.

[b] Correlation coefficients from COMPARE algorithm analyses of averaged total growth inhibition (TGI) mean graph obtained from quadruplicate screening results against the full 60-cancer cell line panel, using the mean value for dolastatin 10 as the seed for all correlations.

[c] Murine L1210 (lymphocytic leukemia cells).

[d] Inhibition of the polymerization of purified, bovine brain tubulin.

[e] ED_{50} value for isodolastatin-(6R) against murine P388 leukemia cells. This compound was not tested on other assays listed before.

[f] *Pro–PEA* corresponds to the phenethylamide of L-proline.

C-terminus was found to be essential for antitumor activity, and the corresponding derivative, described by both Pettit[113,114] and Miyazaki,[118,119] has quickly advanced as a drug candidate (soblidotin, **37**; Figure 11.6), currently in phase II clinical trials. The length of the alkyl chain between the amide and phenyl groups does appear to be important for antitumor activity (derivatives **43**, **44**, **37**, and **48**), whereas the effect of aryl substitution is less obvious (derivatives **45**–**47**). Several amino acid methyl esters are also adequate replacement groups for the usual C-terminus, although the nature of the amino acid employed [e.g., aryl (Phe-OMe, **52**), alkyl (Ile-OMe, **55**), or sulfur-containing (Met-OMe, **54**)] does not appear to have a significant effect on activity. Interestingly, C-terminal replacement groups containing basic functionality (**50** and **51**) exhibited markedly reduced antineoplastic activity and furthermore showed very little correlation to the activity profile of the parent peptide. Derivatives in which the *Dap* subunit was either omitted (**58**) or replaced with proline (**57**) were ineffective. Modification to certain positions of the other subunits also produced derivatives that showed antitumor activity comparable with that of dolastatin 10. However, none of the modifications described resulted in any meaningful simplification of the core structure. It is interesting to note that one of the active *Dov*-modified, synthetic analogs (Me_2Ile N-terminus) described by Pettit et al.[114] has since been discovered as a naturally occurring cyanobacterial metabolite (symplostatin 1, **35**; Figure 11.7).[45] A summary of some SARs for dolastatin 10 is given in Figure 11.8.

Preparation of a single crystal of the (6R)-isomer of dolastatin 10 [isodolastatin-(6R), **42**] afforded the first opportunity for study of the three-dimensional conformation of this peptide, and a molecular modeling study was undertaken by Pettit and Srirangam. Computer-assisted modeling studies for this isomer of dolastatin 10, supported by data from an x-ray crystal structure, revealed a ~21 kcal/mol energy barrier between *cis* and *trans* conformers, visible by NMR at room temperature. Interestingly, the crystalline structure of isodolastatin-(6R) contains all *trans*-amide bonds except for the *Dil–Dap* bond, which proved to be *cis*.[112] Following this work on stereoisomer **42**, Poncet et al. reported a detailed molecular modeling study on the natural stereoisomer of both dolastatins 10 and 15, aimed at elucidation of the structural requirements for antitumor activity. The preferred, low-energy conformations of these peptides in DMSO-d_6 solution were determined via two-dimensional NMR measurements, followed by molecular dynamic simulations.[115] These calculations confirmed that the two conformers observed for dolastatin 10 in solution are a result of *cis–trans* isomerization of the *Dil–Dap* amide bond, with an energy barrier of 8 kcal/mol in favor of the *cis* conformer.

The unique, *cis–trans* isomerization of dolastatin 10 could potentially provide insights into the active conformation of the peptide in association with its presumed intracellular target tubulin. Poncet synthesized a cyclic derivative of the peptide (**39**), joined through a threonine-like ester linkage between the "*Dov*" and "*Doe*" residues, to probe the effect of locking the backbone in a folded conformation (Figure 11.9).[117] Although the resulting compound was completely inactive, it is possible that *cis–trans* isomerization of dolastatin 10 plays a central role in its interaction with tubulin, a mechanism that will likely be more well-defined after further studies. Among the D10/D15 hybrid compounds **40** and **41** prepared by Poncet (Figure 11.9), both peptides retained partial antitumor activity, whereas only peptide **41** (*Dov–Val–Dil–Pro–Hiva–Dpy*) retained capacity to inhibit tubulin polymerization *in vitro*.[117] This result appears to support Hamel's assertion that the *Dil* residue is critical for molecular interactions between the peptide and tubulin.[86]

Because dolastatins 11–14, dolastatins 16–18, and Yamada's series of *D. auricularia* metabolites have not undergone extensive biochemical evaluation to date, less is presently known about SARs for these compounds. Recently, Russo et al. in Italy began preliminary studies aimed at elucidation of SAR for dolastatins 11 and 12 using molecular mechanics and dynamic calculations in aqueous solution.[120] Now that Bates et al. have devised a total synthesis of dolastatins 11 and 12,[66] the door remains open for further elucidation of their unique biochemical effects on actin through preparation of synthetic derivatives. These and other advances should help provide more insight into the specific mechanisms of action for these as yet largely unstudied peptides.

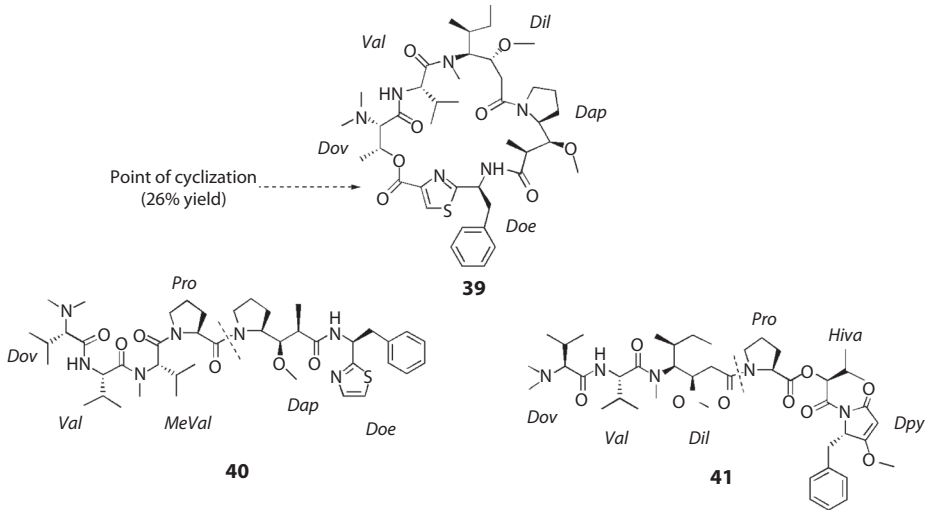

FIGURE 11.9 **(See color insert.)** Dolastatin 10 cyclic derivative and D-10/D-15 hybrid compounds.

Similar to dolastatin 10, efforts toward understanding SARs for dolastatin 15 are further advanced than for other members of this series, and a number of research groups have prepared derivatives and published studies. In contrast to dolastatin 10, dolastatin 15 was found to be surprisingly insensitive to structural and stereochemical modifications at the C-terminus (Table 11.6 and Figure 11.10). Change in the configuration of the stereogenic centers that comprise the *Hiva* and *Dpy* unit was found to minimally affect *in vitro* antineoplastic activity (compounds **59–61**).[121] As with dolastatin 10, a slight trend favoring the phenethylamine C-terminus over other arylalkyl chain lengths was

TABLE 11.6
Survey of Dolastatin 15 N-Terminus Modifications and Effect on Inhibition of Tumor Cell Proliferation and Tubulin Polymerization

No.	N-Terminus	L1210 IC_{50} (n*M*)[a]	P388 ED_{50} (ng/mL)[b]	NCI-H460 ED_{50} (ng/mL)[c]	Tubulin IC_{50} (μg/mL)[d]
1	(7*S*)-Hiva-(4*S*)-Dpy	0.15	2.4	0.28	5.2
59	(7*R*)-Hiva-(4*S*)-Dpy	0.30	—	—	—
60	(7*S*)-Hiva-(4*R*)-Dpy	0.31	—	—	—
61	(7*S*)-Hiva-(4*S*)-Dpy	1.78	—	—	—
62	(7*S*)-Hiva-anilide	3	0.52	0.032	26
63	(7*S*)-Hiva-benzamide	1	0.42	0.25	20
64	(7*S*)-Hiva-phenethylamide	2	0.26	0.044	15
65	(7*S*)-Hiva-phenpropylamide	—	0.38	1.1	—
66	(7*S*)-Lac-phenethylamide	—	0.46	0.37	—
67	L-Val-phenethylamide	—	0.59	2.5	—
68	L-MeVal-phenethylamide	—	>1000	3600	—

[a] Murine L1210 (lymphocytic leukemia cells).
[b] Murine P388 (lymphocytic leukemia cells).
[c] Human nonsmall-cell lung carcinoma.
[d] Inhibition of the polymerization of purified, bovine brain tubulin.

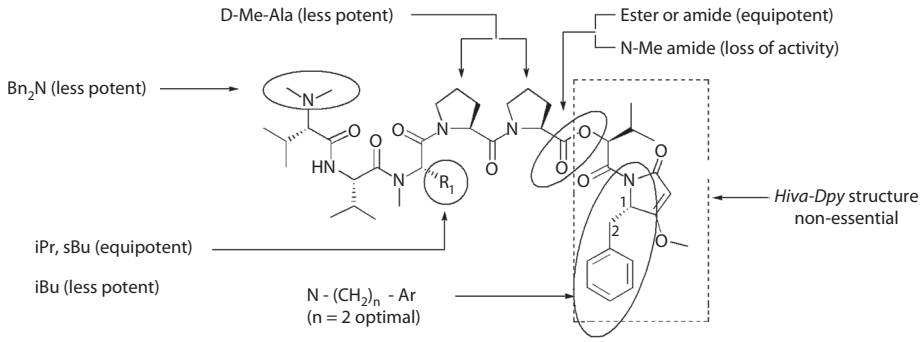

FIGURE 11.10 **(See color insert.)** Effects of structural modifications on dolastatin 15 activity.

observed, but the effect was much more subtle in the case of dolastatin 15 (compounds **62–65**).[122] Results of SAR studies for dolastatin 15 clearly indicate that the structurally complex *Dpy* C terminus plays a limited role in the cell growth inhibitory effects of this peptide.

The interaction of dolastatin 15 with purified tubulin *in vitro* is considerably weaker than that of dolastatin 10 (about 20-fold) and other antimitotic drugs that bind in the vinca domain of tubulin,[99] despite its potent antiproliferative effect on cellular microtubules (one-seventh as active as dolastatin 10, but ten times more potent than the clinically useful anticancer drug vinblastine). Thus far, results from SAR studies on dolastatin 15 have not established a clear connection between cancer cell growth inhibition and a tubulin-based mechanism of action. Although all structural modifications of the C-terminus of dolastatin 15 exhibited potent antineoplastic activity, most showed modest reduction of inhibitory activity against tubulin polymerization. The opposite has been observed for dolastatin 10 derivatives, where potent inhibitory effect on tubulin polymerization (1–4-μM range) has been retained in spite of significant loss of antitumor activity (>1000-fold in some cases).[122] It has been suggested that the potent cytotoxicity and inhibitory effects on microtubule assembly exhibited by dolastatin 15 are not a result of the parent molecule but of a more active metabolite derived from it.[99] In this context, the reduced activity of dolastatin 15 in the purified tubulin assay could be explained by the absence of proteolytic enzymes normally present in cells. Furthermore, the fact that dolastatin 15 is active against prokaryotic cells that lack tubulin indicates a second cellular target. Derivatives **66–68** were prepared by Pettit's group to probe whether intracellular hydrolysis of the ester bond of this depsipeptide might be a necessary condition for *in vitro* activity.[123] Interestingly, replacement of the ester with an *N*-methyl amide function (compound **68**) led to complete loss of antitumor activity. Although the *N*-methyl amide modification would be expected to impart greater stability of the peptide bond toward enzymatic cleavage, conformational changes in the peptide backbone induced by *N*-methylation cannot be ruled out as the cause for the lack of potency in this compound.

Among the most important discoveries made in the dolastatin series is that made by researchers at BASF, who found that the *Hiva–Dpy* units of dolastatin 15 may be completely replaced with a simple benzamide group without loss of activity (cemadotin, LU103793, **38**; Figure 11.6).[124] The progress of this water-soluble D15 derivative through clinical trials in humans is discussed in the next section. Hu et al. have described a series of derivatives based on the structure of cemadotin, in which modifications of the *Dov* (Bn_2Val) and Pro (D-MeAla) residues as well as aromatic ring substitutions were evaluated.[125] Although aromatic ring substituents altered the cytostatic properties only slightly, other modifications described led to more pronounced loss of activity in this series. Kessler et al. have prepared a peptidomimetic compound based on the structure of dolastatin 15, using *N*-substituted glycine monomers, but the resulting peptoid was devoid of cytostatic properties.[126] A summary of dolastatin 15 structural requirements for antitumor activity is shown in Figure 11.10.

The minimum energy, solution-phase conformation of dolastatin 15 has been predicted by Poncet et al., using two-dimensional NMR techniques and molecular dynamics simulations.[115] Despite the known tendency for proline residues to form peptide turn structures because of a decreased energy barrier between *cis* and *trans* amide bond conformations, dolastatin 15, which contains two contiguous proline units, appears to adopt a less-folded, linear shape (all *trans* amide bonds) in solution.[121]

11.6 CLINICAL UPDATE

Of the naturally occurring dolastatins, only dolastatin 10 has progressed to human clinical trials. Although dolastatin 15 has not been studied directly, synthetic derivatives of both dolastatins 10 (soblidotin, **37**) and 15 (cemadotin, **38**) are currently under evaluation in phase II clinical trials. The progress of these studies and the future potential of the dolastatins and its congeners are discussed in this section.

Among the naturally occurring peptides of *D. auricularia*, dolastatin 10 was selected over dolastatin 15 for further evaluation in clinical trials because of its inhibitory effect on cancer cell growth at extremely low concentrations. Preclinical studies on both peptides indicated that myelotoxicity would be a potentially limiting factor, as both compounds were found to inhibit bone marrow cell colony formation at drug concentrations ~100-fold lower than that required for antitumor activity in human tumor cell lines *in vitro*.[127,128] Preclinical animal toxicity evaluations in mice, rats, and dogs showed that myelotoxicity was dose-limiting in all three species, with mice being the least sensitive, and a phase I clinical trial starting dose of 65 μg/M^2 was recommended.[127]

Among phase I patients with advanced solid tumors, a maximum tolerated dose (MTD) was reached at 300 μg/M^2, and granulocytopenia (myelosuppression) was the dose-limiting toxicity, observed in 33% of patients at this dose.[129] Other mild-to-moderate toxicities were also noted, such as fatigue, nausea, and peripheral neuropathy (40% of patients).[128] Clinical pharmacokinetic studies with five patients detected a single dolastatin 10 metabolite, corresponding to a more water-soluble, *N*-desmethyl derivative.[129,130] Dolastatin 10, administered as an intravenous bolus injection, showed a plasma elimination half-life of 5–7 h.[80] Phase II clinical trials for dolastatin 10 in a number of cancer indications (metastatic prostate adenocarcinoma,[131] metastatic melanoma,[132] metastatic colorectal cancer,[133] advanced nonsmall-cell lung carcinoma,[134] and platinum-sensitive ovarian carcinoma[135]) have been completed. The MTD has varied from patient to patient from 300 to 400 μg/M^2. No significant antitumor activity has been observed to date for dolastatin 10, administered as a single agent to patients with advanced solid tumors. Dolastatin 10 does act synergistically with other anticancer substances (e.g., vincristine and bryostatin 1),[95] providing some hope that this highly potent peptide may find use in drug combination therapies.

Structure/activity work by Miyazaki[118,119] and Pettit[136] led to the discovery of the dolastatin 10 synthetic derivative soblidotin (**37**) that is currently in phase II clinical trials. Although less information concerning the results of preclinical work and phase I clinical trials is presently available for soblidotin, a pattern similar to that of dolastatin 10 would be expected because of their close structural analogy. Some preliminary results from a few phase I studies have been recently summarized.[137,138] Soblidotin (single dose, intravenous feed at 1.35–2.4 mg/M^2) was generally well tolerated among patients with advanced solid tumors, and induced antitumor effects were observed.[139] A more recent study conducted with nonsmall-cell lung carcinoma patients has generated some promising results. The drug (single dose, intravenous infusion) was reportedly well tolerated up to 4.8 mg/M^2, and complete or partial responses were seen in 4 of 44 patients.[140,141] These results are a positive sign for how this promising drug may fare in phase II clinical trials, although no further data are presently available.

The third and final drug in the dolastatin family to reach phase II clinical trials in humans as of this writing is the dolastatin 15 derivative cemadotin (**38**). As with dolastatin 10, myelotoxicity (neutrope-

nia) was found to be the principal dose-limiting toxicity, and a MTD of 12.5 mg/M^2 was established for phase II patients.[142] In an earlier phase I clinical study, cardiovascular toxicity and hypertension were the dose-limiting toxicities, but these were later easily controlled via modification of the treatment schedule.[143] Other nonhematologic toxicities were nausea and fatigue and were moderate. Interestingly, the primary metabolite detected for cemadotin is not due to modification of the N-terminus (as with dolastatin 10) but, rather, from loss of the C-terminal benzamide group. This may constitute further evidence that the bioactive species in the case of dolastatin 15 is actually the peptide metabolite resulting from enzymolysis of the *Pro–Hiva* bond (for dolastatin 15) or *Pro*–benzamide bond (for cemadotin), as discussed in Section 11.5. Phase II results have been reported for trials involving patients with nonsmall-cell lung carcinoma and metastatic breast cancer, but no positive responses have been noted with the current dose and schedule.[144,145] Researchers at BASF have also pursued the use of cemadotin in drug combination therapies (e.g., with taxanes).[146] Although the dolastatins have yet to demonstrate clinical efficacy against cancer, it should be noted that these compounds have been studied in biological domains for a relatively short period of time, and in this regard, much of what the dolastatins may ultimately offer for the treatment of human diseases such as cancer remains to be determined.

UPDATE

D. J. Newman

This update will be brief as the original authors performed a thorough coverage of the field up through the middle of 2004. It will cover the two clinical trials that are still listed on the website http://clinicaltrials.gov using dolastatin 10 as the search parameter. It will also cover the current status of three dolastatin derivatives, cemadotin, synthadotin, and auristatin/soblidotin, with particular emphasis on the use of derivatives as "warheads" attached to monoclonal antibodies. The references in this section will continue on from number 147.

Clinical Studies Update (as on 10/2010)

Dolastatin 10

As of early October 2010, there are two clinical trials, NCT00003693 and NCT00003557 still ongoing from November 1999 but not recruiting new patients, where dolastatin 10 is being tested as a single agent. In the 3693 trial, it is being studied at M. D. Anderson as a treatment for various leukemias in a phase I study, and in the 3557 trial, against liver-related carcinomas in a phase II study at the University of Chicago. There have been no updates nor publications related to these trials and the last update listed on the Clinicaltrials website was in July 2008.

Cemadotin

As mentioned in the first edition, this compound (**38**) entered phase II trials but as far as can be found, the clinical development of this compound appears to have ceased. There are no records showing any ongoing or completed trials in the Clinicaltrials website and the only clinical reports are those referred to in the first edition with the final ones being that of Marks et al.[144] and Kerbat et al.[145]

Synthadotin (ILX-651; LU-223651)

As in the case of auristatin/soblidotin which is dealt with next, this compound (**69**; Figure 11.11) has also had a chequered career as companies were brought and sold in recent years. This agent was orally active and advanced to phase II trials against a variety of cancers initially under Ilex and then under Genzyme following their purchase of Ilex. Currently however, those trials have ceased and it

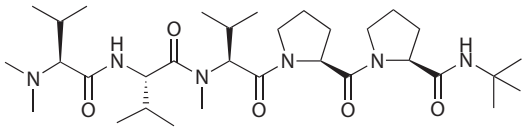

Synthadotin/tasidotin/ILX-651 (**69**)

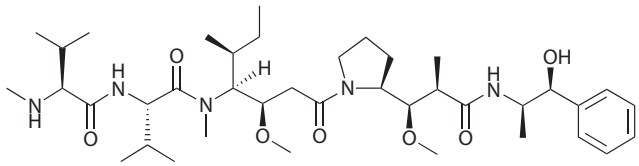

Vedotin/monomethylauristatin E (**70**)

FIGURE 11.11 Synthadotin and vedotin.

is currently at the preclinical level in the United States under Genzyme's auspices, and in the middle of 2008 they reported that it will be investigated as an orally administered antineoplastic agent for patients with advanced, refractory neoplasms based on new preclinical data.

The clinical trials website currently shows three completed phase II trials for this agent under the ILX651 identifier. They are NCT00068211 versus melanoma, NCT00082134 versus hormone-refractory prostate cancer, and NCT00078455 versus non-small-cell lung cancer, but no publications related to these trials have yet been published. What is of interest, however, is the 2007 paper by Ray et al.[147] demonstrating that this compound might in fact be a relatively weak prodrug for the functionally active tasidotin C-carboxylate which is 10–30 times more potent in an *in vitro* assay of purified microtubule dynamics. It will be interesting to see if this finding leads to further work with this molecule or its metabolites/derivatives in due course.

Auristatin PE (Soblidotin, TZT-1027, YHI-201)

As mentioned in the first edition, soblidotin (**37**) was in a number of clinical trials at the phase I and phase II levels. In the Clinicaltrials database, three trials are shown. One was a phase I trial (NCT00072228) against solid tumors that was never started, and the other two were phase II trials that were completed. The first of these (NCT00064220) was against sarcoma with a report published in 2006 demonstrating no confirmed responses,[148] and the second (NCT00061854) was against non small-cell lung cancer. Although the website lists no publications from the latter trial, there was a report from Memorial Sloan Kettering (one of the clinical groups cited as being a study participant) in 2007 that showed no objective responses.[149]

However, demonstrating how compounds that exhibit interesting activities can be further optimized by clever chemistry and biology, the base compound with some subtle modifications such as monomethyl auristatin E (also known as vedotin; **70**; Figure 11.11) with and without a small linker, were used as warheads by Seattle Genetics. Variations differing in the antibody and the specific linker are currently in phase III (brentuximab vedotin; SGN-35), phase II (glembatumumab vedotin; CDX-011), and phase I (PSMA-ADC; MEDI-547 and MN-immunoconjugate) trials, with another (anti-CD19-vcMMAE) in preclinical trials. Using another auristatin PE derivative, auristatin F (where the C-terminal amino acid is now phenylalanine), another monoclonal antibody-warhead combination (1F6-MMAF; SGN-75) is currently in phase I clinical trials and unlike the other two, it does not have a cleavable linker.

Up-to-date reviews and reports of the rationale behind the use of such methods by current leaders in the field, covering the types of "warhead molecules," whether linkers should be cleavable or noncleavable, level of warhead loadings, and so on have flourished in the last 2 or 3 years, and should be consulted by readers who wish to further investigate the utility of these varied approaches.[150–157]

Final Comments

Thus, at this time, although dolastatins and their synthetic chemical analogs appear not to be viable entities as single agent therapies, their lineal descendents, in a chemical sense, the auristatins, are showing significant promise as "warheads" when linked in specific ways to monoclonal antibodies. That this is a feasible route to utilize the exquisite activities of antitumor natural products and overcome to a significant extent, the lack of water solubility of the molecules is now becoming evident with the submission in September 2010 of the herceptin-linked maytansinoid (see Chapter 17 update) for approval by the FDA.[158]

REFERENCES

1. Scheuer, P. J. Ed., *Chemistry of marine natural products*, Academic Press, New York, Vols. I and II, 1973; Vol. III 1980; Vol. IV, 1981; Vol. V. 1983.
2. Faulkner, D. J., Marine natural products, *Nat. Prod. Rep.*, 12, 223, 1995.

3. Roberts, M., Comprising a familiar account of their classification, instincts, and habits, and of their growth and distinguishing characters of their shells, in: *A Popular History of the Mollusca*. Reeve & Benham, London, 1851.
4. Paul, V. J. and Pennings, S. C., Diet-derived chemical defenses in the sea hare *Stylocheilus longicauda* (Quoy and Gaimard 1824), *J. Expl. Mar. Biol. Ecol.*, 151, 227, 1991.
5. Pennings, S. C., Nadeau, M. T., and Paul, V. J., Selectivity and growth of the generalist herbivore *Dolabella auricularia* feeding upon complementary resources, *Ecology*, 74, 879, 1993.
6. Pennings, S. C. and Paul, V. J., Sequestration of dietary secondary metabolites by three species of sea hares: Location, specificity and dynamics, *Mar. Biol.*, 117, 535, 1993.
7. De Nys, R., Steinberg, P. D., Rogers, C. N., Charlton, T. S., and Duncan, M. W., Quantitative variation of secondary metabolites in the sea hare *Aplysia parvula* and its host plant *Delisea pulchra*, *Mar. Ecol. Prog. Ser.*, 130, 135, 1996.
8. Faulkner, D. J., Chemical defenses of marine molluscs, in *Ecological roles of marine natural products*, Paul, V. J., Ed., Comstock Publishing Associates, Ithaca, NY, 1992, 119.
9. Pliny, in *Historica naturalis*, 60 AD, Lib. 9, Lib. 32.
10. Donati, G. and Porfirio, B., Marine pharmacology and toxicology. The dolastatins, *Conchiglia*, 16, 1984.
11. Eales, N. B., Typical british marine plants and animals, aplysia, in: *L.M.B.C. Memoirs* Hardmann, W. A. and Johnstone, J., Eds, Liverpool, England, 1921. Vol. 24.
12. Halstead, B. W., Poisonous sea hares, in *Poisonous and venemous marine animals of the world*, Government Printing Office, Washington, DC, 1965. Vol. 1, 709
13. Sorokin, M., Human poisoning by ingestion of a sea hare (*Dolabella auricularia*), *Toxicon*, 26, 1095, 1998.
14. Pettit, G. R., Day, J. F., Hartwell, J. L., and Wood, H. B., Antineoplastic components of marine animals, *Nature*, 227, 962, 1970.
15. Pettit, G. R., The dolastatins, *Fortschr. Chem. Org. Naturst.*, 70, 1, 1997.
16. Pettit, G. R., Herald, C. L., Ode, R. H., Brown, P., Gust, D. J., and Michel, C., Anti-neoplastic agents. 69. The isolation of loliolide from an Indian Ocean opisthobranch mollusk, *J. Nat. Prod.*, 43, 752, 1980.
17. Pettit, G. R., Kamano, Y., Fujii, Y., Herald, C. L., Inoue, M., Brown, P., Gust, D., et al., Anti-neoplastic agents. 72. Marine animal biosynthetic constituents for cancer chemotherapy, *J. Nat. Prod.*, 44, 482, 1981.
18. Pettit, G. R., Kamano, Y., Herald, C. L., Fujii, Y., Kizu, H., Boyd, M. R., Boettner, F. E., et al., Isolation of dolastatins 10-15 from the marine mollusc *Dolabella auricularia*, *Tetrahedron*, 49, 9151, 1993.
19. Pettit, G. R., Kamano, Y., Herald, C. L., Tuinman, A. A., Boettner, F. E., Kizu, H.,. Schmidt, J. M., Baczynskyj, L., Tomer, K. B., and Bontems, R. J., The isolation and structure of a remarkable marine animal antineoplastic constituent: Dolastatin 10, *J. Am. Chem. Soc.*, 109, 6883, 1987.
20. Pettit, G. R., Xu, J. P., Hogan, F., Williams, M. D., Doubek, D. L., Schmidt, J. M., Cerny, R. L., et al., Isolation and structure of the human cancer cell growth inhibitory cyclodepsipeptide dolastatin 16, *J. Nat. Prod.*, 60, 752, 1997.
21. Pettit, G. R., Xu, J.-P., Hogan, F., and Cerny, R. L., Antineoplastic agents. 369. Isolation and structure of dolastatin 17, *Heterocycles*, 47, 491, 1998.
22. Pettit, G. R., Xu, J-P., Williams, M. D., Hogan, F., Schmidt, J. M., and Cerny, R. L. Antineoplastic agents. 370. Isolation and structure of dolastatin 18, *Bioorg. Med. Chem. Lett*, 7, 827, 1997.
23. Davies-Coleman, M. T., Dzeha, T. M., Gray, C. A., Hess, S., Pannell, L. K., Hendricks, D. T., and Arendse, C. E., Isolation of homodolastatin 16, a new cyclic depsipeptide from a Kenyan collection of *Lyngbya majuscula*, *J. Nat. Prod.*, 66, 712, 2003.
24. Yamada, K. and Kigoshi, H., Bioactive compounds from the sea hares of two genera: *Aplysia* and *Dolabella*, *Bull. Chem. Soc. Japan*, 70, 1479, 1997.
25. Sone, H., Nemoto, T., Ojika, M., and Yamada K., Isolation, structure, and synthesis of dolastatin C, a new depsipeptide from the sea hare *Dolabella auricularia*, *Tetrahedron Lett.*, 34, 8445, 1993.
26. Sone, H., Nemoto, T., Ishiwata, H., Ojika, M., and Yamada, K., et al., Isolation, structure, and synthesis of dolastatin D, a cytotoxic cyclic depsipeptide from the sea hare *Dolabella auricularia*, *Tetrahedron Lett.*, 34, 8449, 1993.
27. Ojika, M., Nemoto, T., Nakamura, M., and Yamada, K., Dolastatin E, a new cyclic hexapeptide isolated from the sea hare *Dolabella auricularia*, *Tetrahedron Lett.*, 36, 5057, 1995.
28. Nakamura, M., Shibata, T., Nakane, K., Nemoto, T., Ojika, M., and Yamada, K., Stereochemistry and total synthesis of dolastatin E, *Tetrahedron Lett.*, 36, 5059, 1995.

29. Mutou, T., Kondo, T., Ojika, M., and Yamada, K., Isolation and stereostructures of dolastatin G and nordolastatin G, cytotoxic 35-membered cyclodepsipeptides from the Japanese sea hare *Dolabella auricularia*, *J. Org. Chem.*, 61, 6340, 1996.
30. Mutou, T., Kondo, T., Shibata, T., Ojika, M., Kigoshi, H., and Yamada, K., Synthesis of dolastatin G and nordolastatin G, cytotoxic 35-membered cyclodepsipeptides of marine origin, *Tetrahedron Lett.*, 37, 7299, 1996.
31. Sone, H., Shibata, T., Fujita, T., Ojika, M., and Yamada, K., Dolastatin H and isodolastatin H, potent cytotoxic peptides from the sea hare *Dolabella auricularia*: isolation, stereo structures, and synthesis, *J. Am. Chem. Soc.*, 118, 1874, 1996.
32. Sone, H., Kigoshi, H., and Yamada, K., Isolation and stereostructure of dolastatin I, a cytotoxic cyclic hexapeptide from the Japanese sea hare *Dolabella auricularia*, *Tetrahedron*, 53, 8149, 1997.
33. Suenaga, K., Tsuyoshi Mutou, T., Takunobu Shibata, T., Takashi Itoh, T., Hideo Kigoshi, H., and Kiyoyuki Yamada, K., Isolation and stereostructure of aurilide, a novel cyclodepsipeptide from the Japanese sea hare I, *Tetrahedron Lett.*, 37, 6771, 1996.
34. Mutou, T., Suenaga, K., Fujita, T., Itoh, T., Takada, N., Hayamizu, K., Kigoshi, H., and Yamada, K., Enantioselective synthesis of aurilide, a cytotoxic 26-membered cyclodepsipeptide of marine origin, *Synlett*, 199, 1997.
35. Sone, H., Kondo, T., Kiryu, M., Ishiwata, H., Ojika, M., and Yamada, K., Dolabellin, a cytotoxic bisthiazole metabolite from the sea hare *Dolabella auricularia*: Structural determination and synthesis, *J. Org. Chem.*, 60, 4774, 1995.
36. Ishiwata, H., Nemoto, T., Ojika, M., and Yamada, K., Isolation and stereostructure of doliculide, a cytotoxic cyclodepsipeptide from the Japanese sea hare *Dolabella auricularia*, *J. Org. Chem.*, 59, 4710, 1994.
37. Ojika, M., Nemoto, T., and Yamada, K., Doliculol-A and doliculol-B, the nonhalogenated C-15 acetogenins with cyclic ether from the sea hare *Dolabella-auricularia*, *Tetrahedron Lett.*, 34, 3461, 1993.
38. Faulkner, D. J., Marine natural-products—metabolites of marine-algae and herbivorous marine mollusks, *Nat. Prod. Rep.*, 1, 251, 1984.
39. Fattorusso, E. and Piattelli, M., Amino acids from marine algae, in: *Marine Natural Products, Chemical and Biological Perspectives*, Scheuer, P. J., Ed., Academic Press, New York, 1980, Vol. III, 95.
40. Mitchell, S. S., Faulkner, D. J., Rubins, K., and Bushman, F. D., Dolastatin 3 and two novel cyclic peptides from a Palauan collection of *Lyngbya majuscula*, *J. Nat. Prod.*, 63, 279, 2000.
41. Luesch, H., Moore, R. E., Paul, V. J., Mooberry, S. L., and Corbett, T. H., Isolation of dolastatin 10 from the marine cyanobacterium *Symploca* species VP642 and total stereochemistry and biological evaluation of its analogue symplostatin 1, *J. Nat. Prod.*, 64, 907, 2001.
42. Harrigan, G. G., Yoshida, W. Y., Moore, R. E., Nagle, D. G., Park, P. U., Biggs, J., Paul, V. J., Mooberry, S. L., Corbett, T. H., and Valeriote, F. A., Isolation, structure determination, and biological activity of dolastatin 12 and lyngbyastatin I from *Lyngbya majuscula Schizothrix calcicola* cyanobacterial assemblages, *J. Nat. Prod.*, 61, 1221, 1998.
43. Nogle, L. M., Williamson, R. T., and Gerwick, W. H., Somamides A and B, two new depsipeptide analogues of dolastatin 13 from a Fijian cyanobacterial assemblage of *Lyngbya majuscula* and *Schizothrix* species, *J. Nat. Prod.*, 64, 716, 2001.
44. Nogle, L. M. and Gerwick, W. H., Isolation of four new cyclic depsipeptides, antanapeptins A-D, and dolastatin 16 from a Madagascan collection of *Lyngbya majuscula*, *J. Nat. Prod.*, 65, 21, 2002.
45. Harrigan, G. G., Luesch, H., Yoshida, W. Y., Moore, R. E., Nagle, Paul, V. J., Mooberry, S. L., Corbett, T. H. and Valeriote, F. A., Symplostatin 1: a dolastatin 10 analogue from the marine cyanobacterium *Symploca hydnoides*, *J. Nat. Prod.*, 61, 1075, 1998.
46. Harrigan, G. G. et al., Symplostatin 2: a dolastatin 13 analogue from the marine cyanobacterium *Symploca hydnoides*, *J. Nat. Prod.*, 62, 655, 1999.
47. Luesch, H., Yoshida, W. Y., Moore, R. E., Paul, V. J., Mooberry, S. L., and Corbett, T. H., Symplostatin 3, a new dolastatin 10 analogue from the marine cyanobacterium *Symploca* sp VP452, *J. Nat. Prod.*, 65, 16, 2002.
48. Luesch, H., Harrigan, G. G., Goetz, G., and Horgen, F. D., The cyanobacterial origin of potent anticancer agents originally isolated from sea hares, *Curr. Med. Chem.*, 9, 1791, 2002.
49. Schmidt, U., Utz, R., Lieberknecht, A., Griesser, H., Potzolli, B., Bahr, J.,Wagner, K., and Fischer, P., Amino acids and peptides; 60. Synthesis of biologically active cyclopeptides; 10. Synthesis of 16 structural isomers of dolastatin 3; ii: synthesis of the linear educts and the cyclopeptides, *Synthesis*, 236, 1987.
50. Hamada, Y., Kato, S., and Shioiri, T., New methods and reagents in organic-synthesis 51. A synthesis of ascidiacyclamide, a cyto-toxic cyclic peptide from ascidian—determination of its absolute-configuration, *Tetrahedron Lett.*, 26, 3223, 1985.

51. Arai, H., Hagmann, W. K., Suguna, H., and Hecht, S. M., Synthesis of the pyrimidine moieties of bleomycin and epibleomycin, *J. Am. Chem. Soc.*, 102, 6631, 1980.
52. Bodanszky, M., Scozzie, J. A., and Muramatsu, I., Dehydroalanine residues in thiostrepton, *J. Antibiot.*, 23, 9, 1970.
53. Pettit, G. R., Kamano, K., Holzapfel, C. W., Van Zyl, W. J., Tuinman, A. A., Herald, C. L., Baczynskyj, L., and Schmidt, J. M., et al., Antineoplastic agents. 150. The structure and synthesis of dolastatin-3, *J. Am. Chem. Soc.*, 109, 7581, 1987.
54. Schmidt, U. and Utz, R., Synthetic studies on the elucidation of the structure and configuration of dolastatin 3, *Angew. Chem. Int. Ed. Eng.*, 23, 725, 1984.
55. Hamada, Y., Kohda, K., and Shioiri, T., Proposed structure of the cyclic peptide dolastatin-3, a powerful cell-growth inhibitor, should be revised, *Tetrahedron Lett.*, 25, 5303, 1984.
56. Holzapfel, C. W. and Van Zyl, W. J., The synthesis and conformation in solution of cyclo[l-pro-l-leu-(gln) thz-(gly)thz-l-val] (dolastatin 3), *Tetrahedron*, 46, 649, 1990.
57. Rinehart, Jr., K. L., Cook, Jr., J. C., Pandey, R. C., Gaudioso, L. A., Meng, H., Moore, M. L., Gloer, J. B., et al., Biologically-active peptides and their mass-spectra, *Pure Appl. Chem.*, 54, 2409, 1982.
58. Pettit, G. R., Dolastatin 10, *Fortschr. Chem. Org. Naturst.*, 70, 14, 1997.
59. Pettit, G. R., Singh, S. B., Hogan, F., Lloyd-Williams, P., Herald, D. L., Burkett, D. D., and Clewlow, P. J., Antineoplastic agents. 189. The absolute-configuration and synthesis of natural (-)-dolastatin-10, *J. Am. Chem. Soc.*, 111, 5463, 1989.
60. Hamada, Y., Hayashi, K., and Shioiri, T., Efficient stereoselective synthesis of dolastatin-10, an antineoplastic peptide from a sea hare, *Tetrahedron Lett.*, 32, 931, 1991.
61. Shioiri, T., Hayashi, K., and Hamada, Y., Stereoselective synthesis of dolastatin 10 and its congeners, *Tetrahedron*, 49, 1913, 1993.
62. Tomioka, K., Kamai, M., and Koga, K., An expeditious synthesis of dolastatin-10, *Tetrahedron Lett.*, 32, 2395, 1991.
63. Roux, F., Maugras, I., Poncet, J., Niel, G., and Jouin, P., Synthesis of dolastatin-10 and [r-doe]-dolastatin-10, *Tetrahedron*, 50, 5345, 1994.
64. Pettit, G. R., Kamano, Y., Kizu, H., Dufresne, C., Herald, C. L., Bontems, R. J., Schmidt, J. M., Boettner, F. E., and Nieman, R. A., Antineoplastic agents. 173. Isolation and structure of the cell growth inhibitory depsipeptides dolastatins 11 and 12, *Heterocycles*, 28, 553, 1989.
65. Bates, R. B. and Gangwar, S., Asymmetric syntheses of 3-amino-2-methylpentanoic acids. Configurations of the beta-amino acid in majusculamide C, 57-normajusculamide C and dolastatins 11 and 12, *Tetrahedron Asymm.*, 4, 69, 1993.
66. Bates, R. B., Brusoe, K. G., Burns, J. J., Caldera, S., Cui, W., Gangwar, S., Gramme, M. R., et al., Dolastatins. 26. Synthesis and stereochemistry of dolastatin 11, *J. Am. Chem Soc.*, 119, 2111, 1997.
67. Carter, D. C., Moore, R. E., Mynderse, J. S., Niemczura, W. P., and Todd, J. S., Structure of majusculamide-C, a cyclic depsipeptide from lyngbya-majuscula, *J. Org. Chem.*, 49, 236, 1984.
68. Mynderse, J. S., Hunt, A. H., and Moore, R. E., 57-normajusculamide-C, a minor cyclic depsipeptide isolated from *Lyngbya majuscula*, *J. Nat. Prod.*, 51, 1299, 1988.
69. Pettit, G. R., Kamano, Y., Herald, C. L., Dufresne, C., Cerny, R. L., Herald, D. L., Schmidt, J. M., and Kizu, H., Antineoplastic agents. 174. Isolation and structure of the cytostatic depsipeptide dolastatin 13 from the sea hare *Dolabella auricularia*, *J. Am. Chem. Soc.*, 111, 5015, 1989.
70. Sih, C. J., Gu, R. L., Grich H. Z., and Brieva, R., Biocatalytic methods for enantioselective synthesis, in: *Stereocontrolled Organic Synthesis*. Trost, B. M., ed., Blackwell Science Publ., 1994, p. 399.
71. Moune, S., Niel, G., Busquet, M., Eggleston, I., and Jouin P., Total synthesis of dolatrienoic acid: A subunit of dolastatin 14, *J. Org. Chem.*, 62, 3332, 1997.
72. Duffield, J. J. and Pettit, G. R., Synthesis of (7s,15s)- and (7r,15s)-dolatrienoic acid, *J. Nat. Prod.*, 64, 472 2001.
73. Pettit, G. R., Herald, D. L., Singh, S. B., Thornton, T. J., and Mullaney, J. T., Antineoplastic agents. 220. Synthesis of natural (-)-dolastatin 15, *J. Am. Chem. Soc.*, 113, 6692, 1991.
74. Patino, N., Frérot, E., Galeotti, N., Poncet, J., Coste, J., Dufour, M.-N., and Jouin, P., Total synthesis of the proposed structure of dolastatin-15, *Tetrahedron*, 48, 4115, 1992.
75. Pettit, G. R., Thornton, T. J., Mullaney, J. T., Boyd, M. R., Herald, D. L., Singh, S-B., and Flahive, E. J., The dolastatins-20 — a convenient synthetic route to dolastatin-15, *Tetrahedron*, 50, 12097, 1994.
76. Akaji, K., Hayashi, Y., Kiso, Y., and Kuriyama, N., Convergent synthesis of dolastatin 15 by solid phase coupling of N-methylamino acid, *Peptide Science*, 35, 9, 1999.

77. Pettit, G. R., Structural modifications of dolastatin 10, *Fortschr. Chem. Org. Naturst.*, 70, 42, 1997.
78. Pettit, G. R., Hogan, F., and Herald, D. L., Synthesis and x-ray crystal structure of the *Dolabella auricularia* peptide dolastatin 18, *J. Org Chem.*, 69, 4019, 2004.
79. Poncet, J., The dolastatins, a family of promising antineoplastic agents, *Current Pharm Design*, 5, 139, 1999.
80. Aherne, G. W., Hardcastle, A., Valenti, M., Bryant, A., Rogers, P., Pettit, G. R., Srirangam, J. K., and Kelland, L. R., Antitumour evaluation of dolastatins 10 and 15 and their measurement in plasma by radioimmunoassay, *Cancer Chemother. Pharmacol.*, 38, 225, 1996.
81. Pietra, F., A secret world, in: *The Natural Products of Marine Life*, Basel, Switzerland, 1990, 39.
82. Yamazaki, M., Iijima, R., and Kosuna, K., Antibacterial and antifungal peptide from *Dolabella auricularia*, Japanese Patent JP10251297, 22 Sep. 1998.
83. Donia, M. and Hamann, M. T., Marine natural products and their potential applications as anti-infective agents, *Lancet Infect. Dis.*, 3, 338, 2003.
84. Fennell, B. J., Carolan, S., Pettit, G. R., and Bell, A., Effects of the antimitotic natural product dolastatin 10, and related peptides, on the human malarial parasite *Plasmodium falciparum*, *J. Antimicrobial Chemother.*, 51, 833, 2003.
85. Hamel, E., Interaction of tubulin with small ligands, in: *Microtubule Proteins*, Avila, J., Ed., CRC Press, Boca Raton, FL, 1990, 89.
86. Bai, R., Pettit, G. R., and Hamel, E., Structure activity studies with chiral isomers and with segments of the antimitotic marine peptide dolastatin-10, *Biochem. Pharmacol.*, 40, 1859, 1990.
87. Bai, R., Pettit, G. R., and Hamel, E., Binding of dolastatin-10 to tubulin at a distinct site for peptide antimitotic agents near the exchangeable nucleotide and vinca alkaloid sites, *J. Biol. Chem.*, 265, 17141, 1990.
88. Quentmeier, H., Brauer, S., Pettit, G. R., and Drexler, H. G., Cytostatic effects of dolastatin 10 and dolastatin 15 on human leukemia cancer cell lines, *Leukemia Lymphoma*, 6, 245, 1992.
89. Steube, K. G., Quentmeier, H., Pettit, G. R., Pietsch, T., Brauer, S., Grunicke, D., Gignac, S., and Drexler, H., Inhibition of cellular proliferation by the natural peptides dolastatin 10 and dolastatin 15, *Mol. Biol. Haematapoiesis*, 2, 567, 1992.
90. Steube, K. G., Grunicke, D., Pietsch, T., Gignac, S. M., Pettit, G. R., and Drexler, H. G., Dolastatin 10 and dolastatin 15: Effect of two natural peptides on growth and differentiation of leukemia cells, *Leukemia*, 6, 1048, 1992.
91. Hu, Z.-B., Gignac, S. M., Quentmeier, H., Pettit, G. R., and Drexler, H. G., Effects of dolastatins on human B-lymphocytic leukemia cell lines, *Leukemia Res.*, 17, 333, 1993.
92. Mohammad, R. M., Varterasian, M. L., Almatchy, V. P., Hannoudi, G. N., Pettit, G. R., and Al-Katib, A., Successful treatment of human chronic lymphocytic leukemia xenografts with combination biological agents auristatin PE and bryostatin 1, *Clin. Cancer Res.*, 4, 1337, 1998.
93. Beckwith, M., Urba, W. J., and Longo, D. L., Growth inhibition of human lymphoma cell lines by the marine natural products dolastatins 10 and 15, *J. Natl. Cancer Inst.*, 85, 483, 1993.
94. Maki, A., Mohammad, R. M., Raza, S., Saleh, M., Govindaraju, K. D., Pettit, G. R., and Al-Katib, A., Effect of dolastatin 10 on human non-Hodgkin's lymphoma cell lines, *Anti-Cancer Drugs*, 7, 344, 1996.
95. Mohammad, R. M., Pettit, G. R., Almatchy, V. P., Wall, N., Varterasian, M. L., and Al-Katib, A., Synergistic interaction of selected marine animal anticancer drugs against human diffuse large cell lymphoma, *Anti-Cancer Drugs*, 9, 149, 1998.
96. Turner, T., Jackson, W. H., Pettit, G. R., Wells, A., and Kraft, A. S.,Treatment of human prostate cancer cells with dolastatin 10, a peptide isolated from a marine shell-less mollusc, *Prostate*, 34, 175, 1998.
97. Hamel, E., Natural products which interact with tubulin in the vinca domain: Maytansine, rhizoxin, phomopsin a, dolastatins 10 and 15 and halichondrin B, *Pharmacol. Ther.*, 55, 31, 1992.
98. Pettit, G. R., Singh, S. B., Hogan, F., and Burkett, D. D., Antineoplastic agents. 205. Chiral modifications of dolastatin-10—the potent cytostatic peptide (19ar)-isodolastatin-10, *J. Med. Chem.*, 33, 3132, 1990.
99. Bai, R., Friedman, S. J., Pettit, G. R., and Hamel, E., Dolastatin-15, a potent antimitotic depsipeptide derived from *Dolabella-auricularia*—interaction with tubulin and effects on cellular microtubules, *Biochem. Pharmacol.*, 43, 2637, 1992.
100. Jordan, M. A., Walker, D., de Aruda, M., Barlozzari, T., and Panda, D., Suppression of microtubule dynamics by binding of cemadotin to tubulin: possible mechanism for its antitumor action, *Biochemistry*, 37, 17571, 1998.
101. Cruz-Monserrate, Z., Mullaney, J. T., Harran, P. G., Pettit, G. R., and Hamel, E., Dolastatin 15 binds in the vinca domain of tubulin as demonstrated by Hummel-Dreyer chromatography, *Eur. J. Biochem.*, 270, 3822, 2003.

102. Haldar, S., Basu, A., and Croce, C. M., Bcl2 is the guardian of microtubule integrity, *Cancer Res.*, 57, 229, 1997.
103. Haldar, S., Basu, A., and Croce, C. M., Serine-70 is one of the critical sites for drug-induced bcl2 phosphorylation in cancer cells, *Cancer Res.*, 58, 1609, 1998.
104. Maki, A., Diwakaran, H., Redman, B., al-Asfar, S., Pettit, G. R., Mohammad, R. M., and al-Katib, A., The bcl-2 and p53 oncoproteins can be modulated by bryostatin-1 and dolastatins in human diffuse large-cell lymphoma, *Anti-Cancer Drugs*, 6, 392, 1995.
105. Ali, M. A., Rosati, R., Pettit, G. R., and Kalemkerian, G. P., Dolastatin 15 induces apoptosis and bcl-2 phosphorylation in small cell lung cancer cell lines, *Anticancer Res.*, 18, 1021, 1998.
106. Mooberry, S. L., Leal, R. M., Tinley, T. L., Luesch, H., Moore, R. E., and Corbett, T. H., The molecular pharmacology of symplostatin 1: a new antimitotic dolastatin 10 analog, *International J. Cancer*, 104, 512, 2003.
107. Watanabe, J., Natsume, T., Fujio, N., Miyasaka, K., and Kobayashi, M., Induction of apoptosis in human cancer cells by TZT-1027, an antimicrotubule agent, *Apoptosis*, 5, 345, 2000.
108. Ikeda, R., Murakoshi, M., Ohtani, M., Tagawa, M., Mikami, T., Natsume, T., Watanabe, J., Kobayashi, M., and Nakayama, T., Induction of apoptosis in mice with B16 melanoma by treatment with the antimicrotubule agent TZT-1027, *Acta Histochem. Cytochem.*, 33, 341, 2000.
109. Otani, M., Natsume, T., Watanabe, J. L., Kobayashi, M., Murakoshi, M., Mikami, T., and Nakayama, T., TZT-1027, an antimicrotubule agent, attacks tumor vasculature and induces tumor cell death, *Jpn. J. Cancer Res*, 91, 837, 2000.
110. Bai, R., Verdier-Pinard, P., Gangwar, S., Stessman, C. C., McClure, K. G., Sausville, E. A., Pettit, G. R., Bates, R. B., and Hamel, E., Dolastatin 11, a marine depsipeptide, arrests cells at cytokinesis and induces hyperpolymerization of purified actin, *Mol. Pharmacol.*, 59, 462, 2001.
111. Boyd, M. R. and Paull, K., Some practical considerations and applications of the National-Cancer-Institute *in-vitro* anticancer drug discovery screen, *Drug Dev. Res.*, 34, 91, 1995.
112. Pettit, G. R., Srirangam, J. K., Herald, D. L., and Hamel, E., The dolastatins. 21. Synthesis, x-ray crystal-structure, and molecular modeling of (6r)-isodolastatin-10, *J. Org. Chem.*, 59, 6127, 1994.
113. Pettit, G. R., Sririrangam, J. K., Barkoczy, J., Williams, M. D., Durkin, K. P., Boyd, M. R., Hamel, E., Schmidt, J. M., and Chapuis, J. C., Antineoplastic agents. 337. Synthesis of dolastatin 10 structural modifications, *Anti-Cancer Drug Design*, 10, 529, 1995.
114. Pettit, G. R., Sririrangam, J. K., Barkoczy, J., Williams, M. D., Boyd, M. R., Hamel, E., Pettit, R. K., et al., Antineoplastic agents 365. Dolastatin 10 SAR probes, *Anti-Cancer Drug Design*, 13, 243, 1998.
115. Alattia, T., Roux, F., Poncet, J., Cavé, A., and Jouin, P., Conformational study of dolastatin-10, *Tetrahedron*, 51, 2593, 1995.
116. Poncet, J., Hortala, L., Busquet, M., Guéritte-Voegelein, F., Thoret, S., Pierré, A., Atassi, G., and Jouin, P., Synthesis and antiproliferative activity of a cyclic analog of dolastatin 10, *Bioorg. Med. Chem. Lett.*, 8, 2855, 1998.
117. Poncet, J., Busquet, M., Roux, F., Pierré, A., Atassi, J., and Jouin, P., Synthesis and biological activity of chimeric structures derived from the cytotoxic natural compounds dolastatin 10 and dolastatin 15, *J. Med. Chem.*, 41, 1524, 1998.
118. Miyazaki, K., Kobayashi, M., Natsume, T., Gondo, M., and Mikami, T., Synthesis and antitumor-activity of novel dolastatin-10 analogs, *Chem. Pharm. Bull.*, 43, 1706, 1995.
119. Kobayashi, M., Natsume, T., Tamaoki, S., Watanabe, J., Asano, H., Mikami, T., Miyasaka, K., et al., Antitumor activity of TZT-1027, a novel dolastatin 10 derivative, *Jpn. J. Cancer Res.*, 88, 316, 1997.
120. Alcaro, S., Marino, T., Ortuso, F., and Russo, N., Theoretical comparison between structural and dynamical features of dolastatins 11 and 12 antineoplastic depsipeptides, *SAR QSAR Environ. Res.*, 14, 475, 2003.
121. Roux, F., Galéotti, N., Poncet, J., Jouin, P., Cros, S., and Zenke, G., Synthesis and in-vitro cytotoxicity of diastereoisomerically modified dolastatin-15 analogs, *Bioorg. Med. Chem. Lett.*, 4, 1947, 1994.
122. Pettit, G. R., Flahive, E. J., Boyd, M. R., Bai, R., Hamel, E., Pettit, R. K., and Schmidt, J. M., Antineoplastic agents 360. Synthesis and cancer cell growth inhibitory studies of dolastatin 15 structural modifications, *Anti-Cancer Drug Design*, 13, 47, 1998.
123. Flahive, E. J., The dolastatins: synthesis and structural modification of dolastatin 15, Ph.D. Dissertation, Arizona State University, Tempe, AZ, 1996.
124. De Arruda, M., Cocchiaro, C. A., Nelson, C. M., Grinnell, C. M., Janssen, B., Haupt, A, and Barlozzari, T., Lu103793 (NSC D-669356): A synthetic peptide that interacts with microtubules and inhibits mitosis, *Cancer Res.*, 55, 3085, 1995.

125. Hu, M. K. and Huang, W.-S., Synthesis and cytostatic properties of structure simplified analogues of dolastatin 15, *J. Peptide Res.*, 54, 460, 1999.
126. Schmitt, J., Bernd, M., Kutscher, B., and Kessler, H., Synthesis of dolastatin 15 mimetic peptoids, *Bioorg. Med. Chem. Lett.*, 8, 385, 1998.
127. Mirsalis, J. C., Schindler-Horvat, J., Hill, J. R., Tomaszewski, J. E., and Donahue, S. J., Toxicity of dolastatin 10 in mice, rats and dogs and its clinical relevance, *Cancer Chemother. Pharmacol.*, 44, 395, 1999.
128. Schwartsmann, G., Brondani da Rocha, A., Mattei, J., and Lopes, R. M., Marine-derived anticancer agents in clinical trials, *Exp. Opin. Investig. Drugs*, 12, 1367, 2003.
129. Madden, T., Tran, H. T., Beck, D., Huie, R., Newman, R. A., Pusztai, L., Wright, J. A., and Abbruzzese, J. L., Novel marine-derived anticancer agents: a phase I clinical, pharmacological and pharmacodynamic study of dolastatin 10, *Clinical Cancer Res.*, 6, 1293, 2000.
130. Garteiz, D. A., Madden, T., Beck, D. E., Huie, W. R., McManus, K. T., Abbruzzee, J. L., Chen, W., and Newman, R. A., Quantitation of dolastatin 10 using HPLC/electrospray ionization mass spectrometry: application in a phase I clinical trial, *Cancer Chemother. Pharmacol.*, 41, 299, 1998.
131. Vaishampayan, U., Michael, G., Du, W., Kraft, A., Hudes, G., Wright, J., and Hussain, M., Phase II study of dolastatin 10 in patients with hormone-refractory metastatic prostrate adenocarcinoma, *Clinical Cancer Res.*, 6, 4205, 2000.
132. Margolin, K., Longmate, J., Synold, T. W., Gandara, D. R., Weber, J., Gonzalez, R., Johansen, M. J., Newman, R., Baratta, T., and Doroshow, J. H., Dolastatin 10 in metastatic melanoma: a phase II and pharmacokinetic trial of the California Cancer Consortium, *Investig. New Drugs*, 19, 335, 2001.
133. Saad, E. D., Kraut, E. H., Hoff, P. M., Moore, D. F., Jones. D., Padzur, R., and Abbruzzese, J., Phase II study of dolastatin-10 as first-line treatment for advanced colorectal cancer, *Am. J.Clin. Oncol.*, 5, 451, 2002.
134. Krug, L. M., Miller, V. A., Kalemkerian, G. P., Kraut, M. J., Ng, K. K., Heelan, R. T., Pizzo, B. A., Perez, W., McClean, N., and Kris, M. G., Phase II study of dolastatin 10 in patients with non-small-cell lung carcinoma, *Ann. Oncol.*, 11, 227, 2000.
135. Hoffman, M. A., Blessing, J. A., and Lentz, S. S., A phase II trial of dolastatin 10 in recurrent platinum-sensitive ovarian carcinoma: A gynecologic oncology group study, *Gynecol. Oncol.*, 89, 95, 2003.
136. Pettit, G. R., Williams, M. D., and Srirangam, J. K., Preparation of dolastatin analog pentapeptide methyl esters as anticancer agents, *Eur. Pat. Appl*., EP 95-305130, 1995.
137. Bayés, M., Rabasseda, X., and Prous, J. R., Gateways to clinical trials, *Methods Find. Exp. Clin. Pharmacol.*, 25, 387, 2003.
138. Bayés, M., Rabasseda, X., and Prous, J. R., Gateways to clinical trials, *Methods Find. Exp. Clin. Pharmacol.*, 26, 53, 2004.
139. De Jonge, M. J. A., van der Gaast, A., Planting, A. S. T., van Doorn, L., Lems, A., Boot, I., Wanders, J., Satomi, M., and Verweij, J., Phase I and pharmacokinetic study of the dolastatin 10 analogue TZT-1027, given on days 1 and 8 of a 3-week cycle in patients with advanced solid tumors, *Clin. Cancer Res*., 11, 3806, 2005.
140. Horti, J., Juhasz, E., and Bodrogi, I., Preliminary results of a phase I trial of TZT-1027, an inhibitor of tubulin polymerization, in patients with advanced non-small cell lung carcinoma, *Proc. Am. Assoc. Cancer Res.*, 43, 2744 (Abs.), 2002.
141. Horti, J., Juhasz, E., and Bodrogi, I., A phase I trial of TZT-1027, an inhibitor of tubulin polymerization, in patients with advanced non-small cell lung cancer (NSCLC), *Proc AACR-NCI-EORTC International Conference on Molecular Targets and CancerTherapeutics*, A255 (Abs.), 2003.
142. Supko, J. G., Lynch, T. J., Clark, J. W., Fram, R., Allen, L. F., Velagapudi, R., Kufe, D. W., and Eder, J. P. Jr., A phase I clinical and pharmacokinetic study of the dolastatin analogue cemadotin administered as a 5-day continuous intravenous infusion, *Cancer Chemother. Pharmacol.*, 46, 319, 2000.
143. Mross, K., Berdel, W. E., and Fiebig, H. H., Phase I clinical and pharmacokinetic study of lu103793 (cemadotin hydrochloride) as an intravenous bolus injection in patients with metastatic solid tumors, *Onkologie*, 19, 405, 1996.
144. Marks, R. S., Graham, D. L., Slaon, J. A., Hillman, S., Fishkoff, S., Krook, J. E., Okuno, S. H., Mailliard, J. A., Fitch, T. R., and Addo, F., A phase II study of the dolastatin 15 analogue lu103793 in the treatment of advanced non-small cell lung cancer, *Am. J. Clin. Oncol.*, 26, 336, 2003.
145. Kerbrat, P., Dieras, V., Pavlidis, N., Ravaud, A., Wanders, J., and Fumoleau, P., Phase II study of LU103793 (dolastatin analogue) in patients with metastatic breast cancer, *Eur. J. Cancer*, 39, 317, 2003.
146. Barlozzari, T. and Haupt, A., Dolastatin-15 derivatives in combination with taxanes, U.S. Patent 6,103, 618, 15 AUG 2000.

147. Ray, A., Okouneva, T., Manna, T., Miller, H. P., Schmid, S., Arthaud, L., Luduena, R., Jordan, M. A., and Wilson, L., Mechanism of action of the microtubule-targeted antimitotic depsipeptide tasidotin (formerly ILX651) and its major metabolite tasidotin C-carboxylate., *Cancer Res.*, 67, 3767, 2007.
148. Patel, S., Keohan, M. L., Saif, M. W., Rushing, D., Baez, L., Feit, K., DeJager, R., and Anderson, S., Phase II study of intravenous TZT-1027 in patients with advanced or metastatic soft-tissue sarcomas with prior exposure to anthracycline-based chemotherapy, *Cancer*, 107, 2881, 2006.
149. Riely, G. J., Gadgeel, S., Rothman, I., Saidman, B., Sabbath, K., Feit, K., Kris, M. G., and Rizvi, N. A., A phase 2 study of TZT-1027, administered weekly to patients with advanced non-small cell lung cancer following treatment with platinum-based chemotherapy, *Lung Cancer*, 55, 181, 2007.
150. Carter, P. J. and Senter, P. D., Antibody-drug conjugates for cancer therapy, *Cancer J.*, 14, 154, 2008.
151. Senter, P. D., Potent antibody drug conjugates for cancer therapy, *Curr. Opin. Chem. Biol.*, 13, 235, 2009.
152. Teicher, B. A., Antibody-drug conjugate targets, *Curr. Can. Drug Targs.*, 9, 982, 2009.
153. Alley, S. C., Okeley, N. M., and Senter, P. D., Antibody-drug conjugates: targeted drug delivery for cancer, *Curr. Opin. Chem. Biol.*, 14, 529, 2010.
154. Gu, J. and Ghayur, T., Rationale and development of multispecific antibody drugs, *Expert Rev. Clin. Pharmacol.*, 3, 491, 2010.
155. Hughes, B., Antibody-drug conjugates for cancer: poised to deliver? *Nat. Rev. Drug. Discov.*, 9, 665, 2010.
156. Lambert, J. M., Antibody-maytansinoid conjugates: A new strategy for the trreatment of cancer, *Drugs Fut.* 35, 471, 2010.
157. Monneret, C., Impact actuel des produits naturels sur la decoverte de nouveaux medicaments anticancereux, *Annal. Pharm.Francaises*, 68, 218, 2010
158. Niculescu-Duvaz, I., Trazuzumab emastine, an antibody-drug conjugate for the treatment of HER2+ metastatic breast cancer, *Curr. Opin. Mol. Therap.*, 12, 350, 2010.

12 Ecteinascidin-743 (Yondelis®), Aplidin®, and Irvalec®

Carmen Cuevas, Andrés Francesch, Carlos M. Galmarini, Pablo Avilés, and Simon Munt

CONTENTS

12.1 Introduction 291
12.2 Ecteinascidin-743 (Yondelis) 292
12.2.1 Background 292
12.2.2 Mechanism of Action 292
12.2.3 Preclinical Drug Development 294
12.2.3.1 *In Vitro* and *In Vivo* Testing 294
12.2.3.2 Preclinical Toxicology 294
12.2.4 Chemical Synthesis 296
12.2.4.1 Synthetic Routes to ET-743 (Yondelis) 296
12.2.5 Clinical Studies 297
12.2.5.1 Yondelis in STS 297
12.2.5.2 Yondelis in Ovarian Cancer 299
12.2.5.3 Safety Profile 300
12.3 Aplidin 300
12.3.1 Background 300
12.3.2 Mechanism of Action 301
12.3.3 Preclinical Drug Development 302
12.3.3.1 *In Vitro* and *In Vivo* Testing 302
12.3.3.2 Preclinical Toxicology 302
12.3.4 Chemical Synthesis 304
12.3.5 Clinical Studies 304
12.4 Irvalec 306
12.4.1 Background 306
12.4.2 Mechanism of Action 306
12.4.3 Preclinical Drug Development 307
12.4.3.1 *In Vitro* and *In Vivo* Testing 307
12.4.3.2 Preclinical Toxicology 307
12.4.4 Chemical Synthesis 308
12.4.5 Clinical Studies 310
References 310

12.1 INTRODUCTION

The natural world, both terrestrial and marine, is a varied and bountiful source for new drugs. Yet until recently only natural products from terrestrial sources have been developed into, or have formed the basis for, modern medicines. The advent of more sophisticated and efficient means to

collect marine organisms over the last few decades has allowed marine biologists, natural products chemists, and medicinal scientists from academia and the pharmaceutical industry to collaborate in unique and enterprising ways to sample the great variety and bounty of intertidal, shallow, and deep-water sea life in the world. Recently, these efforts have resulted in the development of a first generation of drugs from the sea into clinical trials that includes the PharmaMar compounds, Yondelis®, Aplidin®, and Irvalec®.

12.2 ECTEINASCIDIN-743 (YONDELIS)

12.2.1 Background

Yondelis is the first marine anticancer agent approved in the European Union for patients with soft tissue sarcoma (STS) and for the treatment of relapsed ovarian cancer. The antiproliferative properties of the colonial ascidian *Ecteinascidia turbinata* which contains Ecteinascidin-743 (ET-743) were first demonstrated when a crude extract was reported to possess impressive antitumor activity in 1969. *Ecteinascidia turbinata* Herdman (1880; family: Perophoridae) is a colonial ascidian (tunicate) species from the Caribbean and the Mediterranean that belongs to the class Ascidiacea within the subphylum Tunicata (also called Urochordata). Ascidians, or sea squirts, are small, bottom-dwelling soft-bodied marine animals that form colonies comprising many individuals, called zooids. The name tunicate is derived from their characteristic protective covering, or tunic, which functions to a certain extent as an external skeleton and consists of some cells, blood vessels, and a secretion of a variety of proteins and carbohydrates, including tunicin, a cellulose-like polymer—an unusual finding in animals. Within the tunic is the muscular body wall, which controls the opening of the siphons used for feeding. Colonies are formed by asexual reproduction through budding; that is, outgrowths on the parent break off as new individuals. Sexual reproduction, in contrast, leads to a fertilized egg that develops into a free-swimming tadpole larva. The larval stage is brief and is used to find an appropriate place for the adult to live. In 1969, early assays with crude aqueous ethanol extracts of *E. turbinata* showed impressive *in vitro* cytotoxicity against a variety of cancer cell lines. Many unsuccessful attempts at isolation of the active compounds were followed by concerted efforts that led to the characterization of six alkaloids called ecteinascidins 729, 743, 745, 759A, 759B, and 770 by Kenneth Rinehart and his coworkers from the University of Illinois, Urbana-Champaign, of which ET-743 was the most abundant (0.0001% yield; Figure 12.1).[1]

ET-743 (molecular formula: $C_{39}H_{43}N_3O_{11}S$; molecular weight: 761.84u) which has the international nonproprietary name of trabectedin, is being developed under the trademark name of Yondelis, and the full chemical name of [6R-(6α,6aβ,7β,13β,14β,16 α,20R*)]-5-(acetyloxy)-3′,4′,6,6a,7,13,14,16-octahydro-6′,8,14-trihydroxy-7?,9-dimethoxy-4,10,23-trimethyl-spiro[6,16-(epithiopropanoxymethano)-7,13-imino-12H-1,3-dioxolo[7,8]-isoquino[3,2-b][3]benzazocine-20,1(2H)-isoquinolin]-19-one. It is an off-white amorphous powder, hydrophobic, and very soluble in methanol, ethanol, chloroform, ethyl acetate, and acetone.

The novel and unique chemical structure of ecteinascidins is formed by a monobridged pentacyclic skeleton composed of two fused tetrahydroisoquinoline rings linked to a 10-membered lactone bridge through a benzylic sulfide linkage. Most ecteinascidins have an additional tetrahydroisoquinoline ring or tetrahydro-β-carboline attached to the rest of the structure through a spiro ring. This is one of the features distinguishing these molecules from saframycins, safracins, and renieramycins,[2] compounds isolated from bacterial sources and sponges.

12.2.2 Mechanism of Action

In contrast to traditional alkylating agents which bind guanine at the N7 or O6 position in the DNA major groove, ET-743 binds to the exocyclic 2-amino group of guanines in the DNA minor groove through an iminium intermediate generated *in situ* by dehydration of the carbinolamine moiety

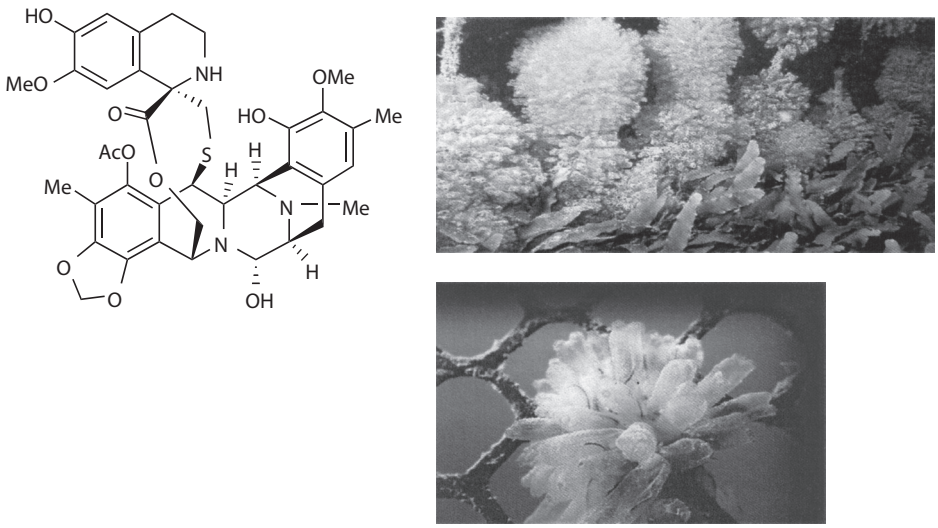

FIGURE 12.1 (**See color insert.**) Structure of ET-743 (Yondelis) and source organism, *Ecteinascidia turbinata*.

present in the monobridge pentacycle skeleton linked to a 10-membered lactone bridge. The carbinolamine moiety is imperative for the pharmacological activity of ET-743, as related compounds without this reactive group (e.g., ET-745) were 100 times less active than trabectedin. The resulting adduct is additionally stabilized through van der Waals interactions and one or more hydrogen bonds between the monobridge pentacycle skeleton with neighboring nucleotides in the same or opposite strand of the DNA double helix, thus creating the equivalent to a functional interstrand crosslink. This type of DNA damage is known to be highly effective in blocking replication and transcription, in forming double-stranded DNA (dsDNA) breaks and in inducing an apoptotic cell death type.[3,4]

The additional tetrahydroisoquinoline ring apparently does not participate in DNA binding and it was proposed to protrude out of the DNA being able to interact with xeroderma pigmentosum complementation group G (XPG) endonuclease, a member of the nucleotide excision repair (NER) system. Molecular modeling studies based on results obtained in Rad13 (ortholog to human XPG) mutants of *Schizosaccharomyces pombe* suggested that the additional tetrahydroisoquinoline forms a hydrogen bond with an arginine residue (Arg961) located in a 46-amino acid region of Rad13.[5] The formation of this Rad13–DNA–trabectedin ternary complex would then induce dsDNA breaks resulting in cell death. The observation that NER-deficient cells are 2–10 times less sensitive to trabectedin is very peculiar for this compound.[6–9] At the clinical level, previous data obtained in sarcoma patients treated with trabectedin showed that high levels of XPG mRNA expression are associated with a better clinical outcome supporting a possible role of XPG as a molecular marker of trabectedin activity.[10]

Structural changes to the DNA caused by trabectedin might also hinder the recognition of transcription factors to specific GC-enriched DNA consensus sequences.[11] Although the binding properties of some transcription factors are unaffected (e.g., MAF, MYB, and MYC), a concentration-dependent inhibition was reported for TBP, E2F, and SRF (10–30 μM), and for the CCAAT box factor NF-Y (50–300 μM). At the cellular level, trabectedin affects the transcription of activated genes.[12] Moreover, trabectedin is apparently blocking the trans-activating ability of chimeric proteins such as FUS-CHOP or EWS1-Fli1 modulating the transcription of genes that should be crucial for tumorigenesis in specific cancer subtypes.[13,14]

12.2.3 Preclinical Drug Development

12.2.3.1 *In Vitro* and *In Vivo* Testing

Preclinical data generated during the development of ET-743 have provided important insight for the selection and design of the clinical trials. Early *in vitro* studies carried out by PharmaMar and the National Cancer Institute (NCI) identified potent (1 pM to 10 nM) activity of ET-743 against cell line subpanels containing murine leukemias and human solid tumors, such as melanoma, breast, non-small cell lung (NSCL), and ovarian cancer. ET-743 was subsequently evaluated in a human tumor colony-forming unit (TCFU) assay derived from surgically ablated primary tumor specimens.[15] Over a range of concentrations (1 nM to 10 μM), ET-743 activity was seen against cancers of the head and neck, ovarian, mesothelioma, breast, kidney, peritoneum, NSCL, melanoma, sarcomas, and primary tumor specimens. The NCI COMPARE analysis of ET-743 (NSC648766) and the Standard Anticancer Agent Database showed significant correlation coefficients (0.962–0.876) to that of the DNA intercalators such as the anthracyclines and the morpholino compounds (NCI data).

ET-743 has been tested in a great variety and number of models against tumors of murine origin (P388 leukemia and B16 melanoma) and human xenografts (melanoma, MEXF 989; NSLC, LXFL 529; breast, MX-1 early and advanced; and ovarian, HOC 22 and HOC 18) (Table 12.1).[16–19]

Drug-resistant lines have also been tested that include melanoma (MEXF 514), NSLC (LXFL 629), and ovarian (HOC 18) tumor lines. These first efforts showed that ET-743 has a broad spectrum of antineoplastic activity, with several tumor types showing selectivity; namely, melanoma, NSCL, and ovarian carcinomas. As a further example of strong activity and long-lasting antitumor effects, the action of ET-743 on human endometrial carcinoma xenografts (HEC-1-B) results in complete regression lasting for more than 125 days. These *in vivo* findings correlate strongly with the results from *in vitro* cross-resistance studies in which ET-743 was very active against many resistant tumors and only moderately cross-resistant to several of the standard agents.[15]

The determination that STSs are more sensitive to ET-743 than other solid tumors was not predicted during the preclinical development of the drug. The finding was serendipitous and came from the prevalence of responding or stable STS patients in the clinical trials. As a result, there has been a considerable effort to confirm this finding to supplement the extensive nonclinical profile already characterized for the antineoplastic effect of ET-743 against other solid tumors. In fact, a variety of sarcomas are differentially sensitive to ET-743, showing IC_{50} potencies in the picomolar and subpicomolar range compared with the nanomolar concentrations established against non-STS solid tumors (Table 12.2).[20,21]

During its clinical development, several *in vivo* studies of ET-743 were performed in representative sarcoma tissues.[21–27] ET-743 shows a strong activity against several sarcoma types, especially chondrosarcomas, where tumor growth can be inhibited as much as 90% at relatively low doses (about 20% maximum tolerated dose [MTD] in mice) and correlates with the *in vitro* findings.[21] In contrast, the *in vivo* effects of ET-743 against some STS models, such as SW634 and UW2237 fibrosarcomas, appear to be less marked than in chondrosarcomas or osteosarcomas.[22]

12.2.3.2 Preclinical Toxicology

Early preclinical toxicology studies were independently carried out both by the NCI (Bethesda, MD)[28,29] and by PharmaMar in collaboration with the New Drug Development Office (Amsterdam). More specific nonclinical studies were performed in collaboration with Johnson & Johnson Pharmaceutical Research & Development. Acute toxicity studies in mice (CD1, MF1), rats (WISTAR, Fisher 344), dogs (beagles), and monkeys (cynomolgus) by intravenous (i.v.) administration, either as a single-bolus dose or using an intermittent five times daily ($d \times 5$) schedule, provided the safe starting dose for phase I clinical trials as 50 $\mu g/m^2$ for a single dose and 10 $\mu g/m^2$ per day for fractionated dose ($d \times 5$) schedules. Furthermore, chronic toxicity studies (three cycles) using several infusion schedules in rats (Sprague–Dawley) and monkeys (Cynomolgus) have been performed as a part of the development plan.

TABLE 12.1
***In Vivo* Antitumor Activity of ET-743 in Murine and Human Tumors**

Cancer Type (Cell Line)	Regimen	Optimal Dose (μg/kg per d)	Antitumor Effect	Tumor-Free Survivors
Leukemia i.p. P388	i.p. qd × 5	27	48% ILS	None
Melanoma				
i.p. B16	i.p. qd × 9	13.4	78% ILS	1/10 (d60)
s.c. MEXF 989[a]	i.v. q4d × 3	100	0.2% T/C	6/6 (d35)
	i.v. (qd × 3) × 2	50	1.8% T/C	none
s.c. MEXF 514[a]	i.v. q4d × 3	100	37% T/C	none
DTIC resistant	i.v. (qd × 3) × 2	50	76% T/C (inactive)	none
NSCL				
s.c. LXFL 529[a]	i.v. q4d × 3	150	0.1% T/C	3/4 (d63)
	i.v. (qd × 3) × 2	50	0.1% T/C	2/4 (d40)
s.c. LXFA 629[b]	i.v. q4d × 3	200	70% T/C (inactive)	none
Ifos resistant	i.v. qd × 3	200	90% T/(inactive)	none
Ovarian				
s.c. HOC 22	i.v. q4d × 3	200	<1.0% T/C	5/6 (d102)
	i.v. (qd × 3) × 3	100	2.0% T/C	3/5 (d102)
s.c. HOC 18	i.v. q4d × 3	200	5.8% T/C	4/8 (d100)
CDDP resistant	i.v. (qd × 3) × 2		11.8% T/C	2/6 (d100)
Breast				
s.c. MX-1 early	i.p. qd × 9	9	no activity	none
	i.p. qd × 5	18	no activity	none
	i.v. qd × 5	40	>160% growth delay	7/10
	i.v. qd × 5	60	0.1% T/C	10/10 (d47)
	i.v. q4d × 3	75	0.1% T/C	9/10 (d23)
s.c. MX-1 advanced[c]	i.v. qd × 1 (d9)	250	203% growth delay	4/10 (d58)
	i.v. qd × 5	50	224% growth delay	3/10 (d58)
	i.v. q3d × 4	41.7	161% growth delay	3/10 (d58)
s.c. G101metastatic[d]	i.v. qd × 1	250	50% (d70) delay	0/10 (d30)
Endometrial s.c. HEC-1-B[e]	i.v. q4d × 3	200	<1% T/C	3/6 (d125)
Prostate s.c. PC-3	i.v. q4d × 3	200	30% T/C	0/6 (d30)
Soft tissue sarcomas				
Chondrosarcoma (CHSA)	i.v. qd × 2	100	24% T/C	ND
Fibrosarcoma (UV2237)	i.v. qd × 1	200	37% T/C	ND
Osteosarcoma (OSA-FH)	i.v. qd × 5	40	33% T/C	ND
Rhabdomyosarc (TE-671)	i.v. qd × 1	300	[toxic]	ND
Reticulocell of ovary (M5076)	i.v. q7d × 2	150	36% T/C	ND

Note: d = study day, i.p. = intraperitoneal, ILS = % increase in life span, i.v. = intravenous, s.c. = subcutaneous, T/C = % of control versus treated tumor volumes.

[a] Fiebig, Freiburg, Germany.

[b] Langdon, Edinburgh, Scotland.

[c] Jacqueline Plowman, National Cancer Institute, Frederick, Maryland.

[d] Josephine Hurst, Goodwin Institute for Cancer Research, Plantation, Florida (unpublished data).

[e] Raffaella Giavazzi, Mario Negri Institute, Milan, Italy.

TABLE 12.2
Comparative *In Vitro* Activity of ET-743 in Human Cancer Cell Lines

Tumor Type	Cell Lines	IC50 Potency
Malignant fibrous histiocytoma	HS-90M/M-8805/M-9005	< 0.1 pM
Fibrosarcoma	HT-1080	< 0.1 pM
Mesenchymal chondrosarcoma	HS-16	4 pM–100 pM
Liposarcoma	HS-18	4 pM–100 pM
Hemangiopericytoma	HS-30	4 pM–100 pM
Mesenchymoma	HS-42	4 pM–100 pM
Colon	HCT-8	10 nM
Colon	HT-29	3 nM
Colon	HCT-16	3 nM
Breast	MCF-7	20 nM

Source: Adapted from Shao, L. et al., in *Proceedings of 93rd American Association for Cancer Research Meeting*, April 6–10, San Francisco, CA, 2002.

ET-743 toxicity, regardless of the animal species tested, is characterized by a common pattern that includes: hepatotoxicity; bone marrow toxicity, both *in vitro*[28,29] and *in vivo*; and damage at the injection site. Qualitative and quantitative differences of this common pattern can be noted depending on the animal species tested.

In rats, gender differences were detectable (although not in other species), with female animals displaying more severe toxicity. Gender differences in rats have also been detected in metabolic behavior.[30] Liver toxicity in rats was characterized by proliferative/inflammatory and epithelial changes in the bile ducts. Cholangitis is mainly found in rats, but not in humans. Bone marrow toxicity has also been detected in rats, and this toxicity shows a tendency to recover after three weeks.

In contrast to rats, monkeys express metabolic profile similarities to humans[31] and are thus considered to be a more relevant and predictive animal model of hepatotoxicity than are rats, and particularly than female rats. The pattern of hepatotoxicity observed in monkeys was also similar to that observed in patients (noncumulative, reversible, predominance of transaminase increase). Bone marrow toxicity was also detected, and it was characterized by myelosuppression (lymphoid depletion in the spleen and thymus, hypocellularity in the bone marrow), with recovery after three weeks.

12.2.4 Chemical Synthesis

Ecteinascidia turbinata has been successfully grown and harvested in aquaculture facilities located along the Mediterranean coast. The purification of the active ingredient is then accomplished on an industrial scale, using chromatographic procedures that represent a more practical and environmentally sound practice than harvesting the creature from the wild. Nevertheless, in recent years several synthetic schemes have been developed for industrial production of ET-743 in the quantities and quality required for a drug product (Yondelis) that will be used in clinical studies worldwide and manufactured for commercialization.

12.2.4.1 Synthetic Routes to ET-743 (Yondelis)

To date, three distinct total synthetic routes to Yondelis (ET-743) have been reported. The seminal work of Corey et al.[32] provided for the first time a total synthesis of this complex molecule. This breakthrough scheme resolved one of the main roadblocks to the synthesis—the cyclization to obtain the 10-membered ring is based on the elegant maneuver of the generation of the short-lived *o*-quinone methide and attack by cysteine thiol. In 2002, Fukuyama et al.[33] published a second total

synthesis of ET-743, based in part on previous efforts targeting members of the saframycins;[34] in which the cyclization reaction undergoes in the conditions previously developed by Danishefsky et al.[35] to converge with the general approach established by Corey for the later stages of the synthesis. Finally in 2006, a highly convergent total synthesis of ET-743 was reported by Zhu et al.[36] as a conclusion of previous investigations on the synthesis of this family of compounds.[37] This third total synthesis has been achieved in 31 steps as the longest linear sequence from 3-methyl catechol. Additionally, two formal syntheses have been described by Danishefsky et al.[38] and Williams et al.[39] who have described the synthesis of an advanced intermediate in the Fukuyama total synthesis and an intermediate of the first formal synthesis, respectively.

The procedures outlined before represent some of the most outstanding work in recent synthetic organic chemistry. However, the long and involved procedures for total synthesis of the molecule represent a tremendous barrier to industrial manufacture of the drug, which is particularly challenging in the face of regulatory requirements for pharmaceuticals. This problem was finally solved with the development of a semisynthetic procedure[40] representing the first industrially feasible route to the manufacture of the drug on a large scale.[41] This semisynthetic approach provides access not only to Yondelis (ET-743) but also to other members of the ecteinascidins and analogous compounds.[42] The procedure uses safracin B, an antibiotic available through fermentation of the bacteria *Pseudomonas fluorescens*, as the starting point. Optimization of the fermentation process, followed by its transformation according to Scheme 12.1, provided a robust, easily scaled-up procedure for manufacturing the drug.

Cyanosafracin B was converted into **2** via a five-step sequence. The amino and phenol groups were protected as the BOC and MOM derivatives, respectively. The hydrolysis of the methoxy-*p*-quinone and subsequent reduction of the *p*-quinone afforded the unstable hydroquinone, which was treated with bromochloromethane to give the methylenedioxy ring. Alkylation of the remaining phenol gave compound **2**. Removal of the BOC and MOM groups from **2** was followed by amide cleavage via an Edman degradation protocol providing **3** in 68% yield. Protection of the phenol with MEMCl allowed for the diazotization of the primary amine for conversion to alcohol **4**. Next, esterification with the protected cysteine produced compound **5**. The synthesis of ET-743 was completed using the chemistry from Corey et al. on similar substrates. A five-step sequence was used to form **9**. Deprotection of the allyl group and oxidation of the phenol, followed by dehydration and cyclization under Swern conditions, gave the intermediate **7**. Simultaneous removal of the MEM and BOC protecting groups was followed by ketone formation. Finally, Pictet–Spengler reaction and carbinolamine formation produced ET-743.

12.2.5 Clinical Studies

Yondelis (Trabectedin, ET-743) is currently commercialized for the treatment of STS and relapsed ovarian cancer in more than 60 countries. Worldwide, more than 12,000 patients have already been treated with this innovative drug. ET-743 is currently being studied in phase II clinical trials for breast cancer, NSCLC, and pediatric indications. Yondelis was granted Orphan Drug designation by the European Commission for the indications of STS and ovarian cancer.

12.2.5.1 Yondelis in STS

STSs are malignant tumors that originate in the soft tissues of the body. Soft tissues connect, support, and surround other body structures. The soft tissues include muscle, fat, blood vessels, nerves, tendons, and synovial tissues. The annual incidence of STS in Europe is approximately 0.004% (4 in 100,000 people).[43] Five-year overall survival (OS) rates are in the order of 50–60%, irrespective of disease stage at diagnosis. Within two to three years from diagnosis, approximately 30–50% of patients develop metastases despite optimal treatment for localized disease.[44]

The first paper which reported clinical activity of trabectedin in STS was published in 2001 by Delaloge et al.[45] This study included 29 patients with advanced, highly pretreated disease (12

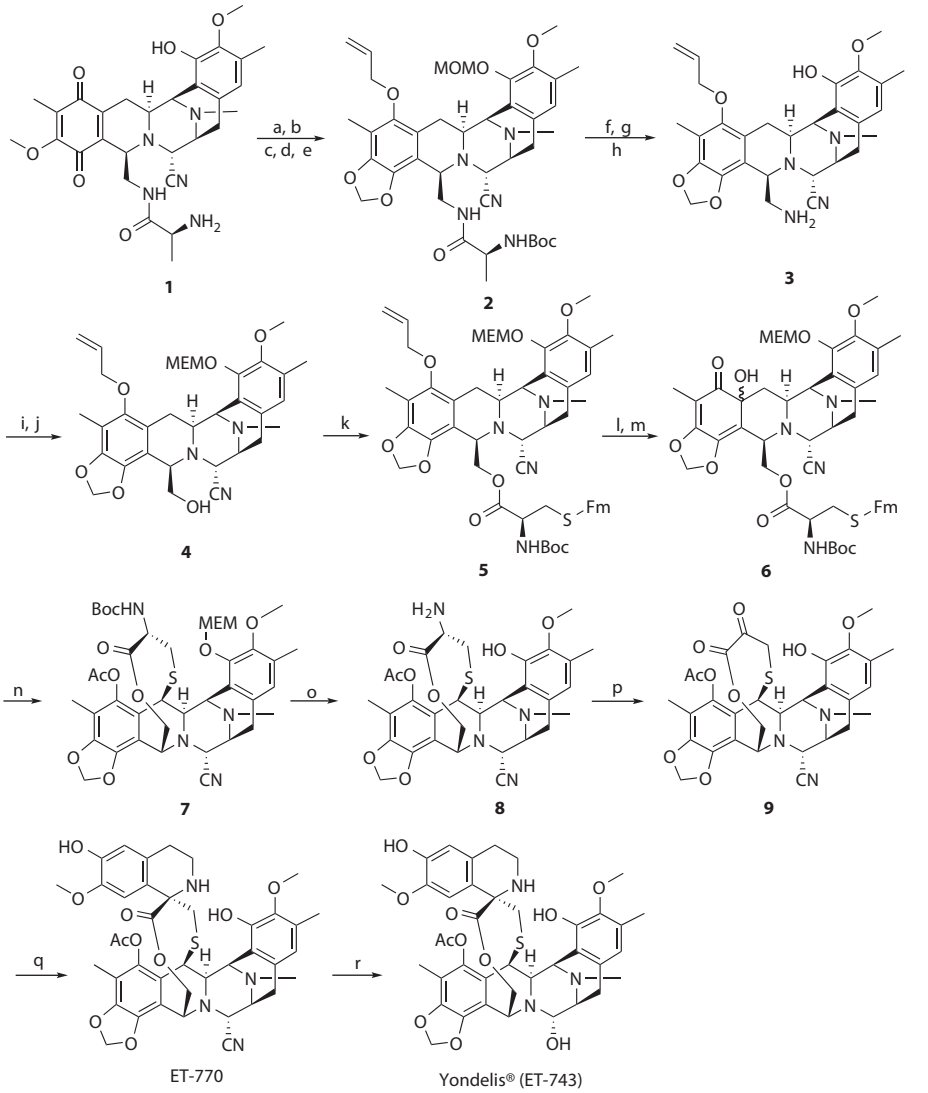

Reagents: (a) Boc_2O, EtOH, 23°C, 23 h, 81%; (b) MOMBr, *i*-Pr_2NEt, DMAP, CH_3CN, 40°C, 6 h, 83%; (c) NaOH 1M, MeOH, 20°C, 2.5 h, 68%; (d) H_2, 10% Pd/C, 23°C, 2 h; $ClBrCH_2$, Cs_2CO_3, DMF, 110°C, 2.5 h; (e) Allyl bromide, Cs_2CO_3, DMF, 23°C, 3 h, 56% for two steps; (f) TFA, CH_2Cl_2, 23°C, 4 h, 95%; (g) Phenylisothiocyanate, CH_2Cl_2, 23°C, 3 h, 87%; (h) HCl/Dioxane 4.3M, 23°C, 1 h, 82%; (i) MEMCl, *i*-Pr_2NEt, DMAP,CH_3CN, 23°C, 6 h, 88%; (j) $NaNO_2$, AcOH, THF, H_2O, 0°C, 3 h, 50%; (k) *(S)*-*N*-(*tert*-butoxycarbonyl)-*S*-(9-fluorenyl-methyl)cysteine, EDC·HCl, DMAP, CH_2Cl_2, 23°C, 2 h, 95%; (l) *n*-Bu_3SnH, $PdCl_2(PPh_3)_2$, AcOH,CH_2Cl_2, 23°C, 15 min, 90%; (m) $(PhSeO)_2O$, CH_2Cl_2, –10°C, 15 min, 91%; (n) DMSO, Tf_2O, CH_2Cl_2, –40°C, 35min; *i*-Pr_2NEt, 0°C, 45 min; *t*-BuOH, 0°C, 5 min; $(CH_3N)_2C$=N-t-Bu, 23°C, 40 min; Ac_2O, 23°C, 1 h, 58%; (o) *p*-TsOH, $CHCl_3$, 23°C, 1 h, 71%; (p) [*N*-methylpyridinium-4-carboxaldehyde]$^+I^-$, DBU, $(CO_2H)_2$, 23°C, 4 h, 57%;(q) 3-Hydroxy-4-methoxyphenylethylamine, silica gel, EtOH, 23°C, 12 h, 90%; (r) $AgNO_3$, CH_3CN, H_2O, 23°C,16 h, 90%.

SCHEME 12.1 Semisynthesis of ET-743 from cyanosafracin B.

patients entered in the phase I trial and 17 patients entered in a compassionate-use program). Overall, the author observed four partial responses (PR) (14%) and ten disease stabilizations (SD; 34%) lasting more than two months. The median time to progression (TTP) was 2.8 months. Eight patients (28%) were progression-free at 6 months and four (14%) were progression-free at 12 months. These

results were quite impressive considering that all patients had received both doxorubicin and an alkylating agent prior to treatment with trabectedin.

A pooled analysis of three nonrandomized phase II studies suggested a slightly higher efficacy for trabectedin in liposarcoma relative to other histological types, although the number within each of the other sarcoma types were too small to draw firm conclusions. Subsequently, a randomized, phase II study was conducted to evaluate the efficacy of trabectedin in a more homogeneous population of patients with liposarcoma and leiomyosarcoma.[46] Two regimens were compared, 1.5 mg/m^2, 24 h i.v. every three weeks (q3wk 24 h) and 0.58 mg/m^2, 3 h i.v. for three consecutive weeks in a three-week cycle (qwk 3 h). TTP was the primary efficacy endpoint based on confirmed independent review of images. A total of 270 patients were randomized, representing the largest randomized trial ever performed in patients with STS in a well-defined population of patients in whom anthracyclines and ifosfamide had failed, and the only clinical trial specifically conducted in liposarcoma/leiomyosarcoma. This randomized clinical trial showed that trabectedin can provide a clinical benefit to patients with sarcomas, especially leiomyosarcomas and liposarcomas, after failure of all conventional treatments. Although both dosing regimens of trabectedin showed efficacy in this trial, the data showed superior disease control with the q3wk 24 h regimen (median TTP: 3.7 vs. 2.3 months, for qwk 24 h and qwk 3 h, respectively; hazard ratio [HR]: 0.734, 95% confidence interval [CI]: 0.554–0.974; $p = 0.0302$). Apart from significant TTP differences, the benefits from trabectedin therapy were further highlighted by progression-free survival (PFS) rates at three months (51.5% in q3wk 24h; 44.7% in qwk 3 h) and six months (35% in q3wk 24 h; 27.5% in qwk 3 h) largely exceeding the criteria established by the EORTC-STBSG to define an active agent in pretreated STS.

Results of an exploratory, pooled analysis that assessed the efficacy of Yondelis and the tumor growth rate in patients with advanced STS participating in three pivotal phase II trials have been released.[47] These trials used 1.5 mg/m^2 of Yondelis in a 24-h infusion regimen every three weeks. Of the 183 patients with progressive disease evaluated, 7.7% ($n = 14$) achieved objective response (>50% tumor shrinkage), a further 7.7% ($n = 14$) achieved minor response (25–50% tumor shrinkage), and 36.1% ($n = 66$) had stabilization of the disease with a median duration of nine months. Therefore, in total, 51.4% ($n = 94$) of patients showed clinical benefit in terms of tumor growth control from treatment with Yondelis. The six-month PFS rate, an endpoint that assesses the percentage of patients whose disease has not progressed by a defined time point, was 19.8%, which is favorable according to results of an European Organization for Research and Treatment of Cancer study that considers drugs with a six-month PFS rate above 14% as efficacious, and those below 8% as inactive.[48] Following Yondelis treatment, 47.5% and 29.3% of patients with advanced, metastatic disease were alive after one and two years, respectively. Median OS time was 10.3 months, with 29% of patients surviving at two years or beyond. Yondelis proved particularly effective in cases of advanced sarcoma that had relapsed or that were resistant to conventional therapy. Phase I and II trials showed that a shorter treatment schedule (3-h infusions at 1.3 mg/m^2 every three weeks) was feasible.

12.2.5.2 Yondelis in Ovarian Cancer

Ovarian cancer is one of the deadliest gynecological cancers. Unfortunately, detection of ovarian cancer is difficult, and the disease is often diagnosed too late for successful treatment. Although with the current standard of care (debulking surgery followed by platinum-based chemotherapy) most of the patients achieve a complete clinical remission, eventually the majority of them will relapse and die owing to their disease. After recurrence, one of the most important prognostic factors is the platinum-free interval (PFI), the time between the last course of platinum regimen and recurrence. Patients who relapse before six months after platinum treatment are classified as platinum-resistant and those who relapse after six months are considered as platinum-sensitive. This classification is very important as the objective and the regimen of treatment is different across the groups.[49]

For platinum-sensitive patients, the treatment of choice is a combination of platinum agent with paclitaxel, pegylated liposomal doxorubicin (PLD), or gemcitabine, as all of these are superior to a platinum agent alone in terms of overall response rate (ORR) and PFS. As cure is not a realistic goal, the objective of any treatment is to improve the TTP and OS. However, approximately 15–17% of sensitive patients will develop hypersensitivity reactions during second-line or greater carboplatin-based treatment for recurrent disease precluding its use; therefore, it is necessary to find an effective alternative for this group of women. Resistant ovarian cancer patients are a group with a very poor prognosis where the treatment is just palliative. Salvage chemotherapy with nonplatinum agents, such as weekly paclitaxel, docetaxel, topotecan, PLD, gemcitabine, and etoposide, mostly results in short-lived response rates of approximately 10–20% and a poor survival. These results justify the need for new therapeutic options with a completely new structure and mechanism of action. Trabectedin achieved an ORR of nearly 30% in patients with platinum-sensitive relapsed ovarian cancer.

A randomized, multicenter, phase III trial (OVA-301) evaluated the combination of trabectedin plus PLD versus PLD alone in relapsed ovarian cancer, with PFS by independent radiology review as the primary endpoint.[50] When combined with PLD, trabectedin improved PFS over PLD alone, with a 21% risk reduction of disease progression (DP) or death (HR = 0.79; 95% CI = 0.65–0.96; $p = 0.0190$; median 7.3 vs. 5.8 months) and adequate tolerability. In the platinum-sensitive, the risk reduction of DP or death was 27% (HR = 0.73; 95% CI = 0.56–0.95; $p = 0.0170$; median PFS 9.2 vs. 7.5 months). A protocol-specified interim analysis of OS was conducted with 300 events (vs. 520 required for the final OS analysis) showing a 15% reduction in the risk of death with the combination (HR = 0.85; $p = 0.1506$). Based mainly on these results, the European Union Commission granted marketing authorization for trabectedin combined with PLD for the treatment of patients with relapsed, platinum-sensitive ovarian cancer in October 2009.[51]

In other indications such as breast and prostate cancer, Yondelis is being developed trying to identify the patients who should respond to the drug treatment by measuring levels of the endonuclease XPG. Yondelis is also being tested in pediatric indications.

12.2.5.3 Safety Profile

In all clinical studies, Yondelis has shown a good safety and tolerability profile. The most frequent adverse event appears to be neutropenia, which is reversible. Transaminase elevations were also reported but were transient. No mucositis, alopecia, neurotoxicity, cardiotoxicity, or cumulative toxicities have been observed.

12.3 APLIDIN

12.3.1 Background

Aplidin (plitidepsin) is a potent depsipeptide that was isolated from a Mediterranean tunicate, *Aplidium albicans*.[52] This compound is structurally related to the Didemnins, agents that were previously isolated from the Caribbean marine tunicate *Trididemnum solidum*.[53,54] The structures of the didemnins were reported to contain a 23-membered macrocycle with an attached side chain. The macrocycle is made up of six subunits, (*S*)-Leu, (*S*)-Pro, (1*S*,2*R*)-Thr, (*S*)-N-Me-Tyr(Me), (3*S*,4*R*,5*S*)-Isostatin (Ist), and (2*S*,4*S*)-3-oxo-4-hydroxy-2,5-dimethylhexanoic acid, also known as α-(α-hydroxyisovaleryl)propionic acid (Hip). The side chain, whose first amino acid is always (*R*)-N-Me-Leu, is joined to the Thr of the macrocycle, and its structure differentiates the various didemnins. Aplidin contains pyruvil-L-Pro as the side chain (Figure 12.2).

Aplidin (molecular formula: $C_{57}H_{87}N_7O_{15}$; molecular weight: 1110.34u) has the registered name Aplidin (also known as plitidepsin), the common name dehydrodidemnin B, and the chemical name (2*S*)-*N*-{(1*R*)-1-[({(3*S*,6*R*,7*S*,10*R*,11*S*,15*S*,17*S*,20*S*,25a*S*)-11-hydroxy-20-isobutyl-15-isopropyl-3-(4-methoxybenzyl)-2,6,17-trimethyl-10-[(1*S*)-1-methylpropyl]-1,4,8,13,16,18,21-heptaoxodocosahydro-

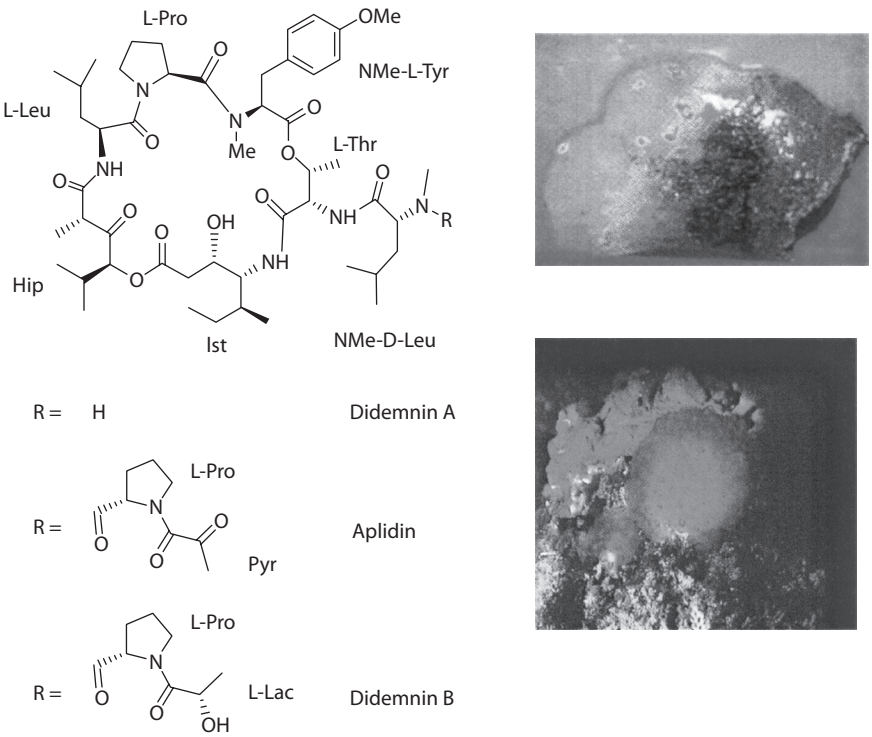

FIGURE 12.2 (**See color insert.**) Structure and source organism of Aplidin.

1*H*-pyrrolo[2,1-*f*][1,15,4,7,10,20]dioxatetraazacyclotricosin-7-yl}amino)carbonyl]-3-methylbutyl}-*N*-methyl-1-pyruvoyl-2-pyrrolidinecarboxamide. Several investigators have reported their results of various biological activities for a wide variety of didemnins.[55–57] Among them, Aplidin exhibited enhanced cytotoxic activity *in vitro* against several solid tumor and leukemic cell lines with IC_{50} values that were about tenfold more potent than those for didemnin B. This enhanced level of *in vitro* potency focused attention on further use of the Aplidin congener. The compound was then chosen for development as an antineoplastic agent because of its antitumor activity, and in early 1999, Aplidin entered phase I clinical trials in Europe and Canada.

12.3.2 Mechanism of Action

Aplidin induces cell death by triggering the mitochondrial apoptotic pathway resulting in cytochrome C release, poly [ADP-ribose] polymerase (PARP) cleavage, and chromatin fragmentation.[58,59] Aplidin activates caspase-3, -7, -8, and -9, and both the intrinsic and the extrinsic pathways seem to mediate apoptosis induction.[60,61] However, caspase-independent pathways are involved, as pan-caspase inhibitors such as Benzyloxycarbonyl-Val-Ala-Asp(OMe) (ZVAD) can only partially inhibit Aplidin-induced apoptosis.[62] At the molecular level, Aplidin induces a specific cellular stress response program including the rapid, strong, and sustained activation of the serine/threonine kinases c-Jun N-terminal kinase (JNK), a member of the mitogen-activated protein kinase family. The rapid activation of JNK induced by Aplidin treatment was observed in different tumor cell line models.[61,59] By using a series of inhibitors and mouse embryo fibroblasts (MEFs) lacking one or more kinases, JNK was confirmed to be a key component of the apoptotic process induced by Aplidin.[63] The search for early targets of Aplidin that could be responsible or at least involved in the activation of JNK rendered the identification of the Rac1 small GTPase. Aplidin causes a rapid (1–2 min) and transient activation of Rac1, and also but less of Cdc42, but not of RhoA or Ras.[64]

Rac1 activation is necessary for JNK activation in several human cancer cells, and was also found in JNK-deficient MEFs, indicating that it precedes and does not require JNK activity. Rac1 downregulation by either transfection of small interfering RNA (siRNA) duplexes or by the use of a specific Rac1 inhibitor consistently diminished JNK activation and apoptosis induction by the drug. Thus, Rac1 seems to play a crucial role in Aplidin action. Suárez et al.[65] also showed that Aplidin presents a moderately high-affinity binding site(s) in HeLa and MDA-MB-231 cells. The analysis of binding kinetics indicates that Aplidin first binds to a receptor probably located at the plasma membrane and then distributes to the cytosol.

The early activation of Rac1 and JNK can be blocked by either adding reduced glutathione (GSH) to the culture medium or by treating cells with compounds that increase the intracellular GSH level.[63,64] Conversely, L-buthionine-sulfoximine (BSO), a compound that decreases the cellular content of GSH, potentiates the activation of those Aplidin targets. Moreover, exogenous GSH prevented the loss of mitochondrial membrane potential and cell death caused by the drug, which strongly supports a critical role of GSH in its cytotoxic action. Aplidin disrupts cellular glutathione homeostasis by increasing the ratio of oxidized to reduced forms as a consequence of the alteration of glutathione peroxidase and glutathione reductase activities and the increase of GSH extrusion to the medium. Interestingly, antioxidants unrelated to the control of glutathione homeostasis do not affect Aplidin action. Direct measurements demonstrated that Aplidin induces oxidative stress by increasing intracellular reactive oxygen specie (ROS) concentration and oxidation of lipids and DNA in MDA-MB-231 cells[64] and induces ROS also in lymphoma cells.[66] In summary, Aplidin induces a GSH-dependent oxidative stress that causes the activation of Rac1 and later of JNK that is sustained by MKP-1 downregulation.

12.3.3 Preclinical Drug Development

12.3.3.1 *In Vitro* and *In Vivo* Testing

In vitro studies have shown cytotoxic effects of plitidepsin (Aplidin) against a broad panel of cell lines with values of $IC_{50} \leq 1$ nM. Plitidepsin was particularly active against cell lines of multiple myeloma, human leukemia and lymphoma, as well as against pancreas, NSCL, breast, melanoma, sarcoma, bladder, gastric, ovarian, and colon tumor cell lines.[61,67,68] *In vitro* combination studies also showed synergism of plitidepsin when combined with other agents, such as melphalan, dexamethasone, lenalidomide, and bortezomib in cell lines of multiple myeloma.[61]

In vivo studies showed antitumor effect of plitidepsin in animal models of multiple myeloma (as a single agent or in combination with dexamethasone), T-cell lymphoma, and primary myelofibrosis (PMF).[60,69–71] Moreover, plitidepsin's combinations with gemcitabine (pancreas), sorafenib (renal), and bevacizumab (NSCLC, renal, breast, and ovary) showed synergic or additive *in vivo* antitumor activity.[72–78]

12.3.3.2 Preclinical Toxicology

Intravenous administration of plitidepsin to male rats did not affect significantly either respiratory rate or tidal volume. Significant decreases in tidal volume and respiratory rate were detected, however, at 24 h postdosing with 1.50 mg/kg of plitidepsin.[79] In a modified Irwin's test, i.v. administration of plitidepsin at the higher dose of 1.5 mg/kg to male rats produced occasional findings up to 24 h post administration (grooming, piloerection, decreased touch response, passivity, hypothermia, and decreased locomotor activity); these clinical signs were always slight in degree.[80] Plitidepsin had no relevant effects on the potassium channel in human ether-a-go-go-related gene (hERG)-transfected cells or in the action potential morphology of isolated cardiac Purkinje fibers from dogs.[81,82] Escalating doses of plitidepsin on RR, QTc, VP/dtmax and dLVP/dtmin in a guinea pig Langendorff preparation[83] showed a slight, concentration-dependent increase in the QT interval. The QTc(F) interval increased slightly after perfusion of 10^{-5} M. Coronary blood flow decreased in a concentration-dependent manner. The estimate of inotropy, dLVP/dtmax, decreased slightly at a

plitidepsin concentration of 10^{-5} M. Moreover, a slight increase of dLVP/dtmin was seen at 10^{-5} M. The effect of plitidepsin on cardiovascular parameters was evaluated in conscious, telemetered dogs.[84] Plitidepsin increased heart rate (HR) between 2 and 48 h after administration of the high dose (0.03 mg/kg). As expected, given the increase in HR, there were decreases in the PR interval, QRS duration, RR interval, and uncorrected QT interval. To correct for variances in HR, QTcF, and QTcQ were calculated. There were no significant effects on QTcF at either of the doses of plitidepsin studied. Only small decreases in QTcQ were detected in the high dose group at 2 and 6 h postdose. A complete scan of the lead II electrocardiogram (ECG) waveforms for the vehicle and the high dose level of plitidepsin (0.03 mg/kg) was performed, and no abnormalities consistent with cardiovascular toxicity were observed during plitidepsin infusion up to 8 h after plitidepsin administration.

The toxicity of plitidepsin was assessed in mice, rats, and dogs.[85–94] Single, fractionated (five daily doses), and multicycle i.v. bolus injections in mice, rats, and dogs induced partially reversible alterations in the reticuloendothelial system, bone marrow (mainly leukopenia), gastrointestinal tract, liver, testes, and/or pancreas as well as inflammatory reactions at the injection site in mice. MTDs are summarized in Table 12.3. In one multiple-cycle study in rats[92] (three cycles of five consecutive treatment days) mortality was observed at 0.07 mg/kg, with anorexia, ataxia, dehydration and tremors. Leukopenia (mainly due to lymphopenia), anemia, and thrombocytopenia, were apparent in most treated animals, particularly males and confirmed by hematopoieteic tissue depletion at histopathology. Other target organs were dose-dependently affected: heart (cardiomyopathy), pancreas (necrosis and secretory material depletion), skeletal muscle (degeneration and chronic inflammation), male genital tract, pituitary gland (endocrine cell vacuolation and endocrine cell cytoplasm depletion), and injection-site (inflammation, edema, necrosis). In another multiple-cycle study in rats[93] (12 cycles, each cycle being a single i.v. bolus dose followed by a two-week observation period) results showed dose-dependent decreases (up to 0.4 mg/kg) in body weight, as well as leukopenia, anemia, thrombocytosis, and reticulocytosis. Leukopenia and thrombocytosis and partial thromboplastin time did not completely recover four weeks after the last drug administration. Increases of some metabolic parameters and electrolytes, such as a persistent increase in cholesterol and blood urea nitrogen (in males), as well as decrease in creatinine were also observed at the dose level of 0.4 mg/kg. No alterations were detected in the ophthalmological and ECG evaluations. Histopathology evaluation revealed lymphoid depletion and/or extramedullary hematopoiesis, as well as brown liver pigmentation and periportal fibrosis. Single hepatocytic necrosis was also observed in some animals at the end of treatment and at the end of recovery at 0.4 mg/kg. Focal, moderate myofiber degeneration in the soleum muscle was seen in a male after 0.4 mg/kg, and cardiomyopathy was reported in one female of the 0.1 mg/kg group and two of the 0.4 mg/kg groups.

TABLE 12.3
Maximum Tolerated Doses (MTDs) in Mice, Rats, and Dogs after Single, Fractionated Dose, and Multiple Cycles of Plitidepsin (Aplidin)

		MTD	
Species	**Schedule**	**mg/kg**	**mg/m²**
Mice	Single dose	0.625	1.875
	Five daily doses	0.220	0.660
Rats	Single dose	0.57	3.42
	Five daily doses	0.140	0.840
	Three cycles of five daily doses	0.035	0.21
Dogs	Five daily doses	>0.04	>0.8
	Three cycles of five daily doses	0.02	0.4

In the multiple-cycle studies in the dog[94] (three cycles of five consecutive treatment days) no mortality was observed up to 0.03 mg/kg/day but dehydration, decreased activity, swollen foreleg (injection site), vomiting, and hypersensitivity occurred (redness/swelling of head/abdomen/paws, head shaking, rubbing of head/face/body on run walls/floor), suggesting that this dose exceeded the MTD (Table 12.3). Serum creatinine, triglycerides, and cholesterol levels dose-dependently decreased. No treatment-related hematology changes were observed. Ophthalmologic and ECG parameters were unaffected by treatment. Dose-dependent microscopic lesions in the pancreas, liver, testes, and thymus were noted.

12.3.4 Chemical Synthesis

Aplidin belongs to the didemnin family,[95] and as a result of the biological activity of these compounds, several research laboratories have made them synthetic targets. Rinehart et al. reported the first total synthesis of the didemnins in 1987. Subsequently, different research groups published several syntheses, differing mainly in the selection of the two amino acids to achieve macrocyclization (Figure 12.3).

To date, the highest-yielding cyclization was reported by Schmidt et al.[96–98] and by Jou et al.[99] The first group synthesized didemnin A, B, and C, and Jou et al. described a process to obtain didemnin A and Aplidin (dehydrodidemnin B); the uniqueness of this synthesis is the use of new coupling reagents based on uranium and phosphonium salts. With this process, it is now possible to prepare a large number of analogs.

The synthesis published by Jou et al.[99] involved the synthesis of the Boc-protected didemnin macrocycle, followed by its coupling with Boc-(*R*)-N-Me-Leu-OH to give Boc-didemnin A, which was coupled with Pyr-Pro-OH to afford Aplidin (Scheme 12.2).

12.3.5 Clinical Studies

Aplidin is currently under clinical investigation. In different phase I and phase II clinical trials, Aplidin has shown antitumor activity in neuroendocrine tumors, neuroblastoma, advanced malignant melanoma, clear cell renal carcinoma, relapsed/refractory multiple myeloma, and relapsed/refractory peripheral T-cell lymphoma. A pivotal randomized phase III trial comparing Aplidin in combination with dexamethasone against dexamethasone was started in June 2010 in patients with

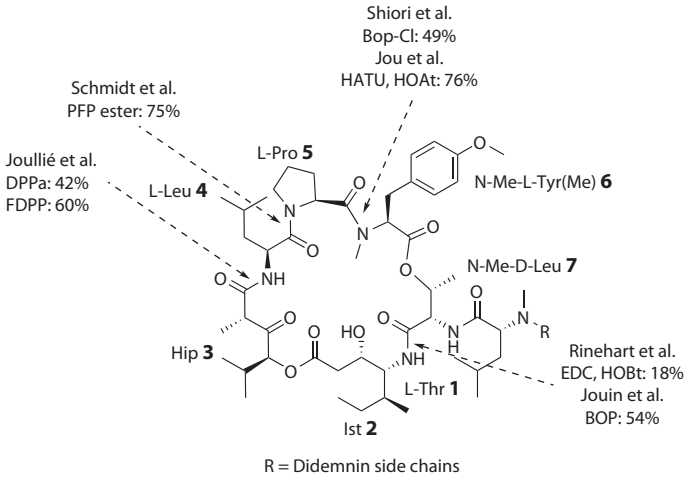

FIGURE 12.3 Amino acids to achieve the cyclization of Aplidin.

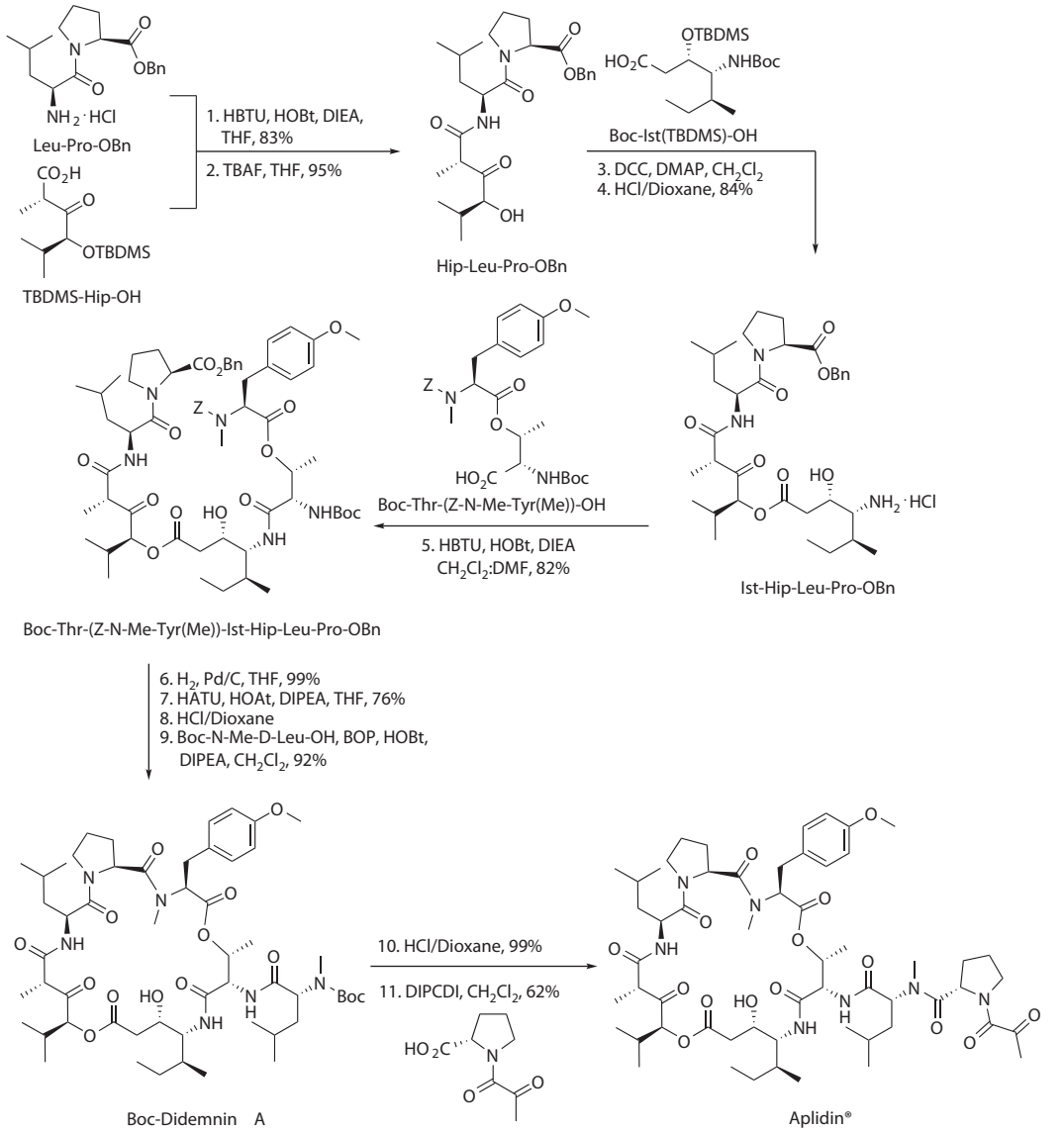

SCHEME 12.2 Synthesis of Aplidin.

relapsed/refractory multiple myeloma. Additionally, a new phase II study in patients with myelofibrosis has been started to confirm clinically available preclinical data in this indication.

As a single agent, Aplidin has been investigated in four i.v. treatment schedules: 24-h infusion q2wk, 3-h infusion q2wk, 1-h infusion weekly (days 1, 8, and 15) for three weeks q4wk, and 1-h infusion daily for 5 days q3wk. Of these studies, two schedules have been selected for further phase II and phase III clinical trials: 3-h infusion q2wk (recommended dose: 5 mg/m^2) and 1-h infusion weekly (recommended dose: 3.2 mg/m^2).

Regarding the safety profile of Aplidin, the main dose-limiting toxicity (DLT) found at the dose schedules proposed for further development consisted of musculoskeletal adverse events. These included myalgia and/or muscle weakness, often associated with elevated creatine phosphokinase (CPK) levels, although transient and reversible muscular events were generally self-limiting and typically resolved within 1–3 weeks.

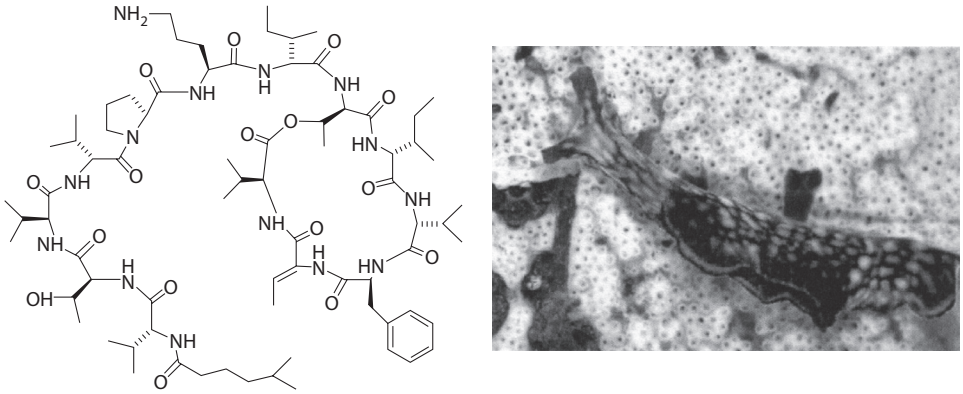

FIGURE 12.4 (**See color insert.**) Structure and source organism of Irvalec.

12.4 IRVALEC

12.4.1 Background

Irvalec (Elisidepsin trifluoroacetate; PM02734) is a synthetic cyclic depsipeptide of the Kahalalide family, Kahalalide F being the only member of the family with important bioactivity. Irvalec is a head-to-side chain cyclodepsipeptide, with a complex structure, comprising six amino acids, among these (*Z*)-didehydro-α-aminobutyric acid (*Z*-Dhb) (formed from dehydration of a Thr residue), as a cyclic part between the carboxylic acid of a L-Val (**1**) and the secondary alcohol of the D-allo-Thr (**6**), and an exocyclic chain of seven amino acids with (*S*)-4-methylhexanoic acid as a terminal aliphatic acid fatty group (Figure 12.4).[100,101] Kahalalide F, together with a number of other natural Kahalalides, was discovered in the mollusk *Elysia rufescens* (a sea slug; a marine gastropod of the ophistobranchia subclass) collected at Kahala (Muanalua Bay) in O'ahu (Hawai'i).[102] Several species of animals of this class are known to acquire, process, and accumulate chemicals produced by the algae on which they feed. Surprisingly, some species are able to retain chloroplasts from these algae that remain active in photosynthesis within the animal for prolonged periods of time.[103] In the case of Kahalalide F, the compound is found in the algae *(Bryopsis pennata)* on which the *Elysia* mollusks feed, albeit in much reduced concentration.[104] In this natural setting, a biological role has been proposed for Kahalalides as a deterrent to the feeding behavior of predators of the *Elysia* nudibranchs.

Irvalec (Elisidepsin trifluoroacetate; molecular formula: $C_{77}H_{125}F_3N_{14}O_{18}$; molecular weight: 1591.89u) has the chemical name, (*R*)-*N*-((*S*)-5-amino-1-((2*R*,3*S*)-1-((3*S*,9*S*,12*R*,15*R*,18*R*,19*R*,*Z*)-9-benzyl-15-*sec*-butyl-6-ethylidene-3,12-diisopropyl-19-methyl-2,5,8,11,14,17-hexaoxo-1-oxa-4,7,10,13,16-pentaazacyclononadecan-18-ylamino)-3-methyl-1-oxopentan-2-ylamino)-1-oxopentan-2-yl)-1-((2*R*,5*S*,8*S*,11*R*,16*S*)-8-((*R*)-1-hydroxyethyl)-2,5,11-triisopropyl-16-methyl-4,7,10,13-tetraoxo-3,6,9,12-tetraazaoctadecane)pyrrolidine-2-carboxamide trifluoroacetate.

12.4.2 Mechanism of Action

Exposure of tumor cells to Irvalec induces necrotic cell death, a process associated with rapid loss of membrane integrity and subsequent cell permeabilization.[105,106] In dose–response experiments using different tumor cell lines, very similar IC_{50} values were obtained after short (30 min) and long (72 h) hours of exposure to the drug, suggesting that the compound exerts its cytotoxic effect immediately after drug treatment. Tumor cells exposed to effective concentrations of Irvalec underwent rapid and dramatic morphological changes, including cell blebbing, severe swelling, and plasma membrane permeabilization that irrevocably lead to cell lysis. Interestingly,

membrane damage was observed only after reaching a threshold concentration of around 1–5 μM in several cell lines and only in the continuous presence of the compound in the culture medium. Altogether, these results suggest that Irvalec induces a rapid imbalance of the physiologic stability of the plasma membrane in tumor cells, causing severe alterations that lead to a necrotic cell death. These results confirm those previously obtained in the yeast *Saccharomyces cerevisiae*,[107] where cells treated with elisidepsin had rapid necrosis-like death, with accumulation of internal small vesicles. A systematic screen of a set of 4,848 viable *S. cerevisiae* haploid deletion mutants was conducted to identify genes involved in sensitivity or resistance to elisidepsin. Several of the 76 identified genes were related to lipid metabolism or vesicle trafficking from the Golgi apparatus. A mutant strain lacking the sphingolipid fatty acyl hydroxylase SCS7 was found to be the most resistant to elisidepsin, whereas overexpression of SCS7 rendered the cells hypersensitive.[107] These results suggested that elisidepsin exerts its potent necrotic cytotoxic activity by inducing rapid and severe membrane damage that appears to involve 2-hydroxy fatty acids located at the cell membrane.

12.4.3 Preclinical Drug Development

12.4.3.1 *In Vitro* and *In Vivo* Testing

Preliminary *in vitro* studies[108] identified elisidepsin as a new antiproliferative drug demonstrating activity against a broad spectrum of solid tumor types (including breast, colon, lung, neuroblastoma, prostate, sarcoma, and thyroid cancer) with IC_{50} values ranging from 0.01 to 1 μM. Based on these *in vitro* data, *in vivo* experiments with hollow fiber (HF) and human tumor xenografts were performed. In the HF system, elisidepsin demonstrated statistically significant antitumor activity against human hepatocellular carcinoma, hepatoma, and pancreatic tumor cell lines. In murine xenograft models using human cell types such as breast, lung, prostate, and melanoma, elisidepsin showed statistically significant activity.[108–110]

The antiproliferative effects of several combinations of elisidepsin with cytotoxics and targeted therapeutics classically used in the treatment of cancer were evaluated to support the clinical use of this compound. The effects of sequential and simultaneous exposure to elisidepsin combined with oxaliplatin, cisplatin, gemcitabine, 5-fluorouracil (5-FU), rapamycin, lapatinib, and sunitinib were studied in a panel of colon, breast, ovarian, lung, prostate, head and neck, and pancreatic cancer cell lines.[111] Elisidepsin strongly potentiated the antiproliferative activity of platinum compounds (oxaliplatin and cisplatin), gemcitabine, and targeted therapies such as rapamycin and lapatinib. The combination with sunitinib showed at least an additive effect. Another study demonstrated that tumor cell lines marginally sensitive to gefitinib and erlotinib retained sensitivity to elisidepsin, thereby suggesting a lack of or partial cross-resistance between these drugs.[111]

12.4.3.2 Preclinical Toxicology

The effect on respiratory function of elisidepsin administered as a single i.v. bolus injection was assessed in rats by recording changes in respiratory rate and/or tidal volume at 15 and 60 min after administration.[112] Intravenous elisidepsin administered to male rats (0.075 and 0.150 mg/kg) did not significantly affect either respiratory rate or tidal volume. The effect of elisidepsin administration on gross behavioral and physiological state was assessed by recording changes based on the Irwin test in rats: no changes were observed in male rats receiving doses of 0.075 and 0.150 mg/kg.[113] The cardiovascular safety evaluation of elisidepsin was carried out both *in vitro* (hERG assay) and in dogs (cardiovascular function).[114,115] *In vitro* data showed a similar percentage of the hERG tail current in cells exposed to 1 μM of elisidepsin compared with vehicle-treated cells. The effect of elisidepsin on cardiovascular parameters (arterial blood pressure, heart rate, and lead II ECG) was evaluated in conscious, telemetered dogs. No clinical signs or ECG findings were observed in any of the animals following i.v. bolus administration of placebo or elisidepsin at doses of 0.075 and 0.100 mg/kg.

TABLE 12.4
Maximum Tolerated Doses (MTDs) Calculated for Irvalec® in Different Animal Species

		MTD, mg/kg (mg/m²)	
Species	**Gender**	**Intravenous SB**	**Intravenous 24-h Infusion**
Rat, SD	M	0.251 (1.5)	0.8 (4.8)
	F	0.249 (1.49)	0.8 (4.8)
Dog, Beagle	M	0.11 (2.2)	0.6 (12)
	F	0.11 (2.2)	1.2 (24)

Note: F, female; M, male; SD, Sprague Dawley; SB, single bolus.

Elisidepsin was tested in rats and dogs treated i.v. both as a bolus and as a 24-h infusion in both single- and multiple-cycle studies.[116–125] The MTDs in rats and dogs are shown in Table 12.4. Toxicity findings associated with elisidepsin were similar between genders both in terms of frequency and severity. The most common clinical signs associated with elisidepsin administration were vomiting, soft feces, dehydration, and slight decreases in food consumption and body weight. The onset of these symptoms was 1–3 days after administration, and animals returned to normal thereafter. No evidence for a higher frequency of these symptoms occurred during multiple-cycle studies. Across species, liver and kidney were the target organs for toxicity, as noted by clinical chemistry changes evidenced by significant dose-dependent increases in alanine aminotransferase (ALT), γ-glutamyltransferase (GGT), blood urea nitrogen (BUN), and creatinine. These changes were recorded 3–4 days after administration, with an apparent tendency toward recovery on day 7. Histopathological evaluation performed during the study period, either prior to a second dose or at the end of the recovery period, demonstrated no liver alterations and only minor renal changes. No signs of accumulation in the increases in enzyme levels were seen in multiple-cycle studies, despite the use of a weekly schedule. No elisidepsin-related hematotoxicity was noted either by peripheral blood examination or by bone marrow staining (for any dose or administration schedule used). Although injection-site changes were noted predominantly in dogs receiving bolus doses (24-h infusion studies were carried out with catheterized animals), no such inflammatory changes were observed in rats. However, in a formal study in male New Zealand White rabbits, elisidepsin showed potential for causing irritation after both i.v. and perivenous administration.[126]

12.4.4 Chemical Synthesis

Irvalec is synthesized in a linear solid-phase synthesis on a 2-chlorotrityl chloride-resin (ClTrt-Cl or Barlos resin).[101] The elongation of the peptide chain is carried out using Fmoc/*t*Bu strategy. HOBt/DIPCDI is used for the amide formation. The D-allo-Thr (**6**) is introduced without protection of the hydroxyl group. Esterification with Alloc-Val-OH takes place quantitatively after two or three coupling reactions with DIPCDI/DIPEA/DMAP. After the incorporation of the (*S*)-4-methylhexanoic acid, the Alloc group is removed with $Pd(PPh_3)_4$ and $PhSiH_3$, and the dipeptide Alloc-Phe-(*Z*)-Dhb-OH, obtained in solution from Alloc-Phe-OH and H-Thr-O*t*Bu with EDC and subsequent dehydration with EDC in the presence of CuCl and treatment with TFA, is coupled with HOAt/DIPCDI. After cleavage of the peptide from the resin under mild acidic conditions, the cyclization and final deprotection are performed in solution. Although the macrocyclization could be carried out at any position except L-Phe (**3**) and (*Z*)-Dhb (**2**), doing so between L-Phe (**3**) and D-Val (**4**) looked to be the most favorable option. The reagents for cyclization are HOBt/DIPCDI (Scheme 12.3). In 2006, several new improved synthetic routes based on convergent approaches with distinct orthogonal protection schemes for the preparation of Kahalalide analogs have been described.[127]

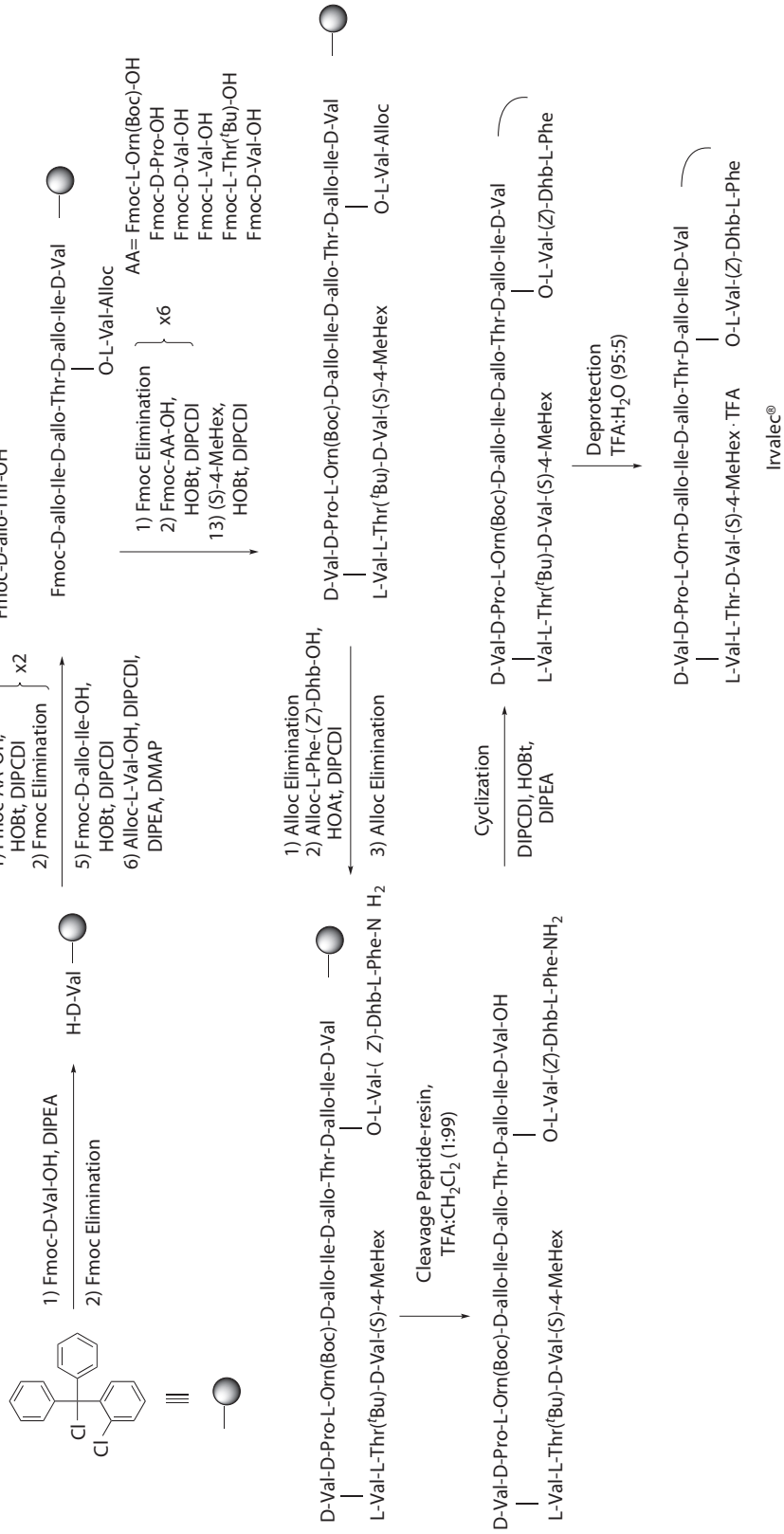

SCHEME 12.3 Synthesis of Irvalec.

These strategies allow a better control and characterization of the intermediates because more reactions are performed in solution. Those solid-phase methodologies are easily scaled up, and are applicable to the generation of a wide variety of new analogs.[128]

12.4.5 Clinical Studies

Two phase I trials are currently evaluating elisidepsin as a single-agent i.v. infusion in patients with advanced solid tumors.[129,130] In the first of these trials, patients were treated with a 30-min or a 3-h i.v. infusion using an q3wk (one dose every three weeks) schedule. DLTs consisted of grade 3–4 asymptomatic and reversible transaminase elevations, which were associated with early plasma concentrations.[129] Once the analysis of data from this first study had found no relevant correlation between plasma clearance and body surface area (BSA), all ongoing clinical trials were amended to switch to a flat dose. This trial is currently evaluating a 3-h infusion schedule with BSA-independent dosing. In the second single-agent phase I trial, patients with advanced solid tumors were treated with elisidepsin as a 24-h i.v. infusion q3wk.[130] DLTs consisted of grade 3 transaminase increases. Based on the safety data available, the most common elisidepsin-related adverse events were transaminase increases (mainly ALT), asthenia, nausea, and pruritus: most were grade ≤ 2. Transaminase increases were asymptomatic and transient, as they appeared approximately 48 h after dosing and lasted for more than 12 days. None of these patients had treatment-related increases in other liver enzymes or liver function tests (e.g., bilirubin, alkaline phosphatase) or in coagulation tests, or acute or fatal liver failure. Hence, the available preliminary safety data for elisidepsin indicate an acceptable safety profile.

A phase II trial is currently ongoing evaluating elisidepsin in patients with squamous NSCLC progressing after at least one line of platinum-based chemotherapy.[130] Furthermore, two phase I trials are currently evaluating elisidepsin in combination with drugs frequently used in NSCLC, such as erlotinib, carboplatin, or gemcitabine.

Preliminary evidence of activity in esophageal/gastric cancer has been reported for elisidepsin in phase I trials. One long-lasting complete response was found in a patient with a large-cell undifferentiated carcinoma of the esophagus and multiple lymph node metastases treated with elisidepsin for 24 h q3wk, with a TTP and OS of 31 months at last follow-up.[130] Furthermore, stable disease lasting longer than three months was found in one patient with esophageal cancer[129] and one patient with gastric cancer.[130] On the basis of these results, a phase Ib/II trial is currently being conducted in patients with unresectable, locally advanced/metastatic esophageal cancer, gastric cancer, or gastroesophageal junction cancer after at least one prior line of systemic therapy. Other tumors in which stable disease lasting longer than three months was found in phase I trials are colorectal adenocarcinoma, pancreatic cancer, pleural mesothelioma, prostate adenocarcinoma, and STS.

REFERENCES

1. Rinehart, K.L., Holt, T.G., Fregeau, N.L., Stroh, J.G., Keifer, P.A., Sun, F., Li, L.H., and Martin, D.G., Ecteinascidins 729, 743, 745, 759A, 759B, and 770: potent antitumor agents from the Caribbean tunicate *Ecteinascidia turbinata*, *J. Org. Chem.*, 55, 4512–4515, 1990. Rinehart, K.L., Holt, T.G., Fregeau, N.L., Stroh, J.G., Keifer, P.A., Sun, F., Li, L.H., and Martin, D.G., Ecteinascidins 729, 743, 745, 759A, 759B, and 770: potent antitumor agents from the Caribbean tunicate *Ecteinascidia turbinata* [*Erratum to document cited in CA113(9):75189d*], *J. Org. Chem.*, 56, 1676, 1991.
2. Scott, J.D. and Williams, R.M., Chemistry and biology of the tetrahydroisoquinoline antitumor antibiotics, *Chem. Rev.*, 102, 1669–1730, 2002.
3. De Silva, I.U., McHugh, P.J., Clingen, P.H., and Hartley, J.A., Defining the roles of nucleotide excision repair and recombination in the repair of DNA interstrand cross-links in mammalian cells, *Mol. Cell. Biol.*, 20, 7980–7990, 2000.
4. Casado, J.A., Río, P., Marco, E., García-Hernández, V., Domingo A., Pérez, L., Tercero, J.C., Vaquero, J.J., Albella, B., Gago, F., and Bueren, J.A., Relevance of the Fanconi anemia pathway in the response of human cells to trabectedin, *Mol. Cancer Ther.*, 7, 1309–1318, 2008.

5. Herrero, A.B., Martin-Castellanos, C., Marco, E., Gago, F., and Moreno, S., Cross-talk between nucleotide excision and homologous recombination DNA repair pathways in the mechanism of action of antitumor trabectedin, *Cancer Res.*, 66, 8155–8162, 2006.
6. Damia, G. and D'Incalci, M., Targeting DNA repair as a promising approach in cancer therapy, *Eur. J. Cancer*, 43, 1791–1801, 2007.
7. Damia, G., Silvestri, S., Carrassa, L., Filiberti, L., Faircloth, G.T., Liberi, G., Foiani, M., and D'Incalci, M., Unique pattern of ET-743 activity in different cellular systems with defined deficiencies in DNA-repair pathways, *Int. J. Cancer*, 92, 583–588, 2001.
8. Erba, E., Bergamaschi, D., Bassano, L., Damia, G., Ronzoni, S., Faircloth, G.T., and D'Incalci, M., Ecteinascidin-743 (ET-743), a natural marine compound, with a unique mechanism of action, *Eur. J. Cancer*, 37, 97–105, 2001.
9. Takebayashi, Y., Goldwasser, F., Urasaki, Y., Kohlhagen, G., and Pommier, Y., Ecteinascidin 743 induces protein-linked DNA breaks in human colon carcinoma HCT116 cells and is cytotoxic independently of topoisomerase I expression, *Clin. Cancer Res.*, 7, 185–191, 2001.
10. Rosell, R., Martinez, N., Rodriguez, S., Chaib, I., Grosso, F., Taron, M., Mendez, P., et al., Expression of XPG mRNA and protein as potential biomarker of response to trabectedin in sarcoma patients. Abstract no. C127. 19th AACR-NCI-EORTC International Conference on "Molecular Targets and Cancer Therapeutics," Oct 22–26, San Francisco, CA, USA. 2007.
11. Bonfanti, M., La Valle, E., Fernandez Sousa Faro, J.M., Faircloth, G., Caretti, G., Mantovani, R., and D'Incalci, M., Effect of ecteinascidin-743 on the interaction between DNA binding proteins and DNA, *Anticancer Drug Res.*, 14, 179–186, 1999.
12. Scotto, K.W., The MDR1 gene: Transcriptional activation and pharmacological intervention, *Br. J. Cancer*, 86 (Suppl. 1), S9 (Abstract. no. S22), 2002.
13. Griffin, L.B., Grohar, P., Pommier, Y., Khanna, C., Khan, J., and Helman, L.J., ET-743 modulates EWS-FLi1 activity in Ewing's sarcoma cells, Abstract no. 1501. In Proceedings of 100th American Association for Cancer Research Meeting, April 18–22, Denver, CO, USA. 2009.
14. Forni, C., Minuzzo, M., Virdis, E., Tamborini, E., Simone, M., Tavecchio, M., Erba, E., et al., Trabectedin (ET-743) promotes differentiation in myxoid liposarcoma tumors, *Mol. Cancer Ther.*, 8, 449–457, 2009.
15. Izbicka, E., Lawrence, R., Davidson, K., Cerna1, C., Gomez, L., Faircloth, G.T., Jimeno, J., Weitman, S., and Von Hoff, D.D., Incomplete cross-resistance between ET-743 and standard chemotherapeutic agents against primary tumors in human tumor cloning assay, *Ann. Oncol.*, 9 (Suppl. 2), Abstract no. 130, 1998.
16. Valoti, G., Nicoletti, M.I., Pellegrino, A., Jimeno, J., Hendriks, H., D'Incalci, M., Faircloth, G., and Giavazzi, R., Ecteinascidin-743, a new marine natural product with potent antitumor activity on human ovarian carcinoma xenografts, *Clin. Cancer Res.*, 4, 1977–1983, 1998.
17. Hendriks, H.R., Fiebig, H.H., Giavazzi, R., Langdon, S.P., Jimeno, J.M., and Faircloth, G.T., High antitumor activity of ET-743 against human tumor xenografts from melanoma, non-small cell lung and ovarian cancer, *Ann. Oncol.*, 10, 1233–1240, 1999.
18. Riccardi, R., Colombo, T., Meco, D., Giavazzi, R., Riccardi, A., Faircloth, G.T., Jimeno, J., Erba, E., and D'Incalci, M., Effective combinations of ET-743 and doxorubicin for tumor growth inhibitions against murine and human sarcomas in athymic mice, Abstract no. 1132. In *Proceedings of 92nd American Association for Cancer Research Meeting*, March 24–28, New Orleans, LA, USA. 2001.
19. D'Incalci, M., Colombo, T., Ubezio, P., Nicoletti, I., Giavazzi, R., Erba, E., Ferrarese, L., et al., The combination of Yondelis and cisplatin is synergistic against human tumor xenografts, *Eur. J. Cancer*, 39, 1920–1926, 2003.
20. Li, W.W., Takahashi, N., Jhanwar, S., Cordon-Cardo, C., Elisseyeff, Y., Jimeno, J., Faircloth, G., and Bertino, J.R., Sensitivity of soft tissue sarcoma cell lines to chemotherapeutic agents: identification of ecteinascidin 743 as a potent cytotoxic agent, *Clin. Cancer Res.*, 7, 2908–2911, 2001.
21. Takahashi, N., Li, W.W., Banerjee, D., Scotto, K.W., and Bertino, J.R., Sequence-dependent enhancement of cytotoxicity produced by ecteinascidin 743 with doxorubicin or paclitaxel in soft tissue sarcoma cells, *Clin. Cancer Res.*, 7, 3251–3257, 2001.
22. Faircloth, G.T., *In vivo* study using tumor containing hollow fibers in the nude mouse, Study 02E01HF, PharmaMar data on file. 2001.
23. Shao, L., Weissbach, L., Faircloth, G.T., and Hornicek, F., *In vitro* invasiveness of chondrosarcoma altered by Ecteinascidin-743, Abstract no. 2676. In Proceedings of 93rd American Association for Cancer Research Meeting, April 6–10, San Francisco, CA, USA. 2002.
24. Faircloth, G.T., Grant, W., and Hornicek, F., *In vivo* combinations of chemotherapeutic agents with Ecteinascidin 743 (Et743) against solid tumors, Abstract no. 387. AACR-NCI-EORTC Conference on "Molecular Targets and Cancer Therapeutics," October 29–November 2, Miami, FL, USA. 2001.

25. Faircloth, G.T., Grant, W., Jimeno, J.M., and Fernández Sousa-Faro, J.M., Dexamethasone potentiates the activity of Ecteinascidin 743 in preclinical melanoma and osteosarcoma models, Abstract no. 379. In Proceedings of 93rd American Association for Cancer Research Meeting, April 6–10, San Francisco, CA, USA. 2002.
26. Morioka, H., Weissbach, L., Vogel, T., Nielsen, G.P., Faircloth, G.T., Shao, L., and Hornicek, F.J., Antiangiogenesis treatment combined with chemotherapy produces chondrosarcoma necrosis, *Clin. Cancer Res.*, 9, 1211–1217, 2003.
27. Jimeno, J.M., Grant, W., and Faircloth, G.T., Enhancing the preclinical *in vivo* antitumor activity of Ecteinascidin 743, a marine natural product currently in phase II clinical trials, Abstract no. 306. AACR-NCI-EORTC Conference on "Molecular Targets and Cancer Therapeutics" November 16–19, Washington D.C., USA. 1999.
28. Ghielmini, M., Colli, E., Erba, E., Bergamaschi, D., Pampallona, S., Jimeno, J., Faircloth, G., and Sessa, C., *In vitro* schedule dependancy of myelotoxicity and cytotoxicity of Ecteinascidin 743, *Ann. Oncol.*, 9, 989–993, 1998.
29. Albella, B., Faircloth, G., López-Lázaro, L., Guzmán, C., Jimeno, J., and Bueren, J.A., *In vitro* toxicity of ET743 and Apldine, two marine-derived antineoplastics, on human bone marrow haematopoietic progenitors: comparison with the clinical results, *Eur. J. Cancer*, 38, 1395–1404, 2002.
30. Vermeir, M., Hendrickx, J., Hurkmans, R., Van Houdt, J., Zwijsen, C., Bode, N., Aviles, P., et al., An interspecies comparison of the metabolism of the anticancer agent Yondelis™ (Trabectedin, ET-743). Abstract No. WP66, 13th International Conference on Cytochromes P450: Biochemistry, Biophysics and Drug Metabolism, Prague, Czech Republic, June 29–July 3, 2003.
31. Vermeir, M., Hemeryck, A., Cuyckens, F., Francesch, A., Bockx, M., Van Houdt, J., Steemans, K., Mannens, G., Avilés, P., and De Coster, R., *In vitro* studies on the metabolism of trabectedin (YONDELIS) in monkey and man, including human CYP reaction phenotyping, *Biochem. Pharmacol.*,77, 1642–1654, 2009.
32. Corey, E.J., Gin, D.Y., and Kania, R.S., Enantioselective total synthesis of Ecteinascidin 743, *J. Am. Chem. Soc.*, 118, 9202–9203, 1996.
33. Endo, A., Yanagisawa, A., Abe, M., Tohma, S., Kan, T., and Fukuyama, T., Total synthesis of Ecteinascidin 743, *J. Am. Chem. Soc.*, 124, 6552–6554, 2002.
34. Fukuyama, T. and Sachleben, R.A., Total Synthesis of (±)-Saframycin B, *J. Am. Chem. Soc.*, 104, 4957–4958, 1982.
35. Zhou, B., Guo. J., and Danishefsky, S.J., Studies directed to the total synthesis of ET 743 and analogues thereof: an expeditious route to the ABFGH subunit, *Org. Lett.*, 4, 43–46, 2002.
36. Chen, J., Chen, X., Bois-Choussy, M., and Zhu, J., Total synthesis of Ecteinascidin 743*, J. Am. Chem. Soc.*, 128, 87–89, 2006.
37. Chen, X., Chen, J., De Paolis, M., and Zhu, J., Synthetic studies toward Ecteinascidin 743, *J. Org. Chem.*, 70, 4397–4408, 2005.
38. Zheng, S., Chan, C., Furuuchi, T., Wright, B.J.D, Zhou, B., Guo, J., and Danishefsky, S.J,, Stereospecific formal total synthesis of Ecteinascidin 743, *Angew. Chem., Int. Ed.*, 45, 1754–1759, 2006.
39. Fishlock, D. and Williams, R.M., Synthetic studies on Et-743. Assembly of the pentacyclic core and a formal total synthesis, *J. Org. Chem.*, 73, 9594–9600, 2008.
40. Cuevas, C., Pérez, M., Martín, M.J., Chicharro, J.L., Fernández-Rivas, C., Flores, M., Francesch, A., et al., Synthesis of Ecteinascidin ET-743 and Phthalascidin Pt-650 from Cyanosafracin B, *Org. Lett.*, 2, 2545–2548, 2000.
41. Cuevas, C., and Francesch, A., Development of Yondelis (trabectedin, ET-743). A semisynthetic process solves the supply problem, *Nat. Prod. Rep.*, 26, 322–337, 2009.
42. Menchaca, R., Martínez, V., Rodríguez, A., Rodríguez, N., Flores, M., Gallego, P., Manzanares, I., and Cuevas, C., Synthesis of natural Ecteinascidins (ET-729, ET-745, ET-759B, ET-736, ET-637, ET-594) from Cyanosafracin B, *J. Org. Chem.*, 68, 8859–8866, 2003.
43. Fletcher, C.D.M., Unni, K.K., and Mertens, M., *Pathology and Genetics of Tumours of Soft Tissue and Bone*. Lyon, France, IARC Press, 2002.
44. Blay, J.-Y., Trabectedin: An emerging therapeutic option in soft tissue sarcoma, *Eur. J. Clin. Med. Oncol.*, 1, 1–7, 2009.
45. Delaloge, S., Yovine, A., Taamma, A., Riofrio, M., Brain, E., Raymond, E., Cottu, P., et al., Ecteinascidin-743: A marine-derived compound in advanced, pretreated sarcoma patients-preliminary evidence of activity, *J. Clin. Oncol.*, 19, 1248–1255, 2001.

46. Demetri, G.D., Chawla, S.P., von Mehren, M., Ritch, P, Baker, L.H., Blay, J.Y., Hande, K.R., et al., Efficacy and safety of trabectedin in patients with advanced or metastatic liposarcoma or leiomyosarcoma after failure of prior anthracyclines and ifosfamide: results of a randomized phase II study of two different schedules, *J. Clin. Oncol.*, 27, 4188–4196, 2009.
47. Lopez-Martin, A.J., Verweij, J., Blay, J., Le Cesne, A., Judson, I., Misset, J., Seiden, M., et al., An exploratory analysis of tumor growth rate (TGR) variations induced by trabectedin (ecteinascidin-743, ET-743) in patients (pts) with pretreated advanced soft tissue sarcoma (PASTS), Abstract no. 3293. American Society of Clinical Oncology (ASCO), 39th Annual Meeting, May 31-June 3. Chicago, IL, USA. 2003.
48. Van Glabbeke, M., Verweij, J., Judson, I., and Nielsen, O.S., On behalf of the EORTC Soft Tissue and Bone Sarcoma Group. Progression-free rate as the principal end-point for phase II trials in soft-tissue sarcomas, *Eur. J. Cancer*, 38, 543–549, 2002.
49. Del Campo, J.M., Muñoz-Couselo, E., Diaz de Corcuera, I., and Oaknin, A., Trabectedin combined with liposomal doxorubicin in women with relapsed ovarian cancer, *Expert Rev. Anticancer Ther.*, 10, 795–805, 2010.
50. Kaye, S.B., Colombo, N., Monk, B.J., Tjulandin, S., Kong, B., Roy, M., Chan, S., et al., Trabectedin plus pegylated liposomal doxorubicin in relapsed ovarian cancer delays third-line chemotherapy and prolongs the platinum-free interval, *Ann Oncol.*, 22, 49–58, 2011.
51. European Medicines Agency (EMA). Assessment report for Yondelis. International non-propietary name/Common name: trabectedin. Procedure. No. EMEA/H/C/000773-II/0008. http://www.ema.europa.eu/docs/en_GB/document_library/EPAR_-_Product_Information/human/000773/WC500045832.pdf. 2010.
52. Rinehart, K.L. and Lithgow-Berelloni, A.M., Novel antiviral and cytotoxic agent, PCT Int. Pat. Appl. WO 91.04985, Apr. 18, 1991; GB Appl. 89/22,026, Sept. 29, 1989; Chem. Abstr., 1991, 115, 248086q.
53. Rinehart, K.L., Gloer, J.B., Carter Cook Jr., J., Mizsak, S.A., and Scahill, T.A., Structures of the didemnins, antiviral and cytotoxic depsipeptides from a Caribbean tunicate, *J. Am. Chem. Soc.*, 103, 1857–1859, 1981.
54. Rinehart, K.L., Kishore, V., Bible, K.C., Sakai, R., Sullins, D.W., and Li, K-M., Didemnins and tunichlorin: novel natural products from the marine tunicate *Trididemnum solidum*, *J. Nat. Prod.*, 51, 1–21, 1988.
55. Urdiales, J.L., Morata, P., Núñez De Castro, I., and Sánchez-Jiménez, F., Antiproliferative effect of dehydrodidemnin B (DDB), a depsipeptide isolated from Mediterranean tunicates, *Cancer Lett.*, 102, 31–37, 1996.
56. Faircloth, G.T., Rinehart, K., Nuñez de Castro, I., and Jimeno, J., Dehydrodidemnin B, a new marine derived antitumor agent with activity against experimental tumor models, *Ann. Oncol.*, 7 (Suppl. 1), 34 (Abstract no. 111), 1996.
57. Sakai, R., Rinehart, K.L., Kishore, V., Kundu, B., Faircloth, G., Gloer, J.B., Carney, J.R., et al., Structure activity relationships of didemnins, *J. Med. Chem.*, 39, 2819–2834, 1996.
58. Garcia-Fernandez, L.F., Losada, A., Alcaide, V., Alvarez, A.M., Cuadrado, A., González, L., Nakayama, K., et al., Aplidin™ induces the mitochondrial apoptotic pathway via oxidative stress-mediated JNK and p38 activation and protein kinase C δ, *Oncogene*, 21, 7533–7544, 2002.
59. Gajate, C. and Mollinedo, F., Rapid and selective apoptosis in human leukemic cells induced by Aplidine through a Fas/CD95- and mitochondrial-mediated mechanism, *Clin. Cancer Res.*, 9, 1535–1545, 2003.
60. Caers, J., Menu, E., De Raeve, H., Lepage, D., Van Valckenborgh, E., Van Camp, B., Alvarez, E., and Vanderkerken, K., Antitumor and antiangiogenic effects of Aplidin in the 5TMM syngeneic models of multiple myeloma, *Br. J. Cancer*, 98, 1966–1974, 2008.
61. Mitsiades, C.S., Ocio, E.M., Pandiella, A., Maiso, P., Gajate, C., Garayoa, M., Vilanova, D., et al., Aplidin, a marine organism-derived compound with potent antimyeloma activity *in vitro* and *in vivo*, *Cancer Res.*, 68, 5216–5525, 2008.
62. Cuadrado, A.J., Garcia-Fernandez, L.F., Gonzalez, L., Suarez, Y., Losada, A., Alcaide, V., Martinez, T., et al., Aplidin induces apoptosis in human cancer cells via glutathione depletion and sustained activation of the epidermal growth factor receptor, Src, JNK, and p38 MAPK, *J. Biol. Chem.*, 278, 241–250, 2003.
63. Cuadrado, A., González, L., Suárez, Y., Martínez, T., and Muñoz, A., JNK activation is critical for Aplidin-induced apoptosis, *Oncogene*, 23, 4673–4680, 2004.
64. Gonzalez-Santiago, L., Suárez, Y., Zarich, N., Muñoz-Alonso, M.J., Cuadrado, A., Martínez, T., Goya, L., et al., Aplidin induces JNK-dependent apoptosis in human breast cancer cells via alteration of glutathione homeostasis, Rac1 GTPase activation, and MKP-1 phosphatase downregulation, *Cell Death Differ.*, 13, 1968–1981, 2006.

65. Suárez, Y., González-Santiago, L., Zarich, N., Dávalos, A., Aranda, J.F., Alonso, M.A., Lasunción, M.A., Rojas, J.M., and Muñoz, A., Plitidepsin cellular binding and Rac1/JNK pathway activation depend on membrane cholesterol content, *Mol. Pharmacol.*, 70, 1654–1663, 2006.
66. Humeniuk, R., Menon, L.G., Mishra, P.J., Saydam, G., Longo-Sorbello, G.S., Elisseyeff, Y., Lewis, L.D., et al., Aplidin synergizes with cytosine arabinoside: Functional relevance of mitochondria in Aplidin-induced cytotoxicity, *Leukemia*, 21, 2399–2405, 2007.
67. Muñoz-Alonso, M.J., González-Santiago, L., Martínez, T., Losada, A., Galmarini, C.M., and Muñoz, A., The mechanism of action of plitidepsin, *Curr. Opin. Investig. Drugs*, 10, 536–542, 2009.
68. Maier, A., *In vitro* evaluation of PM00104 (Zalypsis®), PM02734, and Aplidin (PM90001, Plitidepsin) for anticancer activity in human tumor xenografts using a clonogenic assay. P62D. PharmaMar data on file. 2007.
69. Sanchez, E. and Berenson, J., Use of human myeloma tumors growing in SCID mice to determine the in vivo effects of Aplidin (APLD) in combination with dexamethasone. PharmaMar data on file. 2009.
70. Verrucci, M., Pancrazzi., A, Aracil, M., Martelli, F., Guglielmelli, P., Zingariello, M., Ghinassi, B., et al., CXCR4-independent rescue of the myeloproliferative defect of the gata1low myelofibrosis mouse model by Aplidin, *J. Cell Physiol.*, 225, 490–499, 2010.
71. Maghazachi, A.A., *In vitro* and *in vivo* evaluation of aplidin alone and in combination with rituxan in human T cell lymphoma. 22-0977-PMM-IA, B, C and D. PharmaMar data on file. 2007.
72. Guillen, M.J., Efficacy study of Aplidin (PM90001), Bevacizamab (Avastin) and Temsirolimus (Torisel) administered as single agents and in combination against MRI-H-121, subcutaneous human renal xenograft model in mice. Study No PUSA00780. PharmaMar data on file. 2007.
73. Guillen, M.J., Efficacy study of Aplidin (PM90001) and Bevacizamab (Avastin) administered as single agents and in combination against A2780, human ovarian xenograft model in mice. Study No PUSA00784. PharmaMar data on file. 2008.
74. Guillen, M.J., Response of Aplidin (PM90001) administered alone and in combination with SOC agents: Avastin and Torisel in the subcutaneously implanted human breast xenograft model, MDA-MB-231. Study No PUSA00807. PharmaMar data on file. 2008.
75. Guillen, M.J., Response of Aplidin (PM90001) administered alone and in combination with SOC agents: Avastin and Torisel in the subcutaneously implanted human NSCLC xenograft model, NCI-H-460 in mice. Study No PUSA00798. PharmaMar data on file. 2008.
76. Guillen, M.J., Response of Aplidin (PM90001) administered alone and in combination with SOC agents: Avastin in the subcutaneously implanted human ovarian xenograft model, SK-OV-3. Study No PUSA00803. PharmaMar data on file. 2008.
77. Guillen, M.J., Response of Aplidin (PM90001) Administered Alone and in Combination with SOC Agent: Nexavar® (Sorafenib) in the Subcutaneously Implanted Human Melanoma Xenograft Model, LOX-IMVI. Study No PUSA00828. PharmaMar data on file. 2008.
78. Mishra, P.J., Longo-Sorbello, G.S.A., Mishra, P.J., Aracil, M., Paz de Paz, M.F., Bertino, J.R., and Banerjee, D., Synergistic action of plitidepsin and gemcitabine against pancreatic cancer *in vitro* and *in vivo*. Abstract no. 4501. In Proceedings of 100th American Association for Cancer Research Meeting, April 18–22, Denver, CO, USA. 2009.
79. Mejer, C., The effects of Aplidine on the respiratory rate and tidal volume in Sprague Dawley rats. SPR04-001. PharmaMar data on file. 2004.
80. Mejer, C., The effects of Aplidine in the Irwin test in Sprague Dawley rats. SPI04-001. PharmaMar data on file. 2004.
81. Yao, J., Effects of Aplidine on HERG tail current recorded from stably transfected HEK293 cells. SPH03-032. PharmaMar data on file. 2004.
82. Love, S.D., Effects of Aplidine on action potential parameters in dog isolated cardiac Purkinje fibers. SPP03-014. PharmaMar data on file. 2004.
83. Roche, B., Exploratory study of the effects of escalating doses of Aplidin on: RR, QTc, VP/dtmax and dLVP/dtmin in a Guinea Pig Langendorff Preparation. SPLG06-003. PharmaMar data on file. 2007.
84. Hoagland, K.M., The cardiovascular effects of Aplidine in conscious, telemetered Beagle dogs. SPT03-020. PharmaMar data on file. 2004.
85. Robbins, M.C., A single dose toxicity study in the mouse by the intravenous route (with Aplidine). Bibra Report No. 3170/1/2/97. PharmaMar data on file. 1997.
86. Robbins, M.C., Single dose intravenous toxicity study of three test substance (Aplidin) in mice. BIBRA 3170/2/2/98. PharmaMar data on file. 1998.
87. Robbins, M.C., A single toxicity study in the mouse by the intravenous route (with Aplidine). BIBRA Report No. 3170/3/2/98. PharmaMar data on file. 1998.

88. Robbins, M.C., A single dose toxicity study in the rat by the intravenous route (with Aplidine). BIBRA Report No. 3170/4/2/98. BIBRA International, Woodmansterne Road, Carshalton, Surrey UK. PharmaMar data on file. 1998.
89. Robbins, M.C., A multiple dose toxicity study in the mouse by the intravenous route (with Aplidine). BIBRA Report No. 3170/5/2/98. PharmaMar data on file. 1998.
90. Robbins, M.C., A multiple dose toxicity study in the rat by the intravenous route (with Aplidine). BIBRA Report No. 3170/6/2/98. PharmaMar data on file. 1998.
91. Brown, A.P., Intravenous toxicity study of Aplidine administered for five consecutive days in Beagle dogs. UIC/TRL Study No.: 291. PharmaMar data on file. 1998.
92. Lyubimov, A.V., Three cycle toxicity study of Aplidine via intravenous administration to male and female CD rats. UIC/TRL Study No.: 421. PharmaMar data on file. 2002.
93. Sisti, R., Aplidin (Plitidepsin). Multiple-cycle toxicity study following 12 cycles of administration by intravenous route to SD rats with two or four weeks of recovery. RTC70760. PharmaMar data on file. 2009.
94. Lyubimov, A.V., Three cycle toxicity of Aplidin via intravenous administration to Beagle dogs. UIC/TRL 419. PharmaMar data on file. 2002.
95. Vera, M.D. and Joullié, M.M., Natural products as probes of cell biology: 20 years of didemnin research, *Med. Res. Rev.*, 22, 102–145, 2002.
96. Schmidt, U., Kroner, M., and Griesser, H., Total synthesis of the didemnins—I. Synthesis of the peptolide ring, *Tetrahedron Lett.*, 29, 3057–3060, 1988.
97. Schmidt, U., Kroner, M., and Griesser, H., Total synthesis of the didemnins—II. Synthesis of didemnins A, B, C and prolyldidemnin A, *Tetrahedron Lett.*, 29, 4407–4408, 1988.
98. Schmidt, U., Kroner, M., and Griesser, H., Total synthesis of the didemnins—III. Synthesis of proptected (2*R*,3*S*)-Alloisoleucine and (3*S*,4*R*,5*S*)-Isostatine derivatives-amino acids from hydroxy acids, *Synthesis*, 832–835, 1989.
99. Jou, G., González, I., Albericio, F., Lloyd-Williams, P., and Giralt, E., Total synthesis of dehydrodidemnin B. Use of uranium and phosphonium salt coupling reagents in peptide synthesis in solution, *J. Org. Chem.*, 62, 354–366, 1997.
100. Hamann, M.T. and Scheuer, P.J., Kahalalide F: A bioactive depsipeptide from the sacoglossan mollusk *Elysia rufescens* and the green alga *Bryopsis* sp., *J. Am. Chem. Soc.*, 115, 5825–5826, 1993.
101. López-Macià, Á., Jiménez, J.C., Royo, M., Giralt, E., and Albericio, F., Synthesis and structural determination of Kahalalide F, *J. Am. Chem. Soc.*, 123, 11398–11401, 2001.
102. Hamann, M.T., Otto, C.S., Scheuer, P.J., and Dunbar, D.C., Kahalalides: bioactive peptides from a marine mollusk *Elysia rufescens* and its alga diet *Bryopsis* sp., *J. Org. Chem.*, 61, 6594–6600, 1996.
103. Green, B.J., Li, W-Y, Manhart, J.R., Fox, T.C., Summer, E.J., Kennedy, R.A., Pierce, S.K., and Rumpho, M.E., Mollusc-algal chloroplast endosymbiosis. Photosynthesis, thylakoid protein maintenance, and chloroplast gene expression continue for many months in the absence of the algal nucleus, *Plant Physiol.*, 124, 331–342, 2000.
104. Becerro, M.A., Goetz, G., Paul, V.J., and Scheuer, P.J., Chemical defences of the sacoglossan mollusk *Elysia rufescens* and its host alga *Bryopsis* sp., *J. Chem. Ecology*, 27, 2287–2299, 2001.
105. Molina-Guijarro, J.M., Moneo, V., Martínez-Leal, J.F., Cuevas, C., García-Fernández, L.F., and Galmarini, C.M., PM02734, a new marine-derived antitumoral compound, has rapid effects on membrane integrity and permeability in tumor cells. Abstract no. 888. In Proceedings of 100th American Association for Cancer Research Meeting, April 18–22, Denver, CO, USA. 2009.
106. Molina-Guijarro, J.M., Moneo, V., Martínez-Leal, J.F., Cuevas, C., García-Fernández, L.F., and Galmarini, C.M., Modulation of the early cytotoxic effects of Irvalec by zinc and DIDS in lung tumor cells. Abstract no. 4454. In Proceedings of 101th American Association for Cancer Research Meeting, April 17–21, Washington, D.C., USA. 2010.
107. Herrero, A.B., Astudillo, A.M., Balboa, M.A., Cuevas, C., Balsinde, J., and Moreno, S., Levels of SCS7/FA2H-mediated fatty acid 2-hydroxylation determine the sensitivity of cells to antitumor PM02734, *Cancer Res.*, 68, 9779–9787, 2008.
108. Sasak, H, Yin, J., Elices, M., LePage, D., Cuevas Marchante, C., Avilés, P., and Faircloth, G., PM02734 cytotoxicity in vitro and pharmacokinetics. Abstract no. 1911. In Proceedings of 97th American Association for Cancer Research Meeting, April 1–5, Washington, D.C., USA. 2006.
109. Ling, Y.H., Aracil, M., Jimeno, J., Perez-Soler, R., and Zou, Y., Molecular pharmacodynamics of PM02734 (elisidepsin) as single agent and in combination with erlotinib; synergistic activity in human non-small cell lung cancer cell lines and xenograft models, *Eur. J. Cancer*, 45, 1855–1864, 2009.

110. Elices, M., Lepage, D.J., Grant, W., Alvarez, E., Guillen, M.J., Cuevas, C., Aviles, P., and Faircloth, G., Activity of PM02734 against human breast and prostate tumors. Abstract no. 1107. In Proceedings of 97th American Association for Cancer Research Meeting, April 1–5, Washington, D.C., USA. 2006.
111. Serova, M., Astorgues-Xerri, L., Koumaravel, J., Aracil, M., Faivre, S., and Raymond, E., Irvalec, a novel marine cyclic peptide, enhances the antiproliferative effects of other anticancer drugs in human cancer cell lines. Abstract no. 4569. In Proceedings of 100th American Association for Cancer Research Meeting, April 18–22, Denver, CO, USA. 2009.
112. Mejer, C., The Effects of PM02734 on Respiratory Rate and Tidal Volume in Sprague Dawley Rats. SPR04-024. PharmaMar data on file. 2005.
113. Mejer, C., The Effects of PM02734 in the Irwin Test in Sprague Dawley Rats. SPI04-026. PharmaMar data on file. 2005.
114. Gayheart-Walsten, P., The Cardiovascular Effects of PM02734 in Conscious, Telemeterd Beagle Dogs. SPT04-032. PharmaMar data on file. 2005.
115. Yao, J., Effects of PM02734 on HERG Tail Current Recorded from Stably Transfected HEK293 Cells. SPH04-033. PharmaMar data on file. 2005.
116. LaRochelle, A.L., Twenty-Four Hour Intravenous Infusion Maximum Tolerated Dose (MTD) Study of PM02734 in Rats. APA00006. PharmaMar data on file. 2005.
117. LaRochelle, A.L., Pilot Twenty-Four Hour Intravenous Infusion Toxicity Study of PM02734 in Rats. APA00008. PharmaMar data on file. 2005.
118. Bonnette, K.L., Single Dose Intravenous Maximum Tolerated Dose (MTD) Study of PM02734 in Dogs. APA00001. PharmaMar data on file. 2005.
119. Bonnette, K.L., Pilot Single Dose Bolus Intravenous Toxicity Study of PM02734 in Dogs. APA00003. PharmaMar data on file. 2005.
120. Bonnette, K.L., Twenty-Four Hour Continous Intravenous Infusion Maximum Tolerated Dose (MTD) Study of PM02734 in Dogs. APA00007. PharmaMar data on file. 2005.
121. LaRochelle, A.L., Pilot Twenty-Four Hour Intravenous Infusion Study of PM02734 in Dogs. APA00009. PharmaMar data on file. 2005.
122. Bonnette, K.L., A two Cycle Single Dose Bolus Intravenous Toxicity Study of PM02734 in Rats. APA00002. PharmaMar data on file. 2005.
123. LaRochelle, A.L., Two Cycle, Twenty-Four Hour Intravenous Infusion Toxicity Study of PM02734 in Rats. APA00010. PharmaMar data on file. 2005.
124. Bonnette, K.L., A Two Cycle Single Bolus Intravenous Administration Toxicity Study of PM02734 in Dogs. APA00004. PharmaMar data on file. 2005.
125. LaRochelle, A.L., Two-Cycle Twenty-Four Hour Intravenous Infusion Study of PM02734 in Dogs. APA00011. PharmaMar data on file. 2005.
126. Bonnette, K.L., An Acute Intravenous and Perivenous Study in Rabbits with PM02734. APA00005. PharmaMar data on file. 2005.
127. Gracia, C., Isidro-Llobet, A., Cruz, L.J., Acosta, G.A., Álvarez, M., Cuevas, C., Giralt, E., and Albericio, F., Convergent Approaches for the synthesis of the antitumoral peptide, Kahalalide F. Study of Orthogonal Protecting Groups, *J. Org. Chem.*, 71, 7196–7204, 2006.
128. Jiménez, J.C., López-Macià, Á., Gracia, C., Varón, S., Carrascal, M., Caba, J.M., Royo, M., et al., Structure-activity relationship of Kahalalide F synthetic analogues, *J. Med. Chem.*, 51, 4920–4931, 2008.
129. Bruce J.Y., Geary, D., de las Heras, B., Soto, A., Garcia Paramio, P., Yovine, A., Schilsky, R.L., Undevia, S.D., and Ratain, M.J., Phase I study of PM02734: Association of dose-limiting hepatotoxicity with plasma concentrations, *J. Clin. Oncol.*, 2008 ASCO Annual Meeting Proceedings, 26 (Suppl. 15S), Abstract no. 2513, 2008.
130. Evans, T.R., Oaknin, A., Jones, R.J., Vandermeeren, A., Coronado, C., Soto-Matos, A., Germa, J.R., Crawford, D., Frontelo, P., and Salazar, R., Phase I dose-escalating study of PM02734 in a 24-hour infusion schedule every 21 days in advanced solid tumors, *J. Clin. Oncol.*, 2009 ASCO Annual Meeting Proceedings, 27 (Suppl. 15S), Abstract no. 2511, 2009.

13 Discovery of E7389, A Fully Synthetic Macrocyclic Ketone Analog of Halichondrin B*

Melvin J. Yu, Yoshito Kishi, and Bruce A. Littlefield

CONTENTS

13.1 Introduction 317
13.2 Background 318
13.3 Halichondrin Structure–Activity Relationship 319
13.4 Total Synthesis and Compound Supply 320
13.5 Structure–Activity Relationship of Structurally Simplified Analogs 324
13.6 Synthesis of HB Analogs 333
13.7 *In Vitro* Characterization of E7389 333
13.8 *In Vivo* Characterization of E7389 334
13.9 Conclusion 336
Acknowledgments 337
Update 338
References 339

13.1 INTRODUCTION

E7389, a fully synthetic analog of the structurally complex marine natural product halichondrin B (HB), exhibits unique effects on tubulin dynamics, along with striking anticancer activity in preclinical models of human cancer. The nature of E7389's antitumor activity in such models, combined with its novel tubulin-based effects and superiority over paclitaxel in several animal models, indicates that this agent may exhibit a unique spectrum of antitumor activities in the clinic that will differentiate it from existing anticancer drugs.

Limited supply of natural halichondrins from the wild, a serious obstacle common to other structurally complex marine natural products isolated in low yield, represented a critical issue that all but precluded development of these compounds as drug candidates. Three issues in particular affected the halichondrins. These included securing the required absolute amount of material with a consistent impurity profile to support drug development activities, separating the desired halichondrin from other members of the family closely related in structure, and removing highly toxic coisolated metabolites such as okadaic acid (a known contaminant in extracts from *Halichondria okadai*). The limited supply of halichondrins and strong interest on the part of the U.S. National Cancer Institute (NCI) to develop HB as a new anticancer drug created the need to identify alternative sources of this important class of marine natural products.

* This chapter has been updated by David J. Newman, Natural Products Branch, Developmental Therapeutics Program, Division of Cancer Treatment and Diagnosis, National Cancer Institute, Frederick, MD.

Despite the chemical complexity of the halichondrin family, total synthesis represented the most attractive option to not only identify an optimized analog for drug development, but also provide the means for a reliable and renewable source of material. With the ability to address problems at the molecular level, to fine-tune pharmacological properties, and to adjust physicochemical parameters, E7389 was identified as the most promising analog, with biological characteristics matching or surpassing those of the natural product that inspired it. Although the chemical structure of E7389 is significantly less complex than HB, it nevertheless remains a challenging synthetic target. However, contemporary synthetic organic chemistry has both the capacity and the potential to meet this challenge. With preclinical development work completed, clinical evaluation of this novel agent is now underway to establish the therapeutic value of halichondrin-based drugs as anticancer therapeutics.

13.2 BACKGROUND

HB is a polyether macrolide that exhibits remarkable anticancer activity in preclinical animal models of human cancer. First isolated in the mid-1980s from the western Pacific marine sponge *H. okadai* Kadota,[1,2] members of the Halichondrin family were subsequently found in *Axinella* sp.,[3] *Phakellia carteri*,[4] and most recently, *Lissodendoryx* sp.[5] Trace quantities of halichondrins were also detected in an extract of the black New Zealand shallow-water sponge *Raspalia agminata*.[6] Members of the halichondrin family include halichondrins B and C, norhalichondrins A, B, and C, homohalichondrins A, B, and C, halistatins 1 and 2, isohomohalichondrin B, neonorhalichondrin B, neohomohalichondrin B, and 55-methoxyisohomohalichondrin B (Figure 13.1). Differences between members of this family lie primarily in the level of oxygenation at C.10, C.12, and C.13 and in the length of the carbon backbone. Of these compounds, the most potent include HB (**1a**) and homohalichondrin

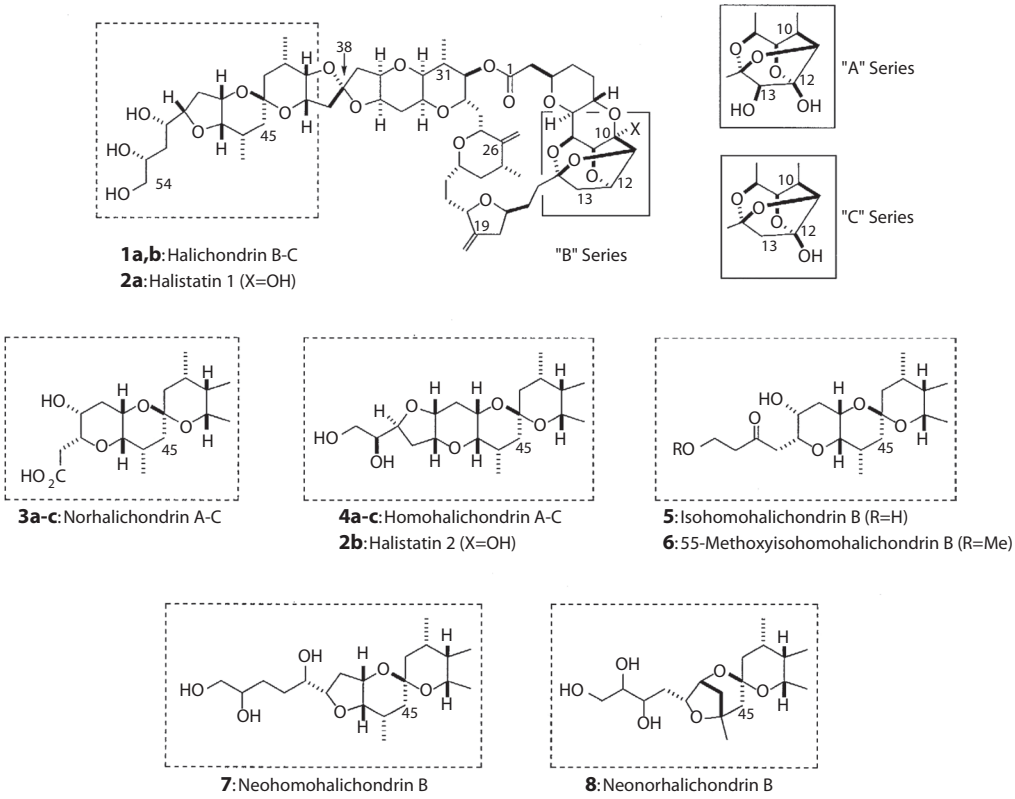

FIGURE 13.1 Halichondrin family (X=H unless otherwise noted).

B (**4b**). The name halipyran was proposed by Pettit et al. for the conserved unsubstituted C.1–C.38 carbon skeleton common to the halichondrin family of marine natural products.[4]

Mechanistically, the halichondrins make up a subtype of tubulin-interactive antimitotic agents with subtle differences in mechanism of action from those of other antimitotics such as the vinca alkaloids.[7] Although classified as a tubulin depolymerizer, the pattern of tubulin interaction by the halichondrins is highly specific.[8] Testing against the 60 human tumor cell lines of the NCI's drug screening program demonstrated that HB exhibited subnanomolar growth-inhibitory activity against a wide variety of cancer cell types *in vitro*, consistent with a tubulin-based antimitotic mechanism.[9] These conclusions were further supported by findings that low micromolar concentrations of the drug inhibited various aspects of tubulin function *in vitro*, including tubulin polymerization, microtubule assembly, β^s-tubulin cross-linking, GTP and vinblastine-binding to tubulin, and tubulin-dependent GTP hydrolysis.[10,11] Although such *in vitro* findings are consistent with a vinca alkaloid-like antitubulin mechanism, they must still be viewed in light of the approximately 10^4-fold discrepancy between the micromolar concentrations required for antitubulin effects *in vitro* and the subnanomolar concentrations that inhibit cell growth. This discrepancy is shared by other tubulin-active drugs and may reflect direct or indirect effects on microtubule dynamics at low drug concentrations rather than net changes in microtubule content seen at higher drug concentrations.[12,13] Other members of the halichondrin family reported to disrupt microtubule networks by preventing microtubule assembly include isohomohalichondrin B.[14]

Recent studies by Jordan et al. with E7389, a synthetic analog of HB, helped shed further light on the unique mechanism of microtubule disruption by the halichondrin-class molecules.[15] Although many tubulin-based antimitotic agents exert their biological effects through direct interactions with microtubules, the halichondrins represented by E7389 suppressed microtubule dynamics by inducing nonproductive tubulin aggregates, leading to suppression of spindle microtubule growth events and reduced microtubule polymer mass. This mechanism differs significantly from that of other tubulin-interactive drugs such as vinblastine or paclitaxel, and is consistent with the highly specific pattern of tubulin interaction by HB reported by Hamel et al. The novel mechanism of E7389 relative to existing tubulin-based drugs further supports the halichondrins as a unique subtype of tubulin-based antimitotics and raises the possibility that compounds from this class may exhibit unique characteristics in the clinic as cancer chemotherapeutic agents.

The high *in vitro* potency of HB is mirrored by its extraordinary anticancer activity in a variety of preclinical animal models. HB was reported by Hirata and Uemura in 1986 to increase mean survival times of mice bearing murine B16 melanoma and P388 and L1210 leukemias.[2] Efficacy in these animal models was also reported in the patent literature by Fujisawa scientists that same year.[16] In 1996, Fodstad et al. described the remarkable activity of halichondrins isolated from natural sources in a number of human tumor xenograft models including melanoma, osteogenic sarcoma, lung cancers, and colon cancers.[7] Synthetic HB prepared by Kishi et al. at Harvard University similarly exhibited impressive activity in human tumor xenograft models.[17] For example, dose-dependent inhibition of subcutaneous LOX human melanoma xenografts was observed in nude mice following intraperitoneal administration (5–25 μg/kg). At 50 μg/kg, tumor growth was completely suppressed, with no visible signs of toxicity.[17]

The extraordinary *in vitro* potency, *in vivo* efficacy, and distinct antitumor profile of the halichondrins in human tumor models led the NCI to select HB for preclinical development as an anticancer chemotherapeutic agent in 1992.

13.3 HALICHONDRIN STRUCTURE–ACTIVITY RELATIONSHIP

Based on limited cytotoxicity data of naturally occurring halichondrins A–C, norhalichondrin A, and homohalichondrin B in B16 melanoma cells *in vitro*, Hirata and Uemura[2] proposed that the 2,6,9-trioxatricyclo[3.3.2.$0^{3,7}$]decane system should be relatively lipophilic (HB-type) and that the terminal moiety should contain two or three hydroxyl groups, but not a carboxylate, for maximum

expression of antitumor activity. Because the length of the halichondrin molecules was estimated to be 30–35Å, corresponding to half the distance of a lipid biomembrane, Hirata and Uemura speculated that the 2,6,9-trioxatricyclo[3.3.2.0^{3,7}]decane portion of the molecule may be important for insertion into the lipid bilayer.

Activity in the NCI 60–human tumor cell line panel of several naturally occurring and semisynthetic halichondrin derivatives was summarized in a review by Munro.[6] Hydrolysis of the macrolactone ring to the corresponding seco acid and reduction of the exo-olefin groups at C.19 and C.26 were both detrimental to *in vitro* biological activity. Acid-induced rearrangement of homohalichondrin B similarly provided products with diminished biological activity. Treatment with excess trifluoroacetic acid in CH_2Cl_2 at 20°C, for example, led to spiroacetal epimerization at C.38 or rearrangement of the 2,6,9-trioxatricyclo[3.3.2.0^{3,7}]decane ring system to a furan derivative.[18] Of the two acid-induced rearrangement pathways, epimerization at C.38 was reportedly more detrimental to biological acvity, affording compounds with a two-log shift in GI_{50} values in the NCI 60–human tumor cell line panel, along with correspondingly major changes in molecular conformation. Extrapolating these results to other naturally occurring members of the halichondrin family, Munro speculated that epimerization at C.38 would, in general, lead to halichondrin derivatives with diminished biological activity. For example, the C.38 epimer of isohomohalichondrin was less active against murine leukemia P388 cells *in vitro* compared with natural material.[5] However, minor modifications to the terminal region of the halichondrins were well tolerated, with minimal impact on *in vitro* potency.

Using HB as the seed compound, correlation coefficients from a COMPARE analysis using a GI_{50}-centered mean graph profile as a qualitative index of antimitotic ability were plotted against GI_{50} values for CCRF-CEM cells as an index of cytotoxicity. The resulting scatter did not allow Munro et al. to draw meaningful conclusions regarding structure–activity relationships for these compounds based on subtle differences in the antimitotic mean graph profile relative to HB. However, significant differences in the average solution conformation in $CDCl_3$ were noted for the less cytotoxic compounds despite similar COMPARE correlation coefficients. Thus, Munro concluded that conformational changes resulting from structural modifications diminished biological activity without altering the antimitotic profile characteristic of HB.

13.4 TOTAL SYNTHESIS AND COMPOUND SUPPLY

Because of the extraordinary *in vivo* potency of the halichondrins, the amount of material required to support preclinical development and eventual clinical investigation was estimated to be approximately 10 g.[6] Assuming success in clinical trials, supply of the halichondrins to meet commercial needs was similarly estimated to be relatively small, at 1–5 kg/year. However, securing even these modest amounts through collection from the wild was determined to be unlikely because of the extremely low yield of halichondrins isolated from natural sources, the low abundance of known HB-producing sponges in the world, and the environmental effect of subjecting deep-sea sponges to large-scale harvesting, with risk of extinction. As a result, compound supply represented a significant obstacle for both development and possible future commercialization of HB as an anticancer drug. Although initial aquaculture feasibility trials on *Lissodendoryx* sp. 1 demonstrated the potential for halichondrins to be isolated from a cultured sponge,[6] the ability of scale-up operations to meet commercial demands of bulk drug substance that satisfy purity specifications in a reliable, economic, and consistent manner remains unknown.

The difficulties associated with securing the needed absolute amount of material for development and possible commercialization are not unique to the halichondrins[19] and represent only one aspect of the supply issue surrounding natural products isolated in extremely low yield from the producing organism. For example, separation of the desired halichondrin (e.g., HB) from other closely related family members, and the need to remove structurally unrelated but highly potent coisolated bioactive metabolites, added purification concerns to the list of compound supply challenges associated with

collection from the wild or through aquaculture techniques. These three issues made development of the halichondrins difficult; unfortunately, NCI's collaborative efforts to identify more widespread sources of the natural product met with only limited success, placing the program at risk of stalling at an early stage of preclinical development and leaving compound supply a serious concern for the NCI Drug Development Group (http://dtp.nci.nih.gov/docs/ddg/ddg_descript.html). Hirata and Uemura proposed that symbiotic microorganisms rather than the sponge itself may be responsible for producing the halichondrins as secondary metabolites.[2] Although the isolation of halichondrins from several marine sponges supported this proposal, no reports regarding the isolation, tissue culture, or fermentation of the putative producing organism or organisms have appeared in the literature, making this approach an unlikely near-term solution.

With compound supply an obstacle for preclinical development of this promising class of anticancer agents, alternative sources of the natural product were critically needed. The extraordinary biological activity of the halichondrins coupled with the extremely challenging and unique structural architecture of these compounds attracted the attention of chemistry research groups throughout the world. Although a number of laboratories reported synthetic studies on the halichondrins,[20–23] the only successful total synthesis to date was reported by Kishi et al. in 1992 for the total synthesis of HB and norhalichondrin B.[20] Kishi's approach was highly convergent, bringing together four major fragments corresponding to the C.1–C.13, C.14–C.26, C.27–C.38, and C.39–C.54 regions of the molecule for final assembly (Figure 13.2). The convergent nature of this approach allowed the chemistry of individual fragments to be further optimized independent of one another, with minimal effect on late-stage coupling or protecting group strategies.[20] In addition, Kishi's synthesis was

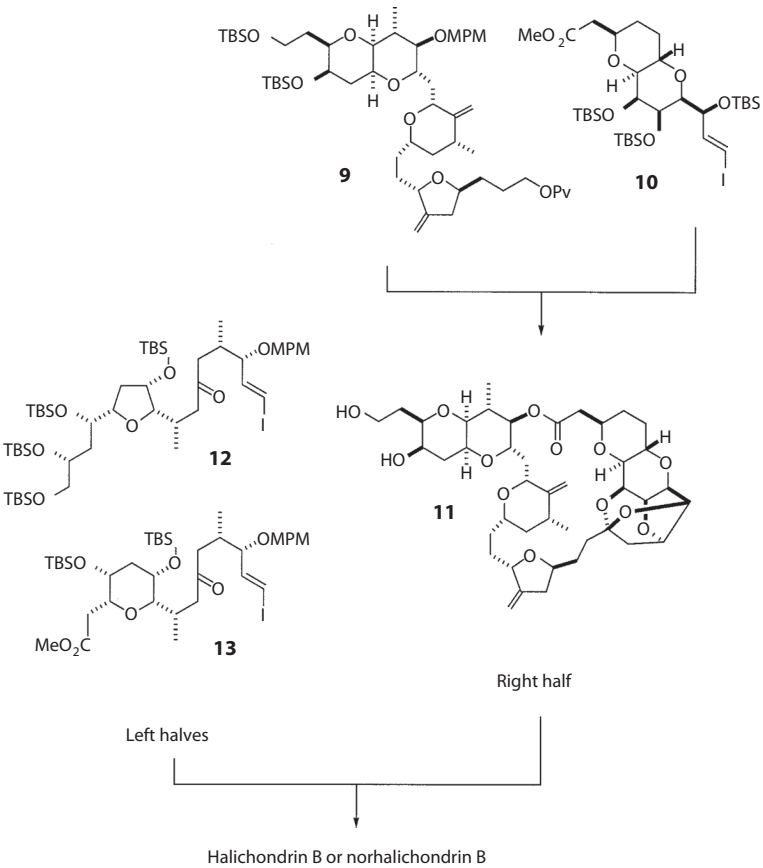

FIGURE 13.2 Kishi total synthesis of HB and norhalichondrin B.

extremely flexible, allowing structural modifications to be made in a modular fashion, thereby facilitating the use of key stockpiled intermediates to prepare different members of the halichondrin family (e.g., synthesis of HB or norhalichondrin B from common "right half" intermediate **11**).

The availability of pure natural product via total synthesis was an important factor in the NCI Decision Network Committee's decision to select HB for preclinical development in March 1992.[24] Total synthesis provided not only a reliable source of material free from potentially toxic coisolated contaminants such as okadaic acid, but also the tools for directed structure modification and the opportunity to identify novel analogs with optimized biopharmaceutical and physicochemical properties not accessible through semisynthesis or derivatization of the natural product itself. The ability to address problems at the molecular level, to fine-tune pharmacological properties as well as metabolic and chemical stability, aqueous solubility, and compound purity, were all essential factors for identifying and bringing the best possible analog forward for clinical investigation.

Although a number of synthetic intermediates and model systems were generated in connection with the synthetic efforts launched by research groups worldwide, biological data for only a handful of compounds were reported in the literature. In 1992, synthetic HB and several synthetic intermediates from the Kishi group at Harvard University were kindly provided to Eisai Research Institute for *in vitro* and *in vivo* biological evaluation as anticancer agents. As expected, potent cell growth-inhibitory activity was observed for synthetic HB. Surprisingly, however, synthetic intermediate **11** corresponding to the C.1–C.38 "right half" fragment of the natural product exhibited *in vitro* activity within an order of magnitude of the natural product in a 3–4 days growth-inhibition assay, using DLD-1 human colon cancer cells.[20,25,26] This compound represented the first example of a structurally simplified synthetic analog of HB exhibiting potent antiproliferative activity, thereby providing experimental evidence that biological activity was associated with the macrocyclic moiety. Both HB and **11** blocked cells at the G2/M phase of the cell cycle, both disrupted normal mitotic spindle architecture through microtubule destabilization with few if any effects on other phases of the cell cycle, and both exhibited a similar profile in the NCI 60–cell line screen. The exciting discovery of a structurally simplified HB fragment that retains the potent cell growth-inhibitory activity of the natural product formed the basis for a research program at Eisai Research Institute to identify novel halichondrin-based anticancer agents using chemistry technology developed in the Kishi Laboratory at Harvard University.

Results obtained with biotinylated macrolactone analog **14** (Figure 13.3) provided the first direct proof of any halichondrin class molecule binding directly to tubulin itself.[27] Under the affinity chromatography conditions, it was not possible to identify the tubulin subtype targeted by the halichondrin macrolactone, as binding to either the α- or the β-tubulin subtype present in α/β-tubulin heterodimers would result in retention of both. The pattern of cell growth inhibition, cell cycle effects, mitotic spindle disruption, and affinity chromatography results taken together indicated that the structurally simplified macrolactone analogs share a similar or identical mechanism to parental HB. Thus, the structural elements necessary for anticancer biological activity reside in the

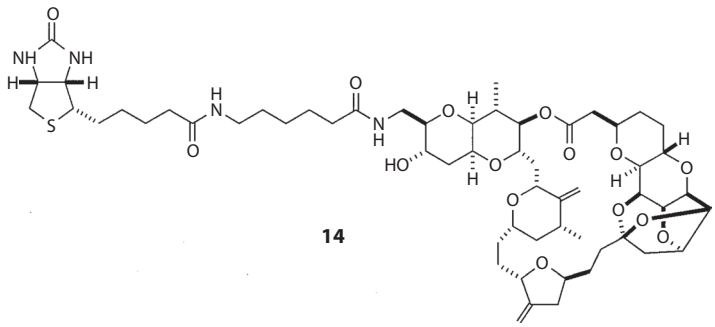

FIGURE 13.3 Biotinylated derivative of compound **11**.

macrocyclic sector of the molecule, providing a clear and compelling starting point for a structure–activity relationship investigation to identify the minimum pharmacophoric substructure for this family of marine natural products.

The discovery that a structurally simplified and synthetically accessible fragment of HB retained potent anticancer activity created the possibility that supply problems associated with the natural product itself could be circumvented. Specifically, if readily accessible halichondrin analogs that retain the full spectrum of remarkable biological activity associated with this family of compounds could be identified through total synthesis, then clinical evaluation of the halichondrin class of marine natural products could proceed with an optimized derivative to determine their value as chemotherapeutic agents in humans.

Horita and Yonemitsu in 1997 described a similar approach from their laboratory that bifurcated HB into partially overlapping polyether and macrolactone units (Figure 13.4).[28] Although the synthesis for each (compounds **15** and **16**, respectively) was reported in the literature, biological activity was presented only for early precursors rather than for the target compounds themselves (Figure 13.5 and Table 13.1). Interestingly, activity was noted for intermediates associated with both sections, although those corresponding to the polyether unit exhibited a higher level of cytotoxicity against KB and L1210 cells relative to those corresponding to the macrolactone region. Polyether analogs corresponding to the C.37–C.54 region of HB were described in the patent literature as antitumor agents with micromolar activity against a panel of 39 human tumor cell lines[29] and were shown in a university publication to have modest activity against MCF-7 breast and KE-4 esophagus cancer

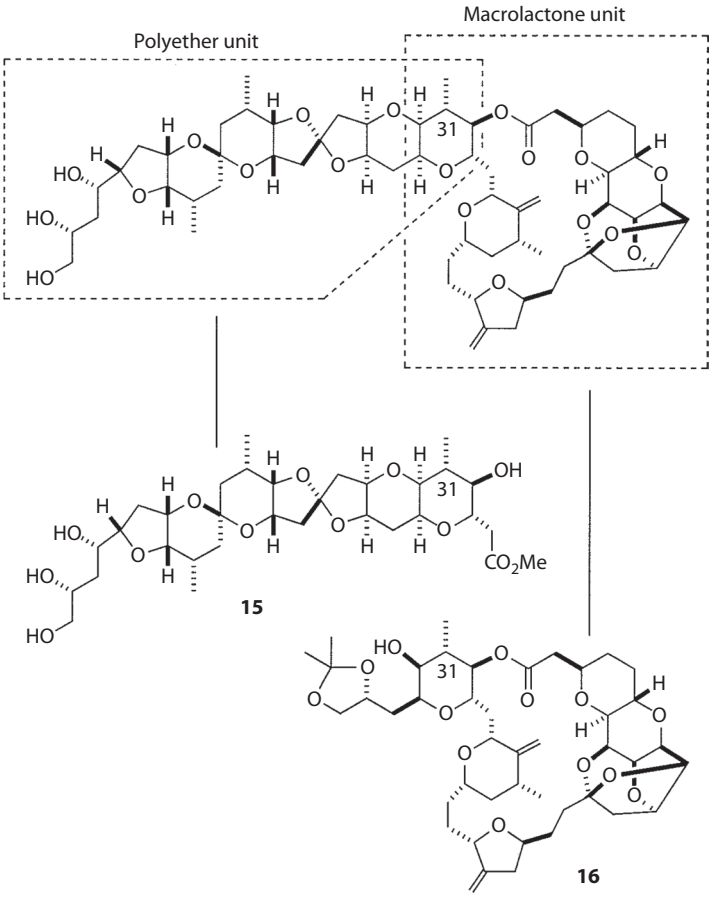

FIGURE 13.4 Yonemitsu synthetic study.

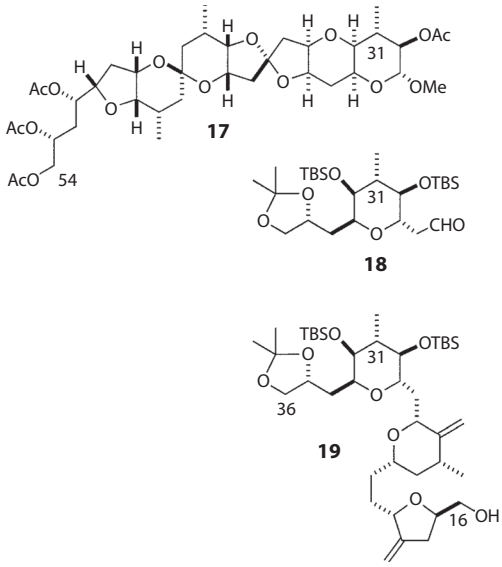

FIGURE 13.5 Representative synthetic intermediates reported by Yonemitsu et al. (Adapted from Horita, K., Nishibe, S., and Yonemitsu, O., Research on anti-tumor active site of marine source natural product, halichondrin B., *International Congress Series*, 1157 (Towards Natural Research in the 21st Century), 327, 1998.)

cells.[30] Because no details regarding mechanism of action for these compounds were provided, it is unclear whether any of the fragments inhibited cell growth through a tubulin-based antimitotic mechanism associated with the natural product.

13.5 STRUCTURE–ACTIVITY RELATIONSHIP OF STRUCTURALLY SIMPLIFIED ANALOGS

Despite the *in vitro* similarities, and in contrast to HB, compound **11** was not active in the *in vivo* LOX human melanoma xenograft model. Cell growth-inhibitory activity for both HB and **11** were similar under continuous exposure conditions in the 3–4 days cell growth assay. Flow cytometric analysis of U937 human histiocytic lymphoma cells, however, revealed a clear difference in ability of the two compounds to maintain a complete mitotic block (CMB) 10 h after drug washout.[31] Although a 10 nM concentration of HB was sufficient to induce and maintain a CMB, concentrations of **11** as high as 1 μM (highest tested concentration) were ineffective

TABLE 13.1
***In Vitro* Activity of HB Synthetic Intermediates**

	IC_{50} (nM)	
Compound	**KB**	**L1210**
17	8.3	0.64
18	3.9	3.1
19	> 100	28

Source: Adapted from Horita, K., Nishibe, S., and Yonemitsu, O., Research on anti-tumor active site of marine source natural product, halichondrin B., *International Congress Series*, 1157 (Towards Natural Research in the 21st Century), 327, 1998.

against this challenge. Thus, in contrast to the natural product, the antimitotic effects of **11** were reversible on washout. Cell viability dose–response curves 5 days postwashout tracked 10-h postwashout rather than 0-h prewashout IC_{99} values, indicating that long-term cell viability was dependent on continued maintenance of a CMB, rather than its initial induction. The reversible nature of **11** indicated that cell growth inhibition would only occur under continuous exposure conditions and that tumor inhibitory activity *in vivo* would cease when drug concentrations in blood fell below a certain critical threshold. On the basis of this working hypothesis, a proprietary cell-based assay was established at Eisai Research Institute that allowed measurement of a compound's ability to maintain a CMB following drug washout as an index of potential antitumor efficacy in *in vivo* settings, using standard intermittent dosing schedules.[32]

Macrolactone analogs modified at the C.30–C.38 region of the molecule were subsequently screened for both intrinsic cell growth-inhibitory activity under continuous exposure conditions as well as the ability to induce an irreversible CMB (Figure 13.6 and Table 13.2).[33] Although intrinsic potency was relatively insensitive to variations in this region of the molecule, the ability to induce an irreversible CMB was structure-specific. For example, compound **20**, prepared by the Kishi group at Harvard University in connection with an improved synthesis of the macrolactone fragment of HB, was the first structurally simplified macrolactone analog found to induce an irreversible CMB (postwashout $IC_{99} = 220$ nM). With a shortened side chain at C.36 and an epimeric hydroxyl group at C.35, this compound represented two structural changes from lead compound **11**, which exhibited a postwashout IC_{99} value greater than 1000 nM. Inverting the C.35 hydroxyl group of **11** alone (cf. **11** and **21**) was not sufficient to improve activity in the mitotic block reversibility assay. Consistent with the idea that induction of an irreversible CMB would permit manifestation of *in vivo* activity, compound **20** exhibited good antitumor activity in the LOX human melanoma xenograft model.[34] In contrast, analog **22**, a direct substructure of the natural product, exhibited a nearly identical *in vitro* profile to diol **11**, as did methoxyl derivative **23**. Increasing the size of the C.31 methyl substituent to

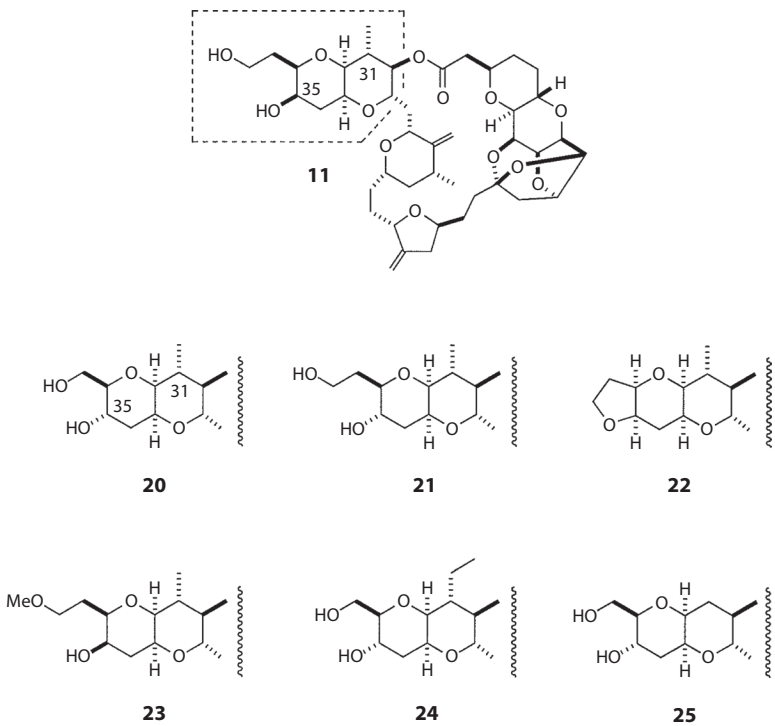

FIGURE 13.6 Representative octahydropyrano[3,2-b]pyran macrolactone analogs.

TABLE 13.2
***In Vitro* Biological Activity of Octahydropyrano[3,2-b]Pyran Macrolactone Analogs**

Compound	Intrinsic Potency, DLD-1 IC_{50} (nM)[a]	Mitotic Block Reversibility		
		U937 IC_{99} 0 h (nM)[b]	U937 IC_{99} 10 h (nM)[c]	Reversibility Ratio
11	4.6	30	>880	>29
20	3.4	9	220	24
21	3.6	10	>1000	>100
22	2.6	20	>1000	>50
23	1.2	7	>650	>93
24	6.0	10	1000	100
25	610.0	—	—	—
26	9.1	30	>1000	>33
27	59	300	>1000	>3
28	650	—	—	—

[a] Growth-inhibitory potency against DLD-1 cells after 3–4 days of continuous drug exposure.
[b] Induction of CMB in U937 cells after 12 h of drug exposure (0 h of washout).
[c] Maintenance of CMB 10 h after drug washout.

an ethyl group (e.g., **24**) led to a modest loss of potency, but removing this group altogether to give compound **25** reduced activity by over two orders of magnitude.

In addition to improving the *in vitro* profile of macrolactone (**11**), structural simplicity and compound accessibility were also major factors driving the structure–activity relationship investigation. For example, if the C.19, C.25, or C.26 substituents of compound **11** could be removed without significantly affecting biological activity (Figure 13.7), then the synthesis of the compounds could be simplified with enhanced access to these compounds. Analogs **26** and **27** indicated that complete removal of the C.19 and C.26 exo-olefins was tolerated, but removal of the C.25 methyl group to give macrolactone **28** reduced activity 100-fold (Table 13.2). Because modifying centers contained directly within the macrocyclic core uniformly led to analogs with equivalent or reduced activity, it

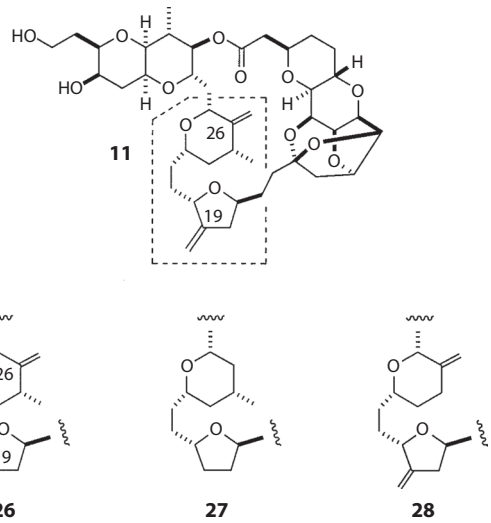

FIGURE 13.7 Representative deletion macrolactone analogs.

was hypothesized that the macrocyclic ring may represent the minimum pharmacophoric substructure of the halichondrins for cell growth-inhibitory activity. It should be noted, however, that these results apply only to the particular macrolactone analogs synthesized and tested. The possibility exists that other modifications (e.g., substitution patterns or conversion of the macrolactone ring to the corresponding macrolactam, macrocyclic ketone, carbocyclic ring, etc.) may lead to analogs where the same changes may not negatively affect activity.

As a result, the macrolactone ring was fixed and held constant as modifications to the fused C.29–C.32 pyran sector were explored. In support of this hypothesis, compound **29** (Figure 13.8) with a single tetrahydropyran ring in place of the C.29–C.36 octahydropyrano[3,2-b]pyran ring system exhibited *in vitro* biological activity comparable with lead compound **20** in terms of both intrinsic potency and ability to induce an irreversible CMB (Table 13.3). Modifications to the tetrahydropyran ring substituents, especially with regard to the C.32 hydroxyl group, however, had little effect on intrinsic potency, but a significant effect on the compound's reversibility characteristics.

The earlier structure–activity relationship investigation around the original octahydropyrano [3,2-b]pyran series of analogs demonstrated the importance of the C.31 substituent. Because small changes in substituent size (e.g., methyl to ethyl) were tolerated, extrapolation to the tetrahydropyran series suggested that replacing the C.31 methyl group with a methoxyl substituent would allow more ready access from commercially available carbohydrate precursors without compromising the biological activity of the final compound. The C.31 methoxyl derivative **30** was found to be equipotent with the corresponding C.31 methyl analog **29**, supporting the interchangeability of these two groups at this center of the molecule.

As observed with previous macrolactone analogs, modifications to the tetrahydropyran ring had no effect on intrinsic cell growth-inhibitory potency. Individually converting each of the hydroxyl groups of diol **30** to methyl ethers **31** and **32**, in contrast, provided highly reversible compounds, as measured by the U937 mitotic block reversibility assay. Shortening the C.33 side chain to a one-

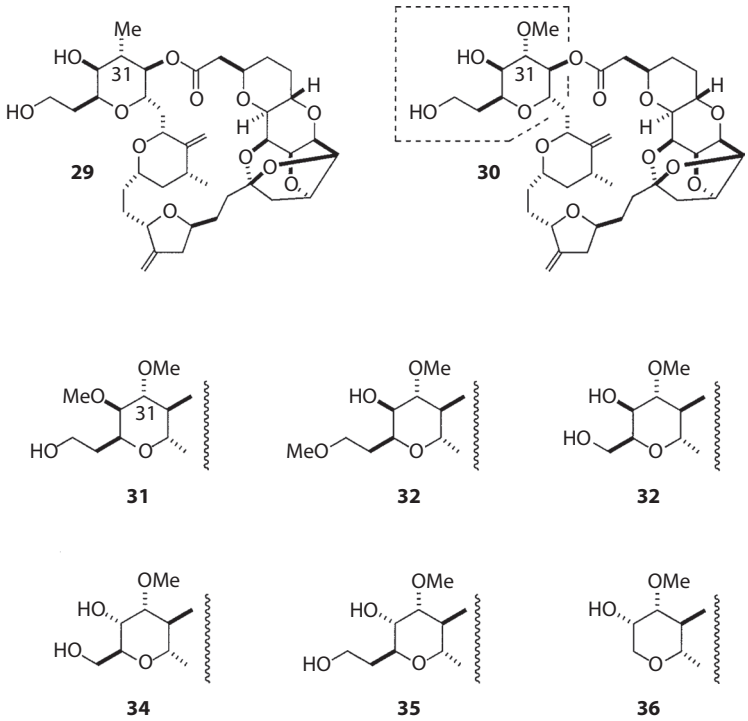

FIGURE 13.8 Representative tetrahydropyran macrolactone analogs.

TABLE 13.3
***In Vitro* Biological Activity of Tetrahydropyran and Tetrahydrofuran Macrolactone Analogs**

Compound	Intrinsic Potency, DLD-1 IC_{50} (nM)[a]	Mitotic Block Reversibility		
		U937 IC_{99}, 0 h (nM)[b]	U937 IC_{99}, 10 h (nM)[c]	Reversibility Ratio
		Tetrahydropyran Series		
29	2.5	10	170	17
30	1.8	10	300	30
31	2.1	10	> 1000	> 100
32	1.8	10	> 1000	> 100
33	2.6	10	300	30
34	2.0	3	65	22
35	1.8	2	100	50
36	> 1000	—	—	—
		Tetrahydrofuran Series		
37	1.0	3	100	33
38	> 1000	—	—	—
39	0.97	7	100	14
40	6.4	10	100	10
41	1.4	3	30	10
42	> 1000	—	—	—
43	220	—	—	—
44	0.67	1.5	15	10

[a] Growth-inhibitory potency against DLD-1 cells after 3–4 days of continuous drug exposure.
[b] Induction of CMB in U937 cells after 12 h of drug exposure (0 h of washout).
[c] Maintenance of CMB 10 h after drug washout.

carbon-lower homolog or inverting the hydroxyl stereochemistry at C.32 had little effect (e.g., **33**–**35**), but removing the C.33 side chain altogether (i.e., **36**) led to complete loss of activity.

Because incremental changes to the C.29–C.33 tetrahydropyran ring system did not provide a clear direction for improvement, an alternative strategy was pursued based on a working hypothesis that the C.31 substituent played a critical role in stabilizing the bioactive conformation of the macrolactone. As noted earlier, presence of the C.31 substituent was critical for good *in vitro* biological activity, albeit with a degree of steric tolerance. Thus, if the bioactive conformation could be reinforced by an alternative ring system, then the apparent potency limitations associated with the tetrahydropyran analogs might be circumvented.

The x-ray crystal structure of norhalichondrin A *p*-bromophenacyl ester reported in 1985 provided an empirically derived starting point for conformational analysis of the C.29–C.33 tetrahydropyran ring.[1] Although the solid-state conformation may not necessarily represent the bioactive conformation of the halichondrins, it does represent a reasonable low-energy structure for examining the octahydropyrano[3,2-b]pyran ring conformation. ^{1}H-nuclear magnetic resonance studies reported by Munro indicate that the average solution conformation of HB in $CDCl_3$ may be similar to the solid-state conformation of norhalichondrin A *p*-bromophenacyl ester.[6] In the x-ray structure, the C.29–C.33 tetrahydropyran ring adopts a twist boat conformation that places the C.31 methyl group in a pseudoequatorial position.[1,35] Although a tetrahydropyran ring can adopt a similar twist boat conformation, the tetrahydrofuran ring would be expected to do so with less conformational freedom (Figure 13.9). By stabilizing the pseudoequatorial orientation of the C.31 methyl group

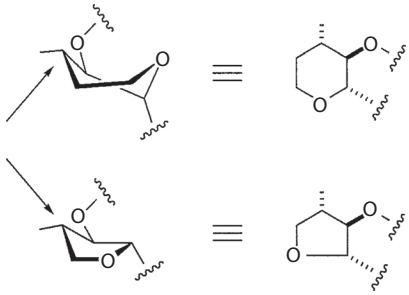

FIGURE 13.9 Conformational analysis of tetrahydropyran and tetrahydrofuran analogs.

relative to the macrocyclic ring, the tetrahydrofuran analogs might be expected to exhibit superior biological activity relative to the tetrahydropyran derivatives based on favorable entropic factors.

Consistent with this working hypothesis, the *in vitro* biological activity of tetrahydrofuran **37** (Figure 13.10) was virtually indistinguishable from that of tetrahydropyran **34**. Inverting the stereocenter at C.29 to give compound **38**, however, provided a compound that was inactive at the highest concentration tested, consistent with the need to maintain a particular low-energy macrolactone ring conformation (these results apply only to the particular macrolactone analogs synthesized and tested). Extending the C.32 hydroxymethyl side chain by either one carbon (e.g., **39**) or to a vicinal propanediol (e.g., **40** and **41**) had little effect, albeit showing a modest difference between the C.34 *R*- and *S*-isomers in the DLD-1 cell growth assay. As expected, based on conformational arguments, activity was critically dependent on the configuration at C.30 and C.31 (e.g., **42** and **43**, respectively; these results apply only to the particular macrolactone analogs synthesized and tested). Further structural and stereochemical optimization ultimately led to tetrahydrofuran **44**, whose intrinsic potency and ability to maintain a CMB exceeded those of the tetrahydropyran derivatives.

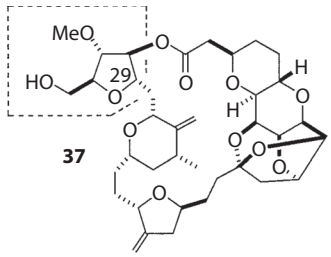

37

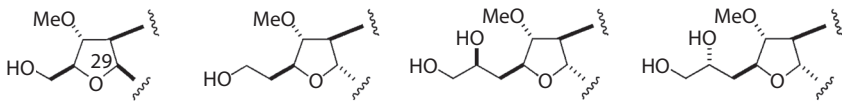

38 **38** **40** **41**

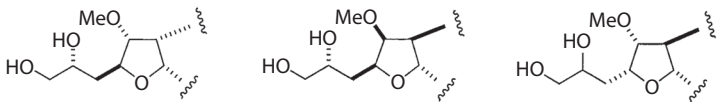

42 **43** **44**

FIGURE 13.10 Representative tetrahydrofuran macrolactone analogs.

Compounds **30** and **44**, representatives from the tetrahydropyran and tetrahydrofuran series, respectively, were evaluated in the LOX human melanoma xenograft model. Unexpectedly, both failed to demonstrate *in vivo* efficacy despite an equal or superior *in vitro* profile relative to lead compound **20**. Although several explanations for this lack of *in vivo* efficacy in the mouse xenograft model were possible, instability of the ester bond in mouse serum was regarded as the most likely explanation. In support of this hypothesis, activity of the octahydropyrano[3,2-b]pyran series of macrolactone analogs (e.g., **11**) was for the most part unaffected by inclusion of up to 1% (v/v) mouse serum in the 3–4 days growth-inhibition assay using DLD-1 human colon carcinoma cells. However, activities of the simplified tetrahydropyran series of macrolactones were completely abrogated by mouse serum concentrations as low as 0.01–0.05% in the cell culture medium.[36] Elimination of biological activity did not occur with either bovine or human sera, regardless of heat inactivation status, consistent with high levels of nonspecific esterases present in mouse serum (18 U/mg protein) compared with bovine (0.3 U/mg) or human sera (0.6 U/mg). As the seco acid of macrolactone **11** was not active *in vitro*, lack of *in vivo* efficacy for compounds **30** and **44** in the mouse xenograft model was attributed to sensitivity of the macrolactone ring to nonspecific esterases present in mouse serum.

The 3–4 days DLD-1 human colon carcinoma cell growth assay was adapted to provide a functional measure of compound stability in the presence of mouse serum. At a fixed drug concentration of 100 n*M*, analogs were examined for cell growth-inhibitory activity in the presence of varying concentrations of mouse serum. The "mouse serum IC_{50} value" from this assay corresponded to the percentage of mouse serum needed to suppress 100 nM drug-mediated cell growth inhibition by 50%. Both the tetrahydropyran and tetrahydrofuran series of compounds were found to be highly sensitive to mouse serum inactivation, with compounds **35** and **37** exhibiting mouse serum IC_{50} values of just 0.002%. However, the reasons underlying the stability of **11** to nonspecific esterases present in mouse serum relative to the sensitivity seen in structurally simplified tetrahydropyran or tetrahydrofuran analogs were not well understood. Although conformational factors may play a role, molecular modeling failed to provide a clear explanation for the striking loss of cell growth-inhibitory activity in the presence of mouse serum esterases, although speculative, protein-binding calculations indicate that differential low-affinity binding of these compounds to serum proteins with nonspecific esterase activity may account at least in part for their observed behavior.

Attempts to further improve the *in vitro* biological profile of the macrolactones met with limited success. As summarized in Figure 13.11, most changes were detrimental to biological activity, with greater latitude observed for those centers external to the C.1–C.30 macrolactone ring (e.g., C.32–C.38). Because minimal opportunities existed to modify the 2,6,9-trioxatricyclo[3.3.2.$0^{3,7}$]decane ring system without significantly altering the global conformation of the molecule, and as members of the halichondrin family with oxygenation at C.10, C.12, or C.13 (e.g., halichondrin A, halistatins 1–2) were less potent relative to their nonhydroxylated counterparts, the C.1–C.13 fragment of HB

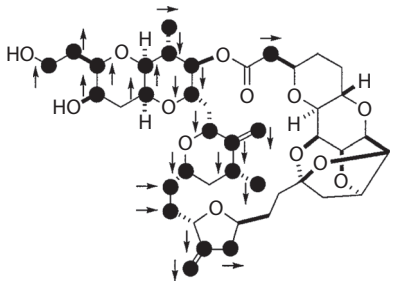

FIGURE 13.11 Closed circles indicate carbon centers that were modified to explore structure–activity relationships. The arrows indicate whether changes ultimately led to an increase, decrease, or no effect on *in vitro* potency.

was held constant as structure–activity relationships were explored around the remainder of the molecule. Despite extensive investigation, instability of the macrolactone ring remained problematic.

Lacking a predictive model with sufficient resolution to guide structure modification efforts, nonhydrolyzable ester bioisosteres were evaluated to identify derivatives that retain activity in the presence of mouse serum. As expected, the C.1 amide, hydroxyl, ether, and ketone analogs exhibited improved stability against nonspecific esterases. However, of the surrogate groups examined, only the ketone bioisostere provided analogs with sufficient *in vitro* potency to warrant further investigation.[32]

From these studies, compound **45** (ER-076349, NSC 707390) emerged as the prototypical macrocyclic ketone for *in vivo* evaluation (Figure 13.12). This analog exhibited antitumor effects in a variety of human tumor xenograft models including MDA-MB-435 breast carcinoma, COLO-205 colon carcinoma, LOX melanoma, and NIH:OVCAR-3 ovarian carcinoma, with no evidence of toxicity based on body weight or water consumption at the doses tested.[27]

Consistent with the bifurcation model of HB, in which the macrocyclic region represented the minimum pharmacophoric substructure for biological activity, structural modifications to regions of the molecule distant from the macrocyclic ring (e.g., the C.32 side chain) had little effect on the *in vitro* biological activity. For example, treatment of **45** with *p*-toluenesulfonyl chloride and several nucleophiles afforded a variety of derivatives differing at C.35 but exhibiting a nearly identical *in vitro* biological profile (Table 13.4).[37] Inverting the C.34 stereocenter (e.g., **46**) similarly had little effect on potency, as did cleavage of the C.34–C.35 vicinal diol to furnish alcohol **50**.

Treatment of **45** with *p*-toluenesulfonyl chloride followed by ammonia, however, provided an amine (compound **51**; E7389, previously ER-086526, also NSC-707389) that for the first time exhibited a reversibility ratio of 1, indicating that even a 10-h drug washout had no effect on the compound's ability to maintain a CMB (Figure 13.13). Several other amine derivatives were subsequently prepared and also found to exhibit a low reversibility ratio (e.g., **52**). In addition to conferring superior reversibility characteristics to this series, the amino group also provided a convenient handle for late-stage derivatization (e.g., acylation). Although simple amides of **51** were highly potent *in vitro* (Figure 13.14), they exhibited diminished *in vivo* activity in human tumor xenograft models (data not shown). From the

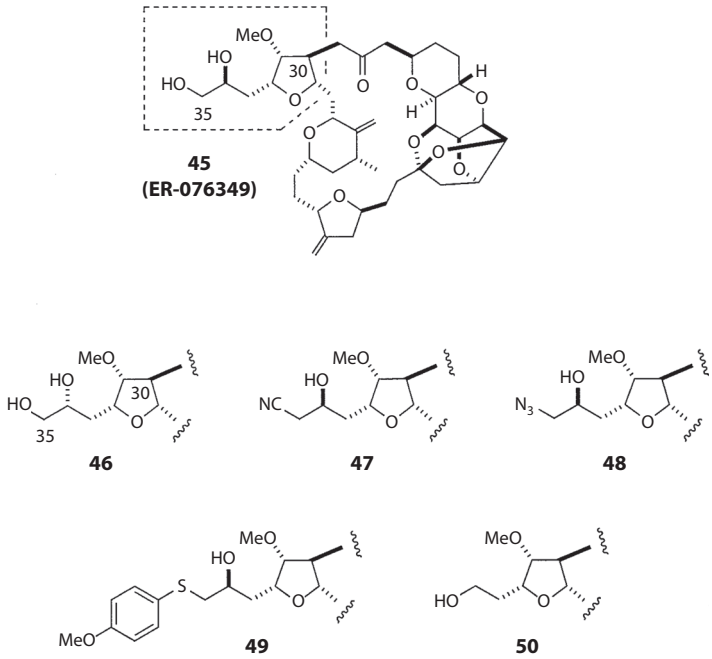

FIGURE 13.12 Representative macrocyclic ketone analogs.

TABLE 13.4
***In Vitro* Biological Activity of Macrocyclic Ketone Analogs**

Compound	Intrinsic Potency, DLD-1 IC_{50} (nM)[a]	Mitotic Block Reversibility		
		U937 IC_{99}, 0 h (nM)[b]	U937 IC_{99}, 10 h (nM)[c]	Reversibility Ratio
45	1.0	3	38	13
46	1.9	3	100	33
47	0.49	2.0	30	15
48	0.53	3	30	10
49	0.71	3	30	10
50	0.66	3	100	33
51 (E7389)	20	11	11	1
52	3.3	10	10	1
53	1.2	1	10	10
54	0.47	1	10	10
55	0.43	3	10	3.3
56	1.3	3	30	10
57	0.69	3	20	6.7
58	0.72	2	10	5
59	0.87	3	10	3.3
60	1.8	3	30	10

[a] Growth-inhibitory potency against DLD-1 cells after 3–4 d continuous drug exposure.
[b] Induction of CMB in U937 cells after 12 h drug exposure (0 h of washout).
[c] Maintenance of CMB 10 h after drug washout.

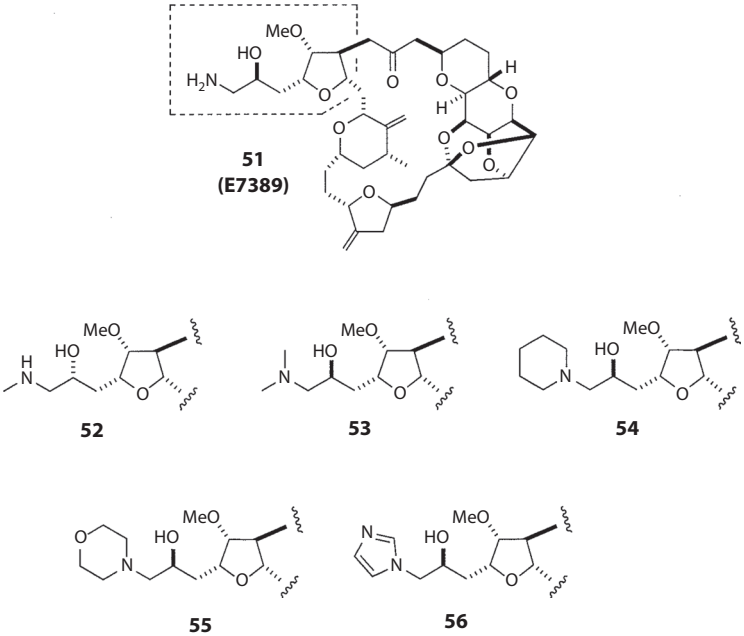

FIGURE 13.13 Representative C.35 amine analogs.

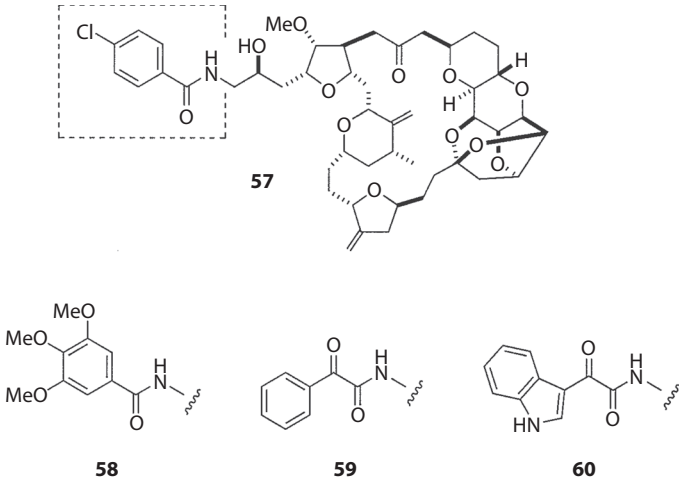

FIGURE 13.14 Representative C.35 amide analogs.

analogs prepared, compound **51** (E7389) emerged as the most promising candidate and was therefore selected for preclinical development by Eisai Co., Ltd., as a new anticancer chemotherapeutic agent.

13.6 SYNTHESIS OF HB ANALOGS

The macrocyclic ketone analogs were prepared in a highly convergent manner, taking advantage of key building blocks, protecting group strategies, and carbon–carbon bond disconnections developed by Kishi et al. for the total synthesis of HB and norhalichondrin B (Figure 13.15). Having established the minimum pharmacophore for cytotoxic activity, the C.1–C.13 and C.14–C.26 synthetic intermediates were fixed and stockpiled, allowing final coupling of the three key fragments to proceed under a standard set of conditions. In this manner, the synthesis of new analogs was reduced to preparation of various C.27–C.35 tetrahydrofuran derivatives for conversion to final product. For example, aldehyde **61** was coupled with vinyl iodide **62** under Nozaki–Hiyama–Kishi conditions[38,39] and cyclized with base. Removal of the MPM protecting group and introduction of the sulfone moiety afforded intermediate **63**. Coupling with C.1–C.13 aldehyde **64** and functional group modification around the C.1 ketone provided an intermediate that underwent a smooth intramolecular Nozaki–Hiyama–Kishi reaction to close the macrocyclic ring between C.13 and C.14. Finally, treatment with tetrabutylammonium fluoride and pyridinium *p*-toluenesulfonate generated the 2,6,9-trioxatricyclo[3.3.2.0^{3,7}]decane system to furnish **45** in good yield. Modification of the C.32 side chain subsequently afforded the desired macrocyclic ketone analogs.

13.7 *IN VITRO* CHARACTERIZATION OF E7389

The halichondrins exhibited a unique pattern of interaction with tubulin compared with other antimitotic drugs,[10] indicating that E7389 may similarly demonstrate unique interactions with tubulin and microtubules. Both E7389 and HB shared low- to subnanomolar cell growth-inhibitory activity against multiple human tumor cell lines *in vitro*, both performed similarly in the NCI 60-cell line screen, both induced G_2/M cell cycle arrest with mitotic spindle disruption consistent with a tubulin-based antimitotic mechanism, and both directly inhibited tubulin polymerization with nearly identical IC_{50} values.

Recent work by Jordan et al. revealed that E7389 suppressed microtubule dynamics through a unique mechanism that differed significantly from those of other tubulin-active drugs such as paclitaxel and vinblastine.[15] For example, unlike other antimitotic drugs, this compound induced the formation of nonproductive tubulin aggregates from soluble α/β-tubulin heterodimers that

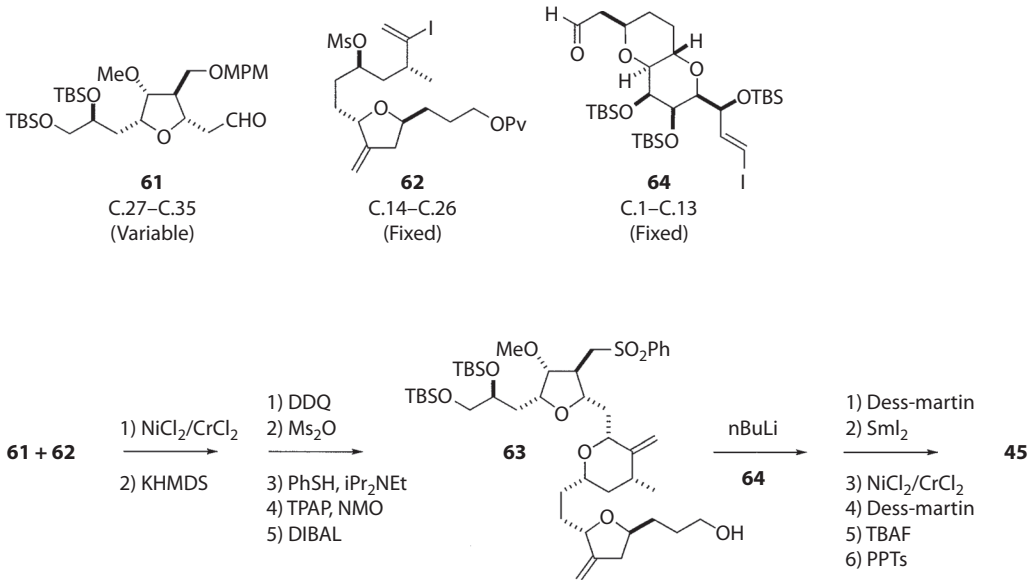

FIGURE 13.15 Synthesis of macrocyclic ketone analogs.

effectively reduced the concentration of soluble tubulin available for productive microtubule growth. Interestingly, there was no effect on treadmilling of microtubules *in vitro*, and in living cells E7389 did not alter catastrophe and rescue frequencies or the shortening events of microtubule dynamic instability at the concentrations tested. The unique characteristics of E7389 in these studies further emphasized the mechanistic differences that set the halichondrin class of compounds apart from other tubulin-interactive agents. Because the role of microtubule-associated proteins and microtubule-regulatory proteins in tubulin aggregate formation induced by E7389 remains unclear at this time, further studies will be needed to elucidate what effects, if any, this agent may have on the interactions between such proteins and microtubules in the context of drug-induced alterations in microtubule function and dynamics. In addition, studies with radiolabeled E7389 may help clarify whether it binds directly to microtubules or only to soluble tubulin heterodimers.

In vitro metabolism studies using a series of human enzyme preparations including liver microsomal preparations, S9 fractions, recombinant drug-metabolizing cytochrome P450 and phase 2 conjugative enzymes, and primary human hepatocytes indicate that E7389 is mainly metabolized by CYP3A4 at pharmacologically relevant concentrations. Suppression of CYP3A4 activity was modest, with an apparent K_i of 3–10 μM, as determined by form-specific nifedipine dehydration, testosterone 6β-hydroxylation, and *R*-warfarin 10-hydroxylation. No induction of CYP1A and CYP3A enzymes was observed immunochemically and enzymatically using primary human hepatocytes. Thus, based on a low anticipated therapeutic dose in humans, clinical drug–drug interactions with E7389 are anticipated to be unlikely.[40]

13.8 *IN VIVO* CHARACTERIZATION OF E7389

The subnanomolar growth-inhibitory activity of E7389 *in vitro* was reflected in the marked antitumor activity of this agent *in vivo* at 0.05–1 mg/kg against several human cancer xenografts, including MDA-MB-435 breast cancer, COLO 205 colon cancer, LOX melanoma, and NIH:OVCAR-3 ovarian cancer (Figure 13.16).[27]

In the MDA-MB-435 breast cancer model (Figure 13.16a), treatment with E7389 led to regression of measurable tumors that were present at the start of dosing. No evidence of toxicity was observed

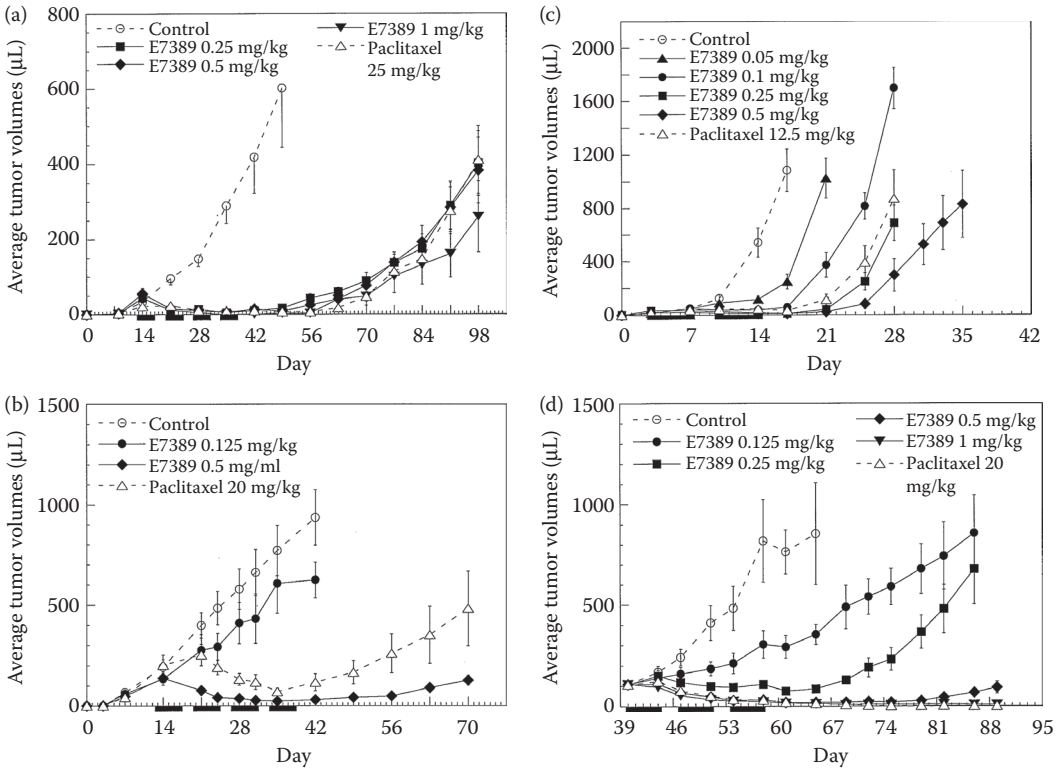

FIGURE 13.16 Inhibition of human tumor xenograft growth *in vivo* by E7389 and paclitaxel. Nude mice bearing MDA-MB-435 breast cancer (a), COLO 205 colon cancer (b), LOX melanoma (c), and NIH:OVCAR-3 ovarian cancer (d). Periods of dosing are indicated by gray bars underlying the *x* axes. COLO 205 and MDA-MB-435 models: E7389 was administered intravenously (MDA-MB-435) or intraperitoneally (COLO 205), using a q2d × 3 schedule for four weekly cycles, beginning on day 13. LOX model: E7389 was administered by daily intraperitoneal injection on days 3–7 and 10–14 inclusive. NIH:OVCAR-3 model: E7389 was administered intravenously beginning on day 40 and continuing on a q2d × 3 schedule for three weekly cycles. Control groups in all the studies received appropriate vehicle injections. Paclitaxel was administered at its empirically determined MTD for each treatment regimen in all the experiments. Plotted mean tumor volumes occurring after onset of any complete remissions represent averages of only those animals continuing to bear measurable tumors. (Adapted from Towle, M.J. et al., *Cancer Res.*, 61, 1013, 2001.)

at any dose based on body weight losses or decreased water consumption. Notably, all doses of E7389 over a fourfold range were either equally efficacious or superior to paclitaxel, which was dosed at its empirically determined maximum tolerated dose (MTD). In contrast, paclitaxel exhibited complete tumor suppression only over a narrow 1.7-fold dose range in this model (data not shown). The ability of E7389 to completely suppress tumor growth at several doses below the MTD is unusual for a cytotoxic agent and may be a consequence of its unique mechanism of action.

In the COLO 205 colon cancer xenograft model (Figure 13.16b), E7389 also showed frank regression and long-term suppression of tumor regrowth superior to that seen with paclitaxel at its empirically determined MTD. As in the MDA-MB-435 model, no evidence of toxicity based on body weight losses or decreased water consumption was observed. In the LOX melanoma model (Figure 13.16c), treatment with E7389 led to complete tumor suppression over a fivefold dose range, again representing an unusually wide therapeutic window for a cytotoxic agent. In this model, tumor regrowth rates in the 0.5 mg/kg E7389 group were delayed significantly beyond that seen with 12.5 mg/kg paclitaxel. Finally, in the NIH:OVCAR-3 ovarian cancer xenograft model (Figure 13.16d), E7389 led to complete tumor suppression equivalent to paclitaxel, both during dosing and throughout the regrowth phase.

The ability of E7389 to induce complete tumor suppression over a relatively wide dose range below the MTD is in sharp contrast to the behavior of standard cytotoxic drugs, irrespective of mechanistic class. Expression of *in vivo* anticancer efficacy by paclitaxel, doxorubicin, or the vinca alkaloids, for example, required dosing at or near the MTD, reflecting a delicate balance between efficacy and toxicity. Although speculative, the exceptionally wide therapeutic window for E7389 in preclinical xenograft models may be related to its novel mode of interaction with tubulin and raises the possibility that this agent may exhibit unique characteristics in the clinic that will distinguish it from existing tubulin-based chemotherapeutic agents.

13.9 CONCLUSION

In the 18 years since Hirata and Uemura first described the halichondrins, each of the challenges associated with bringing this class of structurally complex marine natural products through the discovery and preclinical development pipeline was successfully met with dramatic results. The first—and to date only—total synthesis of HB reported by Kishi et al. provided the basis for directed structure modifications by Eisai scientists to transform the original polyether macrolactone to a structurally simplified macrocyclic ketone through a rational stepwise series of modifications that did not compromise the natural product's remarkable biological profile. Starting from synthetic intermediate **11** prepared in connection with Kishi's total synthesis, the minimum pharmacophoric substructure of the halichondrins was determined to be the C.1–C.34 macrolactone fragment. Optimization of the C.29–C.38 ring system ultimately led to structurally simplified macrolactones that retained the natural product's extraordinary biological activity. Stabilization of the macrolactone ring against serum inactivation and final structure optimization afforded a series of highly potent analogs from which E7389 emerged as the most promising, with outstanding pharmacological, toxicological, and physicochemical characteristics.

With the identification of an optimized fully synthetic drug candidate, the obstacles commonly encountered during the development of structurally complex marine natural products were circumvented.[19] For example, limited compound supply was a critical issue that all but precluded development of HB as an anticancer agent in the early 1990s. Access to sufficient quantity of the producing organism to secure the needed absolute amount of material in a reliable, consistent, and economic manner; separation of the desired drug substance from other structurally related members of the halichondrin family; and removing trace amounts of highly toxic coisolated contaminants to ensure safety were contributing factors that made collection from the wild or through aquaculture techniques impractical, difficult, or unknown. Total synthesis, however, allowed ready access to halichondrin analogs with a defined and consistent impurity profile in sufficient quantity to support all preclinical research activities, satisfy quality criteria, and prevent compound supply from becoming a critical obstacle in the path for clinical evaluation.

Despite significant simplification relative to the natural product that inspired it, the chemical structure of E7389 remains a synthetically challenging target that exceeds the structural complexity of any other totally synthetic drug on the market today. Whereas success in clinical trials will unequivocally establish the potential of E7389 to become an exciting and important drug in the war on cancer, it will be the development of an economically feasible route for possible commercial production that will determine the long-term success of this program. Although hurdles remain, contemporary synthetic organic chemistry has both the capacity and the potential to meet this challenge.[20]

Tubulin-based antimitotics such as paclitaxel represent a class of agents that is clinically proven. In several human tumor xenograft animal models, E7389 exhibited superior efficacy to paclitaxel, with antitumor activity observed at dose levels well below its MTD. The exceptionally wide therapeutic window of E7389 in preclinical animal models, combined with its novel mechanism of tubulin heterodimer aggregation and superior efficacy to paclitaxel, raises the possibility that E7389 may exhibit a unique profile in the clinic that will differentiate it from other anticancer drugs.

With preclinical development completed and work well underway to address future compound supply needs, the stage is finally set to establish the therapeutic value of halichondrin-based agents in humans. E7389 is currently undergoing phase I clinical trials as an anticancer chemotherapeutic agent with first-in-man studies initiated collaboratively between Eisai Co., Ltd., and NCI.[41] If results in the clinic parallel the outstanding preclinical activity observed in animal models, then E7389 will offer new hope for cancer patients and their families and will help bring the dream of getting drugs from the sea another step closer to reality.

ACKNOWLEDGMENTS

The discovery and development of E7389 was possible only through the dedication, vision, and spirit of innovation shared by the many Eisai scientists who made this human healthcare program a reality. In addition, we express our appreciation for valuable assistance of the NCI through a collaborative research and development agreement to help bring the halichondrin class of marine natural products from laboratory concept to clinical investigative drug.

UPDATE

D. J. Newman

Due to unforeseen circumstances, Dr. Melvin Yu of Eisai Research Institute was unable to update the chapter from the first edition, so the following update has been produced from publications that have appeared in the last few years (effectively from 2005 to the middle of 2010). For convenience, the citations from this update continue on from the last 2004 reference, starting at reference number 42.

Synthetic Routes to Eribulin

The work leading up to the identification of eribulin and synthesis of the agent were given in detail in the earlier part of this chapter. However, over the last two years or so, there have been three publications from the Kishi group detailing improved methods for the synthesis of eribulin, and although these are written from an academic perspective, they do consider the relative costs of production.[42–44]

In addition to the work mentioned before from Kishi's group on the synthesis of eribulin, there was an extensive coverage of the patent routes to this molecule, with some duplication of the work presented in the earlier part of this chapter, in the review published by Wang et al. in 2007.[45] This report was followed in early 2009 by an excellent review from the Phillips Group at Colorado of the published syntheses by many groups working on HB, norhalichondrin B, and E7389.[46] This review was closely followed by a report on the total synthesis of the close homolog norhalichondrin B from the same laboratory.[47]

Biochemical Studies on Eribulin

In 2005, Jordan et al. reported that suppression of microtubule growth was the primary antimitotic mechanism of E7389, with differential effects due to concentration when studied in MCF7 cells. At low concentrations, eribulin potently inhibited microtubule dynamics resulting in prolonged arrest of mitosis and inducing apoptosis, whereas at tenfold of the IC_{50} value (or higher concentrations), it induced depolymerization,[48,49] with extension of the experiments to demonstrate eribulin's interaction with centromere dynamics.[50] In the same time frame, Jordan's group and others expanded studies to demonstrate that E7389/eribulin and HB could be modeled into a site close to the vinca site in tubulin,[51] which was extended using analytical ultracentrifugation techniques by Alday and Correia. Their data strongly suggested that eribulin is a strong inhibitor of the 1:2 stathmin:tubulin complex, and may well be a global inhibitor of tubulin polymer formation as a result of disruption of tubulin–tubulin contacts at the interdimer interface.[52] What was also of interest in the latter paper was the report that the penultimate precursor of eribulin (ER-076349), where the group on the left-hand side chain is an hydroxyl rather than an amino substituent, is not as potent an inhibitor of the stathmin–tubulin complex formation, and though it also perturbs tubulin–tubulin contacts, it appears to do so in a more polymer-specific manner.

That the actual interaction of eribulin with tubulin is even more complex is shown by the data reported by Jordan's group in a 2010 paper.[53] By use of ^{3}H-eribulin, they demonstrated a very high affinity site ($K_d = 400 \pm 200$ nM) on 25% of the tubulin mass (which might be the $\alpha\beta_{III}$ tubulin dimer) with a stoichiometry of 0.26 ± 0.12 eribulin per tubulin dimer. Another high affinity site ($K_d = 3.5 \pm 0.6$ μM; stoichiometry of 14.7 ± 1.3 eribulin:tubulin dimer) was also identified together with a low affinity site ($K_d = \sim 46 \pm 28$ μM; stoichiometry of 1.3 ± 0.4 saturable sites per tubulin dimer).

The binding isotherm is highly complex and may be so due to competition for the eribulin between soluble tubulin and microtubules, though there is photo- and electron-micrographic evidence in the paper, and in earlier ones from the same group, for binding to the plus end of microtubules and preferentially to β-tubulin. This is concordant with the ultracentrifugation data reported

before.[52] As mentioned in the paper by Smith et al.,[53] further experimentation will be necessary to explain these complex results, including the inhibition of eribulin binding to microtubles *in vitro* by vinblastine when the eribulin concentration is <5 μM versus the reverse when >5 μM.

Clinical Studies with E7389/Eribulin

To date, there have been two major reviews on eribulin mesylate (the salt form used for clinical trials), with the first published in 2007 by Wang et al.[45] and the second by Cigler and Vahdar in 2010,[54] together with a more clinically oriented article on breast cancer treatments.[55]

In the intervening years E7389/eribulin continued through a series of over 20 clinical trials, some with full reports published on Phase I[56–58] and Phase II trials with heavily pretreated patients[59,60] and others with only abstracts to date.[57,61–74]

In late March 2010, Eisai submitted applications to the U.S. FDA, the EMEA (EU), and the Japanese FDA for approval of eribulin as a treatment for refractory breast cancer. The submission was based on data from the pivotal and global in nature, Phase III "EMBRACE" (Eisai Metastatic Breast Cancer Study Assessing Physician's Choice Versus E7389) study.[75] This study was an open-label, randomized, parallel two-arm, multicenter study with a total of 762 female patients. The participants were definitely not naïve to chemotherapy as they had to have experienced prior recurrent or metastatic breast cancer, and had to have been previously treated with at least two chemotherapy regimens, including anthracyclines and taxanes.

The study met its primary endpoint of demonstrating a statistically significant improvement in overall survival in eribulin mesylate-treated patients compared with the treatment under "The Physician's Choice (TPC)" of drug regimens, which was included following recognition of the heterogeneous nature of the patient population, as well as the need for clinicians to tailor treatment regimes for individual patients.

In this study, patients were treated either with IV eribulin (administered over 2–5 min on days 1 and 8 repeating 21 days) or with TPC. The latter was defined as any single agent chemotherapy, suitable hormonal treatment, or any biological therapy approved for the treatment of cancer; this arm also included palliative treatment or radiotherapy administered according to best local practices.

The submission to the FDA was given priority status for review in June 2010, and at the time of writing (mid-November 2010), the FDA just announced approval of eribulin for second-line therapy in resistant breast cancer. No further information is available for the other submissions, nor for two earlier submissions to Switzerland and Singapore in the middle of 2009.

Even though these applications for approval have been submitted, inspection of the NCI's clinical trials database (http://clinicaltrials.gov) shows that there are 18 trials still listed as of the end of August 2010. Of these, seven are at Phase I, three are at Phase I/II, seven are at Phase II, and one is a compassionate use protocol for patients with advanced breast cancers that are refractory to all other marketed therapies.

Thus, almost 10 years after NCI and Eisai began clinical trials of this extremely complex synthetic compound, that was based on the structure of the marine sponge-derived HB, it now has approval as a chemotherapeutic in the United States, and in a similar manner to other chemotherapeutics at similar stages of their development it is still a part of a very active clinical trials program.

REFERENCES

1. Uemura, D., Takahashi, K., Yamamoto, T., Katayama, C., Tanaka, J., Okumura, Y., and Hirata, Y., Norhalichondrin A: An antitumor polyether macrolide from a marine sponge, *J. Am. Chem. Soc.*, 107, 4796, 1985.
2. Hirata, Y. and Uemura, D., Halichondrins—antitumor polyether macrolides from a marine sponge, *Pure Appl. Chem.*, 58, 701, 1986.

3. Pettit, G.R., Herald, C.L., Boyd, M.R., Leet, J.E., Dufresne, C., Doubek, D.L., Schmidt, J.M. Cerny, R.L., Hooper, J.N.A., and Rutzler, K.C., Isolation and structure of the cell growth inhibitory constituents from the western pacific marine sponge *Axinella* sp., *J. Med. Chem.*, 34, 3339, 1991.
4. Pettit, G.R., Tan, R., Gao, F., Williams, M.D., Doubek, D.L., Boyd, M.R., Schmidt, J.M. et al., Isolation and structure of halistatin 1 from the eastern Indian Ocean marine sponge *Phakellia carteri*, *J. Org. Chem.*, 58, 2538, 1993.
5. (a) Litaudon, M., Hickford, S.J.H., Lill, R,E., Lake, R.J., Blunt, J.W., and Munro, M.H.G. Antitumor polyether macrolides: new and hemisynthetic halichondrins from the New Zealand deep-water sponge *Lissodendoryx* sp., *J. Org. Chem.*, 62, 1868, 1997; (b) Gravelos, D.G., Lake, R.J., Blunt, J.W., Munro, M.H.G., and Litaudon, M.S.P., Halichondrins: cytotoxic polyether macrolides, European Patent Application, EP 0 572 109, 1993.
6. Hart, J.B., Lill, R.E., Hickford, S.J.H., Blunt, J.W., and Munro, M.H.G., The halichondrins: chemistry, biology, supply and delivery, in *Drugs from the Sea*, Fusetani, N., Ed., Karger, New York, 2000, 134.
7. Fodstad, Ø., Dreistol, K., Pettit, G.R., Shoemaker, R.H., and Boyd, M.R., Comparative antitumor activities of halichondrins and vinblastine against human tumor xenografts, *J. Exp. Ther. Oncol.*, 1, 119, 1996.
8. Hamel, E., Natural products which interact iwth tubulin in the vinca domain: maytansine, rhizoxin, phomopsin A, dolastatins 10 and 15 and halichondrin B, *Pharmacol. Ther.*, 55, 31, 1992.
9. Bai, R.L., Paull, K.D., Herald, C.L., Malspeis, L., Petit, G.R., and Hamel, E., Halichondrin B and homohalichondrin B, marine natural products binding in the vinca domain of tubulin. Discovery of tubulin-based mechanism of action by analysis of differential cytotoxicity data, *J. Biol. Chem.*, 266, 15882, 1991.
10. Ludueña, R.F., Roach, M.C., Prasad, V., and Pettit, G.R., Interaction of halichondrin B and homohalichondrin B with bovine brain tubulin, *Biochem. Pharmacol.*, 45, 421, 1993.
11. Bai, R., Cichacz, Z.A., Herald, C.L., Pettit, G.R., and Hamel, E., Spongistatin 1, a highly cytotoxic, sponge-derived, marine natural product that inhibits mitosis, microtubule assembly, and the binding of vinblastine to tubulin, *Mol. Pharmacol.*, 44, 757, 1993.
12. Jordan, M.A., Thrower, D., and Wilson, L., Mechanism of inhibition of cell proliferation by vinca alkaloids, *Cancer Res.*, 51, 2212, 1991.
13. Jordan, M.A., Toso, R.J., Thrower, D., and Wilson, L., Mechanism of mitotic block and inhibition of cell proliferation by taxol at low concentrations, *Proc. Natl. Acad. Sci. U.S.A.*, 90, 9552, 1993.
14. García-Rocha, M., García-Gravalos, M.D., and Avila, J., Characterization of antimitotic products from marine organisms that disorganize the microtubule network: Ecteinascidin 743, isohomohalichondrin-B and LL-15, *Br. J. Cancer*, 73, 875, 1996.
15. Kamath, K., Okouneva, T., Miller, H., Davis, C., Littlefield, B.A., Wilson, L., and Jordan, M.A., E7389, a synthetic analog of halichondrin B, suppresses microtubule dynamics in living MCF7 cells by a novel mechanism, presented at the annual meeting of the American Association for Cancer Research, Washington, DC, July 11–14, 2003, LB-58.
16. Kikuchi, H., Manda, T., Tsukitani, Y., and Yoshida, K., Halichondin-B with antitumour activity—obtained by extracting *Halichondria okadai* with organic solvent then halichondin B is isolated, Japanese Patent JP 61191687; Tsukitani, Y., Manda, T., Yoshida, K. and Kikuchi, H., Japanese Patent 92001751.
17. Towle, M.J., Aalfs, K.K., Budrow, J.A., Kishi, Y., and Littlefield, B.A., *In vitro* and *in vivo* anticancer properties and cell cycle effects of synthetic halichondrin B, presented at the annual meeting of the American Association for Cancer Research, Toronto, Ontario, March 18–22, 1995, 2342.
18. Hart, J.B., Blunt, J.W., and Munro, M.H.G., Acid-catalyzed reactions of homohalichondrin B, a marine sponge-derived antitumor polyether macrolide, *J. Org. Chem.*, 61, 2888, 1996.
19. Fusetani, N., Introduction, in *Drugs from the Sea*, Fusetani, N., Ed., Karger, New York, 2000, 1.
20. (a) Aicher, T.D. and Kishi, Y., Synthetic studies towards halichondrins, *Tetrahedron Lett.*, 28, 3463, 1987; (b) Aicher, T.D., Buszek, K.R., Fang, F.G., Forsyth, C.J., Jung, S.H., Kishi, Y., Matelich, M.C., Scola, P.M., Spero, D.M., and Yoon, S.K., Total synthesis of halichondrin B and norhalichondrin B., *J. Am. Chem. Soc.*, 114, 3162, 1992; (c) Aicher, T.D., Buszek, K.R., Fang, F.G., Forsyth, C.J., Jung, S.H., Kishi, Y., and Scola, P.M., Synthetic studies towards halichondrins: synthesis of the C.27-C.38 segment, *Tetrahedron Lett.*, 33, 1549, 1992; (d) Buszek, K.R., Synthetic studies towards halichondrins: synthesis of the left half of halichondrins, *Tetrahedron Lett.*, 33, 1553, 1992; (e) Fang, F.G., Kishi, Y., Matclich, M.C., Scola, P.M., Synthetic studies towards halichondrins: synthesis of the left halves of norhalichondrins and homohalichondrins, *Tetrahedron Lett.*, 33, 1557, 1992; (f) Duan, J.J. and Kishi, Y., Synthetic studies on halichondrins: A new practical synthesis of the C-1–C-12 segment, *Tetrahedron Lett.*, 34, 7541, 1993; (g) Chen, C., Tagami, K., and Kishi, Y., Ni(II)/Cr(II)-mediated coupling reaction: an asymmetric process, *J. Org. Chem.*, 60, 5386, 1995; (h) Stamos, D.P. and Kishi, Y., Synthetic studies on halichondrins: A practical synthesis of the C.1-C.13 segment, *Tetrahedron Lett.*, 37, 8643, 1996; (i) Stamos,

D.P. and Kishi, Y., Synthetic studies on halichondrins: A practical synthesis of the C.1-C.13 segment, *Tetrahedron Lett.*, 37, 8643, 1996; (j) Stamos, D.P., Taylor, A.G., and Kishi, Y., A mild preparation of vinyliodides from vinylsilanes, *Tetrahedron Lett.*, 37, 8647, 1996; (k) Stamos, D.P., Chen, S.S., and Kishi, Y., New synthetic route to the C.14–C.38 segment of halichondrins, *J. Org. Chem.*, 62, 7552, 1997; (l) Stamos, D.P., Sheng, X.C., Chen, S.S., and Kishi, Y., Ni(II)/Cr(II)-mediated coupling reaction: beneficial effects of 4-tert-butylpyridine as an additive and development of new and improved workup procedures, *Tetrahedron Lett.*, 38, 6355, 1997; (m) Stamos, D.P., Chen, S.S., and Kishi, Y., New synthetic route to the C.14-C.38 segment of halichondrins, *J. Org. Chem.*, 62, 7552, 1997; (n) Xie, C., Nowak, P., and Kishi, Y., Synthesis of the C20-C26 building block of halichondrins via a regiospecific and stereoselective S_N2'; reaction, *Org. Lett.*, 4, 4427, 2002; (o) Wan, Z.-K., Choi, H., Kang, F., Nakajima, K., Demeke, D., and Kishi, Y., Asymmetric Ni(II)/Cr(II)-mediated coupling reaction: stoichiometric process, *Org. Lett.*, 4, 4431, 2002; (p) Choi, H., Nakajima, K., Demeke, D., Kang, F., Jun, H., Wan, Z., and Kishi, Y., Asymmetric Ni(II)/Cr(II)-mediated coupling reaction: Catalytic process, *Org. Lett.*, 4, 4435, 2002; (q) Choi, H., Demeke, D., Kang, F., Kishi, Y., Nakajima, K., Nowak, P., Wan, Z., and Xie, C., Synthetic studies on the marine natural product halichondrins, *Pure Appl. Chem.*, 75, 1, 2003.

21. (a) Kim, S. and Salomon, R.G., Total synthesis of halichondrins: highly stereoselective construction of a homochiral pentasubstituted H-ring pyran intermediate from -D-glucose, *Tetrahedron Lett.*, 30, 6279, 1989; (b) Cooper, A.J. and Salomon, R.G., Total synthesis of halichondrins: Enantioselective construction of a homochiral pentacyclic C1-C15 intermediate from D-ribose, *Tetrahedron Lett.*, 31, 3813, 1990; (c) DiFranco, E., Ravikumar, V.T., and Salomon, R.G., Total synthesis of halichondrins: Enantioselective construction of a homochiral tetracyclic KLMN-ring intermediate from D-mannitol, *Tetrahedron Lett.*, 34, 3247, 1993; (d) Cooper, A.J., Pan, W., and Salomon, R.G., Total synthesis of halichondrin B from common sugars: an F-ring intermediate from D-glucose and efficient construction of the C1 to C21 segment, *Tetrahedron Lett.*, 34, 8193, 1993.
22. (a) Burke, S.D., Buchanan, J.L., and Rovin, J.D., Synthesis of a C(22)-C(34) halichondrin precursor via a double dioxanone-to-dihydropyran rearrangement, *Tetrahedron Lett.*, 32, 3961, 1991; (b) Burke, S.D., Jung, K.W., Phillips, J.R., and Perri, R.E., An expeditious synthesis of the C(1)-C(14) subunit of halichondrin B, *Tetrahedron Lett.*, 35, 703, 1994; (c) Burke, S.D., Zhang, G., and Buchanan, J.L, Enantioselective synthesis of a halichondrin B C(20)–C(36) precursor, *Tetrahedron Lett.*, 36, 7023, 1995; (d) Burke, S.D., Philips, J.R., Quinn, K.J., Zhang, G., Jung, K.W., Buchanan, J.L., and Perri, R.E., Synthetic studies toward complex polyether macrolides of marine origin, *Spec. Publ. R. Soc. Chem.*, 198 (Anti-Infectives), 73, 1997; (e) Burke, S.D., Austad, B.C., and Hart, A.C., An expeditious synthesis of the C(38)-C(54) halichondrin B subunit, *J. Org. Chem.*, 63, 6770, 1998; (f) Burke, S.D., Quinn, K.J., and Chen, V.J., Synthesis of a C(22)-C(34) halichondrin B precursor via ring opening-double ring closing metathesis, *J. Org. Chem.*, 63, 8626, 1998; (g) Burke, S.D., Jung, K.W., Lambert, W.T., Phillips, J.R., and Klovning, J.J., Halichondrin B: Synthesis of the C(1)-C(15) subunit, *J. Org. Chem.*, 65, 4070, 2000; (h) Austad, B.C., Hart, A.C., and Burke, S.D., Halichondrin B: Synthesis of the C(37)-C(54) subunit, *Tetrahedron*, 58, 2011, 2002; (i) Jiang, L. and Burke, S.D., A novel route to the F-ring of halichondrin B. Diastereoselection in Pd(0)-mediated meso and C2 diol desymmetrization, *Org. Lett.*, 4, 3411, 2002; (j) Jiang, L., Martinelli, J.R., and Burke, S.D., A practical synthesis of the F-ring of halichondrin B via ozonolytic desymmetrization of a C2-symmetric dihydroxycyclohexene, *J. Org. Chem.*, 68, 1150, 2003; (k) Lambert, W.T. and Burke, S.D., Halichondrin B: Synthesis of a C1-C14 model via desymmetrization of (+)-conduritol E, *Org. Lett.*, 5, 515, 2003.
23. (a) Horita, K., Hachiya, S., Nagasawa, M., Hikota, M., and Yonemitsu, O., Chiral synthesis of polyketide-derived natural products. 46. Synthetic studies of halichondrin B, an antitumor polyether macrolide isolated from a marine sponge. 1. Stereoselective synthesis of the C1-C13 fragment via construction of the B and A rings by kinetically and thermodynamically controlled intramolecular Michael reactions, *Synlett*, 38, 1994; (b) Horita, K., Nagasawa, M., Hachiya, S., and Yonemitsu, O., Chiral synthesis of polyketide-derived natural products. 47. Synthetic studies of halichondrin B, an antitumor polyether macrolide isolated from a marine sponge. 2. Efficient synthesis of C16-C26 fragments via construction of the D ring by a highly stereocontrolled iodoetherification, *Synlett*, 40, 1994; (c) Horita, K., Chiral synthesis of polyketide-derived natural products. 49. Synthetic studies of halichondrin B, an antitumor polyether macrolide isolated from a marine sponge. 4. Synthesis of the C37-C54 subunit via stereoselective construction of three consecutive J, K, and L rings, *Synlett*, 46, 1994; (d) Horita, K., Sakurai, Y., Nagasawa, M., Hachiya, S., and Yonemitsu, O., Chiral synthesis of polyketide-derived natural products. 48. Synthetic studies of halichondrin B, an antitumor polyether macrolide isolated from a marine sponge. 3. Synthesis of C27-C36 subunit via completely stereoselective C-glycosylation to the F ring, *Synlett*, 43, 1994; (e) Horita, K., Hachiya, S., Ohihara, K., Yoshida, Y., Nagasawa, M., and Yonemitsu, O., Synthetic studies of halichondrin B, an antitumor polyether

macrolide isolated from a marine sponge. 5. A highly concise and efficient synthesis of the C37-C54 tricyclic JKL-ring part, *Heterocycles*, 42, 99, 1996; (f) Horita, K., Hachiya, S., Yamazaki, T., Naitou, T., Uenishi, J., and Yonemitsu, O., Synthetic studies of halichondrin B, an antitumor polyether macrolide isolated from a marine sponge. 6. Synthesis of the C1-C15 unit via stereoselective construction of the B and A rings by kinetically and thermodynamically controlled Michael reactions with the aid of computational search for dominant conformers, *Chem. Pharm. Bull.*, 45, 1265, 1997; (g) Horita, K., Sakurai, Y., Nagasawa, M., and Yonemitsu, O., Synthetic studies of halichondrin B, an antitumor polyether macrolide isolated from a marine sponge. 7. Synthesis of two C27-C36 units via construction of the F ring and completely stereoselective C-glycosylation using mixed Lewis acids, *Chem. Pharm. Bull.*, 45, 1558, 1997; (h) Horita, K., Nagasawa, M., Hachiya, S., Sakurai, Y., Yamazaki, T., Uenishi, J., and Yonemitsu, O., Synthetic studies of halichondrin B, an antitumor polyether macrolide isolated from a marine sponge. 8. Synthesis of the lactone part (C1-C36) via Horner-Emmons coupling between C1-C15 and C16-C36 fragments and Yamaguchi lactonization, *Tetrahedron Lett.*, 38, 8965, 1997; (i) Horita, K., Nagasawa, M., Sakurai, Y., and Yonemitsu, O., Synthetic studies on halichondrin B, an antitumor polyether macrolide isolated from a marine sponge. 9. Synthesis of the C16-C36 unit via stereoselective construction of the D and E rings, *Chem. Pharm. Bull.*, 46, 1199, 1998; (j) Horita, K., Nishibe, S., and Yonemitsu, O., Research on antitumor active site of marine source natural product, halichondrin B. *International Congress Series*, 1157 (Towards Natural Medicine Research in the 21st Century), 327, 1998; (k) Yonemitsu, O., Yamazaki, T., and Uenishi, J.-I., On the stereoselective construction of the B and A rings of halichondrin B. A PM3 study, *Heterocycles*, 49, 89, 1998; (l) Horita, K., Nishibe, S., and Yonemitsu, O., Synthetic study of a highly antitumorigenic marine phytochemical, halichondrin B, in *Phytochemicals and Phytopharmaceuticals*, Shahidi, F. and Ho, C.-T., Eds., AOCS Press, Champaign, IL, 2000, Chapter 35.

24. Michael R. Boyd, Personal communication, 1992.
25. Towle, M. J., Kishi, Y., and Littlefield, B. A., Unpublished observations, 1992.
26. Fang, F., Fang, F. G., Forsyth, C. J., Kishi, Y., Scola, P. M., and Yoon, S.K., New halichondrin intermediates and derivs.—for inhibiting tumour growth esp. of melanoma, fibrosarcoma, monocytic leukaemia, colon, ovarian or breast carcinoma osteosarcoma and RAS-transforming fibroblast, PCT Patent, WO 1993017690; Kishi, Y., Fang, F.G., Forsyth, C.J., Scola, P.M., and Yoon, S.K., Synthesis of halichondrin B and norhalichondrin B, U.S. Patent 5338865; Kishi, Y., Fang, F.G., Forsyth, C.J., Scola, P.M., and Yoon, S.K., Halichondrins and related compounds, U.S. Patent 5436238.
27. Towle, M.J., Salvato, K.A., Budrow, J., Wels, B.F., Kuznetsov, G., Aalfs, K.K., Welsh, S. et al., *In vitro* and *in vivo* anticancer activities of synthetic macrocyclic ketone analogs of halichondrin B, *Cancer Res.*, 61, 1013, 2001.
28. Horita, K., Nishibe, S., and Yonemitsu, O., Research on anti-tumor active site of marine source natural product, halichondrin B, International Congress Series, 1157 (Towards Natural Medicine Research in the 21st Century), 327, 1998.
29. Hotta, K., Takahashi, N., and Nishizawa, M., Anti-tumor agents, Japanese Patent JP 2003261447, 2003.
30. Horita, K., Ohta, N., Takahashi, N., Noguchi, Y., et al., Research on anti-tumor active site of marine source compound, halichondrin B. Inhibitory activity of C37-C54 part derivatives toward the breast and the esophagus cancer cell lines, *Bull. Marine Biomed. Inst. Sapporo Med. Univ.*, 5, 35, 2002.
31. Towle, M.J., Salvato, K.A., Budrow, J., Wels, B.F., Aalfs, K.K., Zheng, W., Seletsky, B.M. et al., *In vivo* anticancer activity of synthetic halichondrin B macrocyclic ketone analogs ER-076349 and ER-086526 correlates with ability to induce irreversible mitotic blocks, presented at the annual meeting of the American Association for Cancer Research, New Orleans, LA, March 24–28, 2001. Abstract 1976.
32. (a) Littlefield, B.A., Palme, M.H., Seletsky, B.M., Towle, M.J., Yu, M.J., and Zheng, W., U.S. Patent 6214865, 2001; (b) Littlefield, B.A., Palme, M.H., Seletsky, B.M., Towle, M.J., Yu, M.J., and Zheng, W., U.S. Patent 6365759, 2002; (c) Littlefield, B.A., Palme, M.H., Seletsky, B.M., Towle, M.J., Yu, M.J., and Zheng, W., U.S. Patent 6469182, 2002; (d) Littlefield, B.A. and Towle, M.J., U.S. Patent 6653341, 2003.
33. Wang, Y., Habgood, G.J., Christ, W.J., Kishi, Y., Littlefield, B.A., Yu, M.J., Structure-activity relationships of halichondrin B analogs: modifications at C.30-C38, *Bioorg. Med. Chem. Lett.*, 10, 1029, 2000.
34. Eisai Research Institute, 1995.
35. Supplementary crystallographic data for norhalichondrin A *p*-bromophenacyl ester (CCDC 231897). http://www.ccdc.cam.ac.uk/data_request/cif
36. Towle, M.J., Wels, B. F., Cheng, H., Budrow, J., Zheng, W., Seletsky, B. M., Hawkins, L. D., et al., Halichondrin B macrocyclic ketone analog E7389: Medicinal chemistry repair of lactone ester instability generated during structural simplification to clinical candidate, presented at the annual meeting of the American Association for Cancer Research, San Francisco, CA, April 6–10, 2002, 5721.

37. Zheng, W., Seletsky, B. M., Palme, M. H., Habgood, G.J., Singer, L.A., DiPietro, L.V., Chen, J.J. et al., Synthetic macrocyclic ketone analogs of halichondrin B: structure-activity relationships, presented at the annual meeting of the American Association for Cancer Research, San Francisco, CA, April 1–5, 2000, 1915.
38. (a) Jin, H, Uenishi, J., Christ, W.J., Kishi, Y., Catalytic effect of nickel(II) chloride and palladium(II) acetate on chromium(II)-mediated coupling reaction of iodo olefins with aldehydes, *J. Am. Chem. Soc.*, 108, 5644, 1986; (b) Takai, K., Tagashira, M., Kuroda, T., Oshima, K., Utimoto, K., and Nozaki, H., Reactions of alkenylchromium reagents prepared from alkenyl trifluoromethanesulfonates (triflates) with chromium(II) chloride under nickel catalysis, *J. Am. Chem. Soc.*, 108, 6048, 1986.
39. (a) Nozaki, H. and Takai, K., Nucleophilic addition of organochromium reagents to carbonyl compounds, *Proc. Jpn. Acad.*, 76, 123, 2000; (b) Fürstner, A., Carbon-carbon bond formations involving organochromium(III) reagents, *Chem. Rev.*, 99, 991, 1999; (c) Wessjohann, L.A. and Scheid, G., Recent advances in chromium(II)- and chromium(III)-mediated organic synthesis, *Synthesis* 1, 1999; (d) Avalos, M., Babiano, R., Cintas, P., Jimenez, J.L., and Palacios, J.C., Synthetic variations based on low-valent chromium: New developments, *Chem. Soc. Rev.*, 28, 169, 1999; (e) Saccomano, N.A., Organochromium reagents, in *Comprehensive Organic Synthesi*s, Trost, B.M., Fleming, I., Eds., Pergamon Press, Oxford, 1991; vol. 1, Chapter 1.6.
40. Zhang, Z.-Y., King, B.M., Pelletier, R.D., and Wong, N., Characterization of *in vitro* metabolism of an anticancer agent E7389: prediction of the potential risk of clinical drug-drug interactions, presented at the 12th North American meeting of the International Society for the Study of Xenobiotics, Providence, RI, October 12–16, 2003, 367.
41. Synold, T.W., Lawrence, J., Xi, B., Colevas, A.D., Lewis, M.D., and Doroshow, J.H., Human pharmacokinetics of E7389 (halichondrin B analog), a novel anti-microtubule agent undergoing phase I investigation in the California Cancer Consortium (CCC), presented at the American Society of Clinical Oncology, Chicago, IL, May 31–June 3, 2003, 575.
42. Yang, Y.-R., Kim, D.-S., and Kishi, Y., Second generation synthesis of C27-C35 building block of E7389, a synthetic Halichondrin analogue, *Org. Lett.*, 11 (20), 4516, 2009.
43. Kim, D.-S., Dong, C.-G., Kim, J.T., Guo, H., Huang, J., Tiseni, P.S., and Kishi, Y., New syntheses of E7389 C14-C35 and Halichondrin C14-C38 building blocks: Double-Inversion approach, *J. Am. Chem. Soc.*, 131, 15636, 2009.
44. Dong, C.-G., Henderson, J.A., Kaburagi, Y., Sasaki, T., Kim, D.-S., Kim, J.T., Urabe, D., Guo, H., and Kishi, Y., New syntheses of E7389 C14-C35 and Halichondrin C14-C38 building blocks: Reductive cyclization and Oxy-Michael cyclization approaches, *J. Am. Chem. Soc.*, 131, 15642, 2009.
45. Wang, Y., Serradell, N., Bolos, J., and Rosa, E., Eribulin mesilate, *Drugs Fut.*, 32 (8), 681, 2007.
46. Jackson, K.L., Henderson, J.A., and Phillips, A.J., The Halichondrins and E7389, *Chem. Rev.*, 109, 3044, 2009.
47. Jackson, K.L., Henderson, J.A., Motoyoshi, H., and Phillips, A.J., A total synthesis of Norhalichondrin B, *Angew. Chem. Int. Ed.*, 48, 2346, 2009.
48. Jordan, M.A., Kamath, K., Manna, T., Okouneva, T., Miller, H.P., Davis, C., Littlefield, B.A., and Wilson, L., The primary antimitotic mechanism of action of the synthetic halichondrin E7389 is suppression of microtubule growth, *Mol. Cancer Ther.*, 4, 1086, 2005.
49. Jordan, M.A. and Kamath, K., How do microtubule-targeted drugs work? An overview, *Curr. Cancer Drug Targets*, 7, 730, 2007.
50. Okouneva, T., Azarenko, O., Wilson, L., Littlefield, B.A., and Jordan, M.A., Inhibition of centromere dynamics by Eribulin (E7389) during mitotic metaphase, *Mol. Cancer Ther.*, 7, 2003, 2008.
51. Dabydeen, D.A., Burnett, J.C., Bai, R.L., Verdier-Pinard, P., Hackford, S.J.H., Pettit, G.R., Blunt, J.W., Munro, M.H.G., Gussio, R., and Hamel, E., Comparison of the activities of the truncated Halichondrin B analog NSC 707389 (E7389) with those of the parent compound and a proposed binding site on tubulin, *Mol. Pharmacol.*, 70, 1866, 2006.
52. Allday, P.H. and Correia, J.J., Macromolecular interaction of Halichondrin B analogues Eribulin (E7389) and ER-076349 with tubulin by analytical ultracentrifugation, *Biochemistry*, 48, 7927, 2009.
53. Smith, J.A., Wilson, L., Azarenko, O., Zhu, X., Lewis, B.M., Littlefield, B.A., and Jordan, M.A., Eribulin binds at microtubule ends to a single site on tubulin to suppress dynamic instability, *Biochemistry*, 49, 1331, 2010.
54. Cigler, T. and Vahdat, L.T., Erybulin mesylate for the treatment of breast cancer, *Expert Opin. Pharmacother.*, 11 (9), 15872010.
55. Fernández, Y., Cueva, J., Palomo, A. G., Ramos, M., de Juan, A., Calvo, L., García-Mata, J., García-Teijido, P., Peláez, I., and García-Estévez, L., Novel therapeutic approaches to the treatment of metastatic breast cancer, *Cancer Treat. Rev.*, 36 (1), 33, 2010.

56. Goel, S., Mita, A.C., Mita, M., Rowinsky, E. K., Chu, Q. S., Wong, N., Desjardins, C. et al., A phase I study of eribulin mesylate (E7389), a mechanistically novel inhibitor of microtubule dynamics, in patients with advanced solid malignancies, *Clin. Cancer Res.*, 15 (12), 4207, 2009.
57. Synold, T.W., Morgan, R.J., Newman, E.M., Lenz, H.J., Gandara, D.R., Colevas, A.D., Lewis, M.D., and Doroshow, J.H., A phase I pharmacokinetic and target validation study of the novel anti-tubulin agent E7389: A California Cancer Consortium trial, *J. Clin. Oncol.*, 23 (16, Suppl.), Abst 3036, 2005.
58. Tan, A.R., Rubin, E.H., Walton, D.C., Shuster, D.E., Wong, Y.N., Fang, F., Ashworth, S., and Rosen, L.S., Phase I study of eribulin mesylate administered once every 21 days in patients with advanced solid tumors., *Clin. Cancer Res.*, 15, 4213, 2009.
59. Vahdat, L.T., Pruitt, B., Fabian, C.J., Rivera, R.R., Smith, D.A., Tan-Chiu, E., Wright, J., et al., Phase II study of eribulin mesylate, a halichondrin B analog, in patients with metastatic breast cancer previously treated with an anthracycline and a taxane, *J. Clin. Oncol.*, 27, 2954, 2009.
60. Arnold, S.M., Moon, J., Williamson, S.K., Atkins, J.N., Ou, S.-H.I., LeBlanc, M., and Urba, S.G., Phase II evaluation of eribulin mesylate (E7389, NSC707389) in patients with metastatic or recurrent squamous cell carcinoma of the head and neck: Southwest Oncology Group trial S0618, *Invest. New Drugs*, 29 (2), 352, 2010.
61. Elsayed, Y.A., Rosen, L., Rajeev, V., Wiggins, L., Liang, E., DesJardins, C., Woeppel, S., and Kornowski, A., Phase I study of a new halichondrin B analog, E7389, administered by 1-hour IV infusion every 21 days, *Eur. J. Cancer Suppl.*, 2 (8), Abst 535, 2004.
62. Desai, K.K., Goel, S., Mita, A., Silberman, S., Sicam, J., Woeppel, S., Macapinlac, M., Berg, K., Rowinski, E., and Mani, S., Dose escalation and pharmacokinetic (PK) study of E7389, a microtubule-binding drug in patients (pts) with advanced solid tumors, *Proc. Am. Soc. Clin. Oncol.*, Abst 3090, 2005.
63. Silberman, S.L., O'Shaughnessy, J., and Vahdat, L. E7389, a novel anti-tubulin, is safe and effective in patients with refractory breast cancer, *Proc. 28th Annu. San Antonio Breast Cancer Sym.*, Abst 1063, 2005.
64. Blum, J., Forero, L., Heiskala, M.K., Meneses, N., Chandrawansa, K., Fang, F., Shapiro, G., Fields, S. Z., Silberman, S., and Vahdat, L., E7389, a novel anti-tubulin, in patients with refractory breast cancer, *Proc. Am. Soc. Clin. Oncol.*, Abst 653, 2006.
65. Das, A., Spira, A., Iannotti, N., Savin, M., Zang, E., Datta, K., Shapiro, G., Patturajan, M., and Silberman, S., A phase II study of a novel anti-tubulin, E7389, in patients with advanced non-small cell lung cancer (NSCLC), *Proc. Am. Soc. Clin. Oncol.*, Abst 7106, 2006.
66. Cortes, J.A., Campone, M., Twelves, C., Vahdat, L.T., Blum, J.M., Rivera, R.R., Shuster, D.E., Wanders, J., Fang, F., and Allison, M.A.K., Eribulin mesylate (E7389) in patients with locally advanced or metastatic breast cancer previously treated with an anthracycline and a taxane: Phase II neuropathy data, *Ann. Oncol.*, 19 (Suppl. 8), Abst 156P, 2008.
67. Goel, R., Vidal, L., Welch, S., Laurie, S., Siu, L., Jonker, D., Srinivasan, R., Wang, L., Fortin, C., and Oza, A.M., Phase I study of E7389/gemcitabine combination in patients with advanced solid tumours, *Eur. J. Cancer Suppl.*, 6 (12), Abst 417, 2008.
68. Minami, H., Mukohara, T., Nagai, S., Mukai, H., and Namiki, M., A phase I study of eribulin mesylate (E7389) in patients with refractory cancers, *Eur. J. Cancer Suppl.*, 6 (12), Abst .446, 2008.
69. Vahdat, L.T., Twelves, C., Allison, M.K., Cortes, J.A., Campone, M., Shuster, D.E., Wanders, J., Fang, F., Gurnani, R.D., and Blum, J.L., Phase II study of eribulin mesylate (E7389) in patients (pts) with locally advanced or metastatic breast cancer (MBC) previously treated with anthracycline, taxane, and capecitabine therapy, *J. Clin. Oncol.*, 26 (15, Suppl.), Abst 1084, 2008.
70. Gitlitz, B.J., Davies, A.M., Belani, C.P., Argiris, A., Ramalingam, S.S., Hoffman, P.C., Koczwas, M., Groshen, S.G., and Gandara, D.R., A phase II study of the halichondrin B analog, E7389, in patients (pts) with advanced non-small cell lung cancer (NSCLC) previously treated with a taxane: A California consortium/university of Pittsburgh/university of Chicago NCI/CTEP sponsored trial, *J. Clin. Oncol.*, 27 (15, Suppl.), Abst 8056, 2009.
71. Gitlitz, B.J., Davies, A.M., Belani, C.P., Athanassios, A., Ramalingam, S.S., Hoffman, P.C., Koczywas, M., Groshen, S.G., and Gandara, D.R., Notable progression free survival (PFS) and disease control rate (DCR) with the Halichondrin B analogue Eribulin Mesylate in advanced non-small cell lung cancer (NSCLC) patients (pts) previously treated with a taxane, *Proc. 13th World Conf. Lung Cancer*, Abst. PD3.3.8, 2009.
72. Hensley, M.L., Kravetz, S., Sima, C., Tew, W., Pereira, L., Sabbatini, P., Whalen, C., Aghajanian, C.A., Zarwan, C., and Berlin, S., Eribulin mesylate (halichondrin B analog E7389) in platinum-resistant epithelial ovarian cancer (PR-EOC): A CTEP-sponsored phase II study, *J. Clin. Oncol.*, 27 (15, Suppl.), Abst. 5561, 2009.

73. Schoffski, P., Ray-Coquard, I.L., Cioffi, A., Bin Bui, N., Bauer, S., Hartmann, J. T., Sciot, R., Wanders, J., Druyts, D., and Hohenberger, P., Activity of eribulin mesylate (E7389) in patients with soft tissue sarcoma (STS): Phase II studies of the European Organisation for Research and Treatment of Cancer Soft Tissue and Bone Sarcoma Group (EORTC 62052), *J. Clin. Oncol.*, 28 (15, Suppl.), Abst 10031, 2010.
74. Witteveen, P., Marchetti, S., Mergui-Roelvink, M., Reyderman, L., Copalu, W., Wanders, J., Jenner, A., Edwards, G., Schellens, J.H., and Voest, E.E., Eribulin mesylate pharmacokinetics in patients with hepatic impairment, *J. Clin. Oncol.*, 28 (15, Suppl.), Abst. 2582, 2010.
75. Twelves, C., Cortes, J., Vahdat, L.T., Wanders, J., Akerele, C., and Kaufman, P.A., Phase III trials of eribulin mesylate (E7389) in extensively pretreated patients with locally recurrent or metastatic breast cancer, *Clin. Breast Cancer*, 10 (2), 160–163, 2010.

14 HTI-286 (Taltobulin), A Synthetic Analog of the Antimitotic Natural Product Hemiasterlin

Raymond J. Andersen, David E. Williams, Wendy K. Strangman, and Michel Roberge

CONTENTS

14.1 Introduction 347
14.2 Natural Product Lead Structures 347
14.3 Biological Activity of the Natural Products 349
14.4 Synthesis of Hemiasterlin 351
14.5 Synthesis of Analogs and SAR 355
14.6 Biological Activity of HTI-286 357
14.7 Preclinical and Clinical Development of HTI-286 357
14.8 Summary 359
Acknowledgment 360
References 360

14.1 INTRODUCTION

HTI-286 (**1**) is a synthetic experimental anticancer drug that progressed to phase II clinical trials for the treatment of nonsmall-cell lung cancer.[1] It shows activity in a wide variety of tumor xenograft models, including several multidrug-resistant tumors. The lead structure for the development of HTI-286 was the sponge tripeptide hemiasterlin (**2**), a microtubule depolymerizing agent that kills cells by causing mitotic arrest leading to apoptosis. The sequence of discoveries that led to the development of HTI-286 and a profile of its biological activities are described next.

14.2 NATURAL PRODUCT LEAD STRUCTURES

The hemiasterlins, criamides, and milnamides are a small family of tri- and tetrapeptide cytotoxins isolated from a variety of marine sponges. Hemiasterlin (**2**) was first isolated by Kashman et al. in 1994 from the sponge *Hemiasterella minor* (Kirkpatrick) collected in Sodwana Bay, South Africa.[2] At virtually the same time, Crews et al. reported the isolation of milnamide A (**3**) from the sponge *Auletta* cf. *constricta* collected in Milne Bay, Papua New Guinea,[3a] and subsequently Crews' group reported the isolation of milnamide C (**3a**) from the same *Auletta* sp.[3b] Both source sponges also contained cyclic depsipeptide cytotoxins. *Hemiasterella minor* yielded jaspamide (jasplakinolide) (**4**) and geodiamolide TA (**5**) in addition to hemiasterlin (**2**), while *A. constricta* contained jaspamide (**4**) and milnamide A (**3**).

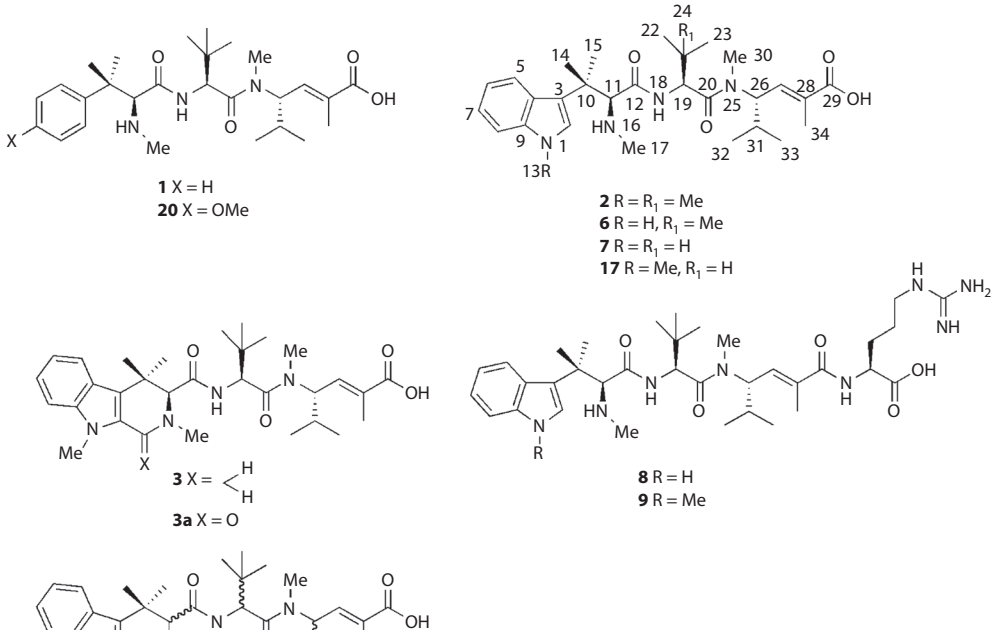

STRUCTURE 14.1

Hemiasterlin (**2**) is a tripeptide comprised of the rare amino acid *tert*-leucine and the two novel amino acids 4-amino-2,5-dimethylhex-2-enoic acid and *N,N′*,β,β-tetramethyltryptophan. *Tert*-Leu had been previously reported only from the discodermins,[4] isolated from the marine sponge *Discodermia kiiensis*, and the bottromycin peptides, produced by cultured actinomycetes.[5] Milnamide A (**3**) has a β-carboline, formally derived from *N,N′*,β,β-tetramethyltryptophan via a Pictet Spengler condensation with formaldehyde, in place of the *N,N′*,β,β-tetramethyltryptophan residue in hemiasterlin (**2**). The 4-amino-2,5-dimethylhex-2-enoic acid residue in **2** and **3** appears to have a biogenetic origin involving *N*-methylvaline and propionic acid-building blocks. There were no relative or absolute configurations assigned to the amino acids in hemiasterlin (**2**) or milnamide A (**3**) in the original reports of their structures. Kashman noted there was an NOE observed between the olefinic methyl (H-34) and tryptophan *N*-methyl (H-17) proton resonances in hemiasterlin (**2**), suggesting a cyclic conformation of the C-11 to C-29 peptide backbone, probably stabilized by an electrostatic attraction between the spatially close *C*-terminal carboxylate anion and *N*-terminal *N*-methyl ammonium cation of the zwitterionic linear peptide.[2]

In 1995, Andersen et al. reported the isolation of hemiasterlin (**2**), hemiasterlins A (**6**) and B (**7**), criamides A (**8**) and B (**9**), and geodiamolides A (**10**) to G (**16**) from the sponge *Cymbastela* sp. collected on reefs off Madang, Papua New Guinea.[6] All three amino acids in hemiasterlin were shown to have the L-configuration by a combination of Marfey's analysis on the natural product and single-crystal x-ray diffraction analysis of hemiasterlin methyl ester.[7] It was also shown that the arginine residue in the criamides had the L-configuration. The solid-state conformation of hemiasterlin methyl ester has an extended linear peptide backbone, which supports Kashman's suggestion that ionic interactions play an important role in the formation of a cyclic peptide backbone conformation for hemiasterlin in solution.

Boyd et al. reported finding hemiasterlins in two sponges also collected in Papua New Guinea.[8] An *Auletta* sp. yielded the known compounds hemiasterlin (**2**), hemiasterlin A (**6**), and several geodiamolides, along with the new tripeptide hemiasterlin C (**17**). Two *Siphonochalina* spp. were also found to contain the same hemiasterlin tripeptides **2**, **6**, and **17** along with geodiamolides.

No evidence for the presence of milnamide A (**3**) or hemiasterlin B (**7**) was found in any of the extracts studied. Ireland's group reported isolating jaspamide, hemiasterlin (**2**), milnamide A (**3**), and the new compound milnamide D (**18**) from specimens of *Cymbastela* sp. collected in Milne Bay, Papua New Guinea.[9]

Table 14.1 lists the taxonomic classification of the sponges that have been the source of hemiasterlins and milnamides.[10] The source sponges in the genera *Auletta* and *Cymbastela* belong to the same family *Axinellidae* and they are, therefore, closely related taxonomically. However, the sponges *H. minor* and *Siphonochalina* sp. belong to different orders, and each is in a different order than *Auletta* and *Cymbastela*. Therefore, the genera *Hemiasterella*, *Siphonochalina*, and *Cymbastela/Auletta* are taxonomically very distant, which suggests a microbial rather than sponge-cell origin for the hemiasterlins/milnamides. To date, all occurrences of hemiasterlins/milnamides have been accompanied by cyclic depsipeptides in the jaspamide/geodiamolide family. There is a report of cultured myxobacteria making chondramides [e.g., chondramide A (**19**)], which are close analogs of jaspamide.[11] This strongly supports a microbial origin for the jaspamide/geodiamolide cyclic depsipeptides. The absolute fidelity in the co-occurrence of the hemiasterlin/milnamide and jaspamide/geodiamolide classes of peptides perhaps indicates that there is a single microorganism in each sponge that makes both families. The variation in metabolite content from one source sponge to another might then result either from microbial strain or growth condition differences at each site.

14.3 BIOLOGICAL ACTIVITY OF THE NATURAL PRODUCTS

Kashman reported that hemiasterlin (**2**) showed *in vitro* cytotoxicity against murine leukemia P388 cells at a concentration of ≈19 nM.[2] However, he cautioned that his sample might have contained

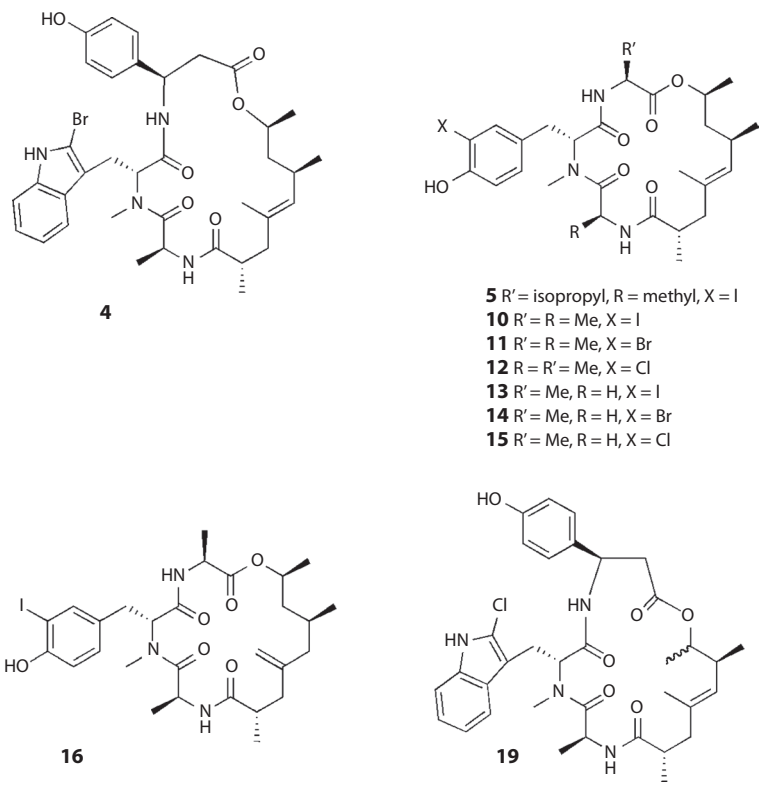

STRUCTURE 14.2

TABLE 14.1
Source Sponges Taxonomy

Research Group	Collection Site	Genus/Species	Class	Order	Family	Compounds
Kashman (1994)	Sodwana Bay, South Africa	*Hemiasterella minor*	Demospongiae	Hadromerida	Hemiasterellidae	Hemiasterlin (**2**) Geodiamolide TA (**5**)
Crews (1994)	Milne Bay, Papua New Guinea	*Auletta* cf. *constricta*	Demospongiae	Halichondrida	Axinellidae	Milnamide A (**3**) Jaspamide (**4**)
Andersen (1995)	Madang, Papua New Guinea	*Cymbastela* sp.	Demospongiae	Halichondrida	Axinellidae	Hemiasterlins (**2**, **6**, **7**) Criamides (**8**, **9**) Geodiamolides (**10–16**)
Boyd (1999)	Papua New Guinea	*Auletta* sp.	Demospongiae	Halichondrida	Axinellidae	Hemiasterlins (**2**, **6**, **17**) Geodiamolides
Boyd (1999)	Papua New Guinea	*Siphonochalina* sp.	Demospongiae	Haplosclerida	Callyspongiidae	Hemiasterlins (**2**, **6**, **17**) Geodiamolides
Ireland (2003)	Milne Bay, Papua New Guinea	*Cymbastela* sp.	Demospongiae	Halichondrida	Axinellidae	Hemiasterlin (**2**) Milnamide D (**18**) Jaspamide (**4**)

impurities of the cytotoxic depsipeptide geodiamolide TA (**5**), so the assays needed to be repeated when additional hemiasterlin became available. Andersen et al. isolated sufficient quantities of hemiasterlin from *Cymbastela* to allow the first determination of accurate IC_{50} for its *in vitro* cytotoxicity.[6] They reported an IC_{50} of 87 pM versus P388, over two orders of magnitude lower than Kashman's value. Potent activity was also observed against a small panel of human cancer cell lines (breast cancer MCF-7, IC_{50} = 169 nM; glioblastoma/astrocytoma U373, IC_{50} = 23 nM; ovarian carcinoma HEY, IC_{50} = 3 nM). The tetrapeptide criamides (**8** and **9**) were found to be roughly a 100-fold less potent than hemiasterlin. Crews reported that milnamide A (**3**) also had *in vitro* cytotoxicity against P388 (IC_{50} 1.4 = μM) and a small panel of human tumor cell lines (IC_{50} = 5.4–7.9 μM), but its potency was modest compared with hemiasterlin.[3] Ireland found that milnamide D (**18**) (IC_{50} = 67 nM) was more potent than milnamide A (**3**) (IC_{50} = 1600 nM) against human colon carcinoma HCT-116 cells *in vitro*, but that both were less potent than hemiasterlin (**2**) (IC_{50} = 6.8 nM), confirming that the presence of the β-carboline *N*-terminus in **3** and **18** decreased activity relative to **2**.[9]

Andersen and Kashman isolated the hemiasterlins as cytotoxic agents with potent subnanomolar to nanomolar activity against P388 mouse leukemia and other cell lines.[2,6] However, the structure of these compounds and their potent cytotoxic activity gave no clue to their mechanism of action. Roberge et al. examined the effects of hemiasterlins on cell cycle progression in human mammary carcinoma MCF-7 cells and found that hemiasterlin, hemiasterlin A, and hemiasterlin B all block cells in mitosis at the same concentrations that showed cytotoxicity.[12] Examination of the hemiasterlin mitotic arrest phenotype using immunofluorescence microscopy showed that the cells arrested at a metaphase-like stage with effects on the morphology of the mitotic spindle that were similar to those caused by tubulin-targeting agents such as vinblastine and nocodazole. High concentrations

of hemiasterlin caused complete microtubule depolymerization. At low hemiasterlin concentrations, cells displayed bipolar spindles with long astral microtubules or multiple asters. Chromosomes failed to align at metaphase and were unable to proceed through later stages of mitosis because of activation of the spindle checkpoint. This study concluded that hemiasterlins exert their cytotoxic effects by inhibiting spindle microtubule dynamics at mitosis.

The study by Anderson[12] implied, but did not demonstrate, that hemiasterlin targets microtubules directly. Lassota at Wyeth subsequently showed that hemiasterlin inhibits the *in vitro* assembly of tubulin into microtubules and noncompetitively inhibits vincristine binding to tubulin.[13] Researchers at the National Cancer Institute (NCI) then examined in detail the interaction of hemiasterlin with tubulin *in vitro*. Gamble et al. showed that hemiasterlin, hemiasterlin A, and hemiasterlin C potently inhibited tubulin polymerization *in vitro* (IC_{50} = 1μM).[8] Bai et al.[14] confirmed that hemiasterlin inhibits noncompetitively the binding of vinblastine to tubulin and inhibits competitively the binding of dolastatatin 10, indicating that hemiasterlin binding causes steric interference with the binding of vinca alkaloids to tubulin.[15] They further demonstrated that hemiasterlin inhibits nucleotide exchange on β-tubulin and that it induces the formation of tubulin aggregates with a ring-like structure and a diameter of about 40 nm. Overall, these effects resembled, but were not identical to, those of dolastatin and cryptophycin, which bind to the same site in tubulin.

The tubulin aggregates induced by hemiasterlin *in vitro* were shown to be closed, single-walled ring-like nanostructures containing 14 α,β-tubulin dimers.[16] These rings form at high concentrations and are unstable—they dissociate even at a relatively high hemiasterlin concentration of 100 nM. This is unlike the rings induced by cryptophycin, which are very stable, and those induced by dolastatin, which have an intermediate stability. As the tubulin rings are induced only at hemiasterlin concentrations about 100-fold above the concentration necessary to induce mitotic arrest and to inhibit cell proliferation, they likely do not contribute to hemiasterlin's cytotoxicity.[16]

The first *in vivo* studies of hemiasterlin were carried out by Theresa Allen at the University of Alberta. As reported by Ireland et al.,[17] she found high antileukemic activity in an *in vivo* P388 murine leukemia model (%T/C 308 with five doses at 0.45 μg per mouse). Hemiasterlin also showed activity in an *in vivo* Gzhi (metastatic murine breast cancer) model: 60% of the mice were long-term survivors with five doses at 1.0 μg per mouse.

14.4 SYNTHESIS OF HEMIASTERLIN

The potent *in vitro* and *in vivo* cytotoxic activity of hemiasterlin, its ability to depolymerize microtubules, a validated anticancer target, and its relatively simple but novel tripeptide structure, made it an attractive target for total synthesis and structure–activity relationship (SAR)-driven modification. A reasonably practical synthesis of hemiasterlin and structural analogs was also required to provide sufficient quantities of compounds for preclinical evaluation and ultimately clinical trials. Andersen and Piers reported the first total synthesis of hemiasterlin in 1997.[18,19] The synthesis employed a convergent approach that involved independent preparation of appropriately protected forms of the novel *N*-terminal tetramethyltryptophan and *C*-terminal 4-amino-2,5-dimethylhex-2-enoic acid residues, followed by peptide coupling with the commercially available L-*tert*-leucine.

The synthesis of Boc-protected tetramethyltryptophan starting from indole-3-acetic acid is outlined in Scheme 14.1. Methylation, first with diazomethane and then with potassium hexamethylsilazide and methyl iodide, introduced the side chain gem-dimethyl and indole *N*-methyl substituents present in the desired tetramethyltryptophan residue. Homologation of the permethylated indole acetic acid was accomplished in a straightforward fashion to give an intermediate indole-3-propionic acid derivative that contained the carbon skeleton of the final amino acid. Introduction of the α-amino functionality with the correct L-configuration was carried out using Evan's methodology. The Evan's chiral auxiliary was introduced by first making a mixed anhydride with 2,2-dimethylpropionyl chloride, which was then treated with the lithiated isopropyl oxazolidone to give an amide. Sequential treatment of the amide with base and 2,4,6-triisopropylbenzenesulfonyl azide produced

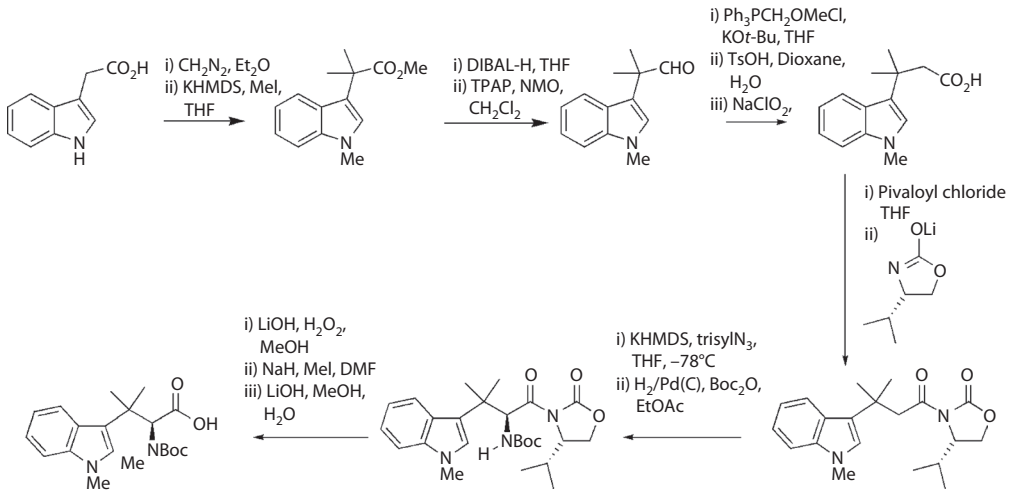

SCHEME 14.1 Synthesis of Boc-tetramethyltryptophan.

an α-azide, which was reduced *in situ* to an amine, and then reacted with di-*tert*-butyl dicarbonate to give the Boc-protected α-amine functionality with the correct configuration. The chiral auxiliary was removed with lithium hydroperoxide and the resulting acid was bismethylated. Hydrolysis of the ester formed in the methylation reaction gave Boc-protected (L)-*N,N′*,β,β-tetramethyltryptophan ready for peptide coupling.

Scheme 14.2 shows the synthesis of Boc-protected 4-amino-2,5-dimethylhex-2-enoic acid. Commercially available (L)-*N*-Boc-*N*-methylvaline was first converted into the Weinreb amide followed by reduction with $LiAlH_4$ to give the corresponding aldehyde. A Wittig reaction on the aldehyde gave the fully protected *C*-terminal amino acid residue with high stereoselectivity.

The reactions involved in coupling the *N*-Boc-amino acids and deprotection to form the desired tripeptide hemiasterlin (**2**) are shown in Scheme 14.3. In the discussions that follow, the *N*-terminal *N,N′*,β,β-tetramethyltryptophan is designated as the "A" residue, *tert*-leucine as "B," and 4-amino-2,5-dimethylhex-2-enoic acid as "C." Formation of the *N*-Boc-B-*C*-OEt dipeptide was accomplished by removal of the *N*-Boc group of the fully protected C residue with TFA, followed by coupling with *N*-Boc-amino acid B as either the mixed anhydride or in the presence of the uronium coupling agent HATU (not shown[19]). Fully protected hemiasterlin resulted from treatment of the TFA salt of the dipeptide B-*C*-OEt with the *N*-Boc-protected amino acid A using PyBOP® as the coupling agent. Deprotected hemiasterlin (**2**) was obtained by saponification of the ethyl ester followed by removal of the Boc group with TFA.

A second, shorter, and more efficient synthesis of hemiasterlin (**2**), which takes advantage of *N*-benzothiazol-2-sulfonyl (Bts)-protected amino acid derivatives, was subsequently reported by Vedejs' group in 2001.[20] The Vedejs approach to hemiasterlin (**2**) outlined in Scheme 14.4 parallels the Andersen synthesis, passing through many of the same intermediates. Commercially available (S)-valinol is the starting point for the Vedejs synthesis of the ethyl ester of 4-amino-2,5-dimethylhex-2-enoic acid.

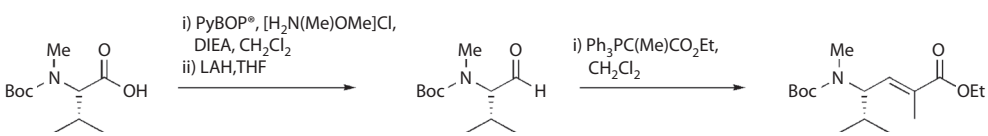

SCHEME 14.2 Synthesis of Boc-4-amino-2,5-dimethylhex-2-enoic acid.

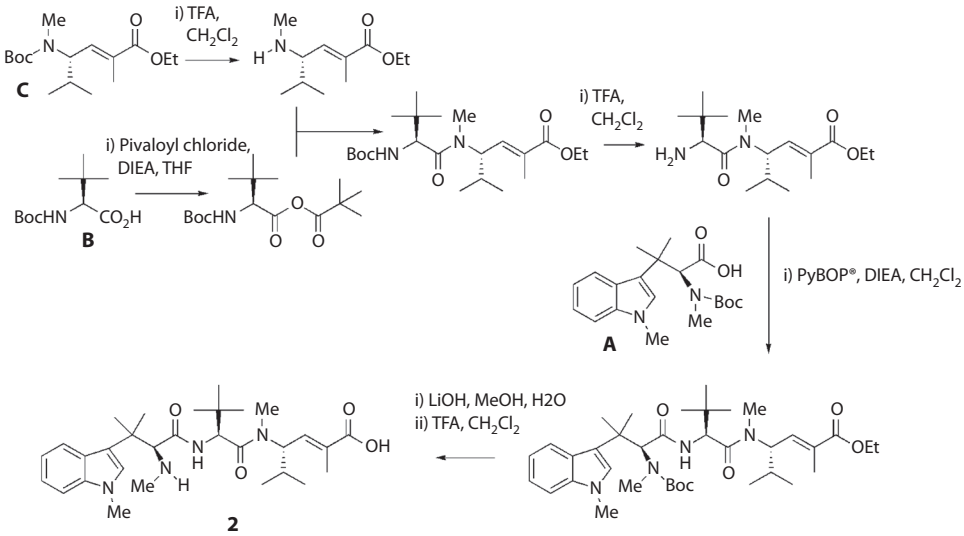

SCHEME 14.3 Andersen synthesis of hemiasterlin.[18,19]

Bts-protected (S)-valinol was readily *N*-methylated under very mild conditions by treatment with iodomethane and potassium carbonate in DMF. Oxidation using either Dess–Martin periodinane or Swern conditions gave the corresponding aldehyde, which was subjected to the same ester-stabilized Wittig reaction employed by Andersen. Removal of the Bts protecting group by treatment with $PhSH/K_2CO_3$ afforded the "C" residue ethyl ester ready for peptide coupling.

L-*tert*-Leucine was protected as its Bts amide and the free carboxylic acid was converted to an acid chloride in preparation for peptide coupling. Biphasic conditions ($NaHCO_3$–Na_2CO_3, CH_2Cl_2–H_2O)

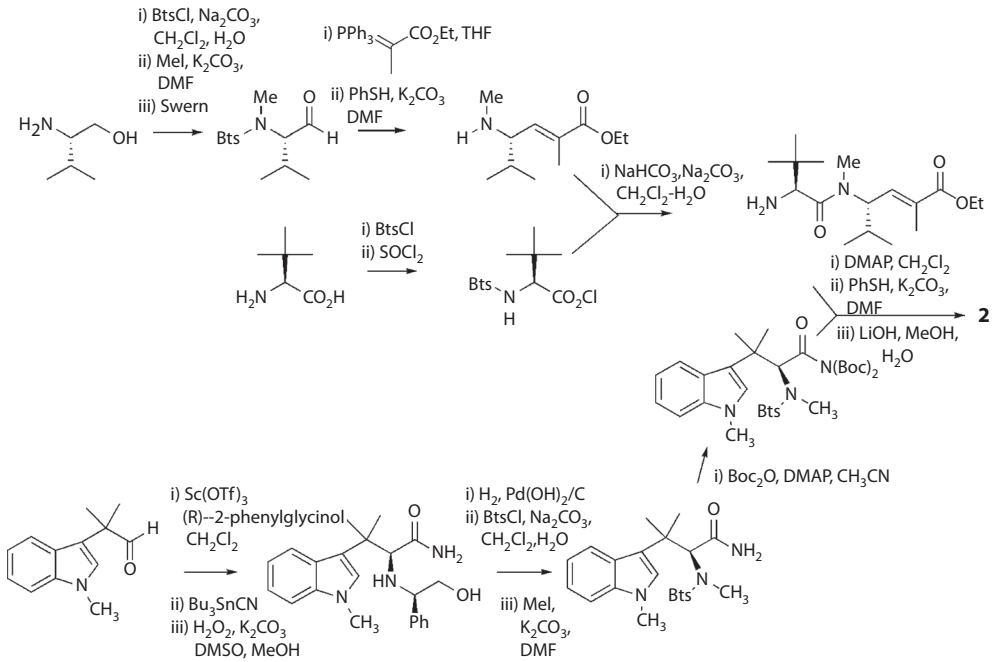

SCHEME 14.4 Vedejs synthesis of hemiasterlin.[20]

were used to couple the activated L-*tert*-leucine with the "C" residue amine. This coupling reaction, involving a *N*-methyl amine, proceeded in higher yield (86%) than the mixed anhydride coupling (69%) employed by Andersen to make the same peptide bond. Removal of the Bts-protecting group by treatment with $PhSH/K_2CO_3$ gave the "BC" dipeptide ethyl ester ready for coupling to the "A" residue.

Synthesis of a protected *N,N′*,β,β-tetramethyltryptophan "A" residue started with the trimethylated indole-3-acetaldehyde intermediate from the Andersen synthesis. An asymmetric Strecker sequence using (*R*)-2-phenylglycinol as the chiral auxiliary and Bu_3SnCN as a source of cyanide was employed to introduce the α-amino group with the required stereochemistry. The resulting nitrile was hydrolyzed to a primary amide with $H_2O_2/K_2CO_3.1.5H_2O$ in 10:1 MeOH:DMSO and the chiral auxiliary was removed by hydrogenolysis to give a primary α-amine. Treatment of the amine with BtsCl followed by methylation with MeI/K_2CO_3 gave the *N*-Bts-*N*-methyl amide, which was converted to the *bis*-Boc derivative by reaction with Boc_2O/DMAP in CH_3CN. The *bis*-Boc amide was reactive enough that with DMAP catalysis it directly formed a peptide bond with the amino group of the "BC" dipeptide ethyl ester (97% yield). Straightforward removal of the Bts ($PhSH/K_2CO_3$) and ethyl ester (LiOH) protecting groups gave hemiasterlin (**2**).

Durst's group has reported two approaches to a convergent asymmetric synthesis of the *N,N′*,β,β-tetramethyltryptophan "A" residue in hemiasterlin (**2**) (Scheme 14.5).[21]

The key sequence of reactions in the first approach are a $SnCl_4$-mediated ring opening of a cyanoepoxide in the presence of *N*-methylindole to give a cyanohydrin, followed by hydrolysis with NaOH to give the trimethylated indole-3-acetaldehyde intermediate from the Andersen and Vedejs syntheses. This intermediate was then converted into the *N*-Boc methyl ester derivative of *N,N′*,β,β-tetramethyltryptophan by a chiral Strecker synthesis similar to that employed by Vedejs. Durst's second approach involved the use of a glycidic ester in place of the cyanoepoxide to directly generate an α-hydroxy methyl ester (Scheme 14.5). Mitsunobu azidization of the α-hydroxy ester followed by reduction with triphenylphosphine in wet THF gave the methyl ester of *N,N′*,β,β-tetramethyltryptophan. Reaction of optically active glycidic ester with *N*-methyl indole gave the α-hydroxy methyl ester with the same optical purity as the glycidic ester. Durst proposed that further transformation of this compound via Mitsunobu azidization and reduction would lead to enantiomerically enriched *N,N′*,β,β-tetramethyltryptophan methyl ester, although this was not verified experimentally.

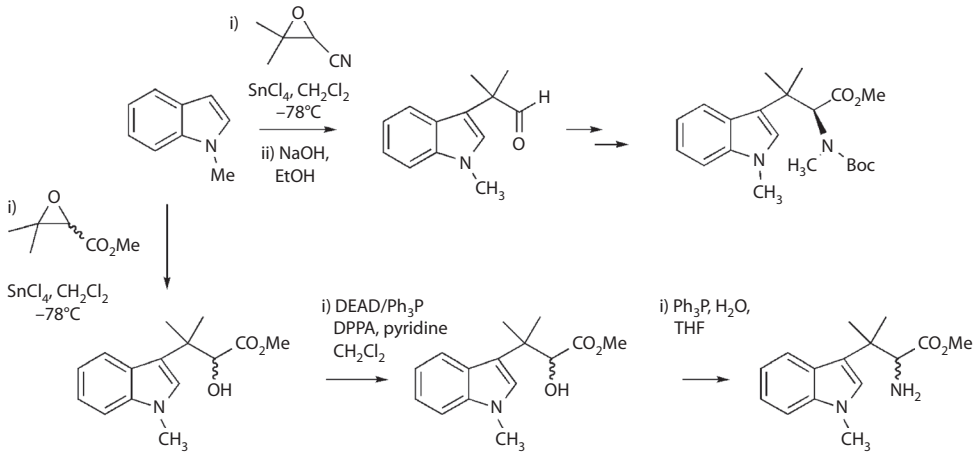

SCHEME 14.5 Synthesis of the *N,N′*,β,β-tetramethyltryptophan residue of hemiasterlin.

14.5 SYNTHESIS OF ANALOGS AND SAR

The convergent nature of the Andersen synthesis[18] of hemiasterlin made it ideally suited for preparing analogs to probe the structural requirements for potent antimitotic activity. Using this synthesis, each of the A, B, and C amino acid residues was altered in turn to prepare a small library of roughly 30 tripeptides that were assessed for biological activity.[19] The synthetic modifications focused on the unique structural features of the natural product hemiasterlin. These included the extensive methylation of the *N*-terminal tryptophan residue, in particular the β,β-dimethylation, the presence of the 4-amino-2,5-dimethylhex-2-enoic acid residue at the *C*-terminus, and occurrence of the rare *tert*-leucine residue in the center of the tripeptide. At the outset, it was felt that these structural features might play important roles in protecting hemiasterlin from proteolysis and in stabilizing a biologically active conformation. A major objective of the analog synthesis program at the University of British Columbia (UBC) was to identify a compound that was more potent and easier to synthesize than the natural product hemiasterlin (**2**).

The development of a convenient cell-based assay for the quantitative determination of cells arrested in mitosis[22] enabled determination of the antimitotic activity of the synthetic hemiasterlin analogs prepared at UBC. A comparison of the IC_{50} of these compounds for antimitotic activity with their IC_{50} for cytotoxicity showed a remarkably linear relation ($r = 0.958$) over a concentration range of almost six orders of magnitude (Figure 14.1).[19] This quantitative relation between antimitotic activity and cytotoxic activity provided strong evidence that the sole mechanism of cytotoxicity of this class of compounds is antimitotic activity, that is, that the hemiasterlins probably have no secondary cellular targets of relevance to cell proliferation or survival.

The synthetic analog study identified structural elements that are critical for potent activity and regions where single structural changes could be made without loss of potent activity (Figure 14.2). It was found that the tryptophan β-methyl substituents, the *N*-methyl substituent on the tryptophan α-amino group, and the *C*-26 isopropyl substituent were all extremely important for potent biological activity. In addition, L-configurations for the *N,N′*,β,β-tetramethyltryptophan and 4-amino-2,5-dimethylhex-2-enoic acid residues, as well as the presence of the $\Delta^{23,24}$ alkene, were required for maximal activity. Conversely, the *C*-terminal carboxylic acid could be converted to a methyl ester, the *N*-25 methyl subsituent could be removed, or the *tert*-leucine residue could be replaced with valine or butyrine as single structural changes without any significant loss in potency. Replacing the

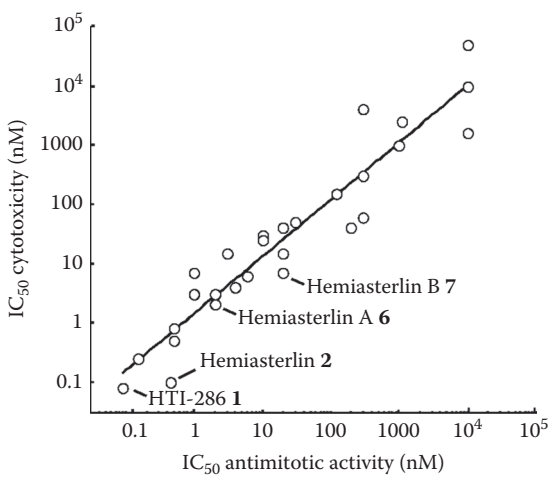

FIGURE 14.1 Plot of *in vitro* cytotoxicity versus antimitotic activity against human breast cancer MCF-7 cells expressing mutant p53, for natural hemiasterlins, HTI-286, and other synthetic analogs (unlabeled circles) generated by Nieman et al.[19]

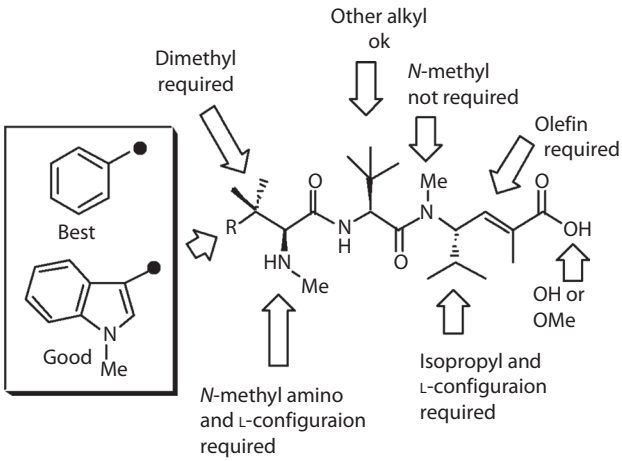

FIGURE 14.2 Structural requirements for optimal cytotoxicity (IC_{50} < 1 nM) and antimitotic activity (IC_{50} < 1 nM) of hemiasterlin analogs.

N-methylindole fragment of the tetramethyltryptophan residue with either methyl or phenyl groups was also well tolerated.

Only one of the synthetic tripeptide analogs tested was more potent than hemiasterlin against MCF-7 mp53 cells. This compound, designated SPA110 (synthetic peptide analog 110), was the phenylalanine analog of hemiasterlin.[19,25] The synthesis of SPA110 was considerably shorter and more efficient than that of hemiasterlin, primarily due to the fact that the carbon skeleton of the β,β-dimethylphenylalanine *N*-terminal residue could be prepared in a single high yield step from benzene and 3-methyl-2-butenoic acid as shown in Scheme 14.6. SPA110 was roughly three-fold more potent than hemiasterlin in Roberge's cell-based antimitotic assay (SPA110, IC_{50} = 0.08 nM; hemiasterlin, IC_{50} = 0.3 nM). On the basis of its relative ease of synthesis and enhanced potency, Wyeth Pharmaceuticals licensed SPA110 from UBC and they gave it the code number HTI-286 (Hemiasterlin Tubulin Inhibitor 286).

The medicinal chemistry group at Wyeth prepared many analogs of HTI-286 (subsequently named Taltobulin by Wyeth) as part of their clinical development program.[26–28] They divided the molecule into the A, B, C, and D fragments as shown in Figure 14.3, and made systematic variations in each of the segments independently. Biological evaluation of their analogs provided further refinement of the SAR for the hemiasterlin/HTI-286 pharmacophore. The general trends observed were: (1) changing the configurations of the amino acids of the A–B–C segments from α*,β*,γ* = *S*,*S*,*S* resulted in reduction of activity; (2) both the *gem*-dimethyl and *N*-methyl groups in the A segment are necessary; (3) a sterically hindered alkyl substituent in the B segment is requisite for activity—*tert*-butyl is best; (4) removal of the *N*-methyl group in the C segment decreases activity; and (5) the configuration of the D segment olefin prefers to be E. One analog, named HTI-042 (**20**), showed slightly superior *in vivo* activity in mouse xenografts with multidrug-resistant cell lines compared with HTI-286.

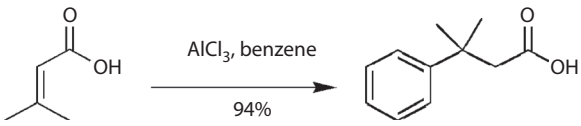

SCHEME 14.6 Synthesis of β,β-dimethylphenylalanine *N*-terminal residue of HTI 286.

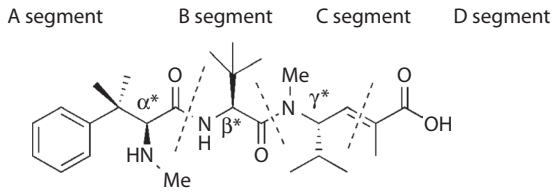

FIGURE 14.3 Segment analysis of HTI-286 used in the Wyeth SAR study.

As part of their SAR investigations, the Wyeth group also made several hybrids of HTI-286 and dolastatins that showed potent *in vitro* cytotoxicity.[23] Qie et al.[24] and Simoni et al.[29] have synthesized HTI-286 analogs with structural variations in the A segment that showed significant activity against cancer cell lines *in vitro*.

14.6 BIOLOGICAL ACTIVITY OF HTI-286

Loganzo et al. published an in-depth study of the tubulin-binding and antiproliferative properties of HTI-286.[30] HTI-286 potently inhibited tubulin polymerization *in vitro* (about 50% at 0.1 μM and totally at 1 μM), about 10-fold more potently than reported by others for hemiasterlin (IC_{50} = 0.98 μM).[8] The effects of HTI-286 on the morphology of mitotic cells were similar to those described for hemiasterlin by Anderson.[12] Flow cytometry showed that HTI-286 caused a pronounced accumulation of cells in the G_2 and/or M phases of the cell cycle after 24 h, consistent with mitotic arrest as the mechanism of action. After 48 h, there was an increase in apoptotic cells.

The antiproliferative activity of HTI-286 was evaluated at Wyeth against a panel of 18 tumor cell lines.[30] The compound showed broad antiproliferative activity, independently of tumor origin, with an average IC_{50} of 2.5 ± 2.1 nM. HTI-286 was more potent than paclitaxel (IC_{50} = 128 ± 369 nM) for all cell lines. Importantly, cells expressing P-glycoprotein, and consequently resistant to many drugs including paclitaxel, retained nearly complete sensitivity to HTI-286. In addition, the KB-8-5 cell line that has been selected for expression of drug efflux pumps by chronic drug exposure was resistant to paclitaxel, docetaxel, vinblastine, vinorelbine, dolastatin-10, colchicine, and doxorubicin, but retained sensitivity to HTI-286. The KB-V1 cell line that expresses very high levels of P-glycoprotein showed resistance (81-fold) to HTI-286, but much less resistance than to paclitaxel (1400–1800-fold). HTI-286 was selected for further preclinical development over other hemiasterlin analogs in large part because of this ability to inhibit the growth of cell lines expressing moderate to high levels of P-glycoprotein.

Researchers at Wyeth[31] found that tritium-labeled benzophenone photoaffinity analogs of HTI-286 specifically and solely photolabel α-tubulin. The binding site maps to sheet 8-helix 10 region of α-tubulin, a region of lateral and longitudinal contacts with other tubulin subunits. In contrast, the binding sites for colchicine are at the α–β-tubulin interface and the binding site for paclitaxel is within β-tubulin. This is the first evidence that a tubulin-binding peptide interacts with α-tubulin and is consistent with the observation that mutations in α-tubulin have been reported in HTI-286-resistant cells.[32,33] Physical methods, including STD-NOE experiments have been used to further probe the binding of HTI-286 and analogs to tubulin.[34,35] The STD-NOE experiments showed that the bound and solution conformations of HTI-286 closely matched the solid-state conformation of the methyl ester of hemiasterlin[7] and they provided support for the SAR data generated from analog synthesis.[19,25–28]

14.7 PRECLINICAL AND CLINICAL DEVELOPMENT OF HTI-286

The initial encouraging *in vivo* efficacy of hemiasterlin in the mouse leukemia P388 model reported by Coleman et al.,[6] combined with the availability of HTI-286, a potent, water-soluble, and more readily synthesized analog, prompted Wyeth to examine the ability of HTI-286 to inhibit tumor

growth in a variety of mouse models.[30] HTI-286 administered intravenously has *in vivo* efficacy against a variety of xenograft tumor models, including LOX-IMVI melanoma, KB-3-1 epidermoid carcinoma, PC3-MM2 prostate carcinoma, SW620 colon carcinoma, U87 glioma, MCF-7 breast carcinoma, and LOVO colon carcinoma. Moreover, HTI-286 was able to inhibit the growth of even large established tumors derived from LOX-IMVI, KB-3-1, LOVO, and PC3MM2. HTI-286 administered for 4 days inhibited the growth of 2.5 g LOX-IMVI tumors and subsequent dosing caused 93% tumor regression. Subsequent studies by Gleave et al. reported promising *in vivo* activity for HTI-286 in mouse models of high-grade bladder cancer[36] and prostate cancer,[37] and Vashist et al. found HTI-286 very effective in mouse models of liver cancer.[38] These groups concluded that HTI-286 is a strong candidate for evaluation in patients with bladder, prostate, or liver cancer.

In keeping with results observed with cell lines in culture, HTI-286 also displayed efficacy against tumors derived from cell lines with inherent or acquired multidrug resistance; KB-8-5 tumors, MX-1W human breast carcinoma, DLD-1 human colon carcinoma, and HCT-15 human colon carcinoma all overexpress P-glycoprotein and showed resistance to paclitaxel or vincristine, but were sensitive to HTI-286.[30] Interestingly, ovarian carcinoma cells resistant to paclitaxel or epothilone, and an A549 lung carcinoma line selected for epothilone resistance because of mutations in the α-tubulin gene, also retained sensitivity to HTI-286.[30]

In addition to targeting cancer cells directly, some microtubule-depolymerizing agents, notably combretastatin A4 phosphate, cause collapse of the tumor vasculature.[39] Targeting the vasculature contributes to killing cancer cells by shutting down blood flow to the tumor. Bert Vogelstein's group has shown that a single dose of HTI-286 (1.7 mg/kg) administered intravenously in mice bearing subcutaneous xenografts of HCT-116 cells caused a complete inhibition of blood flow to the tumors.[40] This effect appeared specific to the tumor vasculature as blood vessels in the skin overlying the tumors was unaffected. This effect occurred rapidly, within 3 h of HTI-286 injection, and was, therefore not due to inhibition of vasculature endothelial cell proliferation. HTI-286 also did not destroy endothelial cells, suggesting that disruption of the microtubule network of the tumor endothelial cells is the cause of vasculature collapse.[40] HTI-286 caused a large increase in tumor hypoxia and rapid hemorrhagic necrosis, indicating that targeting of the tumor vasculature is an important determinant of the antitumor activity of HTI-286.

High nitric oxide synthase activity in tumors seems to confer resistance to combretastatin A4 phosphate.[41] For this reason, Dang et al. examined the effects of combining a lower dose of HTI-286 (1 mg/kg) and the nitric synthase inhibitor L-NNA on xenograft growth. L-NNA significantly enhanced the response to this low dose of HTI-286, without adding toxicity. Moreover, combination treatment with spores of *C. novyi-NT*, a strain of anaerobic bacteria that grow only in hypoxic areas of tumor and can kill tumor cells, further substantially improved the therapeutic effect of L-NNA plus low-dose HTI-286.[40] Wyeth also examined the metabolism of HTI-286 *in vitro* in liver microsomes from a variety of animal species, and *in vivo* in rats and dogs. HTI-286 was metabolized to a major biologically inactive *N*-demethylated species.[42]

Wyeth's preclinical studies also showed that HTI-286 has efficacy when administered orally.[30] These favorable preclinical parameters, combined with the relative ease of synthesis and water solubility of HTI-286, suggested that HTI-286 may have clinical utility in patients, particularly those with intrinsic or acquired resistance to paclitaxel.

A phase I clinical trial was carried out in 2002 with patients with metastatic or advanced-stage malignant solid tumors to assess the safety, tolerability, and pharmacokinetics of HTI-286. HTI-286 dissolved in saline was administered intravenously over 30 min once every 21 days at doses ranging from 0.06 to 2.0 mg/m.^{2} This investigation has been published in abstract form by Ratain et al.[43] Pain, hypertension, and neutropenia were observed as dose-limiting toxicities. Preliminary pharmacokinetic data indicated considerable interindividual variability in clearance, steady-state volume of distribution, and half-life. Serum concentrations above 0.5 ng/mL were associated with neutropenia. The study recommended a phase II dose of 1.5 mg/m^2 and additional studies to determine the basis for the marked interindividual variability in clearance.

An additional phase I dose escalation study of HTI-286 administered in combination with carboplatin was announced, but the results have not been published. A phase II open-label study of HTI-286 as a single agent for the treatment of nonsmall-cell lung cancer for disease reoccurrence following platinum-based therapy was carried out by Wyeth.[1] This trial was suspended before completion and no published explanation exists.

14.8 SUMMARY

Natural products continue to be an important source of lead structures for the development of new experimental drugs for the treatment of cancer.[44] The development path leading to HTI-286 illustrates some of the challenges and opportunities encountered in bringing a marine natural product-derived drug to clinical trials.[45]

Marine sponges, which are the most primitive metazoans in the oceans, are one of the richest source of new marine natural product structures.[44,46] Secondary metabolites isolated from sponge tissues can be either true metabolites of the sponge's own enzymes or metabolites of microorganisms living in association with the sponge. Large-scale wild harvest of the source sponge is environmentally unacceptable, and the problems associated with sponge aquaculture and with laboratory culture of sponge-associated microorganisms, make it difficult to routinely use nature's biosynthetic machinery to make sponge-derived compounds in bulk. Therefore, the major practical source of sponge secondary metabolites for drug development at the moment is via laboratory synthesis. Consequently, the current goal of examining sponge-derived natural products as part of drug discovery programs is primarily to find "chemical inspiration" about new pharmacophores. A lot of research aimed at overcoming the limitations of culturing sponges and their associated microorganisms, partly involving genetic approaches to cloning entire biosynthetic pathways, is ongoing so this situation might well change in the near future. As suggested before, hemiasterlin, which was the "chemical inspiration" for the HTI-286 antimitotic pharmacophore, is presumably a microbial secondary metabolite. Several attempts by the Andersen group at UBC to isolate and culture a hemiasterlin-producing microorganism from *Cymbastela* tissues have all failed.

A number of features of hemiasterlin made it stand out as an extremely exciting natural product lead structure for an anticancer drug development program. The first properties that attracted attention were its exceptionally potent *in vitro* and *in vivo* cytotoxicities against P388 and its relatively simple tripeptide structure. Identification of tubulin as its molecular target elevated the interest in the compound and really provided the impetus for initiating the synthetic program. It is interesting to speculate whether a tripeptide antimitotic agent such as HTI-286 would have ever emerged from a combinatorial chemistry screening program. Some of the first combinatorial libraries were comprised of small peptides made from protein amino acids and a Trp–Val–Val tripeptide would have been a logical compound to make as part of a small peptide library. However, the SAR studies on hemiasterlin showed that such an unmodified tripeptide would not have shown significant activity in a cytotoxin or cell-based antimitotic screen. Nature revealed through the natural product hemiasterlin the additional requirements of extensive β- and *N*-methylation, along with modification of the *C*-terminal valine residue, which are necessary to create potent antimitotic activity and likely proteolytic stability starting from this simple tripeptide template. These combined modifications are unlikely to have been part of a combinatorial synthesis program prior to the "chemical inspiration" provided by the discovery of the natural product hemiasterlin.

Lack of a reliable industrial-scale source of the natural compound or bioactive synthetic analogs is often a major impediment to developing a natural product lead into a drug. The relatively easy synthetic accessibility to hemiasterlin and analogs played an important role in moving the development of this class of antimitotic peptides forward. Synthesis provided hemiasterlin and selected analogs in sufficient quantities for more detailed preclinical *in vitro* and *in vivo* evaluation and guaranteed an unlimited supply of compound for human trials and eventual clinical use. It is important to recognize that the natural product hemiasterlin already had very potent *in vitro* and

in vivo activity against human tumor cell lines, so nature had done most of the work of optimizing the SAR for this pharmacophore. Analog synthesis did identify HTI-286, which shows an incremental improvement in activity profile, but all other analogs made and tested at UBC showed a loss of activity relative to the natural product.[19] The Wyeth medicinal chemistry program did identify other hemiasterlin analogs such as HTI-042 with biological activity superior to the natural product lead compound.[24–26]

Two important milestones in the preclinical decision process to move ahead with HTI-286 were its superior *in vitro* cytotoxicity profile versus multidrug-resistant human cancer cells lines relative to the natural product hemiasterlin, and the fact that it retained activity against taxol and vinca alkaloid-resistant cell lines in mouse tumor xenograft models. Other desirable attributes were its chemical stability and solubility in saline, making formulation straightforward, and its oral activity in mouse models. The discovery that it interacts with α-tubulin distinguished it mechanistically from other tubulin depolymerization agents and raised its development profile.

HTI-286 appears to be a very promising experimental anticancer drug. It represents a new "natural product inspired" chemical structural class of antimitoic agents that target tubulin and inhibit its polymerization into microtubules. HTI-286 shows excellent intravenous and oral activity against drug-sensitive and multidrug-resistant human tumors in mouse xenograft models, both preventing the growth of newly implanted tumors and also regressing well-established tumors. The compound successfully completed a phase I clinical trial, which established a maximum tolerated dose in humans and identified the dose-limiting toxicities. A partial phase II clinical trial with HTI-286 for treatment of nonsmall-cell lung cancer for disease reoccurrence following platinum-based therapy was carried out by Wyeth, but it was suspended early. No explanation was give for the termination of the trial, but it presumably was motivated by lack of sufficient efficacy data to warrant continuation. As with all experimental drugs, there was the hope that the high level of efficacy observed for HTI-286 in preclinical animal models would translate into real benefit for human cancer patients resulting from the discovery of the inspirational natural product hemiasterlin. Only time and further clinical evaluation of HTI-286 and other hemiasterlin analogs[47] will tell if this hope is realized.

ACKNOWLEDGMENT

Financial support for the research at UBC was provided by the NCI of Canada (MR, RJA), the National Institute of Health (USA, RJA), and the Natural Sciences and Engineering Research Council of Canada (RJA, EP). The authors wish to thank Theresa Allen, Ed Piers, Hilary Anderson, John Coleman, Mike LeBlanc, Dilip de Silva, Debra Wallace, Lynette Lim, and Jim Nieman, who all played important roles in the research leading to HTI-286 (SPA-110) at UBC. Wyeth Pharmaceuticals has been a wonderful partner in taking HTI-286 from a basic laboratory discovery to clinical trials. Many individuals at Wyeth, too numerous to mention, made major contributions to the basic science of HTI-286 and its preclinical development. Several others who deserve special mention are Phil Frost, Lee Greenberger, Frank Loganzo, Carolyn Discafani, Arie Zask, and Semiramis Ayral-Kaloustian.

REFERENCES

1. http://www.hrcc.on.ca/ActiveTrials.asp.
2. Talpir, R., Benayahu, Y., Kashman, Y., Pannell, L., Hemiasterlin and geodiamolide TA: Two new cytotoxic peptides from the marine sponge hemiasterella minor (Kirkpatrick), *Tetrahedron Lett.*, 35, 4453, 1994.
3. (a) Crews, P., Farias, J. J., Emrich, R., Keifer, P. A., Milnamide A, an unusual cytotoxic tripeptide from the marine sponge *Auletta cf constricta*, *J. Org. Chem.*, 59, 2932, 1994. (b) Sonnenschein, R. N., Farias, J. J., Tenny, K., Mooberry, S. L., Lobkovsky, E., Clardy, J., Crew, P., A further study of the cytotoxic constituents of a milnamide-producing sponge, *Org. Lett.*, 6, 779, 2004.

4. Matsunaga, S., Fusetani, N., Konosu, S., Bioactive metabolites VI. Structure elucidation of discodermin A, an antimicrobial peptide from the marine sponge *Discodermia kiiensis*, *Tetrahedron Lett.*, 25, 5165, 1984.
5. Kaneda, M., Studies on the bottromycins I. proton and carbon-13 NMR assignments of bottromycin A2, the main component of the complex, *J. Antibiot.*, 45, 792, 1992.
6. Coleman, J. E., de Silva, E. D., Kong, F., Andersen, R. J., Cytotoxic peptides from the marine sponge *Cymbastela* sp., *Tetrahedron*, 51, 10653, 1995.
7. Coleman, J. E., Patrick, B. O., Andersen, R. J., Rettic, S. J., Hemiasterlin methyl ester, *Acta Crystal.*, 52, 1525, 1996.
8. Gamble, W. R., Durso, N. A., Fuller, R. W., Westergaard, C. K., Johnson, T. R., Sackett, D. L., Hamel, E., Cardellina II, J. H., Boyd, M. R., Cytotoxic and tubulin-interactive hemiasterlins from *Auletta* sp. and *Siphonochalina* spp. sponges, *Bioorg. Med. Chem.*, 7, 1611, 1999.
9. Chevallier, C., Richardson, A. D., Edler, M. C., Hamel, E., Harper, M. K., Ireland, C. M., A new cytotoxic and tubulin-interactive milnamide derivative from a marine sponge *Cymbastela* sp., *Org. Lett.*, 5, 3737, 2003.
10. Hooper, J. N. A., van Soest, R. W. M., *Systema Porifera, a Guide to the Classification of Sponges*, Kluwer Academic/Plenum, New York, 2002.
11. Kunze, B., Jansen, R., Sasse, F., Holfe, G., Richenbach, H., Chondramines, A-D., new antifungal and cytostatic depsipeptides from *Chondromyces crocatus* (Myxobacteria). Production, physico-chemical and biological properties, *J. Antibiot.*, 48, 1262, 1995.
12. Anderson, H. J., Coleman, J. E., Andersen, R. J., Roberge, M., Cytotoxic peptides hemiasterlin, hemiasterlin A and hemiasterlin B induce mitotic arrest and abnormal spindle formation, *Cancer Chemother. Pharmacol.*, 39, 223, 1997.
13. Peter Lassota, unpublished results (personal communication).
14. Bai, R., Durso, N. A., Sackett, D. L., Hamel, E., Interactions of the sponge-derived antimitotic tripeptide hemiasterlin with tubulin: Comparison with dolastatin 10 and cryptophycin 1, *Biochemistry*, 38, 14302, 1999.
15. Hamel, E., Interactions of antimitotic peptides and depsipeptides with tubulin, *Biopolymers*, 66, 142, 2002.
16. Boukari, H., Nossal, R., Sackett, D. L., Stability of drug-induced tubulin rings by fluorescence correlation spectroscopy, *Biochemistry*, 42, 1292, 2003.
17. Ireland, C. M., Aalbersberg, W., Andersen R. J., Ayral-Kaloustian, S., Berlinck, R. G. S., Bernan, V., Carter, G. et al., Anticancer agents from unique natural products sources, *Pharmaceutical Biol.*, 41, Supplement, 15–48, 2003.
18. Andersen, R. J., Coleman, J. E., Total synthesis of (-)-hemiasterlin, a structurally novel tripeptide that exhibits potent cytotoxic activity, *Tetrahedron Lett.*, 38, 317, 1997.
19. Nieman, J., Coleman, J. E., Wallace, D. J., Pers, E., Lim, L. Y., Roberge, M., Andersen, R.J., Synthesis and antimitotic/cytotoxic activity of hemiasterlin analogs, *J. Nat. Prod.*, 66, 183, 2003.
20. Vedejs, E., Kongkittingam, C., A total synthesis of (-)-hemiasterlin using *N*-Bts methodology, *J. Org. Chem.*, 66, 7355, 2001.
21. Reddy, R., Jaquith, J. B., Neelagiri, V. R., Saleh-Hanna, S., Durst, T., Asymmetric synthesis of the highly methylated tryptophan portion of the hemiasterlin tripeptides, *Org. Lett.*, 4, 695, 2002.
22. Roberge, M., Cinel, B., Anderson, H. J., Lim, L., Jiang, X., Xu, L., Bigg, C. M., Kelly, M. T., Andersen, R. J., Cell-based screen for antimitotic agents and identification of analogues of rhizoxin, eleutherobin and paclitaxel in natural extracts, *Cancer Res.*, 60, 5052, 2000.
23. Zask, A., Kaplan, J., Musto, S., Loganzo, F., Hybrids of the hemiasterlin analogue taltobulin and the dolastatins are potent antimicrotubule agents. *J. Am. Chem. Soc.*, 127, 17667, 2005.
24. Qie. J., Zhou, W., Zhou, X., He, J., Zhang, Y., Liu, K., Hemiasterlin analogues with unnatural amino acids at the N-terminal and their inhibitory activity on tumor cells, *Int. J. Pept. Res. Ther.*, 15, 187, 2009.
25. The synthesis of HTI-286 (SPA 110) was first reported in Andersen, R. J., Piers, E., Nieman, J., Coleman, J., Roberge, M., WO Patent 99/32509, 1999.
26. Zask, A., Birnberg, G., Cheung, K., Kaplan, J., Niu. C., Norton, E., Suayan, R. et al., Synthesis and biological activity of analogues of the antimicrotubule agent N,β,β-trimethyl-L-phenylalanyl-N^1-[(1S,2E)-3-carboxy-1-isopropylbut-2-enyl]- N^1,3-dimethyl-L-valinamide (HTI-286), *J. Med. Chem.*, 47, 4774, 2004.
27. Yamashita, A., Nortton, E. B., Kaplan, J. A., Niu, C., Loganzo, F., Hernandez, R., Beyer, C. F. et al., Synthesis and activity of novel analogs of hemiasterlin as inhibitors of tubulin polymerization: modification of the A segment, *Bioorg. Med. Chem. Lett.*, 14, 5317, 2004.

28. Zask, A., Brinberg, G., Cheung, K., Kaplan, J., Niu, C., Norton, E., Yamashita, A. et al., D-piece modifications of the hemiasterlin analog HTI-286 produce potent tubulin inhibitors, *Bioorg. Med. Chem. Lett.*, 14, 4353, 2004.
29. Simoni, D., Lee, R. M., Durrant, D. E., Chi, N-W., Baruchallo, R., Rondanin, R., Rullo, C., Marchetti, P., Versatile synthesis of new cytotoxic agents structurally related to hemiasterlins, *Bioorg. Med. Chem. Lett.*, 20, 3431, 2010.
30. Loganzo, F., Discafani, C. M., Annable, T., Byeyer, C., Musto, S., Hari, M., Tan, X. et al., HTI-286, a synthetic analog of the tripeptide hemiasterlin, is a potent antimicrotubule agent that circumvents P-glycoprotein-mediated resistance *in vitro* and *in vivo*, *Cancer Res.*, 63, 1838, 2003.
31. Nunes, M., Kaplan, J., Wooters, J., Hari, M., Minnick Jr., A. A., May, M. K., Shi, C. et al., Two photoaffinity analogues of the tripeptide hemiasterlin, exclusively label α-tubulin, *Biochem.*, 44, 6844, 2005.
32. Prouchynsky, M. S., Kim, J-H., Nogales, E., Annable, T., Loganzo, F., Greenberger, L. M., Sackett, D. L., Fojo, T., Tumor cells reistant to a microtubule-depolymerizing hemiasterlin analogue, HTI-286, have mutations in α- or β-tubulin and increased microtubule stability, *Biochem*. 43, 13944, 2004.
33. Loganzo, F., Hari, M., Annable, T., Tan, X., Morilla, D. B., Musto, S., Zask, A. et al., Cells resistant to HTI-286 do not overexpress P-glycoprotein but have reduced drug accumulation and a point mutation in α-tubulin, *Mol. Can. Ther*., 3, 1319, 2004.
34. Lo, M.-C., Aulabaugh, A., Krishnamurthy, G., Kaplan, J., Zask, A., Smith, R. P., Ellestad, G., Probing the interaction of HTI-286 with tubulin using a stilbene analogue, *J. Am. Chem. Soc.* 126, 9898, 2004.
35. Milton, M. J., Williamson, R. T., Koehn, F. E., Mapping the bound conformation and protein interactions of microtubule destabilizing peptides by STD-NMR spectroscopy, *Bioorg. Med. Chem. Lett.*, 16, 4279, 2006.
36. Hadaschik, B. A., Adamat, H., Fazli, L., Fradet, Y., Andersen, R. J., Gleave, M. E., So, A. I., Intravesical chemotherapy of high-grade bladder cancer with HTI-286, a synthetic analogue of the marine sponge product hemiasterlin, *Clin. Cancer Res*., 14, 1510, 2008.
37. Hadaschik, B. A., Ettinger, S., Sowery, R. D., Zoubeidi, A., Andersen, R. J., Roberge, M., Gleave, M. E., Targeting prostate cancer with HTI-286, a synthetic analog of the marine sponge product hemiasterlin, *Int. J. Cancer* 122, 2368, 2008.
38. Vashist, Y. K., Tiffon, C., Stoupis, C., Redaelli, C. A., Inhibition of hepatic tumor cell proliferation *in vitro* and tumor growth *in vivo* by taltobulin, a synthetic analogue of the tripeptide hemiasterlin, *World J. Gastroenterol.*, 12, 6771, 2006.
39. Giggs, J., Metcalfe, J. C., Hesketh, R., Targeting tumour vasculature: The development of combretastatin A4, *Lancet Oncol.*, 2, 82, 2001.
40. Dang, L. H., Bettegowda, C., Agrawal, N., Cheong, I., Huso, D., Frost, P., Loganzo, F. et al., Targeting vascular and avascular compartments of tumors with *C. novyi-NT* and anti-microtubule agents, *Cancer Biol. Ther.*, 3, 326, 2004.
41. Parkins, C. S., Holder, A. L., Hill, S. A., Chaplin, D. J., Tozer, G. M., Determinants of anti-vascular action by combretastatin A4 phosphate: Role of nitric oxide, *Br. J. Cancer*, 83, 811, 2000.
42. Wang, C. P., Talaat, R., Wang, J., Lin, M., Hultin, T., Scatina, J. A., *In vitro* and *in vivo* metabolism of HTI-286, an antimicrotubule anticancer agent, *Drug Metabol. Rev.*, 35 Supplement 2, 42, 2003.
43. Ratain, M. J., Undevia, S., Janisch, L., Roman, S., Mayer, P., Buckwalter, M., Foss, D., Hamilton, B. L., Fischer, J., Bukowski, R. M., Phase 1 and pharmacological study of HTI-286, a novel antimicrotubule agent: correlation of neutropenia with time above a threshold serum concentration, *Proc. Am. Soc. Clin. Oncol.*, 22, 129, 2003.
44. Newman, D. J., Cragg, G. M., Snader, K. M., Natural Products as Sources of New Drugs over the Period 1981-2002, *J. Nat. Prod.*, 66, 1022, 2003.
45. Andersen, R. J., Williams, D. E., in *Chemistry in the Marine Environment*, Vol. 13, R. E. Hester and R. M. Harrison, Eds., The Royal Society of Chemistry, Cambridge, 2000, 55.
46. Blunt, J., Copp, B., Munro, M., Northcote, P. T., Princep, M., Marine natural products, *Nat. Prod. Rep.*, 20, 1, 2003.
47. Kuznetsov, G., TenDyke, K., Towle, M. J., Cheung, H., Liu, J., Marsh, J. P., Schiller, S. E. et al., Tubulin-based antimitotic mechanism of E7974, a novel analogue of the marine sponge natural product hemiasterlin, *Mol. Can. Ther.*, 8, 2852, 2009.

15 The Actinomycins*

Anthony B. Mauger and Helmut Lackner†

CONTENTS

15.1 Historical Introduction 363
15.2 Separation and Nomenclature 364
15.3 Structures 365
15.4 Conformation 366
15.5 Mechanism of Biological Action 366
15.6 *In Vitro* Antitumor Activity 368
15.7 *In Vivo* Antitumor Activity and Toxicity 368
15.8 Synthesis 368
15.9 Analogs 369
15.9.1 Directed Biosynthesis 369
15.9.2 Partial Synthesis 369
15.9.3 Total Synthesis 370
15.10 Structure–Activity Relationships 371
15.10.1 Introduction 371
15.10.2 Natural Actinomycin Variants 372
15.10.3 Chromophoric Analogs 373
15.10.4 Peptidic Analogs 374
15.11 Clinical Applications of Actinomycins 374
References 375

15.1 HISTORICAL INTRODUCTION

The actinomycins, a family of structurally related chromopeptide antibiotics with a common phenoxazinone chromophore attached to two pentapeptide lactone moieties (Figure 15.1), vary in their amino acid content (Table 15.1). They emerged from the pioneering work of Selman Waksman on soil microorganisms, and in particular from his work on the *Streptomyces*. The first actinomycin, isolated in 1940 from *Streptomyces antibioticus*,[1,2] was the first of several antibiotics discovered by Waksman, the first crystalline antibiotic, and the first to display antitumor activity. Many other actinomycins have since been isolated from other *Streptomyces* species, and it was also found in an unrelated genus, *Micromonospora*.[3]

The first actinomycin was described as a red crystalline substance active against Gram-positive microorganisms,[2] but its toxicity[4] precluded its clinical use as an antibiotic. Interest in the actinomycins revived in 1952 when the antitumor activity of another actinomycin (C) in mouse and rat tumors was found by Hackmann[5] and when Schulte reported the first clinical studies.[6] The discovery that actinomycin inhibits DNA-primed RNA synthesis[7,8] resulted in its widespread use in studies of macromolecular biosynthesis and virus replication.[9]

---

* This chapter has been updated by Anthony B. Mauger in collaboration with Gordon M. Cragg, Natural Products Branch, Developmental Therapeutics Program, Division of Cancer Treatment and Diagnosis, National Cancer Institute, Frederick, MD.

† Deceased.

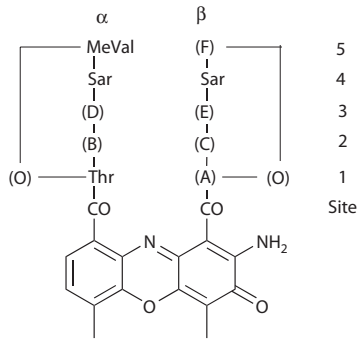

FIGURE 15.1 Structures of 18 naturally occurring actinomycins (see Table 15.1).

15.2 SEPARATION AND NOMENCLATURE

With the first actinomycin preparation designated A, subsequent isolates from different species or strains of *Streptomyces* were termed B,[10] C,[11] D,[12] I,[13] X,[14] Z,[15] and so forth. That they were mixtures was first shown when actinomycin C separated into components C_1, C_2, and C_3 in countercurrent distribution.[16,17] Paper partition chromatographic studies confirmed that most other actinomycin preparations were also multicomponent complexes.[16,18–21] Techniques for their separation have been reviewed.[22]

TABLE 15.1
Structures of Natural Actinomycins (See Figure 15.1)

Actinomycin	A	B	C	D	E	F
$I = X_{0\beta}$	Thr	D-Val	D-Val	Pro	Hyp	MeVal
$X_{0\delta}$	Thr	D-Val	D-Val	Pro	*a*Hyp	MeVal
$II = F_8$	Thr	D-Val	D-Val	Sar	Sar	MeVal
$III^a = F_9$	Thr	D-Val	D-Val	Pro	Sar	MeVal
$IV = X_1 = C_1 = D$	Thr	D-Val	D-Val	Pro	Pro	MeVal
$V = X_2$	Thr	D-Val	D-Val	Pro	4-oxo-Pro	MeVal
X_{1a}	Thr	D-Val	D-Val	Sar	4-oxo-Pro	MeVal
$X_{0\gamma}$	Thr	D-Val	D-Val	Sar	Pro	MeVal
$VI = C_2$	Thr	D-Val	D-*a*Ile	Pro	Pro	MeVal
$i\text{-}C_2$	Thr	D-*a*Ile	D-Val	Pro	Pro	MeVal
$VII = C_3$	Thr	D-*a*Ile	D-*a*Ile	Pro	Pro	MeVal
Z_1	4-OH-Thr	D-Val	D-Val	3-OH-5-MePro	4-oxo-5-MePro	MeAla
Z_2	Thr	D-Val	D-Val	3-OH-5-MePro	4-oxo-5-MePro	MeAla
Z_3	4-Cl-Thr	D-Val	D-Val	3-OH-5-MePro	4-oxo-5-MePro	MeAla
Z_4	Thr	D-Val	D-Val	5-MePro	4-oxo-5-MePro	MeAla
Z_5	4-Cl-Thr	D-Val	D-Val	5-MePro	4-oxo-5-MePro	MeAla
ZP	Thr	D-Val	D-Val	5-MePro	5-MePro	MeVal
G^b	4-OH-Thr	D-Val	D-Val	Pro	3-OH-5-MePro	MeAla

Nonstandard amino acid abbreviations: MeVal = *N*-methylvaline; MeAla = *N*-methylalanine; 5-MePro = 5-methylproline; all amino acids are L except where prefixed by "D."

[a] Actinomycin III is a mixture of two isomers with Pro and Sar interchangeable at sites D and E.

[b] Actinomycin G refers to the product from *Streptomyces HKI-0155*.

This situation was simplified when it was found that different complexes had components in common. Thus, actinomycins A, B, and X contained the same five compounds, albeit in different proportions, and a system of nomenclature was proposed[23] that named them actinomycins I through V in the order of increasing lipophilicity. The actinomycin C components were named IV, VI, and VII, of which only IV was also present in the A, B, and X complexes. Actinomycin D was found to consist solely of IV. The five components of the actinomycin Z complex lie outside this system and are termed Z_1 through Z_5.

While some 26 species of *Streptomyces* and *Micromonospora* have been reported to produce various forms of actinomycins, recent papers have reported that newly isolated strains are capable of producing significant quantities of predominantly one major form;[24] thus, a strain of *Streptomyces griseoruber* isolated from a soil sample associated with the roots of *Azadirachta indica* yielded actinomycin D in titers of 210 mg L^{-1}. This compares with 152 mg L^{-1} of mainly actinomycin D isolated from *Streptomyces parvulus*.[25] Both these yields were obtained under nonoptimized fermentation conditions, and significant improvement can be anticipated through medium optimization. Praveen et al. have also reported the isolation of an actinomycin-D-producing strain, characterized as *Streptomyces sindenensis*, from soil, which, when subjected to UV irradiation, produced a mutant yielding 400 mg L^{-1} as compared with 80 mg L^{-1} produced by the parent;[26] optimization of the production medium increased the yield to 850 mg L^{-1}.

15.3 STRUCTURES

The structures of the best-characterized actinomycins are shown in Figure 15.1 and Table 15.1. The elucidation of the structure of actinomycin C_3 (VII) in 1956 by Brockmann et al. was a notable achievement in the era before nuclear magnetic resonance and mass spectrometry were available.[27] The structure comprises a chromophoric 2-aminophenoxazin-3 one-ring system bearing two methyl groups and two identical pentapeptide lactone moieties. The chromophore, including the two carboxyls, is termed actinocin, so an actinomycin can be described as an actinocinyl-*bis*(pentapeptide lactone).

The structure of actinomycin D (IV; also known as dactinomycin), which has been abbreviated "AMD," was found to be identical to that of C_3, except that both D-*allo*-Ile residues are replaced by D-Val.[28] As distinct from *iso*-actinomycins such as D (IV) and C_3 (VII), the *aniso*-actinomycin C_2 (VI)[29] has a minor regioisomer i-C_2 (originally termed C_{2a}).[30] The two isomers were distinguished via oxidative degradation of the chromophore, permitting separation of the two peptides.[31]

The structures of actinomycins I and V emerged from studies on the reduction of actinomycin X_2 in various ways to generate $X_{0\beta}$ (I), $X_{0\delta}$, and X_1 (IV).[32] The oxygenated proline residues were located in the β-peptide by oxidative degradation of the chromophore. These and other experiments indicated that X_2 contains 4-oxoproline, which is usually destroyed during hydrolysis, and this was confirmed[33] by its isolation. Minor components of the X complex termed $X_{0\gamma}$ and X_{1a} were also described[34] (Table 15.1).

Actinomycins II and III are trace components of the A, B, and X complexes and were characterized after addition of sarcosine to the culture medium for *S. antibioticus* markedly increased their relative concentrations.[35] The added sarcosine acted as a biosynthetic precursor, replacing one or both proline residues.[36] That this involved no change in amino acid sequence was also confirmed.[37] Chromatography revealed that the *aniso*-actinomycin III was a mixture of major and minor regioisomers.[38]

The actinomycin Z complex contains at least five components comprising a far greater diversity of amino acid content than actinomycins I–VII. Early studies[15] revealed that they differ from the other actinomycins in that they all contain *N*-methylalanine, but no proline. Instead, there were several unusual proline congeners found in these actinomycins, including *cis*-5-MePro,[39,40] 4-oxo-5-MePro,[41,42] and *trans*-3-hydroxy-*cis*-5-MePro.[43,44] Moreover, 4-hydroxy-Thr[45] was found in Z_1. More recently, two-dimensional nuclear magnetic resonance and mass spectrometry techniques permitted

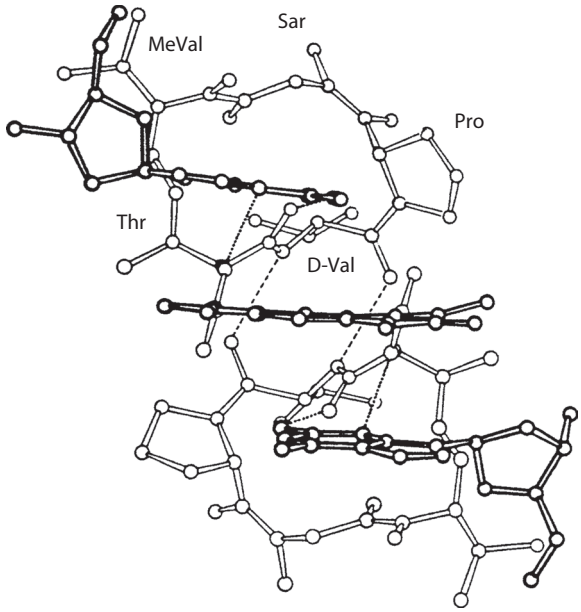

FIGURE 15.2 X-ray crystallographic structure of the 1:2 complex of actinomycin D with deoxyguanosine.[53] The actinomycin chromophore and the deoxyguanosine molecules are shown in bold. Hydrogen bonds are shown as dotted lines. (Reprinted from *J. Mol. Biol*, 68, Jain, S.C. and Sobell, H.M., Stereochemistry of actinomycin binding to DNA. I. Refinement and further structural details of the actinomycin-deoxyguanosine crystalline complex, 1, Copyright (1972), with permission from Elsevier.)

the elucidation of the structures of actinomycins Z_1 through Z_5 and unexpectedly revealed that Z_3 and Z_5 contained 4-chloro-Thr.[46] In addition, actinomycin G from *S. HKI-0155* has been found to have an α-peptide, which is similar to that of AMD, and a Z-type β-peptide.[47] Another actinomycin named ZP has 5-MePro in both peptides but otherwise is identical to AMD.[48]

Numerous other actinomycins have been described, but they are less well characterized structurally than those included in Table 15.1. Information on them is available in several reviews.[49–52]

15.4 CONFORMATION

The first information on the conformation of an actinomycin (D) emerged from an x-ray crystallographic study of its complex with deoxyguanosine (Figure 15.2).[53] Later, x-ray studies of uncomplexed actinomycins D,[54,55] X_2,[56] and Z_3 (Figure 15.3)[55] indicated that their conformations were similar except for an orientation change in the ester linkages. The molecule possesses pseudo-C2 symmetry, and the two peptide moieties are held in unique juxtaposition by two antiparallel hydrogen bonds between the D-Val NH in one peptide and the D-Val C=O in the other, and vice versa. The D-Val-Pro and Pro-Sar peptide bonds are *cis*. Nuclear magnetic resonance studies of actinomycins[57] and of actinomycin–DNA complexes[58] indicate an essentially similar conformation in solution that is remarkably stable in solvents of different polarity.

15.5 MECHANISM OF BIOLOGICAL ACTION

The biological activity of the actinomycins is exerted by inhibition of DNA-dependent RNA synthesis,[7,8] which thereby inhibits protein synthesis.[8] This effect is explained by the strong binding of actinomycin to double-helical DNA.[59,60] This complexation has usually been detected by absorption spectroscopy (bathochromic shift of about 20 nm in the visible maximum of an actinomycin

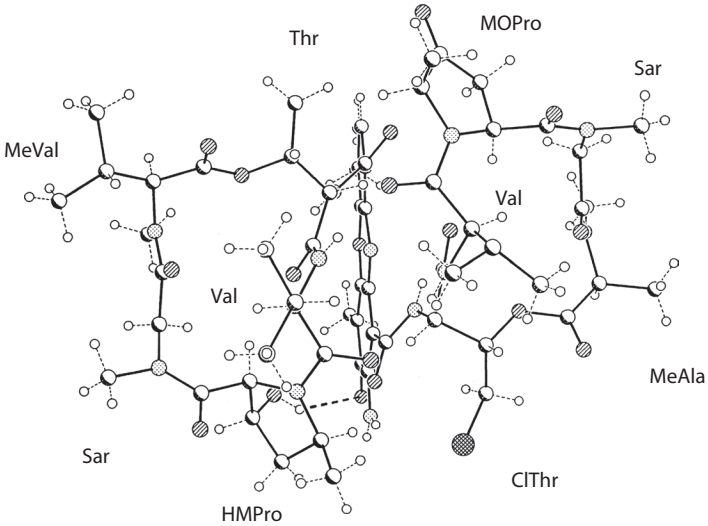

FIGURE 15.3 High-resolution x-ray crystallographic structure of actinomycin Z_3, shown from the chromophoric side of the molecule with the β-peptide ring on the right.[55] *Abbreviations:* MOPro = *cis*-5-methyl-4-oxo-L-proline; HMPro = *trans*-3-hydroxy-*cis*-5-methyl-L-proline (Table 15.1).

normally at 440 nm)[7,61,62] or by elevation in the thermal denaturation temperature (T_m) of the DNA.[63,64] It is required that the DNA be helical[65,66] and that it contains guanine residues.[65,67,68] An intercalative model for the actinomycin–DNA complex was proposed[69] in which the actinomycin chromophore is inserted adjacent to a G–C pair, and this hypothesis was supported by several solution studies involving equilibrium, kinetic and hydrodynamic techniques, and sedimentation coefficients.[70]

Interaction of deoxyguanosine with AMD in solution produces spectral shifts similar to those with DNA.[71] It was therefore of much interest when the 2:1 complex was obtained in crystalline form for x-ray studies.[53] The structure that emerged (Figure 15.2) has approximate twofold symmetry, with the AMD chromophore "sandwiched" between the two guanine ring systems. The complex is held together by π-complex interactions between the three ring systems, by hydrogen bonds between the guanine 2-amino groups and the threonine carbonyl oxygens, and by hydrophobic interactions. This structure provided a model for the geometry of the AMD–DNA interaction, and this model is supported by x-ray structures of DNA complexes of AMD with d(GC)[72] and d(ATGCAT).[73]

The hydrophobic interactions that enhance the binding of actinomycins in the narrow groove of DNA depend on the hydrophobic inner surface of the peptide units, and the nature of the outer surfaces, when the binding occurs near the pause or rho-dependent termination sites of the DNA, terminates transcription by RNA polymerase.[74] Moreover, actinomycins belong to a class of antineoplastic agents that inhibit both topoisomerases I and II. It forms a ternary complex of topoisomerase II, inducing DNA strand breaks,[75] and it also stimulates topoisomerase I-mediated DNA cleavage.[76] Studies have also been reported on the binding of actinomycin D to single-stranded DNA.[77] Recently, evidence has emerged of the capability of actinomycin to downregulate the effect of the transcription factors TBP and Sp1 by blocking access to their specific binding sites.[78]

The DNA structural motif known as the G-quadruplex has recently been identified as a novel target for the discovery and design of new classes of anticancer agents, and DNA sequences capable of forming G-quadruplex structures are located in biologically relevant regions throughout the genome.[79] Recent studies have shown that actinomycin D interacts with oncogenic promoter G-quadruplex DNA to repress gene expression,[80] and binds to the Na^+ and K^+ forms of the G-quadruplex DNA, inducing changes in both their structure and stability.[81]

15.6 *IN VITRO* ANTITUMOR ACTIVITY

Early studies (1958) showed that AMD displays equal growth inhibitory activity against both normal and malignant cells.[82,83] The cytotoxic effects of several actinomycins were compared in HeLa cells.[84] More recently, AMD and several other actinomycins have been evaluated in the 60 human tumor cell line screening system[85] of the National Cancer Institute (NCI). For AMD, the mean molar log GI_{50} (50% growth inhibition), averaged over many experiments, was –8.73. The corresponding numbers for the various panels of cell lines (mean values from several lines) were leukemia: –9.2; nonsmall-cell lung: –8.6; small-cell lung: –8.8; colon: –8.7; central nervous system (CNS): –9.0; melanoma: –8.9; ovarian: –8.4; renal: –8.5; prostate: –8.6; and breast: –8.7. Thus, the most sensitive cell lines were those of leukemia, CNS cancers, and melanoma. In the COMPARE program,[86] AMD most closely resembles other topoisomerase II inhibitors.

15.7 *IN VIVO* ANTITUMOR ACTIVITY AND TOXICITY

The first observations of antitumor activity of an actinomycin (C) involved the suppression of the Ehrlich carcinoma in mice and the Wilms' tumor in rats.[5,87] These were quickly followed by numerous studies in various laboratories; the early work has been reviewed.[88] Among the best responders were the Ridgway osteogenic carcinoma in mice[89] and the Wilms' tumor in rats,[90] especially when combined with radiation.[91] Other experimental tumors susceptible to actinomycins include the P388 and L1210 leukemias, B16 melanoma, and adenocarcinoma 755.[92] Actinomycins C_1 (AMD), C_2, and C_3 were equally efficacious.

Actinomycins are highly toxic;[4] the intravenous LD_{50} of AMD in mice and rats are 1.2 and 0.6 mg kg^{-1} per day, respectively, and the corresponding subcutaneous figures are 1.4 and 0.80.[93] In common with many other antitumor agents, the toxic effects manifest primarily in rapidly proliferating tissues, such as the bone marrow, intestinal mucosa, and lymphoid organs.

15.8 SYNTHESIS

The first synthesis of an actinomycin (C_3) involved the oxidative coupling of two molecules of a 3-hydroxy-4-methylanthraniloyl-*O*-pentapeptide, followed by cyclization of both peptide moieties at the Sar-MeVal peptide bonds[94,95] (Figure 15.4). Interestingly, this route failed to distinguish between the accepted structure for actinomycins and an alternate version that had been proposed,[96,97] in which the C-terminus of one peptide is lactonized by the Thr OH of the other, and *vice versa*, forming a cyclodecapeptide dilactone. Subsequently, several unambiguous syntheses of actinomycins have been described involving a pentapeptide lactone derivative as the key intermediate. In the

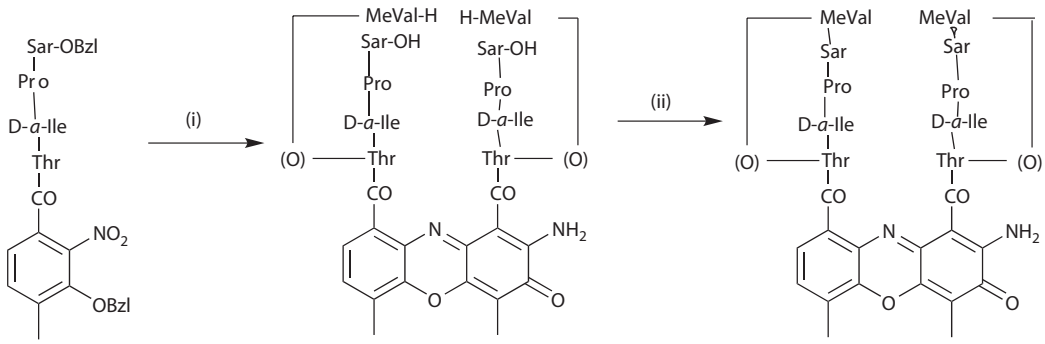

FIGURE 15.4 First total synthesis of an actinomycin (C_3 = VII).[95] Reagents: (i) Cbz-MeVal-OH/carbonyldiimidazole, then H_2/Pd, then $K_3Fe(CN)_6$; (ii) $ClCOOEt/Bu_3N$.

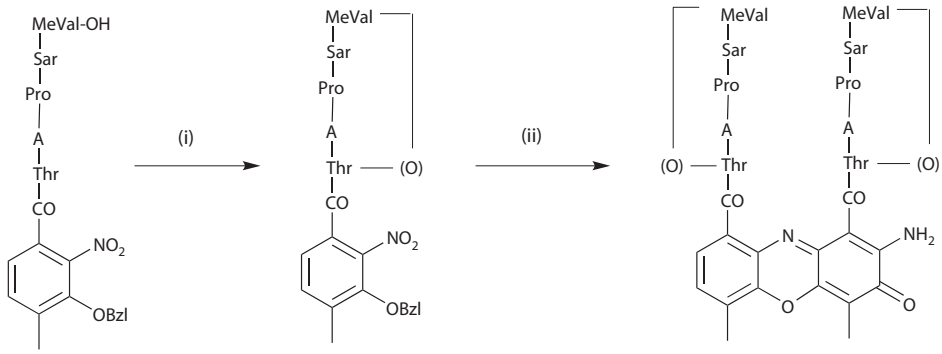

FIGURE 15.5 Synthesis of actinomycins C_1, C_2, i-C_2 and C_3.[98] A = D-Val or D-*a*Ile. Reagents: (i) AcCl/imidazole; (ii) H_2/Pd, then $K_3Fe(CN)_6$.

first example[98] (Figure 15.5), the 3-benzyloxy-4-methylanthraniloyl-pentapeptides were lactonized in syntheses of actinomycins C_1, C_2, i-C_2, and C_3. Analogous peptide lactones were subsequently synthesized in higher yields via cyclization at the Pro-Sar[99] or D-Val-Pro[100] peptide bonds. This intermediate can also be constructed from the cyclic pentapeptide by acid-catalyzed *N,O*-acyl shift followed by acylation of the Thr amino group.[101] Regioselective syntheses of actinomycins C_2 and i-C_2 have been reported,[102,103] as well as that of $X_{0\beta}$.[56]

15.9 ANALOGS

15.9.1 Directed Biosynthesis

The amino acid content of actinomycins can be manipulated by the addition of certain amino acids to the medium in which the producing organism is cultured, a method also known as "controlled biosynthesis."[104] Addition of isoleucine to cultures of *Streptomyces chrysomallus* generated new actinomycins, termed E_1 and E_2,[105] containing one and two N-Me-*allo*-Ile residues (respectively) in place of N-MeVal.[106] Similar studies with *Streptomyces antibioticus* and *Streptomyces parvulus* uncovered a more complex situation, in which D-Ile and D-*allo*-Ile were both able to replace D-Val.[107] Addition of sarcosine to *S. chrysomallus* cultures produced a mixture in which one or both prolines of C_2 and C_3 were replaced by sarcosine, and the products were termed (respectively) F_3 and F_1 (analogs of C_2) and F_4 and F_2 (analogs of C_3).[106,108]

One or both of the proline residues in actinomycins can be replaced by several Pro analogs using directed biosynthesis. They include the *cis*- and *trans*-isomers of 4-methyl-,[109] 4-chloro-, and 4-bromo-prolines;[38] thiazolidine-4-carboxylic acid;[110] azetidine-2-carboxylic acid; and pipecolic acid.[104] When one Pro is replaced, the product is a mixture of two difficultly separable regioisomers. In the case of the 4-substituted prolines, only the four analogs formed using *cis*- and *trans*-4-MePro were characterized.[109] Following the early observation[111] that new actinomycins were formed by *S. antibioticus* in the presence of azetidine-2-carboxylic acid, two analogs, named azetomycins I and II, were isolated,[112] with one or both prolines (respectively) replaced by azetidine-2-carboxylic acid. When pipecolic acid is added to *S. antibioticus* cultures, not only does it replace Pro but actinomycins containing 4-hydroxy- and 4-oxo-pipecolic acid are generated as well[113] (Table 15.2). This is analogous to the presence of Hyp and 4-oxo-Pro (respectively) in the natural actinomycins I and V.

15.9.2 Partial Synthesis

Mild acid hydrolysis of actinomycins replaces the chromophoric NH_2 by OH, and subsequent treatment with thionyl chloride produces 2-chloro-2-deaminoactinomycin.[114] Treatment of this

TABLE 15.2
Biosynthetic Actinomycin Analogs[a] from *Streptomyces antibioticus* with Pipecolic Acid[111]

Actinomycin	Proline	Pipecolic Acid	4-OH-Pipecolic Acid	4-Oxo-Pipecolic Acid
Pip 1α	0	1	0	1
Pip 1β	1	1	0	0
Pip 1γ	0	1	1	0
Pip 1δ	1	0	0	1
Pip 1ε	1	0	1	0
Pip 2	0	2	0	0

[a] The number of residues of each amino acid at the two 3-sites are shown; the remainder of each structure is similar to that of actinomycin D.

compound with a variety of primary and secondary amines provided 34 2-*N*-substituted actinomycins.[115–119] In addition to its hydrogenation to 2-deaminoactinomycin,[114] the 2-chloro derivative is also an intermediate in the preparation of analogs substituted with Cl and Br in the 7-position.[120] Other groups substituted in the 7-position include nitro,[115,121] amino,[116,121] hydroxy,[116] and methoxy.[122] *N*-Acetyl, *N*-pivaloyl, and *N*-stearoyl derivatives of 7-amino-AMD have been described,[70] as well as nine *N*-alkyl and *N*-aryl derivatives.[123] 7-Hydroxy-8-amino-AMD[124] and nine *O*-alkyl and four *O*-acyl derivatives of 7-hydroxy-AMD have also been reported.[119]

Hydrogenation of actinomycin produces dihydroactinomycin, which, unlike actinomycin, can be acetylated. Subsequent reoxidation furnishes *N*-acetyl-actinomycin.[125] Dihydroactinomycin reacts with α-ketoacids to generate tetracyclic analogs with a fused oxazine ring.[115,126,127] Reaction of AMD with aldehydes leads to tetracyclic analogs with a fused oxazole ring, and further manipulations produced related compounds substituted in the 7 and 8 positions.[124,127,128] Some of these tetracyclic analogs are shown in Figure 15.6.

The lactone rings of actinomycins were opened with alkali to produce actinomycinic acids[129] from which dimethyl esters and di-*O*-acetyl derivatives have also been prepared.[125] One or both lactone rings can also be opened by microbial degradation by *Actinoplanes* species.[130] The peptide lactones of actinomycin C_3 have been cleaved at the Sar-MeVal peptide bond with cold, concentrated HCl to produce the *bis-seco*-actinomycin.[131]

The OH groups of Hyp and *allo*-Hyp in actinomycins $X_{0\beta}$ and $X_{0\delta}$ have been converted to their *O*-acetyl and *O*-hexadecanoyl derivatives.[32,132] Likewise, an *O*-acetate and di-*O*-acetate have been prepared from actinomycin Z_1.[42] The 4-oxo-5-MePro residue in this actinomycin has been reduced to two diastereoisomers of 4-OH-5-MePro, and a triacetate of the resulting actinomycins was prepared.[133] The 4-oxo-Pro in actinomycin $X_{1\alpha}$ has been reduced to Hyp, of which the *O*-acetyl derivative has also been produced.[34] Actinocinyl-gramicidin S has been described;[134] the two couplings were effected at the ornithine δ-NH_2 groups.

15.9.3 Total Synthesis

The two chromophoric methyl groups of AMD have been replaced by H, Br, OMe, Et, and *t*-Bu.[135] Moreover, the 6-Me and both 4- and 6-Me groups have been replaced by CF_3.[136] An analog termed *pseudo*-actinomycin C_1 has been synthesized in which the chromophoric methyls and the peptide moieties are exchanged.[137] In another analog, the actinocinyl chromophore is replaced by 4-methylphenazine-1,9-dicarboxylic acid.[138]

A number of peptidic analogs of actinomycin have been synthesized by methods similar to those used for the natural actinomycins (Table 15.3); they include enantio-AMD.[139]

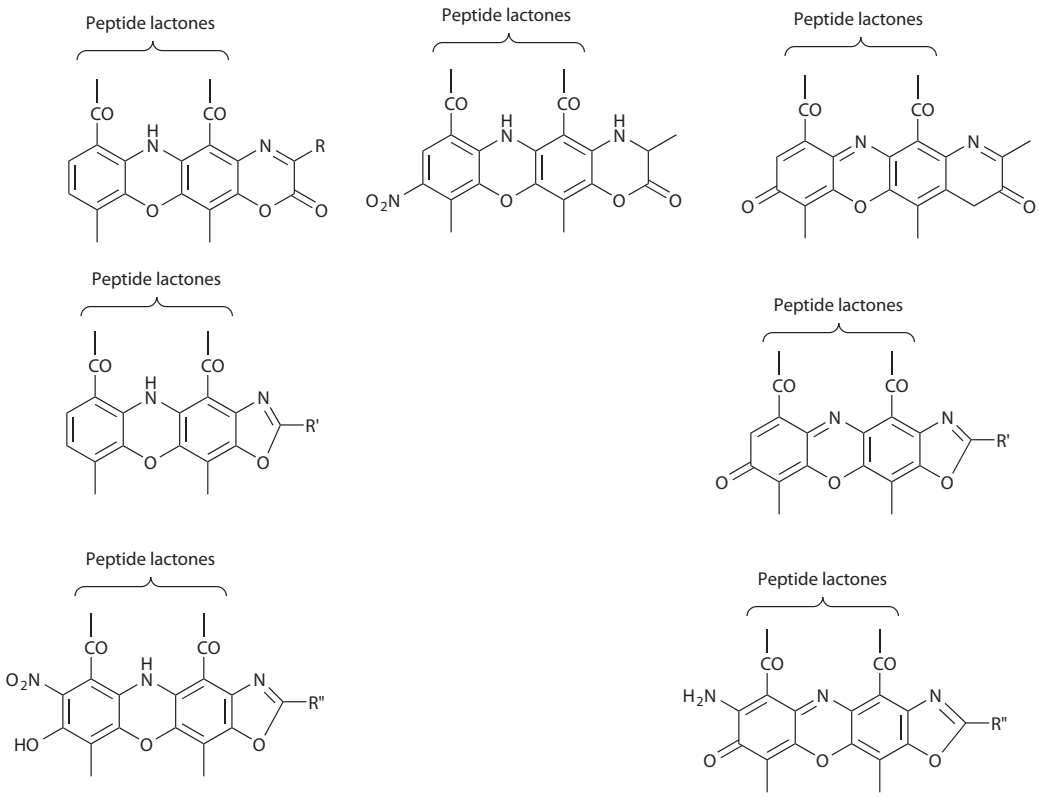

FIGURE 15.6 Tetracyclic analogs of actinomycin D. R = H, CH_3, C_2H_5, CH_2F, *n*-C_6H_{13}, CH_2COOH, CH_2CH_2COOH, C_6H_5, C_6F_5, *o*-ClC_6H_4, *m*-ClC_6H_4, *p*-ClC_6H_4, 2,4-$Cl_2C_6H_3$, 2-naphthyl; R′ = CH_3, C_6H_5, C_6F_5; R″ = CH_3, C_6H_5, CH_2COOH, $CH_2CONH(CH_2)_4NH_2$.

15.10 STRUCTURE–ACTIVITY RELATIONSHIPS

15.10.1 Introduction

For biological activity mimicking the natural actinomycins, the chromophore and both intact cyclopeptide moieties are required. Even the scission of one peptide lactone abolishes biological activity.[102,130] Some actinocinyl derivatives bind to DNA but are inactive. In the case of actinomine (actinocinyl-*bis*[diethylaminoethylamide]),[70] this phenomenon was shown to derive from the rapid rate of dissociation from its complex with DNA, which was 1000 times faster than that of AMD. Thermodynamic and other studies[65,73] indicated an important hydrophobic interaction between the peptide lactones of actinomycins and DNA, and their biological activity depends on the slow dissociation of the complex.

The number of actinomycin analogs that have been described is very large (>100), and the review that follows is not exhaustive. A more detailed review of the work reported through 1977 has appeared.[51] Natural actinomycins and their analogs have been evaluated in a variety of ways, including binding to DNA, inhibition of RNA synthesis, and antimicrobial and antitumor activities. Because antitumor activity is of primary interest, for those compounds for which such data are available, other activities are usually omitted. For other compounds, antimicrobial data, albeit a poor predictor of antitumor activity, are provided. Some analogs described before, which are biologically inactive, are not discussed next. In many cases, analogs were produced in insufficient

TABLE 15.3
Amino Acid Content of Synthetic Peptidic Actinomycin Analogs

Site 1	Site 2	Site 3	Site 4	Site 5	References
Thr	D-Val	α-Hyp, β-Pro	Sar	MeVal	56
Thr	D-Val	Hyp	Sar	MeVal	56
Ser	D-Val	Pro	Sar	MeVal	140
Dpr	D-Val	Pro	Sar	MeVal	141
Dbu	D-Val	Pro	Sar	MeVal	142
Thr	D-Ala	Pro	Sar	MeVal	140
Thr	D-Leu	Pro	Sar	MeVal	140
Thr	D-Thr	Pro	Sar	MeVal	143
Thr	D-Val	Meg	Sar	MeVal	143
Thr	D-Val	Pro	Gly	Val	144
Thr	D-Val	Pro	Sar	MeAla	145
Thr	D-Val	Pro	Sar	MeLeu	143
D-Thr	Val	D-Pro	Sar	D-MeVal	139

Nonstandard amino acid abbreviations: Dpr = L-2,3-diaminopropionic acid; Dbu = L-2,3-diamino-*n*-butyric acid; Meg = *N*-[2-(methoxycarbonyl)ethyl]-glycine.

quantities for *in vivo* evaluation, and none reached clinical trial, although some partially synthetic analogs surpassed AMD in *in vivo* antitumor activity.

15.10.2 Natural Actinomycin Variants

Comparative biological data for actinomycins I–VII are shown in Table 15.4.[146,147] In addition, comparison of II, III, and IV in several mouse ascitic tumors revealed that in the most sensitive tumor, the Gardner lymphosarcoma, these actinomycins had comparable efficacy.[148] These data indicate that replacement of the β-Pro by Hyp or by sarcosine reduces toxicity, antitumor potency, and antimicrobial activity, whereas antitumor efficacy remains about the same. In contrast, replacement by 4-oxo-Pro increases toxicity and antimicrobial activity but reduces antitumor efficacy. More recent work[46] comparing actinomycins Z_1, Z_3, and Z_5 with AMD is shown in Table 15.5. Actinomycin Z_3 is several times as potent as AMD against all three human tumor cell lines studied, as well as against

TABLE 15.4
Biological Activities of Actinomycins I–VII[a]

Actinomycin	Toxicity	Antitumor Efficacy[b]	*Streptomyces aureus*[c]	*Streptomyces subtilis*[c]
I = $X_{0\beta}$	10	+	25	5–15
II	10	++	45	35
III	50	++	35	25–33
IV = AMD = X_1 = C_1	100	++	100	100
V = X_2	800	±	200	200
VI = C_2	100	++	70	90
VII = C_3	70	++	95	100

[a] Numerals indicate activity relative to AMD = 100.
[b] Evaluated by increased life span in mice implanted with leukemia P388, leukemia L1210, or B16 melanoma.
[c] Antimicrobial activities.

TABLE 15.5
Cytotoxicities (Micromolar) in Three Human Tumor Cell Lines and Minimal Inhibitory Concentrations (MICs) (μg mL^{-1}) against *Bacillus subtilis* for Actinomycins D, Z_1, Z_3, and Z_5

Actinomycin and Level	HMO2 (Stomach)	HEP G2 (Liver)	MCF 7 (Breast)	Antimicrobial MIC
D				
GI50	0.2	1.0	0.5	0.78
TGI	0.8	4.0	2.2	
LC50	>50	>50	>50	
Z_1				
GI50	0.75	0.95	<0.5	12.5
TGI	5.8	5.5	>50	
LC50	>50	>50	>50	
Z_3				
GI50	<0.1	<0.1	<0.1	0.20
TGI	<0.1	1.4	<0.1	
LC50	0.28	>50	0.5	
Z_5				
GI50	<0.1	1.5	<0.1	0.75
TGI	<0.1	10	0.12	
LC50	0.50	>50	0.5	

Bacillus subtilis. Z_1 is considerably less active, and Z_5 is roughly comparable with AMD. In earlier studies,[149] Z_1 and Z_5 were less effective than AMD in inhibiting RNA synthesis in *B. subtilis* and in HeLa cells. The lower activity of Z_1 probably results from the presence of 4-hydroxythreonine in a location where its OH group is close to the chromophoric amino group.[55]

15.10.3 Chromophoric Analogs

The importance of the chromophoric 2-NH_2 group is illustrated by the lack of biological activity when it is replaced by H, OH, or Cl[114] or is acylated.[125] Most 2-*N*-alkylated actinomycins were only tested against *B. subtilis* and were at least tenfold less active that the natural variants.[115,117] However, 2-*N*-γ-hydroxypropyl-AMD, although possessing only 10% of the antimicrobial activity of AMD, was equal in antitumor activity.[118] Moreover, in P388 leukemia (mice), 2-*N*-3′-amino-*n*-propyl-AMD surpassed AMD in terms of increased life span (ILS).[119] Replacement of the chromophoric Me groups by H or OMe weakened binding of the analog to DNA and reduced antimicrobial activity to 1–5% of that of AMD, whereas their replacement by Et reduced antimicrobial activity to 30–35%, and the di-*t*-Bu analog lacked activity, presumably because these bulky groups obstruct DNA intercalation.[135] Despite the nearly equal size of Me and CF_3 groups, antibacterial and cytotoxic activities of the 6-CF_3 and 4, 6-di-CF_3 analogs were reduced to 25% and almost 0% (respectively) of the parent actinomycin, probably because of electronic effects.[136]

Substitution in the chromophoric 7-position produces a variety of effects. 7-Chloroactinomycin C_3[120] and 7-nitroactinomycin C_2[116] have about half the antimicrobial activity of the parent compounds, whereas that of 7-bromoactinomycin C_3[120] is 50% higher. 7-Nitro- and 7-amino-AMD were roughly comparable with AMD in *in vivo* antitumor activity.[150] *In vivo* antitumor studies (mice, P388) of nine *N*-substituted 7-amino-AMDs gave ILS values superior to those of AMD for 7-amino-AMD and 7-*N*-(3′,4′-dichlorophenyl)amino-AMD.[123] In similar studies of 7-hydroxy-AMD and its *O*-alkyl and *O*-acyl derivatives, superior ILS values were seen in 7-hydroxy-AMD and 7-adamantoyloxy-AMD.[119]

No rationale was proposed for the enhanced efficacy resulting from these bulky substitutions in the chromophoric 7-position.

Chromophoric analogs of AMD bearing a fourth oxazinone ring hydrolyze to AMD above pH 7. In P388 murine leukemia, the compounds with R = CH_2F and C_6H_5 (Figure 15.6) had ILS values superior to that of AMD.[126] These analogs presumably act as AMD prodrugs, but their enhanced efficacy has not been explained. Dihydro-AMD analogs bearing a fourth oxazole ring were inactive unless the A ring was oxidized to the iminoquinone, which is metabolized to 7-hydroxy-AMD.[127] The 8-amino-iminoquinones had antitumor activity superior to that of AMD when R″ = C_6H_5 or $CH_2CONH(CH_2)_4NH_2$ (Figure 15.6), presumably resulting from their metabolism to 7-hydroxy-8-amino-AMD.[128]

15.10.4 Peptidic Analogs

Synthetic variations at the Thr sites of actinomycin involving replacement by Ser, Dpr, or Dbu (Table 15.3) gave antimicrobial activities of 20%, 10%, and 10% (respectively) of that of AMD.[140–142] Antitumor potency of the Dbu analog was 10–20 times lower than that of AMD. At the D-Val sites, replacement by D-Ala or D-Leu reduces antimicrobial activities to 1% and 10% (respectively) of that of AMD,[140] and D-Thr produces a reduction to 10–20% of that of AMD.[143]

Replacement of one Pro by pipecolic acid (Pip 1β) has little effect on antimicrobial activity, whereas replacement of both (Pip 2) reduces this activity 5- to 15-fold, and replacement by one 4-ketopipecolic acid (Pip 1δ) reduces it further.[151] The *in vivo* antitumor efficacy of Pip 1 is comparable with that of AMD at an eightfold higher dosage, whereas Pip 2 is less active.[92] The *in vivo* antitumor activity of the compounds in which one or both prolines were replaced by azetidine-2-carboxylic acid, termed azetomycins I and II, respectively, have been extensively evaluated; azetomycin I, the more active of the two, was found equivalent to AMD in some experiments[152] and somewhat superior in others.[153] Actinomycins in which one or both prolines were replaced by *cis*- or *trans*-4-MePro (termed K_{1c}, K_{2c}, K_{1t}, and K_{2t}, respectively) had lower antimicrobial activity than AMD in the sequence AMD > K_{1t} > K_{1c} > K_{2t} > K_{2c}.[109]

Replacement of both MeVal residues by MeLeu[143] produced much stronger binding to DNA than AMD, and this analog was at least tenfold more potent than AMD in the NCI *in vitro* screen comprising 60 human tumor cell lines.[85] Presumably, the MeLeu side chains enhance hydrophobic interaction with DNA. In contrast, the AMD analog with both MeVal residues replaced by MeAla binds to DNA less strongly than AMD and has approximately tenfold lower antimicrobial activity,[145] indicating a poorer hydrophobic interaction with DNA. This effect does not prevent actinomycins Z_3 and Z_5, both of which have one MeVal replaced by MeAla, from being at least as active as AMD, but there are other structural differences, including additional methyl groups in the 5-position of both prolines.[46]

15.11 CLINICAL APPLICATIONS OF ACTINOMYCINS

Many early clinical studies with actinomycins C and D in a variety of cancers demonstrated that their effectiveness was most prominent in trophoblastic tumors in females[154] (including methotrexate-resistant choriocarcinoma[155]), in metastatic carcinoma of the testis,[154,156,157] and in Wilms' tumor (nephroblastoma) in children.[158] In rhabdomyosarcoma, efficacy was enhanced by combination with vincristine.[159] Cures were obtained in Wilms' tumor by a combination of surgery, radiotherapy, and actinomycin therapy.[160,161] The most effective route of administration is intravenous. Advances that have been made in the management of Wilms' tumor are discussed by Gommersall et al.[162]

Actinomycin D, also known as Dactinomycin and Cosmegen, soon became the only form of actinomycin in clinical use (http://www.cancer.gov/drugdictionary/?CdrID=39675). It is still in use in therapy of the aforementioned tumors, as well as in treatment of Ewing's sarcoma. Side-effects include bone marrow depression, oral and intestinal lesions, skin reactions, alopecia, and

immunosuppression. As a consequence, in common with other classical anticancer drugs, its effectiveness is constrained by dose-limiting toxicity. Nonetheless, many complete remissions have occurred, and 188 clinical trials are listed at: http://www.cancer.gov/search/ResultsClinicalTrials.aspx?protocolsearchid=7231396. Currently (January 2009), there are 15 ongoing clinical trials, involving treatment of Wilms' tumor, rhabdomyosarcoma, tumors of the Ewing's family[163,164], and pediatric cancers, with dactinomycin, either alone or in combination with other agents, such as vincristine, cyclophospamide, ifosfamide, and doxorubicin, and with or without radiation and/or surgery (http://www.cancer.gov/search/ResultsClinicalTrials.aspx?protocolsearchid=7231312). Pulse dactinomycin was found to be an effective salvage treatment of patients with low-risk gestational trophoblastic neoplasia (GTN) who had failed methotrexate therapy.[165]

For five decades isolated limb perfusion (ILP) has been effectively used for the treatment of patients with advanced melanoma and sarcoma confined to a limb, the advantage being that high-dose regional chemotherapy with agents such as dactinomycin can be administered without causing serious systemic side effects.[166] To achieve the benefits of ILP while minimizing its major disadvantages (ILP involves a complex and invasive operative procedure), isolated limb infusion (ILI), which is a simplified and minimally invasive procedure, was developed and implemented in the early 1990s by Thompson et al. in Australia.[167] The procedure has been reviewed,[168] and recent applications in the treatment of melanoma using melphalan and dactinomycin have been reported.[169,170]

REFERENCES

1. Waksman, S.A. and Woodruff, H.B., Bacteriostatic and bacteriocidal substances produced by a soil actinomyces. *Proc. Soc. Exptl. Biol. Med.*, 45, 609, 1940.
2. Waksman, S.A. and Woodruff, H.B., *Actinomyces antibioticus*, a new soil organism antagonistic to pathogenic and nonpathogenic bacteria. *J. Bacteriol.*, 42, 231, 1941.
3. Fisher, W.P., Charney, J., and Bolhofer, W.A., An actinomycin from a species of the genus *Micromonospora. Antibiot. Chemother.*, 1, 571, 1951.
4. Waksman, S.A., Robinson, H., Metzger, H.J., and Woodruff, H.B., Toxicity of actinomycin. *Proc. Soc. Exptl. Biol. Med.*, 47, 261, 1941.
5. Hackmann, C., Experimentelle untersuchungen über die wirkung von actinomycin C. *Z. Krebsforsch.*, 58, 607, 1952.
6. Schulte, G., Erfahrungen mit neuen zytostatischen mitteln bei hämoblastosen und carcinomen und die abgrenzung ihrer wirkungen gegen roentgentherapie. *Z. Krebsforsch.*, 58, 500, 1952.
7. Kirk, J.M., The mode of action of actinomycin D. *Biochim. Biophys. Acta*,, 42, 167, 1960.
8. Slotnick, I.J., Mechanism of action of actinomycin D in microbiological systems. *Ann. N.Y. Acad. Sci.*, 89, 342, 1960.
9. Shatkin, A.J. The effects of actinomycin on virus replication. In *Actinomycin*, Waksman, S. A., Ed. Interscience Publishers: New York, 1968; p 69.
10. Lehr, K. and Burger, J., The isolation of a crystalline actinomycin-like antibiotic. *J. Arch. Biochem.*, 23, 503, 1949.
11. Brockmann, H. and Grubhofer, N., Actinomycin C. *Naturwiss.*, 36, 376, 1949.
12. Manaker, R.A., Gregory, F.J., Vining, L.C., and Waksman, S.A., Actinomycin. III. The production and properties of a new actinomycin. *Antibiot. Annu.*, 853, 1954/55.
13. Brockmann, H. and Gröne, H., Reine actinomycine. *Naturwiss.*, 41, 65, 1954.
14. Brockmann, H., Linge, H., and Gröne, H., Zur kenntnis des actinomycins X. *Naturwiss.*, 40, 224, 1953.
15. Bossi, R., Hutter, R., Ketter-Schierlein, W., Neipp, L., and Zahner, H., Stoffwechselprodukte von actinomyceten, 14. Mitt. actinomycin Z. *Helv. Chim. Acta*, 41, 1645, 1958.
16. Brockmann, H., Grubhofer, N., Kalbe 11, H., and Kass, W., Über das actinomycin C (antibiotica aus actinomyceten, V. Mitt.). *Chem. Ber.*, 84, 260, 1951.
17. Brockmann, H. and Pfennig, N., Auftrennung von actinomycin C durch gegenstromverteilung. *Naturwiss.*, 39, 429, 1952.
18. Vining, L.C. and Waksman, S.A., Paper chromatographic identification of the actinomycins. *Science*, 120, 389, 1954.
19. Gregory, F.J., Vining, L.C., and Waksman, S.A., Actinomycin. IV. Classification of the actinomycins by paper chromatography. *Antibiot. Chemother.*, 5, 409, 1955.

20. Vining, L.C., Gregory, F.J., and Waksman, S.A., Actinomycin. V. Chromatographic separation of the actinomycin complexes. *Antibiot. Chemother.*, 5, 417, 1955.
21. Roussos, G.G. and Vining, L.C., Isolation and properties of pure actinomycins. *J. Chem. Soc.*, 2469, 1956.
22. Mauger, A.B. and Katz, E. Actinomycins, in *Antibiotics: Isolation, Separation and Purification*. In *J. Chromatogr Library*, Wagman, G.H. a. W., M.J., Ed. Elsevier: New York, 1978; Vol. 15.
23. Waksman, S.A., Katz, E., and Vining, L.C., Nomenclature of actinomycins. *Proc. Natl. Acad. Sci. U.S.A.*, 44, 602, 1958.
24. Praveen, V. and Tripathi, C.K.M., Studies on the production of actinomycin-D by *Streptomyces griseoruber*—A novel source. *Lett. Appl. Microbiol.*, 49, 450, 2009.
25. Williams, W.K. and Katz, E., Development of a chemically defined medium for the synthesis of actinomycin-D by *Streptomyces parvulus. Antimicrob. Agents Chemother.*, 11, 281, 1977.
26. Praveen, V., Tripathi, C.K.M., Bihari, V., and Srivastava, S.C., Production of actinomycin-D by the mutant of a new isolate of *Streptomyces sindenensis. Brazilian J. Microbiol.*, 39, 689, 2008.
27. Brockmann, H., Bohnsack, G., Franck, B., Grone, H., Muxfeldt, H., and Suling, C., Zur konstitution der actinomycine. *Angew. Chem.*, 68, 70, 1956.
28. Bullock, E. and Johnson, A.W., The structure of actinomycin D. *J. Chem. Soc.*, 3280, 1957.
29. Brockmann, H., Boldt, P., and Petras, H.-S., Die aminosäuresequenz von actinomycin C_1 und actinomycin C_2. *Naturwiss.*, 47, 62, 1960.
30. Brockmann, H. and Franck, B., Actinomycin C_{2a}, ein isomeres des actinomycins C_2. *Naturwiss.*, 47, 15, 1960.
31. Brockmann, H. and Boldt, P., Oxidative abspaltung des β-pentapeptidlactonringes aus actinomycin C_2 und C_3; ein beweis für die bis-pentapeptidlacton-struktur der actinomycine. *Chem. Ber.*, 101, 1940, 1968.
32. Brockmann, H. and Manegold, J.H., Ueberfuehrung von actinomycin X_2 in die actinomycine C_1, $X_{0\beta}$ und $X_{0\beta}$; actinomycine XXIII. *Chem. Ber.*, 93, 2971, 1960.
33. Diegelman, R., Mauger, A., and Katz, E., Isolation and identification of oxoproline in actinomycin X_2 (V) hydrolysates. *J. Antibiot.*, 22, 85, 1969.
34. Brockmann, H. and Manegold, J.H., Actinomycin X_{1a} and $X_{0\beta}$. *Chem. Ber.*, 95, 1081, 1962.
35. Waksman, S.A., Katz, E., Goss, W.A., Pugh, L.H., Solotorovsky, M., Auerbach, O., Johnson, A.W., and Mauger, A., Directed formation of the actinomycins—chemical structure and biological activities. *Science*, 129, 1290, 1959.
36. Johnson, A.W. and Mauger, A.B., The isolation and structure of actinomycins II and III. *Biochem. J.*, 73, 535, 1959.
37. Mauger, A.B., Degradation of peptides to diketopiperazines: application of pyrolysis-gas chromatography to sequence determination in actinomycins. *J. Chem. Soc. Chem. Commun.*, 39, 1971.
38. Katz, E., and Mauger, A.B., unpublished data. 1977.
39. Brockmann, H. and Stähler, E.A., Zur konstitution des actinomycins Z_5. *Tetrahedron Lett.*, 2567, 1973.
40. Katz, E., Mason, K.T., and Mauger, A.B., Identification of *cis*-5-methylproline in hydrolysates of actinomycin Z_5. *Biochem. Biophys. Res. Commun.*, 52, 819, 1973.
41. Brockmann, H. and Stähler, E.A., 4-Oxo-5-methylprolin, ein baustein des actinomycins Z_1. *Naturwiss.*, 52, 391, 1965.
42. Brockmann, H. and Manegold, J.H., Actinomycine, XXV; antibiotica aus actinomyceten, LIV. Actinomycin Z_1; zur quantitativen aminosäureanalyse der actinomycine. *Hoppe-Seyler's Z. Physiol. Chem.*, 343, 86, 1965.
43. Katz, E., Mason, K.T., and Mauger, A.B., 3-Hydroxy-5-methylproline, a new amino acid identified as a component of actinomycin Z_1. *Biochem. Biophys. Res. Commun.*, 63, 502, 1975.
44. Mauger, A.B., Stuart, O.A., Katz, E., and Mason, K.T., Synthesis and stereochemistry of 3-hydroxy-5-methylproline, a new naturally occurring imino acid. *J. Org. Chem.*, 42, 1000, 1977.
45. Katz, E., Mason, K.T., and Mauger, A.B., The presence of α-amino-β,γ-dihydroxybutyric acid in hydrolysates of actinomycin Z_1. *J. Antibiot.*, 27, 952, 1974.
46. Lackner, H., Bahner, I., Shigematsu, N., Pannell, L.K., and Mauger, A.B., Structures of five components of the actinomycin Z complex from *Streptomyces fradiae*, two of which contain 4-chlorothreonine. *J. Nat. Prod.*, 63, 352, 2000.
47. Lackner, H., Hulsmann, H., Heinze, S., Simon, H., Bar, H., Zimmer, C., and Grafe, U., A new actinomycin-type chromopeptide from *Streptomyces* Sp. HKI-0155. *J. Antibiot.*, 53, 84, 2000.
48. Hanada, M., Sugawara, K., Nishiyama, Y., Kamei, H., Hatori, M., and Konishi, M., Protactin, a new antibiotic metabolite and a possible precursor of the actinomycins. *J. Antibiot.*, 45, 20, 1992.
49. Brockmann, H., Die actinomycine. *Fortschr. Chem. Org. Naturst.*, 18, 1, 1960.

50. Umezawa, H. and Japan Scientific Societies Press, State College Pennsylvania, 1967 and Univ. Park Press, Baltimore, MD, *Index of Antibiotics from Actinomycetes*. Vol. I and II, 1978.
51. Meienhofer, J. and Atherton, E. Structure-activity relationships in the actinomycins. In *Structure-Activity Relationships among the Semisynthetic Antibiotics*, Perlman, D., Ed. John Wiley & Sons: New York, 1977; p 427.
52. Mauger, A.B. The actinomycins. In *Topics in Antibiotic Chemistry*, Sammes, P.G., Ed. Ellis Horwood: Chichester, 1980; Vol. 5, p 223.
53. Jain, S.C. and Sobell, H.M., Stereochemistry of actinomycin binding to DNA. I. Refinement and further structural details of the actinomycin-deoxyguanosine crystalline complex. *J. Mol. Biol.*, 68, 1, 1972.
54. Ginell, S., Lessinger, L., and Berman, H.M., The crystal and molecular structure of the anticancer drug actinomycin D—some explanations for its unusual properties. *Biopolymers*, 27, 843, 1988.
55. Schäfer, M., Sheldrick, G.M., Bahner, I., and Lackner, H., Crystal structures of actinomycin D and actinomycin Z_3. *Angew. Chem. Internat. Ed.*, 37, 2381, 1998.
56. Lifferth, A., Bahner, I., Lackner, H., and Schafer, M., Synthese und struktur von prolinring-modifizierten actinomycinen des X-typs. *Z. Naturforsch.*, 54b, 681, 1999.
57. Lackner, H., Three-dimensional structure of the actinomycins. *Angew. Chem. Int. Ed.*, 14, 375, 1975.
58. Liu, X., Chen, H., and Patel, D.J., Solution structure of actinomycin-DNA complexes: drug intercalation at isolated G-C sites. *J. Biomol. NMR*, 1, 323, 1991.
59. Kawamata, J. and Imanishi, M., Interactions of actinomycin with deoxyribonucleic acid. *Nature*, 187, 1112, 1960.
60. Kersten, H., Kersten, W., and Rauen, H.M., Action of nucleic acids on the inhibition of growth by actinomycin of *Neurospora crassa. Nature*, 187, 60, 1960.
61. Rauen, H.M., Kersten, H., and Kersten, W., Zur wirkungsweise von actinomycinen. *Hoppe-Seyler's Z. Physiol. Chem.*, 321, 139, 1960.
62. Kawamata, J. and Imanishi, M., Mechanism of action of actinomycin, with special reference to its interaction with deoxyribonucleic acid. *Biken J.*, 4, 13, 1961.
63. Reich, E., Franklin, R., Shatkin, A.J., and Tatum, E.L., Actinomycin: Effect of actinomycin D on cellular nucleic acid synthesis and virus production. *Science*, 134, 556, 1961.
64. Haselkorn, R., Actinomycin D as a probe for nucleic acid secondary structure. *Science*, 143, 682, 1964.
65. Reich, E. and Goldberg, I.H., Actinomycin and nucleic acid function. *Prog. Nucleic Acid Res. Mol. Biol.*, 3, 183, 1964.
66. Gellert, M., Smith, C.E., Neville, D., and Felsenfeld, G., Actinomycin binding to DNA: Mechanism and specificity. *J. Mol. Biol.*, 11, 445, 1965.
67. Goldberg, I.H., Rabinowitz, M., and Reich, E., Basis of actinomycin action. I. DNA binding and inhibition of RNA-polymerase synthetic reactions by actinomycin. *Proc. Natl. Acad. Sci. U.S.A.*, 48, 2094, 1962.
68. Cerami, A., Reich, E., Ward, D.C., and Goldberg, I.H., The interaction of actinomycin with DNA: Requirement for the 2-amino group of purines. *Proc. Natl. Acad. Sci. U.S.A.*, 57, 1036, 1967.
69. Kahan, E., Kahan, F.M., and Hurwitz, J., The role of deoxyribonucleic acid in ribonucleic acid synthesis. VI. Specificity of action of actinomycin D. *J. Biol. Chem.*, 238, 2491, 1963.
70. Müller, W. and Crothers, D.M., Studies on the binding of actinomycin and related compounds to DNA. *J. Mol. Biol.*, 35, 251, 1968.
71. Kersten, W., Interaction of actinomycin C with constituents of nucleic acids. *Biochim. Biophys. Acta*,, 47, 610, 1961.
72. Takusagawa, F., Dabrow, M., Neidle, S., and Berman, H.M., The structure of a pseudo intercalated complex between actinomycin and the DNA binding sequence d(GpC). *Nature*, 296, 466, 1982.
73. Takusagawa, F., Goldstein, B.M., Youngster, S., Jones, R.A., and Berman, H.M., Crystallization and preliminary X-ray study of a complex between d(ATGCAT) and actinomycin D. *J. Biol. Chem.*, 259, 4714, 1984.
74. Takusagawa, F., The role of the cyclic depsipeptide rings in antibiotics. *J. Antibiot.*, 38, 1596, 1985.
75. Ross, W.E., Glaubiger, D., and Kohn, K.W., Qualitative and quantitative aspects of intercalator-induced DNA strand breaks. *Biochim. Biophys. Acta*,, 562, 41, 1979.
76. Wassermann, K., Markovits, J., Jaxel, C., Capranico, G., Kohn, K.W., and Pommier, Y., Effects of morpholinyl doxorubicins, doxorubicin and actinomycin D on mammalian DNA topoisomerases I and II. *Mol. Pharmacol.*, 38, 38, 1990.
77. Wadkins, R.M., Jares-Erijman, E.A., Klement, R., Rudiger, A., and Jovin, T.M., Actinomycin D binding to single-stranded DNA: sequence specificity and hemi-intercalation model from fluorescence and 1H NMR spectroscopy. *J. Mol. Biol.*, 262, 53, 1996.

78. Gniazdowski, M., Denny, W.A., Nelson, S.M., and Czyz, M., Transcription factors as targets for DNA-interacting drugs. *Curr. Med. Chem.*, 10, 909, 2003.
79. Han, H.H., Hurley, L.H., G-quadruplex DNA: A potential target for anti-cancer drug design. *Trends Pharmacol. Sci.*, 21, 136, 2000.
80. Kang, H.-J. and Park, H.-J., Novel molecular mechanism for actinomycin D activity as an oncogenic promoter G-quadruplex binder. *Biochemistry*, 48, 7392, 2009.
81. Hudson, J.S., Brooks, S.C., and Graves, D.E., Interactions of actinomycin D with human telomeric G-quadruplex DNA. *Biochemistry*, 48, 4440, 2009.
82. Foley, G.E. and Eagle, H., The cytotoxicity of anti-tumor agents for normal human and animal cells in first tissue culture passage. *Cancer Res.*, 18, 1012, 1958.
83. Eagle, H. and Foley, G.E., Cytotoxicity in human cell cultures as a primary screen for the detection of anti-tumor agents. *Cancer Res.*, 18, 1017, 1958.
84. Reich, E., Goldberg, I.H., and Rabinowitz, M., Structure-activity correlations of actinomycins and their derivatives. *Nature*, 196, 743, 1962.
85. Monks, A., Scudiero, D., Skehan, P., Shoemaker, R., Paull, K., Vistica, D., Hose, C., et al., Feasibility of a high-flux anticancer drug screen utilizing a diverse panel of human tumor cell lines in culture. *J. Natl. Cancer Inst.*, 83, 757, 1991.
86. Paull, K.D., Shoemaker, R.H., Hodes, L., Monks, A., Scudiero, D.A., Rubinstein, L., Plowman, J., and Boyd, M.R., Display and analysis of patterns of differential activity of drugs against human tumor cell lines: development of mean graph and COMPARE algorithm. *J. Natl. Cancer Inst.*, 81, 1088, 1989.
87. Hackmann, C., HBF 386 (Actinomycin C), ein cytostatisch wirksamer naturstoff. *Strahlentherapie*, 90, 296, 1953.
88. Stock, J.A., Antitumor antibiotics. *Exptl. Chemother.*, 4, 239, 1966.
89. Sugiura, K. and Schmidt, M.S., Effects of antibiotics on the growth of a variety of mouse and rat tumors. *Proc. Am. Assoc. Cancer Res.*, 2, 151, 1956.
90. Hirono, I., Kachi, H., Shibuya, C., and Nishio, Y., Antitumor effect of actinomycin D on transplantable Wilm's tumor in rats. *Gann.*, 59, 473, 1968.
91. Priestly, J.B., The laboratory basis for the clinical treatment of Wilms tumor. *J. Urol*, 107, 696, 1972.
92. Goldin, A. and Johnson, R., Evaluation of actinomycins in experimental systems. *Cancer Chemother. Reps.*, 58, 63, 1974.
93. Philips, F.S., Schwartz, H.S., Sternberg, S.S., and Tan, C.T.C., The toxicity of actinomycin D. *Ann. N.Y. Acad. Sci.*, 89, 348, 1960.
94. Brockmann, H. and Lackner, H., Totalsynthese von actinomycin C_3. *Naturwiss*, 47, 230, 1960.
95. Brockmann, H. and Lackner, H., Totalsynthese von actinomycin C_3 über bis-seco-actinomycin C_3. *Chem. Ber.*, 100, 353, 1967.
96. Bachmann, H.G. and Müller, W., X-ray diffraction of actinomycin C_3. *Nature*, 201, 261, 1964.
97. Perutz, M.F., X-ray diffraction of actinomycin C_3. *Nature*, 201, 814, 1964.
98. Brockmann, H. and Lackner, H., Totalsynthese der actinomycine C_1, C_2, i-C_2 und C_3 über N-(2-amino-3-hydroxy-4-methylbenzoyl)-pentapeptidlactone; ein weiterer beweis für die bispentapeptidstruktur der actinomycine. *Chem. Ber.*, 101, 2231, 1968.
99. Meienhofer, J., Synthesis of actinomycin and analogs. III. A total synthesis of actinomycin D (C_1) *via* peptide cyclization between proline and sarcosine. *J. Am. Chem. Soc.*, 92, 3771, 1970.
100. Vlasov, G.P., Lashkov, V.N., and Glibin, E.N., Synthesis of actinomycin D and its peptide analogs. IV. Synthesis of de(di-3′-proline)actinomycin D. *Zh. Org. Khim. S.S.S.R.*, 15, 983, 1979.
101. Mauger, A.B. and Stuart, O.A., Synthesis of an actinomycin-related peptide lactone from the corresponding cyclic peptide by N,O-acyl shift. *Int. J. Peptide Protein Res.*, 34, 196, 1989.
102. Lackner, H., Totalsynthese von aniso-actinocinyl-peptiden und aniso-actinomycinen über deuterium-markierte vorstufen. *Chem. Ber.*, 103, 2476, 1970.
103. Lackner, H., Synthesen von selectiv deuterierten pentapeptidlactonen und stellungsspezifisch im α- oder β-peptidring markierten actinomycinen. *Chem. Ber.*, 104, 3653, 1971.
104. Katz, E., Controlled biosynthesis of actinomycins. *Cancer Chemother. Rep.*, 58, 83, 1974.
105. Schmidt-Kastner, G., Actinomycin E und actinomycin F, zwei neue biosynthetische actinomycingemische. *Naturwiss.*, 43, 131, 1956.
106. Katz, E., Kawai, Y., and Shoji, J., Configuration of the N-methylisoleucine in the actinomycins. *J. Biochem. Biophys. Res. Commun.*, 43, 1035, 1971.
107. Yajima, T., Grigg, M.A., and Katz, E., Biosynthesis of antibiotic peptides with isoleucine isomers. *Arch. Biochem. Biophys.*, 151, 565, 1972.

108. Schmidt-Kastner, G., The production of actinomycins by controlled biosynthesis: the F actinomycins. *Ann. N.Y. Acad. Sci.*, 89, 299, 1960.
109. Katz, E., Williams, W.K., Mason, K.T., and Mauger, A.B., Novel actinomycins formed by biosynthetic incorporation of *cis*- and *trans*-4-methylproline. *Antimicrob. Agents Chemother.*, 11, 1056, 1977.
110. Nishimura, J.S. and Bowers, W.F., Evidence for the incorporation of L-thiazolidine-4-carboxylate into actinomycins by *Streptomyces antibioticus. Biochem. Biophys. Res. Commun.*, 28, 665, 1967.
111. Katz, E., Biogenesis of the actinomycins. *Ann. N.Y. Acad. Sci.*, 89, 304, 1960.
112. Formica, J.V. and Apple, M.A., Production, isolation and properties of azetomycins. *Antimicrob. Agents Chemother.*, 9, 214, 1976.
113. Formica, J.V. and Katz, E., Isolation, purification, and characterization of pipecolic acid-containing actinomycins, Pip 2, Pip 1α and Pip 1β. *J. Biol. Chem.*, 248, 2066, 1973.
114. Brockmann, H., Gröne, H., and Pampus, G., Chloractinomycine. *Chem. Ber.*, 91, 1916, 1958.
115. Brockmann, H., Pampus, G., and Mecke, R., Actinomycine, XXII; antibiotica aus actinomyceten, XLIV: N-Alkyl-actinomycine. *Chem. Ber.*, 92, 3082, 1959.
116. Brockmann, H., Müller, W., and Peterssen-Borstel, H., Actinomycin-derivate aus dihydroactinomycinen. *Tetrahedron Lett.*, 3531, 1966.
117. Brockmann, H., Hocks, P., and Müller, W., N-2-Substituierte actinomycine. *Chem. Ber.*, 100, 1051, 1967.
118. Moore, S., Kondo, M., Copeland, M., Meienhofer, J., and Johnson, R.K., Synthesis and antitumor activity of 2-deamino- and N^2-(γ-hydroxypropyl)actinomycin D. *J. Med. Chem.*, 18, 1098, 1975.
119. Sengupta, S.K., Anderson, J.E., Kogan, Y., Trites, D.H., Beltz, W.R., and Madhavarao, M.S., N^2- and C-7-substituted actinomycin D analogues: Synthesis, DNA-binding affinity, and biochemical and biological properties. Structure-activity relationship. *J. Med. Chem.*, 24, 1052, 1981.
120. Brockmann, H., Ammann, J., and Müller, W., 7-Chlor- und 7-brom-actinomycine. *Tetrahedron Lett.*, 3595, 1966.
121. Sengupta, S.K., Tinter, S.K., Ramsey, P.G., and Modest, E.J., Synthesis and DNA-binding properties of 7-amino-actinomycin D - a selective fluorescent binding agent. *Fed. Proc., Fed. Am. Soc. Exptl. Biol.*, 30, 342, 1971.
122. Müller, W., Bindung von actinomycin und actinomycin-derivaten an desoxyribonucleinsäuren. *Naturwiss.*, 49, 156, 1962.
123. Madhavarao, M.S., Chaykovsky, M., and Sengupta, S.K., N^7-Substituted 7-aminoactinomycin D analogs. Synthesis and biological properties. *J. Med. Chem.*, 21, 958, 1978.
124. Sengupta, S.K., Kelly, C., and Sehgal, R.K., "Reverse" and "Symmetrical" analogs of actinomycin D: Metabolic activation and *in vitro* and *in vivo* tumor growth inhibitory activities. *J. Med. Chem.*, 28, 620, 1985.
125. Brockmann, H. and Franck, B., Hydrierende acetylierung von actinomycin. *Angew. Chem.*, 68, 68, 1956.
126. Sengupta, S.K., Trites, D.H., Madhavarao, M.S., and Beltz, W.R., Actinomycin D oxazinones as improved antitumor agents. *J. Med. Chem.*, 22, 797, 1979.
127. Sengupta, S.K., Madhavarao, M.S., Kelly, C., and Blondin, J., Tetracyclic chromophoric analogs of actinomycin D: Synthesis, structure elucidation and interconvertability from one form to another, antitumor activity, and structure-activity relationships. *J. Med. Chem.*, 26, 1631, 1983.
128. Sengupta, S.K., Kogan, Y., Kelly, C., and Szabo, J., New actinomycin D analogs as superior chemotherapeutic agents against primary and advanced colon tumors and colon xenografts in nude mice. *J. Med. Chem.*, 31, 768, 1988.
129. Brockmann, H. and Franck, B., Aufspaltung der actinomycine zu actinomycinsäuren. *Angew. Chem.*, 68, 68, 1956.
130. Perlman, D., Mauger, A.B., and Weissbach, H., Microbial transformations of peptide antibiotics. I. Degradation of actinomycins by *Actinoplanes* species. *Antimicrob. Agents Chemother.*, 581, 1966.
131. Brockmann, H. and Sunderkötter, W., Abbau von actinomycin C_3 mit konzentrierter salzsäure. *Naturwiss.*, 47, 229, 1960.
132. Brockmann, H., Pampus, G., and Manegold, J.H., Actinomycin $X_{0\beta}$; zur systematik und nomenklatur der actinomycine. *Chem. Ber.*, 92, 1294, 1959.
133. Brockmann, H. and Stähler, E.A., 3-Hydroxy-4-oxo-5-methylprolin als baustein von actinomycin Z_1. *Tetrahedron Lett.*, 3585, 1973.
134. Mauger, A.B. and Wade, R., The synthesis of actinomycin analogs. Part II. Actinocyl-gramicidin S. *J. Chem. Soc.*, 1406, 1966.

135. Brockmann, H. and Seela, F., 4,6-Didesmethyl-actinomycin C_1 und dessen 4,6-dimethoxy-, 4,6-diäthyl- und 4,6-di-*tert*-butyl-derivat. *Chem. Ber.*, 104, 2751, 1971.
136. Giencke, A. and Lackner, H., Desmethyl(trifluormethyl)-actinomycine. *Liebigs Ann. Chem.*, 569, 1990.
137. Brockmann, H. and Schulze, E., Synthese von pseudo-actinomycin C_1. *Tetrahedron Lett.*, 1489, 1971.
138. Mosher, C.W., Lee, D., Enanoza, R.M., Sturm, P.A., and Kuhlmann, K.F., A phenazine analog of actinomycin D. *J. Med. Chem.*, 22, 918, 1979.
139. Brockmann, H. and Schramm, W., Synthese von actinomycin-(thr-Val-pro-sar-meval), dem antipoden von actinomycin C_1. *Tetrahedron Lett.*, 2331, 1966.
140. Brockmann, H. and Lackner, H., Aufbau von actinomycinen über actinomycinsäuren; ein zweiter syntheseweg, *Chem. Ber.*, 101, 1312, 1968.
141. Moore, S., Patel, R. P., Atherton, E., Kondo, M., Meienhofer, J., Blau, L., Bittman, R., and Johnson, R. K., Synthesis and some properties and antitumor effects of the actinomycin lactam analog [di(1′-L-α,β-diaminopropionic acid)]actinomycin D, *J. Med. Chem.*, 19, 766, 1976.
142. Atherton, E., Patel, R.P., Sano, Y., and Meienhofer, J., Actinomycin D lactam, [1′1′-bis(*threo*-α,β-diaminobutyric acid)]actinomycin D, *J. Med. Chem.*, 16, 355, 1973.
143. Mauger, A.B. and Stuart, O.A., Synthesis and properties of some peptide analogs of actinomycin D, *J. Med. Chem.*, 34, 1297, 1991.
144. Mosher, C.W. and Goodman, M., Synthesis of [4′,4′-bis(glycine), 5′,5′-bis(valine)]actinomycin D, a tetra-N-demethylactinomycin, *J. Org. Chem.*, 37, 2928, 1972.
145. Mauger, A.B., Stuart, O.A., Ferretti, J.A., and Silverton, J.V., Conformation and dimerization of actinomycin-related peptide lactones in solution and in the solid state, *J. Am. Chem. Soc.*, 107, 7154, 1985.
146. Pugh, L.H., Katz, E., and Waksman, S.A., Antibiotic and cytostatic properties of the actinomycins. *J. Bacteriol.*, 72, 660, 1956.
147. Katz, E. and Pugh, L.H., Variations on a theme. The actinomycins. *Appl. Microbiol.*, 9, 263, 1961.
148. Pugh, L.H. and Solotorovsky, M., Comparative effects of actinomycins II, III and IV on several ascitic tumors in mice. *Ann. N.Y. Acad. Sci.*, 89, 373, 1960.
149. Mason, K., Katz, E., and Mauger, A.B., Studies on the biological activities of actinomycins Z_1 and Z_5. *Arch. Biochem. Biophys.*, 160, 402, 1974.
150. Modest, E.J. and Sengupta, S.K., 7-Substituted actinomycin D (NSC-3053) analogs as fluorescent DNA-binding and experimental antitumor agents. *Cancer Chemother. Reps. Part I*, 58, 35, 1974.
151. Formica, J.V., Shatkin, A.J., and Katz, E., Actinomycin analogs containing pipecolic acid: relationship of structure to biological activity. *J. Bacteriol.*, 95, 2139, 1968.
152. Johnson, R.K. private communication.
153. Rose, W.C., Trader, M.W., Laster Jr., R.W., and Schabel Jr., F.M., Comparative antitumor activity of actinomycin analogs in mice bearing Ridgeway osteogenic sarcoma or P388 leukemia. *Cancer Treatment Reps.*, 62, 779, 1978.
154. Li, M.C., Management of choriocarcinoma and related tumors of uterus and testis. *Med. Clin. N. Am.*, 45, 661, 1961.
155. Ross, G.T., Stohlbach, L.L., and Hertz, R., Actinomycin in the treatment of methotrexate-resistant trophoblastic disease in women. *Cancer Res.*, 22, 1015, 1962.
156. Li, M.C., Whitmore Jr., W.F., Golbey, R., and Grabstald, H., Effects of combined drug therapy of metastatic cancer of the testis. *J. Am. Med. Assoc.*, 174, 1291, 1960.
157. MacKenzie, A.R., Chemotherapy of metastatic testis cancer—results in 154 patients. *Cancer Chemother. Rep.*, 19, 1369, 1966.
158. Tan, C.T.C., Dargeon, H.W., and Burchenal, J.H., The effect of actinomycin D in cancer in childhood. *Pediatrics*, 24, 544, 1959.
159. James, D.H., Hustu, O., Wrenn Jr., E.L., and Johnson, W.W., Childhood malignant tumors. Concurrent chemotherapy with dactinomycin and vincristine sulfate. *J. Am. Med. Assoc.*, 197, 1043, 1966.
160. Farber, S., Chemotherapy in the treatment of leukemia and Wilms' tumor. *J. Am. Med. Assoc.*, 198, 826, 1966.
161. Fernbach, D.J. and Martyn, D.T., Role of d actinomycin in the improved survival of children with Wilms' tumor. *J. Am. Med. Assoc.*, 195, 1005, 1966.
162. Gommersall, L.M., Arya, M., Mushtaq, I., and Duffy, P., Current challenges in Wilms' tumor management. *Nat. Clin. Pract. Oncol.*, 2, 298, 2005.
163. Krasin, M.J., Dasvbodoff, A.M., Rodriguez-Galindo, C., Billups, C.A., Fuller, C.E., Neel, M.D., and Merchant, T.E., Definitive surgery and multiagent systemic therapy for patients with localized Ewing sarcoma family of tumors: Local outcome and prognostic factors. *Cancer*, 104, 367, 2005.

164. Jmoschovi, M., Trimis, G., Stefanaki, K., Anastasopoulos, J., Syriopoulou, V., Koultouki, E., and Tzortzatou-Stathopolou, F., Favorable outcome of Ewing sarcoma family tumors to multiagent intensive preoperative chemotherapy: A single institution experience. *J. Surgical Oncol.*, 89, 239, 2005.
165. Covens, A., Filiaci, V.L., Burger, R.A., Osborne, R., and Chen, M.D., Phase II trial of pulse dactinomycin as salvage therapy for failed low-risk gestational trophoblastic neoplasia—A Gynecologic Oncology Group study. *Cancer*, 107, 1280, 2006.
166. Vrouenraets, B.C., Nieweg, O.E., and Kroon, B.B.R., Thirty-five years of isolated limb perfusion: Indications and results. *Br. J. Surg.*, 83, 1319, 1996.
167. Thompson, J.F., Kam, P.C., Waugh, R.C., and Harman, R.C., Isolated limb infusion with cytotoxic agents: A simple alternative to isolated limb perfusion. *Semin. Surg. Oncol.*, 14, 238, 1998.
168. Kroon, H.M., and Thompson, J.F., Isolated limb infusion: A review. *J. Surgical Oncol.*, 100, 169, 2009.
169. Kroon, H.M., Lin, D.-Y., Kam, P.C.A., and Thompson, J.F., Safety and efficacy of isolated limb infusion with cytotoxic drugs in elderly patients with advanced locoregional melanoma. *Ann. Surg.*, 249, 1008, 2009.
170. Kroon, H.M., Lin, D.-Y., Kam, P.C.A., and Thompson, J.F., Isolated limb infusion as palliative treatment for advanced limb disease in patients with AJCC stage IV melanoma. *Ann. Surg. Oncol.*, 16, 1193, 2009.

16 Anthracyclines

Federico-Maria Arcamone

CONTENTS

16.1 Introduction 383
16.2 Development of the Anthracycline Drugs 385
16.2.1 Daunorubicin 385
16.2.2 Doxorubicin 385
16.2.3 Second-Generation Antitumor Anthracyclines 385
16.3 Mechanism of Action 386
16.3.1 DNA Complex and Topoisomerase II Poisoning 386
16.3.2 Natural and Acquired Resistance to Anthracyclines 387
16.3.3 Cardiotoxicity 388
16.4 Synthesis of the Drugs 388
16.4.1 Doxorubicin 388
16.4.2 Epirubicin 388
16.4.3 Idarubicin 388
16.5 Medicinal Chemistry of Antitumor Anthracyclines 389
16.5.1 Analogs Modified in the Aglycone Moiety 389
16.5.1.1 Deoxyderivatives 389
16.5.1.2 Fluoroderivatives 390
16.5.2 Analogs Modified in the Sugar Moiety 391
16.5.2.1 Monosaccharide Analogs 391
16.5.2.2 Disaccharide Analogs 393
16.5.3 Anthracycline–Triplex Helix-Forming Oligonucleotide Conjugates 395
16.6 Clinical Activity of Anthracyclines 396
16.6.1 Daunorubicin 397
16.6.2 Doxorubicin 397
16.6.3 Epirubicin 397
16.6.4 Idarubicin 398
16.6.5 Aclacinomycin 399
16.6.6 Sabarubicin 399
16.6.7 Liposomal Anthracyclines 399
16.6.8 Amrubicin 400
References 400

16.1 INTRODUCTION

Anthracycline aminoglycosides represent a wide class of antibiotics obtained by submerged aerobic fermentation of different microorganisms belonging to the genus *Streptomyces* and are called anthracyclines, because the aglycone moiety is a tetracyclic system bearing an anthraquinone chromophore.[1] The anthracyclines are microbial metabolites belonging, from the biogenetic standpoint,

to the large family of the polyketide natural products, comprising a wide range of biologically active structural groups: the antibacterial antibiotics, tetracyclines, and the macrolides of the erythromycin type; immunosuppressants such as FK506; antiparasitic compounds such as monensin; and the avermectins. These molecules are synthesized by multifunctional polyketide synthase enzymes, which catalyze repeated condensation cycles between simple acylthioesters with the formation of a growing carbon chain containing β-keto groups. These keto groups may undergo a number of intramolecular reactions, leading to aromatic derivatives, such as the aglycone of the anthracyclines, the anthracyclinones, and a series of reductive steps. The final products are characterized by a considerable molecular diversity.[2]

The antitumor activity of a biosynthetic anthracycline was first reported in 1959.[3] In fact, different samples of a mixture of red pigments isolated from the cultures of a *Streptomyces* strain at Farmitalia Research Laboratories were found to be active against murine Ehrlich carcinoma and sarcoma 180 test systems. The presence of compounds possessing the hydroxyanthraquinone chromophore was deduced on the basis of the typical electronic spectrum—red in acid and blue in alkaline solutions. The pigments were isolated by countercurrent distribution, and their relationship with the anthracyclines—previously studied and described by different authors, and more precisely with the rhodomycin complex[1]—was established. Subsequently, useful pharmacological properties were found that were associated with the compounds produced by a novel species, *Streptomyces peucetius*, and related strains. Doxorubicin (**Ia**, originally named adriamycin), the best known component of this group, is the 14-hydroxylated derivative of the main fermentation product daunorubicin (**Ib**), and since its registration in the early 1970s, doxorubicin has been one of the most widely used drugs in cancer chemotherapy.[4] (The trademark of doxorubicin formulations in the United States is Adriamycin®.)

The successful therapeutic application of **Ia** stimulated a considerable effort in the chemical and biological studies of the antitumor anthracyclines aimed at the development of better analogs by chemical modification of the parent drugs or by total synthesis of new structurally related compounds. Although **Ia** remains one of the most effective agents in the treatment of a range of solid tumors, different new members of this chemical group, among which epirubicin (**II**) and idarubicin (**III**) are the most important, are presently used in the medical practice. Such new agents were already described in previous books[5,6] and are currently known as second-generation anthracyclines. In 1992, it was observed that an analog truly superior to doxorubicin had not been identified. In fact, after the synthesis and biological testing of hundreds of new anthracycline glycosides in different laboratories, neither an analog with a really improved therapeutic index nor one with a substantially different spectrum of activity had been found.[7] It should be noted that analogs with considerable structural variations were submitted to testing procedures that were mostly limited to murine models of transplantable leukemias, which is possibly not the best way to make an appropriate selection of new interesting compounds. The present tumor type-oriented pharmacological evaluation, based on the use of a large number of human tumor cell lines and on human tumor heterotransplants in nude mice, coupled with rational drug design and closer attention to aspects, such as drug bioavailability, tissue distribution, and pharmacokinetics, might increase the probability of obtaining results closer to the desired goal.[8]

Antitumor activity has also been associated with other biosynthetic anthracyclines generally differing from the daunorubicin–doxorubicin group in the chemical structure of both the tetracyclic aglycone and the sugar moiety, with the latter often present as an oligosaccharide fragment. One such compound, aclacinomycin (ACM), has been introduced in clinical use.[9] The biosynthetic anthracyclines have been reviewed, together with the products of microbial transformations of individual anthracycline antibiotics, by Oki.[10] An overview of the different biosynthetic anthracyclines, describing the producing microorganisms, the chemical structure, and when available, the pharmacological data of over 250 compounds, has been published.[11] A series of outstanding review articles on the fascinating molecular biology of anthracycline biosynthesis is also available.[12–14]

16.2 DEVELOPMENT OF THE ANTHRACYCLINE DRUGS

16.2.1 Daunorubicin

In December 1958 and February 1959, two similar crude preparations, obtained from a different *Streptomyces* species isolated from a soil sample collected in Apulia at Caste del Monte close to the ancient castle of King Frederick II, were shown to be endowed with significant antitumor properties in terms of tumor size reduction and the time of survival of the treated animals versus untreated ones in the above-mentioned mouse tests. The new microorganism and the main compound obtained from the active samples were named *S. peucetius* and daunomycin, respectively, because of the names of the ancient populations living in the region in early historical times, the Peucetii and the Daunii. The significant antitumor activity of daunomycin was confirmed in a wider spectrum of experimental systems.[15] These results stimulated a detailed investigation of the chemical structure of daunomycin to determine the differences between it and the classical anthracyclines, differences that were responsible for the markedly improved pharmacological properties. The products of acid hydrolysis, namely, the aglycone, daunomycinone, and the sugar moiety, daunosamine, were studied by means of chemical degradation reactions and physicochemical analyses. In brief, both fragments were new compounds,[16,17] indicating that the microorganism produced a novel family of anthracycline glycosides. The complete structure and stereochemistry of daunomycin were finally established as represented in **Ib**,[18–20] and they were eventually confirmed by the x-ray diffraction analysis of the corresponding *N*-bromoacetyl derivative.[21] In the meantime, daunomycin was identified with rubidomycin, isolated by French researchers from *Streptomyces coeruleorubidus*.[22] The World Health Organization suggested "daunorubicin" for the compound's name in recognition of the independent contributions from Farmitalia and Rhone-Poulenc laboratories. Clinical studies, showing its high activity in acute leukemias, were presented in a meeting held at St. Louis Hospital in Paris in 1967.[23]

16.2.2 Doxorubicin

Doxorubicin (adriamycin, **Ia**) was isolated as a pigment coproduced with daunorubicin in the culture medium of *S. peucetius*-derived strains. It showed a marked activity in experimental systems and a wide spectrum of antitumor efficacy, especially in solid tumors.[24] Structure **Ia** was determined, *inter alia*, by nuclear magnetic resonance analysis of the aglycone, adriamycinone, and by direct semisynthesis from daunorubicin.[25] Because of the very small quantities of doxorubicin present in the fermentation broths of the wild strains, the semisynthetic process was developed at a pilot plant scale and was eventually scaled up to the industrial scale, starting in the early 1970s. The publications from the Istituto Nazionale Tumori, Milan, concerning laboratory[26] and clinical[27] results aroused high interest, and the efficacy of doxorubicin in a spectrum of solid tumors was highlighted in an International Symposium held in Milan in September 1971. Early experience with doxorubicin in the treatment of human cancer diseases was reviewed by S.K. Carter.[28]

16.2.3 Second-Generation Antitumor Anthracyclines

Daunosamine, 3-amino-2,6-dideoxy-l-lyxo-hexose,[17] is the natural aminosugar present in all anthracycline glycosides produced by the strains belonging to the species *S. peucetius*, the original producer of the daunorubicin group of antibiotics, and related strains.[11] An early approach to new analogs consisted of the synthesis of related aminosugars, differing from daunosamine in stereochemistry or in structure, and of the coupling of the same with the aglycone moiety, with the aim of modifying the pharmacokinetics or metabolism of the natural glycosides. This approach afforded a number of compounds with a wide variation in bioactivity, out of which the analog of structure **II**, containing the aminosugar acosamine, namely, 3-amino-2,6-dideoxy-l-arabino-hexose, was selected for further

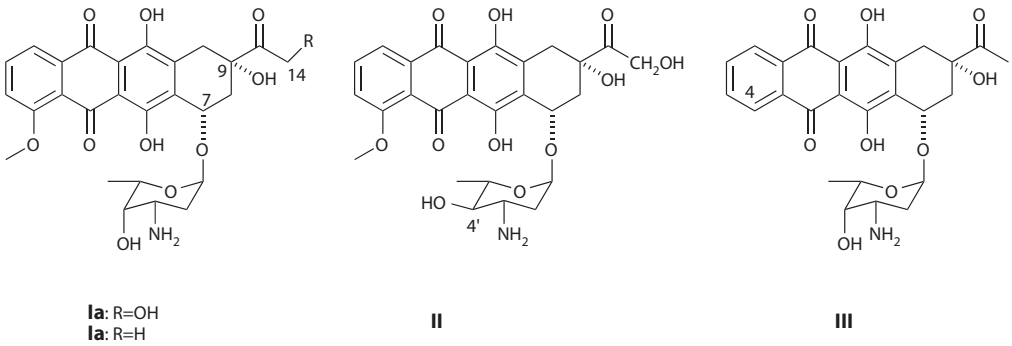

STRUCTURE 16.1 Structures **I** through **III**.

development because of a higher chemotherapeutic index when compared with doxorubicin.[4] The compound, known by the generic name of epirubicin, exhibited superior performance when compared with doxorubicin in experimental models and clinical studies, and was registered in most countries in the 1980s as Farmorubicin® or Pharmorubicin®. However, registration in the United States was obtained only more recently, and the compound is currently marketed in this country as Ellence®.

Daunomycinone, the aglycone of daunorubicin, is characterized by the tetracyclic trihydroxyanthraquinone chromophore typical of natural anthracyclinones, albeit containing specific structural features that identify the daunomycin group of metabolites; namely, the ketone function in the C9 side chain, the absence of a substituent at C10, and the presence of a methoxyl group instead of a hydroxyl at C4. In the closely related carminomycin, the C4 hydroxyl is not methylated. As methods for the total synthesis of daunomycinone and related compounds were made available, it is reasonable that analogs showing no substitution at C4 were prepared and tested. In fact, their synthesis was easier in comparison with that of the natural compounds because of the absence of regioisomers in the construction of the anthraquinone system. The first compound synthesized in this series, 4-demethoxydaunorubicin (**III**) (idarubicin), has been developed to the clinical stage because of its powerful activity in experimental leukemia models and reduced cardiotoxicity. Idarubicin exhibits features rendering this compound unique among clinically available anthracyclines. The results of preclinical studies indicate that the higher lipophilicity of **III** leads to faster accumulation in the nuclei, superior DNA-binding capacity, and consequently greater cytotoxicity compared with **Ib**. A major advantage over the 4-methoxylated parent drug is its ability to partially overcome multidrug resistance. Its major metabolite, idarubicinol, is as active as the parent compound.[29] Idarubicin is marketed with the trademark Zavedos®. As seen below, a 4-demethoxy aglycone has become a favorable structural feature in more recently designed analogs.

16.3 MECHANISM OF ACTION

Anthracyclines, as with several other classes of antitumor agents, work by DNA intercalation, a specific mode of binding in which the drug chromophore is inserted between adjacent DNA base pairs.[30] However, the mechanism of action cannot be described in such a simple way, and the picture appears to be rather more complex.

16.3.1 DNA Complex and Topoisomerase II Poisoning

The binding of anthracyclines to DNA has been extensively studied by a variety of biochemical and biophysical techniques.[31,32] The drug intercalates at a pyrimidine–purine step with a preference for the cytidine–guanosine (CG) sequence and acts as a groove binder, as the sugar moiety interacts with

the minor groove.[33–35] DNA binding is a necessary but not sufficient condition for drug activity. In other words, there is no simple relationship between DNA-binding affinity and cytotoxicity, and a number of different mechanisms have been proposed. In brief, poisoning of topoisomerases is likely to be the mechanism most closely associated with their cytoxicity, although other molecular interactions may play an important role as well. Topoisomerases are enzymes that are involved in the topological interconversions of DNA during DNA transcription and replication; their functions are numerous and important because they are critical for DNA functions and cell survival. It was found that the DNA breaks induced by doxorubicin were associated with the enzyme topoisomerase II.[36] In a study including different anthracyclines, it was found that for all bioactive anthracyclines in the entire SV40 DNA, a single region of prominent cleavage sites lies between nucleotides 4237 and 4294. A good correlation was recorded between cytotoxicity and intensity of topoisomerase II-mediated DNA breakage.[37] All the doxorubicin-stabilized sites had an adenosine at the 3′-terminus of at least one member of each pair of strand breaks that would constitute a topoisomerase II double-strand scission. Conversely, none of the enzyme-only sites had an adenosine simultaneously at the corresponding positions on opposite strands. The requirement of a 3′-adenosine for doxorubicin-stabilized cleavage is therefore incompatible with enzyme-only cleavage and explains the mutual exclusivity of the two classes of sites.[38] The strength of DNA binding does not correlate with the stimulatory effect of anthracyclines on topoisomerase II-mediated DNA cleavage and with the cytotoxic potency. However, drug intercalation is still required for optimal drug activity, indicating that the specific mode of DNA interaction, rather than the strength of binding, is important in determining the cytotoxic potency.[39] On the basis of a study including different semisynthetic doxorubicin analogs, it was concluded that cytotoxic potency of anthracyclines might be the result of an interplay of different factors, namely, the level, the persistence, and the genomic localization of topoisomerase II-mediated DNA cleavage.[40] In conclusion, the main steps of the mode of action of antitumor anthracyclines would be the formation of a drug–DNA–enzyme ternary complex, in which the enzyme is covalently linked to the broken DNA strand, and the consequent DNA damage consisting of protein-associated double-strand breaks that trigger apoptotic cell death.[41,42]

16.3.2 Natural and Acquired Resistance to Anthracyclines

Drug resistance is a major problem in cancer chemotherapy, and it is also clearly apparent in the case of antitumor anthracyclines. A number of important tumors of great clinical importance do not respond to currently available anthracycline drugs. These tumors include colon cancers, lung cancers, pancreatic and renal cancers, and malignant melanoma, to cite only some examples of "naturally resistant" tumors. Other diseases, such as gastric and small cell lung cancers and advanced ovary and breast tumors, are only partially responsive, and often the benefit of drug treatment is marginal. So far, only the classic multidrug resistance phenotype, which is a result of the presence of P-glycoprotein in the plasma membrane (a "pump" that can extrude a wide range of anticancer drugs), has been shown to contribute to resistance in clinical conditions. The other possible mechanisms of resistance are a non-P-glycoprotein-mediated multidrug resistance, a phenotype characterized by the expression of other proteins in the plasma membrane that are also able to extrude anticancer drugs; changes in the intracellular distribution of the drug; glutathione transferases and detoxification mechanisms; low levels of expression or alterations in topoisomerase II; and finally, an increased DNA repair. However, evidence for these mechanisms of resistance in cancer patients is still missing.[43]

A relationship was found between doxorubicin resistance and glutathione transferase activity, but not between doxorubicin resistance and multidrug resistance-associated protein or P-glycoprotein, in human colon adenocarcinoma cell lines,[44] and enzyme-catalyzed formation of the adduct, 7-deoxy-7-*S*-glutathionyl-adriamycinone, may be relevant to tumor cell resistance to doxorubicin.[45] Introduction of HER-2 oncoprotein gene *in vitro* induces resistance to several anticancer drugs, including taxanes, cisplatin, and 5-fluorouracil, in breast cancer cells. Interestingly, in clinical studies, patients with HER-2 oncoprotein overexpression, an important prognostic factor associated

with a poor prognosis in breast cancer, responded better to an anthracycline-based regimen than did patients with low HER-2 expression, and their overall survival was also superior. In addition, treatment with trastuzumab, an anti-HER-2 antibody, increased drug sensitivity to anthracyclines.[46]

16.3.3 Cardiotoxicity

Together with the onset of resistance, a major dose-limiting factor in the repeated treatment with doxorubicin is the development of cardiotoxicity at cumulative dosages higher than 400 mg/m^2. In the mouse, the most prominent and persistent myocardial change induced by repeated doxorubicin administrations was an increased reactivity of the sarcoplasmic reticulum with the zinc iodide–osmium tetroxide reagent that appeared to be related with the observed cardiotoxic effects.[47] The zinc iodide–osmium tetroxide reagent allows the detection of disulfide bonds in polypeptides, cystine, and oxidized glutathione, substances that react more promptly than other potential substrates such as unsaturated lipids and catecholamines. This observation indicates the presence of an oxidative stress that, as already demonstrated by different authors,[48,49] may be caused by a higher than normal oxygen tension in the heart tissue. Excess oxygen could be the result of a long-lasting inhibition of nucleic acid synthesis as that found in the heart tissue of laboratory animals treated with the drug,[50] with a consequent reduction of metabolic consumption of oxygen. Also, inhibition by doxorubicin of mitochondrial DNA transcription leads to a diminished ATP production and consequently to cell damage in high-energy-demanding tissues.[51] In any case, current evidence appears to be consistent with a fundamental role for free radicals, whatever their origin, in the cardiotoxic actions of the anthracyclines.[41]

16.4 SYNTHESIS OF THE DRUGS

16.4.1 Doxorubicin

Doxorubicin (**Ia**) is prepared by semisynthesis starting from biosynthetic daunorubicin (**Ib**), currently obtained in bulk quantities by fermentation of different *Streptomyces* strains, mostly derived from *S. peucetius*. The reaction sequence comprises an electrophilic bromination of **Ib** followed by an acid treatment to give the 14-bromoketone that is converted to **Ia** via the intermediate 14-*O*-formate.[4] As with all commercial anthracyclines, the compound is crystallized to higher than 98% purity as the hydrochloride and is formulated in freeze-dried form with the addition of lactose. Doxorubicin ready-to-use solutions, both with and without stabilizers, have been patented.[52,53]

16.4.2 Epirubicin

Epirubicin (**II**) is prepared by a similar reaction sequence starting from 4-epidaunorubicin, originally prepared by the glycosidation of daunorubicin aglycone, daunomycinone, with *N*,*O*-ditrifluoroacetyl-l-acosaminyl chloride and silver triflate, followed by removal of the protecting trifluoroacetyl groups.[4] A direct conversion of biosynthetic daunorubicin to the 4-epi derivative **VII** has also been carried out.[54] It involves oxidation at C4 of *N*-trifluoroacetyl derivative **IV** to ketone **V** and selective reduction of the latter with sodium borohydride to **VI**, followed by deprotection with base (Scheme 16.1). This procedure is the basis of current industrial production of **II**.

16.4.3 Idarubicin

Idarubicin (**III**) was originally prepared by glycosidation of 4-demethoxydaunomycinone (idarubicinone), which was obtained by total synthesis using a modification of the Wong procedure.[4] A stereoselective synthesis of Wong's tetralin has been published.[55] In contrast, a semisynthetic process useful for the industrial preparation of idarubicinone starting from daunomycinone **VIII**, easily prepared on acid hydrolysis of biosynthetic daunorubicin, has been carried out.[56] As shown in

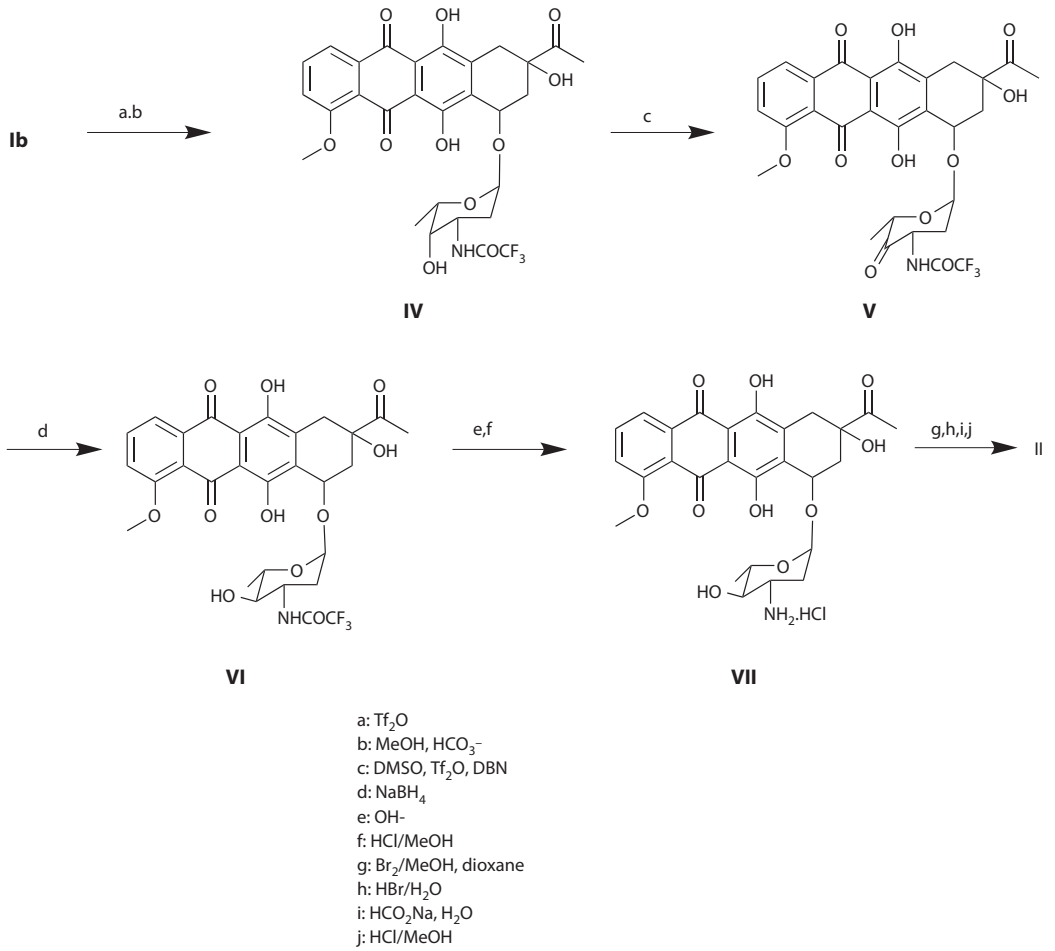

SCHEME 16.1 Semisynthesis of epirubicin.

Scheme 16.2, this process involves demethylation of **VIII** to carminomycinone **IX** and the conversion of the latter to the 13-ethylidene ketal **X** and then to the 4-*O*-triflate **XI**. The subsequent step, leading to 4-deoxy derivative **XII**, is based on the deoxygenation reaction of phenols discovered by Cacchi et al.[57] Removal of the protecting group provides idarubicinone **XIII**, which is glycosylated to **III**. The method is particularly interesting, because daunorubicin is also a source of the aminosugar daunosamine, the other starting material for the synthesis of **III**.

16.5 MEDICINAL CHEMISTRY OF ANTITUMOR ANTHRACYCLINES

16.5.1 Analogs Modified in the Aglycone Moiety

16.5.1.1 Deoxyderivatives

The substitution of a hydroxyl group with a hydrogen atom has been extended to positions 6 and 11, as specific interest in the C6 and C11 deoxyderivatives stems from the hypothesis that antitumor activity or cardiotoxicity of anthracyclines might be related with the redox behavior or with the ability to form metal complexes. Synthesis of the corresponding daunorubicin and doxorubicin analogs led to the conclusion that such modifications, although bearing noticeable consequences on the polarographic behavior or on the chemical outcome of anaerobic quinone reduction, did not result

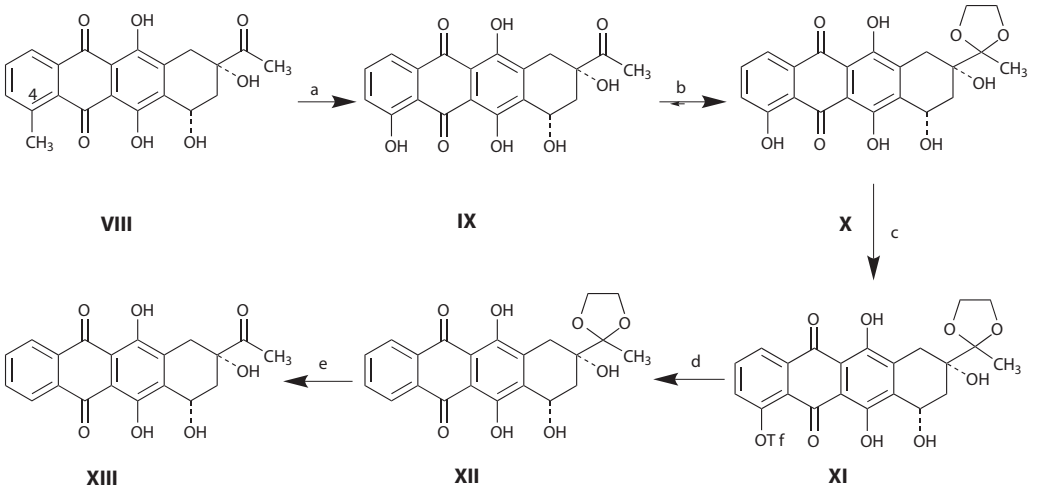

SCHEME 16.2 Semisynthesis of idarubicinone.

in a marked change of bioactivity.[58,59] A significant structural modification in terms of structure–activity relationships was instead the substitution of the C9 hydroxyl group on ring A with a hydrogen atom. In fact, 9-deoxydaunorubicin, although showing the same affinity for DNA and similar electrochemical behavior as the parent daunorubicin, was two orders of magnitude less cytotoxic on cultured HeLa cells. Therefore, it was deduced that the 9-hydroxyl group, which according to the well-known molecular model of the daunorubicin–DNA complex protrudes outside the double helix, might be involved in a specific interaction relevant to the bioactivity of the drug in terms of topoisomerase II blockade in the ternary complex.[60]

16.5.1.2 Fluoroderivatives

According to the established importance of the 9-hydroxyl group mentioned above, a study aimed at the improvement of doxorubicin anticancer activity via introduction of a fluorine atom at the α position with respect to the C9 has been carried out. The substitution of a hydrogen atom with a fluorine at position 8 gave rise to compounds with markedly different chemical and biological properties depending on the stereochemistry at the new chiral center. 8(*S*)-Fluoro aglycones **XIVa** and **XIVb** were obtained from 8,9-oxirane intermediates. These were either prepared by total synthesis when R = H or, in the case of **XIVb**, in enantiomeric (8*S*) form by semisynthesis from "pink compound" **XV** via the corresponding 7,8-epoxide, **XVIa**, and finally **XVIb**. Glycosidation of **XIVa** and **XIVb**, followed by diastereomeric separation when R = H, afforded glycosides **XVIIa** and **XVIIb**, respectively. Compound **XVIIb** was eventually converted to 8(*S*)-fluorodoxorubicin, albeit in low yields because of the inertness toward electrophilic bromination at C14 (possibly a sign of the strong electrostatic effect of the fluorine substitution). A significantly lower cytotoxic potency exhibited by **XVIIa** compared with unsubstituted idarubicin was related to the β conformation of ring A, predominating in the solution of **XVIIa** over the α conformation typical of idarubicin and the other antitumor anthracyclines. To obtain the corresponding epimeric *cis*-8*R*,9*S*-fluorohydrins, Diels–Alder adduct **XVIII** was treated with *N*-bromosuccinimide and tetrabutylammonium dihydrogentrifluoride to give, together with a 8-bromo-9-fluoro derivative, the desired 8-fluoro-9-bromo isomer **XIX** that was converted to the 9,13-epoxide with base. Opening of the oxirane ring with acid and

oxidation of the side chain alcohol gave a ketone that was functionalized at C7 via radical bromination and hydrolysis to give the desired 8,9-*cis*-fluorohydrin **XIVc**. Glycosidation of the latter, followed by separation of diastereomeric glycosides and deprotection, gave 8(*R*)-fluoroidarubicin **XVIIc**, which was found to be as potent as idarubicin in the inhibition of the growth of tumor cell lines *in vitro*. Interestingly, **XVIIc** displayed marked cytotoxic activity against doxorubicin-resistant cell lines (Table 16.1). When delivered intravenously at a dosage of 1.5 mg/kg to immunodepressed mice bearing A2780 human ovarian carcinoma xenografts, the new compound inhibited tumor growth by 93%, whereas in the same system, doxorubicin at 7 mg/kg inhibited by 83% and idarubicin at 1.2 mg/kg inhibited by only 36%. Values of "log cell kill" (difference in mean time required for tumors of treated and control mice to reach 2 g divided by the product of mean doubling time of the tumor and 3.32) were equal to 3 for the 8*R*-fluoro derivative, and to 1.8 for doxorubicin.[61,62]

14-Fluorodoxorubicin **XXI** has been obtained starting from daunomycinone **VIII**, brominated to known **XXa**, whose treatment with $AgBF_4$ and dimethylsulfoxide gave, interestingly, fluoroderivative **XXb**. Bromination and reaction of compound **XXc** with $AgBF_4$ afforded **XXd**. Desired **XXI** was eventually obtained through glycosylation of **XXc** with 1-*p*-nitrobenzoyl-3,4-*N*,*O*-diallyloxycarbonyl daunosamine and treatment of the resulting protected glycoside with the $AgBF_4$-DMSO reagent, followed by removal of the protecting groups.[63] A superior bioactivity of **XXI** in respect to **I** has not been reported.

16.5.2 Analogs Modified in the Sugar Moiety

16.5.2.1 Monosaccharide Analogs

The aminosugar 4-deoxydaunosamine was obtained from daunosamine and used for the preparation of 4-deoxydoxorubicin (esorubicin), a compound showing activity comparable to that of the parent, doxorubicin, and lower cardiotoxicity in experimental studies[5] (albeit not confirmed in clinical phase II studies[64]). Similarly, 4-iodo-4-deoxydoxorubicin, showing promising results in preclinical

TABLE 16.1
Inhibition of Growth of Human Tumor Cell Lines by Doxorubicin (Ia), Idarubicin (III), and Epimeric 8(*S*) and 8(*R*)-Fluoroidarubicins (XVIIa and XVIIc, Respectively)

Cell line	I	III	XVIIa	XVIIc
A2780[a]	13	2.8	14	5
A2780/DX	250	10	60	9
LOVO[b]	41	3	12	3
LOVO/DX	989	20	147	11
MCF-7[c]	13	2	6	3
MCF-7/DX	2460	27	291	16
POVD[d]	37	4	6	9
POVD/DX	350	48	70	9
POGB[d]	16	2	20	2
POGB/DX	390	24	140	4

Note: Results are expressed as IC_{50} values (ng/ml) (adjusted from Ref. 62).
[a] Ovarian tumor.
[b] Colon tumor.
[c] Breast tumor.
[d] Small-cell lung cancer.

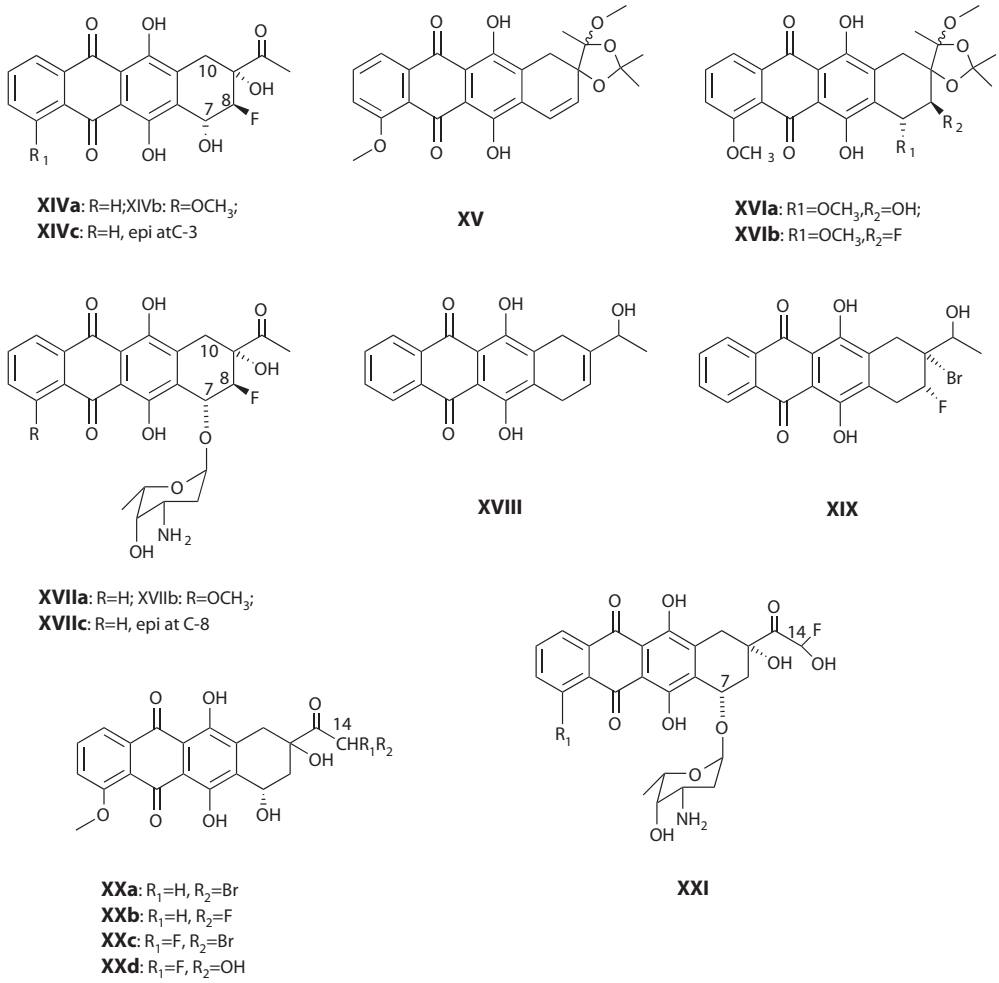

STRUCTURE 16.2 Structures **XIV** through **XXI**.

studies,[65] was also developed up to clinical phase II but did not exhibit therapeutic properties suggesting improved anticancer activity.[66] Instead, the compound was found to be the lead for a novel class of drugs for amyloid-related diseases.[67,68] A doxorubicin derivative named pirarubicin, namely, 4-*O*-dihydropyranyl-doxorubicin, was studied in Japan and has entered into clinical use as a doxorubicin analog endowed with lower side effects.[9] Annamycin **XXII**, a lipophilic iodinated analog, devoid of the sugar amino group and of the methoxy group at C4, was shown, especially when entrapped in liposomes, to be partially effective in cell cultures and in mouse tests against doxorubicin-resistant tumors.[69] Berubicin, the 4′-*O*-benzyl derivative of **Ia**, has been recently shown to cross the blood–brain barrier thus showing potential in the medical treatment of glioblastomas.[70]

An interesting group of analogs is represented by the morpholinyl anthracyclines. These new derivatives were discovered by Acton et al. and found to be about two orders of magnitude more cytotoxic than the known antitumor anthracyclines, very likely owing their high potency to an alkylating mechanism of action.[71] 3′-(2-Methoxy-4-morpholinyl) derivative **XXIII** (nemorubicin) was developed up to the clinical stage because of its high potency and activity in mice inoculated with doxorubicin-resistant P388 leukemia, but a low response rate was observed in patients with tumors endowed with intrinsic resistance to chemotherapy.[72]

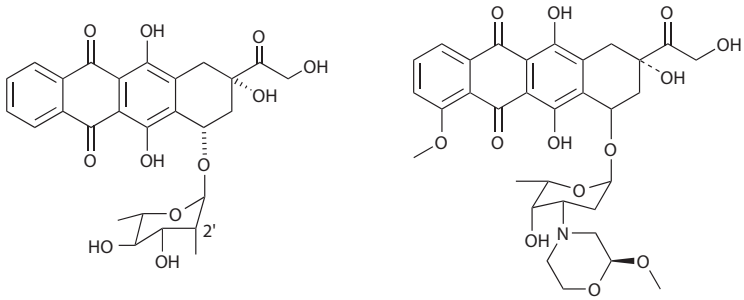

XXII **XXIII**

STRUCTURE 16.3 Structures **XXII** and **XXIII**.

A different, not DNA-related, biochemical mechanism of action has been suggested for the very lipophilic doxorubicin derivative, *N*-benzyldoxorubicin-14-*O*-valerate.[73]

16.5.2.2 Disaccharide Analogs

More recently, attention has been given to analogs containing two sugar residues. Anthracycline disaccharides have been obtained both as biosynthetic products or by semisynthesis. The disaccharide 4-*O*-daunosaminyldaunorubicin was present in the medium of the daunorubicin fermentation, and the same, as well as the corresponding analogs in which the second sugar was acosamine or 2-deoxy-L-rhamnose, was also obtained by semisynthesis and found to be cytotoxic, albeit less potent against murine transplantable leukemias than daunorubicin.[4] Other related glycosides of daunorubicin have been synthesized;[74,75] however, the first bearing a nonaminated sugar directly linked to the aglycone, namely, 7-*O*-(3-*O*-α-L-daunosaminyl-2-deoxy-α,L-rhamnosyl)-daunomycinone, was biologically inactive, apparently because of the different position of the second glycosidic linkage.[76] In fact, as suggested by the DNA-binding geometry and by the conclusions concerning the topoisomerase-related mechanism of action of antitumor anthracyclines, a rational design of disaccharide analogs might be based on the hypothesis that it would be beneficial to increase the molecular recognition properties through a functional enrichment of the portion of the anthracycline molecule involved in the stabilization of the "cleavable ternary complex." Structure activity relationships pointed to the importance of ring A as a "scaffold" determining the orientation of the C7 and C9 substituents, in particular that of the sugar moiety, whose structure and stereochemistry are critical for the stabilization of the ternary complex.[77,78]

Synthesis of disaccharide derivatives of the daunorubicin/doxorubicin and of the 4-demethoxy (idarubicin) series in which the first sugar moiety linked to the aglycon was a nonaminated sugar, namely, 2-deoxy-L-fucose or 2-deoxy-L-rhamnose, and the second moiety was either daunosamine or acosamine or a 3-hydroxy or 4-deoxy analog of these aminosugars, was performed starting from the corresponding aglycon that was glycosylated with the appropriately protected and activated disaccharide.[79] The desired final products were obtained by sequential deprotections and purification. Disaccharide glycosides containing 2-deoxy-L-fucose **XXIVa,b** exhibited superior pharmacological properties in respect to the stereoisomers **XXVa,b** containing 2-deoxy-L-rhamnose.[80]

7-*O*-(α-L-daunosaminyl-α(1-4)-2-deoxy-L-fucosyl)-4-demethoxyadriamycinone **XXIVc** was synthesized as shown in Scheme 16.3 and was developed to the clinical stage because of its favorable pharmacological properties. The high activity of **XXIVc** was related to the activation of p53-independent apoptosis.[81] The new compound exhibited, especially at selected DNA sites, a more marked topoisomerase II-mediated cleavage that was accompanied by a superior antitumor efficacy in the experimental systems when compared with doxorubicin. Very significant activity was found

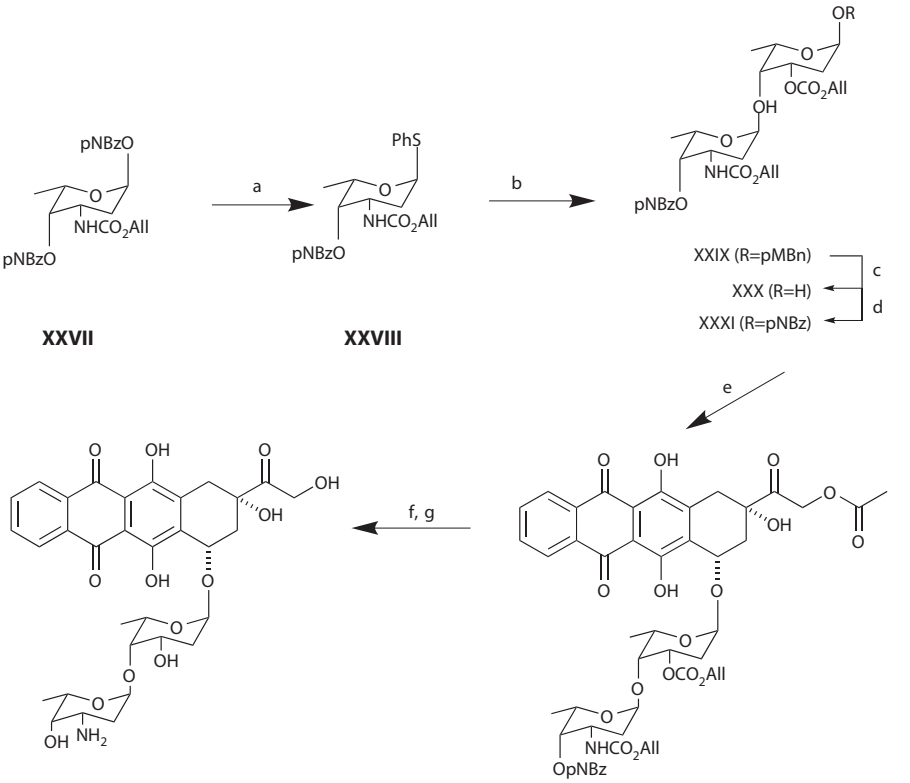

a: PhSTMS, TMSOTf, CH_2Cl_2
b: p-methoxybenzyl 3-O-allyloxycarbonyl-2-deoxy-L-fucoside, IDCP, CH_2Cl_2, Et_2O
c: $Ce(NH_4)(NO_3)_6$, MeCN, H_2O
d: pNBzCl, py
e: 14-acetoxyidarubicinone, TMSOTf, MS, CH_2Cl_2, Et_2O, -10° (R=pNBz)
f: 0.5M K_2CO_3
g: $(Ph_3P)Pd$, Me_2NTMS, AcOTMS, CH_2Cl_2

SCHEME 16.3 Synthesis of 7-*O*-(-L-daunosaminyl-(1-4)-2-deoxy-L-fucosyl)-4-demethoxy-adriamycinone.

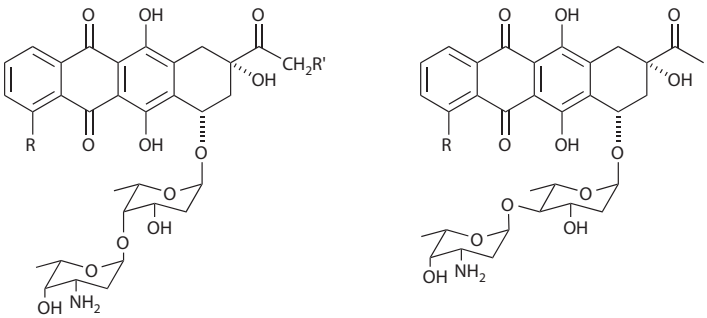

XXIVa: R = H; R' = H
XXIVb: R = OCH_3; R' = H
XXIVc: R = H; R' = OH

XXVa: R = H
XXVb: R = OCH_3

STRUCTURE 16.4 Structures **XXIV** and **XXV**.

against a spectrum of human tumors such as breast, ovary, and lung cancer xenografts in athymic nude mice, where the compound appeared markedly superior to doxorubicin in inhibiting tumor growth and in terms of an increased number of disease-free survivors among treated animals.[82] The generic name selected for **XXIVc** by World Health Organization is "sabarubicin."[83,84]

Spectrophotometric and fluorescence titrations with calf thymus DNA,[85] and with the d(CGATCG) hexamer of **XXIVc**, have revealed spectral patterns very similar to those obtained with doxorubicin, implying that the binding mechanism and the stability of the resulting complexes are nearly the same. X-ray diffraction data of the orange–red crystals of the sabarubicin–hexamer complex[86] allowed the definition of the asymmetric unit containing two DNA strands forming 1 duplex, two bound drugs, and thirty-five solvent molecules. Similar to the well-known complexes of other antitumor anthracyclines with the same DNA hexamer, intercalation occurs at each end of the DNA duplex in the CpG steps, with the drug chromophoric system perpendicular to the long axis of stacked base pairs. However, the two drug molecules appear to have different conformations, and the two binding sites show large differences. In one site, both sugar rings lie in the minor groove, whereas in the other site, the arrangement of the drug is such that the first sugar resides in the minor groove and, although rotated by about 45° around the O7-C1 bond with respect to the corresponding doxorubicin complex, is in the chair conformation with the 3-hydroxyl group still in van der Waals contact with the guanine residue. The second sugar protrudes out in the solvent region where the amino and hydroxyl groups interact with two water molecules (Figure 16.1).

Interestingly, a tight interaction takes place between the amino group of the disaccharide moiety and a guanine residue of a second DNA molecule, different from the one where the drug is intercalated. As a consequence, in the crystals, the end-over-end stacked duplexes do not run parallel, as in other crystallized anthracycline–DNA complexes, but are crossing each other at right angles along the tetragonal *c*-axis, leading to the formation of two layers of stacked duplexes mutually perpendicular to one another. The packing contacts include the amino group on the second sugar that is directly hydrogen bonded to N7 and, through a bridging water, to O6 of a guanine, providing the first example of an anthracycline/DNA complex in which a cross-link with a second DNA helix has been observed. It seems, therefore, that the second sugar may exert interactions with other cellular targets in close proximity with DNA.

16.5.3 Anthracycline–Triplex Helix-Forming Oligonucleotide Conjugates

Triplex helix-forming oligonucleotides (TFOs) that bind to homopurine:homopyrimidine sequences in DNA in a sequence-specific manner can be used to selectively inhibit gene expression and provide the opportunity for rational design of novel DNA sequence-specific cancer therapeutics. Chemical modifications of the TFO that would enhance triplex stability without affecting sequence specificity, such as conjugation with an anthracycline molecule, further increase the potential

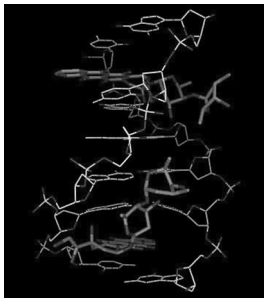

FIGURE 16.1 (See color insert.) Representation of the sabarubicin intercalation complex with d(CGATCG)2 according to an x-ray crystal diffraction study. (Drawing courtesy of Dr. Giovanni Ughetto, Laboratorio del CNR di Montelibretti, Rome.)

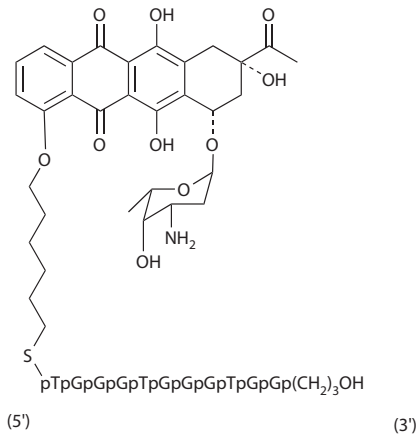

XXVI

STRUCTURE 16.5 Structure **XXVI**.

efficacy of this approach.[87] The resulting conjugates may correctly position the TFO moiety in the major groove of the duplex and allow it to form Hoogsteen hydrogen bonds with the complementary bases of the purine-rich strand of the target DNA while allowing ring A of the intercalated anthracycline, together with the sugar moiety, to protrude into the minor groove, as in the well-known model of the daunomycin–DNA complex. When the aminosugar is lacking (i.e., the TFO is conjugated with a nonglycosylated anthracyclinone), the stabilization of the triple helix is still obtained, albeit one order of magnitude lower.[88]

In a recent study, DNA binding and antigene activity of anthracycline-conjugated TFOs targeted to a sequence near the major P2 promoter in the *c-myc* gene were synthesized. GT-rich 11-mer TFOs were covalently attached through a hexamethylene bridge at the hydroxyl on position 4 of carminomycin. As shown by footprinting and electrophoretic experiments, as well as by spectroscopic measurements, conjugate **XXVI** had high binding affinity and formed a much more stable triplex than the nonconjugated TFO. Binding of **XXVI** was also highly sequence specific, as indicated by the fact that it protected a single region corresponding to the 11-basepair target sequence in the *c-myc* promoter. Conjugates with different TFOs, which were partially complementary to the *c-myc* target sequence, bound with much lower affinity than **XXVI**. The latter inhibited transcription from the P2 promoter in *in vitro* transcription assays and also inhibited transcription in luciferase reporter assays when cotransfected into prostate cancer cells along with a pGL-myc promoter reporter plasmid, but it did not affect the activity of the control pRL-SV40 plasmid. These data indicate that attachment of the anthracycline to the TFO increased its binding affinity and allowed the formation of a very stable complex with duplex DNA. Moreover, **XXVI** was able to selectively inhibit transcription of the *c-myc* gene both *in vitro* and in cultured cells. These results encourage further testing of this approach for the development of novel antigene cancer therapeutics.[89]

16.6 CLINICAL ACTIVITY OF ANTHRACYCLINES

Since the first clinical trials, daunorubicin and doxorubicin have gained rapid acceptance as major therapeutic agents in the medical treatment of cancer. Both drugs, but especially doxorubicin, have been widely used as part of combination regimens for the effective treatment of acute nonlymphocytic leukemia, Hodgkin and non-Hodgkin lymphomas, breast cancer, and sarcomas.[90] Epirubicin, idarubicin, and liposomal doxorubicin offer less toxic and, in some instances, more effective alternatives to older anthracyclines for leukemia, breast cancer, ovarian cancer, and other diseases.[91]

16.6.1 Daunorubicin

Daunorubicin (**Ib**), the first anthracycline introduced into therapeutic use, is endowed with a potent antitumor activity whose spectrum is narrower than that of doxorubicin and is accompanied by a significant hematological toxicity. The compound exhibits delayed cardiotoxicity. Main indications are acute leukemias, but significant activity was recorded against neuroblastomas and rhabdomyosarcomas. Induction of remission in over 70% of patients with acute lymphoblastic leukemia is obtained on treatment with daunorubicin, vincristine, and prednisone, with disease-free survival at 5 yr in up to 45% of patients receiving a consolidation/intensification therapy after remission.[92] Intensive induction chemotherapy using 7-d courses of cytarabine and daunorubicin or amsacrine produces remission in 60–85% of patients with acute myelogenous leukemia, a condition that was invariably fatal 30 yr ago. Median remission duration is 9–16 mo. In some series, 20–40% of patients are in continuous remission for 2 yr or more; many of these patients remain in remission for 5 yr or longer, and some may be cured.[93]

16.6.2 Doxorubicin

A notable feature of the antitumor properties of doxorubicin (**Ia**) is the wide spectrum of activity including (as particularly responsive) acute leukemias, Hodgkin and non-Hodgkin lymphomas, lung microcytomas, soft-tissue sarcomas, Ewing's tumor, thyroid carcinoma, ovarian cancer, breast cancer, rhinopharyngeal tumors, Wilms' tumor, and other pediatric malignancies. It was recognized early on that in these diseases, doxorubicin shows efficacy when administered alone as a slow intravenous injection every 3 wk at a dosage of 65 mg/m^2, with its most usual administration being, however, in combination with other active agents.[94] Out of 113 drug combinations containing doxorubicin (Adriamycin) already used in clinical studies worldwide at the end of the first decade after the original demonstration of therapeutic efficacy of the drug, cyclophosphamide, an alkylating agent, was the most frequent component (54 combinations), followed by the spindle poison vincristine or other vinca alkaloids, such as vinblastine (42 combinations), the metabolic inhibitor 5-fluorouracyl (24 combinations), bleomycin and *cis*-platinum (22 combinations each), and methotrexate (12 combinations), with other less frequent components being mitomycin, etoposide, or nitrosoureas.[95] Doxorubicin was frequently accompanied by cyclophosphamide and vincristine or by 5-fluorouracyl in the treatment of breast cancer (the acronyms used for the main combinations are FAC and VAC). Cyclophosphamide and vincristine or etoposide were the most frequent components in the treatment of small cell lung tumors, whereas doxorubicin was accompanied by cyclophosphamide and methotrexate or either *cis*-platinum or mitomycin or a nitrosourea in the case of the less responsive nonsmall cell lung cancer. In the low respondent gastrointestinal tract malignancies, doxorubicin was combined with 5-fluorouracyl and mitomycin or a nitrosourea and with cyclophosphamide, a vinca alkaloid, bleomycin, and prednisone in the generally more responsive lymphomas. *cis*-Platinum and cyclophosphamide were mainly associated with doxorubicin in the treatment of genital tract tumors.

Doxorubicin is characterized by a rapid distribution phase and a slow elimination phase. The successive half-lives of doxorubicin in plasma are approximately 5 min, 1 h, and 30 h. Total plasma clearance is about 30 L/h/m^2, and its total volume of distribution is approximately 15 L/kg. As the other anthracyclines, the drug is excreted mostly through the bile, and special care is taken in patients with hepatic dysfunction.[96] Doxorubicinol, the product of the reduction of the 13-keto group to a secondary alcohol function, is the major human metabolite of doxorubicin, albeit present in plasma at concentrations well below those of the parent drug.[97]

16.6.3 Epirubicin

Phase II studies of epirubicin (**II**) indicated that the drug produces a pattern of acute toxicity qualitatively similar to but quantitatively lower than that of doxorubicin at identical doses, the most

frequently employed dose schedules being 75 or 90 mg/m^2 intravenously every 3 wk. Epirubicin showed activity in a variety of tumors, such as breast carcinoma, soft-tissue sarcomas, lymphomas, leukemias, ovarian cancer, and gastric cancer, and preliminary evidence of activity was found in melanoma, rectal cancer, and pancreatic cancer, indicating a broad spectrum of activity. As to chronic cardiac toxicity, preliminary findings from a randomized comparison of the two drugs in breast cancer indicated that epirubicin might have a lower cumulative cardiotoxicity than doxorubicin. According to the first clinical studies, pharmacokinetics of epirubicin in human patients showed a multiexponential decrease of plasma levels, with the same pattern being observed for the metabolite epidoxorubicinol, together with a high plasma clearance (0.9–1.4 L/min), a terminal half-life of about 30–40 h, and a large volume of distribution.[98] According to a subsequent review,[99] to achieve hematological equitoxicity of the two drugs, the dose of epirubicin should be approximately 20% higher than that of doxorubicin, giving rise to a higher dosage level for epirubicin. In contrast, epirubicin is significantly less cardiotoxic than doxorubicin. Thus, the maximum cumulative dose, which for doxorubicin is 500 mg/m^2, for epirubicin is close to 1000 mg/m^2. More recent conclusions indicate that epirubicin, used alone or in combination with other cytotoxic agents in the treatment of a variety of malignancies, is better tolerated than, and achieves equivalent objective response rates and overall median survival to, similar doxorubicin-containing regimens in the treatment of advanced and early breast cancer, nonsmall cell lung cancer, small cell lung cancer, non-Hodgkin lymphoma, ovarian cancer, gastric cancer, and nonresectable primary hepatocellular carcinoma.

Dose-intensive epirubicin-containing regimens, which have been designed because of the drug's lower myelosuppression and cardiotoxicity and the definite dose–response relationship of anthracyclines, have produced high response rates in early breast cancer, a potentially curable malignancy, as well as advanced breast and lung cancers. Furthermore, such improved response rates have improved quality of life in some clinical settings, but whether this leads to prolonged survival is yet to be determined.[100] The metabolism of epirubicin is characterized by a biotransformation to relatively or totally inactive metabolites, including a 13-dihydro derivative, epirubicinol, two glucuronides, and four aglycones. Quantitatively, the glucuronides of epirubicin and epirubicinol are very important, and this pathway, which is unique to epirubicin metabolism in humans, might explain the better tolerability of this drug compared with doxorubicin. Epirubicin pharmacokinetics may be described by a three-compartment model, with median half-life values of 3.2 min, 1.2 h, and 32 h for each phase. Total plasma clearance is 46 L/h/m^2, and the volume of distribution at steady state is 1000 L/m^2. The pharmacokinetics of epirubicin appear to be linear for doses up to 150–180 mg/m^2, which is the maximal tolerated dose.[101]

16.6.4 Idarubicin

Idarubicin (**III**) is currently used in the medical treatment of acute nonlymphocytic leukemia in adults. Idarubicin is at least as effective as daunorubicin in this disease, and two studies indicate greater activity and longer survival with an idarubicin–cytarabine regimen than with a daunorubicin–cytarabine regimen. The drug is active in acute lymphocytic leukemia, lymphomas, and breast cancer. Reportedly, idarubicin is more potent and less cardiotoxic than daunorubicin or doxorubicin. However, a maximum cumulative dose, to prevent chronic cardiomyopathy, has not yet been defined. Unlike the other clinically useful anthracyclines, idarubicin has significant oral bioavailability (average 28%), and an oral dosage form has been developed.[102] The oral formulation has demonstrated efficacy in advanced breast cancer, non-Hodgkin lymphoma, and myelodysplastic syndromes as well as in first-line induction therapy of acute myelogenous leukemia. It also has a potential for ameliorating blast crisis of chronic myelogenous leukemia and in multiple myeloma. The most frequent acute adverse effects associated with oral idarubicin are those commonly found with anthracyclines, but there appears to be minimal significant cardiotoxicity. Available data concerning oral idarubicin in hematological malignancies and advanced breast cancer are sufficiently encouraging to warrant further research.[103]

16.6.5 Aclacinomycin

ACM has been extensively evaluated in patients with relapsed leukemia and advanced malignant lymphoma. Analysis of results compiled from Europe, Japan, and the United States shows that ACM is probably equivalent to doxorubicin for remission induction of patients with relapsed acute nonlymphoblastic leukemia. The antitumor activity of ACM in patients with acute lymphoblastic leukemia or malignant lymphoma who have previously received doxorubicin or daunorubicin is low, and the issue of whether ACM lacks clinical cross-resistance to other anthracyclines remains unresolved. Acute cardiac arrhythmias have been observed following the administration of ACM, but congestive cardiomyopathy has been uncommon. It has been reported that ACM has fulfilled its early expectations of antileukemic activity and reduced toxicity.[104]

16.6.6 Sabarubicin

Clinical tolerability of weekly dosed sabarubicin (**XXIVc**) has been determined by researchers at EORTC, who reported the results of a phase I study and recommended intravenous dosages of 30 and 40 mg/m^2 for three consecutive weeks followed by 1 wk rest in, respectively, pretreated and naïve patients.[105] Pharmacokinetics of sabarubicin were studied in patients from two different phase I dose schedules, one in which the drug was administered once in every 3 wk (the current schedule of anthracyclines), and the other in which it was administered once in every week for 3 wk, followed by 1 wk rest. The plasma peak concentration levels and AUC after each dosage showed linear relationship with the administered dose. Plasma concentrations were particularly high, in ranges of 0.474–0.612 μg/mL for the lowest (4 mg/m^2) and 9.538–21.587 μg/mL for the highest (110 mg/m^2) doses used. There was no accumulation of the drug before the next infusion in the weekly regimen. The mean elimination half-life was 20.7 h, which is significantly shorter than that for doxorubicin or epirubicin. The volume of distribution, much smaller than that of the said anthracyclines, was 95.6 L/m^2 and showed a standard deviation of 43.4 L/m^2. In fact, a particularly high inter-patient variation of pharmacokinetic parameters was found.[106]

A dosage of 80–90 mg/m^2 every 3 wk was used in poor-prognosis patients with advanced or metastatic ovarian cancer who had received prior chemotherapy. Out of 15 evaluable patients, one partial response and nine stabilizations of the disease were recorded.[107] A study in prostate cancer patients indicated that the short intravenous infusion of 80 mg/m^2 sabarubicin every 3 wk resulted in 9 PSA responses, 10 stable disease, and 14 disease progression. Cardiotoxicity and neutropenia were observed.[108] The activity of sabarubicin has been demonstrated acting as a single agent in a poor-prognosis population of patients with lung cancers. The drug was well tolerated when used at an intravenous dose of 80–90 mg/m^2 every 3 wk in patients with nonsmall cell lung cancer, as second-line therapy, and with small cell lung cancer as the first-line therapy, with dose-limiting toxicity being hematological. One partial response and five stable diseases were observed in 16 evaluable patients with nonsmall cell lung cancer, and one complete response, nine partial responses, and three stable diseases in 21 evaluable, pretreated small cell lung cancer patients.[109,110]

16.6.7 Liposomal Anthracyclines

Liposomes are closed vesicular lipidic structures that envelop water-soluble molecules. Liposomal anthracyclines have been extensively studied in humans with a variety of cancer types, including one containing daunorubicin and two preparations containing doxorubicin. Results have indicated that liposomal encapsulation may lead to toxicity attenuation while retaining or even enhancing the efficacy of the parent anthracyclines. Approved indications have been achieved for liposomal daunorubicin against AIDS-related Kaposi sarcoma and for liposomal doxorubicin against AIDS-related Kaposi sarcoma and ovarian cancers.[111] Pegylated liposomal doxorubicin shows a pharmacokinetic profile characterized by an extended circulation time and a reduced volume of distribution. The

pharmacokinetic profile in humans at doses between 10 and 80 mg/m^2 is biphasic, exhibiting an initial phase with a half-life of 1–3 h and a second phase with a half-life of 30–90 h. The AUC after a dose of 50 mg/m^2 is reported to be approximately 300-fold greater than that with free drug. Clearance and volume of distribution are drastically reduced (at least 250-fold and 60-fold, respectively). The toxicity profile is characterized by dose-limiting mucosal and cutaneous toxicities, mild myelosuppression, and decreased cardiotoxicity compared with free doxorubicin and minimal alopecia.[112] A retrospective study on 40 patients indicated that pegylated liposomal doxorubicin at a dosage of 40–45 mg/m^2 every 4 wk is clinically active and well tolerated in women with metastatic breast cancer.[113]

16.6.8 Amrubicin

Finally, mention should be made of amrubicin, a totally synthetic idarubicin analog in which an hydroxyl group replaces the amino group at C-3′ and an amino group replaces the C9 hydroxyl group.[114] The compound exhibited high potency in *in vitro* and *in vivo* laboratory experiments.[115,116] It has been registered and is currently marketed in Japan as a clinically useful agent in the treatment of small cell lung cancer.[117]

REFERENCES

1. Brockmann, H., Anthracyclinone und anthracycline (Rhodomycinone, Pyrromycinone und Ihre Glycoside), in *Forschritte der Chemie Organische Naturstoffe*, Zechmeister, L. Ed., Springer, Vienna, Vol. 21, 1963, pp. 121–182.
2. O'Hagan, D., *The Polyketide Metabolites*, Ellis Horwood, Chichester, 1991.
3. Arcamone, F., Di Marco, A., Gaetani, M., and Scotti, T., Isolamento ed attività antitumorale di un antibiotico da Streptomyces sp., *Giorn. Microbiol.*, 9, 83, 1961.
4. Arcamone, F., *Doxorubicin Anticancer Antibiotics*, De Stevens, G. Ed., Academic Press, New York, 1981, pp. 1–369.
5. Arcamone, F., The development of new antitumor anthracyclines, in *Anticancer Agents Based on Natural Products Models*, Cassady, J. and Douros, J. Eds., Academic Press, New York, 1980, chapter 1.
6. Arcamone, F. and Penco, S., Synthesis of new doxorubicin analogs, in *Anthracycline and Anthracenedione-based Anticancer Agents*, Lown, J.W. Ed., Elsevier, Amsterdam, 1988, chapter 1.
7. Weiss, R.B., The anthracyclines: Will we ever find a better doxorubicin? *Semin. Oncol.*, 19, 670, 1992.
8. Arcamone, F., Animati, F., Capranico, G., Lombardi, P., Pratesi, G., Manzini, S., Supino, R., and Zunino, F., New developments in antitumor anthracyclines, *Pharmacol. Ther.*, 76, 117, 1997.
9. Takeuchi, T., Antitumor antibiotics discovered and studied at the Institute of Microbial Chemistry, *J. Cancer Res. Clin. Oncol.*, 121, 505, 1995.
10. Oki, T., Antitumor anthracycline antibiotics from microbial origin, in *Anthracycline and Anthracenedione-based Anticancer Agents*, Lown, J.W. Ed., Elsevier, Amsterdam, 1988, p. 103.
11. Arcamone, F. and Cassinelli, G., Biosynthetic anthracyclines, *Curr. Med. Chem.*, 5, 391, 1998.
12. Fujii, I. and Ebizuka, Y., Anthracycline biosynthesis in *Streptomyces galilaeus*, *Chem. Rev.*, 97, 2511, 1997.
13. Hutchinson, C.R., Biosynthetic studies of daunorubicin and tetracenomycin C, *Chem. Rev.*, 97, 2525, 1997.
14. Hopwood, D.A., Genetic contributions to understanding polyketide synthase, *Chem. Rev.*, 97, 2465, 1997.
15. Di Marco, A., Gaetani, M., Dorigotti, L., Soldati, M., and Bellini, O., Studi sperimentali sull'attività antineoplastica del nuovo antibiotico daunomicina, *Tumori*, 49, 203, 1963.
16. Arcamone, F., Franceschi, G., Orezzi, P., Cassinelli, G., Barbieri, W., and Mondelli, R., Daunomycin. I. The structure of daunomycinone, *J. Am. Chem. Soc.*, 86, 5334, 1964.
17. Arcamone, F., Cassinelli, G., Orezzi, P., Franceschi, G., and Mondelli, R., Daunomycin. II. The structure and stereochemistry of daunosamine, *J. Am. Chem. Soc.*, 86, 5335, 1964.
18. Arcamone, F., Franceschi, G., Orezzi, P., Penco, S., and Redaelli, S., The structure of daunomycin, *Tetrahedron Lett.*, 30, 3349, 1968.

19. Arcamone, F., Cassinelli, G., Orezzi, P., and Mondelli, R., The total absolute configuration of daunomycin, *Tetrahedron Lett*., 30, 3353, 1968.
20. Arcamone, F., Cassinelli, G., Franceschi, G., Mondelli, R., Orezzi, P., and Penco, S., Struttura e stereochimica della daunomicina, *Gazz. Chim. Ital*., 100, 848, 1970.
21. Angiuli, R., Foresti, E., Riva diSanseverino, L., Isaacs, N.W., Kennard, O., Motherwell, W.D.S., Wampler, D.L., and Arcamone, F., Structure of daunomycin; x-ray analysis of N-Br-acetyl-daunomycin solvate, *Nat. New Biol*., 234, 78, 1971.
22. Dubost, M., Ganter, P., Maral, R., Ninet, L., Pinnert, S., Preud'homme, J., and Werner, G.H., Un nouvel antibiotique à propriétés cytostatiques, *C. R. Acad. Sci. (Paris)*, 257, 1813, 1963.
23. Bernard, J., Paul, R., Boiron, M., Jacquillat, C., and Maral, R., *Recent results in cancer research: Rubidomycin*, Springer, Berlin, 1969.
24. Arcamone, F., Cassinelli, G., Fantini, G., Grein, A., Orezzi, P., Pol, C., and Spalla, C., Adriamycin, 14-hydroxydaunomycin, a new antitumor antibiotic from *S. peucetius var. caesius*, *Biotechnol. Bioeng*., 11, 1101, 1969.
25. Arcamone, F., Franceschi, G., Penco, S., and Selva, A., Adriamycin (14-hydroxy-daunomycin), a novel antitumor antibiotic, *Tetrahedron Lett*., 13, 1007, 1969.
26. Di Marco, A., Gaetani, M., and Scarpinato, B.M., A new antibiotic with antitumor activity, *Cancer Chemother. Rep*., 53, 33, 1969.
27. Bonadonna, G., Monfardini, S., de Lena, M., and Fossati-Bellani, F., Clinical evaluation of Adriamycin a new antitumor antibiotic, *Brit. Med. J.*, 3, 503, 1969.
28. Carter, S.K., Adriamycin—A review, *J. Nat. Cancer Inst*., 55, 1265, 1975.
29. Borchmann, P., Hübel, K., Schnell, R., and Engert, A., Idarubicin: A brief overview on pharmacology and clinical use, *Int. J. Clin. Pharmacol. Ther.*, 3, 80, 1997.
30. Wang, A.H.J., Intercalative drug binding to DNA, *Curr. Opin. Struct. Biol*., 2, 361, 1992.
31. Stutter, E., Schuetz, H., and Berg, H., Quantitative determination of cooperative anthracycline-DNA binding, in *Anthracycline and Anthracenedione-based Anticancer Agents*, Lown, J.W. Ed., Elsevier, Amsterdam, 1988, p. 245.
32. Ughetto, G., X.-Ray diffraction analysis of anthracycline-oligonucleotide complexes, in *Anthracycline and Anthracenedione-based Anticancer Agents*, Lown, J.W. Ed., Elsevier, Amsterdam, 1988, p. 296.
33. Pullman, B., Binding affinities and sequence selectivity in the interaction of antitumor anthracyclines and anthracenediones with double stranded polynucleotides and DNA, in *Anthracycline and Anthracenedione-based Anticancer Agents*, Lown, J.W. Ed., Elsevier, Amsterdam, 1988, p. 371.
34. Chaires, J.B., Herrera, J.E., and Waring, J.M., Preferential binding of daunomycin to 5′ at CG and 5′ at GC sequences revealed by footprinting titration experiments, *Biochemistry*, 29, 6145, 1990.
35. Frederick, C.A., Williams, L.D., Ughetto, G., Van der Marel, G.A., Van Boom, J.H., Rich, A., and Wang, A.H.J., The structural comparison of anticancer drug-DNA complexes: Adriamycin and daunomycin, *Biochemistry*, 29, 2538, 1990.
36. Tewey, K.M., Rowe, T.C., Yang, L., Halligan, B.D., and Liu, L.F., Adriamycin induced DNA damage mediated by mammalian DNA topoisomerase II, *Science*, 226, 466, 1984.
37. Capranico, G., Kohn, K.W., Pommier, Y., and Zunino, F., Sequence selective topoisomerase Ii inhibition by anthracycline derivatives in SV 40 DNA: Relationship with DNA binding affinity and cytotoxicity, *Biochemistry*, 29, 562, 1990.
38. Capranico, G., Kohn, K.W., and Pommier, Y., Local sequence requirements for DNA cleavage by mammalian topoisomerase II in the presence of doxorubicin, *Nucleic Acids Res.*, 22, 6611, 1990.
39. Zunino, F. and Capranico, G., DNA topoisomerase II as the primary target of anti-tumor anthracyclines, *Anticancer Drug Design*, 4, 307, 1990.
40. Binaschi, M., Capranico, G., Dal Bo, L., and Zunino, F., Relationship between lethal effects and topoisomerase II-mediated double-stranded DNA breaks produced by anthracyclines with different sequence specificity, *Mol. Pharmacol*., 6, 1053, 1997.
41. Gerwitz, D.A., A critical evaluation of the mechanisms of action proposed for the antitumor effects of the anthracyclines antibiotics Adriamycin and daunorubicin, *Biochem. Pharmacol*., 57, 727, 1992.
42. Pommier, Y., DNA topoisomerase II inhibitors, in *Cancer Therapeutics, Experimental and Clinical Agents*, Techter, B.A. Ed., Humana Press, Totowa, NJ, 153, 1997.
43. Nielsen, D., Maare, C., and Skovsgaard, T., Cellular resistance to anthracyclines, *Gen. Pharmacol.*, 27, 255, 1996.
44. Beaumont, P.O., Moore, M.J., Ahmad, K., Payne, M.M., Lee, C., and Riddick, D.S., Role of glutathione S-transferases in the resistance of human colon cancer cell lines to doxorubicin, *Cancer Res*., 58, 947, 1998.

45. Gaudiano, G., Resing, K., and Koch, T.H., Reaction of reduced anthracyclines with glutathione—Formation of aglycone conjugates, *J. Am. Chem. Soc.*, 116, 6537, 1994.
46. Kim, R., The role of HER-2 oncoprotein in drug-sensitivity in breast cancer, *Oncol. Rep*., 9, 3, 2002.
47. Bellini, O. and Solcia, E., Early and late sarcoplasmic reticulum changes in doxorubicin cardiomyopathy, *Virchows Arch. (Cell Pathol.)*, 49, 137, 1985.
48. Ishikawa, T. and Sies, H., Cardiac transport of glutathione disulfide and S-conjugates. Studies with isolated perfused rat heart during hydroperoxide metabolism, *J. Biol. Chem*., 239, 3838, 1984.
49. Olson, R.D., MacDonald, J.S., van Boxtel, C.J., Boerth, R.C., Harbison, R.D., Slonim, A.E., Freeman, R.W., and Oates, J.A., Regulatory role of glutathione and soluble sulfidryl groups in the toxicity of Adriamycin, *J. Pharmacol. Exp. Ther.*, 215, 450, 1980.
50. Formelli, F., Zedeck, M.S., Sternberg, S.S., and Philips, F.S., Effect of Adriamycin on DNA synthesis in mouse and rat heart, *Cancer Res*., 38, 3286, 1978.
51. Ellis, C.N., Ellis, M.B., and Blakemore, W.S., Effect of Adriamycin on heart mitochondrial DNA, *Biochem. J.*, 245, 309, 1987.
52. Gatti, G., Oldani, D., Bottoni, G., Confalonieri, C., Gambini, L., and De Ponti, R., Injectable stabilized solutions containing an antitumor anthracycline glycoside, BP 2178311 (Feb. 11, 1987), *Chem. Abs*., 107, 223275, 1997.
53. Gatti, G., Oldani, D., Bottoni, G., Confalonieri, C., Gambini, L., and De Ponti, R., Ready to use injections containing anthracycline glycosides in acidic solution, Germ. Offen. 3741037 (Jun. 9, 1988), *Chem. Abs*., 110, 141560, 2000.
54. Suarato, A., Penco, S., Vigevani, A., and Arcamone, F., Anthracycline chemistry: Direct conversion of daunorubicin into the L-*arabino*, L-*ribo*, and L-*lyxo* analogues, and selective deoxygenation at C-4, *Carbohydr. Res*., 98, C1–C3, 1981.
55. Badalassi, F., Crotti, P., Di Bugno, C., D'Arata, F., Bavero, L., and, Ramacciotti, A., Efficient enantioselective synthesis of (R)-2-hydroxy-5,8-dimethoxy-1,2,3,4-tetrahydronaphthalene, the key intermediate in the synthesis of anthracycline antibiotics, *Tetrahedr. Asymm.*, 12, 3155, 2001.
56. Cabri, W., De Bernardinis, S., Francalanci, F., and Penco, S., Process for preparing anthracyclinones, U.S. Patent 5,180,758 (Jan. 19, 1993).
57. Cacchi, S., Piattini, P.G., Morera, E., and Ortar, G., Palladium-catalyzed triethylammonium formate reduction of aryl triflates, a selective method for the deoxygenation of phenols, *Tetrahedron Lett.*, 27, 5541, 1986.
58. Arcamone, F. and Penco, S., Chemical derivatives of anticancer antibiotics with different DNA binding properties, in *Molecular Mechanisms of Carcinogenic and Antitumor Activity*, Chagas, C. and Pullman, B. Eds., Pontificiae Academiae Scientiarum Scripta Varia, Vatican City, Vol. 70, 1987, p. 225.
59. Arcamone, F. and Penco, S., Relationship of structure to anticancer activity and toxicity in anthracyclines, *Gann Monogr. Cancer Res*., 36, 81, 1989.
60. Capranico, G., De Isabella, P., Penco, S., Tinelli, S., and Zunino, F., Role of DNA breakage to cytotoxicity of doxorubicin, 9-deoxydoxorubicin, and 4-demethyl-6-deoxydoxorubicin in murine leukemia P388 cells, *Cancer Res*., 49, 2022, 1989.
61. Pasqui, F., Canfarini, F., Giolitti, A., Guidi, A., Pestellini, V., and Arcamone, F., Synthesis of ring A fluorinated anthracyclines, *Tetrahedron*, 52, 185, 1996.
62. Animati, F., Arcamone, F., Bigioni, M., Capranico, G., Caserini, C., De Cesare, M., Lombardi, P. et al., Biochemical and pharmacological activity of novel 8-fluoroanthracyclines: Influence of stereochemistry and conformation, *Mol. Pharmacol*., 50, 603, 1996.
63. Berettoni, M., Cipollone, A., Olivieri, L., Palomba, D., Arcamone, F., Maggi, C.A., and Animati, F., Synthesis of 14-fluorodoxorubicin, *Tetrahedron Lett.*, 43, 2867, 2002.
64. Ringenberg, Q.S., Propert, K.J., Muss, H.B., Weiss, R.B., Schilsky, R.L., Modeas, C., Perry, M.C., Norton, L., and Green, M., Clinical cardiotoxicity of esorubicin (4-deoxydoxorubicin, DxDx): Prospective studies with serial gated heart scans and reports of selected cases. A Cancer and Leukemia Group B report, *Invest. New Drugs*, 8, 221, 1990.
65. Barbieri, B., Giuliani, F.C., Bordoni, T., Casazza, A.M., Geroni, C., Bellini, O., Sparato, A., Gioia, B., Penco, S., and Arcamone, F., Chemical and biological characterization of 4-iodo-4-deoxydoxorubicin, *Cancer Res*., 47, 4001, 1987.
66. Sessa, C., Calabresi, F., Cavalli, F., Cerny, T., Liati, P., Skovsgaard, T., Sorio, R., and Kaye, S.B., Phase II studies of 4-iodo-4-deoxydoxorubicin in advanced non-small cell lung, colon and breast cancers, *Ann. Oncol*., 2, 727, 1991.
67. Merlini, G., Ascari, E., Amboldi, N., Bellotti, V., Arbustivi, E., Perfetti, V., Ferrari, M., Zorzoli, I., Marinane, M.G., and Garini, P., Interaction of the anthracycline 4-iodo-4-deoxydoxorubicin with amyloid fibrils: Inhibition of amyloidogenesis, *Proc. Natl. Acad. Sci. U.S.A*., 92, 2959, 1995.

68. Gertz, M.A. and Lacy, M.Q., A multicenter phase II trial of 4'-iodo-4'-deoxydoxorubicin (IDOX) in primary amyloidosis (AL), *Amyloid*, 9, 24, 2002.
69. Priebe, W., Skibicki, P., Varela, O., Neamati, N., Sznaidman, M., Dziewiszek, K., Grynkiewicz, G. et al., Non-cross-resistant anthracyclines with reduced basicity and increased stability of the glycosidic bond, in *ACS Symposium Series 574: Anthracycline Antibiotics, New Analogues, Methods of Delivery, and Mechanism of Action*, Priebe, W. Ed., American Chemical Society, Washington, DC, 1995, pp. 14–46.
70. Kazerooni, R., Conrad, C., Johansen, M.J., Sakamoto, M., Fokt, I., Schroeder, C., Thapar, N., Meyer, C., Priebe, W., and Madden, T., Hematologic pharmacodynamics linked to the pharmacokinetics of berubicin, a blood–brain barrier penetrating anthracycline active against high grade glioma, in phase I/II clinical trials. *Eur. J. Cancer*, 6(12 Supp.), 187, 2008.
71. Acton, M., Wasserman, K., and Newman, R.A., Morpholinyl anthracyclines, in *Anthracycline and Anthracenedione-based Anticancer Agent*s, Lown, W. Ed., Elsevier, Amsterdam, 1988, pp 55–101.
72. (a) Bakker, M., Droz, J.P., Hanauske, A.R., Verweij, J., van Oosterom, A.T., Groen, H.J., Pacciarini, M.A. et al., Broad phase II and pharmacokinetic study of methoxy-morpholino doxorubicin (FCE 23762-MMRDX) in non small cell lung cancer, renal cancer and other solid tumor patients, *Br. J. Cancer*, 77, 139, 1998. (b) Broggini, M., Nemorubicin, Anthracycline Chemistry and Biology II, in *Topics in Current Chemistry*, Krohn, K. Ed., Springer, Berlin, Vol. 283, 2008, p. 191.
73. Roaten, J.B., Interaction of the novel anthracycline antitumor agent N-benzyladriamycin-14-valerate with the C1-regulatory domain of protein kinase C: Structural requirements, isoform specificity, and correlation with drug cytotoxicity, *Mol. Cancer Therapeut.*, 1, 483, 2002.
74. Boivin, J., Monneret, C., and Pais, M., Approche de la synthèse d'anthracyclines oligosaccharidiques. Hemisynthèse de la 4-O-(2.deoxy-l-fucosyl)-daunorubicine, *Tetrahedron*, 37, 4219, 1981.
75. El Khadem, H.S. and Matsura, D., Synthesis of 7-(3-amino-2,3,6-trideoxy-4-O-(2,6-dideoxy-α-L-lyxo-hexopyranosyl)-α-L-lyxo-hexopyranosyl)-daunomycinone, *Carbohydr. Res.*, 101, C1, 1982.
76. Horton, D., Priebe, W., Sznaidman, M.L., and Varela, O., Synthesis and antitumor activity of anthracycline disaccharide glycosides containing daunosamine, *J. Antibiotics*, 46, 1720, 1993.
77. Capranico, G., Supino, R., Binaschi, M., Capolongo, L., Grandi, M., Suarato, A., and Zunino, F., Influence of structural modifications at the 3 and 4 positions of doxorubicin on the drug ability to trap topoisomerase II and to overcome drug resistance, *Mol. Pharmacol.*, 45, 908, 1994.
78. Capranico, G., Butelli, E., and Zunino, F., Change of sequence specificity of daunorubicin-stimulated topoisomerase II DNA cleavage by epimerisation of the amino group of the sugar moiety, *Cancer Res.*, 55, 312, 1995.
79. Animati, F., Arcamone, F., Berettoni, M., Cipollone, A., Franciotti, M., and Lombardi, P., New anthracycline disaccharides. Synthesis of L-daunosaminyl-α(1-4)-2-deoxy-L-rhamnosyl and of L-daunosaminyl-α(1-4)-2-deoxy-L-fucosyl daunorubicin analogues, *J. Chem. Soc. Perkin Trans. I*, 1327, 1996.
80. Arcamone, F., Animati, F., Bigioni, M., Capranico, G., Caserini, C., Cipollone, A., De Cesare, M. et al., Configurational requirements of the sugar moiety for the pharmacological activity of anthracycline disaccharides, *Biochem. Pharmacol.*, 57, 1133, 1999.
81. Arcamone, F., Animati, F., Berettoni, M., Bigioni, M., Capranico, G., Casazza, A.M., Caserini, C. et al., A doxorubicin disaccharide analog: Apoptosis related improvement of efficacy in vivo, *J. Natl. Cancer Inst.*, 89, 1217, 1997.
82. (a) Pratesi, G., De Cesare, M., Caserini, C., Perego, P., Dal Bo, L., Polizzi, D., Supino, R. et al., Improved efficacy and enlarged spectrum of activity of a novel anthracycline disaccharide analogue of doxorubicin against human tumor xenografts, *Clin. Cancer Res.*, 4, 2833, 1998. (b) Pratesi, G., Bigioni, M., Salvatore, C., Bullo, A., Bellarosa, D., Iafrate, E., Animati, F. et al., A comparative study of cellular and molecular pharmacology of doxorubicin and MEN 10755, a disaccharide analogue, *Biochem. Pharmacol.*, 62, 63, 2001.
83. Arcamone, F., Sabarubicin, in Anthracycline Chemistry and Biology II, *Topics in Current Chemistry*, Krohn, K. Ed., Springer, Berlin, Vol. 283, 2008, p. 171.
84. Cirillo, R., Sacco, G., Venturella, S., Brightwell, J., Giachetti, A., and Manzini, S., Comparison of doxorubicin and MEN 10755-induced long term progressive cardiotoxicity in the rat, *J. Cardiovasc. Pharmacol.*, 35, 100, 2000.
85. Messori, L., Temperini, C., Piccioli, F., Orioli, P., Di Bugno, C., and Animati, F., Solution chemistry and DNA binding properties of MEN 10755, a novel disaccharide analogue of doxorubicin, *Bioorg. Med. Chem.*, 9, 938, 2001.
86. Temperini, C., Messori, L., Orioli, P., Di Bugno, C., Animati, F., and Ughetto, G., The crystal structure of the complex between a disaccharide anthracycline and the DNA hexamer d(CGATCG) reveals two different binding sites involving two DNA duplexes, *Nucleic Acids Res.*, 31, 1464, 2003.

87. Garbesi, A., Bonazzi, S., Zanella, S., Capobianco, M.L., Giannini, G., and Arcamone, F., Synthesis and binding properties of conjugates between oligodeoxynucleotides and daunorubicin derivatives, *Nucleic Acids Res*., 25, 2121, 1997.
88. Capobianco, M.L., De Champdoré, M., Francini, L., Lena, S., Garbesi, A., and Arcamone, F., New TFO conjugates containing a carminomycinone derived chromophore, *J. Bioconjugate Chem*., 12, 523, 2001.
89. Napoli, S., Negri, U., Arcamone, F., Capobianco, M.L., Carbone, G.M., and Catapano, C.V., Growth inhibition and apoptosis induced by daunomycin-conjugated triplex-forming oligonucleotides targeting the *c-myc* gene in prostate cancer cells. *Nucleic Acid Res.*, 34, 734, 2006.
90. Young, R.C., Ozols, R.F., and Myers, C.E., Medical progress: The anthracycline antineoplastic drugs, *New Engl. J. Med*., 305, 149, 1981.
91. Geffen, D.B. and Man, S., New drugs for the treatment of cancer, 1990–2001, *Isr. Med. Assoc. J.*, 4, 1124, 2002.
92. Hoelzer, D. and Gale, R.P., Acute lymphoblastic leukemia in adults: Recent progress, future directions, *Semin. Hematol*., 24, 27, 1987.
93. Gale, R.P. and Foon, K.A., Therapy of acute myelogenous leukaemia, *Semin. Hematol*., 24, 40, 1987.
94. Bonadonna, G., Principi di chemioterapia antitumorale, in *Manuale di Oncologia Medica*, Bonadonna, G. and Robustelli della Cuna, G. Eds., Masson Italia, Milan, 1981, chapter 18.
95. Beretta, G., *Cancer Chemotherapy Regimens*, Farmitalia-Carlo Erba, Milan, 1983.
96. Robert, J. and Gianni, L., Pharmacokinetics and metabolism of anthracyclines, *Cancer Surv*., 17, 219, 1993.
97. Gill, P., Favre, R., Durand, A., Iliadis, A., Cano, J.P., and Carcassone, Y., Time dependency of Adriamycin and adriamycinol kinetics, *Cancer Chemother. Pharmacol*., 10, 120, 1983.
98. Ganzina, F., 4′-Epidoxorubicin, a new analogue of doxorubicin: A preliminary overview of preclinical and clinical data, *Cancer Treat. Rev*., 10, 1, 1983.
99. Mouridsen, H.T., Alfthan, C., Basthold, L., Bergh, J., Dalmark, M., Eksborg, S., Hellsten, S. et al., Current status of epirubicin (Farmorubicin) in the treatment of solid tumours, *Acta Oncol*., 29, 257, 1990.
100. Plosker, G.L. and Fauld, D., Epirubicin. A review of its pharmacodynamic and pharmacokinetic properties, and therapeutic use in cancer chemotherapy, *Drugs*, 45, 788, 1993.
101. Robert, J., Clinical pharmacokinetics of epirubicin, *Clin. Pharmacokinet*., 26, 428, 1994.
102. Cersosimo, R.J., Idarubicin: An anthracycline antineoplastic agent, *Clin. Pharm*., 11, 152, 1992.
103. Buckley, M.M. and Lamb, H.M., Oral idarubicin. A review of its pharmacological properties and clinical efficacy in the treatment of haematological malignancies and advanced breast cancer, *Drugs Aging*, 11, 61, 1997.
104. Warrell, Jr., R.P., Aclacinomycin A: Clinical development of a novel anthracycline antibiotic in the haematological cancers, *Drugs Exp. Clin. Res*., 12, 275, 1986.
105. Schrivers, D., Alfthan, C., Basthold, L., Bergh, J., Dalmark, M., Eksborg, S., Hellsten, S. et al., Phase I study of MEN-10755, a new anthracycline in patients with solid tumors: A report from the European Organization for Research and Treatment of Cancer, Early Clinical Studies Group, *Ann. Oncol.*, 13, 385, 2002.
106. Bos, A.M.E., De Vrie, E.G.E., Dombernovsky, P., Aamdal, S., Uge, D.R.A., Shuijvers, D., Wanders, J. et al., Pharmacokinetics of MEN-10755, a novel anthracycline disaccharide analogue, in two phase I studies in adults with advanced solid tumours, *Cancer Chemother. Pharmacol*., 48, 361, 2001.
107. Caponigro, F., Willems, P., Sorio, R., Floquet, A., van Belle, S., Demol, J., Tambaro, R. et al., A phase II study of sabarubicin (MEN 10755) as second line therapy in patients with locally advanced or metastatic platinum/taxane resistant ovarian cancer. *Invest. New Drugs*, 23, 85, 2005.
108. Fiedler, W., Tchen, N., Bloch, J., Fargeot, P., Sorio, R., Vermorken, J.B., Collette, L., Lacombe, D., and Twelves, C., A study from the EORTC new drug development group: Open label phase Ii study of sabarubicin (MEN-10755) in patients with progressive hormone refractory prostate cancer, *Eur. J. Cancer*, 42, 200, 2006.
109. Tjan-Heijnen, V.C.G., Gerritsen, A., ten Valde, G.P.M., Giaccone, G., Gamucci, T., Comandini, A., Capriati, A., Mordiva, A., Nurmohamed, S., and Ruland-Adank, S., A phase II study with MEN 10755 as second line therapy in advanced non-small cell lung cancer (NSCLC), 27th ESMO Congress, Nice (France) Oct. 2002. Abstr. 542P, *Ann. Oncol*., 13, 55, 2002.
110. Dickgreber, N.J., Welte, T., Gillissen, A., Dunlop, D., Eberhardt, W., Wagner, T., Swinson, D., Capriati, A., and O'Byrne, K., Phase II open-label study of MEN-10755 in patients with small cell lung cancer extensive disease, *Proc. Am. Soc. Clin. Oncol*., 2003, 22,703.
111. Muggia, F.M., Liposomal encapsulated anthracyclines: New therapeutic horizons, *Curr. Oncol. Rep*., 3, 156, 2001.

112. Gabizon, A., Shmeeda, H., and Barenholz, Y., Pharmacokinetics of pegylated liposomal Doxorubicin: Review of animal and human studies, *Clin. Pharmacokinet*., 42, 419, 2003.
113. Perez, A.T., Domenech, G.H., Frankel, C., and Vogel, C.L., Pegylated liposomal doxorubicin (Doxil) for metastatic breast cancer: The Cancer Research Network, Inc. experience, *Cancer Invest*., 20(Suppl. 2), 22, 2002.
114. Ishizumi, K., Ohashi, N., and Tanno, N., Stereospecific total synthesis of 9-aminoanthracyclines: (+)-9-amino-9-deoxydaunomycin and related compounds, *J. Org. Chem.* 52, 4477. 1987.
115. Morisada, S., Yanagi, Y., Noguchi, T., Kashiwazaki, Y., and Fukui, M., and Antitumor activities of a novel 9-aminoanthracycline (SM-5887) against mouse experimental tumors and human tumor xenografts, *Jpn. J. Cancer Res.* 80, 69, 1989.
116. Yamaoka, T., Hanada, M., Ichii, S., Morisada, S., Noguchi, T., and Yanagi, Y., Cytotoxicity of amrubicin, a novel 9-aminoanthracycline, and its active metabolite amrubicinol on human tumour cells, *Jpn. J. Cancer Res.*, 89, 1067, 1998.
117. Yana, T., Negoro, S., Takada, M., Yokota, S., Takada, Y., Sugiura, T., Yamamoto, H. et al., Phase II study of amrubicin in previously untreated patients with extensive-disease small cell lung cancer: West Japan Thoracic Oncology Group study, *Invest. New Drugs*, 25, 253, 2007.

17 Ansamitocins (Maytansinoids)

Tin-Wein Yu, Heinz G. Floss, Gordon M. Cragg, and David J. Newman

CONTENTS

17.1 Introduction 407
17.2 Naturally Occurring Maytansinoids 407
17.3 Biological Activity and Mechanism of Action 409
17.4 Total Synthesis 410
17.5 Medicinal Chemistry: Structure Modification, Structure–Activity Relationships, and Metabolism 410
17.6 Preclinical and Clinical Developments 414
17.7 Biosynthesis 418
References 421

17.1 INTRODUCTION

The maytansinoids represent a family of antitumor agents of extraordinary potency. Following the discovery of the parent compound, maytansine, in 1972,[1] the chemistry and biology of the maytansinoids were the subjects of intense studies in the 1970s and early 1980s, culminating in clinical trials of maytansine against a variety of human cancers. After the disappointing outcome and eventual termination of the phase II clinical trials, interest in these compounds subsided considerably. The last decade has brought a certain resurgence of interest in the maytansinoids, which were shown to have considerable potential as "warheads" in immunoconjugates with tumor-specific antibodies—an application that is currently under intense investigation. Other studies are addressing the biosynthesis of the maytansinoids, its genetic control, and the role of plants versus microorganisms in their formation.

The earlier work, from the initial discovery to about 1984, has been summarized in several authoritative reviews.[2–5] This chapter only briefly covers some of these earlier works and focuses primarily on the more recent developments in this field, which have occurred since these first reviews were published.

17.2 NATURALLY OCCURRING MAYTANSINOIDS

In 1972, Kupchan et al.,[1] working under the auspices of the National Cancer Institute (NCI), reported the isolation and structure elucidation of maytansine (**1**) (Figure 17.1). They followed up on the observation of activity *in vitro* against KB cells and *in vivo* against mouse L1210 and P388 leukemia, mouse sarcoma 180, and Lewis lung carcinoma and rat Walker 256 carcinosarcoma of extracts of *Maytenus serrata* (Celastraceae) collected in Ethiopia in 1961/1962. Bioassay-guided fractionation led to the isolation of **1** as the principal active constituent in a yield of 0.2 mg/kg of dried plant material. The targeted isolation of such a trace compound was only possible because of its potent cytotoxic

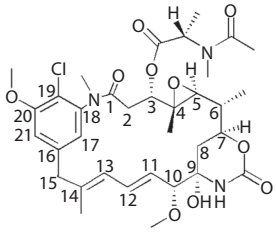

Maytansine (1)

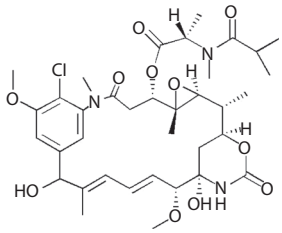

Colubrinol (2)

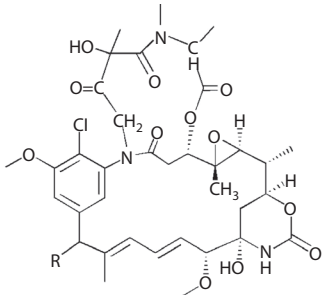

R=OCH_3, N-Methyltrenudone (3)
R=H, Maytanbicyclinol (8)

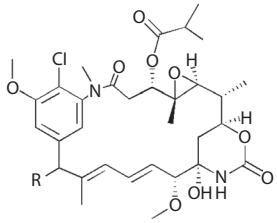

R=H, Ansamitocin P-3 (4)
R=OCH_3, 15-Methoxyansamitocin P-3 (5)

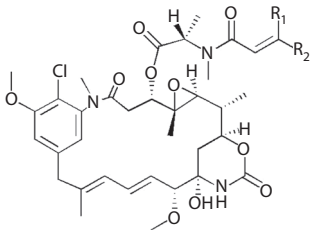

R_1=CH_2CH_3, R_2=CH_3, Mallotusine (6)
R_1=CH_3, R_2=CH_2CH_3, Isomallotusine (7)

FIGURE 17.1 Structures of naturally occurring maytansinoids.

activity (ED_{50}: 10^{-4}–10^{-5} μg/mL against KB cells). The structure of **1** was determined primarily by x-ray crystallography. Subsequently, other *Maytenus* species (e.g., *Maytenus buchananii*), as well as another Celastraceae, *Putterlickia verrucosa*, were established as better sources of **1**, containing seven to eight times higher levels of the compound.[3]

Following the discovery of maytansine, substantial numbers of analogs were also isolated from the same or related plant sources. Most of these contain different C3 ester side chains, lack the ester side chain or the *N*-methyl group, or carry a hydroxy/methoxy substituent at C15. Members of two other plant families, *Colubrina texensis* (Rhamnaceae) and *Trewia nudiflora* (Euphorbiaceae), also yielded maytansinoids—the former some 15-oxygenated compounds, such as colubrinol (**2**),[6] and the latter structures with cyclized ester moieties, such as *N*-methyltrenudone (**3**).[7]

The structures of the maytansinoids are unusual for higher plant products but closely resemble microbial metabolites of the ansamycin family.[8] This raised questions as to the true biosynthetic origin of these compounds and led to a search for microbial producers of maytansinoids. This search culminated in a report by scientists at Takeda Chemical Industries[9] on the isolation of a microorganism originally designated a *Nocardia* species but later reclassified as *Actinosynnema*

pretiosum (Actinomycetes),[10] which produces a series of compounds, the ansamitocins (e.g., ansamitocin P-3, **4**), with structures closely resembling and, in some cases, identical to those of plant-derived maytansinoids. Again, these compounds, to the extent that they carry ester side chains at C3, such as **4**, are very potent cytotoxic agents.

As of early 2004, 49 fully characterized, naturally occurring maytansinoids had been reported in the literature.[11] Most of these were isolated during the 1970s and early 1980s, and their structures are listed in the earlier reviews.[3–5] Since then, only five new compounds have been discovered, and these represent minor variations of known structures. Two groups reported the isolation of **4** from several species of mosses,[12,13] together with three related maytansinoids including one new compound: 15-methoxyansamitocin P-3 (**5**).[12] Feng et al.[14] reported two new compounds, mallotusine (**6**) and isomallotusine (**7**), from *Mallotus anomalus*, and Sneden and colleagues[15] isolated 2-*N*-demethylmaytanbutine (normaytanbutine) and, notably, maytanbicyclinol (**8**), from *M. buchananii*. There are also allusions to additional microbial maytansinoids in the literature (e.g., ansamitocin S-3 carrying a carbamoylated pentose moiety in place of the *N*-methyl group of **4**),[16] but details of their characterization have apparently not been published.

The most recent review on the chemistry and biology of individual agents is that of Kirschning et al. in September of 2008.[17] Included in that review are structures of and citations to some unusual microbial metabolites such as the first *N*-demethyl-*N*-β-D-glucopyranosyl ansamitocins P-1[18] and P-2,[19] as well as the unusual ansacarbamitocins A–F. The ansacarbamitocin variants were isolated from an *Amycolatopsis* sp., and have the same macrocyclic core as the ansamitocins with variations on the glycoside, together with two variations A1 and B1, which lack the 4,5 epoxide substituent found in the A–F compounds and which have a modest antifungal activity against phytopathogenic fungi.[20]

17.3 BIOLOGICAL ACTIVITY AND MECHANISM OF ACTION

The antitumor activity of maytansine and the ansamitocins has been discussed extensively in previous reviews.[2–5] **1** showed significant inhibitory activity against solid tumors, Lewis lung carcinoma, and B16 melanocarcinoma and antileukemic activity against P388 lymphocytic leukemia over a large (50- to 100-fold) dose range.[21,22] In the 60-human cancer cell line screen of the NCI,[23] **1** showed an activity pattern indicative of tubulin-interactive agents.[24] Related compounds carrying the C3 ester function (e.g., maytanprine, maytanbutine, and normaytansine) exhibited a similar activity spectrum and potency as **1**.[25] The 15-oxygenated maytansinoids colubrinol (**2**) and colubrinol acetate isolated from *C. texensis* also showed potencies comparable to those of **1** against KB cells *in vitro* and P388 leukemia *in vivo*.[6] Similarly, the bicyclic maytansinoids isolated from *T. nudiflora* and *M. buchananii* retain activity against P388 leukemia and KB cells.[7,15] The ansamitocins P-3 and P-4 exhibit a very similar activity spectrum and dose range as maytansine (e.g., antitumor activity against P388 leukemia *in vivo* at daily doses as low as 0.8 μg/kg), and they are also active against B16 melanoma, sarcoma 180, Ehrlich carcinoma, and P815 mastocytoma, although not very active against L1210 leukemia.[9]

It was established early on that maytansine[26–28] and ansamitocin P-3[29] inhibit cell division by binding to tubulin, blocking the assembly of microtubules. The cells are arrested in metaphase; the cytological changes resemble those induced by vincristine. Maytansine competitively inhibits vincristine binding to tubulin, and vincristine—but not colchicine—competitively inhibits tubulin binding of **1**.[30] Thus, maytansinoids apparently bind to tubulin at a site overlapping the vinca alkaloids binding site and different from the colchicine binding site. The binding site of the vinca alkaloids has been mapped to the β-subunit of tubulin,[31] and maytansine also binds to this subunit.[32] Several studies have explored features of the β-tubulin structure that are important for maytansinoid binding/activity (e.g., a conserved asparagine residue[33,34] and key sulfhydryl groups[35]). Fluorescent and photoaffinity probes based on ansamitocin P-3 have been described as reagents for probing the tubulin structure.[36] Because tubulin binding of maytansinoids correlates with their activity against

P388 leukemia[37,38] and no other primary effects were apparent, the interaction with tubulin is considered the principal mechanism of antitumor action of the maytansinoids.[3,26]

In addition to their antitumor activity, the maytansinoids also show inhibitory activity against other eukaryotic systems, such as fungi and yeasts, protozoa, insects, and plants, but they have little if any antibacterial activity.[39] Among a large number of fungi and yeasts tested, the yeast *Filobasidium uniguttulatum* (IFO 0699) was selected as a particularly sensitive test organism for the bioassay of maytansinoids. An inhibition zone of 20 mm was obtained with 45 ng of ansamitocin P-4.[40] The antitubulinic activity of maytansinoids can be tested using protozoa, such as *Tetrahymena pyriformis*, which have cilia containing microtubule bundles. Deciliated *Tetrahymena* naturally recover their cilia, and hence motility, within 60 min, and this process is inhibited by maytansinoids (e.g., 100% by 1 μM **4**).[41,42] A similar assay observes axopod retraction in *Actinophris sol* or *Actinosphaerium eichhorni*.[43] Insecticidal activity against members of the Lepidoptera and Coleoptera and against the chicken body louse was reported for extracts and isolated maytansinoids from *T. nudiflora* seeds.[44]

17.4 TOTAL SYNTHESIS

The decade following the original report on the isolation of **1** saw intense efforts aimed at the structure modification of the naturally occurring maytansinoids and at the total synthesis of this class of compounds. The work published up to 1983 has been summarized,[3,5] and in particular detail in the review by Reider and Roland.[4] Two groups, those of Meyers and of Corey, reported the total synthesis of (±) and (–)-*N*-methylmaysenine (not a naturally occurring maytansinoid).[45–47] The first synthesis of a natural maytansinoid, (±)-maysine, was reported by Meyers et al. in 1979,[48] followed in short order by syntheses of (±)-maytansinol (Meyers)[49] and (–)-maytansine (Corey)[50] in 1980. A third group, that of Isobe and Goto, also completed a total synthesis of (±)-maytansinol in 1982.[51] These approaches all converged on an aminoaldehyde or aminoester intermediate containing the complete functionalized structural framework except carbons 1 and 2, which were introduced and ring-closed to the macrocyclic lactam in different ways.[4] In a stereocontrolled synthesis of (–)-maytansinol reported by Isobe and colleagues in 1984, such an intermediate was prepared stereospecifically from D-mannose.[52] Other approaches to the assembly of the macrolactam structure of the maytansinoids were explored (e.g., by the groups of Ho,[4] Barton,[4] Fried,[53] Ganem,[4] Confalone,[54] Goodwin et al.,[55] and Hodgson et al.[56]) but did not lead to completed syntheses. Subsequent to the early synthetic work, two more total syntheses were reported. Gu's group in Shanghai completed a synthesis of maytansine in 1988 (Figure 17.2),[57] and Bénéchie and Khuong-Huu, building on the earlier efforts of the group at Gif-sur Yvette, reported a new synthesis of (–)-maytansinol in 1996 (Figure 17.3).[58] However, all these syntheses, although challenging and creative, are lengthy and low yielding and neither solved the supply issue nor contributed significantly to the generation of structural analogs for structure–activity studies.

17.5 MEDICINAL CHEMISTRY: STRUCTURE MODIFICATION, STRUCTURE–ACTIVITY RELATIONSHIPS, AND METABOLISM

Despite the small amounts of material available from the plant sources, the Kupchan group explored the chemistry of maytansine to generate some analogs for preliminary structure–activity relationship studies. The 9-OH group was converted into various ethers, all of which showed no significant cytotoxic activity. Attempts to cleave the C3 ester group by hydrolysis led instead to elimination to give the olefin, maysine. The ester was cleaved successfully by $LiAlH_4$ reduction at low temperature to give the alcohol, maytansinol. $LiAlH_4$ reduction under more vigorous conditions led to the corresponding deschloro compound. None of the compounds lacking the ester side chain had significant activity, whereas numerous naturally occurring analogs with different ester groups all showed potent activity. All this chemistry has been described in detail in the previous reviews.[3–5]

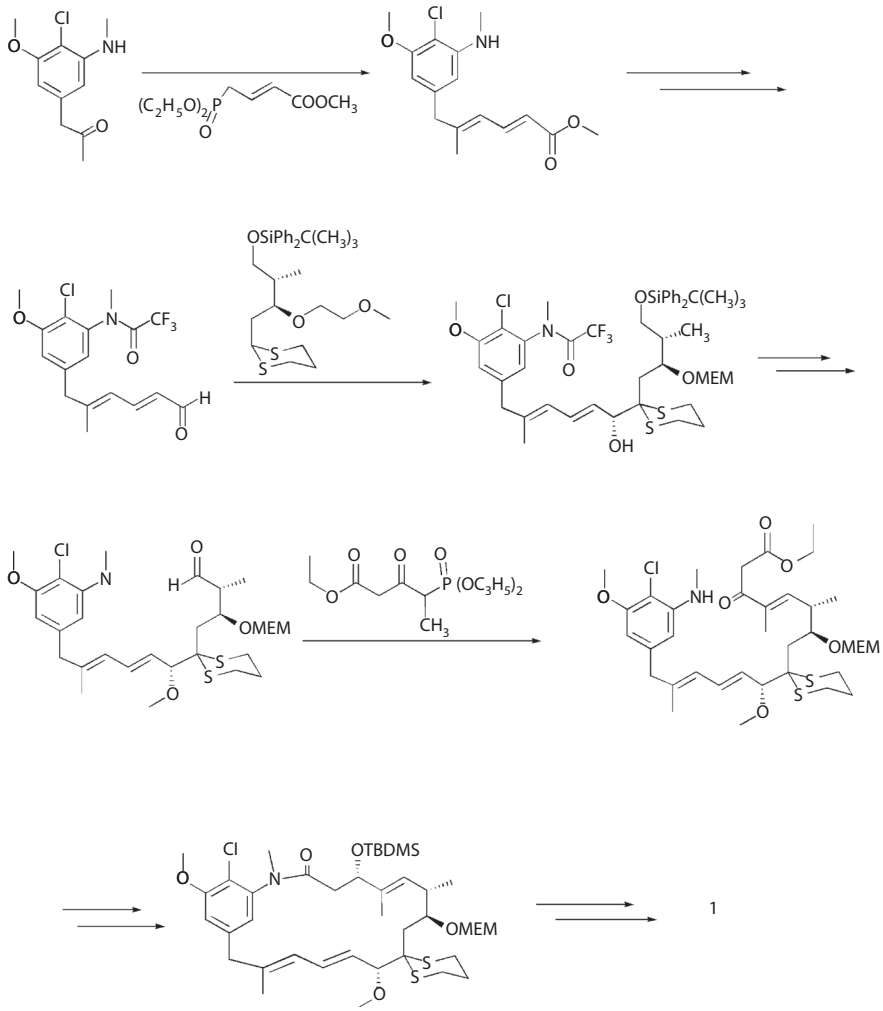

FIGURE 17.2 Total synthesis of maytansine by Gu et al.[57]

With access to more starting material, compound **4** from the microbial fermentation, scientists at Takeda Chemical Industries explored the structure–antitumor activity of the maytansinoids in more detail. Through chemical and microbial transformations, the researchers prepared a large number of analogs of **4** and tested their antitumor activity, as reported in a series of publications[5,59–64] and a large number of patents.[11] Microbial transformations of **4** led to *N*-demethylation,[59] 20-*O*-demethylation,[60] 15-hydroxylation with either *R* or *S* stereochemistry,[57] and 3-*O*-deacylation.[59] Except for the deacylated compounds, all these transformation products retained significant antitumor activity. The 3-, 15-, and 20-hydroxy compounds served as starting materials for the synthesis of large numbers of alkyl and acyl derivatives at these positions, most of them showing varying degrees of biological activity.[64] Interestingly, modifications of the 3-*O*-ester moiety modulated the activity of the molecule, with some compounds of low *in vitro* activity having high *in vivo* activity. One compound, the 3-*O*-phenylglycinate ester, showed a two to four times better activity than that of **1**.[64] Removal of the epoxide function to give an E-4,5-double bond did not abolish the activity,[62] but inversion of the stereochemistry at C3 by oxidation of maytansinol to the 3-ketone, reduction with $NaBH_4$, and reesterification gave 3-epiansamitocin P-3, which was devoid of cytotoxic activity.[63]

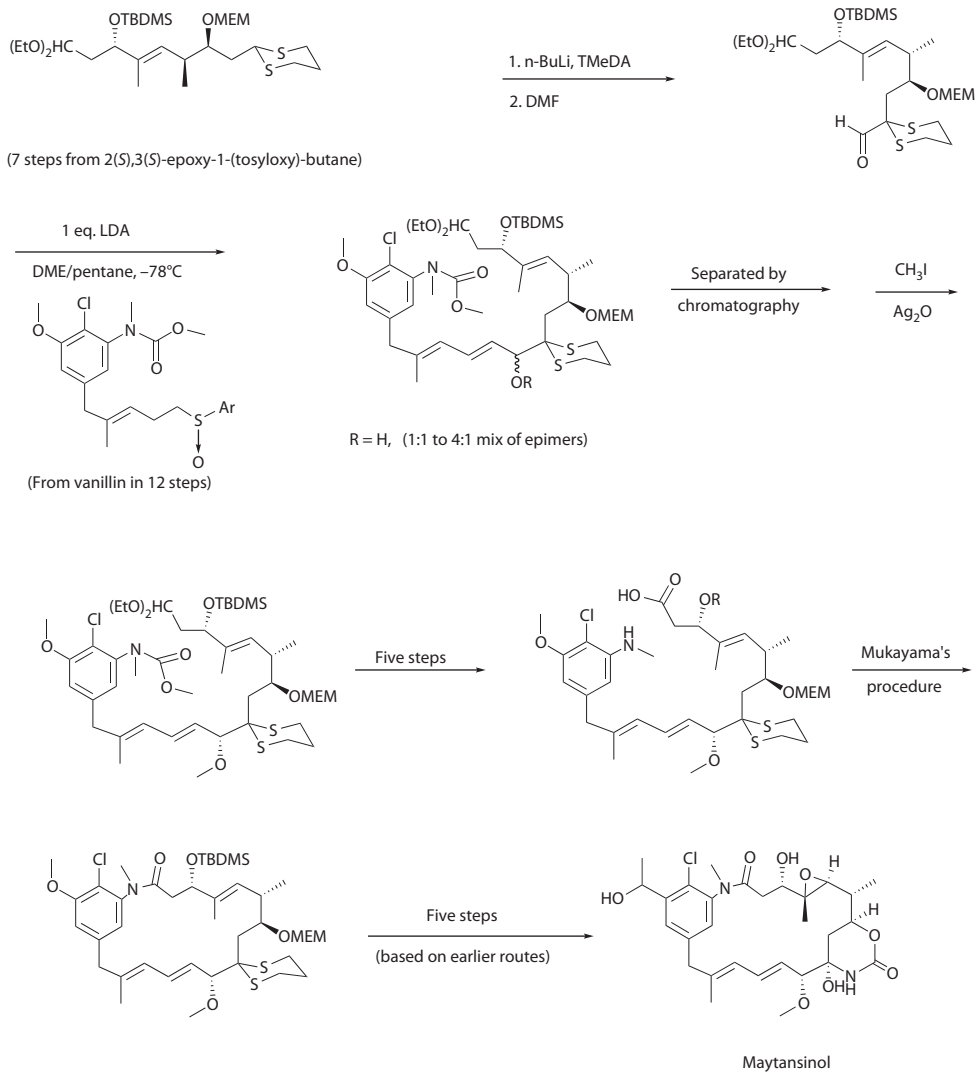

FIGURE 17.3 Total synthesis of (–)-maytansinol by Bénéchie and Khuong-Huu.[58]

Deschloro compounds were also prepared by reduction of **4** with excess $LiAlH_4$ followed by reesterification, with little effect on the biological activity.[65]

More recently, Sneden and colleagues explored further the reductive chemistry of maytansinoids (Figure 17.4).[66,67] Reduction of maytanbutine, the analog of **1** with an *N*-isobutyryl instead of the *N*-acetyl group, with lithium borohydride/lithium triethylborohydride (10:1) cleaved the carbinolamide function to give the 7-carbamoyloxy-9-hydroxy derivative with a 1000-fold decrease in cytotoxic activity.[66] In contrast, hydrogenation of **1** over Pd/C generated 11,12,13,14-tetrahydromaytansine, with little effect on the biological activity.[67] The structure–antitumor activity relationships of the maytansinoids revealed by all these studies can be summarized, as shown in Figure 17.5. An ester group at the 3-position and an unblocked carbinolamide function at C9 are absolute requirements for potent antitumor activity; most other functional group modifications have either no or only a modulating effect on the biological activity.

Suchocki and Sneden also examined the long-term stability of **1**, showing that in outdated clinical samples 40% of the maytansine had decomposed, mostly by elimination of the C3 side chain to

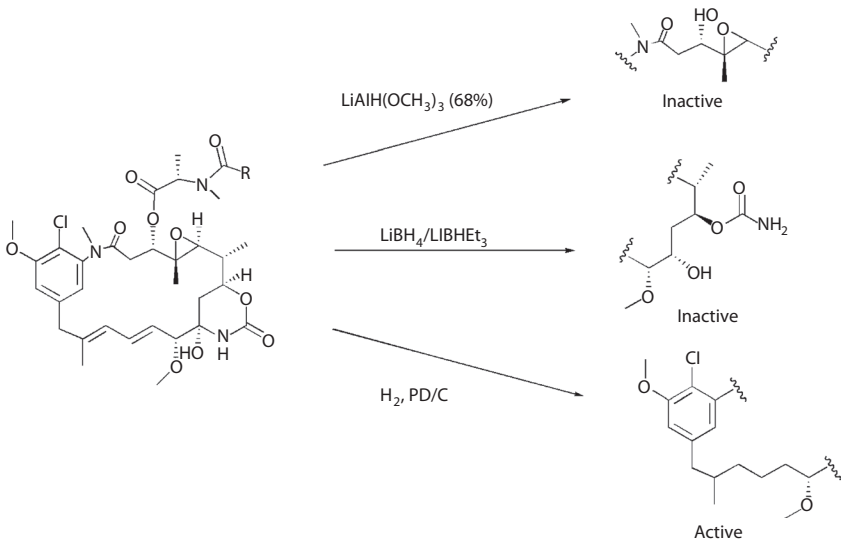

FIGURE 17.4 Reductive modifications of maytansinoids.[66,67,69]

give maysine.[68] One report[69] and a patent[70] deal with improved methods for the preparation of maytansinol (Figure 17.3), an important starting material for the synthesis of immunoconjugates of maytansinoids (*vide infra*).[71]

The structural complexity of many bioactive natural products often precludes the use of exclusively totally synthetic or semisynthetic approaches to the preparation of analogs for the development of natural product libraries. An interesting approach to overcoming such limitations combines chemical semisynthesis with biosynthesis using genetically engineered microorganisms, so-called mutational biosynthesis or mutasynthesis. The biosynthesis of ansamitocin P-3 is primed by a starter unit, 3-amino-5-hydroxybenzoic acid (AHBA), that originates from a shikimate-type biosynthetic pathway so that blocked mutants can be generated without affecting the modules of the polyketide biosynthetic gene cluster (PKS1; see Section 17.7 for a detailed discussion of the biosynthetic process).

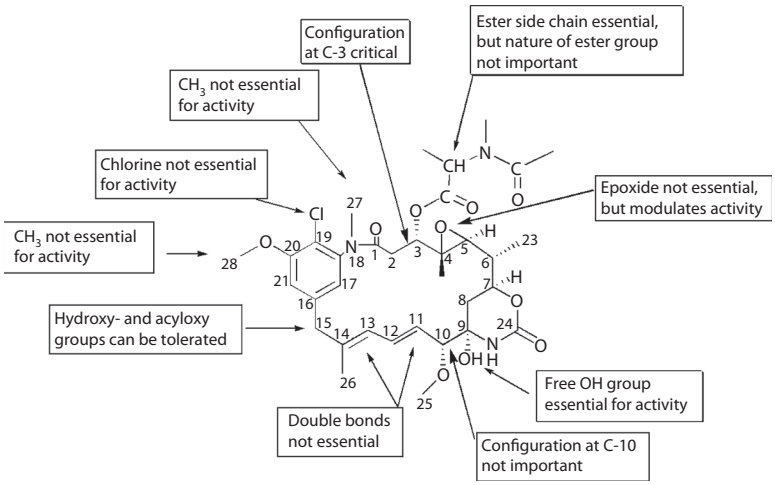

FIGURE 17.5 Summary of the structure–antitumor activity relationships of maytansinoids.

By feeding the appropriate 3-amino-4-halobenzoic acids to growing cultures of an AHBA-blocked mutant of *A. pretiosum* (HGF073), 19-fluoro-, chloro-, and bromo-analogs of 20-demethoxy-AP-3 were obtained.[72] Each analog showed strong antitumor activity against several cancer cell lines, with 19-fluoro-20-demethoxyansamitocin being the most active, exhibiting comparable picomolar activity to ansamitocin P-3. Pd-catalyzed Stille coupling of the bromo derivative with tributylvinyl stannane afforded the corresponding, equally active 19-vinyl derivative in good yield, illustrating not only that mutasynthesis can provide new natural product analogs for further testing, but also that these analogs can serve as substrates for introduction of new functional groups through the application of appropriate semisynthetic chemistry.

Although maytansine progressed all the way to phase II clinical trials, until 2005 there were no data in the literature on the mammalian metabolism of the compound. The reasons probably were that the amounts of material available at the time were extremely small and that the analytical techniques then available were not sensitive enough to follow the metabolism of a compound that is active at such low concentrations. In 2005, Chan and colleagues reported on the *in vitro* metabolism of maytansine and ansamitocin P-3 after incubation with rat and human liver microsomes in the presence of NADPH, and with rat and human plasma and whole blood, using liquid chromatography/multistage mass spectrometry.[71] Unchanged ansamitocin P-3 and 11 metabolites and unchanged maytansine and seven metabolites were detected and the structures of some metabolites were tentatively assigned on the basis of multistage electrospray ion-trap mass fragmentation data and, in some cases, accurate mass measurement.[71] In the case of ansamitocin P-3, incubation with rat and human liver microsomes in the presence of NADPH gave 10-*O*-demethylansamitocin P-3 as the primary metabolite, with additional minor metabolites resulting from hydroxylation, *N*- or 20-*O*-demethylation and combinations thereof. Only 20% was converted to its metabolites in rat liver microsomes compared with 70% in human liver microsomes. In contrast, no differences were seen between rat and human liver microsome metabolism of maytansine, with primary metabolism being *N*-demethylation in the ester side chain, and additional minor metabolites being formed through oxidation of the side-chain *N*-methyl to an *N*-formyl group, loss of the ester side chain and demethylations on the macrocycle.[71] These results are summarized in Figure 17.6. Incubation of either compound with rat or human blood or plasma gave no detectable metabolites, but ansamitocin P-3 was metabolized mainly to maytansinol on treatment with rat liver homogenate, and the 10-*O*-demethyl derivative was the primary urinary metabolite following i.v. bolus administration to rats *in vivo*.[71]

17.6 PRECLINICAL AND CLINICAL DEVELOPMENTS

Given the high potency of maytansine against various tumor types, including some solid tumors, the development of the compound for clinical trials was a high priority of the NCI. Following the isolation of larger, although still limited, quantities of **1** and satisfactory preclinical pharmacological and toxicological evaluation, the compound was entered into phase I clinical trials in patients with advanced disease refractory to conventional therapy in 1975.[2,3] The tolerated dose was established as 1–2 mg/m^2; observed side effects were primarily gastrointestinal toxicity, neurotoxicity, nausea, vomiting, and diarrhea; and a few patients showed promising partial responses. This led to the scheduling of a large number of phase II trials of **1** alone and in combination with other agents. These gave rather disappointing results, showing no substantial clinical benefits.[73–89] As summarized in a 1984 report by the NCI to the Food and Drug Administration on the Investigational New Drug Application for maytansine,[90] the evaluation of the compound as a single agent against 36 different types of tumors in 819 patients showed only one complete response and 20 partial responses while at the same time revealing substantial gastrointestinal and neurological toxicity. At this point, the NCI terminated the clinical trials of **1**.

The 1990s have seen a certain resurgence of clinical interest in the maytansinoids, specifically as cytotoxic agents ("warheads") for antibody-directed targeted delivery to tumor cells. The antibody-targeted delivery approach, although conceptually appealing, has had limited practical

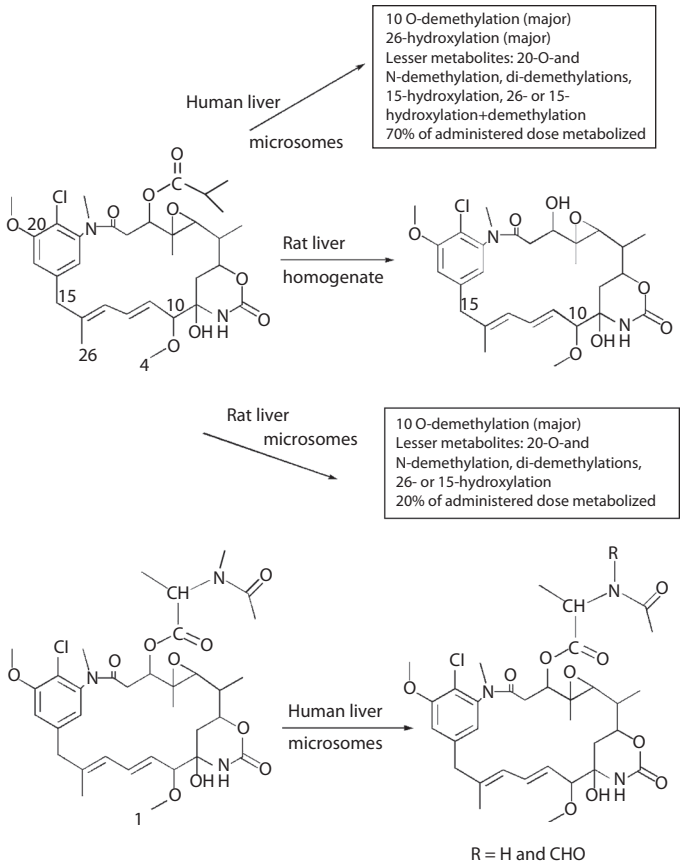

FIGURE 17.6 (**See color insert.**) Results on the mammalian metabolism of ansamitocin P-3 and maytansine.[71]

success, because the amount of drug that can be delivered to the target by an antibody is too small for most clinically used anticancer drugs to be effective. To overcome this problem, the warhead should be a highly potent drug, such as a maytansinoid. At the same time, the target-specific delivery holds the promise of minimizing the general toxic effects of the drug. Two approaches have been explored.

Iwasa and colleagues at Takeda[16] developed a bispecific monoclonal antibody that recognizes both ansamitocin P-3 and the human transferrin receptor, which is highly expressed on various human tumor cells. The **4** targeted to human A431 epidermoid carcinoma xenografts in nude mice was more effective than unconjugated **4** and eventually eradicated this tumor while at the same time showing reduced side effects.

An alternative approach was pursued by Chari et al.[91] at ImmunoGen, Inc., who modified maytansine for conjugation to antibodies or receptor agonists through disulfide linkages to the ester side chain. As shown in Figure 17.7, maytansinol generated either from **1** or **4** was converted using procedures detailed in the patent literature[92,93] into a compound, designated DM1, with a methyl disulfide function in the ester side chain. DM1, on reduction with dithiothreitol gives the corresponding thiol, which can be conjugated to an antibody through either thioether or, preferably, disulfide linkages. The effectiveness of this approach was demonstrated with conjugates to the TA.1, 3E9, and A7 antibodies directed against the *c-erb-2* oncogene protein, the human transferrin receptor, and human colon cancer cell lines, respectively. Multiple DM1 molecules could be conjugated to the TA.1 antibody (one to six molecules per antibody) and gave cytotoxicities against SB-BR-3 breast cancer cells

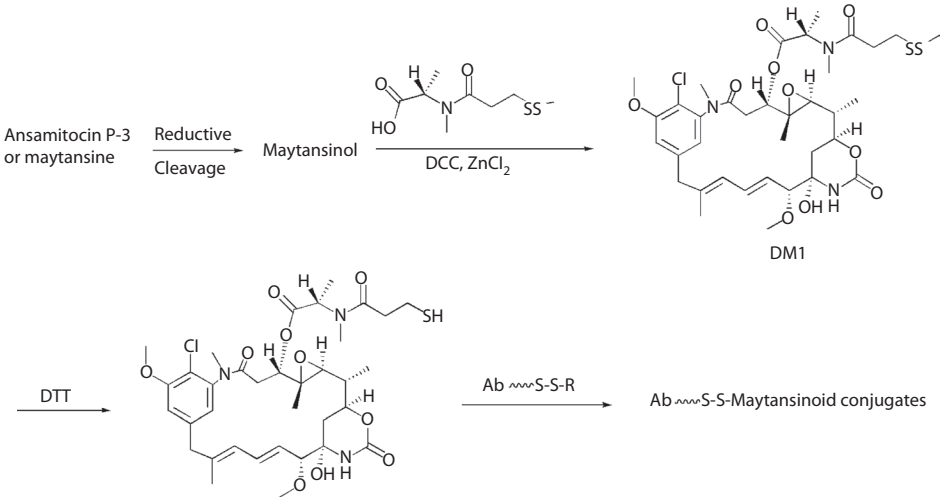

FIGURE 17.7 Structural modification of maytansinoids for conjugation to antibodies and receptor-specific carriers.[91–94]

up to IC_{50} 1.2×10^{-11} M, which were antagonized by the unconjugated antibody and dependent on expression of the target epitope.[91] Subsequently, encouraging preclinical results were presented with a DM1 conjugate to the monoclonal antibody huC242, which recognizes a glycoprotein expressed in human colorectal cancers.[94] The huC242–DM1 conjugate cured mice carrying xenografts of the COLO 205 human colon tumor, even very large tumors, at doses that showed very little toxicity. Effectiveness against two other colon tumor types was also demonstrated. The ImmunoGen technology was considered clinically promising and has been licensed to a number of major pharmaceutical companies.[95] Several different DM1 conjugates are now undergoing clinical trials.[96–99] The ImmunoGen group also reported a DM1 conjugate to a folate derivative designed to target cancer cells that overexpress the folate receptor.[100]

Insight into the mechanism of action of antibody–maytansinoid (DM1 and DM4) conjugates in general has been gained by the demonstration that lysosomal processing is required for their activity, irrespective of the linker. Thus, both thioether- and disulfide-linked conjugates are efficiently degraded in lysosomes to yield the intact maytansinoid drug and the linker attached to lysine.[101] In addition, huC242 disulfide-linked conjugates (e.g., huC242–SPDB–DM4) have been found to show significantly enhanced antitumor activity compared with that shown by thioether-linked conjugates (e.g., huC242–SMCC–DM1). The authors observed that the lysine adduct is the only metabolite formed from the thioether-linked DM1 conjugate, whereas the lysine metabolite formed from the disulfide-linked DM4 conjugate is reduced and *S*-methylated, yielding a lipophilic, potently cytotoxic metabolite, *S*-methyl-DM4; they postulated that this may account for latter's enhanced antitumor activity.[101] HuC242-DM4 has undergone a phase I clinical trial for the treatment of CanAg-expressing tumors such as carcinomas of the colon and pancreas. It was well tolerated at the 168-mg/m^2 dose level, but the maximum tolerated dose has yet to be defined. Some patients experienced ocular toxicity, and approaches to address this effect are being planned.[102] A further phase I trial of this agent is ongoing in patients with inoperable or metastatic colorectal cancer, pancreatic cancer, or other solid tumors (http://www.cancer.gov/drugdictionary/?CdrID=492706). The DM4-conjugated anti-Cripto monoclonal antibody, BIIB015, is in a phase I study in patients with relapsed/refractory solid tumors (http://www.cancer.gov/drugdictionary/?CdrID=596550). Cripto, a member of the EGF-CFC family of growth factor-like molecules, plays a key role in signaling pathways of certain transforming growth factor-beta superfamily members, and is overexpressed in carcinomas such as those of the breast, ovary, stomach, lung, and pancreas, while its expression is absent in normal tissues.

Using A549 human lung tumor and HT-29 human colon carcinoma xenografts in nude rats, Chen et al. have demonstrated that CNTO 95–maytansinoid immunoconjugates are potent antitumor agents against α_v integrin-expressing human carcinomas.[103] It is anticipated that these effects may ultimately be extended to other tumor types, such as melanoma, ovarian, and breast carcinoma, which overexpress α_v integrin. Due to the possibility of tumor antivascular or antiangiogenic effects being responsible for their efficacy, the potential may exist for treating a still broader array of cancers.

Two drugs, trastuzumab (Herceptin®) and lapatinib (Tykerb), are currently approved for the treatment of HER2-positive breast cancer, but they are not effective for all patients suffering from this disease. In this respect, the *in vitro* and *in vivo* efficacy, pharmacokinetics, and toxicity of trastuzumab–maytansinoid conjugates using disulfide and thioether linkers have been evaluated.[104] Trastuzumab linked to DM1 through a nonreducible thioether linkage, trastuzumab–MCC–DM1, was shown to be active in trastuzumab-sensitive and trastuzumab-refractory models of HER2-overexpressing cancer, and surprisingly showed favorable pharmacokinetic and safety profiles when compared with disulfide-linked trastuzumab conjugates (e.g., trastuzumab–SPP–DM1). Trastuzumab–MCC–DM1 was well tolerated and has shown some clinical responses in a phase I clinical trial;[105] it is currently in seven clinical trials (http://www.cancer.gov/drugdictionary/?CdrID=564399). These include: a phase III trial in patients with HER2-positive locally advanced or metastatic breast cancer in comparison with treatment with capecitabine plus lapatinib; a phase II trial in combination with pertuzumab in patients with HER2-positive locally advanced or metastatic breast cancer who have previously received trastuzumab; a phase II study of efficacy and safety in comparison with trastuzumab (Herceptin) and docetaxel (Taxotere®) in patients with metastatic HER2-positive breast cancer who have not received prior chemotherapy for metastatic disease; a phase II study in patients with HER2-positive locally advanced or metastatic breast cancer, and its safety and tolerability when used in combination with pertuzumab in patients with early disease progression; and three phase I trials in combination with agents, such as docetaxel, paclitaxel, and pertuzumab.

The promise evident in the use of antibody drug conjugates in cancer therapy has been the subject of several reviews, and readers are referred to them for further details of developments in this area.[106] In early 2010, investigators at ImmunoGen reported in detail on the various metabolites of the conjugates referred to above, extending the information given by Erickson et al.[101] and further demonstrating excellent *in vivo* activity in a preclinical mouse model of non-Hodgkin's lymphoma.[107,108] In addition to these reports and the review by Lambert (below),[109] the 2009 review by Senter[106] covering requirements for such conjugates from both the warhead and Mab aspects was expanded by Alley et al. in 2010[110] and further refined by Caravella and Lugovskoy in 2010.[111]

The 2010 review by Lambert109 (superscript) gives the current, most complete listing of the preclinical/clinical status of these agents which is summarized below; where available, the number of patients treated through the end of 2009 is included. Through the end of 2009, there have been 14 DM1- or DM4-linked agents that have been reported in preclinical through clinical trials. Of these, four currently fall into the preclinical area: SAR-566658 from Sanofi-Aventis directed against Muc-1; plus two from Amgen and one from Bayer whose details have not yet been released. Three have been discontinued after phase I programs: SB-408075, cantuzumab mertansine, 96 patients from GSK; bivatuzumab mertansine, 62 patients from Boehringer Ingelheim; and MLN-2704, 84 patients from Millenium Pharmaceuticals.

Five are listed as in phase I: SAR-3419, 38 patients from Sanofi-Aventis; IMGN-388, 32 patients from Immunogen; IMGN-633 (AVE-9633), 39 patients from Immunogen/Sanofi-Aventis; BT-062 from Biotest-AG; BIIB-015 from Biotest-Idec. Two more from Immunogen are in phase I/II trials: IMGN-901 (lorvotuzumab mertansine) 142 patients, and IMGN-242 with 45 patients. A more recent review in the "News and Analysis" section of the journal *Nature Reviews: Drug Discovery* in September 2010 indicates that SAR-3419 and IMGN-901 are now in phase II.[112]

The 14th and most advanced of the DM-linked conjugates (09/2010 currently in phase III) is the one from Genentech/Roche known as T-DM1 or trastuzumab emtansine, which is formally equivalent to the warhead mentioned in Polson et al.[108] but linked to the well-known clinical agent

trastuzumab and referred to earlier in the section. As a result of the data from the phase II trial known as TDM4374g on patients who had failed at least two Her2+ treatments (trastuzumab and the tyrosine kinase inhibitor lapatinib), a biological license application (BLA, equivalent to the NDA application for small molecules) has now been submitted to the FDA by Genentech for marketing approval as a treatment for Her2+ breast cancer. Details of the agent and results to the end of 2009 were reported by Lambert as mentioned above,[109] and in more detail by Niculescu-Duvaz[113] in another 2010 review that is contemporary with Lambert's, and from a slightly less scientific aspect in the article by Hughes.[112]

Thus, although maytansine itself has not been successful as a small molecule drug, its potential as a warhead is now being investigated in many different cancer etiologies, and hopefully, very soon one or more of these constructs will be approved for use by the FDA or its equivalent in other countries.

17.7 BIOSYNTHESIS

The biosynthesis of ansamitocins has been studied in *A. pretiosum* by feeding experiments with labeled precursors, which established the building blocks from which the molecule is generated. The maytansinoids are ansamacrolides that are assembled on a polyketide synthase (PKS) from an aromatic starter unit, AHBA,[114] by chain extension with three acetate units, three propionate units, and one "glycolate" extender unit.[115] Functional groups added to the polyketide backbone include three methyl groups from methionine,[115] a cyclic carbinolamide from the carbamoyl group of citrulline[115] and the ester side chain at C3, which is derived from the corresponding fatty acid or its precursor amino acid.[116] The spectrum of the maytansinol esters produced in the fermentation could be strongly influenced by feeding the respective acid (e.g., isobutyric acid for ansamitocin P-3) or one of its precursors (e.g., isobutyraldehyde, isobutanol, or valine) to direct the fermentation towards predominant (up to 90%) production of a single ansamitocin.[116]

On the basis of knowledge about the biosynthesis of AHBA in the rifamycin producer, *Amycolatopsis mediterranei*,[117–119] the gene cluster encoding ansamitocin biosynthesis was cloned from *A. pretiosum*, using the AHBA synthase gene as a probe.[120] Analysis of the cloned DNA revealed the presence of the relevant genes in two clusters, I and II, each carrying an AHBA synthase homologue (Figure 17.8a). The clusters are separated by a 30-kilobase nonessential DNA segment. Cluster I contains the majority of the biosynthetic genes, including four large type I PKS genes (*asmA–D*), which together with the cognate downloading enzyme, encoded by *asm9*, are predicted to catalyze the assembly of the required linear octaketide and its release and cyclization to proansamitocin (Figure 17.8b). Also present are some, but not all, of the AHBA synthesis genes (*asm22–24*), the genes required to synthesize the substrate for the third chain extension step incorporating the "glycolate" extender unit (*asm13–17*), genes for the post-PKS modifications of proansamitocin into **4** (*asm7,10–12,19,21*), and potential regulatory (*asm2,8,18,29,31,34*) and transport/resistance genes (*asm4,5,35*). Cluster II only contains the remaining genes essential for AHBA biosynthesis (*asm43–45,47*); potential regulatory (*asm39,40,48*) and transport/resistance genes (*asm41,42*) present can only affect the AHBA supply, as the deletion of cluster II gave a nonproducing mutant in which full **4** production could be restored by supplementation with AHBA.[120]

On the basis of analogy to the other chain extension substrates, malonyl-CoA for acetate and methylmalonyl-CoA for propionate units, one would predict the substrate for incorporation of "glycolate" units to be 2-hydroxy- or 2-methoxymalonyl-CoA. This, however, is not the case, as the corresponding *N*-acetylcysteamine thioesters were not incorporated into **4**.[121] By comparison with the gene cluster for FK520,[122] which also contains "glycolate" extender units, the products encoded by *asm13–17* were recognized as probably involved in forming the substrate for this unusual chain extension step. *Asm14* encodes a unique acyl carrier protein, which could substitute for the coenzyme A moiety as a carrier of the hydroxy- or methoxymalonate unit. Inactivation of each of these genes and phenotypic analysis of the mutants confirmed this deduction, showing loss of **4** production in each mutant, but formation of 10-demethoxy-**4** in a low yield in the *asm13*, *asm15*, *asm16*, and *asm17*

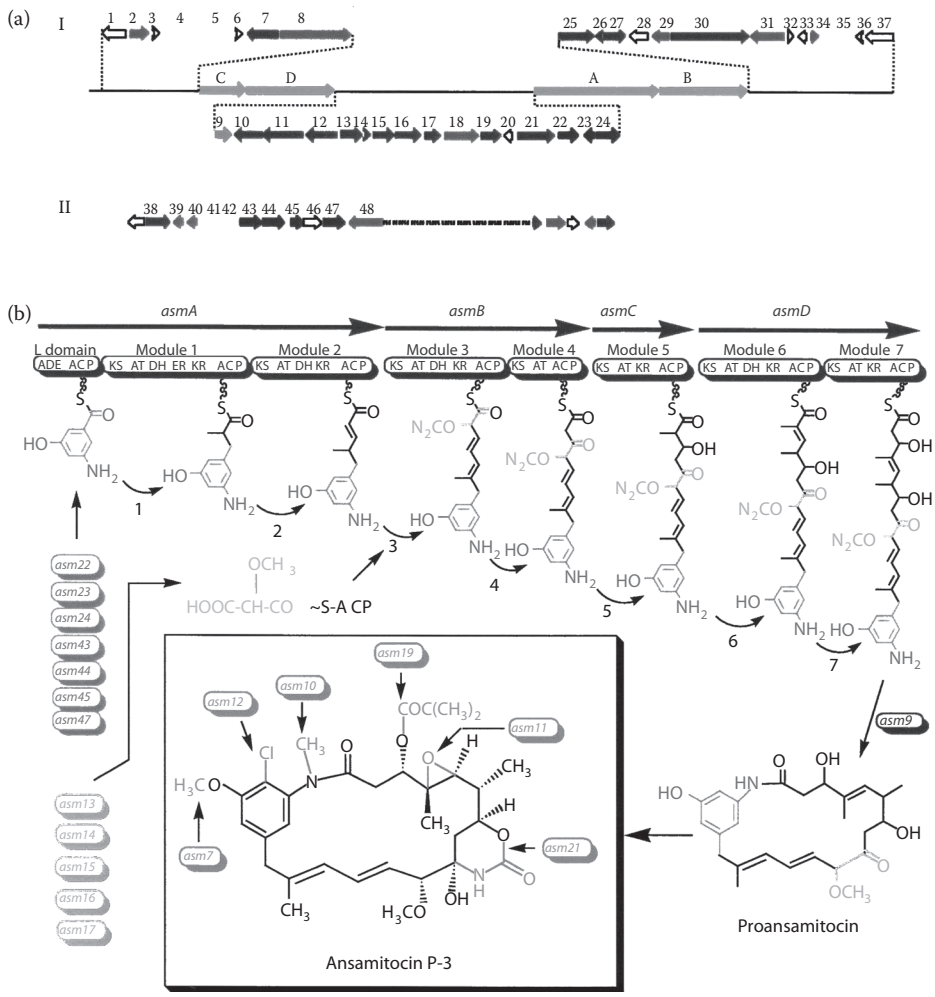

FIGURE 17.8 (**See color insert.**) Biosynthesis of ansamitocin P-3: (a) the ansamitocin biosynthetic gene cluster from *Actinosynnema pretiosum*; (b) assembly of proansamitocin on a type I PKS and post-PKS modification to ansamitocin.[120]

mutants. 10-Demethoxy-**4** was not formed in the *asm14* mutant, indicating that the unique *asm14*-encoded ACP is necessary for the aberrant incorporation of malonyl-CoA in the absence of the "glycolate" substrate.[11,121] *Asm13–17* are not only indispensable but also sufficient to generate this "glycolate" substrate, as shown in *Streptomyces lividans* by coexpression of an *asm13–17* cassette[123] with a cassette of the erythromycin PKS, modified by replacement of the methylmalonate-specific AT6 with the presumably hydroxymalonate-specific AT8 domain of the FK520 PKS.[124] The cotransformant produced a new compound, 2-methoxy-2-desmethyl-6-deoxyerythronolide B, resulting from the incorporation of a "glycolate" in place of the terminal propionate unit. Deletion of the methyltransferase gene *asm17* from the *asm13–17* cassette gave no new product, indicating that the hydroxymalonate moiety must be methylated before incorporation.[123] Hence the substrate for the third chain extension step must be 2-methoxymalonyl-ACP, which is formed from an intermediate of the glycolytic pathway, 1,3-bisphosphoglycerate, as shown in Figure 17.9.[125,126]

The mechanism of polyketide assembly was further probed by feeding a series of synthetic diketide, triketide, and tetraketide potential intermediates, as their *N*-acetylcysteamine thioesters, to an

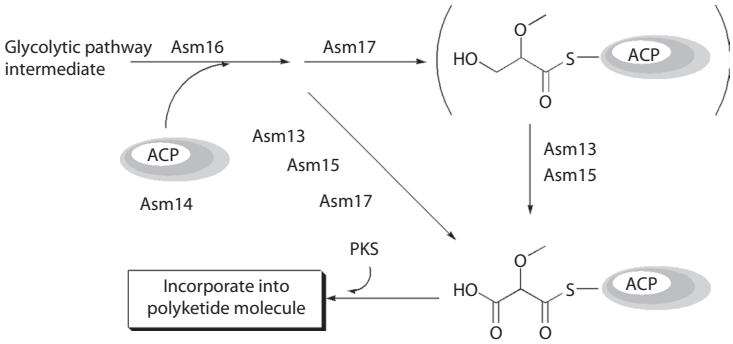

FIGURE 17.9 (**See color insert.**) Formation of 2-methoxymalonyl-ACP, the substrate for the incorporation of the "glycolate" chain extension unit into ansamitocin.[123]

AHBA-blocked mutant of *A. pretiosum*. These experiments revealed that the cryptic stereochemistry of the PKS-bound diketide intermediate is *R*,[127] and that the unusual shift of two conjugated double bonds from the 10,12 to the 11,13 position (ansamitocin numbering) occurs as part of the third chain extension step on the asm PKS.[128] The group of Kirschning also synthesized the *N*-acetylcysteamine thioester of *seco*-proansamitocin,[129] the corresponding free acid and the *N*-acetylcysteamine thioester of *seco*-20-desoxyproansamitocin, and demonstrated their cyclization and further conversion into ansamitocins by an AHBA-deficient mutant of *A. pretiosum*.[130] The Kirschning group also reported the synthesis of proansamitocin and a number of its analogs and their conversion into the corresponding ansamitocins by the same mutant.[131,132]

The enzymes catalyzing the post-PKS modification steps from proansamitocin to **4** and the order in which they function were examined by inactivation of each corresponding gene and, in some cases, by heterologous expression in *Escherichia coli* and characterization of the enzymatic activity.[133,134] Halogenation and carbamoylation, catalyzed by Asm12 and Asm21, respectively, appear to be the first and second step in the sequence. As predicted by the results of Hatano et al.,[116] the acyltransferase Asm19 catalyzing the addition of the ester side chain is rather promiscuous regarding its acyl substrate. Surprisingly, this reaction is not the terminal biosynthetic step, as expected from the natural occurrence of maytansinol, but occurs before the epoxidation by Asm11 and *N*-methylation by Asm10.[131] The predominant pathway from proansamitocin to **4** is depicted in Figure 17.10. However, many of these post-PKS modifying enzymes are not highly substrate-specific; hence, alternate minor pathways to **4** also operate, resulting in a metabolic grid.[134]

The results delineated above provide the tools for the genetic manipulation of the biosynthetic pathway to maytansinoids to generate structural analogs for biologic evaluation, which would be difficult to synthesize chemically. Such genetic manipulations could increase the structural diversity by altering the polyketide backbone and its functionality, or the downstream modifications of the macrolide.

The question of the biosynthetic source of the maytansinoids isolated from higher plants has been investigated by Leistner and colleagues in *Putterlickia* species.[43] Several lines of indirect evidence indicate that at least the polyketide framework of **1** is not biosynthesized by the plant, although the plants may have a role in determining the final structures elaborated: greenhouse-grown plants do not contain maytansine;[43] cell cultures of *Maytenus*[135,136] and *Putterlickia*[43] species do not produce maytansinoids; the **1**-content of individual *Putterlickia* plants (three species) varied dramatically, a phenomenon apparently also encountered by the U.S. Department of Agriculture workers who recollected *Maytenus* species for large-scale isolation of **1**;[43] and a polymerase chain reaction-based search for AHBA synthase-homologous genes in the plant genome gave negative results.[43]

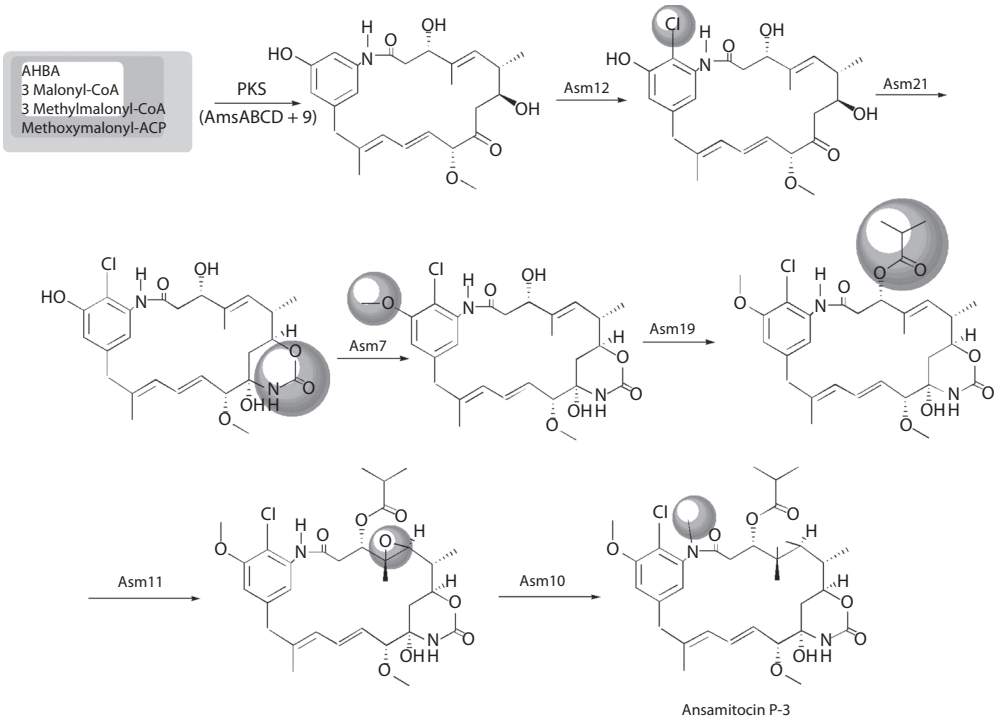

FIGURE 17.10 (**See color insert.**) The sequence of post-PKS modification reactions converting proansamitocin into ansamitocin P-3.[123,134]

The focus is now on the isolation and screening of microorganisms found in, on, or near **1**-producing plants. None of a substantial number of fungal endosymbionts isolated from three *Putterlickia* species carried an AHBA synthase homologue in its genome. Among the bacterial community of *P. verrucosa* and *P. retrospinosa*, one promising candidate was isolated from the rhizosphere and identified as *Kitasatospora putterlickiae* sp. nov.[137] Several ansamitocin-specific gene homologues were found in its genome, but the ability to produce maytansinoids has not yet been demonstrated for this organism.[11]

Three novel ansamitocin glycosides, carrying a β-D-glucosyl group in place of the *N*-methyl group attached to the macrolactam amide nitrogen, have been isolated from *A. pretiosum*.[18,19] Asm25 was identified as the responsible *N*-glycosyltransferase gene, and it has been shown to have broad substrate specificity toward other ansamycins and synthetic indolin-2-ones. [138]

REFERENCES

1. Kupchan, S.M., Komoda, Y., Court, W.A., Thomas, G.J., Smith, R.M., Karim, A., Gilmore, C.J., Haltiwanger, R.C., and Bryan, R.F., Maytansine, a novel antileukemic ansa macrolide from *Maytenus ovatus*. *J. Am. Chem. Soc.*, 94, 1354, 1972.
2. Issell, B.F. and Crooke, S.T., Maytansine. *Cancer Treat. Rev.*, 5, 199, 1978.
3. Komoda, Y. and Kishi, T., Maytansinoids. In *Anticancer Agents Based on Natural Product Models*, Douros, J. and Cassady, J.M., Eds. Academic Press: New York, 1980; pp 353.
4. Reider, P.J. and Roland, D.M., Maytansinoids. In *The Alkaloids*, Brossi, A., Ed. Academic Press: New York, 1984; Vol. 23, pp 71.
5. Smith Jr., C.R. and Powell, R.G., Chemistry and pharmacology of maytansinoid alkaloids. In *Alkaloids*, Pelletier, S.W., Ed. John Wiley and Sons: New York, 1984; Vol. 2, pp 149.

6. Wani, M.C., Taylor, H.L., and Wall, M.E., Plant antitumor agents: Colubrinol acetate and colubrinol, antileukaemic ansa macrolides from *Colubrina texensis. J. Chem. Soc. Chem. Commun.*, 370, 1973.
7. Powell, R.G., Weisleder, D., Smith Jr., C.R., Kozlowski, J., and Rohwedder, W.K., Treflorine, trenudine, and *N*-methyltrenudone: Novel maytansinoid tumor inhibitors containing two fused macrocyclic rings. *J. Am. Chem. Soc.*, 104, 4929, 1982.
8. Rinehart Jr., K.L. and Shield, L.S., Chemistry of the ansamycin antibiotics. *Fortschr. Chem. Org. Nat.*, 33, 231, 1976.
9. Higashide, E., Asai, M., Ootsu, K., Tanida, S., Kozai, Y., Hasegawa, T., Kishi, T., Sugino, Y., and Yoneda, M., Ansamitocins, a group of novel maytansinoid antibiotics with antitumor properties from *Nocardia. Nature*, 270, 721, 1977.
10. Hasegawa, T., Tanida, S., Hatano, K., Higashide, E., and Yoneda, M., Motile actinomycetes: *Actinosynnema pretiosum* subsp. *pretiosum* sp. nov., subsp. nov., and *Actinosynnema pretiosum* subsp. *auranticum* subsp. nov. *Int. J. Syst. Bacteriol.*, 33, 314, 1983.
11. Cassady, J.M., Chan, K.K., Floss, H.G., and Leistner, E., Recent developments in the maytansinoid antitumor agents. *Chem. Pharm. Bull.*, 52, 1, 2004.
12. Sakai, K., Ichikawa, T., Yamada, K., Yamashita, M., Tanimoto, M., Hikita, A., Ijuin, Y., and Kondo, K., Antitumor principles in mosses: The first isolation and identification of maytansinoids, including a novel 15-methoxyansamitocin P-3. *J. Nat. Prod.*, 51, 845, 1988.
13. Suwanborirux, K., Chang, C.-J., Spjut, R.W., and Cassady, J.M., Ansamitocin P-3, a maytansinoid, from *Claopodium crispifolium* and *Anomodon attenuatus* or associated actinomycetes. *Experientia*, 46, 117, 1990.
14. Feng, S.C., et al., Studies on the chemical constituents of *Mallotus anomalus*. II. Structures of the antitumor components from *Mallotus anomalus. Chinese Chem. Lett.*, 5, 743, 1994.
15. Larson, G.M., Schaneberg, B.T., and Sneden, A.T., Two new maytansinoids from *Maytenus buchananii. J. Nat. Prod.*, 62, 361, 1999.
16. Okamoto, K., Harada, K., Ikeyama, S., and Iwasa, S., Therapeutic effect of ansamitocin targeted to tumor by a bispecific monoclonal antibody. *Jpn. J. Cancer Res.*, 83, 761, 1992.
17. Kirschning, A., Harmrolfs, K., and Knobloch, T., The chemistry and biology of the maytansinoid antitumor agents. *C. R. Chimie,* 11, 1523, 2008.
18. Lu, C., Bai, L., and Shen, Y., A novel amide N-glycoside of ansamitocins from *Actinosynnema pretiosum. J. Antibiot.*, 57, 348, 2004.
19. Ma, J., Zhao, P.J., and Shen, Y.M., New amide N-glycosides of ansamitocins identified from *Actinosynnema pretiosum*, *Arch. Pharm. Res.*, 30, 670–673, 2007.
20. Snipes, C.E., Duebelbeis, D.O., Olson, M., Hahn, D.R., Dent III, W.H., Gilbert, J.R., Werk, T.L., Davis, G.E., Lee-Lu, R., and Graupner, P.R., The ansacarbamitocins: polar ansamitocin derivatives, *J. Nat. Prod.*, 70, 1578, 2007.
21. Kupchan, S.M., Komoda, Y., Branfman, A.R., Dailey Jr., R.G., and Zimmerly, V.A., Novel maytansinoids. Structural interrelations and requirements for antileukemic activity. *J. Am. Chem. Soc.*, 96, 3706, 1974.
22. Kupchan, S.M., Komoda, Y., Thomas, G.J., and Hintz, H.P.J., Maytanprine and maytanbutine, new antileukemic ansa macrolides from *Maytenus buchananii. J. C. S. Chem. Comm.*, 1065, 1972.
23. Boyd, M.R. and Paull, K.D., Some practical considerations and applications of the National Cancer Institute *in vitro* anticancer drug discovery screen. *Drug Dev. Res.*, 34, 91, 1995.
24. Cragg, G.M., personal communication. 2002.
25. Kupchan, S.M., Komoda, Y., Branfman, A.R., Sneden, A.T., Court, W.A., Thomas, G.J., Hintz, H.P., Smith, R.M., and Karim, A., The maytansinoids. Isolation, structural elucidation, and chemical interrelation of novel ansa macrolides. *J. Org. Chem.*, 42, 2349, 1977.
26. Wolpert-DeFilippes, M.K., Adamson, R.H., Cysyk, R.L., and Johns, D.G., Initial studies on the cytotoxic action of maytansine, a novel ansa macrolide. *Biochem. Pharmacol.*, 24, 751, 1975.
27. Remillard, S., Rebhun, L., Howie, G.A., and Kupchan, S.M., Antimitotic activity of the potent tumor inhibitor maytansine. *Science*, 189, 1002, 1975.
28. Wolpert-DeFilippes, M.K., Bono Jr., V.H., Dion, R.L., and Johns, D.G., Initial studies on maytansine-induced metaphase arrest in L1210 murine leukemia cells. *Biochem. Pharmacol.*, 24, 1735, 1975.
29. Ootsu, K., Kozai, Y., Takeuchi, M., Ikeyama, S., Igarashi, K., Tsukamoto, K., Sugino, Y., Tashiro, T., Tsukagoshi, S., and Sakurai, Y., Effects of new antimitotic antibiotics, ansamitocins, on the growth of murine tumors *in vivo* and on the assembly of microtubules *in vitro. Cancer Res.*, 40, 1707, 1980.
30. Mandelbaum-Shavit, F., Wolpert-DeFilippes, M.K., and Johns, D.G., Binding of maytansine to rat brain tubulin. *Biochem. Biophys. Res. Commun.*, 72, 47, 1976.

31. Rai, S.S. and Wolff, J., Localization of the vinblastine-binding site on beta-tubulin. *J. Biol. Chem.*, 271, 14707, 1996.
32. Hamel, E., +Natural products which interact with tubulin in the vinca domain: Maytansine, rhizoxin, phomopsin A, dolastatin 10 and 15 and halichondrin B. *Pharmacol. Therap.*, 55, 31, 1992.
33. Takahashi, M., Matsumoto, S., Iwasaki, S., and Yahara, I., Molecular basis for determining the sensitivity of eucaryotes to the antimitotic drug rhizoxin. *Mol. Gen. Genet.*, 222, 169, 1990.
34. Li, Y., Kobayashi, H., Hashimoto, Y., and Iwasaki, S., Binding selectivity of rhizoxin, phomopsin A, vinblastine, and ansamitocin P-3 to fungal tubulins: Differential interactions of these antimitotic agents with brain and fungal tubulins. *Biochem. Biophys. Res. Comm.*, 187, 722, 1992.
35. Luduena, R.F. and Roach, M.C., Tubulin sulfhydryl groups as probes and targets for antimitotic and antimicrotubule agents. *Pharmacol. Ther.*, 49, 133, 1991.
36. Sawada, T., Kato, Y., Kobayashi, H., Hashimoto, Y., Watanabe, T., Sugiyama, Y., and Iwasaki, S., A fluorescent probe and a photoaffinity labeling reagent to study the binding site of maytansine and rhioxin on tubulin. *Bioconjugate Chem.*, 4, 284, 1993.
37. Ikeyama, S. and Takeuchi, M., Antitubulin activities of ansamitocins and maytansinoids. *Biochem. Pharmacol.*, 30, 2421, 1981.
38. York, J., Wolpert-DeFilippes, M.K., Johns, D.G., and Sethi, V.S., Binding of maytansinoids to tubulin. *Biochem. Pharmacol.*, 30, 3239, 1981.
39. Tanida, S., Hasegawa, T., Hatano, K., Higashide, E., and Yoneda, M., Ansamitocins, maytansinoid antitumor antibiotics. Producing organism, fermentation, and antimicrobial activities. *J. Antibiot.*, 33, 192, 1980.
40. Hatano, K., Higashide, E., and Yoneda, M., Bioassay of ansamitocin P-3, an antitumor antibiotic. *Agric. Biol. Chem.*, 48, 1889, 1984.
41. Tanida, S., Higashide, E., and Yoneda, M., Inhibition of cilia regeneration of *Tetrahymena* by ansamitocins, new antitumor antibiotics. *Antimicrob. Agents Chemother.*, 16, 101, 1979.
42. Tanida, S., Hasegawa, T., and Higashide, E., A simple method for determining antitubulinic activities of ansamitocins and related compounds using a cilia regeneration system with deciliated *Tetrahymena. Agric. Biol. Chem.*, 44, 1847, 1980.
43. Pullen, C.B., Schmitz, P., Hoffmann, D., Meurer, K., Boettcher, T., von Bamberg, D., Pereira, A.M., de Castro França, S., Hauser, M., Geertsema, H., van Wyk, A., Mahmud, T., Floss, H.G., and Leistner, E., Occurrence and non-detectability of maytansinoids in individual plants of the genera *Maytenus* and *Putterlickia. Phytochemistry*, 62, 377, 2003.
44. Freedman, B., Reed, D.K., Powell, R.G., Madrigal, R.V., and Smith, C.R., Biological activities of *Trewia nudiflora* extracts against certain economically important insect pests. *J. Chem. Ecol.*, 8, 409, 1982.
45. Corey, E.J., Weigel, L.O., Floyd, D., and Bock, M.G., The total synthesis of (±)-*N*-methylmaysenine. *J. Am. Chem. Soc.*, 100, 2916, 1978.
46. Meyers, A.I., Roland, D.M., Comins, D.L., Henning, R., Fleming, M.P., and Shimizu, K., Progress toward the total synthesis of maytansinoids. Synthesis of (±)-4,5-deoxymaysine (*N*-methylmaysenine). *J. Am. Chem. Soc.*, 101, 4732, 1979.
47. Corey, E.J., Weigel, L.O., Chamberlin, A.R., and Lipshutz, B., Total synthesis of ()-*N*-methylmaysenine. *J. Am. Chem. Soc.*, 102, 1439, 1980.
48. Meyers, A.I., Comins, D.L., Roland, D.M., Henning, R., and Shimizu, K., Total synthesis of (±)-maysine. *J. Am. Chem. Soc.*, 101, 7104, 1979.
49. Meyers, A.I., Reider, P.J., and Campbell, A.L., Total synthesis of (±)-maytansinol. The common precursor to the maytansinoids. *J. Am. Chem. Soc.*, 102, 6597, 1980.
50. Corey, E.J., Weigel, L.O., Chamberlin, A.R., Cho, H., and Hua, D.H., Total synthesis of maytansine. *J. Am. Chem. Soc.*, 102, 6613, 1980.
51. Isobe, M., Kitamura, M., and Goto, T., Stereocontrolled total synthesis of (±)-maytansinol. *J. Am. Chem. Soc.*, 104, 4997, 1982.
52. Kitamura, M., Isobe, M., Ichikawa, Y., and Goto, T., Stereocontrolled total synthesis of (-)-maytansinol. *J. Am. Chem. Soc.*, 106, 3252, 1984.
53. Petrakis, K.S. and Fried, J., A novel synthesis of the cyclic carbinolamide moiety of the maytansinoids. *Tetrahedron Lett.*, 24, 3065, 1983; and references cited therein.
54. Confalone, P.N., The use of heterocyclic chemistry in the synthesis of natural and unnatural products. *J. Heterocyclic Chem.*, 27, 31, 1990; and references cited therein.
55. Goodwin, T.E., Cousins, K.R., Crane, H.M., Eason, P.O., Freyaldenhoven, T.E., Harmon, C.C., King, B.K., LaRocca, C.D., Lile, R.L., Orlicek, S.G., Pelton, R.W., Shedd, O.L., Swanson, J.S., and Thompson, J.W., Synthesis of two new maytansinoid model compounds from carbohydrate precursors. *J. Carbohydr. Chem.*, 17, 323, 1998; and references cited therein.

56. Hodgson, D.M., Parsons, P.J., and Stones, P.A., A short and efficient synthesis of the C-3 to C-10 portion of the maytansinoids. *Tetrahedron Lett.*, 47, 4133, 1991.
57. Gu, X., Pan, B., Zhou, Q., Bai, D., and Gao, Y., Studies on the total synthesis of maytansinoids (IV)—Synthesis of maytansine. *Sci. Sinica, Ser. B.*, 31, 1342, 1988; and references cited therein.
58. Bénéchie, M. and Khuong-Huu, F., Total synthesis of ()-maytansinol. *J. Org. Chem.*, 61, 7133, 1996.
59. Nakahama, K., Izawa, M., Asai, M., Kida, M., and Kishi, T., Microbial conversion of ansamitocin. *J. Antibiot.*, 34, 1581, 1981.
60. Izawa, M., Nakahama, K., Kasahara, F., Asai, M., and Kishi, T., Demethylation of ansamitocins and related compounds. *J. Antibiot.*, 34, 1587, 1981.
61. Izawa, M., Wada, Y., Kasahara, F., Asai, M., and Kishi, T., Hydroxylation of ansamitocin P-3. *J. Antibiot.*, 34, 1591, 1981.
62. Kawai, A., Akimoto, H., Hashimoto, N., and Nomura, H., Chemical modification of ansamitocins. I. Synthesis and properties of 4,4-deoxymaytansinoids. *Chem. Pharm. Bull.*, 32, 2194, 1984.
63. Akimoto, H., Kawai, A., Hashimoto, N., and Nomura, H., Chemical modification of ansamitocins. II. Synthesis of 3-epimaytansinoids *via* 3-maytansinones. *Chem. Pharm. Bull.*, 32, 2565, 1984.
64. Kawai, A., Akimoto, H., Kozai, Y., Ootsu, K., Tanida, S., Hashimoto, N., and Nomura, H., Chemical modification of ansamitocins. III. Synthesis and biological effects of 3-acyl esters of maytansinol. *Chem. Pharm. Bull.*, 32, 3441, 1984.
65. Miyashita, O. and Akimoto, H., Dechloromaytansinoids. Takeda Chemical Industries, Ltd., Japan, European Patent, EP19800528, 1980.
66. Suchocki, J.A. and Sneden, A.T., New maytansinoids: Reduction products of the C(9)-carbinolamide. *J. Org. Chem.*, 53, 4116, 1988.
67. Schaneberg, B.T. and Sneden, A.T., In *Abstracts*, 218th ACS Natl. Meeting, New Orleans, Aug. 22–26, 1999; New Orleans, Aug. 22–26, 1999.
68. Suchocki, J.A. and Sneden, A.T., Characterization of decomposition products of maytansine. *J. Pharm. Sci.*, 76, 738, 1987.
69. Sneden, A.T., Synthetic modifications of biologically interesting natural products. *Synletters*, 5, 313, 1993.
70. Terfloth, G. and SmithKline Beecham Corp., USA, Process for preparation and purification of maytansinol, Int. Appl. WO 02/074775 A1, 2002.
71. Liu, Z., Floss, H.G., Cassady, J.M., and Chan, K.K., Metabolism studies of the anti-tumor agent maytansine and its analog ansamitocin P-3 using liquid chromatography/tandem mass spectrometry. *J. Mass Spec.*, 40, 389, 2005.
72. Taft, F., Brünjes, M., Floss, H.G., Czempinski, N., Grond, S., Sasse, F., and Kirschning, A., Highly active ansamitocin derivatives: Mutasynthesis using an AHBA-blocked mutant. *ChemBioChem*, 9, 1057, 2008.
73. O'Connell, M.J., Rubin, S.A., and Moertel, C.G., Phase II trial of maytansine in patients with advanced colorectal carcinoma. *Cancer Treat. Rep.*, 62, 1237, 1978.
74. Cabanillas, F., Bodey, G.P., Burgess, M.A., and Freireich, E.J., Results of a phase II study of maytansine in patients with breast carcinoma and melanoma. *Cancer Treat. Rep.*, 63, 507, 1979.
75. Creagen, E.T., Fleming, T.R., Edmonson, T.R., and Ingle, J.N., Phase II evaluation of maytansine in patients with advanced head and neck cancer. *Cancer Treat. Rep.*, 63, 2061, 1979.
76. Neidhart, J.A., Laufman, L.R., Vaughn, C., and McCracken, J.D., Minimal single-agent activity of maytansine in refractory breast cancer: A Southwest Oncology Group study. *Cancer Treat. Rep.*, 64, 675, 1980.
77. Ahmann, D.L., Frytak, S., Kvols, L.K., Hahn, R.G., Edmonson, J.H., Bisel, H.F., and Creagan, E.T., Phase II study of maytansine and chlorozotocin in patients with disseminated malignant melanoma. *Cancer Treat. Rep.*, 64, 721, 1980.
78. Franklin, R., Samson, M.K., Fraile, R.J., Abu-Zahra, H., O'Bryan, R., and Baker, L.H., A phase I-II study of maytansine utilizing a weekly schedule. *Cancer Res.*, 46, 1104, 1980.
79. Rosenthal, S., Harris, D.T., Horton, J., and Glick, J.H., Phase II study of maytansine in patients with advanced lymphomas: An Eastern Cooperative Oncology Group pilot study. *Cancer Treat. Rep.*, 64, 1115, 1980.
80. Edmonson, J.H., Rubin, J., Kvols, L.K., O'Connell, M.J., Frytak, S., and Green, S.J., Phase II study of maytansine in advanced breast cancer. *Cancer Treat. Rep.*, 65, 536, 1981.
81. Borden, E.C., Ash, A., Enterline, H.T., Rosenbaum, C., Laucius, J.F., Paul, A.R., Falkson, G., and Lerner, H., Phase II evaluation of dibromodulcitol, ICRF-159, and maytansine for sarcomas. *Am. J. Clin. Oncol.*, 5, 417, 1982.

82. Creech, R.H., Stanley, K., Vogl, S.E., Ettinger, D.S., Bonomi, D.S., and Salazar, O., Phase II study of cisplatin, maytansine, and chlorozotocin in small cell lung carcinoma (EST 2578). *Cancer Treat. Rep.*, 66, 1417, 1982.
83. Ratanatharathorn, V., Gad-el-Mawla, N., Wilson, H.E., Bonnet, J.D., Rivkin, S.E., and Mass, R., Phase II evaluation of maytansine in refractory non-Hodgkin's lymphoma: A Southwest Oncology Group study. *Cancer Treat. Rep.*, 66, 1687, 1982.
84. Thigpen, J.T., Ehrlich, C.E., Creasman, W.T., Curry, S., and Blessing, J.A., Phase II study of maytansine in the treatment of advanced or recurrent adenocarcinoma of the ovary: A Gynecology Oncology Group study. *Am. J. Clin. Oncol.*, 6, 273, 1983.
85. Edmonson, J.H., Hahn, R.G., Creagan, E.T., and O'Connell, M.J., Phase II study of maytansine in advanced sarcomas. *Cancer Treat. Rep.*, 67, 401, 1983.
86. Thigpen, J.T., Ehrlich, C.E., Conroy, J., and Blessing, J.A., Phase II study of maytansine in the treatment of advanced or recurrent squamous cell carcinoma of the cervix. *Am. J. Clin. Oncol.*, 6, 427, 1983.
87. Sabio, H., Frankel, L., Sexauer, C., Faletta, J., and Kim, T.H., Maytansine in refractory childhood acute lymphocytic leukemia: A Pediatric Oncology Group study. *Cancer Treat. Rep.*, 67, 1045, 1983.
88. Ravry, M.J., Omura, G.A., and Birch, R., Phase II evaluation of maytansine (NSC 153858) in advanced cancer: A Southwestern Cancer Study Group trial. *Am. J. Clin. Oncol.*, 8, 148, 1985.
89. Gastrointestinal Tumor Study Group, Phase II trials of maytansine, low-dose chlorozotocin, and high-dose chlorozotocin as single agents against advanced measurable adenocarcinoma of the pancreas. *Cancer Treatment Rep.*, 69, 417, 1985.
90. Anon., Annual Report to the FDA by DCT, NCI, on Maytansine, NSC 153858, IND 11857, February 1984.
91. Chari, R.J., Martell, B.A., Gross, J.L., Cook, S.B., Shah, S.A., Blättler, W.A., McKenzie, S.J., and Goldmacher, V.S., Immunoconjugates containing novel maytansinoids: Promising anticancer drugs. *Cancer Res.*, 52, 127, 1992.
92. Chari, R.J., Goldmacher, V.S., Lambert, J.M., and Blättler, W.A., Cytotoxic agents comprising maytansinoids and their therapeutic use, ImmunoGen, Inc., U.S. Patent 5,208,020, 1993.
93. Chari, R.J. and Widdison, W.C., Process for the preparation and purification of thiol-containing maytansinoids, ImmunoGen, Inc., U.S. Patent 6,333,410, 2001.
94. Liu, C., Tadayoni, B.M., Bourret, L.A., Mattocks, K.M., Derr, S.M., Widdison, W.C., Kedersha, N.L., Ariniello, P.D., Goldmacher, V.S., Lambert, J.M., Blättler, W.A., and Chari, R.V., Eradication of large colon tumor xenografts by targeted delivery of maytansinoids. *Proc. Natl. Acad. Sci. U.S.A.*, 93, 8618, 1996.
95. ImmunoGen website: http://www.immunogen.com, Accessed September 15, 2010.
96. Liu, C. and Chari, R.J., The development of antibody delivery systems to target cancer with highly potent maytansinoids. *Expert Opin. Investig. Drugs*, 6, 169, 1997.
97. Johnson, R., Progress in targeted anticancer therapy using immunotoxins. *Pharmaceut. J.*, 265, 490, 2000.
98. Erickson, S. and Schwall, R. Humanized anti-ErbB2 antibody-maytansinoid conjugates and uses thereof in cancer therapy, Genentech, Inc., WO 2000, U.S. 17229, 2001.
99. Ross, S., Spencer, S.D., Holcomb, I., Tan, C., Hongo, J., Devaux, B., Rangell, L., Keller, G.A., Schow, P., Steeves, R.M., Lutz, R.J., Frantz, G., Hillan, K., Peale, F., Tobin, P., Eberhard, D., Rubin, M.A., Lasky, L.A., and Koeppen, H., Prostate stem cell antigen as therapy target: Tissue expression and *in vivo* efficacy of an immunoconjugate. *Cancer Res.*, 62, 2546, 2002.
100. Ladino, C.A., Ravi, L., Chari, V.J., Bourret, L.A., Kedersha, N.L., and Goldmacher, V.S., Folate-maytansinoids: Target-selective drugs of low molecular weight. *Int. J. Cancer*, 73, 859, 1997.
101. Erickson, H.K., Park, P.U., Widdison, W.C., Kovtun, Y.V., Garrett, L.M., Hoffman, K., Lutz, R.J., Goldmacher, V.S., and Blättler, W.A., Antibody-maytansinoid conjugates are activated in targeted cancer cells by lysosomal degradation and linker-dependent intracellular processing. *Cancer Res.*, 66, 4426, 2006.
102. Mita, M.M., Ricart, A.D., Mita, A.C., Patnaik, A., Sarantopoulos, J., Sankhala, K., Fram, R.J., Qin, A., Watermill, J., and Tolcher, A.W., A phase I study of a CanAg-targeted immunoconjugate, huC242-DM4, in patients with Can Ag-expressing solid tumors. *J. Clin. Oncol.*, 25, No. 18S, 3062, 2007.
103. Chen, Q., Millar, H.J., McCabe, F.L., Manning, C.D., Steeves, R., Lai, K., Kellogg, B., Lutz, R.J., Trikha, M., Nakada, M.T., and Anderson, G.M., Alpha v integrin-targeted immunoconjugates regress established human tumors in xenograft models. *Clin. Cancer Res.*, 13, 3689, 2007.
104. Lewis Phillips, G.D., Li, G., Dugger, D.L., Crocker, L.M., Parsons, K.L., Mai, E., Blättler, W.A., Lambert, J.M., Chari, R.V.J., Lutz, R.J., Wong, W.L.T., Jacobson, F.S., Koeppen, H., Schwall, R.H., Kenkare-Mitra, S.R., Spencer, S.D., and Sliwkowski, M.X., Targeting HER2-positive breast cancer with trastuzumab-DM1, an antibody-cytotoxic drug conjugate. *Cancer Res.*, 68, 9280, 2008.

105. Beeram, M., Krop, I., Modi, S., Tolcher, A., Rabbee, N., Girish, S., Tibbitts, J., Holden, S., Lutzker, S., and Burris, H., A phase I study of trastuzumab-MCC-DM1 (T-DM1), a first-in-class HER2 antibody-drug conjugate (ADC), in patients (pts) with HER2+ metastatic breast cancer (BC). *J. Clin. Oncol.*, 25, No. 18S (June 20 Suppl.), 1042, 2007.
106. Teicher, B.A., Antibody-drug conjugate targets. *Curr. Cancer Drug Targ.*, 9, 982, 2009; Senter, P.D., Potent antibody drug conjugates for cancer therapy. *Curr. Opin. Chem. Biol.*, 13, 235, 2009; Zhiqiang, A., Ed., *Therapeutic Monoclonal Antibodies: From the Bench to the Clinic*. John Wiley & Sons, Inc.: Hoboken, NJ, 2009.
107. Erickson, H.K., Widdison, W.C., Mayo, M.F., Whiteman, K., Audette, C., Wilhelm, S.D., and Singh, R., Tumor delivery and *in vivo* processing of disulfide-linked and thioether-linked antibody-maytansinoid conjugates. *Bioconjugate Chem.*, 21, 84, 2010.
108. Polson, A.G., Williams, M., Gray, A.M., Fuji, R.N., Poon, K.A., McBride, J., Raab, H., Januario, T., Go, M., Lau, J., Yu, S.-F., Du, C., Fuh, F., Tan, C., Wu, Y., Liang, W.-C., Prabhu, S., Stephan, J.-P., Hongo, J.-A., Dere, R.C., Deng, R., Cullen, M., de Tute, R., Bennett, F., Rawstron, A., Jack, A., and Ebens, A., Anti-CD22-MCC-DM1: An antibody-drug conjugate with a stable linker for the treatment of non-Hodgkin's lymphoma. *Leukemia* 24, 1566, 2010.
109. Lambert, J.M., Antibody-maytansinoid conjugates: A new strategy for the trreatment of cancer. *Drugs Fut.*, 35, No. 6, 471, 2010.
110. Alley, S.C., Okeley, N.M., and Senter, P.D., Antibody-drug conjugates: Targeted drug delivery for cancer. *Curr. Opin. Chem. Biol.*, 14, 529, 2010.
111. Caravella, J. and Lugovskoy, A., Design of next-generation protein therapeutics. *Curr. Opin. Chem. Biol.*, 14, 520, 2010.
112. Hughes, B., Antibody-drug conjugates for cancer: Poised to deliver? *Nat. Rev. Drug. Discov.*, 9, 665, 2010.
113. Niculescu-Duvaz, I., Trazuzumab emastine, an antibody-drug conjugate for the treatment of HER2+ metastatic breast cancer. *Curr. Opin. Mol. Therap.*, 12, 350, 2010.
114. Hatano, K., Akiyama, S.-I., Asai, M., and Rickards, R.W., Biosynthetic origin of aminobenzenoid nucleus (C7N-unit) of ansamitocin, a group of novel maytansinoid antibiotics. *J. Antibiot.*, 35, 1415, 1982.
115. Hatano, K., Mizuta, E., Akiyama, S.-I., Higashide, E., and Nakao, Y., Biosynthetic origin of the *ansa*-structure of ansamitocin P-3. *Agric. Biol. Chem.*, 49, 327, 1985.
116. Hatano, K., Higashide, E., Akiyama, S.-I., and Yoneda, M., Selective accumulation of ansamitocins P-2, P-3 and P-4, and biosynthetic origins of their acyl moieties. *Agric. Biol. Chem.*, 48, 1721, 1984.
117. Yu, T.-W., Müller, R., Müller, M., Zhang, X., Draeger, G., Kim, C.-G., Leistner, E., and Floss, H.G., Mutational analysis and reconstituted expression of the biosynthetic genes involved in the formation of 3-amino-5-hydroxybenzoic acid, the starter unit of rifamycin biosynthesis in *Amycolatopsis mediterranei* S699. *J. Biol. Chem.*, 276, 12546, 2001.
118. Guo, J. and Frost, J.W., Kanosamine biosynthesis: A likely source of the aminoshikimate pathway's nitrogen atom. *J. Am. Chem. Soc.*, 124, 10642, 2002.
119. Arakawa, K., Müller, R., Mahmud, T., Yu, T.-W., and Floss, H.G., Characterization of the early stage aminoshikimate pathway in the formation of 3-amino-5-hydroxybenzoic acid: The RifN protein specifically converts kanosamine into kanosamine 6-phosphate. *J. Am. Chem. Soc.*, 124, 10644, 2002.
120. Yu, T.-W., Bai, L., Clade, D., Hoffmann, D., Toelzer, S., Trinh, K.Q., Xu, J., Moss, S.J., Leistner, E., and Floss, H.G., The biosynthetic gene cluster of the maytansinoid antitumor agent ansamitocin from *Actinosynnema pretiosum. Proc. Natl. Acad. Sci. U.S.A.*, 99, 7968, 2002.
121. Carroll, B.J., Moss, S.J., Bai, L., Kato, Y., Toelzer, S., Yu, T.-W., and Floss, H.G., Identification of a set of genes involved in the formation of the substrate for the incorporation of the unusual "glycolate" chain extension unit in ansamitocin biosynthesis. *J. Am. Chem. Soc.*, 124, 4176, 2002.
122. Wu, K., Chung, L., Revill, W.P., Katz, L., and Reeves, C.D., The FK520 gene cluster of *Streptomyces hygroscopicus* var. *ascomyceticus* (ATTC 14891) contains genes for biosynthesis of unusual polyketide extender units. *Gene*, 251, 81, 2000.
123. Kato, Y., Bai, L., Xue, Q., Revill, W.P., Yu, T.-W., and Floss, H.G., Functional expression of genes involved in the biosynthesis of the novel polyketide chain extension unit, methoxymalonyl-acyl carrier protein, and engineered biosynthesis of 2-desmethyl-2-methoxy-6-deoxyerythronolide B. *J. Am. Chem. Soc.*, 124, 5268, 2002.
124. Reeves, C.D., Chung, L.M., Liu, Y., Xue, O., Carney, J.R., Revill, W.P., and Katz, L., A new substrate specificity for acyl transferase domains of the ascomycin polyketide synthase in *Streptomyces hygroscopicus. J. Biol. Chem.*, 277, 9155, 2002.

125. Dorrestein, P.C., Van Lanen, S.G., Li, W., Zhao, C., Deng, Z., Shen, B., and Kelleher, N.L., The bifunctional glyceryl transferase/phosphatase OzmB belonging to the HAD superfamily that diverts 1,3-bisphosphoglycerate into polyketide biosynthesis. *J. Am. Chem. Soc.*, 128, 10386, 2006.
126. Wenzel, S.C., Williamson, R.M., Grünanger, C., Xu, J., Gerth, K., Martinez, R.A., Moss, S.J., Carroll, B.J., Grond, S., Unkefer, C.J., Müller, R., and Floss, H.G., On the biosynthetic origin of methoxymalonyl-acyl carrier protein, the substrate for incorporation of "glycolate" units into ansamitocin and soraphen A. *J. Am. Chem. Soc.*, 128, 14325, 2006.
127. Kubota, T., Brünjes, M., Frenzel, T., Xu, J., Kirschning, A., and Floss, H.G., Determination of the cryptic stereochemistry of the first PKS chain extension step in ansamitocin biosynthesis by *Actinosynnema pretiosum. ChemBiochem*, 7, 1221, 2006.
128. Taft, F., Brünjes, M., Knobloch, T., Floss, H.G., and Kirschning, A., Timing of the $\Delta_{10,12}$-$\Delta_{11,13}$ double bond migration during ansamitocin biosynthesis in *Actinosynnema pretiosum. J. Am. Chem. Soc.*, 131, 3812, 2009.
129. Frenzel, T., Brünjes, M., Quitschalle, M., and Kirschning, A., Synthesis of the N-acetylcysteamine thioester of *seco*-proansamitocin. *Org. Lett*, 8, 135, 2005.
130. Harmrolfs, M., Brünjes, M., Dräger, G., Floss, H.G., Sasse, F., Taft, F., and Kirschning, A., *In vivo* cyclization of synthetic *seco*-proansamitocins to ansamitocin macrolactams by *Actinosynnema pretiosum. ChemBiochem*, 11, 2517, 2010.
131. Meyer, A., Brünjes, M., Taft, F., Frenzel, T., Sasse, F., and Kirschning, A., Chemoenzymatic approaches toward dechloroansamitocin P3. *Org. Lett.*, 9, 1489, 2007.
132. Meyer, A. and Kirschning, A., Total syntheses of new proansamitocin derivatives by ring-closing metathesis. *Synletters*, 8, 1264, 2007.
133. Moss, S.J., Bai, L., Toelzer, S., Carroll, B.J., Mahmud, T., Yu, T.-W., and Floss, H.G., Identification of Asm19 as an acyltransferase attaching the biologically essential ester side chain of ansamitocins using *N*-desmethyl-4,5-desepoxymaytansinol, not maytansinol, as its substrate. *J. Am. Chem. Soc.*, 124, 6544, 2002.
134. Spiteller, P., Bai, L., Shang, G., Carroll, B.J., Yu, T.-W., and Floss, H.G., The post-polyketide synthase modification steps in the biosynthesis of the antitumor agent ansamitocin by *Actinosynnema pretiosum. J. Am. Chem. Soc.*, 125, 14236, 2003.
135. Kutney, J.P., Beale, M.H., Salisbury, P.J., Stuart, K.L., Worth, B.R., Townsley, P.M., Chalmers, W.T., Nilsson, K., and Jacoli, G.G., Isolation and characterization of natural products from plant tissue cultures of *Maytenus buchananii. Phytochemistry*, 20, 653, 1981.
136. Dymowski, W. and Furmanowa, M., Searching for cytostatic substances in plant tissue of *Maytenus molina* by *in vitro* culture. III. Release of substances from active biological fractions from the callus extract of *Maytenus wallichiana* R. and B. *Acta Pol. Pharm.*, 47, 51, 1990.
137. Groth, I., Schütze, B., Boettcher, T., Pullen, C.B., Rodriguez, C., Leistner, E., and Goodfellow, M., *Kitasatospora putterlickiae* sp. *nov*., isolated from rhizosphere soil, transfer of *Streptomyces kifunensis* to the genus *Kitasatospora* as *Kitasatospora kifunensis* comb. nov., and amended description of *Streptomyces aureofaciens* Duggar 1948. *Int. J. Syst. Evol. Microbiol.*, 53, 2033, 2003.
138. Zhao, P., Bai, L., Ma, J., Zeng, Y., Li, L., Zhang, Y., Lu, C., and Floss, H.G., Amide N-glycosylation by Asm25, an N-glycosyltransferase of ansamitocins. *Chem. Biol.*, 15, 863, 2008.

18 Benzoquinone Ansamycins

Kenneth M. Snader

CONTENTS

18.1 Introduction 429
18.2 Mechanism of Action 430
18.3 Medicinal Chemistry 432
18.3.1 New Natural Products 433
18.3.2 Mutasynthesis Products 433
18.3.3 Biosynthetic Engineering Products 434
18.3.4 Synthetic and Semisynthetic Products 440
18.3.5 Nonansamycin Products 446
18.3.6 Metabolic Studies 447
18.4 Clinical Trials 447
References 448

18.1 INTRODUCTION

The discovery of the ability of geldanamycin (GM, **1**; Figure 18.1)[1] to inhibit the chaperone protein, Hsp90,[2] and thus cause death of cancer cells has caused an extraordinary interest in the benzoquinone ansamycins (BAs) as candidates for drug development. At the time of this first review,[3] there were only two candidates in clinical trials, 17-allylamino-17-demethoxygeldanamycin (17-AAG, **2**; Figure 18.1) and 17-dimethylamino-17-demethoxygeldanamycin (17-DMAG, **3**; Figure 18.1). In the following six years, there have been hundreds of modified products prepared and tested, and the promise of potential broad spectrum activity against cancer still looks promising, although no candidate has been unblemished in clinical testing yet. The abundance of new research has also stimulated several excellent reviews that describe not only the BAs,[4,5] but also the intense study done on heat shock protein 90 (Hsp90), its role in both normal and malignant cells, and its impact on the search for other molecules with Hsp90-inhibition activity.[6]

Ansamycins have been defined as cyclic molecules with long aliphatic chains that connect two opposite points of an aromatic ring, like a handle or ansa (thus derives the name).[7] In the case of the BAs, the large ring is a lactam that forms by polyketide chain elongation from the starting aromatic product 3-amino-5-hydroxybenzoic acid (AHBA), itself derived from the shikimic acid pathway. While both the quinone and hydroquinone forms have been isolated from various culture broths, the hydroquinones are often highly susceptible to oxidation during the purification process possibly leading to the preponderance of quinones reported.

With the reports on numerous total syntheses as well as of the x-ray studies on the co-crystallization of Hsp90 with GM,[8] the semisynthetic derivative 17-DMAG,[9] and macbecin,[10] there is no further doubt about the stereochemistry of the various BAs that have been reported. To finalize this aspect of the chemistry, the structures of the known BAs are shown in Figure 18.2.

Indeed, the intense interest in the development of the BAs as classic medicinal chemistry pharmacophores has prompted several excellent reviews on Hsp90 inhibitors. The recent review by Amolins and Blagg[4] details the discovery of at least a dozen natural products that have been shown to inhibit Hsp90. Similarly, Drysdale and Brough[5] have elaborated on several other classes of

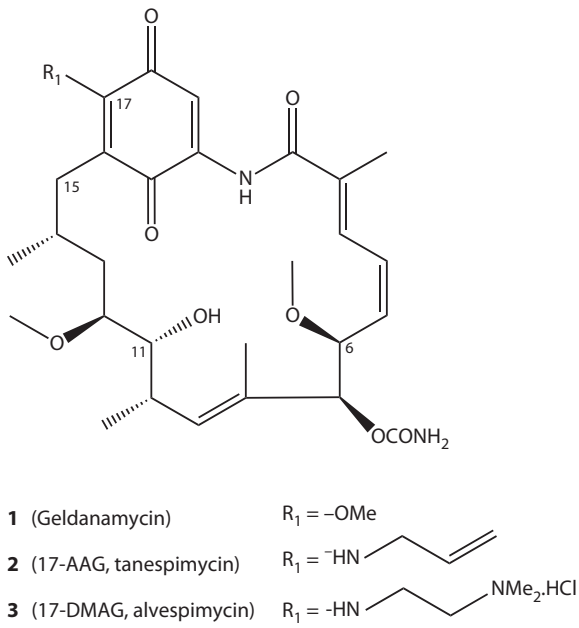

FIGURE 18.1 Structures **1** through **3**.

compounds, including natural products that are under active research as Hsp90 inhibitors. A short summary of these classes will be given later in this review. The success of the BAs as potential drug candidates has even prompted one group at Ensemble Discovery to propose, in a very timely review, that the whole group of natural product macrocycles are "underexploited" as candidates for drug discovery.[6] They go well beyond the group of BAs to include such macrocycles as vancomycin, amphotericin, and epothilone to cite a few interesting and current discoveries. The field of medicinal chemistry is increasingly moving towards molecular screening procedures based on a growing number of known molecular targets, and the concept of virtual screening using three-dimensional modeling is rapidly coming to the forefront of drug discovery.

From the perspective of the development of BAs as anticancer agents, this review will update the status of the understanding of Hsp90 and other chaperone proteins and highlight the considerable increase in the number of new natural and unnatural compounds that have evolved since the last review in 2003.

18.2 MECHANISM OF ACTION

Nothing has driven the interest in BAs more directly than their ability to bind to and inhibit the action of Hsp90. There are currently four known heat shock proteins: Hsp90 is a family of at least two proteins (found in the cytoplasm), Grp94 (found in the endoplasmic reticulum [ER]), and Trap-1 (found in the mitochondria). The cytoplasmic chaperones exist as dimers and each are comprised of three domains: the N-terminal domain, which contains the ATP-binding site; the middle domain, which recognizes the client protein; and the C-terminal domain, which affects the dimerization (Chart 18.1). Hsp90 is the most abundant of the chaperones comprising 1–2% of total cellular protein in normal cells and increases to 4–6% when cells are under stress.[11,12] The ATP-binding site in the N-terminal region of Hsp90 contains a unique binding pocket that binds both ATP and ADP. Conformational changes that occur during the conversion of ATP to ADP regulate the ability of Hsp90 to bind to its client proteins and thus regulate its ability to protect or repair the clients. When the middle domain recognizes and binds a client protein, it causes a conversion of ADP to ATP,

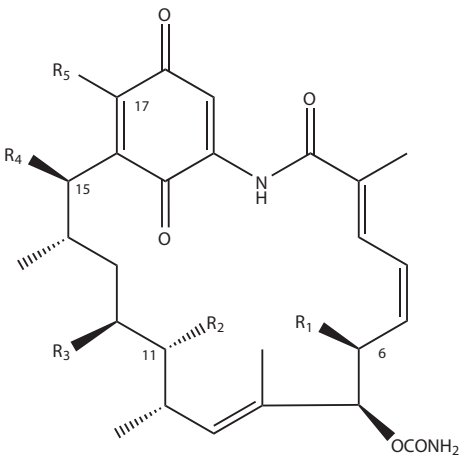

	R_1 (C6)	R_2 (C11)	R_3 (C12)	R_4 (C15)	R_5 (C17)
Quinones					
Geldanamycin	OMe	OH	OMe	H	OMe
Herbimycin A (TAN 420F)	OMe	OMe	OMe	OMe	H
Herbimycin C (TAN 420D)	OMe	OH	OMe	H	H
Macbecin 1	Me	OMe	OMe	OMe	H
TAN 420B	OMe	OH	OH	OMe	H
Hydroquinones					
Macbecin 2	Me	OMe	OMe	OMe	H
TAN 420A	OMe	OH	OH	OMe	H
TAN 420C	OMe	OH	OMe	OMe	H
TAN 420E	OMe	OMe	OMe	OMe	H

FIGURE 18.2 Known benzoquinone ansamycins.

which in turn causes a conformational change in the overall complex. The complex then effects a maturation of the client protein.

GM was the first inhibitor found that binds to the N-terminal-binding pocket blocking the conversion of ADP to ATP and preventing the client protein from binding to the chaperone.[2,13] This interference prevents the protective chaperone effect of Hsp90 and allows degradation of the client protein through ubiquitination and a cascade of proteosome degradation events, ultimately leading to cell apoptosis.

A large number of client proteins make this target for chemotherapy very attractive. The client proteins include kinases, steroid hormone receptors, and transcription factors that are directly related to malignancy. This client group also includes many mutated oncogenic proteins including, but not limited to, Her-2, Raf-1, mutant B-Raf, mutant p53, ErbB2, and Bcr-Abl.[11] For a current list of over 100 client proteins that interact with the Hsp90 chaperone, see the website maintained by Picard.[14] This broad target of effects is a major attraction of Hsp90 inhibitors because it offers the opportunity to block a range of critical cancer pathways. It has prompted at least one researcher to propose that it impacts all of the "hallmark traits" of malignancy (Table 18.1) and offers "broad spectrum" anticancer activity.[15]

The broad spectrum of effects that inhibition of Hsp90 offers is summarized by Workman[15] in which are included a description of the various proteins that serve as "clients" for the Hsp90 chaperone. Also included are suggestions that compounds that selectively induce client protein

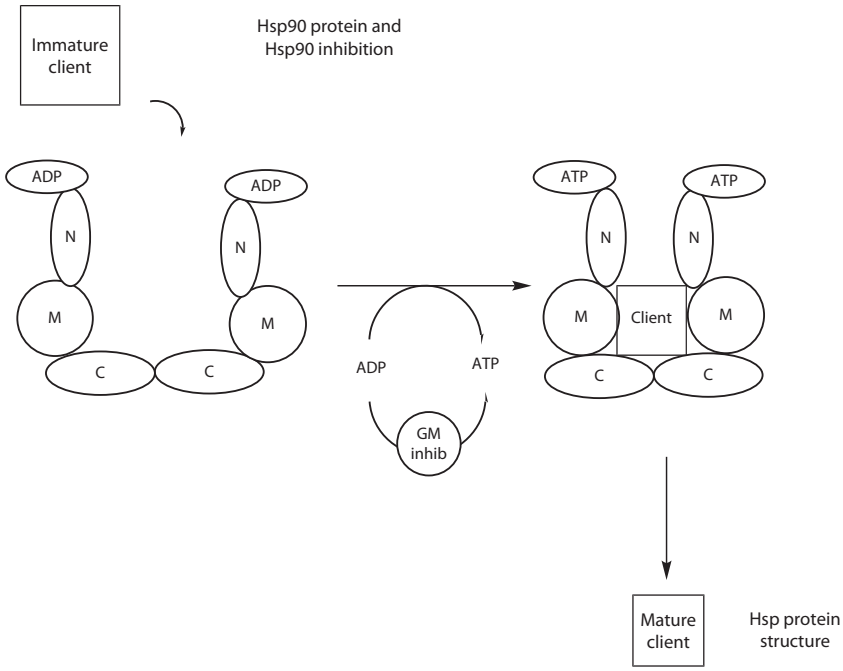

CHART 18.1 HSP protein structure.

degradation might favor cytoprotective pathways for the treatment of other conditions like Alzheimer's or Huntingdon's Disease. Indeed some publications[16] suggest that the GM could have an effect on diabetes and neurodegenerative disorders such as Parkinson's and Alzheimer's diseases by upregulating ER function and enhancing the elimination of unfolded proteins that accumulate during an ER stress response. The downregulation of some cancer proteins such as ErbB2 has been reported by investigators[17] and is just the beginning of more discoveries that will be forthcoming.

18.3 MEDICINAL CHEMISTRY

With the availability of a rapid *in vitro* test for binding to Hsp90, it is not surprising that there have been many new ansamycin-derived products discovered and produced. Both naturally occurring and "unnatural natural products" have been prepared as well as numerous synthetic and semisynthetic analogs. These have been organized into four categories: new natural products, mutasynthesis products, biosynthetic engineering products, and synthetic and semisynthetic products, plus a group of nonansamycin products.

TABLE 18.1
Hallmark Trait of Cancer

Examples of Relevant Hsp90	Client Proteins
Self-sufficiency in growth signals	ErbB2, Raf-1, Akt
Insensitivity to growth suppression signals	Plk, Wee1, Myt1
Evasion of apoptosis	RIP, Akt
Acquisition of limitless replicative potential	HTERT
Sustained angiogenesis	Hif-1α, FAK, Akt
Invasion and metastasis	Met

18.3.1 New Natural Products

Natural evolution of organisms allows for the discovery of new ansamycins to be isolated from the culture of microorganisms. One of the more interesting early discoveries was reblastatin (**4**) reported in 2000 by two groups, one as a minor component from a subspecies of GM-producing *Streptomyces hygroscopicus*[18] and the other from a *Streptomyces* sp.[19]

Both groups used cell cytotoxicity in their discovery process but further studies by multiple groups have verified the inhibition of Hsp90. Also produced in the culture by the GlaxoWellcome group were the two additional products 17-demethoxylebstatin (**7**) and 17-demethylreblastatin (**8**) (see footnote on Figure 18.3 regarding error in names). Of interest is the reporting of these 4,5-dihydro ansamycins with implications about the biosynthesis pathway.

One additional ansamycin, autolytimycin (**6**), has been reported, along with two known compounds, lebstatin (**5**) and 17-*O*-demethylgeldanamycin from *Streptomyces autolyticus*.[20] No biological activity for **5** was reported but the other two products have been studied by other investigators.

18.3.2 Mutasynthesis Products

With the growing research on polyketide biosynthesis and with the identification and cloning of the genes required for the biosynthesis of GM,[21] it was inevitable that mutasynthesis be explored as a tool to make new and novel ansamycin analogs. Eichner et al.[22] used mutational biosynthesis with a AHBA-blocked GM-producing mutant of *S. hygroscopicus*. By supplementing the culture with a variety of 3-aminobenzoic acids, they obtained 13 new compounds related to reblastatin.

The new products were tested *in vitro* against a panel of human tumor cell lines and the three most active compounds **9**, **10**, and **11** showed activity comparable to GM and reblastatin (Figure 18.4).

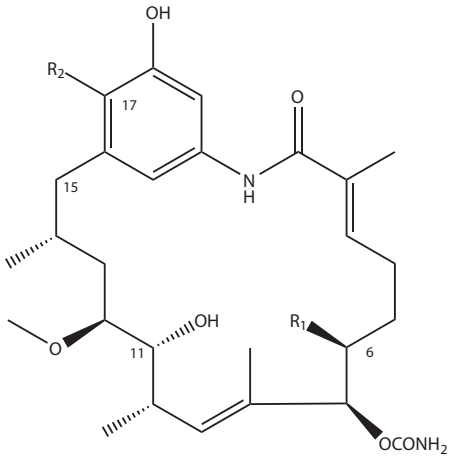

		R_1 (C6)	R_2 (C17)
4	Reblastatin	OMe	OMe
5	Lebstatin[a]	OMe	OMe
6	Autolytimycin[a]	OMe	H
7	19-Demethoxylebstatin[b]	OMe	H
8	19-Demethylreblastatin[b]	OH	OMe

a. In original publicatio n[20], stereochemistry at C6 is inverted but subsequent publications contradict this assignment. b. In original publication[19], the names are incorrect and should be 17-demethoxylebstatin and 17-demethylreblastatin, respectively.

FIGURE 18.3 New natural ansamycins.

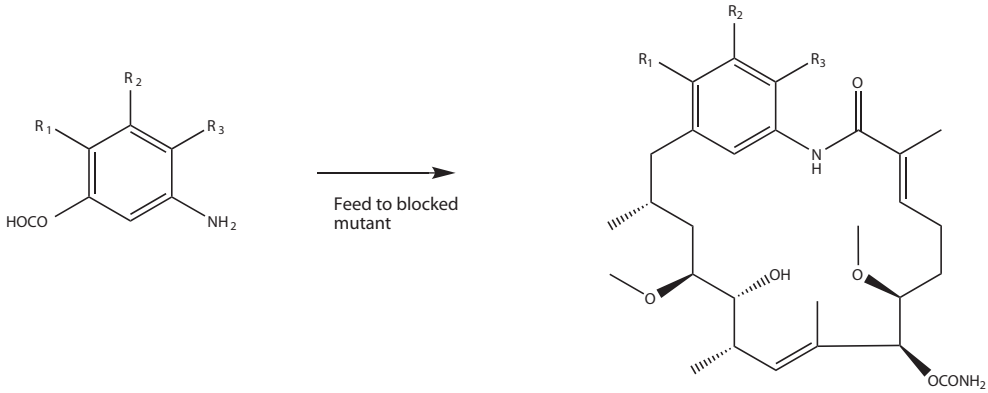

				IC$_{50}$(nM)					
	R 1	R 2	R 3	KB-3-1	U-937	PC-3	SK-OV-3	MCF-7	A-431
9	H	OMe	H	109	188	n.d.	113	38	60
10	H	H	F	73	62	42	54	18	62
11	OH	Br	H	34	21	36	46	120	17
4 (Reblastatin)	OMe	OH	H	53	9	18	125	n.d.	18

FIGURE 18.4 Some active mutasynthesis products related to reblastatin.

Of note is that feeding precursors that carried an electrophillic group ortho to the amine in AHBA tended to produce only the uncyclized seco-acid with all the expected polyketide substituents.

Similarly, a group from Kosan[23] developed an AHBA-deficient mutant of the GM-producing strain. They then fed these cultures with a panel of approximately 30 substituted 3-aminobenzoic acids. Ten of the precursors were incorporated into non-BAs. After testing for binding to purified recombinant human Hsp90α N-terminal domain as well as *in vitro* cytotoxicity against a panel of cancer cell lines in comparison with 17-AAG and 17-DMAG, five products were considered significantly interesting for further study. One liability of BAs is that their activity is dependent upon reductive activation to the hydroquinone by the enzyme NAD(P)H/quinone oxidoreductase 1 (NQO1).[24–27] Since lack of this enzyme occurs in as much as 25% of some populations of cancer patients, this group developed an *in vitro* cell line to test for this unique activity. While 17-AAG and 17-DMAG were relatively inactive in this test ($IC_{50} > 1000$ nM), these new non-BAs generally showed good cytotoxicity (IC_{50}: 89–1200 nM). Some representative values for the five best products (**12–16**) are given in Figure 18.5.

One of the early reports by Korean investigators[28] used an AHBA synthase gene-activated mutant of GM-producing *S. hygroscopicus*. They fed nine precursor benzoic acids and obtained five unique reblastatin-type products. They also found two uncyclized seco acids when they fed hydroxybenzoic acid precursors rather than aminobenzoic acid precursors. Similarly, no products were obtained when feeding ortho aminobenzoic acids (Figure 18.6).

No cytotoxicity or Hsp90-binding studies were reported and all structures were inferred from mass spectroscopy data, except for compounds **17** and **22** where sufficient sample was obtained to allow ^{1}H and ^{13}C NMR studies. This allowed the assignment of these samples as reblastatin analogs. Interestingly, both **17** and **22** were obtained on feeding the mutant 3-aminobenzoic acid.

18.3.3 Biosynthetic Engineering Products

One of the newest and perhaps the most exciting ways to generate new biosynthetic products is by biosynthetic engineering or combinatorial biosynthesis. This process of isolating the biosynthetic

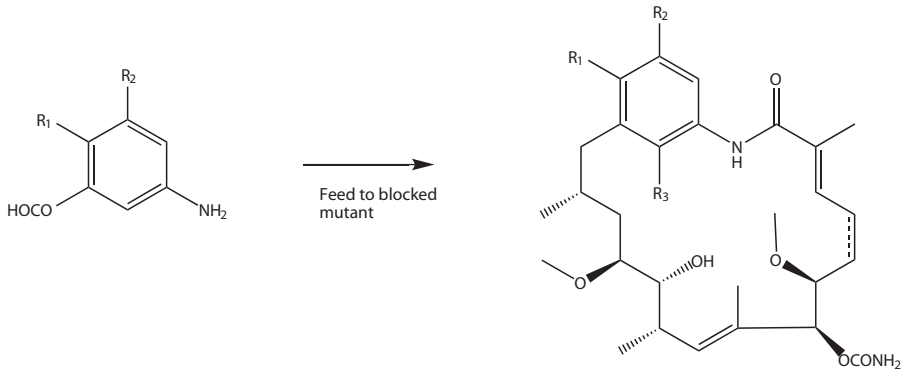

12 - 16

	R_1	R_2	R_3	K_D (nM)	IC_{50} (nM) SKOV-3	MCF-7	MDA-468 (NQO1 minus)	NCI-H596 (NQO1 minus)
17-AAG (2)				160	240	58	1500	1600
17-DMAG (3)				87	122	71	1600	1100
12 (4,5-Dihydro)	OH	Cl	H	n.d.	141	57	89	190
13 (4,5-Unsa'td.)	OH	Cl	H	n.d.	350	330	443	710
14 (4,5-Dihydro)	H	H	H	5.4	320	139	190	390
15 (4,5-Dihydro)	OH	H	H	0.8	840	610	420	1200
16 (4,5-Unsat'd.)	OH	H	H	2.5	158	87	160	325

FIGURE 18.5 Non-benzoquinone ansamycin Hsp90 inhibitors from genetic engineering of *Streptomyces hygroscopicus*.

sequence into genetic modules and then modifying or reshuffling the modules to produce new biosynthetic products holds enormous potential for medicinal chemistry. The greatest amount of experience is with the polyketide synthase (PKS) pathway, and BAs are produced by adding a PKS

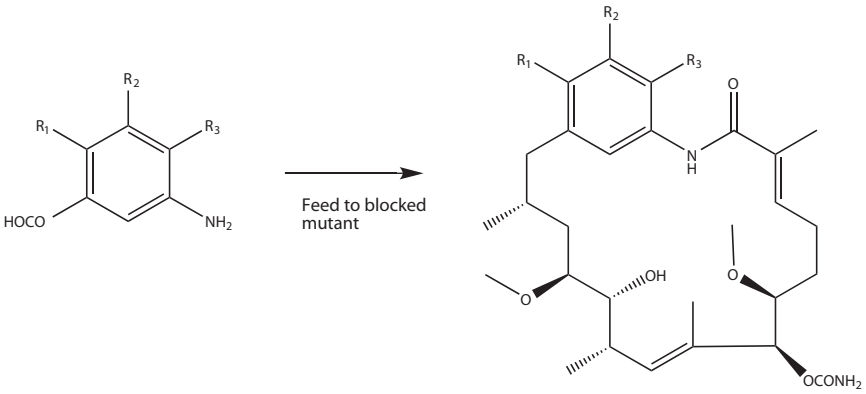

17 - 22

	R_1	R_2	R_3
17	H	H	H
18	H	NH_2	H
19	H	H	OH
20	H	H	NH_2
21	H	H	Cl
22	OH	H	H

FIGURE 18.6 Novel reblastatin-type mutasynthesis products.

process to a glucose-shikimate product, AHBA. This has led several groups to apply these techniques to GM-producing organisms.

The Kosan group[29] have isolated and characterized the geldanamycin polyketide synthase (GdmPKS) gene cluster in *S. hygroscopicus*. They subsequently divided this cluster into seven modules, four that utilize methylmalonyl CoA, two that utilize methoxymalonyl CoA, and a single module that utilizes malonyl CoA. This is sequentially described in Figure 18.7.

They then made AT substitutions of the acyl transferase domains in six of the seven modules. Four of these substitutions led to four sites of derivatization and the seven derivatives shown in Figure 18.8. AT substitutions in mods 1, 4, and 5 led to deletions of the groups at C14, C8, and C6 in the GM structure, respectively. AT substitutions in mod 7 led to three different compounds (**23–25**), each with deletions of the C2 methyl group but which varied due to post-PKS processing as shown in Figure 18.8.

The various analogs were evaluated for both binding affinity to Hsp90 and cytoxicity against SKBr3 cells *in vitro*. All the products were substantially less cytotoxic than 17-AAG; however, one compound, KOSN 1559 (**25**), showed an eightfold greater binding affinity than 17-AAG (Km = 16 vs. 1300 nM).

A group from Korea Research Institute of Bioscience and Biotechnology[30] focused on the post-PKS genes of GM-producing *S. hygroscopicus*. They isolated and identified four genes from the post-PKS processing set, which they labeled gel 8, 1, 7, and 16. They were able to isolate the proposed progeldanamycin (**26**) as the major product from a gel 7,8 knockout mutant (Δgel 7,8). By using selective knockouts of gels 7, 8, or 16, they were able to produce sequential quinone formation

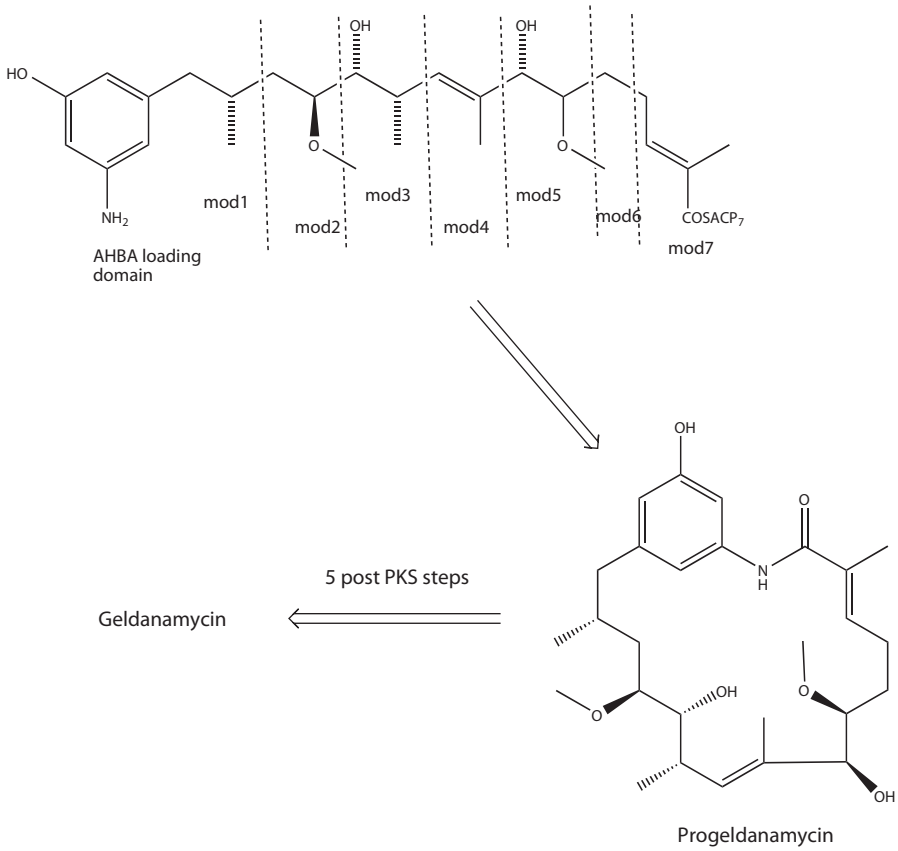

FIGURE 18.7 Geldanamycin polyketide synthase (GdmPKS) gene cluster from *S. hygroscopicus*.

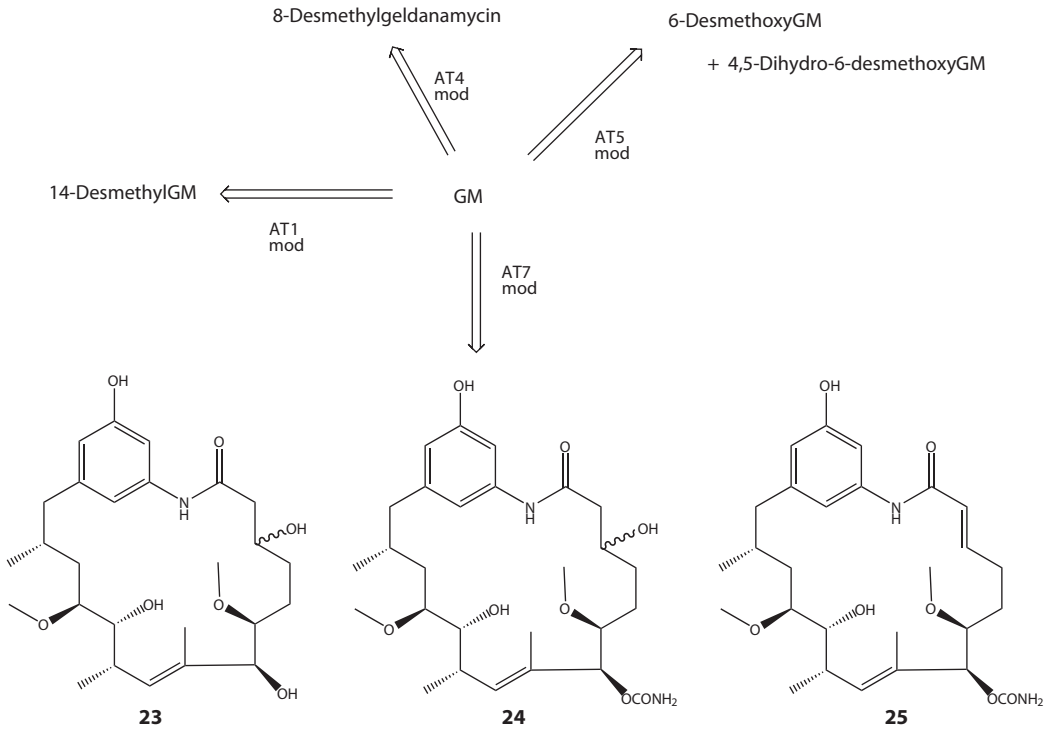

FIGURE 18.8 Products formed by GdmPKS genetic manipulation.

or carbamoylation and thus produce either 17-demethoxyreblastatin (**28**) or 4,5-dihydro-7-decarbamoylgeldanamycin (**27**) as shown in Figure 18.9.

To illustrate how the biosynthesis gene clusters can vary greatly in different organisms, the group at Biotica Technology, Ltd.[31] studied the macbecin producer *Actinosynnema pretiosum*. They reasoned that there were two important reasons for targeting macbecin over the more heavily studied 17-AAG. First, all the first-generation BAs feature the toxic pharmacophore, benzoquinone. This can undergo redox recycling involving NAD(P)H/quinone oxidoreductase (NQO1) as was mentioned earlier. Not only does this lead to cytotoxic superoxide radical generation but it also allows a mechanism for drug resistance, reduction in NQO1 expression levels. Secondly, facile conjugation with nucleophiles such as glutathione or other thiols provide a deactivation and cellular depletion pathway. Their strategy was to use genetic inactivation of the monooxygenase responsible for hydroxylation of the phenolic precursor in the biosynthetic pathway, thus inhibiting formation of the quinone.

The macbecin gene cluster was identified. It was different from others reported in that all the sequences are present in one cluster, unlike those of GM or herbimycin where the post-PKS cluster is separate. They fully sequenced the gene cluster and then used molecular genetic manipulation to delete the gene target mbcM to yield a stable producing strain. Fermentation of this strain produced two new nonquinone macbecin analogs, **30** and **31** (Figure 18.10).

They continued on to produce a series of mutant strains containing different combinations of post-PKS genes and isolated an additional seven products that were all quinones containing structural variations at C15 and C11, some accompanied by olefin formation at C4-C5. These products were helpful in establishing the preferred order of biosynthetic steps, which they now propose as: C7-*O*-carbamoylation, C21-oxidation, C4,5-desaturation, C15-hydroxylation, and C11/C15-*O*-methylation.

Since their original goal was the preparation of nonquinone products, compounds **30** and **31** were evaluated for anticancer activity. *In vitro* cytotoxicity was measured against six cancer cell lines and **30** was essentially equal to macbecin while the C15-hydroxy derivative was much less potent. When

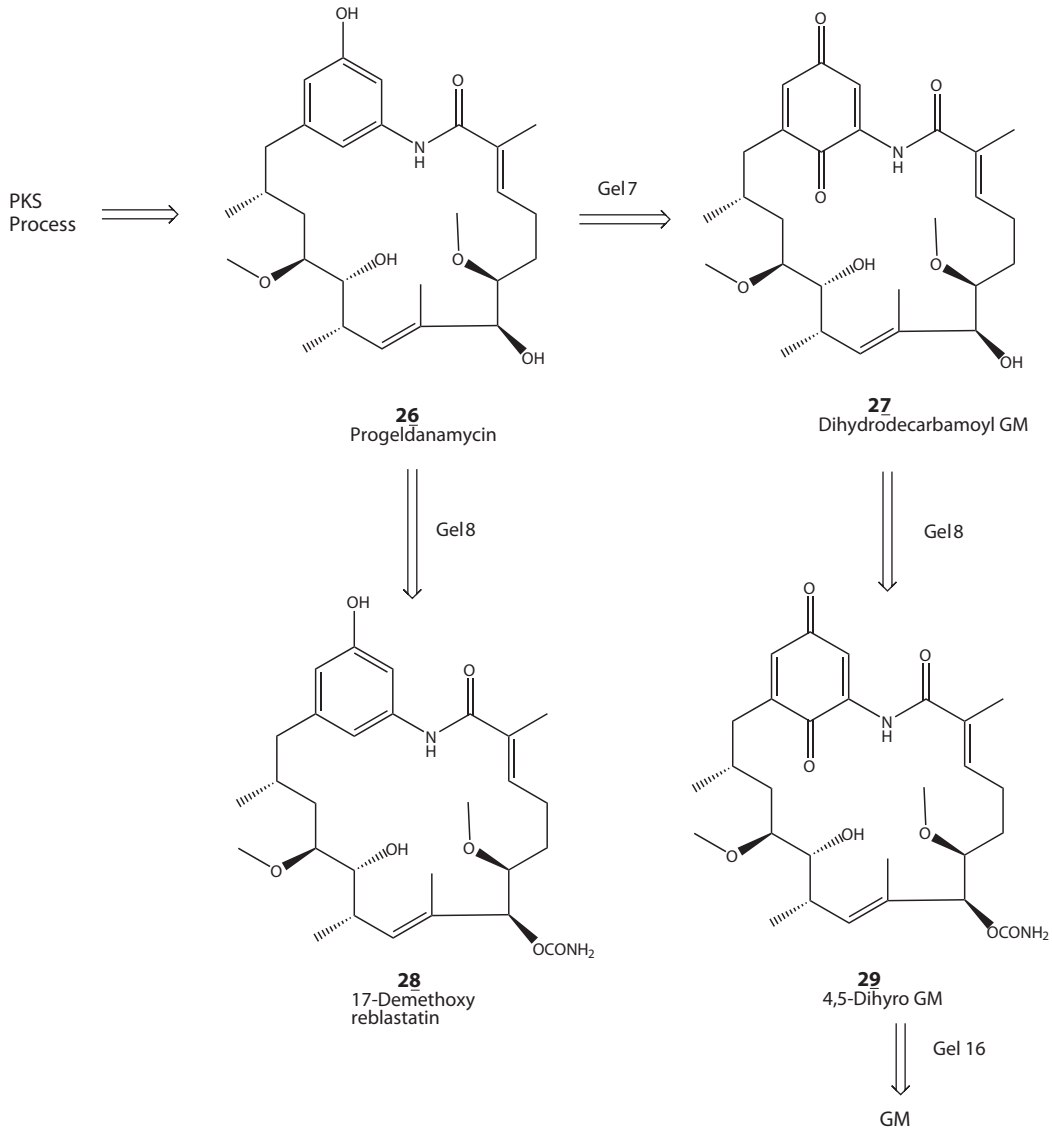

FIGURE 18.9 Products of manipulation of the post-PKS genes of GM-producing *S. hygroscopicus*.

comparing the binding with yeast Hsp90, both **30** and **31** showed strong binding. Superimposition of the x-ray crystal of Hsp90 bound **30** and macbecin showed negligible differences. Preliminary *in vivo* studies showed no toxicity for **30** at 250 mg/kg/day while macbecin was toxic at 10–20 mg/kg/day. They also reported equivalent *in vivo* tumor efficacy at 1/3 the MTD of 29 (85 mg/kg) when compared with 17-AAG at its MTD of 50 mg/kg. Further development of **30** is proposed.

Most recently,[32] a group from KRIBB also reported on extension of their studies to the production of C15 modified GMs. They examined the PKS biosynthesis sequences, specifically using site-directed mutagenesis on DH1, the first step in chain elongation. As others have reported, they also identified seven modules encoded by three genes in their *S. hygroscopicus* strain. They also confirmed that the three genes (gel A–C) assemble the polyketide precursor and then an amide synthase closes the macrolactam to produce progeldanamycin. They disrupted the DH1 domain by a single amino acid substitution and their mutations produced **32** and **33**. Further introduction of double mutations in gel 7 and

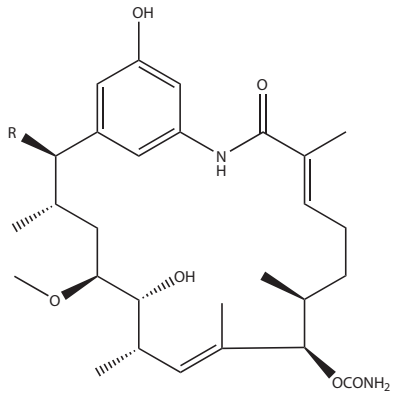

	R	IC_{50}(mM)	K_D(nM)
30	H	0.02	3
31	OH	3.79	6
Macbecin		0.02	5

FIGURE 18.10 New non-quinone macbecin analogs formed by manipulation of the macbecin gene cluster in *Actinosynnema pretiosum*.

gel 8 (post-PKS) produced two additional compounds, **34** and **35**. Mutation in gel 7 alone produced **34** while disruption of gel 7 and gel 8 produced the decarbamoyl **35** (Figure 18.11).

When evaluated for binding to yeast Hsp90, compounds **32**, **33**, and **35** were inactive up to 50 μM. Compound **34**, however, showed an IC_{50} of 0.7 μM versus GM alone whose IC_{50} was 3.2 μM, a 40-fold improvement in binding. No cytotoxicity data were reported.

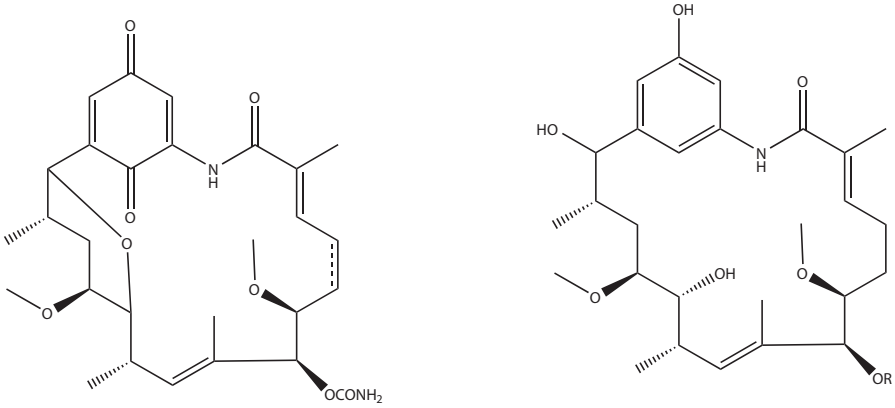

			R
32	DHQ1	4,5-Dihydro	
33	DHQ2	4,5-Unsaturated	
34	DHQ3		$CONH_2$
35	DHQ4		H

FIGURE 18.11 C15 modified GMs produced by site-directed mutagenesis of the DH1 domain of the PKS gene cluster from *S. hygroscopicus*.

18.3.4 Synthetic and Semisynthetic Products

In the previous review,[3] there were several total syntheses reported for BAs. Since then, only one additional synthesis has been reported and that was undertaken because the target, reblastatin (**4**), has several unique chemical features that make it an attractive drug candidate compared with the other BAs, macbecin or herbimycin. Reblastatin is not a benzoquinone but rather an aromatic phenol and does not contain the C2–C5 dieneoate embedded within the ansa ring. Therefore, the group at Boston University reported the first enantioselective synthesis of reblastatin.[33]

The C1–C7 fragment was prepared from the available chiral lactone **36** by conversion to the aldehyde, chain extension with the appropriate Wittig reagent to add the C1–C3 of the ansa chain and then conversion of the blocked diol to the methoxyaldehyde **37** by Meerwein alkylation and gentle oxidation (Figure 18.12).

For a convergent synthesis, the C8–C21 chain was constructed from the benzaldehyde, **38** through the application of two crotylation additions to produce syn-homoallylic alcohols with appropriate stereochemistry. Thus **38** was coupled to the *R*,*R*-crotylsilane to give the alcohol, **39**. The benzylic alcohol was removed by ionic deoxygenation and then further modified to give the aldehyde, **40**. A second crotylation with the *S*,*S*-crotylboronate, **41**, gave the syn-homoallylic alcohol, **42**. Chain extension of MOM-protected intermediates then gave the synthon, **43**, ready for convergent synthesis (Figure 18.13).

Coupling the two synthons **37** and **43** was accomplished by hydrozirconation with Cp_2ZrHCl to give the secoester **44** with only slight epimerization at C10.

Ring closure was effected with cuprous iodide after converting **44** to the amide. Deblocking and conversion to the carbamate ultimately produced reblastatin (**4**). The overall process was achieved in 25 steps and offers ample opportunity for modification of the ansa ring in unique ways (Figure 18.14).

In a more traditional approach, a group at Kosan reexamined the sensitivity of GM to nucleophiles.[34] They prepared over 60 substitutions at C17 to complete their studies on 17-AAG and 17-DMAG and its susceptibility for nucleophillic substitution of the 17-methoxy group of GM. This was considered important because the co-crystallization x-ray examination of 17-DMAG with Hsp90 showed that the C17 position is not protected but is solvent exposed, leaving it vulnerable to nucleophillic displacement.

The various derivatives were evaluated for cytotoxicity and for binding to Hsp90. In summary, the most attractive analog was 17-DMAG. However, several important observations were made from the study. First, the treatment of GM with sterically hindered secondary amines such as *N*,*N*,*N*′-trimethylethylene diamine gave exclusively the C19-substituted product. Secondly, there was a substantial discrepancy between *in vitro* cytotoxicity against SKBr3 cells and Hsp90 binding. They attribute this to the importance of pharmacokinetics citing the observation that GM tends to accumulate in the cytosol at concentrations up to 100-fold greater than extracellular concentrations. Third, in agreement with earlier reports,[35] the cytotoxicity diminished rapidly for amines with bulk-

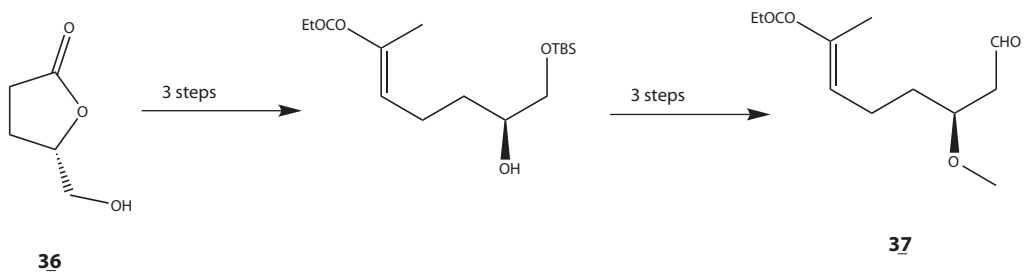

FIGURE 18.12 Synthesis of the C1-C7 fragment **37** of reblastatin.

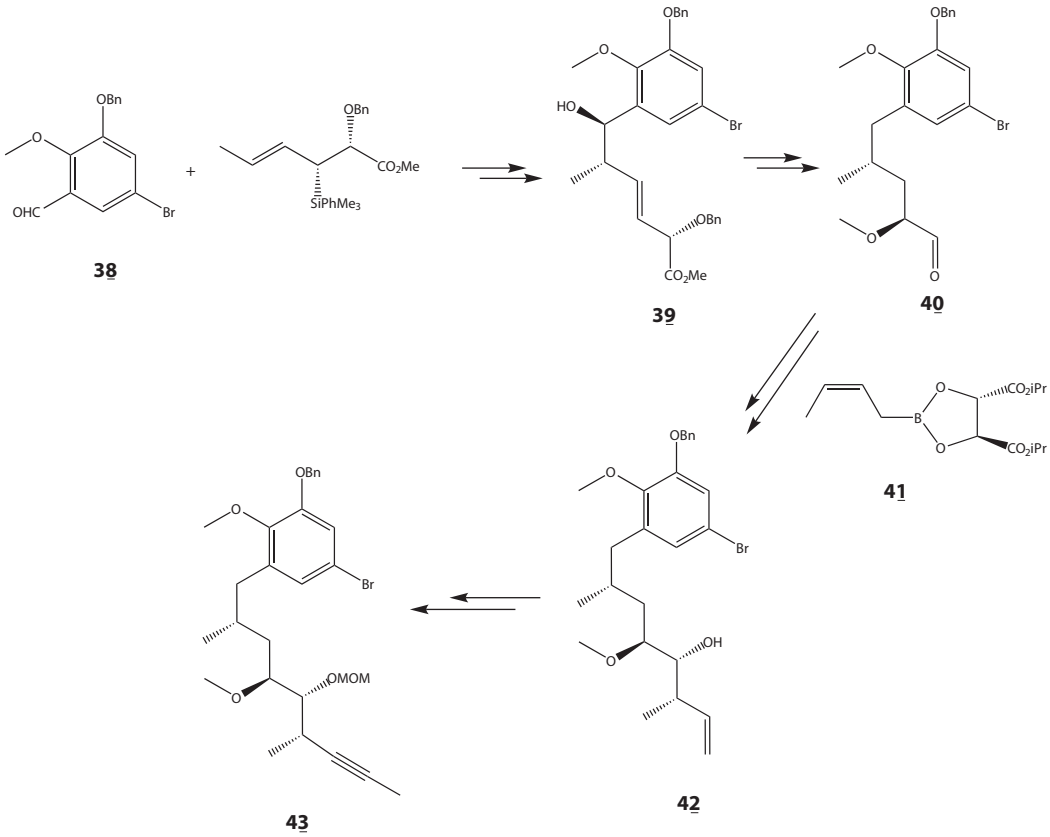

FIGURE 18.13 Synthesis of the C8-C21 chain synthon **43** of reblastatin.

ier substituents, even though Hsp90 binding remained high. Overall, they found more than 20 amino analogs with IC_{50} against SKBr3 of <100 nM, which compares favorably with 17-AAG (IC_{50} = 33 nM) and 17-DMAG (IC_{50} = 24 nM).

In a later report,[36] the same group reported on their modifications of the C11 site of GM. They found that the C11 hydroxyl of either GM or 17-AAG can be selectively alkylated using the Meerwein salt and the proton sponge, 1,8-bis-(dimethylamino)naphthalene. Similarly, the C11

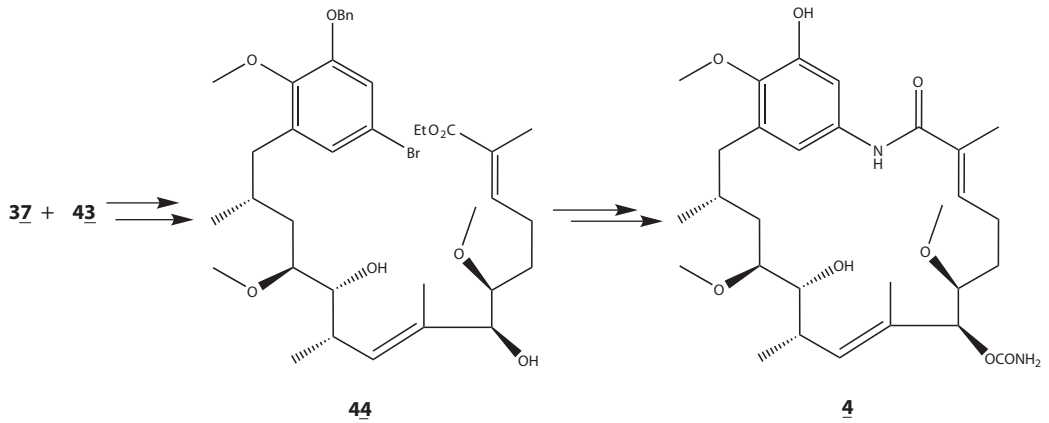

FIGURE 18.14 Completion of the convergent synthesis of reblastatin.

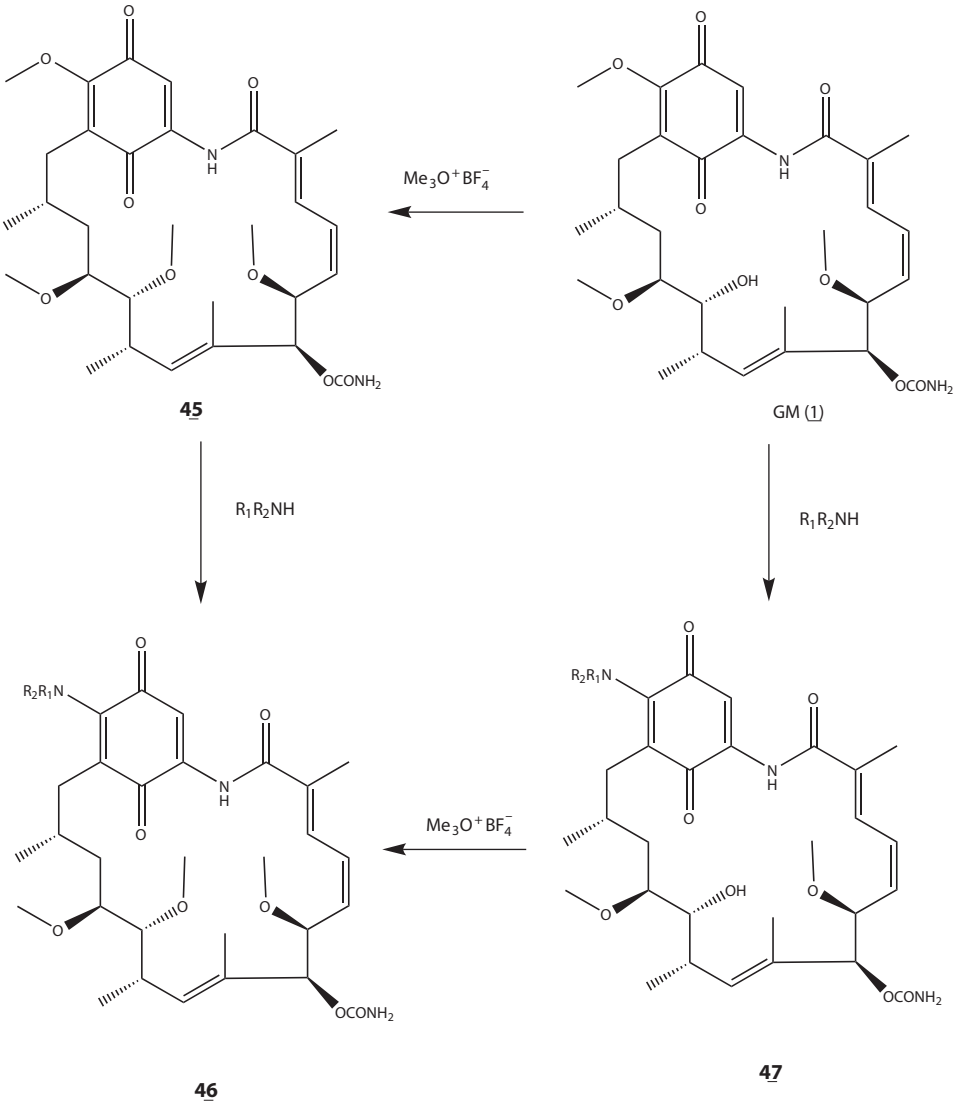

FIGURE 18.15a Modifications of the C11 site of GM.

hydroxyl of 17-aminogeldanamycins (**47**) can readily be acylated to form esters (**48**), carbazates (**49**), or, by oxidation, ketones (**50**), which can then be converted to amines (**51**) or oximes as shown in Figure 18.15a and b.

They report having prepared over 250 analogs and evaluating these for cytotoxicity against SKBr3 cells and binding affinity to Hsp90. Several conclusions were reported. Converting C11 to the methyl ether does not significantly reduce binding to Hsp90 nor the cytotoxicity. However, bulkier ethers do. They postulated that this is because the C11 methoxy can still bind to the Lys58 of Hsp90 while bulkier groups interfere with this binding. Secondly, C11 ketones or oximes have significantly reduced binding to Hsp90 and subsequently reduced cytotoxicity. C11 esters lost binding almost totally, but the readily hydrolyzable esters still showed some degree of cytotoxicity. Interestingly, the C11 carbazate showed reasonable but diminished binding to Hsp90, $K_D = 5\ \mu M$

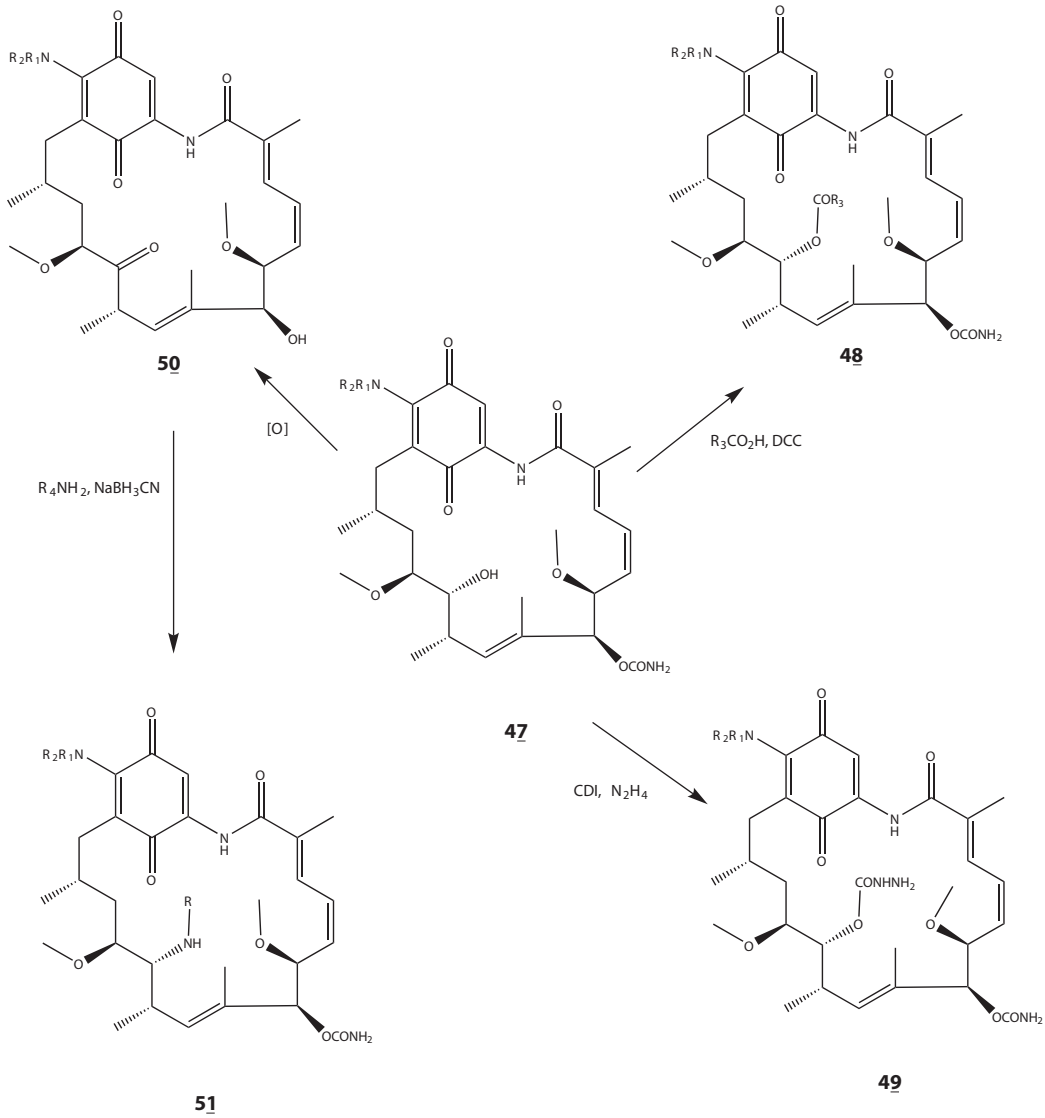

FIGURE 18.15b Further modifications of the C11 site of GM.

versus $K_D = 0.5\ \mu M$ for 17-DMAG. However, the carbazate showed no cytotoxicity once again pointing out the significance of pharmacokinetics.

Using a semisynthetic approach, a group from Conforma Therapeutics prepared a series of 17-amidates using a three-step sequence on the primary metabolite of GM, 17-AG.[37] First was reduction to the hydroquinone, followed by acylation, and then gentle reoxidation to the quinone with Cu^{2+} to give **52** (Figure 18.16).

The group reported over 25 analogs and evaluated them for biological activity in three assays: (a) a Her-2 degradation assay in MCF7 tumor cells (one of the effects of inhibiting the ATPase activity of Hsp90), (b) a competitive binding assay with recombinant Hsp90 using biotinylated GM, and (c) cytotoxicity against MCF7 tumor cells. Interesting candidates were further evaluated *in vivo* against mouse xenografts. They identified two products as their most interesting candidates, **52a** and **52b**. While they were substantially less active in the Her-2 assay, they exhibited good binding to rHsp90

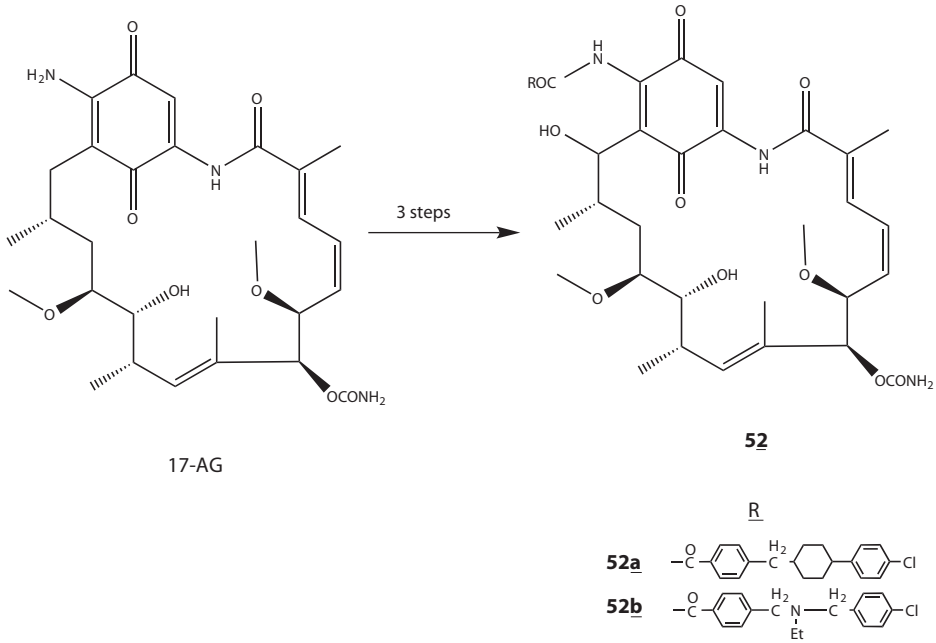

FIGURE 18.16 Preparation of GM 17-amidates.

(IC_{50} ~ 1 μM) as well as lysate Hsp90. These compounds also had good cytotoxic effects against MCF7 *in vitro* with IC_{50} values of 0.15 and 0.2 μM, respectively. Subsequent *in vivo* testing showed activity at 20 mg/kg and further development is reported underway.

In an effort to improve drug delivery to cells, a group from Ohio State University prepared a series of C17 adducts that terminated in a carbohydrate.[38] The objective was to deliver a GM prodrug with a bulky substituent at C17 that would not bind to Hsp90 unless the appropriate enzyme for sugar cleavage was delivered via the ADEPT (antibody-directed enzyme prodrug therapy) technique. Suitably blocked sugars were converted to the trichloroacetamidate as illustrated in Figure 18.17 with glucose.

Subsequent conversion to the amine **53** then gave a suitable precursor for nucleophillic attack on GM to produce the prodrug **54**. Three different sugars were incorporated: glucose, galactose, and lactose. Several lengths of linkers were also examined and the two carbon spacer was optimal. As a control, it was shown that the glucose conjugate showed good activity against a panel of four cancer cell lines with IC_{50}s ranging from 0.07 to 0.75 μM as expected due to the ubiquitous presence of glucosidase in cells. Similarly, the galactose and lactose conjugates were inactive *in vitro*, unless β-galactosidase was added to the culture fluid. Unfortunately, there were no data presented on the actual ADEPT experiment.

In another clever manipulation to improve the insolubility problems of GMs, a group from Infinity Pharmaceuticals[39] recognized that the C17 amino group could be made basic enough to form stable salts if the benzoquinone was reduced to a hydroquinone. They subsequently converted 17-AAG to the new hydroquinone, hydrochloride (**55**), which they have named IPI-504 (Figure 18.18). They also performed the same conversion on the metabolites 17-AG and the diol of 17-AG. When they compared the binding with Hsp90 or canine Grp94, the binding was almost twofold stronger for the hydroquinone and virtually the same for the metabolites. The hydroquinone IPI-504 was also shown to be present at about 60% throughout the duration time of the

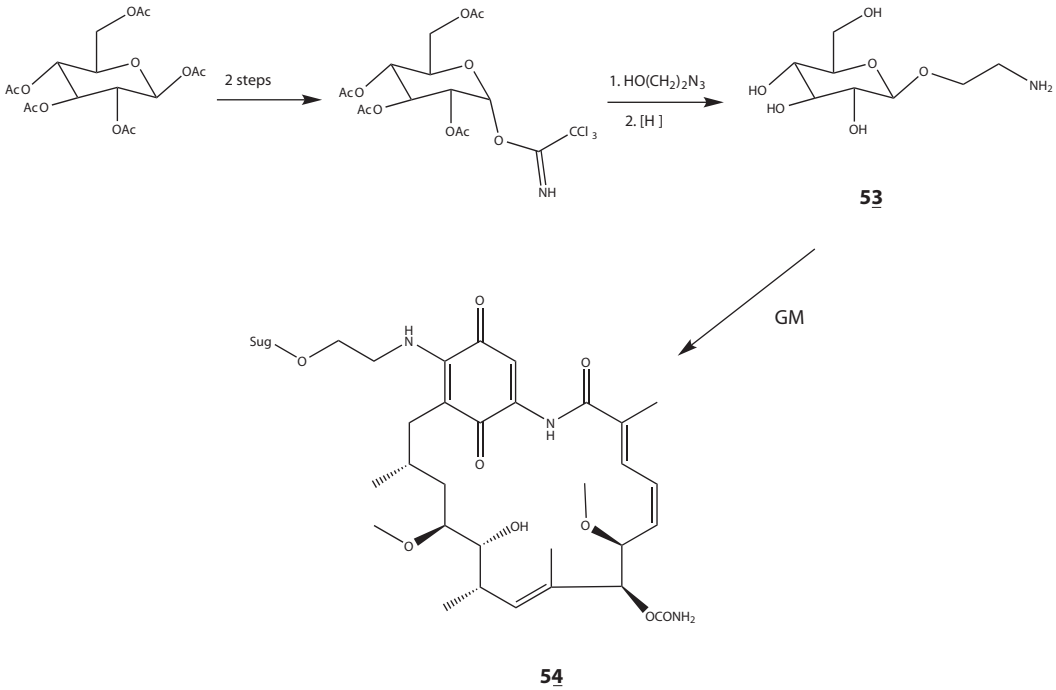

FIGURE 18.17 Preparation of C17 carbohydrate-geldanamycin conjugates.

assay. There was also good correlation between apparent binding efficiency and *in vitro* cytotoxicity. IPI-504 is currently in clinical trials.[4]

Similarly, a group from Johnson & Johnson studied the binding of GM and 17-AAG in the quinone and hydroquinone forms.[27] They found a 40-fold increase in binding for dihydrogeldanamycin vs. GM (K_D: 3 and 143 nM, respectively) and a similar increase for dihydro-17-AAG versus its quinone (K_D: 50 and 2000 nM, respectively). Various reducing agents gave similar results. They also observed that approximately 68% of labeled 17-AAG was found as dihydroquinone in MCF7 cells.

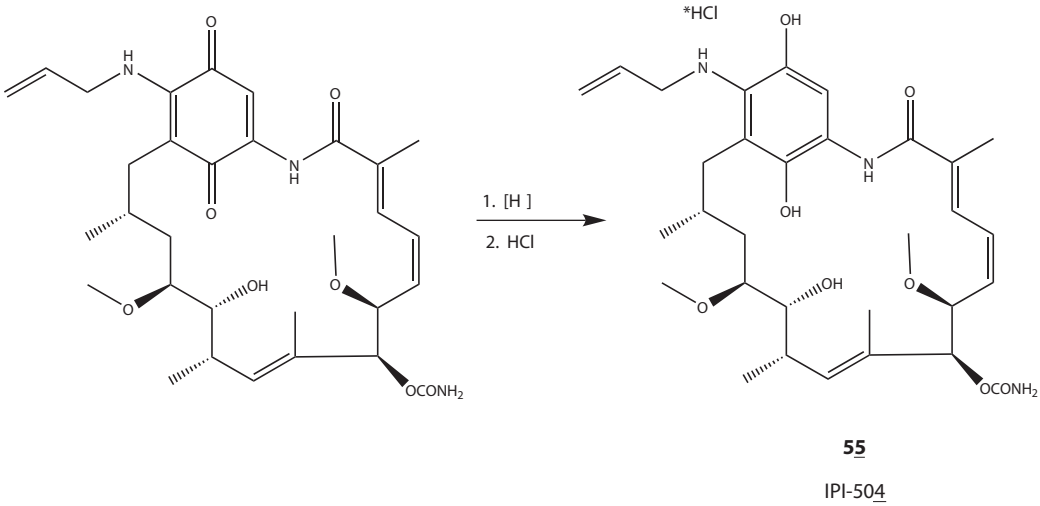

FIGURE 18.18 Synthesis of hydroquinone derivative of 17-amino-17-demethoxygeldanamycin, IPI504.

They propose that this increased hydroquinone binding affinity contributes to the preferential accumulation of 17-AAG in tumor tissue *in vivo*.

Recently, a group from Chulalongkorn University studied the neurotrophic and neuroprotective effects of a series of GM analogs.[40] They obtained their starting materials from a new mangrove-harvested *Streptomyces* sp. They isolated GM, 17-hydroxygeldanamycin, and its hydroquinone. A series of C17 and C19 derivatives were prepared by nucleophillic displacement on GM using either a group of alkoxides to C17 or C17, C19 bisalkoxy GMs. Using several alkyl amines, they were also able to prepare similar C17 or C17, C19 bisalkylamino derivatives, most of which have been previously reported. These were studied for their neurotoxic or neuroprotective effects on cultured P19-derived neurons. Virtually all of the alkylamino GMs showed neurotoxicity based on a loss of cell viability while the monoalkoxy GMs showed slight increases in viability at 1 nM concentrations. Further testing showed that they all exhibited cytotoxicity against P19-derived neurons *in vitro* when concentrations were increased above 1 μM.

Only **56e** (Figure 18.19) showed no neurotoxicity or cytotoxicity at concentrations up to 1 μM. Additionally, it promoted cell viability when dosed at 1 nM on cells that were co-treated with paclitaxel at its toxic dose. In this case, there was actually an increase of cell viability to 120%. The authors do not offer an explanation for this neuroprotective activity but are undertaking further investigation.

18.3.5 Nonansamycin Products

Finally, it should be noted that the discovery of inhibition of Hsp90 by BAs has encouraged the search for other molecules that bind and inhibit Hsp90. In the previous review radicicol, a group of purines labeled PU3 and two chromones were noted as research discoveries. With the increased availability of binding assays, this pool of new therapeutic leads has grown markedly. Two excellent reviews of these new candidates have been published and are recommended,[4,5] since they emphasize these other molecular classes which are not based on the ansamycin structure. The various groups in which Hsp90 inhibition has been discovered include purines, resorcinols (radicicol, pocchonin, etc.), coumermycins, derrubone, gedunin, and celastrol.

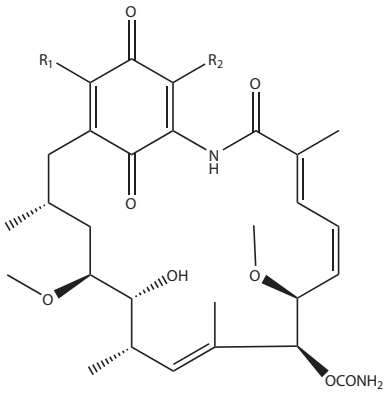

	R1	R2
56a (1, GM)	OMe	H
56b	OEt	H
56c	OPr	H
56d	OCH2Ph	H
56e	OMe	OMe

FIGURE 18.19 C17-alkloxy and C17, C19-bisalkoxy GMs.

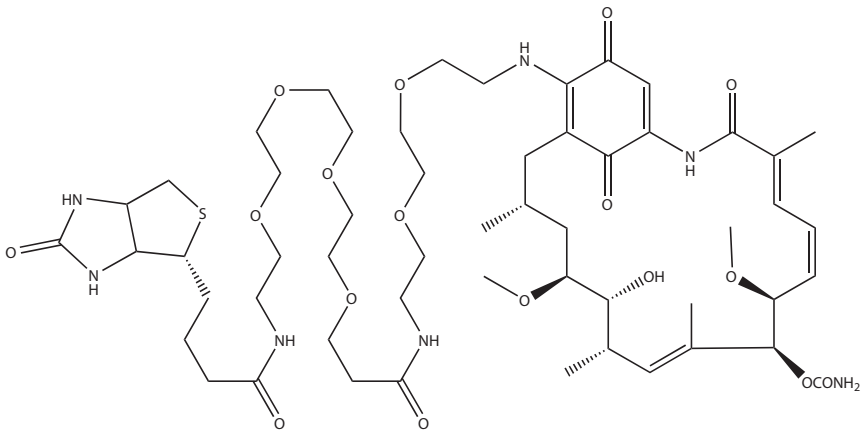

57

FIGURE 18.20 Biotinylated GM derivative.

18.3.6 Metabolic Studies

It was noted earlier that 17-AG and the glycol of 17-AAG are the two major metabolites formed from GM and 17-AAG.[39] In order to study metabolism further, the biotinylated derivative of GM was prepared and characterized.[41] They were looking for additional proteins that bind GM and prepared a series of four photolabile and four nonphotolabile derivatives. Compound **57** (Figure 18.20) had the optimal tether length to capture and release Hsp90.

Using this probe, they examined Jurkat A3 cell lysate and found several proteins that bind and release the probe. Further work to identify these proteins is ongoing.

In an attempt to further understand the metabolic elimination of GM and 17-AAG, the group at U.S. FDA studied the reaction of GM with the thiol group of glutathione.[42] They demonstrated that addition occurred to form the C19 adduct and they evaluated the kinetics for the reaction. They propose that this is a major defensive pathway since preincubation of GMs with sulfhydril containing compounds deactivates their cytotoxicity.

18.4 CLINICAL TRIALS

Original clinical trials of GM were abandoned due to hepatotoxicity and poor delivery systems.[43] The current status of clinical trials can be obtained from the government website (http://clinicaltrials.gov) which, at the time of this writing, indicated that there are nine current trials with tanespimycin (17-AAG). Seven have been completed,[44] one dose escalation trial was terminated due to toxicity, and one, directed at patients with advanced solid tumors or non-Hodgkin's lymphoma, is still active but not recruiting any additional patients.

Of more interest now are the current trials of retaspimycin (IPI-504), which is the water-soluble salt of dihydro-17-AAG. An Expert Opinion review has recently been published,[12] which summarized the advantages of this drug product. There are currently four ongoing phase I/II trials active as of October 2009 that are not recruiting or are closed. There are three additional phase I and II trials that are actively recruiting. In the summary, retaspimycin was shown to have its most promising effects in gastrointestinal stroma tumors (GIST) where they obtained a 70% disease control in a phase I dose escalation study. This prompted a phase III study on metastatic nonresectible GIST, resistant to imatinib or sunitinib but was terminated early due to observed toxicity. There are still

phase I and II trials underway for non-small-cell lung carcinoma and breast cancers. Future trials are planned based on the positive activity observed against diffuse large B-cell lymphoma, mantle cell lymphoma, melanoma, leukemia, and pancreatic cancers. Additionally, combination trials with paclitaxel are still in progress. While retaspimycin still retains toxicity problems, it is currently the best clinical trials candidate.

REFERENCES

1. DeBoer, C., Muelman, P.A., Wnuk, R.J., and Peterson, D.H., Geldanamycin, a new antibiotic, *J. Antibiot. (Tokyo)*, 23, 442, 1970.
2. Whitesell, L., Mimnaugh, E.G., DeCosta, B., Myers, C.E., and Neckers, L.M., Inhibition of heat shock protein Hsp90-ppv60v-src heteroprotein complex formation by benzoquinone ansamycins, *Proc. Natl. Acad. Sci. USA*, 91, 8324, 1994.
3. Snader, K.M., Benzoquinone ansamycins, in *Anticancer Agents from Natural Products*, Cragg, G.M., Kingston, D.G.I., and Newman, D.J., Eds., Taylor and Francis, Boca Raton, 2005, chap. 18.
4. Amolins, M.W. and Blagg, B.S.J., Natural product inhibitors of Hsp90: Potential leads for drug discovery, *Mini Rev. Med. Chem.*, 9, 140, 2009.
5. Drysdale, M.J. and Brough, P.A., Medicinal chemistry of Hsp90 inhibitors, *Curr. Top. Med. Chem.*, 8, 859, 2008.
6. Driggers, E.M., Hale, S.P., Lee, J., and Terrett, N.K., The exploration of macrocycles for drug discovery—An underexploited structural class, *Nat. Rev. Drug Discov.*, 7, 608, 2008.
7. Lancini, G. and Parenti, F., *Antibiotics: An Integrated View*, Springer-Verlag, New York, 1982, chap. 5.
8. Roe, S.M., Prodromou, C., O'Brien, R., Ladbury, J.E., Piper, P.W., and Pearl, L.H., Structural basis for inhibition of the Hsp90 molecular chaperone by the antitumor antibiotics radicicol and geldanamycin, *J. Med. Chem.*, 42, 260, 1999.
9. Jez, J.M., Chen, J.C., Rastelli, G., Stroud, R.M., and Santi, D.V., Crystal structure and molecular modeling of 17-DMAG in complex with human Hsp90, *Chem. Biol.*, 10, 361, 2003.
10. Martin, C.J., Gaisser, S., Challis, I.F., Carletti, I., Wilkinson, B., Gregory, M., Prodromou, C. et al., Molecular characterization of Macbecin as an Hsp90 inhibitor, *J. Med. Chem*., 51, 2853, 2008.
11. Taldone, T., Sun, W., and Chiosis, G., Discovery and development of heat shock protein 90 inhibitors, *Bioorg. Med. Chem.*, 17, 2225, 2009.
12. Hanson, B.E. and Vesole, D.H., Retaspimycin hydrochloride (IPI-504): A novel heat shock protein inhibitor as an anticancer agent, *Expert Opin. Investig. Drugs*, 18, 1375, 2009.
13. Neckers, L.M., Schulte, T.W., and Mimnaugh, E., Geldanamycin as a potential anticancer agent: Its molecular target and biochemical activity, *Investig. New Drugs*, 17, 361, 1999.
14. Picard, D., Hsp90 interactors, http://www.picard.ch/downloads (accessed in May 2011).
15. (a) Workman, P., Combinatorial attack on multistep oncogenesis by inhibiting the Hsp90 molecular chaperone, *Cancer Lett.*, 206, 149, 2004; (b) Workman, P., Burrows, F., Neckers, L., and Rosen, N., Combinatorial therapeutic exploitation of oncogene addictin and tumor stress, *Ann. N. Y. Acad. Sci.*, 1113, 202, 2007.
16. Hosoi, T., Hyoda, K. Okuma, Y., Nomura, Y., and Ozawa, K., Geldanamycin induces CHOP expression through a 4-(2-aminoethyl)-benzenesulfonyl fluoride-responsive serine protease, *Cell Res.*, 17, 184, 2007.
17. Pedersen, N.M., Madshus, I.H., Haslekas, C., and Stang, E., Geldanamycin-induced down-regulation of ErbB2 from the plasma membrane is Clathrin dependent but proteasomal activity independent, *Mol. Cancer Res.*, 6, 491, 2008.
18. Takatsu, T., Ohtsuki, M., Muramatsu, A., Enokita, R., and Kurakata, S., Reblastatin, a novel benzenoid ansamycin-type cell cycle inhibitor, *J. Antibiot.*, 53, 1310, 2000.
19. Stead, P., Latif, S., Blackaby, A.P., Sidebottom, P.J., Deakin, A., Taylor, N.L., Life, P. et al., Discovery of novel ansamycins possessing potent inhibitory activity in a cell-based Oncostatin M signalling assay, *J. Antibiot.*, 53, 657, 2000.
20. Li, M.G., Wu, S.H., Zhao, L.X., Zhang, Q., Li, W.J., Cui, Z.L., Xu, L.H., Wu, D.G., and Jiang, C.L., Isolatin and structure elucidation of Autolytimycin, a new compound produced by *Streptomyces autolyticus* JX-47, *Chin. Chem. Lett.*, 12, 903, 2001.

21. Rascher, A., Hu, Z., Viswanathan, N., Schirmer, A., Reid, R., Nierman, W.C., Lewis, M., and Hutchinson, C.R., Cloning and characterization of a gene cluster for geldanamycin production in *Streptomyces hygroscopicus* NRRL 3602, *FEMS Microbiol. Lett.*, 218, 223, 2003.
22. Eichner, S., Floss, H.G., Sasse, F., and Kirschning, A., New, highly active nonbenzoquinone geldanamycin derivatives by using mutasynthesis, *ChemBioChem*, 10, 1801, 2009.
23. Menzella, H.G., Tran, T.-T., Carney, J.R., Lau-Wee, J., Galazzo, J., Reeves, C.D., Carreras, C. et al., Potent non-benzoquinone ansamycin Heat Shock Protein 90 inhibitors from genetic engineering of *Streptomyces hygroscopicus*, *J. Med. Chem.*, 52, 1518, 2009.
24. Guo, W., Reigan, P., Siegel, D., Zirrolli, J., Gustafson, D., and Ross, D., Formation of 17-allylamino-dethoxygeldanamycin (17-AAG)hydroquinone by NAD(P)H:quinone oxidoreductase 1: Role of 17-AAG hydroquinone in heat shock protein 90 inhibition, *Cancer Res.*, 65, 10006, 2005.
25. Guo, W., Riegen, P., Siegel, D., Zirrolli, J., Gustafson, D., and Ross, D., The bioreduction of a series of benzoquinone ansamycins by NAD(P)H:quinone oxidoreductase 1 to more potent heat shock protein 90 inhibitors, the hydroquinone ansamycins, *Mol. Pharmacol.*, 70, 1194, 2006.
26. Kelland, L.R., Sharp, S.Y., Rogers, P.M., Myers, T.G., and Workman, P., DT-Diaphorase expression and tumor cell sensitivity to 17-allylamino, 17-demethoxygeldanamycin, an inhibitor of heat shock protein 90, *J. Natl. Cancer Inst.*, 91, 1940, 1999.
27. Maroney, A.C., Marugan, J.J., Mezzasalma, T.M., Barnakov, A.N., Garrabrant, T.A., Weaner, L.E., Jones, W.J., Barnakova, L.A., Koblish, H.K., Todd, M.J., Masucci, J.A., Deckman, I.C., Galemmo Jr., R.A., and Johnson, D.L., Dihydroquinone ansamycins: Toward resolving the conflict between low in vitro affinity and high cellular potency of geldanamycin derivatives, *Biochemistry*, 45, 5678, 2006.
28. Kim, W., Lee, J.S., Lee, D., Cai, Z.F., Shin, J.C., Lee, K., Lee, C.-H. et al., Mutasynthesis of Geldanamycin by the disruption of a gene producing starter unit: Generation of structural diversity at the benzoquinone ring, *ChemBioChem*, 8, 1491, 2007.
29. Patel, K., Piagentini, M., Rascher, A., Tian, Z.-Q., Buchanan, G.O., Regentin, R., Hu, Z., Hutchinson, C.R., and McDaniel, R., Engineered biosynthesis of Geldanamycin analogs for Hsp90 inhibition, *Chem. Biol.*, 11, 1625, 2004.
30. Shin, J.C., Na, Z., Lee, D., Kim, W., Lee, K., Shen, Y.-M., Paik, S.-G., Hong, Y.-S., and Lee, J.J., Characterization of tailoring genes involved in the modification of geldanamycin polyketide in *Streptomyces hygroscopicus* JCM4427, *J. Microbiol. Biotechnol.*, 18, 1101, 2008.
31. Zhang, M.-Q., Gaisser, S., Nur-E-Alam, M., Sheehan, L.S., Vousden, W.A., Gaitatzis, N., Peck, G. et al., Optimizing natural products by biosynthetic engineering: Discovery of nonquinone Hsp90 inhibitors, *J. Med. Chem.*, 51, 5494, 2008.
32. Kim, W., Lee, D., Hong, S.S., Na, Z., Shin, J.C., Roh, S.H., Wu, C-Z. et al., Rational biosynthetic engineering for optimization of geldanamycin analogues, *ChemBioChem*, 10, 1243, 2009.
33. Wrona, I.E., Gabarda, A.E., Evano, G., and Panek, J.S., Total synthesis of Reblastatin, *J. Am. Chem. Soc.*, 127, 15026, 2005.
34. Tian, Z.-Q., Liu, Y., Zhang, D., Wang, Z., Dong, S.D., Carreras, C.W., Zhou, Y., Rastelli, G., Santi, D.V., and Myles, D.C., Synthesis and biological activities of novel 17-aminogeldanamycin derivatives, *Bioorg. Med. Chem.*, 12, 5317, 2004.
35. Schnur, R.C., Corman, M.L., Gallaschun, R.J., Cooper, B.A., Dee, M.F., Doty, J.L., Muzzi, M.L. et al., Inhibition of the oncogene product p185erbB-2 *in vitro* and *in vivo* by geldanamycin and dihydrogeldanamycin derivatives, *J. Med. Chem.*, 38, 3806, 1995.
36. Tian, A.-Q., Wang, Z., MacMillan, K.S., Zhou, Y., Carreras, C.W., Mueller, T., Myles, D.C., and Liu, Y., Potent cytotoxic C-11 modified geldanamycin analogues, *J. Med. Chem.*, 52, 3265, 2009.
37. Le Brazidec, J.-Y., Lamal, A., Busch, D., Thao, L., Zhang, L., Timony, G., Grecko, R. et al., Synthesis and biological evaluation of a new class of Geldanamycin derivatives as potent inhibitors of Hsp90, *J. Med. Chem.*, 47, 3865, 2004.
38. Cheng, H., Cao, X., Xian, M., Fang, L., Cai, T.B., Ji, J.J., Tunac, J.B., Sun, D., and Wang, P.G., Synthesis and enzyme-specific activation of carbohydrate-geldanamycin conjugates with potent anticancer activity, *J. Med. Chem.*, 48, 645, 2005.
39. Ge, J., Normant, E., Porter, J.R., Ali, J.A., Dembski, M.S., Gao, Y., Georges, A.T. et al., Design, synthesis, and biological evaluation of hydroquinone derivatives of 17-amino-17-demoethoxygeldanamycin as potent, water-soluble inhibitors of Hsp90, *J. Med. Chem.*, 49, 4606, 2006.
40. Tadtong, S., Meksuriyen, D., Tanasupawat, S., Isobe, M., and Suwanborirux, K., Geldanamycin derivatives and neuroprotective effect on cultured P19-derived neurons, *Bioorg. Med. Chem. Lett.*, 17, 2939, 2007.

41. Clevenger, R.C., Raibel, J.M., Peck, A.M., and Blagg, B.S.J., Biotinylated Geldanamycin, *J. Org. Chem.*, 69, 4375, 2004.
42. Cysyk, R.L., Parker, R.J., Barchi Jr., J.J., Steeg, P.S., Hartman, N.R., and Strong, J.M., Reaction of geldanamycin and C17-substituted analogues with glutathione: Product identifications and pharmacological implications, *Chem. Res. Toxicol*., 19, 376, 2006.
43. Supko, J.G., Hickman, R.L., Grever, M.R., and Malspeis, L., Preclinical pharmacological evaluation of geldanamycin as an antitumor agent, *Cancer Chemother. Pharmacol.*, 36, 305, 1995.
44. Sausville, E.A., Tomaszewski, J.E., and Ivy, P., Clinical development of 17-allylamino-17-demethoxygeldanamycin, *Curr. Cancer Drug Targets*, 3, 377, 2003.

19 Bleomycin Group Antitumor Agents

Sidney M. Hecht

CONTENTS

19.1 Introduction 451
19.2 Mechanism of Action 453
19.2.1 BLM Activation 453
19.2.2 DNA Binding and Degradation 453
19.2.2.1 Chemistry of DNA Degradation 453
19.2.2.2 Modes of DNA Binding 455
19.2.2.3 DNAs Strongly Bound by BLM 456
19.2.3 RNA Degradation 458
19.2.3.1 Transfer RNAs and tRNA Precursor Transcripts 458
19.2.3.2 Other RNA Substrates for BLM 459
19.2.3.3 Chemistry of RNA Cleavage 460
19.2.4 Protein Synthesis Inhibition and Antiviral Properties 460
19.3 Biosynthesis 461
19.4 Development of BLMs as Novel Antitumor Agents 461
19.5 Synthesis and Structure–Activity Studies 464
19.5.1 Solution- and Solid-Phase Syntheses 464
19.5.2 Study of Individual "Amino Acid" Constituents 466
19.5.2.1 Bithiazole Moiety and C-Substituent 466
19.5.2.2 Linker Domain 467
19.5.2.3 Metal-Binding Domain 468
19.5.3 Newly Reported Analogs 468
19.5.4 BLM Combinatorial Library 468
19.6 Clinical Applications 469
19.7 Conclusions 470
Acknowledgment 470
References 470

19.1 INTRODUCTION

The bleomycins (BLMs) are a family of antitumor antibiotics first isolated from *Streptomyces verticillus* by Umezawa and colleagues.[1,2] As illustrated (Figure 19.1), the BLMs are glycosylated oligopeptides, having extensively modified amino acid constituents. Some of these are derived biosynthetically from proteinogenic amino acids such as the bithiazole moiety, which is formed by dehydrative cyclization and oxidation of β-alanylcysteinylcysteine.[3] However, more recent studies have revealed that the biosynthesis also depends in part on transformations used to assemble polyketide antibiotics,[4] and the biosyntheses of the BLM group antibiotics tallysomycin (TLM) and zorbamycin have also been reported recently.[5–9]

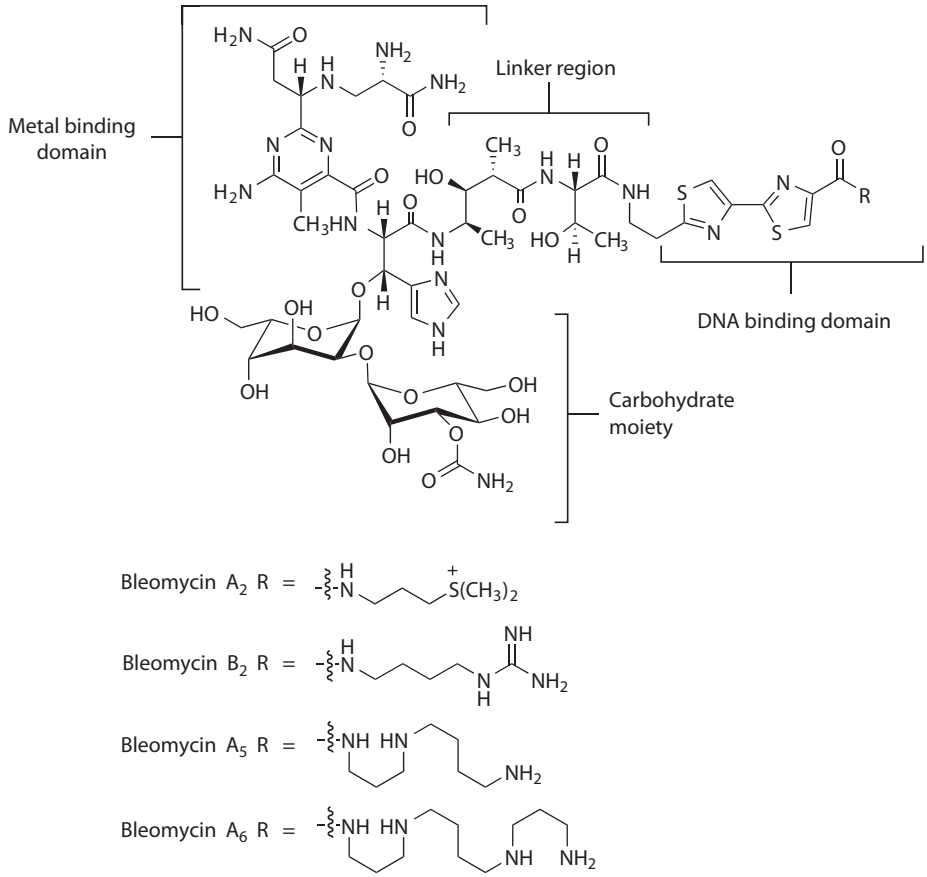

FIGURE 19.1 Structures of some naturally occurring BLMs.

The BLMs exhibit characteristic sequence-selective DNA binding and degradation properties, and this has long been thought to constitute the basis for the antitumor activity of this class of compounds. DNA affinity resides to a significant extent in the "tripeptide S"[10,11] portion of BLM, comprised of the contiguous threonine, bithiazole, and C-terminal moieties. The N-terminus of BLM consists of the pyrimidoblamic acid and glycosylated β-hydroxyhistidine moieties, which are responsible for metal chelation and oxygen activation. These domains also bind to DNA and actually constitute the primary determinant of the sequence selectivity of DNA cleavage by BLM.[12–15] The N- and C-terminal domains of BLM are connected by a linker, (2*S*, 3*S*, 4*R*)-4-amino-3-hydroxy-2-methylvaleric acid; it has been shown convincingly that this linker assumes a compact, folded structure that is essential for efficient sequence-selective DNA cleavage by BLM.[16,17]

While DNA cleavage by BLM has been studied extensively for some time, in the past few years there have been important insights into the nature of DNA binding. This has included x-ray crystallographic studies,[18] and studies with modified BLMs whose potential modes of action with DNA are limited structurally.[19] The emerging picture is that BLM may interact with DNA in multiple binding modes.[18–21] A further aspect of BLM–DNA interaction that has been studied is the nature of DNAs bound preferentially by BLM when DNA is in substantial excess,[22,23] a circumstance that likely reflects the situation in a therapeutic setting. Studies of RNA cleavage by BLM have also continued, and the identity of the transfer RNA that is the most sensitive to cleavage by activated Fe·BLM has been established.[24]

Finally, in a study that may prove to have important implications for the design of improved therapeutic agents, the carbohydrate moiety of BLM has been shown to be essential for the targeting of tumor cells.[25]

19.2 MECHANISM OF ACTION

Early mechanistic studies of BLM explored several biochemical effects of this class of compounds. However, the finding that BLM could mediate damage to DNA in cell-free systems[26,27] and in cultured cells[28–30] focused efforts on a detailed characterization of this process. More recently, it has been appreciated that certain RNAs are highly selective substrates for cleavage by BLM,[24,31–33] and RNA cleavage has continued to receive significant attention.

19.2.1 BLM Activation

The activation of BLM for the degradation of DNA and RNA can be accomplished by admixture of an aqueous solution of BLM with an Fe^{2+} salt and oxygen in the presence of a reductant, or else by treating BLM with Fe^{3+} + H_2O_2. While activated BLM, the last intermediate detected prior to DNA strand scission, has been considered to be a ferric–hydroperoxo complex (BLM–Fe^{III}–OOH)[34] based on analyses carried out by a number of techniques, there is still some question of whether the ferric–hydroperoxo complex is converted to some other species via (homolytic or heterolytic) O–O bond cleavage prior to the initiation of DNA strand scission. A recent study utilizing DFT (density functional theory) calculations has addressed this issue and concluded that heterolytic cleavage of the O–O bond, leading to what is formally a BLM–Fe^{V}=O species, should be facile.[35]

As noted above, the nature of the activated Fe·BLM has been the subject of considerable debate.[36] One useful insight derives from the observation that activated Fe·BLM mediates chemical transformations of small molecules in a fashion most similar to that of cytochrome P450 and its analogs.[37–39] This includes the oxidation/oxygenation of compounds such as stilbene and styrene, and the NIH shift of deuterium in *p*-deuterioanisole.[39] In further analogy with cytochrome P450 model compounds, Fe(III)·BLM can be activated with H_2O_2[40,41] and with oxygen surrogates such as periodate and iodosylbenzene.[39]

19.2.2 DNA Binding and Degradation

19.2.2.1 Chemistry of DNA Degradation

BLM-mediated DNA degradation requires a metal ion, which forms a complex with the N-terminal domain of BLM (cf., Figure 19.1). The first metalloBLM studied was Fe(II)·BLM,[42–44] but Cu(I)·BLM,[37,45] Mn(II)·BLM,[46,47] and VO(IV)·BLM[48] have also been shown to effect DNA degradation. Although not studied definitively, these metalloBLMs appear to effect DNA degradation in the same fashion as Fe(II)·BLM.

The chemistry of DNA degradation by activated Fe·BLM is sequence selective and involves primarily a subset of 5′-GT-3′ and 5′-GC-3′ sequences; it has been studied using DNA oligonucleotides containing a limited number of cleavage sites.[26] Two pathways for Fe·BLM-mediated DNA degradation have been defined. Shown in Figure 19.2 is a pathway that leads to frank DNA strand scission, illustrated using the self-complementary octanucleotide d(CGCTAGCG).[49] The substrate shown in Figure 19.2 was cleaved quite efficiently by activated Fe·BLM, and predominantly at the two 5′-GC-3′ sequences. The observed products, *trans*-3-(cytosin-1′-yl)propenal-(**I**), 5′-GMP (**II**), and a CpG derivative terminating at its 3′-end with a 3′-(phosphoro-2′-*O*-glycolate) moiety (**III**) (pathway a) were verified by comparison with authentic synthetic standards.[12,50] The yield of base propenal was approximately equal to the sum of the yields of **II** and **III**.[12,41] The mechanistic scheme shown in Figure 19.2 rationalizes the nature and amounts of products obtained. Initial abstraction of a H atom would afford a C-4′ deoxyribose radical that could combine with O_2 to form a C-4′ hydroperoxy radical. Reduction and protonation of this intermediate, or recombination with a H atom, would afford a transient C-4′ hydroperoxide, the latter of which would be expected to undergo a Criegee-type rearrangement with scission of the C3′–C4′ deoxyribose bond. Conversion of the resulting hemiacetal to the aldehyde, and elimination of elements of glycolic acid, would then afford the observed products.

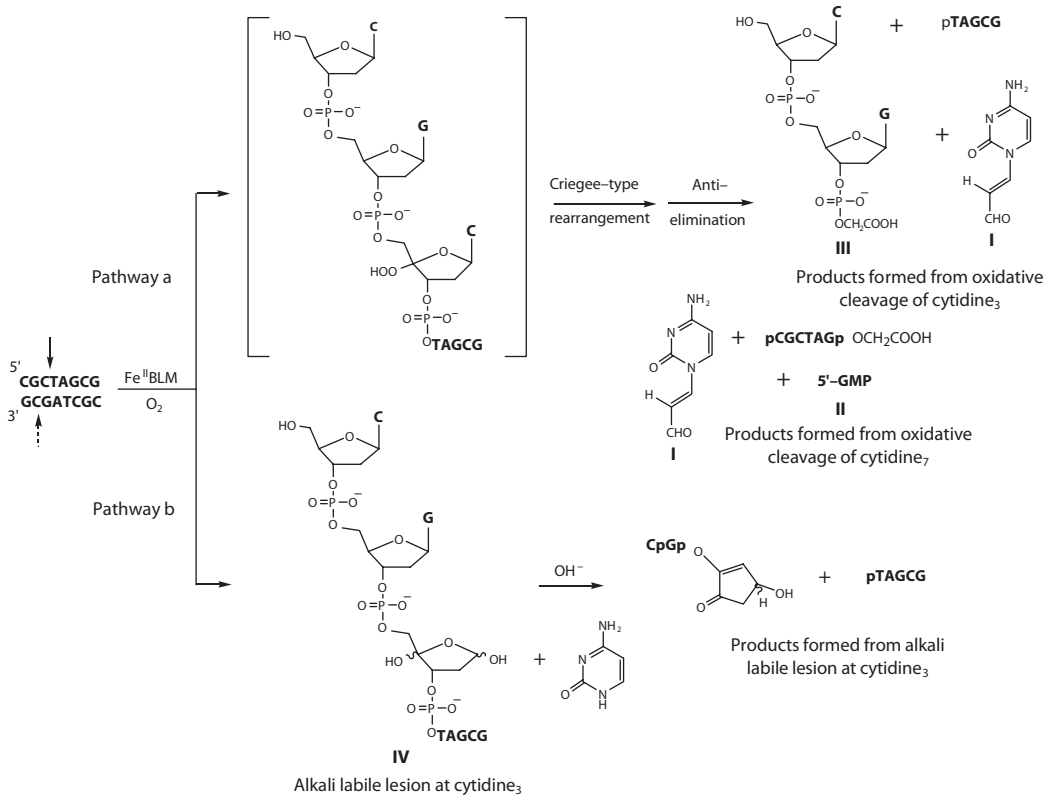

FIGURE 19.2 Pathways leading to (a) frank strand scission of DNA by Fe·BLM and (b) to the formation and base-induced decomposition of the alkali-labile lesion.

It may be noted that in the example shown in Figure 19.2, $CpGp_{CH_2COOH}$ (**III**) would result only from cleavage at cytidine$_3$, while 5′-GMP would result only from cleavage at cytidine$_7$.

In addition to these products shown in Figure 19.2, another set of products was also formed (pathway b).[51–54] These included free cytosine and a DNA lesion denoted the alkali-labile lesion (**IV**), since subsequent treatment with alkali resulted in strand scission. Strand scission was found to occur at the same sites as those outlined in pathway a. In fact, the proportion of frank strand scission products and alkali-labile lesions was a function of oxygen tension; higher oxygen tension favored frank strand scission products.[52–54] The alkali-labile lesion (**IV**) presumably arose from depurination of 4′-OH deoxycytidine (Figure 19.2, pathway b). Since the ratio of products formed via the two pathways was influenced by the amount of oxygen available, the two pathways likely have a common intermediate.[55,56] It seems likely that in the absence of sufficient O_2, the initially formed C-4′ deoxyribose radical undergoes a further one electron oxidation to afford the carbocation.[57–59] The latter could then react with water, affording the putative 4′-OH deoxycytidine intermediate. Independent support for the intermediacy of a C4′-deoxyribose radical has been obtained by the use of a C4′-deuterated DNA oligonucleotide as a substrate for Fe(II)·BLM.[60] A primary kinetic isotope effect was observed at individual thymidine residues, indicating that abstraction of the C4′-H is actually rate limiting for Fe·BLM-mediated DNA degradation.

A recent publication from the Greenberg laboratory[61] has shown that C4′-oxidized basic sites (i.e., of type **IV** in Figure 19.2) can undergo interstrand cross-linking, with the efficiency of the reaction influenced by the proximal DNA sequence. Clearly, a lesion of this type could in principle contribute to the cytotoxic potential of the BLMs. Another study pertinent to the issue of BLM-mediated cytotoxicity involves pathways available for the repair of BLM-damaged DNA. Povirk et al.[62] have

recently demonstrated that Artemis nuclease, which is required for V(D)J recombination, and the for repair of some radiation-induced DNA breaks, is capable of repairing 3′-phosphoglycolate-terminated DNA double-strand breaks (which are formed both by BLM and ionizing radiation[63]).

It is interesting to note that while activated Fe·BLM is capable of effecting both the oxidation and oxygenation of small molecules,[64,65] the degradation of DNA according to the pathways shown in Figure 19.2 involves only DNA substrate oxidation.[59] Dioxygen is required both for Fe(II)·BLM activation and for reaction with the putative C-4′ deoxyribose radical, but is apparently not transferred to DNA from the oxygenated metalloBLM.

A recent study by Burger and Drlica[66] has provided additional data concerning the role of oxygen species in BLM activation and the subsequent action of the activated species. Specifically, they found that superoxide, generated either by a genetic deficiency of superoxide dismutase, or by addition of the superoxide generator plumbagin, attenuated the lethality of BLM toward *Escherichia coli*. Given that superoxide can increase the concentration of peroxide through spontaneous or enzymatic dismutation (which can lead to increased levels of deleterious ·OH), and that superoxide has also been reported to be able to activate Fe(III)·BLM,[67] this finding is both surprising and intriguing.

The catalytic cycle for Fe(II)·BLM has been studied using electrochemical activation at a glassy carbon electrode.[68] This permitted correlation of the number of electrons consumed and DNA oligonucleotide products produced, under conditions where each Fe·BLM molecule was employed up to ~13 times in producing DNA lesions. In the electrochemical system, it was also clear that Fe(II)·BLM could not be activated reductively once it had bound to DNA. Thus, the obligatory order of events must have been Fe(II)·BLM binding by O_2, reduction to afford activated Fe·BLM, and then DNA binding and cleavage.[68]

While the individual metalloBLMs noted above all cleave DNA in a superficially similar fashion, for most metalloBLMs other than Fe·BLM there is a paucity of information on which to base mechanistic comparisons. Those species that have been studied to some extent include Cu(I)·BLM, which has been shown to form a metal complex with BLM quite different than that formed by Fe(II),[45,69] to undergo aerobic activation much less quickly than Fe(II)·BLM,[37] and to produce sequence-specific DNA lesions in different ratios.[37] Co(III)·BLM has a significantly higher DNA affinity than other metalloBLMs,[70] requires light but not oxygen for DNA cleavage,[71–74] binds and cleaves DNA at some sites distinct from those targeted by Fe(II)·BLM,[75] and cleaves DNA with minimal production of the compounds formed in Figure 19.2.[74] This metalloBLM has also been postulated to employ a reactive species different than activated Fe·BLM.[75] Accordingly, mechanistic generalization between metalloBLMs should be made only with great caution.

19.2.2.2 Modes of DNA Binding

An additional noteworthy feature of DNA cleavage by Fe(II)·BLM is the formation of double-strand DNA breaks. The proportion of double-strand cleavage is a function both of the specific BLM congener[76] and DNA substrate employed;[77–80] under favorable circumstances, such breaks can constitute up to 20% of all DNA lesions. It has been demonstrated convincingly that double-strand cleavage results from a specific set of mechanistic events at a DNA sequence conducive to such cleavage,[77–80] and not from the random accumulation of single-strand breaks. For some DNA sequences, it has been argued that a significant rearrangement of structure must occur after the first break to orient the activated BLM in a fashion conducive to the cleavage of a second strand.[80,81] However, at least for one substrate, this would seem to be unnecessary. The Hecht laboratory has described a hairpin oligonucleotide that underwent 43% double-strand cleavage from a bound conformation in which BLM was found to be oriented close to the cleavage sites on both strands.[20]

The idea that double-strand breaks in DNA can be induced by BLMs in different DNA-binding modes has gained support from a recent study by Chen et al.[19] These workers employed a BLM derivative containing a β-cyclodextrin appended to the end of the BLM C-terminal substituent. They found that unlike BLM A_2 and A_5, this derivative mediated double-strand DNA breaks by cooperative binding of a second BLM molecule to the DNA to mediate cleavage on the second strand.

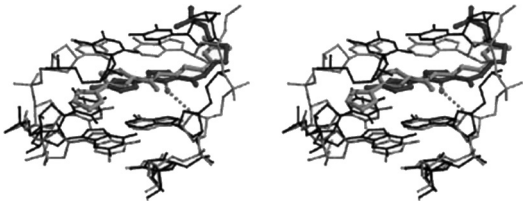

FIGURE 19.3 (**See color insert.**) Stereodiagram of superimposed 5-GTT sites in DNA oligonucleotides d(ATTAGTTATAACTAAT)$_2$ (gray, with BLM in blue) and d(ATTTAGTTAACTAAAT)$_2$ (black, with BLM in orange) with associated BLM bithiazole moieties and C-terminal substituents.

Modes of BLM binding to DNA have represented a more general issue in the field for some time. Strong evidence exists for intercalative binding, especially for Co·BLM derivatives studied in complex with DNA by NMR.[82,83] Nonetheless, other NMR studies involving different metalloBLMs have given results more consistent with minor groove binding,[20,84–86] and biochemical results obtained with BLMs tethered to solid surfaces,[21] or containing reactive groups within the bithiazole moiety[87] have afforded DNA modifications that seem incompatible with an intercalative binding mode. Recently, complexes of Co(III)·BLM B_2 with each of two DNA oligonucleotides [d(ATTAGTTATAACTAAT)$_2$ and d(ATTTAGTTAACTAAAT)$_2$] were analyzed by x-ray crystallography.[18] The bithiazole moieties were intercalated in both complexes, albeit in two rather different modes (Figure 19.3); in one structure this intercalative binding was independent of well-ordered binding of the metal-binding domain to the minor groove. While the differences in the two bound BLM structures are not fully understood at the present time, the technique used to obtain these structures is of great potential importance, especially if it is used to define the mode(s) of binding of BLM to DNA sequences of potential therapeutic relevance (*vide infra*).

19.2.2.3 DNAs Strongly Bound by BLM

While the degradation of DNAs by metalloBLMs has been studied extensively, and several studies have addressed the modes of binding of (metallo)BLMs to several different oligonucleotides, much less is known about those DNAs to which BLM binds preferentially. Given that the clinical dose of BLM is quite low (5 μmol), it is logical to think that DNA binding selectivity will be important in a clinical setting, and that the DNAs degraded by BLM will be a subset of those bound preferentially.

Two strategies have been described recently to identify those DNAs bound avidly by BLM. The first involved the application of a high-throughput fluorescent intercalator displacement (HT-FID) assay described by Boger et al.[88] Utilization of this assay with Co(III)·BLM B_2 by Lewis and Long[89] with a library of 256 DNA hairpins containing a cassette of four variable base pairs revealed a considerable variation of DNA-binding affinities for Co·BLM. Across a range of Co·BLM concentrations, 14 of the 15 best Co·BLM-binding DNA hairpins contained at least two 5′-GT or 5′-GC sites in the duplex stem. One currently unexplained observation was the buffer dependence of the assay for Co·BLM; Na cacodylate buffer afforded the preference noted above, while selection in the presence of Tris·HCl buffers (which have been used in other HT-FID analyses) failed to afford a consistent profile.

An analogous study was reported by the Hecht laboratory.[22,23] This also employed DNA hairpins, but involved a strategy amenable to the study of significantly larger randomized structural domains. As shown in Figure 19.4, a partial DNA hairpin was synthesized chemically, and included a region of eight nucleotides in which all four DNA nucleotides were incorporated in equal proportions. The partial duplex region of the hairpin was then converted to a full duplex via the action of DNA polymerase (Klenow fragment), which created complete hairpins with full complementarity. The library of 64-nucleotide hairpins thus produced should have contained 4^8 (=65,536) unique sequences. The library of DNA hairpins was passed through a column containing BLM A_5 immobilized on Sepharose beads, and the retained DNAs were removed from the column by washing with 1 M aqueous NaCl solution. The DNA hairpin had been designed such that the randomized region was flanked by DNA

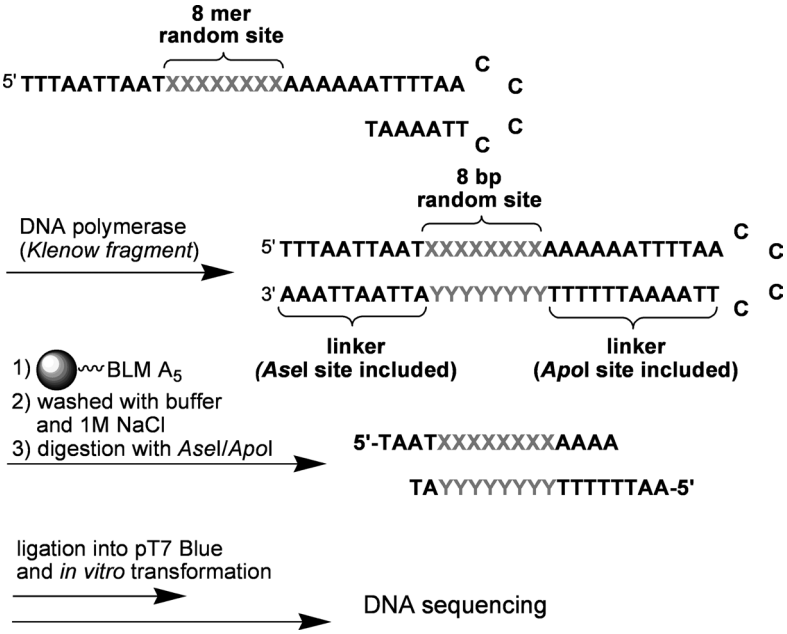

FIGURE 19.4 (**See color insert.**) Scheme used for the selection of hairpin DNAs that bind tightly to BLM.

restriction endonuclease sites; treatment with the relevant enzymes afforded the DNA duplexes, having sticky ends. These were introduced into a DNA plasmid that had been linearized to produce the same sticky ends. Following ligation, the plasmids were transformed into *E. coli* and colonies were isolated; the recovered amplified plasmid DNAs were sequenced in the previously randomized region. The ability of these DNAs to bind strongly to BLM was verified by competition with a 16-nt (profluorescent) DNA hairpin[90] that had been shown to be cleaved efficiently by Fe(II)·BLM.

As shown in Table 19.1 for 10 of these hairpin DNAs, the sequences within the previously randomized regions were not at all typical of those associated with DNAs that are cleaved efficiently

TABLE 19.1
Specific BLM Binding Sequences in 64-Nucleotide Hairpin DNA Isolated from Resin-Linked BLM A_5

5' TTTAATTAATXXXXXXXXAAAAAATTTTAA
3' AAATTAATTAYYYYYYYYTTTTTTAAAATT

1	5' AGATCATG 3' TCTAGTAC	6	5' CTACTAAA 3' GATGATTT
2	5' CGTGACGC 3' GCACTGCG	7	5' TACGCGCA 3' ATGCGCGT
3	5' TAAGTGGG 3' ATTCACCC	8	5' GGGTACCT 3' CCCATGGA
4	5' GAGAGGAT 3' CTCTCCTA	9	5' CGTTGTTA 3' GCAACAAT
5	5' ACAGAATA 3' TGTCTTAT	10	5' CGCCATTG 3' GCGGTAAC

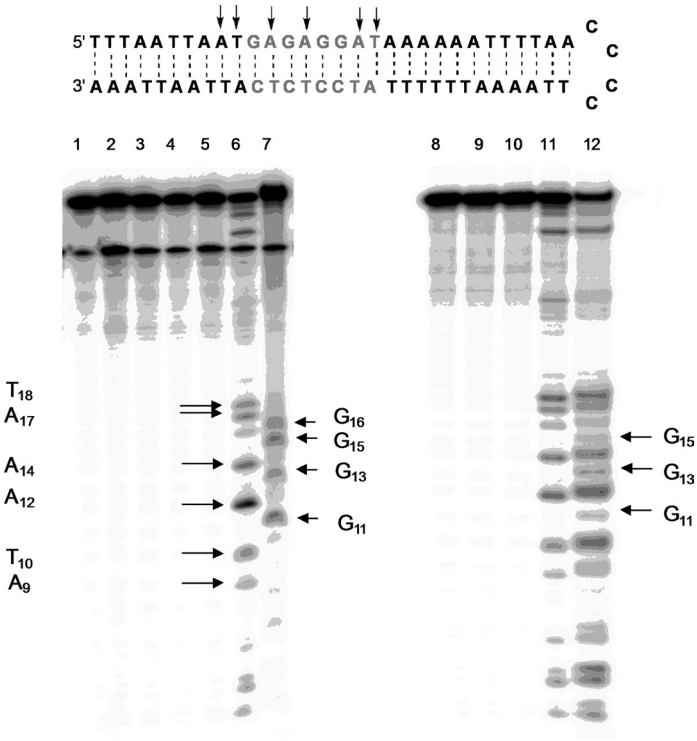

FIGURE 19.5 (**See color insert.**) Sequence-selective cleavage of [5′-^{32}P]-end labeled 64-nt hairpin DNA **4** by BLM A_5. Lane 1, radiolabeled **4** alone; lane 2, 20 μM Fe^{2+}; lane 3, 5 μM BLM A_5; lane 4, 5 μM Fe(II)·BLM A_5; lane 5, 20 μM BLM A_5; lane 6, 20 μM Fe(II)·BLM A_5; lane 7, G lane; Lane 8, radiolabeled **4** alone; lane 9, 20 μM Fe^{2+}; lane 10, 20 μM BLM A_5; lane 11, 20 μM Fe(II)·BLM A_5; lane 12, 20 μM Fe(II)·BLM A_5, followed treatment with 0.2 M *n*-butylamine.

by Fe(II)·BLM; they were AT-rich rather than the GT- and GC-rich regions associated with efficient cleavage. The 10 DNA hairpins were then subjected to degradation by the action of Fe(II)·BLM, and the results were analyzed by polyacrylamide gel electrophoresis.

As illustrated in Figure 19.5 for DNA hairpin **4**, the sites of cleavage of these strongly bound DNAs did not include a disproportionate number of 5′-GT and 5′-GC sites. Further, as shown in the right-hand panel of Figure 19.5, there were three sites that did not undergo DNA strand scission at all (pathway a in Figure 19.2), but which formed alkali-labile lesions (pathway b in Figure 19.2). Thus both the sites of cleavage, and the relative chemistries of cleavage were found to be different for these strongly bound DNAs, than for DNAs identified because they were cleaved efficiently by Fe·BLM. As noted above, the clinical dose of BLM is such that DNA is likely to be in significant excess relative to BLM in a clinical setting. These findings may well necessitate re-evaluation of those parameters of BLM action deemed important for the antitumor efficacy of the drug.

19.2.3 RNA Degradation

19.2.3.1 Transfer RNAs and tRNA Precursor Transcripts

Following an initial report by Magliozzo et al.[91] in which a high (300 μM) concentration of activated Fe·BLM was shown to effect limited degradation of yeast $tRNA^{Phe}$ and a few other tRNA isoacceptors, the Hecht laboratory carried out a systematic study of RNA degradation by Fe(II)·BLM.[31–33,92,93] For transfer RNAs and tRNA precursor transcripts, most of the species studied were refractory to activated Fe·BLM at all tested concentrations. A few tRNAs were cleaved with

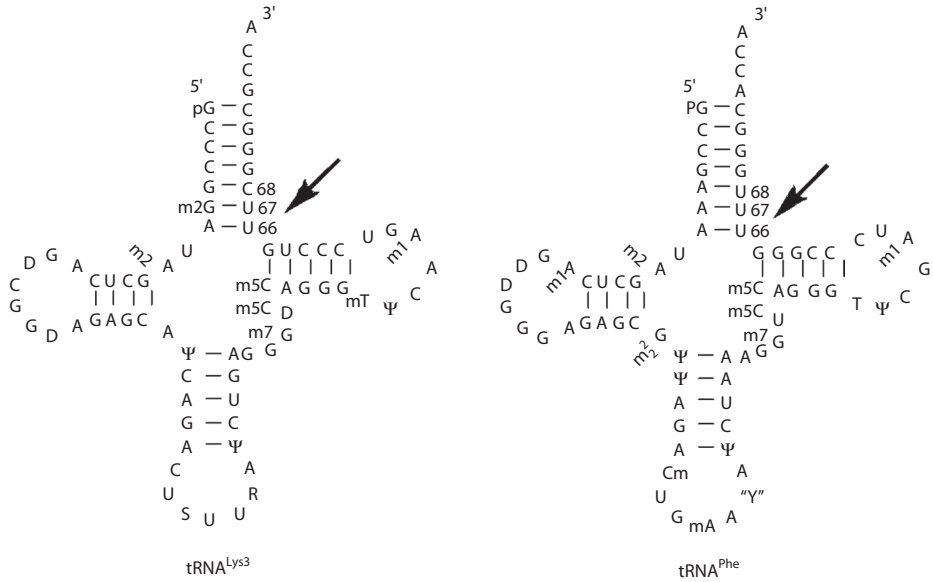

FIGURE 19.6 Chicken tRNA isoacceptors found to be the most susceptible to cleavage by Fe(II)·BLM. The arrows indicate the primary cleavage positions.

modest efficiency, notably a *Schizosaccharomyces pombe* amber suppressor $tRNA^{Ser}$ construct and mature *E. coli* $tRNA_1^{His}$.[32] By far the most efficient cleavage was achieved with a *Bacillus subtilis* $tRNA^{His}$ precursor, which was cleaved with surprising efficiency at U_{35}, and weakly at several other positions.[31,32] While examples of cleavage occurred in many positions of the cloverleaf structure of tRNA, and for sequences not well represented in DNA cleavage studies, the majority of cleavage sites involved 5′-G·pyr-3′ sequences and were located at what are believed to be the junctions between single- and double-stranded regions of the tRNAs.[15,31,32,92,93]

Given the evidence that some tRNA degraded by Fe·BLM could represent an important locus for the action of the drug (*vide infra*), it seemed important to identify the specific tRNA isoacceptor(s) that were highly susceptible to degradation by BLM. This was performed using mixtures of partially fractionated chicken tRNAs, which are highly homologous to the cognate human tRNAs. As shown in Figure 19.6, two tRNA isoacceptors ($tRNA_3^{Lys}$ and $tRNA^{Phe}$) were found to be the most susceptible to cleavage, and both were cleaved selectively at U_{66}.[24] As had been shown earlier for yeast $tRNA^{Phe}$,[94] in the presence of physiological concentrations of Mg^{2+}, cleavage by Fe·BLM was suppressed. In contrast, $tRNA_3^{Lys}$ was still cleaved even at relatively high Mg^{2+} concentrations. While the above study was carried out with fractionated chicken tRNAs, chicken and human $tRNA_3^{Lys}$ have the same structure.[95] $tRNA_3^{Lys}$ appears to be highly susceptible to cleavage by Fe·BLM, and may plausibly constitute a therapeutically relevant locus for the drug.

19.2.3.2 Other RNA Substrates for BLM

While most of the studies of RNA cleavage by BLM have involved tRNAs, several other RNAs have been tested as substrates. Perhaps the most successful of these has been yeast 5S ribosomal RNA that was found to be cleaved quite efficiently at three sites by Fe(II)·BLM.[32] Interestingly, each of the three cleavage sites involved the uridine moiety in 5′-GUA-3′ sequences, and each had a one-base bulge on the cleaved strand one or two nucleosides to the 3′-side of the cleavage site. However, it has not been shown that any rRNA within an intact ribosome is cleaved by Fe(II)·BLM, and studies of the effects of Fe(II)·BLM on a eukaryotic protein-synthesizing system suggested that ribosomes are not a primary target for BLM (*vide infra*).[96]

Several messenger RNAs have been studied as substrates for Fe(II)·BLM. RNAs found to undergo cleavage have included HIV-1 reverse transcriptase mRNA,[31] the iron regulatory element of bullfrog ferritin mRNA,[97] firefly luciferase mRNA,[96] and *E. coli* dihydrofolate reductase mRNA.[98] Also studied has been the cleavage of an RNA–DNA heteroduplex prepared by reverse transcription of *E. coli* 5S rRNA.[33] Both the RNA and DNA strands were cleaved under comparable conditions and at a limited number of sites. Significantly, cleavage of the RNA strand of the heteroduplex involved cleavage sites different than those observed for the original rRNA, indicating that cleavage must actually have involved a heteroduplex structure.

19.2.3.3 Chemistry of RNA Cleavage

The chemistry of RNA cleavage by Fe(II)·BLM has been studied less intensively than that of DNA, but a few useful observations have been made. By the use of yeast 5S rRNA ^{32}P-labeled alternatively at the 5′- and 3′-ends, it was shown that the mobility of individual bands was consistent with that to be expected if the chemistry of RNA cleavage was analogous to that of DNA.[32] This conclusion was also supported by experiments using the self-complementary oligonucleotide CGCTAGCC in which deoxycytidine$_3$ was replaced by ribocytidine.[31] A more detailed analysis indicated the formation of an additional product putatively formed by initial abstraction of C1′ H from ribocytidine$_3$.[99,100] Repetition of this experiment using C_3-*ara* CGCTAGCG indicated formation of the same product, and in enhanced yield. Not yet resolved experimentally is the issue of the formation of an alkali-labile lesion from RNA analogous to the intermediate formed from DNA (Figure 19.2). While the intrinsic lability of the RNA internucleotide linkage to alkali precludes the use of this reagent to unmask the alkali-labile lesion selectively, it has been shown by admixture of hydrazine to Fe·BLM-treated *B. subtilis* tRNA^{His} precursor transcript that some currently uncharacterized lesion is present.[100]

One particularly surprising finding has been reported by Keck and Hecht.[101] While all of the foregoing examples of RNA cleavage by Fe·BLM involve oxidative degradation, this report documents the ability of BLM A_2 to mediate RNA strand scission at a number of sites in the absence of any added metal ion. Cleavage was actually found to be suppressed by admixture of metal ions that bind to BLM. Analysis of the nature of the formed cleavage products indicated that each contained a 2′,3′-cyclic phosphate at the 3′-end. Logically, these might be thought to have resulted from a phosphoryl transfer reaction in which the internucleotide phosphate linkage at certain positions underwent nucleophilic attack by the 2′-OH group of ribose. Oligonucleotide 2′,3′-cyclic phosphate moieties could then form concomitant with RNA strand scission. While the possible relevance of this transformation to the mechanism of action of BLM is unclear, it may be noted that the facility of this transformation was entirely comparable to that involving oxidative RNA cleavage by Fe(II)·BLM.

19.2.4 Protein Synthesis Inhibition and Antiviral Properties

The ability of Fe(II)·BLM to cleave some tRNAs, mRNAs, and rRNAs suggested that this metalloBLM might be able to inhibit the synthesis of proteins. This was studied in a DNA-independent cell-free protein biosynthesizing system containing rabbit reticulocyte lysate and programmed with luciferase mRNA.[96] Treatment with 100 μM BLM A_5 alone reduced luciferase synthesis by ~26%, due to either adventitious metal ions or non-oxidative RNA cleavage, as described above. Treatment with 50 μM Fe(II)·BLM A_5 reduced protein synthesis by about 68%, and 100 μM Fe(II)·BLM A_5 caused ~86% reduction. To determine which RNA(s) had been affected by Fe(II)·BLM A_5, the reaction mixtures were treated with additional ribosomes, luciferase mRNA, or a mixture of tRNA isoacceptors following Fe(II)·BLM treatment. Only admixture of tRNAs had any effect in restoring luciferase synthesis. Production of this protein was completely restored for the reaction mixtures treated with 50 μM Fe(II)·BLM, and partially restored for the 100 μM treatment. Thus one or more transfer RNAs may represent a critical cellular target for BLM.

In this context, it is interesting to note that the antitumor ribonuclease onconase[102–106] has been employed in an experiment analogous to the one summarized above for BLM; virtually identical results were obtained.[107] Because onconase and BLM have been shown to have remarkably similar cytotoxicity profiles toward a panel of cultured tumor cells,[96] the specific tRNAs cleaved by both agents were compared. The two antitumor agents were found to effect the cleavage of several tRNAs in common, although a comparison of cleavage patterns with one isoacceptor revealed cleavage at quite different sites in that tRNA.

It is interesting to note that following treatment of uninfected or HIV-1-infected H9 lymphocytes with onconase, $tRNA_3^{Lys}$ was found to be cleaved by onconase.[108–110] This event may well form the basis for the reported inhibition of viral replication[111,112] and antiviral activity[113] of onconase. As discussed above, this same tRNA isoacceptor was found to be exceptionally sensitive to cleavage by Fe·BLM.[24] In this context, it is interesting that BLM has also been reported to have antiviral activity toward HIV, and to sensitize drug-resistant HIV strains to clinically used antiviral agents.[114] While the mechanism of the antiviral activity of BLM has not been reported, oxidative degradation of $tRNA_3^{Lys}$ may plausibly be relevant.

19.3 BIOSYNTHESIS

The Shen laboratory has continued its studies on the biosynthesis of the BLMs and has achieved some notable successes. Genetic engineering of the biosynthetic pathway in the producer strain (*S. verticillus*) would provide facile access to new derivatives. However, it has not been possible to realize this goal, because the producing strain has been refractory to the introduction of plasmid DNA. Recently, Galm et al.[115] have described the construction of a producer strain by the intergeneric *E. coli–Streptomyces* conjugation under optimized conditions. In addition to potentially providing access to novel BLM analogs for study as potential antitumor agents, it was shown that the strategy could also provide important mechanistic insights. In particular, manipulation of this strain afforded an in-frame *blmD* deletion mutant strain (*S. verticillus* SB5) that produced a decarbamoyl BLM. This permitted a revised biosynthetic pathway for the disaccharide moiety of BLM to be proposed (Figure 19.7).

Also studied by the Shen laboratory has been the synthesis of the BLM group antibiotic TLM. *Streptoalloteichus hindustanus* E465-94 ATCC 31158 was found to contain an 80.2-kbase region containing 40 open-reading frames, 30 of which were assigned to the TLM biosynthetic gene cluster. These included genes encoding nine nonribosomal peptide synthase modules and one polyketide synthase module, genes encoding seven enzymes for sugar biosynthesis and attachment, and other genes encoding other biosynthesis, regulatory, and resistance proteins.[5–7] Of particular interest was the functional characterization of the *tlmK* gene, which attaches talose to the nascent carbinol. A deletion mutant accumulated two major metabolites, TLM K-1 and TLM K-2, which must reflect the instability of the putative carbinolamine intermediate (Figure 19.8).[6]

Finally, a study of the biosynthetic gene cluster of the BLM group antibiotic zorbamycin was carried out in *Streptomyces flavoviridis* ATCC 21892, permitting the assigned structure of zorbamycin to be established more firmly.[8,9] In common with the phleomycins (PLM, *vide infra*), the zorbamycins contains a thiazolinylthiazole moiety, rather than the bithiazole present in BLM.

19.4 DEVELOPMENT OF BLMs AS NOVEL ANTITUMOR AGENTS

The earliest natural products identified in the BLM family were the PLMs; they contain a thiazolinylthiazole moiety rather than the BLM bithiazole (cf., Figures 19.1 and 19.9). The PLMs and BLMs each contain several different C-substituents, as illustrated in Figures 19.1 and 19.9. While the PLMs and BLMs cleave DNA with similar characteristics as regards sequence selectivity, individual congeners do display different biochemical properties, even at the level of cell culture.[116] This presumably reflects a number of factors, such as cellular uptake mechanisms selective for certain types of

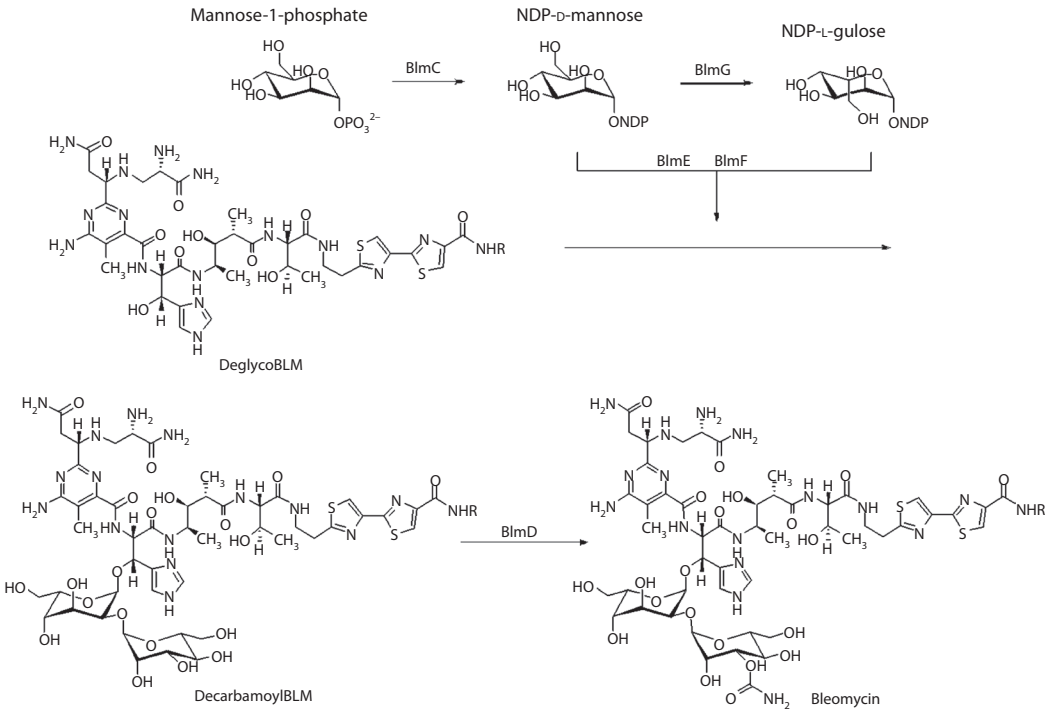

FIGURE 19.7 Proposed pathway for the biosynthesis of the carbohydrate moiety of BLM.

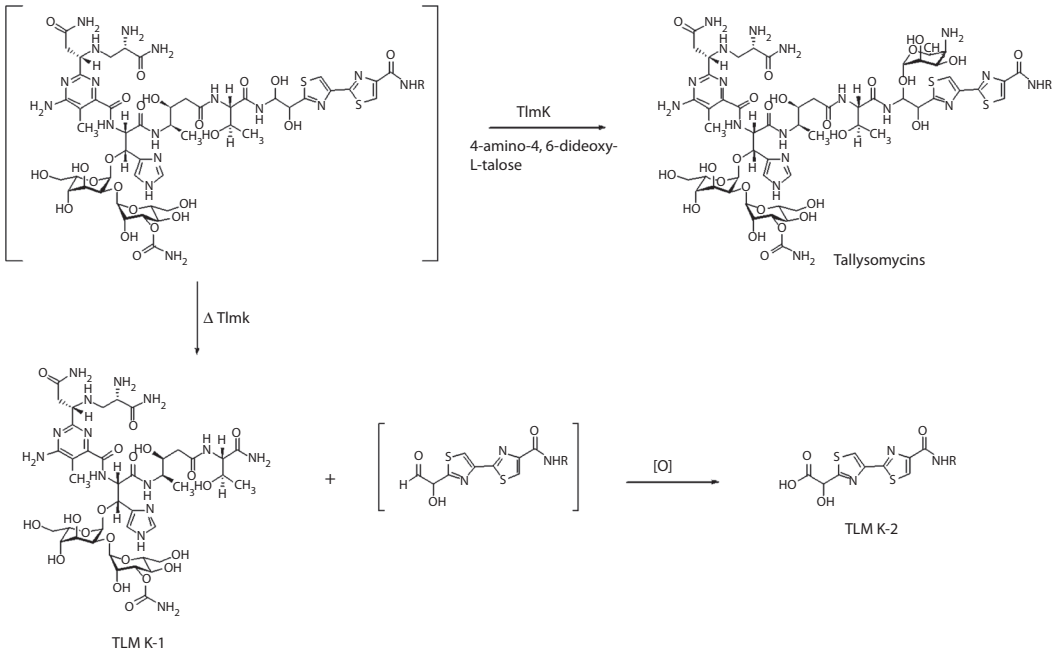

FIGURE 19.8 Function of TlmK in the biosynthesis of tallysomycin, and instability of the putative carbinolamine intermediate.

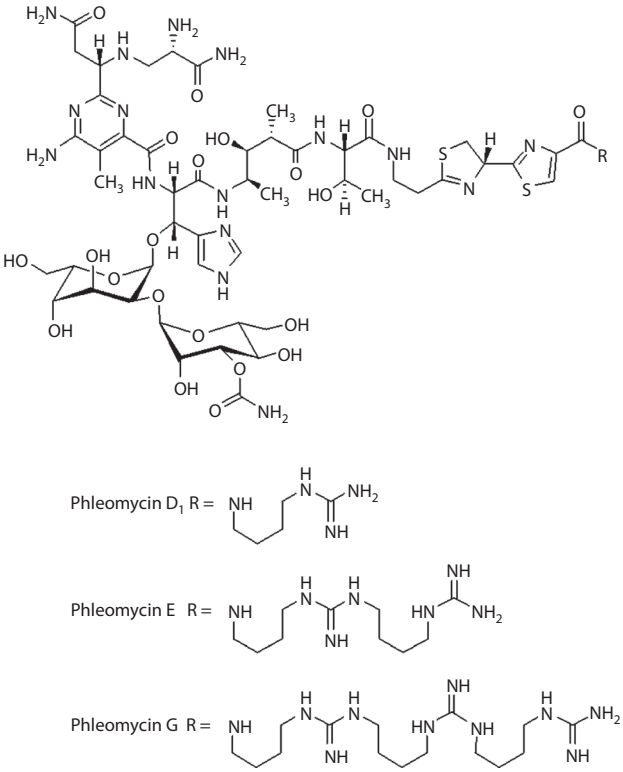

FIGURE 19.9 Structures of some naturally occurring PLMs.

BLM congeners.[117] The PLMs exhibited unacceptable toxicity when tested as a mixture of congeners. Further, the thiazoline moiety is susceptible to hydrolytic ring opening, and possibly also to racemization. For these reasons, attention was focused on the BLMs as clinical candidates.

When they were first isolated, the complexity of the BLM structure precluded their total chemical synthesis. Accordingly, most of the congeners studied were natural variants that differed exclusively at the C-terminus (Figure 19.1). Additionally, it was also found that analogs differing at the C-terminus could be prepared by fermentation via inclusion in the incubation medium of a high concentration of the amine intended for incorporation at the BLM C-terminus.[118] Semisynthetic BLMs differing at the C-terminus were also accessible following initial chemical removal of the C-substituent of BLM A_2; this was accomplished by means of a series of chemical transformations to afford bleomycinic acid.[119–121] Bleomycinic acid was also accessible by treatment of BLM B_2 with an acylagmatine hydrolase.[122] Polyamine condensation with bleomycinic acid, for example, then afforded new BLM analogs.

While most of the initial BLM structural modifications were limited to alterations at the C-terminus, several other types of transformations of the naturally derived BLMs were reported. These included the preparation of epiBLM, iso- and decarbamoylBLMs, as well as deamido- and depyruvamideBLMs (Figure 19.10).[118] These analogs were found to differ somewhat in their animal organ distribution profiles, as well as in their intrinsic biological properties.[123] One of the most remarkable was deglycoBLM, the simplified analog lacking the carbohydrate moiety.[124,125] This species was found to mediate DNA cleavage with almost the same sequence selectivity as BLM itself, and to produce the same chemical products.[125,126] Nonetheless, recent studies with this analog suggest that it may function biologically in some contexts in a fashion quite distinct from BLM itself.[127,128]

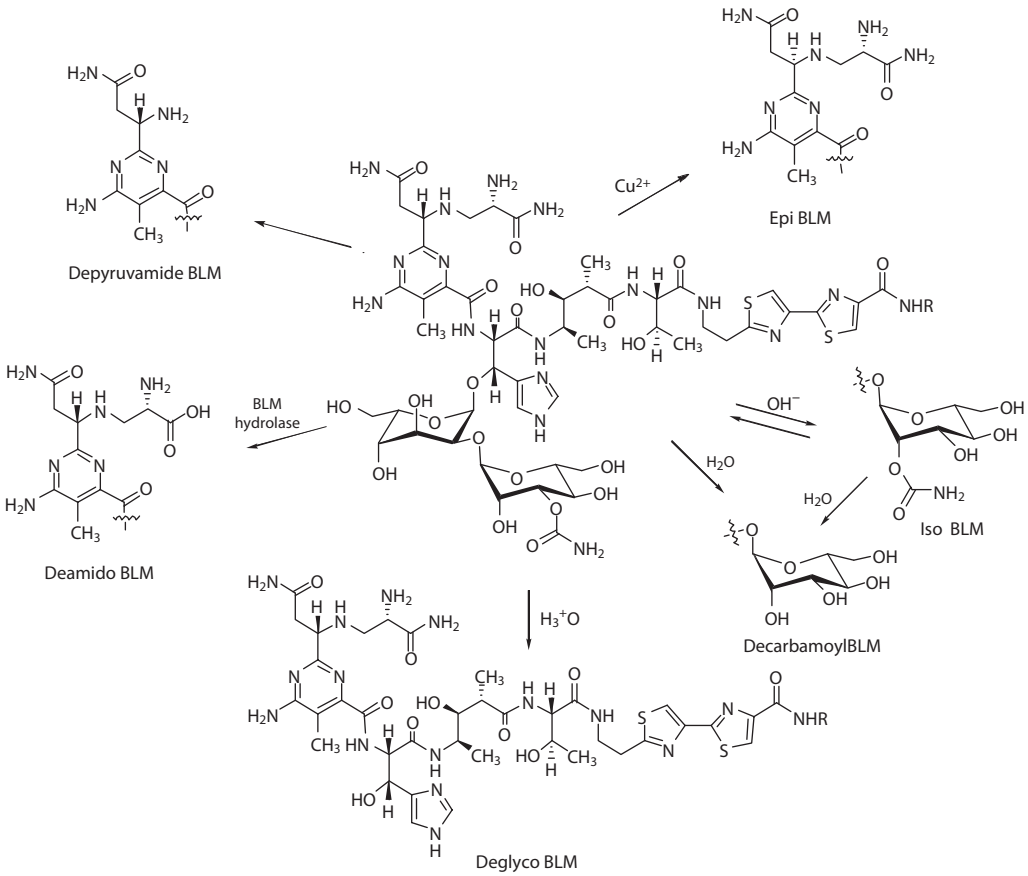

FIGURE 19.10 Analogs of BLM accessible by semisynthesis from BLM itself.

Other naturally occurring variants of the BLMs were also identified. Perhaps the best known are the TLMs, which have progressed to clinical trials. As shown (Figure 19.8), the TLMs have a third carbohydrate moiety (a talose residue), which is attached to the peptide backbone of TLM via a carbinolamide linkage, the latter of which has been shown to be unstable in the absence of the talose moiety (*vide supra*). In common with the BLMs, the TLMs cleave DNA predominantly at 5′-GC-3′ and 5′-GT-3′, but with somewhat altered patterns of preferred sites of cleavage.[129]

In the United States, Europe, and Japan, BLM is utilized clinically as a mixture of congeners that differ at the C-terminus. The major constituents are BLM A_2 (~60–65%) and BLM B_2 (~30%). This mixture was reported to exhibit efficacy better than single congeners in animal tumor models.[130] It has also been reported that BLM congeners having free amino groups within the C-substituent exhibited enhanced pulmonary toxicity, an observation that led to the preparation and evaluation of analogs such as liblomycin[131] and BAPP.[121,123] Interestingly, BLM A_5 (which has free amino groups within the C-substituent in the form of a spermidine moiety) is used clinically in Russia and China.

19.5 SYNTHESIS AND STRUCTURE–ACTIVITY STUDIES

19.5.1 Solution- and Solid-Phase Syntheses

Three laboratories have reported solution-phase syntheses of naturally occurring BLMs. The first two were reported in 1982 by the Umezawa[132] and Hecht[133] laboratories. The development of methodology

relevant to the synthesis of BLM has continued to the present time. To date, two additional syntheses of BLM have been described by the Boger[134] and Hecht[135] laboratories, as well as the syntheses of closely related compounds.[76,135–137] Of special interest has been the report of the total synthesis of deamido-BLM, the sole reported catabolite formed following the therapeutic administration of BLM.[137]

An important advance in the synthesis of BLM congeners occurred in 2000 with the first report of the preparation of a deglycobleomycin by solid-phase synthesis.[138] The synthesis involved the use of Tentagel resin functionalized with a trityl linker. The "amino acid" constituents of BLM were condensed stepwise onto the resin-bound linker from the C-terminus. Following Boc pyrimido-blamic acid addition,[139] the formed deglycoBLM A_5 was deblocked and cleaved from the resin with trifluoroacetic acid/trisopropylsilane/water/dimethylsulfide.[138]

While the use of a linker incorporating a trityl group provided access to deglycoBLM, there were some limitations to this strategy. The most critical was the obligatory cleavage of deglycoBLM from the resin concomitant with removal of the Boc protecting group. The use of a dimedone-based resin linker, cleavable by treatment with hydrazine, proved successful in permitting the elaboration of fully protected deglycoBLMs attached to a Tentagel support (Figure 19.11).[140] As shown, after

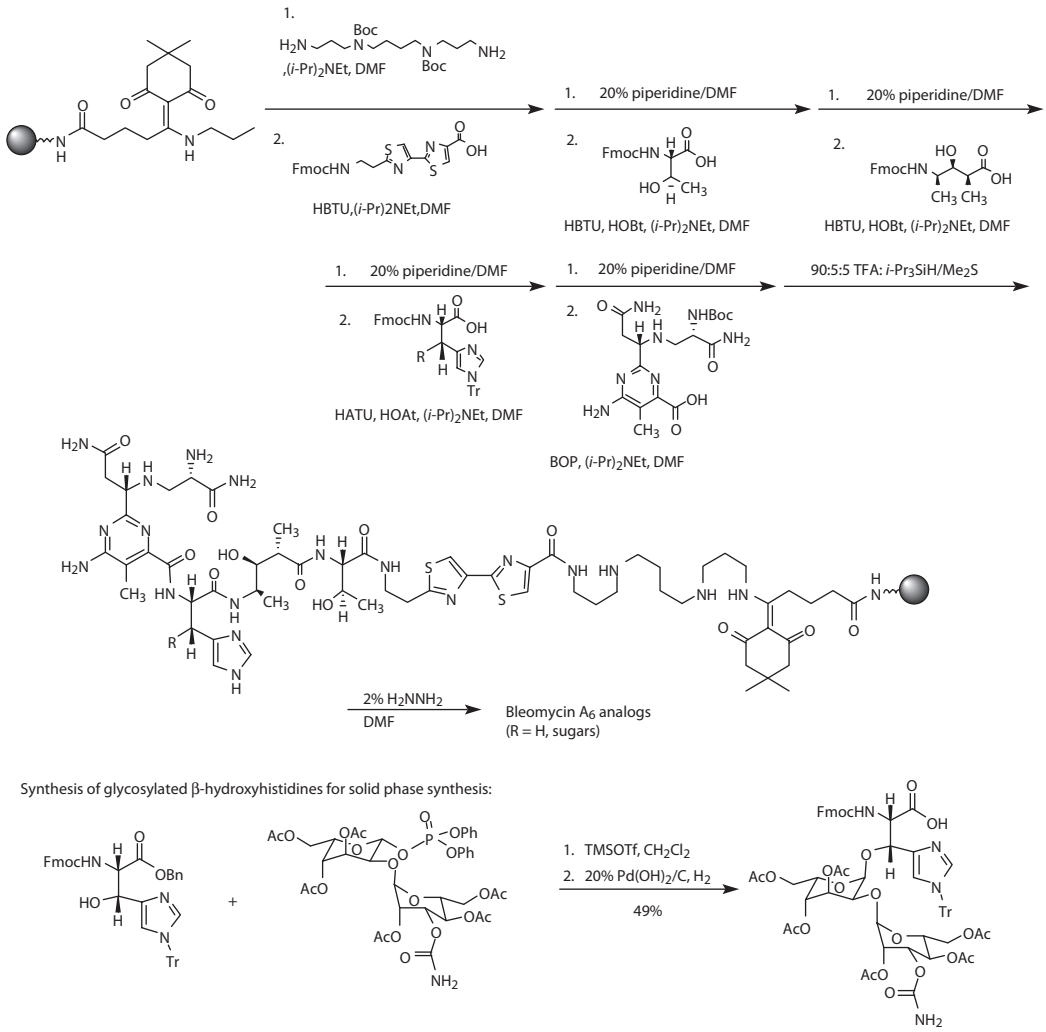

FIGURE 19.11 Scheme employed for the solid-phase synthesis of deglycoBLM and glycosylated BLMs.

attachment of each Fmoc-protected fragment to the resin-bound linker, subsequent treatment with piperidine effected Fmoc cleavage and formation of a dibenzofulvene–piperidine adduct, which has been characterized spectroscopically.[141] This permitted the determination of stepwise coupling yields. The synthesis of deglycoBLM $A_{2'\text{-a}}$ was realized in 68% overall yield using this procedure.[140] In parallel, a study of the C-substituent permitted determination of the C-substituent optimal to enable on-resin assay of the synthesized deglycoBLM.[142]

Another study addressed the issue of preparing glycosylated BLMs by solid-phase synthesis. As outlined in Figure 19.11, this was realized by preparing a suitably protected β-hydroxyhistidine derivative containing the disaccharide moiety present in BLM. The synthesis was based on earlier syntheses described by Ohno[143] and Boger,[144] but used protecting groups compatible with solid-phase synthesis. In this fashion, BLM A_5 was synthesized in a reasonable yield,[145] and with greater facility than the respective solution-phase synthesis.[135] As described in a section below, this strategy has also been employed successfully to prepare carbohydrate analogs of BLM.

As regards the preparation of other BLM group antibiotics, the absolute stereochemistry of the methine H in the thiazoline moiety of PLM has been determined,[146] potentially enabling the total synthesis of PLM. Additionally, Sznaidman and Hecht[147] have reported a strategy for elaborating the glycosylcarbinolamide moiety of TLM, in spite of the documented instability of the carbinolamide moiety itself.[6]

19.5.2 Study of Individual "Amino Acid" Constituents

19.5.2.1 Bithiazole Moiety and C-Substituent

Systematic alteration of the bithiazole moiety has not been reported, although several studies have shaped our present understanding of the way in which this moiety functions in DNA binding. These include photochemical transformations of the bithiazole moiety[148,149] and replacement with mono- and bishalogenated bithiazoles.[87] While neither of these types of alterations affected obvious changes in the DNA-binding properties of the derived (deglyco)BLMs under dark conditions, irradiation of the deglycoBLMs containing halogenated thiazoles permitted confirmation that these structural elements can reside in the minor groove of DNA.[87]

The ability of the tripeptide S moiety of BLM (consisting of the threonine, bithiazole, and C-terminal substituent) to bind DNA with an affinity similar to that of BLM[10,11] argues that much of the DNA-binding affinity of BLM resides within this domain. The finding that deglycoBLM analogs containing monothiazole constituents cleaved DNA inefficiently and without demonstrable sequence selectivity was fully consistent with this view.[150] Replacement of the bithiazole moiety with a pyrrole-based heterocyclic system resulted in a change in sequence selectivity to afford cleavage at sequences reminiscent of the sequence-selective binding of distamycin and netropsin.[151,152]

Based on these observations, it might have been reasonable to conclude that the sequence selectivity of DNA cleavage by the (deglyco)BLMs is determined by the bithiazole moiety, as actually suggested in an early study.[153] However, there are now a few lines of experimentation that make it clear that the actual situation is more complex. These include the findings that photolysis of halogenated bithiazoles in the presence of DNA resulted in sequence-selective DNA damage, albeit not with a sequence selectivity characteristic of BLM.[154,155] Also, an analog of the pyrimidoblamic acid moiety effected sequence-selective cleavage of DNA in the same fashion as BLM.[14] In addition, BLM congeners having the same bithiazole + C-terminus, but differing in their metal-binding domains, exhibited altered strand selectivity of DNA cleavage.[12]

Perhaps the most compelling evidence was obtained for a series of analogs of deglycoBLM in which the threonine moiety was replaced by glycine or oligoglycine, thus systematically altering the distance between the metal-binding and bithiazole domains.[13] If increasing the number of glycines between the two binding domains caused them on average to be at greater distances from each

other when bound to a DNA substrate, the pattern of DNA cleavage should then reflect which binding partner (i.e., the metal-binding domain or bithiazole) is the predominant structural element in defining the sequence selectivity of DNA binding. It was shown experimentally that all of the analogs were cleaved at the same sites, arguing that the metal-binding domain is the primary determinant of the sequence selectivity of DNA binding by BLM.[13]

The above finding that strongly bound DNAs have altered patterns and BLM binding and cleavage, relative to the sites of cleavage observed when excess BLM is employed, has added an additional level of complexity to the interpretation of DNA cleavage studies. Most published studies measure only DNA cleavage, and so reflect the overall efficiency of both processes when BLM is in excess. Thus, the selectivity for preferred cleavage at 5′-GC-3′ and 5′-GT-3′ sequences in the presence of excess BLM may well reflect the reality that rate-limiting DNA cleavage[60] by BLM occurs the most effectively at the widest, shallowest part of the minor groove.[15] This suggestion is supported by the observation that BLM cleaves DNA and RNA duplexes most efficiently at sites having a widened minor groove. Examples might be thought to include DNA[156] and RNA bulges,[32] sites of DNA platination,[157] the 5′-junction of a DNA triplex structure with its DNA duplex target,[158] and the putative junctions between single- and double-stranded structures in RNAs.[31,32]

Naturally occurring BLMs have several different C-substituents most of which are polyamines, or polyamines containing guanidine moieties. Virtually all of the naturally occurring BLMs have C-substituents that are charged at physiological pH, and the charged C-substituent is clearly important for productive binding to the (negatively charged) nucleic acid substrates for BLM. BLM congeners lacking positively charged C-substituents, notably (deglyco)BLM demethyl A_2, have been demonstrated to produce less DNA cleavage.[116]

Although not studied in a thorough fashion, it appears that two positively charged substituents within the C-substituent[142] that are appropriately positioned[159] are sufficient to support DNA cleavage by that (deglyco)BLM congener in an optimal fashion. While the nature of the C-substituent has often been ignored in studies of (deglyco)BLM, cell culture studies make it clear that this substituent is of considerable importance from the perspective of medicinal chemistry.[116] As noted above, in some cases, this may be a function of differences in mechanisms of cellular uptake based on the structure of the C-substituent.[117]

19.5.2.2 Linker Domain

Several lines of evidence have suggested that (deglyco)BLM assumes a folded conformation when it is bound to a DNA duplex substrate.[16,17,82,86] The structural elements that control this folded conformation have been defined convincingly by studies from the Boger and Stubbe laboratories.[16,17] Alterations of the threonine moiety did not affect the sequence selectivity of DNA cleavage, but did effect efficiency of cleavage, as shown earlier by the Hecht laboratory.[13] The ratio of single- to double-strand cleavage was also affected by changes in the threonine moiety.[16] Careful analysis of the effect of substituents within the methylvalerate moiety indicated that substituents in the 2- and 4-positions are critical in facilitating folding into a stable conformation optimal for DNA cleavage.[16,17] A related effort has been made to exploit the putative folded conformation of (deglyco)BLM by the preparation of conformationally rigid analogs containing structurally altered methylvalerate moieties.[160,161] Although the prepared analogs were capable of binding Fe^{2+} and activating oxygen for transfer to low molecular weight substrates, none mediated sequence-selective DNA cleavage in the same fashion as BLM. The most likely interpretation is that none of the analogs was a sufficiently good mimic of the preferred folded conformation of BLM to permit efficient DNA cleavage to proceed. It is also possible that productive DNA binding and cleavage by BLM may actually require some flexibility within the ligand for mechanistic reasons. In either case, this structural domain of BLM may be of utility in differentiating the binding of different classes of substrates (e.g., DNA and RNA) by BLM.

19.5.2.3 Metal-Binding Domain

The metal-binding domain of BLM is comprised of pyrimidoblamic acid and (glycosylated) β-hydroxyhistidine moieties. Many of the early analogs of BLM, prepared by semisynthesis from naturally occurring BLMs, were altered within this domain, but relatively little has been done to vary this domain systematically.

Changes made within the β-hydroxyhistidine domain of (deglyco)BLM have mainly involved those reported by Boger and colleagues. These have been important in defining the role of the ⊠-nitrogen of the imidazole moiety in sequence-selective DNA cleavage,[162] consistent with the role of this N atom as a metal ion ligand, and the lack of importance of the OH group of β-hydroxyhistidine to the function of deglycoBLM as a DNA cleaving agent.[163]

Some reports have appeared that are pertinent to the role(s) of the disaccharide moiety of BLM. These have included two studies in which monosaccharide derivatives have been prepared that explored the role of the L-gulose moiety. Both found that monosaccharide analogs of BLM containing L-gulose attached to β-hydroxyhistidine were the most effective in maintaining potency of DNA cleavage.[136,145] This monosaccharide analog was also found to be more efficient in cleaving a good RNA substrate for BLM than congeners containing D-mannose or L-rhamnose.[145] It seems clear that the carbohydrate moiety of BLM is exceptionally important in determining the efficiency of RNA cleavage by individual BLM analogs.

Recently, the Hecht laboratory has reported the results of experiments in which BLM A_5 was attached to microbubbles through the C-substituent and used to mediate binding to monolayers of cultured mammalian cells. These BLM-derivatized microbubbles were found to adhere to monolayers of MCF-7 breast cancer cells, but not to a comparable cell line (MCF-10A) of normal breast cells.[25] The same observation of selective binding was reported for three additional sets of cancer and normal cell lines. Interestingly, microbubbles derivatized with deglycoBLM A_5 were not observed to adhere to MCF-7 or MCF-10A cells. The clear implication of this observation is that the disaccharide moiety of BLM is required for selective binding to tumor cells.

19.5.3 Newly Reported Analogs

Few new analogs of BLM have been reported via solution-phase synthesis since the solid-phase synthesis of BLM has been described.[164] However, Xu et al. have reported interesting new derivatives prepared by semisynthesis from naturally occurring BLMs. These have included acylated derivatives of the C-terminal amine in BLM A_6 (containing a spermine C-substituent),[165] and several C-terminal amino acid and peptide derivatives of BLM A_5.[166] The latter derivatives exhibited good *in vitro* cytotoxic potency versus four lines of cultured cells, especially versus the MDA-MB-435 cell line, where the derivatives were all at least several-fold more potent than BLM A_5.[166]

19.5.4 BLM Combinatorial Library

The studies described above provide a good starting point for a program of systematic modification of BLM structure to identify analogs with improved properties, but do little to guide the synthesis of analogs differing from BLM at multiple sites. Given the complexity of the BLM structure, it is reasonable to expect that multiple alterations may afford BLM analogs with unique properties. Accordingly, the Hecht laboratory utilized its solid-phase BLM synthesis methodology (Figure 19.11) to prepare a library of 108 deglycoBLM analogs through parallel solid-phase synthesis.[164] The library, prepared with the spermine C-substituent of BLM A_6, involved the use of three analogs of the bithiazole moiety, three analogs of threonine, three analogs of the methylvalerate moiety, and four analogs of β-hydroxyhistidine (Figure 19.12).

The analogs were assayed for their abilities to relax supercoiled plasmid DNA, affect sequence-selective DNA cleavage, mediate double-strand DNA breaks and affect the degradation of

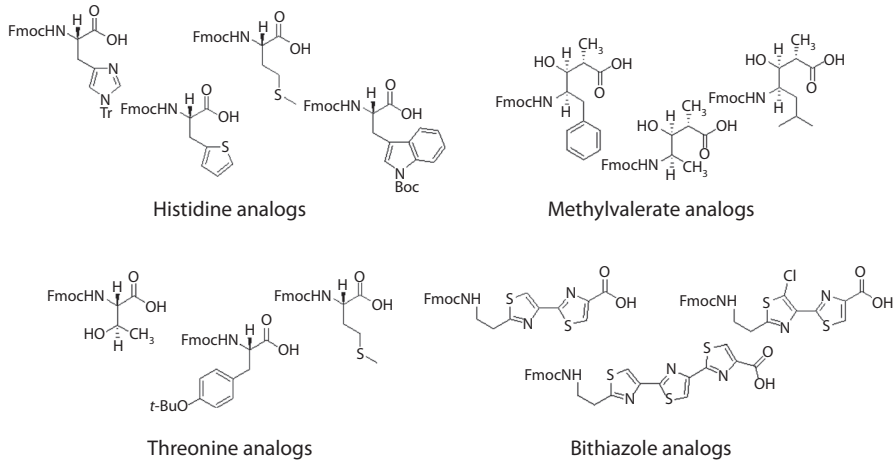

FIGURE 19.12 Building blocks used for the preparation of a deglycoBLM library.

$tRNA_3^{Lys}$.[24] Several important lessons were learned from the analysis of this library.[167] In spite of earlier reports[13,16,17] that replacement of threonine in the linker region resulted in less efficient DNA cleavage, replacement of threonine with methionine and tyrosine resulted in enhanced cleavage potential. Several of the analogs also exhibited novel DNA cleavage sites not shared by deglycoBLM itself, and some of the analogs containing multiple aromatic substituents were noted to shift the DNA bands, consistent with the interpretation that they bound to DNA more avidly than deglycoBLM itself. While none of the library members effected the oxidative degradation of $tRNA_3^{Lys}$ in the presence of Fe^{2+}, some of them were capable of mediating the hydrolytic cleavage of the RNA substrate in the absence of metal ions, as noted previously for BLM itself.[101] Critically, for any amino acid constituent whose inclusion rendered the parent molecule (deglycoBLM) poorly functional in DNA cleavage, no combination of changes elsewhere in the molecule was capable of restoring function. This observation has important practical implications for the design of more sophisticated BLM libraries.

The ability to prepare parallel libraries of BLMs on beads should be readily extensible to mix-and-split libraries, that is, libraries containing mixtures of beads each of which contains multiple copies of a single (deglyco)BLM congener. In concert with the use of DNA molecular beacons already described as substrates for BLM,[168] it should in principle be possible to identify BLM congeners with improved properties by a process of *selection* rather than *design*. Clearly, the realization of this strategy could dramatically accelerate the development of a more complete understanding of the medicinal chemistry of BLM.

19.6 CLINICAL APPLICATIONS

BLM has been employed in the clinic as an antitumor agent for more than 30 years; the early studies and major findings have been summarized in two books.[169,170] BLM was found to have clinically apparent activity as a single agent when used to treat squamous cell carcinomas, including those of the skin, and head and neck.[171] Although initial studies involved limited numbers of patients, good response rates were also observed in the treatment of primary brain tumors and superficial bladder tumors.

A more usual application for BLM at the present time is in combination with other antitumor agents. BLM is effective as part of a regimen for the treatment of Hodgkin's lymphomas, testicular cancers, germ cell ovarian cancers, and some non-Hodgkin's lymphomas.[172,173] One feature that has promoted the study of BLM as an agent in combination therapy is its lack of myelosuppressive

activity. Pulmonary fibrosis, observable in about 10% of patients, is generally the dose-limiting toxicity for BLM in the clinic.[174,175]

BLM is well established in the clinic as an antitumor agent in certain regimens, where it has been shown to contribute to favorable clinical outcomes. A good example is its activity in the treatment of germ cell carcinomas.[176] In spite of its long history of clinical trials and applications, new uses continue to be sought for this agent. Numerous clinical trials have been reported within the past several years for a variety of indications, and a recent focus has involved the use of localized administration of the drug, which should minimize toxic side effects. Recent trials include those involving BLM treatment of complicated hemangiomas[177] and the treatment of craniopharyngiomas in children.[178] Other recent examples of clinical trials involving local administration of BLM have included the treatment of cutaneous warts[179] and lymphangioma,[180] and the sclerotherapy of microcystic lymphatic malformation in oral and facial regions.[181]

BLM has been used with cisplatin and vinblastine in a comparative study for the treatment of epithelial ovarian cancer,[182] and with etoposide and cisplatin for the treatment of advanced disseminated germ cell tumors.[183,184] Other studies include the use of BLM in combination with radiotherapy for the treatment of patients with inoperable head and neck cancer.[185] Following reports that the toxicity of BLM in cultured cells was increased dramatically by electroporation,[186] this technique has also been incorporated into clinical trials.[187] Recent clinical trials involving electrochemotherapy include the treatment of head and neck cancers,[188] and cutaneous and subcutaneous metastases including metastatic melanomas.[187,189,190] The response rates in these trials generally seem quite favorable.[191]

19.7 CONCLUSIONS

Although the BLMs have now been studied for more than four decades, a significant level of research activity is still readily apparent, and important new insights have been obtained recently. These include a better understanding of the specific RNA that may constitute a therapeutic target for BLM, the finding that DNA binding and cleavage under therapeutically relevant conditions involves DNA sequences quite different than what has been reported traditionally, and the recognition that BLM likely exhibits multiple binding modes in its interaction with DNA. Recent studies of BLMs altered in the carbohydrate moiety underscore the likely role of this structural element in tumor targeting, and possibly in defining the cytotoxic mechanism(s) of the drug. In addition to providing insights into the BLM biosynthesis, the increasingly successful manipulation of the genes for BLM biosynthesis should also afford access to a broader variety of analogs for characterization. The construction of larger synthetic combinational BLM libraries will certainly also provide access to BLMs will altered properties in DNA and RNA cleavage, and can guide the search for new clinically useful agents.

ACKNOWLEDGMENT

Work in our laboratory on bleomycin is supported by NIH Research Grant CA140471, awarded by the National Cancer Institute.

REFERENCES

1. Umezawa, H., Thirty-five years with bioactive microbial products, *Heterocycles*, 13, 17, 1979.
2. Crooke, S. T., Bleomycin: A brief review, in *Bleomycin: Current Status and New Developments*, Carter, S. K., Crooke, S. T., and Umezawa, H., Eds., Academic, New York, 1978, pp. 1–8.
3. Fujii, A., Biogenetic aspects of bleomycin-phleomycin group antibiotics, in *Bleomycin: Chemical, Biochemical and Biological Aspects*, Hecht, S. M., Ed., Springer-Verlag, New York, 1979, pp. 75–91.

4. Shen, B., Du, L., Sanchez, C., Edwards, D. J., Chen, M., and Murrell, J. M., Cloning and characterization of the bleomycin biosynthetic gene cluster from *Streptomyces verticillus* ATCC15003, *J. Nat. Prod.*, 65, 422, 2002.
5. Tao, M., Wang, L., Wendt-Pienkowski, E., George, N. P., Galm, U., Zhang, G., Coughlin, J. M., and Shen, B., The tallysomycin biosynthetic gene cluster from *Streptoalloteichus hindustanus* E465-94 ATCC 31158 unveiling new insights into the biosynthesis of the bleomycin family of antitumor antibiotics, *Mol. BioSyst*., 3, 60, 2007.
6. Wang, L., Tao, M., Wendt-Pienkoski, E., Galm, U., Coughlin, J. M., and Shen, B., Functional characterization of *tlmK* unveiling unstable carbinolamide intermediates in the tallysomycin biosynthetic pathway, *J. Biol. Chem*., 284, 8256, 2009.
7. Tao, M., Wang, L., Wendt-Pienkowski, E., Zhang, N., Yang, D., Galm, U., Coughlin, J. M., Xu, Z., and Shen, B., Functional characterization of *tlmH* in *Streptoalloteichus hindustanus* E465-94 ATCC 31158 unveiling new insight into tallysomycin biosynthesis and affording a novel bleomycin analog, *Mol. BioSyst*., 6, 349, 2010.
8. Wang, L., Yun, B.-S., George, N. P., Pienkowski, E. W., Galm, U., Oh, T.-J., Coughlin, J. M., Zhang, G., Tao, M., and Shen, B., Glycopeptide antitumor antibiotic zorbamycin from *Streptomyces flavoviridis* ATCC 21892: strain improvement and structure elucidation, *J. Nat. Prod*., 70, 402, 2007.
9. Galm, U., Wendt-Pienkowski, E., Wang, L., George, N. P., Oh, T.-J., Yi, F., Tao, M., Coughlin, J. M., and Shen, B., The biosynthetic gene cluster of zorbamycin, a member of the bleomycin family of antitumor antibiotics, from *Streptomyces flavoviridis* ATCC 21892, *Mol. BioSyst*., 5, 77, 2009.
10. Chien, M., Grollman, A. P., and Horwitz, S. B., Bleomycin-DNA interactions: Fluorescence and proton magnetic resonance studies, *Biochemistry*, 16, 3641, 1977.
11. Boger, D., Colletti, S. L., Honda, T., and Menezes, R. F., Total synthesis of bleomycin A_2 and related agents. 1. Synthesis and DNA binding properties of the extended C-terminus: Tripeptide S, tetrapeptide S, pentapeptides S, and related agents, *J. Am. Chem. Soc.*, 116, 5607, 1994.
12. Sugiyama, H., Kilkuskie, R. E., Chang, L. H., Ma, L. T., Hecht, S. M., van der Marel, G. A., and van Boom, J. H., DNA strand scission by bleomycin: Catalytic cleavage and strand selectivity, *J. Am. Chem. Soc.*, 108, 3852, 1986.
13. Carter, B. J., Murty, V. S., Reddy, K. S., Wang, S. N., and Hecht, S. M., A role for the metal binding domain of bleomycin in determining the DNA sequence selectivity of Fe-bleomycin, *J. Biol. Chem.*, 265, 4193, 1990.
14. Guajardo, R. J., Hudson, S. E., Brown, S. J., and Mascharak, P. K., $[Fe(PMA)]^{n+}$(n = 1,2): Good models of Fe-bleomycins and examples of mononuclear non-heme iron complexes with significant O_2-activation capabilities, *J. Am. Chem. Soc.*, 115, 7971, 1993.
15. Hecht, S. M., RNA degradation by bleomycin, a naturally occurring bioconjugate, *Bioconjugate Chem.*, 5, 513, 1994.
16. Boger, D. L., Ramsey, T. M., Cai, H., Hoehn, S. T., and Stubbe, J., A systematic evaluation of the bleomycin A_2 L-threonine side chain: Its role in preorganization of a compact conformation implicated in sequence-selective DNA cleavage, *J. Am. Chem. Soc.*, 120, 9139, 1998.
17. Boger, D. L., Ramsey, T. M., Cai, H., Hoehn, S. T., and Stubbe, J., Definition of the effect and role of the bleomycin A_2 valerate substituents: Preorganization of a rigid, compact conformation implicated in sequence-selective DNA cleavage, *J. Am. Chem. Soc.*, 120, 9149, 1998.
18. Goodwin, K. D., Lewis, M. A., Long, E. C., and Georgiadis, M. M., Crystal structure of DNA-bound Co(III)·bleomycin B_2: Insights on intercalation and minor groove binding, *Proc. Natl. Acad. Sci. U.S.A.*, 105, 5052, 2008.
19. Chen, J., Ghorai, M. K., Kenney, G., and Stubbe, J., Mechanistic studies on bleomycin-mediated DNA damage: Multiple binding modes can result in double-stranded DNA cleavage, *Nucleic Acids Res*., 36, 3781, 2008.
20. Keck, M. V., Manderville, R. A., and Hecht, S. M., Chemical and structural characterization of the interaction of bleomycin A_2 with $d(CGCGAATTCGCG)_2$. Efficient, double-strand DNA cleavage accessible without structural reorganization, *J. Am. Chem. Soc.*, 123, 8690, 2001.
21. Abraham, A. T., Zhou, X., and Hecht, S. M., DNA cleavage by Fe(II)·bleomycin conjugated to a solid support, *J. Am. Chem. Soc.*, 121, 1982, 1999.
22. Akiyama, Y., Ma, Q., Edgar, E., Laikhter, A., and Hecht, S. M., Identification of strong DNA binding motifs for bleomycin, *J. Am. Chem. Soc*., 130, 9650, 2008.
23. Ma, Q., Akiyama, Y., Xu, Z., Konishi, K., and Hecht, S. M., Identification and cleavage site analysis of DNA sequences bound strongly by bleomycin, *J. Am. Chem. Soc*., 131, 2013, 2009.
24. Tao, Z.-F., Konishi, K., Keith, G., and Hecht, S. M., An efficient mammalian transfer RNA target for bleomycin, *J. Am. Chem. Soc*., 128, 14806, 2006.

25. Chapuis, J.-C., Schmaltz, R. M., Tsosie, K. S., Belohlavek, M., and Hecht, S. M., Carbohydrate dependent targeting of cancer cells by bleomycin-microbubble conjugates, *J. Am. Chem. Soc*., 131, 2438, 2009.
26. Natrajan, A. and Hecht, S. M., Bleomycin: Mechanism of polynucleotide recognition and oxidative degradation, in *Molecular Aspects of Anticancer Drug-DNA Interactions*, Neidle, S. and Waring, M., Eds., MacMillan, London, 1994, pp. 197–242.
27. Hecht, S. M., Bleomycin: New perspectives on the mechanism of action, *J. Nat. Prod.*, 63, 158, 2000.
28. Barranco, S. C. and Humphrey, R. M., Effects of bleomycin on survival and cell progression in Chinese hamster cells, *Cancer Res.*, 31, 1218, 1971.
29. Hittelman, W. N. and Rao, P. N., Bleomycin-induced damage in prematurely condensed chromosomes and its relation to cell cycle progression in CHO [Chinese hamster ovary] cells, *Cancer Res.*, 34, 3433, 1974.
30. Barlogie, B., Drewinko, B., Schumann, J., and Freireich, E J., Pulse cytophotomeric analysis of cell cycle perturbation with bleomycin *in vitro*, *Cancer Res.*, 36, 1182, 1976.
31. Carter, B. J., de Vroom, E., Long, E. C., van der Marel, G. A., van Boom, J. H., and Hecht, S. M., Site-specific cleavage of RNA by Fe(II)·bleomycin, *Proc. Natl. Acad. Sci. U.S.A.*, 87, 9373, 1990.
32. Holmes, C. E., Carter, B. J., and Hecht, S. M., Characterization of iron(II)-bleomycin-mediated RNA strand scission, *Biochemistry*, 32, 4293, 1993.
33. Morgan, M. and Hecht, S. M., Iron(II)bleomycin-mediated degradation of a DNA-RNA heteroduplex, *Biochemistry*, 33, 10286, 1994.
34. Decker, A., Chow, M. S., Kemsley, J. N., Lehnert, N., and Solomon, E. I., Direct hydrogen-atom abstraction by activated bleomycin: An experimental and computational study, *J. Am. Chem. Soc*., 128, 4719, 2006.
35. Kumar, D., Hirao, H., Shaik, S., and Kozlowski, P. M., Proton-shuffle mechanism of O–O activation for formation of a high-valent oxo–iron species of bleomycin, *J. Am. Chem. Soc*., 128, 16148, 2006.
36. Claussen, C. A. and Long, E. C., Nucleic acid recognition by metal complexes of bleomycin, *Chem. Rev.*, 99, 2797, 1999.
37. Ehrenfeld, G. M., Shipley, J. B., Heimbrook, D. C., Sugiyama, H., Long, E. C., Van Boom, J. H., Van der Marel, G. A., Oppenheimer, N. J., and Hecht, S. M., Copper dependent cleavage of DNA by bleomycin, *Biochemistry*, 26, 931, 1987.
38. Murugesan, N., Ehrenfeld, G. M., and Hecht, S. M., Oxygen transfer from bleomycin-metal complexes, *J. Biol. Chem.*, 257, 8600, 1982.
39. Murugesan, N. and Hecht, S. M., Bleomycin as an oxene transferase: Catalytic oxygen transfer to olefins, *J. Am. Chem. Soc.*, 107, 493, 1985.
40. Burger, R. M., Peisach, J., and Horwitz, S. B., Activated bleomycin: A transient complex of drug, iron, and oxygen that degrades DNA, *J. Biol. Chem.*, 256, 11636, 1981.
41. Natrajan, A., Hecht, S. M., van der Marel, G. A., and van Boom, J. H., A study of O_2 vs H_2O_2-supported activation of Fe·bleomycin, *J. Am. Chem. Soc*., 112, 3997, 1990.
42. Ishida, R. and Takahashi, T., Increased DNA chain breakage by combined action of bleomycin and superoxide radical, *Biochem. Biophys. Res. Commun.*, 66, 1432, 1975.
43. Sausville, E. A., Peisach, J., and Horwitz, S. B., Effect of chelating agents and metal ions on the degradation of DNA by bleomycin, *Biochemistry*, 17, 2740, 1978.
44. Sausville, E. A., Stein, R. W., Peisach, J., and Horwitz, S. B., Properties and products of the degradation of DNA by bleomycin and iron (II), *Biochemistry*, 17, 2746, 1978.
45. Ehrenfeld, G. M., Rodriguez, L. O., Hecht, S. M., Chang, C., Basus, V. J., and Oppenheimer, N. J., Copper (I)-bleomycin: Structurally unique complex that mediates oxidative DNA strand scission, *Biochemistry*, 24, 81, 1985.
46. Ehrenfeld, G. M., Murugesan, N., and Hecht, S. M., Activation of oxygen and mediation of DNA degradation by manganese-bleomycin, *Inorg. Chem.*, 23, 1496, 1984.
47. Burger, R. M., Freedman, J. H., Horwitz, S. B., and Peisach, J., DNA degradation by manganese (II)-bleomycin plus peroxide, *Inorg. Chem.*, 23, 2215, 1984.
48. Kuwahara, J., Suzuki, T., and Sugiura, Y., Effective DNA cleavage by bleomycin-vanadium (IV) complex plus hydrogen peroxide, *Biochem. Biophys. Res. Commun.*, 129, 368, 1985.
49. Sugiyama, H., Kilkuskie, R. E., Hecht, S. M., van der Marel, G. A., and van Boom, J. H., An efficient, site-specific DNA target for bleomycin, *J. Am. Chem. Soc.*, 107, 7765, 1985.
50. Sugiyama, H., Ehrenfeld, G. M., Shipley, J. B., Kilkuskie, R. E., Chang, L. H., and Hecht, S. M., DNA strand scission by bleomycin group antibiotics, *J. Nat. Prod.*, 48, 869, 1985.
51. Sugiyama, H., Xu, C., Murugesan, N., and Hecht, S. M., Structure of the alkali-labile product formed during Fe(II)·bleomycin-mediated DNA strand scission, *J. Am. Chem. Soc.*, 107, 4104, 1985.

52. Rabow, L., Stubbe, J., Kozarich, J. W., and Gerlt, J. A., Identification of the alkali-labile product accompanying cytosine release during bleomycin-mediated degradation of d(CGCGCG), *J. Am. Chem. Soc.*, 108, 7130, 1986.
53. Sugiyama, H., Xu, C., Murugesan, N., Hecht, S. M., van der Marel, G. A., and van Boom, J. H., Chemistry of the alkali-labile lesion formed from iron(II)-bleomycin and d(CGCTTTAAAGCG), *Biochemistry*, 27, 58, 1988.
54. Burger, R. M., Peisach, J., and Horwitz, S. B., Stoichiometry of DNA strand scission and aldehyde formation by bleomycin, *J. Biol. Chem.*, 257, 8612, 1982.
55. Wu, J. C., Kozarich, J. W., and Stubbe, J., The mechanism of free base formation from DNA by bleomycin: A proposal based on site specific tritium release from poly(dA.dU), *J. Biol. Chem.*, 258, 4694, 1983.
56. Wu, J. C., Stubbe, J., and Kozarich, J. W., Mechanism of bleomycin: Evidence for 4′-ketone formation in poly(dA-dU) associated exclusively with free base release, *Biochemistry*, 24, 7569, 1985.
57. Rabow, L. E., Stubbe, J., and Kozarich, J. W., Identification and quantitation of lesion accompanying base release in bleomycin-mediated DNA degradation, *J. Am. Chem. Soc.*, 112, 3196, 1990.
58. Rabow, L. E., Stubbe, J., Kozarich, J. W., and McGall, G. H., Identification of the source of oxygen in the alkaline-labile product accompanying cytosine release during bleomycin-mediated oxidative degradation of d(CGCGCG), *J. Am. Chem. Soc.*, 112, 3203, 1990.
59. Kane, S. A. and Hecht, S. M., Polynucleotide recognition and degradation by bleomycin, *Prog. Nucleic Acid Res. Mol. Biol.*, 49, 313, 1994.
60. Kozarich, J. W., Worth, L., Jr., Frank, B. L., Christner, D. F., Vanderwall, D. E., and Stubbe, J., Sequence-specific isotope effects on the cleavage of DNA by bleomycin, *Science*, 245, 1396, 1989.
61. Sczepanski, J. T., Jacobs, A. C., Majumdar, A., and Greenberg, M. M., Scope and mechanism of interstrand cross-link formation by the C4′-oxidized abasic site, *J. Am. Chem. Soc.*, 131, 11132, 2009.
62. Povirk, L. F., Zhou, T., Zhou, R., Cowan, M. J., and Yannone, S. M., Processing of 3′-phosphoglycolate-terminated DNA double strand breaks by Artemis nuclease, *J. Biol. Chem.*, 282, 3547, 2007.
63. Henner, W. D., Rodriguez, L. O., Hecht, S. M., and Haseltine, W. A., γ Ray induced deoxyribonucleic acid strand breaks: 3′-Glycolate termini, *J. Biol. Chem.*, 258, 711, 1983.
64. Heimbrook, D. C., Mulholland, R. L., and Hecht, S. M, Multiple pathways in the oxidation of *cis*-stilbene by Fe·bleomycin, *J. Am. Chem. Soc.*, 108, 7839, 1986.
65. Heimbrook, D. C., Carr, S. A., Mentzer, M. A., Long, E. C., and Hecht, S. M., On the mechanism of oxygenation of *cis*-stilbene by Fe·bleomycin, *Inorg. Chem.*, 26, 3835, 1987.
66. Burger, R. M., and Drlica, K., Superoxide protects *Escherichia coli* from bleomycin mediated lethality, *J. Inorg. Biochem.*, 103, 1273, 2009.
67. Sugiura, Y., Suzuki, T., Kuwahara, J., and Tanaka, H. *Biochem. Biophys. Res. Commun.*, 105, 1511, 1982.
68. Van Atta, R. B., Long, E. C., Hecht, S. M., Van der Marel, G. A., and Van Boom, J. H., Electrochemical activation of oxygenated Fe·bleomycin, *J. Am. Chem. Soc.*, 111, 2722, 1989.
69. Oppenheimer, N. J., Chang, C., Rodriguez, L. O., and Hecht, S. M., Copper(I)·bleomycin: A structurally unique redox-active complex, *J. Biol. Chem.*, 256, 1514, 1981.
70. Wu, W., Vanderwall, D. E., Lui, S. M., Tang, X.-J., Turner, C. J., Kozarich, J. W., and Stubbe, J., Studies of Co·bleomyicn A_2 green: Its detailed structural characterization by NMR and molecular modeling and its sequence-specific interaction with DNA oligonucleotides, *J. Am. Chem. Soc.*, 118, 1268, 1996.
71. Chang, C.-H. and Meares, C. F., Light-induced nicking of deoxyribonucleic acid by cobalt(III)bleomycins, *Biochemistry*, 21, 6332, 1982.
72. Chang, C.-H., and Meares, C. F., Cobalt-bleomycins and deoxyribonucleic acid: Sequence-dependent interactions, action spectrum for nicking, and indifference to oxygen, *Biochemistry*, 23, 2268, 1984.
73. Subramanian, R. and Meares, C. F., Photosensitization of cobalt bleomycin, *J. Am. Chem. Soc.*, 108, 6427, 1986.
74. Saito, I., Morii, T., Sugiyama, H., Matsuura, T., Meares, C. F., and Hecht, S. M., Photoinduced DNA strand scission by cobalt bleomycin green complex, *J. Am. Chem. Soc.*, 111, 2307, 1989.
75. McLean, M. J., Dar, A., and Waring, M. J., Differences between sites of binding to DNA and strand cleavage for complexes of bleomycin with iron or cobalt, *J. Mol. Recog.*, 1, 184, 1989.
76. Boger, D. L., Honda, T., Menezes, R. F., and Colletti, S. L., Total synthesis of bleomycin A_2 and related agents. 3. Synthesis and comparative evaluation of deglycobleomycin A_2, epideglycobleomycin A_2, deglycobleomycin A_1, and desacetamido-, descarboxamido-, desmethyl-, and desimidazolyldeglycobleomycin A_2, *J. Am. Chem. Soc.*, 116, 5631, 1994.
77. Povirk, L. F., Han, Y.-H., and Steighner, R. J., Structure of bleomycin-induced DNA double-strand breaks: Predominance of blunt ends and single-base 5′ extensions, *Biochemistry*, 28, 5808, 1989.

78. Steighner, R. J. and Povirk, L. F., Bleomycin-induced DNA lesions at mutational hot spots: Implications for the mechanism of double-strand cleavage, *Proc. Natl. Acad. Sci. U.S.A.*, 87, 8350, 1990.
79. Absalon, M. J., Kozarich, J. W., and Stubbe, J., Sequence specific double-strand cleavage of DNA by Fe-bleomycin. 1. The detection of sequence-specific double-strand breaks using hairpin oligonucleotides, *Biochemistry*, 34, 2065, 1995.
80. Absalon, M. J., Wu, W., Kozarich, J. W., and Stubbe, J., Sequence-specific double-strand cleavage of DNA by Fe-bleomycin. 2. Mechanism and dynamics, *Biochemistry*, 34, 2076, 1995.
81. Hoehn, S. T., Junker, H.-D., Bunt, R. C., Turner, C. J., and Stubbe, J., Solution structure of Co(III)-bleomycin-OOH bound to a phosphoglycolate lesion containing oligonucleotide: Implications for bleomycin-induced double-strand DNA cleavage, *Biochemistry*, 40, 5894, 2001.
82. Lui, S. M., Vanderwall, D. E., Wu, W., Tang, X.-J., Turner, C. J., Kozarich, J. W., and Stubbe, J., Structural characterization of Co·bleomycin A_2 brown: Free and bound to d(CCAGGCCTGG), *J. Am. Chem. Soc.*, 199, 9603, 1997.
83. Wu, W., Vanderwall, D. E., Teramoto, S., Lui, S. M., Hoehn, S., Tang, X.-J., Turner, C. J., Boger, D. L., Kozarich, J. W., and Stubbe, J., NMR studies of Co·deglycobleomycin A_2 green and its complex with d(CCAGGCCTGG), *J. Am. Chem. Soc.*, 120, 2239, 1998.
84. Oppenheimer, N. J., Rodriguez, L. O., and Hecht, S. M., Structural studies of "active complex" of bleomycin: An assignment of the ligands to the ferrous ion in a ferrous-bleomycin-carbon monoxide complex, *Proc. Natl. Acad. Sci. U.S.A.*, 76, 5616, 1979.
85. Manderville, R. A., Ellena, J. F., and Hecht, S. M., Interaction of Zn(II)·bleomycin with $d(CGCTAGCG)_2$: A binding model based on NMR experiments and restrained molecular dynamics calculations, *J. Am. Chem. Soc.*, 117, 7891, 1995.
86. Sucheck, S. J., Ellena, J. F., and Hecht, S. M., Characterization of Zn(II)·deglycobleomycin A_2 and interaction with $d(CGCTAGCG)_2$: Direct evidence for minor groove binding of the bithiazole moiety, *J. Am. Chem. Soc.*, 120, 7450, 1998.
87. Zuber, G., Quada, J. C., Jr., and Hecht, S. M., Sequence selective cleavage of a DNA octanucleotide by chlorinated bithiazoles and bleomycins, *J. Am. Chem. Soc.*, 120, 9368, 1998.
88. Boger, D. L., Fink, B. E., Brunette, S. R., Tse, W. C., and Hedrick, M. P., A simple, high-resolution method for establishing DNA binding affinity and sequence selectivity, *J. Am. Chem. Soc*., 123, 5878, 2001.
89. Lewis, M. A. and Long, E. C., Fluorescent intercalator displacement analyses of DNA binding by the peptide-derived natural products netropsin, actinomycin, and bleomycin, *Bioorg. Med. Chem*., 14, 3481, 2006.
90. Akiyama, Y., Ma, Q., Edgar, E., Laikhter, A., and Hecht, S. M., A novel DNA hairpin substrate for bleomycin, *Org. Lett*., 10, 2127, 2008.
91. Magliozzo, R. S., Peisach, J., and Ciriolo, M. R., Transfer RNA is cleaved by activated bleomycin, *Mol. Pharmacol.*, 35, 428, 1989.
92. Carter, B. J., Reddy, K. S., and Hecht, S. M., Polynucleotide recognition and strand scission by Fe·bleomycin, *Tetrahedron*, 47, 2463, 1991.
93. Carter, B. J., Holmes, C. E., Van Atta, R. B., Dange, V., and Hecht, S. M., Metal-catalyzed polynucleotide strand scission, *Nucleos. Nucleot.*, 10, 215, 1991.
94. Hüttenhofer, A., Hudson, S., Noller, H. F., and Mascharak, P. K., Cleavage of tRNA by Fe(II)-bleomycin, *J. Biol. Chem.*, 267, 24471, 1992.
95. Benás, P., Bec, G., Keith, G., Marquet, R., Ehresmann, C., Ehresmann, B., and Dumas, P., The crystal structure of HIV reverse-transcription primer tRNA(Lys,3. shows a canonical anticodon loop, *RNA*, 6, 1347, 2000.
96. Abraham, A. T., Lin, J.-J., Newton, D. L., Rybak, S., and Hecht, S. M., RNA cleavage and inhibition of protein synthesis by bleomycin, *Chem. Biol.*, 10, 45, 2003.
97. Dix, D. J., Lin, P. N., McKenzie, A. R., Walden, W. E., and Theil, E. C., The influence of the base-paired flanking region on structure and function of the ferritin mRNA iron regulatory element, *J. Mol. Biol.*, 231, 230, 1993.
98. Snow, A., Characterization of the cellular loci of bleomycin-mediated damage. Ph.D. Thesis, University of Virginia, 1995.
99. Duff, R. J., de Vroom, E., Geluk, A., Hecht, S. M., van der Marel, G. A., and van Boom, J. H., Evidence for C-1′ hydrogen abstraction from modified oligonucleotides by Fe·bleomycin, *J. Am. Chem. Soc.*, 115, 3350, 1993.
100. Holmes, C. E., Duff, R. J., van der Marel, G. A., van Boom, J., and Hecht, S.M., On the chemistry of RNA degradation by Fe(II)·BLM, *Bioorg. Med. Chem.*, 5, 1235, 1997.

101. Keck, M. V. and Hecht, S. M., Sequence-specific hydrolysis of yeast $tRNA^{Phe}$ mediated by metal free bleomycin, *Biochemistry*, 34, 12029, 1995.
102. Ardelt, W., Mikulski, S. M., and Shogen, K., Amino-acid-sequence of an antitumor protein from rana-pipiens oocytes and early embryos-homology to pancreatic ribonucleases, *J. Biol. Chem.*, 266, 245, 1991.
103. Darzynkiewicz, Z., Carter, S. P., Mikulski, S. M., Ardelt, W. J., and Shogen, K., Cystostatic and cytotoxic effects of pannon P-30: A novel anticancer agent, *Cell Tissue Kinet.*, 21, 169, 1988.
104. Mikulski, S. M., Viera, A., Ardelt, W., Menduke, H., and Shogen, K., Tamoxifen and trifluoroperazine (stelazine) potentiate cystostatic cytotoxic effects of P-30 protein: A novel protein possessing antitumor activity, *Cell Tissue Kinet.*, 23, 237, 1990.
105. Mikulski, S. M., Ardelt, W., Shogen, K., Bernstein, E. H., and Menduke, H., Striking increase of survival of mice bearing M109 madison carcinoma treated with a novel protein from amphibian embryos, *J. Natl. Cancer Inst.*, 82, 151, 1990.
106. Mikulski, S. M., Grossman, A. M., Carter, P. W., Shogen, K., and Costanzi, J. J., Phase-1 human clinical trial of onconase (R) (P-30 protein) administered intravenously on a weekly schedule in cancer patients with solid tumors, *Int. J. Oncol.*, 3, 57, 1993.
107. Lin, J.-J., Newton, D. L., Mikulski, S. M., Kung, H.-F., Youle, R. J., and Rybak, S. M., Characterization of the mechanism of cellular and cell free protein synthesis inhibition by an anti-tumor ribonuclease, *Biochem. Biophys. Res. Commun.*, 204, 156, 1994.
108. Saxena, S. K., Sirdeshmukh, R., Ardelt, W., Mikulski, S. M., Shogen, K., and Youle, R. J., Entry into cells and selective degradation of tRNAs by a cytotoxic member of the RNase A family, *J. Biol. Chem.*, 277, 15142, 2002.
109. Suhasini, A. N. and Sirdeshmukh, R., Onconase action on $tRNA^{Lys3}$, the primer for HIV-1 reverse transcription, *Biochem. Biophys. Res. Commun.*, 363, 304, 2007.
110. Suhasini, A. N. and Sirdeshmukh, R., Transfer RNA cleavages by onconase reveal unusual cleavage sites, *J. Biol. Chem.*, 281, 12201, 2006.
111. Saxena, S. K., Gravell, M., Wu, Y.-N., Mikulski, S. M., Shogen, K., Ardelt, W., and Youle, R. J., Inhibition of HIV-1 production and selective degradation of viral RNA by an amphibian ribonuclease, *J. Biol. Chem.*, 271, 20783, 1996.
112. Tafech, A., Bassett, T., Sparanese, D., and Lee, C. H., Destroying RNA as a therapeutic approach, *Curr. Med. Chem.*, 13, 863, 2006.
113. Youle, R. J., Wu, Y.-N., Mikulski, S. M., Shogen, K., Hamilton, R. S., Newton, D., D'Alessio, G., and Gravell, M., RNase inhibition of human immunodeficiency virus infection of H9 cells, *Proc. Natl. Acad. Sci. U.S.A.*, 91, 6012, 1994.
114. Georgiou, N. A., Van der Bruggen, T., Healy, D. M. C., van Tienen, C., de Bie, P., Oudshoorn, M., Marx, J. J. M., and van Asbeck, B. S., Bleomycin has antiviral properties against drug-resistant HIV strains and sensitizes virus to currently used antiviral agents, *Int. J. Antimicrob. Agents*, 27, 63, 2006.
115. Galm, U., Wang, L., Wendt-Pienkowski, E., Yang, R., Liu, W., Tao, M., Coughlin, J. M., and Shen, B., *In vivo* manipulation of the bleomycin biosynthetic gene cluster in *Streptomyces verticillus* ATCC15003 revealing new insights into its biosynthetic pathway, *J. Biol. Chem.*, 283, 28236, 2008.
116. Berry, D. E., Chang, L.-H., and Hecht, S. M., DNA damage and growth inhibition in cultured human cells by bleomycin congeners, *Biochemistry*, 24, 3207, 1985.
117. Aouida, M., Poulin, R., and Ramotar, D., The human carnitine transporter SLC22A16 mediates high affinity uptake of the anticancer polyamine analog bleomycin-A5, *J. Biol. Chem.*, 285, 6275, 2010.
118. Hecht, S. M., Bleomycin group antitumor agents, in *Cancer Chemotherapeutic Agents*, Foye, W. O., Ed., American Chemical Society, Washington, DC, 1995, pp 369–388.
119. Takita, T., Fujii, A., Fukuoka, T., and Umezawa, H., Chemical cleavage of bleomycin to bleomycinic acid and synthesis of new bleomycins, *J. Antibiot.*, 26, 252, 1973.
120. Tanaka, W. and Takita, T., Pepleomycin, the second generation bleomycin chemically derived from bleomycin A_2, *Heterocycles*, 13, 469, 1979.
121. Umezawa, H., Recent chemical studies of bioactive microbial products: Genetics, active structures, development of effective agents with potential usefulness, *Heterocycles*, 13, 23, 1979.
122. Umezawa, H., Takahashi, Y., Fuji, A., Saino, T., Shirai, T., and Takita, T., Preparation of bleomycinic acid: Hydrolysis of bleomycin B_2 by a fusarium acylagmatine amidohydrolase, *J. Antibiot.*, 26, 117, 1973.
123. Tanaka, W., Development of new bleomycins with potential clinical utility, *J. Antibiot.*, 30, S-41, 1977.
124. Saito, S., Umezawa, Y., Morishima, H., Takita, T., Umezawa, H., Narita, M., Otsuka, M., Kobayashi, S., and Ohno, M., A new synthesis of deglyco-bleomycin A_2 aiming at the total synthesis of bleomycin, *Tetrahedron Lett.*, 23, 529, 1982.

125. Aoyagi, Y., Suguna, H., Murugesan, N., Ehrenfeld, G. M., Chang, L. H., Ohgi, T., Shekhani, M. S., Kirkup, M. P., and Hecht, S. M., Deglycobleomycin: Total synthesis and oxygen transfer properties of an active bleomycin analog, *J. Am. Chem. Soc.*, 104, 5237, 1982.
126. Oppenheimer, N. J., Chang, C., Chang, L.-H., Ehrenfeld, G., Rodriguez, L. O., and Hecht, S. M., Deglycobleomycin: Degradation of DNA and formation of a structurally unique Fe(II)·CO complex, *J. Biol. Chem.*, 257, 1606, 1982.
127. Brahim, S., Prévotat, L., Yatouji, S., Mérino, D., Cortier, M., Rébé, C., Micheau, O., Kenani, A., and Bettaieb, A., Deglycosylated bleomycin induces apoptosis in lymphoma cell via c-jun NH_2-terminal kinase but not reactive oxygen species, *Biochem. Pharmacol.*, 74, 1445, 2007.
128. Brahim, S., Bettaieb, A., and Kenani, A., Deglycosylated bleomycin triggers apoptosis in laryngeal carcinoma cells in a caspase and reactive oxygen species independent manner, *J. Oral Pathol. Med.*, 37, 352, 2008.
129. Kross, J., Henner, W. D., Hecht, S. M., and Haseltine, W. A., Specificity of deoxyribonucleic acid cleavage by bleomycin, phleomycin and tallysomycin, *Biochemistry*, 21, 4310, 1982.
130. Umezawa, H., Advances in bleomycin studies, in *Bleomycin: Chemical, Biochemical and Biological Aspects*, Hecht, S. M., Ed., Springer-Verlag, New York, 1979, pp 24–36.
131. Takahashi, K., Ekimoto, H., Minamide, S., Nishikawa, N., Kuramochi, H., Motegi, A., Nakatani, T., Takita, T., Takeuchi, T., and Umezawa, H., Liblomycin, a new analog of bleomycin, *Cancer Treat. Rev.*, 14, 169, 1987.
132. Takita, T., Umezawa, Y., Saito, S., Morishima, H., Naganawa, H., Umezawa, H., Tsuchiya, T., et al., Total synthesis of bleomycin A_2, *Tetrahedron Lett.*, 23, 521, 1982.
133. Aoyagi, Y., Katano, K., Suguna, H., Primeau, J., Chang, L. H., and Hecht, S. M., Total synthesis of bleomycin, *J. Am. Chem. Soc.*, 104, 5537, 1982.
134. Boger, D. L. and Honda, T., Total synthesis of bleomycin A_2 and related agents. 4. Synthesis of the disaccharide subunit 2-O-(3-O-carbamoyl-α-D-mannopyranosyl)-L-gulopyranose and completion of the total synthesis of bleomycin A_2, *J. Am. Chem. Soc.*, 116, 5647, 1994.
135. Katano, K., An, H., Aoyagi, Y., Overhand, M., Sucheck, S. J., Stevens, W. C., Jr., Hess, C. D., Zhou, X., and Hecht, S. M., Total synthesis of bleomycin group antibiotics. Total synthesis of bleomycin demethyl A_2, bleomycin A_2, and decarbamoyl bleomycin demethyl A_2, *J. Am. Chem. Soc.*, 120, 11285, 1998.
136. Boger, D. L., Teramoto, S., and Zhou, J., Key synthetic analogs of bleomycin A_2 that directly address the effect and role of the disaccharide: Demannosylbleomycin A_2 and α-D-mannopyranosyldeglycobleomycin A_2, *J. Am. Chem. Soc.*, 117, 7344, 1995.
137. Zou, Y., Fahmi, N. E., Vialas, C., Miller, G. M., and Hecht, S. M., Total synthesis of deamido bleomycin A_2, the major catabolite of the antitumor agent bleomycin, *J. Am. Chem. Soc.*, 124, 9476, 2002.
138. Leitheiser, C. J., Rishel, M. J., Wu, X., and Hecht, S. M., Solid phase synthesis of bleomycin group antibiotics: Elaboration of deglycobleomycin A_5, *Org. Lett.*, 2, 3397, 2000.
139. Aoyagi, Y., Chorghade, M. S., Padmapriya, A. A., Suguna, H., and Hecht, S. M., Synthesis of pyrimidoblamic acid and epipyrimidoblamic acid, *J. Org. Chem.*, 55, 6291, 1990.
140. Smith, K. L., Tao, Z.-F., Hashimoto, S., Leitheiser, C. J., Wu, X., and Hecht, S. M., Deglycobleomycin: Solid-phase synthesis and DNA cleavage by the resin-bound ligand, *Org. Lett.*, 4, 1079, 2002.
141. Gordeev, M. F., Luehr, G. W., Hui, H. C., Gordon, E. M., and Patel, D. V., Combinatorial chemistry of natural products: Solid phase synthesis of D-and L-cycloserine derivatives, *Tetrahedron*, 54, 15879, 1998.
142. Tao, Z.-F., Leitheiser, C. J., Smith, K. L., Hashimoto, S., and Hecht, S. M., Solid phase synthesis of deglycobleomycins: A C-terminal tetraamine linker that permits direct evaluation of resin-bound bleomycins, *Bioconjugate Chem.*, 13, 426, 2002.
143. Owa, T., Otsuka, M., and Ohno, M., An efficient synthesis of *erythro*-β-hydroxy-L-histidine, the pivotal amino acid of bleomycin-Fe(II)-O_2 complex, *Chem. Lett.*, 1873, 1988.
144. Boger, D. L. and Menezes, R. F., Synthesis of tri- and tetrapeptide S: The extended C-terminus of bleomycin A_2, *J. Org. Chem.*, 57, 4331, 1992.
145. Thomas, C. J., Chizhov, A. O., Leitheiser, C. J., Rishel, M. J., Konishi, K., Tao, Z.-F., and Hecht, S. M., Solid phase synthesis of bleomycin A_5 and three monosaccharide analogs: Exploring the role of the carbohydrate moiety in RNA cleavage, *J. Am. Chem. Soc.*, 124, 12926, 2002.
146. Hamamichi, N. and Hecht, S. M., Determination of the absolute configuration of the thiazolinylthiazole moiety of phleomycin, *J. Am. Chem. Soc.*, 115, 12605, 1993.
147. Sznaidman, M. L. and Hecht, S. M., Studies on the total synthesis of tallysomycin. Synthesis of the threonylbithiazole moiety containing a structurally unique glycosylcarbinolamide, *Org. Lett.*, 3, 2811, 2001.
148. Morii, T., Matsuura, T., Saito, I., Suzuki, T., Kuwahara, J., and Sugiura, Y., Phototransformed bleomycin antibiotics: Structure and DNA cleavage activity, *J. Am. Chem. Soc.*, 108, 7089, 1986.

149. Morii, T., Saito, I., Matsuura, T., Kuwahara, J., and Sugiura, Y., New lumibleomycin-containing thiazolylisothiazole ring, *J. Am. Chem. Soc.*, 109, 938, 1987.
150. Hamamichi, N., Natrajan, A., and Hecht, S. M., On the role of individual bleomycin thiazoles in oxygen activation and DNA cleavage, *J. Am. Chem. Soc.*, 114, 6278, 1992.
151. Otsuka, M., Masuda, T., Haupt, A., Ohno, M., Shiraki, T., Sugiura, Y., and Maeda, K., Man-designed bleomycin with altered sequence specificity in DNA cleavage, *J. Am. Chem. Soc.*, 112, 838, 1990.
152. Owa, T., Haupt, A., Otsuka, M., Kobayashi, S., Tomioka, N., Itai, A., Ohno, M. et al., Man-designed bleomycins: Significance of the binding sites as enzyme models and of the stereochemistry of the linker moiety, *Tetrahedron*, 48, 1193, 1992.
153. Kuwahara, J. and Sugiura, Y., Sequence-specific recognition and cleavage of DNA by metallobleomycin: Minor groove binding and possible interaction mode, *Proc. Natl. Acad. Sci. U.S.A.*, 85, 2459, 1988.
154. Quada, J. C., Jr., Zuber, G. F., and Hecht, S. M., Interaction of bleomycin with DNA, *Pure Appl. Chem.*, 70, 307, 1998.
155. Quada, J. C., Jr., Boturyn, D., and Hecht, S. M., Photoactivated DNA cleavage by compounds structurally related to the bithiazole moiety of bleomycin, *Bioorg. Med. Chem.*, 9, 2303, 2001.
156. Williams, L. D. and Goldberg, I. H., Selective strand scission by intercalating drugs at DNA bulges, *Biochemistry*, 27, 3004, 1988.
157. Gold, B., Dange, V., Moore, M., A., Eastman, A., van der Marel, G. A., van Boom, J. H., and Hecht, S. M., Alteration of bleomycin cleavage specificity in a platinated DNA oligomer of defined structure, *J. Am. Chem. Soc.*, 110, 2347, 1988.
158. Kane, S. A., Hecht, S. M., Sun, J.-S., Garestier, T., and Helene, C., Specific cleavage of a DNA triple helix by Fe^{II}·bleomycin, *Biochemistry*, 34, 16715, 1995.
159. Kross, J., Henner, W. D., Haseltine, W. A., Rodriquez, L., Levin, M. D., and Hecht, S. M., Structural basis for the DNA affinity of bleomycins, *Biochemistry*, 21, 3711, 1982.
160. Rishel, M. J., Thomas, C. J., Tao, Z.-F., Vialas, C., Leitheiser, C. J., and Hecht, S. M., Conformationally constrained analogs of bleomycin A_5, *J. Am. Chem. Soc.*, 125, 10194, 2003.
161. Cagir, A., Tao, Z.-F., Sucheck, S. J., and Hecht, S. M., Solid-phase synthesis and biochemical evaluation of conformationally constrained analogs of deglycobleomycin A_5, *Bioorg. Med. Chem.*, 11, 5179, 2003.
162. Boger, D. L., Ramsey, T. M., and Cai, H., Synthesis and evaluation of potential N^{π} and N^{σ} metal chelation sites with the beta-hydroxy-L-histidine subunit of bleomyin A_2: Functional characterization of imidazole N^{π} metal complexation, *Bioorg. Med. Chem.*, 4, 195, 1996.
163. Boger, D. L., Teramoto, S., and Cai, H., Synthesis and evaluation of deglycobleomycin A_2 analogs containing a tertiary *N*-methyl amide and simple ester replacement for the L-histidine secondary amide: Direct functional characterization of the requirement for secondary amide metal complexation, *Bioorg. Med. Chem.*, 4, 179, 1996.
164. Leitheiser, C. J., Smith, K. L., Rishel, M., J., Hashimoto, S., Konishi, K., Thomas, C., Li, C., McCormick, M., and Hecht, S. M., Solid phase synthesis of bleomycin group antibiotics. Construction of a 108-member deglycobleomycin library, *J. Am. Chem. Soc.*, 125, 8218, 2003.
165. Xu, Z.-D., Wang, M., Xiao, S.-L., Zhang, Y.-J., and Yang, M., Novel bleomycin analogs: Synthesis, antitumor activity, and interaction with DNA, *Helv. Chim. Acta*, 87, 2834, 2004.
166. Xu, Z.-D., Wang, M., Xiao, S.-L., and Yang, M., Novel peptide derivatives of bleomycin A_5: Synthesis, antitumor activity and interaction with DNA, *Bioorg. Med. Chem. Lett.*, 15, 3996, 2005.
167. Ma, Q., Xu, Z., Schroeder, B. R., Sun, W., Wei, F., Hashimoto, S., Konishi, K., Leitheiser, C. J., and Hecht, S. M., Biochemical evaluation of a 108-member deglycobleomycin library: Viability of a selection strategy for identifying bleomycin analogs with altered properties, *J. Am. Chem. Soc.*, 129, 12439, 2007.
168. Hashimoto, S., Wang, B., and Hecht, S. M., Kinetics of DNA cleavage by Fe(II)·bleomycins, *J. Am. Chem. Soc.*, 123, 7437, 2001.
169. Carter, S. K., Crooke, S. T., and Umezawa, H., Eds., *Bleomycin: Current Status and New Developments*, Academic Press, Orlando, FL, 1978.
170. Sikic, B. I., Rozencweig, M., and Carter, S. K., Eds., *Bleomycin Chemotherapy*, Academic Press, Orlando, FL, 1985.
171. Bennett, J. M. and Reich, S. D., Bleomycin, *Ann. Intern. Med.*, 90, 945, 1979.
172. Einhorn, L. H. and Donohue, J., Cis-diamminedichloroplatinum, vinblastine, and bleomycin combination chemotherapy in disseminated testicular cancer, *Ann. Intern. Med.*, 87, 293, 1977.
173. Carlson, R. W., Sikic, B. I., Turbow, M. M., and Ballon, S. C., Combination cisplatin, vinblastine, and bleomycin chemotherapy (PVB) for malignant germ-cell tumors of the ovary, *J. Clin. Oncol.*, 1, 645, 1983.

174. Comis, R. L., Kuppinger, M. S., Ginsberg, S. J., Crooke, S. T., Gilbert, R., Auchincloss, J. H., and Prestayko, A. W., Role of single-breath carbon monoxide-diffusing capacity in monitoring the pulmonary effects of bleomycin in germ cell tumor patients, *Cancer Res.*, 39, 5076, 1979.
175. Muggia, F. M., Louie, A. C., and Sikic, B. I., Pulmonary toxicity of antitumor agents, *Cancer Treat. Rev.*, 10, 221, 1982.
176. Levi, J. A., Raghavan, D., Harvey, V., Thompson, D., Sandeman, T., Gill, G., Stuart-Harris, R., Snyder, R., Byrne, M., and Kerestes, Z., The importance of bleomycin in combination chemotherapy for good-prognosis germ cell carcinoma, *J. Clin. Oncol.*, 11, 1300, 1993.
177. Omidvari, S., Nezakatgoo, N., Ahmadloo, N., Mohammadianpanah, M., and Mosalaei, A., Role of intralesional bleomycin in the treatment of complicated hemangiomas: Prospective clinical study, *Dermatologic. Surg*., 31, 499, 2005.
178. Hukin, J., Steinbok, P., Lafay-Cousin, L., Henderson, G., Strother, D., Mercier, C., Samson, Y., Howes, W., and Bouffet, E., Intracystic bleomycin therapy for craniopharyngioma in children: The Canadian experience, *Cancer*, 109, 2124, 2007.
179. Dhar, S. B., Rashid, M. M., Islam, A., and Bhuiyan, M., Intralesional bleomycin in the treatment of cutaneous warts: A randomized clinical trial comparing it with cryotherapy, *Ind. J. Dermatol. Venereol. Leprol*., 75, 262, 2009.
180. Baskin, D., Tander, B., and Bankaoglu, M., Local bleomycin injection in the treatment of lymphangioma, *Eur. J. Ped. Surg*., 15, 383, 2005.
181. Bai, Y., Jia, J., Huang, X. X., Alsharif, M. J., Zhao, J. H., and Zhao, Y. F., Sclerotherapy of microcystic lymphatic malformations in oral and facial regions, *J. Oral Maxillo. Surg*., 67, 251, 2009.
182. Tokuhashi, Y., Kikkawa, F., Tamakoshi, K., Suganuma, N., Kuzuya, K., Arii, Y., Kawai, M. et al., A randomized trial of cisplatin, vinblastine, and bleomycin versus cyclophosphamide, aclacinomycin, and cisplatin in eipthelial ovarian cancer, *Oncology*, 54, 281, 1997.
183. Nichols, C. R., Catalano, P. J., Crawford, E. D., Vogelzang, N. J., Einhorn, L. H., and Loehrer, P. J., Randomized comparison of cisplatin and etopside and either bleomycin or ifosfamide in treatment of advanced disseminated germ cell tumors: And Eastern Cooperative Oncology Group, Southwest Oncology Group, and Cancer and Leukemia Group B study, *J. Clin. Oncol.*, 16, 1287, 1998.
184. Christian, J. A., Huddart, R. A., Norman, A., Mason, M., Fossa, S., Aass, N., Nicholl, E. J., Dearnaley, D. P., and Horwich, A., Intensive induction chemotherapy with CBOP/BEP in patients with poor prognosis germ cell tumors, *J. Clin. Oncol.*, 21, 871, 2003.
185. Minatel, E., Gigante, M., Franchin, G., Gobitti, C., Mascarin, M., Bujor, L., Barzan, L., and Trovo, M. G., Combined radiotherapy and bleomycin in patients with inoperable head and neck cancer with unfavourable prognostic factors and severe symptoms, *Oral Oncol.*, 34, 119, 1998.
186. Poddevin, B., Orlowski, S., Belehradek, J., Jr., and Mir, L. M., Very high cytotoxicity of bleomycin introduced into the cytosol of cells in culture, *Biochem. Pharmacol.*, 42, 567, 1991.
187. Campana, L. G., Mocellin, S., Basso, M., Puccetti, O., De Salvo, G. L., Chiarion-Sileni, V., Vecchiato, A., Corti, L., Rossi, C. R., and Nitti, D., Bleomycin-based electrochemotherapy: Clinical outcome from a single institution's experience with 52 patients, *Ann. Surg. Oncol*., 16, 191, 2009.
188. Tijink, B. M., De Bree, R., Van Dongen, G. A., and Leemans, C. R., How we do it: Chemo-electroporation in the head and neck for otherwise untreatable patients, *Clin. Otolaryngol*., 31, 447, 2006.
189. Quaglino, P., Mortera, C., Osella-Abate, S., Barberis, M., Illengo, M., Rissone, M., Savola, P., and Bernengo, M. G., Electrochemotherapy with intravenous bleomycin in the local treatment of skin melanoma metastases, *Ann. Surg. Oncol*., 15, 2215, 2008.
190. Byrne, C. M., Thompson, J. F., Johnston, H., Hersey, P., Quinn, M. J., Hughes, T. M., and McCarthy, W. H., Treatment of metastatic melanoma using electroporation therapy with bleomycin (electrochemotherapy), *Melanoma Res*., 15, 45, 2005.
191. For additional information concerning current clinical trials, see: http://www.clinicaltrials.gov. Enter "cancer AND bleomycin."

20 Biochemical and Biological Evaluation of (+)-CC-1065 Analogs and Conjugates with Polyamides*

Rohtash Kumar and J. William Lown

CONTENTS

20.1 Introduction 479
20.2 Drug–DNA Interactions 481
20.3 Modification in the Pharmacophore Unit 482
20.3.1 CPI Analogs 482
20.3.2 Enantiomers of CPI Analogs 486
20.3.3 CC-1065 Analogs 486
20.3.4 Further Analogs 489
20.4 Interaction of CC-1065 with Chromatin 489
20.5 Polyamide Conjugates and Related Sequence Directed Structures 492
20.6 Bisalkylators (Dimers) 498
20.7 Structural Characterization of Drug DNA Complexes 498
20.8 Cellular and Pharmacological Studies 501
20.8.1 *In Vitro* Studies 501
20.8.2 *In Vivo* Studies 504
20.9 Development of Potential Targeted Therapies 505
20.10 Clinical Studies 505
20.11 Conclusions and Prospects 506
References 506

20.1 INTRODUCTION

CC-1065 (**1**) is an extremely potent antitumor antibiotic isolated from *Streptomyces zelensis* by Upjohn Company.[1,2] It is one of the most potent anticancer compounds having a wide spectrum of activities against tumor cells *in vitro* and *in vivo* as well as against microbial organisms.[3,4] Structurally, the CC-1065 molecule consists of three repeating pyrroloindole subunits, one of which contains the DNA reactive cyclopropylpyrroloindole (CPI) moiety (**2**), while the other two subunits mediate noncovalent binding interactions with DNA. CC-1065 alkylates the N3 position of adenine with its reactive cyclopropyl group in the minor groove of double helical DNA in a sequence-specific manner with a consensus sequence of 5-(T/A)(T/A) A* (where the asterisk indicates the site of alkylation). The preferred site of alkylation by CC-1065 was determined to be the 5-TTA* sequence.[4–10]

* This chapter has been updated by Gordon M. Cragg, Natural Products Branch, Developmental Therapeutics Program, Division of Cancer Treatment and Diagnosis, National Cancer Institute, Frederick, MD.

Despite the highly potent activity of CC-1065 *in vitro*[3,11] and *in vivo*,[2] clinical development was precluded by an unusual hepatotoxicity, which led to delayed death in mice at therapeutic doses.[12] Subsequently, an aggressive and highly successful synthetic program at the Upjohn company provided a series of three new compounds that appeared to be more suitable for clinical development. These agents, adozelesin (**3**), U-71184 (**4**), and U-80224 (**5**), have been shown to have improved antitumor efficacy over CC-1065 and do not show delayed lethality.[13,14]

Duocarmycin (**6a**), duocarmycin/SA (**6b**), and pyrindamycin (**7**) are structurally related natural products, with **6a** and **6b** possessing the CC-1065-DNA reactive cyclopropane ring.[15,16] The structural element of CC-1065 that produces delayed toxicity has been elucidated, but its biochemical mechanism is still unknown. Yatakemycin (**8**), the newest and most potent member of this structural class, was isolated from the culture broth of *Streptomyces* sp. TP-AO356.[17] Total synthesis led to a revision of its structure, and an asymmetric total synthesis has been reported.[18] A number of CC-1065 analogs, which maintain potent antitumor activity without exhibiting delayed death, were subsequently synthesized, and the unique feature of all these synthetic analogs is the cyclopropyl indole moiety (CPI; **2**). Bizelesin (**9**) is a bifunctional analog, shows good antitumor efficacy both *in vitro*

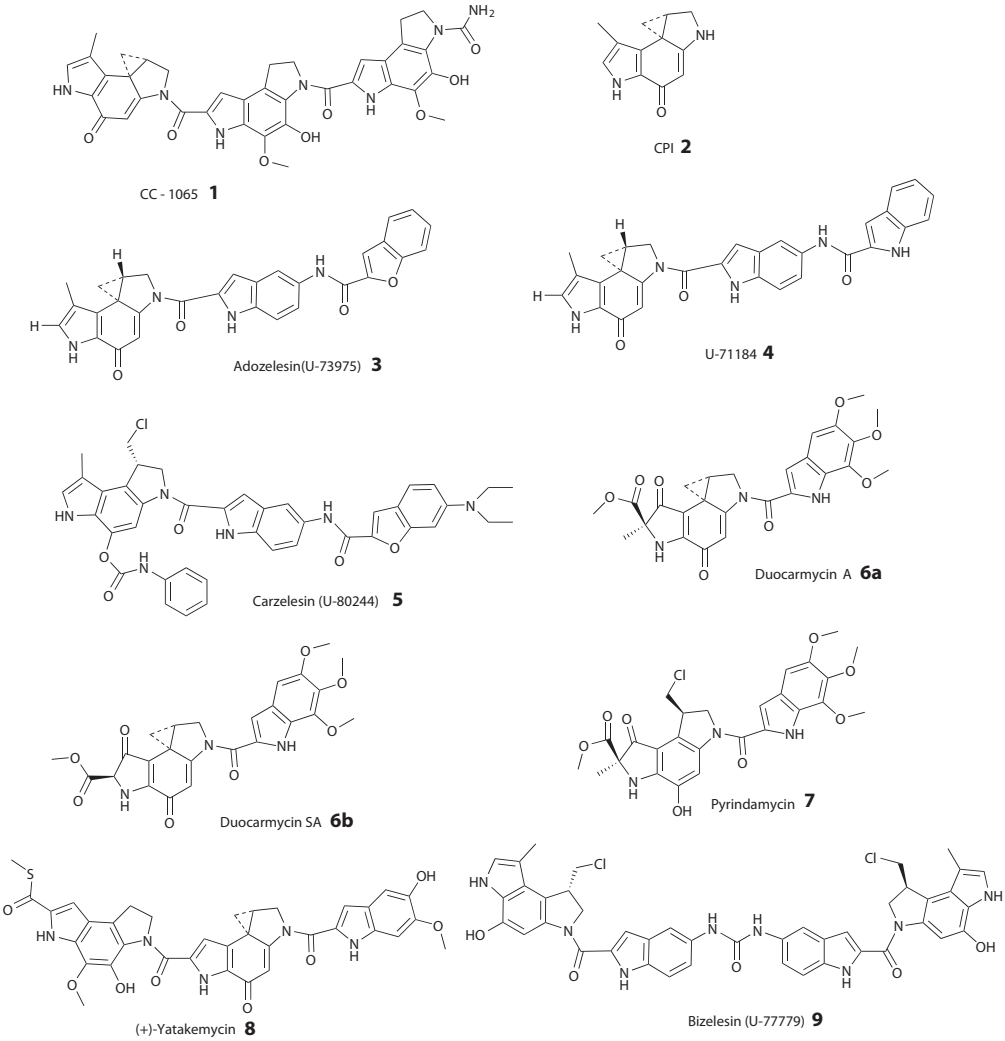

STRUCTURES 1–9

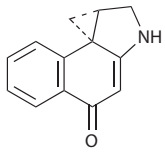

CBI 10

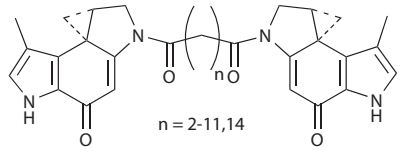

CPI-CPI 11

STRUCTURES 10 and 11

and *in vivo*, and is generally 20- to 30-fold more potent than adozelesin (a monofunctional analog) when tested against human carcinoma cells.[19] Adozelesin (**3**) is currently in phase II clinical trials, and bizelesin (**9**) is currently in phase I clinical trials.

Certain synthetic analogs of CC-1065 and duocarmycin, including dimeric structures, show promise and are also currently undergoing clinical trials,[19] indicating that synthetic efforts in this area can be useful. A new class of agents bearing the 1,2,9,9a-tetrahydrocyclopropa[*c*]benz[*e*]indole-4-one (**10**) pharmacophore (CBI) has been synthesized.[20]

In this chapter, in addition to delineating the cytotoxic and antitumor activities of CC-1065, we also examine the most recent analogs of CPI and CBI and their cytotoxicities. Certain CPI–polyamide conjugates have shown good cytotoxic potency;[21,22] therefore, we also describe various new CPI and CBI polyamide conjugates. Since CPI–CPI dimers (**11**) were very active against tumor cells, a large number of CBI–CBI dimers with varying lengths of the aliphatic chain linkers and with specific polyamides were synthesized in our group, and their cytotoxic properties against tumor cells are summarized below.

20.2 DRUG–DNA INTERACTIONS

The mechanisms of cytotoxic action of CC-1065 and its analogs have been shown to involve binding to the minor groove of DNA and alkylation at the N-3 position of adenine with concomitant opening of the reactive CPI unit (Figure 20.1). Thermal treatment of this covalently modified DNA results in depurination of the alkylated bases followed by strand cleavage, producing a 5-phosphate and 3-modified deoxyribose.[4,5,23]

Both enantiomers primarily alkylate N-3 of adenine, but the orientation of the drug is different. For the natural (+) enantiomer, the B and C subunits lie on the 5 site of alkylation and on the 3 site for the (–) enantiomer, as shown by DNA footprinting. They also show different sequence selectivity, although both prefer AT-rich sites. However, (+) and (–) analogs that contain only the A subunit do not show different sequence selectivity, demonstrating the importance of the B and C subunits in determining the site of alkylation. The unnatural enantiomer appears to be less reactive and provides less stabilization of the DNA helix as judged by the change in melting temperature of the alkylated DNA. A slight increase in the amount of alkylation on guanine was observed for (–)-CC-1065. Only the natural enantiomer appears to cause delayed death.[7,12,24,25]

Recent studies have shown that many analogs of CC-1065 reversibly alkylate DNA. However, CC-1065 itself appears to alkylate DNA irreversibly under the conditions tested. This difference is attributed to the strong noncovalent binding of CC-1065, which either prevents the reverse reaction after alkylation has occurred or keeps the drug bound so that it realkylates the same site. Boger and Johnson have suggested that irreversibility of the alkylation may be related to the delayed toxicity of some of these compounds.[26]

Several studies have shown that the unnatural enantiomers or epimers of this class of compounds also alkylate DNA and possess cytotoxic activity. Terashima's group synthesized (+)-duocarmycin A and its three possible stereoisomers and compared their *in vitro* cytotoxicities against P388 murine leukemia, demonstrating that both compounds bearing natural configurations at the cyclopropane moiety were more potent than those having unnatural configurations. This result indicated the importance of chirality in the cyclopropyl ring in duocarmycin A.[27,28]

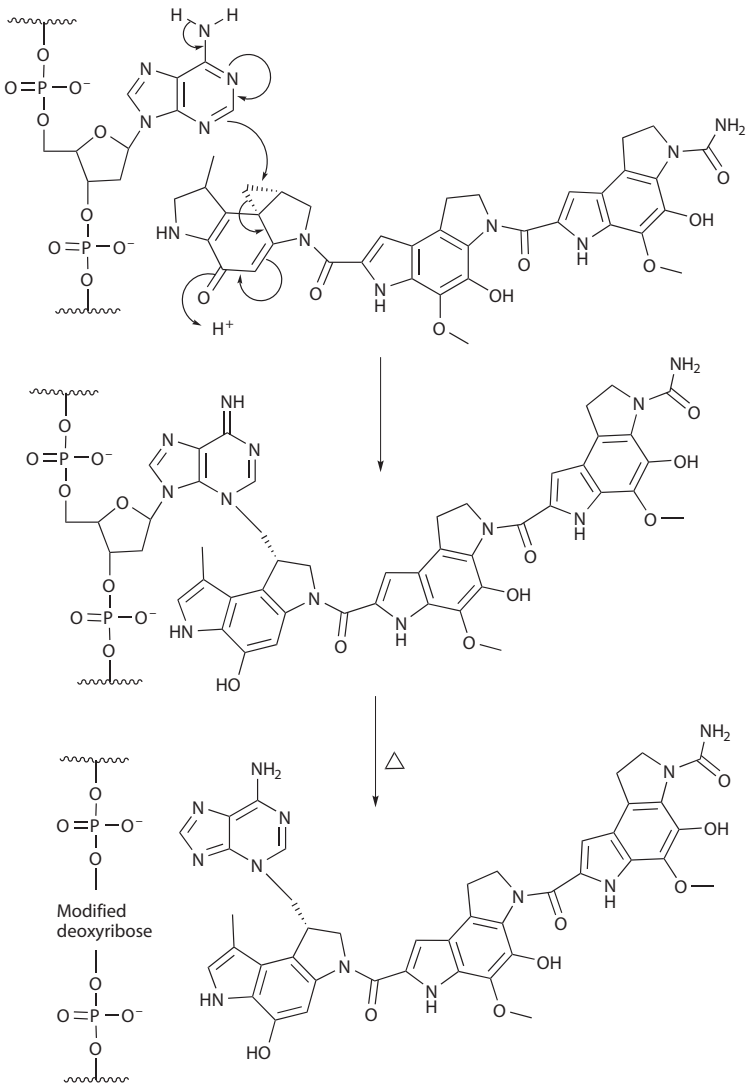

FIGURE 20.1 The mechanisms of cytotoxic action of CC-1065 and its analogs.

Boger and Johnson[26] synthesized both enantiomers of CC-1065 and duocarmycin A, duocarmycin SA, and epimers of duocarmycin A, and compared cytotoxic potencies against L1210 and relative DNA alkylation efficiencies. In the case of duocarmycin A, both (–) forms, which had opposite chirality in the cyclopropyl ring to that of natural (+)-duocarmycin A, had almost no effect on the DNA alkylation and cytotoxic potency. In the case of duocarmycin SA, the natural enantiomer was found to alkylate DNA at concentrations approximately 10 times that required for the nonnatural products.[29]

20.3 MODIFICATION IN THE PHARMACOPHORE UNIT

20.3.1 CPI Analogs

Compounds derived from the pharmacophore of CC-1065 but bearing different electron-withdrawing constituents in the benzene ring and different leaving groups on the C3 methylene

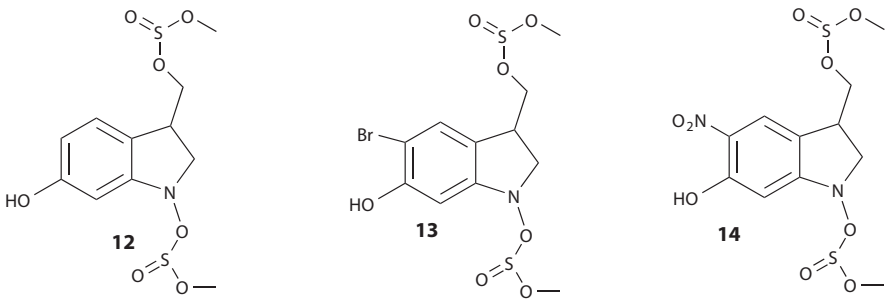

STRUCTURES 12–14

have been synthesized and evaluated.[30] These synthetic agents were less reactive at the common preferred sites than CC-1065, and higher concentrations are required to produce detectable cleavage. On the basis of alkylation intensities and densitometric data, the overall binding intensity is in the order of CC-1065 > **13** > **14** > **12**. From those experiments, it appears that there are two factors that are critical for the formation of the cyclopropane ring by cyclization: the first is the electron density of the benzoyl moiety where an electron-withdrawing group retards the cyclization, whereas an electron-donating group promotes the cyclization, and the second factor is the leaving ability of the group on the C3 methylene carbon. A better leaving group will favor the cyclization.

The evidence from gel electrophoresis showed that when supercoiled PM2 DNA is incubated with **12**, **13**, **14**, and CC-1065 at 80 μM for 20 h, the CCC DNA form was completely converted to OC DNA. This indicated that, like CC-1065, **12**, **13**, and **14** also exert their cytotoxicity through covalent binding to DNA. However, additional binding at the G residues by these synthetic analogs may represent an alternative or additional mechanism for this recognition of DNA.[31,32] In this connection, the DNA sequence specificity of the pyrrolo[1,4]benzodiazepine antitumor antibiotics, which bind through N2 of guanine, has been supported by theoretical calculations.[33]

A series of N-substituted CPI-analogs (**15–41**) has been synthesized, and certain structural features have been identified that affect reactivity toward nucleophiles and those influencing noncovalent interactions with DNA. Those features have then been related to biological activity and potency.[13] Table 20.1 lists the biological activities of CC-1065 and the racemic CPI analogs. Solvolytic reactivity is indicated by the pseudo-first-order rate constant for acid-catalyzed opening of the cyclopropyl ring in methanolic buffer. When CC-1065 is incubated with calf thymus DNA (CT-DNA) for 24 h at 25°C (Table 20.1), the observed induced circular dichroism (ICD) is entirely caused by the binding. Although the racemic analogs display no circular dichroism (CD) on their own, in the presence of DNA some of them show significant ICD. From the ICD, it appears that two structural features of the CPI moiety strongly influence DNA binding, the size of the ring attached to the pyrrolidine nitrogen of CPI, and the length of the aromatic amide chain. An ICD is almost exclusively associated with structures having a five-membered heteroaryl ring attached to CPI. Methyl substituents on the five-membered ring significantly diminish the ICD, as is also the case when the nitrogen atom is replaced with oxygen or sulfur. Analogs with six-membered rings attached to CPI fail to show an appreciable ICD. Table 20.1 shows that cytotoxic potency is qualitatively correlated to DNA binding.

The DNA alkylation selectivity of the analogs of (+) CC-1065 has been studied.[34,35] The sites of alkylation of double-stranded DNA were examined for simple derivatives of 7-methyl-1,2,8, 8a-tetrahydrocycloprop[1,2-C]pyrrolo[2,2-e]indole-4(5H)-one (CPI; **2**), (+) CC-1065 (**1**), and 1,2,7,7a-tetrahydrocycloprop[1,2-C]indole-4-one (CI; **42**) left-hand subunits. It was found that the CI subunit of the agents is a much more reactive alkylating agent than the natural CPI alkylation

TABLE 20.1
Physicochemical and Biological Properties of Racemic CC-1065 and CPI Analogs[SL1]

No.	*R*	Formula	R_2^a	$K \times 10^{5b}$	ICD × 10^{3c}	ID_{50}^d	P388 *In Vivo*[e] OD[f]	P388 *In Vivo*[e] %ILS[g]
		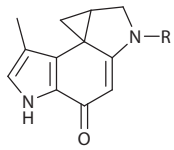						
15	$(PDE\text{-}I)_2$	$C_{37}H_{33}N_7O_8$	0.39		280	0.07	0.1	62
16	SO_2Me	$C_{13}H_{14}N_2O_3S$	0.82	0.3	0	100	25	60
17	SO_2Ph	$C_{18}H_{16}N_2O_3S$	0.58			900		
18	H	$C_{12}H_{12}N_2O$	0.87	Stable	0	900	10 (HDT)	NAw
19	$CO_2C(CH_3)_3$	$C_{17}H_{20}N_2O_3$	0.35	0.5	0	300		
20	$COCH_3$	$C_{14}H_{14}N_2O_2$	0.90		0	20	3	45
21	$CO(CH_2)_8CH_3$	$C_{22}H_{30}N_2O_2$	0.07		0	100	40 (HDT)	NA
22	COPh	$C_{19}H_{16}N_2O_2$	0.63	0.9	<1	3	12	71
23	CO-4-(NHCOPh)C_6H_4	$C_{26}H_{21}N_3O_3$	0.42		11	0.5	0.5	83
24	CO-2-pyridyl	$C_{18}H_{15}N_3O_2$	0.76	1.2	0	10	15	69
25	CO-2-naphthyl	$C_{23}H_{18}N_2O_2$	0.46		0	7	6	73
26	CO-2-quinolyl	$C_{22}H_{17}N_3O_2$	0.50	1.2	1	10	6	142
27	CO-6-(NHCO$(CH_2)_4CH_3$)-2-quinolyl	$C_{28}H_{28}N_4O_3$	0.15		[h]	100	21	127
28	CO-2-pyrrolyl	$C_{17}H_{15}N_3O_2$	0.70		10	2	1	71
29	CO-2-indolyl	$C_{21}H_{17}N_3O_2$	0.45	1.0	36	0.2	0.4	90
30	CO-1-Me-2-indolyl	$C_{22}H_{19}N_3O_2$	0.43	1.0	3	10	8	44
31	CO-2-benzofuranyl	$C_{21}H_{16}N_2O_3$	0.47	1.1	6	0.04	0.25	110
32	CO-2-benzothiophenyl	$C_{21}H_{16}N_2O_2S$	0.41	1.1	7	0.3	0.80	100
33	CO-3-Me-2-indenyl	$C_{23}H_{20}N_2O_2$	0.39		4	30	17 (HDT)	NA
		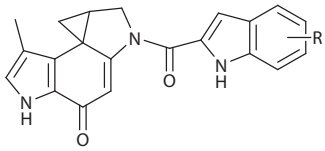						
34	5-OMe	$C_{22}H_{19}N_3O_3$	0.47	1.0	22	0.01	0.05	95
35	6-OH, 7-OMe	$C_{22}H_{19}N_3O_4$	0.63	1.0	37	0.1	0.05	55
36	5-$NHCONH_2$	$C_{22}H_{19}N_5O_3$	0.89	1.0	47	0.6	0.06	65
37	5-NHCOPh	$C_{28}H_{22}N_4O_3$	0.43		36	0.07	0.05	82
38	5-NHCO-2-indolyl	$C_{30}H_{23}N_5O_3$	0.30	[i]	70	0.01	0.05	159 (4)

TABLE 20.1 (continued)
Physicochemical and Biological Properties of Racemic CC-1065 and CPI Analogs[SL1]

							P388 *In Vivo*[e]	
No.	***R***	**Formula**	R_2^a	$K \times 10^{5b}$	$ICD \times 10^{3c}$	ID_{50}^d	**OD**[f]	**%ILS**[g]
39	5-NHCO-2-benzofuranyl	$C_{30}H_{22}N_4O_4$	0.30	1.0	50	0.02	0.05	170 (1)
40	5-NHCO-5-($NHCONH_2$)-2-indolyl	$C_{31}H_{25}N_7O_4$			75	0.3	0.1	121 (2)
41	5-NHCO-5-(NHCOPh)-2-indolyl	$C_{37}H_{28}N_6O_4$	0.30		33	0.01	0.1	77

Note: HDT, highest dose tested, toxicity not reached; NA, no activity.

[a] Chromatographic measure of lipophilicity determined by liquid–liquid chromatography on C_{18}-bonded silica gel.

[b] Pseudo-first-order rate constant, in seconds[1], for solvolytic ring opening at pH3, followed spectrophotometrically.

[c] Molar ellipticity, in the presence of CT-DNA.

[d] $ID_{50,}$ the nanomolar concentration of drug required to inhibit, by 50%, the growth of murine L1210 leukemia cells in a 3-d assay.

[e] Drug given by interperitoneal injection to mice implanted interperitoneally with 10^6 P388 leukemia cells.

[f] Optimum dose in milligrams per kilogram per day, given on days 1, 5, and 9.

[g] Percentage increase in life span of treated animals over that of control mice bearing tumor, when treated at the optimal dose. Numbers in parentheses are the numbers of mice that survived for 30 d.

[h] Extreme insolubility of the drug gave anomalous and irreproducible results.

[i] The drug was not soluble in this medium in the concentration range used.

subunit of CC-1065. The simple derivatives **43**, **44**, **45**, and **46** of CI were found to alkylate double-stranded DNA under milder conditions than did simple derivatives of CPI, and the marked similarities in CI and CPI DNA alkylation profiles indicate that CI represents the minimum pharmacophore of CPI. By use of the Fe(III)-$CDPI_3$ EDTA (FeIII-**43**, FeIII-**44**), they demonstrated that the noncovalent binding is a prerequisite for DNA alkylations. The relative cleavage efficiency observed with Fe(III)-**47** was found to parallel the relative alkylation efficiency of (+)- or net (–)-CC-1065.

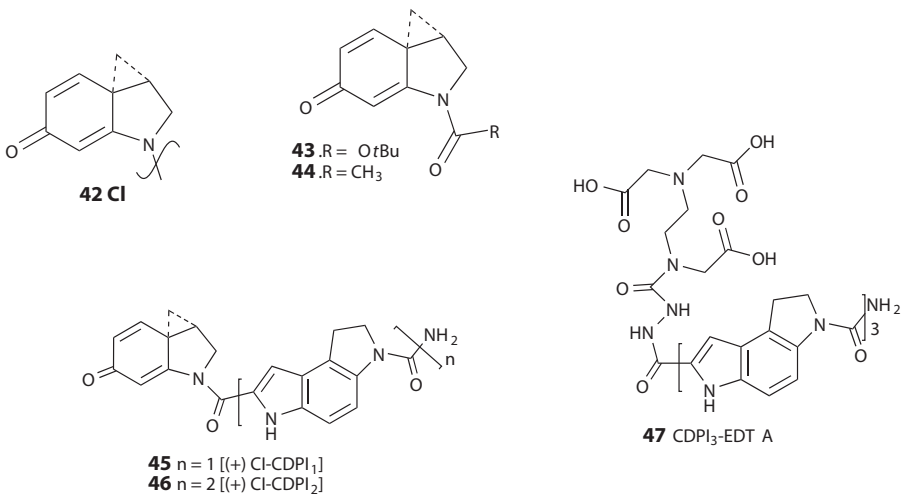

STRUCTURES 42–47

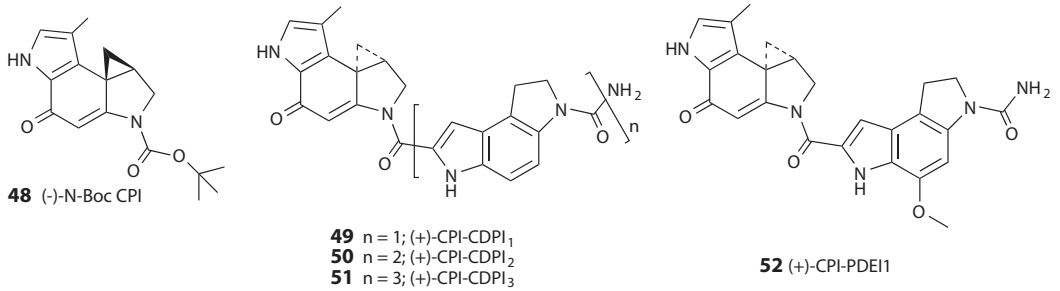

STRUCTURES 48–52

20.3.2 Enantiomers of CPI Analogs

Boger's group[36] made a detailed evaluation of the DNA-alkylation selectivity of (+)-CC-1065 and its enantiomer (–) CC-1065 and a series of analogs (**48**–**52**) possessing the CPI alkylation subunit. The natural enantiomers bind in the minor groove in the 3 → 5 direction starting from the adenine N3 alkylation site across a 2-base (N-Boc-CPI **48**; i.e., 5-AA), 3.5-base (CPI-CDPI$_1$ **49**/CPI-PDEI$_1$ **52**; i.e., 5-AAA), 5-base (CC-1065/CPI-CDPI$_2$ **50**; i.e., 5-AAAAA), or 6.5-base (CPI-CDPI$_3$ **51**; i.e., 5-AAAAAA) AT-rich site. In contrast, the unnatural enantiomers bind in the reverse 5 → 3 direction in the minor groove, and the binding site starts at the first 5 base preceding the adenine N3 alkylation site and extends across the alkylation site to the adjacent 3 base covering an AT-rich site of 2 bases (N-Boc-CPI **48**; i.e., 5AA), 5 bases (CC-1065/CPI-CDPI$_2$; i.e., 5-AAAAA), or 6.5 bases (CPI-CDPI$_3$; i.e., 5-AAAAAA). Three-dimensional models of natural and unnatural enantiomer alkylations clearly illustrate the offset binding sites. A simple model for the CC-1065 DNA alkylation reaction that accommodates the behavior of both enantiomers is provided, in which the sequence selectivity is derived from the noncovalent binding selectivity of the agents in the narrower sterically more accessible AT-rich minor groove. The inherent steric accessibility to the adenine N3-alkylation site accompanies deep penetration of the agent into the minor groove within the AT-rich site (Figure 20.2).

In the DNA-binding and cytotoxic activity studies of two enantiomers of bis-indole analogs of CC-1065, the isomer with the same stereochemical configuration as natural (+)-CC-1065 was a potent cytotoxic agent, but its enantiomer was essentially inactive.[37] Both enantiomers showed significant binding to DNA, but the biologically less active isomer showed less overall binding. In all cases, the agents preferred AT-rich DNA, and all bound to similar regions in DNA, as evidenced by the positions of drug-initiated thermal breaks in single end-labeled fragments of Phi X174 RF DNA. The overall similarity in site specificity for binding of the structurally diverse agents indicates that much of the specificity observed in the binding of the agent to DNA lies in the DNA itself.

20.3.3 CC-1065 Analogs

A simple method to detect CPI-binding sites on double-stranded DNA has been devised.[8] The technique uses a modified form of bacteriophage T7 polymerase to synthesize a radiolabeled nascent strand from double-stranded DNA that has been allowed to react *in vitro* with the CC-1065 analog U-73,975 (adozelesin; **3**). The reaction products were electrophoresed on sequencing gels containing 8 M urea and visualized by autoradiography. The transit of this DNA polymerase is inhibited at the sites where CPIs are bound to the template strand. The positions of polymerase inhibition can be determined by comparison of CPI-treated and -untreated DNA reactions. This modified dideoxynucleotide technique has been used to establish the sequence selectivity of U-73,975.

Bizelesin (U-77,779; **9**) is a symmetrical dimer of the spirocyclopropyl alkylating subunit of (+)-CC-1065 in which the linker consists of two indole subunits separated by a ureido group. A

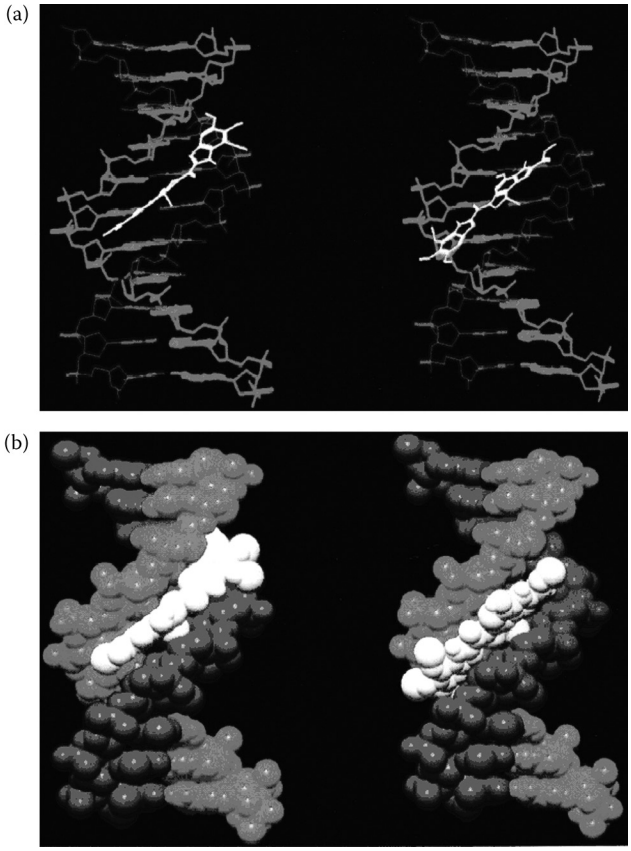

FIGURE 20.2 **(See color insert.)** Comparison stick and space-filling models of the (+)-duocarmycin SA (left) and ent-()-duocarmycin SA (right) alkylation at the same site within w794DNA: duplex 5-d(GACTAATTTTT). The natural enantiomer binding extends in the 3 → 5 direction from the adenine N3 alkylation site 5-CTAA. The unnatural enantiomer binding extends in the 5 → 3 direction across the site 5-AATT.

comparison of bizelesin with a monoalkylating analog of (+)-CC-1065[38] shows that it appears to have increased sequence selectivity such that monoalkylating compounds like (+)-CC-1065 react at more than one site. In contrast, however, bizelesin reacts only at sites where there are two suitably positioned alkylation sites. Bizelesin generally forms interstrand cross-links (ISCs) with adenine primarily spaced 6 bp apart (including the covalently modified adenines) while occupying the intervening minor groove.

Bizelesin alkylates DNA through guanine in restriction fragments in which there is a suitably positioned adenine contained in a highly reactive monoalkylation sequence 5-TTTTT N*, and in which N was G, C, or T. Such fragments were prepared to evaluate the cross-linking potential of bizelesin at nonadenine bases. Kinetic analysis of monoalkylation and cross-linking events demonstrates that it is the reaction at N (guanine or cytosine) that results in the cross-link that is the slow step. On the basis of this analysis and the normal unreactivity of guanine and cytosine to alkylation by the CPI alkylating moiety of (+)-CC-1065, the molecular mechanism for this type of cross-linking reaction most probably involves a covalent immobilization of the second alkylating arm in a proximity-driven reaction.

The sequence selectivity for DNA-ISCs by bizelesin was determined by sequencing gel analysis[39] and showed that bizelesin induced two distinct forms of DNA-ISC, one of which spanned six nucleotides and linked two adenine N3-positions within an AT-rich sequence, and the second spanned seven nucleotides, also linking two adenine N3-positions, with a preference for contiguous runs of adenines.

Three major six-nucleotide DNA-ISCs were identified and found to occur within 5-TAATTA-3, 5-TAAATA-3, and 5-TAAAAA-3 sequences. The major seven-nucleotide DNA-ISC was found to occur within 5-TAAAAAA-3 sequences, and within this sequence, the formation of the seven-nucleotide DNA-ISC was preferred over the six-nucleotide DNA-ISC by a ratio of approximately 2:1. DNA-ISC formation within adenine tracts eliminated the inherent DNA bending associated with such sequences. Further, chemical probing of each isolated DNA-ISC with diethyl pyrocarbonate (A-specific) and potassium permanganate (T-specific) showed that the major DNA conformational changes, such as helical distortion, were localized within the cross-linked sequence.

These results indicate that a significant degree of DNA distortion may also be demonstrated[40] and that covalent DNA adducts induced by bizelesin at the adenine N3-position undergo two subsequent competing reactions. One reaction causes DNA strand cleavage via depurination, and one reaction proceeds through loss of the DNA adduct (adduct reversal with restoration of DNA integrity). The results were obtained by studying the chemical stability of synthetic oligonucleotides, which contained either a distinct monofunctional adduct or DNA-ISCs. Quantification of adduct reversal was performed on the basis that drug-modified DNA, on exposure to heat followed by hot piperidine treatment, was resistant to strand cleavage at the site of alkylation. The rate of adduct reversal was found to increase with increasing temperature and was found to be maximum at 70°–80°C. The rate of adduct reversal was also found to increase with increasing pH and ionic strength. Adduct reversal was favored in DNA containing cross-links, whereas rapid depurination occurred preferentially within monofunctionally alkylated DNA.

The ligand-mediated polymerase chain reaction technique has been used to map drug-induced DNA alkylation sites in single-copy genes at the nucleotide level in human cells.[41–43] This technique has been used to map the alkylation sites induced by adozelesin and bizelesin within DNA in human cells.[44] The pattern of the drug alkylation sites is mapped within the human PGK1 and P53 genes, with the monofunctional alkylating agent, adozelisin, alkylating genomic DNA predominantly within 5-(A/T)(A/T) A* (A* = alkylated adenine) sequences, and additional sites of alkylation were observed within 5-(A/T)(G/C)(A/T) A* sequences; however, these were considered to represent sites of medium-to-low preference. In contrast, bizelesin, a bifunctional analog capable of both DNA monofunctional alkylation and DNA-ISC formation, was also found to alkylate 5-(A/T) (A/T) A* sequences. Putative bizelesin DNA-ISC sites indicated that AT-rich sequences are preferred in the intervening sequence between the two cross-linked adenines. Both six- and seven-nucleotide regions were identified as putative sites of DNA-ISC formation, with 5-TTTTTTA*, 5-TTTATCA*, and 5-GTACTAA* sequences being preferred. Nonadenine bases were not observed as potential intracellular sites of either DNA interstrand cross-linking formation or monofunctional alkylation.

The DNA base pair preferences of the antitumor antibiotic CC-1065 and two analogs of CC-1065 were studied by following the rate of covalent bond formation (N3 adenine adduct) with DNA oligomers containing the 5-NNTTA* and 5-NNAAA* sequences (N = nucleotide).[45] The rate of adduct formation of CC-1065 is greatly affected by DNA base changes at the fourth and fifth positions of the binding sites for the 5-NNAAA sequences, but not the 5-NNTTA sequences. However, an analog of the CC-1065 ring system, with additional methylene and oxygen substituents, shows similar rates of adduct formation for all sequences. A second analog of CC-1065, containing a fused three-ring system, but not the methylene and oxygen substituents of CC-1065, shows similar rates of adduct formation, with the same sequence dependence as CC-1065, but does not distinguish between the sequence to the degree shown by CC-1065. Adduct formation of CC-1065, but not the analogs, competes with a reversibly bound species. Thymine bases to the 3 side of a potentially reactive adenine or cytosine base at the fifth position from the bonding adenine create reversible binding sites that decrease the rate of adduct formation of CC-1065. The sequence 5-GCGAATT binds CC-1065 only reversibly. This sequence can compete for CC-1065 with covalent bonding sequences if the sites are located in different oligomers, or if the sites are located (overlapped or not overlapped) in the same oligomer. The results of these competitive binding experiments indicate that the transfer of CC-1065 from the reversible binding site to the covalent bonding site with both sites

located on a single DNA duplex, not overlapped, occurs through an equilibrium of CC-1065 in solution, not by migration of CC-1065 in the minor groove.

A number of indirect observations that indicate a conformational acceleration in the action of CC-1065 and its analogs have been summarized by Boger et al.[46,47] The DNA alkylation reaction is derived in part from a DNA-binding-induced conformational change in the agents, which substantially increases their inherent reactivity. The ground-state destabilization results from a binding-induced twist in the linkage N2 amide and requires a rigid extended N2-amide substituent, which disrupts the vinylogous amide stabilization and activates the agents for DNA alkylation.

The CT-DNA and poly(dI-dC) · poly(dI-dC) binding properties of the natural antitumor antibiotic and selected analogs of CC-1065, U-66,664, U-68,819, U-66,694, and U-65,415 were studied by CD and absorbance methods.[48] The results indicate that the intense long-wavelength DNA-induced CD band of these molecules originates from a chiral electronic transition, which is delocalized over the whole molecule. Both the covalently bound species exhibit the characteristic spectral behavior of an inherently disymmetric chromophore when these agents bind within the minor groove of B-form DNA. This mechanism of optical activity accounts for why CC-1065 shows a weak CD in buffer but a very intense induced CD at long wavelength when bound to DNA, why the intensity of the induced CD of CC-1065 analogs depends on how many fused ring systems the analog contains, and why covalently bound analogs, having the mirror image configuration of the natural configuration, also exhibit an intense, positive, induced CD at long wavelength.

20.3.4 Further Analogs

Recent studies by the Boger group on the synthesis of extended anthracene (CNI; **53**) and phenanthrene (iso-CNI; **54**) analogs of CBI have been reported.[49] The duocarmycin analogs incorporating the CNI pharmacophore [(+)-CNI-TMI] exhibited potent cytotoxicity ($IC_{50} = 30$ pM) similar to the corresponding CBI analog, whereas the iso-CNI analog was >10-fold less active. The Boger group has also synthesized *N*-acyl *O*-aminophenol derivatives of prodrugs of CBI-TMI and CBI-indole$_2$ (**55** and **56**, respectively) representing members of a new class of reductively activated prodrugs of the duocarmycin and CC-1065 structural class. The expectation that hypoxic tumor environments, with their higher concentration of "reducing" nucleophiles (e.g., thiols), are capable of activating such derivatives, thereby increasing their sensitivity to the prodrug treatment, has been confirmed by preliminary *in vitro* and *in vivo* studies.[50] These prodrugs offer potential advantages related to controlled or targeted release *in vivo*. Another 2007 contribution from this group was aimed at the synthesis of predictably more potent analogs of CC-1065, and entailed the synthesis of the thieno analogs of the MeCPI alkylation subunit found in CC-1065, namely 7-methyl-1,2,8,8a-tetrahydrocyclopropa[*c*]thieno[3,2-e]indol-4-one (MeCTI; **57**) and its isomer 6-methyl-1,2,8,8a-tetrahydrocyclopropa[*c*]thieno[2,3-e]indol-4-one (iso-MeCTI; **58**). They were found to be five to six times more stable than MeCPI, and when incorporated into the key analogs of the natural products they provided derivatives that exceeded the potency of the corresponding MeCPI derivatives (3- to 10-fold).[51] A number of other analogs are discussed in the following section.

20.4 INTERACTION OF CC-1065 WITH CHROMATIN

Most of the CC-1065 studies have used natural DNA or synthetic oligonucleotides for binding studies. However, nuclear DNA does not exist as naked DNA but is packaged as chromatin. Chromatin consists of repeating nucleosome subunits composed of an interior core of histones, around which are wrapped approximately 140 bp of the B-form DNA. Moy et al.[52] reported on the interactions of CC-1065 and adozelesin with DNA, chromatin, and histones. CD-binding studies show that CC-1065 and adozelesin bind to P388 chromatin and that induced CD spectra are similar to those obtained when CC-1065 binds to P388 DNA and many synthetic polynucleotides. The intensity of the induced CD spectra and the rate of conversion of reversibly bound drug to irreversibly bound drug are less

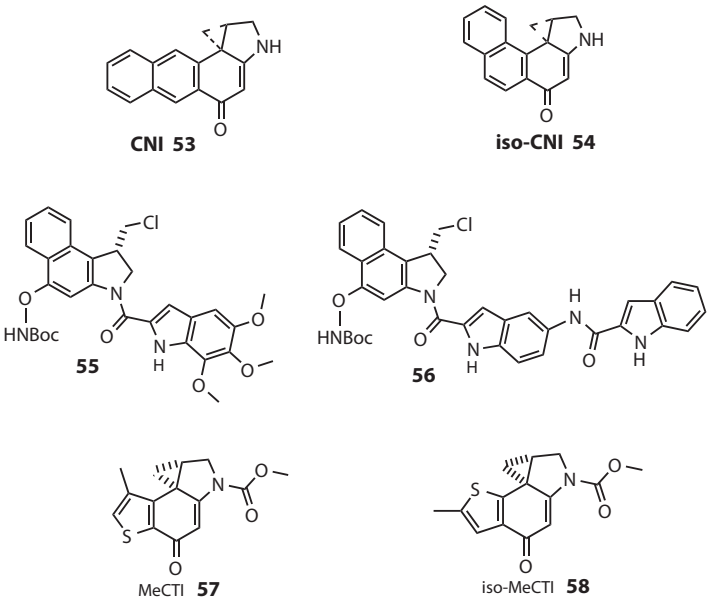

STRUCTURES 53–58

for chromatin than for naked DNA. Because the histones themselves do not bind CC-1065, this indicates that histones act indirectly to restrict the binding of CC-1065 to chromatin. This could occur because fewer binding sites are available on chromatin when compared with free DNA or because of a less dissymmetric environment of chromatin. It was assumed that a good fit in the minor groove leads to a more chiral environment for the drug chromophore and, hence, a more intense induced CD.

A new type of CC-1065 analog, **59**–**65**, where the CPI moiety is replaced by 1,2-dihydro-1-(chloromethyl)-5-hydroxy-8-methyl-3H-furano[3,2-c]indole (CFI), has been synthesized.[53] The major site of alkylation with W794 duplex DNA for **62** and (+)-CC-1065 proved to be identical. 5-d(AATTA) 3-alkylation occurs at the 3 adenine and agent binding is in the 3′ → 5′ direction. The profile of DNA alkylation selectivity for **59** also proved to be identical to that of adozelesin (**3**). However, compound **65** exhibited a different and less selective profile of DNA alkylation. The high-affinity site for **65** with W794 duplex DNA was 5′-(AATTT)-3′, with alkylation at the 5 adenine and agent binding in 5′ → 3′ direction. The profile of DNA alkylation exhibited by **65** proved essentially identical to that of the unnatural enantiomers (–)-CC-1065 and (–)-CPI-CDPI3.[24] A more significant distinction between **59** and **65** is the relative efficiency or intensity of DNA alkylation. Consistent with the relative *in vitro* cytotoxic potency of **59**, it proved to be comparable or slightly less effective

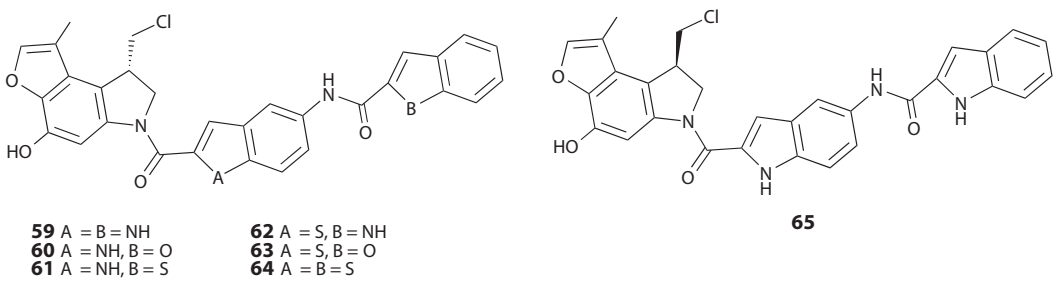

STRUCTURES 59–65

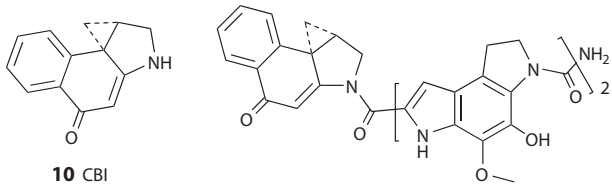

10 CBI

66 CBI-PDEI$_2$

STRUCTURES 10 and 66

(one to five times) at alkylating the duplex DNA than (+)-CC-1065 and much more effective than compound **65**.

A new CBI (1,2,9,9a-tetrahydrocyclopropa[*c*]benz[*e*]indole-4-one; **10**) analog of CC-1065, CBI-PDEI$_2$ (**66**), has been synthesized and evaluated.[20] Compound **66** was shown to have similar DNA sequence selectivity and structural effects on DNA as (+)-CC-1065. The effect of CBI-PDE-I dimer was also compared with (+)-CC-1065 in the inhibition of duplex unwinding by helicase II and nick sealing by T4 ligase and found to be quantitatively similar. The *in vitro* and *in vivo* potencies of CBI compounds correspond very closely to the corresponding CPI derivatives.

A number of 1,2,9,9a-tetrahydrocyclopropa[*c*]benz[*e*]indole-4-one (CBI; **10**)-based and 9a-chloromethyl-1,2,9,9a-tetrahydrocyclopropa[*c*]benz[*e*]indole-4-one (C2BI; **67**)-based analogs of CC-1065, (**51**) and **68**, have been synthesized and evaluated by Boger et al.[54,55] It was found that CBI analogs are four times more stable and potent than the corresponding CPI analogs. Similarly, the CBI-based agents alkylate DNA with unaltered sequence selectivity at an enhanced rate with greater efficiency than the corresponding CPI analogs. In comparison with the CBI-based agents, the C$_2$BI-based agents proved to be approximately 100–10,000 times less effective at DNA alkylation and 100–10,000 times less potent in cytotoxicity assays. These effects are suggested to be the consequence of a significant steric deceleration of the adenine N3-alkylation reaction attributed to the additional 9a-chloromethyl substituent. Consistent with this interpretation, the noncovalent binding constant of C$_2$BI-CDPI$_2$ (**68**) for poly[dA]-poly[DT] proved nearly identical to CDPI$_3$ under kinetic binding conditions, and prolonged incubation of C$_2$BI-CDPI$_2$ (**68**) with poly[dA]-poly[dT] (72 h, 25°C) provided covalent complexes with a helix stabilization comparable to that observed with (+)- or (–)-CPI-CDPI$_2$, indicating that the size of the C$_2$BI subunit inhibits, but does not preclude, productive DNA alkylation.

A library of 132 CBI (1,2,9,9a-tetrahydrocyclopropa[*c*]benzo[*e*]indole-4-one) analogs of CC-1065 and the duocarmycins was prepared using the solution-phase technology of acid–base liquid–liquid extraction for the isolation and purification steps (Figure 20.3).[56] The 132 analogs constituted a systematic study of the DNA-binding domain with the incorporation of dimers composed of monocyclic, bicyclic, and tricyclic (hetero) aromatic subunits. From their examination, clear trends in cytotoxic potency and DNA alkylation efficiency emerged, highlighting the importance of the first-attached DNA-binding subunit (A subunit): tricyclic is more active than bicyclic, which in turn is

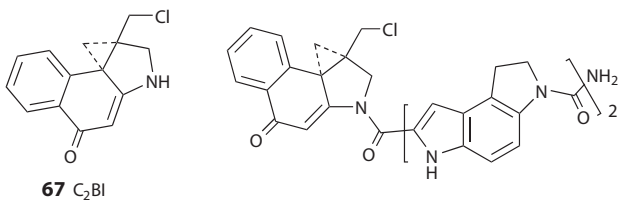

67 C$_2$BI

68 C$_2$BI-CDPI$_2$

STRUCTURES 67 and 68

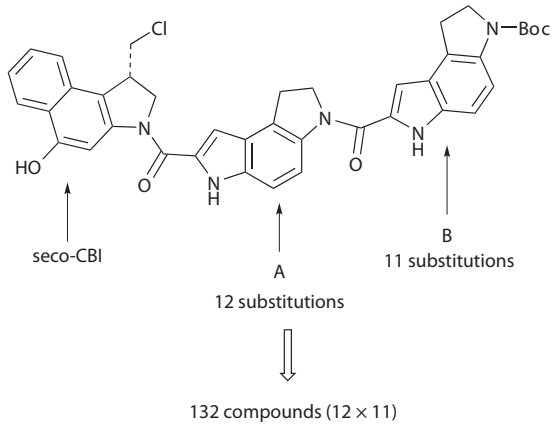

FIGURE 20.3 Solution-phase synthesis of 132 CC-1065 analogs based on CBI. All the compounds were purified by liquid–liquid acid–base extraction.

far more active than monocyclic (hetero) aromatic subunits. Notably, the trends observed in the cytotoxic potencies paralleled those observed in the relative efficiencies of DNA alkylation. Their interpretation of these results is that the trends represent the partitioning of the role of the DNA-binding subunits into two distinct contributions, the first of which is derived from an increase in DNA-binding selectivity and affinity, which leads to potency enhancements of 10- to 100-fold and is embodied in the monocyclic series. The second, which is additionally embodied in the bicyclic and tricyclic heteroaromatic subunits, is a contribution to the catalysis of the DNA alkylation reaction that provides additional enhancements of 100- to 1000-fold. The total enhancements thus exceed 25,000-fold. Aside from the significance of these observations in the design of future CC-1065/duocarmycin analogs, their importance to the design of hybrid structures containing the CC-1065/duocarmycin alkylation subunit should not be underestimated. Those that lack an attached bicyclic or tricyclic A subunit, that is, duocarmycin/distamycin hybrids, can be expected to be intrinsically poor or slow DNA alkylating agents.

20.5 POLYAMIDE CONJUGATES AND RELATED SEQUENCE DIRECTED STRUCTURES

In a novel approach to explore the properties of cyclopropylindole (CPI), Lown et al. envisaged certain CC-1065 analogs, **69–78**, in which different numbers of *N*-methylpyrrole amide (a DNA sequence recognizing moiety) groups are attached with different linkers to the CPI moiety.[21] They postulated that the positively charged functionality of the protonated dimethylamino group in the oligopeptide might contribute to reduced cytotoxic potency by reducing intracellular accessibility and, therefore, should be replaced by an uncharged moiety. It was also considered likely that the linker between the CPI unit and the oligopeptide would be important to the binding potency of the conjugate molecules to DNA to maintain proper contact over the whole of the molecular recognition region.[57] The extent and the relative rates of DNA cleavage following alkylation and thermal treatment of these conjugates were determined by agarose gel mobility shift assay and high-resolution polyacrylamide gel electrophoresis and contrasted with that of CC-1065. The CPI–*N*-methyl pyrrole agents avoid the major alkylation sites of CC-1065, but all alkylate the minor CC-1065 site of 5ATAA and exhibit a consensus sequence of 5-NA/TA/TA. The cytotoxicities of these compounds were determined against KB human tumor cells *in vitro*. Compound **74** bearing a 4-butyramide group in the *N*-methyl pyrrole is 100 times more potent than compound **75**, which lacks an amide group, whereas compound **78**, which bears a rigid trans double-bond linker is 1000 times more potent than its flexible ethyl-linked counterpart **77**.

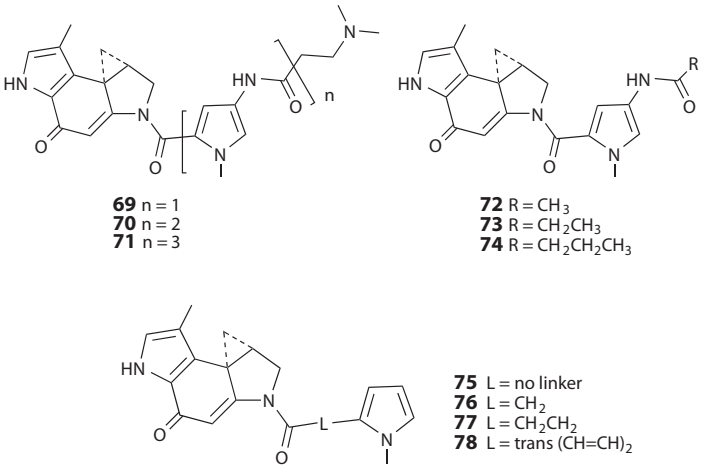

STRUCTURES 69–78

Sugiyama's group synthesized the novel hybrid molecules **79**–**80**, and they alkylate the 3-end of A in AT-rich sequences, as does the parent duocarmycin. More significantly, these hybrids alkylate G residues of predetermined DNA sequences effectively and with high specificity by formation of a heterodimer with distamycin.[58] They also synthesized compounds **81** and **82**,[59] which were designed to alkylate the target sequences (A/T) G $(A/T)_2$N(A/G) and (A/T) G (A/T) CN (A/G), respectively, according to Dervan's ring-pairing rule. High-resolution denaturing gel electrophoresis indicated that compound **81** exclusively alkylated the 5-TGTAA**A**A-3 within a 400-bp DNA fragment. Similarly, alkylation of **82** occurred exclusively at the G of the 5AGTCA**GA**-3 sequence with efficiency at the nanomolar concentration (Figure 20.4).

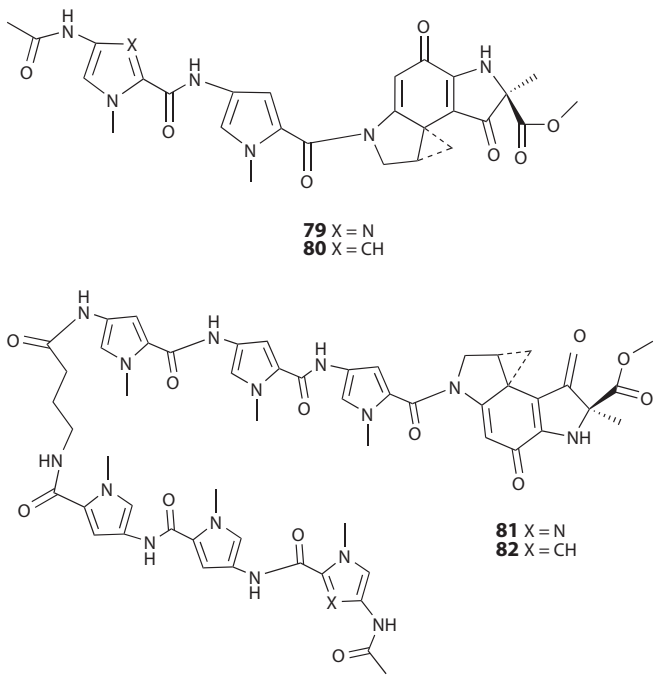

STRUCTURES 79–82

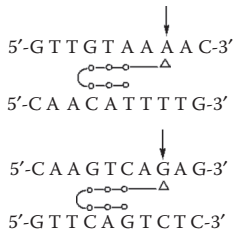

FIGURE 20.4 DNA alkylation sites of 81 and 82.

Recently, Bando et al.[60] developed a novel type of DNA interstrand cross-linking agent by synthesizing dimers of a pyrrole (Py)/imidazole (Im)–diamide–CPI conjugate, ImPyLDu86 (**83**), using seven different linkers for connection (Figure 20.5). The tetramethylene linker compound, **84**, efficiently produces DNA-ISCs at the 9-bp sequence, 5-PyGGC(T/A)GCCPu-3, but only in the presence of a partner triamide, ImImPy. For efficient cross-linking by **84** with ImImPy, one AT base pair between two recognition sites was required to accommodate the linker region. Elimination of the AT base pair and insertion of an additional AT base pair, and substitution with the GC base pair, significantly reduced the degree of cross-linking. The sequence specificity of the interstrand cross-linking by **84** was also examined in the presence of various triamides. The presence of ImImIm slightly reduced the formation of a cross-linked product compared with ImImPy. The mismatch partners ImPyPy and PyImPy did not produce an ISC product with **84**, whereas ImPyPy and PyImPy induced efficient alkylation at their matching site with **84**.

The interstrand cross-linking abilities of **84** were further examined using denaturing polyacrylamide gel electrophoresis with 5-Texas Red-labeled 400- and 67-bp DNA fragments. The sequencing gel analysis of the 400-bp DNA fragment with ImImPy demonstrated that **84** alkylates several sites on the top and bottom strands, including one interstrand cross-linkage on longer DNA fragments. A simple method using biotin-labeled complementary strands was developed (Figure 20.6) and produced a band corresponding to the interstrand cross-linked site on both top and bottom strands. Densitometric analysis indicated that the ISCs in the observed alkylation bands was approximately 40% of the total. This compound efficiently cross-linked both strands at the target sequence. This system consisted of a 1:2 complex of the alkylating agent and its partner ImImPy and caused an interstrand cross-linking in a sequence-specific fashion according to the base pair recognition rule of Py–Im polyamides (Figure 20.7).

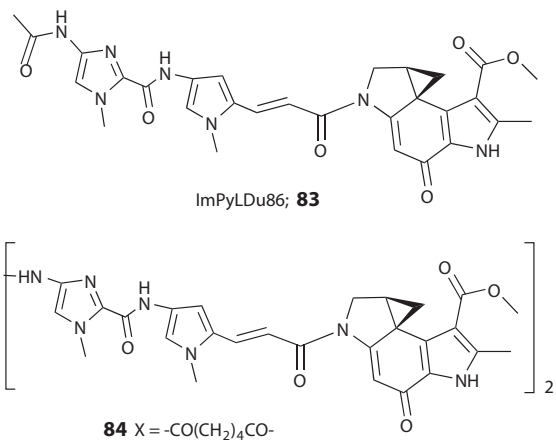

STRUCTURES 83 and 84

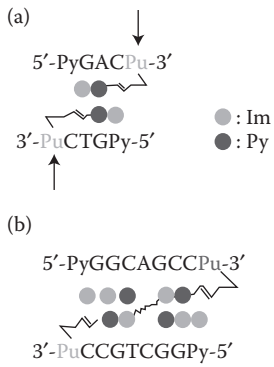

FIGURE 20.5 **(See color insert.)** (a) The chemical structure of ImPyLDu86 83 and a schematic representation of the recognition of the 5-PyGACPu-3 sequence by the homodimer of 83. The arrows indicate the site where alkylation takes place. (b) A putative binding mode of the 1:2 complex of covalent dimer of 83, 84, with ImImPy to 5-PyGGCAGCCPu-3 sequence.

A series of hybrid agents, **85–92**, of CC-1065 has been synthesized and evaluated and incorporate the CBI analog of the DNA-alkylation subunit of the CC-1065 linked to the C-terminus di- and tripeptide S-DNA-binding domain of bleomycin A2.[61] The attachment of the DNA-binding domain of bleomycin A2 did not alter the DNA-alkylation selectivity of the CBI alkylation's subunit (5AA > 5TA), nor did it enhance the selectivity that approaches the 5-bp AT-rich alkylation's selectivity of CC-1065.

A new class of hybridization-triggered cross-linkable oligodeoxyribonucleotides (ODNs) that are conjugated to the reactive cyclopropylindole (CPI) has been synthesized and studied for their properties.[62] Here, the authors conjugated racemic CPI to ODNs via a terminal phosphorothioate at

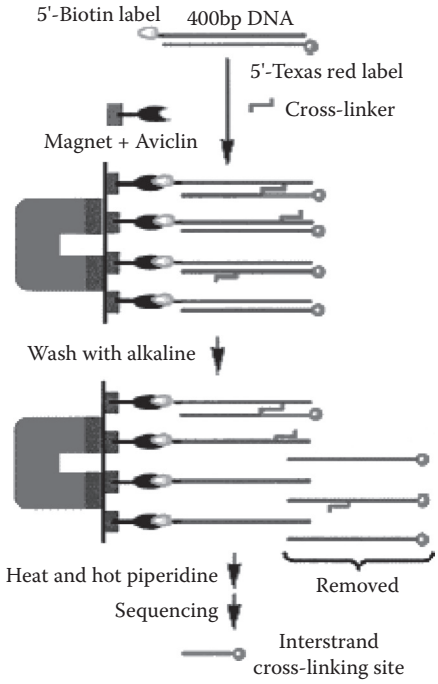

FIGURE 20.6 **(See color insert.)** Determination of interstrand cross-linking sites.

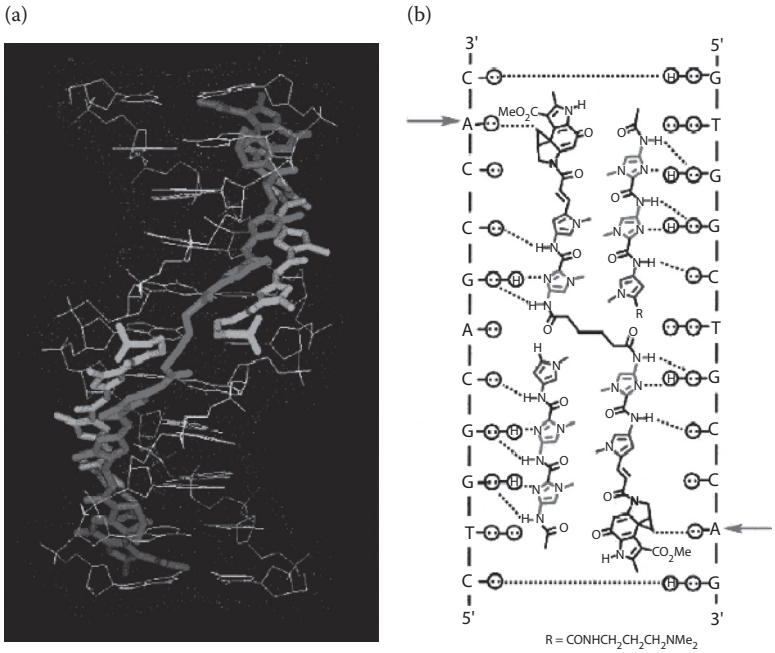

FIGURE 20.7 **(See color insert.)** (a) Energy-minimized structure of 84-ImImPy$_2$-d(CTGGCTGCCAC)/d(GTGGCAGCCAG) interstrand cross-linked complex. DNA is drawn in white. Py and Im residues of 84 and ImImPy are drawn in blue and red, respectively. (b) A DNA interstrand cross-linking mode of the 1:2 complex of 84 with ImImPy.

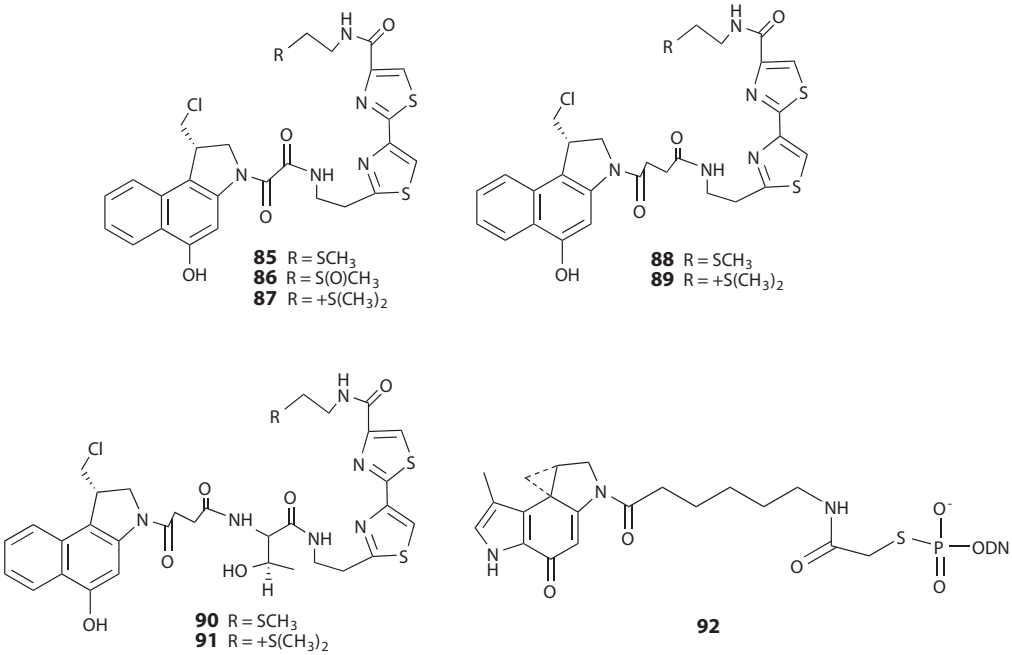

STRUCTURES 85–92

either the 3- or 5-end of ODNs (**92**). This replaces the minor groove binding B and C subunits of CC-1065 with many more sequence-specific binding agents (ODN). These conjugates were stable in aqueous solution at neutral pH even in the presence of strong nucleophiles. When a 3-CPI–ODN conjugate was hybridized to a complementary DNA strand at 37°C, the CPI moiety alkylated nearby adenine bases of the complement efficiently and rapidly, with a half-life of a few minutes. CPI–ODN conjugates are highly effective sequence-specific inhibitors of single-stranded viral DNA replication or gene-selective inhibitors of transcription initiation.

Lown and coworkers[63–65] synthesized a bis-functionalized precursor of CBI, **93**, and with this precursor synthesized bis-polyamide CBI conjugates of symmetrical **94** and unsymmetrical **95** types by incorporating pyrrole rings on both sides for AT specificity and pyrrole on one side and imidazole on the other side of CBI for mixed sequence recognition. The authors also explored[66,67] solid-phase techniques for the synthesis of seco-CBI **97** and conjugates, which bears two polyamide moieties on either side of the pharmacophore **96** through an intermediate **98**. Lown et al.[21,22] have demonstrated that incorporation of a vinyl linker between CPI or CBI and the carrier dramatically enhances the efficiency of DNA alkylation as well as cytotoxicity. In confirmation of this significant finding, a diamide–CPI conjugate possessing a vinyl linker **99** was also synthesized by Tao et al.[68] Molecular modeling indicated that the insertion of a vinyl linker (L) between polyamide and CPI adjusts the location of the cyclopropane ring of the conjugates and in this way improves the alkylation efficacy of the conjugates. Sequence-selective alkylation of double-stranded DNA by **99** was investigated by high-resolution denaturing gel electrophoresis, using 400-bp DNA fragments. Highly efficient alkylation predominantly occurs simultaneously at the purines of the 5-PyG(A/T) Cpu-3 site on both strands at nanomolar concentrations of **99**. These results indicate that the homodimer of conjugate **99** dialkylates both strands according to Dervan's pairing rule,[69] together with a new mode of recognition in which the Im–vinyl linker (L) pair target G/C base pairs. In addition to the major dialkylation sites, a minor alkylation site was also observed at 5-GT(A/T)

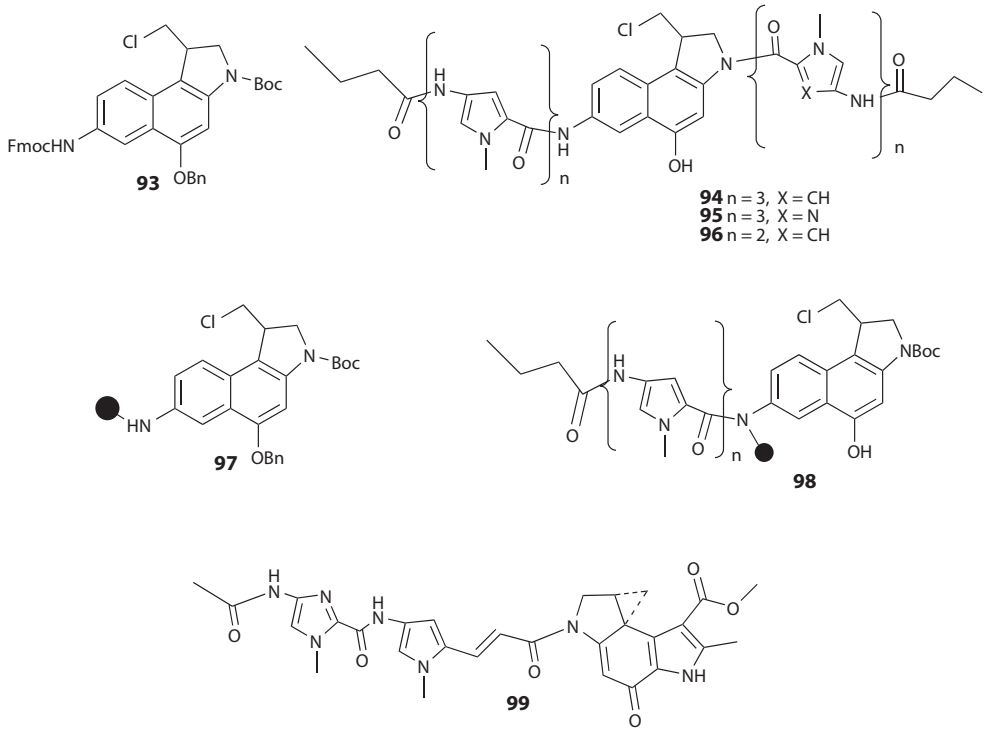

STRUCTURES 93–99

GC-3. This alkylation can be explained by an analogous slipped homodimer recognition mode in which the L–L pair recognizes the A/T base pair. High-performance liquid chromatography analysis revealed that the conjugate **99** simultaneously alkylates GN3/AN3 of the target sequences on both strands of ODNs.

Eight-ring hairpin polyamides conjugated with seco-CBI were prepared by Chang and Dervan.[70] Alkylation yields and specificity were determined on a restriction fragment containing a 6-bp match and mismatch series. Alkylation was observed at a single adenine flanking the polyamide binding site, and strand-selective cleavage could be achieved on the basis of the enantiomer of seco-CBI conjugate; a near quantitative cleavage was observed after 12 h.

20.6 BISALKYLATORS (DIMERS)

The CPI bisalkylator, U-77,779 (bizelesin), in which the two alkylating moieties are connected with a rigid linker 1,3-bis-(2-carbonyl-1H-indole-5-yl) urea group, showed promising antitumor activity,[19,71] and this compound is in clinical trials. Boger et al.[72] synthesized a series of four dimers, **100**–**103**, derived from head-to-tail coupling of the two enantiomers of duocarmycin SA alkylation subunits. All the agents proved to be potent in cytotoxicity assays and displayed a two- to threefold higher activity than duocarmycin SA. CPI dimers have shown good cytotoxic and antitumor activities, and now it is well documented that the activity of the dimeric drugs is strongly related to the length and the position of the linker. To investigate the structure–activity relationship systematically, Lown and coworkers[65,66,73–75] have designed three types of seco-CBI dimers, namely, C7-C7, N3-N3, and N3-C7 **104**–**109**, which contain two racemic CBI moieties linked from two different positions by a flexible methylene chain of variable length and with *n* numbers of pyrrole, imidazole, or thiazole moieties with the polyamides. Dimers, which are connected by a flexible methylene chain, are generally more active against human cancer cell lines when compared with the corresponding monomer, connected to a polyamide. Recently, Lown and coworkers developed the glycosylated water-soluble versions of seco-CBI polyamide conjugates (unpublished work), **110**–**111**, which are more active against the human cancer cell lines when compared with their nonwater-soluble versions.

A set of 10 compounds, each combining the seco-1,2,9,9a-tetrahydrocyclopropa[*c*]benz[*e*]indol-4-one (seco-CBI) and pyrrolo[2,1-c]benzodiazepine pharmacophores (**112**), were designed and prepared.[76] These compounds were anticipated to cross-link between N3 of adenine and N2 of guanine in the minor groove of DNA. The compounds, which differ in the chain length separating the two alkylation subunits, and the configuration of the CBI portion, showed great variation in cellular toxicity (over four orders of magnitude in a cell line panel), with the most potent example exhibiting IC_{50}s in the picomolar range. Cytotoxicity correlated with the ability of the compounds to cross-link naked DNA. Cross-linking was also observed in living cells, at much lower concentrations than for a related symmetrical pyrrolo[2,1-c]benzodiazepine dimer. A thermal cleavage assay was used to assess sequence selectivity, demonstrating that the CBI portion controlled the alkylation sites, whereas the pyrrolo[2,1-c]benzodiazepine substituent increased the overall efficiency of alkylation. Several compounds were tested for *in vivo* activity using a tumor growth delay assay against WiDr human colon carcinoma xenografts, with one compound (the most cytotoxic and most efficient cross-linker) showing a statistically significant increase in survival time following a single intravenous dose.

20.7 STRUCTURAL CHARACTERIZATION OF DRUG DNA COMPLEXES

Bizelesin forms an adduct with d-$(CGTAATTACG)_2$ and ^1H nuclear magnetic resonance (NMR) analysis of this adduct indicated that adenines 6 bp apart on opposite DNA strands are cross-linked, yielding two major adducts differing in the central duplex region (5AATT3).[77] In the major product, both adenines are *syn* oriented and Hoogsteen base paired to thymines (5HG model), whereas the other adduct contains an *anti*-oriented AT-step adenine that shows no evidence of hydrogen bonding with pairing thymines (50P model). Bizelesin's size, rigidity, and cross-linking properties restrict

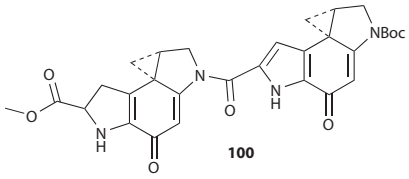

100

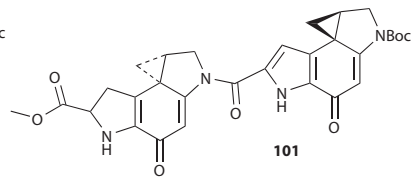

101

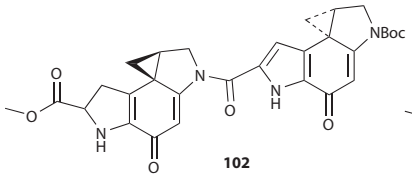

102

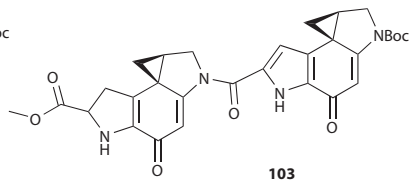

103

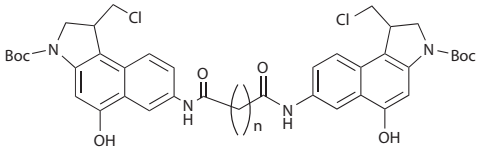

104 n = 3, 4, 5,6

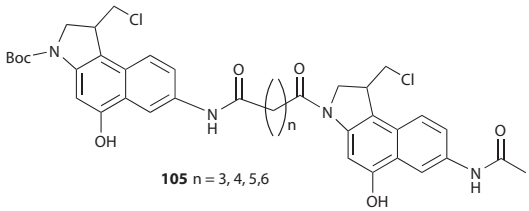

105 n = 3, 4, 5,6

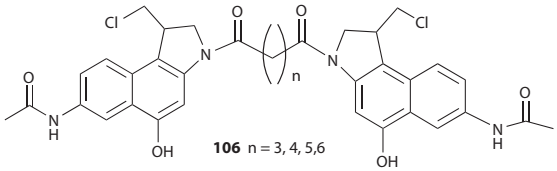

106 n = 3, 4, 5,6

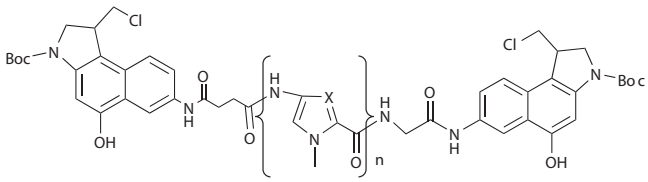

107 X = CH or N, n = 1, 2,3

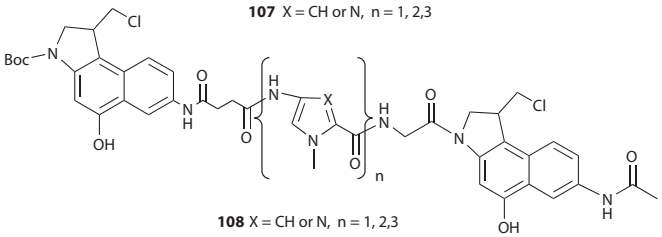

108 X = CH or N, n = 1, 2,3

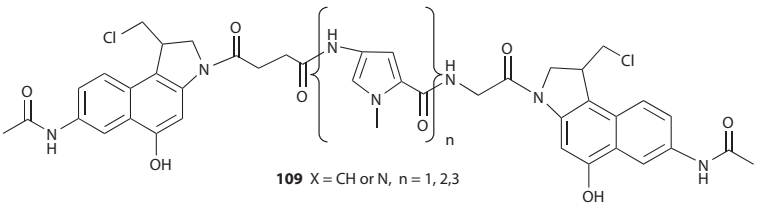

109 X = CH or N, n = 1, 2,3

STRUCTURES 100–109

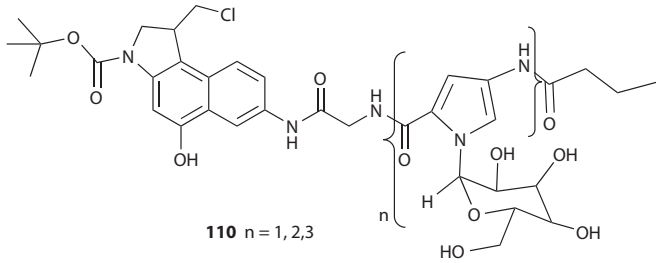

110 n = 1, 2,3

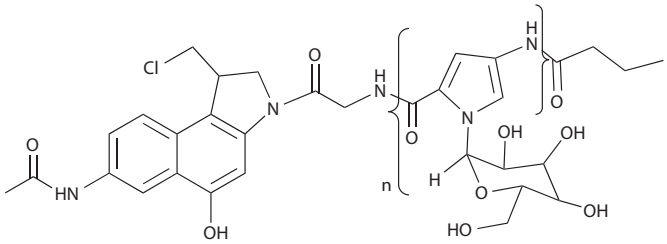

111 n = 1, 2,3

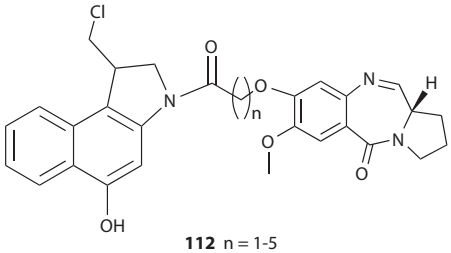

112 n = 1-5

STRUCTURES 110–112

the DNA adduct's range of motion and freeze out DNA conformations adopted during the cross-linking process. In several sequences, bizelesin cross-links and shows overwhelming preference for a 7-bp sequence over a possible 6-bp sequence[78] (Figure 20.8).

The role of the central GC base pairs in the formation of the 7-bp cross-link was investigated using two-dimensional ^{1}H NMR studies that concentrated on the 7-bp cross-link formed with the sequence 5TTAGTTA-3. ^{1}H NMR analysis coupled with restrained molecular dynamics provided evidence for distortion around the covalently modified adenines. The modified bases are twisted toward the center of the duplex adduct because of distortion, and this effectively reduces the cross-linked distance. The restrained molecular dynamics study also showed that a hydrogen bond is formed between the exocyclic amine of the central guanine and the carbonyl of the ureylene linker. It is possible to speculate on the role of the central GC bases in this sequence preference and to propose a mechanism by which bizelesin forms a 7-bp rather than a 6-bp cross-link with 5-TTAGTTA-3 on the basis of the observation of the distortion in the duplex and the hydrogen bonding between the drug and DNA.

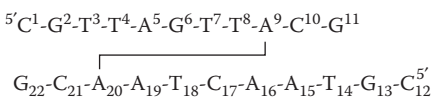

FIGURE 20.8 Cross-linking of adenines 6 bp apart on opposite DNA strands.

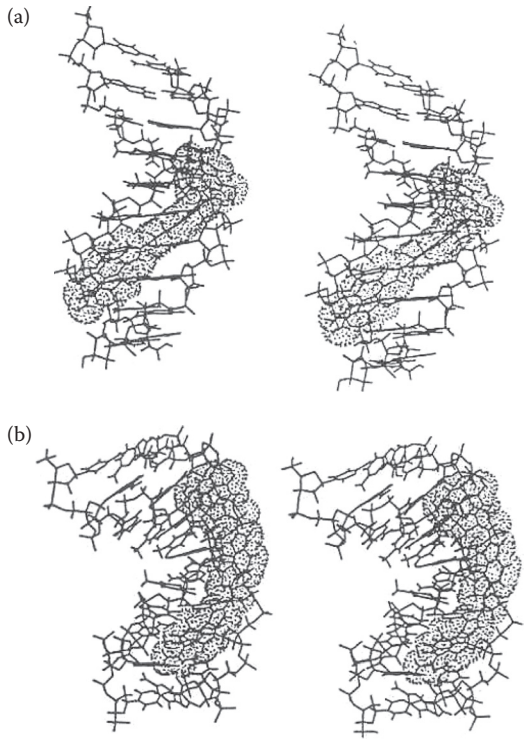

FIGURE 20.9 Stereoviews of (a) the initial model involving docking of the CPI-CDPI$_2$ (dotted van der Waals surface is shown) to a regular B-DNA decamer and (b) NOESY distance restrained, MORASS hybrid matrix/molecular dynamics final refined structure of the decamer-CPI-CDPI$_2$ complex starting from the initial model. The A strand C1 is depicted in the upper left of the structures, with the minor groove at A17 facing away or to the right of the viewer. Note the sharp bend in the duplex near the site of alkylation in B.

Multidimensional NMR studies of the CPI-CDPI2 · d-(CGCTTAAGCG)$_2$ complex indicate that CPI-CDPI$_2$ binds to the decamer in the same manner as CC-1065[79] (Figure 20.9). The effect of CPI-CDPI$_2$ on the ^{1}H and ^{31}P spectra of the decamer was consistent with a minor groove-binding motif, with the drug alkylating at A17 with CDPI rings oriented toward the 5-end of the alkylated strand. NMR data indicate formation of one major and one minor adduct. The minor adduct formation could represent drug alkylation of the DNA at a secondary site or alternative orientation of the rings.

20.8 CELLULAR AND PHARMACOLOGICAL STUDIES

20.8.1 *In Vitro* Studies

Adozelesin (**3**) is an extremely potent cytotoxic agent that causes 90% lethality after 2-h exposure *in vitro* of Chinese hamster ovary (CHO) and lung (V79), mouse melanoma (B16), and human carcinoma (A2780) cells at 0.33, 0.19, 0.2, and 0.25 ng/mL, respectively. The relative drug sensitivity of the cell lines (A2780 > V79, B16, CHO) was correlated to the relative amounts of [^{3}H]adozelesin that alkylated DNA. The greater sensitivity of A2780 resulted in greater cell kill at comparable DNA alkylation levels. Phase-specific toxicity studies show that adozelesin was least lethal to CHO cell in mitosis and very early G1. Lethality increased as the cell progressed through G1 and was maximum in late G1 and early S. Adozelesin had three different effects on the progression of CHO, V79, B16, and A2780 through the cell cycle: it slowed progression through S, which resulted in significantly increasing the percentage of S-phase cells (though this effect was transient); cell progression was

blocked in G2 for a long time period; and the response of the cell lines to G2 block differed. CHO and V79 cells escaped G2 block by dividing and became tetraploid. In contrast, B16 and A2780 cells remained blocked in G2 and did not become tetraploid. Subsequent G2 blockade was followed by a succession of events (polyploidy and unbalanced growth) that resulted in cell death.

The cell-cycle kinetics have been studied by flow cytometry[80] and were performed on five human gynecological cancer cell lines, AN3, AE7, BG1, HEC1A, and SKUT1B, with exposure to adozelesin at near confluency at 0, 0.1, 0.2, 0.5, 1.0, and 5*X*, with $X = 10$ pg/mL as a reference concentration for 90 min. Cell samples were taken by trypsinization at 0, 24, 48, 72, 96, and 168 h for flow cytometry. The results revealed that there was a spectrum of cell-cycle perturbations that included biphasic S and G2 blocks, reverse dose-dependent G2 blocks, and a sequential relationship of S and G2 blocks. This study demonstrated that the cell kinetics response to adozelesin depended on several variables, such as cell lines, drug sensitivity, concentrations, and sampling time.

The effects of CC-1065 (**1**) and its analogs U-66,664, U-66,819, U-66,694, and U-71,184 (**4**) have been studied on the inhibition of CHO cell survival, cell progression, and their phase-specific toxicity.[81,82] Lethality of these compounds after 2-h drug exposure was in the following order (50% lethal dose in nanomolars in parentheses), CC-1065 (0.06) > U-71,184 (1.3) > U-66,694 (3.2) > U-68,819 (171) > U-66,664 (>1200). The phase-specific cytotoxicity of U-71,184 and U-66,694 was different from that of CC-1065. CC-1065 was most cytotoxic to cells in M and early G1, and toxicity decreased as cells entered late G1 and S. In contrast, U-66,694 and U-71,184 were most toxic to cells in late G1. The biochemical and cellular effects of U-71,184 were then studied in detail; after 2-h exposure to 3 ng/mL, 90% cell kill or growth inhibition was observed, whereas 100 ng/mL was needed for similar inhibition of DNA and RNA synthesis. This discrepancy between the doses indicated that the inhibition of nucleic acid synthesis may not be causally related to lethality. Further studies showed that when the drug was removed after 2-h exposure, DNA synthesis continued to be inhibited, whereas RNA and protein synthesis reached levels higher than the control. Therefore, it is likely that the stimulation of RNA combined with protein synthesis leads to unbalanced growth and cell death.

The adozelesin (**3**) cytotoxic potency was compared with doxorubicin, cisplatin, 5-fluorouracil, and cytoxan by the adenosine triphosphate chemosensitivity assay in 10 gynecologic-cancer cell lines.[83] By comparing the mean drug concentrations required to reduce the adenosine triphosphate concentrations by 50%, adozelesin was found to be approximately 100 times more potent than doxorubicin, cisplatin, 5-fluorouracil, or cytoxan. Similarly, experiments designed to investigate the cytotoxicity of adozelesin on fresh cervical and ovarian carcinoma samples demonstrated that at least a 4000-fold lower level of this agent was required compared with cisplatin in the same experiment,[84] with similar results being found when the adenosine triphosphate assay referred to earlier was used with 10 gynecologic cancer cell lines.[85]

The cytotoxicity against CHO cells of several agents combined with adozelesin has been reported.[86] The additive, synergistic, or antagonistic nature of the combined drug effect was determined for most combinations using the median effect principle. In experiments with alkylating agents, combinations of adozelesin with melphalan or cisplatin were usually additive or slightly synergistic. Adozelesin–tetraplatin combinations were synergistic at several different ratios of exposure to drug. By using methylxanthines, adozelesin combined synergistically with noncytotoxic doses of caffeine and pentoxifylline and resulted in several logs increase in adozelesin cytotoxicity. In experiments with hypomethylating agents, adozelesin combined synergistically with 5-azacytidine (5-aza-CR) and 5-aza-2-deoxy cytidine (5-aza-2-CdR), and combinations of adozelesin with tetraplatin or 5-aza-2-CdR were also tested against B16 melanoma cell *in vitro* and were found to be additive and synergistic, respectively.

Hematopoietic clonal assays were used to evaluate the effects of bizelesin on granulocyte-macrophage (CFU-gm) colony formation.[87] Marrow cells were exposed *in vitro* to bizelesin (**9**) (0.001–1000 nM) for 1 or 8 h and were then assayed for colony formation. There was a 3-log difference in drug concentration at which 100% colony inhibition occurred (1 or 8 h) for murine CFU-gm versus

human or canine CFU-gm. The IC_{70} value after an 8-h bizelesin exposure for human CFU-gm (0.006 ± 0.002 nM) was 2220 times lower than for murine CFU-gm (13.32 ± 8.31 nM). At any given concentration, an 8-h drug exposure resulted in greater colony inhibition than a 1-h exposure for all species ($P < 0.05$). Increasing exposure time from 1 to 8 h increased toxicity to human and canine CFU-gm much more than to murine CFU-gm. The results of these *in vitro* clonal assays were quantitatively consistent with those seen in whole animal studies, indicating that bizelesin could be a potent myelosuppressive agent in the clinic. Because the dose-limiting toxicity in preclinical models is myelosuppression, and because the *in vitro* sensitivity of human and canine CFU-gm is similar, the canine maximum tolerated dose is better than the murine maximum tolerated dose to determine a safe starting dose for phase I clinical trials.

The DNA damage and differential cytotoxicity produced in human carcinoma cells by adozelesin and bizelesin have been studied.[88] The concentration of adozelesin required to produce a 1-log cell kill in six human tumor cell lines varied from 20 to 60 pM, whereas with bizelesin, the comparable concentrations ranged from 1 to 20 pM. The cytotoxicity of adozelesin and bizelesin was found to be independent of the guanine *O*6-alkyl transferase phenotype. The sensitivities of the BE and HT-29 human colon carcinoma cells were increased when the time of drug exposure was varied from 2 to 6 h, with DNA-ISCs, as measured by the technique of alkaline elution, only detected when HT-29 or BE cells were exposed to extremely high concentrations of bizelesin for 6 h.

The cytotoxic actions of adozelesin (**3**) against the human colon (HT-29, DLD-1) and lung (SK) carcinoma cell lines have been studied.[89] The concentrations of adozelesin that produced 50% cell kill for 4- and 24-h exposures were in the range of 0.001–0.02 ng/mL for both colon and lung carcinoma cells, indicating that this analog is a very potent cytotoxic agent. Because most clinical regimens for tumor therapy consist of several drugs, the antineoplastic action of adozelesin in combination with 5-aza-2-CdR, a potent inhibitor of DNA methylation, or cytosine arabinoside (Ara-C), a potent inhibitor of DNA synthesis, was examined. The adozelesin plus 5-Aza-CdR combination showed a synergistic effect on cytotoxicity against DLD-1 colon carcinoma cells for both a 6- and 24-h exposure. However, the combination of adozelesin and Ara-C for a 6-h exposure showed an antagonistic effect, whereas 24-h exposure showed a synergistic effect. These preclinical results provided some preliminary data on possible drugs that might be useful in combination with adozelesin in clinical trials.

Bis-indolyl-(seco)-1,2,9a-tetrahydrocyclopropa[*c*]benz[*e*]indole-4-one compounds are synthetic analogs of CC-1065 that are highly cytotoxic toward a broad spectrum of tumor cell lines. One of these compounds, DC1, was conjugated to antibodies via novel cleavable disulfide linkers. Conjugates of DC1 with the murine mAbs anti-Bu and N901 directed against tumor-associated antigens CD19 and CD56, respectively, proved to be extremely potent and antigen selective in killing target cells in culture.[90] DC1 conjugates with humanized versions of anti-B4 and N901 antibodies were also examined and shown to be as cytotoxic and selective as the respective murine antibody conjugates. The anti-B4-DC1 conjugate showed antitumor efficacy in an aggressive metastatic human B-cell lymphoma survival model in SCID mice and completely cured animals bearing large tumors. Anti-B4-DC1 was considerably more effective in this tumor model than doxorubicin, cyclophosphamide, etoposide, or vincristine at their maximum tolerated doses.

The mutagenicity for V-79 cell (6-thioguanine resistance and salmonella histidine auxotropy or aza guanine resistance) of selected CPI analogs was compared with DNA-binding activity, and the structure–activity relationship was determined. The compounds CC-1065, U-62,736, U-66,866, U-66,694, U-67,786, and U-68,415 all have an A segment with an intact cyclopropyl group and different B segments,[91] whereas the cyclopropyl group is absent from U-66,226 and U-63,360. This absence of the cyclopropyl ring diminished the cytotoxic and mutagenic potency of the compounds such that U-63,360 was nearly three orders of magnitude less potent than CC-1065 in V-79 cells. For the compounds with an intact cyclopropyl group, the order of cytotoxic and mutagenic potency in V79 cells generally correlated with binding to CT-DNA and increased with the length of the B segment; the order of cytotoxicity being CC-1065 > U-68,415 > U-66,694 > U-66,866 > U-62,736.

These results show that an electrophilic carbon afforded by an intact cyclopropyl group of this type is necessary, but not sufficient to account for the high cytotoxic and mutagenic potency of CC-1065 and U-68,415. The size and characteristics of the B segment also affect the potency. The authors speculate that the more cytotoxic analogs are less mutagenic, because they may have greater structure directed binding to less mutable DNA sites in the minor groove.

20.8.2 *In Vivo* Studies

The analog of CPI or its kinetically equivalent ring opened seco precursor, carzelesin (**5**), was evaluated against a series of human xenografts growing at the subcutaneous sites.[92] The model consisted of seven colon adenocarcinomas and six pediatric rhabdomyosarcomas. Carzelesin was given a single intravenous injection, and the tumor volumes were determined at seven-day intervals. At the highest dose (0.5 mg/kg), the dose producing 10% lethality (LD10), carzelesin significantly inhibited growth in four of the colon tumor lines; in contrast, on lowering the dose to 0.25 mg/kg, only two of the seven colon adenocarcinomas exhibited significant growth inhibition. However, with the rhabdomyosarcoma lines, all were significantly arrested in growth. There was no apparent cross-resistance to carzelesin in two rhabdomyosarcomas selected for vincristin resistance (RH 12/VCR, Rh 18/VCR) or in Rh 28/LPAM xenografts selected for primary resistance to the bifunctional alkylating agent, melphalan. Carzelesin maintained full activity against Rh 18/Topo tumors selected *in situ* for resistance to topotecan.

Adozelesin (**3**), which was selected from a series of analogs of CC-1065 for its superior *in vivo* and antitumor activity, was highly active when administered intravenously against intraperitoneal or subcutaneous implanted murine tumors, including L1210 leukemia, B16 melanoma, MS076 sarcoma, and colon 38 carcinoma, and produced long-term survivors in mice bearing intravenous inoculated L1210 and Lewis lung carcinomas.[14] In addition, modest activity was shown against the highly drug-resistant pancreas 02 carcinoma. Adozelesin was also highly effective against human tumor xenografts, implanted subcutaneously in athymic (nude) mice, including colon CX-1 adenocarcinoma, lung LX-1 tumor, clear cell caki-1 carcinoma, and ovarian 2780 carcinoma. Its broad spectrum of *in vivo* activity compared favorably with the three widely used antitumor drugs: cisplatin, cyclophosphamide, and doxorubicin. Adozelesin appeared to be more effective than these drugs in the treatment of various resistant tumors such as subcutaneously implanted mouse B16 melanoma, pancreatic 02 carcinoma, human colon CX-1, and human lung LX-1 tumor xenografts, and based on its high potency and high efficacy, it was chosen for clinical investigation and development.

The mutagenic potential of the antitumor compounds CC-1065 and adozelesin were assessed[93] to track the *in vivo* fate of their unique modifications at the nucleotide level. Mice were inoculated with a single therapeutic dose of these agents and sacrificed at 18 h, 3 d, or 15 d for extraction and analysis of liver DNA. Although undetectable at 18 h post-treatment, by 72 h a threefold increase in mutant frequency was observed in drug-treated animals such that sequence analysis of drug-induced mutations could be performed and a direct comparison made between *in vitro* and *in vivo* DNA alkylation. Base substitution involving guanine or cytosine accounted for 64% of the 41 mutations that occurred at a cyclopropylindole alkylation site, whereas 23 mutations occurred one to four nucleotides from a potentially alkylated adenine.

Following intravenous administration of bizelesin (15 μg/kg) to male CD2F1 mice, the plasma elimination of cytotoxic activity resulting from bizelesin in the L1210 cell bioassay was described by a two-compartment open model;[94] the A-phase ($t_{1/2}$ A) and B-phase ($t_{1/2}$ B) half-lives, steady-state volume distribution, and total body clearance were 3.5 min, 7.3 h, 7.641 mL/kg, and 16.3 mL/min/kg, respectively. The drug level following intraperitoneal administration was at least 10 times lower than that resulting from intravenous infusion. Following intravenous or intraperitoneal administration, the recovery of material in urine was <0.1% of the delivered dose. The low urine recovery indicated an extensive interaction of the parent drug and other reactive species with macromolecules or further metabolism or degradation to inactive species.

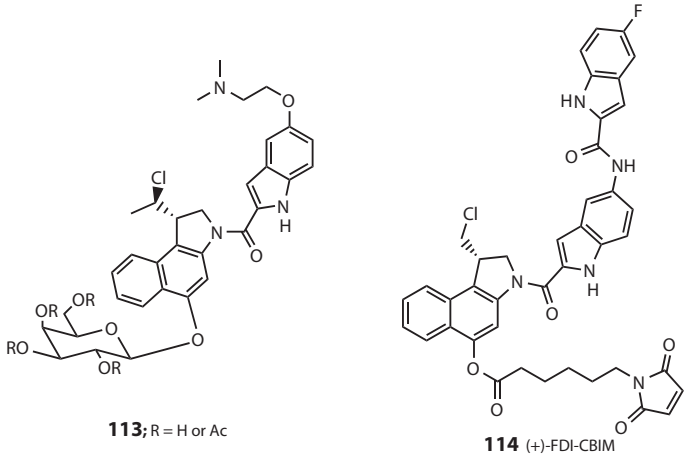

STRUCTURES 113 and 114

20.9 DEVELOPMENT OF POTENTIAL TARGETED THERAPIES

Antibody-directed enzyme prodrug therapy (ADEPT) involves the administration of conjugates of appropriate enzymes and monoclonal antibodies that bind to tumor-associated antigens. Following clearance of any remaining unbound conjugate from the blood stream, a prodrug is administered. Selective transformation of the prodrug to the corresponding highly cytotoxic compound is achieved by the targeted antibody–enzyme conjugate bound to the tumor, thereby leading to the selective killing of tumor cells.[95] Tietze and Krewer have designed and evaluated a series of novel glycosidic prodrugs (e.g., **113** and compare structures **110** and **111**) based on analogs of CC-1065 and the duocarmycins. These prodrugs are up to 4800 times less toxic than the corresponding drugs liberated in the presence of the activating enzyme (e.g., β-d-galactosidase), which exhibit high cytotoxicity, with IC_{50} values of as low as 16 pM.[96,97]

Wang et al. have reported the synthesis of prodrug of the CC-1065 analog, (+)-FDI-CBIM (114), which formed an albumin conjugate when added to human albumin *in vitro*. The prodrug showed significantly improved antitumor efficacy compared with the free drug in animal models using syngeneic animal tumors and human ovarian xenografted tumor cells.[98]

20.10 CLINICAL STUDIES

Adozelesin is a potent synthetic analog that was chosen for clinical development, because it had a preclinical antitumor spectrum that was similar to CC-1065 at therapeutic doses but did not produce deaths. Phase I evaluations using a variety of adozelesin treatment schedules have been reported.[99,100] Adozelesin was given as a 10-min intravenous infusion for five consecutive days every 21 d on recovery from toxicity. The dose range evaluated was 6–30 μg/m^2 per day. All patients had refractory solid tumors and had received prior cytotoxic drug treatment. Thirty-three patients (22 men, 11 women) were entered in the study, and 87 courses of treatment were initiated. Dose-limiting toxicity was cumulative myelosuppression (leukopenia, thrombocytopenia). The maximum tolerated dose was 30 μg/m^2 per day. The only other significant toxicity was an anaphylactoid syndrome that occurred in two patients. A partial response was observed in a patient with refractory soft-tissue sarcoma. The recommended phase II starting dose of adozelesin using 10-min intravenous infusion for five consecutive days was 25 μg/m^2 per day, to be repeated every four to six weeks to allow recovery from myelotoxicity. Phase II clinical trials were performed in the 1990s against metastatic breast cancer, metastatic small cell lung cancer, and untreated advanced gastric adenocarcinoma

(http://www.cancer.gov/search/ResultsClinicalTrials.aspx?protocolsearchid=7259745). Marginal efficacy was reported in the treatment of metastatic breast cancer,[101] while there are no published reports recorded in PubMed for the other two phase II trials.

Two phase I trials of bizelesin against advanced cancer were performed in 2002 (http://www.cancer.gov/search/ResultsClinicalTrials.aspx?protocolsearchid=7258274). The dose-limiting toxicity observed was neutropenia, and the drug was well tolerated. Though no objective responses were noted, both teams of investigators appeared to favor further study,[102,103] but no further trials have been recorded in PubMed.

While there have been three phase I studies of carzelesin reported in PubMed, thus far only one report of a phase II clinical trial has appeared. In this trial, carzelesin was used as second- or third-line chemotherapy in patients with breast, ovarian, head and neck cancer, and non-Hodgkin's lymphoma, and as first-line chemotherapy in patients with colorectal and gastric cancer and melanoma. While the drug was well tolerated, no significant responses were observed in any of the tumors studied.[104] As of late September 2004, carzelesin was the only agent that was still listed as being in clinical trials; it was quoted in the Prous Integrity™ database as being in phase II and under "active development," but as of January, 2010, no reports have been recorded in PubMed.

20.11 CONCLUSIONS AND PROSPECTS

The sequence selectivity inherent in even the simplest minor groove ligands has enabled them to be used as probes of DNA structure and dynamics. From these data has arisen the concept of devising sequence-specific agents such as polyamides capable of single-gene recognition, and thus of being targeted to single deleterious genes. An extensive series of studies has led to the development of synthetic approaches to the natural products CC-1065 and the duocarmycins. The present understanding of the origin of the properties of the natural products emerged from the design and evaluation of synthetic substrates and agents containing systematic structural modifications, in addition to extensive studies conducted on the natural product themselves. As a consequence of these efforts, and despite expectations of the unique behavior of the natural products, potent and efficacious antitumor activity has not only been observed with such analogs, but both their potency and efficacy may even exceed those of the natural products. This illustrates that their useful properties may be enhanced by well-founded and well-designed structural modifications. The active units, when coupled with certain appropriate linkers as dimers, have proven to be even more potent and are in clinical trials. Conjugating the pharmacophore unit of CC-1065 with the DNA-binding polyamides indicates a promising additional approach for developing new types of sequence-specific DNA alkylating agents. The evident advantages of single-gene agents for molecular medicine will determine much of the future emphasis of this area, provided the formidable problems of converting them into pharmacologically acceptable drugs can be overcome.

REFERENCES

1. Hanka, L.J., Dietz, A., Gerpheide, S.A., Kuentzel, S.L., and Martin, D.G., CC-1065 (NSC-298223), a new antitumor antibiotic: Production, *in vitro* biological activity, microbiological assays and taxonomy of the producing microorganisms. *J. Antibiot.*, 31, 1211, 1978.
2. Martin, D.G., Bikes, C., Gerpheide, S.A., Hanka, L.J., Krueger, W.C., McGovren, J.P., Mizsak, S.A., Neil, G.L., Stewart, J.C., and Visser, J., CC-1065 (NSC 298223), a potent new antitumor agent: Improved production and isolation, characterization and antitumor activity. *J. Antibiot.*, 34, 1119, 1981.
3. Bhuyan, B.K., Newell, K.A., Crampton, S.L., and Von Hoff, D.D., CC-1065 (NSC-298223), a most potent antitumor agent, kinetics of inhibition of growth DNA synthesis, and cell survival. *Cancer Res.*, 42, 3532, 1982.
4. Reynolds, V.L., Molineux, I.J., Kaplan, D.J., Swenson, D.H., and Hurley, L.H., Reaction of the antitumor antibiotic CC-1065 with DNA location of the site of thermally induced strand breakage analysis of DNA sequence specificity. *Biochemistry*, 24, 6228, 1985.

5. Hurley, L.H., Reynolds, V.L., Swenson, D.H., Petzold, G.L., and Scahill, T.A., Reaction of the antitumor antibiotic CC-1065 with DNA: Structure of a DNA adduct with DNA sequence specificity. *Science*, 226, 843, 1984.
6. Hurley, L.H., Lee, C.S., McGovren, J.P., Warpehoski, M.A., Mitchell, M.A., Kelly, R.C., and Aristoff, P.A., Molecular basis for sequence-specific DNA alkylation by CC-1065. *Biochemistry*, 27, 3886, 1988.
7. Hurley, L.H., Warpehoski, M.A., Lee, C.S., McGovren, J.P., Scahill, T.A., Kelly, R.C., Mitchell, M.A., Wicnienski, N.A., and Gebhard, I., Sequence specificity of DNA alkylation by the unnatural enantiomer of CC-1065 and its synthetic analogs. *J. Am. Chem. Soc.*, 112, 4633, 1990.
8. Weiland, K.L. and Dooley, J.P., *In vitro* and *in vivo* DNA binding by the CC-1065 analogue U-73975. *Biochemistry*, 30, 7559, 1991.
9. Boger, D.L., Munk, S.A., and Zarrinmayeh, H., (+)-CC-1065 DNA alkylation: Key studies demonstrating a no covalent binding selectivity contribution to the alkylation selectivity. *J. Am. Chem. Soc.*, 113, 3980, 1991.
10. Boger, D.L., Munk, S.A., Zarrinmayeh, H., Ishizaki, T., Haught, H., and Bina, M., An alternative and convenient strategy for generation of substantial quantities of singly5-^{32}P-end labeled double stranded DNA for binding studies. Development of a protocol for examination of functional features of (+)-CC-1065 and ducaromycins that contribute to their sequence selective DNA alkylation properties. *Tetrahedron*, 47, 2661, 1991.
11. Li, H., Swenson, D.H., Schpok, S.L., Kuentzel, S.L., Dayton, B.D., and Krueger, W.C., CC-1065 (NSC 298223), a novel antitumor agent that interacts strongly with double-stranded DNA. *Cancer Res.*, 42, 999, 1982.
12. McGovren, J.P., Clarke, G.L., Pratt, E.A., and DeKoning, T.F., Preliminary toxicity studies with the DNA-binding antibiotic, CC-1065. *J. Antibiot.*, 37, 63, 1984.
13. Warpehoski, M.A., Gebhard, I., Kelly, R.C., Krueger, W.C., Li, L.H., McGovren, J.P., Prairie, M.D., Wicnienski, N., and Wierenga, W., Stereoelectronic factors influencing the biological activity and DNA interaction of synthetic antitumor agents modeled on CC-1065. *J. Med. Chem.*, 31, 590, 1988.
14. Li, L.H., Kelly, R.C., Warpehoski, M.A., McGovren, J.P., Gebhard, I., and DeKoning, T.F., Adozelesin, a selected lead among cyclopropyl pyrroleindole analogs of the DNA binding antibiotic, CC-1065. *Invest. New Drugs*, 9, 137, 1991.
15. Ichimura, M., Ogawa, T., Takahashi, K., Kobayashi, E., Kawamoto, I., Yasuzawa, T., Takahashi, I., and Nakano, H., Duocarmycin SA, a new antitumor antibiotic from *Streptomyces* sp. *J. Antibiot.*, 43, 1037, 1990.
16. Sugiyama, H., Hosoda, M., Saito, I., Asai, A., and Saito, H., Covalent alkylation of DNA with duocarmycin A. Identification of a basic site structure. *Tetrahedron Lett.*, 31, 7197, 1990.
17. Igarashi, Y., Futamata, K., Fujita, T., Sekine, A., Senda, H., Naoki, H., and Furumai, T., Yatakemycin, a novel antifungal antibiotic produced by *Streptomyces* sp. TP-A0356. *J. Antibiot.*, 56, 107 – 113, 2003.
18. Tichenor, M.S., Trzupek, J.D., Kastrinsky, D.B., Shiga, F., Hwang, I., and Boger, D.L., Asymmetric total synthesis of (+)- and ent-(-)-yatakemycin and duocarmycin SA: Evaluation of yatakemycin key partial structures and its unnatural enantiomer. *J. Am. Chem. Soc.*, 128, 15683, 2006.
19. Mitchell, M.A., Kelly, R.C., Wicnienski, N.A., Hatzenbuhler, N.T., Williams, M.G., Petzold, G.L., Slightom, J.L., and Siemieniak, D.R., Synthesis and DNA cross-linking by a rigid CPI dimer. *J. Am. Chem. Soc.*, 113, 8994, 1991.
20. Aristoff, P.A., Johnson, P.D., Sun, D., and Hurley, L.H., Synthesis and biochemical evaluation of the CBI-PDE-I dimer, a benzannelated analog of (+)-CC-1065 that also produces delayed toxicity in mice. *J. Med. Chem.*, 36, 1956, 1993.
21. Wang, Y., Gupta, R., Huang, L., Luo, W., and Lown, J. W., Design, synthesis, cytotoxic properties and preliminary DNA sequencing evaluation of cpi-n-methyl pyrrole hybrids. Enhancing effect of a trans double bond linker and role of the terminal amide functionality on cytotoxic potency. *Anticancer Drug Des.*, 11, 15, 1996.
22. Iida, H. and Lown, J.W., Design and synthesis of cyclopropylpyrroloindole (CPI)-lexitropsin conjugates and related structure. *Synth. Org. Chem.*, 1, 1998.
23. Reynolds, V.L., McGovren, J.P., and Hurley, L.H., The chemistry, mechanism of action and biological properties of CC-1065, a potent antitumor antibiotic. *J. Antibiot.*, 39, 319, 1986.
24. Boger, D.L., Coleman, R.S., Invergo, B.J., Sakya, S.M., Ishizaki, T., Munk, S.A., Zarrinmayeh, H., Kitos, P.A., and Thompson, S.C., Synthesis and evaluation of aborted and extended CC-1065 functional analogs: (+)- and (-)-cpi-pde-i1, (+)- and (-)-cpi-cdpi1, and (+-.)-, (+)-, and (-)-CPI-CDPI3. Preparation of key partial structures and definition of an additional functional role of the CC-1065 central and right-hand subunits. *J. Am. Chem. Soc.*, 112, 4623, 1990.

25. Boger, D.L., Johnson, D.S., and Yun, W., (+)- and ent-(-)-duocarmycin SA and (+)- and ent-(−)-n-boc-dsa DNA alkylation properties. Alkylation site models that accommodate the offset at-rich adenine N3 alkylation selectivity of the enantiomeric agents. *J. Am. Chem. Soc.*, 116, 1635, 1994.
26. Boger, D.L. and Johnson, D.S., CC-1065 and the duocarmycins: Understanding their biological function through the mechanistic studies. *Angew. Chem. Int. Ed. Engl.*, 35, 1439, 1996.
27. Fukuda, Y., Itoh, Y., Nakatani, K., and Tershima, S., Synthetic studies on duocarmycin. 1. Total synthesis of dl-duocarmycin A and its 2-epimer. *Tetrahedron*, 50, 2793, 1994.
28. Fukuda, Y., Nakatani, K., and Tershima, S., Synthetic studies on duocarmycin. 2. Synthesis and cytotoxicity of natural (+)-duocarmycin A and its three possible stereoisomers. *Tetrahedron*, 50, 2809, 1994.
29. Boger, D.L. and Mesini, P., DNA alkylation properties of CC-1065 and duocarmycin analogs incorporating the 2,3,10,10a-tetrahydrocyclopropa[d]benzo[f]quinol-5-one alkylation subunit: Identification of subtle structural features that contribute to the regioselectivity of the adenine N3 alkylation reaction. *J. Am. Chem. Soc.*, 117, 11647, 1995.
30. Wang, Y., Gupta, R., Huang, L., and Lown, J.W. CC-1065 functional analogues possessing different electron withdrawing substituents and leaving groups: Synthesis, kinetics and sequence specificity of reaction with DNA and biological evaluation. *J. Med. Chem.*, 36, 4172, 1993.
31. Lown, J.W., Krowicki, K., Bhat, U.G., Skorobogaty, A., Ward, B., and Dabrowiak, J., Molecular recognition between oligopeptides and nucleic acids: Novel imidazole containing oligopeptides related to netropsin that exhibited altered DNA sequence specificity. *Biochemistry*, 25, 7408, 1986.
32. Sugiyama, H., Ohmori, K., Chan, K.L., Hosoda, M., Asai, A., Saito, H., and Saito, I., A novel guanine N3 alkylation by antitumor antibiotic duocarmycin a. *Tetrahedron Lett.*, 34, 2179, 1993.
33. Dickerson, R.E., Kopka, M.L., and Pjura, P.E., The major and minor grooves of the DNA helix as conduits for information transfer, in *DNA Ligand Interaction, from Drugs to Proteins*, Guschlbauer, W. and. Saenger, W., Eds., Plenum Press, New York, 1987, 45.
34. Boger, D.L., Zarrinmayeh, H., Munk, S.A., Kitos, P.A., and Suntornwat, O., Demonstration of a pronounced effect of nonvovalent binding selectivity on the (+) CC-1065 DNA alkylation and identification of the pharmacophore of the alkylation subunit. *Proc. Natl. Acad. Sci. U.S.A.*, 88, 1431, 1991.
35. Boger, D.L., Zhou, J., and Cai, H., Demonstration and defination of the noncovalent binding selectivity of agents related to CC-1065 by an affinity cleavage agent: Noncovalent binding coincidental with alkylation. *Bioorg. Med. Chem.*, 4, 859, 1996.
36. Boger, D.L., Johnson, D.S., Yun, W., and Tarby, C.M., Molecular basis for sequence selective DNA alkylation by (+)- and enant-(-)-CC-1065 and related agents: Alkylation site models that accommodate the offest at-rich adenine n3 alkylation selectivity. *Bioorg. Med. Chem.*, 2, 115, 1994.
37. Swenson, D.H., Petzold, G.L., Williams, M.G., Li, L.H., Prairie, M.D., and Krueger, W.C., Evaluation of DNA binding characteristics of some CC-1065 analogues. *Chem. Biol. Interact.*, 67, 199, 1988.
38. Ding, Z.M. and Hurley, L.H., DNA interstrand cross-linking, DNA sequence specificity, and induced conformational changes produced by dimeric analogue of (+)-CC-1065. *Anticancer Drug Design*, 6, 427, 1991.
39. Lee, C.S. and Gibson, N.W., Nucleotide preferences for DNA interstrand crosslinking induced by the cyclopropyl pyrrole indole analogue U-77, 779. *Biochemistry*, 32, 2592, 1993.
40. Lee, C.S. and Gibson, N.W., DNA interstrand cross-links induced by the cyclopropyl pyrroloindole antitumor agent bizelisin are reversible upon exposure to alkali. *Biochemistry*, 32, 9108, 1993.
41. Muller, P.R. and Wold, B., *In vivo* footprinting of a muscle specific enhancer by ligation mediated PCR. *Science*, 246, 780, 1989.
42. Pfeifer, G.P., Steigerwald, S.D., Mueller, P.R., Wold, B., and Riggs, A.D., Genomic sequencing and methylation analysis by ligation mediated PCR. *Science*, 246, 810, 1989.
43. Garrity, P.A. and Wold, B.J., Effects of different DNA polymerases in ligation mediated PCR: Enhanced genomic sequencing and *in vivo* footprinting. *Proc. Natl. Acad. Sci. U.S.A.*, 89, 1021, 1992.
44. Lee, C.S., Pfeifer, G.P., and Gibson, N.W., Mapping of DNA alkylation sites induced by adozelesin and bizelesin in human cells by ligation-mediated polymerase chain reaction. *Biochemistry*, 33, 6024, 1994.
45. Krueger, W.C., Hatzenbuhler, N.T., Prairie, M.D., and Shea, M.H., DNA sequence recognition by the antitumor antibiotic CC-1065 and analogues of CC-1065. *Chem. Biol. Interact.*, 79, 265, 1991.
46. Boger, D.L. and Johnson, D.S., CC-1065 and duocarmycins: Unraveling the keys to a new class of naturally derived DNA alkylating agents. *Proc. Natl. Acad. Sci. U.S.A.*, 92, 3642, 1995.
47. Boger, D.L. and Garbaccio, R.M., Catalysis of the CC-1065 and duocarmycin DNA alkylation reaction: DNA binding induced conformational change in the agent results inactivation. *Bioorg. Med. Chem.*, 5, 263, 1997.
48. Krueger, W.C. and Prairie, M.D., The origin of the DNA induced circular dichroism of CC-1065 and analogues. *Chem. Biol. Interact.*, 79, 137, 1991.

49. Gauss, C.M., Hamasaki, A., Parrish, J.P., MacMillan, K.S., Rayl, T.J., Hwang, I., and Boger, D.L., Synthesis and preliminary evaluation of duocarmycin analogues incorporating the 1,2,11,11a-tetrahydrocyclo-propa[c]naphtho[2,3-e]indol-4-one (CNI) and 1,2,11,11a-tetrahydrocyclopropa[c]naphtho[1,2-e] indol-4-one (iso-CNI) alkylation subunits. *Tetrahedron*, 65, 6591, 2009.
50. Jin, W., Trzupek, J.D., Rayl, T.J., Broward, M.A., Vielhauer, G.A., Weir, S.J., Hwang, I., and Boger, D.L., A unique class of duocarmycin and CC-1065 analogues subject to reductive activation. *J. Am. Chem. Soc.*, 129, 15391, 2007.
51. Tichenor, M.S., MacMillan, K.S., Stover, J.S., Wolkenberg, S.E., Pavani, M.G., Zanella, L., Zaid, A.N., et al., Rational design, synthesis, and evaluation of key analogues of CC-1065 and the duocarmycins. *J. Am. Chem. Soc.*, 129, 14092, 2007.
52. Moy, B.C., Prairie, M.D., Krueger, W.C., and Bhuyan, B.K., Interaction of CC-1065 and its analogues with mouse DNA and chromatin. *Cancer Res.*, 49, 1983, 1989.
53. Mohamdi, F., Spees, M.M., Staten, G.S., Marder, P., Kipka, J.K., Johnson, D.A., Boger, D.L., and Zarrinmayeh, H., Total synthesis and biological properties of novel antineoplastic (chloromethyl)furanoindolines, an asymmetric hydroboration mediated synthesis of the alkylation subunit. *J. Med. Chem.*, 37, 232, 1994.
54. Boger, D.L., Johnson, D.S., Palanki, M.S., Kitos, P.A., Chang, J., and Dowell, P., Evaluation of functional analogues of CC-1065 and the duocarmycins incorporating the cross-linking 9a-chloromethyl-1, 2,9,9a-tetrahydrocyclopropa[c] benz [e] indole-4-one (C2BI) alkylation subunit. *Bioorg. Med. Chem.*, 1, 27, 1993.
55. Boger, D.L., Yun, W., and Han, N., 1,2,9,9a-tetrahydro cyclopropa[c] benz [e] indole-4-one (CBI) analogues of CC-1065 and the duocarmycins: Synthesis and evaluation. *Bioorg. Med. Chem.*, 3, 1429, 1995.
56. Boger, D.L., Schmitt, H.W., Fink, B.E., and Hedrick, M.P., Parallel synthesis and evaluation of 132 (+)-1,2,9,9a-tetrahydrocyclopropa[c]benz[e]indol-4-one (CBI) analogues of CC-1065 and the duocarmycins defining the contribution of the DNA-binding domain. *J. Org. Chem.*, 66, 6654, 2001.
57. Reddy, B.S.P., Sharma, S.K., and Lown, J.W., Recent developments in sequence selective minor groove DNA effectors. *Curr. Med. Chem.*, 8, 475, 2001.
58. Tao, Z.F., Tsuyoshi Fujiwara, T., Saito, I., and Sugiyama, H., Sequence-specific DNA alkylation by hybrid molecules between segment A of duocarmycin A and pyrrole/imidazole diamide. *Angew. Chem. Int. Ed. Engl.*, 38, 650, 1999.
59. Tao, Z.F., Tsuyoshi Fujiwara, T., Saito, I., and Sugiyama, H., Rational design of sequence-specific DNA alkylating agents based on duocarmycin A and pyrrole-imidazole hairpin polyamides. *J. Am. Chem. Soc.*, 121, 4961, 1999.
60. Bando, T., Narita, A., Saito, I., and Sugiyama, H., Highly efficient sequence-specific DNA interstrand cross-linking by pyrrole/imidazole CPI conjugates. *J. Am. Chem. Soc.*, 125, 3471, 2003.
61. Boger, D.L. and Han, N., CC-1065/duocarmycin and bleomycin A_2 hybrid agents. Lack of enhancement of DNA alkylation by attachment to non-complementary DNA binding subunits. *Bioorg. Med. Chem.*, 5, 233, 1997.
62. Lukhatanov, E.A., Podyminogin, M.A., Kutyavin, I.V., Meyer, R.B., and Gamper, H.B., Rapid and efficient hybridization-triggered cross linking within a DNA duplex by an oligodeoxyribonucleotide bearing a conjugated cyclopropyl pyrrole indole. *Nucleic Acids Res.*, 24, 683, 1996.
63. Jia, G., Iida, H., and Lown, J.W., Synthesis of bis-lexitropsin-1,2,9,9a-tetrahydrocyclo-propa[c]benz[e] indole-4-one (CBI) conjugates. *Heterocycl. Comm.*, 4, 1998.
64. Jia, G., Iida, H., and Lown, J.W., Synthesis of an unsymmetrical bis-lexitropsin-1,2,9,9a-tetrahydrocyclo-propa[c]benz[e]indole-4-one (CBI) conjugates. *Chem. Comm.*, 119, 1999.
65. Jia, G., Iida, H., and Lown, J.W., Design and synthesis of 1,2,9,9a-tetrahydrocyclo-propa[c]benz[e] indole-4-one (seco-CBI) dimers. *Heterocycl. Comm.*, 5, 497, 1999.
66. Jia, G., Iida, H., and Lown, J.W., Solid-phase synthesis of 1-chloromethyl-1,2-dihydro-3h-benz[e]indole (seco-CBI) and polyamide conjugate. *Synletters*, 603, 2000.
67. Jia, G. and Lown, J.W., Design, synthesis and cytotoxicity evaluation of 1-chloromethyl-5-hydroxy-1,2-dihydro-3h-benz[e]indole (seco-CBI) dimers. *Bioorg. Med. Chem.*, 8, 1607, 2000.
68. Tao, Z.F., Saito, I., and Sugiyama, H., Highly cooperative DNA dialkylation by the homodimer of imidazole-pyrrole diamide-CPI conjugate with vinyl linker. *J. Am. Chem. Soc.*, 122, 1602, 2000.
69. Wemmer, D.E. and Dervan, P.B., Targeting the minor groove of DNA. *Curr. Opin. Struct. Biol.*, 7, 355, 1997.
70. Chang, A.Y. and Dervan, P.B., Strand selective cleavage of DNA by diastereomers of hairpin polyamide-seco-CBI conjugates. *J. Am. Chem. Soc.*, 122, 4856, 2000.

71. Mitchell, M.A., Johnson, P.D., Williams, M.G., and Aristoff, P.A., Interstrand DNA cross-linking with dimers of the spirocyclopropyl alkylating moiety of CC-1065. *J. Am. Chem. Soc.*, 111, 6428, 1989.
72. Boger, D.L., Searcey, M., Tse, W.C., and Jin, Q., Bifunctional alkylating agents derived from duocarmycin SA: Potent antitumor activity with altered sequence selectivity. *Bioorg. Med. Chem. Lett.*, 10, 495, 2000.
73. Kumar, R. and Lown, J.W., Design and synthesis of bis 1-chloromethyl-5-hydroxy-1, 2-dihydro-3h-benz [e] indole (seco-CBI)-pyrrole polyamide conjugates. *Org. Lett.*, 4, 1851, 2002.
74. Kumar, R. and Lown, J.W., Synthesis of novel thiazole-contaning bis 1-chloromethyl-5-hydroxy-1, 2-dihydro-3h-benz [e] indole (seco-CBI)-polyamide conjugates, as anticancer agents. *Heterocycl. Commun.*, 8, 521, 2003.
75. Kumar, R. and Lown, J.W., Synthesis and cytotoxicity evaluation of novel c7-c7, c7-n3 & n3-n3 dimers of 1-chloromethyl-5-hydroxy-1,2-dihydro-3h-benz [e]indole (seco-CBI) with pyrrole and imidazole polyamide conjugates. *Org. Biomol. Chem.*, 1, 2630, 2003.
76. Tercel, M., Stribbling, S.M., Sheppard, H., Siim, B.G., Wu, K., Pullen, S.M., Botting, K.J., Wilson, W.R., and Denny, W.A., Unsymmetrical DNA cross-linking agents: Combination of the CBI and PBD pharmacophores. *J. Med. Chem.*, 46, 2132, 2003.
77. Seaman, F.C. and Hurley, L.H., Interstrand cross-linking by bizelesin produces a Watson-Crick to Hoogsteen base pairing transition region in d(CGTAATTACG)$_2$. *Biochemistry*, 32, 12577, 1993.
78. Thompson, A.S., Fan, J.Y., Sun, D., Hansen, M., and Hurley, L.H., Determination of structural role of the internal guanine-cytosine base pair in recognition of a seven base pair sequence cross-linked by bizelesin. *Biochemistry*, 34, 11005, 1995.v
79. Powers, R. and Gorenstein, D.G., Two-dimensional ^{1}H and ^{31}P NMR spectra restrained molecular dynamics structure of covalent CPI-CDPI2-oligodeoxy ribonucleotide decamer complex. *Biochemistry*, 29, 9994, 1990.
80. Nguyen, H.N., Sevin, B.U., Averette, H., Perras, J., Ramos, R., and Donato, D., Spectrum of cell-cycle kinetics of alkylating agent adozelesin in gynecological cancer cell lines: Correlation with drug induced cytotoxicity. *J. Cancer Res. Clin. Oncol.*, 118, 515, 1992.
81. Adams, E.G., Bardiner, G.J., and Bhuyan, B.K., Effects of U-71, 184 and several other CC-1065 analogues on cell survival and cell cycle of Chinese hamster ovary cells. *Cancer Res.*, 48, 109, 1988.
82. Zsido, T.J., Beerman, T.A., Meegan, R.L., Woynarowski, J.M., and Baker, R.M., Resistance of CHO cells expressing p-glycoprotein to cyclopropylpyrroloindole (CPI) alkylating agents. *Biochem. Pharmacol.*, 43, 1817, 1992.
83. Nguyen, H.N., Sevin, B.U., Averette, H., Perras, J., Hightower, R., Ramos, R., Donato, D., and Penalver, M., *In vitro* evaluation of novel chemotherapeutic agent, adozelesin, in gynecologic-cancer cell lines. *Cancer Chemother. Pharmacol.*, 30, 37, 1992.
84. Hightower, R.D., Sevin, B.U., Perras, J.P., Untch, M., Angioli, R., Ramos, R., and Averette, H., Comparison of U-73,975 and cisplatin cytotoxicity in fresh cervical and ovarian carcinoma specimens with ATP-chemosensitivity assay. *Gynecol. Oncol.*, 47, 186, 1992.
85. Hightower, R.D., Sevin, B.U., Perras, J., Nguyen, H., Angioli, R., Untch, M., and Averette, H., *In vitro* evaluation of the novel chemotherapeutic agents U-73, 975, U-77, 779, and U-80, 244 in gynecologic cancer cell lines. *Cancer Invest.*, 11, 276, 1993.
86. Smith, K.S., Folz, B.A., Adams, E.G., and Bhuyan, B.K., Synergistic and additive combinations of several antitumor drugs and other agents with the potent alkylating agent adozelesin. *Cancer Chemother. Pharmacol.*, 35, 471, 1995.
87. Volpe, D.A., Tomaszewski, J.E., Parchment, R.E., Garg, A., Flora, K.P., Murphy, M.J., and Grieshaber, C.K., Myelotoxic effects of the bifunctional alkylating agent bizelesin on human, canine and murine myeloid progenitor cells. *Cancer Chemother. Pharmacol.*, 39, 143, 1996.
88. Lee, C.S. and Gibson, N.W., DNA damage and differential cytotoxicity produced in human carcinoma cells by CC-1065 analogues, U-73, 975 and U-77, 779. *Cancer. Res.*, 51, 6586, 1991.
89. Cote, S. and Momparler, R.L., Evaluation of the antineoplastic activity of adozelesin alone and in combination with 5-aza-2-deoxycytidine and cytosine arabinoside on DLD-1 human colon carcinoma cells. *Anticancer Drugs*, 4, 327, 1993.
90. Chari, R.V., Jackel, K.A., Bourret, L.A., Derr, S.M., Tadayoni, B.M., Mattocks, K.M., Shah, S.A., Liu, C., Blättler, W.A., and Goldmacher, V.S., Enhancement of the selectivity and antitumor efficacy of a CC-1065 analogue through immuno conjugate formation. *Cancer Res.*, 55, 4079, 1995.
91. Harbach, P.R., Zimmer, D.M., Mazurek, J.H., and Bhuyan, B.K., Mutagenicity of the antitumor antibiotic CC-1065 and its analogues in mammalian (V79) cells and bacteria. *Cancer Res.*, 48, 32, 1988.

92. Houghton, P.J., Cheshire, P.J., Hallman, J.D.N., and Houghton, J.A., Therapeutic efficacy of the cyclopropylpyrroloindole, carzelesin, against xenografts derived from adult and childhood solid tumors. *Cancer Chemother. Pharmacol.*, 36, 45, 1995.
93. Monroe, T.J. and Mitchell, M.A., *In vivo* mutagenesis induced by CC-1065 and adozelesin DNA alkylation in a transgenic mouse model. *Cancer Res.*, 53, 5690, 1993.
94. Walker, D.L., Reid, J.M., and Ames, M.M., Preclinical pharmacology of bizelesin, a potent bifunctional analogue of the DNA-binding antibiotic CC-1065. *Cancer Chemother. Pharmacol.*, 34, 317, 1994.
95. Bagshawe, K.D., Antibody-directed enzyme prodrug therapy (ADEPT) of cancer. *Expert Rev. Anticancer Ther.*, 6, 1421, 2006.
96. Tietze, L.F. and Krewer, B., Novel analogues of CC-1065 and the duocarmycins for the use in targeted tumour therapies. *Anticancer Agents Med. Chem.*, 9, 304, 2009.
97. Tietze, L.F. and Krewer, B., Antibody-directed enzyme prodrug therapy: A promising approach for a selective treatment of cancer based on prodrugs and monoclonal antibodies. *Chem. Biol. Drug Design*, 74, 205, 2009.
98. Wang, J., Jiang, X., Jiang, S., Cai, H., Han, L., Li, Z., Tian, W., Jiang, W., Zhang, Z., Xiao, Y., Wright, S.C., and Larrick, J.W., Synthesis and antitumor activity evaluations of albumin-binding prodrugs of CC-1065 analog. *Bioorg. Med. Chem.*, 16, 6552, 2008.
99. Shamdas, G.J., Alberts, D.S., Modlano, M., Wiggins, C., Power, J., Kasunic, D.A., Elfring, G.L., and Earhart, R.H., Phase I study of adozelesin (U-73, 975) in patients with solid tumors. *Anticancer Drugs*, 5, 10, 1994.
100. Foster, B.J., LoRusso, P.M., Poplin, E., Zalupski, M., Valdivieso, M., Wozniak, A., Flaherty, L., Kasunic, D.A., Earhart, R.H., and Baker, L.H., Phase I trial of adozelesin using the treatment schedule of daily × 5 every three weeks. *Invest. New Drugs*, 13, 321, 1996.
101. Cristofanilli, M., Bryan, W.J., Miller, L.L., Chang, A.Y., Gradishar, W.J., Kufe, D.W., and Hortobagyi, G.N., Phase II study of adozelesin in untreated metastatic breast cancer. *Anticancer Drugs*, 9, 779, 1998.
102. Schwartz, G.H., Patnaik, A., Hammond, L.A., Rizzo, J., Berg, K., Von Hoff, D.D., and Rowinsky, E.K., A phase I study of bizelesin, a highly potent and selective DNA-interactive agent, in patients with advanced solid malignancies. *Ann. Oncol.*, 14, 775, 2003.
103. Pitot, H.C., Reid, J.M., Sloan, J.A., Ames, M.M., Adjei, A.A., Rubin, J., Bagniewski, P.G., Atherton, P., Rayson, D., Goldberg, R.M., and Erlichman, C., A Phase I study of bizelesin (NSC 615291) in patients with advanced solid tumors. *Clin. Cancer Res.*, 8, 712, 2002.
104. Pavlidis, N., Aamdal, S., Awada, A., Calvert, H., Fumoleau, P., Sorio, R., Punt, C., et al., Carzelesin phase II study in advanced breast, ovarian, colorectal, gastric, head and neck cancer, non-Hodgkin's lymphoma and malignant melanoma: A study of the EORTC early clinical studies group (ECSG). *Cancer Chemother. Pharmacol.*, 46, 167, 2000.

21 Epothilone, A Myxobacterial Metabolite with Promising Antitumor Activity

Gerhard Höfle and Hans Reichenbach

CONTENTS

21.1 Introduction 513
21.2 Natural Epothilones 515
21.3 Biosynthesis 518
21.4 Mechanism of Action 521
21.5 Total Synthesis and Semisynthesis 529
21.5.1 Total Synthesis 529
21.5.2 Semisynthesis 533
21.6 Structure–Activity Relationships 541
21.7 Preclinical Studies 547
21.8 Clinical Studies 549
21.8.1 Epothilone B-Lactam (BMS 247550, Ixabepilone, Ixempra) 550
21.8.2 Epothilone B (EPO906, Patupilone) 553
21.8.3 Epothilone D (KOS-862) 554
21.8.4 ZK-EPO (Sagopilone) 555
21.8.5 21-Aminoepothilone B (BMS-310705) 555
21.8.6 Dehydelone (KOS-1584) 556
Acknowledgments 556
References 556

21.1 INTRODUCTION

Epothilone is a secondary metabolite of the myxobacterium *Sorangium cellulosum*. It is a macrolactone of a novel structural type characterized by an epoxy and a ketogroup in the lactone ring and a side chain with a thiazole ring (Figure 21.1), functional groups from which the name epo-thi-lone was coined.[1] Two main variants, epothilone A (**1a**) and epothilone B (**1b**) are normally isolated from the bacterial culture.[2,3] The B variant is a homolog with an extra methyl group at the epoxide that makes it more active by a factor of 5–10. Similarly, minor and trace components are always observed as pairs of homologs with the B-series being invariably more active.[4] Epothilone, originally spelled epothilon, was discovered by us in 1987 because of its antifungal activity. Its structure was first disclosed in 1991 in the Annual Scientific Report of our institute, Gesellschaft für Biotechnologische Forschung (GBF).[1] The structure was elucidated mainly by spectroscopic methods and corroborated by x-ray crystallography, which also provided the absolute configuration.[3] Besides antifungal activity, strong cytotoxicity against mammalian cells was also reported. A German patent was filed in November 1991 (granted in May 1994), and an international one in November 1992,[5] although it was withdrawn in April 1994, because the impressive antitumor activity of the epothilones was not

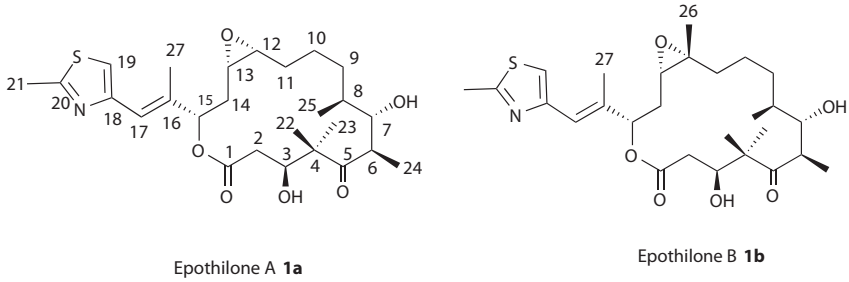

FIGURE 21.1 Structures of the major epothilones.

yet known, and there was limited interest in purely cytotoxic compounds. The patent strain, *S. cellulosum* So ce90, was deposited at the German Culture Collection (Deutsche Sammlung von Mikroorganismen und Zellkulturen, DSMZ) in Braunschweig in October 1991, under number DSM 6773, and has since been sent to many laboratories all over the world.

The discovery of epothilone was the result of a decade of basic research at the GBF with the aim of identifying new producers of diverse secondary metabolites among bacteria. This has indeed been achieved with the discovery that myxobacteria synthesize a wealth of compounds with a wide variety of chemical structures, many of them novel and with unusual and, in many respects, interesting mechanisms of action. Thus far, we have isolated and characterized more than 600 different compounds from those organisms representing around 120 structural types,[6] and it is quite obvious that our many publications have stimulated more intensive investigation of myxobacteria for secondary metabolites.

In the 1980s and 1990s, Taxol® (paclitaxel; see Chapter 6) was developed into a very successful antitumor drug with a new mechanism of action, namely, stimulation of tubulin polymerization and stabilization of microtubuli (MT). As Taxol initially had to be produced from the bark of slow-growing Pacific yew trees, and there was little chance of development of an economically viable total synthesis, several pharmaceutical companies started screening for Taxol mimics from diverse natural sources, at first without any success in spite of the enormous numbers of compounds and extracts tested.[7] Colleagues at Merck Sharp and Dohme screened extracts from myxobacteria, having obtained access to the collection of *Sorangium* strains of Dr. John E. Peterson, a retired botanist and professor at Emporia State University in Kansas, who had worked on those organisms 30 years ago. They soon found the desired activity, and with the small quantities of substance they could recover from plate cultures, they elucidated the structure, only to find out that they had rediscovered epothilone. They retained our name, just adding the "e," and cited our patent. The publication of their results, including the mechanism of action,[8] which we had failed to determine, started an avalanche of patents and publications on total synthesis, biosynthesis, genetics, molecular biology, biochemistry, and preclinical and clinical work,[9] which still is increasing in volume, with the focus shifted to structural modifications, structure–activity relationships (SAR), and clinical studies.[11]

It soon turned out that epothilone has several properties that could make it superior to Taxol. It acts at very low doses (in the nano- to picomolar range), is active against multidrug resistance (MDR), including Taxol-resistant cancer cells, and is more water-soluble, so that certain derivatives can even be administered orally. Further, it can be produced by fermentation without difficulty, and, as a smaller and simpler molecule, is also accessible by total synthesis, enabling the production of many variants (so far more than 1000).

The epothilone story after publication of the 1995 Merck article[8] is a good example of the often overlooked fact that basic research and its transfer to practice is far from a straightforward process. When the Merck group discovered our patents, they terminated the project without contacting us regarding possible collaboration. Later, we ourselves tried to interest four major German, a Swiss, and three U.S. pharmaceutical companies in the possibility of collaboration in epothilone development, supplying test material to each company. After over 18 months of consideration, we finally came to an

1985	Dr. Reichenbach at GBF isolates *Sorangium cellulosum* strain So ce90 from a soil sample
1987	The strain is screened positive for antifungal activity, epothilone A and B were isolated, and their structures elucidated by Dr. Gerth and Dr. Bedorf
1991	Immunosuppresive activity studied at Ciba Geigy
	First publication of structure in *Sci. Ann. Rep.* of GBF
1992	Application tests and field trials for plant protection by Ciba-Geigy
1994	Work on epothilones terminated at GBF, international patent application abandoned
	Good activity in NCI 60 cell line antitumor screening
1995	Rediscovery of epothilone A and B as Taxol mimics at MSD
	Disclosure of the absolute configuration as personal communications by Dr. Höfle
1996	First total syntheses by the Danishefsky, Nicolaou, and Schinzer groups
1997	Large scale production at GBF by fermentation
	Joint semisynthesis program started at BMS and GBF
1999	Clinical trials with natural, synthetic, and semisynthetic epothilones commence
2000	Biosynthesis genes cloned by Novartis and Kosan
2003	Phase II/III clinical trials with epothilone B-lactam (ixabepilone)
2007	FDA approval of ixabepilone for the treatment of breast cancer under the brand name Ixempra™
2010	Five natural, synthetic and semisynthetic epothilones in advanced clinical trials

FIGURE 21.2 Timeline for epothilone discovery and development.

agreement with Bristol-Myers Squibb. The Swiss (Novartis) and one of the German companies (Schering) soon started independent epothilone projects, Schering using total synthesis, and Novartis with material produced by fermentation, using our patent strain, So ce90. By early 1997, we had already developed fermentation and separation processes with mutant strains, allowing us to produce 10 g amounts of pure epothilones A and B.[9c] The yields could later be increased using traditional methods to several hundred milligrams per liter, so that, contrary to statements in the literature, it was possible to produce all the material needed for development and future applications using *S. cellulosum*, which can be cultivated without problems on cheap media based on soy meal in industrial bioreactors up to the 40-m^3 scale. The time course of epothilone discovery and development is shown in Figure 21.2.

21.2 NATURAL EPOTHILONES

The epothilones were discovered in cultures of the myxobacterium *S. cellulosum*. Myxobacteria are Gram-negative bacteria that move by gliding along surfaces and are notable for their highly developed intercellular communication systems and their ability to construct, under unfavorable living conditions, in a cooperative action involving hundreds of thousands of cells, fruiting bodies of a remarkably sophisticated shape and structure.[12] The epothilone-producing organism (Figure 21.3), strain So ce90, is a cellulose degrader, and was isolated at the GBF in 1985 from a soil sample collected on the banks of the Zambesi river in southern Africa. In addition to epothilones A and B, the strain synthesized in abundance a family of novel spiroketal polyene polyketides, named spirangiens,[1,13] which also showed antifungal effects and cytotoxicity. The epothilones aroused immediate interest because of their strong immunosuppressive effect and good activity against oomycetes, important parasites of agricultural plants.[5] Both effects lacked practical applications, however, because of the high toxicity of the compounds. The need for gram amounts of epothilones for relevant tests had already led at that time to the establishment of a production and isolation process at the GBF; however, because of the presence of an excess of spirangiens, the isolation of pure compounds was cumbersome and only achieved by multistep chromatography.

The discovery in 1995 that *S. cellulosum* strain SMP44 also synthesizes epothilones made a second producer strain available.[8] This strain is used practically for all studies in the United States with the exception of the BMS/GBF project and synthetic material. Initially, epothilone production with SMP44

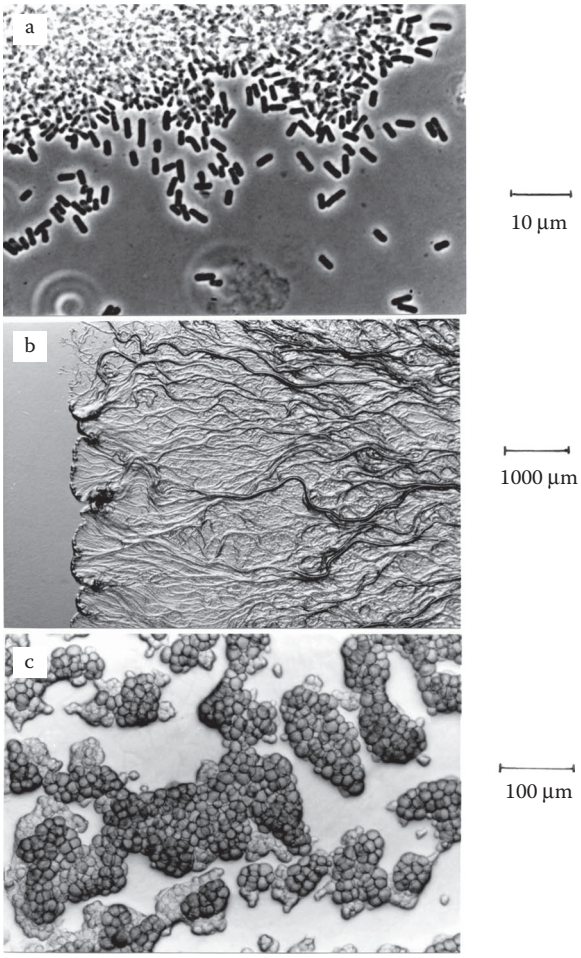

FIGURE 21.3 The myxobacterium, *Sorangium cellulosum*, producer of epothilone. (a) Vegetative cells; (b) vegetative, spreading swarm colony; (c) fruiting bodies, consisting of tiny sporangioles.

was performed in large (150 mm) Petri dishes on agar for 10 d at 28°C. From 80 plates, 2.7 mg of pure epothilone A and 0.9 mg of epothilone B could be recovered, which was sufficient to elucidate the structures by nuclear magnetic resonance and mass spectroscopy.[8] Similarly, the initial yields of epothilones in liquid cultures of the GBF strain were rather low (2 mg/L). As a first step in yield improvement, strain So ce90 was mutated to eliminate spirangien synthesis, which competed for precursors (the first spirangien negative mutant was obtained in October 1996).[14] This was possible only after the strain had been adapted to grow in liquid media in a single cell suspension and to develop colonies from individual cells after plating, which are both time-consuming procedures in myxobacteria.

Parallel to strain improvement, a first optimization of the fermentation medium was undertaken. Cellulose-degrading *S. cellulosum* is much more versatile metabolically than most myxobacteria, notably *Myxococcus xanthus*, and grows on complex as well as on very simple media. Our first production medium consisted of defatted soybean meal, potato starch, glucose, yeast extract, and mineral salts.[2] As epothilones are excreted into the broth, a hydrophobic adsorber resin, Amberlite XAD-16, was added during fermentation. The resin increased yields by a factor of 5 by avoiding feedback inhibition by the end product and prevention of its degradation.[9p,15] The medium was later improved, among others, by adding skim milk powder.[16] Production was during log and early stationary phase, with yields of 22 mg/L epothilone A and 11 mg/L epothilone B.[2] The generation time

was around 16 h, and cell densities up to 2×10^9 were achieved. After 7 d of fermentation, the resin was harvested by sieving, and the epothilones were extracted with methanol and processed further. Later, the yields could be increased substantially by further optimizing the medium, and especially by a mutation program during which more than 24,000 mutant clones were generated by treatment either with ultraviolet light or nitrosoguanidine, and were characterized by high-performance liquid chromatography analysis.[17] Thereby, not only high producers but also clones with defective biosynthetic pathways were obtained,[15–17] among them strains that produced epothilone A only, but none that produced solely epothilone B. The same was observed with about 40 further epothilone producers discovered among the 1700 *S. cellulosum* strains of the GBF collection. The positive strains came from soil samples collected on four continents, and represented between 1% and 2.5% of all strains depending on the area of origin.[9p] The various strains differed not only in the epothilone pattern, but also in the physiology of production. Thus, for example, epothilone synthesis is stimulated by glucose in So ce90 but inhibited in strain So ce1198.[9p] So far, epothilones have not been found in any other myxobacterial species nor any other organism.

From highly producing *S. cellulosum* strains, small amounts of epothilones C (**2a**), D (**2b**), E (**3a**), and F (**3b**) (Figure 21.4) were isolated in addition to epothilones A and B.[4,18] Whereas in C and D, the epoxide is replaced by a *cis* double bond, an additional hydroxyl group is present at the thiazole methyl group in the variants E and F. Later, desoxyepothilones **2** and hydroxyepothilones **3** became readily available by fermentation of a P450-defective mutant,[17] and by biotransformation with *S. cellulosum*,[15] respectively. This greatly facilitates their isolation, but separation of the homologous pairs still requires careful reversed-phase chromatography.

From a large-scale fermentation (700 L) of So ce90 mutant B2, 35 variants could be isolated in very small amounts in addition to epothilones A–F.[4] Of those, only epothilones C_7 and C_9 may be regarded as regular biosynthetic products carrying extra hydroxyl groups at C14β and C27. The majority of the other variants result from aberrant biosynthesis. They lack methyl groups, carry extra methyl groups, have an oxazole instead of a thiazole ring and extra double bonds, and have reduced (by two C-atoms) or expanded ring sizes (epothilones K and I). Several small open-chain molecules are obviously derived from biosynthetic intermediates that had escaped from the enzyme complex.[4] Recently, from large-scale fermentation of a new *S. cellulosum* strain, So0157-2, for the first time epothilone glycosides were isolated, and identified as epothilone A, B, C 3-α-D-arabinosides.[19a] Another *S. cellulosum* strain, AHB125, from the Anhui area in China was found to produce epothilone D and other anticancer substances.[19b]

The epothilones A–F are colorless solids, readily soluble in polar organic solvents, and stable at ambient temperature in the pH range of 5–9. Epothilones A, B, and D are crystalline with melting points in the range of 76–128°C depending on the solvents of crystallization (the exact melting point of epothilone A is 76–78°C [ethyl acetate/toluene], and 85–87°C [methanol/water]).[3,20–22] Several crystal structures are available for crystals from lipophilic and polar solvents exhibiting different conformations (Figure 21.14, Section 21.5).[3,21] Aqueous solubility depends crucially on the presence

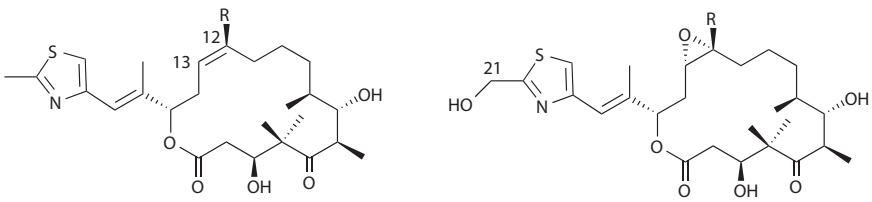

Epothilone C **2a** R = H
Epothilone D **2b** R = CH_3

Epothilone E **3a** R = H
Epothilone F **3b** R = CH_3

FIGURE 21.4 Structures of minor epothilones.

of epoxide and C12 methyl groups, and range from 700 mg/L for epothilone A and 200 mg/L for B to 16 mg/L for epothilone D.[3,22] Thus, epothilone D is about as poorly water-soluble as paclitaxel (6–30 mg/L),[23] posing similar problems with its administration at therapeutically useful doses. Nevertheless, because of its promising therapeutic window, epothilone D was identified very early as a candidate for clinical studies by Danishefsky's group.[24] Total synthesis was upscaled and production by fermentation optimized. Under favorable conditions, our So ce90 P450-defective mutant produced 70 mg/L of epothilone D.

21.3 BIOSYNTHESIS

Biogenesis of epothilones has been studied in *S. cellulosum* on three levels: actual biosynthesis using feeding experiments and blocked mutants; analysis of the genes coding for the relevant enzymes (the genes were cloned and sequenced from both producer strains, So ce90 and SMP44); and *in vitro* synthesis using part of the enzymatic apparatus cloned and expressed in *Escherichia coli*.

By feeding ^{13}C and radioactively labeled precursors to strain So ce90, it was quickly established that the carbon chain is synthesized from acetate, propionate, and cysteine (Figure 21.5).[16] Methyl C21 comes from acetate, methyl C22 from *S*-adenosyl methionine, and all other methyls arise from propionate. This is also the case with methyl C26 at the epoxide site. The biochemical reason for the indiscriminate incorporation of acetate and propionate at this site, leading to mixtures of epothilones A and B, is still unknown. So far it was not possible to isolate strains or mutants that synthesize exclusively the more active epothilone B, although mutants restricted to epothilone A are available.[16] Only recently, could it be demonstrated by genetic engineering that a sufficient supply of propionyl-CoA is crucial for epothilone B synthesis. Thus, the epothilone A:B ratio could be shifted from about 1:1 to 1:127 by cloning the gene of propionyl-CoA synthetase from *Ralstonia* (*Burkholderia*, *Pseudomonas*) *solanacearum* into *S. cellulosum* So ce90. However, yields of only up to 1 mg/L epothilone B were obtained.[25] For large-scale production of epothilone B, certain *S. cellulosum* mutants in combination with a low-dose sodium propionate feeding are still used. Under these conditions, the original A to B ratio of 2:1 is shifted to over 1:1,[26] making the laborious separation somewhat easier.

Epothilone synthesis starts by joining cysteine and acetate to yield a methylthiazole. This requires participation of a nonribosomal peptide synthetase (NRPS). The rest of the molecule is essentially provided by polyketide synthase (PKS) modules.[16] As was corroborated by the genetic approach, the whole biosynthetic machinery consists of a huge hybrid multienzyme complex composed of one NRPS and eight PKS modules (Scheme 21.1). The oxygen of the epoxy group is introduced by a post-PKS monooxygenase using molecular oxygen. The PKS module responsible for this section of the molecule has, however, no dehydratase (DH) sequence that could produce the double bond required as the substrate of the monooxygenase. Since we could isolate two epothilone fragments, one with a hydroxyl on C13, the other with a C12/C13 double bond, which is perhaps produced by a DH in another module, the substrate of the monooxygenase may arise in this way.[17]

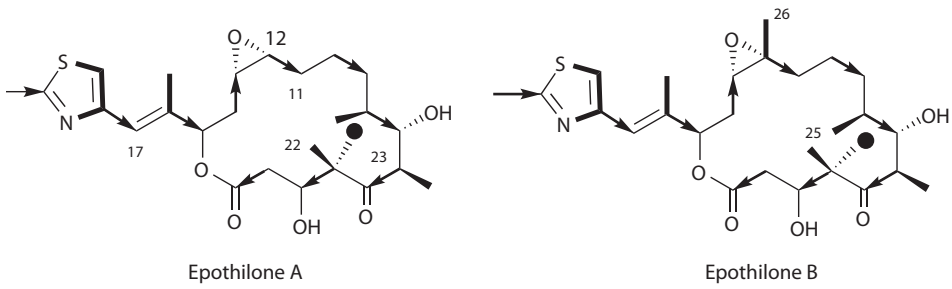

FIGURE 21.5 Incorporation of acetate, propionate, methionine, and cysteine in epothilone A and B.

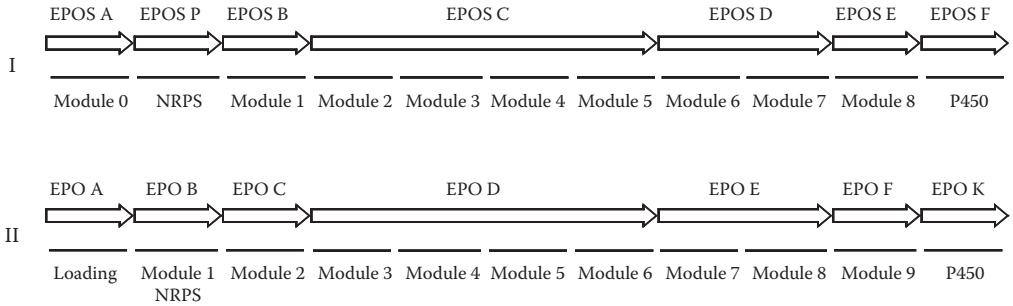

SCHEME 21.1 Analysis and assignment of epothilone biosynthesis genes by the Novartis (I) and Kosan groups (II).

The dehydration must happen at an early stage because the hydroxy precursors of epothilones C and D could not be detected.[17] Increasing amounts of epothilones A or B in the medium inhibit *de novo* synthesis of those molecules. At the same time, epothilones C and D, present only in traces in the control, rise to very high levels.[17] Obviously, the monooxygenase responsible for the introduction of the epoxy group is feedback inhibited by epothilones A and B, and epothilones C and D are the end products of the PKS. When epothilones C or D are fed to the nonproducing So ce90 C2 mutant, the compounds are bound immediately to the cells and transformed into epothilones A/B. The monooxygenase is found only in epothilone-producing strains and has never been seen in other *Sorangium* strains.[17] It appears that epothilone C has a higher affinity for the monooxygenase than epothilone D, as it is preferentially epoxidized, and that even slight and remote changes in the molecule may prevent epoxidation. The block mutant D48 is defective in its monooxydase and is thus a producer of epothilones C and D.[17]

In cultures of So ce90 without XAD resin, yields of epothilones A/B go down dramatically because the excreted material is degraded starting with the opening of the lactone ring by an esterase, which can be demonstrated in the culture supernatant. Next, the epoxide is hydrolyzed to the 12,13-diol followed by a rapid breakdown of the entire molecule.[15] Lactone hydrolysis by esterases is also the predominant metabolism in mammalian systems, as first observed by us with mouse serum and pig liver esterase.[27] Similarly, epothilone D may be hydrolyzed by a mouse liver microsome preparation.[28] In cultures of So ce90 without XAD resin, a small proportion of the epothilones A/B is hydroxylated at C21 to give epothilones E/F.[15] This transformation is caused by an epothilone A/B-induced monooxygenase, which appears to be a P450 enzyme, because it is inhibited when iconazole is added to the culture.[15] A screening of 95 wild strains of *S. cellulosum* showed that this monooxygenase is widely distributed among nonproducing *Sorangium* strains. A practical process for the conversion of epothilones A/B to E/F was developed later by BMS using cultures of the bacterium *Amycolata autotrophica* (formerly *Nocardia autotrophica*),[29] and applied by Kosan for the hydroxylation of other epothilone variants in the side chain and in the macrocycle.[30]

In contrast to So ce90, such detailed biosynthetic studies are not available for strain SMP44. However, the epothilone genes have been cloned and sequenced from both producer strains, So ce90[31] and SMP44.[32] Both sequences are patented.[33,34] As will be discussed below, the SMP44 genes have been investigated and modified extensively after cloning in the heterologous host, *M. xanthus*.

Good summaries of the organization of the epothilone gene cluster are available[31,32,35] (Scheme 21.1), and details need not be discussed here. Briefly, in SMP44, all seven genes required for epothilone synthesis, *epoA* to *epoF* and *epoK* are clustered together in a 56-kilobase-pair stretch of DNA.[32] *EpoA* is the loading domain, *epoB* the NRPS module, and *epoC* to *epoF* are PKS modules. Overall, there are nine modules plus the loading domain and *epoK*, a P450 monooxygenase responsible for the introduction of the epoxy group. All genes are transcribed in one direction and probably in one operon. A methyl transferase domain in module 8 (*epoE*) may be responsible for the introduction of one of the methyl groups on C4. When EpoK was expressed in *E. coli*, the isolated

protein could be used to epoxidize epothilone D into epothilone B.[32] There is an anomaly in the sequence of PKS module 4: the DH required for the introduction of the C12/13 double bond of the PKS end product is lacking. The hypothesis that the DH of the neighboring module 5 may be responsible for creating that double bond has recently been proven by destroying that domain.[36] Although the exact mechanism of the enzymatic reaction is not yet elucidated, a forward–backward shuffling of the growing chain between modules 4 and 5 is suggested. Another anomaly is found in module 9 (Epo F) where the DH and enoyl reductase (ER) are inactive[32] ([3-^{13}C, 3-^{18}O]-labeled epothilones were isolated after feeding of [1-^{13}C, 1-^{18}O]propionate[22]).

The Novartis group sequencing the So ce90 epothilone genes used a slightly different nomenclature for the same general organization of the gene cluster (Scheme 21.1).[31] In this case also, transcription is unidirectional. It is suggested that all those genes form one operon of more than 56 kilobase pairs. The finished polyketide, epothilone C/D, appears to be released from the PKS by a thioesterase; a sequence showing conserved motifs of that enzyme has been identified next to module 8 in *epoE*.[31] A methyltransferase domain in *epoD* is required to produce one of the gem methyl groups at C4. The sequence of *epoF* indicates a cytochrome P450 oxygenase. A short distance in front and behind the epothilone genes, two ORFs, *orf3* and *orf14*, seem to code for transport proteins that may be involved in export of epothilone from the producing cell.[31] In summary, the genetic apparatus for epothilone synthesis is remarkably similar, in fact almost identical, in two producing strains of *S. cellulosum*, although they are of completely different origin. Among 56,000 base pairs, only 407 (= 0.7%) differ in the two gene clusters, which is an astonishing and very unusual correspondence not yet seen with any other *Sorangium* compounds (Rolf Müller, personal communication).

The epothilone gene cluster from SMP44 was cloned and expressed in the heterologous host *Streptomyces coelicolor* that replicated 10-fold faster; however, it produced only around 0.1 mg/L of epothilones.[37] Later the *M. xanthus* system was found superior and amenable to make structural variants by manipulating the gene cluster.[38] Thus, by inactivating the monooxygenase gene, strains were obtained that synthesized only epothilones C and D.[38] Most remarkably, and contrary to So ce90 and SMP44, these strains produce significantly more epothilone D than C,[38] and respond to feeding of acetate and propionate by preferentially producing epothilone C or D, respectively.[39] Similarly, feeding of serine can replace cysteine leading preferentially to the oxazole analogs, epothilones H_1 and H_2.[39] From these results, it may be concluded that the enzymes handling the amino acid and the C12,C13-building blocks are promiscuous, so that the outcome of feedings crucially depends on the availability of the activated precursors at the site of biosynthesis. By feeding of propionate to So ce90, the epothilone A:B ratio could only be shifted from 2:1 to 1:2,[26] and feeding of serine did not increase the formation of the oxazole variants.[14,26a] In this respect, *M. xanthus* is clearly more flexible and superior to *S. cellulosum*. Also the oxygen supply during fermentation of *M. xanthus* has a strong influence on the products formed. At 50% oxygen saturation, epothilones B and D were formed with yields of 48 and 3 mg/L, while with oxygen depletion 30 mg/L epothilone D and no B was produced.[40]

Using site-specific mutation, the P450-defective *M. xanthus* strain was further modified by inactivating the ER domain in module 5 to make 10,11-didehydro-epoD (= Epo490).[41] Inactivating the ketoreductase domain in module 6 produced 9-keto-epothilones C and D and their 4-desmethyl analogs, 9-keto-10,11-didehydro-epothilone D, and two fragmentary epothilones. In addition, small amounts of a tetrahydrofuran derivative was isolated, which was formed from 10,11-didehydroepothilone B by rearrangement involving the C6 hydroxy group.[42] Several of the analogs created by those different methods are also known as trace components from So ce90 fermentations.[4]

From a practical point of view, epothilone D was and is still a very important fermentation product. Because of a promising therapeutic window, it was introduced into clinical trials by Kosan Biosciences, but was later dropped in favor of its 9,10-didehydro analog (dehydelone), and recently revitalized as a potential anti-Alzheimer drug by BMS.[43] Independently, it was discovered that low doses of epothilone D are able to reverse the symptoms of schizophrenia in a mouse model.[44]

Although the original production of epothilones C and D by *M. xanthus* was below 1 mg/L, the yields could be increased by further mutations,[38] and media[39,45] and process[46–48] optimization. In particular, feeding of methyl oleate as carbon source increased the yield to 27 mg/L and later to 90 mg/L.[47,48] Predictably, the presence of residual methyl oleate complicates workup and isolation; thus only 63 mg/L of epothilone D could be recovered.

Further, it was demonstrated that an *E. coli* strain engineered to express the last half of the epothilone biosynthetic pathway is able to process an advanced precursor to epothilone C.[49] In the future, this approach may possibly allow for the exclusive production of epothilone D and its analogs from simple synthetic precursors, thus avoiding tedious separation of C/D homologs. The genes of the first three modules of the cluster, EpoA, EpoB, and EpoC, were expressed in *E. coli*, the resulting proteins purified, and their enzymatic reactions studied *in vitro*.[35,50–54] Products were usually obtained in minute quantities but could be identified by comparison with synthetic material. The system is of particular interest because it allows the study of PKS/NRPS/PKS interfaces in this hybrid multienzyme complex. It turned out that the individual enzymes of the epothilone cluster show considerable flexibility with respect to their substrate specificity, which could be useful for combinatorial biosynthesis. However, before application, the problem of producing reasonable yields has to be solved.

In another study, it was demonstrated that the base sequence of the KS domain of *epoB* in So ce90 (corresponds to *epoC* in SMP44) differs in several respects from the KS domains of all other epothilone modules.[55] While those cluster closely together, as is the rule in PKS genes, the *epoB* KS goes with PKS modules of other organisms. Also, the *epoB* KS deviates significantly in its GC composition. This was taken as a hint that the *epoB* KS sequence may have been introduced into a rudimentary epothilone gene sequence by horizontal gene transfer. Also, the exact position of epothilone bound to a protein could be analyzed for the first time.[56] The crystal structure of the P450EpoK monooxygenase was analyzed in the free form and with substrate and product bound. The enzyme has a very large binding cavity, but otherwise resembles other P450 enzymes, particularly P450EryF from the erythromycin cluster (30% identity, 48% similarity).

21.4 MECHANISM OF ACTION

The biological and biochemical effects of the epothilones have been studied in many laboratories in the United States and in Europe applying diverse experimental methods, and results are not always strictly comparable. Clearly, individual cell lines and the various epothilone analogs behave quite differently. Nevertheless, the overall picture is fairly consistent and, as a rule, safe generalizations can be made. In the following discussion, frequent reference is made to synthetic and structure–activity studies discussed in detail in Sections 21.4 and 21.5, respectively.

Epothilone does not act on bacteria, and among the filamentous fungi and yeasts tested, only *Mucor hiemalis* (Zygomycetes) responded (minimal inhibitory concentration 20 μg/mL).[2] In greenhouse experiments, various oomycetes were also inhibited. The cytotoxicity of the epothilones in animal cell cultures was noted immediately after their discovery,[1,2,5] but the effects they produce on the tubulin cytoskeleton were only realized much later.[8] In the beginning, only the two main fermentation products, epothilones A and B, were available for study. Although epothilone B differs only in an additional methyl group on C13, its efficacy in cell culture assays is consistently higher by a factor of 5–10.[4,8,9e,1,57–62] This difference also remains with analogs of the two, for example, epothilones C and D[4,17,57,60,63] or the oxazole derivatives,[4,64,65] and is even seen in binding and polymerization experiments with tubulin.[58] The epothilones act on a wide variety of cell types including many human tumor cell lines. The concentration range for cytotoxicity is IC_{50} = 0.3–4 ng/mL,[111] or 1.3–17 nM[8,9l,57–59] for epothilone A, and 0.1–1.5 ng/mL,[4] or 0.06–0.9 nM for epothilone B.[8,9l,57–59] The figures for Taxol are 0.2–95 nM.[8,57,58] (The molecular weights are: Taxol 854, epothilone A 494, epothilone B 508, i.e., Taxol is 1.73 and 1.68 times larger than epothilones A and B). The efficacy of Taxol equals that of epothilone A and is clearly less than that of epothilone B.[8,57,58]

For instance, with 0.05–0.06 versus 0.22–0.6 nM, epothilone B is 6- to 10-fold more active than Taxol against human prostate cancer cells.[63] It came as a big surprise and is of considerable practical relevance that the epothilones still act on Taxol-resistant and MDR cells in general.[8,58] Although the resistant cell lines tolerated hundred to several thousand-fold higher concentrations of the selective agent, such as Taxol, vinblastine, or adriamycin, resistance to epothilones rose only by a factor of 1.5–10, and rarely higher. For epothilones C and D, it was even found to decrease in some instances.[57] It was reported that epothilone B-lactam and epothilone C-lactam lose activity on drug-resistant cell lines,[59,66,67] but this was not corroborated by another study using several drug-resistant human cancer cell lines.[68] *In vivo* studies also did not support that statement. Epothilone B-lactam indeed shows about the same activity as epothilone A. Resistance to epothilone itself will be discussed below.

The epothilones promote tubulin polymerization and stabilize MTs, as does Taxol. The morphological changes produced in treated cells resemble those affected by Taxol. In interphase cells, massive bundles of MTs arise in the cytoplasm, apparently randomly and independent from centrosomes, originating from multiple nucleation centers.[8,58,69,70] This transformation can already be seen 2 h after application, and after 24 h, virtually all MTs are in bundles (epothilone B).[58] When cells are kept at 4°C, their MTs decay completely within 1 h, but in the presence of 25 μM epothilone A, epothilone B, or Taxol, they remain stable.[8] Already 2 h after the addition of epothilones, mitotic defects can be observed, reaching a maximum after 6 h.[58]

At concentrations of 10 μM, normal spindles are no longer seen.[58] The organization of MTs in mitotic cells differs from that in interphase cells, so that a considerable turnover of tubulin still must occur in spite of the MT-stabilizing effect of the drug.[8,58] An explanation could be that, before mitosis, MT-destabilizing proteins, such as katanin or stathmin/op18, are activated, or that MTs are stabilized less rigorously, perhaps because MT-associated proteins (MAPs) have dissociated after having become phosphorylated.[66] Multipolar spindles arise in a concentration range from 5 nM to 1 μM.[8] The spindles produced in the presence of epothilone A, epothilone B, or Taxol seem to differ somewhat in their morphology.[58] The result of those mitotic aberrations is an arrest of the cell cycle at the G_2–M stage (e.g., with 100 nM epothilone A or B after 72 h).[8,58,70,63] The DNA content is then 4n.[63] The mitotic blockade is complete after 8 h (at the ID_{50}, 7.5 nM of epothilone B-lactam,[68] or, in another system, after 20 h at 3.5 nM epothilone B[71]). Mitotic arrest and cytotoxicity are seen at much lower doses than aberrations in interphase MTs (e.g., at 3–30 nM vs. 6–40 nM vs. more than 1 μM, respectively).[8] A certain percentage of cells seem to pass through aberrant mitosis and become arrested in the following G_1 phase as multimininucleate cells.[8] With epothilone B at its $IC_{50,}$ 38% of cells become multimininucleate, and with epothilone A and Taxol, 10–15% do so. Delayed mitosis takes place in those cells 24–30 h after the addition of the drug, and although they die, too, they do so after a longer time. The phenomenon is preceded by an aberrant chromosome alignment in metaphase, and is probably related to apoptotic fragmentation of nuclei discussed below. In MCT7 cell cultures, 2.5% of control cells are in mitosis.[71] When epothilone B is added, many cells enter mitosis but do not progress beyond metaphase. The ratio of anaphase to metaphase cells in the control was 0.18; with 1 nM epothilone B, 0.03; and at 3 nM, 0. Many of the cells that were not blocked in mitosis became multinucleate, probably because of an abortive mitosis. The behavior of cells exposed to epothilone B at a dose too low to lead to mitotic arrest is of considerable practical interest. In this case, multipolar spindles are induced, resulting in aneuploid cells that are also not viable.[72]

The epothilones lead to apoptosis as indicated by DNA ladders. The DNA is nicked specifically in G_2–M-blocked cells.[8] Further, fragmentation of the cell nuclei is seen. This can be monitored automatically by an image analyzer.[73] With L926 mouse fibroblasts, fragmentation of nuclei can be seen already after 1 d and reaches its maximum after 2 d (100 ng/mL epothilone B). Fragmentation increases linearly with the logarithm of concentration between 1 and 1000 ng/mL epothilone A.[73] Treated cells appear to remain vital for some time, at least the reduction of tetrazolium salts continues in mouse macrophages unrestricted for 48 h (epothilone B, 0.02–20 ng/mL).[70]

A comparison of epothilones B and D showed that the total uptake of epothilone B is higher by a factor of 4.[74] In addition, the intracellular distribution of the two compounds differs dramatically. Although nearly all of epothilone D is found in the protein fraction of the cytosol, almost 50% of the epothilone B resides in the nucleus.[74] This different behavior was corroborated by a more detailed study using tritiated 6-propyl-epothilones B and D (pEpts B and D), which show almost the same inhibitory effects as the natural 6-methyl analogs.[75] The study compared two cell lines, A431 (human epidermoid) and NCI/Adr (human mammary carcinoma, Taxol-resistant up to more than 1 μM). Epothilone D and pEpt D acted much more slowly than epothilone B and pEpt B, which produced almost maximal and lasting growth inhibition after only 4 h exposure in A431 cells. Drug uptake and intracellular pools turned out to be dose-dependent. Efflux of pEpt D was faster (almost complete after 60 min) than that of pEpt B, 60–70% of which was still inside the cells after 4 h when the loading dose was high (70 nM). When it was low (3.5 nM), NCI/Adr in contrast to A431 cells lost pEpt B quickly. This demonstrates that the two cell lines have different transport mechanisms for the two analogs. Apparently, the export pump of NCI/Adr cells becomes blocked when pEpt B is present in high concentrations.

In both cell lines, there seems to exist an MDR1-independent, yet verapamil-sensitive, export. Verapamil, a Ca antagonist and inhibitor of the MDR1 phosphoglycoprotein (Pgp) shuttle, stimulates the uptake of both drugs at low drug concentrations, but at high concentrations stimulates uptake only of pEpt D. Intracellular pools may reach up to 100 pmol/10^6 cells. Drug distribution was the same in both cell lines: pEpt D (and Taxol) was mainly in the soluble part of the cytosol (80%), and only little was in the nucleus (5–15%), whereas half of the pEpt B was in the nucleus (40–50% vs. 40–60% in the cytosol); there it was located on nuclear proteins, presumably tubulin, and nothing was on the DNA. This distribution may contribute to the differences in drug transport and efficacy of the two analogs.

The influence of epothilone B on MT dynamics was directly measured on time-lapse photographs of MTC7 cells that were stably transfected with green-fluorescent-protein α-tubulin.[71] Cells were analyzed 6 h after the addition of the drug when the intracellular equilibrium was reached. The growth rate of MTs in control cells was 13.3 μm/min, the shortening rate 21 μm/min, and dynamicity (= length of growth + length of shortening during total observation period per minute) 10.4 μm/min. With 2 nM epothilone B, those figures were reduced to 8.3, 19.3, and 6.3 μm/min, and with 3.6 nM to 7.5, 14.9, and 3.9 μm/min. Thus, while under all conditions, MTs shortened twice as fast as they grew, epothilone B clearly reduced MT dynamics. Also, at 3.6 nM, most MTs were completely stabile, although their ends showed minute (below 5 μm/min) changes in length (they "chatted"). The few MTs that still were dynamic grew and shortened more slowly and for shorter lengths of time; also, pause times, at which no changes occurred, became longer. The concentration and time scales of the MT effects correlate closely with those of mitotic arrest, and it was concluded that the reduction of MT dynamics is the direct cause of mitotic arrest. Spindle MTs may be particularly sensitive to interference with their dynamics, because they have to grow for a longer time and to greater lengths than interphase MTs. Essentially, the same reactions as just described for epothilone B were seen with Taxol, only at somewhat higher concentrations.

However similar the reactions of cells to Taxol and epothilone are, still they are not identical. An example is the behavior of mouse macrophages (*in vitro*).[70] At very high doses (0.1–10 μg/mL), Taxol stimulates the macrophages to react as they do to endotoxins; for example, to synthesize nitric oxide (*Salmonella typhimurium* lipopolysaccharide has this effect at 1–10 ng/mL). Epothilone B (up to 10 μg/mL) neither induces macrophages to release nitric oxide nor prevents it when they are treated with lipopolysaccharide, yet epothilone B acts normally on MTs inside the cell (at 12.5 ng/mL). Also, the degrees of resistance of normal cells to epothilone and Taxol do not always match.[76]

Studies on the effects of epothilones on isolated tubulin *in vitro* showed that the drugs make tubulin polymerize under conditions not applicable in the absence of the drug; for instance, in the absence of GTP[8,58] or MAPs or both, and in the presence of Ca^{++} (3 mM)[8] and at low temperatures

(0°C).[58] They stabilize existing MTs at cold temperatures (4°C for 30 min,[8] 0°C for at least 1 h[58]), with epothilone B doing so even after the addition of 5 mM $CaCl_2$ (not however epothilone A or Taxol).[58] Although initial studies suggested that epothilone A is more effective than epothilone B,[8] this was later corrected when purified tubulin was used.[47] The observed effects resemble those produced by Taxol, and indeed it was shown that epothilones displace [^{3}H]-Taxol from polymerized tubulin[8,58] (apparent K_i values, depending on the method of data analysis: epothilone A, 1.4/0.6 μM; epothilone B, 0.7/0.4 μM; docetaxel, 1.2 μM).[58] This indicates that the epothilones dock to the binding site of Taxol (i.e., β-tubulin), although initially allosteric effects or overlapping binding sites could not be excluded, and that epothilone B binds more tightly than epothilone A and Taxol. More thorough studies showed that while epothilone A is close to Taxol in efficacy, there still are subtle differences.[58] Thus, for example, in experiments without GTP but with MAPs, epothilone A causes better polymerization than Taxol (both epothilones allow assembly at 10°C, maximum at 25°C, whereas Taxol produces no MTs below 25°C, maximum at 37°C), or, with GTP but without MAPs at 25°C, Taxol is more active than epothilone A (epothilone B is already near its maximum) and reaches its maximum at 37°C, when it is twice as active as epothilone A. In the absence of both MAPs and GTP, significant polymerization takes place with all three drugs only at higher concentrations (i.e., more than 10 μM per 10 μM tubulin, which was the ratio in the former experiments).

Polymerization in the absence of GTP is somewhat enigmatic. There are two GTPs bound to the tubulin dimer: one on α-tubulin at the α,β-interface, which is neither exchangeable nor hydrolyzable, and one near the carboxy end of β-tubulin that is exchangeable and becomes hydrolyzed to GDP soon after the addition of the heterodimer to the plus end of the growing MT (which is capped with GTP-tubulin). It appears that the GTP hydrolysis changes the shape of the dimer from straight to (in the free form) bean shaped.[77] This in turn may introduce some stress in the MT, may produce the helical arrangement of the protofilaments, and may be a prerequisite for decay of the MT. Epothilone also reduces the number of protofilaments in MTs formed *in vitro* from 55% with 14 (control) to 67% with 13 (20 μM epothilone B, 10 μM tubulin).[77] The idea that the epothilones stimulate nucleation of tubulin polymerization is supported by two further experiments.[58] The critical concentration of tubulin, $[T]_{cr}$ (i.e., the lowest concentration at which polymerization begins under standard conditions), is regarded to be proportional to nucleation. The $[T]_{cr}$ was, without drug, 3 μM, and in the presence of any one of the three drugs, <1 μM; in the presence of only MAPs or only GTP, $[T]_{cr}$, with Taxol or epothilone A, was 1.4–1.7/4.3–4.5 μM, and with epothilone B, 0.8/2 μM. Without both MAPs and GTP, $[T]_{cr}$, with Taxol, was 22 μM, with epothilone A 19 μM, and with epothilone B 7.4 μM.

In addition, the average length of the MTs formed in the presence of the three drugs was measured in electron microscopic pictures. With MAPs and GTP but without drugs, the MTs were 4.3 μm long, with epothilones A or B, 2.8 and 1.1 μm, and with Taxol, 1.9 μm (i.e., shorter than with epothilone A). When GTP was lacking, the MTs became longer, and without MAPs even more so, yet with epothilone B, they were always half as long as with the other drugs. The morphology of the MTs was the same with or without drug, namely, tubules with occasional ribbon-like open sections.

In summary, the experiments just described demonstrate that the epothilones bind to, or close to, the Taxol site on β-tubulin, that they (also) bind to polymerized tubulin, that they seem to stimulate nucleation, and that MAPs are not required for drug binding. There is an obvious discrepancy between the concentrations effective in producing cytotoxicity and mitotic arrest (lower nM range) and those interfering with MT turnover *in vitro* (μM range). This may be explained by a several hundred-fold accumulation of epothilones inside the cells.[74,78] When HeLa cells, containing about 25 μM tubulin, were exposed to 10 nM epothilone, the drug reached intracellular saturation levels after 2 h. The cells then contained 4.22 μM epothilone A, or 2.55 μM epothilone B, respectively. Exposure to 100 nM drug reversed the relative internal levels to 17 μM epothilone A, or 26 μM epothilone B.[78] Thus, even at relatively low doses, both drugs reached intracellular concentrations sufficient to disturb MT dynamicity, which may lead to a lasting mitotic arrest after a short exposure of the cells to the drug.

In recent years, a much better understanding of the molecular interaction between Taxol/epothilone and β-tubulin has been gained. The yeast, *Saccharomyces cerevisiae*, is not inhibited by epothilone B (up to 150 μM), which is likely a result of a lack of uptake of the drug,[79,80] as purified yeast tubulin is induced by epothilone B to polymerize *in vitro* (EC_{50} = 1.3 μM in the presence of 5 μM tubulin and 50 μM GTP; with bovine brain tubulin, the EC_{50} is 1.2 μM).[69] Interestingly, Taxol has no such effect. Epothilone B reduces the dynamicity of yeast tubulin by a factor of 9.[80] In the presence of epothilone B, yeast tubulin also assembles without GTP. Yeast contains only one β-tubulin gene, and its β-tubulin differs in 124 amino acids from mammalian brain tubulin. With 75% similarity, it is close enough to coassemble into MTs. By analyzing available data on Taxol binding to bovine brain β-tubulin, 5 amino acids that differed in yeast tubulin were assumed to be responsible for preventing Taxol binding. Those amino acids were exchanged by site-specific mutation, namely, Ala19 to Lys19, Thr23 to Val23, Gly26 to Asp26, Asn227 to His227, and Tyr270 to Phe270.[79] The mutated yeast tubulin now polymerized with Taxol (EC_{50} = 1.55 μM, at 5 μM tubulin under conditions that do not allow spontaneous assembly) even more efficiently than bovine brain tubulin, which is perhaps a consequence of the 5–10% lower critical concentration of yeast tubulin. The EC_{50} of epothilone B remained the same (1.45 μM) with yeast wild type and mutant tubulin. The molar-binding ratio of Taxol:tubulin for wild-type yeast tubulin was 0.13, and for mutant tubulin it was 1.01, which was identical to that for bovine brain tubulin.[79] Radioactive Taxol bound to mutant MTs could be replaced almost completely by a 10-fold excess of epothilone B.[79] Clearly, the five inserted amino acids are not required for epothilone binding but are essential for the interaction of Taxol with β-tubulin. This shows that the binding site of epothilone need not be exactly identical with that of Taxol. The unaltered EC_{50} of epothilone B for the mutant tubulin seems to indicate that epothilone indeed binds at a slightly different location to tubulin.

Efforts have been made to identify the binding site of epothilone by mapping point mutations conferring resistance. The studies concentrated on the highly variable carboxy end of the otherwise conserved 450 amino acids of α- and β-tubulin, because this is the location of the nucleotide- and MAP-binding sites. Also, this part of the molecule is important for MT stability, because it is responsible for lateral contact of the protofilaments. In addition, most residues involved in Taxol binding have been located in this area. The mutants showed an increase in epothilone tolerance by a factor of 20–470.[81–83] Several of them had at the same time become hypersensitive to MT-destabilizing drugs (colchicine, vinblastine) or become outright epothilone-dependent.[82,83] This was explained by a destabilizing effect of the mutation that is counteracted by the stabilizing activity of epothilone (or Taxol).[84]

The drug-resistant cell lines grow more slowly than the parent lines.[82] Expression of the MDR1 (Pgp) and the MPR (multidrug-resistance-associated protein, another membrane protein) export systems is not increased[82,83] or even absent.[81] Also, there is no reduction of intracellular [^{3}H]-Taxol accumulation.[83] All this means that resistance is most likely caused by reduced epothilone binding. This has been shown to be the case by determining the percentage of polymerized tubulin, which decreased with increasing resistance from 28% (parental) to 6.9%.[84] In one cell line selected against 300 nM epothilone D, the mutated tubulin did not bind epothilone to any extent and also could not be stimulated to polymerize by the drug.[83] As a rule, epothilone resistance goes parallel to Taxol resistance,[83] but sometimes considerable discrepancies were observed—even more so with respect to docetaxel.[81,82,83]

Usually, only one point mutation was discovered in resistant cell lines, but occasionally two could arise.[83] Most mutations were expressed on the protein level.[83] The identified amino acid exchanges were usually close to the M loop and on helices H7 and H9. Thus, the mutated residues were indeed near the Taxol-binding site. Thr274 appears to be particularly critical for epothilone binding; it lies exactly at the site of interaction between β-tubulin and the C7-OH of Taxol.[81] The mapped mutations concerned a considerable variety of residues (see Table 21.1). This may be because epothilone resistance is a more complex phenomenon than it may seem at first sight. For one thing, resistance may vary with different cell types, among others, because they vary in their

TABLE 21.1
Amino Acids in β-Tubulin Suspected to Be Involved in Epothilone Binding

Method	Responsible Amino Acids	Isotype	Reference
Resistant mutants	Thr274 to Ile, Arg282 to Gln		81
Resistant mutants	Pro173 to Ala, Gln292 to Lys, Tyr422 to Tyr/Lys (heterozygotous)	βI	82
Resistant mutants	Pro173 to Pro/Ala, Tyr422 to Tyr/Lys	βI	85, 86
Resistant mutants	Ala231 to Thr, Gln292 to Glu	βI	83
Predicted from epothilone binding to P450epoK	Leu217, His229, Thr276, Arg284		56
Not required in yeast tubulin (in contrast to Taxol)	Lys19, Val23, Asp26, His227, Phe270		79

β-tubulin isotype composition, including posttranslational modifications. Not until 2003 did it become possible to determine the exact isotype profile of an experimental cell line by liquid chromatography combined with electrospray ionization mass spectrometry.[85] This permits assurance that the isotypes present in the genome are really expressed under the conditions of the experiment, which is not necessarily the case.[87] The isotypes are encoded by different genes, and the various genes are preferentially expressed in specific cell types. They are more than 80% homologous and vary mainly at their carboxy ends. The isotypes differ in conformation, assembly, dynamics, and ligand binding.[74] Among the seven known isotypes of β-tubulin, isotype I appears to be the preferred target of epothilone,[82,83,85] and that of Taxol.[74] In HeLa cells, the prominent isotypes of β-tubulin were I and IVb. Two epothilone-resistant sublines contained the same isotypes with a separate heterozygotous mutation, each in I. It could be shown that the mutant alleles were expressed, and apparently at a higher level than the wild type.[85]

Altered expression of isotypes[84] and changes in posttranslational modification of β-tubulin,[85] which could influence binding of MAPs, have to be considered as possibilities in producing resistance, although this has not yet been shown for epothilone. Nor can one be sure that tubulin mutations that lead to drug resistance are located in the β-isomer. In a Taxol-resistant, Taxol-dependent A549 cell line, the β1-tubulin was unaltered, and Taxol still bound to it, but there was a Ser379 to Arg exchange in the Kα1 isotype of α-tubulin.[84] Interestingly, overexpression of βIII-tubulin is found in many cases of cancer and appears to play a role in taxane resistance, for example, in breast, prostate, and NSCLC.[86] βIII-tubulin synthesis may be stimulated in hypoxic microenvironments within a cancer, so that tumor growth by itself may be responsible for an excess in βIII. It seems that ixabepilone blocks dynamicity of βIII tubulin and thus still is active in those cancers.

A major contribution to resistance may come from altered binding of MAPs to tubulin. MAPs may stabilize or destabilize MTs, and mutations in tubulin could influence the interaction between the two proteins. But of course, there could also be mutations in the MAPs themselves; in the enzymes that activate or deactivate them, usually kinases and phosphatases; or in the systems that control the expression of MAPs. There is experimental evidence that those assumptions are not mere theory. In the Taxol-resistant (and Taxol-dependent) cell lines, A549-T12 and A549-T24, a rise in MT dynamicity is seen in the absence of Taxol.[84,85] In this case, the responsible mutation is in the α-tubulin. The point mutation is near the carboxy end and presumably at a site of MAP4 and stathmin interaction. In response to rising Taxol concentrations (2 nM is required for survival), the status of the two regulatory proteins is also changed. Whereas the active, hyperphosphorylated form of stathmin (which destabilizes MTs) was barely detectable, the intracellular level of the nonphosphorylated, inactive form increased twofold, and the phosphorylated, and therefore inactive, form of MAP4 (which is an MT stabilizer) had clearly risen.[84] In another study, it was shown that tubulin-interactive drugs, like epothilone A, lead to phosphorylation of MAP4, probably by a mitotic kinase.[87] The phosphorylated

MAP4 dissociates from the MTs, which then become disorganized. Drug-resistant cells do not phosphorylate MAP4, and their MTs remain intact with MAP4 associated.

At very high doses, however, the same events as in sensitive cells take place, which shows that the interaction between tubulin and MAP4 is undisturbed. Also, expression of MAP4 is not influenced by the drugs in sensitive and resistant cells. Thus, it appears that MAP4 takes part in the drug-induced killing process, and resistance is somehow connected with the failure to phosphorylate the molecule. Although the exact mechanism of this sequence of events is not yet understood, it is obvious that the binding of epothilone to tubulin activates downstream events that contribute to cytotoxicity.

In a more general approach, genes that were overexpressed in epothilone A-resistant cell lines were identified by analyzing cDNA microarrays.[76,88,89] The STAT1 gene, interferon-inducible genes, and an MT-associated GTPase were found to be upregulated. The latter perhaps contributes to resistance by destabilizing MTs in the resistant cells. Another study, also using cDNA microarrays, demonstrated that 41 genes had an altered expression after epothilone B (10 nM) treatment of cells, and that many of them were connected with the tumor necrosis factor (TNF) stress response pathway.[88]

An important determinant in epothilone resistance could be the regulation of transport systems (i.e., of the membrane proteins involved in uptake and thus intracellular accumulation of the drug), and of the MDR1 and MPR machinery responsible for export. The latter are of particular interest in connection with epothilone, because they appear to be much less active on epothilone than on other cytotoxic drugs, including Taxol.

Studies on epothilone resistance repeatedly demonstrated that intracellular accumulation of tritium-labeled Taxol was unimpaired.[83] Thus, in those cases, resistance could not be attributed to impeded uptake of the drug. Similar experiments have been carried out with tritium-labeled epothilone analogs.[74,75] [^{3}H]- 6-propyl epothilones B and D were used to study uptake by nonresistant A431 (human epidermoid) and doxorubicin (adriamycin)-resistant NCI/Adr tumor cells (which also are resistant to epothilones).[74] The resulting picture turned out to be rather complex, as pointed out already. In several epothilone B-resistant A549 and HeLa cell lines, the MDR1 gene was not expressed at all, and although the MRP system was expressed, its level of expression did not increase after the cells became epothilone-resistant.[82] Also, in epothilone D-resistant leukemia cell lines, no rise in the levels of the MDR1 and MRP systems was seen, which could have explained resistance.[83] In fact, it already had been discovered that epothilones are not substrates for Pgp.[8,58] A human neuroblastoma cell line that was constitutive for MDR1 still responded to epothilone A, but not to Taxol.[69] The level of Pgp even rose during drug treatment (i.e., MDR1 was induced by epothilone A). In contrast to epothilone, calcein was exported from the cells ever more efficiently the higher the Pgp levels became, which proved that the transport system was fully functional. Thus, it seems that the cellular export systems do not play a major role in epothilone resistance, nor is there evidence that impaired uptake may be a decisive factor.

How does epothilone kill cells? All studies dealing with the killing mechanism of epothilone agree that the drug binds to MTs within cells, which leads to mitotic arrest by disorganization of the normal turnover of tubulin; to an accumulation of the cell population in the G_2–M phase of the cell cycle; to a decay of the cell nuclei; and to apoptosis. However, there still remains to be explained how exactly apoptosis is achieved, and whether apoptosis is the only way by which epothilones become cytotoxic. The answer is of more than academic interest, as it may have implications for the treatment of cancer. Thus far, no fully consistent picture can be presented. Among other reasons, this may be because investigators dealing with that problem used different cell types and various epothilone analogs.

It appears that the tumor suppressor protein, p53, does not play a role in the killing of cells by epothilone, as human neuroblastoma cell lines, which constitutively sequester p53 in the cytoplasm and thus prevent its effect as an intranuclear transcription factor, still were fully sensitive to epothilone A (and Taxol).[69] In contrast, it was shown that, although cells with mutated p53 normally become less sensitive to cytostatic compounds, their sensitivity to epothilone B (and Taxol) rises, perhaps because a higher proportion of cells with mutant p53 is in mitosis—the target of epothilone.[90]

Apoptosis is a rather complex phenomenon induced by a receptor-mediated extrinsic or a mitochondrial pathway, and it is modulated by a large number of proteins. Very briefly (for more details, see, e.g., Refs. 91 and 92), the extrinsic pathway starts with death receptors (e.g., DR4 and DR5) in the cell membrane. They are activated by binding a death ligand (e.g., Apo2-2L/TRAIL = TNF-related apoptosis-inducing ligand) and then, after several more steps, form a death-initiating signaling complex, which results in autocatalytic activation of initiator caspase 8, and the following effector caspase cascade finally triggers apoptosis.

The mitochondrial pathway begins with the release of cytochrome c from mitochondria into the cytosol. This, which again involves several steps, leads to the formation of apoptosomes (consisting of oligomers of APAF-1[apoptotic protease-activating factor-1]), which activate initiator caspase 9 and, in turn, executioner caspase 3 (and caspase 7). Those caspases cleave a number of cellular proteins and finally lead to apoptosis. The sequence is modulated by the Bcl-2 and IAP protein families. One study applying (water soluble) epothilone B-amine (BMS 310705) on ovarian carcinoma cells taken from a patient who no longer responded to treatment with platinum and Taxol demonstrated that the drug killed the cells *via* the mitochondrial pathway of apoptosis.[91] The cells were exposed for 1 h to 10–500 nM of the drug and then incubated in drug-free medium. After 24 h, more than 25% of cells showed apoptosis, and after 96 h, 90% were dead. An increase in activity of initiator caspase 9 and effector caspase 3, but not of initiator caspase 8 (typical for the extrinsic pathway) was seen. Also, 12 h after treatment, cytochrome c was detected in the cytosol. Another study using epothilone B-lactam on cell-cycle-synchronized human ovarian carcinoma cells found not only indicators of the mitochondrial pathway (leakage of cytochrome c into the cytosol, activation of caspase 3, and downregulation of the protective proteins survivin, cIAP1 and XIAP, which inhibit caspase 3, caspase 7, and caspase 9), but also a rise of the death receptors DR4 and DR5 in the cytoplasmic membrane, which sensitized the cells to the death ligand, Apo2-2L/TRAIL.[92] Thus, in this case, the extrinsic pathway seemed also to be in operation. The study also showed that epothilone B-lactam is active on Taxol-resistant cells.

Still another study showed a role of the Bcl-2 family of apoptosis-modulating proteins in the killing process.[93] Again, epothilone B-lactam was used. The drug induced a conformational change in the proapoptotic Bax protein, which resulted in its transfer from the cytosol into mitochondria and a concomitant release of cytochrome c from mitochondria into the cytosol, with the consequences pointed out above. Apoptosis could be mitigated by overexpression of Bcl-2, and enhanced by the Bcl-2 antagonist, BAK-BH3 peptide. The conclusion was that epothilone B-lactam induces apoptosis by a Bcl-2-suppressible pathway, and that treatment of breast cancer can perhaps be improved by a combined therapy with epothilone B-lactam and a Bcl-2 antagonist. Involvement of the Bcl-2 family was also seen when human ovarian carcinoma cells were treated with epothilone A.[87] The epothilone A–tubulin interaction, which must be unimpaired, results in inactivation of the prosurvival proteins Bcl-2 and Bcl-x_L by phosphorylation, and in lowering of the Mcl-1 level by increased turnover. As Mcl-1 inactivates the proapoptotic Bax protein by forming a complex with it, reduced Mcl-1 and a concomitant overexpression of Bax clearly would support apoptosis. Typically, in resistant cells, Mcl-1 remains high in the presence of epothilone A, Bax is lowered, and Bcl-x_L is not phosphorylated.

In contrast to the studies just discussed, the authors of an investigation of the effects of epothilone B on nonsmall-cell lung cancer cells concluded that epothilone kills the cells by a yet unknown, caspase-independent mechanism.[94] At low doses, cytotoxic effects (disruption of the MT cytoskeleton, arrest of cells in the G_2–M phase, aberrant mitosis, multinucleated cells) are seen rather soon, before 24 h after the addition of the drug, yet symptoms of apoptosis (nuclear condensation, apoptotic bodies, cytochrome c release, cleavage of poly [ADP-ribose] polymerase, activation of caspase 3 and caspase 9) appear only much later, and therefore may be just side effects. Furthermore, the cells would still die when the mitochondrial or the extrinsic pathway of apoptosis was neutralized by overexpression of the antiapoptotic proteins, Bcl-2 or Bcl-x_L, or of the dominant negative FAS-associated death domain. Even the caspases could be blocked by natural (response modifier A) or artificial (Z-Val-Ala-Asp-fluoromethylketone) antagonists without interfering with cell death. If this

hypothesis is correct, drugs may be found that induce that mechanism more efficiently and, thus, may be even more beneficial in cancer therapy.

Several studies report synergistic effects between epothilone and other drugs, which may become of interest in cancer therapy. Many solid tumors show interstitial hypertension, which impedes transfer of drugs from capillaries to tumor tissue. This high interstitial fluid pressure appears to be mediated by the activity of platelet-derived growth factor, the receptors of which are expressed in many solid tumors. The tyrosine kinase inhibitor, STI571 (Novartis Pharma), blocks the kinase activity of those receptors, which results in lowered interstitial fluid pressure and improves the uptake of drugs by the tumor. When severe combined immunodeficiency (SCID) mice with human anaplastic thyroid carcinoma were treated with a combination of epothilone B and STI571, the tumors became more than 40% smaller than after treatment with epothilone B alone.[95] The level of epothilone B in the tumor increased threefold, but remained unchanged in liver, kidney, and the intestinal tract. However, STI571 (100–150 mg/kg) had to be administered on three consecutive days at a minimum, and its effects faded away 2 d after the last application.

The synthetic flavonoid, flavopiridol, has aroused considerable interest in recent years on account of its antitumor activity. It arrests cells in the G_1–S (or G_2–M) phase of the cell cycle and induces apoptosis. The mechanism appears to be the inhibition of mRNA synthesis, perhaps by blocking transcriptional elongation or by binding to duplex DNA. In consequence of this, cyclins and antiapoptotic members of the IAP and Bcl-2 families of proteins are downregulated.[96] Further, flavopiridol blocks cyclin-dependent kinases and brings about conformational changes of Bax, with the sequels outlined above. In human breast cancer cells, flavopiridol (100–500 nM) acted synergistically with epothilone B (20 nM) in inducing apoptosis, but only when applied after, and not in advance of, that drug.[96] In a Bcl-2 overexpressing cell line, epothilone B and flavopiridol, alone or in sequence, induced only minor apoptosis, which demonstrates again that Bcl-2 acts as an epothilone antagonist.

Specific farnesyl transferase inhibitors are potent antitumor drugs. The explanation is that they prevent posttranslational farnesylation of certain proteins (e.g., of the p21ras family), which is a prerequisite of their insertion into the cell membrane. With human breast cancer cells, it was shown that those inhibitors (e.g., L-744,822; Merck) increase sensitivity to antimitotic drugs, such as Taxol and epothilone.[97] The synergistic effect was additive. It is speculated that this happens because a farnesylated protein controls the checkpoint of mitosis. Also, human prostate cancer cells, including a line that was rather resistant to L-744,822, became considerably more sensitive to the drug when they were pretreated with epothilones.[63]

This was regarded as a promising strategy for therapy of advanced prostate cancer. A broad synergistic effect was seen in colon cancer cells treated with a combination of epothilone D and 5-fluorouracil.[98]

Histone-deacetylase inhibitors, like LAQ824 (Novartis), lead to altered gene expression, with changes in the levels of several important regulatory proteins. As a result, they enhance epothilone B-induced apoptosis in human breast cancer cells.[99]

Epothilone B-lactam sensitizes human lung cancer cells to radiation, *in vitro* as well as *in vivo* (athymic nude mice).[100] *In vitro*, the induction of apoptosis by drug and radiation was additive, and a higher dose of the drug for a shorter exposure time was more efficient than a lower dose for a longer time. The *in vivo* effect is considered to be a result of a combination of mitotic arrest and reoxygenation of the tumor, so that the timing of the irradiation after drug exposure becomes a critical factor.

21.5 TOTAL SYNTHESIS AND SEMISYNTHESIS

21.5.1 Total Synthesis

The discovery of the epothilones as the first Taxol mimics, and reports of their promising pharmacological properties, triggered enormous world-wide synthetic activities in late 1995. With seven stereogenic centers in a 16-membered macrocycle, their total synthesis appeared, though challenging,

to be far less difficult than that of Taxol. Thus, many groups entered the field and made epothilone probably the most often synthesized natural product in recent years. Apart from preliminary synthetic studies, more focused work started in late 1995 when the absolute configuration became available from our lab (before publication in July 1996, the absolute configuration of epothilone A and B had been communicated to interested scientists from October 1995 on). First total syntheses of epothilone A and, later, epothilone B were reported by the groups of Danishefsky, Nicolaou, and Schinzer in 1996 and 1997.[9a] Key bond- forming steps in these early syntheses were macrolactonization, a highly diastereoselective C6–C7 aldol reaction, and olefin metathesis at C12–C13. Soon after, macroaldolization forming the C2–C3 bond and a novel B-alkyl Suzuki coupling of C11–C12 were introduced by the Danishefsky group. Over the years, these basic approaches have been developed further by the original authors and adopted by many other groups for their own synthetic strategies. Many more alternatives were developed, omitting only a few carbon–carbon bonds not used in the assembly of the macrocycle and the attachment of the thiazole side chain (Figure 21.6). Thanks to the efforts of many groups, the early synthetic strategies mentioned above proved their value and were applied in the syntheses of structural analogs and adapted to a plant-scale synthesis. It is beyond the scope of this review to discuss in detail the more than 20 direct and formal total syntheses published and reviewed before 2005[9a,b,d,f,j–n], and until 2010.[10a,k,l,o] However, a few points on crucial bond-forming strategies should be made.

In most syntheses, the first strategic goals are, as in the biosynthesis, the 12,13-olefins epothilones C and D (occasionally named also dEpoA and dEpoB, **2a**, **2b**), which are epoxidized in a more or less stereoselective manner to epothilones A and B.[105,107,111,136,137] A particular challenge is the stereocontrolled synthesis of the trisubstituted *Z* olefin in the epothilone D series for which a variety of approaches have been developed. Traditional reactions like Wittig olefination or ring-closing olefin

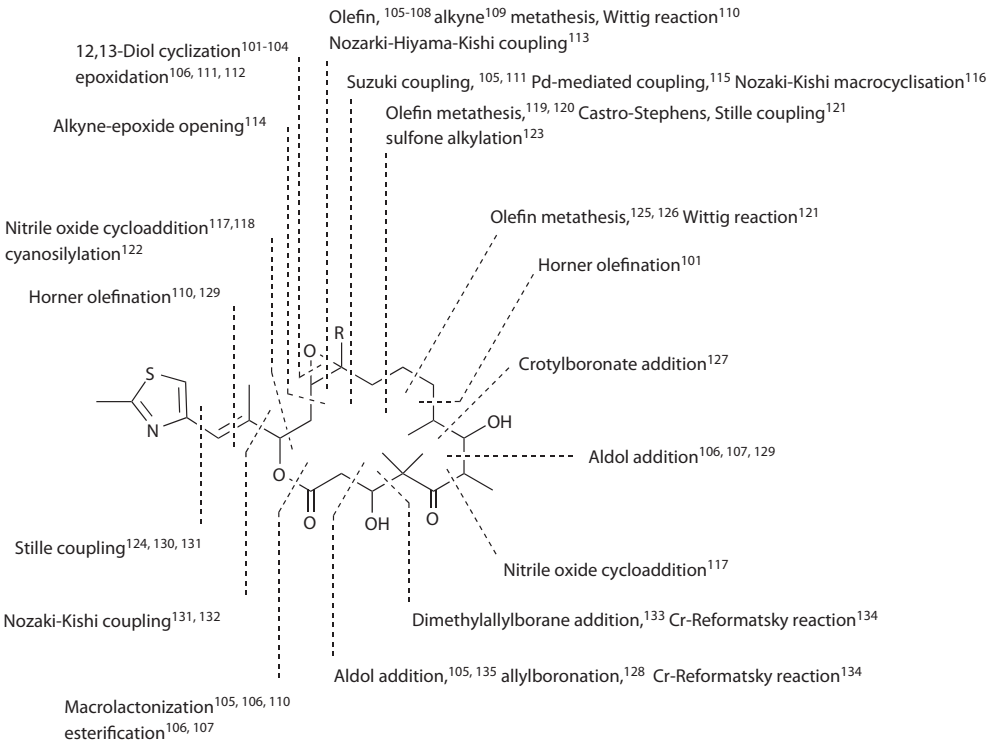

FIGURE 21.6 C,C- and C,O-bond-forming strategies in the total synthesis of epothilones.

metathesis (RCM) proceed with low-to-moderate stereoselectivity and require chromatographic separation of the *E*/*Z* isomers. One of the recent solutions to this problem is to generate a 12,13-fused β-lactone with the appropriate configuration, which undergoes a Grob-type fragmentation to give exclusively the *Z* olefin.[138] To improve the unsatisfactory *Z* selectivity of RCM in macrocyclizations, smaller-ring intermediates were envisaged to generate the 12,13-double bond. Thus, a "silicon tethered" RCM gave a 9-membered disiloxane ring intermediate with an improved *E*/*Z* ratio of 1:5,[139,140] whereas perfect stereocontrol was achieved by RCM of a C15-OH methacryl ester to give an unsaturated 6-membered lactone intermediate.[141] In another stereoselective approach, the C12,13 olefin is introduced by propyne using a modified Normant alkylation.[142] Avoiding epothilone D as an intermediate, the epoxide of epothilone B is generated in a final step from a protected 12,13-diol of appropriate configuration.[140] Alternatively, the sensitive epoxide is introduced at an early stage with high stereoselectivity, and, with the necessary precautions, carried through the synthesis by Mulzer's group.[101]

Soon after completion of the synthesis of the four major epothilones A–D, the groups of Danishefsky and Nicolaou and others started to explore SAR for cytotoxicity and tubulin binding. Following their own philosophies, either a limited number of selected analogs[60] or large libraries were synthesized *via* combinatorial chemistry.[187] In this work, all stereocenters were probed for their relevance for biological activity, the alkyl groups on C8[143] and C16[144,145] were removed, or new ones were added at C10[146] and C14.[146,147] Further, the C6[75] and C12 methyl groups were replaced by larger alkyl, alkenyl, alkynyl, and functionalized alkyl groups,[60,126,130,144,148–152] and 11-hydroxy and 11-fluoro groups[116] were introduced. Stille coupling of C17/C18 allowed the attachment of a great variety of 5- and 6-membered heterocyclic side chains, optionally carrying additional substituents.[124,130,145] The observation that substituents at C19, like methyl in **4** (Figure 21.7), entirely abolish biological activity[153] indicated that the *syn* conformation of H19 and Me27 seen in solution and in the crystal structure (**II**, Figure 21.14) is crucial for tubulin binding. Evidently, this conformation may be locked by interconnecting C19 with C27. This was realized in 2000 by Altmann et al.[154] at Novartis with the synthesis of benzothiazole (**5**), benzoxazole, and quinoline analogs. Independently, at that time, the same strategy was pursued by Klar et al. at Schering,[75] leading, after additional modification of the C6 side chain, to the highly active benzothiazol analog ZK-EPO (Sagopilone),[155] which is presently in phase II/III clinical trials as an anticancer drug.

Whereas 12,13-trans olefins (**17**; Figure 21.7) and the epoxides derived from them were regularly unwanted byproducts in the RCM,[60,156] Altmann et al.[157] synthesized them in a stereoselective manner to prove their unexpected biological activity. The epoxides were also made from the *trans* olefins, as well as the *cis*- and *trans*-substituted cyclopropanes,[131,132,158–161] cyclobutanes,[132,160] and aziridine analogs.[162]

To rigidify the macrocycle and enforce certain conformations, 12,13-benzo (**6**),[163] 9,10,11-benzo (**7**),[75] 10,11,12-benzo (**8**),[75,164] 8,9,10-furano (**9**),[165] and 10,11-cyclopropano[119] analogs were synthesized (Figure 21.7). Similarly, the C4 geminal dimethyl groups were integrated in a cyclopropane ring.[64,65] By insertion of a methylene group, the C6 and C8 methyl groups were linked to form a cyclohexanol **10**,[166] and C4,C6 to form a cyclohexanone **11**.[102] Modest conformational strain was introduced by extra *trans* double bonds at C9,C10 (**16**),[126,167,168] and C10,C11 (**14**),[119] whereas epothilones with a C9,C10 (**19**),[169] or a C12,C13 (**20**)[109] alkyne bond, prepared *en route* to epothilones B and D, are profoundly distorted (Figure 21.7). The same applies to a C9,C10 *cis* double bond (**15**),[169] although this is not anticipated from the planar drawing. On the other hand, based on computer models, the tubulin-binding conformation was preadjusted by a methylene group linking C14 and C17 (**12**, X = N, CH),[170] and a five atom bridge linking the methyl groups C22 and C26 (**13**, X = CH_2, CO).[171] As isosteric replacements, oxygen was introduced for C10,[172] and nitrogen for the C16-oxygen to give lactam **22**.[62] Further, C4, C12, and C13 were replaced by nitrogen leading to lactams and amines **23**,[173] and **24a**,[9q] and **24b**.[174] (Figure 21.8). A variety of other functional group manipulations by semisynthesis, including compounds **18** and **21**, will be discussed in the following section.

Occasionally, building blocks taken from natural products were utilized, such as geraniol,[114] nerol,[134,175] and carene[176] in the northern ring segment. The use of pantolactone[75,177] for the C1–C5

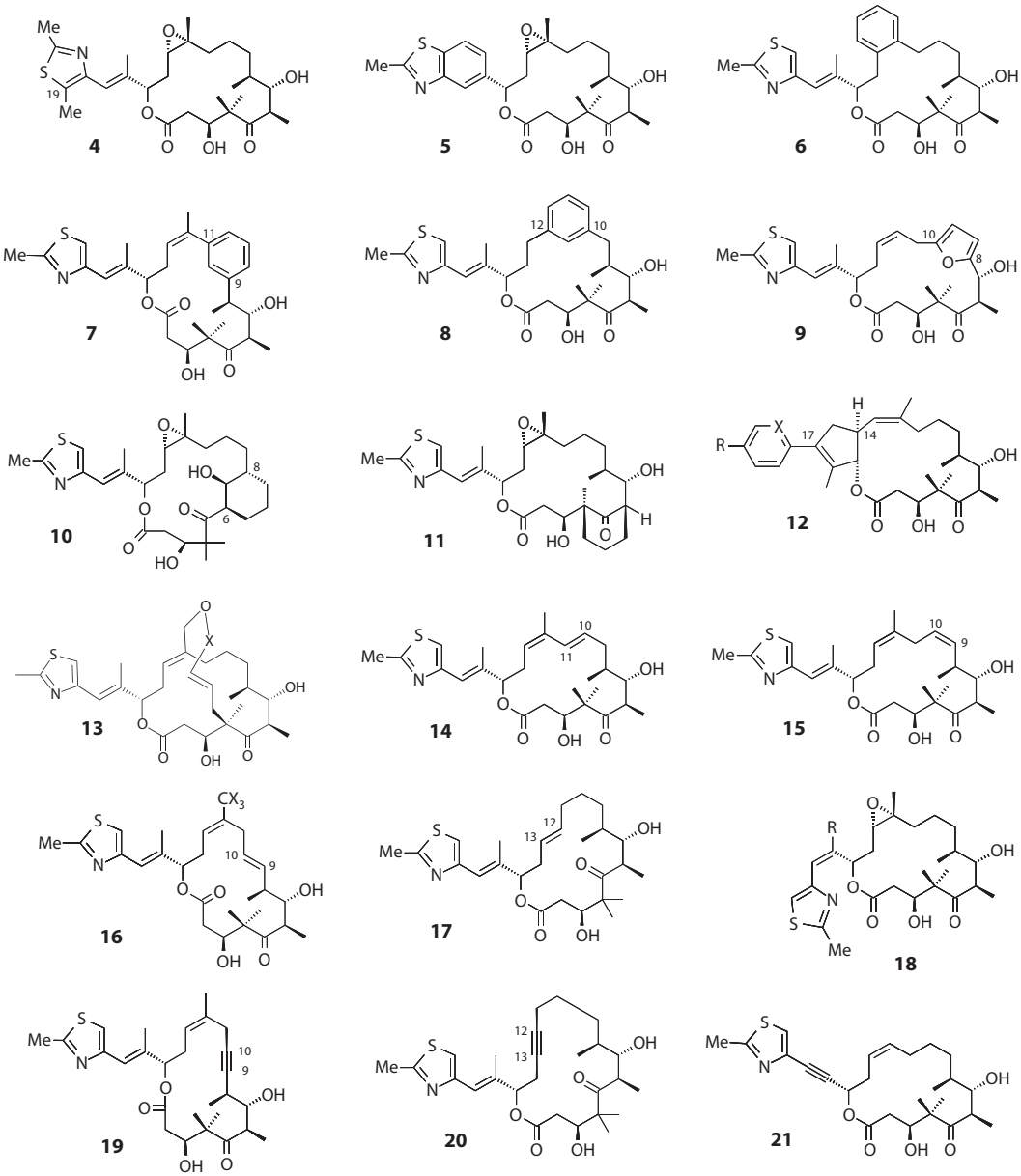

FIGURE 21.7 Conformationally restrained epothilone analogs (for clarity only one C12 homolog, and either the C12,C13 olefin or epoxide version is shown).

ring segment and of diethyl (*S*)-malate[75,178] for the C13–C16 segment provided the C3 and C15 stereocenters. In one and the same synthesis, both northwestern and southeastern ring segments were constructed from glucose by extensive functional group manipulations performed by Ermolenko and Potier.[179] Chemoenzymatic methods were applied to establish the desired configuration at the C3, C7, and C15 hydroxyl groups. Thus, resolution of racemates was achieved by commercial esterases and lipases,[180,181] by a genetically engineered lipase,[182] or in case of C15, by a catalytic aldolase antibody.[183–185] An aldolase-catalyzed asymmetric synthesis was developed by Liu and Wong,[186] providing building blocks with the C7 and C15 stereocenters in an enantiomerically pure form. In a polymer supported synthesis of an epothilone C-based library, Nicolaou et al.[156,187]

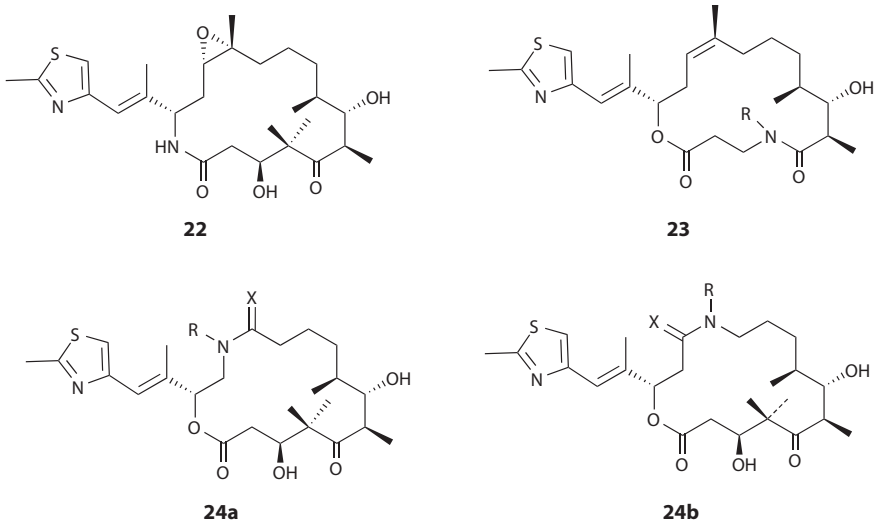

FIGURE 21.8 Epothilone aza-analogs.

used an olefinic linker to the polymer support, which is cleaved in the final step by participation in an olefin metathesis cyclization. In this way, only successfully cyclized molecules are released from the polymer to give immediately pure products.

In an alternative approach, Ley et al.[188] synthesized epothilone B, using polymer-supported reagents and scavengers, while the growing product was kept in solution. Thus, tedious extraction and purification steps were avoided, making this approach amenable for large-scale synthesis. However, the advantages of the overall process may be doubtful in terms of cost-effectiveness when costs for the preparation and regeneration of the polymer reagents are included.

In summary, during the past 14 years of epothilone synthesis, around 550 original papers and 220 reviews have been published, and 480 patents filed and, in part, granted. Apart from academic syntheses of natural epothilones and the development of new synthetic methods, far more than 1000 epothilone analogs may have been synthesized for SAR studies and in search of clinically useful analogs. For two compounds, ZK-EPO (Sagopilone) and 9,10-dehydro-epothilone D (dehydelone), large-scale processes were developed, taken to plant-level production, and introduced into clinical trials by Schering and Kosan Biosciences in collaboration with Roche (Figure 21.16).

21.5.2 Semisynthesis

In the course of strain and process optimization at the GBF starting in late 1995, epothilone A and B became available in larger amounts and were used for semisynthesis. Also a block-mutant strain was developed supplying epothilones C and D.[17] Since 1997, a broad semisynthesis program was pursued in collaboration with Bristol-Myers Squibb. Later, based on material from strain SMP44 and *M. xanthus*, Kosan Biosciences contributed on a smaller scale to semisynthesis. Remarkably, up to now, no reports on semisyntheses have been published by Novartis, even though they must have produced epothilones by large-scale fermentation of a strain derived from So ce90 since the late nineties.[189]

Early one-step transformations were performed at the GBF with epothilones A and B, including mono- and diacylation of the 3,7-dihydroxy groups, Swern oxidation to 3,5- and 5,7-diketones, and borohydride reduction of the C5 ketone to a 1:1 mixture of epimeric alcohols.[190] Similarly, solvolysis of the epoxide produced mixtures of stereoisomeric diols (cat. H_2SO_4), chlorohydrins (HCl), or rearranged 14-membered lactones (TFA, BF_3OEt_2). Dihydroxylation of epothilone C with OsO_4/NMO

gave a 2:1 mixture of epimeric *cis* diols. 12,13-Dihydro-epothilone C was formed selectively with diimine, whereas catalytic reduction produced complex mixtures because of hydrogenolysis of the allylic ester moiety.[191] Hydrolysis of the lactone in epothilones A–D was achieved by LiOH in MeOH/H_2O to give *seco*-acid **25**, and depending on reaction time, by retroaldol reactions, the C7 aldehyde and C5 isopropyl-ketone fragments (**27**, **28**; Scheme 21.2).[22] Whereas the stereocenter C6 was conserved in **28**, that on C8 was completely racemized in **27**. However, prolonged basic hydrolysis in the presence of sodium borohydride gave the corresponding alcohol **26** with 98% ee.[22] To our frustration, all these derivatives were devoid of significant biological activity.

Contrary to basic hydrolysis, a very clean cleavage of epothilone A–D to *seco*-acids was achieved on a preparative scale with pig liver esterase.[192–194] Interestingly, epothilone A could be restored by Yamaguchi macrolactonization of the 3,7-nonprotected *seco*-acid **25** (X = O, R = Me) in 25% yield.[194] Although C3 and C7 hydroxyl groups occupy β-positions to carbonyl groups, they are not eliminated under these and other more rigorous conditions. Under very mild conditions, the *N*-acetylcysteamine thioester of *seco*-epothilone C is cyclized but, in part, also hydrolyzed with cloned thioesterase from *S. cellulosum*.[195] Apart from preparative utility, the sensitivity of the lactone bond to esterases was identified very early as a problem in animal studies and possible future clinical application.[192] The remedy obviously was isosteric replacements in the carboxyl group or introduction of steric hinderance next to it. Up to now, only the conversion of the lactone to a lactam has been realized. In a short and very elegant reaction sequence, Vite, Borzilleri, and coworkers at BMS transformed epothilone B lactone to the lactam. Using palladium chemistry, the allylic lactone was opened and the C15 oxygen replaced by azide with overall retention of configuration. Reduction of the azide **29** to an amine, and cyclization by standard peptide chemistry, produced the lactam **22** in good yield (Scheme 21.3).[62] Remarkably, the whole sequence did not require 3,7-OH protection

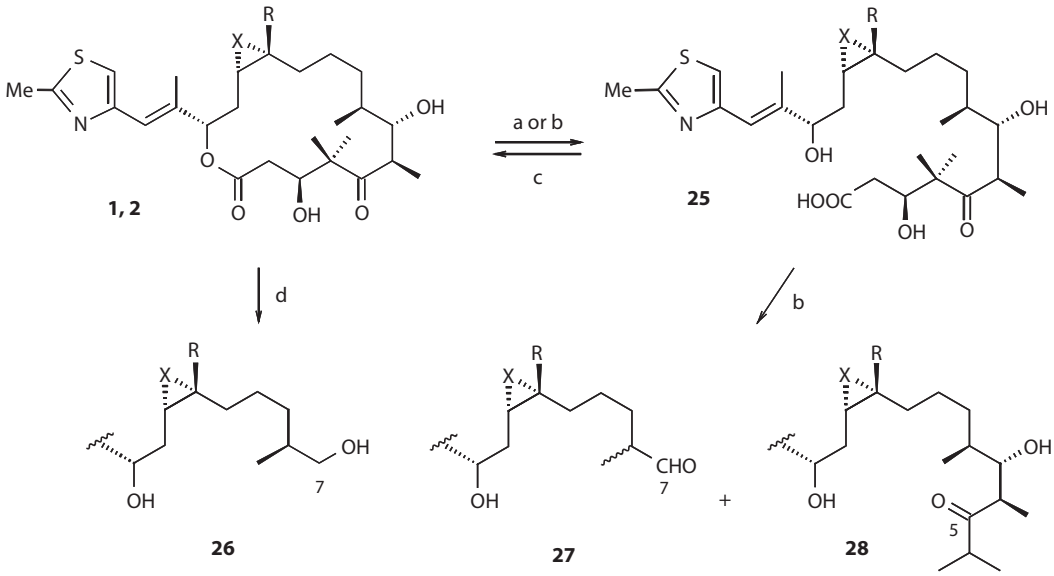

SCHEME 21.2 Lactone cleavage and retro-aldol reactions of epothilone.

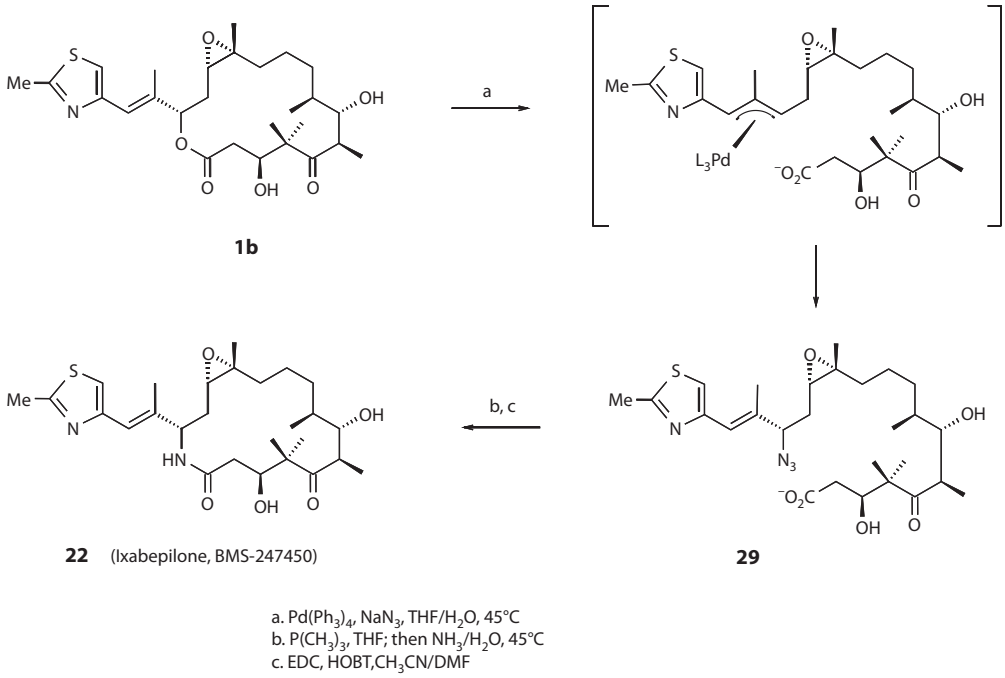

SCHEME 21.3 Lactone to lactam conversion of epothilone B.

and could be performed as a one-pot reaction. Because of its favorable cytotoxic and pharmacological profile, epothilone B-lactam **22** (BMS-247550, ixabepilone) was introduced into clinical trials in 2000,[11k] and was approved by the FDA for the treatment of metastatic or locally advanced breast cancer in 2007.

Alternative approaches to lactone stabilization started with 3,7-diformyl epothilones **30**, which on treatment with DBU gave in good yields *trans*-2,3-olefins **31**.[194] As Michael acceptors nucleophiles like cyanide are readily added to give a 1:1 mixture of 3α- and 3β-cyano epothilones **32a** and **32b** (Scheme 21.4).[196] Both stereoisomers were not of sufficient activity to be developed further.

Another ideal target for versatile structural modification was the 12,13-epoxide and the corresponding olefin in the epothilones A–D. Immediately after isolation, we investigated the epoxidation of epothilones C and D with dimethyl dioxirane and MCPBA to see what the outcome of the epoxidation in the ongoing total syntheses would be. Whereas a clean reaction with dimethyl

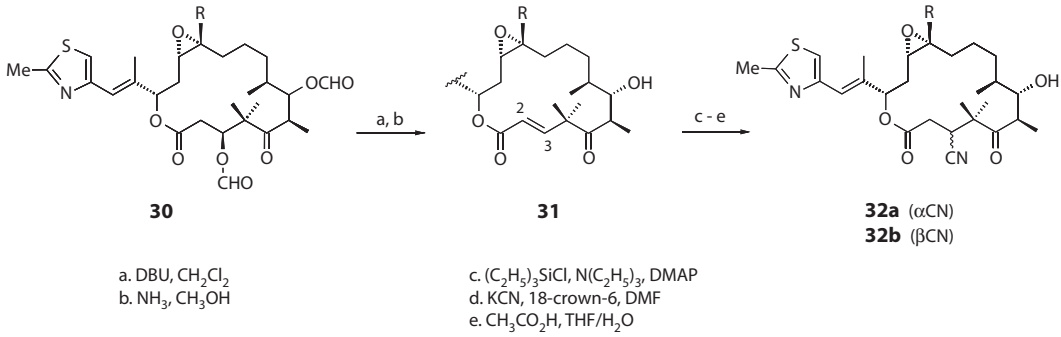

SCHEME 21.4 Synthesis of 2,3-unsaturated and 3-desoxy-3-cyano-epothilones.

dioxirane at –20°C gave predominantly the natural α-epoxides besides the β-isomers,[137] MCPBA produced significant amounts of byproducts, particularly with a slight excess of MCPBA at temperatures up to 50°C. The byproducts were identified as stereoisomers of the 16,17-epoxides, 12,13,16,17-bisepoxides, and thiazole *N*-oxides.[61,107,112,197] Starting from epothilones A and B, the *N*-oxides **33** were isolated in 50–55% yield, and found to be valuable intermediates in the functionalization of the C21 methyl group (see below).[61] Expectedly, the nucleophilic nitrogen in **1** could be methylated with Meerwein's salt to give *N*-methylthiazolium tetrafluoroborate **34**.[198] Contrary to epoxidation, cyclopropanation of the C12,C13 double bond of epothilone C (and D) turned out to be a tough problem, but was eventually achieved in low yield with dibromo- and dichlorocarbene generated under phase-transfer conditions to give exclusively α-cyclopropanes **35**.[159] Subsequently, the halogen from **35a** was removed by tin hydride reduction to **35b** (Figure 21.9). Starting with the unnatural epothilone A β-epoxide, the α-episulfide was obtained in moderate yield by reaction with an excess of ammonium isothiocyanate in acetonitrile at 120°C.[22,199] Due to the inversion of both stereocenters, the episulfide has the natural configuration. Both the cyclopropane and episulfide turned out to be as active as the epoxide, thus ruling out that the epoxide forms a covalent or hydrogen bond with tubulin.

The epoxide in epothilone A was regioselectively opened to bromohydrin **37** with $MgBr_2$ in ether; oxidation to the bromoketone, α-addition of cyanide followed by ring closure gave the *trans*-like cyanoepoxide **36**.[196] Its structure was proven by x-ray crystallography. Alternatively, the bromohydrin was converted to the azido alcohol, then Mitsunobu inversion and mesylation of the C12-OH set the stage for phosphine reduction of the azide and cyclization to aziridine **38a** with the natural α-configuration.[162] Subsequently, the nitrogen was alkylated and acylated with a broad range of residues to **38b** (Scheme 21.5).

The aziridines are generally as active as the parent epoxide, some even more so in tubulin-binding and cytotoxicity assays. For that reason, an aziridine was selected for a tumor-targeting approach aiming at the folate receptor of tumor cells, originally developed by Leamon et al. at Endocyte for vinblastine and mitomycin.[200a] BMS and Endocyte have collaborated in the synthesis of a folate epothilone aziridine conjugate with a peptidic spacer incorporating a disulfide bridge named Epofolate (**39**; Figure 21.10).[200b] After uptake by cancer cells, the disulfide and carbonate bonds are cleaved, and a highly active *N*-(2-hydroxyethyl)-aziridine derivative is released. Preclinical *in vitro* and *in vivo* data have been published so far only in a patent appplication.[200b] Nevertheless, the conjugate **39** was introduced into clinical trials in 2007, and is currently in phase I/II studies.[201] Similarly, epothilone analogs with a benzimidazole side chain carrying a *N*-hydroxyethyl substituent for prodrug design and tumor targeting have been prepared by total synthesis.[202]

Whereas epoxidation of the C12,C13 double bond is the final step in the epothilones A and B biosynthesis and in many total syntheses, it was desirable to use the rich supply of epothilones A and B from fermentation for the reverse reaction. This was achieved by the BMS group in good yield

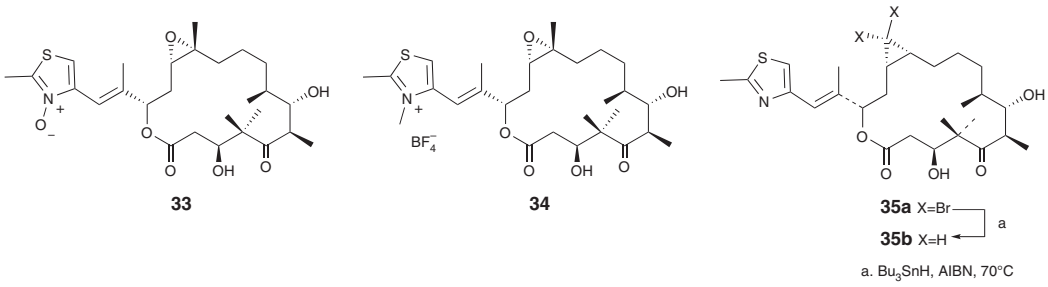

FIGURE 21.9 Epothilone thiazole-*N*-derivatives and 12,13-cyclopropanes.

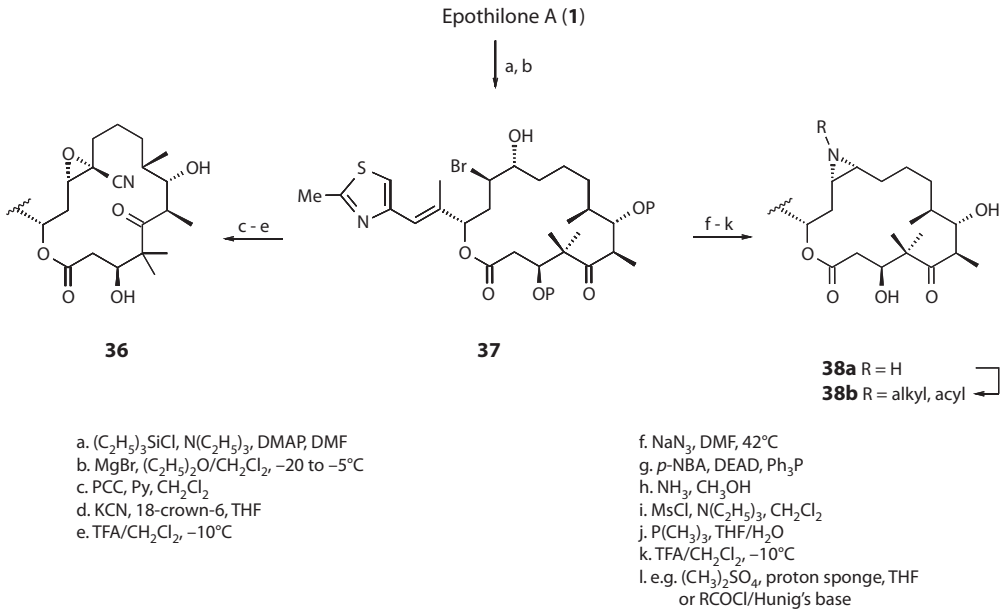

SCHEME 21.5 Synthesis of 12-cyano- and 12,13-aziridino-epothilone A analogs.

and retention of (*Z*)-configuration by the reduction of unprotected **1a** and **1b** with $TiCp_2Cl_2$/Mg and WCl_6/*n*-butyl lithium to epothilone C and D (**2a** and **2b**), respectively (Scheme 21.6).[159]

Cleavage of the C12,C13 double bond of epothilones C and D by either ozonation or with OsO_4/$Pb(OAc)_4$ or, alternatively, diol formation and periodate cleavage of epothilones A and B gave valuable C12 aldehyde and ketone-building blocks **40**. During this reaction sequence, the lactone bond was cleaved with PLE (pig liver esterase) or basic hydrolysis. Subsequently, synthetic ring segments were introduced by Wittig condensation[203] or, after methylenation, olefin metathesis.[204] Further, amino-substituted ring segments were introduced at C12 to provide, after lactonizatation, 13-aza-epothilones such as lactam **24a**.[9q] In an entirely different approach, building blocks from the degradation of epothilones and other myxobacterial compounds were used to synthesize "natural product-like" combinatorial libraries for high-throughput screenings.[205] Attempts to functionalize the 12,13- (or 16,17) double bond of epothilones C and D by an ene-reaction with singlet oxygen failed, and the products were recovered unchanged.[22]

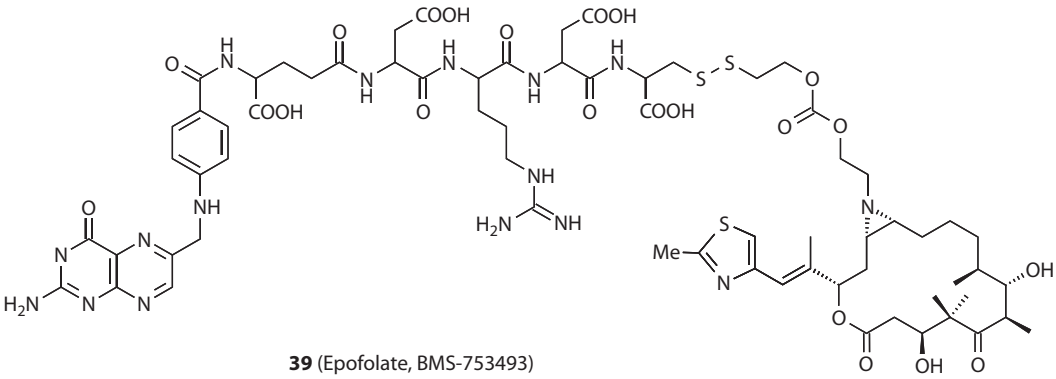

FIGURE 21.10 Epothilone-folate conjugate.

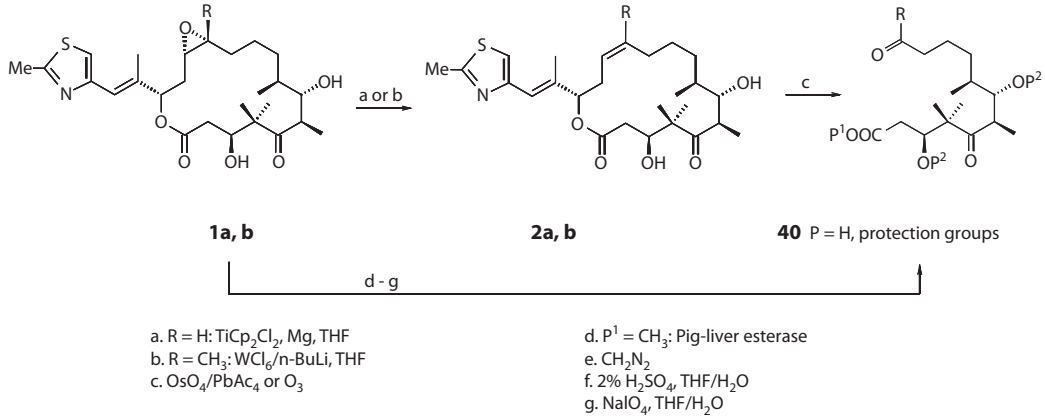

SCHEME 21.6 Degradation of epothilones A–D to the C1–C12 ring segment.

Inspired by the RCM in the total syntheses of epothilones, the reverse reaction was investigated in the presence of an excess of ethylene and second-generation Grubbs's catalysts. The expected *seco*-diene **41** was obtained in good yield and processed further by replacement of the C13–C15 ring segment with a synthetic analog **43** to give **45**. In this reaction sequence, ester cleavage to **42** was achieved by a TBSOTf-induced fragmentation at 30°C. RCM afforded, for example, the alkyne analog **44** of epothilone C along with the C12/C13 *trans* isomer (1:1; Scheme 21.7). Subsequently, **44** was epoxidized to the alkyne analog of epothilone A.[206] More direct modifications of the linker

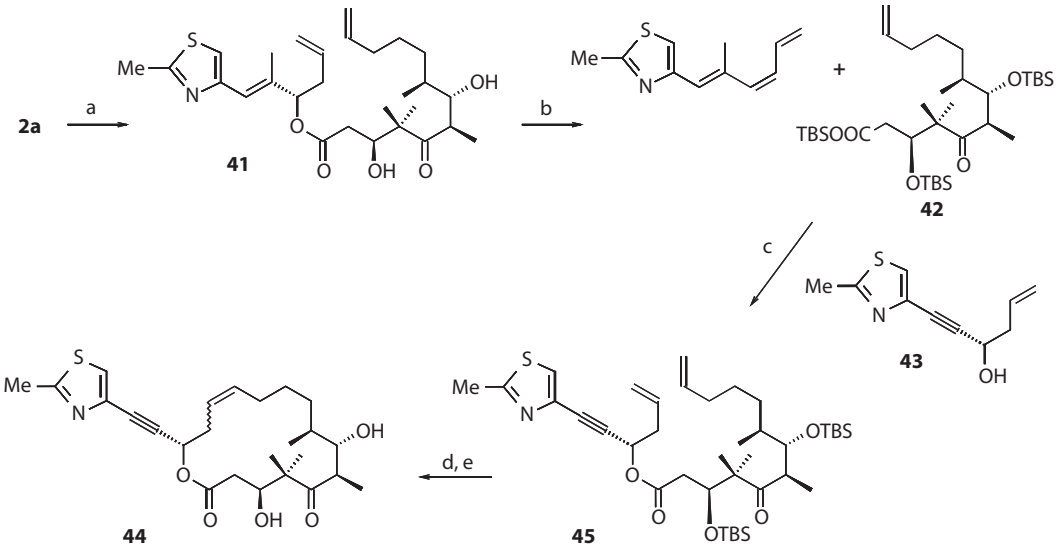

SCHEME 21.7 Synthesis of the 16,17-alkyne analog of epothilone C.

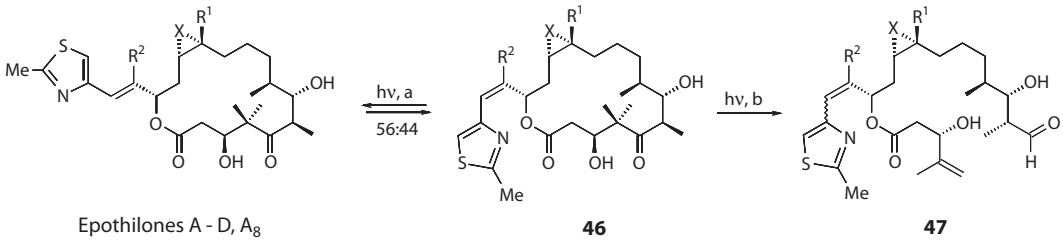

SCHEME 21.8 Photochemical isomerisations of epothilone C.

group C16,C17 were catalytic hydrogenation, epoxidation followed by reduction to a 16-hydroxyl group, and its elimination to give a C16 exomethylene derivative.[190] Several epothilones, including the 16-desmethyl analog of epothilones A and C, could be isomerized to 6:4 mixtures with their *Z*-isomers **46** by benzophenone-sensitized irradiation with a high-pressure mercury lamp (Scheme 21.8).[206] On prolonged irradiation, a byproduct accumulated, which was isolated in 50% yield, and idenified as aldehyde **47** formed by a Norrish Type II cleavage.[22]

A very promising entry to side-chain modification seemed to be the ozonolysis of epothilones A and B to give the C16-ketones **48**.[190] However, apart from the formation of standard carbonyl derivatives of the acetyl group like oximes and esters, after reduction to the alcohol, new side chains could not be introduced by Wittig, and Wittig–Horner condensation. Only methylenation worked well, indicating steric reasons for the failure. On the other hand, Wittig-like condensation with the boron analog $(C_2H_4O_2B)_2CHLi$ did work, yielding vinyl boronic acid **50** as a 7:3 *E/Z* mixture (Scheme 21.9). For the introduction of side chains by Suzuki coupling of **50** reactive iodo compounds, such as iodo

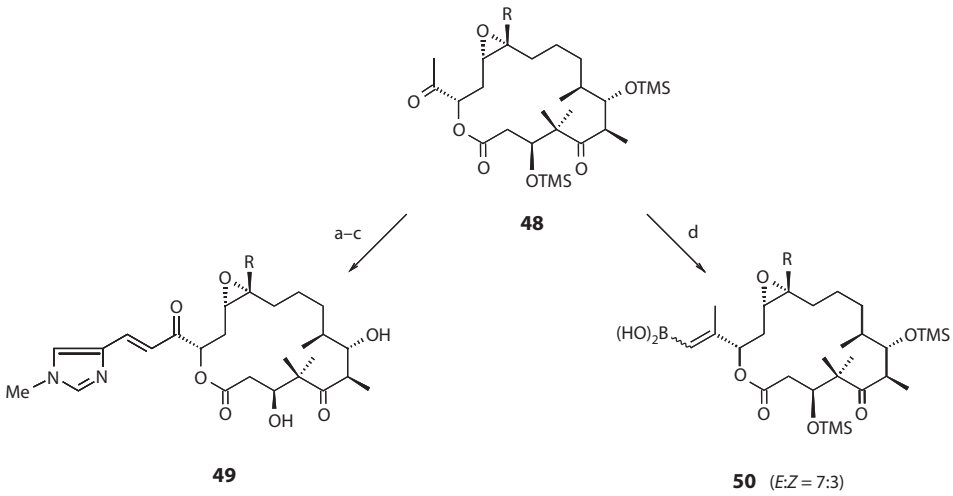

SCHEME 21.9 Aldol condensation and boron-analog olefination of a 15-acetyl epothilone analog.

benzene, were required. Otherwise, **48** was transformed by *N*-iodosuccinimide to the corresponding iodovinyl epothilone that could be introduced in Stille couplings,[197] as described by Nicolaou et al.[130,131] Moreover, modified side chains could be attached by aldol condensation of the methyl ketone in **48** with synthetic aldehydes to give, for example, imidazole **49**.[197]

Initially, modification of the thiazole ring other than by replacement seemed hardly possible in the presence of the sensitive functional groups in the macrocycle. However, with *n*-butyl and *t*-butyl lithium at low temperatures, deprotonation of C19 and, to a lesser extent, of the C21 methyl was possible. After quenching the anions with deuterium chloride or carbon and heteroatom electrophiles, the corresponding derivatives were obtained in moderate to low yields.[153,198]

An unexpected, more selective access to C21 derivatives was opened by a Polonovsky-type rearrangement of the epothilone A and B thiazole *N*-oxides **33**. On treatment with acetic anhydride, the oxygen is transposed as an acetoxy residue to the C21 methyl. On mild hydrolysis, epothilones E and F (**3a**,**b**) were obtained.[61] It should be mentioned that all steps including *N*-oxidation with peracids were carried out without 3,7-OH protection (Scheme 21.10). Alternatively, C21 hydroxylation, was achieved at BMS by biotransformation using *A. autotrophica* and other *Actinomyces* strains.[29] In addition to C21, *A. autotrophica* also hydroxylates the C9 and C14 positions, and the C12 methyl group.[30]

Starting from semisynthetic epothilones E and F, Nicole Glaser at the GBF prepared a diverse library of more than 80 side-chain-modified epothilones,[198] which are outlined below. As benzylic-like alcohols, the nonprotected epothilones E and F were smoothly oxidized to the corresponding aldehydes and carboxylic acids by manganese dioxide and sodium chlorite, respectively. From epothilones E and F, a variety of esters and alkyl ethers, thioethers, and a glucoside were prepared. All halogens from fluorine to iodine were introduced by tosylation and nucleophlic displacement, or, for fluorine, with DAST. The C21 azides were obtained from the alcohols in a one-pot reaction with phosphoryl azide, subsequently reduced to the amines **51** with hydrogen and Lindlar catalyst, and further modified by alkylation and acylation. The majority of these C21 derivatives showed high activity in cell culture assays, and some also showed promising results in mouse tumor models.

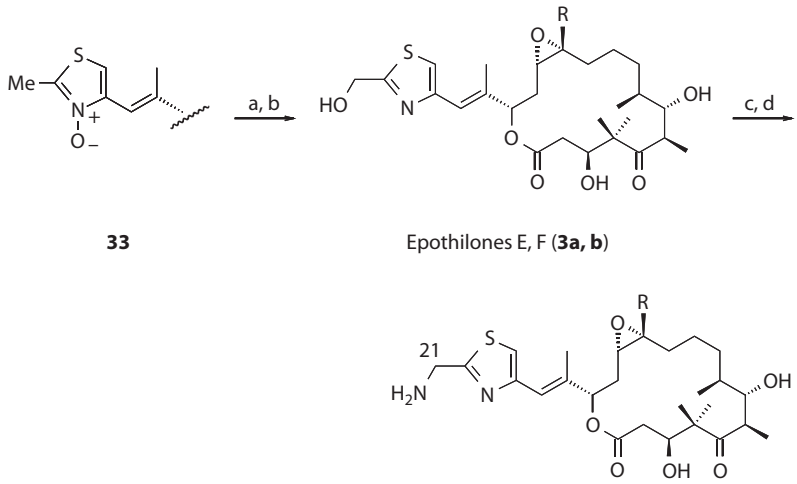

SCHEME 21.10 Conversion of epothilone-*N*-oxides to 21-aminoepothilones.

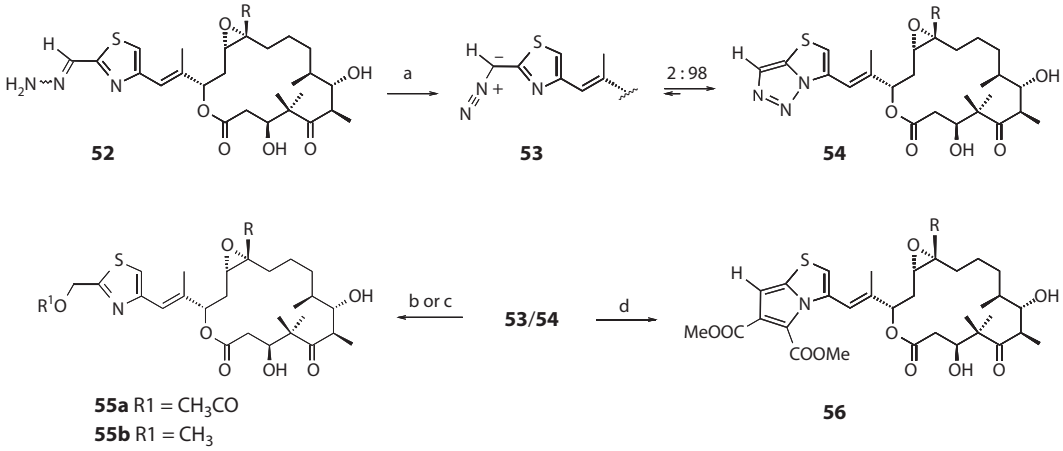

a. NiO_2, CH_2Cl_2
b. CH_3COOH
c. CH_3OH, hν, >260 nm
d. Dimethyl acetylenedicarboxylate, CH_2Cl_2, RT

SCHEME 21.11 Synthesis and decomposition of 21-diazoepothilones.

Epothilone B 21-amine (**51a**, BMS-310705) is eightfold more stable than **1b** *in vitro* against PLE, and entered clinical trials in 2000.

Similarly to epothilones E and F, the corresponding C21 aldehydes were extensively modified to *E*/*Z* oximes and hydrazones, and, using various C,C-coupling techniques, to C21 alkyl-, alkenyl- and alkynyl-substituted thiazole analogs. The hydrazone **52** was smoothly oxidized with nickel peroxide to the diazo compound **53**, which exists in equilibrium with the cyclo-tautomer **54** and may be trapped by a cycloaddition to dimethyl acetylenedicarboxylate to give pyrrolothiazole **56** or reacted with acetic acid to give ester **55a**. The diazo compound **53**(**54**) was stable as a solid or in solution at room temperature, but is decomposed on irradiation ($\lambda > 260$ nm) in methanol to give the epothilone E 21-methyl ether (**55**; Scheme 21.11). Fortunately, **53** (**54**) shows high cytotoxic activity, and thus may be used for photoaffinity labeling of tubulin.

In an attempt to occupy simultaneously two adjacent binding sites on MTs, epothilone dimers with variable spacers were designed (Figure 21.11).[198] However, the plan was not further pursued when it turned out that epothilone E with diglycol substituents on the 21-hydroxy group **57**, and the dimer **58** were inactive in the tubulin polymerization assay. Similarly, C7-OH esters **59** of epothilone A with various dicarboxylic acids were inactive.[207] The moderate cytotoxic activity of **57**–**59** is presumably caused by partial ester hydrolysis to epothilones E and A during the 72-h incubation with tumor cells. Contrary to that, epothilone C17,C17′ dimer **60** (Figure 21.11) which was obtained as side product from Stille coupling of a 17-iodo building block surprisingly showed remarkable activity in the tubulin polymerization assay.[145]

21.6 STRUCTURE–ACTIVITY RELATIONSHIPS

Investigation of SAR started very early at the GBF with more than 39 natural epothilones isolated from large-scale fermentations and simple one-step semisynthetic derivatives. Shortly after, the Danishefsky and Nicolaou groups published biological data for a great variety of analogs, and industrial groups at BMS, Kosan, Novartis, and Schering followed. Unfortunately, the data generated for cytotoxicity/growth inhibition by different groups are hardly comparable on a quantitative basis

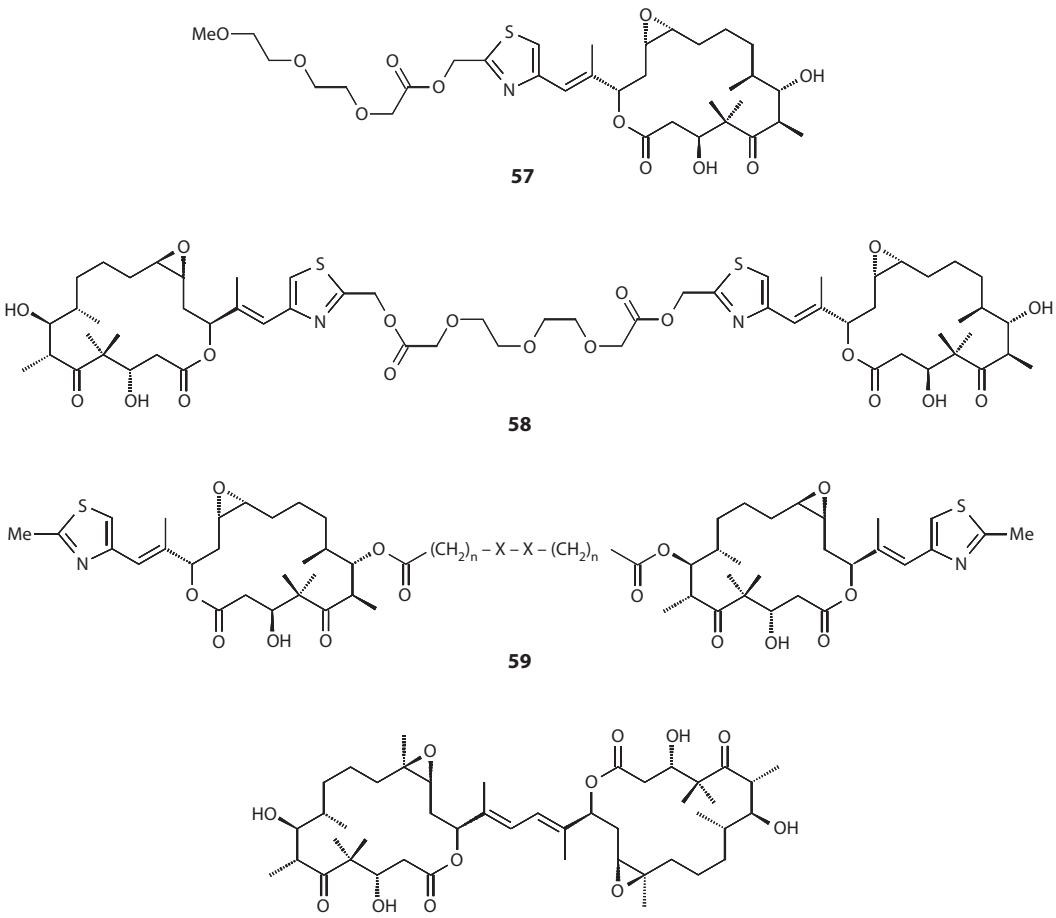

FIGURE 21.11 Pegylated epothilone E and epothilone C21-OH, C7-OH, and C17,C17′ dimers.

due to the broad range of sensitivity of the various cell lines, and experimental conditions applied. *In vitro* tubulin polymerization assays depend even more on a variety of parameters, such as the origin and isotype composition of the tubulin used, presence of MAPs, other ingredients, and the experimental setup.[158,208] Clearly, in the search for clinically useful derivatives, activity against multidrug-resistant cell lines is most important; however, these data are even less comparable for compounds from different laboratories. Therefore, in the following discussion, we only classify cytotoxic activity against sensitive tumor cell lines into four broad categories: high (>20% of the activity of the parent compound), moderate (5–20%), low (1–5%), and inactive (<1%).

Most natural epothilones have been isolated in two variants, having either hydrogen on C12 (Epo A series) or a methyl group (Epo B series). The same applies for epothilones from total synthesis and semisynthesis. Regardless of structure, epothilones of the B series are more active in cytotoxicity and tubulin polymerization assays by a factor of 5–20. Therefore, most *in vivo* studies and clinical trials have been performed with compounds from the B series. Only the aziridine derivative, Epofolate **39** (Figure 21.10), which is in phase I/II clinical trials, belongs to the A series.

Structural modifications affecting the activity of epothilones are summarized in Figures 21.12 and 21.13. It is generally accepted that a 16-membered macrocycle and the configuration of its seven stereocenters are prerequisites for biological activity.[124] However, moderate activity was observed with certain 18-membered epothilones, whereas 14-, 15-, and 17-membered analogs were very

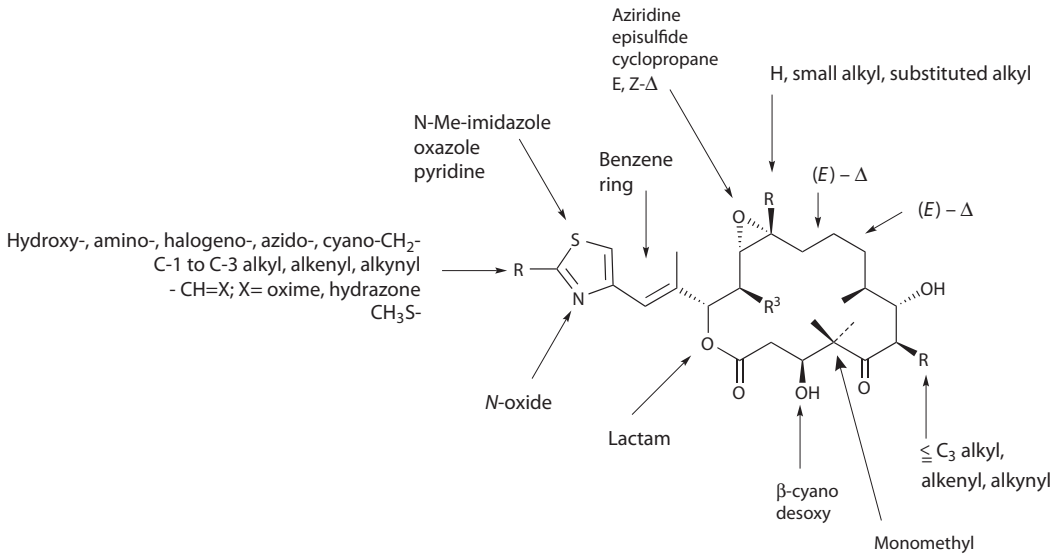

FIGURE 21.12 Epothilone modifications resulting in high to moderate activity.

weakly active or inactive.[124,209] Replacement of the lactone group of epothilone B, D, and F by a lactam reduces cytotoxic activity and tubulin binding only slightly by a factor of 1:3 to 1:10, while other properties such as resistance to esterase cleavage, therapeutic window, protein binding, or p.o. efficacy are improved.[62,68] Remarkably, lactam analogs obtained by total synthesis rather than semi-synthesis seem to be less active, in particular against MDR cell lines.[59,210] No other isosteric replacements of the lactone group like ethers or ketones have been reported thus far.

Epothilones with a (*E*)-2,3-double bond from elimination of the 3-hydroxyl and 3-desoxy derivatives are still moderately active, which indicates that the 3-hydroxyl is neither a hydrogen bridge donor nor an acceptor in the tubulin-bound state of epothilone. Nevertheless, there are significant steric restraints: whereas the 3β-cyano analogs with natural configuration are highly active, the 3α-cyano analogs are inactive.[196] Similarly, for steric reasons, ester and ether derivatives of the C3 and C7 hydroxyl groups are inactive. Oxidation of the C3 and C7 hydroxyl groups to ketones, and borohydride reduction of the C5 ketone to the epimeric alcohols lead to complete loss of activity. Both epimeric 4-desmethylepothilones A_1 and A_2 are highly active,[4] whereas replacement of 8-Me by hydrogen, or formation of a cyclopropane by linking C22 and C23 drastically, reduces the activity.[64,65] The loss of activity can be rationalized by conformational changes induced by the absence of the 6-Me/8-Me *syn* interaction and change of the C3/C4/C5 bond angles. Most remarkably, increasing steric bulk at C6 of epothilone B by an ethyl substituent leads to fourfold activity compared with the parent compound, whereas allyl and propyl derivatives are slightly less active than the parent compound.[75]

In the crystal structure and in solution, the carbon backbone C8–C12 adopts a nearly anti-periplanar conformation, and it is thus not too surprising that the C9/C10[126,167,168] and C10/C11[4,119,120] *trans* olefins are highly active, whereas the C9/C10 *cis* isomer is inactive,[169] as is the alkyne.[169] The C10 oxa-analog is also for no obvious reasons inactive.[172] Next to the side chain, the C12/C13 epoxide and olefin turned out to be most flexible and have been modified extensively. Thus, replacement of the epoxide by cyclopropane,[131,159,160] episulfide,[22] aziridine, *N*-acyl, and *N*-alkyl aziridine[162] retains or even improves cytotoxic activity, a fact that rules out an early hypothesis of covalent binding to tubulin protein *via* epoxide opening. Also cyclobutane analogs[160] and 12,13-oazolines[211] are highly active, whereas acetonides of 12,13-diols[140] are less, and a 12,13-benzo analog[163] was inactive. Epoxides and all other related analogs in the unnatural β-configuration are inactive. The desoxyepothilones C and D (**2a** and **2b**) are less active in cell assays by a factor of 5–40; however, they

are as active or even more active than the epoxides in the tubulin assay.[60,108,187,212] Most surprisingly, desoxyepothilones in the unnatural (*E*)-configuration of the double bond are also highly active, as well as the corresponding epoxides, provided the natural configuration of C13 is retained.[156,157]

The presence of the C12 methyl is extremely important for the high *in vitro* and *in vivo* activity of the epothilone B series. It may be replaced, however, with retention of activity by small alkyl, alkenyl, and alkynyl groups or modified by the introduction of halogen and oxygen substituents.[60,148,152] Interestingly, the fluorescent epothilone D analog with a bulky *m*-dimethylaminobenzoyloxy substituent at the C12 methyl group is still about as active as Taxol.[213] An extra methyl in the 14α position reduces activity slightly, whereas a 14β methyl causes refolding of the corresponding ring segment and loss of activity.[146] The vinyl spacer C16/C17 in the side chain and its (*E*)-configuration are of crucial importance for biological activity,[60,206] whereas the C16 methyl group seems not to be important.[4,145] Epothilone analogs lacking the spacer,[60,214] or ones extended by one atom,[197] or containing an alkyne spacer,[206] 16,17-epoxides,[187,190] or conformationally flexible spacers with a C16/C17 single bond,[190] are inactive. The conformationally restrained epothilone analogs **7–13**, **15**, and **18–21** (Figure 21.7) are also more or less inactive.

The thiazole may be replaced by an oxazole or α-pyridyl without loss of activity whereas the β- and γ-pyridyl analogs are only moderately active or inactive.[4,64,65,75,130] From these early findings, it was concluded that the position of the nitrogen in the natural epothilones is a prerequisite for activity by acting as a hydrogen bond acceptor in the tubulin bound state. In support of this, *N*-methylthiazolium epothilone B is inactive, whereas thiazole-*N*-oxides are still active with the *N*-oxide oxygen acting as a hydrogen bond acceptor.[198] The same applies to the triazolo-thiazole analog **54**.[198] Later, a variety of highly active 5- and 6-membered heterocyclic analogs were synthesized having a nitrogen atom in the required position. Apart from positional isomerism, conformational restraints may place the nitrogen out of its preferred orientation resulting in complete loss of activity. This is the case with C19-substituted thiazole analogs like **4**[153] or accordingly substituted pyridyl analogs.[130] On the other hand, the nitrogen may be locked in its optimal position by condensation of the heterocycle with a benzene ring, conferring high activity to the resulting benzothiazoles (like **5**), -oxazoles, -imidazoles, and -quinolines.[75,154,215] A disturbing point in this otherwise consistent picture is that the quinoline analog of epothilone D with the nitrogen in the "unnatural" para position is expectedly 100-fold less active, whereas both regioisomers of the quinoline analogs of epothilone B are highly active.[216,217]

The C20 methyl of the natural thiazole side chain may be replaced by hydrogen, small alkyl, alkenyl, or alkynyl groups,[198] or heteroatom substituents like methylsulfanyl with retention of high

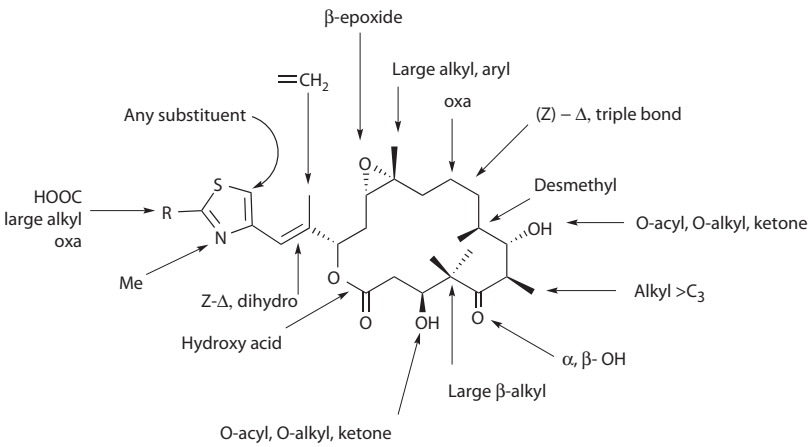

FIGURE 21.13 Epothilone modifications resulting in low activity and loss of activity.

activity.[161] In general, three-atom (except hydrogen) residues are still highly to moderately active, whereas bigger ones are weakly active or inactive.[198] The methyl group C21 may be modified by a variety of halogen, oxygen, nitrogen, and sulfur substituents or oxidized to the aldehyde and further derivatized without loss of activity, provided the space demand of the entire residue does not exceed three to four atoms.[198] The thiazole-20-carboxylic acid derivative is inactive.[198]

Studies on the solution conformation of epothilone A started even before the absolute configuration was published. Thus, Georg's group predicted the relative configuration and conformation of epothilone A on the basis of nuclear magnetic resonance measurements and molecular dynamics calculations.[218] One of the proposed structures showed the correct relative configuration for the independent western and eastern ring segments. We found NOEs (Nuclear Overhauser effects) and coupling constants of epothilone B in DMSO/D_2O solution in good agreement with a conformation similar to that in the crystal.[3] Only the thiazole side chain is apparently rotating around both its single bonds. Interestingly, the conformation of the side chain is strikingly different in crystals grown from lipophilic or from polar solvents. Whereas in crystals from dichloromethane/petroleum ether, H17 and H19 are *syn*-periplanar-oriented and the side chain adopts an equatorial position (Figure 21.14, **I**),[3] in crystals from methanol/water H17 and H19 are *anti*-periplanar-oriented, and the side chain adopts a more axial position with regard to the macrocycle (Figure 21.14, **II**),[21] The conformation of epothilone B in a (poly)crystalline state has recently been determined by magic-angle spinning (MAS) NMR and expectedly (the crystals have been obtained from dichloromethane) found to be identical to conformer **I** from x-ray analysis.[219] In a detailed conformational analysis of epothilone A in CD_2Cl_2 and DMSO/D_2O, Taylor and Zajicek[220] added a second minor conformer, designated **B**, with the 3-OH rotated from an axial to an equatorial position, accompanied by rotations in the C6/C7 segment. Interestingly, an equatorial 3-OH is also found in the crystal structure of epothilone B-*N*-oxide where it is stabilized by a hydrogen bond to the *N*-oxide oxygen, while the conformation around C6–C8 is not significantly influenced.[61] Apparently, a weak intramolecular hydrogen bond of the C3-OH to the thiazole nitrogen is also able to stabilize a C3-OH_{eq} conformation in $CDCl_3$ solution, as we found in (21*R*,*S*)-diastereomeric C21-substituted epothilone A and B derivatives.[198] Thus, in the 20-epoxyethyl epothilone A analog, the 3-OH nuclear magnetic resonance signal appears duplicated, and a strong NOE is observed between 17H and 3H. The latter indicates a C16–C19 *syn*-periplanar conformation as it is observed in the crystal structure of epothilone B from aqueous methanol (Figure 21.14, **II**).

The early observation that epothilones can displace tubulin-bound taxol suggested that both are bound to the same or overlapping binding sites.[8] This immediately triggered the search for a common pharmacophore and the bioactive conformation of the epothilones by modeling experiments. Based on the crystal structure of both molecules, NMR data, and the supposed homology of

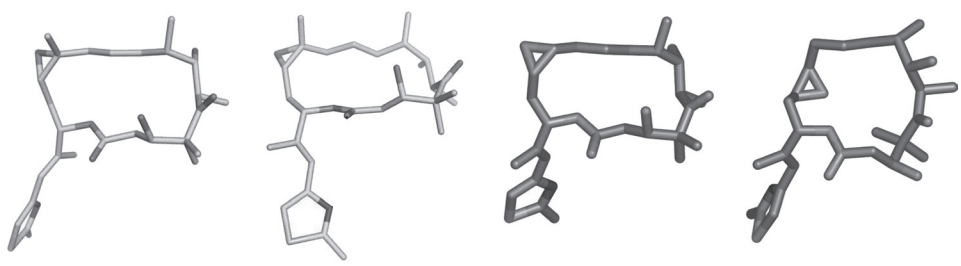

I II III IV

FIGURE 21.14 (See color insert.) Crystal structure of epothilone B from dichloromethane/petroleum ether (I), methanol/water (II), and the tubulin-bound structures of epothilone A from NMR (III), and electron crystallography (IV). (Modeling by W.-D. Schubert.)

structural features like a geminal dimethyl group, an epoxide/oxetane, and thiazole/phenyl groups, several of models were proposed,[221–225] and, in part, corroborated by mapping of cross-resistance to certain amino acid replacements in β-tubulin.[81,83,226,227] Also, a tubulin point mutation outside the Taxol-binding site was observed that confers high resistance to both Taxol and epothilone.[84] Later, SAR were included in the modeling studies,[146,226,228–231] and specific epothilone derivatives were designed to challenge the various proposals.[147,166,171] In view of the flexibility of the macrocycle and the side chain, the number of functional groups present, and the spacious tubulin-binding site (epothilone is only about half the size of Taxol), it is not surprising that a variety of plausible models were proposed.[232–235] Several fluorescent probes such as **61**,[236] **62a**,[213] and **63**[198] have been synthesized and characterized, but not employed in mechanistic studies so far (Figure 21.15).

In 2003, the first direct observation of the tubulin-bound conformation of epothilone A was reported by the Griesinger's group.[237,238] From sophisticated nuclear magnetic resonance measurements (of transferred NOEs and transferred cross-correlation rates) of free and tubulin-bound epothilone A in rapid exchange, the dihedral angles, and thus the conformation of bound epothilone was obtained (Figure 21.14, **III**). It resembles that in the crystal structure **I** (Figure 21.14), with a C16,C19 *syn*-orientation of the thiazole as in the crystal structure **II**, and with an equatorial C3-OH as in the "minor conformer" proposed by Taylor and Zajicek.[219] Similarly, the binding mode of epothilone A was investigated by the analysis of interligand-transferred NOEs (INPHARMA method) observed in mixtures with tubulin and baccatin III as a model for Taxol. More than 19 intermolecular NOEs correlate thiazole protons with the phenyl and geminal dimethyl protons of baccatin III, as well as phenyl protons of baccatin III with C22–C25 methyl protons of epothilone.[239] This abundance of NOEs could be an indication that one or both compounds are bound in more than one position in the tubulin-binding site, or that more than one binding site is involved.[240] Nevertheless, modeling was followed up, including also structural information from the Taxol–tubulin complex derived from electron crystallography.[241a] In conclusion, the binding mode of epothilone A partially resembles the latter, with the thiazole occupying roughly the position of the 3′-benzoyl group of Taxol, stacked face to face with the imidazole ring of His227. The C3-OH is in equatorial orientation, and is not embedded in hydrogen bonds, which is in good agreement with SAR results.[215,241b] The C7-OH is located next to Thr274 and Arg282 in good agreement with

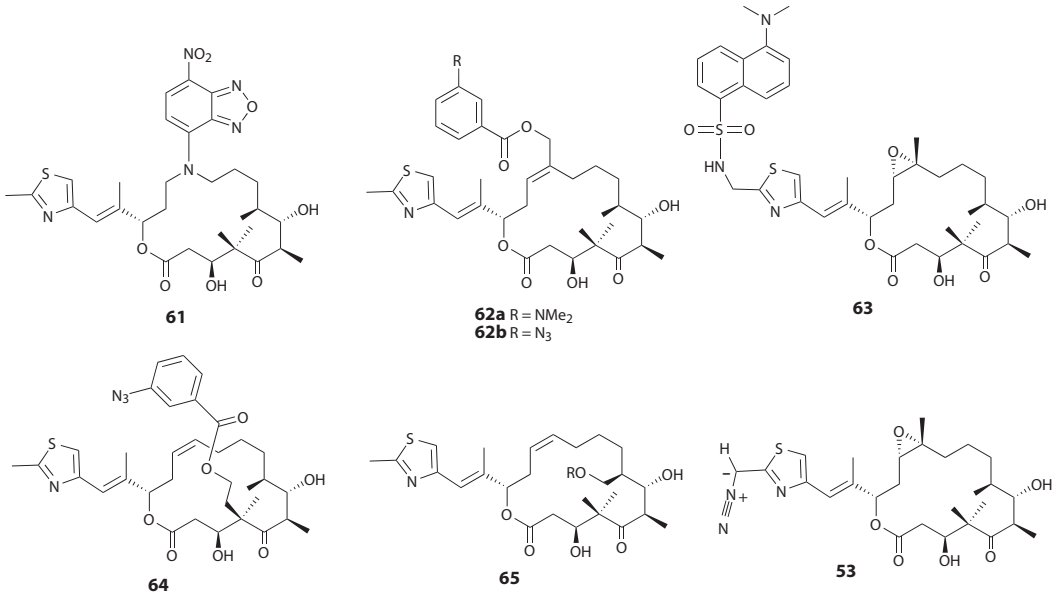

FIGURE 21.15 Fluorescent and photoreactive epothilone derivatives.

cross-resistant tubulin mutants in these positions.[241a] However, there are also critical points casting doubts on the relevance of the NMR/modeling results. Clearly, the NMR effects are mediated by protons of the tubulin, but its own structure as soluble monomer, oligomer, or MT sheets is not well defined in these NMR studies. Also, the second low-affinity binding site for Taxol[240] may be involved in the ligand exchange,[242] which has not yet been considered in this work.

In 2004, the groups of Snyder and Downing derived the conformation and binding mode of epothilone A on tubulin by electron crystallography (Figure 21.14, **IV**).[243] As reported for the structure determination of the Taxol/α,β-tubulin complex,[244] two-dimensional crystals of tubulin heterodimers were obtained by adding Zn^{2+} in the presence of an excess of epothilone A. Due to the low resolution, the structure could only be solved with the help of NMR data and extensive modeling. As expected, epothilone binds within the well-known Taxol-binding site making a series of hydrogen bonds between the protein and the C3-OH, C7-OH, 5-ketone, and the lactone carbonyl. The epoxide is folded inward, and the thiazole nitrogen forms a hydrogen bond to the imidazole of His227. This conformation and binding mode is in profound contradiction to that derived from NMR measurements in the presence of tubulin. However, it is compatible with a selection of SAR, and perfectly explains the requirement of a nitrogen *anti*-periplanar to C15 for biological activity. This is corroborated by the high activity of the conformationally locked benzothiazole and quinoline analogs,[75,154] and by the inactivity of C19 methyl-substituted thiazole and pyridine analogs, which, for steric reasons, cannot adopt this conformation. Interestingly, the opposite, a C16–C19 anti-periplanar conformation of epothilone D and B, is adopted in the crystal structures of the complex with cytochrome P450Epok,[56] the biosynthetic enzyme that introduces the 12,13-epoxide.

To date, it cannot be predicted which of the two contradictory proposals for the structure of the epothilone tubulin complex will prevail, if any. After all, the structure derived from electron crystallography also has its shortcomings, as there are antiparallel protofilaments in the crystal instead of natural parallel ones that may distort the binding site, as well as the far-reaching modeling of the epothilone conformation. Experiments to pin down the true configuration of epothilones in the binding site by photoaffinity labeling with **62b**,[245] **64**,[246] **65**,[247] and **53**[198] (Figure 21.15) have been in vain, so far. What is needed now are photolabile epothilone derivatives with high binding affinity producing short-lived reactive intermediates. Also, solid-state NMR investigations of MTs loaded with different isotope-labeled epothilones might allow new insights into the structure and alignment of epothilone in its binding site.

21.7 PRECLINICAL STUDIES

Epothilone effects, as far as they are published, have been determined mostly in athymic nude mice but occasionally also in SCID mice, nude rats, and Beagle dogs, in most cases with xenografts of human cancer cells. The data are even more heterogeneous than those with cell cultures because of differences of the methods and schedules of application and because of the kinds of cancer cells, epothilone analogs, and experimental animals used. The studies established, nevertheless, that epothilones act *in vivo*; that they inhibit human cancers, often resulting in cures of the animals; and that they are superior to Taxol and other cytostatic drugs in many cases, especially with MDR tumors. SCID mice tolerate epothilone B well at a dose of 0.3 mg/kg; at 1 mg/kg, weight loss is observed; and at 3 mg/kg, the animals show serious toxic effects (once per week, subcutaneously, vehicle 30% PEG, 70% 0.9% NaCl solution).[83]

In a preliminary study on nude mice, a dose of 0.6 mg/kg epothilone B, daily for 4 d, intraperitoneally (i.p.), killed all animals, whereas all survived treatment with 25 mg/kg epothilone D, daily for 5 d.[46] It was suggested that the epoxy group at C12/C13 may be responsible for high *in vivo* toxicity.[55] Apart from leukopenia (43% decrease of lymphocytes), no hematological or other pathological changes in various organs were seen with either drug.[46] Toxicity of epothilone B could be mitigated by an altered administration schedule: at 0.6 mg/kg, five times every second day, i.p., in DMSO, only three of seven mice died, and with the same dosage, but intravenously (i.v.), all animals

survived. While epothilone D treatment resulted in appreciable regression and even cures of human mammary and ovarian carcinoma xenografts, epothilone B had a too narrow therapeutic window for good antitumor effects. The mode of administration was later optimized, namely, i.v. by infusion over 6 h rather than by injection, using the vehicle cremophor–ethanol.[23a,56]

The efficacy of epothilones is most impressive against MDR tumors. Thus, in nude mice, epothilone D was >35,000-fold more active than Taxol against MDR human adenocarcinoma. It was also fully curative for human T-cell leukemia.[23a] A comparison of several epothilones, Taxol, and other cytostatic drugs showed superior performance of epothilone D and its C21-OH analog (dEpothilone F) in many cases.[23a,b] Epothilone D (30 mg/kg i.v.) was better than Taxol in controlling xenografts in nude mice of human solid lung, mammary, and one of two ovarian adenocarcinomas, and in particular of MDR sublines. It was inferior to Taxol, however, against colon, colon adeno, prostate adeno, and one of two ovarian adenocarcinoma lines. Complete remission was only achieved with MX-1 mammary carcinoma (as well as by Taxol). Epothilone D was superior to Taxol, with complete remission, in four human leukemias, including MDR lines, and was inferior to Taxol only in the HL-60 line. Epothilone B and epothilone B-lactam were much less successful because of their narrow therapeutic windows (but see below). The same study showed that resistance to epothilone D developed only very slowly and to low levels (twofold in 21 mo).[56] In mouse plasma, epothilone D was quickly inactivated ($t_{1/2}$ = 20 min), probably because of esterase activity, but was much more stable in human plasma ($t_{1/2} \geq 3$ h).[56] Beagle dogs fully tolerated a single dose of 2–6 mg/kg i.v. (40–120 mg/m^2); they developed diarrhea and leukopenia and lost weight at 12 mg/kg (240 mg/m^2); and 20 mg/kg (400 mg/m^2) produced severe toxic effects (e.g., necrosis of the intestinal mucosa, cell decay in the bone marrow) and was lethal.[56] At 6 mg/kg, $t_{1/2}$ was >5 h, and plasma concentrations after 24 h were 0.045 μg/mL (0.092 μM), which is 10 times the IC_{50} (0.0095 μM) for leukemia cells.[56]

Also, more effective epothilone analogs have been tested.[152] Introduction of a C9,C10 *trans* double bond in epothilone D (= dehydelone) makes the compound not only 10 times more active against MX-1 mammary carcinoma xenografts in nude mice, but also more toxic (with a maximum tolerated dose [MTD] of 3 mg/kg, vs. 30 mg/kg of epothilone D). Also, although the compound may lead to a complete remission of tumors, they often return later. Performance was much improved by also replacing the CH_3 on C12 by CF_3, and thiazole by isoxazole (fludelone and iso-fludelone), which bestows higher stability ($t_{1/2}$ = 212 min in mouse plasma, 10.5 h in human plasma; epothilone D, 46 min) and bioavailability (solubility in water: 20 μg/mL; epothilone D: 9.4 μg/mL). Thus, for example, with xenografts of slow-growing human lung carcinoma A549, two treatments with six doses of 25 mg/kg iso-fludelone administered every second day spaced 8 d apart resulted in 99.5% remission and, after two more doses, in complete elimination of the tumor (epothilone D failed to eradicate the tumor). With seven doses of 20 mg/kg administered every second day, the growth of a Taxol-resistant subline was completely suppressed, and the tumor size reduced by 24%.[152,248,249]

Another novel compound, semisynthetic C21 thiomethyl epothilone B (ABJ879), has been proposed by Novartis for a phase I clinical study.[250] It shows about the same tubulin-polymerizing activity as Taxol but is clearly more potent in blocking cell proliferation in cultures (average IC_{50} for seven human carcinoma cell lines: 0.09 vs. 4.7 nM of Taxol). The drug is fully active on MDR1 cells and lines with resistance resulting from β-tubulin mutations. In nude mice, single-dose treatment (2–3 mg/kg i.v. 6–7 d after implantation of the tumor) produces transient but long-lasting remission (25–95%). Positive effects were seen with slow-growing lung adenocarcinoma H-596, colon tumor HT-29, and large-cell lung tumor H-460. A preliminary pharmacokinetics–pharmacodynamics drug-response model has also been presented.[251] Doses of 1.5 and 1.8 mg/kg, every second week, were acceptable, but 1.5 and 2 mg/kg, once a week, caused intolerable weight losses. The drug penetrates tissues, where its level becomes 10 times higher than in plasma, and is retained there for a long time, so that plasma concentrations are not representative of tissue exposure—a fact that may be true also for other epothilone analogs.

The controversy about the efficacy of epothilone B-lactam (BMS-247550) has been fueled by decidedly positive results reported by BMS scientists.[252] In addition to various established tumor cell lines, three primary xenografts from biopsies were tested. A human ovarian carcinoma, Pat-7, from a patient who no longer responded to Taxol and other cytostatic drugs was highly responsive to epothilone B-lactam in nude mice at the optimal dose of 4.8–6.3 mg/kg, administered i.v. five times every second day (the optimal dose of Taxol is 24–36 mg/kg). The log cell kill (LCK) was 2.9 (Taxol, 0.8). The same tumor in nude rats at the optimal dose of 3 mg/kg, administered i.v. two times 8 d apart, could be eradicated in four of six animals (LCK > 5; Taxol, LCK = 2.2, no cures [0/6]). Good LCK values and growth delays were also seen in nude mice with Taxol-resistant human ovarian and colon carcinomas. Also, in several other instances of Taxol-sensitive tumors in nude mice, the animals could be cured, and high LCK values (>6.3) were seen, even when the compound was not better than Taxol. Furthermore, epothilone B-lactam gave excellent results when administered orally. At the MTD (60–80 mg/kg, five times every second day), epothilone B-lactam was highly active on the Pat-7 xenograft (LCK = 3.1, growth delay of 32.8 d); in comparison, Taxol given i.v had an LCK = 1.3, growth delay of 9.8 d, and was orally inactive. HCT116 colon carcinoma was eradicated in all eight mice treated with 90 mg/kg, five times every second day (equivalent to the best i.v. regimen). In contrast to epothilones A and B, epothilone B-lactam is completely stable in rodent and human plasma and in liver microsomal preparations, and shows clearly reduced toxicity.[252]

Epothilone D, too, was reported to be active in rats and Beagle dogs after oral administration.[253] The drug was well tolerated, and >50% (dogs) and 10–20% (rats) were found in the blood stream, with half-lives of 9–11 h (dogs) and 6 h (rats), respectively. A study by the Sloan-Kettering Institute for Cancer Research yielded far fewer positive results for epothilone B-lactam compared with epothilone D.[55] Thus, an i.v. infusion of 6 mg/kg of the B-lactam "somewhat" inhibited the growth of MX-1 mammary tumor xenografts in nude mice, but no remission was seen, and not much improvement was observed with doses near the MTD (9 mg/kg). Similar results were obtained with K562 leukemia, but cures were observed when the animals were treated subsequently with C21-OH epothilone D (30 mg/kg).

A study, to date only *in vitro*, indicates that the dosing regime could have a massive influence on tumor angiogenesis and metastasis.[254] Human vascular endothelial cell lines were more efficiently killed by a "metronomic" administration of cytostatic drugs, including epothilone B; that is, by extended (144 h) application of low (10–100 pM) concentrations rather than high doses for a short time (24 h). IC_{50} values were thus reduced to 25–140 pM, although those for tumor cells and fibroblasts remained high (550 pM to >1 nM); thus this strategy appears to selectively affect endothelial cells.

Not much has been published about the metabolic fate of epothilones in animals. Degradation of epothilone B (10 mg/kg i.v.) in the liver of nude mice was studied by capillary high-performance liquid chromatography combined with mass spectrometry.[255] One hour after administration, three metabolites could be recovered and identified guided by a key fragment at *m/z* 166, an acylium ion derived from the very stable thiazole side chain. The following degradation pathway was reconstructed: opening of the epoxide; opening of the macrolactone ring to the hydroxycarboxylic acid; reduction of the C5-keto group, and reaction of the C5-hydroxy group with the carboxylic acid group to give a 6-membered lactone ring or, after conjugation with taurine, to yield a 6-membered lactam ring at the end of the chain.

21.8 CLINICAL STUDIES

Eight epothilone analogs have been introduced into clinical studies (Figure 21.16), two of them just five years after the discovery of their Taxol-like mechanism of action. Epothilone B (**1b**, EPO906, Patupilone, Novartis) started phase I trials, beginning early in 1999, followed by phase II[256,257,259] and, recently, phase III. Epothilone B-lactam (**22**, BMS-247550, Ixabepilone, Bristol-Myers Squibb) was started in phase I trials in October 1999, and completed in September 2000; phase I trials in

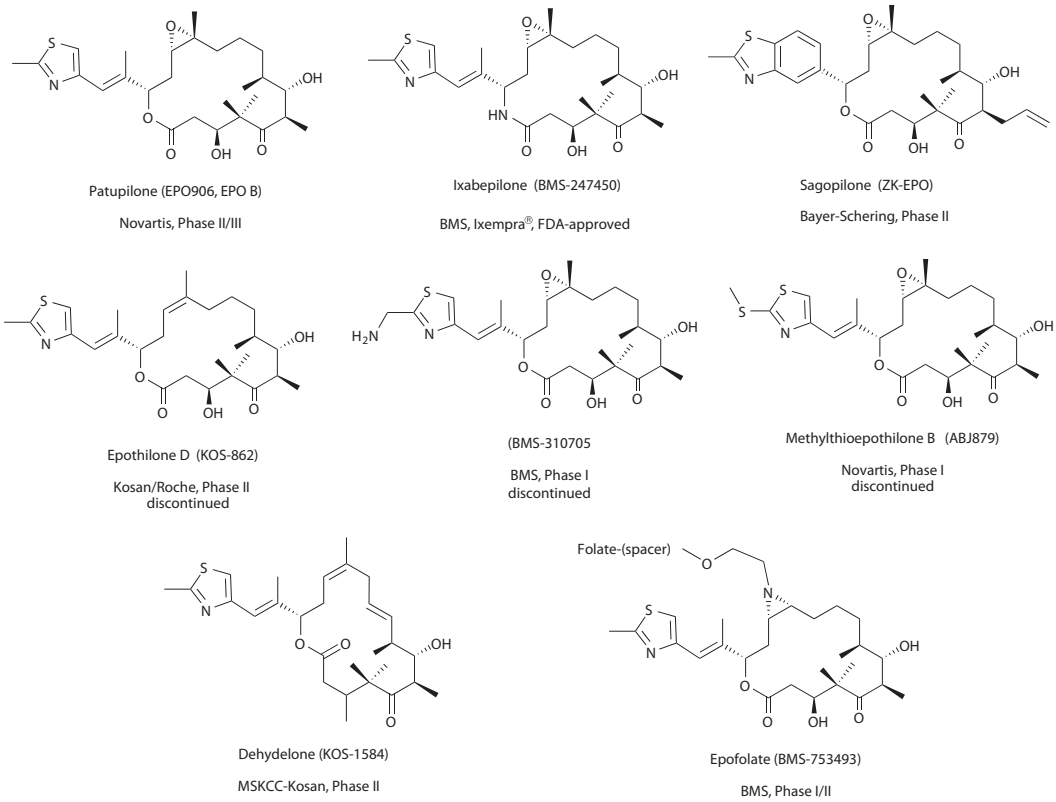

FIGURE 21.16 Epothilones in clinical trials.

children started in April 2002; phase II trials have been ongoing since February 2001, and in 2002, there were 15 National Cancer Institute-sponsored phase II studies; it progressed through phase III.[11a,b,k] This is the only epothilone analog so far that has obtained approval (FDA, October 2007) for the treatment of advanced and metastatic breast cancer resistant to taxanes and anthracyclines, alone or in combination with capecitabine, and is now on the market under the name Ixempra.

The epothilones have been tested in patients with many different carcinomas, mostly solid tumors, including MDR cases and, as such, difficult to treat (e.g., cervical adenocarcinomas of the squamous type).[258,259] The responses have varied between complete and partial remission, tumor stabilization, reduction of CA 125 levels (cancer antigen found at elevated levels in the blood of many cancer patients, especially those with ovarian cancer), and continued growth. The individual epothilone analogs appear to differ in the MTDs, the dose-limiting toxicities (DLTs), the side effects, half-lives in patients, and efficacy. It may still be too early to assess the relative effectiveness of the drugs conclusively. Although most data are only published as abstracts, several excellent reviews summarize the many available results,[11] so that details need not be repeated here.

21.8.1 Epothilone B-Lactam (BMS 247550, Ixabepilone, Ixempra)

Initially, the MTD of epothilone B-lactam was estimated to be 6 mg/m^2 when administered i.v. over 1 h, daily for 5 d every 3 wk.[260] At 8 mg/m^2 dose-limiting neutropenia was seen, but many patients tolerated higher doses when the drug was administered in combination with filgrastim (granulocyte colony-stimulating factor, which mitigates myelosuppression and neutropenia). Other side effects were peripheral neuropathy, fatigue, nausea, stomatitis, myalgia, and arthralgia, usually in mild

forms.[11a,260,261] DLT was neutropenia. Two patients died of sepsis, probably as a consequence of neutropenia. In earlier phase II studies, mild to moderate, mostly reversible sensory and motor neuropathies (especially serious when too high a dose was chosen: 50 mg/m^2 every 3 wk[262]) caused much concern.[262–265] Efforts to predict neurological complications by applying various tests were not fully satisfactory.[266] The acceptable weekly dose may be 20–30 mg/m^2. The drug was quickly absorbed by the tissue, where its half-life was 24–48 h, whereas $t_{1/2}$ in the plasma was only 16.8 h. This was also supported by a study that analyzed effects in peripheral blood mononuclear cells (PBMCs) in patients.[267] It showed that MTs formed bundles 1 h after administration (at the already toxic dose of 50 mg/m^2 i.v. over 1 h, once a week every 3 wk, in 70% of cells; at 40 mg/m^2 in 63%), but after 24 h, the effect was much reduced (to 25% and 16–23%, respectively). Cytotoxic effects followed MT bundling with a time delay but were expressed within 24 h: cleavage of poly(ADP-ribose)polymerase, indicating cell death (apoptosis and necrosis), was at base level after 1 h (3%) but rose to 28% of cells after 24 h. For the treatment of progressive metastatic prostate cancer, a dose of 35 mg/m^2 i.v. over 3 h, once every 3 wk (five cycles) in combination with estramustine phosphate (an estradiol analog without affinity to the estradiol receptor) is recommended.[261] Positive responses and decline in prostate-specific antigen levels were seen in 40–60% of patients. It appears that in aqueous solution, the epothilone B-lactam rearranges by an intramolecular reaction of the amide group with the epoxide [273] and becomes inactive, so that the timing of treatment has to be carefully planned.

Eventually, the safe dosage turned out to be 40 mg/m^2 i.v., once every 3 wk, formulated in Cremophor-EL, initially recommended for phase II but also used in phase III and in clinical practice (breast cancer). DLT was mainly up to grade 4 neutropenia and grade 1–2 peripheral neuropathy. It appears that neutropenia can be mitigated by an extended infusion time, namely, 3 h instead of 1 h.[268,269] The explanation may be that a sustained blood plasma level of ixabepilone above 15 ng/mL favors neutropenia.[270] A study on Japanese patients with various tumors showed no deviations of their responses to ixabepilone from what is known for American and European patients. This result was indeed to be expected because the drug is decomposed by the Cyp3A4 system present in almost all humans.[268] In a phase I study, 18 children, aged 2–18 yr, with recalcitrant solid tumors were treated with 3.5 up to 10 mg/m^2 ixabepilone i.v. for 1 h daily for 5 d every 3 wk.[271] DLT began to appear at 10 mg/m^2 (one case of neutropenia), but 8 mg/m^2 was well tolerated. Pharmacokinetics resembled those of adults: $t_{1/2} = 14.8 \pm 6$ h, CL 29.3 L/h · m^2. As pharmacokinetic data vary with the application schedule and the individual patient, the published studies on adults are not strictly comparable. In one study,[270] a linear relationship was seen between dose (7.4–56 mg/m^2 i.v., 1 h every 3 wk), C_{max}, and *AUC*. The plasma concentration declined in a bi-(to tri-)phasic exponential pattern, with a steep initial segment (within 10 h, suggesting rapid tissue binding) followed by a much flatter branch (for the next 60 h due to degradation and excretion of the products *via* feces). With doses of 14.6/40/56 mg/m^2, $t_{1/2}$ was 17–19/34–37/32–38 h, C_{max} 83–142/327–426/834–897 ng/mL, CL 17.5–19.5/17.9–23.2/20.9–21.6 L/h · m^2, V_{ss} 775–1581/809–948/636–679 L/m^2 (suggesting preferential distribution of the drug in tissues), and *AUC* 747–836/1756–2643/2709–2937 h · ng/mL. Also, in another study,[268] a higher than proportional increase of C_{max} between 40 and 50 mg/m^2 was found which may explain the DLT of 50 mg/m^2. In this study, 15–50 mg/m^2 i.v., 3 h every 3 wk, were tested. With 15/40/50 mg/m^2, $t_{1/2}$ was 36/43/29 h; C_{max} 62/313/583 ng/mL; CL 49/32/12 L/h · m^2, V_{ss} 1912/1171/365 L/m^2; and *AUC* 567/2301/6324 ng · h/mL. Again, there was a fast initial decline of the plasma concentration followed by a much slower reduction over a long time. With all tested doses, the plasma concentration soon fell to <4% of the initial C_{max}. An early study on the pharmacokinetic parameters of ixabepilone determined for the doses of 14.8/40/50 mg/m^2 (i.v., 1 h every 3 wk), $t_{1/2}$ 42/35/40 h, C_{max} 56/312/546 ng/mL, CL 46.3/21.1/25.8 L/h · m^2, V_{ss} 2525/1213/932 L/m^2, and *AUC* 319/2558/2242 ng · h/mL. The values found in cycle 2 were similar but not identical. The plasma concentration 8 h after infusion was <10% of C_{max}. The recommended dose for phase II studies was clearly 40 mg/m^2. Bioavailability after oral application was 41% (solution) and 37% (suspension), and the plasma concentration profile (doses 15–50 mg/m^2) was very similar to that

after i.v. infusion. Tubulin polymerization in PBMCs, a measure of ixabepilone effects, was around 10% half an hour after oral administration (25 mg/m^2 solution or 50 mg/m^2 suspension) and was thus lower (or slower!) than after i.v. injection (20% for 25 mg/m^2 within 30 min).[269]

A first analysis of the relation between ixabepilone plasma concentration and the effects on tubulin polymerization in normal and tumor cells (after an i.v. infusion of 40 mg/m^2 within 1 h)[272,273] showed that MT bundle formation (MBF, as an easy to determine parameter) in PBMCs is fast, reversible, and dose- and time-dependent. It reaches a maximum shortly after infusion (around 50% of cells) and falls back to base line within 45 h. MBF in tumor cells is higher than in PBMCs 24–72 h after infusion, but then also goes down to zero. The percentage of MBF in PBMCs correlates with severity of side effects: an MBF of 53% at the end of infusion (corresponding to a plasma concentration of 625 ng/mL) appears to correlate positively with the risk of 2–4 grade neutropenia, one of 41% with grade 0–1. This suggests that a longer infusion time could be less harmful. While CL correlates positively with MBF in tumor cells, correlation of C_{max} and *AUC* is negative reflecting various complications in the transfer of the drug from blood to tumor (e.g., accessibility, uptake, presence of different types of β-tubulin).

While MBF in PBMCs is proportional to ixabepilone plasma concentration over a wide dose and exposure range, there is no general correlation with MBF in tumor cells, so that the PBMC parameter is not a suitable measure of efficacy of the drug. The important question: who would possibly profit from ixabepilone treatment, is not yet definitely settled. Various biochemical processes have been considered in breast cancer (and other) patients for predictive significance, however often with too small sample sizes. After tubulin polymerization, the terminal amino acid, tyrosine, is removed from α-tubulin, and the penultimate glutamic acid becomes exposed. Also Lsy40 is then posttranslationally acetylated. Both events are indicators of polymerization. Among 67 patients with renal cell carcinoma, after exposure to ixabepilone (6 mg/m^2 i.v., days 1–5 every 3 wk), α-tubulin acetylation rose to 2- to 100-fold, Glu tubulin to 2- to 25-fold, and overall α-tubulin by a factor of 2–10 indicating a stimulation of tubulin synthesis by ixabepilone, and proving that the drug really entered the tumor cells.[274] Yet α-tubulin acetylation was not found to be a reliable indicator of therapeutic efficacy in breast cancer patients (nor was the tau1 or p59 level of expression).[275, 276] In contrast, the expression of estrogen receptor 1 (ER) appears to be a good indicator of ixabepilone success. In breast cancer patients, its level correlates inversely with the response to the drug. The level of ER expression can, however, not be determined reliably by biochemical tests but has to be controlled by gene expression profiling. In this way, a 37% positive and a 92% negative predictive value for the appearance of metastases could be achieved.[277–280] Another indicator in breast cancer cases is the receptor tyrosine kinase, HER2 (= Neu = erbB2), which, due to gene amplification, is 10- to 100-fold overexpressed in 30% of patients. This means a poor prognosis.[281] HER2 may be blocked by herceptin (= trastuzumab), a humanized monoclonal antibody. At least in xenografts (mice), a combination of ixabepilone and herceptin produced substantial therapeutic synergism.[282] The ultimate tool for predicting breast cancer response to ixabepilone will probably be the analysis of gene expression profiles. Already, it is possible to differentiate between breast cancer patients who run a high risk or a low risk to develop metastases, and thus to restrict chemotherapy to high-risk patients and save the others from unnecessary suffering and high costs.[277,283] In 18 human breast cancer cell lines, about 200 genes were found to correlate positively or negatively with ixabepilone sensitivity. This number could be reduced to two sets of 26 and 20 genes that predicted response to ixabepilone.[280] In a study by the Netherlands Cancer Institute, the gene expression profiles of 78 breast cancer patients were analyzed. From biopsies, total RNA was isolated, and the cDNA produced from it was hybridized with 25,000 gene fragments. Around 5000 genes showed modified expression in comparison with healthy women, 231 of which were significant for the prediction of a later relapse, but 70 genes were sufficient for a reliable risk assessment. The later international evaluation included more than 1000 patients. About 45% were classified as low risk, and 96% of those would survive the following 10 yr without metastases. Far less than 1% of them would profit from chemotherapy. Of the high-risk group, only 50% would survive without relapse, but also half of the

remaining 50% can be saved by hormone and chemotherapy. Difficult to treat patients with triple negative (ER–PR–HER2) breast cancer still respond to ixabepilone. In the rather common case of overexpression of those receptors, combination with a targeted agent is promising.[282] Thus in cell cultures, cytostatic trastuzumab (= herceptin) raised the cytotoxic effect of ixabepilone twofold. A similar result was obtained with xenografts.[281] In another study on cultured adult bovine aortic endothelial cells and an *in vivo* angiogenesis model, ixabepilone showed better antiangiogenetic properties than paclitaxel, and this activity (and antitumor efficacy) was further stimulated by combination with bevacizumab (= Avastin), which binds to and thus inactivates VEGF.[274] A significant synergism was seen in colon GEO tumors between ixabepilone and cetuximab (= Erbitox), an inhibitor of an EGF receptor, a tyrosine kinase overexpressed in 80% of cells in colon carcinomas.[285] Of particular interest is the combination of ixabepilone and capecitabine, a prodrug of 5-fluorouracil, which blocks DNA synthesis. While ixabepilone was modestly active (LCK 0.8) on xenografts of human colon GEO tumors (mice), together with capecitabine (in this case, inactive alone: LCK 0.4), a substantial therapeutic synergism (LCK 1.9) was achieved.[285] In patients resistant to anthracyclines and taxanes, far better results were obtained with a combination of ixabepilone and capecitabine than with each drug by itself.[273] This strategy is limited by the fact that 75% of such patients are also resistant to capecitabine. But ixabepilone was still active in 50% of 126 breast cancer patients with metastases, who no longer responded to paclitaxel, anthracycline, and capecitabine.[286] In a phase III study on 752 patients with metastatic breast cancer pretreated with taxanes and anthracyclines, treatment with ixabepilone plus capecitabine clearly resulted in better responses than with capecitabine alone.[287,288] Results of this kind were decisive for FDA approval of ixabepilone. With the same combination, 62 metastatic breast cancer patients, 44% of them ER–PR–HER2 negative, showed encouraging responses. A dosage of 40 mg/m^2 ixabepilone, i.v. 3 h, every 3 wk plus 2000 mg/m^2 capecitabine, p.o. on days 1–14, every 3 wk is recommended with manageable side effects.[289,290] Caution is indicated with liver dysfunction cases. Ixabepilone then should be reduced to 10 mg/m^2 every 3 wk.[291] While the efficacy of ixabepilone in the presence of MDR proteins is somewhat lower than that of epothilone B, this turns out to be an advantage, because tissues of the gastrointestinal tract protect themselves from harmful drugs by the Pgp pump.[284] This may explain why the DLT of epothilone B is diarrhea, and not neutropenia.

Another type of cancer that responded favorably to ixabepilone was hormone refractory prostate cancer in patients with metastases but without prior chemotherapy.[292–294] Combination with estramustine phosphate turned out to be superior to ixabepilone alone. Also, because there is no cross-resistance between epothilones and taxanes, application of, for example, ixabepilone and docetaxel, appears to be a meaningful approach. In fact, some patients benefit from a taxane after negative results with ixabepilone.[294] Positive results are also reported for ixabepilone treatment of patients with taxane[262,276] and anthracycline[264] resistant MBC, and with NSCLC.[265] After it was discovered that many types of cancer, for example, many forms of ovarian, lung, colon, and breast cancers, overexpress the folate receptor, drug conjugates with folic acid were used to administer cytotoxic or diagnostic agents more directly to tumors in order to achieve a higher drug density in the tumor and to reduce side effects. A conjugate with epothilone-12,13-aziridine (Section 21.5.2; Figure 21.10) alone or in combination with ixabepilone or bevacizumab gave encouraging results in cell cultures and in rodents.[10g,201] The conjugate was introduced in phase I and II clinical evaluations. Conjugates of another myxobacterial cytotoxic compound, tubulysin, that leads to decay of MTs, are equally very promising.[295]

21.8.2 Epothilone B (EPO906, Patupilone)

Epothilone B was chosen very early by Novartis for clinical development, and has now reached phase III trials. It is the more efficacious one of the two main fermentation products of *S. cellulosum* strain So ce90, and has been used in many basic studies on the mechanism of action of the epothilones as well as in preclinical and clinical studies. Excellent reviews on these topics are available.[11]

The nonmodified natural product is more sensitive to cleavage by esterases than ixabepilone, yet is much more stable in humans than in rodents: blood concentration declines in a multiphasic pattern with an initial $t_{1/2}$ of 7 min, followed by a terminal $t_{1/2}$ of 4–5 d.[257,296] A rapid tissue distribution is also indicated by a high V_{ss} of >1000 L/m^2.[257] Epothilone B is highly resistant to export from cells, and was not effectively recognized by any one of seven tested multidrug transporters including Pgp[297] (which, as already pointed out, is not necessarily an advantage). Also, it is much more toxic than ixabepilone and, while being more efficacious, has a narrower therapeutic window. Patupilone was applied in the clinic i.v. with short infusion times. It may be formulated in polyethylene glycol-300 (instead of Cremophor-EL), which minimizes carrier-related adverse effects.[294] Various time schedules were tested. In phase I trials, doses were usually very low: 0.5 to 2.5 (MTD) mg/m^2, weekly for 3 wk and the fourth week off.[257,296,298,299] The recommended dose for phase II was 10 mg/m^2 (MTD) i.v., 20 min every 3 wk.[300–304] DLT was mostly diarrhea, as well as gastrointestinal hemorrhages, nausea, hyponatremia, but only rarely hematological problems. Even though patupilone treatment was not yet fully optimized in those trials, many cancers responded more or less favorably to the drug, for example, ovarian, breast and colon cancers,[296] NSCLC,[302,303] hepatic cell carcinoma,[304] colorectal,[301] gastric,[305] and hormone refractory prostate cancers.[294,306] Patupilone crosses the blood–brain barrier and acts on recurrent or progressive brain metastases.[303,307] In some trials, patupilone was combined with other anticancer drugs, such as capecitabine, gemcitabine, or estramustine with good results. There has been little reported about the drug recently, so it was concluded that it had been dropped from further development,[10t] but the compound is still found in the portfolio of Novartis. In fact, it has been reported to be in a phase III trial with platinum-resistant ovarian cancer. There was no excretion of unaltered compound *via* the kidneys (<0.1%).

21.8.3 Epothilone D (KOS-862)

Epothilone D is the immediate biosynthetic precursor of epothilone B and is obtained in poor yields from fermentations of *S. cellulosum* strain So ce90. Larger quantities are available by total synthesis, by fermentation of a blocked mutant,[17] or a recombinant strain of the myxobacterium *M. xanthus* in which the gene (*P450 EpoK*) of the epoxidase is deleted.[47,48] Several phase I trials have been performed beginning in October 2001, and phase II studies on metastatic breast cancer, NSCLC, and colorectal cancer were initiated in December 2003 through a collaboration between Kosan and Hoffmann-La Roche. The project was discontinued in October 2007 at the time of FDA approval of ixabepilone. Details of preclinical and early phase I studies are summarized in an excellent review.[11h] While epothilone D is quickly cleaved in the blood of various rodents, it is fairly stable in dog and human plasma in which it is bound to proteins.[308] In animal experiments, p.o. administration was successfully used, but in clinical trials the drug was always administered i.v. Permissible doses were much higher than with ixabepilone and patupilone. The recommended dose for phase II is 100 mg/m^2 i.v., 90 min weekly in 3 of 4 wk (MBC).[309] About 120 mg/m^2 once every 3 wk was also possible with tolerable adverse events, but 125 mg/m^2 every 3 wk was not tolerated. Side effects were mainly neurological: ataxia, cognitive and perceptual disturbances, and peripheral neuropathies, but other effects included anemia, nausea, diarrhea, fatigue, and neutropenia. Those events, however, were not cumulative and, as a rule, resolved within 1 wk. The CNS effects are obviously connected with the fact that the drug easily crosses the blood–brain barrier and accumulates and persists in the brain for longer periods. In a phase II study on 37 patients suffering from metastatic breast cancer conducted between February 2004 and April 2005, four patients (14%) experienced a PR, two of them with hepatic metastases (tumor reduction >50%). One further patient showed an unconfirmed PR.[309] Pharmacokinetic data are similar to those reported for other epothilones, and the DLT was neurotoxicity. Similar results were reported for a second trial with 13 MBC patients.[310] After it was discovered that certain disorders of the brain are connected with a decay of MTs in the neurons, the observed good brain penetration of epothilone D and its long half-life (in sharp contrast to paclitaxel) prompted studies on its influence on CNS disturbances. The results are

potentially of great practical consequence. In a schizophrenia model with STOP-null mice (STOP is a MAP contributing to MT stability), epothilone D had a dramatic effect on mouse behavior parallel to improvements in synaptic functions.[311] In a recent patent,[312] BMS claims beneficial effects of epothilone D on tau-associated diseases and in particular Alzheimer's disease. This claim is based on the good brain penetration and retention of epothilone D, on experiments with a mouse model, and the present knowledge about Alzheimer's disease.[313] The animals showed behavioral and brain-histological improvements after epothilone D treatment. Most importantly, in both mouse models, the desired effects were observed at very low, subtoxic doses of epothilone D.

21.8.4 ZK-EPO (Sagopilone)

ZK-EPO was originally invented by the Schering company in Berlin (Schering AG; *sag*opilone) and is now in clinical development by Bayer-Schering. It is a fully synthetic compound produced in 22 steps with a final overall yield of 0.9%,[155] and was chosen from 350 active synthetic variants for clinical development because of its outstanding preclinical performance reflecting high efficacy, rapid tissue distribution, resistance to export from cells by efflux pumps and thus good activity on MDR cells, and, in general, an acceptable therapeutic window.[155,314] A detailed review on sagopilone including the clinical studies is available.[10e,11f] Sagopilone has been in phase I clinical trials since 2004/2005,[306,307] and in phase II since 2005/2006 covering a variety of cancers.[10e,11f] Some aspects are of particular interest. Thus, sagopilone rapidly crosses the blood–brain barrier, at least in mice and rats, and reaches almost the same concentration in the brain as in the plasma (the ratio *AUC* brain/ *AUC* blood was 0.8). The drug was active on intracranial xenografts of human brain tumors and brain metastases of various cancers, and therefore is being studied in a phase II trial on patients with gliablastoma.[317,318] In a mouse model, sagopilone inhibited the growth of bone metastases as well as bone resorption.[319] Again this effect is being investigated in phase II clinical trials. Details about the administration of the drug and its behavior in the human body are reported in publications of the first phase I study.[314–316] As the compound is more soluble in water than ixabepilone, it can be formulated without Cremophor-EL, so avoiding alleviating premedication. Standard administration was i.v. 30 min once every 3 wk with escalating doses beginning with 0.6 mg/m^2. The MTD was 22 mg/m^2 and the recommended dose for phase II was 16.5 mg/m^2 (much lower than for ixabepilone). The DLT was peripheral sensory neuropathy. Because with ixabepilone neuropenia could be mitigated by a longer infusion time; nine patients were treated with a 3-h infusion, but without a significant difference in the side effects. Other adverse events were nausea, vomiting, diarrhea, hyponatremia, and in some instances, ataxia of CNS origin (disturbance of coordinated movement), which was attributed to transfusion of the drug into the brain. Neutropenia played only a minor role. Pharmacokinetic data still are preliminary, but so far much as expected. After infusion, the plasma concentration drops very quickly ($t_{1/2} = 3$ min), which is followed by a long terminal phase ($t_{1/2} = 52–83$ h). The peak plasma concentration after the 3-h infusion was five times lower than after the 30-min infusion. Also, a V_{ss} of 2309–3765 L, and a CL of 665–1232 mL/min suggested a fast tissue distribution and a slow release. Serum binding and accumulation was not evident. The 53 patients in the study suffered from many different types of cancer and were all pretreated. Yet three PRs (partial responses, two breast and one renal cell cancer) and 11 SDs (stable diseases, for 42–161 d) were achieved (five head and neck cancers, two cholangiocarcinomas, and one of each adrenal gland, NSCLC, uveal melanoma, and ovarian cancer). In a recent patent application, claims were also made for the treatment of osteoporosis and related diseases by ZK-EPO-type compounds.[320]

21.8.5 21-Aminoepothilone B (BMS-310705)

A water-soluble, esterase-resistant derivative, 21-aminoepothilone B was made public in 2002[321] and tested in phase I clinical trials[11i,322,323] but was then shelved in favor of ixabepilone. In cell cultures, over 25% of cells showed apoptosis 24 h after a 1 h exposure to 0.05 μM of the drug, which

was better than with paclitaxel.[91] Apoptosis was induced *via* the mitochondrial pathway. An acceptable application schedule in the clinic was 40 mg/m^2 i.v., 15 min every 3 wk. In one study,[322b] a CR was obtained in one of five NSCLC patients and PRs in one of six ovarian, one of three breast, and no responses in eight colon, seven melanoma, and four renal cancers. In a second study,[323] PRs were observed in one of three breast, one stomach, and no responses in six colon, four ovarian, two cervix, and two pancreas cancer cases. Side effects were usually tolerable, mainly neutropenia (DLT), sensory neuropathy, and diarrhea (DLT). Preliminary pharmacokinetics were dose-dependent. After a dose of 40 mg/m^2 (30 mg/m^2), $t_{1/2}$ was 42 (33) h, C_{max} 3936 (3433) ng/mL, CL 277 (283) mL/min · m^2, V_{ss} 433 (494) L/m^2, and *AUC* 2823 (2105) ng · h/mL.

21.8.6 Dehydelone (KOS-1584)

A derivative of epothilone D, 9,10-didehydro epothilone D (dehydelone), entered the clinic by the end of 2004. The drug is formulated with cyclodextrin. In two phase I trials, administration was i.v., for 1 and 3 h, respectively. The dosage was rather low, either 0.8–7.5 mg/m^2 on days 1, 8, and 15 every 4 wk,[324] or 0.8–11.3 mg/m^2 once every 3 wk.[325] With these regimes, the MTD was not reached. Dehydelone is more active, more stable, and shows better tumor penetration than epothilone D. Several cases of SD with various tumors were achieved in the trials. Adverse effects were mainly gastrointestinal: diarrhea, nausea, anorexia, constipation, but no neutropenia and—in contrast to epothilone D—no neurotoxicity or CNS effects at these low doses. The preliminary pharmacokinetic data show, at a dose of 5 mg/m^2, a $t_{1/2}$ of 17.7–18.5 h, a C_{max} of 78–122 ng/mL, a V_{ss} of 504–741 L, a CL of 19.7–30 L/h, and an AUC_{tot} of 631–688 ng h/mL. MBF at the end of infusion was lower (40–50%) than with epothilone D, but then also the dosage was very different. A derivative of dehydelone, fludelone (26-trifluordehydelone, KOS-1591), seems to have a much better therapeutic index than dehydelone, at least in mouse experiments.[10n,r,111,248]

ACKNOWLEDGMENTS

We thank all members of the former groups of Natural Product Biology, Natural Product Chemistry, the Bio-Plant and Instrumental Analytics at the GBF (now HZI) for their contributions in the epothilone project. Financial support from Bristol-Myers Squibb and the Fonds der Chemischen Industrie is gratefully acknowledged.

REFERENCES

1. Höfle, G., Biologically active secondary metabolites from myxobacteria—Isolation and structure elucidation, in *Scientific Annual Report of the GBF*, Walsdorff, H.-J., Ed., Braunschweig, Germany, 1991, pp. 65–68.
2. Gerth, K., Bedorf, N., Höfle, G., Irschik, H., Reichenbach, H., Epothilones A and B: Antifungal and cytotoxic compounds from *Sorangium cellulosum* (Myxobacteria), *J. Antibiot.*, 49, 560, 1996.
3. Höfle, G., Bedorf, N., Steinmetz, H., Schomburg, D., Gerth, K., Reichenbach, H., Epothilone A and B—Novel 16-membered macrolides with cytotoxic activity: Isolation, crystal structure, and conformation in solution, *Angew. Chem. Int. Ed.*, 35, 1567, 1996. The stereochemical assignments of the 22-Me and 23-Me have to be interchanged; see Refs. 220 and 237.
4. Hardt, I.H., Steinmetz, H., Gerth, K., Sasse, F., Reichenbach, H., Höfle, G., New natural epothilones from *Sorangium cellulosum*, strains So ce90/B2 and So ce90/D13: Isolation, structure elucidation, and SAR studies, *J. Nat. Prod.*, 64, 847, 2001.
5. Höfle, G., Bedorf, N., Gerth, K., Reichenbach, H., German Patent 4138042, filed Nov. 11, 1991, granted Oct. 14, 1993; World Patent 9310121 filed Nov. 19, 1992.
6. Reichenbach, H., Höfle, G., Biologically active secondary metabolites from myxobacteria, *Biotech. Adv.*, 11, 219, 1993; Höfle, G., Reichenbach, H., The biosynthetic potential of the myxobacteria, in *Sekundärmetabolismus bei Mikroorganismen*, Kuhn, W., Fiedler, H.-P., Eds., Attempto Verlag, Tübingen,

1995, pp. 61–78; Reichenbach, H., Höfle, G., Myxobacteria as producers of secondary metabolites, in *Drug Discovery from Nature*, Grabley, S., Thiericke, R., Eds., Springer-Verlag, Berlin Heidelberg, 1999, pp. 149–179.

7. Lavelle, F., What's new about new tubulin/microtubules binding agents? *Exp. Opin. Invest. Drugs*, 4, 771, 1995.
8. Bollag, D.M., McQueney, P.A., Zhu, J., Hensens, O., Koupal, L., Liesch, J., Goetz, M., Lazarides, E., Woods, C.M., Epothilones, a new class of microtubule-stabilizing agents with a Taxol-like mechanism of action, *Cancer Res.*, 55, 2325, 1995.
9. (a) Nicolaou, K.C., Roschangar, F., Vourloumis, D., Chemical biology of epothilones, *Angew. Chem. Int. Ed. Engl.* 37, 2014, 1998; (b) Mulzer, J., Martin, H.J., Berger, M., Progress in the synthesis of chiral heterocyclic natural products: Epothilone B and tartrolon B, *J. Heterocycl. Chem.*, 36, 1421, 1999; (c) G. Höfle, Epothilone—A natural product on the road to becoming a medicine, in *Scientific Annual Report of the GBF*, Jonas, R., Ed., Braunschweig, Germany, 1999/2000, pp. 21–34; (d) Altmann, K.-H., Bold, G., Caravatti, G., End, N., Flörsheimer, A., Guagnano, V., O'Reily, T., Wartmann, M., Epothilones and their analogs—potential new weapons in the fight against cancer, *Chimia*, 54, 612, 2000; (e) Altmann, K.-H., Wartmann, M., O'Reilly, T., Epothilones and related structures—A new class of microtubule inhibitors with potent *in vivo* antitumor activity, *Biochim. Biophys. Acta*, 1470, M79, 2000; (f) Mulzer, J., Epothilone B and its derivatives as novel antitumor drugs: Total and partial synthesis and biological evaluation, *Monatsh. Chem.*, 131, 205, 2000; (g) Winssinger, N., Nicolaou, K.C., Epothilones and sarcodictyns: From combinatorial libraries to designed analogs, *Am. Chem. Soc.*, chap. 9, 148–170, 2001; (h) Altmann, K.-H., Microtubule-stabilizing agents: A growing class of important anticancer drugs, *Curr. Opin. Chem. Biol.*, 5, 424, 2001; (i) Stachel, S.J., Biswas, K., Danishefsky, S.J., The epothilones, eleutherobins, and related types of molecules, *Curr. Pharm. Des.*, 7, 1277, 2001; (j) Nicolaou, K.C., Ritzén, A., Namoto, K., Recent development in the chemistry, biology and medicine of the epothilones, *Chem. Commun.*, 1523, 2001; (k) Flörsheimer, A., Altmann, K.-H., Epothilones and their analogs—A new class of promising microtubule inhibitors, *Expert Opin. Ther. Patents*, 11, 951, 2001; (l) Wartmann, M., Altmann, K.-H., The biology and medicinal chemistry of epothilones, *Curr. Med. Chem. Anti-Cancer Agents*, 2, 123, 2002; (m) Altmann, K.-H., Epothilone B and its analogs—A new family of anticancer agents, *Med. Chem.*, 3, 149, 2003; (n) Mulzer, J., Martin, H.J., Lessons learned from macrolide synthesis, *Chem. Rec.*, 3, 258, 2004; (o) Rivkin, A., Cho, J.S., Gabarda, A.E., Yoshimura, F., Danishefsky, S.J., Application of ring-closing metathesis reactions in the synthesis of epothilones, *J. Nat. Prod.*, 67, 139, 2004; (p) Gerth, K., Pradella, S., Perlova, O., Beyer, S., Müller, R., Myxobacteria, proficient producers of novel natural products with various biological activities past and future biotechnological aspects with the focus on the genus *Sorangium*, *J. Biotechnol.*, 106, 233, 2003; (q) Vite, G.D., Borzilleri, R.M., Kim, S.-H., Regueiro-Ren, A., Humphreys, W.G., Lee, F.Y.F., Epothilones A and B: Springbord for semisynthesis of promising antimitotic agents, in *Anticancer Agents—Frontiers in Cancer Chemotherapy*, Ojima, I., Vite, G.D., Altmann, K.-H., Eds., ACS Symposium Series 796, American Chemical Society, Washington, DC, 2001, p. 148.
10. (a) Altmann, K.-H., Cachoux, F., Feyen, F., Gertsch, J., Kuzniewski, C.N., Wartmann, M., Natural products as leads to anticancer drug discovery: Discovery of new chemotypes of microtubule stabilizers through reengineering of the epothilone scaffold, *Chimia*, 64, 8, 2010. (b) Altmann, K.-H., The epothilones: An outstanding family of anti-tumor agents, in *Progress in the Chemistry of Organic Natural Products*, Kinghorn, A.D., Falk, H., Kobayashi, J., Eds., Springer, Wien, 2009; (c) Hunt, J.T., Discovery of ixabepilone, *Mol. Cancer Ther.*, 8, 275, 2009; (d) Borzilleri, R.M., Vite, G.D., Case history: Discovery of ixabepilone (Ixempra™), a first-in-class epothilone analog for treatment of metastatic breast cancer, *Ann. Rep. Med. Chem.*, 44, 301, 2009; (e) Galmarini, C.M., Sagopilone, a microtubule stabilizer for the potential treatment of cancer, *Curr. Opin. Invest. Drugs*, 10, 1359, 2009; (f) Sabatini, P., Spriggs, D.R., Epothilones: Better or more of the same?, *J. Clin. Oncol.*, 27, 1, 2009; (g) Reichenbach, H., Höfle, G., Discovery and development of the epothilones, *Drugs in R&D*, 9, 1, 2008; (h) Leamon, C.P., Folate-targeted drug strategies for the treatment of cancer, *Curr. Opin. Invest. Drugs.*, 9, 1277, 2008; (i) Altmann, K.-H., Pfeiffer, B., Arseniyadis, S., Pratt, B.A., Nicolaou, K.C., The chemistry and biology of epothilones—The wheel keeps turning, *ChemMedChem.*, 2, 396, 2007; (j) Watkins, E.B., Chittiboyina, A.G., Avery, M.A., Recent developments in the synthesis of epothilones and related analogues, *Eur. J. Org. Chem.*, 4071, 2006; (k) Altmann, K.-H., Cachoux, F., Caravatti, G., Isarno, T., Wartmann, M., Recent developments in the chemistry and biology of epothilones, *ARKIVOC*, 8, 131, 2006; (l) Luduvico, I., Le Hyaric, M., De Almeida, M.V., Da Silva, A.D., Synthetic methodologies for the preparation of epothilones and analogues, *ChemInform*, 37, 49, 2006; (m) Nicolaou, K.C., Pratt, B.A., Arseniyadis, S., Wartmann, M., O'Brate, A., Giannakakou, P., Molecular design and chemical synthesis of a highly potent epothilone, *ChemMedChem.*, 1, 41, 2006; (n) Rivkin, A., Chou, T.-C., Danishefsky, S.J., On the remarkable antitumor properties of

fludelone: How we got there, *Angew. Chem. Int. Ed*., 44, 2838, 2005; (o) Watkins, E.B., Chittiboyina, A.G., Jung, J.-C., Avery, M.A., The epothilones and related analogues—A review of their syntheses and anticancer activities, *Curr. Pharm. Des*., 11, 1615, 2005; (p) Kolman, A., Activity of epothilones, *Curr. Opin. Invest. Drugs*, 6, 616, 2005; (q) Heinz, D.H., Schubert, W.D., Höfle, G., Much anticipated—The bioactive conformation of epothilone and its binding to tubulin, *Angew. Chem. Int. Ed.*, *44*, 1298, 2005; (r) Cho, Y.S., Wu, K.-D., Moore, M.A.S., Chou, T.-C., Danishefsky, S.J., Second-generation epothilones: Discovery of fludelone and its extraordinary antitumor properties, *Drugs Future*, 30, 737, 2005; (s) Feyen, F., Cachoux, F., Gertsch, J., Wartmann, M., Altmann, K.-H., Epothilones as lead structures for the synthesis-based discovery of new chemotypes for microtubule stabilisation, *Acc. Chem. Res*., 41, 21, 2008; (t) Kingston, D.G.I., Tubulin-interactive natural products as anticancer agents, *J. Nat Prod.*, 72, 507, 2009.

11. (a) Frye, D.K., Advances in breast cancer treatment: The emerging role of ixabepilone, *Expert Rev. Anticancer Ther*., 10, 23, 2010; (b) Michaud, L.B., The epothilones: How pharmacology relates to clinical utility, *Ann. Pharmacother.*, 43, 1294, 2009; (c) Fumoleau, P., Treatment beyond taxanes, emerging new cytotoxic agents, *Eur. J. Cancer*, Suppl. 7, 8, 2009; (d) Perez, E.A., Impact, mechanisms, and novel chemotherapy strategies for overcoming resistance to anthracyclines and taxanes in metastatic breast cancer. *Breast Cancer Res. Treat*., 8, 2086, 2008; (e) Cheng, K.L., Bradley, T., Budmann, D.R., Novel microtubule-targeting agents—The epothilones, *Biologics Targets Ther.*, 2, 789, 2008; (f) Gianni, L., Ixabepilone and the narrow path to developing new cytotoxic drugs, *J. Clin. Oncol.*, 25, 3389, 2007; (g) Kuppens, I.E.L.M., Current state of the art of new tubulin inhibitors in the clinic, *Curr. Clin. Pharmacol*., 1, 57, 2006; (h) Kolman, A., Epothilone D Kosan/Roche, *Curr. Opin. Invest. Drugs*, 5, 657, 2004; (i) Kolman, A., BMS-310705 Bristol-Myers Squibb/GBF, *Curr. Opin. Invest. Drugs*., 5, 1292, 2004; (j) Goodin, S., Kane, M.P., Rubin, E.H., Epothilones: Mechanism of action and biological activity, *J. Clin. Oncol.*, 22, 2015, 2004; (k) Lin, N., Brakora, K., Seiden, M., BMS-247550 Bristol-Myers Squibb/GBF, *Curr. Opin. Invest. Drugs*, 4, 746, 2003; (l) Borzilleri, R.M., Vite, G.D., Epothilones: New tubulin polymerisation agents in preclinical and clinical development, *Drugs Future*, 27, 1149, 2002.
12. (a) Reichenbach, H., Order Myxococcales, in *Bergey's Manual of Systematic Bacteriology*, 2nd edition, Garrity, G., Ed., Springer-Verlag, New York, 2004; (b) *Myxobacteria II*, Dworkin, M., Kaiser, D., Eds., American Society for Microbiology, Washington, DC, 1993, pp. 1–404.
13. Höfle, G., Bedorf, N., Gerth, K., Reichenbach, H., (GBF) German Patent 4211056 (1993).
14. Gerth, K., unpublished results.
15. Gerth, K., Steinmetz, H., Höfle, G., Reichenbach, H., Studies on the biosynthesis of epothilones: Hydroxylation of epo A and B to epothilones E and F, *J. Antibiot*., 55, 41, 2002.
16. Gerth, K., Steinmetz, H., Höfle, G., Reichenbach, H., Studies on the biosynthesis of epothilones: The biosynthetic origin of the carbon skeleton, *J. Antibiot.*, 53, 1373, 2000.
17. Gerth, K., Steinmetz, H., Höfle, G., Reichenbach, H., Studies on the biosynthesis of epothilones: The PKS and epothilone C/D monooxygenase, *J. Antibiot*., 54, 144, 2001.
18. Reichenbach, H., Höfle, G., Gerth, K., Steinmetz, H., (GBF) German Patent Application 19647580.5 (Nov. 18, 1996).
19. (a) Wang, J., Zhang, H., Ying, L., Wang, C., Jiang, N., Zhou, Y., Wang, H., Bai, H., Five new epothilone metabolites from *Sorangium cellulosum* strain So0157-2, *J. Antibiot.*, 62, 483, 2009; (b) Guo, W.-J., Guo, W.-J., Tao, G.-J., Tao, W.-Y., Cui, F.-J., Jin, X.-C., Bi, F., Xu, Z.-H., Ao, Z.-H., A myxobacterium strain *Sorangium cellulosum* AHB125 producing epothilone D and other anticancer substances, *Nat. Prod. Res*., 21, 1256, 2007.
20. Hofmann, H., Mahnke, M., Memmert, K., Petersen, F., Schupp, T., Küsters, E., Mutz, M., (Novartis) World Patent 9942602 (1999).
21. Hecht, H.-J., Höfle, G., unpublished results; Crystallographic data of the structure have been deposited with the Cambridge Crystallographic Data Centre as supplementary publication no. CCDC-241333 and CCDC-241334.Copies of the data can be obtained free of charge on application to CCDC, 12 Union Road, Cambridge CB2 1EZ, UK (fax: (+44)1223-336-033; e-mail: deposit@ccdc.cam.ac.uk).
22. Höfle, G., Kiffe, M., Steinmetz, H., unpublished results.
23. Straubing, R.M., Biopharmaceutics of paclitaxel (Taxol): Formulation, activity, and pharmacokinetics, in *Taxol, Science Application*, Suffness, M., Ed., CRC Press, Boca Raton, 1995, p. 238.
24. (a) Chou, T.-C., Zhang, X.-G., Harris, C.R., Kuduk, S.D., Balog, A., Savin, K.A., Bertino, J.R., Danishefsky, S.J., Desoxyepothilone B is curative against human tumor xenografts that are refractory to paclitaxel, *Proc. Natl. Acad. Sci. U.S.A.*, 95, 15798, 1998; (b) Lee, C.B., Chou, T.-C., Zhang, X.-G., Wang, Z.-G., Kuduk, S.D., Chapell, M.D., Stachel, S.J., Danishefsky, S.J., Total synthesis and antitumor activity of 12,13-desoxyepothilone F: An unexpected solvolysis problem at C15, mediated by remote substitution at C21, *J. Org. Chem.*, 65, 6525, 2000.

25. Han, S.J., Woo, P.S., Woo, K.B., Jun, S.S., Selective production of epothilone B by heterologous expression of propionyl-CoA synthetase in *Sorangium cellulosum*, *J. Microbiol. Biotechnol*., 18, 135, 2008.
26. (a) Gerth, K., Irschik, H., unpublished results from 1996 and 1997; (b) Benigni, D., Stankavage, R., Chiang, S.-J., Hou, H., Eagan, B., Gu, D., Hou, D. et al., (BMS) U.S. Patent 2004/0132146A1.
27. Sasse, F., Höfle, G., unpublished results obtained in 1996.
28. Wang, H., Wang, Z., Wang, S., Li, M., Nan, L., Rhie, J.K., Covey, J.M., Zhang, R., Hill, D.L., Preclinical pharmacology of epothilone D, a novel tubulin-stabilizing antitumor agent, *Cancer Chemother. Pharmacol*., 56, 255, 2005.
29. Li, W., Matson, J.A., Huang, X., Lam, K.S., McClure, G., (BMS) Int. Pat. Appl., WO 00/39276 (July 6, 2000).
30. Tang, L., Qiu, R.-G., Li, Y., Katz, L., Generation of novel epothilone analogs with cytotoxic activity by biotransformation, *J. Antibiot*., 56, 16, 2003.
31. Molnar, I., Schupp, T., Ono, M., Zirkle, R.E., Milnamow, M., Nowak-Thomspon, B., Engel, N. et al., The biosynthetic gene cluster for the microtubule-stabilizing agents epothilones A and B from *Sorangium cellulosum* So ce90, *Chem. Biol*., 7, 97, 2000.
32. Julien, B., Shah, S., Ziermann, R., Goldman, R., Katz, L., Khosla, C., Isolation and characterization of the epothilone biosynthetic gene cluster from *Sorangium cellulosum*, *Gene*, 249, 153, 2000.
33. Schupp, T., Ligon, J., Molnar, I., Zirkle, R., Görlach, J., Cyr, D., World Patent 9966028-A3 (Dec. 23, 1999), (Novartis AG).
34. Julien, B., Katz, L., Khosla, C., Tang, L., Ziermann, R., World Patent 200031247-A3 (June 2, 2000), (Kosan Bioscience).
35. Walsh, C.T., O'Connor, S.E., Schneider, T.L., Polyketide-nonribosomal peptide epothilone antitumor agents: The EpoA, B, C subunits, *J. Ind. Microbiol. Biotechnol.*, 30, 448, 2003.
36. Tang, L., Ward, S., Chung, L., Carney, J.R., Li, Y., Reid, R., Katz, L., Elucidating the mechanism of *cis* double bond formation in epothilone biosynthesis, *J. Am. Chem. Soc.*, 126, 46, 2004.
37. Tang, L., Shah, S., Chung, L., Carney, J., Katz, L., Khosla, C., Julien, B., Cloning and heterologous expression of the epothilone gene cluster, *Science*, 287, 640, 2000.
38. Julien, B., Shah, S., Heterologous expression of epothilone biosynthetic genes in *Myxococcus xanthus*, *Antimicrob. Agents Chemother*., 46, 2772, 2002; Tang, L., Chung, L., Carney, J.R., Starks, C.M., Licari, P., Generation of new epothilones by genetic engineering of a polyketide synthase in *Myxococcus xanthus*, *J. Antibiot*., 58, 178, 2005.
39. Frykman, S.A., Tsuruta, H., Lau, J., Regentin, R., Ou, S., Reeves, C., Carney, J., Santi, D., Licari, P., Modulation of epothilone analog production through media design, *J. Ind. Microbiol. Biotechnol.*, 28, 17, 2002.
40. Frykman, S.A., Tsuruta, H., Starks, C.M., Regentin, R., Carney, J.R., Licari, P.J., Control of secondary metabolite congener distributions via modulation of the dissolved oxygen tension, *Biotechnol. Prog*., 18, 913, 2002.
41. Arslanian, R.L., Tang, L., Blough, S., Ma, W., Qiu, R.-G., Katz, L., Carney, J.R., A new cytotoxic epothilone from modified polyketide synthases heterologously expressed in *Myxococcus xanthus*, *J. Nat. Prod*., 65, 1061, 2002.
42. Starks, C.M., Zhou, Y., Liu, F., Licari, P.J., Isolation and characterization of new epothilone analogs from recombinant *Myxococcus xanthus* fermentations, *J. Nat. Prod.*, 66, 1313, 2003.
43. Albright, Ch.F., Barten, D.M., Lee, F.Y., (BMS) Use of epothilone D in treating tau-associated diseases including Alzheimer's disease, WO 2009/132253A1.
44. Andrieux, A., Salin, P., Schweitzer, A., Begou, M., Pachaud, B., Brun, P., Gory-Faure, S. et al., Microtubule stabilizer ameliorates synaptic function and behavior in a mouse model for schizophrenia, *Biol. Psychiat.*, 60, 1224, 2006.
45. Regentin, R., Frykman, S., Lau, J., Tsuruta, H., Licari, P., Nutrient regulation of epothilone biosynthesis in heterologous and native production strains, *Appl. Microbiol. Biotechnol*., 61, 451, 2003.
46. Lau, J., Frykman, S., Regentin, R., Ou, S., Tsuruta, H., Licari, P., Optimizing the heterologous production of epothilone D *in Myxococcus xanthus*, *Biotechnol. Bioeng*., 78, 280, 2002.
47. Arslanian, R.L., Parker, C.D., Wang, P.K., McIntire, J.R., Lau, J., Starks, C., Licari, P.J., Large-scale isolation and crystallization of epothilone D from *Myxococcus xanthus* cultures, *J. Nat. Prod*., 65, 570, 2002.
48. Frykman, S.A., Tsuruta, H., Licari, P.J., Assessment of fed-batch, semicontinuous, and continuous epothilone D production process, *Biotechnol. Prog*., 21, 1102, 2005.

49. Boddy, C.N., Hotta, K., Tse, M.L., Watts, R.E., Khosla, C., Precursor-directed biosynthesis of epothilone in *Escherichia coli*, *J. Am. Chem. Soc.*, 126, 7436, 2004; Mutka, S.C., Carney, J.R., Liu, Y., Kennedy, J., Heterologous production of epothilone C and D in *Escherichia coli*, *Biochemistry*, 45, 1321, 2006.
50. O'Connor, S.E., Walsh, C.T., Liu, F., Biosynthesis of epothilone intermediates with alternate starter units: Engineering polyketide-nonribosomal interfaces, *Angew. Chem. Int. Ed.*, 42, 3917, 2003.
51. Schneider, T.L., Walsh, C.T., O'Connor, S.E., Utilization of alternate substrates by the first three modules of the epothilone synthetase assembly line, *J. Am. Chem. Soc*., 124, 11272, 2002.
52. Chen, H., O'Connor, S., Cane, D.E., Walsh, C.T., Epothilone biosynthesis: Assembly of the methylthiazolylcarboxy starter unit on the EpoB subunit, *Chem. Biol*., 8, 899, 2001.
53. O'Connor, S.E., Chen, H., Walsh, C.T., Enzymatic assembly of epothilones: The epoC subunit and reconstitution of the epoA-ACP/B/C polyketide and nonribosomal peptide interfaces, *Biochemistry*, 41, 5685, 2002.
54. Schneider, T.L., Shen, B., Walsh, C.T., Oxidase domains in epothilone and bleomycin biosynthesis: Thiazoline to thiazole oxidation during chain elongation, *Biochemistry*, 42, 9722, 2003.
55. Lopez, J.V., Naturally mosaic operons for secondary metabolite biosynthesis: Variability and putative horizontal transfer of discrete catalytic domains of the epothilone polyketide synthase locus, *Mol. Gen. Genomics*, 270, 420, 2003.
56. Nagano, S., Li, H., Shimizu, H., Nishida, C., Ogura, H., Ortiz de Montelano, P.R., Poulos, T.L., Crystal structures of epothilone D-bound, epothilone B-bound, and substrate-free forms of cytochrome P450epoK, *J. Biol. Chem*., 278, 44886, 2003.
57. Chou, T.-C., Zhang, X.-G., Balog, A., Su, D.-S., Meng, D., Savin, K., Bertino, J.R., Danishefsky, S.J., Desoxyepothilone B: An efficacious microtubule-targeted antitumor agent with a promising *in vivo* profile relative to epothilone B, *Proc. Natl. Acad. Sci. U.S.A.*, 95, 9642, 1998.
58. Kowalski, R.J., Giannakakou, P., Hamel, E., Activities of the microtubule-stabilizing agents epothilones A and B with purified tubulin and in cells resistant to paclitaxel (Taxol), *J. Biol. Chem.*, 272, 2534, 1997.
59. Schinzer, D., Altmann, K.-H., Stuhlmann, F., Bauer, A., Wartmann, M., Synthesis and biological evaluation of aza-epothilones, *ChemBioChem*, 1, 67, 2000.
60. Su, D.-S., Balog, A., Meng, D., Bertinato, P., Danishefsky, S.J., Zheng, Y.-H., Chou, T.-C., He, L., Horwitz, S.B., Structure–activity relationships of the epothilones and the first in vivo comparison with paclitaxel, *Angew. Chem. Int. Ed.*, 36, 2093, 1997.
61. Höfle, G., Glaser, N., Kiffe, M., Hecht, H.-J., Sasse, F., Reichenbach, H., N-oxidation of epothilone A–C and *O*-acyl rearrangement to C-19- and C21-substituted epothilones, *Angew. Chem. Int. Ed.*, 38, 1971, 1999.
62. Borzilleri, R.M., Zheng, X., Schmidt, R.J., Johnson, J.A., Kin, S.-H., DiMarco, J.D., Fairchild, C.R. et al., A novel application of a Pd(0)-catalyzed nucleophilic substitution reaction to the regio- and stereoselective synthesis of lactam analogs of the epothilone natural products, *J. Am. Chem. Soc.*, 122, 8890, 2000.
63. Sepp-Lorenzino, L., Balog, A., Su, D.-S., Meng, D., Timaul, N., Scher, H.I., Danishefsky, S.J., Rosen, N., The microtubule-stabilizing agents epothilones A and B and their desoxy-derivatives induce mitotic arrest and apoptosis in human prostate cancer cells, *Prost. Cancer Prost. Dis.*, 2, 41, 1999.
64. Nicolaou, K.C., Vallberg, H., King, N.P., Roschangar, F., He, Y., Vourloumis, D., Nicolaou, C.G., Total synthesis of oxazole- and cyclopropane-containing epothilone A analogs by the olefin metathesis approach, *Chem. Eur. J.*, 3, 1957, 1997.
65. Nicolaou, K.C., Sarabia, F., Finlay, M.R.V., Nincovic, S., King, N.P., Vourloumis, D., He, Y., Total synthesis of oxazole- and cyclopropane-containing epothilone B analogs by the macrolactonization approach, *Chem. Eur. J.*, 3, 1971, 1997.
66. Stachel, S.J., Lee, C.B., Spassova, M., Chappell, M.D., Bornmann, W.G., Danishefsky, S.J., Chou, T.-C., Guan, J., On the interactivity of complex synthesis and tumor pharmacology in the drug discovery process: Total synthesis and comparative *in vivo* evaluations of the 15-aza epothilones, *J. Org. Chem*., 66, 4369, 2001.
67. Chou, T.-C., O'Connor, O.A., Tong, W.P., Guan, Y., Zhang, Z.-G., Stachel, S.J., Lee, C., Dinshefsky, S.J., The synthesis, discovery, and development of a highly promising class of microtubule stabilisation agents: Curative effects of desoxyepothilones B and F against human tumor xenografts in nude mice, *Proc. Natl. Acad. Sci. U.S.A.*, 98, 8113, 2001.
68. Lee, F.Y.F., Borzilleri, R., Fairchild, C.R., Kim, S.-H., Long, B.H., Reventoe-Suarez, C., Vite, G.D., Rose, W.C., Kramer, R.A., BMS-247550: A novel epothilone analog with a mode of action similar to paclitaxel but possessing superior antitumor efficacy, *Clin. Cancer Res*., 7, 1429, 2001.

69. Wolff, A., Technau, A., Brandner, G., Epothilone A induces apoptosis in neuroblastoma cells with multiple mechanisms of drug resistance, *Int. J. Oncol.*, 11, 123, 1997.
70. Mühlradt, P.F., Sasse, F., Epothilone B stabilizes microtubuli of macrophages like Taxol without showing Taxol-like endotoxin activity, *Cancer Res.*, 57, 3344, 1997.
71. Kamath, K., Jordan, M.A., Suppression of microtubule dynamics by epothilone B is associated with mitotic arrest, *Cancer Res*., 63, 6026, 2003.
72. Chen, J.G., Horwitz, S.B., Differential mitotic responses to microtubule-stabilizing drugs, *Cancer Res.*, 62, 1935, 2002.
73. Iffert, R., Sasse, F., Analyse des Apoptischen Zellkernzerfalls durch Bildverarbeitung, *BIOforum*, 22, 631, 1999.
74. Lichtner, R.B., Rotgeri, A., Bunte, T., Buchmann, B., Hoffmann, J., Schwede, W., Skuballa, W., Klar, U., Subcellular distribution of epothilones in human tumor cells, *Proc. Natl. Acad. Sci. U.S.A.*, 98, 11743, 2001.
75. Klar, U., Skuballa, W., Buchmann, B., Schwede, W., Bunte, T., Hoffmann, J., Lichtner, R.B., Synthesis and biological activity of epothilones, in *Anticancer Agents—Frontiers in Cancer Therapy*, Ojima, I., Vite, G.D., Altmann, K.-H., Eds., ACS Symposium Series 796, American Chemical Society, 2001, pp. 131–146.
76. Atadja, P., Isolation and characterisation of epothilone A resistant cells, *Proc. Am. Assoc. Cancer Res*., 41, 803, 2000.
77. Meurer-Grob, P., Kasparian, J., Wade, R.H., Microtubule structure at improved resolution, *Biochemistry*, 40, 8000, 2001.
78. Wartmann, M., Koppler, J., Lartigot, M., Fabbro, D., Altmann, K.-H., Kawai, R., Kuhnol, J., Ramstein, Aichholz, R., and Blum, W., Epothilones A and B accumulate several hundred fold inside cells, *Proc. Am. Assoc. Cancer Res*., 41, 213, 2000, abstr. 1362.
79. Gupta Jr., M.L., Bode, C.J., Georg, G.I., Himes, R.H., Understanding tubulin-Taxol interactions: Mutations that impart Taxol binding to yeast tubulin, *Proc. Natl. Acad. Sci. U.S.A.*, 100, 6394, 2003.
80. Bode, C.J., Gupta Jr., M.L., Reiff, E.A., Suprenant, S.A., Georg, G.I., Himes, R.H., Epothilone and paclitaxel: Unexpected differences in promoting the assembly and stabilisation of yeast microtubules, *Biochemistry*, 41, 3870, 2002.
81. Giannakakou, P., Gussio, R., Nogales, E., Downing, K.H., Zaharewitz, D., Bollbuck, B., Poy, G., Sackett, D., Nicolaou, K.C., Fojo, T., A common pharmacophore for epothilone and taxanes: Molecular basis for drug resistance conferred by tubulin mutations in human cancer cells, *Proc. Natl. Acad. Sci. U.S.A.*, 97, 2904, 2000.
82. He, L., Huang Yang, C.-P., Horwitz, S.B., Mutations in β-tubulin map to domains involved in regulation of microtubule stability in epothilone-resistant cell lines, *Mol. Cancer Ther.*, 1, 3, 2001.
83. Verrills, N.M., Flemming, C.L., Liu, M., Ivery, M.T., Cobon, G.S., Norris, M.D., Haber, M., Kavallaris, M., Microtubule alterations and mutations induced by desoxyepothilone B: Implications for drug-target interactions, *Chem. Biol.*, 10, 597, 2003.
84. Martello, L.A., Verdier-Pinard, P., Shen, H.-J., He, L., Torres, K., Orr, G.A., Horwitz, S.B., Elevated levels of microtubule destabilizing factors in a Taxol-resistant/dependent A549 cell line with an α-tubulin mutation, *Cancer Res*., 63, 1207, 2003.
85. Verdier-Pinard, P., Wang, F., Burd, B., Angeletti, R.H., Horwitz, S.B., Orr, G.A., Direct analysis of tubulin expression in cancer cell lines by electrospray ionization mass spectrometry, *Biochemistry*, 42, 12019, 2003.
86. Dumontet, C., Jordan, M.A., Lee, F.F., Ixabepilone: Targeting βIII-tubulin expression in taxane-resistant malignancies, *Mol. Cancer Ther*., 8, 17, 2009.
87. Poruchynsky, M.S., Giannakakou, P., Ward, Y., Bulinski, J.C., Telford, W.G., Robey, R.W., Fojo, T., Accompanying protein alterations in malignant cells with a microtubule-polymerizing drug-resistance phenotype and a primary resistance mechanism, *Biochem. Pharmacol*., 62, 1469, 2001.
88. Khabele, D., Lopez-Jonez, M., Yang, W.C., Aragno, D., Gross, S.J., Augenlicht, L.H., Goldberg, G.L., Tumor necrosis factor-α related gene response to epothilone B in ovarian cancer, *Gynecol. Oncol.*, 93, 19, 2004.
89. Atadja, P., Yan-Ncale, Y., Towbin, H., Buxton, F., Cohen, D., Gene expression profiling of epothilone A-resistant cells, *Mechanisms of Drug Resistance in Epilepsy: Lessons from Oncology*, Novartis Foundation Symposium, 2002, pp.119–136.
90. Ioffe, M., Nelson, D., Rao, K., Goodin, S., White, E., DiPaola, R.S., Epothilone induced cytotoxicity is dependent on p53 in prostate cells, *Proc. Am. Assoc. Cancer Res*., 44, abstr. 829, 2003.
91. Uyar, D., Takigawa, N., Mekhail, T., Grabowski, D., Markman, M., Lee, F., Canetta, R., Peck, R., Bukowski, R., Ganapathi, R., Apoptotic pathways of epothilone BMS 310705, *Gynecol. Oncol*., 91, 173, 2003.

92. Griffin, D., Wittmann, S., Guo, F., Nimmanapalli, R., Bali, P., Wang, H.G., Phalla, K., Molecular determinants of epothilone B derivative (BMS 247550) and Apo-2L/TRAIL-induced apoptosis of human ovarian cancer cells, *Gynecol. Oncol.*, 89, 37, 2003.
93. Yamaguchi, H., Paranawithana, S.R., Lee, M.W., Huang, Z., Bhalla, K.N., Wang, H.-G., Epothilone B analog (BMS-247550)-mediated cytotoxicity through induction of bax conformational change in human breast cancer cells, *Cancer Res*., 62, 466, 2002.
94. Bröker, L.E., Huisman, C., Ferreira, C.G., Rodriguez, J.A.Kruyt, F.A.E., Giaccone, G., Late activation of apoptotic pathways plays a negligible role in mediating the cytotoxic effects of discodermolide and epothilone B in non-small cell lung cancer cells, *Cancer Res.*, 62, 4081, 2002.
95. Pietras, K., Stumm, M., Hubert, M., Buchdunger, E., Rubin, K., Heldin, C.-H., McSheehy, P., Wartmann, M., Östman, A., STI571 enhances the therapeutic index of epothilone B by a tumor-selective increase of drug uptake, *Clin. Cancer Res*., 9, 3779, 2003.
96. Wittmann, S., Bali, P., Donapati, S., Nimmanapalli, R., Guo, F., Yamaguchi, H., Huang, M., Jove, R., Wang, H.G., Bhalla, K., Flavopiridol down-regulates antiapoptotic proteins and sensitizes human breast cancer cells to epothilone B-induced apoptosis, *Cancer Res*., 63, 93, 2003.
97. Moasser, M.M., Sepp-Lorenzino, L. Kohl, N.E., Oliff, A., Balog, A., Su, D.-S., Danishefsky, S.J., Rosen, N., Farnesyl transferase inhibitors cause enhanced mitotic sensitivity to Taxol and epothilones, *Proc. Natl. Acad. Sci. U.S.A.*, 95, 1369, 1998.
98. Zhou, Y., Liu, F., Feng, L., Uphoff, J., Ma, W., Hannah, A.L., Johnson Jr., R.G., KOS-862 (epothilone D) with 5-fluorouracil in human colon cancer cell lines: Synergistic antitumor effects, *Proc. Am. Assoc. Cancer Res*., 44, abstr. 2746, 2003.
99. Fuino, I., Bali, P., Wittmann, S., Donapaty, S., Guo, F., Yamaguchi, H., Wang, H.-G., Atadja, P., Bhalla, K., Histone deacetylase inhibitor IAQ824 down-regulates Her-2 and sensitizes human breast cancer cells to trastuzumab, taxotere, gemcitabine, and epothilone B, *Mol. Cancer Ther*., 2, 971, 2003.
100. Kim, J.-C., Kim, J.-S., Saha, D., Cao, Q., Shyr, Y., Choy, H., Potential radiation-sensitizing effect of semisynthetic epothilone B in human lung cancer cells, *Radiother. Oncol*., 68, 305, 2003.
101. Martin, H.J., Drescher, M., Mulzer, J., How stable are epoxides? A novel synthesis of epothilone B, *Angew. Chem. Int. Ed*., 39, 581, 2000.
102. Martin, H.J., Pojarliev, P., Kählig, H., Mulzer, J., The 12,13-diol cyclization approach for a truly stereocontrolled total synthesis of epothilone B and the synthesis of a conformationally restrained analog, *Chem. Eur. J.*, 7, 2261, 2001.
103. Mulzer, J., Karig, G., Pojarliev, P., A novel highly stereoselective total synthesis of epothilone B and of its (12*R*, 13*R*) acetonide, *Tetrahedron Lett*., 41, 7635, 2000.
104. Meng, D., Sorensen, E.J., Bertinato, P., Danishefsky, S.J., Studies toward a synthesis of epothilone A: Use of hydropyran templates for the management of acyclic stereochemical relationships, *J. Org. Chem.*, 61, 7998, 1996.
105. Meng, D., Bertinato, P., Balog, A., Su, D.-S., Kamenecka, T., Sorensen, E.J., Danishefsky, S.J., Total syntheses of epothilones A and B, *J. Am. Chem. Soc.*, 119, 10073, 1997.
106. Schinzer, D., Limberg, A., Bauer, A., Böhm, O.M., Cordes, M., Total synthesis of (-)-epothilone A, *Angew. Chem. Int. Ed.*, 36, 523, 1997.
107. Nicolaou, K.C., He, Y., Vourloumis, D., Vallberg, H., Roschangar, F., Sarabia, F., Ninkovic, S., Yang, Z., Trujillo, J.I., The olefin metathesis approach to epothilone A and its analogues, *J. Am. Chem. Soc*., 119, 7960, 1997.
108. Meng, D., Su, D.-S., Balog, A., Bertinato, P., Sorensen, E.J., Danishefsky, S.J., Zheng, Y.-H., Chou, T.-C., He, L., Horwitz, S.B., Remote effects in macrolide formation through ring-forming olefin metathesis: An application to the synthesis of fully active epothilone congeners, *J. Am. Chem. Soc.*, 119, 2733, 1997.
109. Fürstner, A., Mathes, C., Grela, K., Concise total syntheses of epothilone A and C based on alkyne metathesis, *Chem. Commun*., 1057, 2001.
110. Nicolaou, K.C., Ninkovic, S., Sarabia, F., Vourloumis, D., He, Y., Vallberg, H., Finlay, M.R.V., Yang, Z., Total syntheses of epothilones A and B via a macrolactonization-based strategy, *J. Am. Chem. Soc*., 119, 7974, 1997.
111. Balog, A., Meng, D., Kamenecka, T., Bertinato, P., Su, D.-S., Sorensen, E.J., Danishefsky, S.J., Total synthesis of (-)-epothilone A, *Angew. Chem. Int. Ed.*, 35, 2801, 1996.
112. Yang, Z., He, Y., Vourloumis, D., Vallberg, H., Nicolaou, K.C., Total synthesis of epothilone A: The olefin metathesis approach, *Angew. Chem. Int. Ed.*, 36, 166, 1997.
113. Taylor, R.E., Chen, Y., Total synthesis of epothilones B and D, *Org. Lett.*, 3, 2221, 2001.

114. Liu, Z.-Y., Yu, C.-Z., Yang, J.-D., Chiral synthesis of the C3–13 segment of epothilone A, *Synletters*, 12, 1383, 1997.
115. Schinzer, D., Bauer, A., Schieber, J., Synthesis of epothilones: Stereoselective routes to epothilone B, *Synletters*, 8, 861, 1998.
116. Njardson, J.T., Biswas, K., Danishefsky, S.J., Application of hitherto unexplored macrocyclization strategies in the epothilone series: Novel epothilone analogs by total synthesis, *Chem. Commun*., 2759, 2002.
117. Bode, J.W., Carreira, E.M., Stereoselective syntheses of epothilones A and B via nitrile oxide cycloadditions and related studies, *J. Org. Chem*., 66, 6410, 2001.
118. Bode, J.W., Carreira, E.M., Stereoselective syntheses of epothilone A and B in nitrile oxide cycloadditions and related studies, *J. Am. Chem. Soc.*, 123, 3611, 2001.
119. Biswas, K., Lin, H., Njardsarson, J.T., Chappell, M.D., Chou, T.-C., Guan, Y., Tong, W.P., He, L., Horwitz, S.B., Danishefsky, S.J., Highly concise routes to epothilones: The total synthesis and evaluation of epothilone 490, *J. Am. Chem. Soc.*, 124, 9825, 2002.
120. Yamamoto, K., Biswas, K., Gaul, C., Danishefsky, S.J., Effects of temperature and concentration in some ring closing metathesis reactions, *Tetrahedron Lett*., 44, 3297, 2003.
121. White, J.D., Carter, R.G., Sundermann, K.F., Wartmann, M., Total synthesis of epothilone B, epothilone D, and *cis*- and *trans*-9,10-dehydroepothilone D, *J. Am. Chem. Soc*., 123, 5407, 2001.
122. Sawada, D., Kanai, M., Shibasaki, M., Enantioselective total synthesis of epothilones A and B using multifunctional asymmetric catalysis, *J. Am. Chem. Soc.*, 122, 10521, 2000.
123. Mulzer, J., Mantoulidis, A., Öhler, E., Easy access to the epothilone family—Synthesis of epothilone B, *Tetrahedron Lett.*, 39, 8633, 1998.
124. Nicolaou, K.C., He, J., Roschangar, F., King, N.P., Vourloumis, D., Li, T., Total synthesis of epothilone E and analogs with modified side chains through the Stille coupling reaction, *Angew. Chem. Int. Ed.*, 37, 84, 1998.
125. Bertinato, P., Sorensen, E.J., Meng, D., Danishefsky, S.J., Studies toward a synthesis of epothilone A: Stereocontrolled assembly of the acyl region and models for macrocyclization, *J. Org. Chem.*, 61, 8000, 1996.
126. Sun, J., Sinha, S.C., Stereoselective total synthesis of epothilones by the metathesis approach involving C9–C10 bond formation, *Angew. Chem. Int. Ed*., 41, 1381, 2002; Rivkin, A., Yoshimura, F., Gabarda, A.E., Chou, T.C., Dong, H., Tong, W.P., Danishefsky, S.J., Complex target-oriented total synthesis in the drug discovery process: The discovery of a highly promising family of second generation epothilones, *J. Am. Chem. Soc*., 125, 2899, 2003.
127. May, S.A., Grieco, P.A., Total synthesis of (-)-epothilone B, *Chem. Commun.*, 1597, 1998.
128. Mulzer, J., Mantoulidis, A., Synthesis of the C(1) –C(9) segment of the cytotoxic macrolides epothilon A and B, *Tetrahedron Lett.*, 37, 9179, 1996.
129. Schinzer, D., Limberg, A., Böhm, O.M., Studies towards the total synthesis of epothilones: Asymmetric synthesis of the key fragments, *Chem. Eur. J.*, 2, 1477, 1996.
130. Nicolaou, K.C., Scarpelli, R., Bollbuck, B., Werschkun, B., Pereira, N.M.A., Wartmann, M., Altmann, K.-H., Zaharevitz, D., Gussio, R., Giannakakou, P., Total synthesis of epothilone E and related side-chain modified analogs via a Stille coupling based strategy, *Bioorg. Med. Chem.*, 7, 665, 1999; Nicolaou, K.C., Scarpelli, R., Bollbuck, B., Werschkun, B., Pereira, M.M.A., Wartmann, M., Altmann, K.-H., Zaharevitz, D., Gussio, R., Giannakakou, P., Chemical synthesis and biological properties of pyridine epothilones, *Chem. Biol.*, 7, 593, 2000.
131. Nicolaou, K.C., Ritzen, A., Namoto, K., Buey, R.M., Diaz, J.F., Andreu, J.M., Wartmann, M., Altmann, K.-H., O'Brate, A., Giannakakou, P., Chemical synthesis and biological evaluation of novel epothilone B and *trans*-12,13-cyclopropyl epothilone B analogs, *Tetrahedron*, 58, 6413, 2002.
132. Nicolaou, K.C., Namoto, K., Li, J., Ritzén, A., Ulven, T., Shoji, M., Zaharevitz, D. et al., Synthesis and biological evaluation of 12,13-cyclopropyl and 12,13-cyclobutyl epothilones, *ChemBioChem*., 1, 69, 2001.
133. Ramachandran, P.V., Prabhudas, B., Chandra, J.S., Reddy, M.V.R., Brown, H.C., Preparative-scale synthesis of both antipodes of B-γ,γ-dimethylallyldiisopino-camphenylborane: Application for the synthesis of C_1–C_6 subunit of epothilone, *Tetrahedron Lett*., 45, 1011, 2004.
134. Gabriel, T., Wessjohann, L., The chromium-reformatsky reaction: Asymmetric synthesis of the aldol fragment of the cytotoxic epothilons from 3-(2-bromoacyl)-2-oxazolidinones, *Tetrahedron Lett*., 38, 1363, 1997.
135. Panicker, B., Karle, J.M., Avery, M.A., An unusual reversal of stereoselectivity in a boron mediated aldol reaction: Enenantioselective synthesis of the C_1–C_6 segment of the epothilones, *Tetrahedron*, 56, 7859, 2000.

136. (a) Stachel, S.J., Danishefsky, S.J., Chemo- and stereoselective epoxidation of 12,13-desoxyepothilone B using 2,2-dimethyldioxirane, *Tetrahedron Lett.*, 42, 6785, 2001; (b) Liu, Z.-Y., Chen, Z.-C., Yu, C.-Z., Wang, R.-F., Zhang, R.-Z., Huang, C.-S., Yan, Z., Cao, D.-R., Sun, J.-B., Li, G., Total synthesis of epothilone A through stereospecific epoxidation of the *p*-methoxybenzyl ether of epothilone C, *Chem. Eur. J.*, 8, 3747, 2002.
137. Höfle, G., personal communication to D. Schinzer (TU Braunschweig) in July 1996.
138. Prantz, K., Mulzer, J., Decarboxylative grop-type fragmentations in the synthesis of trisubstituted *Z* olefins: Application to peloruside A, discodermolide and epothilone D, *Angew. Chem. Int. Ed.*, 48, 5030, 2009.
139. Gaich, T., Mulzer, J., Synthesis of epothilones via a silicon-tethered RCM reaction, *Org. Lett.*, 7, 1311, 2005.
140. Gaich, T., Karig, G., Martin, H.J., Mulzer, J., New solutions to the C-12,13 stereoproblem of epothilones B and D; synthesis of a 12,13-diol-acetonide epothilone B analog, *Eur. J. Org. Chem.*, 3372, 2006.
141. Hong, Y.D., Lee, H.W., Lee, I.Y.C., Jung, J.-K., Synthesis of the C11–C21 fragments of epothilones A and B using ring-closing metathesis, *Bull. Kor. Chem. Soc.*, 28, 367, 2007.
142. Valluri, M., Hindupur, R.M., Bijoy, P., Labadie, G., Jung, J.-C., Avery, M.A., Total synthesis of epothilone B, *Org. Lett.*, 3, 3607, 2001; Jung, J.-C., Total synthesis of epothilones B and D, *J. Org. Chem.*, 69, 9269, 2004.
143. Balog, A., Bertinato, P., Su, D.-S., Meng, D., Sorensen, E., Danishefsky, S.J., Zheng, Y.-H., Chou, T.-C., He, L., Horwitz, S.B., Stereoselective syntheses and evaluation of compounds in the 8-desmethylepothilone A. Series: Some surprising observations regarding their chemical and biological properties, *Tetrahedron Lett.*, 38, 4529, 1997.
144. Nicolaou, K.C., Hepworth, D., Finlay, M.R.V., King, N.P., Werschkun, B., Bogot, A., Synthesis of 16-desmethylepothilone B: Improved methodology for the rapid, highly selective and convergent construction of epothilone B and analogs, *Chem. Commun.*, 519, 1999.
145. Nicolaou, K.C., Hepworth, D., King, N.P., Raymond, M., Finlay, V., Scarpelli, R., Manuela, M. et al., Total synthesis of 16-desmethylepothilone B, epothilone B_{10}, epothilone F, and related side chain modified epothilone B analogs, *Chem. Eur. J.*, 6, 2783, 2000.
146. Taylor, R.E., Chen, Y., Galvin, G.M., Pabba, P.K., Conformation–activity relationships in polyketide natural products. Towards the biologically active conformation of epothilone, *Org. Biomol. Chem.*, 2, 127, 2004; Frein, J.D., Taylor, R.E., Sackett, D.L., New sources of chemical diversity inspired by biosynthesis: Rational design of a potent epothilone analogue, *Org. Lett.*, 11, 3186, 2009.
147. Taylor, R.E., Chen, Y., Beatty, A., Myles, D.C., Zhou, Y., Conformation–activity relationships in polyketie natural products: A new perspective on the rational design of epothilone analogs, *J. Am. Chem. Soc.*, 125, 26, 2003.
148. Nicolaou, K.C., Ninkovic, S., Finlay, M.R.V., Sarabia, F., Li, T., Total synthesis of 26-hydroxyepothilone B and related analogs, *Chem. Commun.*, 2343, 1997.
149. Nicolaou, K.C., Finlay, M.R.V., Ninkovic, S., Sarabia, F., Total synthesis of 26-hydroxy-epothilone B and related analogs *via* a macrolactonization based strategy, *Tetrahedron*, 54, 7127, 1998.
150. Chappell, M.D., Harris, C.R., Kuduk, S.D., Balog, A., Wu, Z., Zhang, F., Lee, C.B. et al., Probing the SAR of dEpoB via chemical synthesis: A total synthesis evaluation of C26-(1,3-dioxolanyl)-12,13-desoxyepothilone B, *J. Org. Chem.*, 67, 7730, 2002.
151. Koch, G., Loiseleur, O., Altmann, K.-H., Total synthesis of 26-fluoro-epothilone B, *Synletters*, 4, 693, 2004.
152. Chou, T.-C., Dong, H., Rivkin, A., Yoshimura, F., Gabarda, A.E., Cho, Y.S., Tong, W.P., Danishefsky, S.J., Design and total synthesis of a superior family of epothilone analogs, which eliminate xenograft tumors to a nonrelapsable state, *Angew. Chem. Int. Ed.*, 42, 4762, 2003.
153. Sefkow, M., Höfle, G., Substitutions at the thiazole moiety of epothilone, *Heterocyles*, 48, 2485, 1998.
154. Altmann, K.-H., Bold, G., Caravatti, G., Flörsheimer, A., Guagnano, V., Wartmann, M., Synthesis and biological evaluation of highly potent analogs of epothilones B and D, *Bioorg. Med. Chem. Lett.*, 10, 2765, 2000.
155. Klar, U., Buchmann, B., Schwede, W., Skuballa, W., Hoffmann, J., Lichtner, R.B., Total synthesis and antitumor activity of ZK-EPO: The first fully synthetic epothilone in clinical development, *Angew. Chem. Int. Ed.*, 45, 7942, 2006.
156. Nicolaou, K.C., Winssinger, N., Pastor, J., Ninkovic, S., Sarabia, F., He, Y., Vourloumis, D., Yang, Z., Li, T., Giannakakou, P., Hamel, E., Synthesis of epothilone A and B in solid and solution phase, *Nature*, 387, 268, 1997.

157. Altmann, K.-H., Bold, G., Caravatti, G., Denni, D., Flörsheimer, A., Schmidt, A., Rhis, G., Wartmenn, M., The total synthesis and biological assessment of *trans*-epothilone A, *Helv. Chim. Acta*, 85, 4086, 2002.
158. Buey, R.M., Diaz, J.F., Andreu, J.M., O'Brate, A., Giannakakou, P., Nicolaou, K.C., Sasmal, P.K., Ritzén, A., Namoto, K., Interaction of epothilone analogs with the paclitaxel binding site: Relationship between binding affinity, microtubule stabilisation, and cytotoxicity, *Chem. Biol*., 11, 225, 2004.
159. Johnson, J., Kim, S.-H., Bifano, M., DiMarco, J., Fairchild, C., Gougoutas, J., Lee, F., Long, B., Tokarski, J., Vite, G., Synthesis, structure proof, and biological activity of epothilone cyclopropanes, *Org. Lett.*, *2*, 1537, 2000.
160. Nicolaou, K.C., Namoto, K., Ritzén, A., Ulven, T., Shoji, M., Li, J., D'Amico, G. et al., Chemical synthesis and biological evaluation of *cis*- and *trans*-12,13-cyclopropyl and 12,13-cyclobutyl epothilones and related pyridine side chain analogs, *J. Am. Chem. Soc.*, 123, 9313, 2001.
161. Nicolaou, K.C., Finlay, M.R.V., Ninkovic, S., King, N.P., He, Y., Li, T., Sarabia, F., Vourloumis, D., Design, synthesis, and biological properties of highly potent epothilone B analogs, *Ang. Chem. Int. Ed.*, 42, 4086, 2003; Nicolaou, K.C., Finlay, M.R.V., Ninkovic, S., King, N.P., He, Y., Li, T., Sarabia, F., Vourloumis, D., Synthesis and biological properties of C12,13-cyclopropyl-epothilone A and related epothilones, *Chem. Biol.*, 5, 365, 1998.
162. Regueiro-Ren, A., Borzilleri, M., Zheng, X., Kim, S.-H., Johnson, J.A., Fairchild, C.R., Lee, F.Y.F., Long, B.H., Vite, G.D., Synthesis and biological activity of novel epothilone aziridines, *Org. Lett*., 3, 2693, 2001; Vite, G.D., Kim, S.-H., Höfle, G., (BMS/GBF) U.S. Patent No. 6,498,257 B1, 2002.
163. Glunz, P.W., He, L., Horwitz, S.B., Chakravarty, S., Ojima, I., Chou, T.-C., Danishefsky, S.J., The synthesis and evaluation of 12,13-benzodesoxyepothilone B: A highly convergent route, *Tetrahedron Lett.*, 40, 6895, 1999.
164. End, N., Bold, B., Caravatti, G., Wartmann, M., Altmann, K.-H., Synthetic epothilone analogs with modifications in the northern hemispere and the heterocyclic side-chain-synthesis and biological evaluation, *Fourth International Electronic Conference on Synthetic Organic Chemistry* (ECSOC-4), September 1–30, 2000.
165. Schinzer, D., Bourguet, E., Ducki, S., Synthesis of furano-epothilone D, *Chem. Eur. J.*, 10, 3217, 2004.
166. Zhan, W., Jiang, Y., Brodie, P.J., Kingston, D.G.I., Liotta, D.C., Snyder, J.P., Design and synthesis of C6–C8 bridged epothilone A, *Org. Lett*., 10, 1565, 2008.
167. Rivkin, A., Biswas, K., Chou, T.-C., Danishefsky, S.J., On the introduction of a trifluoromethyl substituent in the epothilone setting: Chemical issues related to ring forming olefin metathesis and earliest biological findings, *Org. Lett*., 4, 4081, 2002.
168. Yoshimura, F., Rivkin, A., Gabarda, A.E., Chou, T.-C., Dong, H., Sukenick, G., Morel, F.F., Taylor, R.E., Danshefsky, S.J., Synthesis and conformational analysis of (*E*)-9,10-dehydroepothilone B: A suggestive link between the chemistry and biology of epothilones, *Angew. Chem. Int. Ed.*, 42, 2518, 2003.
169. White, J.D., Sundermann, K.F., Wartmann, M., Synthesis, conformational analysis, and bioassay of 9,10-didehydroepothilone D, *Org. Lett.*, 4, 995, 2002.
170. Alhamadasheh, M.M., Gupta, S., Hudson, R.A., Perera, L., Tillekeratne, L.M.V., Total synthesis and selective activity of a new class of conformationally restrained epothilones, *Chem. Eur. J*., 14, 570, 2008.
171. Kingston, D.G.I., A natural love of natural products, *J. Org. Chem*., 73, 3975, 2008; Chen, Q.-H., Ganesh, T., Brodie, P., Slebodnick, C., Jiang, Y., Banerjee, A., Bane, S., Snyder, J.P., Kingston, D.G.I., Design, synthesis and biological evaluation of bridged epothilone D analogs, *Org. Biomol. Chem*., 6, 4542, 2008.
172. Quintard, D., Bertrand, P., Vielle, S., Raimbaud, E., Renard, P., Pfeiffer, B., Gesson, J.-P., Enantioselective synthesis of 2,3-dehydro-3-desoxy-10-oxaepothilone D, *Synletters*, 13, 2033, 2003; Quintard, D., Bertrand, P., Bachmann, C., Gesson, J.-P., Synthesis and conformational analysis of macrocycles related to 10-oxa-epothilone, *Eur. J. Org. Chem*., 4762, 2004.
173. Cachoux, F., Schaal, F., Teichert, A., Wagner, T., Altmann, K.-H., Synthesis of 4-aza epothilone D analogs, *Synletters*, 14, 2709, 2004.
174. Altmann, K.-H., Bold, G., Caravatti, G., End, N., Flörsheimer, A., Guagnano, V., O'Reilly, T., Wartmann, M., Epothilones and their analogs—Potential new weapons in the fight against cancer, *Chimia*, 54, 612, 2000; Feyen, F., Jantsch, A., Hauenstein, K., Pfeiffer, B., Altmann, K.-H., Synthesis of 12-aza analogs of epothilones and (E)-9,10-dehydroepothilones, *Tetrahedron*, 64, 7920, 2008.
175. Zhang, H.S., Zhong, C.F., Bao, X.P., Studies of the total synthesis of epothilone B and D: A facile synthesis of C7–C14 and C15–C21 fragments, *Chin. Chem. Lett*., 14, 115, 2003.

176. Akbutina, F.A., Sadretdinov, I.F., Kuznetsov, O.M., Vasil'eva, E.V., Miftakhov, M.S., Approaches to epothilone carboanalogs starting from Δ^3-carene, *Russ. J. Org. Chem.*, 39, 75, 2003.
177. Akbutina, F.A., Sadretdinov, I.F., Selezneva, N.K., Miftakhov, M.S., Chiral synthetic block based on (*R*)-pantolactone, *Mendeleev Commun.*, 151, 2003; Klar, U., Roehr, B., Kuczynski, F., Schwede, W., Berger, M., Skuballa, W., Buchmann, B., Efficient chiral pool synthesis of the C1–C6 fragment of epothilones, *Synthesis*, 301, 2005.
178. Bekish, A.V., Isakov, V.E., Kulinkovich, O.G., A cyclopropanol approach to the synthesis of the C13–C21 fragment of epothilones from diethyl (*S*)-malate, *Tetrahedron Lett.*, 46, 6979, 2005; Hurki, A.L., A cyclopropanol approach to the synthesis of both enantiomers of the C12–C21 fragment of epothilones, *Tetrahedron*, 65, 3518, 2009.
179. Ermolenko, M.S., Potier, P., Synthesis of epothilones B and D from D-glucose, *Tetrahedron Lett.*, 43, 2895, 2002.
180. Machajewski, T.D., Wong, C.-H., Chemoenzymatic synthesis of key epothilone fragments, *Synthesis*, 1469, 1999.
181. Shioji, K., Kawaoka, H., Miura, A., Okuma, K., Synthesis of C1–C6 fragment for epothilone A via lipase-catalyzed optical resolution, *Synth. Comm.*, 31, 3569, 2001.
182. Bornscheuer, U.T., Altenbuchner, J., Meyer, H.H., Directed evolution of an esterase for the stereoselective resolution of a key intermediate in the synthesis of epothilones, *Biotechnol. Bioeng.*, 58, 554, 1998.
183. Sinha, S.C., Sun, J., Wartmann, M., Lerner, R.A., Synthesis of epothilone analogs by antibody-catalyzed resolution of thiazole aldol synthons on a multigram scale. Biological consequences of C-13 alkylation of epothilones, *ChemBioChem.*, 2, 656, 2001.
184. Sinha, S.C., Sun, J., Miller, G., Barbas III, C.F., Lerner, R.A., Storer, R.I., Takemoto, T., et al., Sets of aldolase antibodies with antipodal reactivities. Formal synthesis of epothilone E by large-scale antibody-catalyzed resolution of thiazole aldol, *Org. Lett.*, 1, 1623, 1999.
185. Sinha, S.C., Barbas III, C.F., Lerner, R.A., The antibody catalysis route to the total synthesis of epothilones, *Proc. Natl. Acad. Sci. U.S.A.*, 95, 14603, 1998.
186. Liu, J., Wong, C.-H., Aldolase-catalyzed asymmetric synthesis of novel pyranose synthons as a new entry to heterocycles and epothilones, *Angew. Chem. Int. Ed.*, 41, 1404, 2002.
187. Nicolaou, K.C., Vourloumis, D., Li, T., Pastor, J., Wissinger, N., He, Y., Ninkovic, S. et al., Designed epothilones: Combinatorial synthesis, tubulin assembly properties, and cytotoxic action against Taxol-resistant tumor cells, *Angew. Chem. Int. Ed.*, 36, 2097, 1997.
188. Storer, R.J., Takemoto, T., Jackson, P.S., Brown, D.S., Baxendale, J.R., Ley, S.V., A total synthesis of epothilones using solid-supported reagents and scavengers, *Angew. Chem. Int. Ed.*, 42, 2521, 2003; Storer, R.I., Takemoto, T., Jackson, P.S., Brown, D.S., Baxendale, I.R., Ley, S.V., Multi-step application of immobilized reagents and scavengers: A total synthesis of epothilone C, *Chem. Eur. J.*, 10, 2529, 2004; Garabatos-Perera, J.R., Sáez-Diaz, R.I., Multi-step application of immobilized reagents and scavengers: A total synthesis of epothilones C and A, *Chemtracts Org. Chem.*, 19, 402, 2006.
189. Hofman, H., Mahnke, M., Memmert, K., Petersen, F., Schupp, T., Küsters, E., Mutz, M., (Novartis) Fermentative preparation process for cytostatics and crystal forms thereof, WO 1999/042602 (priority Feb. 19, 1998).
190. Sefkow, M., Kiffe, M., Schummer, D., Höfle, G., Oxidative and reductive transformations of epothilone A, *Bioorg. Med. Chem. Lett.*, 8, 3025, 1998.
191. Sefkow, M., Kiffe, M., Höfle, G., Derivatization of the C12–C13 functional groups of epothilones A, B and C, *Bioorg. Med. Chem. Lett.*, 8, 3031, 1998.
192. Höfle, G., unpublished results from 1996.
193. Vite, G.D., Kim, S.-H., Höfle, G., (BMS/GBF) WO 2001073103A2.
194. Höfle, G., Kiffe, M., (GBF) WO 9719086A1.
195. Boddy, C.N., Schneider, T.L., Hotta, K., Walsh, C.T., Khosla, C., Epothilone C macrolactonization and hydrolysis are catalyzed by the isolated thioesterase domain of epothilone polyketide synthase, *J. Am. Chem. Soc.*, 125, 3428, 2003.
196. Regueiro-Ren, A., Leavitt, K., Kim, S.-H., Höfle, G., Gougoutas, J., DiMarco, J., Lee, F.Y.F., Fairchild, C.R., Long, B.H., Vite, G.D., SAR and pH stability of cyano-substituted epothilones, *Org. Lett.*, 4, 3815, 2002.
197. Höfle, G., Glaser, N., Leibold, T., Sefkow, M., Epothilone A–D and their thiazole-modified analogs as novel anticancer agents, *Pure Appl. Chem.*, 71, 2019, 1999.
198. Glaser, N., *Semisynthese Seitenketten-modifizierter epothilone*, Doctoral Thesis, Technical University of Braunschweig, 2001.

199. Vite, G.D., Kim, S.-H., Höfle, G., (BMS/GBF), U.S. 6,399638B1.
200. (a) Leamon, C.P., Folate-targeted drug strategies for the treatment of cancer, *Curr. Opin. Invest. Drugs*, 9, 1277, 2008; (b) Vite, G.D., Lee, F.Y., Leamon, C.P., (BMS/Endocyte) U.S. 2007/0275904 A1; Vite, G.D., Lee, F.Y., Leamon, C.P., Vlahov, I.R., (BMS/Endocyte), U.S. 2007/0276018 A1.
201. http://www.clinicaltrials.gov/ct2/results?term=bms-753493; http://www.clinicaltrials.gov/ct2/show/NCT00550017
202. Dietrich, S.A., Riediker, L., Gertsch, J., Altmann, K.-H., Synthesis and biological activity of new functionalized epothilones for prodrug design and tumor targeting, *Chimia*, 64, 136, 2010.
203. Vite, G.D., Kim, S.-H., Höfle, G., (BMS/GBF) U.S. Patent, 6399638 B1 (June, 4, 2002).
204. Dong, S.D., Sundermann, K., Smith, K.M.J., Petryka, J., Liu, F., Myles, D.C., Rapid access to epothilone analogs via semisynthetic degradation and reconstruction of epothilone D, *Tetrahedron Lett.*, 45, 1945, 2004.
205. Niggemann, J., Michaelis, K., Frank, R., Zander, N., Höfle, G., Natural product-derived building blocks for combinatorial synthesis. Part 1. Fragmentation of natural products from myxobacteria, *J. Chem. Soc., Perkin Trans.*, 1, 2490, 2002.
206. Karama, U., Höfle, G., Synthesis of epothilone 16,17-alkyne by replacement of the C13–C15(*O*)-ring segment of natural epothilone C, *Eur. J. Org. Chem.*, 1042, 2003.
207. Passarella, D., Comi, D., Cappelletti, G., Cartelli, D., Gertsch, J., Quesada, A.R., Borlak, J., Altmann, K.-H., Synthesis and biological evaluation of epothilone A dimeric compounds, *Bioorg. Med. Chem.*, 17, 7435, 2009.
208. Hamel, E., Evaluation of antimitotic agents by quantitative comparisons of their effects on the polymerisation of purified tubulin, *Cell Biochem. Biophys.*, 38, 1, 2003.
209. (a) Nicolaou, K.C., Sarabia, F., Ninkovic, S., Finlay, M.R.V., Boddy, C.N.C., Probing the ring size of epothilones: Total synthesis of [14]-, [15]-, [17]-, and [18]-epothilones A, *Angew. Chem. Int. Ed.*, 37, 81, 1998; (b) Rivkin, A., Njardarson, J.T., Biswas, K., Chou, T.-C., Danishefsky, S.J., Total syntheses of [17]- and [18]-dehydrodesoxyepothilones B via a concise ring-closing metathesis-based strategy: Correlation of ring size with biological activity in the epothilone series, *J. Org. Chem.*, 67, 7737, 2002.
210. Stachel, S.J., Chappell, M.D., Lee, C.B., Danishefsky, S.J., Chou, T.-C., He, L., Horwitz, S.B., On the total synthesis and preliminary biological evaluations of 15(*R*) and 15(S) Aza-dEpoB: A Mitsunobu inversion at C15 in pre-epothilone fragments, *Org. Lett.*, 2, 1637, 2000.
211. Pfeiffer, B., Hauenstein, K., Merz, P., Gertsch, J., Altmann, K.-H., Synthesis and SAR of C12–C13-oxazoline derivatives of epothilone A, *Bioorg. Med. Chem. Lett.*, 19, 3760, 2009.
212. Su, D.-S., Meng, D., Bertinato, P., Balog, A., Sorensen, E.J., Danishefsky, S.J., Zheng, Y.-H., Chou, T.-C., He, L., Horwitz, S.B., Total synthesis of (-)-epothilone B: An extension of the Suzuki coupling method and insights into structure-activity relationships of the epothilones, *Angew. Chem. Int. Ed.*, 36, 757, 1997.
213. Ganesh, T., Schilling, J.K., Palakodety, R.K., Ravindrs, R.K., Shanker, N., Bane, S., Kongston, D.G.I., Synthesis and biological evaluation of fluorescently labeled epothilone analogs for tubulin binding studies, *Tetrahedron*, 59, 9979, 2003.
214. Hearn, B.R., Zhang, D., Li, Y., Myles, D.C., C-15 Thiazol-4-yl analogues of (E)-9,10-didehydroepothilone D: synthesis and cytotoxicity, *Org. Lett.*, 8. 3057, 2006.
215. Cachoux, F., Isarno, T., Wartmann, M., Altmann, K.-H., Scaffolds for microtubule inhibition through extensive modification of the epothilone template, *Angew. Chem. Int. Ed.*, 44, 7469, 2005.
216. Cachoux, F., Isarno, T., Wartmann, M., Altmann, K.-H., Total synthesis and biological assessment of benzimidazole-based analogues of epothilone A: Ambivalent effects on cancer cell groth inhibition, *ChemBioChem.*, 7, 54, 2006; Dietrich, S.A., Lindauer, R., Stierlin, C., Gertsch, J., Matesanz, R., Notararigo, S., Díaz, J.F., Altmann, K.-H., Epothilone analogues with benzimidazole and quinoline side chains: Chemical synthesis, antiproliferative activity, and interactions with tubulin, *Chem. Eur. J.*, 15, 10144, 2009.
217. Bold, G., Wojeik, S., Caravatti, G., Lindauer, R., Stierlin, C., Gertsch, J., Wartmann, M., Altmann, K.-H., Structure-activity relationships in side-chain-modified epothilone analogues—How important is the position of the nitrogen atom, *ChemMedChem.*, 1, 37, 2006.
218. Victory, S.F., Van der Velde, D.G., Jalluri, R.K., Grunewald, G.L., Georg, G.I., Relative stereochemistry and solution conformation of the novel paclitaxel-like antimitotic agent epothilone A, *Bioorg. Med. Chem. Lett.*, 6, 893, 1996.
219. Lange, A., Schupp, T., Petersen, F., Carlomagno, T., Baldus, M., High-resolution solid-state NMR structure of an anticancer agent, *ChemMedChem.*, 2, 522, 2007.

220. Taylor, R.E., Zajicek, J., Conformational properties of epothilone, *J. Org. Chem.*, 64, 7224, 1999; *ibid.*, 65, 5449, 2000.
221. Winkler, J.D., Axelsen, P.H., A model for the Taxol (paclitaxel)/epothilone pharmacophore, *Bioorg. Med. Chem. Lett.*, 6, 2963, 1996.
222. Ojima, I., Chakravarti, S., Inoue, T., Lin, S., He, L., Horwitz, S.B., Kuduk, S.D., Danishefsky, S.J., A common pharmacophore for cytotoxic natural products that stabilize microtubules, *Proc. Natl. Acad. Sci. U.S.A.*, 96, 4256, 1999.
223. Wang, M., Xia, X., Kim, Y., Hwang, D., Jansen, J.M., Botta, M., Liotta, D.C., Snyder, J.D., A unified and quantitative receptor model for the microtubule binding of paclitaxel and epothilone, *Org. Lett.*, 1, 43, 1999.
224. Jiménez-Barbero, J., Amat-Guerri, F., Snyder, J.P., The solid state, solution and tubulin-bound conformations of agents that promote microtubule stabilisation, *Curr. Med. Chem. Anti-Cancer Agents*, 2, 91, 2002.
225. Lee, K.W., Briggs, J.M., Comparative molecular field analysis (CoMFA) study of epothilones—Tubulin depolymerization inhibitors: Pharmacophore development using 3D QSAR methods, *J. Comput. Aided Mol. Des.*, 15, 41, 2001.
226. He, L., Jagtap, P.G., Kingston, D.G.I., Shen, H.-J., Orr, G.A., Horwitz, S.B., A common pharmacophore for Taxol and the epothilones based on the biological activity of a taxane molecule lacking a C13 side chain, *Biochemistry*, 39, 3972, 2000.
227. Day, W., Mutants yield a pharmacophore model fort he tubulin–paclitaxel binding site, *TiPS*, 21, 321, 2000.
228. Forli, S., Manetti, F., Altmann, K.-H., Botta, M., Evaluation of novel epothilone analogues by means of a common pharmacophor and a QSAR pseudoreceptor model for taxanes and epothilones, *ChemMedChem.*, 5, 35, 2010.
229. Manetti, F., Forli, S., Maccari, L., Corelli, F., Botta, M., 3D QSAR studies of the interaction between β-tubulin and microtubule stabilizing antimitotic agents (MSAA). A combined pharmacophore generation and pseudoreceptor modelling approach applied to taxanes and epothilones, *Il Pharmaco*, 58, 357, 2003.
230. Erdélyi, M., Pfeiffer, B., Hauenstein, K., Fohrer, J., Gertsch, J., Altmann, K.-H., Carlomagno, T., Conformational preferences of natural and C2-modified epothilones in aqueous solution, *J. Med. Chem.*, 51, 1469, 2008.
231. Díaz, J.F., Andreu, J.M., Jiménez-Barbero, J., The interaction of microtubules with stabilizers characterized at biochemical and structural levels, in *Topics in Current Chemistry*, Vol. 286, Carlomagno, T., Ed., Springer-Verlag, Berlin, 2009, p. 121.
232. Heinz, D.H., Schubert, W.-D., Höfle, G., Much anticipated—The bioactive conformation of epothilone and its binding to tubulin, *Angew. Chem. Int. Ed.*, 44, 1298, 2005.
233. Sánches-Pedregal, V.M., Griesinger, Ch., The tubulin binding mode of MT stabilizing and destabilizing agents studied by NMR, in *Topics in Current Chemistry*, Vol. 286, Carlomagno, T., Ed., Springer-Verlag, Berlin, 2009, p. 151.
234. Nettles, J.H., Downing, K.H., The tubulin binding mode of microtubule stabilizing agents studied by electron crystallography, in *Topics in Current Chemistry*, Vol. 286, Carlomagno, T., Ed, Springer-Verlag, Berlin, 2009, p. 209.
235. Botta, M., Forli, S., Magnani, M., Manetti, F., Molecular modeling approaches to study the binding mode on tubulin of microtubule destabilizing and stabilizing agents, in *Topics in Current Chemistry*, Vol. 286, Carlomagno, T., Ed., Springer-Verlag, Berlin, 2009, p. 279.
236. Gertsch, J. Feyen, F., Buetzberger, A., Gerber, B., Pfeiffer, B., Altmann, K.-H., Making epothilone fluoresce: design, synthesis, and biological characterisation of a fluorescent N12-aza-epothilone (azathilone), *ChemBioChem.*, 10, 2513, 2009.
237. Carlomagno, T., Blommers, M.J.J., Meiler, J., Jahnke, W., Schupp, T., Petersen, F., Schinzer, D., Altmann, K.-H., Griesinger, C., The high-resolution solution structure of epothilone A bound to tubulin: An understanding of the structure-activity relationships for a powerful class of antitumor agents, *Angew. Chem. Int. Ed.*, 42, 2511, 2003.
238. Carlomagno, T., Sanchez, V.M., Mlommers, M.J.J., Derivation of dihedral angles from CH-CH dipolar-dipolar cross-correlated relaxation rates: A C–C torsion involving a quaternary carbon atom in epothilone A bound to tubulin, *Angew. Chem. Int. Ed.*, 42, 2515, 2003.
239. Sánchez-Pedregal, V.M., Reese, M., Meiler, J., Blommers, M.J.J., Griesinger, C., Carlomagno, T., The INPHARMA method: Protein-mediated interligand NOEs for pharmacophore mapping, *Angew. Chem. Int. Ed.*, 44, 4172, 2005.
240. Barasoain, I., García-Carril, A.M., Matesanz, R., Maccari, G., Trigili, C., Mori, M., Shi, J, Z. et al., Probing the pore drug binding site of microtubules with fluorescent taxanes: Evidence of two binding poses, *Chem. Biol.*, 17, 243, 2010; Buey, R.M., Calvo, E., Barasoain, I., Pineda, O., Edler, M.C., Matesanz,

R., Cerezo, G. et al., Cyclostreptin binds covalently to microtubule pores and lumenal taxoid binding sites, *Nat. Chem. Biol*., 3, 117, 2007.

241. (a) Reese, M., Sanchez-Pedregal, V., Kubicek, K., Meiler, J., Blommers, M.J.J., Griesinger, C., Carlomagno, T., Structural basis of the activity of the microtubule-stabilizing agent epothilone a studied by NMR spectroscopy in solution, *Angew. Chem. Int. Ed.*, 46, 1864, 2007; (b) Erdély, M., Navarro-Vásquez, A., Pfeiffer, B., Kuzniewski, C.N., Felser, A., Widmer, T., Gertsch, J. et al., The binding mode of side chain- and C3-modified epothilones to tubulin, *ChemMedChem.*, 5, 911, 2010.
242. Kubicek, K., Grimm, S.K., Orts, J., Sasse, F., Carlomagno, T., The tubulin-bound structure of the antimitotic drug tubulysin, *Angew. Chem. Int. Ed.*, 49, 1, 2010.
243. Nettles, J.H., Li, H., Cornett, B., Krahn, J.M., Snyder, J.P., Downing, K.H., The binding mode of epothilone A on α,β-tubulin by electron crystallography, *Science*, 305, 866, 2004.
244. Snyder, J.P., Nettles, J., Cornett, B., Downing, K., Nogales, E., The binding conformation of Taxol in b-tubulin: A model based on electron crystallographic density, *Proc. Natl. Acad. Sci. U.S.A.*, 98, 5312, 2001.
245. Reiff, E.A., Nair, S., Henri, J.T., Greiner, J.F., Reddy, B., Chakrasali, R., David, S.A., Chiu, T.-L., Amin, E.A., Himes, R., Total synthesis and evaluation of C26-hydroxyepothilone D derivatives for photoaffinity labeling of β-tubulin, *J. Org. Chem*., 75, 86, 2010.
246. Hutt, O.E., Inagaki, J., Reddy, B., Nair, S., Reiff, E., Henri, J.T., Greiner, J.F., Vander Velde, D.G., Chiu, T.-L., Amin, E.A., Total synthesis and evaluation of C22-(3-azidobenzoyloxy)methyl epothilone C for photoaffinity labeling of β-Tubulin, *Bioorg. Med. Chem. Lett*., 19, 3293, 2009.
247. Hutt, O.E., Reddy, B.S., Nair, S.K., Reiff, E.A., Henri, J.T., Greiner, J.F., Chiu, T.-L. et al., Total synthesis and evaluation of C25-benzyloxyepothilone C for tubulin assembly and cytotoxicity against MCF-7 breast cancer cells, *Bioorg. Med. Chem. Lett*., 18, 4904, 2008.
248. Chou, T.-C., Zhang, X., Zhong, Z.-Y., Li, Y., Feng, L., Eng, S., Myles, D., Johnson Jr., R., Wu, N., Yin, Y.I., Therapeutic effect against human xanograft tumors in nude mice by the third generation mictotubule stabilizing epothilones, *Proc. Natl. Acad. Sci. U.S.A.*, 105,13157, 2008.
249. Danishefsky, S.J., On the potential of natural products in the discovery of pharma leads: A case for reassessment, *Nat. Prod. Rep.*, 1114, 2010.
250. Wartmann, M., Loretan, J., Reuter, R., Hattenberger, M., Muller, M., Vaxelaire, J. Flörsheimer, A., O'Reily, T., Nicolaou, K.C., Altmann, K.-H., Preclinical pharmacological profile of ABJ879, a novel epothilone B analog with potent and protracted anti-tumor activity, *AACR Annu. Meeting*, Orlando, March 27–31, abstr. 5440, 2004.
251. DiLea, C., Wartmann, M., Maira, S.M., Tanaka, J., Sizer, K., Dugan, M., A PK-PD dose optimization strategy for the microtubule stabilizing agent ABJ879, *AACR Annu. Meeting*, Orlando, March 27–31, abstr. 5132, 2004.
252. Lee, F.Y.F., Smykla, R., Johnston, K., Menard, K., McGlinchey, K., Peterson, R.W., Wiebesiek, A., Vite, G., Fairchild, C.R., Kramer, R., Preclinical efficacy spectrum and pharmacokinetics of ixabepilone, *Cancer Chemother. Pharmacol*., 63, 201, 2009.
253. Johnson Jr., R.G., Carney, J., Zhong, Z., Cropp, G., Sherrill, M., Oral bioavailability of KOS-862 (epothilone D), a potent stabilizer of microtubulin polymerisation in rats and Beagle dogs. *Proc. Am. Assoc. Cancer Res*., 44, abstr. 5339, 2003.
254. Bocci, G., Nicolaou, K.C., Kerbel, R.S., Protracted low-dose effects on human endothelial cell proliferation and survival in vitro reveal a selective antiangiogenic window for various chemotherapeutic drugs, *Cancer Res.*, 62, 6938, 2002.
255. Blum, W., Aichholz, R., Ramstein, P., Kühnöl, J., O'Reily, T., Flörsheimer, A., *In vivo* metabolism of epothilone B in tumor-bearing nude mice: Identification of three new epothilone B metabolites by capillary high-pressure liquid chromatography/mass spectrometry/tandem mass spectrometry, *Rapid Commun. Mass Spectrom*., 15, 41, 2001.
256. Borman, S., First disclosures of clinical candidates, *Chem. Eng. News*, 80, 35, 2002.
257. Rothermel, J., Wartmann, M., Chen, T., Hohneker, J., EPO906 (epothilone B): A promising novel microtubule stabilizer, *Sem. Oncol.*, 30 (Suppl. 6), 51, 2003.
258. Agrawal, M., Edgerly, M., Fojo, T., Kotz, H., Treatment of recurrent cervical adenocarcinoma with BMS-247550, an epothilone B analog, *Gynecol. Oncol*., 90, 96, 2003.
259. Altaha, R., Fojo, T., Reed, E., Abraham, J., Epothilones: A novel class of non-taxane microtubule-stabilizing agents, *Curr. Pharm. Design*, 8, 1707, 2002.
260. Abraham, J., Agrawal, M., Bakke, S., Rutt, A., Edgerly, M., Balis, F.M., Widemann, B. et al., Phase I trial and pharmacokinetic study of BMS-247550, an epothilone B analog, administered intravenously on a daily schedule for five days, *J. Clin. Oncol.*, 21, 1866, 2003.

261. Smaletz, O., Galsky, M., Scher, H.I., DeLaCruz, A., Morris, M.J., Solit, D.B., Davar, U., Schwartz, L., Kelly, W.K., Pilot study of epothilone B analog (BMS-247550) and estramustine phosphate in patients with progressive metastatic prostate cancer following castration, *Ann. Oncol.*, 14, 1518, 2003.
262. Thomas, E., Tabernero, J., Fornier, M., Conté, P., Fumoleau, P., Lluch, A., Vahdat, L.T. et al., Phase II clinical trial of ixabepilone (BMS-247550), an epothilone B analog, in patients with taxane-resistant metastatic breast cancer, *J. Clin. Oncol*., 25, 3399, 2007.
263. Gianni, L., Ixabepilone and the narrow path to developing new cytotoxic drugs, *J. Clin. Oncol.*, 25, 3389, 2007.
264. Roché, H., Yelle, L., Cognetti, F., Mauriac, L., Bunnell, C., Sparano, J., Kerbrat, P. et al., Phase II clinical trial of ixabepilone (BMS-247550), an epothilone b analog, as first-line therapy in patients with metastatic breast cancer previously treated with anthracycline chemotherapy, *J. Clin. Oncol*., 25, 3415, 2007.
265. Vansteenkiste, J., Lara Jr., P.N., Le Chevalier, T., Breton, J.-L., Bonomi, P., Sandler, A.B., Socinski, M.A. et al., Phase II clinical trial of the epothilone b analog ixabepilone, in patients with non-small-cell lung cancer whose tumors have failed first-line platinum-based chemotherapy, *J. Clin. Oncol*., 25, 3448, 2007.
266. Lee, J.J., Low, J.A., Croarkin, E., Parks, R., Berman, A.W., Mannan, N., Steinberg, S.M., Swain, S.M., Changes in neurologic function tests may predict neurotoxicity caused by ixabepilone, *J. Clin. Oncol*., 24, 2084, 2006.
267. McDaid, H.M., Mani, S., Shen, H.-J., Muggia, F., Sonnichsen, D., Horwitz, S.B., Validation of the pharmacodynamics of BMS-247550, an analog of epothilone B, during a phase I clinical study, *Clin. Cancer Res.*, 8, 2035, 2002.
268. Shimizu, T., Yamamoto, N., Yamada, Y., Fujisaka, Y., Yamada, K., Fujiwara, Y., Takayama, K. et al., Phase I clinical and pharmacokinetic study of 3-weekly 3-h infusion of ixabepilone (BMS-247550), an epothilone B analog, in Japanese patients with refractory solid tumors, *Cancer Chemother. Pharmacol*., 61, 751, 2008.
269. Awada, A., Piccart, M.J., Jones, S.F., Peck, R.A., Gil, T., Lebwohl, D., Wu, C.-Y., Burris III, H.A., Phase I dose escalation study of weekly ixabepilone, an epothilone analog, in patients with advanced solid tumors who have failed standard therapy, *Cancer Chemother. Pharmacol*., 63, 417, 2009.
270. Gadgeel, S.M., Wozniak, A., Boinpall, R.R., Wiegand, R., Heilbrun, L.K., Jain, V., Parchment, R., Colevas, D., Cohen, M.B., LoRusso, P.M., Phase I clinical trial of BMS-247550, a derivative of epothilone B, using accelerated titration 2B design, *Clin. Cancer Res*. 11, 6233, 2005.
271. Widemann, B.C., Fox, E., Goodspeed, W.J., Goowin, A., Cohen, M., Fojo, T., Colevas, A.D., Balsi, F.M., Phase I trial of the epothilone B analog BMS-247550 (ixabepilone) in children with refractory solid tumors, *J. Clin. Oncol*., Proc. Suppl. abstr. 8529, 2005.
272. Mani, S., McDaid, H.M., Grossman, A., Muggia, F., Goel, S., Griffin, T., Colevas, D., Horwitz, S.B., Egorin, M.J., Peripheral blood mononuclear and tumor cell pharmacodynamics of the novel epothilone B analogue, ixabepilone, *Ann. Oncol*., 18, 90, 2007;
273. Mani, S., McDaid, H., Hamilton, A., Hochster, H., Cohen, M.B., Khabelle, D., Griffin, T. et al., Phase I clinical and pharmacokinetic study of BMS-247550, a novel derivative of epothilone B, in solid tumors, *Clin. Cancer Res*., 10, 1289, 2004.
274. Fojo, A.T., Menefee, M.E., Poruchynsky, M., Edgery, M., Mickley, L., Li Ning Tapia, E., Merino, M., Balsi, F., Bates, S., A translational study of ixabepilone (BMS-247550) in renal cell cancer (RCC): Assessment of its activity and demonstration of target engagement in tumor cells, *J. Clin. Oncol., 2005 ASCO Annu. Meeting*, 23 (Suppl.), abstr. 4541, 2005.
275. Lee, J.J., Yang, S.X., Low, J.A., Nguyen, D., Berman, A.W., Steinberg, S.M., Swain, S.M., et al., Predictive significance of Tau-1, acetylated α-tubulin, and p53 for response to ixabepilone chemotherapy in breast cancer, *Am. Assoc. Cancer Res*., *2005 ASCO Annu. Meeting Proc*., 46 (Suppl.), abstr. 2176, 2005.
276. Denduluri, N., Low, J.A., Lee, J.J., Berman, A.W., Walshe, J.M., Vatas, U., Chow, C.W., Steinberg, S.M., Yang, S.X., Swain, S.M., Phase II trial of ixabepilone, an epothilone B analog, in patients with metastatic breast cancer previously untreated with taxanes, *J. Clin. Oncol*., 25, 3421, 2007.
277. (a) Baselga, J., Gianni, L., Llombart, A., Manikhas, G., Kubista, E., Steger, G., Lee, H., Ronczka, Xu, L., Clark, E., Galbraith, S., Predicting response to ixabepilone: Genomics study in patients receiving single agent ixabepilone as neoadjuvant treatment for breast cancer, *Breast Cancer Res. Treat.*, 94 (S31–S32), abstr. 305, 2005; (b) Baselga, J., Zambetti, M., Llombart-Cussac, A., Manikhas, G., Kubista, E., Steger, G.G., Makhson, A. et al., Phase II genomics study of ixabepilone as neoadjuvant treatment for breast cancer, *Am. Soc. Clin. Oncol*. 27, 526, 2009.
278. Buyse, M., Loi, S., van't Veer, L., Viale, G., Delorenzi, M., Glas, A.M., d'Assignies, M.S. et al., Validation and clinical utility of a 70-gene prognostic signature for woman with node-negative breast cancer, *J. Nat. Cancer Inst*., 98, 1183, 2006.

279. Lee, H., Xu, L., Wu, S., Paul, B., Baselga, J., Llombart, A., Steger, G.G., Galbraith, S., Clark., E., Predictive biomarker discovery and validation for the targeted chemotherapeutic ixabepilone, *J. Clin. Oncol*., *2006 ASCO Annu. Meeting Proc*., 24 (Suppl.), abstr. 3011, 2006.
280. Lee, J.J., Swain, S.M., The epothilones: Translating from the laboratory to the clinic, *Clin. Cancer Res*., 14, 1618, 2008.
281. Lee, F.Y., Castenada, S., Hawken, D., Hickey, C., Kan, D., Lewin, A., Wen, M.-L. et al., Bevacizumab/ixabepilone (BMS-247550) combination produces synergistic antitumor efficacy in multiple tumor models in vivo and is superior to brevacizumab/paclitaxel combination, *Clin. Cancer Res.*, *2005 ASCO Annu. Meeting Proc*., 11 (Suppl.), abstr. B246, 2005.
282. Lee, F.Y., Castaneda, S., Inigi, I., Kann, D., Paul, B., Wen, M.-L., Fairchild, C., Clark, E., Lee, H., Ixabepilone (BMS-247550) plus trastuzumab combination therapy induces synergistic antitumor efficacy in HER2 dependent breast cancers and is accompanied by modulation of molecular response markers, *Am. Soc. Clin. Oncol. Meeting Proc.*, 24, abstr. 561, 2005.
283. Simon, J., MammaPrint^{R}: Klassifizierung von Mamma-Tumoren durch Genexpressionsanalyse, *Laborwelt*, 8, 27, 2007.
284. Lee, F.Y.F., Borzilleri, R., Fairchild, C.R., Kamath, A., Smykla, R., Kramer, R., Vite, G., Preclinical discovery of ixabepilone, a highly active antineoplastic Agent, *Cancer Chemother. Pharmacol*., 63, 157, 2008.
285. Lee, F.Y., Camusa, A., Castaneda, S., Flefleh, C., Ingio, I., Kan, D., McGlinchey, K. et al. Preclinical efficacy evaluation of ixabepilone (BMS-247550) in combination with cetuximab or capecitabine in human colon and lung carcinoma xenografts, *J. Clin. Oncol., 2006 ASCO Annu. Meeting Proc.*, 24 (Suppl.), abstr. 12017, 2006.
286. Perez, E.A., Lerzo, G., Pivot, X., Thomas, E., Vahdat, L., Bosserman, L., Viens, P. et al., Efficacy and safety of ixabepilone (BMS-247550) in a phase II study of patients with advanced breast cancer resistant to an anthracycline, a taxane, and capecitabine, *J. Clin. Oncol*., 25, 3407, 2007.
287. Thomas, E.S., Gomez, H.L., Li, R.K., Chung, H.-V., Fein, L.E., Chan, V.F., Jassem, J. et al., Ixabepilone plus capecitabine for metastatic breast cancer progressing after anthracycline and taxane treatment, *J. Clin. Oncol*., 25, 5210, 2007.
288. Thomas, E.S., Ixabepilone plus capecitabine for metastatic breast cancer progressing after anthracycline and taxane treatment, *J. Clin. Oncol*., 26, 2223, 2008.
289. Vahdat, L.T., Klimovsky, J., Bunnell, C.A., Phase I/II trial in patients with metastatic breast cancer (MBC) previously treated with a taxane and an anthrecycline: Final safety data, *J. Clin. Oncol., 2006 ASCO Annu. Meeting Proc.*, 24 (Suppl.), abstr. 10528, 2006.
290. Bunnell, C.A., Klimovsky, J., Thomas, E., Final efficacy results of a phase I/II trial of ixabepilone in combination with capecitabine in patients with metastatic breast cancer (MBC) previously treated with a taxane and an anthracycline, *J. Clin. Oncol., 2006 ASCO Annu. Meeting*, 24 (Suppl.), abstr. 10511, 2006; Thoma, E., Tabernero, J., Fornier, M., Conté, P., Fumoleau, P., Lluch, A., Vahdat, L.T. et al., Phase II clinical trial of ixabepilone (BMS-247550), an epothilone B analog, in patients with taxane-resistant metastatic breast cancer, *J. Clin. Oncol*., 25, 3399, 2007.
291. Takimoto, C.H., Liu, P.Y., Lenz, H., Remick, S., Mulkerin, D., Mani, S., Synold, T.W., Ramanathan, R.K., Ivy, P., A phase I pharmacokinetic (PK) study of the epothilone B analogue, ixabepilone (BMS-247550) in patients (pts) with advanced malignancies and varying degrees of hepatic impairment, a SWOG Early Therapeutics Committee and NCI Organ Dysfunction Working Group Trial, *2006 ASCO Annu. Meeting*, 24 (Suppl.), abstr. 2004, 2006.
292. Hussain, M., Dipaola, R.S., Baron, A.D., Higano, C.S., Tchekmediyan, N.S., Miller, J.A., Rothermel, J.D., Ixabepilone (epothilone B analogue BMS-247550) is active in chemotherapy-naive patients with hormone-refractory prostate cancer: A Southwest Oncology Group Trial S0111, *J. Clin. Oncol*., 23, 8724, 2005.
293. Galsky, M.D., Small, E.J., Oh, W.K., Chen, I., Smith, D.C., Colevas, A.D., Martone, L. et al., Multi-institutional randomized phase II trial of the epothilone B analog ixabepilone (BMS-247550) with or without estramustine phosphate in patients with progressive castrate metastatic prostate cancer, *J. Clin. Oncol*., 23, 1439, 2005.
294. Bhandari, M.S., Hussain, M., Epothilones and the next generation of phase III trials for prostate cancer, *BJU Int.*, 96, 296, 2005.
295. Reddy, J.A., Dorton, R., Dawson, A., Vetzel, M., Parker, N., Nicoson, J.S., Westrick, E. et al., In vivo structural activity and optimization studies of folate-tubulysin conjugates, *Mol. Pharm.*, 6, 1518, 2009.

296. Rubin, E.H., Rothermel, J., Tesfaye, F., Chen, T., Hubert, M., Ho, Y.-Y., Hsu, C.-H., Oza, A.M., Phase I dose-finding study of weekly single-agent patupilone in patients with advanced solid tumors, *J. Clin. Oncol*., 23, 9120, 2005.
297. Tanabe, K.M., Millward, M., Allen, J.D., Interactions of patupilone (epothilone B) with multidrug transporter proteins, *Proc. Am. Assoc. Cancer Res*., 46, 3430, 2005.
298. Wojtowicz, M., Rothermel, J.D., Anderson, J., Todd, M., Rubin, E.H., Dipaola, R.S., Phase I dose-escalation trial investigating the safety and tolerability of EPO906 plus estramustine in patients with advanced cancer, *J. Clin. Oncol*., 22, abstr. 4623, 2004.
299. Rinehart, J.J., Rothermel, J.D., Anderson, J., Losusso, P., Phase I dose-escalation trial investigating the safety and tolerability of EPO906 plus gemcitabine in patients with advanced cancer, *J. Clin. Oncol*., 22, abstr. 3100, 2004.
300. Rosen, P.J., Rosen, L.S., Britten, C., Parson, M., Cropp, G.F., McDaid, H., Han, J., Johnson, R.G., Hannah, A.L., KOS-862 (epothilone D): Results of a phase I dose-escalating trial in patients with advanced malignancies, *Proc. Am. Soc. Clin. Oncol.*, 21: abstr. 413, 2002.
301. Casado, E., Tabernero, J., Melichar, B., Bridgewater, J., Bennouna, J., Delord, J., Sopala, M., Sklenar, S.I., Cheung, W., Johori, A., Patupilone in chemotherapy-pretreated patients with advanced colorectal cancer (CRC) receiving nutritional support and intensive diarrhea management: A phase I multicenter trial, *J. Clin. Oncol*., 24, abstr. 3593, 2006.
302. Sánchez, J.M., Mellemgaard, A., Perry, M., Zatloukal, P., Hamm, J., Belani, C.P., Kim, E., Felip, E., Berton, M., Johri, A., Efficacy and safety of patupilone in non-small cell lung cancer (NSCLC): A phase I/II trial, *J. Clin. Oncol., 2006 ASCO Annu. Meeting Proc*., abstr. 7104, 2006.
303. Abrey, L., Wen, P.Y., Govindan, R., Reimers, H.J., Rigas, J.R., John, H., Activity of patupilone for the treatment of recurrent or progressive small cell lung cancer (NSCLC): An open-label, multicenter, phase II study, *J. Clin. Oncol., 2007 ASCO Annu. Meeting Proc.*, abstr. 18058, 2007.
304. Veenok, A.P., Poon, R., Kang, Y.K., Mok, T.S., Chao, Y., de Bedout, S., Harbott, A., Li, J., Johri, A.R., Evaluation of patupilone as monotherapy in patients with advanced hepatobiliary cancer, *J. Clin. Oncol., 2007 ASCO Annu. Meeting Proc*., abstr. 15055, 2007.
305. Hsin, K.W., Boyer, M., Ducreux, M., Liu, M., Soo, R., Yeo, W., Williams, K.J., Johri, A., Efficacy of patupilone in advanced local or metastatic gastric cancer: A phase IIa trial, *J. Clin. Oncol., 2006 ASCO Annu. Meeting Proc.*, abstr. 4969, 2006.
306. Hussain, A., Tangen, C.M., Lara Jr., P.N., Vaishampayan, U.N., Petrylak, D.P., Colevas, A.D., Sakr, W.A., Crawford, E.D., A phase IIa trial of weekly EPO906 in patients with hormone-refractory prostate cancer (HPRC), *J. Clin. Oncol., 2004 ASCO Annu. Meeting Proc*., abstr. 4563, 2004.
307. Perez, E.A., Microtubule inhibitors: Differentiating tubulin-inhibiting agents based on mechanisms of action, clinical activity, and resistance, *Mol. Cancer Ther*., 8, 2086, 2009.
308. Wang, H., Wang, Z., Wang, S., Li, M., Nan, L., Rhie, J.K., Covey, J.M., Zhang, R., Hill, D.L., Preclinical pharmacology of epothilone D, a novel tubulin-stabilizing antitumor agent, *Cancer Chemother. Pharmacol*., 56, 255, 2005.
309. Buzdar, A., Silverman, P., Kaufman, P.A., Waintraub, S., Doyle, S., Kroener, J., Robinson, P., Perez, E., Zhang, X, DeMario, M., A phase II study of KOS-862 (epothilone D) in anthracycline and taxane pretreated metastatic breast cancer: Updated results, *SABCS*, abstr. 1087, 2005.
310. Cortes, J., Climent, M.A., Gomez, P., Ruiz, A., Calvo, E., Zhang, X., Perez, E., Demario, M., Baselga, J., A phase I trial of weekly combination KOS-862 (Epothilone D) and trastuzumab in HER-2 overexpressing malignancies, *J. Clin. Oncol., 2006 ASCO Annu. Meeting Proc*., abstr. 2028, 2006.
311. Andrieux, A., Salin, P., Schweitzer, A, Bégou, M., Pachoud, B., Brun, P., Gory-Fauré, S. et al., Microtubule stabilizer ameliorates synaptic function and behavior in a mouse model for schozophrenia, *Biol. Psychiat.*, 60, 1224, 2006.
312. Albright, C., Barten, D.M., Lee, F.Y., Use of epothilone D in treating tau-associated diseases including Alzheimer's disease, WO 2009/132253A1.
313. Michaelis, M.L., Ansar, S., Chen, Y., Reiff, E.R., Seyb, K.I., Himes, R.H., Audus, K.L., Georg, G.I., β-Amyloid-induced neurodegeneration and protection by structurally diverse microtubule-stabilizing agents, *J. Pharmacol. Exp. Ther.*, 312, 659, 2005.
314. Hoffmann, J., Buchmann, B., Schwede, W., Skuballa, W., Lichtner, R.B., Klar, U., Bosslet, K., Comparative sensitivity of ZK-EPO, a novel synthetic epothilone, and other epothilone derivatives to multidrug resistance mechanisms, *Clin. Cancer Res.*, 11 (24/2 Suppl.), abstr. B236, 2005.
315. Schmid, P., Kiewe, P., Kuehnhardt, D., Korfel, A., Lindemann, S., Giurescu, M., Reif, S., Thiel, E., Possinger, K., A phase I study of the novel, third generation epothilon ZK-EPO in patients with advanced solid tumors, *J. Clin. Oncol., 2005 ASCO Annu. Meeting Proc*., abstr. 2051, 2005.

316. Schmid, P., Kiewe, P., Possinger, K., Korfel, A., Lindemann, S., Giurescu, M., Reif, S., Wiesinger, H., Thiel, E., Kühnhardt, D., Phase I study of the novel, fully synthetic epothilone sagopilone (ZK-EPO) in patients with solid tumors, *Ann. Oncol.*, 21, 633, 2010.
317. Hoffmann, J., Buchmann, B., Schwede, W., Skuballa, W., Lichtner, R.B., Pietsch, H., Klar, U., New synthetic Epothilone Derivative ZK-Epo inhibits breast cancer metastasis, *Proc. Am. Assoc. Cancer Res*., 46, 3424, 2005.
318. Hoffmann, J., Fichtner, I., Lemm, M., Lienau, P., Hess-Stumpp, H., Rotgeri, A, Hofmann, B., Klar, U., Sagopilone crosses the blood-brain barrier *in vivo* to inhibit brain tumor groth and metastases, *Neuro-Oncology*, 11, 158, 2009.
319. Strube, A., Hoffmann, J., Stepina, E., Hauff, P., Klar, U., Käkönen, S.-M., Sagopilone inhibits breast cancer bone metastasis and bone destruction due to simultaneous inhibition of both tumor groth and bone resorption, *Clin. Cancer Res*., 15, 3751, 2009.
320. Kaekoenen, S.-M., Hoffmann, J., Klar, U., (Bayer Schering Pharma) EP 1 930 004A1 (2008).
321. Vite, G.D., The semisynthesis and preclinical evaluation of BMS-310705, an epothilone analog in clinical evaluation. *223rd American Chemical Society National Meeting*, Chicago, April 7, 2002; Lee, F.Y., Vite, G., Gerhard, H., Kim, S.-H., Clark, J., Fager, K., Kennedy, K. et al., The discovery of BMS 310705: A water-soluble and chemically stable semisynthetic epothilone possessing potent parenteral and oral antitumor activity against models of taxane-sensitive and taxane-resistant human tumor in vivo, *Proc. AACR*, 43, 792, 2002.
322. (a) Mekhail, T., Holden, S., Pierson, S., Lee, F., Galbraith, S., Cohen, M., Messina, M. et al., A phase I pharmacokinetic and biologic study of the novel epothilone BMS-310705 in patients with advanced cancer, *Proc. Am. Soc. Clin. Oncol.*, 2002 ASCO Annual Meeting Proceedings, abstr. 408; (b) Mekhail, T., Chung, C., Holden, S., Bukowski, R.M., Eckhardt, S.G., Cunningham, M., Messina, M., Cohen, M., Peck, R., Sikic, B., Phase I trial of novel epothilone B analog BMS-310705 Ivq 21 days, *Proc. Am. Soc. Clin. Oncology, 2003 ASCO Annu. Meeting Proc*., abstr. 515, 2003.
323. Sessa, C., Perotti, A., Lladò, A., Cresta, S., Capri, G., Voi, M., Marsoni, S., Corradino, I., Gianni, L., Phase I clinical study of the novel epothilone B analogue BMS-310705 given on a weekly schedule, *Ann. Oncol.*, 18, 1548, 2007; Sessa, C., Perotti, A., Malossi, A., Capri, G., Cresta, S., De Braud, F., Dall'o', E., Voi, M., Marsoni, S., Gianni, L., Phase I and pharmacokinetic (PK) study of the novel epothilone BMS-310705 in patients (pts) with advanced solid cancer, *Proc. Am. Soc. Clin. Oncol.*, *22*, 130, 2003.
324. Stopek, A., Thomas, E., Jones, S., Cohen, J., Cropp, G., Zhou, Y., Feng, L., Kersey, K., Hannah, H.L., Burris, H., Phase I trial of a novel epothilone, KOS-1584, using a weekly dosing schedule, *J. Clin. Oncol., 2006 ASCO Annu. Meeting Proc*., abstr. 2041, 2006.
325. Villalona-Calero, M., Goel, S,. Schaaf, L., McCracken, B., Desai, K., Copp, G., Zhou, Y., Johnson, R.G., Hannah, A.L., Mani, S., First-in-human phase I trial of a novel epothilone, KOS-1584, *J. Clin. Oncol., 2006 ASCO Annu. Meeting Proc*., abstr. 2003, 2006.

22 Enediynes

Philip R. Hamann, Janis Upeslacis, and Donald B. Borders

CONTENTS

22.1 Introduction 575
22.2 History 575
22.3 Structural Classes and Producing Organisms 578
22.4 Biosynthesis 580
22.5 Total Syntheses 581
22.6 Molecular Mechanisms of Action 590
22.7 Cellular Mechanisms of Action 594
22.8 Preclinical Studies 598
22.9 Clinical Experience 604
22.10 Summary 607
References 608

22.1 INTRODUCTION

The enediyne antitumor antibiotics represent some of the most potent, biologically active natural products ever discovered. These compounds possess both antibacterial and antitumor activities and are related by containing enediyne functionality constrained within 9- or 10-membered rings, with varying degrees of chemical complexity in the remainder of the molecules. Most of these antitumor antibiotics are produced by microorganisms classified as the actinomycetes. The challenging chemical structures of these enediynes, their mechanisms of action, and their biological activity have attracted considerable scientific attention. Two of these compounds, neocarzinostatin and esperamicin A1, were advanced into anticancer clinical trials as single agents. Esperamicin A1 was eventually abandoned from further development because of toxicity issues. However, neocarzinostatin has been approved for human use in Japan for a number of cancer indications, both as the natural product itself as well as a part of a polymer-based conjugate. A monoclonal antibody conjugate of calicheamicin was successful in clinical trials and has been commercialized for the treatment of acute myelogenous leukemia in adults.

This chapter updates our earlier review of enediynes as anticancer agents.[1] We included a number of meeting abstract references in our first offering, even though these are often difficult to retrieve, because much of the scientific and clinical information was only available in that form at the time. However, unless such abstracts have since matured into full scientific papers, we have deleted most such references for this chapter. Some of the other previous reviews covering the enediynes have included a comprehensive summary in book form,[2] as well as a number of focused reviews detailing structure determinations, mechanism of action, synthetic approaches, biosynthesis, and biological activity.[3–10] A book devoted to neocarzinostatin has also been published.[11]

22.2 HISTORY

The structures of the major components of the calicheamicins and esperamicins were published as back-to-back articles in a 1987 issue of the *Journal of the American Chemical Society* based on research at two different pharmaceutical companies.[12–15] It is fortunate that these publications

appeared together since, taken individually, the structures with 10-membered ring enediynes were difficult to believe. These remarkable compounds were structurally quite different from one another but, surprisingly, both had the same novel 10-membered ring enediyne system, an allylic methyl trisulfide group, a hydroxyamino-linked disaccharide unit, and unique amino- and thio-containing carbohydrates (Figure 22.1). In addition, the calicheamicins possessed a highly substituted halobenzene unit. Both classes of compounds showed extremely potent biological activity with a mechanism of action involving free radical damage to DNA at selective sites. In the case of the calicheamicins, a high percentage of the damage involved double-strand cleavage of DNA.[16] In time, the structures of additional members of both families of compounds were elucidated.[17,18]

A key factor in the discovery of the calicheamicin complex in fermentation extracts was a newly developed *in vitro* test termed the biochemical induction assay (BIA) that detected DNA-damaging agents.[19] The assay was extremely sensitive for detecting the very low concentrations of the calicheamicins present in the early fermentation. Even very crude preparations of the complex were significantly more potent in this assay than the reference compounds, and this provided the first

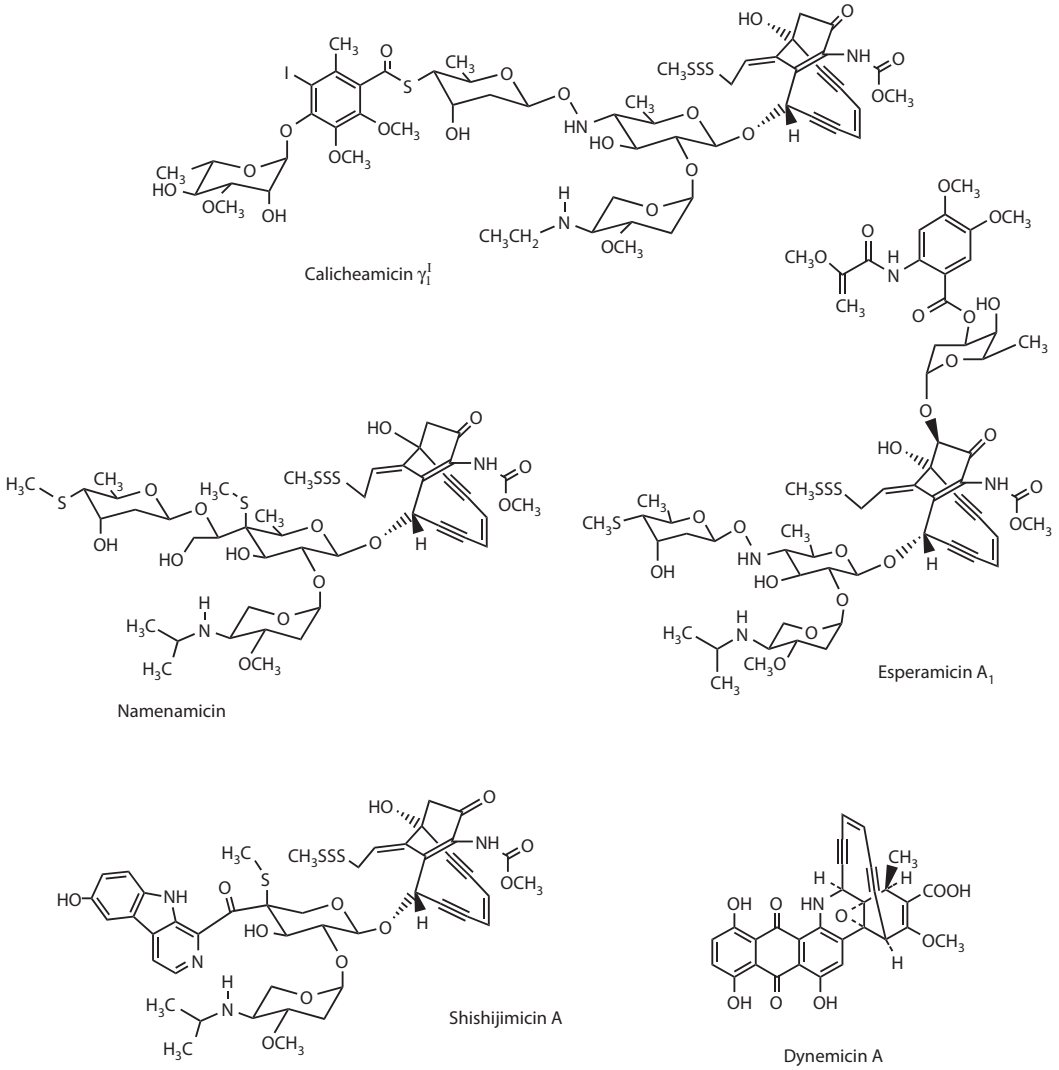

FIGURE 22.1 Structures of representative 10-membered ring enediyne antibiotics.

suggestion that the compounds were novel. Pure calicheamicin γ_1^I was extremely active in the BIA and against Gram-positive bacteria in the pg/mL range.[20,21] It was also very active against Gram-negative bacteria.

Once the structures of calicheamicin and esperamicin were firmly established, the very elegant and earlier structural work with the more remarkable 9-membered ring enediyne chromophoric component and associated apoprotein of the antitumor antibiotic neocarzinostatin could be fully appreciated.[22] This compound could only be isolated along with the apoprotein, which provided stability to the highly reactive 9-membered ring enediyne chromophoric component. It became apparent that calicheamicin and esperamicin represented 10-member ring enediyne antitumor antibiotics that were stable without an associated protein, whereas neocarzinostatin represented another type, the 9-membered chromoprotein enediynes, requiring a protein for stabilization.

A number of the enediyne antibiotics listed in Table 22.1 have various synonyms. The numeric designations were given by the pharmaceutical companies at the initial stages of their investigations

TABLE 22.1
Summary of Enediyne Antibiotics Produced by Various Organisms

Name	Synonyms	Producing Organism	Structure Type[a]
Calicheamicin	LL-E33288 Calichemicin	*Micromonospora echinospora* ssp. calichensis	10-mr enediyne with allylic MeSSS
Esperamicin	BMY 28175 FR900405 FR900406 Veractamycins A and B	*Actinomadura verrucosospora*	10-mr enediyne with allylic MeSSS
Namenamicin		*Polysyncraton lithostrotum* (ascidian)	10-mr enediyne with allylic MeSSS
Shishijimicin		*Didemnum proliferum* (ascidian)	10-mr enediyne with allylic MeSSS
Dynemicin	BU 3420T	*Micromonospora chersina* *Micromonospora globosa*	10-mr enediyne with anthraquinone
Endynamicin		*Micromonospora globosa*	10-mr enediyne with anthraquinone
Uncialamycin		Streptomyces from lichen	10-mr enediyne with anthraquinone
Actinoxanthin		*Streptomyces globisporus*	Presumed 9-mr enediyne with apoprotein
Auromomycin	Macromomycin I	*Streptomyces macromyceticus*	Presumed 9-mr Enediyne with apoprotein
Kedarcidin		*Streptoalloteichus* sp.	9-mr enediyne with apoprotein
Lidamycin	C-1027, C1027	*Streptomyces globisporus* C-1027	9-mr enediyne with apoprotein
Maduropeptin	BBM 1644	*Actinomadura madurae*	9-mr enediyne with apoprotein
Neocarzinostatin	Zinostatin NSC 69856	*Streptomyces carzinostaticus*	9-mr enediyne with apoprotein
Precursors to sporolides A and B		*Salinispora tropica* Marine actinomyces	9-mr enediyne precursor to sporolides
Antibiotic N1999A2		*Streptoverticillium* sp.	9-mr enediyne

[a] 9- and 10-membered rings are abbreviated as 9-mr and 10-mr, respectively.

and then were changed to more conventional names if the compounds showed promise for further development. Thus, the esperamicin complex was originally designated BMY 28175 by Bristol-Myers. Two other companies working on components of the same complex at approximately the same time as Bristol-Myers designated their compounds as FR900405 and FR900406 (Fujisawa) or veractamycins A and B (Parke-Davis). The BMY 28175 designation was subsequently changed to esperamicin and eventually shown to be identical to the products isolated by the other two companies.[23] Lederle Laboratories originally named the LL-E33288 complex "calichemicin" and that name appeared in the initial structure papers. However, a conflict due to a resemblance of that name to that of a chemical company required changing the name to "calicheamicin."

22.3 STRUCTURAL CLASSES AND PRODUCING ORGANISMS

The enediyne antitumor antibiotics fall into two general classes as shown in Table 22.1. Representative examples wherein the conjugated enediyne system is a part of a 10-member macrocycle are shown in Figure 22.1, and examples of the 9-member enediynes identified so far are shown in Figure 22.2. Many of the 10-member ring enediynes are related to calicheamicin and esperamicin and have an allylic methyl trisulfide group that can act as a trigger to initiate the formation of a diradical through cycloaromatization of the core ring. These diradicals are responsible for the resultant DNA damage. Although dynemicin A and endynamicin, differing from each other by virtue of stereochemistry, also possess a 10-member ring enediyne, they contain no methyl trisulfide group to initiate radical formation. Uncialamycin also has these general structural features. Instead, these compounds contain an epoxide and bridging anthraquinone unit that is involved in redox activation, putting them into a different subclass than the other 10-member ring enediynes.

With the exception of antibiotic N1999A2,[24] the 9-member ring enediynes (Figure 22.2) are molecules that are associated noncovalently with coproduced apoproteins that stabilize the chromophores by binding them in a hydrophobic cavity.[25] Although the apoproteins examined so far exhibit significant homology, they differ for each individual antibiotic. For example, the neocarzinostatin, kedarcidin, and lidamycin apoproteins contain 113, 114, and 110 amino acids, respectively.[26–28] The x-ray crystal structure of the neocarzinostatin apoprotein was determined to a resolution of 0.15 nm. The structure of this apoprotein was then compared with crystal structure data for the apoproteins of actinoxanthin and auromomycin to show a three-dimensional similarity to these homologous proteins.[29] The apoproteins stabilize the enediynes in a cellular environment by excluding glutathione from the reaction center through electronic repulsions.[30] Supra C-1027, a significantly stabilized analog of the lidamycin chromoprotein, was prepared by the incorporation of deuterated glycine into the apoprotein.[31] This was accomplished by expressing the di-deutero-Gly apoprotein in *Escherichia coli* containing a vector with the lidamycin apoprotein coding sequence. The di-deutero-Gly apoprotein was then complexed with the chromophore to obtain the chromoprotein. Peptidase activity has also been attributed to the apoproteins, which may help expose the DNA to the enediyne chromophores.[32,33]

The structures of the enediynes have been determined by spectral methods, mainly 2D-NMR and MS techniques, chemical degradations, and, in some cases, x-ray crystallography. Because of the considerable interest in this class of compounds and the challenge of synthesizing these unusual structures, a number of the enediyne antibiotics have been confirmed or revised by total syntheses.

Most of the enediyne antitumor antibiotics are produced by microorganisms classified as actinomycetes. Within this general class, though, there is considerable diversity of genus and species for the organisms that produce the natural products (Table 22.1). Lidamycin, one of the 9-membered ring enediyne antibiotics, was isolated from the fermentation products of *Streptomyces globisporus* C-1027, which was obtained from the soil samples at Qian-jiang County of Hubei Province, China.[34] The antibiotic is named lidamycin but a number of recent publications have referred to it as C-1027 (and, occasionally, C1027), which appears to be the designation for an

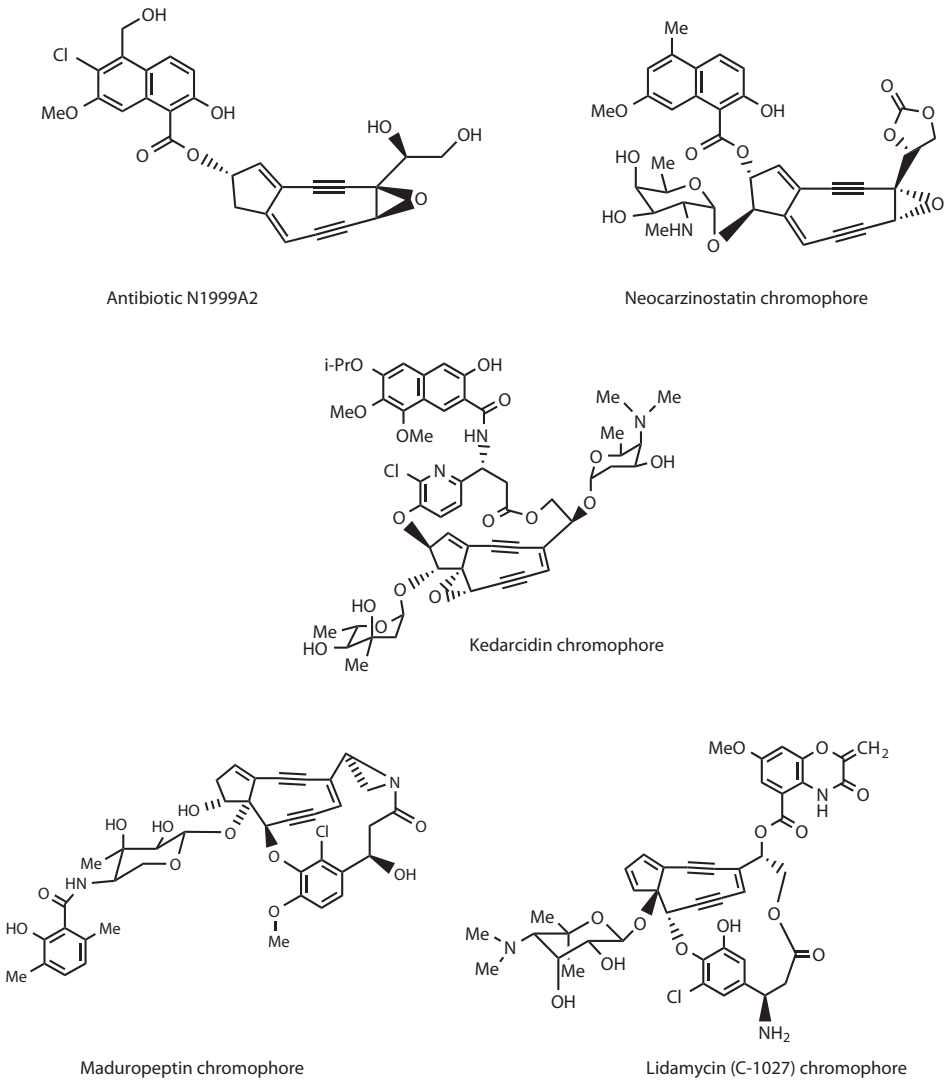

FIGURE 22.2 Structures of representative 9-membered ring enediyne antibiotics.

isolate of the producing organism. Macroscopic organisms have been implicated in producing 10-member ring enediynes related to calicheamicin and esperamicin (Table 22.1). Marine ascidians were credited for producing namenamicin and shishijimicin.[35,36] However, the ascidian that produced namenamicin was later found to coexist with several *Micromonospora* species in a symbiotic relationship, which led to speculation that one of the *Micromonospora* sp. may have actually produced the enediynes rather than the ascidian (Table 22.1). Uncialamycin is a 10-membered ring enediyne similar to dynemicin and was isolated from a streptomyces isolated from the surface of a British Columbia lichen.[37]

One of the most unusual reported results for enediyne derived structures are the sporolides produced by the marine actinomycete *Salinispora tropica*.[38] It is proposed that the sporolides are derived from a gene cluster producing a polyketide synthase (PKS) that forms an enediyne product. The enediyne undergoes further enzymatic transformations followed by a Bergmann rearrangement to give an aromatized nonenediyne unit as part of a polycyclic macrolide ring of the sporolides (see next section).[39]

22.4 BIOSYNTHESIS

The gene clusters for calicheamicin, neocarzinostatin, antibiotic C-1027 (lidamycin), maduropeptin and dynemicin have been cloned and sequenced. This information provides the foundation to understanding the processes involved to form the enzymes and other proteins necessary to conduct the biosynthesis of these remarkable molecules.

Most of the enediyne antibiotics are generated as complexes of related components by the producing organisms (Table 22.1). The various components of the calicheamicin complex, at last count about 20, differ not only by the halogen on the aromatic ring but also by the presence or absence of the terminal sugars. In addition, the amine of the terminal amino sugar is elaborated with either a methyl, ethyl, or isopropyl group. The natural components of the calicheamicin complex contained a bromine atom, an unusual halogen for a terrestrial organism. Attempts to improve fermentation yields by adding potassium iodide to the media resulted in a significant improvement and gave new components containing iodine instead of bromine.[40] Surprisingly, addition of iodide to the fermentation media of esperamicin and dynemicin also resulted in increased fermentation yields, even though these products do not contain a halogen.[23] This suggests that iodide or one of the other halides may be involved in intermediate steps in the biosynthesis of the enediyne antibiotics. $CalO_2$, a putative orsellinic acid P450 oxidase, appears to be involved in the calicheamicin biosynthesis after enzyme $CalO_3$-catalyzed iodination, which may require coenzyme A or an acyl carrier protein bond substrate. In this study, the x-ray structure determination of $CalO_2$ at 2.5 angstrom resolution was reported and was the first crystal structure for a P450 involved in modifying a bacterial iterative type I polyketide product.[41]

Biosynthetic incorporation studies using labeled acetate and other potential polyketide precursors revealed the pathway for assembly of the esperamicin and neocarzinostatin chromophores, and dynemicin biosynthetic precursors.[42–45] These studies are representative of 9- and 10-membered ring enediyne antibiotics. Cloning, sequencing, and characterization of the complete calicheamicin and lidamycin chromophore biosynthesis gene clusters have been reported.[9,46,47,48] The PKSs for these enediynes are quite unique from previously reported PKSs. A comparison of the lidamycin chromophore locus with that of calicheamicin revealed that the enediyne PKSs are highly conserved in spite of producing 9- and 10-membered ring enediynes, respectively. A linear carbonyl-conjugated hexadiene has been characterized that was suggested to be a common precursor for the 10-membered enediynes,[49] and it was suggested that the previously reported pentadecaheptaene was the precursor to the 9-membered ring enediynes.[50] However, other studies showed that the pentadecaheptaene was the only major product shared by PKSs of three different 9- and 10-membered ring enediynes.[51] The divergence of biosynthesis of 9- and 10-membered ring enediynes at the PKS stage has been further questioned and also the legitimacy of either polygene as true precursors on the path to calicheamicin. A more convergent model of enediyne biosynthesis was suggested and supports the contention that the divergence of 9- and 10- member products results from the action of one or more accessory enzymes acting in concert with the enediyne PKS.[52] A phylogenetic tree has been suggested that relates the synthesis of both 9- and 10-member enediynes and yields a genomic method to screen for other enediynes.[53]

The genes from the marine actinomycete *S. tropica* involved in the biosynthesis of the enediyne precursor unit of the sporolides A and B share a strong homology with those from other 9-member ring enediyne PKS gene clusters including lidamycin, neocarzinostatin, and maduropeptin.[39,54] The enediyne produced by the sporolides PKS was proposed to be modified by enzymatic reactions and then a Bergmann cyclization to give part of the nonenediyne polycyclic macrolide found in sporolides A and B.[38]

Exploration of the biosynthesis of other unique structural elements in calicheamicin has led to various unique enzymes involved in those pathways.[55] CalE10, the N-oxidase involved with the hydroxyaminosugar formation, was characterized and confirmed that oxidation occurs at the sugar nucleoside stage prior to glycosyltransfer.[56] This study represents the first characterization of an amino sugar N-oxidase.

The gene cluster responsible for the biosynthesis of antibiotic C-1027 was found to contain a gene that encodes for a new type of aminomutase, which converts L-tyrosine into (*S*)-β-tyrosine.[57] Further biochemical processing of the (*S*)-β-tyrosine converts it to the subunit of C-1027. The x-ray crystal structure of the L-tyrosine 2,3-aminomutase from antibiotic C-1027 was reported, and this study confirmed its homology to ammonia-lyases.[58] The conversion of (*S*)-α-tyrosine to the (*S*)-3-chloro-4,5-dihydroxy-β-phenylalanine moiety of C-1027 is catalyzed by five proteins. One of these proteins is SgcC3, a FAD-dependent halogenase, that acts on a carrier protein-tethered substrate. A sixth protein catalyses the incorporation of this amino acid moiety into the C-1027 chromophore.[59]

In addition, the genes that encode the production of the C-1027 chromophore in *Streptomyces globisporus* C-1027 are clustered with the cagA gene that encodes the antibiotic C-1027 apoprotein.[60] This suggests that some type of genetic coordination exists between production of the chromophore and the apoprotein in this organism.

Sequence analysis of the genes within the neocarzinostatin cluster suggested dNDP-D-mannose as a precursor for the deoxy amino sugar and revealed two distinct type I PKSs. These data supported a convergent model for neocarzinostatin (NCS) chromophore biosynthesis from the deoxy amino sugar, naphthoic acid, and the enediyne core.[61] It was proposed that the biosynthesis of the naphthoic acid moiety and its incorporation into the neocarzinostatin chromophore are catalyzed by five enzymes. Biochemical characterization of one of these enzymes, NcsB1, revealed that it was an *O*-methyltransferase catalyzing regiospecific methylation of its native substrate.[62] Another of these enzymes, NcsB2, involved in the activation of the naphthoic acid moiety exhibited promiscuous substrate specificity with a diverse set of naphthoic acid analogs.[63]

It has been speculated that the C-1027 chromophore is sequestered by binding to a preapoprotein to form a complex that is transported out of the cell by an efflux pump and processed by removing a leader peptide sequence to yield the chromoprotein.[60] This may serve to protect the producing organism from the toxic effects of antibiotic C-1027. Another similar mechanism has been discovered for calicheamicin that may prove to be a general phenomenon. A protein, CalC, is coproduced with calicheamicin that binds to the triggered natural product prior to the Bergman cyclization better than it binds to the intact form, thereby scavenging the triggered form through "self-sacrifice" before it can damage the DNA.[64]

Previous studies with kedarcidin showed that exposure of the producing organism to the chromophore resulted in significantly upregulated apoprotein production, by as much as 10- to 20-fold. However, decoupling of the joint biosynthesis of apoprotein and chromophore has also been achieved. When the neocarzinostatin-producing organism was fermented in a synthetic medium containing $MgSO_4$, the free chromophore was observed in the culture filtrate.

The maduropeptin biosynthetic gene cluster from *Actinomadura madurae* was cloned and sequenced.[65] The biosynthesis of maduropeptin chromophore involves a PKS for the enediyne and a PKS for the 6-methylsalicylic acid. Furthermore, the apoprotein gene was localized within the maduropeptin gene cluster.

The biosynthetic genes encoding the production of dynemicin were cloned and sequenced but, surprisingly, the genes encoding the enediyne and the anthraquinone (see Figure 22.1) were not flanking. This suggested that the location of the genes in *Micromonospora chersina* encoding the enediyne core and the anthraquinone are chromosomally distinct.[66]

22.5 TOTAL SYNTHESES

The novelty of the enediynes, the obvious challenges in the overall structures, the intriguing mechanisms of action, and the dramatic potency of these compounds have led to a flurry of synthetic activity that continues today. A literature search in the CAS database indicated about 1000 articles that have both the keywords enediyne and synthesis. Many of these syntheses are Herculean efforts, especially the syntheses of calicheamicin, which are about 70 steps long. Aside from the development of new synthetic methodology, the enediyne syntheses have served to confirm and sometimes

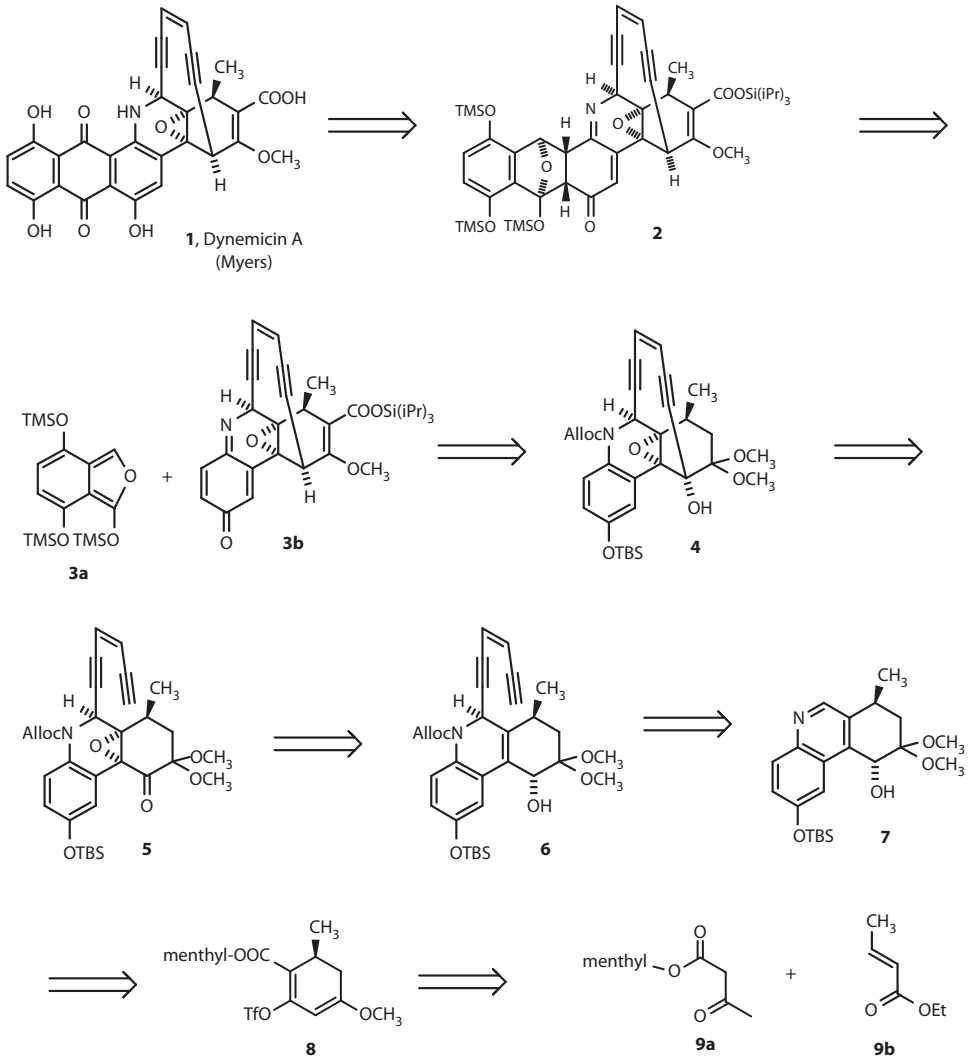

FIGURE 22.3 Myers synthesis of dynemicin.

even correct the structural assignments, have made some of the enediynes more available, have shed light on their mechanisms of action, and have explored their SAR. This has resulted in simplified (e.g., dynemicin[67]) or hybrid molecules (e.g., calicheamicin hybrids) with interesting properties. The synthetic summaries that follow focus primarily on the enediyne portion of these molecules. Each of Figures 22.3 through 22.16 uses independent numbering of the structures. The significant work on the carbohydrates present in many of the enediynes that are the keys to some of their biological properties is not included in the interest of space.

Myers dynemicin synthesis[*] (1995, Figure 22.3).[68,69] The Myers group completed the synthesis of the dynemicin core by the Diels–Alder reaction of isobenzofuran **3a** with the fully elaborated right-hand segment **3b**. Their synthetic strategy required only reaction with MnO_2 plus HF-Et_3N to complete the synthesis. The enediyne ring was closed by intramolecular reaction of the acetylene in compound **5** with the ketone. This reaction left behind an unneeded alcohol, which was later

[*] Each figure uses independent numbering of the structures.

removed. The enediyne was introduced in one piece by reaction of activated quinoline **7** with a magnesium acetylide. The requisite quinoline was ultimately derived by condensation of the unsaturated ester **9b** with menthol ester **9a**. There was little, if any, chiral induction in this reaction, but the desired diastereomer was isolable by crystallization. The overall synthesis was 24 steps in 1–2% yield and confirmed the chirality assignment of dynemicin.

Danishefsky dynemicin synthesis (1996,* Figure 22.4*)*.[70,71] In the retrosynthetic sense, dynemicin A was made by the air oxidation and deprotection of phenol **2**, which was accessible by the annulation of **3b** with the anion of **3a**. Quinone imine **3b** was accessible in six steps from diol **4**, which was the first intermediate in the synthesis containing the enediyne. This was constructed by the double Pd-catalyzed coupling of bis-iodoacetylene **5b** with tin reagent **5a**. Compound **5b** was made in 15 steps from quinoline **6**. In this sequence, one acetylene was introduced via an ethynyl magnesium reagent reacting with the quinoline in the presence of a chloroformate, and the other acetylene was introduced via the Corey–Fuchs procedure. Quinoline **6** was accessed by the treatment of intermediate **7** with ammonia, which itself was made via the oxidative (CAN) rearrangement of the intramolecular Diels–Alder product **8**. The Diels–Alder starting material **9** was made by standard chemistry from commercially available aldehyde **10**. The overall synthesis proceeded in 33 steps to give the deeply blue–violet-colored dynemicin **1** in milligram quantities.

Nicolaou uncialamycin synthesis (2007, Figure 22.5*)*.[72] This synthesis has some overall similarities to the previous syntheses of the related dynemicin A. The final stage of the construction of uncialamycin relied on an AB ring annulation similar to that used by Danishefsky in his dynemicin synthesis. The precursor for the transformation, **2b**, was constructed by adding the enediyne as a unit starting with quinoline **5**. Unfortunately, the stereochemistry of uncialamycin methyl carbinol was unknown at the time of this synthesis, and the approach employed resulted in the wrong isomer, necessitating the inversion of the center from that shown in alcohol **4** to that shown in **3**. The quinoline was derived in five steps from commercially available isatin **5**. Thus, racemic uncialamycin was made in 20 steps. Further work is being carried out to assign the absolute stereochemistry, which is likely to be the same as dynemicin A.

Myers synthesis of neocarzinostatin chromophore (1996, Figure 22.6*)*.[73,74] The Myers group ended their synthesis with a unique glycosylization of alcohol **2** using an amino sugar unprotected on the amino group, followed by deprotection. This aglycone was made in a seven-step sequence from **3** that involved a key deoxygenative rearrangement of an epoxy alcohol to a transposed allylic alcohol. The enediyne in intermediate **4** was made by the intramolecular reaction of a lithium acetylide with the aldehyde. The enediyne/epoxide unit **6b**, which was made from a glyceraldehyde derivative, was initially incorporated via an acetylide reaction with cyclopentenone **6a**. The entire synthesis was about 30 steps long and was the first completed synthesis of an enediyne chromoprotein chromophore.

Kobayashi/Hirama synthesis of neocarzinostatin aglycon (2006, Figure 22.7*)*.[75] This synthesis relied on a penultimate dehydration to generate the final unsaturation with the Martin sulfurane. The naphthoic acid was added to protected alcohol **2**, which was derived from alcohol **3**. This alcohol was derived from the cesium-catalyzed, chelation-controlled, intramolecular reaction of the acetylene and aldehyde in **4**. The lower acetylene was added by the reaction of propargyl magnesium bromide with ketone **5** (with poor stereocontrol). The upper acetylene was added by Pd/Cu coupling of a highly elaborated acetylene with vinyl iodide **6**, which was made in five steps from cyclopentene **7**, the synthesis of which was not described.

Kobayashi/Hirama synthesis of N1999-A2 chromophore (2001, Figure 22.8*)*.[76,77] N1999-A2 is structurally very similar to neocarzinostatin, so it is no surprise that the basic synthesis is similar to the Kobayashi/Hirama synthesis of that enediyne. The main deviation was the incorporation of the upper acetylene second in the conversion of vinyl iodide **6** to a precursor of compound **5**. It appears that the synthesis of vinyl iodide **6** is not published. The naphthoic acid was made in a multistep synthesis from 3-methoxybenzyl alcohol.

Myers synthesis of N1999-A2 chromophore (2006, Figure 22.9*)*.[78] Final elaboration of the enediyne core **2** was routine, but the construction of this core was quite unique. Metalation of vinyl

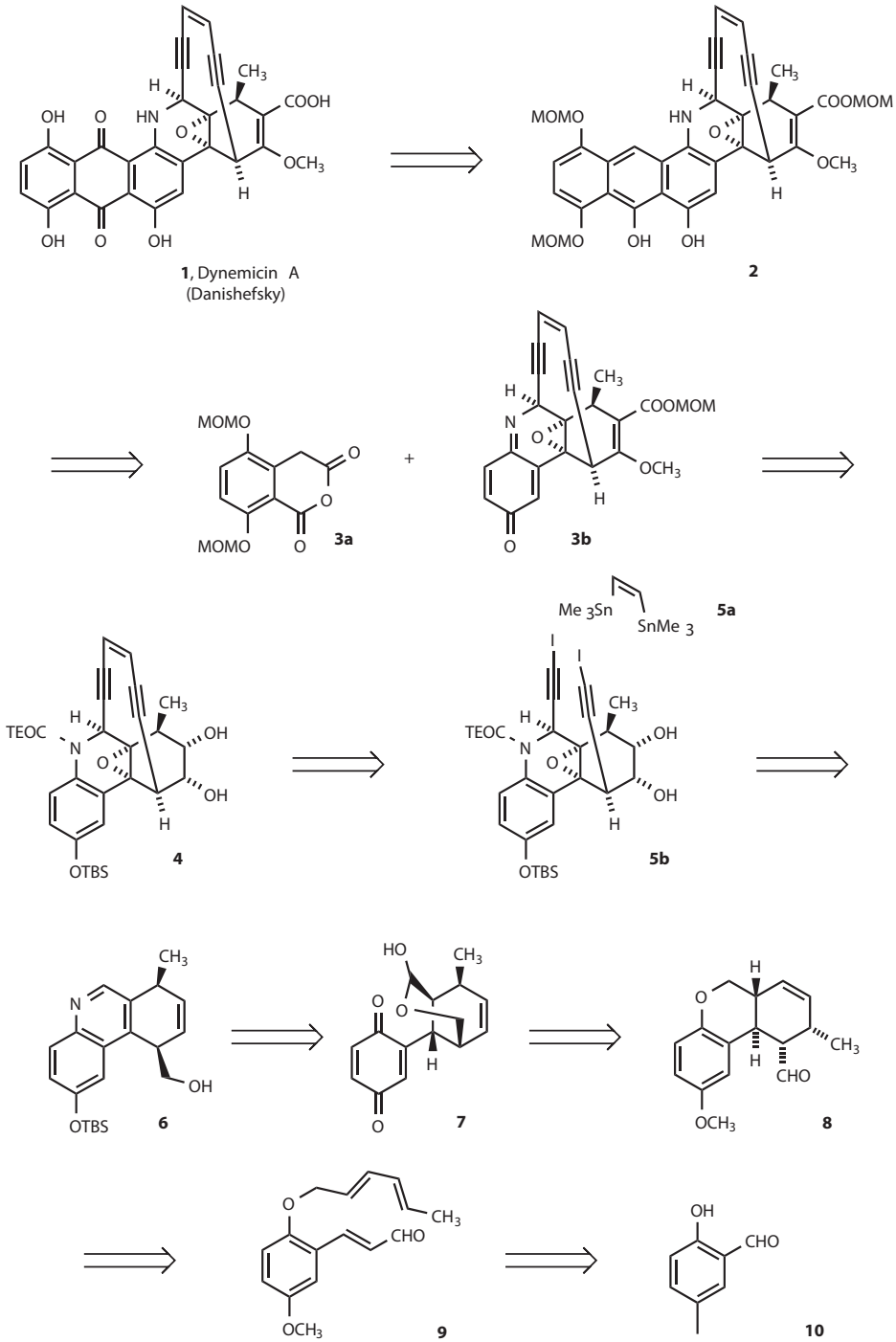

FIGURE 22.4 Danishefsky synthesis of dynemicin.

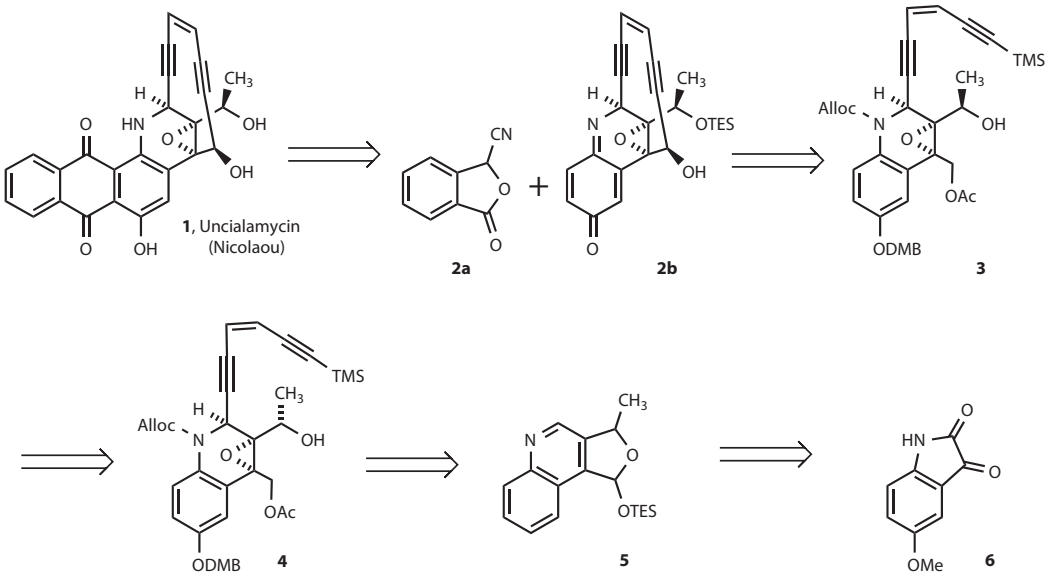

FIGURE 22.5 Nicolaou synthesis of uncialamycin.

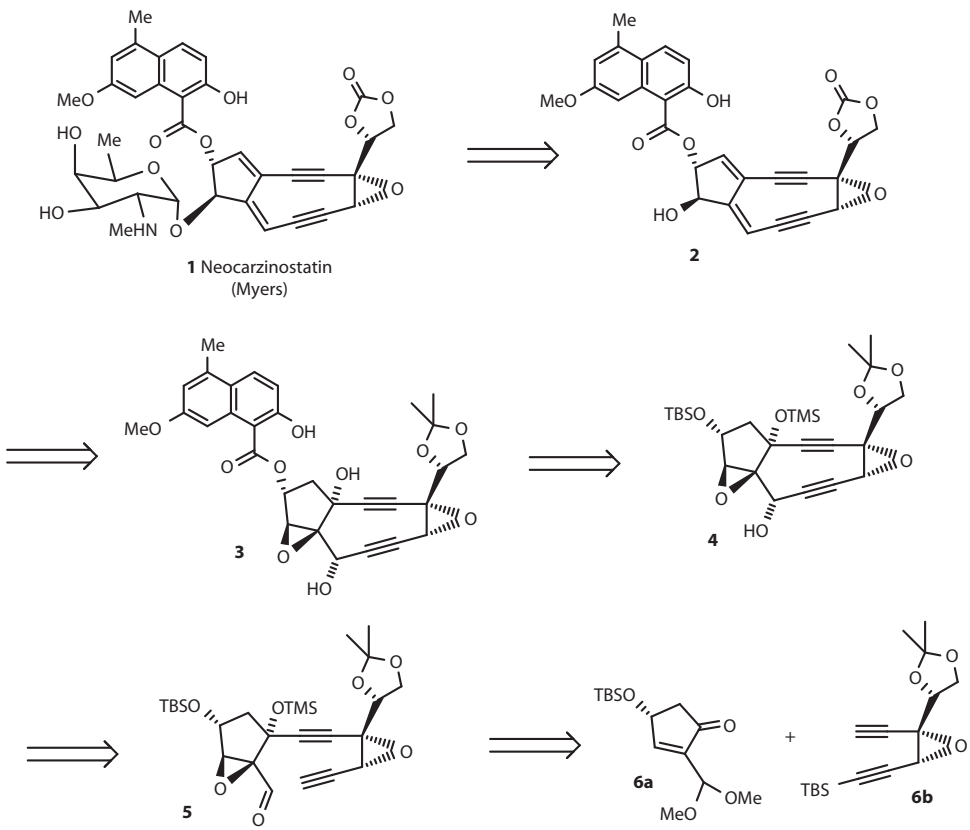

FIGURE 22.6 Myers synthesis of neocarzinostatin.

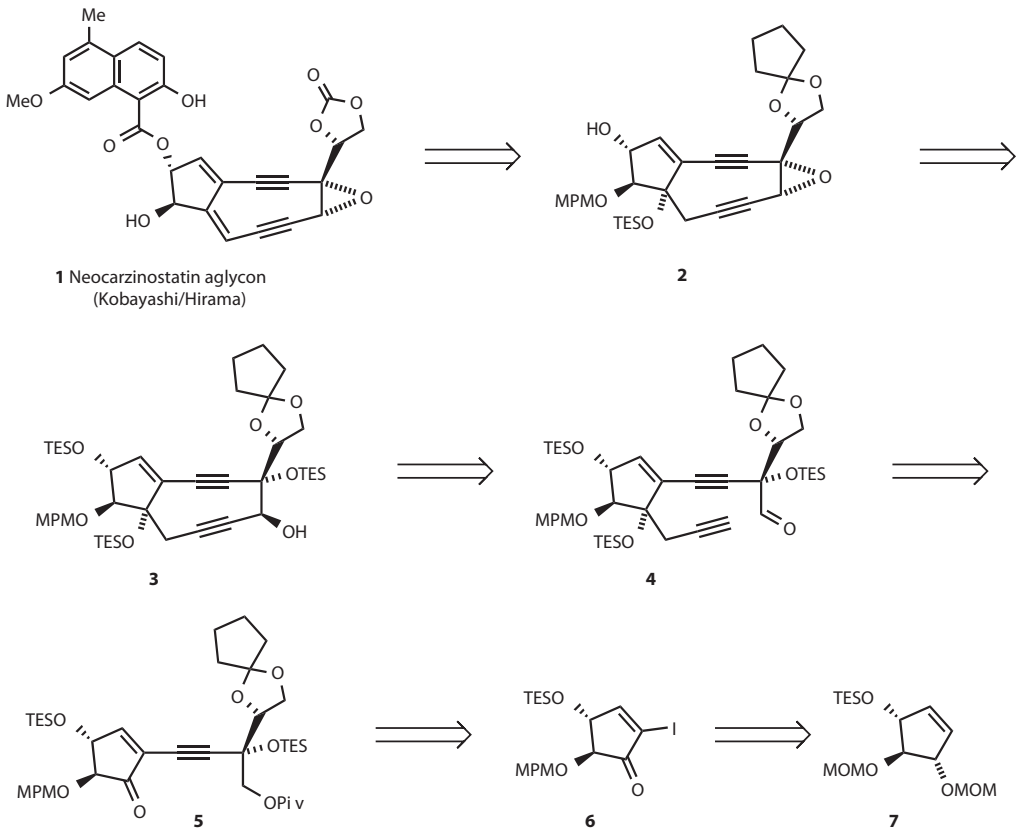

FIGURE 22.7 Kobayashi/Hirama synthesis of neocarzinostatin aglycon.

bromide **3** at low temperature and rapid quenching gave a 30–40% yield of cyclized material that resulted from transannular reaction of the vinyl anion with the acetylene. The diacetylene in **3** was constructed by intramolecular copper-mediated coupling of compound **4**, which itself was made by the Pd/Cu coupling of **5a** and **5b**. These two highly elaborated building blocks were made from **6a** and **6b**, respectively, each of which started with glyceraldehyde.

Hirama synthesis of the C-1027 (lidamycin) chromophore core (2008, Figure 22.10*).*[79,80,81] The Hirama group introduced the enediyne late in the synthesis due to its instability. This was accomplished by the SmI_2 deoxygenation of compound **2** to make the protected C-1027 core compound **1**. The nascent enediyne ring was closed in the context of a macrolactone by the intramolecular reaction of the acetylene in compound **4** with the aldehyde to make compound **3**. Although similar to Hirama's strategy for other enediynes, the presence of the macrolide certainly influenced this reaction due to the rigidity of the system. The prior macrolactonization of compounds **6** to **5** proceeded with significant atropselectivity. This hydroxy acid was built up from iodide **8**, itself derived by iodination of a well-known, commercially available prostaglandin intermediate.

Hirama synthesis of maduropeptin chromophore (2009, Figure 22.11*).*[82,83] Maduropeptin chromophore has been made as the methanol adduct **1b**, which has been shown to be in equilibrium with the conjugated enediyne form. The glycosidic bond was made by reaction of a protected core with a TES-protected glycosyl trichloroimidate. This core was made by protecting group rearrangement of ansa-lactam **2**, which was made in good yield by the reduction and cyclization of azide/activated ester **3**. Compound **3** was made in seven steps from intermediate **4**, which was the result of cesium-mediated ring closure of acetylene/aldehyde **5**. The upper acetylene in **5** was incorporated via the

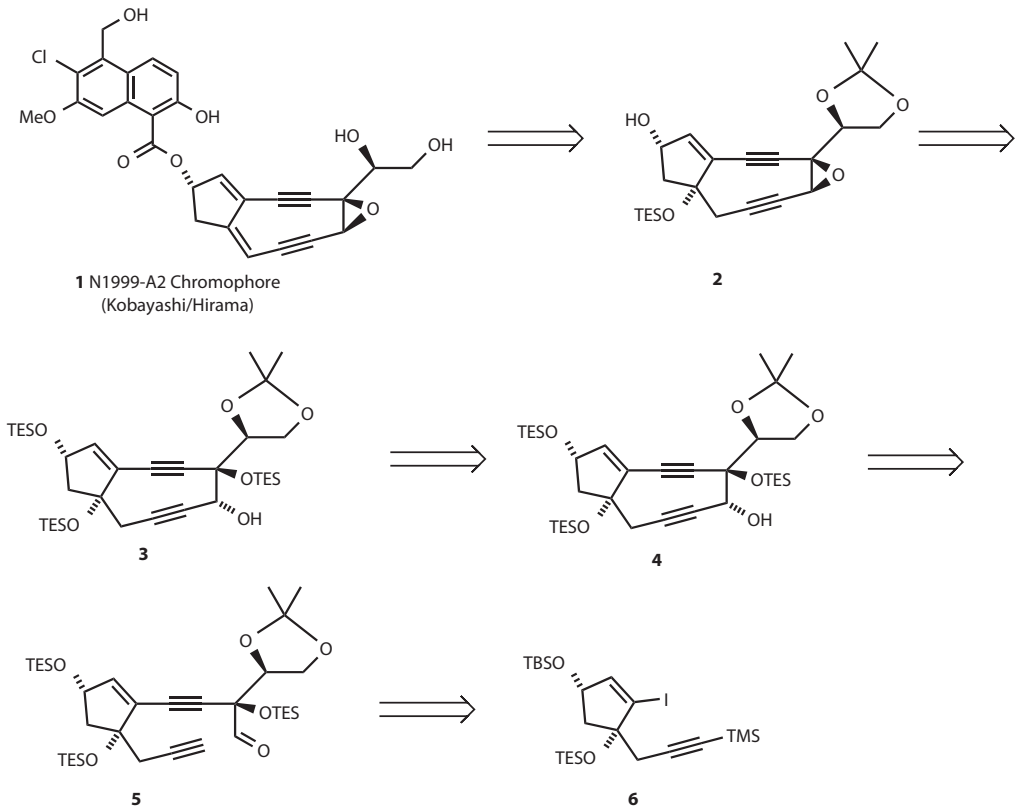

FIGURE 22.8 Kobayashi/Hirama synthesis of N1999-A2.

Sonogashira coupling of a highly elaborated acetylene. The aryl ether in **6** had been installed via cesium fluoride-catalyzed opening of epoxide **7a** (itself the result of numerous synthetic steps) and an elaborated phenol derived from commercially available **7b**. The overall synthesis consisted of over 40 synthetic steps. In the course of this synthesis it was discovered that the amino sugar was the opposite enantiomer from that initially assigned.

Myers synthesis of kedarcidin chromophore (2000, Figure 22.12*).*[84–88] The Myers group initially synthesized the originally proposed structure for kedarcidin and discovered an error had been made in the stereochemical assignment of one of the glycosylated alcohols, and so they made what turned out to be the correct isomer. In the synthesis, the second of the two carbohydrate units was added near the end of the synthesis by the reaction of compounds **2a** and **2b**. This was followed by dehydration and deprotection. In contrast, the kedarosamine (the upper sugar) was carried through most of the synthesis. This included the steps for the construction of the enediyne core, that is, acetylene dimerization and transannular ring closure from intermediate **4** to form enediyne **3**, similar to the Myers group's synthesis of N1999-A2.

Hirama synthesis of kedarcidin chromophore Aglycone (2009).[89] Hirama has published an efficient synthesis of a protected aglycone of kedarcidin chromophore, but his group unfortunately made the originally published isomer and will have to adjust the synthesis accordingly.

Nicolaou synthesis of calicheamicin γ_1^I *(1992,* Figure 22.13*).*[90–95] The first calicheamicin synthesis involved glycosylation of a protected enediyne without the methyl trisulfide in place (**2b**) and a protected glycosyl trichloroacetimidate with the hydroxylamine present as an oxime (**2a**). Enediyne **2b** was made from compound **3**, the lactones of which helped establish the stereochemistry of the involved alcohol. Intramolecular condensation of the acetylene and the aldehyde in

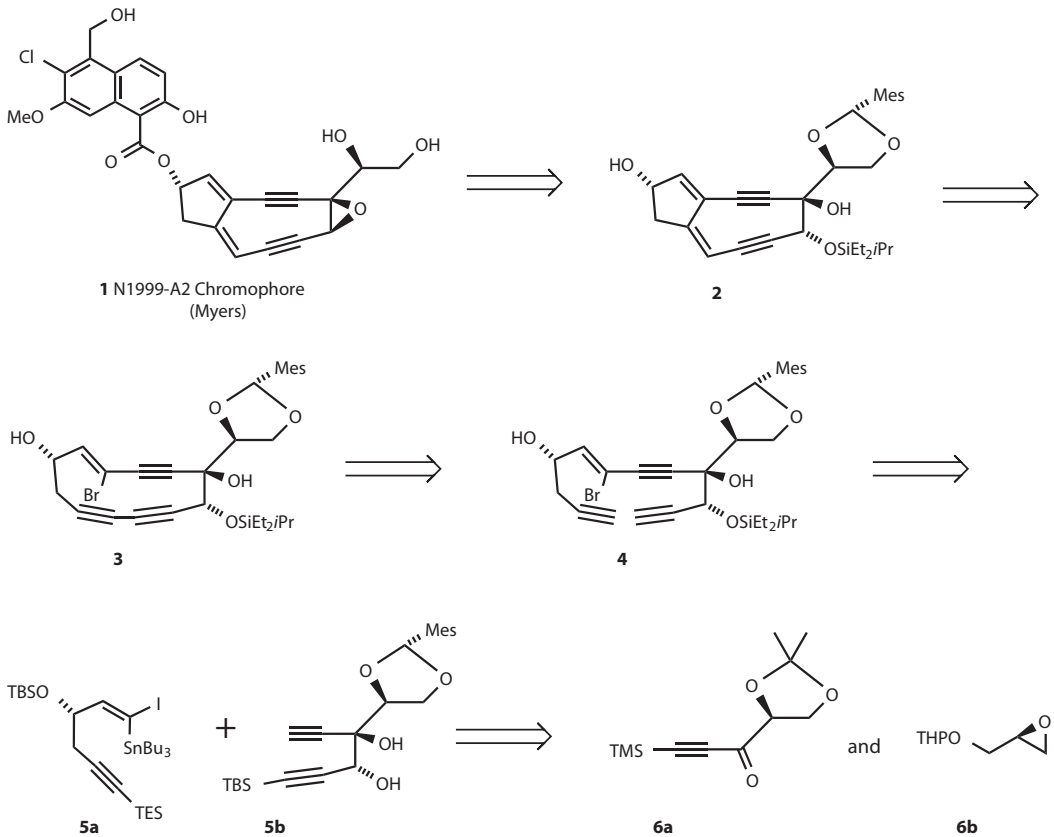

FIGURE 22.9 Myers synthesis of N1999-A2.

intermediate **4** was used to establish the bicyclic core, and the enediyne was initially introduced by the Pd/Cu-catalyzed coupling of a vinyl chloride with acetylene **5**. The core structure of this intermediate was established by intramolecular [3 + 2] cycloaddition of the nitrile oxide derived from oxime **7**, which in turn was derived from compound **8**. Compound **8** was derived from commercially available tetronic acid. The total synthesis was about 70 steps, 35 steps maximum linear, and in ~0.1% yield.

Danishefsky synthesis of calicheamicin γ_1^I *(1994,* Figure 22.14*).*[96–100] Although the Danishefsky calicheamicin synthesis appeared later than that of Nicolaou, his group actually made the aglycone calicheamicinone first. The final synthesis also involved later-stage intermediates, requiring only two deprotection steps after the glycosylation of **2b** with **2a**. The two syntheses of the enediyne core were similar, with the enediyne core being derived in both instances by the annulation of the enediyne piece on a highly functionalized cyclohexane ring, in this case compound **7a**. The ultimate exocyclic allylic trisulfide was present as an epoxide in compounds **5**, **6**, and **7a** in this synthesis, while the enediyne was brought in as a single unit. Overall the strategy for construction of the enediyne core was similar to that of Nicolaou, but with very different protecting groups and nascent functionality.

Other calicheamicinone syntheses. Two other syntheses of calicheamicinone have appeared, which virtually constitute formal syntheses of calicheamicin itself. The one from the Clive group (Figure 22.15)[101,102] forms the enediyne core via the unique double coupling of the diiodide **2** with 1,2-bis(trimethylstannyl)ethylene. Intermediate **2** was made in turn from the advanced cyclohexane derivative **3**, itself the product of a Diels–Alder reaction.

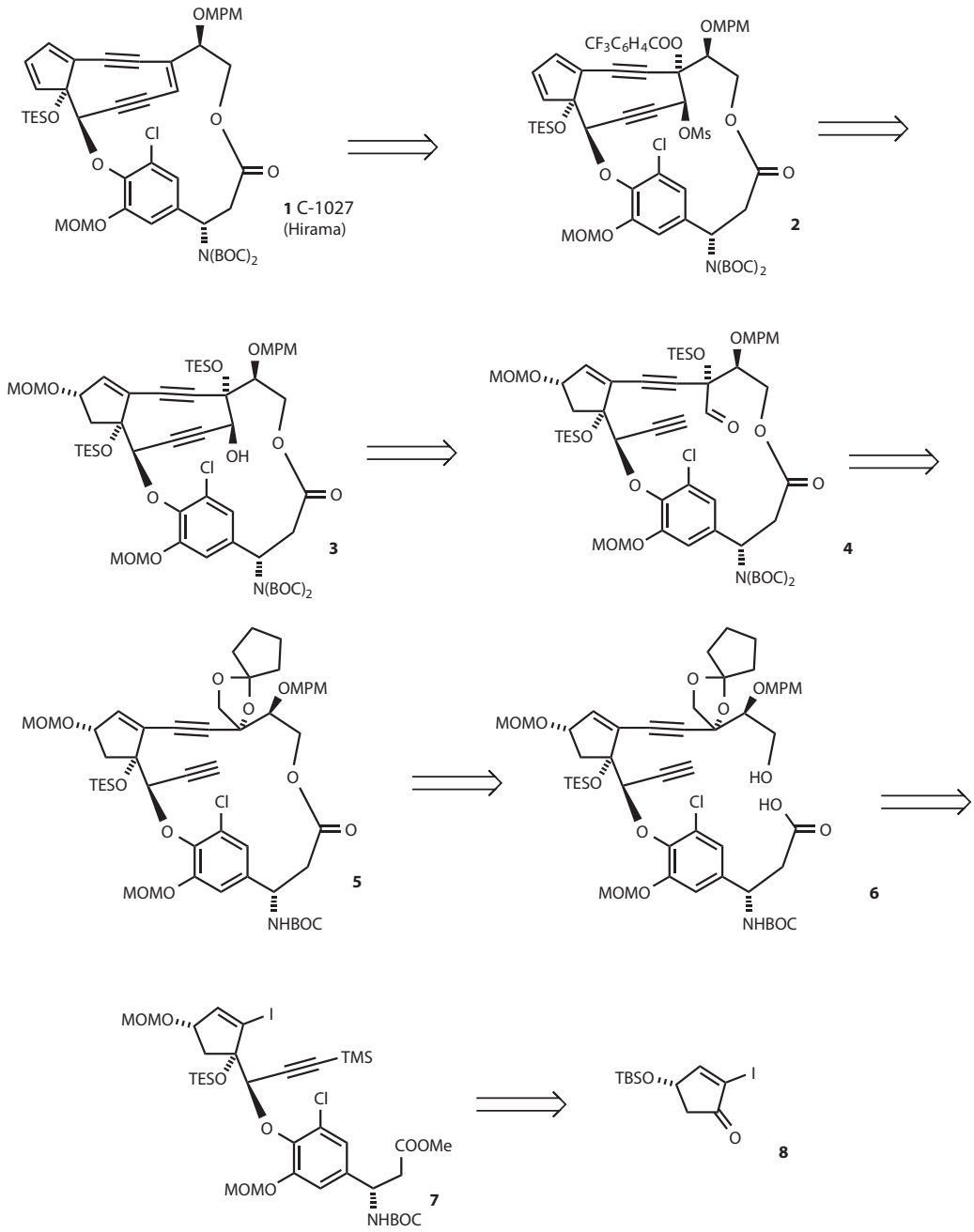

FIGURE 22.10 Hirama synthesis of the C-1027 (lidamycin) core.

The second synthesis is that of the Magnus group (Figure 22.16).[103,104] The most novel step in this synthesis is the late introduction of the carbamate nitrogen by reaction of the enedione derived from compound **1** with $Ph_2Se = NH$. The synthesis of **1** is similar to the syntheses published by Nicolaou and Danishefsky, except for variation in the protecting groups.

The closely related enediyne esperamicin has not been synthesized yet, but the trisaccharide has been made by both Nicolaou's group[105] and Danishefsky's group in collaboration with a group from Bristol-Myers Squibb.[106]

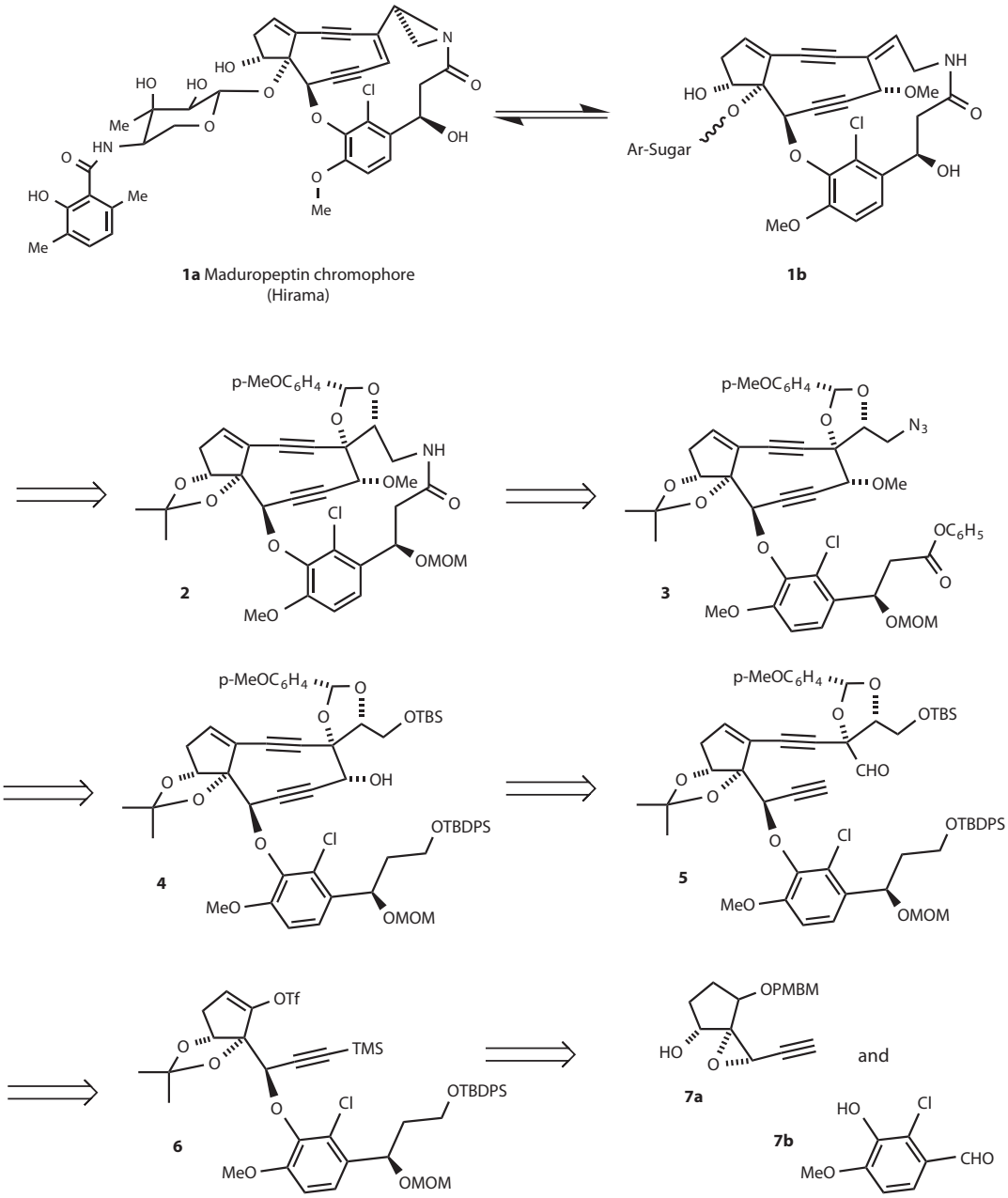

FIGURE 22.11 Hirama synthesis of maduropeptin.

22.6 MOLECULAR MECHANISMS OF ACTION

As a class, the enediynes cause single- and double-strand cleavage of DNA by rearrangement of their core to an aromatic diradical through a Bergman (10-member) or Bergman-like (9-member) cyclization.[107–109] How the molecules interact with DNA differs somewhat. Calicheamicin is the first-known DNA binder that utilizes a carbohydrate sequence to recognize DNA and binds to the minor groove in a nonintercalative manner. In addition, the carbohydrate portion of calicheamicin has a novel pyrimidine selectivity as a result of a shape-dependent induced-fit interaction.[110–114]

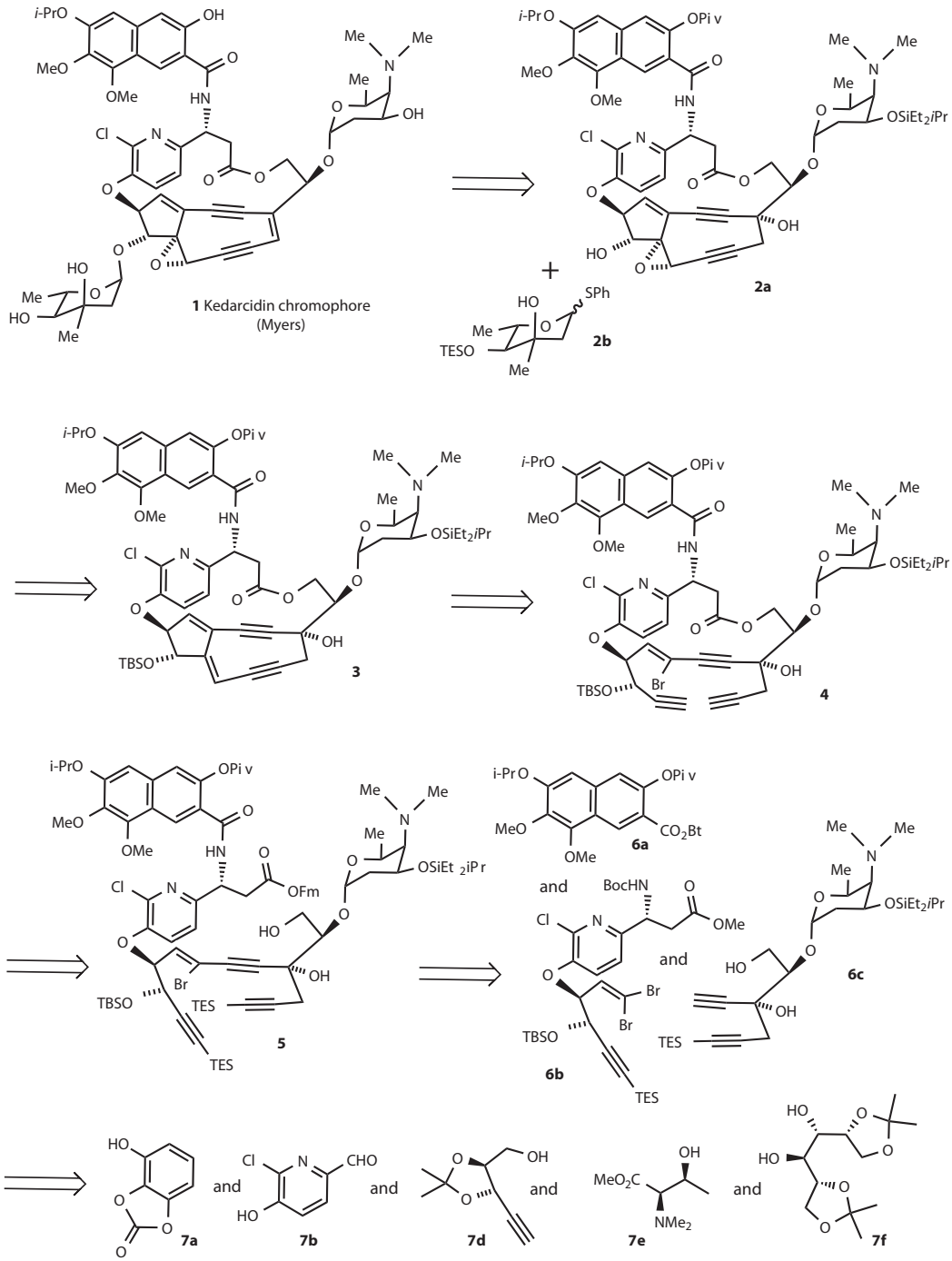

FIGURE 22.12 Myers synthesis of kedarcidin.

Esperamicin binds through a combination of carbohydrate-guided minor groove fit as well as base-pair intercalation, and dynemicin and antibiotic N1999A2 bind through purely intercalative mechanisms.[24,77,115]

Triggering of the methyl trisulfide-containing enediynes within cells requires a reductive cleavage of the trisulfide by glutathione and subsequent rearrangements to form the diradical. This

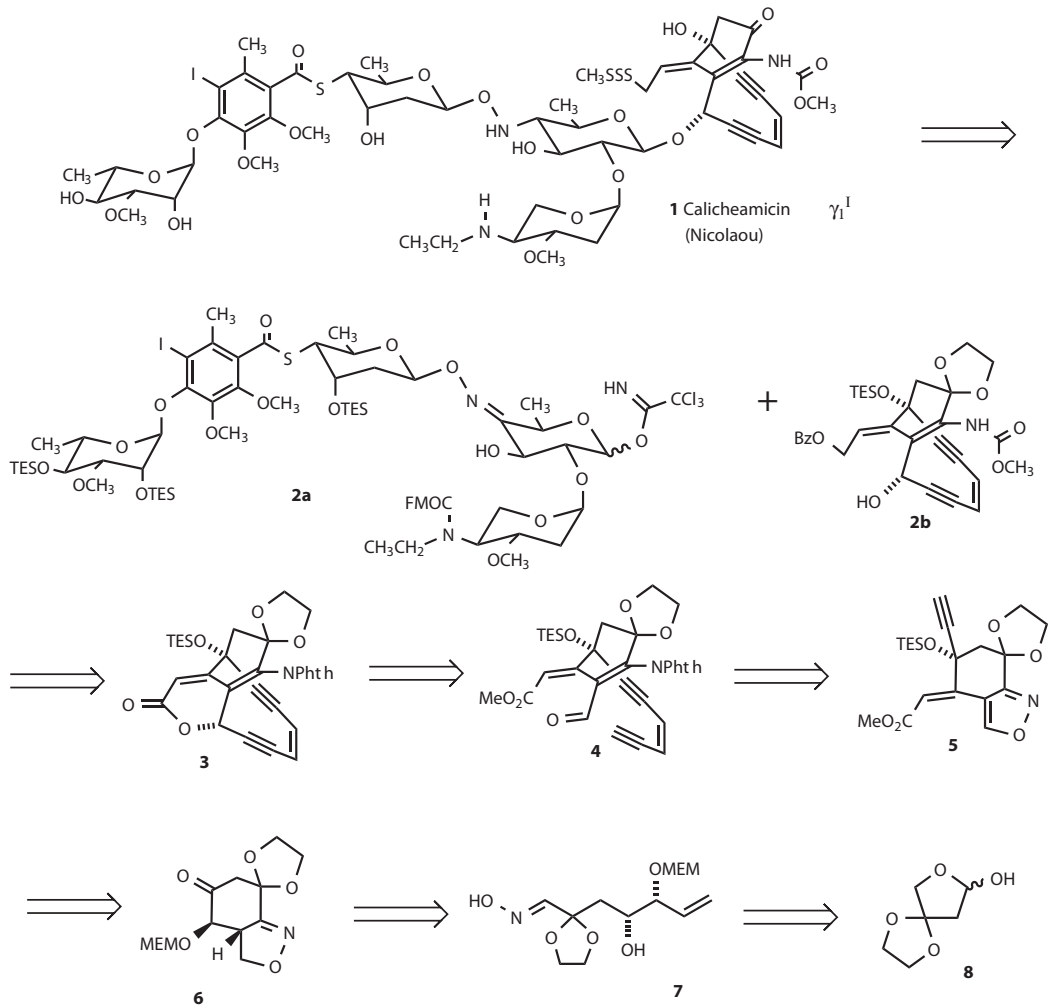

FIGURE 22.13 Nicolaou synthesis of calicheamicin.

chemistry is illustrated for calicheamicin γ_1^I in Figure 22.17. The reduction does not necessarily have to occur with the enediyne prebound to DNA. For example, the pre-Bergman cyclization intermediate for calicheamicin γ_1^I has a half-life of about four seconds.[116] However, how the enediyne and product diradical are positioned in the DNA determines the type of damage that occurs. A diradical that spans both strands produces double-strand breaks, whereas a diradical with access to only one strand leads to single-strand breaks.[16,116,117,118] The structure of a calicheamicin γ_1^I–DNA duplex complex was studied in aqueous solution using 2D-NMR techniques and molecular dynamics calculations. A predominate species of the hairpin duplex complex with DNA containing (TCCT)(AGGA) was observed and gave further insight into the binding and sequence specificity.[119] Additional studies have shown that calicheamicin is triggered in the minor grove resulting in the cyclohexanone adopting a chair rather than a twist-boat form. Triggered calicheamicin can undergo the Bergman cyclization at body temperature only if the chair form is present.[120]

The Bergman cyclization of the dynemicin-like enediynes is the same as illustrated for calicheamicin, but the trigger in this case is reduction of the anthraquinone, which allows the electrons on nitrogen to open the epoxide vinylogously through the aromatic ring.[121,122]

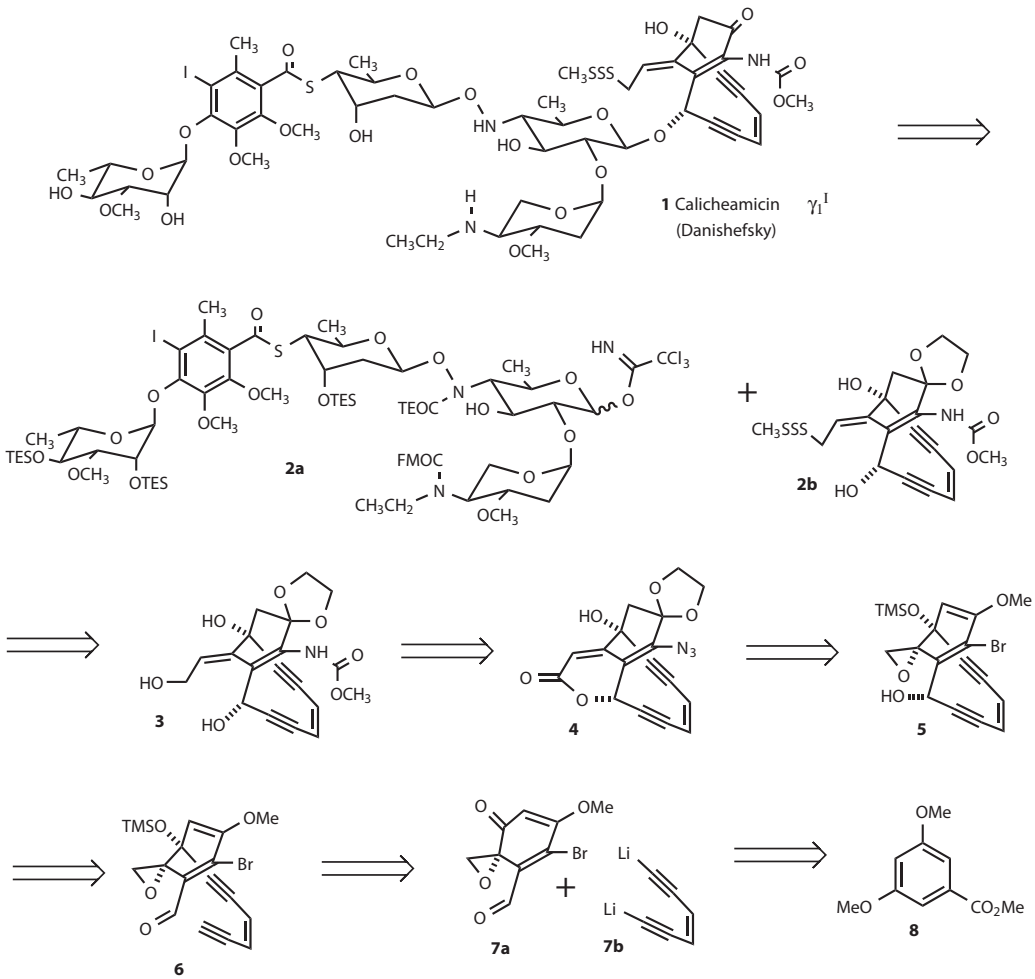

FIGURE 22.14 Danishefsky synthesis of calicheamicin.

Triggering of the 9-membered enediynes involves glutathione just like most of the 10-membered ring enediynes, but in a conjugate addition to the poly-unsaturated system. They all owe their existence to an epoxide functionality (e.g., neocarzinostatin and kedarcidin chromophores) or a bridging chain across the enediyne (e.g., maduropeptin chromophore), or both, which keep the diyne portion of the core separated. The triggering of neocarzinostatin is illustrated in Figure 22.17. As is also true for the 10-membered enediynes, the triggering is achieved by structural changes, such as opening of the epoxide, disruption of the bridging structure, or binding to DNA, that permit the reacting ends of an enediyne to approach within a bonding distance of 2.9 to 3.4 Å.[109]

A review of the interaction of enediynes with DNA has been published.[123] Lidamycin caused sequence-specific double-strand DNA cleavage.[124] However, when oxygen was depleted from the reaction of lidamycin with DNA, sequence-specific covalent DNA drug adducts and DNA interstrand cross-links were formed with the drug.[125] These types of reactions may be important in the central regions of large tumors where relatively anaerobic conditions prevail. Lidamycin cleaved DNA more efficiently in cells than in a cell-free environment. Mixed single- and double-strand breaks were observed in intracellular episomal, mitochondrial, and genomic DNA at low nanomolar concentrations.[126]

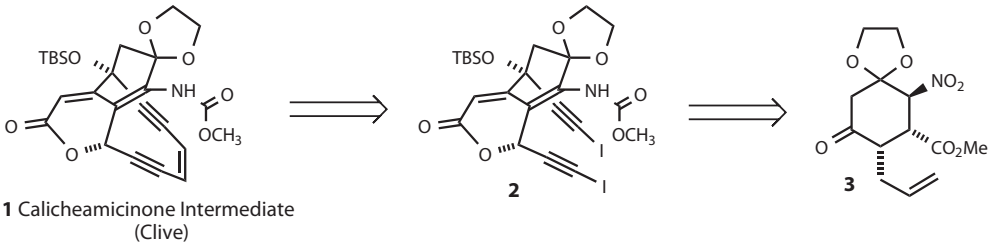

FIGURE 22.15 Clive synthesis of calicheamicinone.

Calicheamicin γ_1^I cleavage of plasmid DNA was not inhibited by excess tRNA or protein, showing that this enediyne specifically targets DNA.[127] The ratio of DNA double- to single-strand breaks caused by calicheamicin γ_1^I in cellular DNA of human fibroblasts was 1:3, close to the 1:2 ratio observed with purified plasmid DNA.[127] In addition, calicheamicin γ_1^I induced a strong double-strand break response in human fibroblasts at concentrations that would deliver <1000 molecules per cell. In these and other studies, however, the cells were fully capable of repairing such breaks.[128]

22.7 CELLULAR MECHANISMS OF ACTION

Enediynes exert their biological effects through free radical damage to DNA, and as a result, they have been compared with radiomimetics. It is clear, however, that the cellular response to each of the various enediynes is unique and differs significantly from the effects of ionizing radiation. Although the traditional responses to DNA damage such as apoptosis (programmed cell death) have been observed, other types of responses occur as well. The specific cellular response is not only, in part, guided by the type of DNA damage induced, but also clearly dependent on the inherent make-up of the cells and the resultant tendencies to follow certain biological pathways.

Lidamycin appears to cause normal apoptosis in HL-60 leukemia cells,[129] but abnormal apoptosis at higher concentrations in BEL-7402 hepatoma cells.[130] Although laddering of DNA and caspase involvement were seen, the nuclear membrane remained intact and no apoptotic bodies were observed. This was ascribed to direct DNA shredding by lidamycin preceding the onset of the actual apoptotic signals. Consistent with this, a separate study indicated that the DNA laddering appears to occur before caspase involvement.[131]

Many of the responses that were ataxia-telangiectasia mutation (ATM) dependent for ionizing radiation and bleomycin, such as p53 phosphorylation, were shown to occur by ATM-independent mechanisms with lidamycin.[132] However, Mylotarg®, an antibody conjugate of calicheamicin, has been shown to cause G2 arrest associated with the ATM/Chk1 and Chk2 phosphorylation pathway and caspase-3 mediated apoptosis or G2 arrest without apoptosis.[133] Lidamycin, as well as neocarzinostatin, has been reported to inhibit DNA replication by an indirect mechanism involving the hyperphosphorylation of replication protein A.[134]

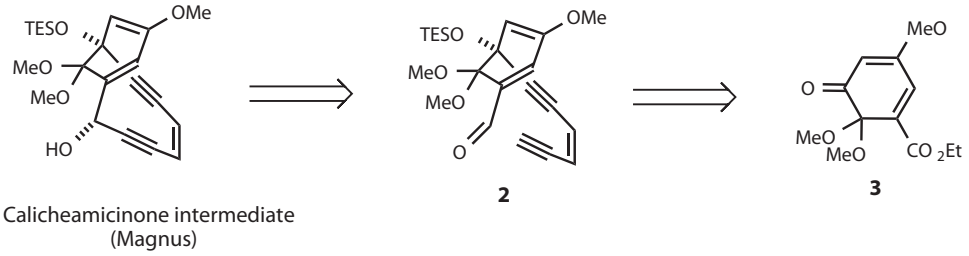

FIGURE 22.16 Magnus synthesis of calicheamicinone.

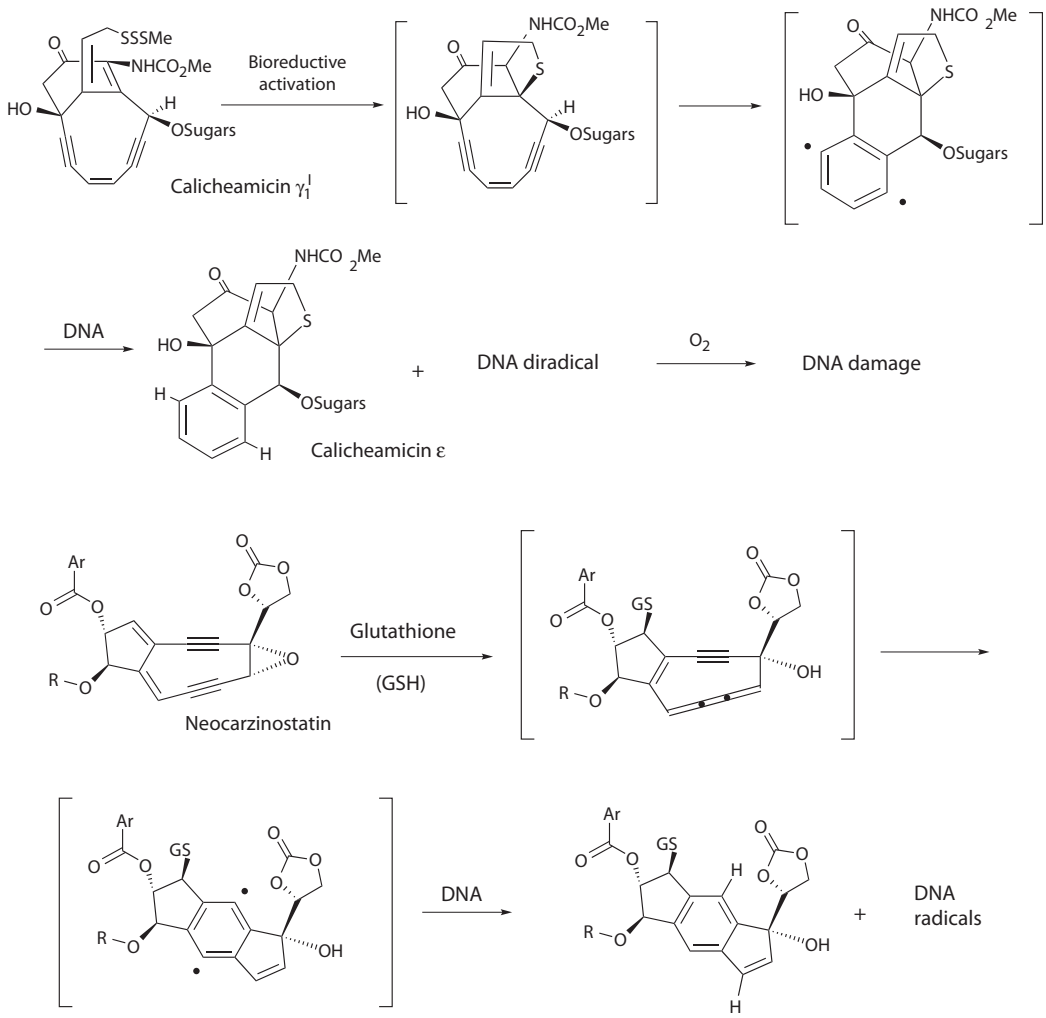

FIGURE 22.17 Diradical formation from calicheamicin γ_1^I/neocarzinostatin and their interaction with DNA.

Dynemicin A induces apoptosis.[67] Curiously though, a series of simplified synthetic analogs of this enediyne appear to induce apoptosis by a non-DNA dependent mechanism,[67] although it is possible that initial DNA damage triggers a secondary mechanism. Other related analogs not capable of generating free radicals were also shown to block apoptosis induced by a variety of unrelated agents, such as the anthracyclines, camptothecin, and Ara-C.

Calicheamicin γ_1^I, as well as other members of this family, show different effects on different cell lines. SH-SY5Y N-type neuroblastoma cells undergo apoptosis at subnanomolar concentrations of the compound, while SH-EP1 S-type neuroblastoma cells proceed to differentiation.[135] The same differential effects were seen for esperamicin A1, dynemicin, and neocarzinostatin. Work in the same labs with this latter agent has demonstrated the involvement of the Bcl-2/caspase-3 pathway in apoptosis of PC12 pheochromocytoma cells.[136]

The synthetic enediyne calicheamicin θ differs from γ_1^I only by having a thioester replacement for the methyl trisulfide. Thus hydrolysis activates this analog as opposed to the reductive mechanism required for the natural calicheamicins. This compound causes apoptosis in Molt-4 leukemia cells as indicated by chromatin condensation and DNA degradation.[137] Other studies have indicated

that calicheamicin θ-induced apoptosis is p53-independent and Bax-dependent, showing the usual cytochrome C release and caspase-3 and -9 involvement.[138]

Upregulation of p53 that correlated with DNA damage has also been reported for calicheamicin γ_1^I.[139] Studies with Mylotarg on bone marrow samples from acute myeloid leukemia (AML) patients indicated a general lack of intrinsic apoptotic potential in these cells and a low rate (25%) of caspase involvement after drug exposure. This may indicate that nonapoptotic mechanisms predominate in this case, or that the inherently low apoptotic potential in many of the samples may be responsible for a lack of clinical response in some patients.[140]

One similarity has been noted between radiation damage and the cellular response to esperamicin and neocarzinostatin. Cytotoxicity for all these treatments shows a dependence on oxygen, making hypoxic cells that occur in the center of solid tumors more resistant.[141] Radiosensitive cells are also more responsive to calicheamicin and neocarzinostatin as well as to bleomycin, although no mechanistic details have been investigated.[142] Although poly(ADP-ribose) polymerase has been reported to be involved in double-strand break repair caused by radiation, it does not appear to be involved in repairing double-strand breaks caused by neocarzinostatin.

Similar to radiation sensitivity, the cytotoxicity of calicheamicin in the form of its antibody conjugate, Mylotarg, has been shown to be cell-cycle dependent.[143] Causing cells to leave G_0 phase and cycle by treatment with interferon or granulocyte-macrophage colony-stimulating factor (CSF) resulted in a more rapid cell death and increased sensitivity.

In marked contrast to radiation sensitivity, neocarzinostatin is more cytotoxic to neuroblastoma cells when Bcl-2 is upregulated, even though Bcl-2 normally renders cells resistant to apoptosis.[144] This has been correlated to an increase in glutathione in these cells, which is responsible for activating neocarzinostatin.[145] Such an increase in sensitivity does not occur for a synthetic enediyne that is activated by a nonreductive pathway. This may not be common for all enediynes or all cell lines. In related work, 6-mercaptodopamine, a thiol taken up by the dopamine pathway, increases the efficacy of neocarzinostatin in neuroblastoma cell lines both *in vitro* and *in vivo*.[146]

Two reports have reaffirmed the importance of cleavable Bcl-2, caspase-3, and the availability of sulfhydryl groups for the potentiation of the apoptotic effects of neocarzinostatin in cancer cells, in spite of the normal role Bcl-2 plays as an antiapoptotic protein.[147,148]

A number of cellular targets for calicheamicin were identified at the time of our last review. Some of these were the activation of the protein kinase ATM and phosphorylation of the Chk1 and Chk2 proteins leading to G2 cell-cycle arrest. Caspase-3 and -9-mediated apoptosis, hypermethylation of replication protein A, upregulation of p53 and Bcl-2, and an increase in glutathione have been ascribed to calicheamicin as well. Subsequent probing has, however, revealed some additional targets for both calicheamicin and Mylotarg. Both agents, when tested at clinically relevant concentrations, led to an apoptotic morphology and activation of caspase-3 signaling in HL60 and NB4 AML cells. In addition, Mylotarg caused pro-apoptotic activation of Bak, Bax, and stress-activated protein kinase p38 in responsive cells.[149]

Responsiveness of AML cells to Mylotarg appears to be, in part, dependent on the expression of Syk kinase. Blocking of Syk using siRNA, even when these cells were initially responsive to Mylotarg, rendered them resistant. 5-Azacytidine, an agent that upregulates Syk, restored sensitivity in some cell populations.[150]

The cellular target on the surface of cells for Mylotarg is the CD33 antigen. An *in vitro* study involving a lentivirus-assisted transfer of DNA for native and mutated forms of CD33 into cells lacking the antigen showed that there exists a quantitative relationship between the levels of CD33 expression and Mylotarg cytotoxicity. Point mutations in the sequences transferred interfered with the internalization of the conjugate as well as its cytotoxicity.[151]

Central to the cytotoxic activity of calicheamicin is the ability to induce cleavage of both strands of DNA simultaneously. Such events are relatively minor compared with the single-stranded breaks seen with this agent but double-strand breaks would appear, at least superficially, as single-hit, lethal events for a target cell. However, DNA is not an isolated, linear entity but packaged around

histones most of the time. So in spite of a double-strand break, the resultant ends of the DNA do not, in general, simply float away from each other and ultimately result in cell death. Cells express several mechanisms for rejoining such strands. Two proteins involved in this process are the DNA-dependent protein kinase (DNA-PK) and the XRCC4-DNA ligase IV complex, for example. Treatment of cells with an inhibitor of the poly(ADP-ribose) polymerase-1 (PARP-1) enzyme resulted in an increase in the cytotoxicity of calicheamicin and suggested that additional mechanisms of double-strand rejoining are operational that involve PARP-1.[152]

No new information regarding the biological activity (nor anything else, for that matter) has appeared since our last review for a number of the enediynes. Such is the case for kedarcidin, maduropeptin, namenamicin, shishijimicin, actomoxanthin, and auromomycin, among others. Even esperamicin and dynemicin have not produced new cellular or *in vivo* anticancer studies. Some of this is due to the extremely small amounts in which these materials were isolated in the first place, with no practical and safe ways to scale them up. Toxicity and stability of many of these agents also played a negative role in their further development. This has not been the case, however, for lidamycin, one of the chromoproteins that still generates considerable interest in the scientific community, particularly in China where it was first discovered. In this regard, many of the research articles involving lidamycin have been published in Chinese but, in most cases, English versions have appeared several years thereafter and, in general, only the latter are summarized here. However, significant studies that have not yet been published in English are included, but only based on their abstracts. A few references hint that lidamycin has attained clinical trial status, although no reports in that regard have, as yet, appeared. All the publications available for lidamycin so far detail only preclinical studies. A review summarizing the discovery, biosynthesis, anticancer activity, and biochemical targets of lidamycin has been published recently, so only the biochemistry and biology that have appeared subsequently are included here.[153]

A dose-dependent inhibition of phosphorylated Akt, leading to the activation of the nuclear transcription factor NF-κB by lidamycin, has been observed in the PANC-1 and SW1990 pancreatic cancer cell lines. In addition, lidamycin resulted in a downregulation of K-ras kinase and the reduction of matrix metalloproteinase-9 activity, the latter enzyme being important for tumor invasiveness.[154]

Activation of the wild-type p53 transcriptional factor by lidamycin has been attributed to the apoptotic cell death induced by this enediyne. Colorectal cancer cells that were either deficient in p53 or contained a mutated version of the enzyme showed resistance to lidamycin. Such effects are triggered by low doses (~10 nmol) of the drug. Higher concentrations of lidamycin lead to rapid apoptosis of cells through DNA strand breaks and cross-links, with little regard for the subtleties of established biological pathways or their checkpoints.[155]

The human colon carcinoma HT-29 cell line has been a particularly rich source of putative lidamycin targets. At a biochemical level, lidamycin induces G2 cell-cycle arrest in these cells, but cells in G1 phase were more sensitive to the drug. This affect is observed concurrently with an increase in phosphorylation of Chk1, Chk2, Cdc25C, and Cdc2 along with elevated transcription of Cdc2 and cyclin B1. The authors found that the p38 MAPK pathway also contributed to the G2 arrest, as evidenced by the concurrent administration of lidamycin with SB203580, a p38 MAPK inhibitor. This combination led to an increase in cells accumulated in the G2 phase and increased the number of apoptotic cells.[156]

Similarly, in a study where the multiple myeloma cell lines U266 and SKO-007 were used, activation of p38 MAPK was also attributed to the activity of lidamycin. In addition, the *c*-Jun NH_2-terminal kinase (JMK) was activated and an increase in the levels of PARP and the caspase-3 and -7 was observed. Taken together, these mechanisms resulted in significant increases in the apoptotic levels of these cells subsequent to lidamycin treatment.[157]

A characteristic of solid tumors is that they tend to develop hypoxic, necrotic cores. Ionizing radiation as a therapy for such tumors is limited since the hypoxic environment prevents the formation of peroxy radicals, the lethal constituent of radiotherapy. Lidamycin is unusual, even among the enediynes, in that it is nearly threefold more cytotoxic toward hypoxic cells compared with tumors

growing in a normal oxygenated environment. By comparison, neocarzinostatin is about fourfold less cytotoxic under hypoxic conditions. This unusual feature of lidamycin has been attributed to its ability to induce both DNA strand breaks as well as cross-links. Although both mechanisms are operational under hypoxic conditions after lidamycin triggering, the DNA cross-linking ability still kills cells, whereas strand breakage, mediated by the benzyne diradical, does not occur as well in an oxygen-poor environment.[158]

As a prelude to possible future clinical studies, a publication combining lidamycin and the epidermal growth factor receptor (EGFR) tyrosine kinase inhibitor, gefitinib, has appeared. Human epidermoid carcinoma A431 (high expresser of EGFR receptors) and human large-cell lung cancer H460 cells (moderate expresser of EGFR receptors) were used for this study. Concurrent downregulation of the EGFR-signaling pathway with gefitinib significantly potentiated the cytotoxic effects of lidamycin. Such effects were more pronounced in the cell line expressing high levels of EGFR receptors, as expected.[159]

22.8 PRECLINICAL STUDIES

The enediynes are among the most cytotoxic compounds known, but they tend to have rather narrow therapeutic windows. As a class, they also exhibit poor pharmacokinetic properties due to their lipophilicity. There has only been limited preclinical pharmacology published for most of the unmodified natural products. Availability of the enediynes themselves has been a deterrent in this regard since fermentation production levels, even after considerable refinement, have remained low compared with most natural products. Studies with semisynthetic derivatives have also been hampered by the same constraints, and, even though totally synthetic routes have been developed for many of the natural enediynes, these have been undertaken for the sheer intellectual challenge of assembling these molecules from available starting materials rather than with any sourcing goals in mind. Two notable exceptions exist to these generalities. The first is calicheamicin θ, a totally synthetic derivative further discussed below. The second is dynemicin A, structurally one of the simplest members of the natural enediynes. Even though the total syntheses reported were well over 20 steps each and still not a practical source for these compounds, they led to a variety of studies designed to identify the minimal structural units necessary for high biological activity. A relatively recent review summarizes both the chemistry and biology of these efforts,[160] so only derivatives designed for tumor targeting are summarized here. It has been such attempts at targeting the enediynes, particularly by attaching them to antibodies, which has given this class of natural products significant medicinal promise.

Relatively few studies using lidamycin in traditional tumor models have appeared. One of these has compared the anticancer activity of lidamycin, its apoprotein, and lidamycin chromophore itself with mitomycin C and adriamycin. The test systems investigated were the human hepatoma BEL-7402 and SMMC-7721 tumors implanted in athymic nude mice and the mouse hepatoma H22 implanted in normal Kunming mice. *In vitro* studies showed that lidamycin itself was 10,000-fold more potent than mitomycin C and adriamycin. Lidamycin and its chromophore were essentially equipotent at comparable doses, whereas the apoprotein was about 10^5 less potent. *In vivo*, similar differences in potency existed, although these were not nearly as pronounced. Lidamycin itself showed high potency: a single 0.05-mg/kg dose of the drug inhibited BEL-7402 tumor growth by nearly 70%, with all test animals surviving the experiment. Similar results were seen with the other two tumor models.[161]

A second study performed using the colon sarcoma 26 model investigated a variety of ways to present this tumor to therapy. Thus, subcutaneous, orthotopic, and intrahepatic models of Colo26 were treated, as well as one involving a hepatic metathesis after intrasplenic transplantation of the same tumor. The level of tumor inhibition by lidamycin, given at the same doses, was the same in the subcutaneous, orthotopic, and intrahepatic models, but the intrasplenic model was more resistant,

showing only ~70% reduction in tumor growth at 0.1 mg/kg (compared with >90% inhibition of the other models at the same dose).[162]

Three reports have evaluated the pharmacokinetics of ^{125}I-labeled lidamycin in mice and rats and differ largely by how the radioactivity in samples was assessed and what pharmacokinetic parameters are listed. Briefly, lidamycin distributes mainly to the kidneys, lungs, and liver, is excreted largely in the urine, and shows a $T_{1/2}$ of ~3 hours in mice. Numerous additional constants are listed.[163–165]

Lidamycin has been conjugated to the murine monoclonal antibody 3G11 and several of its fragments. 3G11 targets type IV collagenase, an enzyme secreted by certain solid tumors to achieve invasiveness. Lidamycin and whole 3G11 were coupled using the *m*-maleimidobenzoyl-*N*-hydroxysuccinimide ester (SMB) bi-functional cross-linking agent. This was tested against the murine carcinoma 26 in female BALB/c mice and the highest dose administered, 0.1 mg/kg, inhibited tumor growth by 81% at the 10-day time point.[166]

Antibody conjugates have been made with a monosulfide bond to native antibody (3G11) as well, or to a Fab or scFv antibody fragment against type IV collagenase.[167,168] These constructs inhibited KB epidermoid cells at 2 fM and decreased the growth of hepatoma 22 xenograft tumors by 90%. An antigastric cancer antibody, 3H11, has also been used for targeting this enediyne.[169] The conjugate had an IC_{50} of 0.02 fM with 400-fold selectivity versus a nontargeting control conjugate and was active against BGC823 gastric cell xenografts. Additional whole antibody constructs have also been summarized in a general review of C-1027.[170]

Two more recent papers describe the construction and expression of a fusion protein between lidamycin apoprotein and the light-chain variable region (VL)[171] as well as the heavy-chain variable (VH) region[172] of murine 3G11. After purification and refolding, both constructs were "energized" by the reincorporation of lidamycin chromophore. The size of these constructs was ~24 kDa, compared with ~170 kDa for the whole antibody conjugate. The VL construct was only tested in normal Kunming mice implanted with murine hepatoma 22 and produced 90% tumor inhibition at the highest dose tested (0.375 mg/kg) on day 18. The VH counterpart was tested in nude mice implanted with human fibrosarcoma HT-1080 cells and a 0.25-mg/kg dose suppressed tumor growth by 76% on day 18.

Lidamycin has also been attached to an RGD-containing nonapeptide. This targeted construct inhibited pulmonary metastases in a PG giant-cell lung carcinoma model.[173]

Dynemicin A has been examined by a different strategy. ADEPT and GDEPT are approaches that use a less cytotoxic prodrug that is activated at the tumor site by an enzyme that is either pretargeted by an antibody or expressed by an introduced or induced gene, respectively. A simplified version of dynemicin missing the anthraquinone and containing an alternate carbamate activating group has been reported.[174] The nitrobenzyl carbamate is activated by nitroreductases.[175] This derivative showed a 90-fold increase in potency in the presence of the enzyme, and it was also 21- to 135-fold more cytotoxic to cell lines that express a nitroreductase.[176] Related simplified versions of dynemicin have been attached to lexitropsins and were cytotoxic to a panel of cancer cell lines in the 20 to 50 μM range.[177] Nuclear uptake was indicated by confocal microscopy.

Calicheamicin and esperamicin have been used to make numerous targeted constructs. Esperamicin has been conjugated to alpha-fetoprotein to make a construct that showed activity both *in vitro* and *in vivo*, where subcutaneous P388 tumors were completely eliminated in over 90% of the animals.[178] Calicheamicin has also been attached to the same protein.[179] This conjugate was cytotoxic to the QOS T-lymphoma cell line at 0.15 nM and was more potent than calicheamicin itself. The structure of the actual alpha-fetoprotein–calicheamicin conjugate is not evident from these reports though. The conjugation methodology and structures reported are not entirely compatible with what is known about the chemistry of calicheamicin, although a disulfide-linked construct attached through lysines can be assumed. An antisense oligodeoxynucleotide conjugate of calicheamicin has also been prepared,[180] but no further details are available.

Nearly all of the antibody conjugates prepared from calicheamicin analogs have been based on semisynthetic modification of the natural products themselves. An *N*-acetyl derivative of calicheamicin γ_1^I has been used most extensively for preparing such constructs, even though this derivative is about one order of magnitude less potent than the corresponding parent molecule.[181] An unusual displacement of the methyl trisulfide functionality by thiols has been used to introduce linkers for eventual antibody conjugation.[182] This transformation has had three beneficial consequences. First, conversion to a disulfide stabilizes the molecule. Second, a wide variety of thiols are useful for this displacement, allowing further tailoring of how readily the reductive activation step can occur, modulating the stability of the construct in serum, and allowing introduction of a functional group for antibody conjugation.[182] Third, the cleavage of the disulfide releases calicheamicin γ_1^I in "triggered" form, significantly limiting the potential half-life of the resultant triggered intermediates.[116]

For conjugates of *N*-acetyl-calicheamicin γ_1^I possessing stabilized (α,α-dimethyl) disulfides, three different synthetic methods have been reported. The first, direct conjugation to aldehyde groups generated by oxidation of carbohydrate residues on the antibodies, gives hydrazone linkages that are capable of releasing drug by mild acid hydrolysis ("carbohydrate" conjugates). The second method is the conjugation of activated esters to lysines on the antibodies to produce constructs with only the disulfide available as a point of drug release ("amide" conjugates). The third method also attaches drug to the lysines, but these conjugates contain an added hydrolytic site of release by virtue of a hydrazone linkage in the center of the linker ("hybrid" conjugates). The carbohydrate-based conjugates were the first to be reported and were capable of curing a number of xenograft tumors.[183]

Two specific examples of the calicheamicin amide conjugates have been published. One was made from an anticanine lymphoma antibody designated 231.[184] This conjugate was curative of canine lymphoma xenografts in mice with no apparent lethality, and all control groups (antibody, free calicheamicin derivative, and admixtures of the two) were essentially inactive.

The second amide-based conjugate, prepared from the anti-PEM (MUC1) antibody CTM01 (aka 7F11C7), entered clinical trials at about the same time as Mylotarg. The original candidate considered for the clinic was constructed by conjugating a hydrazide derivative of calicheamicin through oxidized carbohydrate residues of the antibody, but this was replaced by an amide-based conjugate. Two publications have appeared: one detailing the rationale for selecting an "amide-based" conjugate for the clinic, and the other comparing the murine and humanized versions of the CTM01 conjugate.[185,186] Contrasting the "carbohydrate-based" conjugate, containing both a hydrolytic point of release (the hydrazide bond) and a reductive point of release (the disulfide linkage) side by side with the "amide-based" conjugate, which only contained the disulfide as a point for calicheamicin release, showed that both types of conjugates were highly potent and completely suppressed the growth of a variety of solid tumors. However, the "amide-based" conjugate was somewhat more stable in circulation, and moreover, exhibited better activity against tumor models overexpressing the multidrug resistance (P-gp) phenotype. The "amide-based" conjugate also showed good activity against the cisplatin-resistant ovarian carcinoma subclone A2780DDP. This finding is interesting because the A2780DDP cell line overexpresses glutathione, a reducing agent particularly adept at inactivating cisplatin, but probably inadvertently cleaves the disulfide bond of the linker.[185]

Conjugates of both the murine and humanized versions of CTM01 showed excellent tumor-inhibiting properties, as expected.[186] However, the humanized conjugate exhibited slightly better affinity for the MUC1 antigen and cellular internalization properties, was expected to be considerably less immunogenic in humans than the murine counterpart, and thus led to the selection of the "amide-based," humanized conjugate of calicheamicin (designated CMB-401) for clinical evaluation.

Several examples of "hybrid" calicheamicin conjugates have been reported. One is Mylotarg (formerly CMA-676), the first FDA-approved antibody-targeted chemotherapeutic agent that recognizes the CD33 antigen expressed on differentiated myeloid cells and is used to treat AML.[187,188]

N-acetyl-calicheamicin γ_1^I was converted to the disulfide derivative of α,α-dimethylpropionyl hydrazide and this, in turn, was reacted with 4-(4-acetylphenoxy)-butyric acid (AcBut). Activation of the carboxylic acid as a hydroxysuccinimide ester followed by conjugation to the antibody hP67.6 produced Mylotarg. The product, containing the AcBut "hybrid" linker is relatively stable in circulation, but releases the calicheamicin derivative in the acidic environment of lysosomes.[189] The conditions used for preparing preclinical samples of Mylotarg containing minimal aggregated material have now been published. Earlier conditions for conjugating the AcBut-OSu derivative of *N*-acetyl-calicheamicin γ_1^I to the antibody P67.6 involved using 20% aqueous DMF but yielded about 25% of the conjugate in aggregated form. Three candidates were selected for further study from a group of 11 additives commonly used to prevent the aggregation of proteins by testing their ability to de-aggregate aggregated conjugate. The optimized procedure for the reaction between the P67.6 antibody and NAc-gamma calicheamicin DMH involved using 30% propylene glycol at pH 7.75 in the presence of 60 mM octanoic acid. These conditions produced conjugate with <4% aggregate, containing a loading of 2.5 mol/mol of calicheamicin in a 60% protein yield.[190]

In vitro Mylotarg was superior to the corresponding amide conjugate versus HL-60 promyelocytic leukemia cells[191] and was also an improvement over the corresponding carbohydrate conjugate.[183] It showed an IC_{50} in cell culture against HL-60 cells of 0.46 pg of calicheamicin equivalents per milliliter, was 78,000-fold more selective versus control cells that were equally sensitive to *N*-acetyl-calicheamicin γ_1^I, and was curative of HL-60 xenografts in mice over a wide dose range. Clinical support studies have shown that sensitivity to Mylotarg is cell-cycle dependent and that some internalization can occur through nonspecific endocytosis.[143] Such studies have also largely confirmed the intended mechanism of CD33 targeting and internalization.[192*]

The murine monoclonal antibody m5/44 targets the CD22 antigen of B-cell lymphomas. In addition, the antibody is internalized after targeting, making it a potential candidate for conjugation to calicheamicin. Initial studies in this regard used the murine version m5/44 to select the best linker. Two linkers were examined: the first was the acid-stable "amide-based" linker described above for CMB-401, and the second was the AcBut "hybrid" linker used to construct Mylotarg. A conjugate using the AcBut linker showed potent activity when tested against human B-cell lymphomas implanted into nude mice. In preparation for clinical trials, the corresponding humanized version of the antibody was prepared through CDR grafting onto an IgG_4 kappa framework and was designated g5/44. A calicheamicin conjugate of this construct was more potent than its murine counterpart and was designated CMC-544 for clinical trials, and given the generic name of inotuzumab ozogamicin.[193]

Additional preclinical experiments have been reported for CMC-544. The Ramos B-cell lymphoma, when implanted into severe combined immunodeficient (scid) mice, infiltrates the kidneys, bone marrow, and the CNS, causing hind-limb paralysis within 35 days and ultimately death. CMC-544, when administered up to 15 days after Ramos implantation (but not at 21 days or beyond) prevented this paralysis and B-cell infiltration in diseased scid mice for over 100 days. Mylotarg, which does not target the CD22 antigen and parent antibody g5/44, was ineffective.[194]

The therapeutic potential of CMC-544 has also been explored in models of acute lymphoblastic leukemia (ALL). This cancer is characterized by the expression of the CD22 antigen, which appears to be internalized following antibody binding, along with several other CD antigens. REH cells, an ALL model adapted to *in vivo* growth, were implanted into both nude and scid mice. Experiments

* A report has been published that indicates that "passive," as opposed to active, antigen-dependent targeting of solid tumors might be a viable approach to cancer therapy. Key to this idea was the observation that Mylotarg can inhibit some in vivo solid tumor models that do not express detectable levels of the CD33 antigen. The report summarized experiments conducted in nude mice using 10 tumor cell lines representing six of the major tumor types. Three additional antibody conjugates besides Mylotarg were tested (constructed using the anti-CD22 MoAb G5/44, the anti-CD20 MoAb rituximab, and a nonspecific mouse antibody MOPC-21), and as long as calicheamicin was conjugated through a hydrolytically sensitive linker, these conjugates showed some antitumor effects. Conjugates containing hydrolytically stable linkers were ineffective, as were conjugates prepared using PEGylated Fc fragments or albumin as a carrier. The authors speculate that these antitumor effects are due to the tortuous, leaky nature of tumor vasculature.[284]

in nude mice implanted ip to establish localized ALL tumors, dosing three times at 4-day intervals with 160 μg/kg of CMC-544, resulted in complete regression of tumors, and all animals survived the 102-day observation period. Lower doses were less effective. Scid mice were also used as a model of disseminated disease and similar results were observed (80 μg/kg Q4D × 3). Significant protection from hind-leg paralysis was even seen with doses of 4 μg/kg Q4D × 3.[195]

Rituximab (Biogen-Idec and Genentech) is a chimeric IgG_1 monoclonal antibody used to treat refractory rheumatoid arthritis and non-Hodgkin's lymphoma patients, among other conditions. It recognizes the CD20 antigen expressed on B cells but, unlike CMC-544, rituximab eliminates target cells through effector functions such as antibody-dependent cellular cytotoxicity and complement-dependent cytotoxicity. The two agents were studied individually and in combination in nude mice against B-cell lymphoma. CMC-544 alone was effective at inhibiting both developing and established xenografts, whereas rituximab showed good activity against developing tumors but lesser effects against the established (disseminated) model. Combining CMC-544 and rituximab produced 90% "cures" (mice surviving for 125 days) in a disseminated BCL model.[196]

An obvious extension of this study was to prepare the corresponding calicheamicin conjugate of rituximab and test it in the same BCL model. Both the "hybrid" linking conjugation methodology (the same as for CMC-544) and the "amide-based" linker (same as for CMB-401) were used. Neither methodology interfered with the effector functions of rituximab. Calicheamicin conjugated through the "hybrid" linker significantly improved the activity of rituximab, particularly against the *in vivo* disseminated BCL model compared with unmodified rituximab. However, no improvement in activity over parent rituximab was seen by using the "amide-based" conjugation method for calicheamicin.[197]

The activity of CMC-544 has also been assessed *in vitro* against CD22-expressing isolates obtained from 19 patients with B-cell chronic lymphocytic leukemia, the Daudi and Raji cell lines, and the P-gp-positive cell lines Daudi/MDR and Raji/MDR. All cells expressing the CD22 antigen responded in a dose-dependent manner, a response that was attenuated by the amount of CD22 expressed on a particular cell population. However, cells also expressing the MDR phenotype were less sensitive to CMC-544, a condition that could be reversed by the inclusion of PSC833 or MS209, two MDR modifiers, in test samples.[198]

Another reported calicheamicin conjugate targets the $Lewis^Y$ antigen and uses the antibody designated Hu3S193. This conjugate was more efficacious in several different solid tumor xenograft models (gastric, colon, and prostate) than a control conjugate, producing cures in the gastric model. The $Lewis^Y$ antigen (Le^Y) is expressed on the surface of a variety of carcinomas, including prostate, breast, colon, lung, and ovarian tumors. Calicheamicin was conjugated using the same linker as in Mylotarg to this humanized antibody. *In vitro*, sensitivity of cells toward this conjugate (CMD-193) depended on their expression of the Le^Y antigen. *In vivo*, the conjugate was particularly active against the N87 human gastric tumor xenografts in nude mice, inhibiting tumor growth for over 100 days. Activity was also noted against the LOVO model of colon cancer, as well as the LNCaP prostate carcinoma.[199]

A conjugate between *N*-acetyl-calicheamicin γ_1^I and the anti-CD64 antibody H22 has been constructed using the AcBut linker and assessed for its potential for eliminating macrophages and monocytes in peripheral blood and synovial fluid samples obtained from 12 rheumatoid arthritis patients. Previously, the authors had studied a ricin A-chain conjugate of the same antibody and found that although synovial macrophages were eliminated, the ricin A-chain conjugate had relatively little effect on circulating monocytes. The calicheamicin conjugate, however, eliminated monocytes both at sites of inflammation as well as from circulation. Elimination of both cell types in synovial fluid is desirable as a therapy for rheumatoid arthritis, but the destruction of monocytes in circulation makes the calicheamicin conjugate less appealing for this type of therapy because interfering with normal immune function could be detrimental.[200]

The H8 monoclonal antibody targets the oncofetal protein 5T4, an antigen expressed on a significant number of carcinomas. Conjugates between this antibody and *N*-acetyl-calicheamicin γ_1^I using

both the acid-labile and acid-stable linkers were studied. Several additional modifications were incorporated into the conjugates, such as PEGylation of "relaxed" H8 (to cleave intrachain disulfide bonds) and conjugation through the AcPAc [(3-acetylphenyl)acetic acid] linker. PEGylation significantly decreased the avidity of binding for the conjugate *in vitro*, and this construct was not studied further. *In vivo*, the remaining conjugates showed significant antitumor activity, in most cases extending to complete tumor eradication out beyond 100 days. However, the individual tumors that expressed the 5T4 antigen determined whether the acid-labile or acid-stable conjugate produced the best results.[201]

Four conjugates of the synthetic calicheamicin analog θ have been reported that target three different antigens. This enediyne was also linked to antibodies through a disulfide-containing spacer, but attachment was through the amino sugar residue, which was first modified with *N*-hydroxysuccinimido-3-(2-pyridyldithio)propionate (SPDP). This activated intermediate was then reacted with antibodies that had been modified with iminothiolane to yield the conjugates.[202] One was produced using the chimeric CH 14.18 antibody, where IC_{50} values against three different cell lines ranged from 0.1 to 6 nM. The second, more thoroughly studied conjugate was prepared from antibody 14G2a.[202] This conjugate exhibited an IC_{50} against NXS2 cells of around 0.1 pM, or about 100-fold less cytotoxic than calicheamicin itself, and had some activity in a model of neuroblastoma metastatic to the liver. No data were reported for nontargeting conjugates or control cell lines.

An anti-CD19 conjugate of calicheamicin θ has also been described.[203] The IC_{50} was between 1 and 100 pM and tripled the life span of mice implanted with the BCR/Abl-positive pre-B-cell leukemia Nalm-6. Lastly, an antirenal gamma-glutamyl transferase conjugate made using antibody 138H11 had an IC_{50} of 50 pM against Caki-1 cells, with 40-fold selectivity over a control conjugate and a control cell line.[204] Suppression of tumor growth for at least three weeks was seen in a xenograft model of Caki-1 cells at the maximum tolerated dose where some weight loss was also observed. At a half-maximal dose, a growth delay of two weeks was seen, whereas no significant activity was noted for a nonbinding control conjugate. Mild reduction of the same antibody cleaved some of the surface-accessible disulfide bonds to generate thiols. A calicheamicin θ conjugate has also been constructed through these thiols, showing an IC_{50} of 16 nM against Caki-2 cells.[205] When evaluated against Nalm-6 leukemia cells implanted into scid mice, this conjugate, injected on days 5 and 7 after tumor implantation, completely inhibited leukemia growth out to 100 days, with all animals surviving the therapy. Various controls were either inactive or far less so.[206]

Numerous publications describe neocarzinostatin conjugates, all prepared with the chromophore inside the apoprotein, using the antiadenocarcinoma antibody A7. These have included not only the whole antibody as the targeting unit, but also smaller antigen-recognizing fragments such as $F(ab')_2$s and Fabs as well. All such constructs have been prepared using traditional SPDP-based cross-linking strategies. Whole antibody conjugates of A7 and neocarzinostatin were active in a xenograft model of pancreatic cancer when injected either intravenously (iv) or intratumorally.[207] The same conjugate also showed activity against gastric cell lines.[208] *In vitro*, the conjugate was 10-fold more active against antigen-positive MKN45 cells than antigen-negative MKN1 control cells with an IC_{50} of 70 ng/mL, in neocarzinostatin equivalents. Tumor nodule formation was inhibited by 90% in a disseminated intraperitoneal model. However, the effect was not significantly different than that seen with neocarzinostatin alone, although the diminished toxicity data indicated a wider therapeutic window for the conjugate. This was confirmed in a subsequent report where the MTD was improved by about fivefold, with the conjugate being less toxic, even though the significantly better pharmacokinetic properties would be expected to increase the total exposure to neocarzinostatin.[209] More than twice as much antibody A7 and its conjugate localized to xenografts compared with a control antibody, yet both localized to an antigen-negative tumor in equal amounts.

A neocarzinostatin conjugate prepared from Fab fragments of A7 inhibited colony formation of antigen-positive colon[210] and pancreatic[211] cells in an antigen-specific manner, but the specificity was only about twofold. Modest antigen-specific activity was also seen in xenografts of colorectal

cancer,[212] but complete, antigen-dependent tumor suppression was seen in a pancreatic xenograft model.[213]

The tumor-targeting ability of the Fab construct has been studied relative to whole antibody and a $F(ab')_2$ construct using ^{125}I radiolabeling.[214,215] The Fab conjugate targeted the tumor faster and more radiolabel was associated with the implant at the earlier time points. Of the three, whole antibody showed the least amount of tumor targeting at two hours.[215] So even though Fab fragments are usually considered to be cleared too rapidly for drug targeting, this may be appropriate for neocarzinostatin, which itself has a relative short half-life in circulation. When this Fab conjugate (chFabA7-neocarzinostatin) was administered to cancer patients, kidney toxicity was observed,[210,212] possibly because of the rapid clearance of Fab fragments through the kidneys in general.

In an approach involving targeting through an avidin-biotin system, both neocarzinostatin and an anti-CEA antibody were first biotinylated. Cells were treated with the modified antibody, followed by avidin, and finally the modified neocarzinostatin.[216,217] The multivalent avidin protein binds tightly to both biotinylated molecules stepwise in sandwich fashion. When colon adenocarcinoma cells were treated for 72 hours, no difference was seen with or without the biotinylated antibody. However, when the cells were washed seven minutes after the final exposure, a fivefold increase was seen in the cytotoxicity with the biotinylated antibody compared with controls.[218]

TES-23 is an antibody raised against rat tumor-derived endothelial cells.[219] As such, it targets tumor vasculature in human xenografts about 20 times more effectively than a control antibody. A neocarzinostatin conjugate was active in suppressing KMT-17 fibrosarcoma tumors in rats (the same tumor used for making the antibody) at 17 μg/kg, injected three times.[219] Tumor hemorrhagic necrosis was observed. Less toxicity was seen with the conjugate, even though the activity was not significantly different from neocarzinostatin itself. Antigen-specific distribution of the conjugate to KMT-17 rat and Sarcoma-180 murine tumors was demonstrated,[220] as well as to Meth-A and colon 26 murine tumors.[221] The conjugate was active against Meth-A tumors implanted subcutaneously in mice with three of four survivors in a group treated with 50 μg/kg of neocarzinostatin equivalents.[221]

Four other antibodies have been conjugated to neocarzinostatin.[222] These were prepared using thiol-maleimide coupling to give a monosulfide linkage instead of the disulfides produced by SPDP-based couplings. The antibodies used were 791T/36 (anti-gp72 targeting osteosarcoma and colorectal carcinoma), BW 431/26 (CEA, targeting colon and stomach cancer), SWA11 (anti-SCLC-Ag cluster w4/gp45, targeting small-cell lung cancer), and OV-TL3 (anti-OA3/p85, targeting ovarian carcinoma). The *in vitro* selectivity of the first three conjugates relative to antigen-negative cells was low, while the last one was about eightfold selective over background. The potency of these conjugates ranged from 16 to 5100 ng/mL.

Neocarzinostatin has also been conjugated to transferrin, in this case through a monosulfide between dithiolane and a maleimide.[223] An increase in cytotoxicity was seen compared with neocarzinostatin alone; however, additional experiments with modified incubation conditions and with excess transferrin indicated that the effects were not due to internalization of the conjugate but to neocarzinostatin that had disassociated from the conjugate before cell entry.

22.9 CLINICAL EXPERIENCE

Esperamicin A1 has been examined in phase I and II clinical trials for the treatment of advanced adenocarcinoma of the pancreas.[224–226] Although these three references are for meeting abstracts, this appears to be the only information published about the trials. No clearly demonstrable cases of response were seen in the 14 patients treated. Nausea/vomiting, malaise/fatigue, thrombocytopenia, and hepatic toxicity were the most common side effects.

Neither calicheamicin γ_1^I itself nor other members of this family have been examined in the clinic. Instead, all the clinical experience regarding this enediyne has been based on antibody-targeted forms. Clinical data are available for several such conjugates.

CMB-401, which targets the PEM (MUC-1) antigen with the hCTM01 antibody, has been evaluated through phase II clinical trials. An imaging study was conducted first with ^{111}In-labeled antibody to confirm tumor targeting in ovarian cancer.[227] A 7.6-fold increase of radioactivity in tumor versus normal tissues was seen at 0.1 mg/kg protein dose, and a 14-fold increase was seen at 1 mg/kg. In a phase I trial of CMB-401, 34 patients were pretreated with 35 mg/m^2 of unmodified hCTM01 antibody to clear circulating antigen, followed by doses of the conjugate ranging from 2 to 16 mg/m^2.[228] The MTD was defined by malaise, hematological toxicities, and gastro-intestinal hemorrhage. Four patients had >50% decrease in CA125 levels and three patients showed reduction in tumor bulk. In this trial, the half-life of the conjugate was estimated to be 36 hours, and up to four cycles of treatment led to no allergic reactions with only three increases in antibody titer.[229]

Ovarian cancer patients who had relapsed after standard chemotherapy were treated with 35 mg/m^2 of native antibody followed by 16 mg/m^2 of CMB-401 in a phase II trial.[230] Of the 19 evaluable patients, only four had >50% decreases in CA125 levels and there were no objective responses. Two reasons cited for possible failure were complications arising from the attempts to clear circulating antigen and from the use of an amide-based-linking system for calicheamicin, relying only on the reductive mechanism for drug release. There is no data given to support either of these hypotheses, and numerous other possibilities must certainly exist.

Mylotarg (gemtuzumab ozogamicin) is the first antibody-targeted chemotherapeutic agent registered for humans. It was approved by the FDA in May of 2000 for use in relapsed AML in patients over the age of 60 who no longer respond to conventional chemotherapy.[187,188] Approval was based on phase II data where about 30% of patients achieved a complete remission. Myelosuppression was the dose-limiting toxicity, along with transient, reversible liver effects. A common infusional syndrome seen with most antibody therapies was also observed. Mylotarg is significantly less toxic than traditional chemotherapy, which has resulted in savings regarding hospitalization time and the associated costs.[231,232]

One unusual side effect appears to be associated with the timing of stem-cell transplantation following therapy and has been termed veno-occlusive disease (VOD) or sinusoidal obstruction syndrome. This condition is characterized by the blockage of liver capillaries and is fatal in up to 30% of such cases. A retrospective study of 62 patients who had undergone allogenic stem-cell transplantation revealed that 21% of patients in this study developed symptoms of VOD overall, but this risk was increased to 64% with pretreatment with Mylotarg. None of the patients who underwent stem-cell transplantation more than 3.5 months after Mylotarg therapy (four patients in this study) developed VOD.[233] A recent review of this condition with respect to the side effects of Mylotarg and the timing of stem-cell transplantation has been published.[234] Reviews of Mylotarg efficacy and toxicities have also been published.[235,236]

The lack of a universal response to Mylotarg in AML may have various causes. Some possibilities include P-glycoprotein expression,[237,238,239] other efflux pumps,[240] variations in CD33 levels,[241] and resistance to apoptosis.[133]

Although AML most commonly affects the elderly, Mylotarg has also been examined for pediatric AML as well as ALL.[242] Two studies reported on the use of Mylotarg in children diagnosed with AML, both on a compassionate use basis. The first involved 15 children receiving 4 to 9 mg/m^2 for up to three courses.[243] Relatively few conclusions could be drawn regarding this study because a majority of the patients responding to the treatment underwent immediate stem-cell transplant therapy, and most of them did not survive. The second study involving six patients was not more encouraging in terms of a positive response rate, at least as monotherapy in children.[244]

A final report of the phase II study of Mylotarg on 277 elderly patients in first recurrence with CD33-positive AML concluded that two 9 mg/m^2 doses spaced out by two weeks produced a 26% remission rate with an acceptable safety profile.[245]

A similar study, when repeated in 40 Japanese patients with AML and comparable median age, equally distributed between phase I and II protocols, revealed similar safety, pharmacokinetic, and

remission profiles. However, it was noted that disease-free survivals lasted significantly longer in a subset of these patients compared with their nonoriental counterparts in other studies.[246]

One study has attempted to determine whether dividing the 9-mg/m^2 doses of Mylotarg, given iv on days 1 and 14 at the initiation of therapy, would produce a better response rate against AML than smaller, fractionated doses. In this study, 57 AML patients in their first relapse were treated with three doses of 3 mg/m^2 each of Mylotarg on days 1, 4, and 7 as a single course of therapy. Although dosing was not repeated at the 14-day time point, this therapy was promising because it yielded a comparable response rate, at half the total exposure to Mylotarg, as the approved dosing regimen.[247]

Two studies addressed the importance of the CD33 antigen as the target for Mylotarg. The antibody P67.6, which is the targeting unit of the construct, requires CD33 expression for effective delivery of calicheamicin to AML cells. However, an excess presence of this antigen in peripheral blood, as would be expected when CD33 is shed by replicating or dying cells, binds Mylotarg and prevents it from reaching the bone marrow, the primary repository of AML cells, and significantly reduces cancer cell kill.[248] A second study attempted to find an association between high CD33 expression and the lack of a positive clinical outcome in many patients. The authors concluded that coexpression of the CD33 antigen along with the P-glycoprotein receptor, a hallmark of the multidrug resistance of target cells, was inversely correlated with the sensitivity toward therapy. In spite of high CD33 expression, cells also possessing high levels of P-gp were resistant to Mylotarg, whereas AML cells expressing low levels of P-gp responded well to this therapy.[249]

Mylotarg has been evaluated in combination with various high-dose regimens involving traditional anticancer agents. These include cytarabine,[250] all-*trans*-retinoic acid,[251] IL-11,[252] topotecan/Ara-C,[253] fludarabine/Ara-C/G-CSF/idarubicin,[254] troxatyl,[255] Ara-C/mitoxantrone/amifostine,[256] mitoxantrone/Ara-C/etoposide,[257] imatinib (Gleevec),[258] fludarabine/Ara-C/cyclosporin,[259] Ara-C/idarubicin,[260] and daunorubicin/Ara-C/cyclosporin.[261] These studies were in progress at the writing of our last review[1] but none appear to have matured into preferred treatments over Mylotarg monotherapy. Several new combination studies have been initiated since that time.

Granulocyte CSF (G-CSF), when used as a priming agent to attenuate expression of the CD33 antigen or inhibit P-gp function of AML blast cells isolated from refractory patients, augmented the cytotoxic effects of Mylotarg against these cells.[262] A clinical trial conducted by the same group actually evaluated this combination two years prior to the publication of the *in vitro* results, but the significance of the response, given the small size of the clinical trial (eight patients), is difficult to assess relative to Mylotarg monotherapy.[263]

A substantial number of inhibitors and modulators of various cellular receptors, proteins, and housekeeping enzymes as adjuncts to Mylotarg treatment have been investigated in preclinical studies. Such agents have included farnesyl transferase and Bcl-2 inhibitors, the histone deacetylase inhibitor valproic acid, various FLT-3 receptor inhibitors, interleukin-2, FMS-like tyrosine kinase 3 inhibitors, DNA-hypomethylating agents, antiangiogenesis agents, the anti-CD45 antibody BC8 (to block an antigen coexpressed with CD33), and a host of P-gp modulators including zosuquidar, cyclosporine A, the peripheral benzodiazepine receptor ligand PK11195, and MK-571. A recent review of most such studies has been published.[264] One of these modulators, oblimersen sodium that targets Bcl-2 mRNA, has been evaluated in a nonrandomized Phase II study along with Mylotarg in 48 elderly patients with relapsed AML. No significant improvement over Mylotarg monotherapy was observed.[265]

Acute promyelocytic leukemia (APL) is a subset of AML and occurs in <10% of patients diagnosed with AML. If left untreated, this form of leukemia is fatal but can be treated, at least transiently, with all-trans-retinoic acid (ATRA). Anthracyclines, in combination with ATRA, have been used to prolong remissions, and more recently so has arsenic trioxide (ATO). However, APL blasts express a significant level of the CD33 antigen, the target for Mylotarg. To investigate whether Mylotarg might be useful for this type of leukemia, blast cells from six patients with resistance to ATRA and two with resistance to both ATRA and ATO were isolated and assessed for their

sensitivity. The report concluded that ATRA and ATO-resistant APL responded well to Mylotarg as long as these cells did not express the P-gp multidrug efflux protein.[266]

Three clinical studies have been published so far to exploit this observation and investigate combinations of ATRA, ATO, and Mylotarg in high-risk (relapsed) patients. Complete response rates and long-term survivals were encouraging.[267–269]

A phase I study in nine patients with Le^Y-positive tumors has been published. The primary goal of the study was to assess human biodistribution and clearance parameters at doses of 1.0 and 2.6 mg/m^2 with ^{111}In as the tracer label. Half-life ($T_{1/2}$) was determined to be 108.88 ± 35.67 hours, regardless of dose, with rapid blood clearance and low uptake into tumors. Redosing was performed every three weeks for up to six cycles of therapy, but only one minor response was noted in the study.[270]

Further clinical studies with Mylotarg are not likely to occur. Pfizer, the present owner of Mylotarg, announced in a June 21, 2010 press release that it will voluntarily withdraw the NDA effective on October 15. This decision, made through discussions with the FDA, will minimize future availability of this drug in the United States.

Neocarzinostatin has been examined in the clinic both by itself and as several forms of polymer-based conjugates. The natural product is approved for a number of cancers in Japan, but not elsewhere. These cancers include stomach, pancreas, liver, bladder, and brain, as well as leukemia. The main side effect with neocarzinostatin is myelosuppression. More recently, it has shown some promise in refractory or recurrent AML in combination with enocitabine and aclarubicin with 57% of patients achieving complete remission.[271]

Conjugates of neocarzinostatin and the anticolon antibody A7 have been in clinical trials as well. Patients given whole antibody conjugate between 15 and 90 mg showed no adverse effects, and three out of eight patients with liver metastases secondary to colon cancer showed a decrease in tumor size and three experienced pain relief, but this treatment had no effect on other metastases.[272] However, most of these patients mounted a human antimouse (HAMA) response against the murine antibody itself. Experiments with sera from these patients showed that the HAMA response blocked conjugate cytotoxicity.[273] Such immunological reactions have led to serious problems such as anaphylaxis. A chimeric version of A7 has been constructed (part human sequences, part mouse) and only the antigen-recognizing parts of the antibody (the Fab′ fragments, about one-sixth the size of a whole IgG antibody) have been conjugated to neocarzinostatin. Seven colorectal cancer patients were each administered 18-mg doses of the construct; two of these patients still mounted a high HAMA response. As expected, clearance was more rapid than the corresponding whole A7 conjugate, and no anticancer responses were noted.[274]

SMANCS (*s*tyrene *m*aleic *a*cid copolymer *n*eo*c*arzino*s*tatin conjugate), zinostatin stimalarmar, is approved in Japan for patients with liver cancer or liver metastases, and is being explored for cancers of the kidney, lung, and pancreas. It is coadministered as a mixture with Lipiodol, a heavily iodinated poppy seed oil. Reviews covering the discovery, development, and clinical use of this therapy are available.[275–278] In a phase I study, 12 patients with hepatocellular carcinoma were injected through the hepatic artery starting with 3 mg/m^2 of zinostatin stimalamar. This was, in fact, the highest tolerated dose. No objective responses were noted.[279] A somewhat related approach that has not progressed to clinical trials is the use of chitin derivatives to deliver neocarzinostatin.[280]

22.10 SUMMARY

The isolation and preliminary biological activity of neocarzinostatin as an anticancer agent was first reported in 1965.[281] During subsequent years, the characterization and a low-resolution x-ray crystal structure of this natural product were reported, and the mechanism of DNA cleavage was elucidated. A variety of conjugates were prepared, including SMANCS as well as various antibody-based constructs, in an effort to overcome the short biological half-life of this compound. Clinical trials were initiated with neocarzinostatin, both in Japan as well as in the United States. Yet these

studies were all performed with the conviction that neocarzinostatin was, in fact, an anticancer protein. It was not until 1979 that the protein was shown to be associated with a much smaller chromophoric subunit that was responsible for the observed biological activity,[282] and it took another six years before an enediyne macrocyclic structure was assigned to the chromophore, though without much of the stereochemistry.[22] The last chapter relating to the structure of the molecule was closed in 1998, with the report of the total synthesis of the neocarzinostatin chromophore.[74]

In the meantime, similarities between the neocarzinostatin apoprotein and several other "anticancer proteins" soon led to work that showed that some of these sequestered enediynes as well. But these early enediynes were soon upstaged by the more stable 10-membered ring analogs: isolation and biological activity for esperamicin was published in 1985[283] and its structure in 1987,[13] along with that of calicheamicin γ_1^I the same year.[15] The complex and extremely novel structures of these compounds captured the attention and resources of many major academic total synthesis groups, in a race to be first to construct these molecules. Biochemists and biologists helped elucidate the activity and the mechanisms of action for these compounds. As more members of this family were isolated and their structures were assigned, the mechanisms and pathways by which microorganisms assembled these molecules became an important and ongoing challenge.

What remained, however, was to make the enediynes into useful drugs. In spite of extreme potency, their physical characteristics, their short half-lives, and their narrow therapeutic windows precluded using most of these natural products as drugs themselves. Neocarzinostatin and calicheamicin γ_1^I were eventually converted to anticancer agents approved for human use via conjugation to a polymer and an antibody, respectively. The recently announced withdrawal of Mylotarg from the U.S. market is, of course, disappointing, but a number of new enediyne-based drugs have entered clinical trials in recent years. One or more of these could succeed. We have tried to demonstrate in this review that the research into enediynes continues in an effort to understand the biology of these molecules better and thereby expand their clinical applications.

REFERENCES

1. Hamann, P.R., Upeslacis, J., and Borders, D.B., Enediynes, in *Anticancer Agents from Natural Products*, Cragg, G.M., Kingston, D.G.I., and Newman, D.J., Eds., CRC Press, New York, 2005.
2. Borders, D.B. and Doyle, T.W., Eds., *Enediyne Antibiotics as Antitumor Agents*, Marcel Dekker, Inc., New York, 1995.
3. Lee, M.D., Ellestad, G.A., and Borders, D.B., Calicheamicins: Discovery, structure, chemistry, and interaction with DNA, *Acc. Chem. Res.*, 24, 235, 1991.
4. Nicolaou, K.C. and Dai, W.M., Chemistry and biology of the enediyne anticancer antibiotics, *Angew. Chem., Int. Ed. Engl.*, 30, 1387, 1991.
5. Smith, A.L. and Nicolaou, K.C., The enediyne antibiotics, *J. Med. Chem.*, 39, 2103, 1996.
6. Nicolaou, K.C., Sorensen, E.J., and Winssinger, N., The art and science of organic and natural products synthesis, *J. Chem. Educ.*, 75, 1225, 1998.
7. Xi, Z. and Goldberg, I.H., DNA-damaging enediyne compounds, in *Comprehensive Natural Products Chemistry*, Barton, D.S., Nakanishi, K., and Meth-Cohn, O., Eds., Pergamon Press, Oxford, 1999, 7, 553.
8. Jones, G.B. and Fouad, F.S., Designed enediyne antitumor agents, *Curr. Pharm. Des.*, 8, 2415, 2002.
9. Shen, B., Liu, W., and Nonaka, K., Enediyne natural products: Biosynthesis and prospect towards engineering novel antitumor agents, *Curr. Med. Chem.*, 10, 2317, 2003.
10. Yus, M. and Foubelo, F., Enediyne: Recent developments, *Recent Res. Devel. Organic Chem.*, 6, 205, 2002.
11. Maeda, H., Edo, K., and Ishida, N., Eds., *Neocarzinostatin: The Past, Present and Future of an Anticancer Drug*, Springer-Verlag, New York, 1997.
12. Golik, J., Clardy, J., Dubay, G., Groenewold, G., Kawaguchi, H., Konishi, M., Krishnan, B., Ohkuma, H., Saitoh, K., and Doyle, T.W., Esperamicins, a novel class of potent antitumor antibiotics. 2. Structure of esperamicin X, *J. Am. Chem. Soc.*, 109, 3461, 1987.
13. Golik, J., Dubay, G., Groenewold, G., Kawaguchi, H., Konishi, M., Krishnan, B., Ohkuma, H., Saitoh, K., and Doyle, T.W., Esperamicins, a novel class of potent antitumor antibiotics. 3. Structures of esperamicins A1, A2, and A1b, *J. Am. Chem. Soc.*, 109, 3462, 1987.

14. Lee, M.D., Dunne, T.S., Siegel, M.M., Chang, C.C., Morton, G.O., and Borders, D.B., Calichemicins, a novel family of antitumor antibiotics. 1. Chemistry and partial structure of calichemicin γ_1^I, *J. Am. Chem. Soc.*, 109, 3464, 1987.
15. Lee, M.D., Dunne, T.S., Chang, C.C., Ellestad, G.A., Siegel, M.M., Morton, G.O., McGahren, W.J., and Borders, D.B., Calicheamicin, a novel family of antitumor antibiotics. 2. Chemistry and structure of calicheamicin γ_1^I, *J. Am. Chem. Soc.*, 109, 3466, 1987.
16. Zein, N., Sinha, A.M., McGahren, W.J., and Ellestad, G.A., Calicheamicin γ_1^I: An antitumor antibiotic that cleaves double-stranded DNA site specifically, *Science*, 240, 1198, 1988.
17. Lee, M.D., Dunne, T.S., Chang, C.C., Siegel, M.M., Morton, G.O., Ellestad, G.A., McGahren, W.J., and Borders, D.B., Calicheamicins, a novel family of antitumor antibiotics. 4. Structure elucidation of calicheamicins β_1^{Br}, γ_1^{Br}, α_2^I, α_3^I, β_1^I, γ_1^I, and δ_1^I, *J. Am. Chem. Soc.*, 114, 985, 1992.
18. Golik, J., Beutler, J., Clark, P., Ross, J., Roach, J., Muschik, G., and Lebherz, W.B. III, *Antitumor Antibiotics*, U.S. Patent 5,086,045, 1992.
19. White, R.J., Maiese, W.M., and Greenstein, M., in *Manual of Industrial Microbiology and Biotechnology*, Demain, A.L. and Solomon, N.A., Eds., American Society of Microbiology, Washington, DC, 1986, 24.
20. Lee, M.D., Manning, J.K., Williams, D.R., Kuck, N.A., Testa, R.T., and Borders, D.B., Calicheamicins, a novel family of antitumor antibiotics. 3. Isolation, purification and characterization of calicheamicins β_1^{Br}, γ_1^{Br}, α_2^I, α_3^I, β_1^I, γ_1^I, and δ_1^I, *J. Antibiot.*, 42, 1070, 1989.
21. Maiese, W.M., Lechevalier, M.P., Lechevalier, H.A., Korshalla, J., Kuck, N., Fantini, A., Wildey, M.J., Thomas, J., and Greenstein, M., Calicheamicins, a novel family of antitumor antibiotics: Taxonomy, fermentation and biological properties, *J. Antibiot.*, 42, 558, 1989.
22. Edo, K., Mizugaki, M., Koide, Y., Seto, H., Furihata, K., Otake, N., and Ishida, N., The structure of neocarzinostatin chromophore possessing a novel bicyclo-7.3.0-dodecadiyne system, *Tet. Lett.*, 26, 331, 1985.
23. Lam, K.S. and Forenza, S., Fermentation and isolation of esperamicins, in *Enediyne Antibiotics as Antitumor Agents*, Borders, D.B. and Doyle, T.W., Eds., Marcel Dekker, Inc., New York, 1995, Chap. 10.
24. Ando, T., Ishii, M., Kajiura, T., Kameyama, T., Miwa, K., and Sugiura, Y., A new non-protein enediyne antibiotic N1999A2: Unique enediyne chromophore similar to neocarzinostatin and DNA cleavage feature, *Tet. Lett.*, 39, 6495, 1998.
25. Takashima, H., Amiya, S., and Kobayashi, Y., Neocarzinostatin: Interaction between the antitumor-active chromophore and the carrier protein, *J. Biochem.*, 109, 807, 1991.
26. Hofstead, S.J., Matson, J.A., Malacko, A.R., and Marquardt, H., Kedarcidin, a new chromoprotein antitumor antibiotic. II. Isolation, purification and physico-chemical properties, *J. Antibiot.*, 45, 1250, 1992.
27. Kim, K.H., Kwon, B.M., Myers, A.G., and Rees, D.C., Crystal structure of neocarzinostatin, an antitumor protein-chromophore complex, *Science*, 262, 1042, 1993.
28. Okuno, Y., Otsuka, M., and Sugiura, Y., Computer modeling analysis for enediyne chromophore-apoprotein complex of macromolecular antitumor antibiotic C-1027, *J. Med. Chem.*, 37, 2266, 1994.
29. Teplyakov, A., Obmolova, G., Wilson, K., and Kuromizu, K., Crystal structure of apo-neocarzinostatin at 0.15-nm resolution, *Eur. J. Biochem.*, 213, 737, 1993.
30. Chin, D.H., Rejection by neocarzinostatin protein through charges rather than sizes, *Chem.-Eur. J.*, 5, 1084, 1999.
31. Usuki, T., Inoue, M., Hirama, M., and Tanaka, T., Rational design of supra C-1027: Kinetically stabilized analog of the antitumor enediyne chromoprotein, *J. Am. Chem. Soc.*, 126, 3022, 2004.
32. Zein, N., Casazza, A.M., Doyle, T.W., Leet, J.E., Schroeder, D.R., Solomon, W., and Nadler, S.G., Selective proteolytic activity of the antitumor agent kedarcidin, *Proc. Natl. Acad. Sci. U.S.A.*, 90, 8009, 1993.
33. Sakata, N., Tsuchiya, K.S., Moriya, Y., Hayashi, H., Hori, M., Otani, T., Nagai, M., and Aoyagi, T., Aminopeptidase activity of an antitumor antibiotic, C-1027, *J. Antibiot*., 45, 113, 1992.
34. Gao, R.-J., Li, D.-D., and Zhen, Y.-S., Study on mechanisms of action of enediyne antitumor antibiotic lidamycin, *Zhongguo Xinyao Zazhi*, 15, 1039, 2006.
35. McDonald, L.A., Capson, T.L., Krishnamurthy, G., Ding, W.-D., Ellestad, G.A., Bernan, V.S., Maiese, W.M., Lassota, P., Discafani, C., Kramer, R.A., and Ireland, C.M., Namenamicin, a new enediyne antitumor antibiotic from the marine ascidian Polysyncraton lithostrotum, *J. Am. Chem. Soc.*, 118, 10898, 1996.
36. Oku, N., Matsunaga, S., and Fusetani, N., Shishijimicins, A.-C, novel enediyne antitumor antibiotics from the ascidian *Didemnum proliferum*, *J. Am. Chem. Soc.*, 125, 2044, 2003.
37. Davies, J., Wang, H., Taylor, T., Warabi, K., Huang, X.H., and Andersen, R.J., Uncialamycin, a new enediyne antibiotic, *Org. Lett.*, 7, 5233, 2005.

38. Oh, D.C., Williams, P.G., Kauffman, C.A., Jensen, P.R., and Fenical, W., Cyanosporasides A and B, chloro- and cyano-cyclopenta[a]indene glycosides from the marine actinomycete "Salinispora pacifica," *Org. Lett.*, 8, 1021, 2006.
39. McGlinchey, R.P., Nett, M., and Moore, B.S., Unraveling the biosynthesis of the sporolide cyclohexenone building block, *J. Am. Chem. Soc.*, 130, 2406, 2008.
40. Fantini, A.A. and Testa, R.T., Taxonomy, fermentation and yield improvement, in *Enediyne Antibiotics as Antitumor Agents*, Borders, D.B. and Doyle, T.W., Eds., Marcel Dekker, Inc., New York, 1995, Chap. 3.
41. McCoy. J.G., Johnson, H.D., Singh, S., Bingman, C.A., Lei, I.K., Thorson, J.S., and Phillips, G.N. Jr., Structural characterization of $CalO_2$: A putative orsellinic acid P450 oxidase in the calicheamicin biosynthesis pathway, *Proteins*, 74, 50, 2009.
42. Hensens, O.D., Giner, J.-L., and Goldberg, I.H., Biosynthesis of NCS Chrom A, the chromophore of the antitumor antibiotic neocarzinostatin, *J. Am. Chem. Soc.*, 111, 3295, 1989.
43. Lam, K.S., Veitch, J.A., Golik, J., Krishnan, B., Klohr, S.E., Volk, K.J., Forenza, S., and Doyle, T.W., Biosynthesis of esperamicin A1, an enediyne antitumor antibiotic, *J. Am. Chem. Soc.*, 115, 12340, 1993.
44. Lam, K.S., Gustavson, D.R., Veitch, J.A., and Forenza, S., The effect of cerulenin on the production of esperamicin A_1 by *Actinomadura verrucosospora*, *J. Indust. Microbiol. Biotech.*, 12, 99, 1993.
45. Tokiwa, Y., Miyoshi-Saitoh, M., Kobayashi, H., Sunaga, R., Konishi, M., Oki, T., and Iwasaki, S., Biosynthesis of dynemicin A, a 3-ene-1,5-diyne antitumor antibiotic, *J. Am. Chem. Soc.*, 114, 4107, 1992.
46. Ahlert, J., Shepard, E., Lomovskaya, N., Zazopoulos, E., Staffa, A., Bachmann, B.O., Huang, K. et al., The calicheamicin gene cluster and its iterative type I enediyne PKS, *Science*, 297, 1173, 2002.
47. Liu, W., Christenson, S.D., Standage, S., and Shen, B., Biosynthesis of the enediyne antitumor antibiotic C-1027, *Science*, 297, 1170, 2002.
48. Van Lanen, S.G. and Shen, B., Biosynthesis of enediyne antitumor antibiotics, *Curr. Top. Med. Chem.*, 8, 448, 2008.
49. Kong, R., Goh, L.P., Liew, C.W., Ho, Q.S., Murugan, E., Li, B., Tang, K., and Liang, Z.-X., Characterization of a carbonyl-conjugated polyene precursor in 10-membered enediyne biosynthesis, *J. Am. Chem. Soc.*, 130, 8142, 2008.
50. Zhang, J., Van Lanen, S.G., Ju, J., Liu, W., Dorrestein, P.C., Li, W., Kelleher, N.L., and Shen, B., A phosphopantetheinylating polyketide synthase producing a linear polyene to initiate enediyne antitumor antibiotic biosynthesis, *Proc. Natl. Acad. Sci. U.S.A.*, 105, 1460, 2008.
51. Sun, H., Kong, R., Zhu, D., Lu, M., Ji, Q., Liew, C.W., Lescar, J., Zhong, G., and Liang, Z.-X., Products of the iterative polyketide synthases in 9- and 10-membered enediyne biosynthesis, *Chem. Comm.*, 47, 7399, 2009.
52. Beleccki, K., Crawford, J.M., and Townsend, C.A., Production of octaketide polyenes by the calicheamicin polyketide synthase CalE8: Implications for the biosynthesis of enediyne core structures, *J. Am. Chem. Soc.*, 131, 12564, 2009.
53. Liu, W., Ahlert, J., Gao, Q., Wendt-Pienkowski, E., Shen, B., and Thorson, J.S., Rapid PCR amplification of minimal enediyne polyketide synthase cassettes leads to a predictive familial classification model, *Proc. Natl. Acad. Sci. U.S.A.*, 100, 11959, 2003.
54. Nett, M. and Moore, B.S., Exploring and engineering biosynthetic pathways in the marine actinomycete Salinispora tropica, *Pure Appl. Chem.*, 81, 1075, 2009.
55. Thorson, J.S., Sievers, E.L., Ahlert, J., Shepard, E., Whitwam, R.E., Onwueme, K.C., and Ruppen, M., Understanding and exploiting nature's chemical arsenal: The past, present and future of calicheamicin research, *Curr. Pharm. Des.*, 6, 1841, 2000.
56. Johnson, H.D. and Thorson, J.S., Characterization of CalE10, the N-oxidase involved in the calicheamicin hydroxyaminosugar formation, *J. Am. Chem. Soc.*, 130, 17662, 2008.
57. Christenson, S.D., Liu, W., Toney, M.D., and Shen, B., A novel 4-methylideneimidazole-5-one-containing tyrosine aminomutase in enediyne antitumor antibiotic C-1027 biosynthesis, *J. Am. Chem. Soc.*, 125, 6062, 2003.
58. Christianson, C.V., Montavon, T.J., Van Lanen, S.G., Shen, B., and Bruner, S.D., The structure of L-tyrosine 2,3-aminomutase from the C-1027 enediyne antitumor antibiotic biosynthetic pathway, *Biochemistry*, 46, 7205, 2007.
59. Lin, S., Van Lanen, S.G., and Shen, B., Characterization of the two-component, FAD-dependent monooxygenase SgcC that requires carrier protein-tethered substrates, *J. Am. Chem. Soc.*, 130, 6616, 2008.
60. Liu, W. and Shen, B., Genes for production of the enediyne antitumor antibiotic C-1027 in *Streptomyces lobisporus* are clustered with the cagA gene that encodes the C-1027 apoprotein, *Antimicrob. Agents Chemother.*, 44, 382, 2000.

61. Liu, W., Nonaka, K., Nie, L., Zhang, J., Christenson, S.D., Bae, J., Van Lanen, S.G., Zazopoulos, E., Farnet, C.M., Yang, C.F., and Shen, B., The neocarzinostatin biosynthetic gene cluster from *Streptomyces carzinostaticus* ATCC 15944 involving two iterative type I polyketide synthases, *Chem. Biol.*, 12, 293, 2005.
62. Luo, Y., Lin, S., Zhang, J., Cooke, H.A., Bruner, S.D., and Shen, B., Regiospecific O-methylation of naphthoic acids catalyzed by NcsB1, an O-methyltransferase involved in the biosynthesis of the enediyne antitumor antibiotic neocarzinostatin, *J. Biol. Chem.*, 283, 14694, 2008.
63. Cooke, H.A., Zhang, J., Griffin, M.A., Nonaka, K., Van Lanen, S.G., Shen, B., and Bruner, S.D., Characterization of NcsB2 as a promiscuous naphthoic acid/coenzyme A ligase integral to the biosynthesis of the enediyne antitumor antibiotic neocarzinostatin, *J. Am. Chem. Soc.*, 129, 7728, 2007.
64. Biggins, J.B., Onwueme, K., and Thorson, J.S., Resistance to enediyne antitumor antibiotics by CalC self-sacrifice, *Sci. China, C: Life Sci.*, 301, 1537, 2003.
65. Van Lanen, S.G., Oh, T.-j., Liu, W., Wendt-Pienkowski, E., and Shen, B., Characterization of the maduropeptin biosynthetic gene cluster from *Actinomadura madurae* ATCC 39144 supporting a unifying paradigm for enediyne biosynthesis, *J. Am. Chem. Soc.*, 129, 13082, 2007.
66. Gao, Q. and Thorson, J.S., The biosynthetic genes encoding for the production of the dynemicin enediyne core in *Micromonospora chersina* ATCC53710, *FEMS Microbiol. Lett.*, 282, 105, 2008.
67. Hiatt, A., Merlock, R., Mauch, S., and Wrasidlo, W., Regulation of apoptosis in leukemic cells by analogs of dynemicin A, *Bioorg. Med. Chem.*, 2, 315, 1994.
68. Myers, A.G., Fraley, M.E., Tom, N.J., Cohen, S.B., and Madar, D.J., Synthesis of (+)-dynemicin A and analogs of wide structural variability: Establishment of the absolute configuration of natural dynemicin A, *Chem. Biol.*, 2, 33, 1995.
69. Myers, A.G., Tom, N.J., Fraley, M.E., Cohen, S.B., and Madar, D.J., A convenient synthetic route to (+)-dynemicin A and analogs of wide structural variability, *J. Am. Chem. Soc.*, 119, 6072, 1997.
70. Shair, M.D., Yoon, T.Y., Mosny, K.K., Chou, T.C., and Danishefsky, S.J., The total synthesis of dynemicin A leading to development of a fully contained bioreductively activated enediyne prodrug, *J. Am. Chem. Soc.*, 118, 9509, 1996.
71. Shair, M.D., Yoon, T.-Y., and Danishefsky, S.J., Total synthesis of (±)-dynemicin A, *Angew. Chem., Int. Ed. Engl.*, 34, 1721, 1995.
72. Nicolaou, K.C., Zhang, H., Chen, J.S., Crawford, J.J., and Pasunoori, L., Total synthesis and stereochemistry of uncialamycin, *Angew. Chem., Int. Ed.*, 46, 4704, 2007.
73. Myers, A.G., Hammond, M., Wu, Y., Xiang, J.-N., Harrington, P.M., and Kuo, E.Y., Enantioselective synthesis of neocarzinostatin chromophore aglycone, *J. Am. Chem. Soc.*, 118, 10006, 1996.
74. Myers, A.G., Liang, J., Hammond, M., Harrington, P., Wu, Y., and Kuo, E., Total synthesis of (+)-neocarzinostatin chromophore, *J. Am. Chem. Soc.*, 120, 5319, 1998.
75. Kobayashi, S., Hori, M., Wang, G.X., and Hirama, M., Formal total synthesis of neocarzinostatin chromophore, *J. Org. Chem.*, 71, 636, 2006.
76. Kobayashi, S., Reddy, R.S., Sugiura, Y., Sasaki, D., Miyagawa, N., and Hirama, M., Investigation of the total synthesis of N1999-A2: Implication of stereochemistry, *J. Am. Chem. Soc.*, 123, 2887, 2001.
77. Kobayashi, S., Ashizawa, S., Takahashi, Y., Sugiura, Y., Nagaoka, M., Lear, M.J., and Hirama, M., The first total synthesis of N1999-A2: Absolute stereochemistry and stereochemical implications into DNA cleavage, *J. Am. Chem. Soc.*, 123, 11294, 2001.
78. Ji, N., O'Dowd, H., Rosen, B.M., and Myers, A.G., Enantioselective synthesis of N1999A2, *J. Am. Chem. Soc.*, 128, 14825, 2006.
79. Inoue, M., Sasaki, T., Hatano, S., and Hirama, M., Synthesis of the C-1027 chromophore framework through atropselective macrolactonization, *Angew. Chem., Int. Ed.*, 43, 6500, 2004.
80. Inoue, M., Kikuchi, T., and Hirama, M., Synthesis of the fully functionalized nine-membered diyne core of the C-1027 chromophore, *Tet. Lett.*, 45, 6439, 2004.
81. Inoue, M., Ohashi, I., Kawaguchi, T., and Hirama, M., Total synthesis of the C-1027 chromophore core: Extremely facile enediyne formation through SmI_2-mediated 1,2-elimination, *Angew. Chem., Int. Ed.*, 47, 1777, 2008.
82. Komano, K., Shimamura, S., Inoue, M., and Hirama, M., Total synthesis of the maduropeptin chromophore aglycone, *J. Am. Chem. Soc.*, 129, 14184, 2007.
83. Komano, K., Shimamura, S., Norizuki, Y., Zhao, D., Kabuto, C., Sato, I., and Hirama, H., Total synthesis and structure revision of the (-)-maduropeptin chromophore, *J. Am. Chem. Soc.*, 131, 12072, 2009.
84. Myers, A.G. and Goldberg, S.D., Synthesis of the kedarcidin core structure by a transannular cyclization pathway, *Angew. Chem., Int. Ed.*, 39, 2732, 2000.
85. Myers, A.G., Hogan, P.C., Hurd, A.R., and Goldberg, S.D., Enantioselective synthesis of kedarcidin chromophore aglycone in differentially protected form, *Angew. Chem., Int. Ed.*, 41, 1062, 2002.

86. Ren, F., Hogan, P.C., Anderson, A.J., and Myers, A.G., Synthesis of L-kedarosamine in protected form and its efficient incorporation into an advanced intermediate to kedarcidin chromophore, *Org. Lett.*, 9, 1923, 2007.
87. Myers, A.G. and Horiguchi, Y., Synthesis of the naphthoic acid component of kedarcidin chromophore by routes employing photochemical and thermal electrocyclic ring closure reactions, *Tet. Lett.*, 38, 4363, 1997.
88. Ren, F., Hogan, P.C., Anderson, A.J., and Myer, A.G., Kedarcidin chromophore: Synthesis of its proposed structure and evidence for a stereochemical revision, *J. Am. Chem. Soc.*, 129, 5381, 2007.
89. Ogawa, K., Koyama, Y., Ohashi, I., Sato, I., and Hirama, M., Total synthesis of a protected aglycone of the kedarcidin chromophore, *Angew. Chem., Int. Ed.*, 40, 1110, 2009.
90. Nicolaou, K.C., Groneberg, R.D., Miyazaki, T., Stylianides, N.A., Schulze, T.J., and Stahl, W., Total synthesis of the oligosaccharide fragment of calicheamicin γ_1^I, *J. Am. Chem. Soc.*, 112, 8193, 1990.
91. Smith, A.L., Hwang, C.K., Pitsinos, E., Scarlato, G.R., and Nicolaou, K.C., Enantioselective total synthesis of (-)-calicheamicinone, *J. Am. Chem. Soc.*, 114, 3134, 1992.
92. Nicolaou, K.C., Hummel, C.W., Pitsinos, E.N., Nakada, M., Smith, A.L., Shibayama, K., and Saimoto, H., Total synthesis of calicheamicin γ_1^I, *J. Am. Chem. Soc.*, 114, 10082, 1992.
93. Groneberg, R.D., Miyazaki, T., Stylianides, N.A., Schulze, T.J., Stahl, W., Schreiner, E.P., Suzuki, T., Iwabuchi, Y., Smith, A.L., and Nicolaou, K.C., Total synthesis of calicheamicin γ_1^I. 1. Synthesis of the oligosaccharide fragment, *J. Am. Chem. Soc.*, 115, 7593, 1993.
94. Smith, A.L., Pitsinos, E.N., Hwang, C.K., Mizuno, Y., Saimoto, H., Scarlato, G.G., Suzuki, T., and Nicolaou, K.C., Total synthesis of calicheamicin γ_1^I. 2. Development of an enantioselective route to (-)-calicheamicinone, *J. Am. Chem. Soc.*, 115, 7612, 1993.
95. Nicolaou, K.C., Hummel, C.W., Nakada, M., Shibayama, K., Pitsinos, E.N., Saimoto, H., Mizuno, Y., Baldenius, K.U., and Smith, A.L., Total synthesis of calicheamicin γ_1^I. 3. The final stages, *J. Am. Chem. Soc.*, 115, 7625, 1993.
96. Cabal, M.P., Coleman, R.S., and Danishefsky, S.J., Total synthesis of calicheamicinone: A solution to the problem of the elusive urethane, *J. Am. Chem. Soc.*, 112, 3253, 1990.
97. Halcomb, R.L., Boyer, S.H., and Danishefsky, S.J., Synthesis of the calicheamicin aryltetrasaccharide domain bearing a reducing terminus: Coupling of fully synthetic aglycone and carbohydrate domains by the Schmidt reaction, *Angew. Chem. Int. Ed.*, 31, 338, 1992.
98. Hitchcock, S.A., Boyer, S.H., Chu-Moyer, M.Y., Olson, S.H., and Danishefsky, S.J., A convergent total synthesis of calicheamicin γ_1^I, *Angew. Chem., Int. Ed.*, 33, 858, 1994.
99. Hitchcock, S.A., Chu-Moyer, M.Y., Boyer, S.H., Olson, S.H., and Danishefsky, S.J., A remarkable glycosylation reaction: The total synthesis of calicheamicin γ_1^I, *J. Am. Chem. Soc.*, 117, 5750, 1995.
100. Danishefsky, S.J. and Shair, M.D., Observations in the chemistry and biology of cyclic enediyne antibiotics: Total synthesis of calicheamicin γ_1^I and dynemicin, *J. Org. Chem.*, 61, 16, 1996.
101. Clive, D.L.J., Tao, Y., Bo, Y., Hu, Y.-Z., Selvakumar, N., Sun, S., Daigneault, S., and Wu, Y.-J., Synthetic studies on calicheamicin γ_1^I-synthesis of (−)-calicheamicinone and models representing the four sugars and the aromatic system, *Chem. Comm.*, 2000, 1341, 2000.
102. Clive, D.L.J., Bo, Y., Tao, Y., Daigneault, S., Wu, Y.-J., and Meignan, G., Synthesis of (±)-calicheamicinone by two related methods, *J. Am. Chem. Soc.*, 118, 4904, 1996.
103. Magnus, P., Miknis, G.F., Press, N.J., Grandjean, D., Taylor, G.M., and Harling, J., Synthesis of a protected (±)-calicheamicinone derivative by sequential introduction of functionality into the bicyclo[7.3.1] enediyne core structure, *J. Am. Chem. Soc.*, 119, 6739, 1997.
104. Churcher, I., Hallett, D., and Magnus, P., Synthesis of the enediyne aglycone (±)-calicheamicinone, *J. Am. Chem. Soc.*, 120, 3518, 1998.
105. Nicolaou, K.C. and Clark, D., Total synthesis of the carbohydrate fragments of esperamicin A1, *Angew. Chem., Int. Ed.*, 31, 855, 1992.
106. Halcomb, R.L. Wittman, M.D., Olson, S.H., Danishefsky, S.J., Golik, J., Wong, H., and Vyas, D., Synthesis of the core trisaccharide of esperamicin: Corroboration of the proposed structure for its rearrangement product and stabilization of the core trisaccharide domain, *J. Am. Chem. Soc.*, 113, 5080, 1991.
107. Bergman, R.G., Reactive 1,4-dehydroaromatics, *Acc. Chem. Res.*, 6, 25, 1973.
108. Chen, W.C., Chang, N.Y., and Yu, C.H., Density functional study of Bergman cyclization of enediynes, *J. Phys. Chem. A*, 102, 2584, 1998.
109. Schreiner, P.R., Cyclic enediynes—Relationship between ring size, alkyne carbon distance, and cyclization barrier, *Chem. Comm.*, 483, 1998

110. Biswas, K., Pal, S., Carbeck, J.D., and Kahne, D., The molecular basis for pyrimidine-selective DNA binding: Analysis of calicheamicin oligosaccharide derivatives by capillary electrophoresis, *J. Am. Chem. Soc.*, 122, 8413, 2000.
111. Walker, S.L., Andreotti, A.H., and Kahne, D.E., NMR characterization of calicheamicin bound to DNA, *Tetrahedron*, 50, 1351, 1994.
112. Walker, S., Gupta, V., Kahne, D., and Gange, D., Analysis of hydroxylamine glycosidic linkages: Structural consequences of the NO bond in calicheamicin, *J. Am. Chem. Soc.*, 116, 3197, 1994.
113. Paloma, L.G., Smith, J.A., Chazin, W.J., and Nicolaou, K.C., Interaction of calicheamicin with duplex DNA: Role of the oligosaccharide domain and identification of multiple binding modes, *J. Am. Chem. Soc.*, 116, 3697, 1994.
114. Ikemoto, N., Kumar, R.A., Ling, T.T., Ellestad, G.A., Danishefsky, S.J., and Patel, D.J., Calicheamicin-DNA complexes: Warhead alignment and saccharide recognition of the minor groove, *Proc. Natl. Acad. Sci. U.S.A.*, 92, 10506, 1995.
115. Miyagawa, N., Sasaki, D., Matsuoka, M., Imanishi, M., Ando, T., and Sugiura, Y., DNA cleavage characteristics of non-protein enediyne antibiotic N1999-2A, *Biochem. Biophys. Res. Commun.*, 306, 87, 2003.
116. De Voss, J.J., Hangeland, J.J., and Townsend, C.A., Characterization of the *in vitro* cyclization chemistry of calicheamicin and its relation to DNA cleavage, *J. Am. Chem. Soc.*, 112, 4554, 1990.
117. Zein, N., McGahren, W.J., Morton, G.O., Ashcroft, J., and Ellestad, G.A., Exclusive abstraction of non-exchangeable hydrogens from DNA by calicheamicin γ_1^I, *J. Am. Chem. Soc.*, 111, 6888, 1989.
118. De Voss, J.J., Townsend, C.A., Ding, W.D., Morton, G.O., Ellestad, G.A., Zein, N., Tabor, A.B., and Schreiber, S.L., Site-specific atom transfer from DNA to a bound ligand defines the geometry of a DNA-calicheamicin γ_1^I complex, *J. Am. Chem. Soc.*, 112, 9669, 1990.
119. Kumar, R.A., Ikemoto, N., and Patel, D.J., Solution structure of the calicheamicin γ_1^I-DNA complex, *J. Mol. Biol.*, 265, 187, 1997.
120. Kraka, E., Tuttle, T., and Cremer, D., The reactivity of calicheamicin γ_1^I in the minor groove of DNA: The decisive role of the environment, *Chem.-Eur. J.*, 13, 9256, 2007.
121. Sugiura, Y., Arakawa, T., Uesugi, M., Shiraki, T., Ohkuma, H., and Konishi, M., Reductive and nucleophilic activation products of dynemicin A with methyl thioglycolate. A rational mechanism for DNA cleavage of the thiol-activated dynemicin A, *Biochemistry*, 30, 2989, 1991.
122. Nicolaou, K.C., Dai, W.M., Hong, Y.P., Baldridge, K.K., Siegel, J.S., and Tsay, S.C., Molecular design, chemical synthesis, kinetic studies, calculations, and biological studies of novel enediynes equipped with triggering, detection, and deactivating devices: Model dynemicin A epoxide and cis-diol systems, *J. Am. Chem. Soc.*, 115, 7944, 1993.
123. Cosgrove, J.P. and Dedon, P.C., Binding and reaction of calicheamicin and other enediyne antibiotics with DNA, in *Small Molecule DNA and RNA Binders*, Demeunynck, M., Bailly, C., and Wilson, W.D., Eds., Wiley-VCH Verlag, Weinheim, Germany, 2003, 2, 609.
124. Xu, Y.-J., Zhen, Y.-S., and Goldberg, I.H., C1027 chromophore, a potent new enediyne antitumor antibiotic, induces sequence-specific double-strand DNA cleavage, *Biochemistry*, 33, 5947, 1994.
125. Xu, Y.J., Zhen, Y.S., and Goldberg, I.H., Enediyne C1027 induces the formation of novel covalent DNA interstrand cross-links and monoadducts, *J. Am. Chem. Soc.*, 119, 1133, 1997.
126. Cobuzzi, R.J. Jr., Kotsopoulos, S.K., Otani, T., and Beerman, T.A., Effects of the enediyne C-1027 on intracellular DNA targets, *Biochemistry*, 34, 583, 1995.
127. Elmroth, K., Nygren, J., Mårtensson, S., Ismail, I.H., and Hammarsten, O., Cleavage of cellular DNA by calicheamicin γ_1^I, *DNA Repair*, 2, 363, 2003.
128. Mårtensson, S., Nygren, J., Osheroff, N., and Hammarsten, O., Activation of the DNA-dependent protein kinase by drug-induced and radiation-induced DNA strand breaks, *Radiat. Res.*, 160, 291, 2003.
129. Jiang, B., Li, D.D., and Zhen, Y.S., Induction of apoptosis by enediyne antitumor antibiotic C1027 in HL-60 human promyelocytic leukemia cells, *Biochem. Biophys. Res. Commun.*, 208, 238, 1995.
130. He, Q. and Li, D., Interaction of direct breaking DNA strands and initiating of apoptotic pathway contributed to high potent cytotoxicities of enediyne antibiotic lidamycin (C1027) to human tumor cells, *Proc. Am. Assoc. Cancer Res.*, 42, 643, 2001.
131. Wang, Z., He, Q., Liang, Y., Wang, D., Li, Y.Y., and Li, D., Non-caspase-mediated apoptosis contributes to the potent cytotoxicity of the enediyne antibiotic lidamycin toward human tumor cells, *Biochem. Pharmacol.*, 65, 1767, 2003.
132. Dziegielewski, J. and Beerman, T.A., C-1027-induced activation of DNA-damage responses is ATM-independent, *Proc. Am. Assoc. Cancer Res.*, 42, 199, 2001.

133. Amico, D., Barbui, A.M., Erba, E., Rambaldi, A., Introna, M., and Golay, J., Differential response of human acute myeloid leukemia cells to gemtuzumab ozogamicin *in vitro*: Role of Chk1 and Chk2 phosphorylation and caspase 3, *Blood*, 101, 4589, 2003.
134. McHugh, M.M., Yin, X., Kuo, S.R., Liu, J.S., Melendy, T., and Beerman, T.A., The cellular response to DNA damage induced by the enediynes C-1027 and neocarzinostatin includes hyperphosphorylation and increased nuclear retention of replication protein A (RPA) and trans inhibition of DNA replication, *Biochemistry*, 40, 4792, 2001.
135. Hartsell, T.L., Hinman, L.M., Hamann, P.R., and Schor, N.F., Determinants of the response of neuroblastoma cells to DNA damage: The roles of pre-treatment cell morphology and chemical nature of the damage, *J. Pharmacol. Exp. Ther.*, 277, 1158, 1996.
136. Liang, Y., Yan, C., Nylander, K.D., and Schor, N.F., Early events in Bcl-2-enhanced apoptosis, *Apoptosis*, 8, 609, 2003.
137. Nicolaou, K.C., Li, T., Nakada, M., Hummel, C.W., Hiatt, A., and Wrasidlo, W., Calicheamicin θ_I^I: A rationally designed molecule with extremely potent and selective DNA cleaving properties and apoptosis inducing activity, *Angew. Chem., Int. Ed.*, 33, 183, 1994.
138. Prokop, A., Wrasidlo, W., Lode, H., Herold, R., Lang, F., Henze, G., Dörken, B., Wieder, T., and Daniel, P.T., Induction of apoptosis by enediyne antibiotic calicheamicin θ proceeds through a caspase-mediated mitochondrial amplification loop in an entirely Bax-dependent manner, *Oncogene*, 22, 9107, 2003.
139. Siegel, J., Fritsche, M., Mai, S., Brandner, G., and Hess, R.D., Enhanced p53 activity and accumulation in response to DNA damage upon DNA transfection, *Oncogene*, 11, 1363, 1995.
140. Noël, G., Giocanti, N., Fernet, M., Mégnin-Chanet, F., and Favaudon, V., Poly(ADP-ribose) polymerase (PARP-1) is not involved in DNA double-strand break recovery, *BMC Cell Biology*, http://www.biomedcentral.com/ content/pdf/1471-2121-4-7.pdf, 2003.
141. Batchelder, R.M., Wilson, W.R., Hay, M.P., and Denny, W.A., Oxygen dependence of the cytotoxicity of the enediyne anti-tumour antibiotic esperamicin A-1, *Br. J. Cancer*, 74, S52, 1996.
142. Van Duijn-Goedhart, A., Zdzienicka, M.Z., Sankaranarayanan, K., and van Buul, P.P., Differential responses of Chinese hamster mutagen sensitive cell lines to low and high concentrations of calicheamicin and neocarzinostatin, *Mutat. Res.*, 471, 95, 2000.
143. Jedema, I., Barge, M.Y., van der Velden, V.H.J., Nijmeijer, B.A., van Dongen, J.J.M., Willemze, R., and Falkenburg, J.H.F., Internalization and cell cycle-dependent killing of leukemic cells by Gemtuzumab ozogamicin: Rationale for efficacy in CD33-negative malignancies with endocytic capacity, *Leukemia*,18, 316, 2004
144. Cortazzo, M. and Schor, N.F., Potentiation of enediyne-induced apoptosis and differentiation by Bcl-2, *Cancer Res*., 56, 1199, 1996.
145. Kappen, L.S. and Goldberg, I.H., Activation and inactivation of neocarzinostatin-induced cleavage of DNA, *Nucleic Acids Res.*, 5, 2959, 1978.
146. Schor, N.F., Hartsell, T.L., Will, P., Nylander, K.D., and Certo, J., The use of 6-mercaptodopamine to target neuroblastoma cells for enediyne-induced apoptosis and antineoplastic effect, *Proc. Am. Assoc. Cancer Res.*, 35, 316, 1994.
147. Mi, Z., Hong, B., Mirnics, Z.K., Tyurina, Y.Y., Kagan, V.E., Liang, Y., and Schor, N.F., Bcl-2-mediated potentiation of neocarzinostatin-induced apoptosis: Requirement for caspase-3, sulfhydryl groups, and cleavable Bcl-2, *Cancer Chemother. Pharmacol.*, 57, 357, 2006.
148. Rogers, D., Nylander, K.D., Mi, Z., Hu, T., and Schor, N.F., Molecular predictors of human nervous system cancer responsiveness to enediyne chemotherapy, *Cancer Chemother. Pharmacol.*, 62, 699, 2008.
149. Haag, P., Viktorsson, K., Lindberg, M.L., Kanter, L., Lewensohn, R., and Stenke, L., Deficient activation of Bak and Bax confers resistance to gemtuzumab ozogamicin-induced apoptotic cell death in AML, *Exper. Hematol.*, 37, 755, 2009.
150. Balaian, L. and Ball, E.D., Cytotoxic activity of gemtuzumab ozogamicin (Mylotarg) in acute myeloid leukemia correlates with the expression of protein kinase Syk, *Leukemia*, 20, 2093, 2006.
151. Walter, R.B., Raden, B.W., Kamikura, D.M., Cooper, J.A., and Bernstein, I.D., Influence of CD33 expression levels and ITIM-dependent internalization on gemtuzumab ozogamicin-induced cytotoxicity, *Blood*, 105, 1295, 2005.
152. Audebert, M., Salles, B., and Calsou, P., Involvement of poly(ADP-ribose) polymerase-1 and XRCC1/DNA ligase III in an alternative route for DNA double-strand breaks rejoining, *J. Biol. Chem.*, 279, 55117, 2004.
153. Shao, R.-G. and Zhen, Y.-S., Enediyne anticancer antibiotic lidamycin: Chemistry, biology and pharmacology, *Anti-Cancer Agents Med. Chem.*, 8, 123, 2008.

154. Chen, J., Ouyang, Z.G., Zhang, S.H., and Zhen, Y.S., Down-regulation of the nuclear factor-κB by lidamycin in association with inducing apoptosis in human pancreatic cancer cells and inhibiting xenograft growth, *Oncol. Rep.*, 17, 1445, 2007.
155. Chen, L., Jiang, J., Cheng, C., Yang, A., He, Q., Li, D., and Wang, Z., p53 Dependent and independent apoptosis induced by lidamycin in human colorectal cancer cells, Cancer Biol. Ther., 6, 965, 2007.
156. Liu, X., Bian, C., Ren, K., Jin, H., Li, B., and Shao, R.G., Lidamycin induces marked G2 cell cycle arrest in human colon carcinoma HT-29 cells through activation of p38 MAPK pathway, *Oncol. Rep.*, 17, 597, 2007.
157. Zhen, Y.-Z., Lin, Y.-J., Shang, B.-Y., and Zhen, Y.-S., Enediyne lidamycin induces apoptosis in human multiple myeloma cells through activation of p38 mitogen-activated protein kinase and *c*-Jun NH_2-terminal kinase, *Int. J. Hematol.*, 90, 44, 2009.
158. Beerman, T.A., Gawron, L.S., Shin, S., Shen, B., and McHugh, M.M., C-1027, A radiomimetic enediyne anticancer drug, preferentially targets hypoxic cells, *Cancer Res.*, 69, 593, 2009.
159. Liu, H., Li, L., Li, X.Q., Liu, X.J., and Zhen, Y.S., Enediyne lidamycin enhances the effect of epidermal growth factor receptor tyrosine kinase inhibitor, gefitinib, in epidermoid carcinoma A431 cells and lung carcinoma H460 cells, *Anti-Cancer Drugs*, 20, 41, 2009.
160. Maier, M.E., Bosse, F., and Niestroj, A.J., Design and synthesis of dynemicin analogs, *Eur. J. Org. Chem.*, 1, 1999.
161. Huang, Y.-H., Shang, B.Y., and Zhen, Y.S., Antitumor efficacy of lidamycin on hepatoma and active moiety of its molecule, *World J. Gastroenterol.*, 11, 3980, 2005.
162. Liu, X.-J., Dai, Y., Shang, Y., Li, Y., and Zhen, Y.S., Inhibitory effect of lidamycin on growth of colon carcinoma 26 and hepatic metastasis in mice, *Ai Zheng (Chinese J. Cancer)*, 24, 641, 2005.
163. Liu, Y.-P., Li, Q.S., Huang, Y.R., and Liu, C.X., Tissue distribution and excretion of ^{125}I-lidamycin in mice and rats, *World J. Gastroenterol.*, 11, 3281, 2005.
164. Liu, Y.-P., Li, Q.S., Huang, Y.R., Zhou, M.J., and Liu, C.X., Pharmacokinetics of C-1027 in mice as determined by TCA-RA method, *World J. Gastroenterol.*, 11, 717, 2005.
165. Liu, Y.-P., Li,Q.-S., Huang, Y.-R., Zhou, M.-J., and Liu, C.-X., Determination of lidamycin: Application in mice, *J. Liq. Chromatogr. Relat. Technol.*, 28, 453, 2005.
166. Li, L., Huang, Y.H., Li, Y., Wang, F.Q., Shang, B.Y., and Zhen, Y.S., Antitumor activity of anti-type IV collagenase monoclonal antibody and its lidamycin conjugate against colon carcinoma, *World J. Gastroenterol.*, 11, 4478, 2005.
167. Wang, F., Shang, B., and Zhen, Y., Antitumor effects of the molecule-downsized immunoconjugate composed of lidamycin and Fab' fragment of monoclonal antibody directed against type IV collagenase, *Sci. China, C: Life Sci.*, 47, 66, 2004.
168. Wang, F.-Q., Bo-Yang, S., and Yong-Su, Z., Antitumor effects of the immunoconjugate composed of lidamycin and monoclonal antibody 3G11, *Acta Pharm. Sin.*, 38, 515, 2003.
169. Zhen, Y.S., Shao, R.S., Zhou, X.Z., Wang, N.Q., Liu, T., Zhou, S.Q., and Dong, Z.W., Conjugate of antibiotic C1027 and monoclonal antibody 3H11 shows potent antitumor effect against gastric cancer, *Proc. Am. Assoc. Cancer Res.*, 35, 511 (abst. 3047), 1994.
170. Wang, X.-W. and Xie, H., C-1027, *Drugs Future*, 24, 847, 1999.
171. Miao, Q.F., Shang, B.Y., Ouyang, Z.G., Liu, X.Y., and Zhen, Y.S., Generation and antitumor effects of an engineered and energized fusion protein VL-LDP-AE composed of single-domain antibody and lidamycin, *Sci. China, C: Life Sci.*, 50, 447, 2007.
172. Miao, Q.-f., Liu, X.Y., Shang, B.Y., Ouyang, Z.G., and Zhen, Y.S., An enediyne-energized single-domain antibody-containing fusion protein shows potent antitumor activity, *Anti-Cancer Drugs*, 18, 127, 2007.
173. Zhen, Y.S., Lin, M., Zhen, H.Y., and Wang, X.H., Lidamycin and its RGD-containing peptide conjugate inhibit angiogenesis and metastasis, *Proc. Am. Assoc. Cancer Res.*, 41, 645 (abst. 4098), 2000.
174. Wrasidlo, W., Hiatt, A., Mauch, S., Merlock, R.A., and Nicolaou, K.C., *In vivo* efficacy of novel synthetic enediynes, *Acta Oncol.*, 34, 157, 1995.
175. Hay, M.P., Wilson, W.R., and Denny, W.A., A novel enediyne prodrug for antibody-directed enzyme prodrug therapy (ADEPT) using *E. coli* B nitroreductase, *Bioorg. Med. Chem. Lett.*, 5, 2829, 1995.
176. Hay, M.P., Wilson, W.R., and Denny, W.A., Nitrobenzyl carbamate prodrugs of enediynes for nitroreductase gene-directed enzyme prodrug therapy (GDEPT), *Bioorg. Med. Chem. Lett.*, 9, 3417, 1999.
177. Xie, Y., Miller, G.G., Cubitt, S.A., Soderlind, K.J., Allalunis-Turner, M.J., and Lown, J.W., Enediyne-lexitropsin DNA-targeted anticancer agents: Physicochemical and cytotoxic properties in human neoplastic cells *in vitro*, and intracellular distribution, *Anti-Cancer Drug Des.*, 12, 169, 1997.

178. Severin, S.E., Posypanova, G.A., Sotnichenko, A.I., Shmyrev, I.I., Moskaleva, E.Y., Feldman, N.B., Finakova, G.V. et al., Targeted delivery of esperamicin A1 by using oncofetal protein alpha-fetoprotein, *Eur. J. Cancer*, 33, S89, 1997.
179. Severin, S.E., Moskaleva, E.Yu., Shmyrev, I.I., Posypanova, G.A., Belousova, Yu.V., Sologub, V.K., Luzhkov, Yu.M., Nakachian, R., Andreani, J., and Severin, E.S., Alpha-fetoprotein-mediated targeting of anti-cancer drugs to tumor cells *in vitro*, *Biochem. Mol. Biol. Int.*, 37, 385, 1995.
180. Capson, T. and Ruffner, D., Preparation of calicheamicin-oligodeoxynucleotide conjugates for use as antisense therapeutics, *Pharm. Res. (New York)*, 13, S153, 1996.
181. Durr, F.E., Wallace, R.E., Testa, R.T., and Kuck, N.A., Biological activities of calicheamicin, in *Enediyne Antibiotics as Antitumor Agents*, Borders, D.B. and Doyle, T.W., Eds., Marcel Dekker, Inc., 1995, Chapter. 8.
182. Ellestad, G.A., Hamann, P.R., Zein, N., Morton, G.O., Siegel, M.M., Pastel, M., Borders, D.B., and McGahren, W.J., Reactions of the trisulfide moiety in calicheamicin, *Tet. Lett.*, 30, 3033, 1989.
183. Hinman, L.M,. Hamann, P.R., Wallace, R., Menendez, A.T., Durr, F.E., and Upeslacis, J., Preparation and characterization of monoclonal antibody conjugates of the calicheamicins: A novel and potent family of antitumor antibiotics, *Cancer Res*., 53, 3336, 1993.
184. Jeglum, K.A., Hinman, L.M., Harmann, P.R., and Beyer, C.F., Antitumor effects of a calicheamicin immunoconjugate with anti-canine lymphoma monoclonal antibody 231, *Proc. Am. Assoc. Cancer Res.*, 35, 506 (abst. 3016), 1994.
185. Hamann, P.R., Hinman, L.M., Beyer, C.F., Greenberger, L.M., Lin, C., Lindh, D., Menendez, A.T., Wallace, R., Durr, F.E., and Upeslacis, J., An anti-MUC1 antibody-calicheamicin conjugate for treatment of solid tumors. Choice of linker and overcoming drug resistance, *Bioconjugate Chem.*, 16, 346, 2005.
186. Hamann, P.R., Hinman, L.M., Beyer, C.F., Lindh, D., Upeslacis, J., Shochat, D., and Mountain, A., A calicheamicin conjugate with a fully humanized anti-MUC1 antibody shows potent antitumor effects in breast and ovarian tumor xenografts, *Bioconjugate Chem.*, 16, 354, 2005.
187. Bross, P.F., Beitz, J., Chen, G., Chen, X.H., Duffy, E., Kieffer, L., Roy, S. et al., Approval summary: Gemtuzumab ozogamicin in relapsed acute myeloid leukemia, *Clin. Cancer Res.*, 7, 1490, 2001.
188. Bross, P.F., Beitz, J., Chen, G., Chen, X.H., Duffy, E., Kieffer, L., Roy, S. et al., Approval summary: Gemtuzumab ozogamicin in relapsed acute myeloid leukemia (correction to previous reference), *Clin. Cancer Res.*, 8, 300, 2002.
189. Hamann, P.R., Hinman, L.M., Hollander, I., Beyer, C.F., Lindh, D., Holcomb, R., Hallett, W. et al., Gemtuzumab ozogamicin, a potent and selective anti-CD33 antibody-calicheamicin conjugate for treatment of acute myeloid leukemia, *Bioconjugate Chem.*, 13, 47, 2002.
190. Hollander, I., Kunz, A., and Hamann, P.R., Selection of reaction additives used in the preparation of monomeric antibody-calicheamicin conjugates, *Bioconjugate Chem.*, 19, 358, 2008.
191. Hamann, P.R., Hinman, L.M., Beyer, C.F., Lindh, D., Upeslacis, J., Flowers, D.A., and Bernstein, I., An anti-CD33 antibody-calicheamicin conjugate for treatment of acute myeloid leukemia, choice of linker, *Bioconjugate Chem.*, 13, 40, 2002.
192. van der Velden, V.H.J., Berger, M.S., and Van Dongen, J.J.M., Mylotarg therapy in acute myeloid leukemia: Mechanism of action and implications for future treatment protocols, *Haematol. Blood Transfus.*, 41, 169, 2003.
193. DiJoseph, J.F., Popplewell, A., Tickle, S., Ladyman, H., Lawson, A., Kunz, A., Khandke, K. et al., Antibody-targeted chemotherapy of B-cell lymphoma using calicheamicin conjugated to murine or humanized antibody against CD22, *Cancer Immunol. Immunother.*, 54, 11, 2005.
194. DiJoseph, J.F., Goad, M.E., Dougher, M.M., Boghaert, E.R., Kunz, A., Hamann, P.R., and Damle, N.K., Potent and specific antitumor efficacy of CMC-544, a CD22-targeted immunoconjugate of calicheamicin, against systemically disseminated B-cell lymphoma, *Clin. Cancer Res.*, 10, 8620, 2004.
195. DiJoseph, J.F., Dougher, M.M., Armellino, D.C., Evans, D.Y., and Damle, N.K., Therapeutic potential of CD22-specific antibody-targeted chemotherapy using inotuzumab ozogamicin (CMC-544) for the treatment of acute lymphoblastic leukemia, *Leukemia*, 21, 2240, 2007.
196. DiJoseph, J.F., Dougher, M.M., Kalyandrug, L.B., Armellino, D.C., Boghaert, E.R., Hamann, P.R., Moran, J.K., and Damle, N.K., Antitumor efficacy of a combination of CMC-544 (inotuzumab ozogamicin), a CD22-targeted cytotoxic immunoconjugate of calicheamicin, and rituximab against non-Hodgkin's B-cell lymphoma, *Clin. Cancer Res.*, 12, 242, 2006.
197. DiJoseph, J.F., Dougher, M.M., Armellino, D.C., Kalyandrug, L., Kunz, A., Boghaert, E.R., Hamann, P.R., and Damle, N.K., CD20-specific antibody-targeted chemotherapy of non-Hodgkin's B-cell lymphoma using calicheamicin-conjugated rituximab, *Cancer Immunol. Immunother.*, 56, 1107, 2007.

198. Takeshita, A,. Shinjo, K., Yamakage, N., Ono, T., Hirano, I., Matsui, H., Shigeno, K. et al., CMC-544 (inotuzumab ozogamicin) shows less effect on multidrug resistant cells: Analyses in cell lines and cells from patients with B-cell chronic lymphocytic leukaemia and lymphoma, *Br. J. Haematology*, 146, 34, 2009.
199. Boghaert, E.R., Sridharan, L., Armellino, D.C., Khandke, K.M., DiJoseph, J.F., Kunz, A., Dougher, M.M. et al., Antibody-targeted chemotherapy with the calicheamicin conjugate hu3S193-N-acetyl gamma calicheamicin dimethyl hydrazide targets Lewis^{Y} and eliminates Lewis^{Y}-positive human carcinoma cells and xenografts, *Clin. Cancer Res.*, 10, 4538, 2004.
200. van Roon, J.A., Bijlsma, J.W., van de Winkel, J.G., and Lafeber, F.P., Depletion of synovial macrophages in rheumatoid arthritis by an anti-FcgammaRI-calicheamicin immunoconjugate, *Ann. Rheum. Dis.*, 64, 865, 2005.
201. Boghaert, E.R., Sridharan, L., Khandke, K.M., Armellino, D., Ryan, M.G., Myers, K., Harrop, R. et al., The oncofetal protein, 5T4, is a suitable target for antibody-guided anti-cancer chemotherapy with calicheamicin, *Int. J. Oncol.*, 32, 221, 2008.
202. Lode, H.N., Reisfeld, R.A., Handgretinger, R., Nicolaou, K.C., Gaedicke, G., and Wrasidlo, W., Targeted therapy with a novel enediyne antibiotic calicheamicin θI1 effectively suppresses growth and dissemination of liver metastases in a syngeneic model of murine neuroblastoma, *Cancer Res.*, 58, 2925, 1998.
203. Bernt, K.M., Lode, H.N., Hagemeier, C., Gaedicke, K., and Wrasidlo, W., CD19 targeted calicheamicin theta is effective against high risk ALL, *Blood*, 96, 467a, 2000.
204. Knoll, K., Wrasidlo, W., Scherberich, J.E., Gaedicke, G., and Fischer, P., Targeted therapy of experimental renal cell carcinoma with a novel conjugate of monoclonal antibody 138H11 and calicheamicin θI1, *Cancer Res.*, 60, 6089, 2000.
205. Schmidt, C.S., Wrasidlo, W., Scherberich, J.E., Gaedicke, G., and Fischer, P., Chemoimmunoconjugates with the monoclonal antibody 138H11 for targeting the cytotoxic prodrug calicheamicin θ to renal cell carcinomas, *Tumor Target*, 4, 271, 1999.
206. Bernt, K.M., Prokop, A., Huebener, N., Gaedicke, G., Wrasidlo, W., and Lode, H.N., Eradication of CD19+ leukemia by targeted calicheamicin θ, *Bioconjugate Chem.*, 20, 1587, 2009.
207. Otsuji, E., Yamaguchi, T., Tsuruta, H., Yata, Y., Nishi, H., Okamoto, K., Taniguchi, K. et al., The effect of intravenous and intra-tumoural chemotherapy using a monoclonal antibody-drug conjugate in a xenograft model of pancreatic cancer, *Eur. J. Surg. Oncol.*, 21, 61, 1995.
208. Okamoto, K., Yamaguchi, T., Otsuji, E., Yamaoka, N., Yata, Y., Tsuruta, H., Kitamura, K., and Takahashi, T., Targeted chemotherapy in mice with peritoneally disseminated gastric cancer using monoclonal antibody-drug conjugate, *Cancer Lett.*, 122, 231, 1998.
209. Kitamura, K., Miyagaki, T., Yamaoka, N., Tsurumi, H., Noguchi, A., Yamaguchi, T., and Takahashi, T., The role of monoclonal antibody A7 as a drug modifier in cancer therapy, *Cancer Immunol. Immunother.*, 36, 177, 1993.
210. Yamaguchi, T., Tsurumi, H., Kitamura, K., Otsuji, E., Miyagaki, T., Kotani, T., and Takahashi, T., Production, binding and cytotoxicity of human/mouse chimeric monoclonal antibody-neocarzinostatin conjugate, *Cancer Sci.*, 84, 1190, 1993.
211. Otsuji, E., Yamaguchi, T., Yata, Y., Nishi, H., Okamoto, K., Taniguchi, K., Kato, M. et al., Antitumor effect of neocarzinostatin conjugated to human/mouse chimeric Fab fragments of the monoclonal antibody A7 on human pancreatic carcinoma, *J. Surg. Oncol.*, 57, 230, 1994.
212. Yamaguchi, T., Tsurumi, H., Kotani, T., Yamaoka, N., Otsuji, E., Kitamura, K., and Takahashi, T., *In vivo* efficacy of neocarzinostatin coupled with Fab human/mouse chimeric monoclonal antibody A7 against human colorectal cancer, *Jpn. J. Cancer Res.*, 85, 167, 1994.
213. Otsuji, E., Yamaguchi, T., Tsuruta, H., Yata, Y., Nishi, H., Okamoto, K., Taniguchi, K. et al., Effects of neocarzinostatin-chimeric Fab conjugates on the growth of human pancreatic carcinoma xenografts, *Br. J. Cancer*, 73, 1178, 1996.
214. Otsuji, E., Yamaguchi, T., Yamaoka, N., Tanaguchi, K., Kato, M., Kotani, T., Kitamura, K., and Takahashi, T., Biodistribution of neocarzinostatin conjugated to chimeric Fab fragments of the monoclonal antibody A7 in nude mice bearing human pancreatic cancer xenografts, *Jpn. J. Cancer Res.*, 85, 530, 1994.
215. Otsuji, E., Yamaguchi, T., Tsuruta, H., Yata, Y., Nishi, H., Okamoto, K., Taniguchi, K., Kato, M., Kotani, T., Kitamura, K., and Takahashi, T., Applicability of monoclonal antibody Fab fragments as a carrier of neocarzinostatin in targeting chemotherapy, *J. Surg. Oncol.*, 61, 149, 1996.
216. Otsuji, E., Yamaguchi, Y., Matsumura, H., Yamamoto, K., Tsuruta, H., Yata, Y., Nishi, H., Okamoto, K., Kitamura, K., and Takahashi, T., Distribution of neocarzinostatin conjugated to biotinylated chimeric monoclonal antibody Fab fragments after administration of avidin, *Br. J. Cancer*, 74, 597, 1996.

217. Otsuji, E., Yamaguchi, T., Yamamoto, K., Matsumura, H., Tsuruta, H., Yata, Y., Nishi, H., Okamoto, K., Kitamura, K., and Takahashi, T., Decreased renal accumulation of biotinylated chimeric monoclonal antibody-neocarzinostatin conjugate after administration of avidin, *Jpn. J. Cancer Res.*, 88, 205, 1997.
218. Nakaki, M., Takikawa, H., and Yamanaka, M., Targeting immunotherapy using the avidin-biotin system for a human colon adenocarcinoma *in vitro*, *J. Int. Med. Res.*, 25, 14, 1997.
219. Tsunoda, S., Ohizumi, I., Matsui, J., Koizumi, K., Wakai, Y., Makimoto, H., Tsutsumi, Y. et al., Specific binding of TES-23 antibody to tumour vascular endothelium in mice, rats and human cancer tissue: A novel drug carrier for cancer targeting therapy, *Br. J. Cancer*, 81, 1155, 1999.
220. Makimoto, H., Koizumi, K.-I., Tsunoda, S.-I., Wakai, Y., Matsui, J., Tsutsumi, Y., Nakagawa, S. et al, Tumor vascular targeting using a tumor-tissue endothelium-specific monoclonal antibody as an effective strategy for cancer chemotherapy, *Biochem. Biophys. Res. Commun.*, 260, 346, 1999.
221. Wakai, Y., Matsui, J., Koizumi, K., Tsunoda, S., Makimoto, H., Ohizumi, I., Taniguchi, K. et al., Effective cancer targeting using an anti-tumor tissue vascular endothelium-specific monoclonal antibody (TES-23), *Jpn. J. Cancer Res.*, 91, 1319, 2000.
222. Maibücher, A., Schönlau, F., Gottschalk, U., Köhnlein, W., and Garnett, M.C., Neocarzinostatin immunoconjugates: *In vitro* evaluation of therapeutic potential, *Pharm. Sci. Commun.*, 4, 253, 1994.
223. Schönlau, F., Maibücher, A., Köhnlein, W., and Garnett, M.C., Mechanism of free and conjugated neocarzinostatin activity: Studies on chromophore and protein uptake using a transferrin-neocarzinostatin conjugate, *Z. Naturforsch., C: Biosci.*, 52, 245, 1997.
224. Brown, T., Williams, R., Kelley, S., Sterbenz, K., Wilkins, D., and Coble, D., A phase II trial of BMY-28175 in advanced pancreatic carcinoma, *Proc. Am. Soc. Clin. Oncol.*, 13, 219 (abst. 664), 1994.
225. Melink, T., Tait, N., Engstrom, C., Kelley, S., Skokov, M., Eisenberg, M., and Van Echo, D.A., A phase I trial of BMY-28175 on a single dose schedule, *Proc. Am. Soc. Clin. Oncol.*, 10, 120 (abstr. 348), 1991.
226. Sessa, C., Drozd, E., Gumbrell, L., Durr, R., Bruntsch, U., Kelley, S., and Cavelli, F., Phase I study of BMY-28175 (esperamicin A1) on a single intermittent schedule, *Proc. Am. Soc. Clin. Oncol.*, 9, 66 (abstr. 255), 1990.
227. Van Hof, A.C., Molthoff, C.F.M., Davies, Q., Perkins, A.C., Verheijen, R.H.M., Kenemans, P., den Hollander, W. et al., Biodistribution of ^{111}indium-labeled engineered human antibody CTM01 in ovarian cancer patients: Influence of protein dose, *Cancer Res.*, 56, 5179, 1996.
228. Gillespie, A.M., Broadhead, T.J., Chan, S.Y., Owen, J., Farnsworth, A.P., Sopwith, M., and Coleman, R.E., Phase I open study of the effects of ascending doses of the cytotoxic immunoconjugate CMB-401 (hCTM01-calicheamicin) in patients with epithelial ovarian cancer, *Ann. Oncol.*, 11, 735, 2000.
229. Broadhead, T.J., Gillespie, A.M., Coleman, P.E., Owen, J., Skelton, L., Stephens, S., Farnsworth, A., Sopwith, M., and Chen, S.Y., CNB-401—A new agent for immunotherapy of epithelial ovarian cancer: Immune response and pharmacokinetics, *Br. J. Cancer*, 78, 1998.
230. Chan, S.Y., Gordon, A.N., Coleman, R.E., Hall, J.B., Berger, M.S., Sherman, M.L., Eten, C.B., and Finkler, N.J., A phase 2 study of the cytotoxic immunoconjugate CMB-401 (hCTM01-calicheamicin) in patients with platinum-sensitive recurrent epithelial ovarian carcinoma, *Cancer Immunol. Immunother.*, 52, 243, 2003.
231. Mallick, R., Sievers, E., and Berger, M., A decision analysis of expected cost savings with outpatient administration of gemtuzumab ozogamicin (Mylotarg, CMA-676) in patients in first relapse of acute myeloid leukemia (AML), *Blood*, 96, 439a, 2000.
232. Lang, K., Menzin, J., Earle, C.C., and Mallick, R., Outcomes in patients treated with gemtuzumab ozogamicin for relapsed acute myelogenous leukemia, *Am. J. Health-Syst. Pharm.*, 59, 941, 2002.
233. Wadleigh, M., Richardson, P.G., Zahrieh, D., Lee, S.J., Cutler, C., Ho, V., Alyea, E.P. et al., Prior gemtuzumab ozogamicin exposure significantly increases the risk of veno-occlusive disease in patients who undergo myeloablative allogeneic stem cell transplantation, *Blood*, 102, 1578, 2003.
234. McKoy, J.M., Angelotta, C., Bennett, C.L., Tallman, M.S., Wadleigh, M., Evens, A.M., Kuzel, T.M. et al., Gemtuzumab ozogamicin-associated sinusoidal obstructive syndrome (SOS): An overview from the research on adverse drug events and reports (RADAR) project, *Leuk. Res.*, 31, 599, 2007.
235. Stadtmauer, E.A., Trials with gemtuzumab ozogamicin (Mylotarg®) combined with chemotherapy regimens in acute myeloid leukemia, *Clin. Lymphoma*, 2, S24, 2002.
236. Sievers, E.L., Antibody-targeted chemotherapy of acute myeloid leukemia using gemtuzumab ozogamicin (Mylotarg), *Blood Cells Mol. Dis.*, 31, 7, 2003.
237. Naito, K., Takeshita, A., Shigeno, K., Nakamura, S., Fujisawa, S., Shinjo, K., Yoshida, H. et al., Calicheamicin-conjugated humanized anti-CD33 monoclonal antibody (gemtuzumab ozogamicin, CMA-676) shows cytocidal effect on CD33-positive leukemia cell lines, but is inactive on p-glycoprotein-expressing sublines, *Leukemia*, 14, 1436, 2000.

238. Linenberger, M.L., Hong, T., Flowers, D., Sievers, E.L., Gooley, T.A., Bennett, J.M., Berger, M.S., Leopold, L.H., Appelbaum, F.R., and Bernstein, I.D., Multidrug-resistance phenotype and clinical responses to gemtuzumab ozogamicin, *Blood*, 98, 988, 2001.
239. Matsui, H., Takeshita, A., Naito, K., Shinjo, K., Shigeno, K., Maekawa, M., Yamakawa, Y., Tanimoto, M., Kobayashi, M., Ohnishi, K., and Ohno, R., Reduced effect of gemtuzumab ozogamicin (CMA-676) on p-glycoprotein and/or CD34-positive leukemia cells and its restoration by multidrug resistance modifiers, *Leukemia*, 16, 813, 2002.
240. Walter, R.B., Raden, B.W., Hong, T.C., Flowers, D.A., Bernstein, I.D., and Linenberger, M.L., Multidrug resistance protein attenuates gemtuzumab ozogamicin-induced cytotoxicity in acute myeloid leukemia, *Blood*, 102, 1466, 2003.
241. Jilani, I., Estey, E., Huh, Y., Joe, Y., Manshouri, T., Yared, M., Giles, F. et al., Differences in CD33 intensity between various myeloid neoplasms, *Am. J. Clin. Pathol.*, 118, 560, 2002.
242. Zwaan, C.M., Reinhardt, D., Jürgens, H., Huismans, D.R., Hählen, K., Smith, O.P., Biondi, A., van Wering, E.R., Feingold, J., and Kaspers, G.J.L., Gemtuzumab ozogamicin in pediatric CD33-positive acute lymphoblastic leukemia: First clinical experiences and relation with cellular sensitivity to single agent calicheamicin, *Leukemia*, 17, 468, 2003.
243. Zwaan, C.M., Reinhardt, D., Corbacioglu, S., van Wering, E.R., Bökkerink, J.P.M., Tissing, W.J.E., Samuelsson, U., Feingold, J., Creutzig, U., and Kaspers, G.J.L., Gemtuzumab ozogamicin: First clinical experiences in children with relapsed/refractory acute myeloid leukemia treated on compassionate-use basis, *Blood*, 101, 3868, 2003.
244. Unal, E. and Sahdev, I., Use of gemtuzumab ozogamicin in the treatment of pediatric relapsed/refractory acute myeloid leukemia, *Turk. J. Hematol.*, 25, 36, 2008.
245. Larson, R.A., Sievers, E.L., Stadtmauer, E.A., Löwenberg, B., Estey, E.H., Dombret, H., Theobald, M. et al., Final report of the efficacy and safety of gemtuzumab ozogamicin (Mylotarg) in patients with CD33-positive acute myeloid leukemia in first recurrence, *Cancer*, 104, 1442, 2005.
246. Kobayashi, Y., Tobinai, K., Takeshita, A., Naito, K., Asai, O., Dobashi, N., Furusawa, S. et al., Phase I/II study of humanized anti-CD33 antibody conjugated with calicheamicin, gemtuzumab ozogamicin, in relapsed or refractory acute myeloid leukemia: Final results of Japanese multicenter cooperative study, *Int. J. Hematol.*, 89, 460, 2009.
247. Taksin, A.L., Legrand, O., Raffoux, E., de Revel, T., Thomas, X., Contentin, N., Bouabdallah, R. et al., High efficacy and safety profile of fractionated doses of Mylotarg as induction therapy in patients with relapsed acute myeloblastic leukemia: A prospective study of the alfa group, *Leukemia*, 21, 66, 2007.
248. Van Der Velden, V.H.J., Boeckx, N., Jedema, I., te Marvelde, J.G., Hoogeveen, P.G., Boogaerts, M., and van Dongen, J.J.M., High CD33-antigen loads in peripheral blood limit the efficacy of gemtuzumab ozogamicin (Mylotarg) treatment in acute myeloid leukemia patients, *Leukemia*, 18, 983, 2004.
249. Walter, R.B., Gooley, T.A., van der Velden, V.H.J., Loken, M.R., van Dongen, J.J.M, Flowers, D.A., Bernstein, I.D., and Appelbaum, F.R., CD33 expression and P-glycoprotein-mediated drug efflux inversely correlate and predict clinical outcome in patients with acute myeloid leukemia treated with gemtuzumab ozogamicin monotherapy, *Blood*, 109, 4168, 2007.
250. Leopold, L.H., Berger, M.S., Cheng, S.C., Cortes-Franco, J.E., Giles, F.J., and Estey, E.H., Comparative efficacy and safety of gemtuzumab ozogamicin monotherapy and high-dose cytarabine combination therapy in the treatment of patients with acute myeloid leukemia in first relapse, *Clin. Adv. Hematol. Oncol.*, 1, 220, 2003,
251. Estey, E.H. Giles, F.J., Beran, M., O'Brien, S., Pierce, S.A., Faderl, S.H., Cortes, J.E., and Kantarjian, H.M., Experience with gemtuzumab ozogamicin ("Mylotarg") and all-trans retinoic acid in untreated acute promyelocytic leukemia, *Blood*, 99, 4222, 2002.
252. Estey, E.H., Thall, P.F., Giles, F.J., Wang, X.M., Cortes, J.E., Beran, M., Pierce, S.A., Thomas, D.A., and Kantarjian, H.M., Gemtuzumab ozogamicin with or without interleukin 11 in patients 65 years of age or older with untreated acute myeloid leukemia and high-risk myelodysplastic syndrome: Comparison with idarubicin plus continuous-infusion, high-dose cytosine arabinoside, *Blood*, 99, 4343, 2002.
253. Cortes, J., Tsimberidou, A.M., Alvarez, R., Thomas, D., Beran, M., Kantarjian, H., Estey, E., and Giles, F.J., Mylotarg combined with topotecan and cytarabine in patients with refractory acute myelogenous leukemia, *Cancer Chemother. Pharmacol.*, 50, 497, 2002.
254. Kell, W.J., Burnett, A.K., Chopra, R., Yin, J.A.L., Clark, R.E., Rohatiner, A., Culligan, D., Hunter, A., Prentice, A.G., and Milligan, D.W., A feasibility study of simultaneous administration of gemtuzumab ozogamicin with intensive chemotherapy in induction and consolidation in younger patients with acute myeloid leukemia, *Blood*, 102, 4277, 2002.

255. Giles, F., Garcia-Manero, G., O'Brien, S., Estey, E., and Kantarjian, H., Fatal hepatic veno-occlusive disease in a phase I study of Mylotarg and troxatyl in patients with refractory acute myeloid leukemia or myelodysplastic syndrome, *Acta Haematol. (Basel)*, 108, 164, 2002.
256. Venugopal, P., Gregory, S.A., Loew, J., Raza, A., Adler, S., Enschede, S., Manson, S., Cherian, S., Hsu, W.-T., and Sivaraman, S., Gemtuzumab ozogamycin (GO) combined with intensive induction chemotherapy (CT) using high dose ARA-C (HD Ara-C) and mitoxantrone (MTX) followed by amifostine (ami) in poor prognosis acute myeloid leukemia: Profile of hepatic events, *Proc. Am. Soc. Clin. Oncol.*, 22 (abstr. 2358), 2003.
257. Amadori, S., Sucio, S., Willemze, R., Mandelli, F., Selleslag, D., Stauder, R., Ho, A. et al., Sequential administration of gemtuzumab ozogamicin and conventional chemotherapy as first line therapy in elderly patients with acute myeloid leukemia: A phase II study (AML-15) of the EORTC and GIMEMA leukemia groups, *Haematologica*, 89, 950, 2004.
258. Sallah, A.S., Wan, J.P., Nguyen, N.P., and Sigounas, G., Combination imatinib and gemtuzumab ozogamicin in patients with chronic myeloid leukemia in myeloid blast crisis, *Blood*, 100, 319b (abstr. 4824), 2002.
259. Tsimberidou, A.M., Estey, E., Cortes, J.E., Garcia-Manero, G., Faderl, S., Verstovsek, S., Thomas, D.A. et al., Mylotarg, fludarabine, cytarabine (Ara-C) and cyclosporine (MFAC) regimen as post remission therapy in acute myelogenous leukemia, *Cancer Chemother. Pharmacol.*, 52, 449, 2003.
260. Alvarado, Y., Tsimberidou, A., Kantarjian, H., Cortes, J., Garcia-Manero, G., Faderl, S., Thomas, D., Estey, E., and Giles, F.J., Pilot study of Mylotarg, idarubicin and cytarabine combination regimen in patients with primary resistant or relapsed acute myeloid leukemia, *Cancer Chemother. Pharmacol.*, 51, 87, 2003.
261. Apostolidou, E., Cortes, J., Tsimberidou, A., Estey, E., Kantarjian, H., and Giles, F.J., Pilot study of Gemtuzumab ozogamicin, liposomal daunorubicin, cytarabine and cyclosporine regimen in patients with refractory acute myelogenous leukemia, *Leuk. Res*., 27, 887, 2003.
262. Rutella, S., Bonanno, G., Procoli, A., Mariotti, A., Lucia, M.B., Contemi, A.M., Cauda, R. et al., Granulocyte colony-stimulating factor enhances the *in vitro* cytotoxicity of gemtuzumab ozogamicin against acute myeloid leukemia cell lines and primary blast cells, *Exp. Hematol.*, 34, 54, 2006.
263. Leone, G., Rutella, S., Voso, M.T., Fianchi, L., Scardocci, A., and Pagano, L., *In vivo* priming with granulocyte colony-stimulating factor possibly enhances the effect of gemtuzumab-ozogamicin in acute myeloid leukemia: Results of a pilot study, *Haematologica*, 89, 634, 2004.
264. Shipley, J.L. and Butera, J.N., Acute myelogenous leukemia, *Exper. Hematol.*, 37, 649, 2009.
265. Moore, J., Seiter, K., Kolitz, J., Stock, W., Giles, F., Kalaycio, M., Zenk, D., and Marcucci, G., A phase II study of Bcl-2 antisense (oblimersen sodium) combined with gemtuzumab ozogamicin in older patients with acute myeloid leukemia in first relapse, *Leuk. Res.*, 30, 777, 2006.
266. Takeshita, A., Shinjo, K., Naito, K., Matsui, H., Sahara, N., Shigeno, K., Horii, T. et al., Efficacy of gemtuzumab ozogamicin on ATRA- and arsenic-resistant acute promyelocytic leukemia (APL) cells, *Leukemia*, 19 1306, 2005.
267. Estey, E., Garcia-Manero, G., Ferrajoli, A., Faderl, S., Verstovsek, S., Jones, D., and Kantarjian, H., Use of all-trans retinoic acid plus arsenic trioxide as an alternative to chemotherapy in untreated acute promyelocytic leukemia, *Blood*, 107, 3469, 2006.
268. Aribi, A., Kantarjian, H.M., Estey, E.H., Koller, C.A., Thomas, D.A., Kornblau, S.M., Faderl, S.H., Laddie, N.M., Garcia-Manero, G., and Cortes, J.E., Combination therapy with arsenic trioxide, all-trans retinoic acid, and gemtuzumab ozogamicin in recurrent acute promyelocytic leukemia, *Cancer*, 109, 1355, 2007.
269. Ravandi, F., Estey, E., Jones, D., Faderl, S., O'Brien, S., Fiorentino, J., Pierce, S. et al., Effective treatment of acute promyelocytic leukemia with all-trans-retinoic acid, arsenic trioxide, and gemtuzumab ozogamicin, *J. Clin. Oncol.*, 27, 504, 2009.
270. Herbertson, R.A., Tebbutt, N.C., Lee, F.T., MacFarlane, D.J., Chappell, B., Micallef, N., Lee, S.T. et al., Phase I biodistribution and pharmacokinetic study of Lewis Y-targeting immunoconjugate CMD-193 in patients with advanced epithelial cancers, *Clin. Cancer Res*., 15, 6709, 2009.
271. Takeshita, T., Salvage combination chemotherapy with enocitabine, aclarubicin and neocarzinostatin for recurrent or refractory acute myelogenous leukemia, *Med. J. Kagoshima Univ.*, 52, 33, 2000.
272. Takahashi, T., Yamaguchi, T., Kitamura, K., Suzuyama, H., Honda, M., Yokota, T., Kotanagi, H., Takahashi, M., and Hashimoto, Y., Clinical application of monoclonal antibody-drug conjugates for immunotargeting chemotherapy of colorectal carcinoma, *Cancer*, 61, 881, 1988.
273. Otsuji, E., Tsuruta, H., Toma, A., Kobayashi, S., Okamoto, K., Yata, Y., and Yamagishi, H., Effects of idiotypic human anti-mouse antibody against *in vitro* binding and antitumor activity of a monoclonal antibody-drug conjugate, *Hepatogastroenterology*, 50, 380, 2003.

274. Yata, Y., Otsuji, E., Okamoto, K., Tsuruta, H., Kobayashi, S., Toma, A., and Yamagishi, H., Decreased production of anti-mouse antibody after administration of human/mouse chimeric monoclonal antibody-neocarzinostatin conjugate to human, *Hepatogastroenterology*, 50, 80, 2003.
275. Fang, J., Sawa, T., and Maeda, H., Factors and mechanism of "EPR" effect and the enhanced antitumor effects of macromolecular drugs including SMANCS, *Adv. Exp. Med. Biol.*, 519, 29, 2003.
276. Maeda, H., Sawa, T., and Konno, T., Mechanism of tumor-targeted delivery of macromolecular drugs, including the EPR effect in solid tumor and clinical overview of the prototype polymeric drug SMANCS, *J. Control. Release*, 74, 47, 2001.
277. Maeda, H., SMANCS and polymer-conjugated macromolecular drugs: Advantages in cancer chemotherapy, *Adv. Drug Delivery Rev.*, 46, 169, 2001.
278. Greish, K., Fang, J., Inutsuka, T., Nagamitsu, A., and Maeda, H., Macromolecular therapeutics: Advantages and prospects with special emphasis on solid tumor targeting, *Clin. Pharmacokinet.*, 42, 1089, 2003.
279. Ishii, H., Furuse, J., Nagase, M., Maru, Y., Yoshino, M., and Hayashi, T., A phase I study of hepatic arterial infusion chemotherapy with zinostatin stimalamer alone for hepatocellular carcinoma, *Jpn. J. Clin. Oncol.*, 33, 570, 2003.
280. Seiichi, T., Yoshiaki, M., Masayoshi, J., Norio, N., and Shin-Ichiro, N., Induction of drug-specific antibody and the controlled release of drug by 6-O-carboxymethyl-chitin, *J. Control. Release*, 28, 235, 1994.
281. Nishikawa, T., Kumagai, K., Kudo, A., and Ishida, N., Cytological study on the effect of neocarzinostatin on sarcoma 180 in vivo, *J. Antibiot*., 18, 223, 1965.
282. Napier, M.A., Holmquist, B., Strydom, D.J., and Goldberg, I.H., Neocarzinostatin: Spectral characterization and separation of a non-protein chromophore, *Biochem. Biophys. Res. Commun.*, 89, 635, 1979.
283. Konishi, M., Ohkuma, H., Saitoh, K., Kawaguchi, H., Golik, J., Dubay, G., Groenewold, G., Krishnan, B., and Doyle, T.W., Esperamicins, a novel class of potent antitumor antibiotics. I. Physico-chemical data and partial structure, *J. Antibiot.*, 38, 1605, 1985.
284. Boghaert, E.R., Khandke, K., Sridharan, L., Armellino, D., Dougher, M., Dijoseph, J.F., Kunz, A. et al., Tumoricidal effect of calicheamicin immuno-conjugates using a passive targeting strategy, *Int. J. Oncol*., 28, 675, 2006.

23 The Mitomycins*

William A. Remers

CONTENTS

23.1 Introduction 623
23.2 Mechanism of Action 627
23.3 Analogs and Derivatives 632
23.3.1 Structural Analogs and Derivatives 632
23.3.2 Conjugated Derivatives 633
23.4 Structure–Activity Relationships 635
23.5 Synthesis 637
23.6 Clinical Applications 637
References 639

23.1 INTRODUCTION

In 1956, Hata et al.[1] at the Kitasato Institute isolated mitomycins A and B by chromatography of a mixture compounds from cultures of *Streptomyces caespitosis*. A subsequent investigation on the same organism by Wakaki's group at Kyowa Fermentation Industry yielded mitomycin C, which proved to be the most active anticancer agent among these, and subsequent, natural mitomycins.[2] Mitomycin C (Chart 23.1) was introduced as an anticancer drug by Kyowa, and it caught on rapidly.[3] It was given to an estimated 60% of patients receiving chemotherapy in Japan during the 1960s. In contrast, the first clinical trials in the United States were very unsatisfactory, with 11 patients dying from the effects of myelosuppression.[4] The reason for this serious toxicity was that the mitomycin C was given on the schedule used for 5-fluorouracil—daily injection for five consecutive days—but it has cumulative and delayed toxicity to bone marrow. Bristol-Myers finally received approval in 1974 for clinical use of mitomycin C based on a revised dosage schedule.[5]

The earliest mitomycins all had the azirino[2,3:3,4]pyrrolo[1,2-*a*]indole ring system as their basic skeleton.[6] They were divided into three structural types based on the nature and stereochemistry of their side chains, as shown in Chart 23.1. Thus, mitomycin A and B types differ in the stereochemistry of the side chain,[7] whereas mitomycin G types have only a methylene group.[8] Two mitomycin-like structures (mitomycinoids) with somewhat different skeletons, isomytomycin A and albomitomycin A, were discovered by Kono et al. in 1987, and the somewhat related compound FR-900482 was isolated in 1987 (Chart 23.1).[9]

The complicated systematic chemical names of the mitomycins led investigators to develop a distinctive nomenclature for them. Compounds with the complete skeleton including the aziridine ring, saturation at carbons 9 and 9a, and the quinone oxidation state are called mitosanes,[9] and the corresponding hydroquinones are called leucomitosanes.[10] If the structures are the same, except that there is a 9,9a-double bond, the compounds are called aziridinomitosenes and leucoaziridinomitosenes. If these compounds lack the aziridine ring, they are mitosenes (Figure 23.1).[9]

* This chapter has been updated by Gordon M. Cragg, Natural Products Branch, Developmental Therapeutics Program, Division of Cancer Treatment and Diagnosis, National Cancer Institute Frederick, MD.

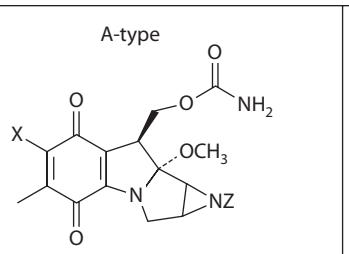

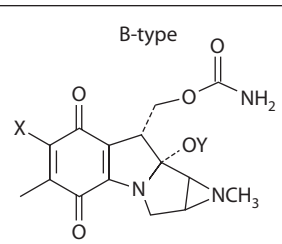

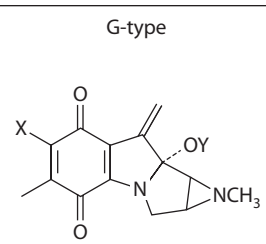

Mitomycin	X	Z	Mitomycin	X	Y	Mitomycin	X	Y
A	CH_3O	H	B	CH_3O	H	G	H_2N	CH_3
C	H_2N	H	D	H_2N	H	H	CH_3O	H
F	CH_3O	CH_3	E	H_2N	CH_3	K	CH_3O	CH_3
Porfiromycin	H_2N	CH_3	I	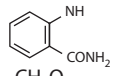	H			
M	CH_3NH	H	J	CH_3O	CH_3			
			L	CH_3NH	H			

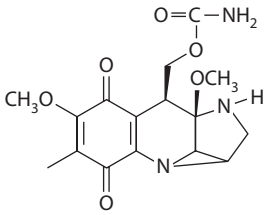

Isomitomycin A

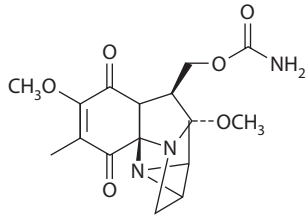

Albomitomycin A

CHART 23.1 Natural mitomycins.

The structures of mitomycins A and B and porfiromycin (Chart 23.1) were elucidated by Webb et al. at American Cyanamid in 1962 and confirmed by Tulinsky's x-ray diffraction analysis.[11] One noteworthy finding in the course of degradative studies on mitomycins was the formation of 1-hydroxy-2-aminomitosenes when the mitomycins were treated with acid (Scheme 23.1).[6] The stereochemistry of these "apomitomycins" and other acid hydrolysis products were determined by Taylor and Remers and by Shaber and Rebek.[12,13] Other chemical transformations of mitomycins that became important in later mode of action studies included selective hydrolysis of the 7-amino group of mitomycin C to a hydroxyl group[14] and selective hydrolysis of the carbamate group to a hydroxyl group (Scheme 23.1).[15] Acylation of the aziridinyl nitrogen of certain mitomycins was used in preparing many conjugates, as described below.

Catalytic reduction of the mitomycin quinone ring produces a leucoaziridinomitosene, which can be reoxidized to an aziridinomitosene.[10] Other two-electron-reduction processes typically afford 1,2-disubstituted mitosenes with the 1-substituent and the stereochemistry dependent on the nucleophile.[16] Reduction of mitomycins in the presence of reactive thiols resulted in replacement of the carbamate group in the side chain, as well as opening of the aziridine ring.[17] Hornemann et al.[18] found that sodium dithionite reduction of mitomycin C afforded a mitosane in which the 9a-methoxy group was replaced by sodium bisulfite (Scheme 23.2). When mitomycin C was reduced at lower pH (5.0), it formed a 2,7-diaminomitosene by trapping a proton from the solvent. Kohn et al. reported that proton capture at C(1) occurs with high stereoselectivity: the proton is added from the opposite

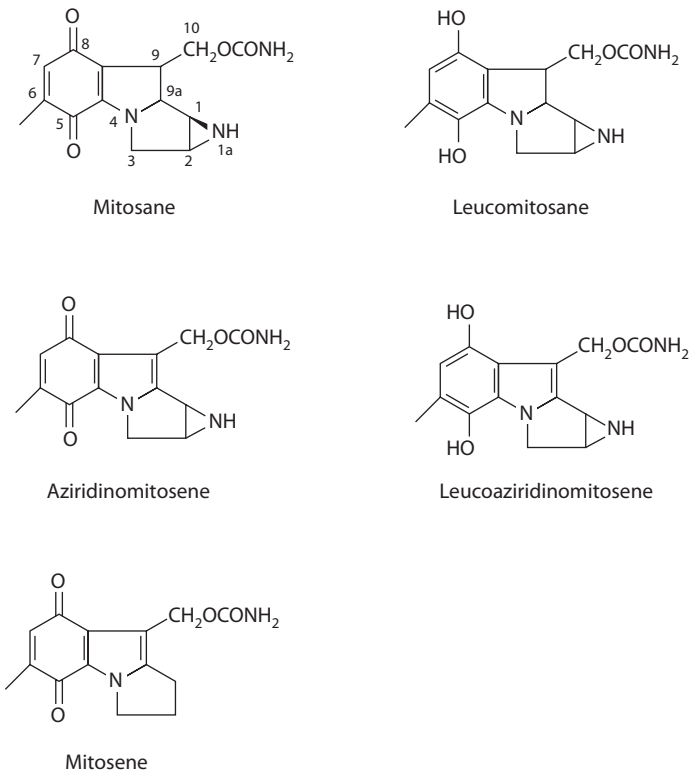

FIGURE 23.1 Nomenclature for mitomycins and derivatives.

side of the ring to the protonated 2-amino group. They suggested further that a quinone methide intermediate participates in this process (Scheme 23.3).[19]

Another interesting discovery by Kohn's group was that mitomycin C analogs containing a second amino group in the C(7) substituent undergo cyclization to give a C(8) imine, provided that there is an appropriate spacer between the two nitrogens (Scheme 23.4).[20] When the two nitrogens were separated by a three-methylene chain in which the central atom was dimethylated, the product was an iminoquinone with an albomitomycin structure (Scheme 23.4).[21]

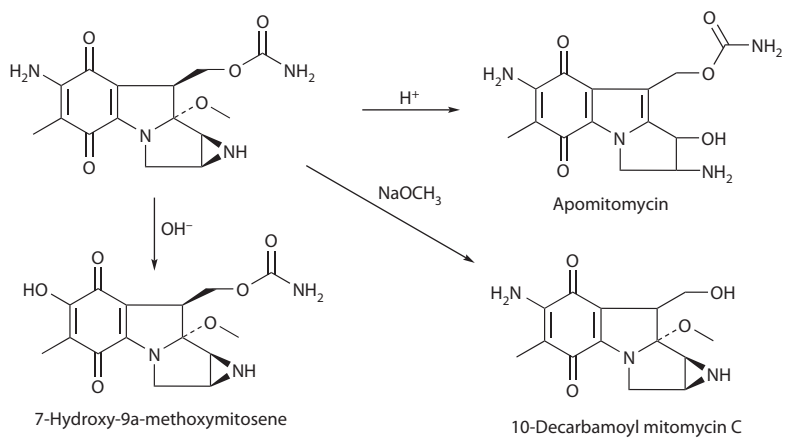

SCHEME 23.1 Chemical transformations of mitomycin C.

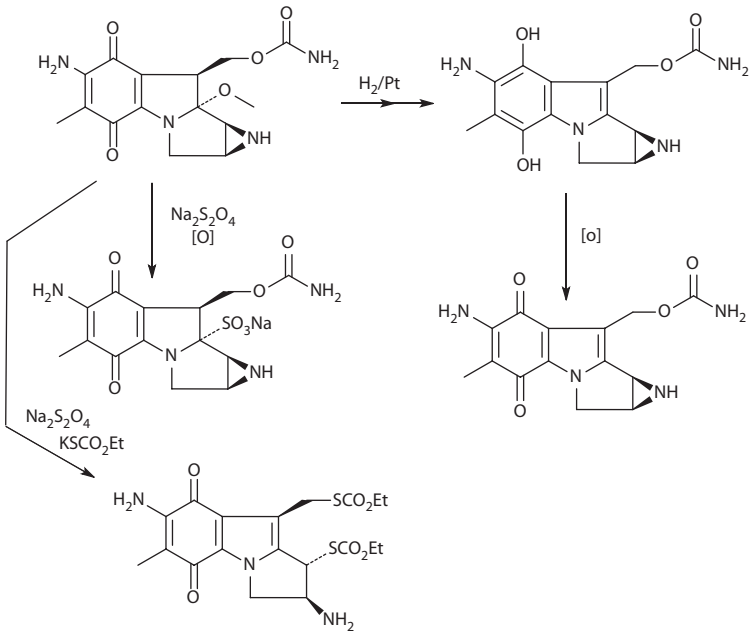

SCHEME 23.2 Reductive transformations of mitomycin C.

Mitomycin C reduction by biological agents such as xanthine oxidase or NADPH-cytochrome C P450 reductase involves an initial one-electron transfer to give a semiquinone radical, which can be detected by electron paramagnetic resonance.[22] Electochemical or catalytic reduction of mitomycin C in inert solvents also produced semiquinone radicals.[23] In biological systems, these species undergo disproportionation to the hydroquinones and quinones.[24]

Early studies on the biosynthesis of mitomycins showed that the *O*-methyl and *N*-methyl groups, but not the *C*-methyl group, are derived from L-methionine.[25] Hornemann et al.[26] then demonstrated that D-glucosamine is incorporated intact into mitomycins, and that L-citrulline donates the intact $CONH_2$ group. More recently, Sherman et al.[27] determined that the aminomethylbenzoquinone

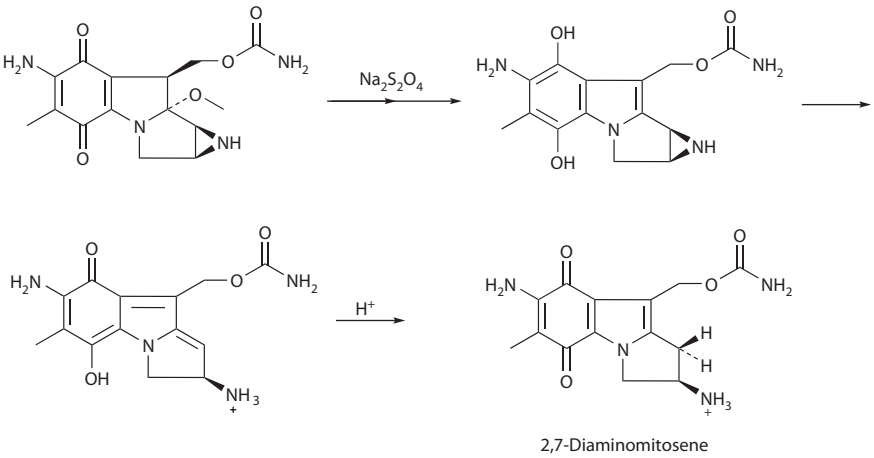

SCHEME 23.3 Formation of 2,7-diaminomitosene.

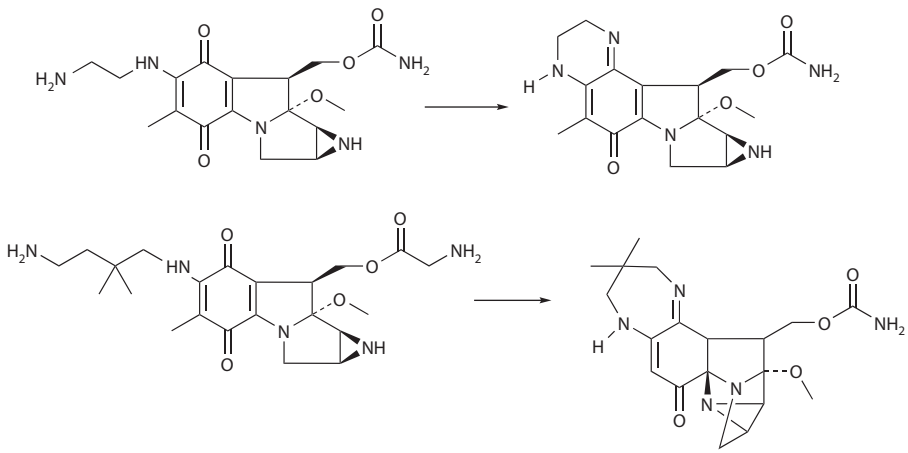

SCHEME 23.4 Cyclization reactions of mitosanes with amino groups on the C(7)-substituent.

unit of mitomycin C comes from 3-amino-5-hydroxybenzoic acid (Figure 23.2). Floss et al.[28] had previously shown that 3-amino-5-hydroxybenzoic acid is formed by a modified shikimate pathway involving 3,4-dideoxy-4-amino-D-arabinoheptulosonic acid-7-phosphate. The Sherman group has shown that the gene, mitN, which has high similarity to methyltransferases, is located within the mitomycin biosynthetic gene cluster. Overexpression of the mitN gene in *Escherichia coli* gave the histidine-tagged protein (MitN), which was purified to homogeneity. Inframe deletion of mitN of the mitomycin biosynthetic pathway generated in *Streptomyces lavendulae* produced a DHS5373 mutant strain, which not only continued the production of mitomycins A and C, but also resulted in the accumulation of a new mitomycin analog, 9-epi-mitomycin C. The function of MitN as an aziridine *N*-methyltransferase was demonstrated by its reaction with 9-epi-mitomycin C in the presence of *S*-adenosylmethionine to yield mitomycin E, as well as the conversion of mitomycin A to mitomycin F under the same reaction conditions. The authors thus concluded that MitN plays an important role in a parallel biosynthetic pathway leading to the production of the subclass of mitomycins with 9α-stereochemistry, but that it is not involved directly in the biosynthesis of mitomycins A and C.[29]

In 1990 Islam and Skibo prepared pyrrolobenzimidazole analogs of mitosenes.[30] The compound with 6-aziridino and 1-carbamoyloxy substituents (Scheme 23.5) was highly potent against human solid-tumor cell lines. It resembled doxorubicin in its DNA-strand cleaving ability and cardiotoxicity.[31] The *S*-enantiomer was selectively toxic over the *R*-enantiomer for ovarian cancer cells.[32]

23.2 MECHANISM OF ACTION

The antimicrobial and antitumor activities of mitomycins result in part from alkylation of DNA. Approximately 10% of their covalent interactions result in cross-linking of double-helical DNA,

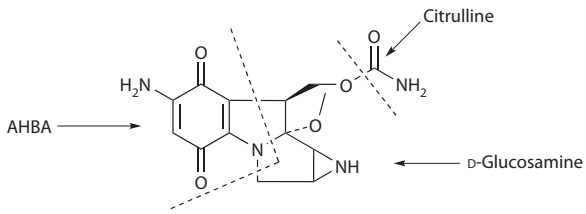

FIGURE 23.2 Biosynthetic precursors of mitomycin C.

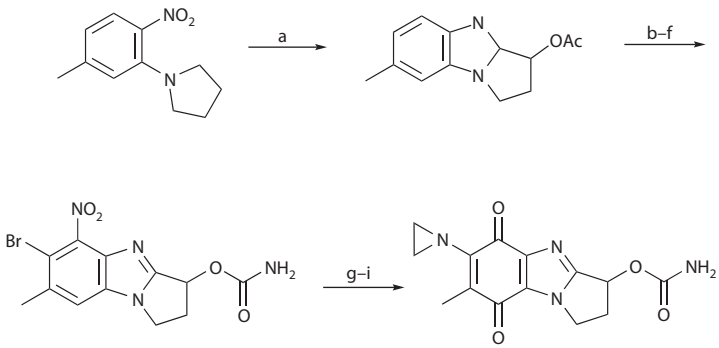

Reagents: (a) Zn Cl_2, Ac_2O; (b) Br_2, HOAc; (c) HNO_3, H_2SO_4; (d) $NaOCH_3$, MeOH; (e) phenyl chloroformate; (f) NH_3, MeOH; (g) H_2, Pd/C; (h) Fremy's salt; (i) aziridine, aerobic MeOH.

SCHEME 23.5 Preparation of 6-aziridino-1-carbamoyloxy-2,3-dihydro-7-methyl-[1,2-a]benzimidazole-5,8-dione.

and the remaining linkages are monofunctional.[33,34] Although alkylation of DNA occurred readily in living cells, this process could not be demonstrated *in vitro* until Iyer and Szybalski[35] discovered that NADPH-dependent cell extracts or chemical-reducing agents were required. Under these conditions, only marginal amounts of mitomycin C were incorporated, and there was no cross-linking. An ingenious solution to this problem in mitomycin activation was provided by Tomasz, who postulated that the initial binding of mitomycins involved semiquinone radicals rather than hydroquinones and devised a method of maximizing the concentration of semiquinone radicals by adding the reducing agent, sodium dithionite, in portions and maintaining an excess of the mitomycin.[36] These conditions produced a high binding ratio of mitomycins, and cross-links were obtained.

The effects of different oxidoreductase enzymes on the activation of mitomycin C were studied. Gustafson and Pritsos found that xanthine dehydrogenase activated it under both aerobic and anaerobic conditions, and they proposed that mitomycin reduction occurs at the NAD^+ site on this enzyme.[37] Enhancement of mitomycin C toxicity by compounds that induce DT-diaphorase was found to occur in tumor cells by Begleiter et al.[38] In contrast, DT-diaphorase downregulation in MKN28 gastric cancer cells produced resistance to mitomycin C.[39] Sartorelli et al.[40] found that in Chinese hamster ovary cells that overexpressed human NADPH:cytochrome C reductase, mitomycin C was highly active under both oxygenated and hypoxic conditions, whereas porfiromycin was markedly more cytotoxic under hypoxic than aerobic conditions.

One-electron reduction to a semiquinone-free radical is catalyzed by the NADPH:cytochrome P450 reductase (P450R). Levels of P450R in human tumors are highly heterogeneous, and a gene therapy to overexpress P450R in tumors and specifically sensitize them to mitomycin C has been developed. Injection of a nonreplicating adenovirus, Ad P450R, engineered to carry human P450R cDNA into MDA468 human breast tumor xenografts increased tumor P450R activity fivefold. Treatment of the virally pretreated tumors with mitomycin C resulted in a markedly enhanced response, clearly demonstrating, at least in a preclinical model, the therapeutic benefit of the virus-mediated P450R gene therapy strategy. This approach has been reviewed by Cowen et al.[41]

In 1964, Iyer and Szybalski proposed a mechanism of action for mitomycins based on bifunctional alkylation and cross-linking of DNA. It involved reduction of the quinone ring to a hydroquinone followed by loss of the elements of methanol to give a mitosene hydroquinone. In this hydroquinone, the aziridine ring opens to provide a carbonium ion that can alkylate DNA. Cross-linking occurs by alkylation of DNA by C(10) of the mitomycin following elimination of the carbamoyloxy group.[35] Moore[42] modified this mechanism to include the intermediacy of quinone methides (Scheme 23.6).

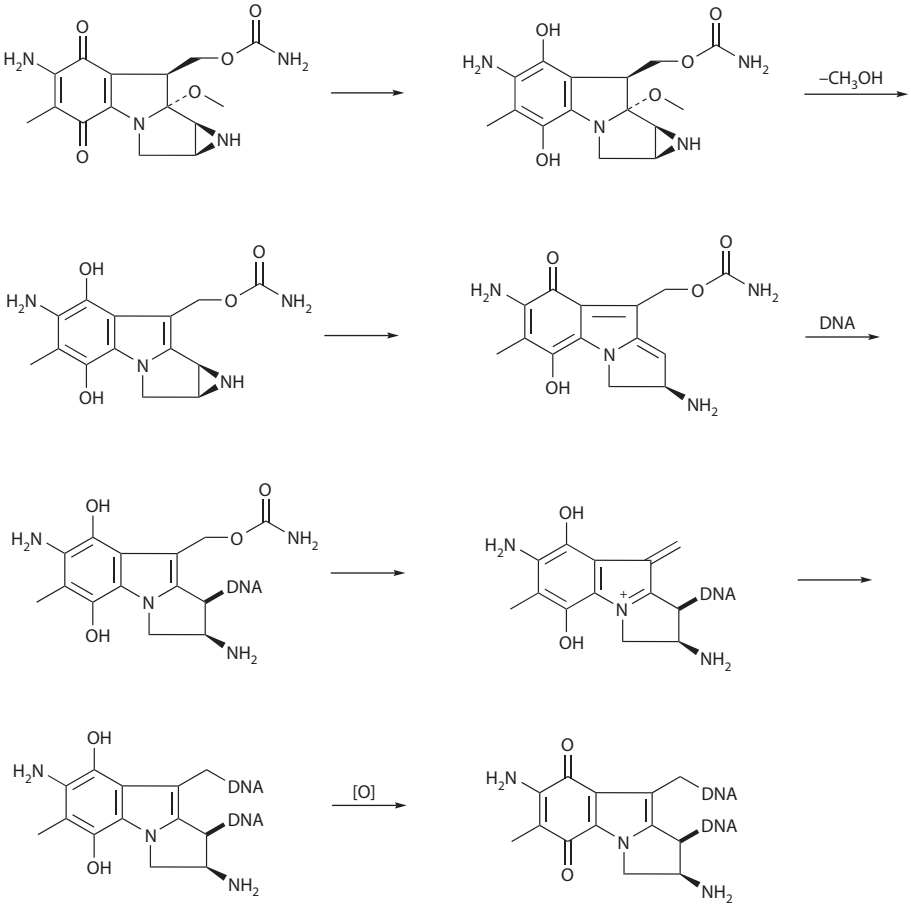

SCHEME 23.6 Proposed mechanism of bifunctional alkylation of DNA by mitomycin C.

Kohn's group found that mitomycin D and mitomycin-9a-sulfonate gave binding profiles comparable to that of mitomycin C under reductive conditions. These results indicated that neither the leaving group at C(9a) nor the stereochemistry at C(9) and C(9a) influence the sites of DNA binding and supported the concept of quinone methide formation before bonding at C(1).[43]

Boryah and Skibo determined the p*K*a values of mitomycin C in its quinone and hydroquinone forms. The quinone form has p*K*a values as follows: 1.2 for the protonated quinone ring, 2.7 for the protonated indole nitrogen, and 7.6 for the protonated aziridine nitrogen. In comparison, the hydroquinone form has p*K*a values of 1.2 for the protonated 7-amino group, 5.1–6.1 for the protonated indole nitrogen, and 9.1 for the protonated aziridine nitrogen. Protonation of the indoline nitrogen in the quinone form prevents the elimination of methanol; however, there is a 10^5-fold increase in the rate constant for methanol elimination in the hydroquinone form. The carbocation resulting from methanol elimination (p*K*a = 7.1) dissociates to a quinone methide. At pH values below 7.1, the carbocation traps water, and at pH values above 7.1, it traps both water and a proton.[44]

The specific atoms involved in the alkylation of DNA by mitomycin C were determined by Tomasz, Nakanishi, and coworkers. They hydrolyzed the mitomycin-bound DNA with enzymes, including snake venom diesterase and alkaline phosphatase, to obtain the mitomycin-bound nucleosides and then elucidated their structures by a variety of analytical methods.[45–50] Monoalkylation occurs preferentially at C(1) of the mitomycin, with the covalent bond formed with the 2-amino group of a guanine residue. Among the three different products isolated in the initial experiments,

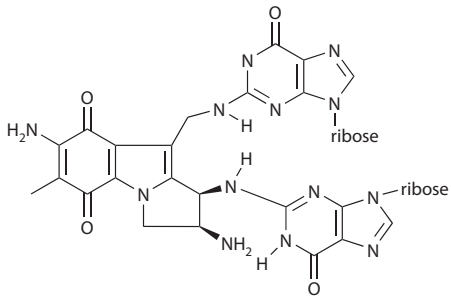

FIGURE 23.3 Main product from cross-linking of DNA by mitomycin C.

the main product had the amino groups attached to C(1) and C(2) of the mitosene moiety in a *cis* orientation. The minor products were the C(1) epimer and the 10-decarbamoyl derivative.[51] Dialkylation with cross-linking involves alkylation of the 2-amino group of guanine in one strand of the DNA double helix by C(1) of mitomycin C and alkylation of the 2-amino group of guanine in the opposite strand by C(10) of the same mitomycin C molecule (Figure 23.3).[52,53] Tomasz et al. isolated a product that had an intrastrand cross-link between the DNA and mitosene. The covalent bonds were between 2-amino groups of guanines and C(1) and C(10) of the mitosene, just as in the intermolecular cross-linked products; however, the DNA double helix was bent at 14.6 degrees near the cross-link site.[52,54] A further monoadduct was isolated from mouse mammary tumor cells. It had the covalent bond formed between C(10) of the mitosene and the 2-amino group of a guanine residue.[55]

The preferred 5-CpG sequence for mitomycin binding and cross-linking DNA was first suggested by molecular-modeling studies,[56] and it was confirmed by chemical and spectroscopic studies in a number of laboratories.[53,57,58] The laboratories of Tomasz and Kohn independently showed that the initial covalent-bonding event occurs at C(1) of the mitomycin in the preferred 5-CpG sequence and is independent of the second bonding step.[59–61] Kohn pointed out that a hydrogen bond between the C(10) carbonyl oxygen of an activated mitomycin and the 2-amino group on a guanine residue in the precovalent complex contributes significantly to the sequence specificity.[61] Substitutions, such as methoxycarbonyl and methanesulfonyl, on the aziridine nitrogen of mitomycin C changed the sequence specificity for DNA binding.[62]

The mechanism of enzymatic reductive activation of mitomycin C was revised by Tomasz et al. in 1997. They found that when mitomycin C was reduced by a variety of chemical and enzymic agents in the presence of *Micrococcus lysodeicticus*, the overall yield of adducts was higher at pH 7.4 than at 5.8, except for DT-diaphorase reduction. The cross-links were always greater at lower pH. From these results, they proposed that three competing pathways for activation afford three different DNA-reactive electrophiles that generate three unique sets of DNA adducts.[63]

DNA alkylation by certain mitomycin C analogs was investigated by Tomasz et al., who reported that, in the absence of reduction, 2,7-diaminomitosene bound to DNA, whereas mitomycin C, mitomycin A, porfiromycin, and certain analogs did not. Protonation of the 2-amino group of 2,7-diaminomitosene strongly affected binding, although the presence of functional groups, including 1-OH and *N*-methyl, did not.[64] Under reductive activation, C(10) of 2,7-diaminomitosene alkylated DNA on N(7) of a guanine residue.[65] Decarbamoyl mitomycin C was surprisingly more cytotoxic than mitomycin C to hypoxic EMT6 mouse mammary tumor cells and CHO cells. The frequency of total adducts was 20- to 30-fold higher with decarbamoyl mitomycin C, although the frequency of cross-links was equal. These results are in contrast to the alkylation of calf thymus DNA *in vitro*, wherein mitomycin C is more reactive.[66] The unnatural enantiomer of mitomycin C formed both a mono and a bis adduct on reduction in the presence of DNA. These adducts were stereoisomers of the main adducts formed by natural mitomycin C.[67] Reduction of racemic 1,10-bisacetoxy-7-methoxymitosene

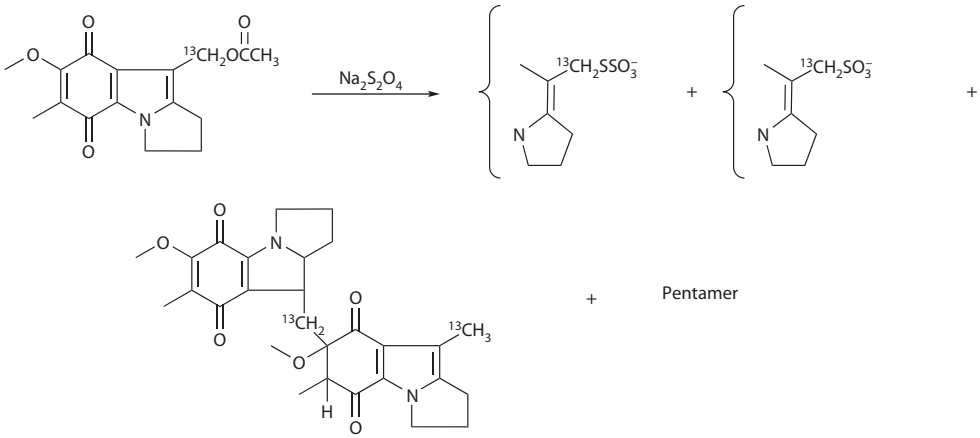

SCHEME 23.7 Products from dithionite reduction of a ^{13}C-labeled mitosene.

in the presence of DNA gave five products. In the two major adducts, the stereochemistry at C(1) was the same as that found for natural mitomycin C adducts, but the C(2) chirality was reversed.[68]

Alkylation sites on reduced mitosenes were assessed by Ouyang and Skibo, using ^{13}C nuclear magnetic resonance. They found that reduction by dithionite gave sulfite esters as well as sulfonates, both the 6-amino group of adenine and the 2-amino group of guanine are alkylated, both nitrogen and oxygen centers in purines residues are alkylated, and the main fate of the iminium ions formed after reduction is head-to-tail polymerization (Scheme 23.7).[69]

Zhu and Skibo found that when indoloquinones with 5-aziridino substituents were reduced to hydroquinones, the fate of this aziridino group and the cytotoxicity were strongly influenced by the adjacent 6-substituent. In the 6-unsubstituted compound, the aziridine ring may assume a conformation in which a 1,5-sigmatropic shift occurs (Scheme 23.8). This shift results in loss of the aziridine ring and drastically reduces cytotoxicity. In contrast, a 6-methyl group provides steric hindrance that prevents the sigmatropic shift and allows the aziridine ring to alkylate DNA, thus retaining cytotoxicity. Similar results were observed for the corresponding benzoquinones and benzimidazolequinones.[70]

The binding of mitomycin C to modified oligonucleotides was investigated. Millard and Beachy found that cross-linking was increased when the cytosines in CpG–CpG were methylated. They suggested that this enhancement resulted from an electronic effect.[71] Oligonucleotides in which 2,6-diaminopurine was substituted for guanine were readily alkylated by reduced mitomycin C. The sequence specificity was TpD (analogous to CpG), and cross-links occurred in TpD · TpD and TpG.CpD regions.[72]

Glutathione does not reduce mitomycin C or form conjugates with it; however, in the presence of chemical or enzymic reducing systems, three monoconjugates and two bisconjugates are formed. Similar results were found with mercaptoethanol or *N*-acetylcysteine. Glutathione accelerated the

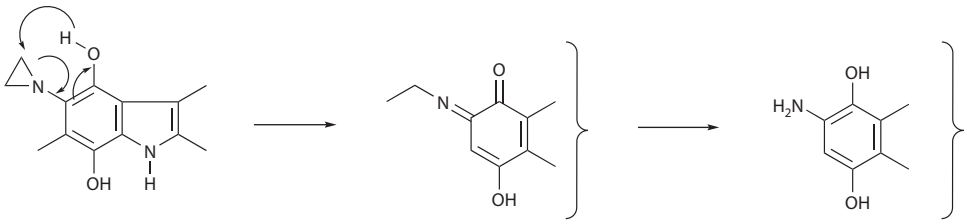

SCHEME 23.8 1,5-Sigmatropic shift in a 5-aziridinoindolohydroquinone.

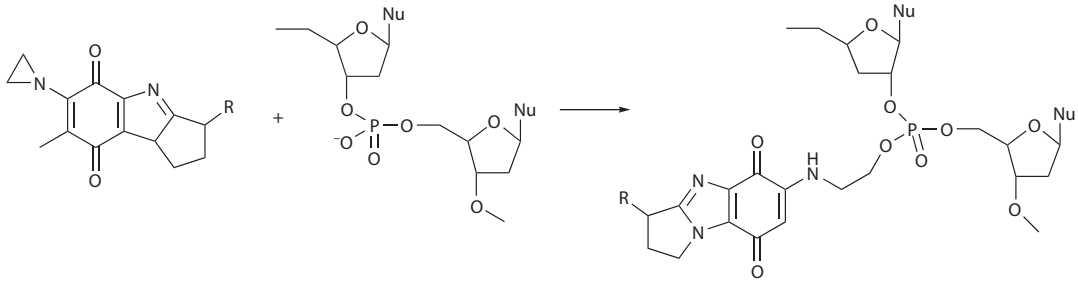

SCHEME 23.9 Alkylation of a phosphate group in DNA by a 6-aziridinopyrrolo[1,2-a]imidazole.

reduction of mitomycin C by "slow" agents such as cytochrome C reductases. Glutathione was considered by Tomasz to be involved in further reduction of the initially formed semiquinone radical.[73] A ternary glutathione–mitomycin–DNA adduct was isolated from the reduction of mitomycin C in the presence of DNA or synthetic duplex oligonucleotides. The mitosene residue was linked to the nucleotide by its C(1) atom, and the glutathione residue was linked to C(10). Overall, glutathione has an inhibitory effect on mitomycin C alkylation of DNA, which may be a factor in mitomycin resistance by tumor cells with high glutathione levels.[74] In support of this idea, Xu et al.[75] found that the cytotoxicity of mitomycin C increased significantly in cells pretreated with ethacrynic acid, which inhibits glutathione transferase and depletes glutathione levels.

The effects of DNA alkylation by mitomycin C on other biological processes were examined by Tomasz et al. The action of DNA polymerases was terminated nearly quantitatively at the nucleotide 3' to each mitomycin monoadduct site on the DNA. These monoadducts do not distort the DNA, but the resulting increase in thermodynamic stability may prevent replication.[76] In selected tissue culture cell lines, mitomycin C and decarbamoylmitomycin C, but not 2,7-diaminomitosene, induced p53 protein levels and increased levels of p21am and Gadd45 mRNA. They also induced apoptosis in ML-1 cells. This marked the first observation that adducts of a multiadduct type of DNA-damaging agent were differentially recognized by DNA damage sensor pathways.[77]

Benzimidazole analogs with 6-aziridino substituents (Scheme 23.9) cleave DNA under reducing conditions, specifically at G + A bases.[78] Skibo and Schultz showed that after reduction of the quinone ring, the aziridino group of these compounds alkylates phosphate groups in the DNA backbone to form phosphotriesters that are labile to hydrolysis. They also alkylate N(7) of guanine and adenine residues. The observed base specificity was attributed to Hoogsteen-type hydrogen bonding of the hydroquinone in the major groove of the DNA double helix.[79]

A second important mechanism of action for mitomycins is the generation under aerobic conditions of superoxide and hydroxyl radicals that can cause DNA strand cleavage.[80–84] This process is promoted by metal ions such as Cu(II) and inhibited by enzymes such as catalase and superoxide dismutase, as well as by free-radical scavengers and metal-ion-sequestering agents.[85] Pritsos and Sartorelli showed that the free radicals generated by quinone antibiotics, including mitomycins, cause cytotoxicity that depends on the extent of DNA damage and the ability of cells to repair the damage.[86] This damage is easier to repair than that caused by mitomycin cross-linking of DNA.

23.3 ANALOGS AND DERIVATIVES

23.3.1 Structural Analogs and Derivatives

The rather broad antitumor spectrum of mitomycin C, together with its serious toxicity, spurred the quest for analogs that might have better therapeutic indices. Hundreds of mitosanes, aziridinomitosenes, and mitosenes, as well as indoloquinones, were synthesized and screened.[87] Despite the

development of numerous compounds with very impressive activity in animal screens, there have been no new clinical agents approved to date.

Among the mitosanes, the position most readily substituted is C(7) in the quinone ring. In particular, the replacement of the 7-methoxy group, as found in mitomycin A, with amines and alkoxides has been much investigated (Scheme 23.10). The earliest studies were by Kinoshita et al.[88–90] Mitomycin A is not produced in quantity by fermentation, but it is readily obtained by hydrolysis of mitomycin C to the 7-hydroxy derivative (Scheme 23.1), followed by *O*-methylation using diazomethane (Scheme 23.10).[14] The corresponding compounds with a methyl group on the aziridine nitrogen can be prepared from porfiromycin. An important feature of the 7-amino analogs is that both the quinone-reduction potential and the lipophilicity can be controlled by varying the substituents on the nitrogen. A large variety of substituted amines, including ethylamines, secondary amines, arylamines, and amidines, were prepared and tested by Remers et al. and by chemists at Bristol-Myers Squibb.[91–100] As discussed in the following sections, the arylamines and amidines were highly potent, and ethylamines bearing disulfide groups were efficacious. New 7-alkoxymitosanes were prepared by alkoxide exchange on mitomycin A or treatment of 7-hydroxymitosane with 3-substituted 1-phenyltriazenes (Scheme 23.10). Many of them showed high potency.[101]

Mitomycin C analogs with structural changes at other positions included acyl derivatives on the aziridine nitrogen,[88] the potent 10-decarbamoyl derivative,[15] which was converted into 10-chloro and 10-bromoderivatives,[102] and the 6-carboxaldehyde.[103]

Aziridinomitosenes corresponding to mitomycin A and its *N*-methyl derivative were prepared from the parent compounds by catalytic reduction and air oxidation. The methoxy group was then replaced by a variety of amines. As described below, potency depended on the ease of quinone reduction.[104] Mitosenes without the aziridine ring, but with substituents at C(1) or at C(1) and C(2), were prepared by total synthesis by Remers et al.[105,106] 1-Acetoxy-mitosenes with a variety of substituents in the quinone ring, and 7-methoxymitosenes with new substituents at C(1) and C(10), were also investigated.[107,108] None of these mitosenes were comparable in activity to the mitosanes.

The earliest work on synthesis and evaluation of mitomycin analogs was conducted by Allen et al. on indoloquinones and directed toward the development of new antibacterial agents. It provided important information on the relative importance of various functional groups in mitomycin-related structures.[109–112]

23.3.2 Conjugated Derivatives

A variety of conjugates has been prepared from mitomycin C in attempts to improve its therapeutic properties. The earliest one, which was prepared by Iwata and Goldberg, involved coupling

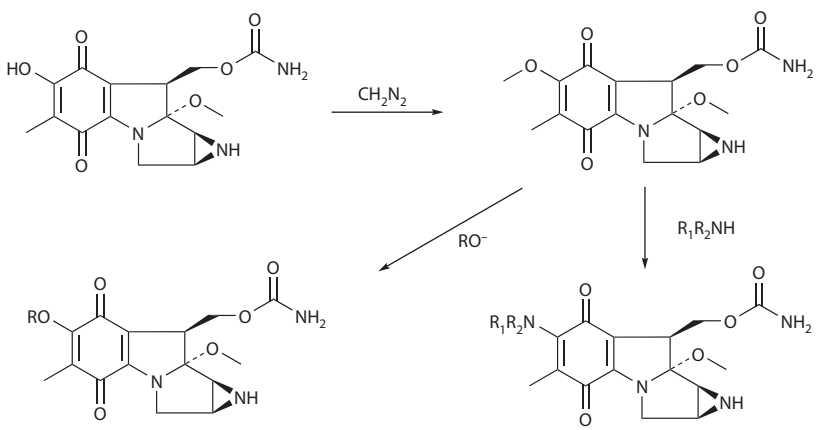

SCHEME 23.10 Preparation of 7-substituted mitosanes.

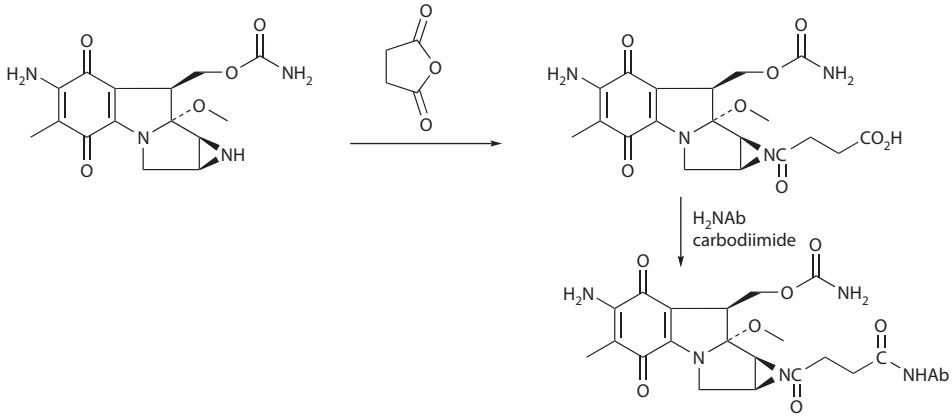

SCHEME 23.11 Synthesis of monoclonal antibody conjugates of mitomycin C.

conconavilin A with *N*(1a)-succinylated mitomycin C in the presence of a carbodiimide. An improved antitumor effect was claimed.[113] Conjugation with bovine-serum albumin required prior acetylation to prevent protein polymerization in the presence of carbodiimides. The conjugate of mitomycin C with glutarated albumin had high mitomycin content, and it was stable.[114]

Many conjugates were based on the delivery of mitomycin C to selected targets using monoclonal antibodies. In general, these conjugates were prepared by substituting the aziridino nitrogen with acyl groups having a free carboxyl group at the other end of the chain and then coupling with an antibody (Scheme 23.11). Sometimes the antibody is linked to an intermediary, which provides many binding sites for the mitomycin. Acylated aziridines are less stable than ordinary amides, and they undergo gradual hydrolysis to liberate mitomycin C at the target. The following conjugates were formed in this manner: monoclonal anti-MM46 immunoglobulin M antibody, with or without serum albumin as intermediary;[115] antialpha-fetoprotein antibody;[116] monoclonal antibody MGb2 with dextran T-40 as intermediary;[117] and antineural cell-adhesion molecule monoclonal antibody.[118] None of these conjugates has become an established therapeutic agent to date, although the MGb2 monoclonal antibody conjugate was reported to have an enhanced activity against human gastric cancer cells in nude mice.[117]

Two types of conjugates were directed toward binding with DNA. Kohn's group treated decarbamoylporfiromycin with carbonyldiimidazole followed by $H_2N(CH_2)_6P{=}S(OH)R$, wherein R is the base sequence for human A-raf-1-gene or human FGFR1 gene.[119] Tomasz et al. prepared conjugates in which 1, 2, or 3 *N*-methylpyrrolecarboxamide units were tethered by five methylene groups to the 7-amino group of mitomycin C. These *N*-methylpyrrole units are found in distamycin, and they direct molecules to AT-rich regions of DNA.[120]

Some derivatives of mitomycin C were prepared to modify its physical properties for improved absorption and distribution. Thus, alkyl and alkenylazacycloalkananone derivatives exhibit improved penetration through rat skin.[121] Another lipophilic substituent was the docosahexenoyl group.[122] Derivatives with hydrophilic properties were prepared by attaching a linear (1–3)-β-D-glucan to the aziridine nitrogen,[123] or a glucopyranosyl group linked through a phenolic group to N(7).[124] A conjugate with dextran, prepared by using $CO(CH_2)_4CH_2NHC(N{=}H)$ as the linker, showed strong affinity to lymph cells.[125] Other hydrophilic mitomycin C derivatives were formed by condensing poly[N5-(2-hydroxyethyl)-L-glutamine] through a tetrapeptide spacer [126] and by coupling a N(1a) succinyl mitomycin C with a chitosan. The latter derivative had high drug content, pH-dependent drug release, and long duration in plasma.[127]

A novel prodrug containing a 1,2-diacyl lipid linked to mitomycin C by a thiolytically cleavable dithiobenzyl carbamate (Figure 23.4) was formulated in STEALTH liposomes. It was

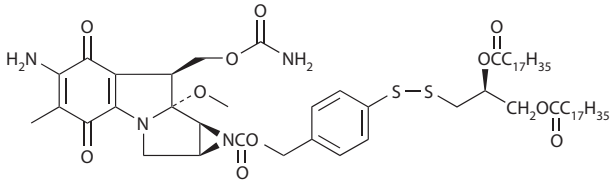

FIGURE 23.4 Thiolytically cleavable lipophilic prodrug of mitomycin C.

reported to be well retained in the liposomes and to show increased tumor inhibition over mitomycin C.[128]

Conjugates of 2,7-diaminomitosenes with cytidine 5-monophosphate and 5-*ara*-CMP were prepared as prodrugs that would liberate both the nucleotides and an alkylating intermediate on reduction. This process actually worked, as shown by liberation of the nucleotides, and the 5-*ara*-CMP conjugate prepared from mitomycin C was more potent than either parent compound (Scheme 23.12).[129,130]

23.4 STRUCTURE–ACTIVITY RELATIONSHIPS

One key to understanding structure–activity relationships among mitomycins and their analogs is that the functional groups are so distributed on the pyrrolo[1,2-a]indole nucleus that they interact with each other in a chain of events that produces potent alkylating functionalities. Another key to understanding is that at least three factors determine antitumor potency. They include the ability to enter cells, which is determined in part by their partition coefficient; the ease of their reduction to reactive intermediates, which is determined by the quinine-reduction potential; and the presence of optimal alkylating groups such as the aziridine ring and the carbamoyloxymethyl substituent.[88,89,97]

Mitomycins are relatively stable in their quinone state; however, as described in Section II, reduction of the quinone ring strongly activates the molecule. The nitrogen atom common to two rings becomes more electron rich and is able to participate in the loss of the 9a-substituent to give a leukoaziridinomitosene, which can undergo opening of the aziridine ring and loss of the carbamoyl group (Scheme 23.6). The ease of reduction of the quinone ring is obviously important in initiating the action of mitomycins, and this can influence the antitumor potency. Thus mitomycin A, which

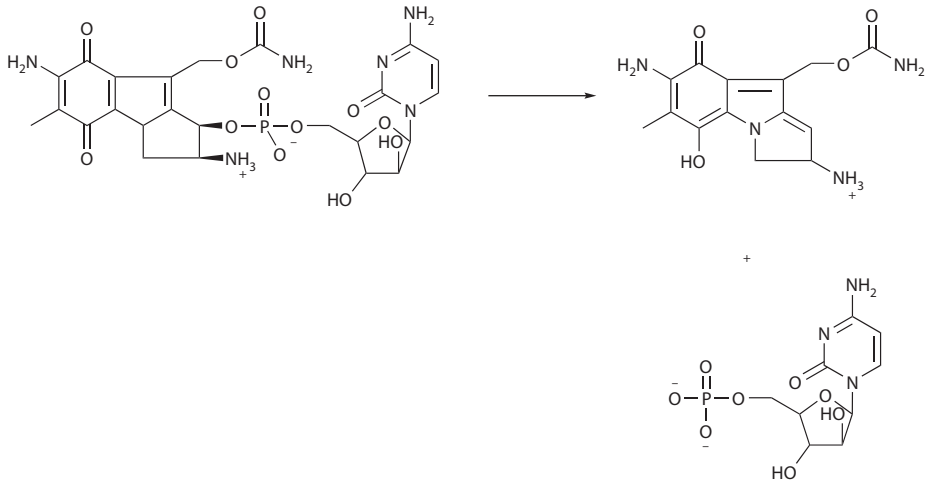

SCHEME 23.12 Prodrug for mitomycin and 5-ara-CMP.

TABLE 23.1
Mitomycins Receiving Clinical Trials

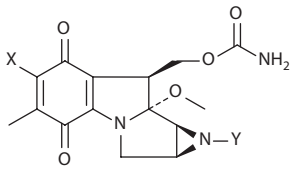

Identification	X	Y
Mitomycin C	H_2N	H
Porfiromycin	H_2N	CH_3
M83	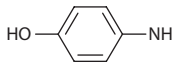	H
BMY-25282	$(CH_3)_2N–C=N–$	H
BMY-25067	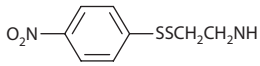	H
KT 6149	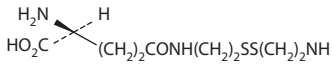	H

has a 7-methoxy substituent and half-wave-reduction potential ($E_{1/2}$) of –0.21 V, is more readily reduced and a more potent cytotoxic agent than mitomycin C, which has a 7-amino group and $E_{1/2}$ of –0.45 V.[93] Kunz et al. subjected a set of 30 mitomycin C and mitomycin A analogs to a QSAR study using multiple linear regression analysis based on cytotoxic potency in a panel of human tumor cells in culture (log $1/C$), $E_{1/2}$, and the logarithm of the partition coefficient (log P). A statistically significant correlation with an equation $\log(1/C) = 10.1 + 6.59E_{1/2} + 0.35 \log P$ was obtained. The parameter $E_{1/2}$ accounted for 48% of the variance, and log P accounted for 21%.[97] When the analysis was limited to mitomycin C analogs, $E_{1/2}$ was the only significant variable, whereas when the analysis was limited to mitomycin A analogs, log P was the only significant variable. These results were explained by the consideration that all of the mitomycin A analogs were 7-alkoxymitosanes with identical low $E_{1/2}$ values, meaning that cell uptake is the controlling factor in their potency, whereas the mitomycin C analogs, being harder to reduce in biological systems, are limited by reduction potential rather than by cell uptake. The nature of the assay system may be crucial in determining the relative potencies of mitomycins, and presumably other types of drugs. Thus, in the murine leukemia assay, the most potent mitomycin C and mitomycin A analogs were the most hydrophilic ones, whereas in the cell culture study described above, the most lipophilic analogs were the most potent ones.[101,131] This result indicates that the more lipophilic compounds may be concentrating in fatty tissues in the mice. It also indicates that optimizing a set of analogs in an *in vitro* assay might not be valuable for subsequent *in vivo* assays.

An ethyleneimino substituent at C(7) in the quinone ring gave especially potent antitumor activity against P-388 leukemia in mice.[93] Skibo and Schultz[78] subsequently showed that this substituent alkylates phosphate groups in the DNA backbone, giving enhanced covalent-binding energy. Quinones bearing an ethyleneimine group are reduced more readily than those with alkylamines.[94] Another C(7) substituent that confers increased antitumor potency to mitomycins is the amidine group, as found in BMY-25282 (Table 23.1).[100,132]

Elimination of the elements of water or methanol from C(9) and C(9a) of mitomycins produces aziridinomitosenes. They have all of the appropriate functionality for efficient DNA cross-linking, but they are less potent than the corresponding mitosanes, because their indoloquinone chromophores are more difficult to reduce than the corresponding benzoquinone chromophores of mito-

sanes.[133] Mitosenes without the aziridine ring are also less potent than mitosanes, although the presence of two alkylating functionalities at C(1) and C(10) permits bisalkylation with cross-linking of DNA. For example, the 1,10-diacetoxymitosene prepared by Orlamans et al.[134] possessed antitumor activity, although the spectrum was more limited than that of mitomycin C. Even indoloquinones with good leaving groups at C(2), which is equivalent to C(1) in mitosenes, have potent antibacterial activity in culture.[135]

Mitosanes lacking the carbamoyl substituent are surprisingly active antitumor agents.[66] Their potency may be explained by facile loss of hydroxide from an activated intermediate to give the same quinonemethide that mitomycins provide. The antitumor activity of mitomycin G, which has only a methylene group for C(10),[8] can be rationalized in the same way.

23.5 SYNTHESIS

The total synthesis of mitomycins has presented a formidable challenge to chemists because of the highly interactive functionality arranged on a compact skeleton. Allen et al. at American Cyanamid made early syntheses of indoloquinines and mitosenes related to the mitomycins, with the goal of producing new antibacterial agents.[136–138] This research was extended by Remers et al. to 1-substituted and 1,2-disubstituted mitosenes.[105,106,139] Groups led by Hirata and by Franck showed how to form the aziriding ring on the pyrrolo[1,2-*a*]indole nucleus.[140,141] Kametani et al.[142] introduced the 9a-methoxy group into the pyrrolo[1,2-*a*]indole system.

The real breakthrough in mitomycin synthesis was the landmark total synthesis of mitomycin C published by Kishi's group in 1977.[143,144] Although this synthesis was quite long, it showed how to solve most of the vexing problems in handling the reactive functionalities of mitomycins. A key step was the transannular closure of the two 5-membered rings of the pyrrolo[1,2-a] indole system from an 8-membered ring (Scheme 23.13). In 1989, Fukuyama and Yang[145] published an elegant and practical synthesis of mitomycin C by a route that went through isomitomycin A (Scheme 23.14). Danishefsky et al. have reported a number of ingenious, but unsuccessful, attempts to synthesize mitomycin C.[146] They did, however, succeed in the total syntheses of mitomycin K and the mitomycin-related compound FR-900482.[147,148]

Synthetic studies covering the past 30 years have recently been reviewed.[149]

23.6 CLINICAL APPLICATIONS

Mitomycin C was very widely used in cancer chemotherapy in Japan during the 1960s, and it subsequently received some important applications in the United States and other countries. It showed a broad spectrum of antitumor activity, although it was seldom the most effective agent against specific tumors. More recently, its use has declined because of its high toxicity and the introduction of newer agents of other chemical types. Nevertheless, it is still effective in cancer chemotherapy, especially in combinations with other anticancer drugs. Reference to mitomycin C in the NCI drug dictionary (http://www.cancer.gov/drugdictionary/?CdrID=42674) showed that, as of August, 2010, 350 trials have been completed, and that 25 trials are ongoing, generally using mitomycin C in

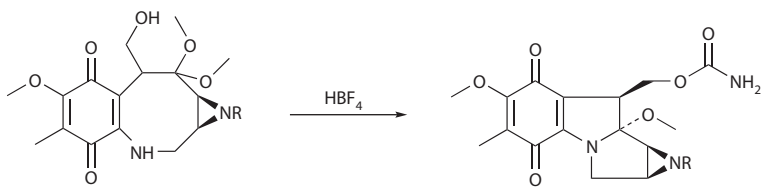

SCHEME 23.13 Formation of the mitosane nucleus in the Kishi synthesis.

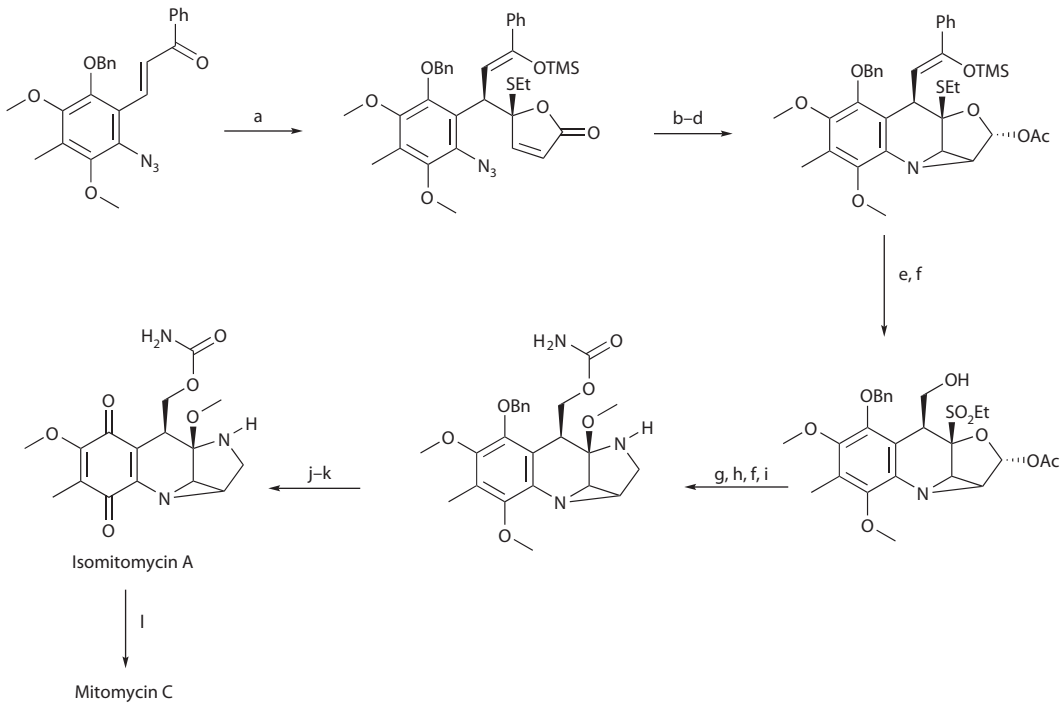

Reagents: (a) 5-Ethylthio-2-trimethylsiloxyfuran, $SnCl_4$, CH_2Cl_2, -78°C; (b) toluene 110°C; (c) DIBAL,14 THF, −78°C; (d) Ac_2O, Py; (e) RuO_2, $NaIO_4$; (f) $NaBH_4$/MeOH; (g) $Cl_3CCONCO$; (h) NH_3/MeOH; (i) $ClSO_3H$/MeOH; (j) H_2, Pd/C; (k) DDQ, acetone-H_2O, −78°C; (l) NH_3, MeOH.

SCHEME 23.14 Total synthesis of mitomycin C.

combination with other anticancer agents. These include 19 phase II, III, and IV trials against various forms of anal, bladder, cholangioc carcinoma, colorectal, gastric, hepatocellular, nasopharyngeal, and pancreatic cancers, and peritoneal carcinomatosis, as well as five phase I trials against bladder, hepatocellular, liver, prostate, and metastatic, unresectable, or recurrent solid tumors.

In 1968, Moertel et al.[150] found that mitomycin C produced objective responses in patients with tumors of the colon, pancreas, stomach, liver, and gallbladder. It also showed activity against non-small-cell lung cancer, some head and neck cancers, breast cancer, and chronic myelogenous leukemia.[151–153] Early et al.[154] showed that mitomycin C is active in topical administration to superficial bladder tumors. Furthermore, systemic activity was found for mitomycin C in advanced biliary, ovarian, and cervical squamous cell carcinoma.[155]

Results of a trial in which patients with squamous cell carcinoma of the head and neck received concurrent postoperative treatment with mitomycin and radiation, when compared with the results of trials in which patients received either radiation alone or radiation with porfiromycin, showed greater locoregional control in the mitomycin arms, although no statistically significant difference in the rates of overall survival or distant metastasis was observed.[156]

Combination regimens, including mitomycin C, have been used against a variety of cancers. One of the most common combinations is the FAM regimen, which contains 5-fluorouracil, Adriamycin, and mitomycin C, and is used in treating gastric and pancreatic carcinomas.[157] Mitomycin C and bleomycin in combination produced response rates up to 80% in cancers of the uterine cervix.[151] The MOB regimen includes mitomycin C, Oncovin, and bleomycin.

Mitomycin C (Mutamycin®) is supplied as lyophilized powder also containing mannitol in 5- and 20-mg vials. It is diluted with sterile water and administered by slow intravenous push or by

continuous intravenous infusion. Extravasation produces severe local necrosis. It is cleared rapidly from the vascular compartment, and the highest level appears in the kidneys, with lower detectable levels found in muscle, intestine, stomach, and eye.[158] The most serious toxicity of mitomycin C is bone marrow suppression, which reduces blood levels of platelets, leukocytes, and erythrocytes.[153] It is delayed and cumulative, which requires careful minimization of lifetime doses to under 50 to 60 mg/m^2. Gastrointestinal disturbances, renal toxicity, and alopecia also occur, and fatigue and drowsiness have been observed.[153,154,158]

The troublesome toxicity of mitomycin C has prompted the synthesis of hundreds of analogs. Among them, four compounds with novel substituents at C(7) have been introduced into clinical trials (Table 23.1). The *p*-hydroxyanilino derivative known as M83 was introduced by Kyowa Hakko Kogyo, and it showed excellent activities in animal models;[92] however, it was not superior to mitomycin C in the clinic. Bristol-Myers Squibb developed the highly potent dimethylamidino derivative, BMY-25282,[132,159] but it was cardiotoxic. Following interesting preclinical studies on the supposed mercaptoethylamino derivative, which was shown to actually be the corresponding disulfide,[100,160] a variety of disulfides cleavable to mercaptoethylamino derivatives was prepared.[161] Bristol-Myers Squibb conducted clinical trials on the [2-(4-nitrophenyl)dithio]ethylamino derivative, BMY-25067,[99] but eventually decided not to pursue it further. The 2-[2-(L-glutamylamino) ethyl]dithioethylamino derivative, KT 6149,[98] was introduced into the clinic by Kyowa Fermentation Industries and is still under investigation.

Porfiromycin was discovered at Upjohn,[162] and they gave it a brief clinical trial. It has much the same pattern of activity and toxicity as mitomycin C, but it is less potent.

REFERENCES

1. Hata, T., Hoshi, T., Kanamori, K., Matsumae, A., Sano, Y., Shima, T., and Sugawara, R., Mitomycin, a new antibiotic from streptomyces. *J. Antibiot. (Tokyo), Ser. A*, 9, 141, 1956.
2. Wakaki, S., Marumo, H., and Tomioka K., Isolation of new fractions of antitumor mitomycins. *Antibiot. Chemother.*, 8, 288, 1958.
3. Frank, W. and Osterberg, A.E., Mitomycin C (NSC-26988)—An evaluation of the Japanese reports. *Cancer Chemother. Rep.*, 9, 114, 1960.
4. Jones, Jr., R., Mitomycin C. A preliminary report of studies of human pharmacology and initial therapeutic trial. *Cancer Chemother. Rep.*, 2, 3, 1959.
5. Sutow, W.W., Wilbur, J.R., Vietti, T.J., Vuthibhagdee, P., Fujimoto, T., and Watanabe, A., Evaluation of dosage schedules of mitomycin C (NSC-26988) in children. *Cancer Chemother. Rep., Part 1*, 55, 285, 1971.
6. Webb, J.S., Cosulich, D.B., Mowat, J.H., Patrick, J.B., Broschard, R.W., Meyer, W.E., Williams, R.P., Wolf, C.F., Fulmor, W., Pidacks, C., and Lancaster, J.E., The structures of mitomycins A, B, C, and porfiromycins—Parts I and II. *J. Am. Chem. Soc.*, 84, 3185, 1962.
7. Yahashi, R. and Matsubara, I., The molecular structure of 7-demethoxy-7-*p*-bromoanilino mitomycin B. *J. Antibiot. (Tokyo)*, 29, 10, 1976.
8. Urakawa, C., Kawanishi, M., Iwasaki, A., Shirahata, K., Nakano, K., Takahashi, S., and Mineura, K., Jpn Kokai Tokkyo Koho, Japanese Patent JP 55015408 19800202, Showa, 1980.
9. Kono, M., Saitoh, Y., Shirahata, K., Arai, Y., and Ishii, S., Albomitomycin A and isomitomycin A: Products of novel intramolecular rearrangement of mitomycin A. *J. Am. Chem. Soc.*, 109, 7224, 1987.
10. Feigelson, G.B., Egbertson, M., Danishefsky, S.J., and Schulte, G., On the reaction of leucomitosenes with osmium tetroxide. A route to novel mitomycins. *J. Org. Chem.*, 53, 3390, 1988.
11. Tulinsky, A. and van den Hende, J.H., The crystal and molecular structure of n-brosylmitomycin A. *J. Am. Chem. Soc.*, 89, 2905, 1967.
12. Taylor, W.G. and Remers, W.A., Structures and stereochemistry of mitomycin hydrolysis products. *Tetrahedron Lett.*, 3483, 1974.
13. Rebek, J., Shaber, S.H., Shue, Y.K., Gehret, J.C., and Zimmerman, S., Total synthesis of a mitosene. *J. Org. Chem.*, 49, 5164, 1984.
14. Garrett, E.R., The physical chemical characterization of the products, equilibria, and kinetics of the complex transformations of the antibiotic porfiromycin. *J. Med. Chem.*, 6, 488, 1963.
15. Kinoshita, S., Uzu, K., Nakano, K., and Takahashi, T., Chemical transformations of mitomycins: Structure-activity relation of mitomycin derivatives. *Prog. Antimicrob. Anticancer Chemother.*, II, 112, 1970.

16. Underberg, W.J.M. and Lingeman, H., Aspects of chemical stability of mitomycin and porfiromycin in solution. *J. Pharm. Sci.*, 72, 549, 1974.
17. Schiltz, P. and Kohn, H., Studies on the reactivity of reductively activated mitomycin C. *J. Am. Chem. Soc.*, 115, 10510, 1993.
18. Hornemann, U., Ho, Y.-K., Mackey, Jr., J.K., and Srivastava, S.C., Studies on the mode of action of mitomycin antibiotics. Reversible conversion of mitomycin C into sodium 7-aminomitosane-9a-sulfonate. *J. Am. Chem. Soc.*, 98, 7069, 1976.
19. Han, I., Russell, D.J., and Kohn, H., Studies on the mechanism of mitomycin C(1) electrophilic transformations: Structure-activity relationships. *J. Org. Chem.*, 57, 1799, 1992.
20. Wang, S. and Kohn, H., Studies on the mechanism of activation of C(7) ethylenediamine substituted mitomycins. Relevance of the proposed mode of action of BMY-25067 and KW-2149. *Tetrahedron Lett.*, 37, 2337, 1996.
21. Wang, S. and Kohn, H., Mitomycin betaines: Synthesis, structure and solvolytic reactivity. *J. Org. Chem.*, 61, 9202, 1996.
22. Pan, S.-S., Andrews, P.A., Glover, C.J., and Bachur, N.R., Reductive activation of mitomycin C and mitomycin C metabolites catalyzed by NADPH-cytochrome P-450 reductase and xanthine oxidase. *J. Biol. Chem.*, 259, 959, 1984.
23. Danishefsky, S.J. and Egbertson, M., The characterization of intermediates in the mitomycin activation cascade: A practical synthesis of an aziridinomitosene. *J. Am. Chem. Soc.*, 108, 4648, 1986.
24. Hoey, B.M., Butler, J., and Swallow, A.J., Reductive activation of mitomycin C. *Biochemistry*, 27, 2608, 1988.
25. Kirsch, E.J. and Korshalla, J.D., Influence of biological methylation on the biosynthesis of mitomycin A. *J. Bacteriol.*, 87, 247, 1964.
26. Hornemann, U., James, P., Kehrer, J.P., Carmen, S., Nunez, C.S., and Ranieri, R.L., D-Glucosamine and L-citrulline, precursors in mitomycin biosynthesis by *Streptomyces verticillatus. J. Am. Chem. Soc.*, 96, 320, 1974.
27. Mao, Y., Varoglu, M., and Sherman, D.H., Mitomycin resistance in *Streptomyces lavendulae* includes a novel drug-binding-protein-dependent export system. *J. Bacteriol.*, 181, 2199, 1999.
28. Kim, C.G., Bergon, K.P., Ahn, Y., Wang, J.J., Shibuya, M., and Floss, H.G., Formation of 3-amino-5-hydroxybenzoic acid, the precursor of mC7 units in ansamycin antibiotics, by a new variant of the shikimate pathway. *J. Am. Chem. Soc.*, 111, 4941, 1992.
29. Sitachitta, N., Lopanik, N.B., Mao, Y., and Sherman, D.H., Analysis of a parallel branch in the mitomycin biosynthetic pathway involving the mitN-encoded aziridine N-methyltransferase. *J. Biol. Chem.*, 282, 20941, 2007.
30. Islam, I. and Skibo, E.B., Synthesis and physical studies of azamitosene and iminoazamitosene reductive alkylating agents. Iminoquinone hydrolytic stability, syn/anti isomerization, and electrochemistry. *J. Org. Chem.*, 55, 3195, 1990.
31. Islam, I., Skibo, E.B., Dorr, R.T., and Alberts, D.S., Structure-activity studies of antitumor agents based on pyrrolo[1,2-a]benzimidazoles: New reductive alkylating DNA cleaving agents. *J. Med. Chem.*, 34, 2954, 1991.
32. Huang, X., Suleman, A., and Skibo, E.B., Rational design of pyrrolo[1,2-a]benzimidazole based antitumor agents targeting the DNA major groove. *Bioorg. Chem.*, 28, 324, 2000.
33. Mercado, C.M. and Tomasz, M., Inhibitory effects of mitomycin-related compounds lacking the C1-C2 aziridine ring. *Antimicrob. Agents Chemother.*, 1, 73, 1972.
34. Szybalski, W. and Iyer, V.N., The mitomycins and porfiromycin, in *Antibiotics I, Mechanism of Action*, Gottlieb, D. and Shaw, P.D., Eds., Springer, New York, 1967, pp. 221–245.
35. Iyer, V.N. and Szybalski, W., Mode of interaction of mitomycin C with deoxyribonucleic acid and other polynucleotides *in vitro. Science*, 145, 55, 1964.
36. Tomasz, M., Mercado, C.M., Olson, J., and Chatterjie, N., Mode of interaction of mitomycin C with deoxyribonucleic acid and other polynucleotides *in vitro. Biochemistry*, 13, 4878, 1974.
37. Gustafson, D.L. and Pritsos, C.A., Kinetics and mechanism of mitomycin C bioactivation by xanthine dehydrogenase under aerobic and hypoxic conditions. *Cancer Res.*, 53, 5470, 1993.
38. Wang, X., Doherty, G.P., Leith, M.K., Curphey T.J., and Begleiter, A., Enhanced cytotoxicity of mitomycin C in human tumor cells with inducers of DT-diaphorase. *Br. J. Cancer*, 80, 1223, 1999.
39. Sagara, N. and Katoh, M., Mitomycin C resistance induced by TCF-3 overexpression in gastric cancer cell line MKN28 is associated with DT-diaphorase down regulation. *Cancer Res.*, 60, 5959, 2000.

40. Belcourt, M.F., Hodnick, W.F., Rockwell, S., and Sartorelli, A.C., Differential toxicity of mitomycin C and porfiromycin to aerobic and hypoxic Chinese hamster ovary cells overexpressing human NADPH:cytotcrome (P-540) reductase. *Proc. Natl. Acad. Sci. U.S.A.*, 93, 456, 1996.
41. Cowen, R.L., Garside, E.G., Fitzpatrick, B., Papadopoulou, M.V., and Williams, K.J., Gene therapy approaches to enhance bioreductive drug treatment. *Br. J. Radiol.*, 81 (Special Issue), S45, 2008.
42. Moore, H.W., Bioactivation as a model for drug design bioreductive alkylation. *Science*, 197, 527, 1977.
43. Li, V.-S., Choi, D., Tang, M.-S., and Kohn, H., Structural requirements for mitomycin C DNA binding. *Biochemistry*, 34, 7120, 1995.
44. Boruah, R.C. and Skibo, E.B., Mitomycin C redox couple pKa values studied by spectrophotometric titration, pH rate profiles, and Nernst-Clark plots. *J. Org. Chem.*, 60, 2232, 1995.
45. Tomasz, M., Lipman, R., McGuinness, B.F., and Nakanishi, K., Isolation and characterization of a major adduct between mitomycin C and DNA. *J. Am. Chem. Soc.*, 110, 5892, 1988.
46. Tomasz, M., Chawla, A.K., and Lipman, R., Mechanism of monofunctional and bifunctional alkylation of DNA by mitomycin C. *Biochemistry*, 27, 3182, 1988.
47. Tomasz, M., Lipman, R., Snyder, J.K., and Nakanishi, K., Full structure of a mitomycin C dinucleotide adduct. Use of differential FT-IR spectroscopy in microscale structural studies. *J. Am. Chem. Soc.*, 105, 2059, 1983.
48. Verdine, G.L. and Nakanishi, K., Use of differential second-derivative UV and FTIR spectroscopy in structural studies with multichromophoric compounds. *J. Am. Chem. Soc.*, 107, 6118, 1985.
49. Tomasz, M., Lipman, R., Verdine, G.L., and Nakanishi, K., Reassignment of the guanine-binding mode of reduced mitomycin C. *Biochemistry*, 25, 4337, 1986.
50. Tomasz, M., Chowdary, D., Lipman, R., Shimotakahara, S., Veiro, D., Walker, V., and Verdine, G.L., Reaction of DNA with chemically or enzymatically activated mitomycin C: Isolation and structure of the major covalent adduct. *Proc. Natl. Acad. Sci. U.S.A.*, 83, 6702, 1986.
51. Borowy-Borowski, H., Lipman, R., Chowdary, D., and Tomasz, M., Duplex oligodeoxyribonucleotides crosslinked by mitomycin C at a single site: Synthesis, properties, and crosslink. *Biochemistry*, 19, 2992, 1990.
52. Norman, B., Live, D., Sastry, M., Lipman, R., Hingerty, B.E., Tomasz, M., Broyde, S., and Patel, D.J., NMR and computational characterization of mitomycin cross-linked to adjacent deoxyguanosines in the minor groove of the d(TACGA).d(TACGA) duplex. *Biochemistry*, 29, 2861, 1990.
53. Weidner, M.F., Millard, J.T., and Hopkins, P.B., Determination at single-nucleotide resolution of the sequence specificity of DNA interstrand cross-linking agents in DNA fragments. *J. Am. Chem. Soc.*, 111, 9720, 1989.
54. Rao, S.N., Singh, U.C., and Kollman, P.A., Conformations of the noncovalent and covalent complexes between mitomycins A and C and $d(GCGCGCGCGC)_2$. *J. Am. Chem. Soc.*, 108, 2058, 1986.
55. McGuiness, B.F., Lipman, R., Goldstein, J., Nakanishi, K., and Tomasz, M., Reductive alkylation of DNA by mitomycin A, a mitomycin with high redox potential. *Biochemistry*, 30, 6444, 1991.
56. Remers, W.A., Rao, S.N., Wunz, T.P., and Kollman, P.A., Conformations of complexes between mitomycins and decanucleotides. 3. Sequence specificity, binding at C-10, and mitomycin analogs. *J. Med. Chem.*, 31, 1612, 1988.
57. Teng, S.P., Woodson, S.A., and Crothers, D.M., DNA sequence specificity for mitomycin crosslinking. *Biochemistry*, 28, 3901, 1989.
58. Borowy-Borowski, H., Lipman, R., and Tomasz, M., Recognition between mitomycin C and specific double-strand DNA sequences for cross-link formation. *Biochemistry*, 29, 2999, 1990.
59. Kumar, S., Johnson, W.S., and Tomasz, M., Orientation isomers of the mitomycin C interstrand cross-links in non-self-complementary DNA. Differential effect of two isomers on restriction endonuclease cleavage at a nearby site. *Biochemistry*, 32, 1364, 1993.
60. Kumar, S., Lipman, R., and Tomasz, M., Recognition of specific DNA sequences by mitomycin C for alkylation. *Biochemistry*, 31, 1399, 1992.
61. Li, V.-S., Choi, D., Wang, Z., Jimenez, L.S., Tang, M.-S., and Kohn, H., Role of the C-10 substituent in mitomycin C-1-DNA binding. *J. Am. Chem. Soc.*, 118, 2326, 1996.
62. Kohn, H., Li, V.S., Schiltz, P., and Tang, M.-S., On the origins of the DNA sequence selectivity of mitomycin monoalkylation transformations. *J. Am. Chem. Soc.*, 114, 9218, 1992.
63. Kumar, S.G., Lipman, R., Cummings, J., and Tomasz, M., Mitomycin C-DNA adducts generated by DT-diaphorase. Revised mechanism of the enzymatic reductive activation of mitomycin C. *Biochemistry*, 36, 14128, 1997.
64. Kumar, G.S., He, Q.-Y., Behr-Ventura, D., and Tomasz M., Binding of 2,7-diaminomitosene to DNA: Model for recognition of DNA by activated DNA. *Biochemistry*, 34, 2662, 1995.

65. Kumar, G.S., Musser, S.M., Cummings, J., and Tomasz, M., 2,7-Diaminomitosene, a monofunctional mitomycin C derivative, alkylates DNA in the major groove. Structure and base-sequence specificity of the DNA adduct and mechanism of alkylation. *J. Am. Chem. Soc.*, 118, 9209, 1996.
66. Palom, Y., Kumar, G.S., Tang, L.-Q., Paz, M.P., Musser, S.M., Rockwell, S., and Tomasz, M., Relative toxicities of DNA cross-links and monoadducts: New insights from studies of decarbamoyl mitomycin C and mitomycin C. *Chem. Res. Toxicol.*, 15, 1398, 2002.
67. Gargulio, D., Musser, S.M., Yang, L., Fukuyama, T., and Tomasz, M., Alkylation and crosslinking of DNA by the unnatural enantiomer of mitomycin C: Mechanism of the DNA-sequence specificity of mitomycins. *J. Am. Chem. Soc.*, 117, 9388, 1995.
68. Maliepaard, M., de Mol, N.J., Tomasz, M., Gargiulo, D., Janssen, L.H.M., van Duynhoven, J.P.M., van Velzen, E.J.J., Verboom, W., and Reinhoudt, D.N., Mitosene-DNA adducts. Characterization of two major DNA adducts formed by 1,10-bis(acetoxy)-7-methoxymitosene upon reductive activation. *Biochemistry*, 36, 9211, 1997.
69. Ouyang, A. and Skibo, E., The iminium ion chemistry of mitosene DNA alkylating agents. Enriched ^{13}C-NMR studies. *Biochemistry*, 39, 5718, 2000.
70. Xing, C. and Skibo, E.B., Sigmatropic reactions of the aziridinyl semiquinone species. Why aziridinyl benzoquinones are metabolically more stable than aziridinyl indoloquinones. *Biochemistry*, 39, 10770, 2000.
71. Millard, J.T. and Beachy, T.M., Selective recognition of m5Cpg dinucleotide sequence in DNA by mitomycin C for alkylation and crosslinking. *Biochemistry*, 32, 12850, 1993.
72. Tomasz, M., Das, A., Tang, K.S., Ford, M.G.J., Minnock, A., Musser, S.M., and Waring, M.J., The purine 2-amino group as the critical recognition element for sequence-specific alkylation and crosslinking of DNA by mitomycin C. *J. Am. Chem. Soc.*, 120, 11581, 1998.
73. Sharma, M. and Tomasz, M., Conjugation of glutathione and other thiols with bioreductively activated mitomycin C. Effect of thiols on reductive activation rate. *Chem. Res. Toxicol.*, 7, 390, 1994.
74. Sharma, M., He, Q.-Y., and Tomasz, M., Effects of glutathione on alkylation and crosslinking of DNA by mitomycin C. Isolation of a ternary glutathione-mitomycin-DNA adduct. *Chem. Res. Toxicol.*, 7, 401, 1994.
75. Xu, B.H., Gupta, V., and Singh, S.V., Mitomycin sensitivity in human bladder cancer cells: Possible role of glutathione and glutathione transferase in resistance. *Arch. Biochem. Biophys.*, 308, 164, 1994.
76. Basu, A.K., Hanrahan, C.J., Malia, S.A., Kumar, S., Bizanek, R., and Tomasz, M., Effect of site specifically located mitomycin C-DNA monoadducts on *in vitro* DNA synthesis by DNA polymerases. *Biochemistry*, 32, 4708, 1993.
77. Abbas, T., Olivier, M., Lopez, J., Houser, S., Xiao, G., Kumar, G.S., Tomasz, M., and Bargonetti, J., Differential activation of p53 by the various adducts of mitomycin C. *J. Biol. Chem.*, 277, 40513, 2002.
78. Skibo, E.B. and Schultz, W.G., Pyrrolo[1,2-a]benzimidazole based aziridinyl quinones. *J. Med. Chem.*, 36, 3050, 1993.
79. Schultz, W.G., Nieman, R.A., and Skibo, E.B., Evidence for DNA phosphate backbone alkylation and cleavage by pyrrolo[1,2-a]benzimidazoles, small molecules capable of causing sequence specific phosphodiester bond hydrolysis. *Proc. Natl. Acad. Sci. U.S.A.*, 92, 11854, 1995.
80. Bachur, N.R., Gordon, S.L., and Gee, M.V., A general mechanism for microsomal activation of quinone anticancer agents to free radicals. *Cancer Res.*, 38, 1745, 1978.
81. Tomasz, M., Hydrogen peroxide generation during the redox cycle of mitomycin C and DNA-bound mitomycin C. *Chem. Biol. Interact.*, 13, 89, 1976.
82. Lown, J.W., The molecular mechanism of antitumor action of the mitomycins, in *Mitomycin C, Current Status and New Developments*, Carter, S.T. and Crooke, S.T., Eds., Academic Press, Orlando, FL, 1979, pp. 5–26.
83. Ueda, K., Morita, J., Yamashita, K., and Komano, T., Inactivation of bacteriophage NX174 by mitomycin C in the presence of sodium hydrosulfite and cupric ions. *Chem. Biol. Interact.*, 29, 145, 1980.
84. Pan, S.-S., Andrews, P.A., and Bachur, N.R., Reduction of mitomycin C by NADPH cytochrome p450 reductase and xanthine oxidase. *Fed. Proc.*, 41, 1541, 1982.
85. Hashimoto, Y., Shudo, K., and Okamoto, T., Structures of modified nucleotides isolated from calf thymus DNA alkylated with reductively activated mitomycin C. *Tetrahedron Lett.*, 23, 677, 1982.
86. Pritsos, C.A. and Sartorelli, A.C., Generation of reactive oxygen radicals through bioactivation of mitomycin antibiotics. *Cancer Res.*, 46, 3528, 1986.
87. Remers, W.A. and Dorr, R.T., Chemistry, biology, and therapeutics of the mitomycins, in *The Alkaloids: Chemical and Biological Perspectives*, Pelletier, S.W., Ed., Wiley, New York, 1988, Vol. 6, pp. 1–74.

88. Kinoshita, S., Uzu, K., Nakano, K., Shimizu, M., Takahashi, T., and Matsui, M., Mitomycin derivatives. 1. Preparation of mitosane and mitosene compounds and their biological activities. *J. Med. Chem.*, 14, 103, 1971.
89. Kinoshita, S., Uzu, K., Nakano, K., and Takahashi, T., Mitomycin derivatives. 2. Derivatives of decarbamoylmitosane and decarbamoylmitosene. *J. Med. Chem.*, 14, 109, 1971.
90. Kojima, R., Driscoll, J., Mantel, N., and Goldin, A., Some structure-activity relationships for mitomycin C (NSC-26980) derivatives in the treatment of l1210 leukemia. *Cancer Chemother. Rep.*, 3, 121, 1972.
91. Iyengar, B.S., Sami, S.M., Remers, W.A., Bradner, W.T., and Schurig, J.E., Mitomycin C and porfiromycin analogs with substituted ethylamines at position 7. *J. Med. Chem.*, 26, 16, 1983.
92. Imai, R., Ashizawa, T., Urakawa, C., Morimoto, M., and Nakamura, N., Antitumor activity of 7-N-phenyl derivatives of mitomycin C in the leukemia p388 system. *Gann.*, 71, 560, 1980.
93. Iyengar, B.S., Lin, H.-J., Cheng, L., Remers, W.A., and Bradner, W.T., Development of new mitomycin C and porfiromycin analogs. *J. Med. Chem.*, 24, 975, 1981.
94. Iyengar, B.S., Sami, S.M., Tarnow, S.E., Remers, W.A., Bradner, W.T., and Schurig, J.E., Mitomycin C analogs with secondary amines at position 7. *J. Med. Chem.*, 26, 1453, 1983.
95. Sami, S.M., Iyengar, B.S., Tarnow, S.E., Remers, W.A., Bradner, W.T., and Schurig, J.E., Mitomycin C analogs with aryl substituents on the 7-amino group. *J. Med. Chem.*, 27, 701, 1984.
96. Iyengar, B.S., Takahashi, T., Remers, W.A., and Bradner, W.T., Metal complexes of mitomycins. *J. Med. Chem.*, 29, 144, 1986.
97. Kunz, K.R., Iyengar, B.S., Dorr, R.T., Alberts, D.S., and Remers, W.A., Structure-activity relationships for mitomycin C and mitomycin A analogs. *J. Med. Chem.*, 34, 2281, 1991.
98. Ishioka, C., Kanumara, R., Konishi, Y., Ishikawa, A., Shibata, H., and Wakui, A., Comparative studies on the action of 7-N-[2-[[2-(-L-glutamylamino)ethyl]dithio]ethyl]mitomycin C and of mitomycin C on cultured NL60-cells and isolated phage and plasmid DNA. *Cancer Chemother. Pharmacol.*, 26, 117, 1990.
99. Bradner, W.T., Rose, W.C., Schurig, J.E., and Florczyk, A.P., Antitumor activity and toxicity in animals of N-7[2-(4-nitrophenyldithio)ethyl]mitomycin C (BMY-25067). *Invest. New Drugs*, 8(Suppl.), S1, 1990.
100. Bradner, W.T., Rose, W.C., Schurig, J.E., Schlein, A., and Huftalen, J.B., Antitumor activity and toxicity in animals of RR-150 (7-cysteaminomitosane), a new mitomycin derivative. *Cancer Res.*, 44, 5619, 1984.
101. Sami, S.M., Iyengar, B.S., Remers, W.A., and Bradner, W.T., Preparation and antitumor activity of new mitomycin A analogs. *J. Med. Chem.*, 30, 168, 1987.
102. Li, V.-S., Choi, D., Wang, Z., Jimenez, L.S., Tang, M.-S., and Kohn, H., The role of the C-10 substituent in mitomycin C-1-DNA bonding. *J. Am. Chem. Soc.*, 118, 2326, 1996.
103. Takanagi, H., Oshima, J., Furuhata, K., Takeda, K., Ogura, H., Komiyama, K., and Hata, T., One step preparation of 6-demethyl-6-formylmitomycin C and cytotoxicity of its derivatives. *J. Antibiot. (Tokyo), Ser. A*, 45, 1815, 1992.
104. Iyengar, B.S., Remers, W.A., and Bradner, W.T., Preparation and antitumor activities of 7-substituted-1-,2-aziridinomitosenes. *J. Med. Chem.*, 29, 1864, 1986.
105. Fost, D.L., Ekwuribe, N.N., and Remers, W.A., Synthesis of 1-substituted-7-methoxymitosenes. *Tetrahedron Lett.*, 131, 1973.
106. Taylor, W.G., Leadbetter, G., Fost, D.L., and Remers, W.A., Mitomycin antibiotics. Synthesis and antineoplastic activity of mitosene analogs of the mitomycins. *J. Med. Chem.*, 20, 138, 1977.
107. Casner, M.L., Remers, W.A., and Bradner, W.T., Synthesis and biological activity of 6-substituted analogs of the mitomycins. *J. Med. Chem.*, 28, 921, 1985.
108. Hodges, J.C., Remers, W.A., and Bradner, W.T., Synthesis and antineoplastic activity of mitosene analogs of the mitomycins. *J. Med. Chem.*, 24, 1184, 1981.
109. Allen, Jr., G.R., Poletto, J.F., and Weiss, M.J., The mitomycin antibiotics. Synthetic studies. II. Synthesis of 7-methoxymitosene, an antibacterial agent. *J. Am. Chem. Soc.*, 86, 3878, 1964.
110. Allen, Jr., G.R. and Weiss, M.J., The mitomycin antibiotics. Synthetic studies. XV. The preparation of a related indoloquinone. *J. Med. Chem.*, 10, 1, 1967.
111. Allen, Jr., G.R. and Weiss, M.J., The mitomycin antibiotics. Synthetic studies XVII. Preparation of 1-(β-substituted ethyl)indoloquinone analogs. *J. Med. Chem.*, 10, 23, 1967.
112. Remers, W.A., Roth, R.H., and Weiss, M.J., The mitomycin antibiotics. Synthetic studies. VIII. Indoloquinone analogs with variations at C-5. *J. Org. Chem.*, 31, 1012, 1966.
113. Iwata, H. and Goldberg, E.P., Tissue-binding macromolecular antitumor drugs for localized therapy: Mitomycin C-concanavalin A conjugates. *Polymer Reprints*, 24, 73, 1983.

114. Kaneko, Y., Tanaka, T., and Iguchi, S., Preparation and properties of a mitomycin C-albumin conjugate. *Chem. Pharm. Bull.*, 38, 2614, 1990.
115. Umemoto, N., Kato, Y., Takeda, Y., Saito, M., and Hara, T., Conjugates of mitomycin C with the immunoglobulin M monomer fragment of a monoclonal anti-MM46 immunoglobulin M antibody with or without serum albumin as intermediary. *J. Appl. Biochem.*, 6, 297, 1984.
116. Tsukada, Y., Characterization of human AFP producing stomach cancer xenotransplanted in nude mice and the effect of mitomycin C and antibody to human AFP of this tumor. *Nippon Shokakibyo Gakki Zasshi*, 82, 18, 1985.
117. Li, S., Zhang, X., Zhang, S., Chen, X., Chen, L., Shu, Y., Zhang, J., and Fan, D., Preparation of antigastric cancer monoclonal antibody MGb2-mitomycin C conjugate with improved antitumor activity. *Bioconjugate Chem.*, 1, 245, 1990.
118. Tanaka, J.-I., Sato, E., Saito, Y., Kusano, T., and Koyama, K., Preparation of a conjugate of mitomycin C and anti-neural cell adhesion molecule monoclonal antibody for specific chemotherapy against biliary tract carcinoma. *Surg. Today*, 28, 1217, 1998.
119. Huh, N., Rege, A.A., Yoo, B., Kogan, T.P., and Kohn, H., Design, synthesis, and evaluation of mitomycin-tethered phosphorothioate oligodeoxynucleotides. *Bioconjugate Chem.*, 7, 659, 1996.
120. Paz, M.M., Das, A., and Tomasz, M., Mitomycin C linked to minor groove binding agents: Synthesis, reductive activation, DNA binding and cross-linking properties and *in vitro* antitumor activity. *Bioorg. Med. Chem.*, 7, 2713, 1999.
121. Okamoto, H., Tsukahara, H., Hashida, M., and Sezaki, H., Effect of 1-alkyl or 1-alkenyl-azocycloalkanone derivatives on penetration of mitomycin C through rat skin. *Chem. Pharm. Bull.*, 35, 4605, 1987.
122. Shikano, M., Onimura, K., Fukai, Y., Hori, M., Fukazawa, H., Mizuno, S., Yazawa, K., and Uehara, Y., 1a-Docosahexaenoyl mitomycin C: A novel inhibitor of protein tyrosine kinase. *Biochem. Biophys. Res. Commun.*, 248, 858, 1998.
123. Nagai, K., Tanaka, J., Kiho, T., and Ukai, S., Synthesis and antitumor activities of mitomycin C (1–3)-beta-D-glucan conjugate. *Chem. Pharm. Bull.*, 40, 986, 1992.
124. Ghiorghis, A., Talebaum, A., and Clarke, R., *In vitro* antineoplastic activity of C-7-substituted mitomycin C analogs MC-77 and MC-62 against human breast-cancer cell lines. *Cancer Chemother. Pharmacol.*, 29, 290, 1992.
125. Yan, Z., et al., Synthesis of the anticancer drug mitomycin C-dextran conjugate with affinity to lymph and studies on its biological properties. *Zhongguo Yaowu Huaxue Zashi*, 9, 240, 1999.
126. Hoste, K., Schacht, E., and Rihova, B., Synthesis and biological evaluation of PEG-substituted macromolecular prodrugs from mitomycin C. *J. Bioact. Compat. Polym.*, 17, 123, 2002.
127. Kato, Y., Onishi, H., and Machida, Y., A novel water-soluble N-succinyl-chitosan-mitomycin C conjugate prepared by direct carbodiimide coupling: Physicochemical properties, antitumor characteristics, and systemic retention. *S.T.P. Pharma Sci.*, 10, 133, 2000.
128. Gabizon, A., Tzemach, D., Horowitz, A.T., Shmeeda, H., and Zalipsky, S., Reduced toxicity and superior therapeutic activity of a mitomycin-C lipid-based prodrug incorporated in pegylated liposomes. *Clin. Cancer Res.*, 12, 1913, 2006.
129. Iyengar, B.S., Dorr, R.T., Remers, W.A., and Kowal, C.D., Nucleotide derivatives of 2,7-diaminomitosene. *J. Med. Chem.*, 31, 1579, 1988.
130. Iyengar, B.S., Dorr, R.T., and Remers, W.A., Additional nucleotide derivatives of mitosenes. Synthesis and activity against parenteral and multidrug resistant L1210 leukemia. *J. Med. Chem.*, 34, 1947, 1991.
131. Bradner, W.T., Remers, W.A., and Vyas, D.M., Structure-activity comparison of mitomycin C and mitomycin A analogs. *Anticancer Res.*, 9, 1095, 1989.
132. Bradner, W.T., Rose, W.C., Schurig, J.E., Florczyk, A.P., Huftalen, J.B., and Catino, J.J., Antitumor activity and toxicity in animals of BMY-25282, a new mitomycin derivative. *Cancer Res.*, 45, 6475, 1985.
133. Remers, W.A., Mitomycins, in *Anticancer Agents Based on Natural Product Models*, Cassady, J.M. and Douros, J.D., Eds., Academic Press, New York, 1980, chapter 4.
134. Orlamans, E.O., Verboom, W., Scheltinga, M.W., Reinhoudt, D.N., Lelieveld, P., Fiebig, H.H., Winterhalter, B.R., Double, J.A., and Bibby, M.C., Synthesis, mechanism of action, and biological evaluation of mitosenes. *J. Med. Chem.*, 32, 1612, 1989.
135. Weiss, M.J., Redin, G., Allen, G., Dornbush, A., Lindsay, H., Poletto, J., Remers, W., Roth, R., and Slobada, A., The mitomycin antibiotics. Synthetic studies. XXII. Antibacterial structure-activity relationships in the indoloquinone series. *J. Med. Chem.*, 11, 742, 1968.
136. Allen, Jr., G.R., Poletto, J.F., and Weiss, M.J., Mitomycin antibiotics. Synthetic studies. III. Related indoloquinones, active antibacterial agents. *J. Am. Chem. Soc.*, 86, 3878, 1964.

137. Allen, Jr., G.R., Poletto, J.F., and Weiss, M.J., Mitomycin antibiotics, Synthetic studies. XVII. Indoloquinones with variants at the 2 position. *J. Org. Chem.*, 30, 2897, 1965.
138. Poletto, J.F., Allen, Jr., G.R., and Weiss, M.J., Mitomycin antibiotics. Synthetic studies. XIX. Synthesis of indoloquinone analogs with certain C-3 variants. *J. Med. Chem.*, 10, 95, 1967.
139. Leadbetter, G., Fost, D.L., Ekwuribe, N.N., and Remers, W.A., Mitomycin antibiotics. Synthesis of 1-substituted 7-methoxymitosenes. *J. Org. Chem.*, 39, 3580, 1974.
140. Hirata, T., Yamada, Y., and Matsui, M., Synthetic studies on mitomycins. Synthesis of aziridinopyrrolo[1,2-a]indoles. *Tetrahedron Lett.*, 19, 1969.
141. Siuta, G.J., Franck, R.W., and Kempton, R.J., Studies directed toward a mitomycin synthesis. *J. Org. Chem.*, 39, 3739, 1974.
142. Kametani, T., Ohsawa, T., Takahashi, K., Ihara, M., and Fukumoto, K., Photooxygenation of 9-keto-7-methoxy-6-methyl-9H-pyrrolo[1,2-a]indole as a synthetic approach to mitomycins. *Heterocycles*, 4, 1637, 1976.
143. Nakatsubo, F., Fukuyama, T., Cocuzza, A.J., and Kishi, Y., Synthetic studies toward mitomycins. 2. Total synthesis of dl-porfiromycin. *J. Am. Chem. Soc.*, 99, 8115, 1977.
144. Fukuyama, T., Nakatsubo, F., Cocuzza, A.J., and Kishi, Y., Synthetic studies toward mitomycins. III. Total synthesis of mitomycins A and C. *Tetrahedron Lett.*, 4295, 1977.
145. Fukuyama, T. and Yang, L., Practical synthesis of (±)-mitomycin C. *J. Am. Chem. Soc.*, 111, 8303, 1989.
146. Danishefsky, S., Chemical explorations driven by an enchantment with mitomycinoids—A twenty year account. *Synlett*, 475, 1995.
147. Benbow, J.W., McClure, K.F., and Danishefsky, S.J., Intramolecular cycloaddition reactions of dienyl nitroso compounds: Application to the synthesis of mitomycin K. *J. Am. Chem. Soc.*, 115, 12305, 1993.
148. McClure, K.F. and Danishefsky, S.J., A novel Heck arylation reaction: Rapid access to congeners of FR 900482. *J. Am. Chem. Soc.*, 115, 6094, 1993.
149. Andrez, J-C., Mitomycins syntheses: A recent update. *Beilstein J. Org. Chem*., 5, 33, 2009.
150. Moertel, C.G., Reitemeir, R.J., and Hahn, R.G., Mitomycin C therapy in advanced gastrointestinal cancer. *J. Am. Med. Assoc.*, 204, 1045, 1968.
151. Doll, D.C., Weiss, R.B., and Issel, B.F., Mitomycin: Ten years after approval for marketing. *J. Clin. Oncol.*, 3, 276, 1985.
152. Miller, T.P., McMahon, L.J., and Livingston, R.B., Extensive adenocarcinoma and large cell undifferentiated carcinoma of the lung treated with 5-FU, vincristine, and mitomycin C. *Cancer Treat. Rep.*, 64, 1241, 1980.
153. Crooke, S.T. and Bradner, W.T., Mitomycin C: A review. *Cancer Treat. Rev.*, 3, 121, 1976.
154. Early, K., Elias, E.G., Mittelman, A., Albert, D., and Murphy, G.P., Mitomycin C in the treatment of metastatic transitional cell carcinoma of urinary bladder. *Cancer Chemother. Pharmacol.*, 31, 1150, 1973.
155. Baker, L.H., Opipari, M.I., and Izbicki, R.M., Phase II study of mitomycin C, vincristine, and bleomycin in advanced squamous cell carcinoma of the uterine cervix. *Cancer Chemother. Pharmacol.*, 38, 2222, 1976.
156. Rewari, A.N., Haffty, B.G., Wilson, L.D., Son, Y.H., Joe, J.K., Ross, D.A., and Papac, R.J., Postoperative concurrent chemoradiotherapy with mitomycin in advanced squamous cell carcinoma of the head and neck: Results from three prospective randomized trials. *Cancer J.*, 12, 123, 2006.
157. MacDonald, J., Schein, P., Ueno, W., and Wooley, P., 5-Fluorouracil (5-FU), mitomycin C (MMC), and Adriamycin (ADR)—FAM: A new combination chemotherapy program for advanced gastric carcinoma (abstract C-11). *Proc. Am. Soc. Clin. Oncol.*, 17, 244, 1976.
158. Dorr, R.T. and Von Hoff, D.D. *Cancer Chemotherapy Handbook*. Appleton and Lange, Norwalk, CT, 1994, 719 pp.
159. Kaplan, M.A. and Vyas, D.M., Crystalline 7-(dimethylaminomethylene)-amino-9a-methoxymitosane. *Ger. Offen. DE*, 3605, 523, 1986.
160. Senter, P.D., Langley, D.R., Manger, W.E., and Vyas, D.M., Reassignment of the structure of the antitumor agent RR-150. *J. Antibiot. (Tokyo), Ser. A*, 41, 199, 1988.
161. Vyas, D.M., Chiang, Y., Benigni, D., Rose, W.C, Bradner, W.T., and Doyle, T.W., Novel disulfide mitosanes as antitumor agents, *Proceedings of the 14th International Congress of Chemotherapy*, *Kyoto, Japan*, *1985*, University of Tokyo Press, Tokyo, Anticancer Section 1, 1986, pp. 485–486.
162. DeBoer, C., Dietz, A., Lummus, N.E., and Savage, G.M. Porfiromycin, a new antibiotic *Antimicrobial Agents Annual, 1960*, Plenum Press, New York, 1961, 17 pp.

24 Staurosporines and Structurally Related Indolocarbazoles as Antitumor Agents*

Michelle Prudhomme

CONTENTS

24.1 Introduction 647
24.2 Mechanisms of Action 649
24.2.1 Staurosporine and UCN-01 649
24.2.2 K-252a 651
24.2.3 Rebeccamycin 651
24.2.4 AT2433-A1 and B1 651
24.3 Total Syntheses of the Natural Products 651
24.4 Development of Drugs from the Natural Products 654
24.5 Clinical Applications 660
24.6 Conclusions 660
Update 661
References 663

24.1 INTRODUCTION

Bacteria and primitive organisms are important sources of various compounds of biological interest. Among the diversity of bacterial metabolites are maleimido- or maleamido-indolocarbazoles. Some of them do not bear any sugar moiety (arcyriaflavins, tjipanazole J, K-252c, and BE-13793C), and others have a carbohydrate moiety linked to only one indole nitrogen (rebeccamycin, AT2433-A1, and AT2433-B1) or to both indole nitrogens (staurosporines, K-252a, and K-252b) (Figure 24.1).[1–6] Staurosporine was isolated from *Streptomyces staurosporeus*[7,8] in 1977, and three years later, arcyriaflavins were obtained from the fruiting bodies of slime molds *Arcyria denudata*.[9] Later, more than 30 microbial staurosporine analogs were isolated from bacterial cultures. Indolocarbazoles have attracted considerable interest since the discovery in 1986 of the inhibitory properties of staurosporine toward protein kinase C (PKC), a kinase involved in many signal transduction pathways leading to a variety of cell responses, such as cell proliferation, differentiation, and gene expression.[10] K-252a and analogs bearing a five-membered ring sugar moiety have been isolated from *Nocardiopsis* and *Streptomyces* species, and they are also PKC inhibitors.[11–13] Staurosporine is a nonselective adenosine triphosphate (ATP)-competitive kinase inhibitor that inhibits the different PKC isoenzymes,

* This chapter has been updated by David J. Newman, Natural Products Branch, Developmental Therapeutics Program, Division of Cancer Treatment and Diagnosis, National Cancer Institute, Frederick, MD.

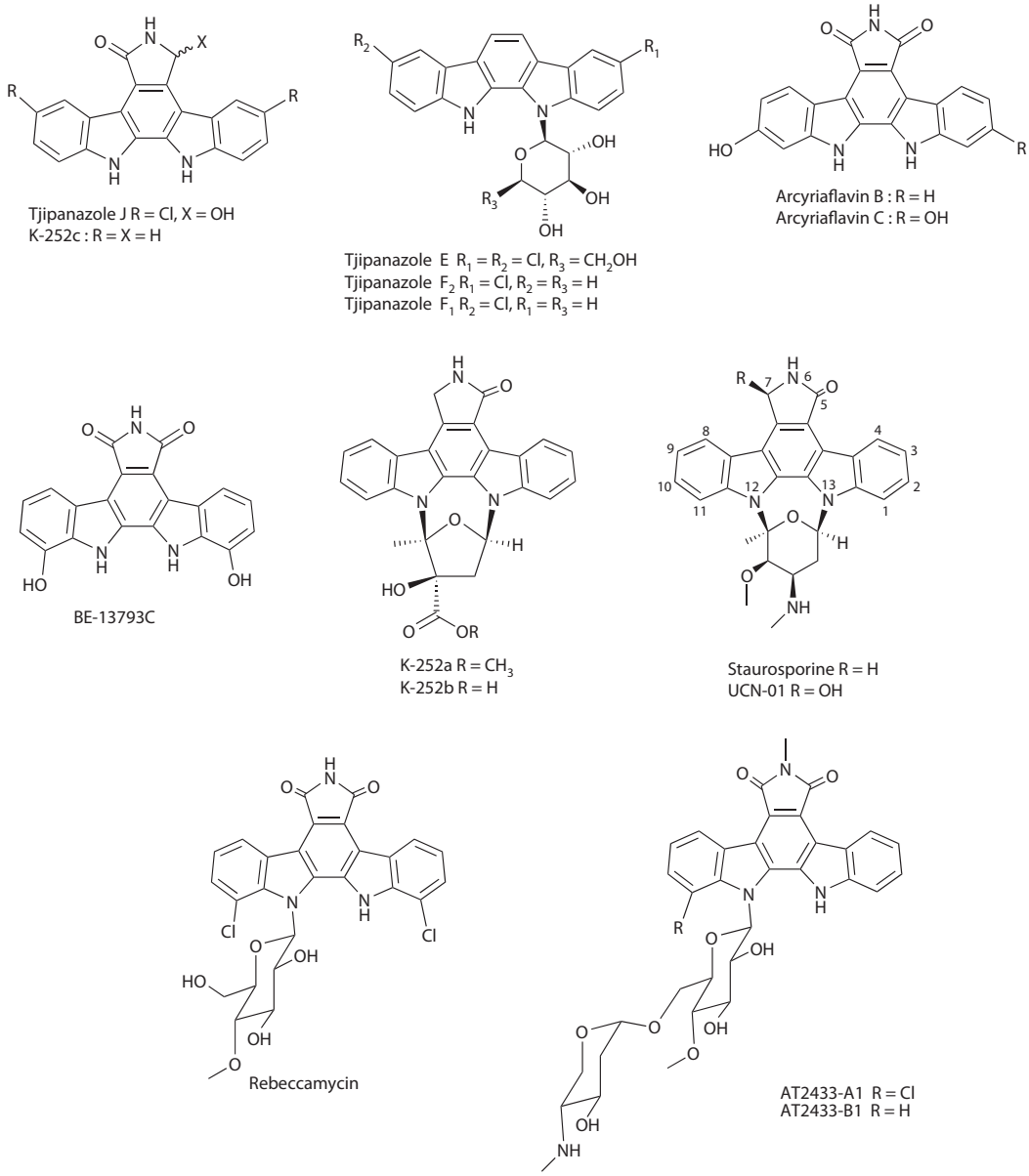

FIGURE 24.1 Indolocarbazoles from natural sources.

cyclin-dependent kinases (CDKs), and tyrosine kinases involved in cell proliferation.[14–17] More recently, it has been shown that UCN-01, a 7-hydroxy staurosporine isolated from cultures of a *Streptomyces* strain,[18] abrogates cell-cycle arrest caused by DNA damage. This results in premature activation of mitosis in DNA-damaged cells, which leads to cell death.[19,20]

The cytotoxicity of rebeccamycin and BE-13793C is linked to their capacity to inhibit topoisomerases, nuclear enzymes that control the topological state of DNA and are involved in various vital processes such as replication and transcription. Rebeccamycin is only a topoisomerase I inhibitor, whereas BE-13793C inhibits both topoisomerase I and II.[21,22] The antibiotics, AT2433-A1 and -B1, structurally related to rebeccamycin, do not inhibit topoisomerases, and their cytotoxicity may be a consequence of their tight intercalative binding to DNA.[23] Because of the promising biological

activities of indolocarbazoles, large structure–activity relationship studies were carried out, which led to the discovery of more potent and more selective molecules. In this chapter, only indolocarbazole compounds bearing a sugar moiety are described.

24.2 MECHANISMS OF ACTION

24.2.1 Staurosporine and UCN-01

Staurosporine, initially described as a PKC inhibitor, proved to be a potent and nonselective ATP-competitive kinase inhibitor. It strongly inhibits serine/threonine kinases such as PKC, PKA, PKG, CDKs, CaMK, MLCK, S6-kinase, ERK-1, and aurora kinases, as well as tyrosine kinases, such as PDGFR, c- and v-Src, EGFR, and many others.[14,24,25] The majority of them are extremely sensitive to staurosporine, with IC_{50} values in the low nanomolar range. The crystal structure of staurosporine in complex with the cyclin-dependent kinase 2 (CDK2) provides insight into the interactions with a variety of kinases. The carbonyl and the NH of the lactam heterocycle seem to be always involved in hydrogen bonds with amino acid residues of all kinases (Figure 24.2).[26] Staurosporine has also been cocrystallized with cAMP-dependent protein kinase PKA and Src tyrosine kinase CSK.[27,28]

More interesting is UCN-01, which exhibits greater selectivity toward protein kinases. UCN-01 inhibits "classic" PKC isoenzymes but has no effect against the "atypical" PKC isoforms, which are only activated on their regulatory domain by phosphatidylserine and phosphatidylinositol-3,4,5-triphosphate.[29] UCN-01 inhibits the growth of various human tumor cell lines. In contrast to staurosporine, UCN-01 is a relatively nonpotent direct inhibitor of CDK1 and CDK2, and it induces

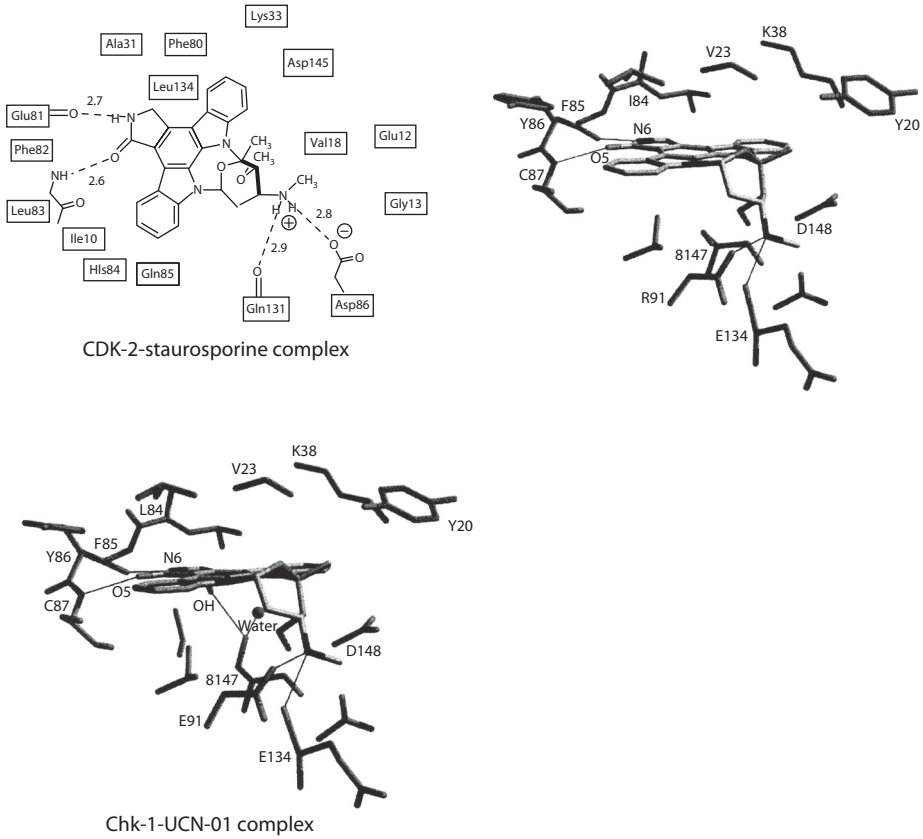

FIGURE 24.2 **(See color insert.)** Crystal structures of staurosporine and UCN-01 complexes with kinases.

preferential G1-phase accumulation and reduction of cellular CDK2 activity by preventing the phosphorylation of Thr160 residue.[30–32] Moreover, UCN-01 abrogates G2 and S checkpoints.[33,34] In the cell cycle of normal cells, three principal checkpoints can be activated in response to DNA damage in the G1, S, and G2 phases. These checkpoints control the ability of cells to arrest the cell cycle, allowing time to repair the DNA. The G1 checkpoint allows DNA repair before DNA replication, the S checkpoint is involved in replication fork regulation, and the G2 checkpoint allows DNA repair before mitosis. The G1 checkpoint is dependent on the activity of p53. The *p53* gene is mutated in nearly half of all human malignancies and in large proportions of premalignant precursor lesions.[35–37] In p53-mutated cancer cells, the G1 checkpoint is lacking, and the G2 checkpoint provides cancer cells with the opportunity to repair their DNA after damage. The combination of a DNA-damaging agent with molecules that can abrogate S and G2 arrest would enhance cytotoxicity selectively in the tumor cells. The arrest in the G2 phase after DNA damage seems to be mediated by Chk1 kinase inhibition.

In the presence of DNA damage, Chk1 is activated by phosphorylation by ATM or ATR (Figure 24.3). Chk1 then phosphorylates and inactivates the Cdc25C phosphatase, thereby preventing activation of the cyclinB1/CDK1 mitotic complex through phosphorylation of Thr-14 and Tyr-15 residues controlled by Wee-1 kinase and Cdc25C phosphatase. Because Wee-1 kinase is relatively resistant to UCN-01,[14,38] this staurosporine analog should inhibit one or several kinases that phosphorylates Cdc25C on the Ser-16 residue (Chk1, Chk2, and cTAK1).[39] It has been shown that UCN-01 inhibits Chk1 and cTAK1 with IC_{50} values of 11 and 27 nM, respectively.[33] Initially, it was suggested that Chk2 was weakly inhibited by UCN-01 (IC_{50}: 1040 nM). A more recent report has shown that UCN-01 efficiently inhibits both Chk1 and Chk2 kinase activity immunoprecipitated from human colon carcinoma HCT116 cells (IC_{50}: about 10 nM); however, inhibition of recombinant Chk2 requires much higher concentrations of UCN-01 (IC_{50}: about 300 nM).[40] In p53 mutant cells, low concentrations of UCN-01 caused S-phase cells to progress to G2 before undergoing mitosis and death, whereas high concentrations caused a direct S-to-M premature mitosis.[34] X-ray structures of Chk1 in complex with staurosporine and UCN-01 have been determined. Both compounds bind in the ATP-binding pocket of the kinase (Figure 24.2).[41] The selectivity of UCN-01 toward Chk1 over CDKs can be a result of the interaction of the hydroxyl group on the lactam heterocycle with the ATP-binding pocket. The inhibition activities of UCN-01 and staurosporine (Ki,app) against Chk1, CDK1, CDK2, and CDK4 have been determined. The Ki,app values for UCN-01 in nanomoles are 5.6, 95, 30, and 3600, respectively, and for staurosporine, the values are

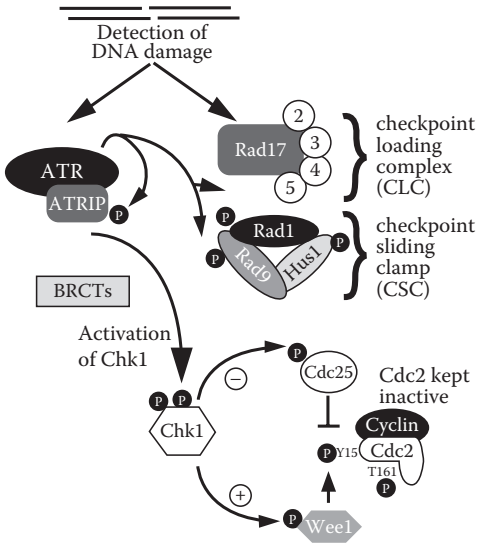

FIGURE 24.3 Activation of Chk1.

7.8, 1.0, 2.9, and 41, respectively.[41] An additional target for the apoptosis-modulating activity of UCN-01 has recently been identified. UCN-01 inhibits 3-phosphoinositide-dependent protein kinase 1 (PDK1), which plays a central role in the regulation of the Akt-PKB survival pathway by phosphorylating Akt on Thr208 residue.[42] The PDK1-Akt survival pathway represents a new and attractive target for cancer chemotherapy.

24.2.2 K-252a

K-252a was originally identified as a PKC inhibitor, but its effects are wide-ranging and include tyrosine kinase receptor TrkA and MLK3 inhibition and activation of PI3K and MEK-signaling pathways. It also induces cell cycle arrest and apoptosis by inhibiting CDK1 and Cdc25C.[11,43–45]

24.2.3 Rebeccamycin

Rebeccamycin was isolated in 1987 from cultures of *Saccharothrix aerocolonigenes*.[46] Its antiproliferative activity against various tumor cell lines is linked to its ability to inhibit topoisomerase I.[47] Although rebeccamycin is structurally related to staurosporine, the biological targets of these microbial metabolites are quite different. Rebeccamycin is inactive against PKC, PKA, and topoisomerase II but inhibits topoisomerase I,[21] whereas staurosporine is a nonselective kinase inhibitor without activity against topoisomerases. Like camptothecin, rebeccamycin is a topoisomerase I poison, stabilizing the enzyme–DNA interaction in the form of a covalent intermediate called "cleavable complex" and preventing the religation of the cleaved DNA strand.[48] More potent and soluble rebeccamycin analogs were prepared either by semisynthesis from rebeccamycin or by total synthesis.[49–51]

24.2.4 AT2433-A1 and B1

AT2433-A1 and B1 (Figure 24.1) have been isolated from cultures of *Actinomadura melliaura*, with two other molecules bearing a primary amine instead of the methylamino group on the deoxysugar moiety.[52] Their antitumor activity was evaluated against transplantable mouse leukemia P388. AT2433-A1 was at least eight times more potent than AT2433-B1. Their cytotoxicity may be a consequence of their tight intercalative binding to DNA, preferentially to GC-rich sequences, but contrary to rebeccamycin, these disaccharide indolocarbazoles have no inhibitory effect on topoisomerase I.[53,54] In contrast to AT2433-B1, its isomer, JDC-277, bearing an axial hydroxyl group instead of an equatorial *N*-methylamino group on the deoxysugar moiety, stimulates topoisomerase I-mediated DNA cleavage mainly at TG sites, showing that sequence-selective DNA interaction and topoisomerase I inhibition depend on the stereochemistry, and the substituents on the disaccharide unit.

24.3 TOTAL SYNTHESES OF THE NATURAL PRODUCTS

Because of the small quantities generally available from the natural sources and because of the possibility to have access to various analogs, total syntheses of natural indolocarbazoles have triggered considerable efforts.[55] Early work centered on aglycon construction.[56–63] The first total synthesis of staurosporine was achieved in 1995 by Danishefsky et al. in 27 steps (Figure 24.4), using sequential indole-Grignard additions to *N*-(benzyloxymethyl)-dibromomaleimide, followed by glycosylation with a 1,2-anhydrosugar, and then photocyclization. Coupling of the sugar moiety with the second indole nitrogen was performed from the exo-glycal intermediate, and after removal of the protective groups, the last step was the reduction of a carbonyl group of the imide heterocycle.[64,65] In 1997, Wood et al.[66,67] reported the synthesis of staurosporine and several natural compounds such as TAN-1030A, K-252a, RK286, and MLR-52 from the same intermediate obtained by cyclofuranosylation of the lactam aglycone in the presence of camphorsulfonic acid. A ring expansion approach was developed that allowed the transformation of a furanosylated indolocarbazole to a pyranosylated derivative (Figure 24.4).

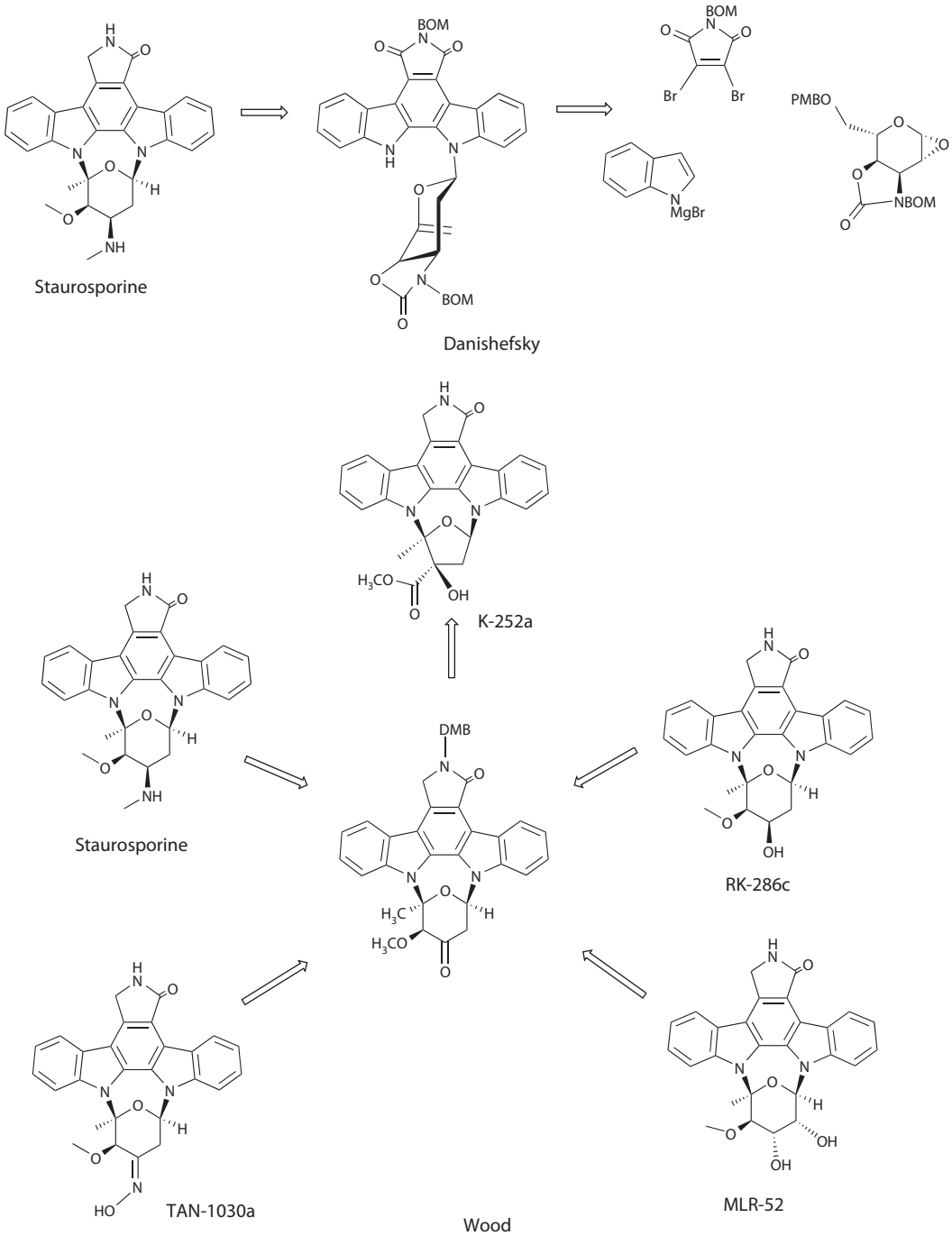

FIGURE 24.4 Total syntheses of staurosporine and related microbial metabolites.

The 23-step stereocontrolled total synthesis of K-252a was described in 1999 starting from indole-3-acetic acid (Figure 24.5).[68] The glycosylation was carried out before the introduction of the second indole moiety provided by tryptamine. The carboxylate substituent of the sugar was introduced via the addition of hydrogen cyanide on a carbonyl group. Four total syntheses of rebeccamycin have been reported (Figure 24.6).[69–71] Kaneko et al. proposed two synthetic approaches to the

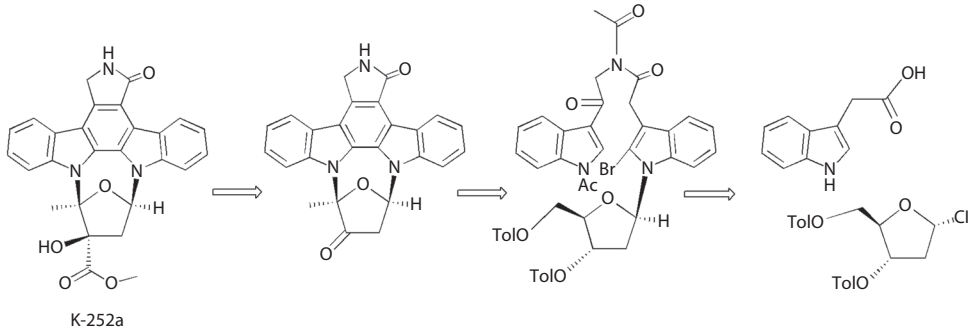

FIGURE 24.5 Total synthesis of K-252a by Kobayashi et al.

chlorinated indolocarbazole aglycone, to which α-bromo sugar was attached via the Koenigs–Knorr method. The chlorinated aglycone was obtained from *N*-benzyloxymethyl-dibromomaleimide and either chloroindole or 7-7-dichloroindigo. Danishefsky's method used a bisindolylmaleimide aglycone that was coupled to an anhydro sugar before photocyclization. Faul et al. performed the glycosylation of 7-chloro-indole-3-acetamide using the anhydro sugar described by Danishefsky before condensation with methyl 7-chloroindole-3-glyoxylate. The oxidative cyclization of the bisindolylmaleimide was carried out using palladium(II) triflate.

The synthesis of tjipanazole E was achieved by Bonjouklian et al. (Figure 24.7).[72] Tjipanazole D, obtained by condensation of *p*-chlorophenylhydrazine and 1,2-cyclohexanedione followed by a Fischer indolization, was further glycosylated using α-bromo-tetraacetylglucose. Tjipanazoles F1 and F2 were synthesized by Gilbert et al. (Figure 24.7).[73,74] Tjipanazole F2 was prepared from 1,2-bis(3-indolyl)ethane via a Mannich cyclization, followed by sequential bromination, glycosylation, oxidation, and halogen exchange. Tjipanazole F1 was synthesized via the same

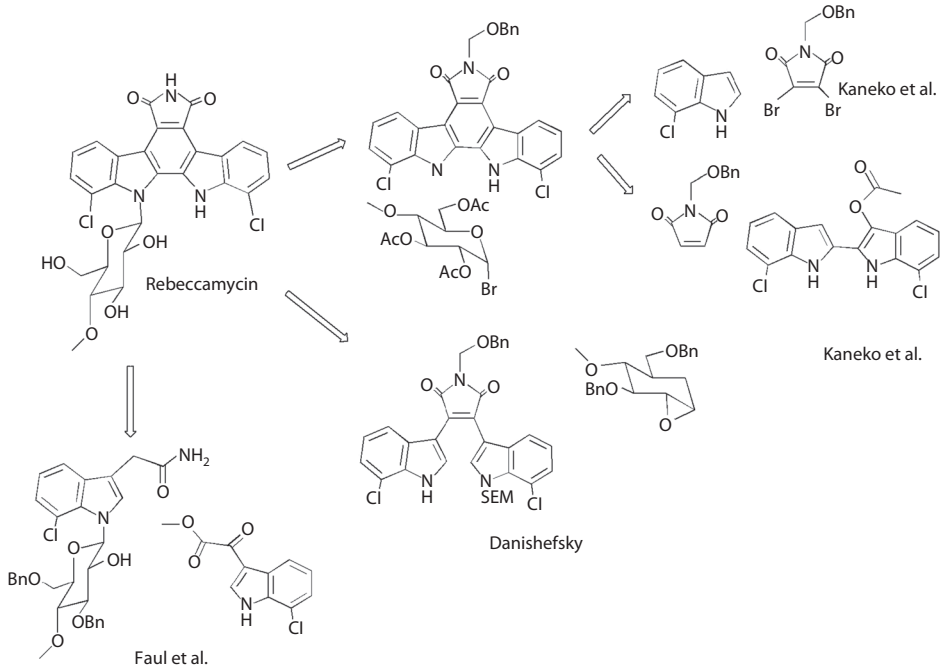

FIGURE 24.6 Total synthesis of rebeccamycin.

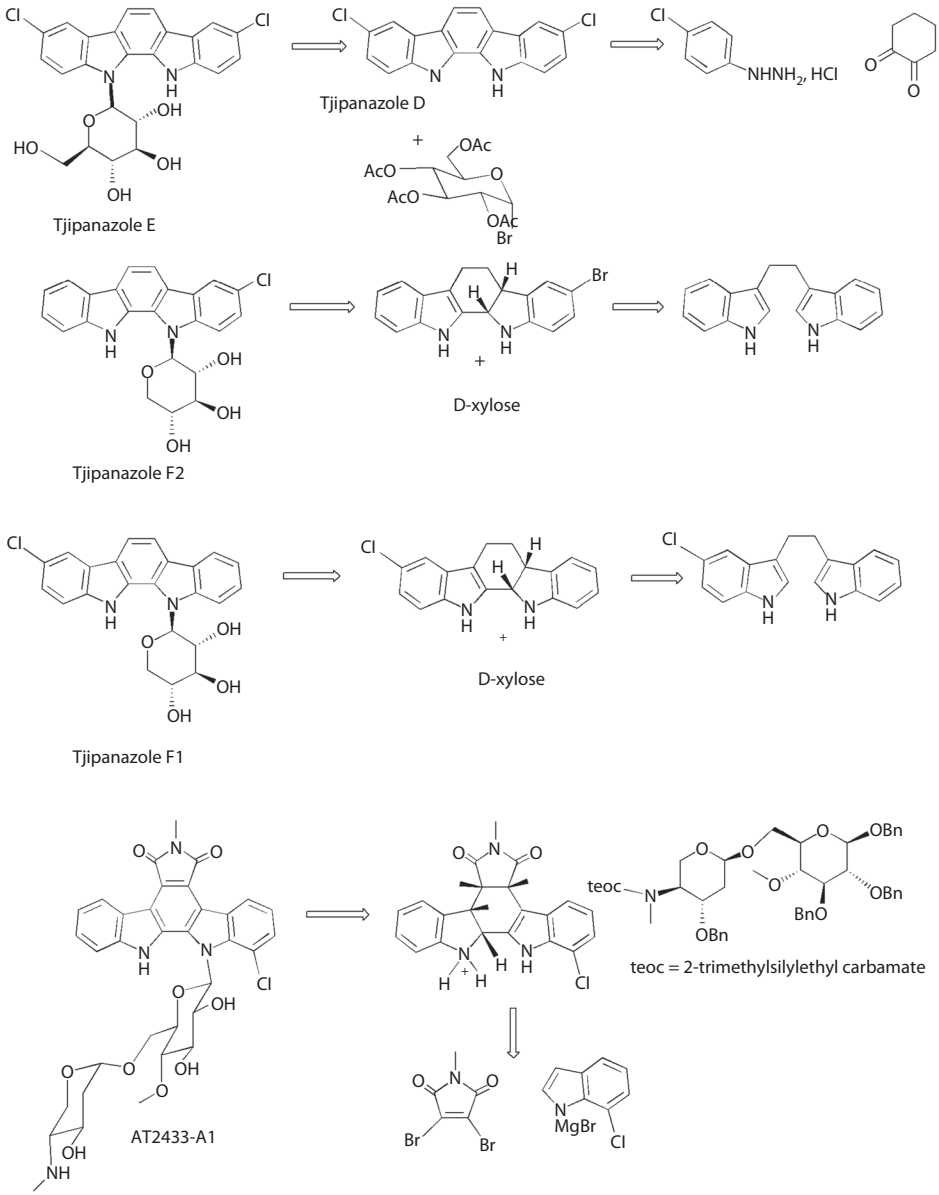

FIGURE 24.7 Syntheses of tjipanazoles E, F1, F2, and AT2433-A1.

sequence of reactions from 1-(5-chloro-indolyl)-2-indolyl-ethane; the halogen atom was introduced at the beginning of the synthesis using 5-chloro-indole. Chisholm and Van Vranken described in 2000 the first total synthesis of AT2433-A1 and B1 via the glycosylation of the indoline intermediate prepared from *N*-methyl-dibromomaleimide and 7-chloro-indolylmagnesium bromide and indolylmagnesium bromide, respectively (Figure 24.7).[75]

24.4 DEVELOPMENT OF DRUGS FROM THE NATURAL PRODUCTS

Structural analogs of staurosporine were synthesized, aiming at higher selectivity. Among them, CGP 41 251 was developed by Novartis (Figure 24.8). CGP 41 251 was less potent but much more

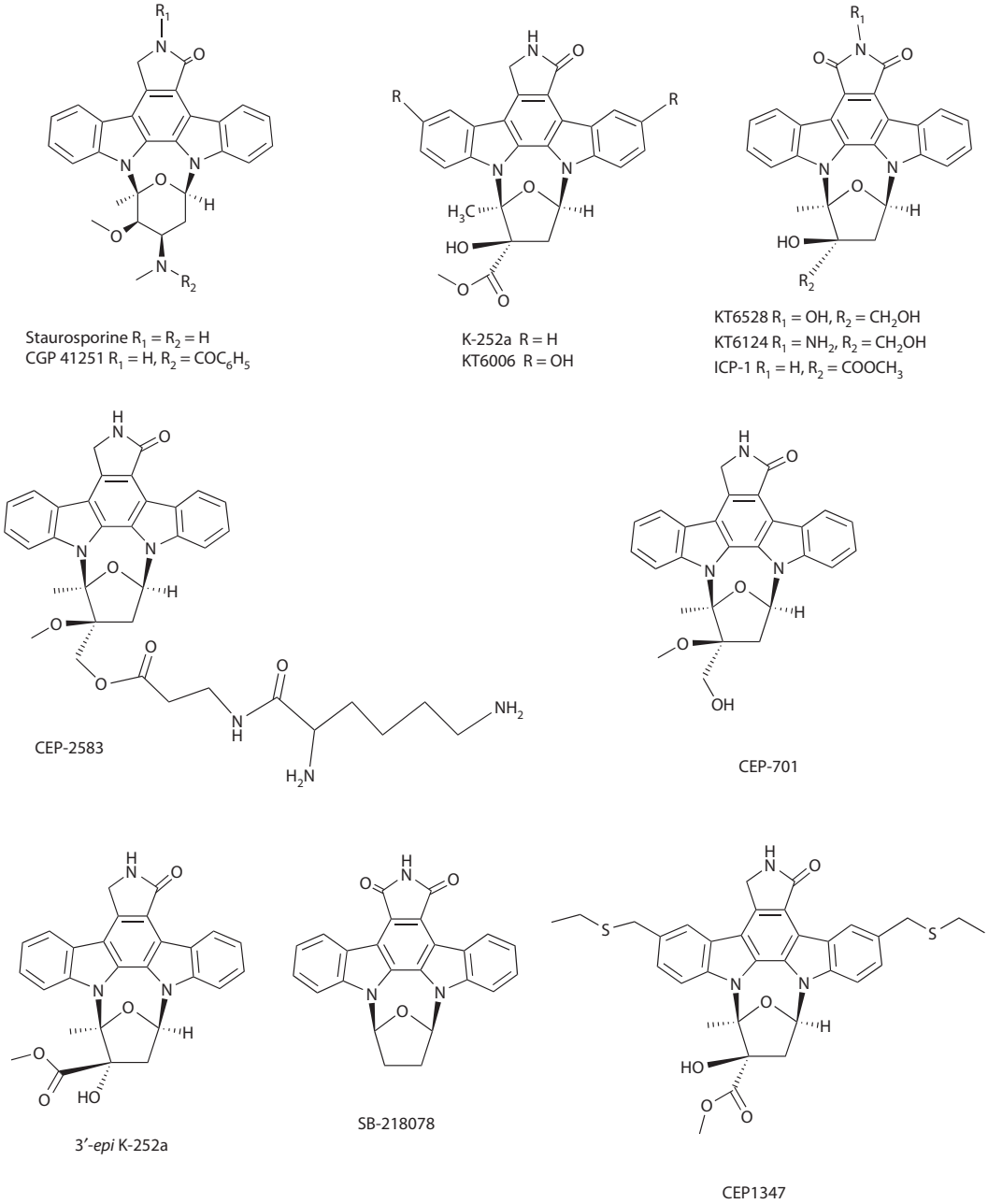

FIGURE 24.8 Indolocarbazoles structurally related to staurosporine and K-252.

selective toward kinases than staurosporine. The antiproliferative activity of staurosporine was three to nine times stronger than that of CGP 41 251. The increased specificity of CGP 41 251 has not resulted in a cell-type-specific antiproliferative effect. *In vivo*, staurosporine and CGP 41 251 were active in the growth inhibition model, with a higher therapeutic index for CGP 41 251 in comparison with staurosporine.[76,77] Like staurosporine, K-252a and UCN-01, CGP 41 251 has no effect on topoisomerase I.[78]

On the contrary, the K-252a derivatives, KT6124, KT6528, and KT6006 (Figure 24.8), are topoisomerase I inhibitors and exhibit quite different effects on the cell cycle of HR-3Y1 cells.[78,79] Staurosporine, CGP 41 251, and K-252a induce G2/M-phase accumulation, whereas UCN-01 exerts a preferential G1-phase block. KT6124 and KT6528, which are weaker PKC inhibitors, induce an S-phase delay, as observed with the topoisomerase I inhibitor camptothecin. KT6006 induces not only the S-phase delay but also G2/M-phase block. SB-218078, in which a tetrahydrofuranyl unit replaces the sugar unit (Figure 24.8), was found to enhance the cytotoxicity of DNA-damaging agents by preventing G2 arrest. As with UCN-01, SB-218078 is a potent inhibitor of human Chk1 kinase (Ki,app = 15 nM),[41] and it abrogates G2 arrest caused by either γ-irradiation or a topoisomerase I inhibitor.[80]

Avid binding of UCN-01 to human plasma proteins, not predicted from the animal studies, limits access to the tumor.[81,82] A screen of related indolocarbazoles showed that ICP-1 (Figure 24.8), a K-252a analog, was also able to abrogate S- and G2-phase arrest and to enhance cytotoxicity induced by cisplatin only in p53-defective cells.[83] In contrast to UCN-01, checkpoint abrogation by ICP-1 was only slightly inhibited by human plasma. CEP-2583 and CEP-701 (Figure 24.8), tyrosine kinase receptor inhibitors developed by Cephalon, are currently undergoing phase II clinical trials.[84,85] This group has recently obtained, by semisynthesis from K-252a, the 3-*epi* diastereoisomer (Figure 24.8). Inverting the 3-alcohol resulted in a 20-nM inhibitor of VEGFR2 and a 1-nM inhibitor of TrkA tyrosine kinase compared with 43 and 13 nM for K-252a, respectively.[86]

CEP1347 is a semisynthetic K-252a derivative (Figure 24.8) bearing two methylthioethyl substituents in the 3 and 9 positions on the planar indolocarbazole. Both K-252a and CP1347 are neuroprotective compounds, and they mediate neuroprotective effects through the activation of neurotrophic-signaling pathways. Both compounds inhibit JNK (*c*-Jun N-terminal kinase) pathway activation through similar mechanisms. Unlike K-252a, however, CP1347 does not inhibit the majority of common kinases such as PKC, PKA, MLCK, and PI-3 kinase, but it directly inhibits PAKs, a family of serine/threonine kinases, in a quite selective manner.[87–89]

BE-13793C (Figure 24.1), a topoisomerase I inhibitor, was isolated from cultures of *Streptoverticillium* species.[90] Modifications were carried out to enhance the solubility and to obtain compounds exhibiting more potent antitumor activities *in vivo*. Glycosylated derivatives ED-110 and NB-506 were prepared, as well as analogs such as J-107088 bearing the hydroxyl groups in various positions on the indolocarbazole framework (Figure 24.9).[91–94] ED-110 and NB-506 stimulate DNA cleavage by topoisomerase I without any effect on topoisomerase II. The replacement of the NHCHO substituent of NB-506 with a longer side chain [$NHCH(CH_2OH)_2$] reinforces the interaction with DNA without affecting the intercalative binding process.[95,96] A NB-506 regioisomer, with the two hydroxyl groups at positions 2 and 10 instead of 1 and 11, has lost its capacity to intercalate into DNA but remains an extremely potent topoisomerase I poison, showing that intercalation into DNA is not required for the inhibition of topoisomerase I by indolocarbazoles. NB-506 and its

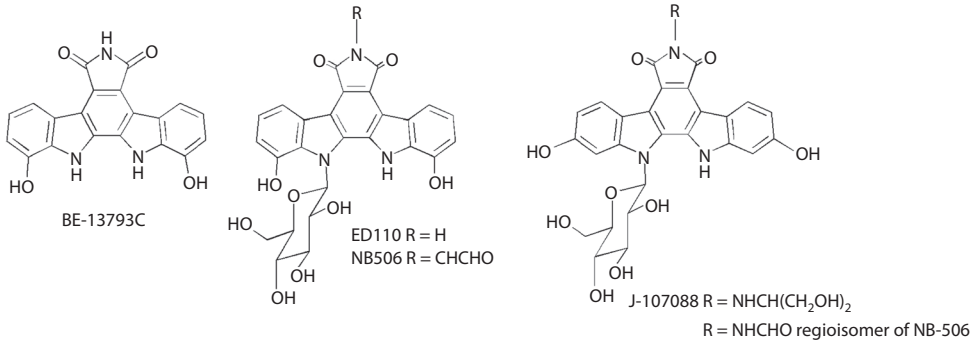

FIGURE 24.9 Chemical structures of BE-13793C, semisynthetic derivatives, and synthetic analogs.

regioisomer stimulate cleavage at different sites on DNA. The 2,10 isomer is up to 100-fold more toxic to tumor cells than the parent NB-506.[97] NB-506 induces apoptosis in leukemia cells via alterations of mitochondrial and caspases functions.[98] The metabolism of NB-506 has been studied, both *in vitro* and *in vivo*, in animals and humans (Figure 24.10).[99,100] In rodent plasma, NB-506 was converted to its deformylated derivative ED-501, whereas in dog and human plasma, it was converted to its anhydride ED-551, an inactive metabolite. It has been suggested that the conversion of NB-506 into anhydride ED-551 is catalyzed by metal ions with the formation of a complex in which the metal ion interacts with the three carbonyl groups. The replacement of the NHCHO group by an $NHCH(CH_2OH)_2$ substituent (compound D; Figure 24.10) significantly reduces the rate of metabolization into the inactive anhydride form.[101] During the course of clinical trials of NB-506, Banyu Pharmaceuticals continued to synthesize NB-506 analogs, and from among several hundred compounds, J-107088 (Figure 24.9), which showed greater inhibitory activity than NB-506 toward topoisomerase I, has recently replaced NB-506 in the clinical trials.[93]

Large structure–activity relationship studies have also been carried out on rebeccamycin analogs prepared either by semisynthesis or by total synthesis.[50,51,102] Biosynthetic studies revealed that rebeccamycin is from two tryptophan, one glucose, and one methionine molecules.[102] Addition of 6-, 5-, or 4-fluorotryptophan to the fermentation broths resulted in rebeccamycin analogs bearing, instead of chlorine atoms, fluorine atoms in the 2 and 10, 3 and 9, and 4 and 8, positions, respectively, on the indolocarbazole unit. Maximal topoisomerase I-induced cytotoxicity is imparted by 3,9-dihalogenated compounds. The 2,10-dihalogenated compounds exhibit less topoisomerase I-selective cytotoxicity, and the 1,11-disubstituted analogs have the least topoisomerase I-dependent cytotoxicity. These observations may be explained by interaction with other cytotoxic targets such as DNA or kinases. The 4,8-dihalogenated compounds are the least cytotoxic and the least active toward topoisomerase I or other targets. The methylation of the 4-hydroxyl group of the sugar moiety has little effect on topoisomerase I inhibition but results in increased cytotoxicity, very likely because of better penetration into the cells. The semisynthetic analog synthesis program developed

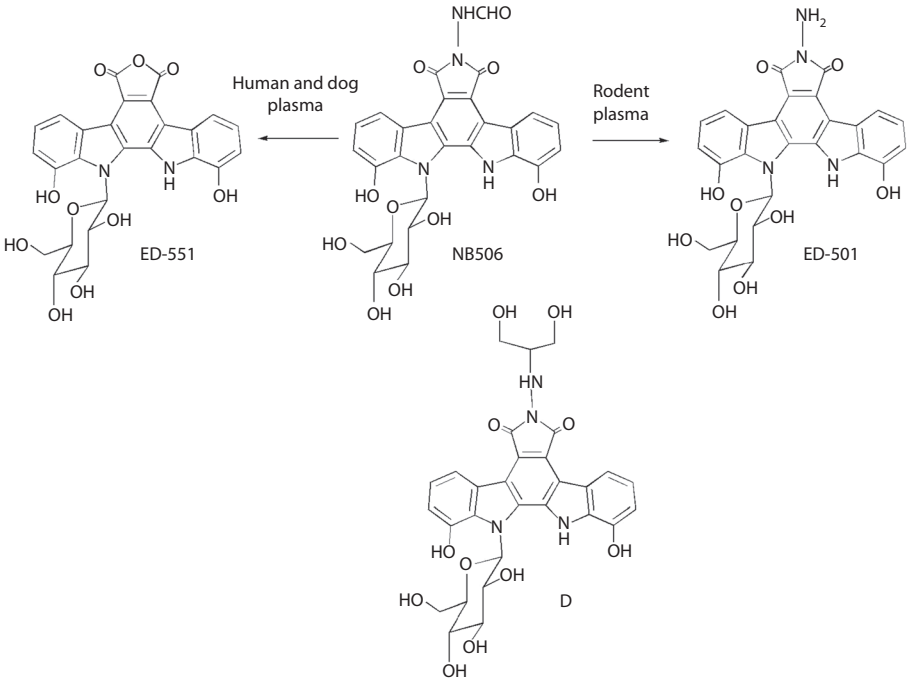

FIGURE 24.10 Metabolism of NB-506.

by Bristol-Myers culminated in the discovery of the 6-*N*-diethylaminoethyl derivative, a water-soluble analog of rebeccamycin.[49]

NSC 655649, a tartrate salt, entered phase I studies (Figure 24.11). This compound has a broad spectrum of activity against solid tumors and, in contrast to rebeccamycin, inhibits topoisomerase II. NCS 655649 is currently undergoing phase II clinical trials for the treatment of hepatobiliary and gall bladder cancers.[102] Interestingly, the introduction of an amino group at the 6-position on the sugar unit (Figure 24.11) strongly enhances the capacity of the drugs to interact with DNA, but almost abolishes their poisoning effect on topoisomerase I, showing that DNA and topoisomerase I represent two independent targets that can both be used for the development of antitumor rebeccamycin derivatives.[103]

The main differences between the structures of rebeccamycin and staurosporine are the sugar moiety linked to one indole nitrogen in rebeccamycin and to both indole nitrogens in staurosporine, and the imide function in the upper heterocycle of rebeccamycin instead of an amide function in staurosporine. These differences should be responsible for their enzyme selectivities. Therefore,

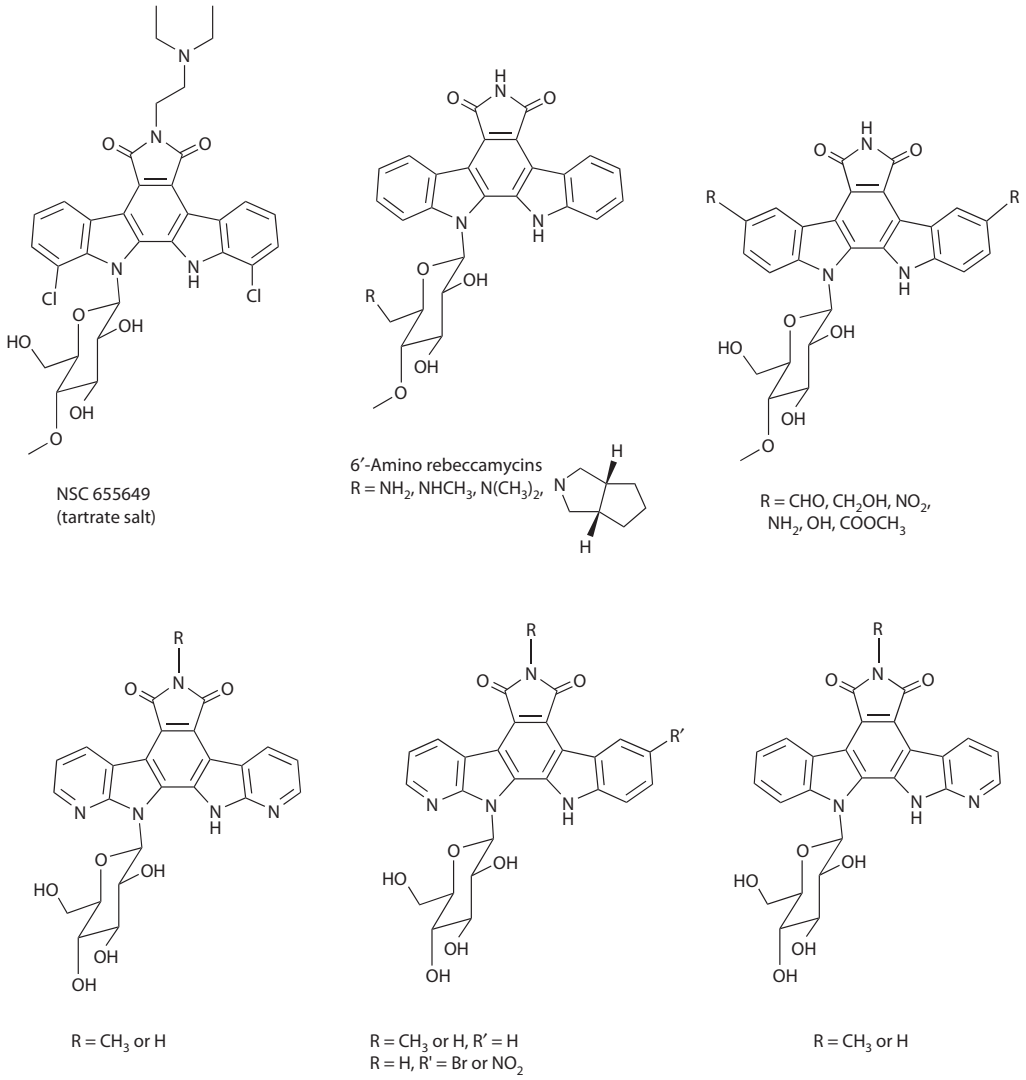

FIGURE 24.11 Semisynthetic rebeccamycin analogs and aza-rebeccamycin obtained by total synthesis.

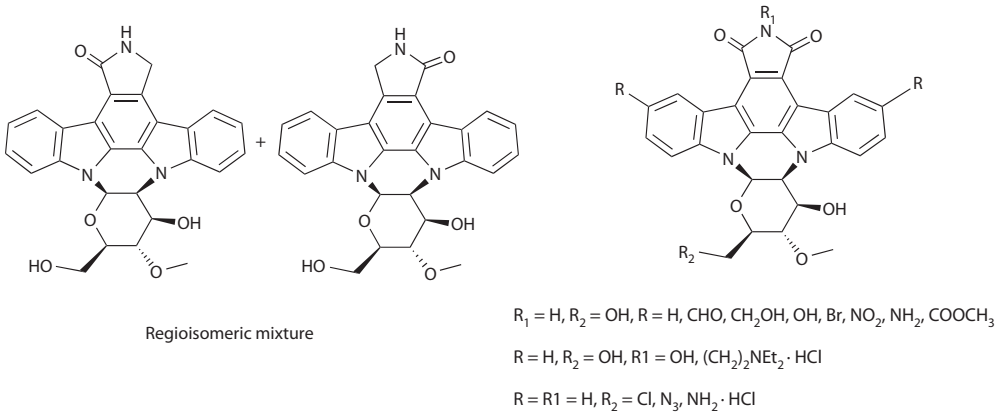

FIGURE 24.12 Staurosporine analogs from rebeccamycin.

structural modifications were performed on rebeccamycin to obtain staurosporine analogs, with the sugar moiety linked to both indole nitrogens (Figure 24.12).[104,105] The antitopoisomerase I activities of the unsubstituted imide and rebeccamycin are in the same range, whereas the activity of the regioisomeric mixture of amides is about 10-fold weaker. There is no doubt that the carbonyl group that distinguishes these compounds must be important for both DNA binding and topoisomerase I inhibition. None of these bridged compounds inhibits PKC. The two cationic molecules, bearing a *N,N*-diethylamino chain at the imide nitrogen or an amino substituent on the sugar moiety, exhibit enhanced affinity for DNA, and this translates at the biological level into a 10-fold higher cytotoxic index; however, they do not inhibit topoisomerase I, in contrast to the parent uncharged derivative ($R' = R'' = OH$), which stimulates DNA single-strand breaks by topoisomerase I.[106] In contrast to rebeccamycin and dechlorinated rebeccamycin, which exhibit nonselective cytotoxicity toward various tumor cell lines, some compounds in this bridged series, such as 3,9-dinitro, 3,9-dihydroxy, and 3,9-diformyl compounds, exhibit a marked selectivity, indicating targets that are differently expressed in the various tumor cell lines.

Substitutions in 3,9-positions on the indolocarbazole framework of rebeccamycin have been carried out (Figure 24.11).[107] Depending on the structural modifications, the rebeccamycin derivatives may or may not exhibit selectivity toward the various tumor cell lines tested. 3,9-Substituents can enhance or abolish the cytotoxicity, but they can also induce selectivity. The 3,9-dihydroxy derivative is not only a DNA-binding topoisomerase I poison, but it also inhibits CDK1/cyclinB and CDK5/p25. It induces accumulation of L1210 cells in the G2 + M phases, which seems to be correlated with CDK1/cyclinB inhibition. This multitarget drug represents a new lead for subsequent drug design in the rebeccamycin series.

Another interesting series is that of the 7-azarebeccamycins obtained by total synthesis.[108,109] Surprisingly, DNA-binding experiments in the monoazaindole series showed major differences between the compounds bearing the carbohydrate moiety on either the azaindole moiety or the indole unit. Compounds with the sugar attached to the indole exhibit higher affinity for DNA and stronger topoisomerase I inhibition than the parent, dechlorinated rebeccamycin. When the sugar is linked to the azaindole, however, DNA-binding properties are abolished and topoisomerase I inhibitory properties are strongly weakened. Even the introduction of a bromo or a nitro group is not sufficient to restore the affinity for DNA; however, these substitutions induced marked topoisomerase I inhibition. Both monoaza or diaza rebeccamycins showed a selective action toward certain cell lines. Their cytotoxic profiles are quite different from those of the parent nonaza compounds, which are nonselective and display similar cytotoxicity against all the tumor cell lines, but like most of rebeccamycin derivatives, they induce a G2 + M arrest. It can be concluded from these studies that if topoisomerase I remains the first target for rebeccamycin derivatives, they certainly have other

biological targets. The first results show that kinases that control the cell cycle should also be targets for rebeccamycin analogs.

24.5 CLINICAL APPLICATIONS

Though there is no indolocarbazole on the market at present, some of them are undergoing clinical trials. Phase I and II trials of UCN-01 have been reported.[110] In a phase I study, where the doses were administered by continuous infusion for 72 hours, a prolonged half-life of 600 hours was observed. The side effects were various, and among them, hyperglycemia needed insulin treatment. However, avid plasma protein binding of UCN-01 dictated a change in dose escalation and administration schedules. Phase I trials with shorter infusions are being completed. In a phase II study, one patient with melanoma achieved a partial response, and encouraging results were obtained in a patient with refractory anaplastic large-cell lymphoma.[111–113] The maximal tolerated and recommended phase II dose was 42.5 mg/m^2 per day for three days. A phase II clinical trial of the staurosporine analog CGP41251 (PKC412) has been reported. The patients with lymphoproliferative disorders were treated at three oral dose levels of 25, 150, and 225 mg/day for 14 days. The results show that the treatment is well tolerated and reduces the tumor load in chronic B-cell malignancies.[114] Rebeccamycin derivative NCS 655649 has entered into phase I and II studies. This drug may be safely given at a maximal tolerated dose of 572 mg/m^2 in both single- and multiple-dose formats. Antitumor activity was observed in two heavily pretreated ovarian cancer patients and, in one patient, with a soft-tissue sarcoma refractory to etoposide and doxorubicin. Preliminary data of a phase I study demonstrated antitumor activity in colorectal carcinoma. A phase II trial evaluated the efficacy of NSC 655649 in patients with advanced previously minimally treated metastatic colorectal cancer. At 500 mg/m^2 once every three weeks, the treatment was inactive.[115–118] A phase II study of NCS-655649 in metastatic renal cell cancer showed a modest antitumor activity of this drug in patients with advanced this cancer.[119]

24.6 CONCLUSIONS

Indolocarbazoles represent a promising class of antitumor agents. Minimal structural modifications are able to modify the biological targets and induce selectivity toward tumor cell lines. Staurosporine is a nonselective kinase inhibitor, whereas the main target for rebeccamycin is topoisomerase I. Rebeccamycin exhibits no selectivity toward the various tumor cell lines, whereas 7-azarebeccamycins in which an indole moiety is replaced by a 7-azaindole unit are highly selective. Other structural modifications on the rebeccamycin framework, such as substitutions in 3,9-positions, may induce selectivity toward the tumor cell lines and strong inhibitory properties toward kinases involved in the progression of the cell cycle. No indolocarbazole has yet been launched on the market, but a staurosporine analog UCN-01 and a rebeccamycin derivative NCS 655649 have entered into phase I and II trials. UCN-01 and a K-252a analog, ICP-1, abrogate the DNA-damage-induced checkpoints to cell-cycle progression in the G2 and in the S phases. This is probably the most important point, because in this manner, indolocarbazoles may exhibit highly selective activity against tumor cells without effect on normal cells, thereby achieving the ultimate goal for antitumor drugs.

UPDATE

D. J. Newman

Since the middle of 2004, there have been a series of very interesting original papers and reviews covering synthetic, biosynthetic, and some clinical data on the indolocarbazoles reported on in the first edition (above) together with other agents that were either not covered or had not had significant work published until after 2004.

This editorial note is not designed to be in any way exhaustive but will note the current status of some molecules referred to earlier and will reference some excellent papers, both original and reviews of various aspects of the field that merit study by interested readers. The references will continue on from number 120 and structures will follow the format and numbering from the first edition.

Modifications of the Indolocarbazole Nucleus by the Prudhomme Group

Shortly after the closing date for the first edition, Prudhomme published an excellent review on the biological targets of antitumor indolocarbazoles,[120] which was followed in 2008 by a thorough discussion on their close chemical relatives, the pyrrolocarbazoles,[121] with an exemplar being granulatimide (Figure 24.13), a compound first reported from marine sources by Berlinck et al. in 1998.[122]

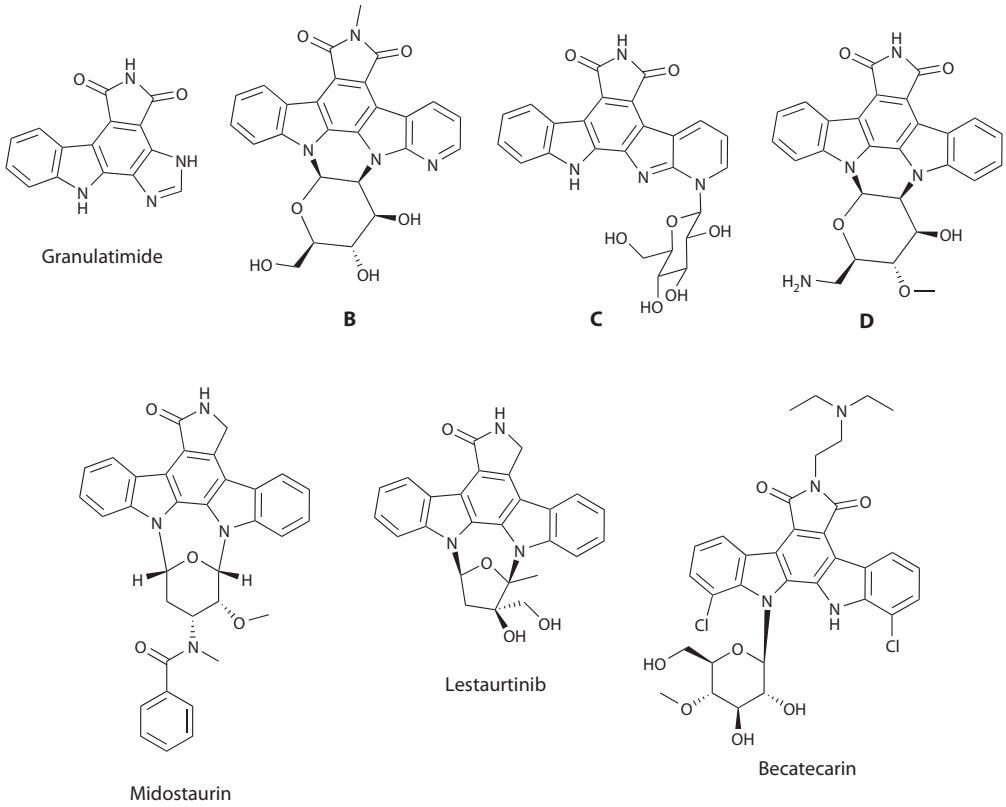

FIGURE 24.13 Further indolocarbazoles and related compounds.

Prior to this latter review, Prudhomme also demonstrated that one could generate quite novel agents resembling indolocarbazoles, such as UCN-01, but with a 7-azaindole moiety, and further modified by attachment of the sugar to both the indole and azaindole nitrogens but with the pyran oxygen of the sugar pointing towards the indole nitrogen (**B**; Figure 24.13).[123] These and other azaindole derivatives related to rebeccamycin (**C**; Figure 24.13) had different biological effects from the nonaza-substituted materials, having lost DNA-binding and topoisomerase I inhibitory activities, but gaining Chk1 inhibitory characteristics in the case of **C** (Figure 24.13), but all exhibited significant cytotoxicities against selected tumor cell lines.[124] Further modifications of the base rebeccamycin molecule to yield agents having both Chk1 inhibitory and DNA-damaging activities, but without the aza substitutions, were then reported by Prudhomme's group in 2008.[125] This was followed in early 2009 by the report of a very simple three-step synthesis of the Chk1 inhibitor (**D**; Figure 24.13) with an IC_{50} value of 2.8 nM by Prudhomme's group starting from rebeccamycin.[126]

Other Pertinent Reviews and Reports

In addition to the papers cited above from the Prudhomme group, other excellent reviews of both the chemistry and biology of the indolocarbazoles and their chemical relatives have been published in the last four to six years, and these too should be consulted. They include a 2007 review by Asche and Demeunynck on the antitumor carbazoles, which covers more than just the indolocarbazoles,[127] and a discussion of the targeting of PKC in relation to cancers of the gastric system, which includes work related to UCN-01 and other derivatives, by Fahrmann in 2008.[128] In that same year, there was a special report in Tetrahedron by Janosik et al.[129] on the recent chemistry and applications of the indolocarbazoles, which led to a very interesting report in early 2009 of indolocarbazole derivatives having fused thio- and selenopyrans that had higher affinities for the aryl hydrocarbon receptor (AhR) than dioxin.[130] It will be interesting to follow such molecules, as there have been reports of antitumor effects via the AhR in work from Meijer's group in prior years when studying indirubins.[131]

In addition to these, there are two reviews, one by the discoverer of staurosporine, Satoshi Omura in 2009, covering the chemical biology of natural indolocarbazoles over the past 30 years,[132] and the other, a truly epic treatise on the chemistry and biology of the carbazole alkaloids, published in 2008 as a single topic volume in the series *The Alkaloids, Chemistry and Biology* by Knolker and Reddy.[133]

Biosynthetic Studies

What is of definite interest is that over the last few years, the gene clusters of some of the indolocarbazole molecules have been fully or partially characterized, adding to data that were in the literature. In a review in 2009, Ryan and Drennan[134] demonstrated the multiplicity of biosynthetic pathways starting from two molecules of tryptophan, which lead to the large number of chemical structures encompassed by the term "bisindole natural products." Contemporaneously with this publication were two papers from Chiu's group in Taiwan demonstrating that they could successfully express variations on the K-252 basic structure by heterologous expression of the sugar transferase pathway in *Escherichia coli*.[135,136]

The full characterization of the rebeccamycin and staurosporine gene clusters and their heterologous expression in *Streptomyces albus* had been reported in the early 2000s by Salas' group working with Rohr and Thorson.[137] Recently, the Salas' group reported on the combinatorial biosyntheses of novel glycosylated indolocarbazoles, where different sugar moieties, rhamnose, olivose, or digitoxose, were linked as in staurosporine or rebeccamycin; all demonstrated antiproliferative or *in vitro* activity against some protein tyrosine kinases, with a maintenance of activity at the nanomolar level and a reduction in the number of kinases inhibited when compared with the parent

staurosporine. Among the compounds, one demonstrated <30 pM activity against Ikkb and one showed subnanomolar activity against JAK2. Both of these compounds had the sugar linked as in staurosporine but the aglycones differed, as did the sugars.[138]

Current Clinical Status (as October 2010)

Although a significant number of staurosporine-like agents have entered clinical trials over the years in the United States, Europe, and Japan, the current status obtained from combination searches of the NCI clinical trials registry and the Thomson-Reuters Integrity® database is that PKC-412 or midostaurin (Figure 24.13) is currently in phase III clinical trials under Novartis for acute myeloid leukemia (AML), with trials against other cancers also underway. The compound now known as lestaurtinib (Figure 24.13) but also known as CEP-701 is currently in phase II/III clinical trials against relapsed AML, and is thought to be an inhibitor of FLT3 among other kinases.[139] In addition, a pegylated derivative of the well-known base molecule, K-252a (Figures 24.1) (which was withdrawn due to toxicity), is currently in phase II clinical trials under the name K-252a-PEG(2K) for atopic dermatitis and psoriasis (which is a proliferative disease).

The compound becatecarin (Figure 24.13) is reportedly still in phase II clinical trials, in spite of having a rather checkered career as companies licensed compounds and then released them to others. It had reached phase III studies under Helsinn and Excelis but now is quoted as being at the phase II level, though a search of the NCI clinical trials database shows 13 completed trials but no action since 2008. This is the only rebeccamycin analog to make it this far in clinical trials to date.

Conclusion

Although the structure of the base indolocarbazole skeleton, as that of staurosporine, was first reported over 30 years ago, this skeleton and its congeners are still being worked on by chemists and biologists. The methodologies of chemical and now combinatorial biosynthesis have the potential to uncover more selective PKC and PTK inhibitors that can enter clinical trials against proliferative diseases. Since the path to antitumor agents is long and definitively nonlinear, these chemical skeletons will continue to yield valuable insight into molecules that should have increased specificity in many signal transduction pathways, and ultimately lead to novel treatment modalities in the future.

REFERENCES

1. Prudhomme, M., Indolocarbazoles as anti-cancer agents, *Curr. Pharm. Des.* 3, 265, 1997, and references provided therein.
2. Williams, D. E., Bernan, V. S., Ritacco, F. V., Maiese, W. M., Greenstein, M., and Andersen, R. J., Holyrines A and B, possible intermediates in staurosporine biosynthesis produced in culture by a marine actinomycete obtained from the North Atlantic Ocean, *Tetrahedron Lett.* 40, 7171, 1999.
3. Schupp, P., Eder, C., Proksch, P., Wray, V., Schneider, B., Herderich, M., and Paul, V., Staurosporine derivatives from the ascidian *Eudistoma toealensis* and predatory flatworm *Pseudoceros* sp., *J. Nat. Prod.* 62, 959, 1999.
4. Cantrell, C. L., Groweiss, A., Gustafson, K. R., and Boyd, M. R., A new staurosporine analog from the prosobranch mollusk *Coriocella nigra*, *Nat. Prod. Lett.* 14, 39, 1999.
5. Hernandez, L. M. C., De La Fuente-Blanco, J. A., Perez-Baz, J., Fernandez-Puentes, J. L., Romero-Millan, F., Espliego-Vazquez, F., Fernandez-Chimeno, R. I., and Garcia-Gravalos, D., 4-*N*-methyl-5-hydroxystaurosporine and 5-hydroxystaurosporine, new indolocarbazole alkaloïds from a marine *Micromonospora* sp. strain, *J. Antibiot.* 53, 895, 2000.
6. Schupp, P., Proksch, P., and Wray, V., Further new staurosporine derivatives from the ascidian *Eudistoma toealensis* and its predatory flatworm *Pseudoceros* sp., *J. Nat. Prod.* 65, 295, 2002.
7. Omura, S., Iwai, Y., Hirano, A., Nakagawa, A., Awaya, J., Tsuchiya, H., Takahashi, Y., and Asuma, R., A new alkaloid AM-2282 of *Streptomyces* origin. Taxonomy, fermentation, isolation and preliminary characterization, *J. Antibiot.* 30, 275, 1977.

8. Furusaki, A., Hashiba, N., Matsumoto, T., Hirano, A., Iwai, Y., and Omura, S., X-ray crystal structure of staurosporine: A new alkaloid from a *Streptomyces* strain, *J. Chem. Soc. Chem. Commun.* 800, 1978.
9. Steglich, W., Steffan, B., Kopanski, L., and Eckhardt, G., Indole pigments from the fruiting bodies of the slime mold *Arcyria denudata*, *Angew. Chem. Int. Ed. Engl.* 19, 459, 1980.
10. Tamaoki, T., Nomoto, H., Takahashi, I., Kato, Y., Morimoto, M., and Tomita, F., Staurosporine, a potent inhibitor of phospholipid/Ca^{++} dependent protein kinase, *Biochem. Biophys. Res. Commun.* 135, 397, 1986.
11. Kase, H., Iwahashi, K., and Matsuda, Y., K-252a, a potent inhibitor of protein kinase C from microbial origin, *J. Antibiot.* 39, 1059, 1986.
12. Cai, Y., Fredenhagen, A., Hug, P., and Peter, H. H., The staurosporine producing strain *Streptomycetes longisporoflavus* produces metabolites related to K-252a. Proposal for biosynthetic intermediates of K-252a, *J. Antibiot.* 49, 1060, 1996.
13. Yasuzawa, T., Iida, T., Yoshida, M., Hirayama, N., Takahashi, M., Shirahata, K., and Sano, H., The structures of the novel protein kinase C inhibitors K-252a, b, c, and d, *J. Antibiot.* 39, 1072, 1986.
14. Gray, N., Detivaud, L., Doerig, C., and Meijer, L., ATP-directed inhibitors of cyclin-dependent kinases, *Curr. Med. Chem.* 6, 859, 1999.
15. Hoehn, P., Ghisalba, O., Moerker, T., and Peter, H. H., 3-Demethoxy-3-hydroxystaurosporine, a novel staurosporine analog produced by a blocked mutant, *J. Antibiot.* 48, 300, 1995.
16. Rialet, V. and Meijer, L., A new screening test for antimitotic compounds using the universal M phase-specific protein kinase, p34cdc2/cyclin Bcdc13, affinity-immobilized on p13suc1-coated microtitration plates, *Anticancer Res.* 11, 1581, 1991.
17. Al-Obeidi, F. A. and Lam, K. S., Development of inhibitors for protein tyrosine kinases, *Oncogene* 19, 5690, 2000.
18. Takahashi, I., Saitoh, Y., Yoshida, M., Sano, H., Nakano, H., Morimoto, M., and Tamaoki, T., UCN-01 and UCN-02, new selective inhibitors of protein kinase C II. Purification, physico-chemical properties, structural determination and biological activities, *J. Antibiot.* 42, 571, 1989.
19. Jackson, J. R., Gilmartin, A., Imburgia, C., Winkler, J. D., Marshall, L. A., and Roshak, A., An indolocarbazole inhibitor of human checkpoint kinase (Chk1) abrogates cell cycle arrest caused by DNA damage, *Cancer Res.* 60, 566, 2000.
20. Yu, L., Orlandi, L., Wang, P., Orr, M. S., Senderowicz, A. M., Sausville, E. A., Silvestrini, R., Watanabe, N., Piwnica-Worms, H., and O'Connor, P. M., UCN-01 abrogates G_2 arrest through a Cdc2-dependent pathway that is associated with inactivation of the Wee1Hu kinase and activation of the Cdc25C phosphatase, *J. Biol. Chem.* 273, 33455, 1998.
21. Rodrigues Pereira, E., Belin, L., Sancelme, M., Prudhomme, M., Ollier, M., Rapp, M., Severe, D., Riou, J., Fabbro, D., and Meyer, T., Structure-activity relationships in a series of substituted indolocarbazoles: Topoisomerase I and protein kinase C inhibition and antitumoral and antimicrobial properties, *J. Med. Chem.* 39, 4471, 1996.
22. Kojiri, K., Kondo, H., Yoshinari, T., Arakawa, H., Nakajima, S., Satoh, F., Kawamura, K., Okura, A., Suda, H., and Okanishi, M., A new antitumor substance, BE-13793C, produced by a streptomycete. Taxonomy, fermentation, isolation, structure determination and biological activity, *J. Antibiot.* 44, 723, 1991.
23. Facompré, M., Carrasco, C., Colson, P., Houssier, C., Chisholm, J. D., Van Vranken, D. L., and Bailly, C., DNA binding and topoisomerase I poisoning activities of novel disaccharide indolocarbazoles, *Mol. Pharmacol.* 62, 1215, 2002.
24. Meggio, F., Deana, A. D., Ruzzene, M., Brunati, A. M., Cesaro, L., Guerra, B. et al., Different susceptibility of protein kinases to staurosporine inhibition. Kinetic studies and molecular bases for the resistance of protein kinase CK2, *Eur. J. Biochem.* 234, 317, 1995.
25. Mahedevan, D., Bearss, D. J., and Vankayalapati, H., Structure-based design of novel anti-cancer agents targeting aurora kinases, *Curr. Med. Chem. Anti-Cancer Agents* 3, 25, 2003.
26. Lawrie, A. M., Noble, M. E. M., Tunnah, P., Brown, N. R., Johnson, L. N., and Endicott, J. A., Protein kinase inhibition by staurosporine revealed in details of the molecular interaction with CDK2, *Nat. Struct. Biol.* 4, 796, 1997.
27. Prade, L., Engh, R. A., Girod, A., Kinzel, V., Huber, R., and Bossemeyer, D., Staurosporine-induced conformational changes of cAMP-dependent protein kinase catalytic subunit explain inhibitory potential, *Structure* 5, 1627, 1997.
28. Lamers, M. B. A. C., Antson, A. A., Hubbard, R. E., Scott, R. K., and Williams, D. H., Structure of the protein tyrosine kinase domain of C-terminal Src kinase (CSK) in complex with staurosporine, *J. Mol. Biol.* 285, 713, 1999.
29. Roy, K. K. and Sausville, E. A., Early development of cyclin dependent kinase modulators, *Curr. Pharm. Des.* 7, 1669, 2001.

30. Akiyama, T., Sugiyama, K., Shimizu, M., Tamaoki, T., and Akinaga, S., G1-checkpoint function including a cyclin-dependent kinase 2 regulatory pathway as potential determinant of 7-hydroxystaurosporine (UCN-01)-induced apoptosis and G1-phase accumulation, *Jpn. J. Cancer Res.* 90, 1364, 1999.
31. Sausville, E. A., Cyclin-dependent kinases: Novel targets for cancer treatment, in Perry, M. Ed., *1999 Educational Book*, American Society for Clinical Oncology, Alexandria, VA, 1999, p. 9.
32. Abe, S., Kubota, T., Otani, Y., Furukawa, T., Watanabe, M., Kumai, K., Akiyama, T., Akinaga, S., and Kitajima, M., UCN-01 (7-hydroxystaurosporine) inhibits *in vivo* growth of human cancer cells through selective perturbation of G1 phase checkpoint machinery, *Jpn. J. Cancer Res.* 92, 537, 2001.
33. Busby, E. C., Leistritz, D. F., Abraham, R. T., Karnitz, L. M., and Sarkaria, J. N., The radiosensitizing agent 7-hydroxystaurosporine (UCN-01) inhibits the DNA damage checkpoint kinase hChk1, *Cancer Res.* 60, 2108, 2000.
34. Kohn, E. A., Ruth, N. D., Brown, M. K., Livingstone, M., and Eastman, A., Abrogation of the S phase DNA damage checkpoint results in S phase progression or premature mitosis depending on the concentration of 7-hydroxystaurosporine and the kinetics of Cdc25C activation, *J. Biol. Chem.* 277, 26553, 2002.
35. Zhou, B.-B. S. and Elledge, S. J., The DNA damage response: Putting checkpoints in perspective, *Nature* 408, 433, 2000.
36. Cuddihy, A. R. and O'Connell, M. J., Cell-cycle responses to DNA damage in G2, *Int. Rev. Cytol*. 222, 99, 2003.
37. Nyberg, K. A., Michelson, R. J., Putman, C. W., and Weinert, T. A., Toward maintaining the genome: DNA damage and replication checkpoints, *Annu. Rev. Genet.* 36, 617, 2002.
38. Graves, P. R., Yu, L., Schwarz, J. K., Gales, J., Sausville, E. A., O'Connor, P. M., and Piwnica-Worms, H., The Chk1 protein kinase and the Cdc25C regulatory pathways are targets of the anticancer agent UCN-01, *J. Biol. Chem.* 275, 5600, 2000.
39. Tenzer, A. and Pruschy, M., Potentiation of DNA-damage-induced cytotoxicity by G2 checkpoint abrogators, *Curr. Med. Chem. Anti-Cancer Agents* 3, 35, 2003.
40. Yu, Q., Rose, J. H., Zhang, H., and Pommier, Y., Inhibition of Chk2 activity and radiation-induced p53 elevation by the cell cycle checkpoint abrogator 7-hydroxystaurosporine (UCN-01), *Proc. Am. Assoc. Cancer Res.* 42, 800, 2001.
41. Zhao, B., Bower, M. J., McDevitt, P. J., Zhao, H., Davis, S. T., Johanson, K. O., Green, S. M., Concha, N. O., and Zhou, B.-B. S., Structural basis for Chk1 inhibition by UCN-01, *J. Biol. Chem.* 277, 46609, 2002.
42. Sato, T., Fujita, N., and Tsuruo, T., Interference with PDK1-Akt survival signaling pathway by UCN-01 (7-hydroxystaurosporine), *Oncogene* 21, 1727, 2002.
43. Roux, P. P., Dorval, G., Boudreau, M., Angers-Loustau, A., Morris, S. J., Makkerh, J., and Barker, P. A., K-252a and CEP1347 are neuroprotective compounds that inhibit mixed-lineage kinase-3 and induce activation of Akt and ERK, *J. Biol. Chem.* 277, 49473, 2002.
44. Angeles, T. S., Kinetics of trkA tyrosine kinase activity and inhibition by K-252a, *Arch. Biochem. Biophys.* 349, 267, 1998.
45. Chin, L. S., Murray, S. F., Doherty, P. F., and Singh, S. K., K-252a induces cell cycle arrest and apoptosis by inhibiting Cdc2 and Cdc25c, *Cancer Invest.* 17, 391, 1999.
46. Bush, J. A., Long, B. H., Catino, J. J., and Bradner, W. T., Production and biological activity of rebeccamycin, a novel antitumor agent, *J. Antibiot.* 40, 668, 1987.
47. Marminon, C., Pierre, A., Pfeiffer, B., Perez, V., Leonce, S., Joubert, A., Bailly, C., Renard, P., Hickman, J., and Prudhomme, M., Syntheses and antiproliferative activities of 7-azarebeccamycin analogs bearing one 7-azaindole moiety, *J. Med. Chem.* 46, 609, 2003.
48. Bailly, C., Riou, J., Colson, P., Houssier, C., Rodrigues-Pereira, E., and Prudhomme, M., DNA cleavage by topoisomerase I in the presence of indolocarbazole derivatives of rebeccamycin, *Biochemistry* 36, 3917, 1997.
49. Kaneko, T., Wong, H., Utzig, J., Schurig, J., and Doyle, T. W., Water soluble derivatives of rebeccamycin, *J. Antibiot.* 43, 125, 1990.
50. Prudhomme, M., Recent developments of rebeccamycin analogs as topoisomerase I inhibitors and antitumor agents, *Curr. Med. Chem.* 7, 1189, 2000.
51. Prudhomme, M., Rebeccamycin analogs as anti-cancer agents, *Eur. J. Med. Chem.* 38, 123, 2003.
52. Matson, J. A., Claridge, C., Bush, J. A., Titus, J., Bradner, W. T., Doyle, T. W., Horan, A. C., and Patel, M., AT2433-A1, AT2433-A2, AT2433-B1, and AT2433-B2 novel antitumor antibiotic compounds produced by *Actinomadura melliaura*. Taxonomy, fermentation, isolation and biological properties, *J. Antibiot.* 42, 1547, 1989.

53. Carrasco, C., Facompré, M., Chisholm, J. D., Van Vranken, D. L., Wilson, W. D., and Bailly, C., DNA sequence recognition by the indolocarbazole antibiotic AT2433-A1 and its diastereoisomer, *Nucleic Acids Res.* 30, 1774, 2002.
54. Facompré, M., Carrasco, C., Colson, P., Houssier, C., Chisholm, J. D., Van Vranken, D. L., and Bailly, C., DNA binding and topoisomerase I poisoning activities of novel disaccharide indolocarbazoles, *Mol. Pharmacol.* 62, 1215, 2002.
55. Knölker, H.-J. and Reddy, K. R., Isolation and synthesis of biologically active carbazole alkaloïds, *Chem. Rev*. 102, 4303, 2002.
56. Sarstedt, B. and Winterfeldt, E., Reactions with indole derivatives XLVIII, a simple synthesis of staurosporin aglycon, *Heterocycles* 20, 469, 1983.
57. Magnus, P. D., Exon, C., and Sear, N. L., Indole-2,3-quinodimethanes. Synthesis of indolocarbazoles for the synthesis of the fused dimeric indole alkaloïd staurosporinone, *Tetrahedron* 39, 3725, 1983.
58. Joyce, R. P., Gainor, J. A., and Weinreb, S. M., Synthesis of the aromatic and monosaccharide moieties of staurosporine, *J. Org. Chem*. 52, 1177, 1987.
59. Brenner, M., Rexhausen, H., Steffan, B., and Steglich, W., Synthesis of arcyriarubin B and related bisindolylmaleimides, *Tetrahedron* 44, 2887, 1988.
60. Hughes, I., Nolan, W. P., and Raphael, R. A., Synthesis of the indolo[2,3-*a*]carbazole natural products staurosporinone and arcyriaflavin B, *J. Chem. Soc. Perkin Trans.* 1, 2475, 1990.
61. Moody, C. J., Rahimtoola, K. F., Porter, B., and Ross, B. C., Synthesis of the staurosporin aglycon, *J. Org. Chem.* 57, 2105, 1992.
62. Mc Combie, S. W., Bishop, R. W., Carr, D., Dobek, E., Kirkup, M. P., Kirschmeier, P., Lin, S., Petrin, J., Rosinski, K., Shankar, B. B., and Wilson, O., Indolocarbazoles. 1. Total synthesis and protein kinase inhibiting characteristics of compounds related to K-252c, *Bioorg. Med. Chem. Lett.* 3, 1537, 1993.
63. Link, J. T., Gallant, M., and Danishefsky, S. J., The first synthesis of a fully functionalized core structure of staurosporine: Sequential indolyl glycosidation by endo and exo glycals, *J. Am. Chem. Soc*. 115, 3782, 1993.
64. Link, J. T., Raghavan, S. and Danishefsky, S. J., First total synthesis of staurosporine and *ent*-staurosporine, *J. Am. Chem. Soc.* 117, 552, 1995.
65. Link, J. T., Raghavan, S., Gallant, M., Danishefsky, S. J., Chou, T. C., and Ballas, L. M., Staurosporine and *ent*-staurosporine: The first total syntheses, prospects for a regioselective approach, and activity profiles, *J. Am. Chem. Soc.* 118, 2825, 1996.
66. Wood, J. L., Stoltz, B. M., Dietrich, H., Pflum, D. A., and Petsch, D. T., Design and implementation of an efficient synthetic approach to furanosylated indolocarbazoles: Total synthesis of (+)- and (-)-K252a, *J. Am. Chem. Soc.* 119, 9641, 1997.
67. Wood, J. L., Stoltz, B. M., Goodman, S. N., and Onwueme, K., Design and implementation of an efficient synthetic approach to pyranosylated indolocarbazoles: Total synthesis of (+)-RK286c, (+)-MLR-52, (+)-staurosporine and (-)-TAN-1030a, *J. Am. Chem. Soc.* 119, 9652, 1997.
68. Kobayashi, Y., Fujimoto, T., and Fukuyama, T., Stereocontrolled total synthesis of (+)-K252a, *J. Am. Chem. Soc.* 121, 6501, 1999.
69. Kaneko, T., Wong, H., Okamoto, K. T., and Clardy, J., Two synthetic approaches to rebeccamycin, *Tetrahedron Lett.* 26, 4015, 1985.
70. Gallant, M., Link, J. T., and Danishefsky, S. J., A stereoselective synthesis of indole-b-*N*-glycosides: An application to the synthesis of rebeccamycin, *J. Org. Chem*. 58, 343, 1993.
71. Faul, M. M., Winneroski, L. L., and Krumrich, C. A., Synthesis of rebeccamycin and 11-dechlororebeccamycin, *J. Org. Chem.* 64, 2465, 1999.
72. Bonjouklian, R., Smitka, T. A., Doolin, L. E., Molloy, R. M., Debono, M., Shaffer, S. A., Moore, R. E., Stewart, J. B., and Patterson, G. M. L., Tjipanazoles, new antifungal agents from the blue-green alga *Tolypothrix tjipanasensis*, *Tetrahedron* 47, 7739, 1991.
73. Gilbert, E. J. and Van Vranken, D. L., Control of dissymmetry in the synthesis of (+)-tjipanazole F2, *J. Am. Chem. Soc*. 118, 5500, 1996.
74. Gilbert, E. J., Ziller, J. W., and Van Vranken, D. L., Cyclizations of unsymmetrical bis-1,2-(3-indolyl) ethanes: Synthesis of (-)-tjipanazole F1, *Tetrahedron* 53, 16553, 1997.
75. Chisholm, J. D. and Van Vranken, D. L., Regiocontrolled synthesis of the antitumor antibiotic AT2433-A1, *J. Org. Chem.* 65, 7541, 2000.
76. Meyer, T., Regenass, U., Fabbro, D., Alteri, E., Rousel, J., Moller, M., Caravatti, G., and Matter, A., A derivative of staurosporine (CGP 41 251) shows selectivity for protein kinase C inhibition and *in vitro* anti-proliferative as well as *in vivo* anti-tumor activity, *Int. J. Cancer* 43, 851, 1989.
77. Hoehn, P., Ghisalba, O., Moerker, T., and Peter, H. H., 3-Demethoxy-3-hydroxystaurosporine, a novel staurosporine analog produced by a blocked mutant, *J. Antibiot.* 48, 300, 1995.

78. Akinaga, S., Diverse effects of indolocarbazole compounds on the cell cycle progression of *ras*-transformed rat fibroblast cells, *J. Antibiot.* 46, 1767, 1993.
79. Yamashita, Y., Fujii, N., Murakata, C., Ashizawa, T., Okabe, M., and Nakano, H., Induction of mammalian DNA topoisomerase I mediated DNA cleavage by antitumor indolocarbazole derivatives, *Biochemistry* 31, 12069, 1992.
80. Jackson, J. R., Gilmartin, A., Imburgia, C., Winkler, J. D., Marshall, L. A., and Roshak, A., An indolocarbazole inhibitor of human checkpoint kinase (Chk1) abrogates cell cycle arrest caused by DNA damage, *Cancer Res.* 60, 566, 2000.
81. Fuse, E., Tanii, H., Kurata, N., Kobayashi, H., Shimada, Y., Tamura, T., Sasaki, Y. et al., Unpredicted clinical pharmacology of UCN-01 caused by specific binding to human α_1-acid glycoprotein, *Cancer Res.* 58, 3248, 1998.
82. Sausville, E., Arbuck, S. G., Messmann, R., Headlee, D., Bauer, K. S., Lush, R. M., Murgo, A. et al., Phase I trial of 72-hour continuous infusion of UCN-01 in patients with refractory neoplasms, *J. Clin. Oncol.* 19, 2319, 2001.
83. Eastman, A., Kohn, E. A., Brown, M. K., Rathman, J., Livingstone, M., Blank, D. H., and Gribble, G. W., A novel indolocarbazole, ICP-1, abrogates DNA damage-induced cell cycle arrest and enhances cytotoxicity: Similarities and differences to the cell cycle checkpoint abrogator UCN-01, *Mol. Cancer Ther.* 1, 1067, 2002.
84. Traxler, P., Bold, G., Buchdunger, E., Caravatti, G., Furet, P., Manley, P., O'Reilly, T., Wood, J., and Zimmermann, J., Tyrosine kinase inhibitors: From rational design to clinical trials, *Med. Res. Rev.* 21, 499, 2001.
85. Laird, A. D. and Cherrington, J. M., Small molecule tyrosine kinase inhibitors: Clinical development of anticancer agents, *Expert Opin. Investig. Drugs* 12, 51, 2003.
86. Gingrich, D. E. and Hudkins, R. L., Synthesis and kinase inhibitory activity of 3-(S)-*epi*-K-252a, *Bioorg. Med. Chem. Lett*. 12, 2829, 2002.
87. Maroney, A. C., Finn, J. P., Connors, T. J., Durkin, J. T., Angeles, T., Gessner, G., Xu, Z. et al., CEP1347 (KT7515), a semi-synthetic inhibitor of the mixed lineage kinase family, *J. Biol. Chem.* 276, 25302, 2001.
88. Roux, P. P., Dorval, G., Boudreau, M., Angers-Loustau, A., Morris, S. J., Makkerh, J., and Barker, P. A., K252a and CP1347 are neuroprotective compounds that inhibit mixed-lineage kinase-3 and induce activation of Akt and ERK, *J. Biol. Chem.* 277, 49473, 2002.
89. Nheu, T. V., He, H., Hirokawa, Y., Tamaki, K., Florin, L., Schmitz, M. L., Suzuki-Takahashi, I. et al., The K252a derivatives, inhibitors for the PAK/MLK kinase family selectively block the growth of RAS transformants, *Cancer J.* 8, 238, 2002.
90. Kojiri, K., Kondo, H., Yoshinari, T., Arakawa, H., Nakajima, S., Satoh, F., Kawamura, K., Okura, A., Suda, H., and Okanishi, M., A new antitumor substance, BE-13793C, produced by a streptomycete. Taxonomy, fermentation, isolation, structure determination and biological activity, *J. Antibiot.* 44, 723, 1991.
91. Tanaka, S., Ohkubo, M., Kojiri, K., Suda, H., Yamada, A., and Uemura, D., A new indolopyrrolocarbazole antitumor substance, ED-110, a derivative of BE-13793C, *J. Antibiot.* 45, 1797, 1992.
92. Kanzawa, F., Nishio, K., Kubota, N., and Saijo, N., Antitumor activities of a new indolocarbazole substance, NB-506, and establishment of NB-506-resistant cell lines, SBC-3/NB, *Cancer Res.* 55, 2806, 1995.
93. Yoshinari, T., Ohkubo, M., Fukasawa, K., Egashira, S., Hara, Y., Matsumoto, M., Nakai, K., Arakawa, H., Morishima, H., and Nishimura, S., Mode of action of a new indolocarbazole anticancer agent, J-107088, targeting topoisomerase I, *Cancer Res.* 59, 4271, 1999.
94. Ohkubo, M., Nishimura, T., Kawamoto, H., Nakano, M., Honma, T., Yoshinari, T., Arakawa, H., Suda, H., Morishima, H., and Nishimura, S., Synthesis and biological activities of NB-506 analogs modified at the glucose group, *Bioorg. Med. Chem. Lett.* 10, 419, 2000.
95. Yoshinari, T., Yamada, A., Uemura, D., Nomura, K., Arakawa, H., Kojiri, K., Yoshida, E., Suda, H., and Okura, A., Induction of topoisomerase I-mediated DNA cleavage by a new indolocarbazole, ED-110, *Cancer Res.* 53, 490, 1993.
96. Bailly, C., Qu, X., Chaires, J. B., Colson, P., Houssier, C., Ohkubo, M., Nishimura, S., and Yoshinari, T., Substitution at the F-ring *N*-imide of the indolocarbazole antitumor drug NB-506 increases the cytotoxicity, DNA binding, and topoisomerase I inhibition activities, *J. Med. Chem.* 42, 2927, 1999.
97. Bailly, C., Dassonneville, L., Colson, P., Houssier, C., Fukasawa, K., Nishimura, S., and Yoshinari, T., Intercalation into DNA is not required for inhibition of topoisomerase I by indolocarbazole antitumor agents, *Cancer Res.* 59, 2853, 1999.
98. Facompré, M., Goossens, J.-F., and Bailly, C., Apoptotic response of HL-60 human leukemia cells to the antitumor drug NB-506, a glycosylated indolocarbazole inhibitor of topoisomerase I, *Biochem. Pharmacol.* 61, 299, 2001.

99. Takenaga, N., Hasegawa, T., Ishii, M., Ishizaki, H., Hata, S., and Kamei, T., *In vitro* metabolism of a new anticancer agent, 6-*N*-formylamino-12,13-dihydro-1,11-dihydroxy-13-(β-D-glucopyranosyl)5*H*-indolo [2,3-*a*]pyrrolo[3,4-*c*]-5,7(6*H*)-dione (NB-506), in mice, rats, dogs and humans, *Drug Metab. Dispos.* 27, 213, 1999.
100. Takenaga, N., Ishii, M., Nakajima, S., Hasegawa, T., Iwasa, R., Ishizaki, H., and Kamei, T., *In vivo* metabolism of a new anticancer agent, 6-*N*-formylamino-12,13-dihydro-1,11-dihydroxy-13-(β-D-glucopyra nosyl)5*H*-indolo[2,3-*a*]pyrrolo[3,4-*c*]-5,7(6*H*)-dione (NB-506), in rats and dogs: Pharmacokinetics, isolation, identification, and quantification of metabolites, *Drug Metab. Dispos.* 27, 205, 1999.
101. Goossens, J.-F., Kluza, J., Vezin, H., Kouach, M., Briand, G., Baldeyrou, B., Wattez, N., and Bailly, C., Plasma stability of two glycosyl indolocarbazole antitumor agents, *Biochem. Pharmacol.* 65, 25, 2003.
102. Long, B. H., Rose, W. C., Vyas, D. M., Matson, J. A., and Forenza, S., Discovery of antitumor indolocarbazoles: Rebeccamycin, NSC 655649, and fluoroindolocarbazoles, *Curr. Med. Chem. Anti-Cancer Agents* 2, 255, 2002.
103. Anizon, F., Moreau, P., Sancelme, M., Laine, W., Bailly, C., and Prudhomme, M., Rebeccamycin analogs bearing amine substituents or other groups on the sugar moiety, *Bioorg. Med. Chem. Lett.* 11, 3709, 2003.
104. Anizon, F., Moreau, P., Sancelme, M., Voldoire, A., Prudhomme, M., Ollier, M., Severe, D. et al., Synthesis, biochemical and biological evaluation of staurosporine analogs from the microbial metabolite rebeccamycin, *Bioorg. Med. Chem. Lett.* 6, 1597, 1998.
105. Marminon, C., Anizon, F., Moreau, P., Leonce, S., Pierre, A., Pfeiffer, B., Renard, P., and Prudhomme, M., Syntheses and antiproliferative activities of new rebeccamycin derivatives with the sugar unit linked to both indole nitrogen, *J. Med. Chem.* 45, 1330, 2002.
106. Facompré, M., Baldeyrou, B., Bailly, C., Anizon, F., Marminon, C., Prudhomme, M., Colson, P., and Houssier, C., DNA targeting of two new antitumor rebeccamycin derivatives, *Eur. J. Med. Chem.* 37, 925, 2002.
107. Moreau, P., Gaillard, N., Marminon, C., Anizon, F., Dias, N., Baldeyrou, B., Bailly, C. et al., Semi-synthesis, topoisomerase I and kinases inhibitory properties, and antiproliferative activities of new rebeccamycin derivatives, *Bioorg. Med. Chem.* 11, 4871, 2003.
108. Marminon, C., Pierre, A., Pfeiffer, B., Perez, V., Leonce, S., Joubert, A., Bailly, C., Renard, P., Hickman, J., and Prudhomme, M., Syntheses and antiproliferative activities of 7-azarebeccamycin analogs bearing one 7-azaindole moiety, *J. Med. Chem.* 46, 609, 2003.
109. Marminon, C., Pierre, A., Pfeiffer, B., Perez, V., Leonce, S., Renard, P., and Prudhomme, M., Syntheses and antiproliferative activities of rebeccamycin analogs bearing two 7-azaindole moieties, *Bioorg. Med. Chem.* 11, 679, 2003.
110. Dancey, J. and Sausville, E. A., Issues and progress with protein kinase inhibitors for cancer treatment, *Nat. Rev. Drug Discov.* 2, 297, 2003.
111. Walder, S., Perspectives for cancer therapies with CDK2 inhibitors, *Drug Resist. Updat.* 4, 347, 2001.
112. Senderowicz, A. M., Preclinical and clinical development of CDK inhibitors, *Proceedings of the 1st International Symposium on Signal Transduction Modulators in Cancer Therapy*, Amsterdam, 2002, p. 41.
113. Sausville, E. A., Elsayed, Y., Monga, M., and Kim, G., Signal transduction-directed cancer treatments, *Ann. Rev. Pharmacol. Toxicol.* 43, 199, 2003.
114. Virchis, A., Ganeshaguru, K., Hart, S., Jones, D., Fletcher, L., Wright, F., Wickremasinghe, R. et al., A novel treatment approach for low grade lymphoproliferative disorders using PKC412 (CGP41251), an inhibitor of protein kinase C, *Hematol. J.* 3, 131, 2002.
115. Merchant, J., Tutsch, K., Dresen, A., Arzoomanian, R., Alberti, D., Feierabend, C., Binger, K. et al., Phase I clinical and pharmacokinetic study of NSC 655649, a rebeccamycin analog, given in both single-dose and multiple dose-formats, *Clin. Cancer Res.* 8, 2193, 2002.
116. Tolcher, A. W., Eckhardt, S. G., Kuhn, J., Hammond, L., Weiss, G., Rizzo, J., Aylesworth, C. et al., Phase I and pharmacokinetic study of NSC 655649, a rebeccamycin analog with topoisomerase inhibitory properties, *J. Clin. Oncol.* 19, 2937, 2001.
117. Dowlati, A., Hoppel, C. L., Ingalls, S. T., Majka, S., Li, X., Sedransk, N., Spiro, T., Gerson, S. L., Ivy, P., and Remick, S. C., Phase I and pharmacokinetic study of rebeccamycin analog NSC 655649 given daily for five consecutive days, *J. Clin. Oncol.* 19, 2309, 2001.
118. Goel, S., Wadler, S., Hoffman, A., Volterra, F., Baker, C., Nazario, E., Ivy, P., Silverman, A., and Mani, S., A phase II study of rebeccamycin analog NSC 655649 in patients with metastatic colorectal cancer, *Invest. New Drugs* 21, 103, 2003.
119. Hussain, M., Vaishampayan, U., Heilbrun, L. K., Jain, V., LoRusso, P. M., Ivy, P., and Flaherty, L., A phase II study of rebeccamycin analog (NSC-655649) in metastatic renal cell cancer, *Invest. New Drugs* 21, 465, 2003.

120. Prudhomme, M., Biological targets of antitumor indolocarbazoles bearing a sugar moiety, *Curr. Med. Chem. Anti-Cancer Agents* 4, 509, 2004.
121. Henon, H., Conchon, E., Hugon, B., Messaoudi, S., Golsteyn, R. M., and Prudhomme, M., Pyrrolocarbazoles as checkpoint 1 kinase inhibitors, *Anti-Cancer Agents Med. Chem.* 8, 577, 2008.
122. Berlinck, R. G. S., Britton, R., Piers, E., Lim, L., Roberge, M., Moreira da Rocha, R., and Andersen, R. J., Granulatimide and isgranulatimide, aromatic alkaloids with G2 checkpoint inhibition activity isolated from the Brazilian ascidian *Didemnum granulatum*: Structure elucidation and synthesis, *J. Org. Chem.* 63, 9850, 1998.
123. Messaoudi, S., Anizon, F., Pfieffer, B., and Prudhomme, M., Synthesis of bridged aza-rebeccamycin analogues, *Tetrahedron* 61, 7304, 2005.
124. Messaoudi, S., Anizon, F., Peixoto, P., David-Cordonnier, M.-H., Golsteyn, R. M., Leonce, S., Pfieffer, B., and Prudhomme, M., Synthesis and biological activities of 7-aza rebeccamycin analogues bearing the sugar moiety on the nitrogen of the pyridine ring, *Bioorg. Med. Chem.* 14, 7551, 2006.
125. Marminon, C., Anizon, F., Moreau, P., Pfieffer, B., Pierre, A., Golsteyn, R. M., Peixoto, P. et al., Rebeccamycin derivatives as dual DNA-damaging agents and potent checkpoint kinase 1 inhibitors, *Mol. Pharmacol.* 74, 1620, 2008.
126. Anizon, F., Golsteyn, R. M., Leonce, S., Pfieffer, B., and Prudhomme, M., A three-step synthesis from rebeccamycin of an efficient checkpoint kinase 1 inhibitor, *Eur. J. Med. Chem.* 44, 2234, 2009.
127. Asche, C. and Demeunynck, M., Antitumor carbazoles, *Anti-Cancer Agents Med. Chem.* 7, 247, 2007.
128. Fahrmann, M., Targeting protein kinase C (PKC) in physiology and cancer of the gastric cell system, *Curr. Med. Chem.* 15, 1175, 2008.
129. Janosik, T., Wahistrom, N., and Bergman, J., Recent progress in the chemistry and applications of indolocarbazoles, *Tetrahedron* 64, 9159, 2008.
130. Wincent, E., Shirani, H., Bergman, J., Rannug, U., and Janosik, T., Synthesis and biological evaluation of fused thio- and selenopyrans as new indolocarbazole analogues with aryl hydrocarbon receptor affinity, *Bioorg. Med. Chem.* 17, 1648, 2009.
131. Knockaert, M., Blondel, M., Bach, S., Leost, M., Elbi, C., Hager, G. L., Nagy, S. R. et al., Independent actions on cyclic-dependent kinases and aryl hydrocarbon receptor mediate the antiproliferative effect of indirubins, *Oncogene* 23, 4400, 2004.
132. Nakano, H. and Omura, S., Chemical biology of natural indolocarbazole products: 30 years since the discovery of staurosporine, *J. Antibiot.* 62, 17, 2009.
133. Knolker, H.-J. and Reddy, K. R., Chemistry and biology of the carbazole alkaloids, in Cordell, G. A. Ed., *The Alkaloids, Chemistry and Biology*, Vol. 65, Academic Press, London, 2008, pp. 1–430.
134. Ryan, K. S. and Drennan, C. L., Divergent pathways in the biosynthesis of bisindole natural products, *Chem. Biol.* 16, 351, 2009.
135. Chiu, H.-T., Chen, Y.-L., Chen, C.-Y., Jin, C., Lee, M.-N., and Lin, Y.-C., Molecular cloning, sequence analysis and functional characterization of the gene cluster for biosynthesis of K252a and its analogs, *Mol. BioSyst.* 5, 1180, 2009.
136. Chiu, H.-T., Lin, Y.-C., Lee, M.-N., Chen, Y.-L., Wang, M.-S., and Lui, C.-C., Biochemical characterization and substrate specificity of the gene cluster for biosyntheses of K-252a and its analogues by *in vitro* heterologous expression system of *Escherichia coli*, *Mol. BioSyst.* 5, 1192, 2009.
137. Salas, A. P., Zhu, L., Sanchez, C., Brana, A. F., Rohr, J., Mendez, C., and Salas, J. P., Deciphering the late steps in the biosynthesis of the anti-tumour indolocarbazole staurosproine: Sugar donor substrate flexibility of the StaG glycosyltransferase, *Mol. Microbiol.* 58, 17, 2005, and references cited therein.
138. Sanchez, C., Salas, A. P., Brana, A. F., Palomino, M., Pineda-Lucena, A., Carbajo, R. J., Mendez, C., Moris, F., and Salas, J. A., Generation of potent and selective kinase inhibitors by combinatorial biosynthesis of glycosylated indolocarbazoles, *Chem. Comm.* 4118, 2009.
139. Pratz, K. W., Sato, T., Murphy, K. M., Stine, A., Rajkhowa, T., and Levis, M., FLT-3 mutant allelic burden and clinical status are predictive of response to FLT3 inhibitors in AML, *Blood* 115, 1425, 2010.

25 Combinatorial Biosynthesis of Anticancer Natural Products

Steven G. Van Lanen and Ben Shen

CONTENTS

25.1 Introduction 671
25.2 Examples of Combinatorial Biosynthesis of Anticancer Natural Products 673
25.2.1 Daunorubicin and Doxorubicin 673
25.2.2 Mithramycins 677
25.2.3 Ansamycins 680
25.2.4 Epothilones 682
25.2.5 Leinamycin 683
25.2.6 Enediynes 684
25.2.7 Aminocoumarins 687
25.3 Summary, Challenges, and Future Prospects 690
Acknowledgments 691
References 691

25.1 INTRODUCTION

Chemotherapy remains a critical component for the treatment of cancer, the estimated cause of one in eight deaths worldwide.[1] Historically, natural products have been excellent sources of chemotherapeutics providing a foundation for anticancer drug discovery and development.[2] However, the increasing incidence of drug resistance[3,4] along with cumulative side effects of certain chemotherapies[4,5] warrants the continued and expanded discovery of new therapeutics. Fortunately, significant progress has been made on several fronts that have allowed the implementation of new strategies for structural diversification. Combinatorial biosynthesis is one such strategy aimed at harnessing the inherent power of microbial genetics and expedient biosynthetic machineries *en route* to natural products with anticancer potential.

Combinatorial biosynthesis encompasses several different and complementary approaches to generate novel compounds.[6–12] However, all these approaches share one feature: they all rely on the manipulation of a microbe's biosynthetic machinery to produce new compounds. Thus, no matter what specific approach is employed, the process of combinatorial biosynthesis begins with the identification of the genes governing the biosynthesis of a given metabolite (Figure 25.1). This has been greatly facilitated by the realization that genes coding for the biosynthesis of a given compound are usually clustered within one region of chromosomal DNA within actinomycetes.[12,13] Typically, a selected gene is inactivated to confirm the identity of the genetic locus and to establish the function of the gene product. Gene inactivation experiments often produce mutant microbes that accumulate biosynthetic intermediates or shunt products (Figure 25.1, I). Although this is usually accomplished in the native producing strain, there have been significant advances in mobilizing biosynthetic gene clusters into genetically amenable hosts for the production of natural products, which, in most cases, dramatically facilitates genetic manipulation.[11,14] In some instances, an additional gene is coexpressed with the endogenous biosynthetic genes leading to the introduction of functionality not

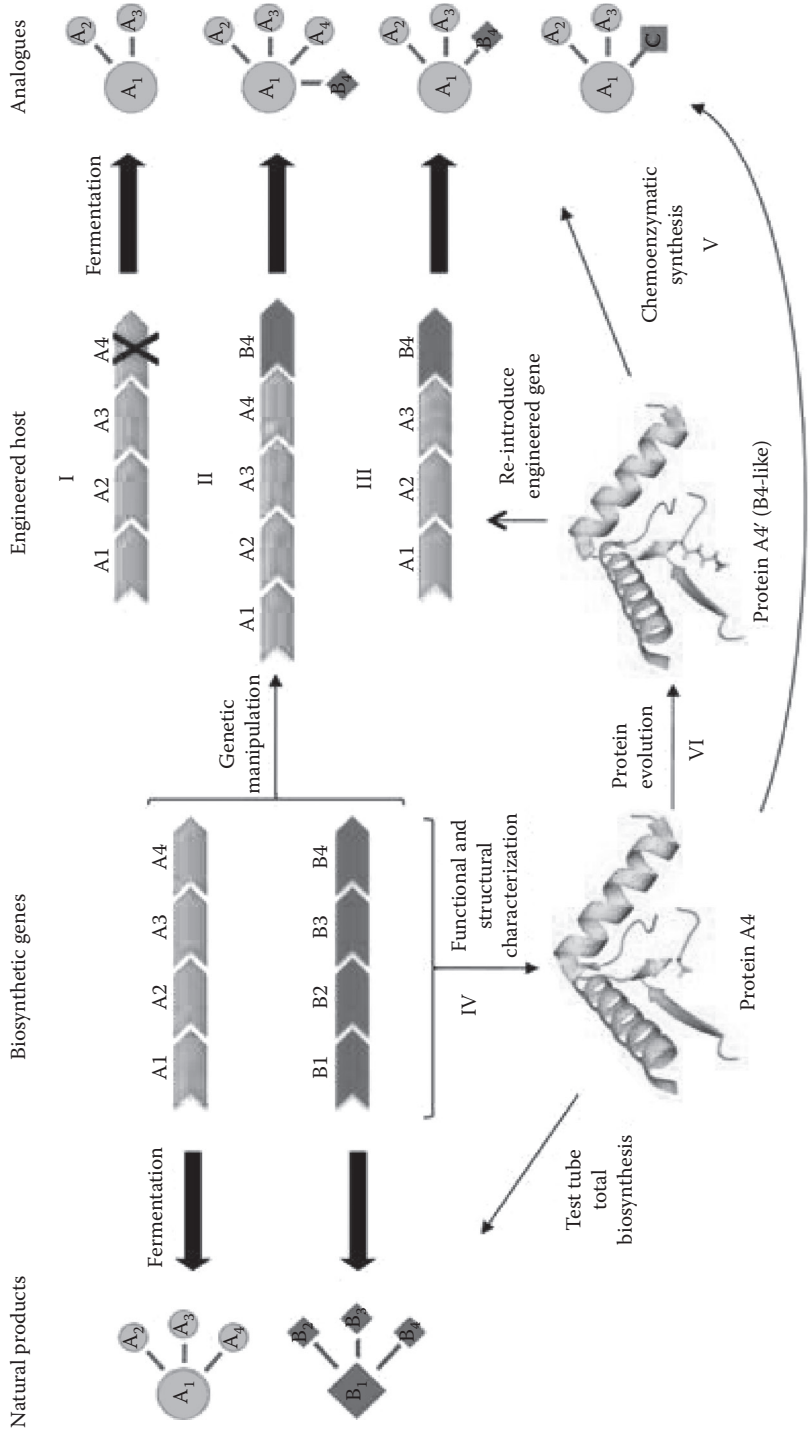

FIGURE 25.1 **(See color insert.)** Potential combinatorial biosynthetic strategies for producing natural products and analogs: I, gene inactivation; II, gene expression; III, cross-complementation; IV, functional and structural characterization of key biosynthetic enzymes; V, chemoenzymatic synthesis; and VI, enzyme engineering by mutagenesis or directed evolution.

observed from the native producer (Figure 25.1, II). Alternatively, an inactivated gene can be cross-complemented with a functionally equivalent gene or related variant to yield new analogs (Figure 25.1, III). Although shown for a single gene, the process can be adapted for multiple genes. Fundamentally, however, in all cases, the successful application of *in vivo* combinatorial biosynthetic methods relies critically on the implementation of robust genetic systems.

Also critical to the success of combinatorial biosynthesis is the functional and mechanistic understanding of individual enzymes. Often, this knowledge is gained by examining the structure and function of recombinant proteins *in vitro* (Figure 25.1, IV). Similar to the dependence of *in vivo* combinatorial biosynthetic strategies on genetic systems, the *in vitro* studies depend on soluble, active protein. In many cases, such as the large multimodular proteins involved in polyketide and nonribosomal peptide biosynthesis, this requirement has hindered significant advances. Nevertheless, the *in vitro* strategy has been successfully used with relatively simpler proteins not only to reconstitute entire biosynthetic pathways requiring several enzymes,[15,16] but also to take advantage of enzyme reaction reversibility and relaxed specificity to generate libraries of structural analogs using a chemoenzymatic approach (Figure 25.1, V).[17,18] Alternatively, a desired enzyme activity can be modified by site-directed mutagenesis or directed evolution (Figure 25.1, VI),[19] which can also lead to new analogs. It can be envisioned that the gene for the evolved enzyme can be reintroduced into the gene cluster to generate new analogs *in vivo*, but this strategy has not yet been explored. Although clearly not as prevalent as *in vivo* genetic manipulation, it is beginning to appear that *in vitro* approaches are opening up new avenues for structural diversification.

This review is an update of our prior report highlighting combinatorial strategies for seven families of anticancer natural products: the anthracyclines, mithramycins, ansamycins, epothilones, leinamycins, enediynes, and aminocoumarins.[20] The goals of this report are (i) to give specific examples of the combinatorial biosynthetic strategies highlighted in Figure 25.1 that have successfully yielded new compounds, and to summarize the biological activity of these new compounds (if reported); and (ii) to summarize the recent advances in our understanding of the biochemical pathways and enzyme mechanism that lead to the final product, which sets the stage for a more rationale utilization of combinatorial biosynthesis. Although a significant amount of background information is provided herein, the reader is referred to our prior report[20] along with several excellent reviews on the fundamentals of natural product biosynthesis and advances in combinatorial biosynthetic strategies.[6–12]

25.2 EXAMPLES OF COMBINATORIAL BIOSYNTHESIS OF ANTICANCER NATURAL PRODUCTS

25.2.1 Daunorubicin and Doxorubicin

Daunorubicin (DNR) and doxorubin (DOX) are model anthracycline polyketides that were initially isolated from a wild-type and mutant strain of *Streptomyces peucetius*, respectively, and consist of a characteristic tetrahydrotetracene-5,12-quinone scaffold (Figure 25.2a; Chapter 16).[21,22] They have been used clinically since the 1960s to treat a wide range of solid tumors and certain hematological malignancies. Since their introduction into the clinic, the efficacy of DNR and DXR has continued to be improved by conjugation to carriers such as liposomes,[23] and recently, it has been demonstrated that coadministration of DNR with the antimetabolite cytarabine improved the duration of survival in young adults with acute myeloid leukemia.[24] Despite this success, long-term treatment with DNR and DOX can result in life-threatening cardiotoxicity.[25] However, following the discovery of DNR and DOX, new anthracyclines have been isolated with structural variations that reduce side effects. For example, aclacinomycin (also known as aclarubicin) isolated from *Streptomyces galilaeus* is a trisaccharide-containing anthracycline associated with significantly less cardiotoxicity, and has been clinically used in Japan (Figure 25.2a).[26] Thus, naturally occurring structural variations of the common tetracyclic core have been shown to alter the biological activity, thus providing the inspiration to rationally design new anthracyclines by combinatorial biosynthesis.

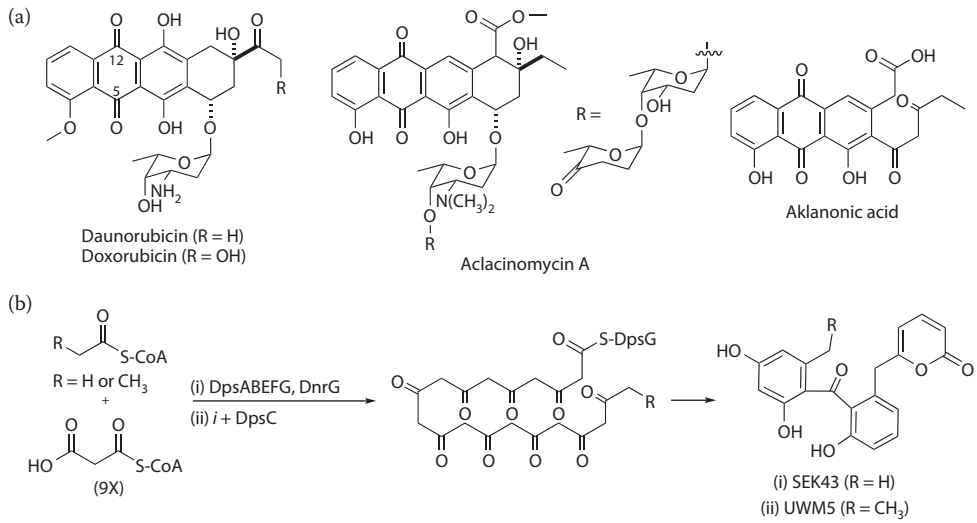

FIGURE 25.2 Anthracycline polyketides: (a) structures of representative anthracyclines and (b) biosynthesis of the polyketide backbone of anthracyclines and aberrantly cyclized decaketides.

The biosynthetic gene cluster for DNR/DOX[27,28] was cloned and sequenced shortly after the gene clusters for the aromatic polyketides actinorhodin[29] and tetracenomycin[30] were reported. Clearly identifiable in all clusters were genes encoding proteins with similarity to bacterial fatty acid synthases (FASs): a ketosynthase α (KS_α) subunit, a KS_β unit (often denoted as the chain length factor), and an acyl carrier protein (ACP), and together with a malonyl-CoA:ACP transacylase that is recruited from the endogenous FAS system; this type II polyketide synthase (PKS) system has been demonstrated to function as an elongation module responsible for multiple rounds of decarboxylative condensation using malonyl-CoA as a substrate.[31] While this mechanism is similar to that of fatty acid biosynthesis, wherein the newly formed β-keto group is completely reduced by a ketoreductase (KR), dehydratase, and enoylreductase enzymes, the polyketide from type II PKSs is not reduced leading to an unstable poly-β-carbonylthioester intermediate that, upon catalysis by discrete cyclases, a KR, aromatases, and oxygenases, results in an isolable polycyclic intermediate, which has been reviewed elsewhere for anthracyclines and related aromatic polyketides.[31,32] This intermediate is subsequently acted on regiospecifically by tailoring enzymes such as methyltransferases and glycosyltransferases to yield the final product.

For the minimal type II PKS system, the biosynthesis of the polyketide backbone is initiated by decarboxylation of malonyl-ACP to yield an acetyl-ACP starter unit such as that observed for tetracenomycin[33] and actinorhodin.[34] In contrast, several type II PKS systems contain a dedicated enzyme with similarity to KS III (FabH) that initiates polyketide biosynthesis by the formation of a nonacetyl primed ACP, and sometimes this initiation module contains a dedicated ACP. Polyketide biosynthesis for DNR/DOX is initiated by the KS III-like enzyme, DpcC, which works in concert with the elongation PKS [(DpsA [KS_α], DpsB [KS_β], and DpsG [ACP]), a KR (DpsE), two cyclases (DpsF and DpsY), and a monooxygenase (DnrG) to produce aklanonic acid (Figure 25.2a), a bona fide biosynthetic intermediate, or, when the gene for *dpsY* is excluded, the 21-carbon, aberrantly cyclized decaketide UWM5 (Figure 25.2b).[35] By heterologously expressing the DNR/DOX elongation PKS in *Streptomyces lividans*, along with *dpsE*, *dpsF*, and *dnrG*, a 20-carbon, aberrantly cyclized decaketide, SEK43, was produced without any aklanonic acid (Figure 25.2b).[35] Thus, by heterologous expression without the KS III homolog, the DNR/DOX PKS system was converted into an acetyl-primed PKS system. By utilizing a cell-free extract of *S. lividans* strains harboring

the same genes that direct the biosynthesis of SEK43, incorporation of purified, recombinant DpsC was sufficient to switch production to UWM5.[36] Furthermore, DpsC was subsequently shown *in vitro* to self-load a propionyl unit from propionyl-CoA to a conserved Ser residue, which is followed by DpcC-catalyzed decarboxylative condensation with malonyl-*S*-DpsG to form the β-ketoacyl-*S*-DpsG priming unit.[36]

The functional characterization of DpsC as the enzyme responsible for nonacetyl priming has now guided the combinatorial biosynthetic experiments of several, related aromatic polyketides produced by type II PKS.[37–39] For example, by combining the initiation module of R1128, an anthracycline-type aromatic polyketide that incorporates a methyl (R1128a), ethyl (R1128b), isopropionyl (R1128c), or propionyl (R1128d) starter unit (Figure 25.3), with the minimal elongation PKS of

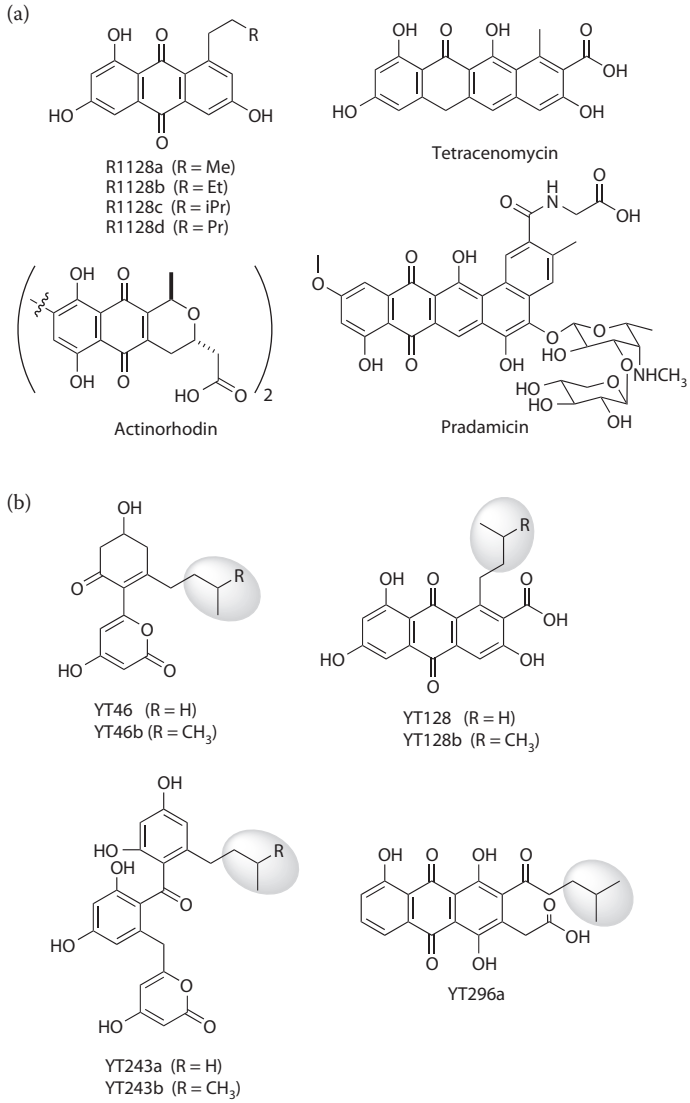

FIGURE 25.3 Aromatic polyketides containing alternative starter units: (a) structures of naturally occurring aromatic polyketides of different backbone lengths and (b) structures of nonacetyl-primed aromatic polyketides that are produced by utilizing the R1128 initiation module and the minimal PKS involved in the biosynthesis of tetracenomycin, actinorhodin, and pradamicin. The engineered starter units are highlighted with ovals.

actinorhodin (an octaketide PKS producing a C_{16} backbone), tetracenomycin (a decaketide PKS producing a C_{20} backbone), and pradamicin (a dodedecaketide PKS producing a C_{24} backbone), a variety of new nonacetyl-primed polyketides were identified.[40,41] Interestingly, in all cases, the KS_α–KS_β compensated for the "bulky" priming unit by catalyzing fewer rounds of decarboxylative condensation. Thus, the R1128 initiation module with (*i*) the actinorhodin PKS produced new hexaketides initiated with propionyl-CoA (YT46) and isobutyryl-CoA (YT46b),[40] (*ii*) the tetracenomicin PKS and R1128 cyclases produced the octaketides YT128 and YT128b,[40] and (*iii*) the pradamycin PKS produced the SEK15-like decaketides YT243a and YT243b (Figure 25.3b).[41] Furthermore, the pradamycin PKS with the R-1128 initiation module, the DNR cyclase DpsY, and other accessory enzymes were able to generate aklanonic acid analog YT296a (Figure 25.3b).[41] Based on these results, along with structural analysis of the actinorhodin KS_α – KS_β that has provided clues to the steric constraints of the binding pocket, it can be concluded that different nonacetyl starter units can be incorporated for most systems and that chain length is not programmed by the number of condensations but by the intrinsic spatial constraints of the KS_α–KS_β.[42]

The manipulation of the biosynthetic enzymes involved in starter unit incorporation has established the general programming rules for type II PKS and simultaneously has led to the isolation of new anthracycline-type and -related polyketides. In addition to these strategies aimed at generating structural variants of the aglycone, enzymatic steps involved in the assembly and incorporation of the lone deoxysugar in DNR/DXR, daunosamine, have also been targeted for combinatorial biosynthesis. Perhaps the best example has been illustrated by the successful generation of an *S. peucetius* mutant strain able to produce 4-epi-DNR and 4-epi-DXR, which was previously shown to have superior anticancer properties compared with the parent structure.[43] In this case, the daunosamine 4-KR *dnmV* was inactivated to generate *S. peucetius* Δ*dnmV* mutant strain that was unable to produce DNR or DXR and accumulated the aglycone intermediate, ε-rhodomycinone (Figure 25.4a). Subsequently, the Δ*dnmV* mutant strain was complemented with *aveE* or *eryBIV*, encoding enzymes required for the biosynthesis of the deoxysugars in avermectin and erythromycin, respectively, that catalyze 4-ketoreduction yielding the opposite stereochemistry relative to DnmV, and fermentation of the resulting strain indeed produced the expected compound in good yields (Figure 25.4b), thus converting the DNR-producing strain to an epirubicin-producing strain and demonstrating that cross-complementation is an excellent strategy for structural diversification.

The glycosylation pattern in other anthracyclines has also been targeted to generate new compounds. The gene cluster for the anthracycline steffimycin from *Streptomyces steffisburgensis* was characterized (Figure 25.4c),[44] and subsequent coexpression of the steffimycin gene cluster with different plasmids containing genes directing the biosynthesis of a variety of deoxysugars led to the production of 12 new steffimycin analogs in the heterologous host, *Streptomyces albus*.[45] Thus, similarly to DNR/DNX, the steffimycin glycosyltransferase incorporated unnatural sugars for attachment to the aglycone, and interestingly, both D- and L-sugars were accepted in this case. One of the new steffimycin analogs, D-digitoxosyl-8-demethoxy-10-deoxysteffimycinone (Figure 25.4c), showed moderately improved antitumor activity against three human tumor cell lines relative to steffimycin. Alternatively, *oleY*, encoding a 3-*O*-methyltransferase, was expressed in *S. steffisburgensis* to give the expected product, 3′-*O*-methylsteffimycin, which also had improved antitumor activity (Figure 25.4c). Finally, the glycosylation pattern for the anthracycline cosmomysin was also targeted in an effort to produce new compounds, but in this case solely by gene inactivations.[46] Cosmomycin contains two unusual trissacharide chains (Figure 25.4d), and inactivation of two genes encoding putative glycosyltransferases led to the isolation of five new anthracyclines. Thus, both cross-complementation and relatively simple gene inactivation has resulted in a library of anthracyclines with unnatural glycosylation patterns.

The biosynthesis of anthracyclines is highlighted by unusual oxidative steps modifying the polycyclic core, and several enzymes catalyzing these oxidations have been characterized within the past decade. For example, the aclacinomycin 10-hydroxylase, which converts 15-demethoxyaclacinomycin A into desmethylaclacinomycin A, has been shown to be a novel substrate-assisted

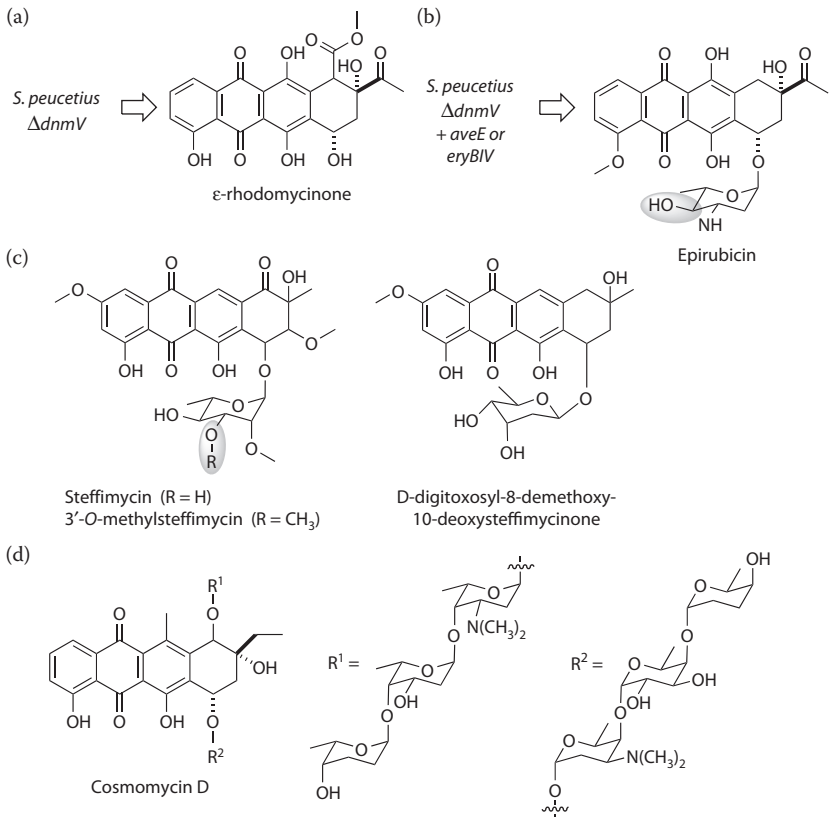

FIGURE 25.4 Anthracycline-type polyketides with modified deoxysugar moieties: (a) structure of the aglycon ε-rhodomycinone produced by gene inactivation of *Streptomyces peucetius*; (b) structure of epirubicin produced by complementation of the indicated *S. peucetius* mutant strain; (c) structures of steffimycin and analogs produced by genetic manipulation; and (d) structure of cosmomycin D containing two unusual trisaccharides attached to the aglycon. The engineered groups are highlighted with ovals.

hydroxylase with the requirement of *S*-adenosyl-L-methionine as a cofactor.[47] Also, the structure for the FAD-dependent aklavinone-11-hydroxylase has been reported.[48] Interestingly, this enzyme is very specific for the aglycone, and the structure suggests a single Arg is the bulky residue that permits entry of the 7-*O*-glycosylated compound. Unexpectedly, mutation of the Arg residue to Ala had no effect on the specific activity with the natural substrate. Although no other potential substrates were tested, the removal of the bulky side chain in the mutant enzyme may yield a protein with relaxed specificity toward glycosylated anthracyclines, and this *in vitro* strategy may yield new glycosylated aklavinone analogs in the near future.

25.2.2 Mithramycins

Mithramycins are aureolic acid polyketides isolated from *Streptomyces argillaceus* with excellent antitumor activity and are clinically used for the treatment of certain types of testicular cancer,[49] chronic and acute myeloid leukemia,[50] Paget's bone disease,[51] and, more recently, pancreatic cancer when combined with bevacizumab, an antibody for vascular endothelial growth factor.[52] The aureolic acids consist of a tricyclic polyketide core (excluding chromocyclomycin) with two oligosaccharide chains of varying lengths (Figure 25.5a).[53] The biologically active structure consists of an aureolic acid dimer complexed with a single Mg^{2+} ion that is able to interact and bind to the minor groove of

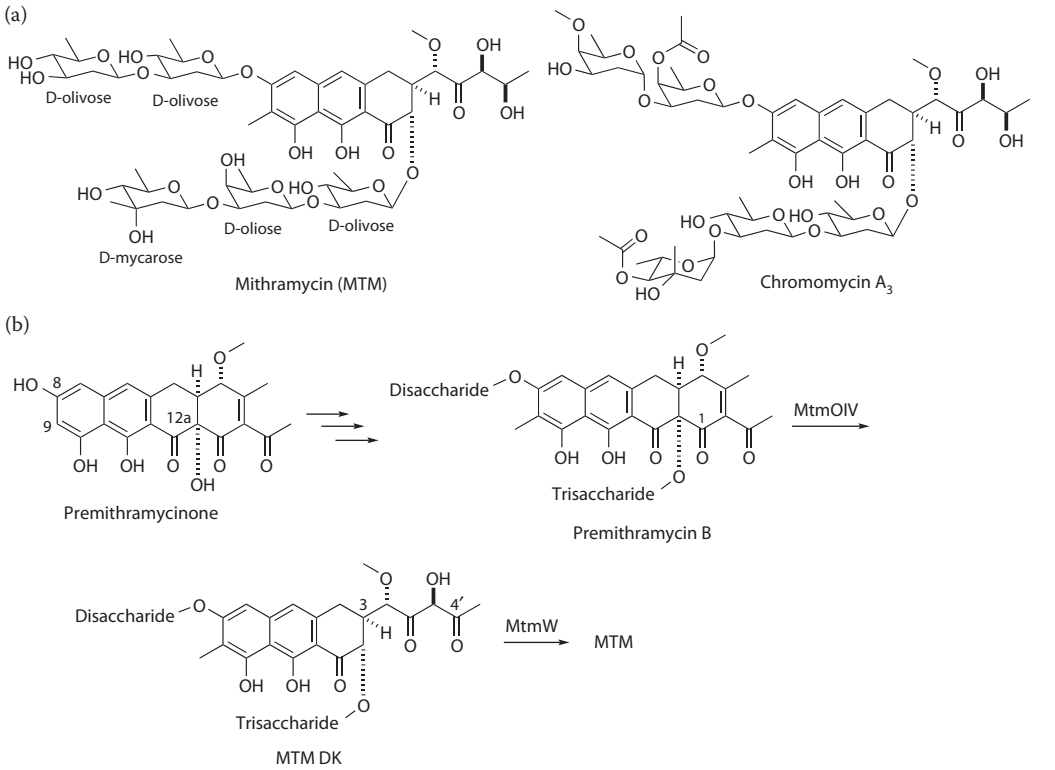

FIGURE 25.5 Aureolic acid polyketides: (a) structures of selected aureolic acid polyketides with identified gene clusters and (b) post-PKS modifications of the premithramycinone aglycon *en route* to mithramycin.

DNA in regions of high GC content. The aureolic acid–DNA complex prohibits DNA processing such as RNA synthesis, thus leading to their potent anticancer properties.

The biosynthetic gene cluster of mithramcyin (MTM)[54] along with the related aureolic acid chromomycin A_3 from *Streptomyces griseus*[55] have been cloned and sequenced (Figure 25.5a). The polyketide scaffold is generated by a type II PKS system in a similar manner to the anthracyclines leading to the first tetracyclic decaketide, premithramycinone, which subsequently undergoes *O*-glycosylation at C-12a and C-8 (Figure 25.5b).[53] For mithramycin biosynthesis, five consecutive glycosylation steps yield tri- and disaccharide moieties, respectively, which is followed by *C*-methylation at C-9 to give premithramycin B. In the penultimate step, the fourth ring at C-1 is oxidatively cleaved by a Baeyer Villager monooxygenase to form MTM DK, and the C-4′-keto group of the newly formed C-3 side chain is reduced by the KR MtmW to yield the final product (Figure 25.5b).

The post-PKS-tailoring steps in MTM biosynthesis have been successfully exploited to generate new analogs. Gene inactivation of *mitW*, encoding the 4′-KR, led to the production of a series of new MTMs, including MTM-SK, demycarosyl-MTM-SK, and MTM-SA.[56] Structural elucidation revealed each derivative was modified within the C-3 side chain, with the MTM-SK and demycarosyl-MTM-SK resulting from a Favorskii-like rearrangement of the β-diketo species that is expected in the absence of MitW, and MTM-SA resulting from a retro-aldol cleavage of the β-diketo species (Figure 25.6a). These compounds were tested using 60 human tumor cell lines to reveal that MTM-SK was more active than mithramycin (three- to ninefold improvement depending on the type of cancer cell line) and, importantly, was more than 1500-fold less toxic than mithramycin.[56] From this same mutant strain, another new compound named MTM-SDK was also isolated, and,

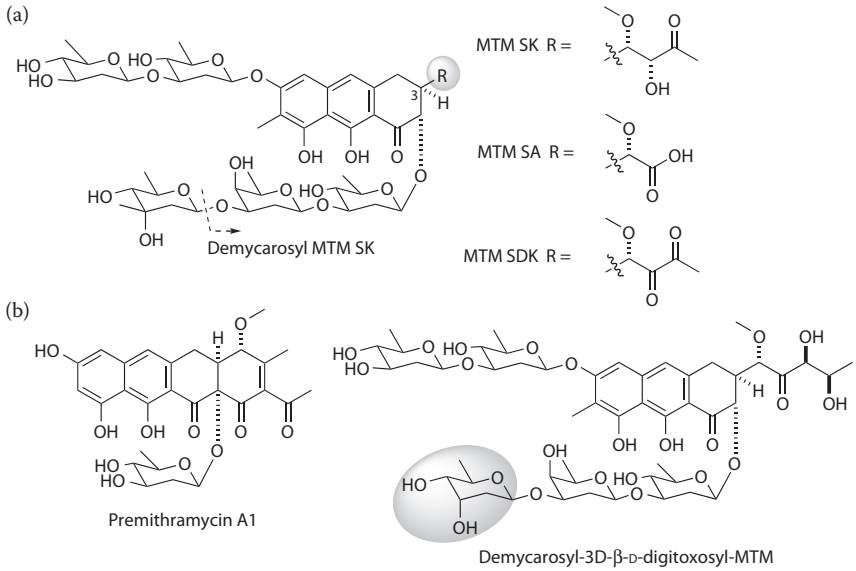

FIGURE 25.6 Novel mithramycins produced by genetic engineering: (a) structures of mithramycins produced upon gene inactivation of *mitW*, encoding a 4′-KR and (b) structures of new mithramycins produced by genetic engineering of the sugar biosynthetic pathways. The engineered groups are highlighted with ovals.

similarly to MTM, was able to selectively interfere with the function of GC-rich DNA-binding transcription factors but at much lower concentrations than MTM.[57] In addition, SDK was a better inhibitor of cell proliferation than MTM and had no detectable cytotoxicity to normal cells. These results suggest SDK may be an effective drug for the treatment of cancers associated with abnormal gene expression due to GC-rich DNA-binding transcription factors.

The post-PKS steps in the biosynthesis of the deoxyhexoses and the glycosylation events of MTM biosynthesis have also been targeted by gene inactivation to yield several new MTM analogs. The genes for *mtmC* and *mtmTIII*, both involved in the biosynthesis of D-mycarose (Figure 25.5a), were inactivated leading to the isolation of new sugar-modified MTMs, ketopremithramycins and ketomithramycins.[58] The gene for *mtmU*, encoding a 2,3-dehydratase involved in the biosynthesis of the three D-olivose sugar moieties, led to the accumulation of premithramycinone (Figure 25.5b), and inactivation of *mtmV*, encoding a putative 4-KR involved in D-oliose biosynthesis, resulted in the accumulation of premithramycinone and the monoglycosylated product, premithramycin A1 (Figure 25.6b).[59] More recently, the wild-type and the Δ*mtmV* mutant strain have been used as hosts for plasmids carrying genes directing the biosynthesis of NDP-activated L-digitoxose that do not normally occur in the pathway, a process that was termed "flooding."[60,61] This strategy led to new mithramycins with altered glycosylation patterns, including an MTM analog containing D-digitoxose as the distal sugar within the trisaccharide, demycarosyl-3D-β-D-digitoxosyl-MTM (Figure 25.6b). This new compound was demonstrated to have improved apoptosis activity with estrogen receptor-positive and -negative human breast cancer cell lines.[61]

Similar to research on anthracycline biosynthesis, the functional identification of proteins and characterization of the enzymes will continue to open up new doors for implementing combinatorial biosynthetic strategies. Perhaps the most interesting aspect of aureolic acid biosynthesis is the conversion of the relatively nontoxic, fully glycosylated tetracyclic precursor to the bioactive tricyclic compound (Figure 25.5). For mithramycin, this reaction is catalyzed by the Baeyer–Villiger monooxygenase MtmOIV, for which a structure has recently been reported.[62] Using structure-inspired site-directed mutagenesis, Phe and Arg residues were individually replaced with an Ala, and the resulting mutant enzymes both had slightly improved second-order rate constants. Although

the biochemical evidence for these results has yet to be determined, this may be the first step in engineering MtmOIV to accommodate different substrates to generate new MTM analogs.

25.2.3 Ansamycins

Rifamycin B from *Amycolatopsis mediterranei* S699, geldanamycin from *Streptomyces hygroscopicus* var. *geldanus* NRRL 3602, and ansamitocin P-3 from *Actinosynnema pretiosum* are representative ansamycin antiobitics that are structurally characterized by an aliphatic ansa bridge with either a benzene (ansamitocin P-3; Chapter 17), benzoquinone (geldanamycin; Chapter 18), or naphthalene (rifamycin B) aromatic ring (Figure 25.7). While rifamycin B and semisynthetic have been employed for nearly 50 years to treat tuberculosis,[63] the latter two compounds of this family are potent anticancer agents. While ansamitocin P-3 inhibits cell division by binding to tubulin,[64] geldanamycin is an inhibitor of heat shock protein 90 (Hsp90),[65,66] which is a molecular chaperone involved in the maturation process of several proteins involved in the control of cell-cycle and transcription regulation. Because of this activity, inhibition by geldanamycin leads to cell-cycle arrest and apoptosis. While geldenamycin and ansamitocin P-3 display a dose-limiting toxicity in humans preventing advancement in clinical trials, a semisynthetic geldanamycin, 17-allylamino-17-demethoxygeldanamycin (17-AAG) is currently being evaluated in phase II/III clinical trials (Figure 25.7).[67,68]

The biosynthetic gene clusters for rifamycin,[69] geldanamycin,[70] and ansamitocin P-3[71] have been cloned and sequenced to reveal this family of compounds is biosynthesized by a modular type I PKS. In contrast to the dissociative architecture and iterative nature of type II aromatic PKS, type I PKS consists of large multimodular proteins, wherein each module minimally consists of KS, AT, and ACP domains that are responsible for the incorporation of one extender unit.[72] Within the PKS of this family, a loading module is present that selects and loads 3-amino-5-hydroxybenoic acid to initiate polyketide extension, and the nascent polyketide tethered to the ACP of the last module serves as the substrate for a discrete amide synthase that catalyzes intramolecular lactamization of the nascent polyketide tethered to the ACP of the last module.[73] The rifamycin PKS consists of 10 extension modules within five proteins with the ATs specifying either methylmalonyl-CoA or malonyl-CoA, and each module contains the expected, additional KR and dehydratase domains that lead to the final degree of saturation observed in the nascent polyketide. On the other hand, the geldanamycin and ansamitocin P-3 PKS consists of seven extension modules within three or four proteins, respectively, with the ATs loading malonyl- and methylmalonyl-CoA and a methoxymalonyl unit that is now known to be derived from 1,3-bisphophoglycerate.[74–76] In all of the cases, several enzymatic post-PKS steps modify the polyketide macrolactam to yield the final product, and many of the genes encoding these enzymes in rifamycin and ansamitocin biosynthesis have been inactivated to make new analogs and delineate the post-PKS steps.[77,78]

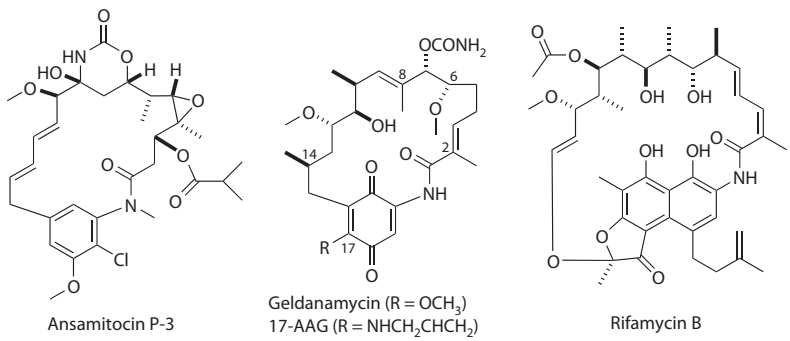

FIGURE 25.7 Structures of selected ansamycin polyketides with identified biosynthetic gene clusters.

As we have previously discussed,[20] combinatorial biosynthesis using several rifamycin and ansamitocin biosynthetic genes along with polypeptide linkers from the 6-deoxyerythronolide B type I PKS and methylmalonyl-CoA biosynthetic genes from *S. coelicolor* resulted in the expected product from the heterologous host *Escherichia coli*.[79] While this proof-of-principle experiment demonstrated the feasibility of rationally designing new compounds using a combinatorial biosynthetic strategy, "simpler" domain-swapping experiments within the geldanamycin-producing strain and gene inactivations have more recently been performed yielding several new analogs.[80,81] In the first example, each AT specifying for nonmalonyl-CoA extender units was individually swapped for a malonyl-CoA-loading AT domain from the rapamycin type I PKS to generate six mutant strains of *S. hygroscopicus* var. *geldanus* NRRL 3602.[80] Four of the mutant strains containing a substituted AT domain in module 1, 4, 5, or 7 resulted in the expected 14-desmethyl, 8-desmethyl, 6-desmethoxy, and 2-desmethyl geldanamycins, respectively. Furthermore, AT substitution of module 7 led to the isolation of the 2-desmethyl-4,5-dihydro analog KOSN1559 that was unable to undergo the post-PKS oxidative tailoring steps at C-17 and C-21 of the phenol (Figure 25.8a), and this new compound was shown to have not only significantly lower cytotoxicity but also increased binding affinity to Hsp90.[80] In a second example, Red/ET mediated recombination was used to effectively inactivate the KR of module 6 by inserting a Y1888F site-directed mutant, and fermentation of the resulting mutant strain not only lead to the accumulation of KOSN1869 containing the expected structural permutation but also prevented activity of the module 7 KR and lacked any post-PKS modification (Figure 25.8a).[81] A slightly different approach has been utilized to generate nonbenzoquinone geldanamycin analogs from a different strain that also produces geldanamycin and for which the biosynthetic gene cluster is known.[82] In this example, the DH domain of the first extension module was inactivated by insertion of the apramycin resistance cassette, which resulted in the abolishment of geldanamycin production. Subsequently, the inactivated DH was replaced *via* a double crossover to restore the wild-type architecture except for one alteration: the expressed module contained a DH domain harboring an H2041Q point mutation, and this His was expected to be critical for NADPH binding. This single point mutation resulted in a mutant strain that produced four new geldanamycin analogs, all of which had the expected structural modification, that is, 15-hydroxygeldanamycin analogs. One of these analogs, DHQ3, which was also not modified by post-PKS-tailoring enzymes to generate the characteristic benzoquinone (Figure 25.8a), had ~5-fold increased inhibition activity using a yeast Hsp90 ATPase assay. Unfortunately, this compound was not tested *in vivo*, and as has been reported for Hsp90 inhibitors, better *in vitro* activity does not necessarily translate to increased *in vivo* efficacy.[83]

Gene inactivation in combination with mutasynthesis has been utilized to prepare new geldanamycin analogs with structural variations in the benzoquinone moiety. An *S. hygroscopicus* var. *geldanus* NRRL 3602 mutant strain was prepared, wherein a subcluster of genes involved in 5-amino-3-hydroxybenzoic acid (AHBA) biosynthesis was inactivated to prepare a nonproducing mutant

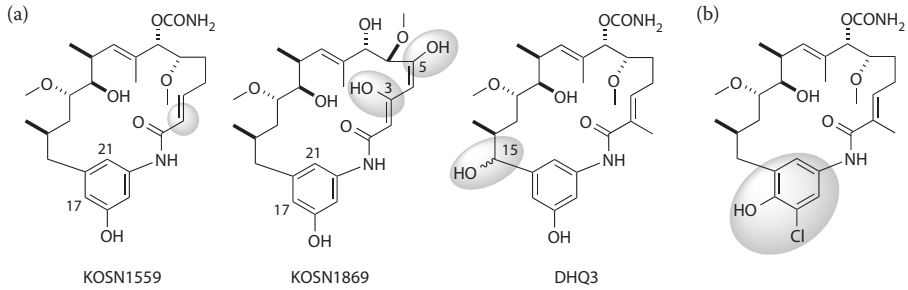

FIGURE 25.8 (See color insert.) Novel ansamycin analogs produced by genetic engineering: (a) structures of geldanamycin analogs produced by engineering the PKS and (b) structure of a geldanamycin analog with a modified benzoquinone moiety produced by mutasynthesis. The engineered groups are highlighted with ovals.

strain that, when AHBA was added to the fermentation media, restored geldanamycin production.[84,85] This result sets the stage to feed AHBA analogs, of which 10 of approximately 30 were incorporated into the geldanamycin polyketide to generate analogs that did not contain the typical benzoquinone moeity.[85] Importantly, the benzoquinone had previously been shown to be a significant factor in the unwanted hepatoxicity associated with the benzoquinone ansamycins,[86] and indeed feeding with 3-amino-5-chlorobenzoic acid resulted in a geldanamycin analog (Figure 25.8b) with comparable *in vitro* potency compared with 17-AAG and 17-(2-dimethylamino)ethylamino-17-demethoxygeldanamycin, two semisynthetic Hsp90 inhibitors in clinical evaluation, and that have higher antiproliferative activity with NQ01 deficient cell lines, and superior efficacy in mouse xenograft models.[85]

Both pre- and post-PKS-modifying steps have been examined *in vitro*. For the former, the initial steps leading to the methylmalonyl extender unit have been revealed by studying homologous enzymes involved in the biosynthesis of oxazolomycin[74] and zwittermycin.[76] Of particular interest is the first reaction catalyzed by an enzyme that belongs to the haloacid dehalogenase superfamily, and the enzyme from the oxazolomycin pathway, OzmB, was shown to use 1,3-bisphosphoglycerate and generate a 3-phosphoglyceryl-*S*-OzmB intermediate. OzmB subsequently catalyzes dephosphorylation to form glyceryl-*S*-OzmB followed by a trans-thioesterification to a holo-ACP. For *in vitro* studies aimed at elucidation of the post-PKS steps, the amide *N*-glycosylation enzyme (Asm25) in ansamitocin P-3 has been characterized.[87] In the parent ansamitocin P-3, the lone amide is *N*-methylated as the terminal step in the biosynthetic pathway; however, a series of *N*-glycosylated ansamitocins have been isolated. This amide *N*-glycosyltransferase was functionally identified and shown to utilize a variety of ansamycin analogs and unusual synthetic lactam derivates. Unfortunately, the resulting products had lower antitumor activity as revealed using an *in vitro* test system.[87]

25.2.4 Epothilones

The epothilones are antifungal antibiotics isolated from the myxobacterium *Sorangium cellulosum*,[88] and consist of a 16-membered macrolactone core with a methylthiazole moiety (Figure 25.9; Chapter 21). Almost immediately after their discovery, the epothilones were demonstrated to be microtubule-stabilizing agents using a similar mechanism of action as taxol.[90] At least seven derivatives of epothilones have entered clinical trials to treat various cancers, and in 2007, one analog (Ixempra™) was approved by the FDA for the treatment of metastatic or locally advanced breast cancer.[89]

The biosynthetic gene cluster for epothilones was identified independently by two groups to reveal five PKS proteins containing a loading module and eight extension modules as well as one discrete protein-containing domain with similarity to nonribosomal peptide synthetase (NRPS).[91,92] Similar to PKS, a minimal module of an NRPS is composed of three domains: an adenylation (A) domain that activates and loads an amino acid to the downstream peptidyl carrier protein (PCP) domain and a condensation (C) domain that catalyzes amide bond formation between adjacent PCP-tethered substrates. The NRPS involved in epothilone biosynthesis has been demonstrated to catalyze incorporation of L-cysteine, which is subsequently condensed with an acetyl unit of the loading module and modified to the thiazole ring by tandem cyclase and oxidase domains located upstream and adjacent to the A domain.[93] Following the first extension and thiazole formation, the macrolide backbone is produced in an analogous fashion to ansamycins, with malonyl- and methylmalonyl-CoA serving as extender units, and the nascent polyketide undergoes intramolecular lactonization that is catalyzed by a thioesterase domain located at the C-terminus of the last extension module. Once released, a P450 oxygenase (EpoK) catalyzes epoxidation at C-12/C-13,[92] although this step is apparently inefficient *in vivo* leading to the formation of minor amounts of nonoxidized epothilones C and D (Figure 25.9).[91] Furthermore, the AT of module 4 is able to load either malonyl- or methylmalonyl-extender units leading to a mixture of epothilones at C-12.[91,92]

The biosynthetic gene cluster with or without *epoK* has now been heterologously expressed in *S. coelicolor* CH999[92] and *Myxococcus xanthus*[94] to yield the expected epothilones, and

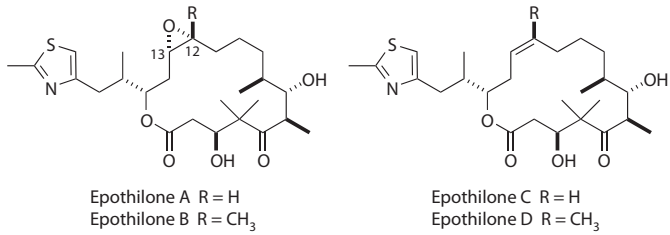

FIGURE 25.9 Structures of selected epothilones.

M. xanthus was used as the host to generate an inactive ER in module 5 by site-directed mutagenesis and an inactive KR domain within module 6 (in the latter case, the experimental details were not reported) to generate several new epothilone analogs with reduced activity.[94,95] More recently, the pathways leading to epothiolones C and D have been reconstructed in *E. coli*.[96,97] In one example, the final four modules (modules 6–9) were expressed in three separate expression vectors in *E. coli* BAP1, which was previously engineered to express *sfp* encoding a phosphopantetheinyl transferase, and an *N*-acetylcysteamine thioester intermediate mimicking the ACP-tethered substrate presented to module 6 was synthesized and included in the fermentation media.[96] The resulting recombinant *E. coli* strain produced epothilone C with yields comparable to the native producing strain. In a separate report, the genes encoding the entire cluster excluding *epoK* were optimized for *E. coli* codon usage, and after splitting the gene *epoD*, encoding a 760-kD protein with four modules, into two separate genes and engineering the linker regions for optimal interaction, epothilone C and D biosynthesis was produced.[97] Unfortunately, yields were quite low (<1 μg/mL) compared with using *S. coelicolor* as a host (50–100 μg/mL), but nevertheless demonstrate the utility of *E. coli* for heterologous production of epothilone-type compounds. Furthermore, the *in vitro* demonstration of the relaxed substrate specificities of the AT of module 6,[98] and the demonstration that EpoA containing the loading module, and EpoB containing the NRPS module, can be replaced with proteins from rapamycin, enterobactin, or yersiniabactin biosynthetic pathways,[99] all suggest that the manipulation of the epothilone assembly line has the potential to generate new analogs.

25.2.5 Leinamycin

Leinamycin, isolated from species of *Streptomyces atroolivaceus*,[100] is a hybrid peptide-polyketide that has potent antitumor activity against several cancer cell lines.[101,102] *In vitro* analysis has demonstrated that leinamycin, upon reductive activation in the presence of thiols, exerts its anticancer activity by an epi-sulfonium ion-mediated DNA alkylation, a mode of action that is unprecedented for thio-dependent DNA cleavage.[103] Further studies have demonstrated that leinamycin alkylates DNA at the N7-position of guanine bases,[104] and binding to DNA also generates leinamycin–guanine adducts that result in the rapid formation of apurinic sites.[105] Recently *in vivo* analysis using MiaPaCa cells has indeed demonstrated that both single- and double-stranded DNA breaks due to the generation of reactive oxygen species and apurinic sites correlate to the potent cytotoxic activity of leinamycin.[106]

The structure of leinamycin consists of an 18-membered macrolactam containing a thiazole ring and an unusual 1,3-dioxo-1,2-dithiolane moiety (Figure 25.10). The identification of the biosynthetic gene cluster in 2002 revealed a hybrid NRPS–PKS system with a novel genetic architecture wherein the six modules of the type I PKS lack the AT domain,[107,108] but instead a discrete AT LnmG loads each ACP domain *in trans*, which has been demonstrated *in vitro*.[109] This AT-less PKS architecture has now been identified in a number of biosynthetic gene clusters for structurally distinct polyketides[110,111] and may provide an entry point for modification of the leinamycin polyketide scaffold.

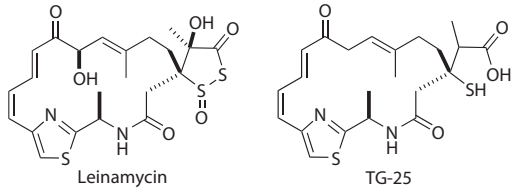

FIGURE 25.10 Structure of leinamycin and TG-25, an engineered analog of leinamycin generated by inactivating the *lnmE* gene.

Several genes within *S. atroolivaceus* have been inactivated to define the gene cluster boundary,[108] confirm the requirement of certain genes for leinamycin biosynthesis, and prepare new leinamycin analogs. For example, inactivation of *lnmE*, encoding a protein of unknown function, resulted in a mutant strain that produced the leinamycin analog, TG-25 (Figure 25.10).[112] Complementary to leinamycin that requires reductive activation for its anticancer activity, TG-25 is a potent DNA-alkylating agent requiring oxidative activation. This unprecedented mode of action by TG-25 to exert its cytoxicity *via* oxidative activation and epi-sulfonium ion-mediated DNA alkylation could be exploited for anticancer drug discovery as demonstrated in killing prostate cancer cells under high oxidative stress.[112]

The highly unusual structure of leinamycin suggests novel enzymatic steps for its biosynthesis, and a few of these unusual biochemical transformations have been characterized *in vitro*. First, a discrete adenylation enzyme LnmQ was demonstrated to initiate the biosynthesis of the hybrid peptide–polyketide backbone by activation and loading of D-Ala to the cognate ACP, which is also a discrete protein.[113] This result revealed a strategy for directly incorporating D-amino acids in bacterial peptides, which is typically carried out by A domains that activate and load L-amino acids that are subsequently modified by an epimerization domain within an NRPS module.[114] Secondly, the tandem ACPs found in module 6 were demonstrated to be functionally equivalent and that only one is needed for leinamycin biosynthesis, but the downstream ACP is the preferred substrate for malonyl-CoA loading by AT in trans.[115] Finally, a new family of bifunctional acyltransferase/decarboxylase enzymes has been identified by the functional characterization of LmnK, which generates propionyl-*S*-ACP from methylmalonyl-CoA resulting in the β-alkyl branch observed in the final product, leinamycin.[116] LnmK, therefore, could be exploited by combinatorial biosynthesis methods to engineer novel polyketides, especially those with β-alkyl branches.

25.2.6 Enediynes

The enediynes are polyketide-derived natural products that represent some of the most cytotoxic compounds ever discovered from microorganisms (Chapter 22).[117–119] Central to the enediynes, of which more than a dozen unique examples are known,[120] is the presence of two acetylenic groups conjugated to a double bond within a 9- or 10-membered carbocycle that typically undergoes a thiol- or nucleophile-dependent Bergmann-type or Myers-Saito-type cycloaromatization leading to either a 2,6- or 3,6-biradical species, as depicted with the model enediynes neocarzinostatin and C-1027 (Figure 25.11a). This biradical species can readily abstract hydrogen atoms from DNA to generate free radicals, and in the presence of molecular oxygen, leads to double- and single-stranded DNA breaks.[117,118] Furthermore, C-1027 has been demonstrated to generate DNA interstrand cross-links, which is significantly enhanced under hypoxic conditions.[121] Currently, a polymer derivative of NCS, a 9-membered enediyne, is utilized clinically in Japan (SMANCS®),[122] and an antibody conjugate of calicheamicin, a 10-membered enediyne, is utilized within the United States (Mylotarg®).[123]

The biosynthetic gene clusters for the 9-membered enediynes C-1027 from *Streptomyces globisporus*,[124] NCS from *Streptomyces carzinostaticus*,[125] and maduropeptin from *Actinomadura*

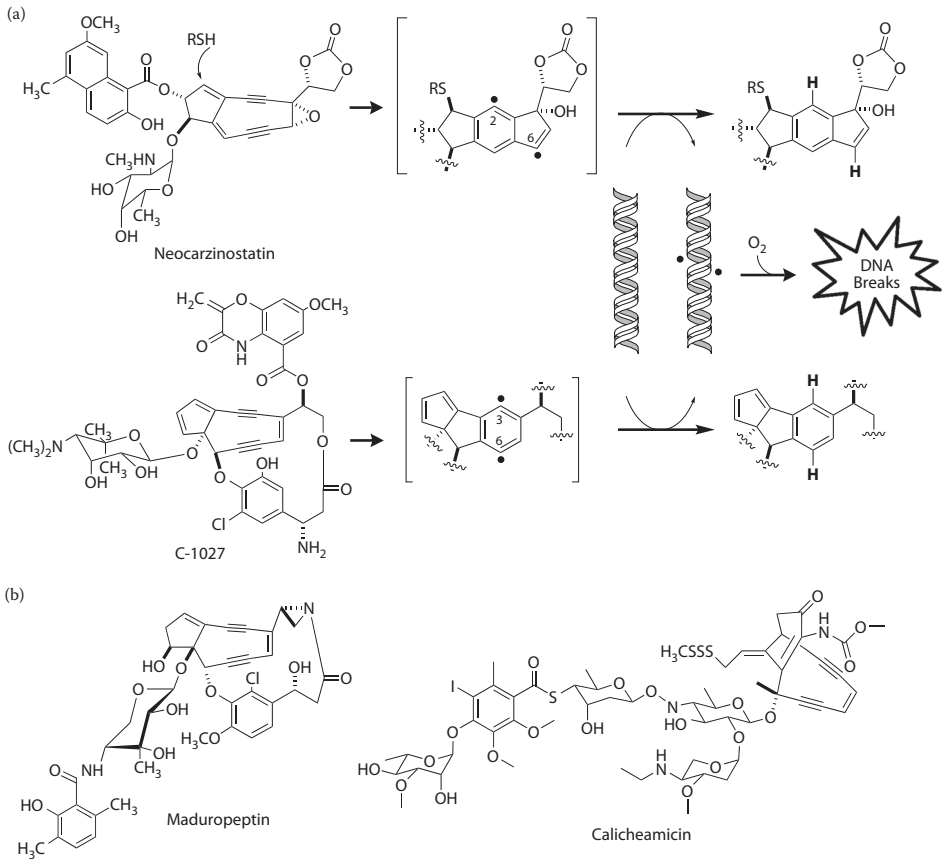

FIGURE 25.11 Structure of representative enediynes: (a) the generation of a diradical species upon an electronic rearrangement of model 9-membered enediynes neocarzinostatin and C-1027 and (b) structure of additional selected enediynes with known biosynthetic gene clusters.

madurae,[126] and the 10-membered enediynes calicheamicin from *Micromonospora echinospora* ssp. *calichensis*[127] and dynemicin from *Micromonospora chersina*[128] have been cloned and sequenced (Figure 25.11a and 11b). A set of homologous genes were identified within the biosynthetic gene clusters for the enediynes, highlighted by an iterative type I PKS (PKSE) containing a novel modular architecture relative to known PKS and a discrete type II thioesterase, and this set of homologous genes has been utilized to design primers for the rapid PCR-amplification of enediyne biosynthetic genes.[129–131] Further analysis of the individual gene clusters has revealed that the enediynes are likely produced utilizing a convergent biosynthetic strategy. For example, in C-1027 biosynthesis, the benzoxazolinate, the α-amino acid, and deoxy aminosugar moieties (see Figure 25.12) are derived from the simple precursors chorismic acid, L-tyrosine, and glucose-1-phosphate prior to attachment to the enediyne core by an acyltransferase, condensation enzyme, and glycosyltransferase, respectively.[120]

A genetic system within the C-1027,[124] NCS,[125] calicheamicin,[127] and dynemicin[128] producing strains has been developed, setting the stage to explore the function of individual genes, determine the cluster boundaries, and generate new analogs by gene inactivation. To date, gene inactivation experiments using the C-1027-producing strain as a host have been the most fruitful for generating and isolating new compounds. Specifically, the benzoxazolinate *O*-methyltransferase and β-amino acid halogenase and hydroxylase have been individually inactivated to yield mutant strains producing the corresponding 7″-desmethyl-, 20′-deschloro-, and 22′-deshydroxy-C-1027 analogs (Figure 25.12).[124,132,133] The ability to induce double-stranded DNA breaks by these

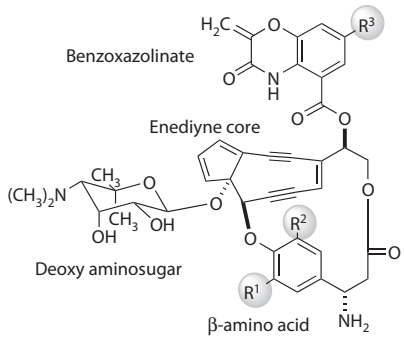

FIGURE 25.12 Structural components of the 9-membered enediyne C-1027 and engineered analogs of C-1027 generated by inactivating selected genes for C-1027 biosynthesis. The engineered groups are highlighted with ovals.

analogs was shown to decrease approximately 50-fold, 4-fold, and 25-fold, respectively; however, the 7″-desmethyl-C-1027, in contrast to 20′-deschloro- and 22′-deshydroxy-C-1027, retained the identical ability to generate DNA interstrand cross-links.[132,133] Not only did these slight modifications change the ratio of double-strand DNA breaks and interstrand cross-links, but they also enabled the discovery of enediyne-mediated DNA interstrand cross-links, an unprecedented mode of action for the enediyne family of anticancer agents. The latter property might prove to be therapeutically advantageous, especially in solid tumors or other poorly oxygenated tumor cells, and C-1027 has indeed been shown to preferentially target hypoxic cancer cells.[121] The ability to modulate the mode of action by subtle structural variations provides the inspiration for other combinatorial techniques to be utilized to generate novel analogs with improved drug properties.

Many of the enzymatic steps involved in C-1027 biosynthesis have now been characterized *in vitro*, including the enzymes that initiate the biosynthesis of each moeity.[131,134–139] Of particular interest is the polyketide origin of the enediyne core, and bioinformatics suggested that PKSE contains KS, AT, KR, and DH domains, from N- to C-terminus, as well as a putative ACP located between the AT and KR domains and a phosphopantetheinyltransferase (PPTase) located at the C-terminus.[131] PPTases incorporate the phosphopantetheine cofactor onto a conserved Ser of an ACP, thus generating a free thiol used to shuffle biosynthetic intermediates. To confirm the identity of the C-1027 cluster, *sgcE*, the gene encoding the PKSE for C-1027 biosynthesis, was inactivated to yield a Δ*sgcE* mutant strain unable to produce C-1027, and subsequently this gene was complemented *in trans* to generate a recombinant strain in which C-1027 production was restored.[124] This set the stage to explore the function of individual domains by site-directed mutagenesis and *in vivo* complementation.[138] Thus, critical residues for the KS, AT, the putative ACP, and the putative PPTase were mutated to Ala, and subsequent complementation of the ΔSgcE mutant strain failed to restore C-1027 production, demonstrating that these residues are essential for the function of SgcE. The identity and function of individual domains was also interrogated *in vitro* by mapping the active sites of the recombinant, wild-type SgcE or site-directed mutants of SgcE using Fourier transform mass spectroscopy.[138] The results provided clear evidence that SgcE contains a novel ACP domain that is modified by a novel PPTase domain *in cis*, and cross-complementation of the ΔSgcE mutant strain with *ncsE* and *mdpE*, the neocarzinostatin and maduropeptin PKSE, respectively, suggests all 9-membered enediyne PKSE have an identical domain architecture and function.[126,138] One of the significant results from these studies is the realization that the ACP and PPTase domains of the 9-membered enediyne PKSE are located on a single polypeptide and a discrete PPTase is not needed

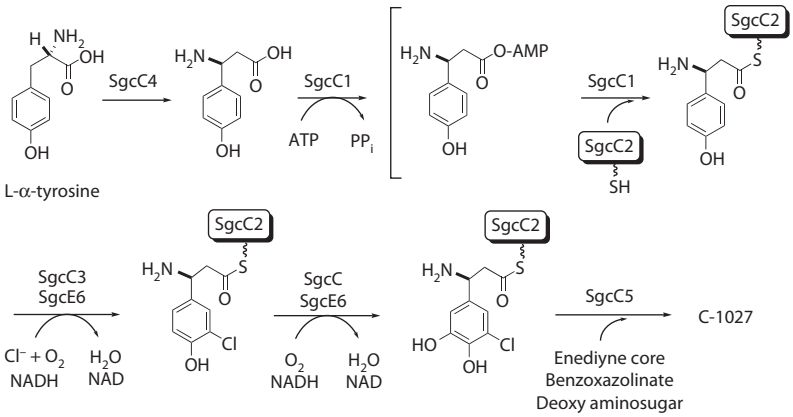

FIGURE 25.13 Biosynthetic pathway leading to the β-amino acid moiety of C-1027.

to form a functional PKS. Indeed, heterologous expression of *sgcE* or *ncsE* along with *sgcE10* or *ncsE10*, which encodes the discrete type II thioesterases, in *E. coli*, *S. lividans*, or *S. albus*, led to the isolation of the new polyene, 1,3,5,7,9,11,13-pentadecaheptaene.[138] Similarly, *in vitro* analysis of recombinant CalE8, the calicheamicin PKSE, and CalE7, the type II thioesterase, revealed the production of a mixture of linear polyenes: the heptaene observed for the 9-membered enediyne PKSE system and a methyl hexaenone of identical chain length.[140–142] It was subsequently shown using several different *in vivo* systems that PKSE–thioester pairs from three 9-membered and two 10-membered enediyne gene clusters all produced the same heptaene, and the PKSE or TE from a 9-membered enediyne system can be freely interchanged with the respective enzyme from a 10-membered enediyne system, supporting a common catalytic function for PKSE by the production of a heptaene.[143] Although it is still not known whether the heptaene or new polyenes are bona fide biosynthetic intermediates or shunt products, the heptaene was demonstrated to be produced in high yields from the native producers of both 9- and 10-membered enediyne-producing strains.[143,144] The results set the stage to explore the assembly of the enediyne core by systematically adding auxiliary enzymes that may lead to the production of advanced intermediates.[138,140–142]

The enzymes involved in the biosynthesis and attachment of the β-amino acid moiety have been functionally assigned, including the new type of aminomutase SgcC4,[135,136] a β-amino acid-activating A enzyme SgcC1,[145,146] FAD- and PCP-dependent halogenase SgcC[147,148] and hydroxylase SgcC3,[148,149] and an ester-bond forming C enzyme SgcC5 (Figure 25.13).[150] A related pathway is observed in maduropeptin biosynthesis,[126] but the variations in regiochemistry and nature of the substitutions make this pathway ideal for combinatorial biosynthetic strategies. Finally, the glycosylation steps in calicheamicin have been analyzed not only to allow for the functional assignment of the glycosylatransferases,[151,152] but also to reveal that certain glycosyltransferases catalyze readily reversible reactions. By exploiting this reversibility, more than 70 calicheamicin analogs were generated,[152] thus demonstrating the feasibility of this *in vitro* chemoenzymatic approach to prepare new enediynes that is likely applicable for the structural diversification of other natural products.

25.2.7 Aminocoumarins

The aminocoumarins were initially discovered based on their antibiotic activity, and the aminocoumarin novobiocin (Albamycin®) has been clinically utilized to treat staphylococci and other Gram-positive infections.[153] The aminocoumarins bind to the ATP-binding site of bacterial DNA gyrase subunit B, a type II topoisomerase, thereby competitively inhibiting the ATPase activity and hence gyrase-catalyzed supercoiling of DNA.[154] In addition, some aminocoumarins inhibit the

ATPase activity of topoisomerase IV, also a type II topoisomerase, thereby restricting the unlinking of daughter chromosomes during replication.[155] During the 1990s, it was realized that novobiocin potentiates the anticancer activity of etopside and teniposide, suggesting a potential role for aminocoumarins in cancer chemotherapy.[156] Since this time, the aminocoumarins have been demonstrated to moderately inhibit the same target as benzoquinone ansamycins, Hsp90, yielding a similar phenotype characterized by a depletion of Hsp90 client proteins.[157] Interestingly, novobiocin binds the C-terminal nucleotide-binding region of Hsp90, which is a unique site relative to the geldamycin-binding N-terminal ATP-binding region.[157] Although the novobiocin–Hsp90 binding interaction is relatively weak, this discovery may nevertheless provide the molecular rationale for previous results demonstrating the potentiation effect observed with novobiocin.

The central feature of this family is the 3-amino-4,7-dihydroxycoumarin moiety that is modified with a variety of structurally unusual groups, such as the *C*-prenylated 4-hydroxybenzoic acid moiety in novobiocin and clorobiocin, the 3-methyl-pyrrole-2,4-dicarboxylic acid moiety in coumermycin, or the aromatic polyketide moieties in simocyclinone D8 and rubradirin (Figure 25.14). The biosynthetic gene cluster for three proven Hsp90 inhibitors of the aminocoumarin family,[157] novobiocin from *Streptomyces spheroides* NCIB 11891,[158] clorobiocin from *Streptomyces roseochromogenes* DSM 12976,[159] and coumermycin A_1 from *Streptomyces rishiriensis* DSM 40489,[160] have been cloned and sequenced. Furthermore, the biosynthetic gene clusters for simocyclinone from *Streptomyces antibioticus* Tü6040[161] and rubradirin from *Streptomyces achromogenes* var. rubradiris NRRL3061,[162] both unusual hybrid polyketide-aminocoumarins, have also been identified. The central feature to all of these compounds is the 3-amino-4,7-dihydroxycoumarin moiety, and much of the functional characterization associated with the assembly of this moiety as well as the assembly and attachment of the peripheral moieties in novobiocin and clorobiocin has been reported and is recently reviewed elsewhere[163]. Of the many strategies employed to generate structural analogs,[164,165] gene inactivation and complementation, *in vitro* chemoenzymatic biosynthesis, and directed evolution have been more recently employed to generate new compounds.

Both clorobiocin and coumermycin A_1 contain a 5-methylpyrrole-2-carboxylic acid moiety, which is replaced by a carbamoyl group in novobiocin (Figure 25.14). The genes involved in the biosynthesis of this moiety have been interrogated by gene inactivation within the clorobiocin-producing

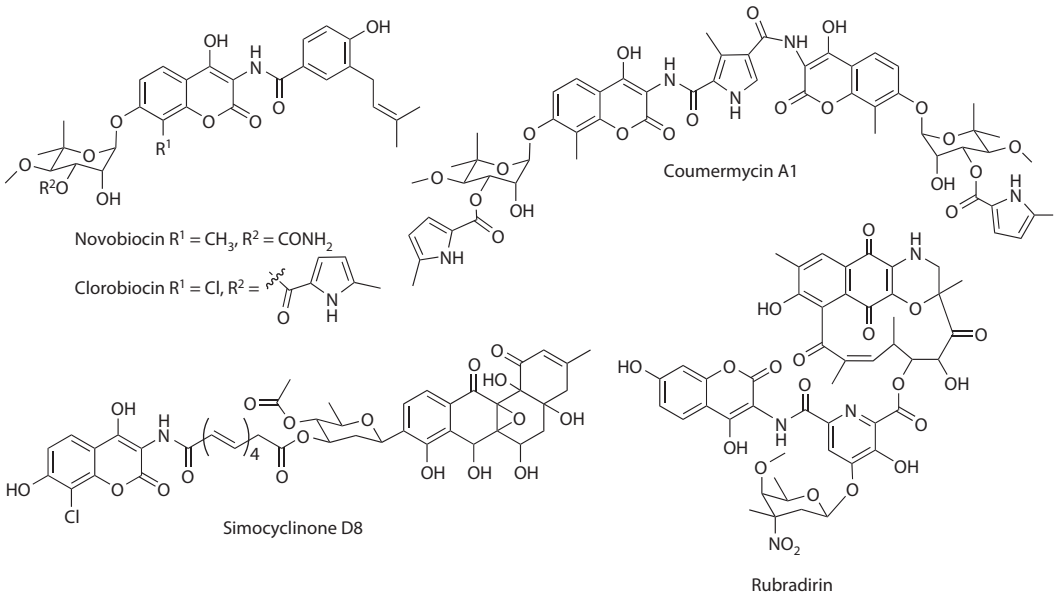

FIGURE 25.14 Structures of selected aminocoumarins.

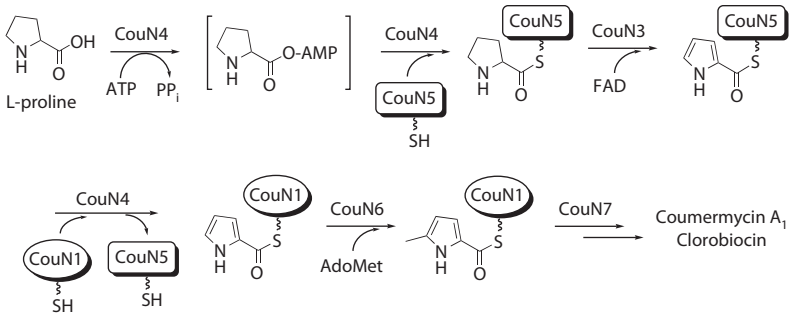

FIGURE 25.15 Biosynthesis of the 5-methylpyrrole-2-carboxylic acid moiety of clorobiocin and coumermycin A_1.

strain,[166,167] and most of the homologous enzymes in coumermycin A_1 biosynthesis have been characterized *in vitro* (Figure 25.15).[168–170] CouN4, similar to adenylation domains of NRPS, has been shown to activate and load proline onto a free-standing holo-PCP (CouN5), which is then oxidized by the FAD-dependent enzyme CouN3 to pyrrolyl-*S*-CouN5.[168] CouN2 next catalyzes transthioesterification to a second PCP (CouN1), and the acyltransferase enzyme CouN7 installs this moiety onto the deoxysugar of the coumermycin scaffold.[169,170] CouN6 likely catalyzes *C*-methylation prior to CouN7-catalyzed transfer, although this enzyme has not been characterized *in vitro*.

Several combinatorial biosynthetic strategies aimed at manipulating the biosynthetic pathway leading to the 5-methylpyrrole-2-carboxylic acid moiety have now been reported. In one example using gene inactivation/complementation, a halogenase gene involved in the biosynthesis of the structurally unique compound hormaomyicn was introduced into the clorobiocin-producing strain as a means to generate novclobiocin 124 containing a desmethyl, chlorinated pyrrole moiety (Figure 25.16). To avoid substrate competition, the *couN6* homolog was inactivated to eliminate the biosynthesis of the 5-methylated pyrrole moiety, and indeed clorobiocin with 5-chloropyrrole-2-carboxylic acid (novclobiocin 124) was isolated (Figure 25.16). In a second example, a chemoenzymatic approach was used to prepare 21 novel novobiocin analogs.[171] Several acyl-*S*-CoA derivatives were synthesized and loaded onto CouN1 using the promiscuous PPTase, Sfp. Subsequently, the acyltransferase CouN7 was used to install these different pyrrole mimics onto the noviose moiety of the aminocoumarin scaffold. Although the antitumor activity was not determined, a couple of these new analogs had activity against Gram-positive bacteria rivaling that of novobiocin.

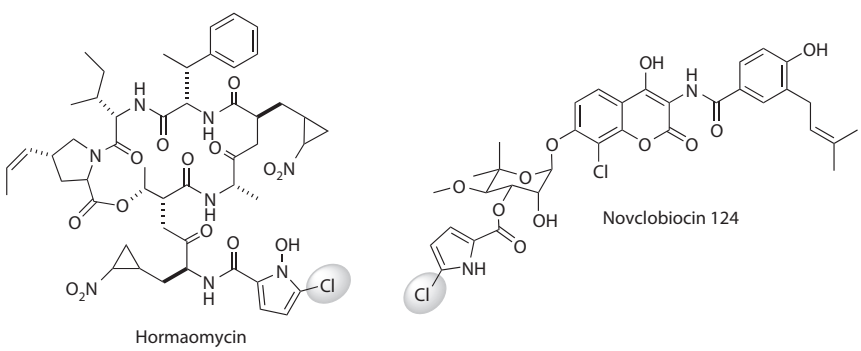

FIGURE 25.16 Structure of hormaomycin containing a chlorinated 5-methylpyrrole-2-carboxylic acid moiety and the novobiocin analog generated by heterologous expression of the hormaomycin halogenase. The engineered chlorine groups are highlighted with ovals.

A directed evolution strategy has been used to generate novobiocin analogs with variation in the novobiose moiety. The oleandomycin glycosyltransferase OleD was shown to utilize novobiocic acid as an aglycon substrate, and a triple mutant was prepared resulting in a fivefold improvement in glucosylation toward the aglycon.[172] This OleD triple mutant was next subjected to single-site saturation mutagenesis, and recombination of selected mutants ultimately resulted in an OleD triple mutant with ~300-fold improved catalytic efficiency toward the aglycon. Using 21 unnatural sugar nucleotides as donors, the OleD triple mutant was able to catalyze the incorporation of 10 of these into the aglycon novobiocic acid, while the wild-type only recognized four donors. Thus, it appears that this approach of directed evolution not only increased the efficiency of catalysis but also increased promiscuity leading to a library of novobiocins with altered sugars.

25.3 SUMMARY, CHALLENGES, AND FUTURE PROSPECTS

The elucidation of the biosynthetic gene cluster for DNR and DXR was achieved <20 years ago, and the biosynthetic gene clusters for the majority of the compounds discussed here have only been identified within the past decade. Within this short time frame, a significant amount of the biosynthetic logic has been established, but nevertheless the biochemical novelties associated with most pathways have delayed the implementation of combinatorial biosynthetic strategies in its truest sense. However, there are clearly some important discoveries that have been highlighted here. For example, it is clear that gene inactivation provides a strategy to rapidly access novel analogs, and often a single inactivation can lead to multiple isolable intermediates or shunt products that have intriguing biological activity. Also clear is that, and rather remarkably, the type II PKS systems in anthracycline and aureolic acid biosynthesis appear to be forgiving with respect to starter units, thus demonstrating that all downstream enzymes have relaxed substrate specificities. In contrast, certain enzymes described here are apparently unable to accommodate changes in the substrate, which is best represented by the post-PKS-tailoring steps in geldenamycin that appear to be quite specific. The *in vitro* characterization and engineering of these "stubborn" enzymes should open up new avenues for combinatorial biosynthesis.

Due to the technical difficulties and significant amount of time required for the implementation of genetic systems for individual strains, one of the great challenges that lies ahead is the development of a universal host that is easy to manipulate, fast growing, and enables high titers. It is clear from the studies with anthracyclines and aureolic acids that the type II PKS system is readily expressed in model hosts *Streptomyces* sp. and *E. coli*, and incremental success has been reported for other types of biosynthetic machinery in bacterial hosts.[11] For example, type I PKSs such as the geldenamycin PKS have been successfully expressed in *E. coli*. However, many of the anticancer natural products discussed here, such as the enediynes or leinamycin, have not been produced in a heterologous host, and thus to date the *in vivo* biosynthetic studies have been limited to genetics within the producing strain. Very recently, the genome of *Stretpomyces avermitilis* was reduced by ~82% and served as host for the heterologous expression of two gene clusters to give recombinant strains that produced greater amounts than the native producing strains.[173] While these results are promising, heterologous expression of a third gene cluster failed, and further studies aimed at understanding the molecular details behind this inconsistency will be critical to developing a universal host.

Remarkable progress has been made toward the realization of combinatorial biosynthesis of anticancer natural products. Both simple and complex genetic manipulations of biosynthetic pathways have been demonstrated to be viable approaches to generate bioactive analogs. The functional and structural characterization of enzymes involved in natural product biosynthesis also continues to expand the opportunities available for manipulating biosynthetic machinery to generate new compounds. Indeed, the characterization of many enzymes has been critical in revealing the molecular details of substrate specificity, which may subsequently be rendered flexible by structure-inspired or random mutagenesis approaches. Once the pathway bottlenecks have been eliminated,

it is envisioned that combinatorial biosynthesis will become an even simpler strategy to rapidly improve the pharmacological properties of natural products to make a better anticancer drug.

ACKNOWLEDGMENTS

Steven Van Lanen is supported in part by ACS IRG-85-001-19. Studies on natural product biosynthesis and engineering in Shen laboratories are supported in part by National Institutes of Health Grants AI51689, CA78747, CA94426, CA106150, and CA113297.

REFERENCES

1. Garcia, M., Jemal, A., Ward, E.M., Center, M.M., Hao, Y., Siegel, R.I., and Thun, M.J., *Global Cancer Facts & Figures 2007*, American Cancer Society, Atlanta, 2007.
2. Cragg, G.M. and Newman, D.J., Nature: A vital source of leads for anticancer drug development, *Phytochem. Rev.*, 8, 313, 2009.
3. Rybak, S. and Shogen, K., Conquering cancer resistance, *Drug Discov. Dev*., 11, 18, 2008.
4. Szakacs, G., Varadi, A., Ozvegy-Laczka, C., and Sarkadi, B., The role of ABC transporters in drug absorption, distribution, metabolism, extretion, and toxicity (ADME-Tox), *Drug Discov. Today*, 13, 379, 2008.
5. Conklin, K. and Nicolson, G.L., Molecular replacement in cancer therapy: Reversing cancer metabolic and mitochondrial dysfunction, fatigue and the adverse effects of cancer therapy, *Curr. Cancer Ther. Rev.*, 4, 66, 2008.
6. Olano, C., Méndez, C., and Salas, J.A., Antitumor compounds from actinomycetes: From gene clusters to new derivatives by combinatorial biosynthesis, *Nat. Prod. Rep*., 26, 628, 2009.
7. Wilkinson, B. and Micklefield, J., Mining and engineering natural-product biosynthetic pathways, *Nat. Chem. Biol.*, 3, 379, 2007.
8. Liu, W. and Yu, Y., Combinatorial biosynthesis of pharmaceutical natural products, in *Biocatalysis for the Pharmaceutical Industry*: *Discovery, Development, and Manufacturing*, Tao, J., Lin, G.-Q., and Liese, A., Eds., John Wiley & Sons, Singapore, 2009, 229.
9. Schnarr, N.A. and Khosla, C., Combinatorial biosynthesis of polyketides and nonribosomal peptides, *Chem. Biol*., 2, 519, 2007.
10. Kennedy, J., Mutasynthesis, chemobiosynthesis, and back to semi-synthesis. Combining synthetic chemistry and biosynthetic engineering for diversifying natural products, *Nat. Prod. Rep*., 25, 25, 2008.
11. Galm, U. and Shen, B., Expression of biosynthetic gene clusters in heterologous hosts for natural product production and combinatorial biosynthesis, *Exp. Opin. Drug Discov*., 1, 409, 2006.
12. Baltz, R.H., Molecular engineering approaches to peptide, polyketide, and other antibiotics, *Nat. Biotech*., 24, 1533, 2006.
13. Van Lanen, S.G. and Shen, B., Microbial genomics for the improvement of natural product discovery, *Curr. Opin. Microbiol.*, 9, 252, 2006.
14. Watanabe, K., Hotta, K., Praseuth, A.P., Koketsu, K., Migita, A., Boddy, C.N., Wang, C.C.C., Oguri, H., and Oikawa, H., Total biosynthesis of antitumor nonribosomal peptides in *Escherichia coli*, *Nat. Chem. Biol.*, 2, 423, 2006.
15. Sattely, E.S., Fischbach, M.A., and Walsh, C.T., Total biosynthesis: In vitro reconstitution of polyketide and nonribosomal peptide pathways, *Nat. Prod. Rep*., 25, 757, 2008.
16. Cheng, Q., Xiang, L., Izumikawa, M., Meluzzi, D., and Moore, B.S., Enzymatic total synthesis of enterocin polyketides, *Nat. Chem. Biol.*, 3, 557, 2007.
17. Kopp, F. and Marahiel, M.A., Where chemistry meets biology: The chemoenzymatic synthesis of nonribosomal peptides and polyketides, *Curr. Opin. Biotechnol.*, 18, 513, 2007.
18. Williams, G.J. and Thorson, J.S., Natural product glycosyltransferases: Properties and applications, *Adv. Enzymol. Rel. Areas Mol. Biol.*, 76, 55, 2009.
19. Williams, G.J., Gantt, R.W., and Thorson, J.S., The impact of enzyme engineering upon natural product glycodiversification, *Curr. Opin. Chem. Biol*., 12, 556, 2008.
20. Thomas, M.G., Bixby, K.A., and Shen, B., Combinatorial biosynthesis of anticancer natural products, in *Anticancer Agents from Natural Products*, Cragg, G.M., Kingston, D.G.I., and Newman, D.J., Eds., CRC Press LLC, Boca Raton, 2005, 519.
21. Di Marco, A., Gaetani, M., Orezzi, P., Scarpinato, B.M., Silvestrini, R., Soldati, M., Dasdia, T., and Valentini, L., "Daunomycin", a new antibiotic of the rhodomycin group, *Nature*, 201, 706, 1964.

22. Arcamone, F., Cassinelli, G., Fantini, G., Grein, A., Orezzi, P., Pol, C., and Spalla, C., Adriamycin, 14-hydroxydaunomycin, a new antitumor antibiotic from *S. peucetius* var. *caesius*, *Biotechnol. Bioeng*., 11, 1101, 1969.
23. Forssen, E.A. and Ross, M.E., Daunoxome treatment of solid tumors: Preclinical and clinical investigations, *J. Lipos. Res.*, 4, 481, 1994.
24. Fernandez, H.F., Sun, Z., Yao, X., Litzow, M.R., Luger, S.M., Paietta, E.M., Racevskis, J. et al., Anthracycline dose intensification in acute myeloid leukemia, *New Engl. J. Med.*, 361, 1249, 2009.
25. Wouters, K.A., Kremer, L.C.M., Miller, T.L., Herman, E.H., and Lipshultz, S.E., Protecting against anthracycline-induced myocardial damage: A review of the most promising strategies, *Br. J. Haematol.*, 131, 561, 2005.
26. Oki, T., Matsuzawa, Y., Yoshimoto, A., Numata, K., Kitamura, I., Hori, S., Takamatsu, A. et al., New antitumor antibiotics, aclacinomycins A and B, *J. Antibiot.*, 28, 830, 1975.
27. Grimm, A., Madduri, K., Ali, A., and Hutchinson, C.R., Characterization of the *Streptomyces peucetius* ATCC 29050 genes encoding doxorubicin polyketide synthase, *Gene*, 151, 1, 1994.
28. Ye, J., Dickens, M.L., Plater, R., Li, Y., Lawrence, J., and Strohl, W.R., Isolation and sequence analysis of polyketide synthase genes from the daunomycin-producing *Streptomyces* sp. strain C5, *J. Bacteriol*., 176, 6270, 1994.
29. Motamedi, H. and Hutchinson, C.R., Cloning and heterologous expression of a gene cluster for the biosynthesis of tetracenomycin C, the anthracycline antitumor antibiotic of *Streptomyces glaucescens*, *Proc. Natl. Acad. Sci. U.S.A*., 84, 4445, 1987.
30. Malpartida, F. and Hopwood, D.A., Molecular cloning of the whole biosynthetic pathway of a Streptomcyes antibiotic and its expression in a heterologous host, *Nature*, 309, 462, 1984.
31. Shen, B., Biosynthesis of aromatic polyketides, in *Topics in Current Chemistry*, 209, Leeper, F.J. and Vederas, J.C., Eds., Springer, Berlin, 2000, 1.
32. Metsä-Ketelä, M., Niemi, J., Mäntsälä, P., and Schneider, G., Anthracycline biosynthesis: Genes, enzymes and mechanisms, in *Topics in Current Chemistry*, 282, Krohn, K., Ed., Springer, Berlin, 2008, 101.
33. Shen, B. and Hutchinson, C.R., Enzymatic synthesis of a bacterial polyketide from acetyl and malonyl coenzyme A, *Science*, 262, 1535, 1993.
34. Carreras, C.W., Pieper, R., and Khosla, C., Efficient synthesis of aromatic polyketides in vitro by the actinorhodin polyketide synthase, *J. Am. Chem. Soc.*, 118, 5158, 1996.
35. Bao, W., Sheldon, P.J., Wendt-Pienkowski, E., and Hutchinson, C.R., The *Streptomyces peucetius dpsC* gene determines the choice of starter unit in biosynthesis of the daunorubicin polyketide, *J. Bacteriol*., 181, 4690, 1999.
36. Bao, W., Sheldon, P.J., and Hutchinson, C.R., Purification and properties of the *Streptomyces peucetius* DpsC β-ketoacyl:acyl carrier protein synthase III that specifies the propionate-starter unit for type II polyketide biosynthesis, *Biochemistry*, 38, 9752, 1999.
37. Xu, Z., Metsä-Ketelä, M., and Hertweck, C., Ketosynthase III as a gateway to engineering the biosynthesis of antitumoral benastatin derivatives, *J. Biotechnol*., 140, 107, 2009.
38. Kalaitzis, J.A., Cheng, Q., Thomas, P.M., Kelleher, N.L., and Moore, B.S., In vitro biosynthesis of unnatural enterocin and wailupemycin polyketides, *J. Nat. Prod*., 72, 469, 2009.
39. Zhang, W. and Tang, Y., Engineering starter units in aromatic polyketides, *ACS Symposium Series*, 955, American Chemical Society, 2007, 231.
40. Tang, Y., Lee, T.S., and Khosla, C., Engineered biosynthesis of regioselectively modified aromatic polyketides using bimodular polyketide synthases, *PLOS Biol.*, 2, 227, 2004.
41. Lee, T.S., Khosla, C., and Tang, Y., Engineered biosynthesis of alkanonic acid analogues, *J. Am. Chem. Soc*., 127, 12254, 2005.
42. Keatinge-Clay, A.T., Maltby, D.A., Medzihradszky, K.F., Khosla, C., and Stroud, R.M., An antibiotic factory caught in action, *Nat. Struct. Mol. Biol*. 11, 888, 2004.
43. Madduri, K., Kennedy, J., Rivola, G., Inventi-Solari, A., Filippini, S., Zanuso, G., Colombo, A.L. et al., Production of the antitumor drug epirubicin (4′-epidoxorubicin) and its precursor by a genetically engineered strain of *Streptomyces peucetius*, *Nat. Biotechnol*., 16, 69, 1998.
44. Gullón, S., Olano, C., Abdelfattah, M.S., Braña, A.F., Rohr, J., Méndez, C., and Salas, J., Isolation, characterization, and heterologous expression of the biosynthesis gene cluster for the antitumor anthracycline steffimycin, *Appl. Environ. Microbiol*., 72, 4172, 2006.
45. Olano, C., Abdelfattah, M.S., Gullón, S., Braña, A.F., Rohr, J., Méndez, C., and Salas, J., Glycosylated derivatives of steffimycin: Insights into the role of the sugar moieties for the biological activity, *ChemBioChem.*, 9, 624, 2008.

46. Garrido, L.M., Lombó, F., Baig, I., Nur-e-Alam, M., Furlan, R.L.A., Borda, C.C., Braña, A.F., J. et al., Insights in the glycosylation steps during biosynthesis of the antitumor anthracycline cosmomycin: Characterization of two glycosyltransferase genes, *Appl. Microbiol. Biotechnol*., 73, 122, 2006.
47. Jansson, A., Koskiniemi, H., Erola, A., Wang, J., Mäntsäläs, P., Schneider, G., and Niemi, J., Aclacinomycin 10-hydroxylase is a novel substrate-assisted hydroxylase requiring S-adenosyl-L-mehtionine as a cofactor, *J. Biol. Chem*., 280, 3636, 2005.
48. Lindqvist, Y., Koskiniemi, H., Jansson, A., Sandalova, T., Schnell, R., Liu, Z., Mäntsäläs, P., Niemi, J., and Schneider, G., Structural basis for substrate recognition and specificity in aklavinone-11-hydroxylase from rhodomycin biosynthesis, *J. Mol. Biol*., 393, 966, 2009.
49. Du Priest, R.W. and Fletcher, W.S., Chemotherapy of testicular germinal tumors, *Oncology*, 28, 147, 1973.
50. Leroy, I., Laurent, G., and Quillet-Mary, A., Mithramycin A activates Fas death pathway in leukemic cell lines, *Apoptosis*, 11, 113, 2006.
51. Ryan, W.G., Paget's disease of bone and fibrous dysplasia, *Curr. Opin. Rheumatol*., 4, 410, 1992.
52. Jia, Z., Zhang, J., Wei, D., Wang, L., Yuan, P., Le, X., Li, Q., Yao, J., and Xie, K., Molecular basis of the synergistic antiangiongenic activity of bevacizumab and mithramycin A, *Cancer Res*., 68, 4878, 2007.
53. Lombó, F., Menéndez, N., Salas, J.A., and Méndez, C., The aureolic acid family of antitumor compounds: Structure, mode of action, biosynthesis, and novel derivatives, *Appl. Microbiol. Biotechnol*., 73, 1, 2006.
54. Lombó, F., Blanco, G., Fernández, E., Méndez, C., and Salas, J.A., Characterization of *Streptomyces argillaceus* genes encoding a polyketide synthase involved in the biosynthesis of the antitumor mithramycin, *Gene*, 172, 87, 1996.
55. Menéndez, N., Nur-e-Alam, M., Braña, A.F., Rohr, J., Salas, J.A., and Méndez, C., Biosynthesis of the antitumor chromomycin A_3 in *Streptomyces griseus*: Analysis of the gene cluster and rational design of novel chromomycin analogs, *Chem. Biol*., 11, 21, 2004.
56. Remsing, L.L, González, A.M., Nur-e-Alam, M., Fernández-Lozano, M.J., Braña, A.F., Rix, U., Oliveira, M.A., Méndez, C., Salas, J.A., and Rohr, J., Mithramycin SK, a novel antitumor drug with improved therapeutic index, mithramycin SA, and demycarosyl-mithramycin SK: Three new products generated in the mithramycin producer *Streptomyces argillaceus* through combinatorial biosynthesis, *J. Am. Chem. Soc*., 125, 5745, 2003.
57. Albertini, V., Jain, A., Vignati, S., Napoli, S., Rinaldi, A., Kwee, I., Nuer-e-Alam, M. et al., Novel GC-rich DNA-binding compound produced by a genetically engineered mutant of the mithramycin producer *Streptomyces argillaceus* exhibits improved transcriptional repressor activity: Implications for cancer therapy, *Nucleic Acids Res*., 34, 1721, 2006.
58. Remsing, L.L., Garcia-Bernardo, J., Gonzalez, A., Künzel, E., Rix, U., Braña, A.F., Bearden, D.W., Méndez, C., Salas, J.A., and Rohr, J., Ketopremithramycins and ketomithramycins, four new aureolic acid-type compounds obtained upon inactivation of two gene involved in the biosynthesis of the deoxysugar moieties of the antitumor drug mithramycin by *Streptomyces argillaceus*, reveal novel insights into post-PKS tailoring steps of the mithramycin biosynthetic pathway, *J. Am. Chem. Soc.*, 124, 1606, 2002.
59. González, A., Remsing, L.L., Lombó, F. Fernández, M.J., Prado, L., Braña, A.F., Künzel, E., Rohr, J., Méndez, C., and Salas, J.A., The *mtmVUC* genes of the mithramycin gene cluster in *Streptomyces argillaceus* are involved in the biosynthesis of the sugar moieties, *Mol. Gen. Genet.*, 264, 827, 2001.
60. Pérez, M., Baig, I., Braña, A.F., Salas, J.A., Rohr, J., and Méndez, C., Generation of new derivatives of the antitumor antibiotic mithramycin by altering the glycosylation pattern through combinatorial biosynthesis, *ChemBioChem.*, 9, 2295, 2008.
61. Baig, I., Pérez, M., Braña, A.F., Gomathinayagam, R., Damodaran, C., Salas, J.A., Méndez, C., and Rohr, J., Mithramycin analogues generated by combinatorial biosynthesis show improved bioactivity, *J. Nat. Prod.*, 71, 199, 2008.
62. Beam, M.P., Bosserman, M.A., Noinaj, N., Wehenkel, M., and Rohr, J., Crystal structure of Baeyer-Villager monooxygenase MtmOIV, the key enzyme of the mithramycin biosynthetic pathway, *Biochemistry*, 48, 4476, 2009.
63. Sepkowitz, K.A., Rafalli, J., Riley, L., Kiehn, T.E., and Armstrong, D., Tuberculosis in the AIDS era, *Clin. Microbiol. Rev.*, 8, 189, 1995.
64. Correia, J.J., Effects of antimitotic agents on tubulin-nucleotide interactions, *Pharmacol. Ther*., 52, 127, 1991.
65. Stebbins, C.E., Russo, A.A., Schneider, C., Rosen, N., Hartl, F.U., and Pavletich, N.P., Crystal structure of an Hsp90-geldanamycin complex: Targeting of a protein chaperone by an antitumor agent, *Cell*, 89, 239, 1997.

66. Supko, J.G., Hickman, R.L., Grever, M.R., and Malspeis, L., Preclinical pharmacologic evaluation of geldanamycin as an antitumor agent, *Cancer Chemother. Pharmacol*., 36, 305, 1995.
67. Gaspar, N., Sharp, S.Y., Pacey, S., Jones, C., Walton, M., Vassal, G., Eccles, S., Pearson, A., and Workman, P., Acquired resistance to 17-allylamino-17-demethoxygeldanamycin (17-AAG, tanespimycin) in glioblastoma cells, *Cancer Res.*, 69, 1966, 2009.
68. Kim, Y.S., Alarcon, S.V., Lee, S., Lee, M.-J., Giaccone, G., Neckers, L., and Trepel, J.B., Update on Hsp90 inhibitors in clinical trial, *Curr. Top. Med. Chem*., 9, 1479, 2009.
69. August, P.R., Tang, L, Yoon, Y.J., Ning, S, Müller, R., Yu, T.-W., Taylor, M. et al., Biosynthesis of the ansamycin antibiotic rifamycin: Deductions from the molecular analysis of the rif biosynthetic gene cluster of *Amycolatopsis mediterranei* S699, *Chem. Biol*., 5, 69, 1998.
70. Rascher, A., Hu, Z., Viswanathan, N., Schirmer, A., Reid, R., Nierman, W.C., Lewis, M., and Hutchinson, C.R., Cloning and characterization of a gene cluster for geldanamycin production in *Streptomyces hygroscopicus* NRRL 3602, *FEMS Microbiol. Lett*., 218, 233, 2008.
71. Yu, T.-W., Bai, L., Clade, D., Hoffmann, D., Toelzer, S., Trinh, K.Q., Xu, J., Moss, S.J., Leistner, E., and Floss, H.G., The biosynthetic gene cluster of the maytansinoid antitumor agent ansamitocin from *Actinosynnema pretiosum*, *Proc. Natl. Acad. Sci. U.S.A*., 99, 7968, 2002.
72. Staunton, J. and Weissmann, K.J., Polyketide biosynthesis: A millennium review, *Nat. Prod. Rep*., 18, 380, 2001.
73. Floss, H.G., From ergot to ansamycins—45 years in biosynthesis, *J. Nat. Prod*., 69, 158, 2006.
74. Dorrestein, P.C., Van Lanen, S.G., Li, W., Zhao, C., Deng, Z., Shen, B., and Kelleher, N.L., The bifunctional glyceryl transferase/phosphates OzmB belonging to the HAD superfamily that diverts 1,3-bisphosphoglycerate into polyketide biosynthesis, *J. Am. Chem. Soc.*, 128, 10386, 2006.
75. Wenzel, S.C., Williamson, R.M., Gruenanger, C., Xu, J., Klaus, G., Martinez, R.A., Moss, S.J., Carroll, B.J., Grond, S., and Unkefer, C.J., On the biosynthetic origin of methoxymalonyl-acyl carrier protein, the substrate for incorporation of "glycolate" units into ansamitocin and soraphen A, *J. Am. Chem. Soc.*, 128, 14325, 2006.
76. Chan, Y.A., Boyne, M.T., Podevels, A.M., Klimowicz, A.K., Handelsman, J., Kelleher, N.L., and Thomas, M.G., Hydroxymalonyl-acyl carrier protein (ACP) and aminomalonyl-ACP are two additional type I polyketide synthase extender units, *Proc. Natl. Acad. Sci. U.S.A.*, 103, 14349, 2006.
77. Spiteller, P., Bai, L., Shang, G., Carroll, B.J., Yu, T.-W., and Floss, H.G., The post-polyketide synthase modification steps in the biosynthesis of the antitumor agent ansamitocin by *Actinosynnema pretiosum*, *J. Am. Chem. Soc*., 125, 14236, 2003.
78. Xu, J., Wan, E., Kim, C.-J., Floss, H.G., and Mahmud, T., Identification of tailoring genes involved in the modification of the polyketide backbone of rifamycin B by *Amycolatopsis mediterranei* S699, *Microbiology*, 151, 2515, 2005.
79. Watanabe, K., Rude, M.A., Walsh, C.T., and Khosla, C., Engineered biosynthesis of an ansamycin polyketide precursor in *Escherichia coli*, *Proc. Natl. Acad. Sci. U.S.A*., 100, 9774, 2003.
80. Patel, K., Piagentini, M., Rascher, A., Tian, Z.-Q., Buchanan, G.O., Regentin, R., Hu, Z., Hutchinson, C.R., and McDaniel, R., Engineered biosynthesis of geldanamycin analogs for Hsp90 inhibition, *Chem. Biol*., 11, 1625, 2004.
81. Vetcher, L., Tain, Z.-Q., McDaniel, R., Rascher, A., Revill, W.P., Hutchinson, R.C., and Hu, Z., Rapid engineering of the geldanamycin biosynthesis pathway by Red/ET recombination and gene complementation, *Appl. Environ. Microbiol*., 71, 1829, 2005.
82. Kim, W., Lee, D., Hong, S.S., Na, Z., Shin, J.C., Roh, S.H., Wu, C.Z. et al., Rational biosynthetic engineering for optimization of geldanamycin analogues, *ChemBioChem.*, 10, 1243, 2009.
83. Maroney, A.C., Marugan, J.J., Mezzasalma, T.M., Barnakov, A.N., Garrabrant, T.A., Weaner, L.E., Jones, W.J. et al., Dihydroquinone ansamycins: Toward resolving the conflict between low in vitro affinity and high cellular potency of geldanamycin derivatives, *Biochemistry*, 45, 5678, 2006.
84. Kim, W., Lee, J.S., Lee, D., Cai, X.F., Shin, J.C., Lee, K., Lee, C.H., Ryu, S., Paik, S.G., Lee, J.J., and Hong, Y.S., Mutasynthesis of geldanamycin by the disruption of a gene producing starter unit: Generation of structural diversity at the benzoquinone ring, *ChemBioChem.*, 8, 1491, 2007.
85. Menzella, H.G., Tran, T.-T., Carney, J.R., Lau-Wee, J., Galazzo, J., Reeves, C.D., Carreras, C. et al., Potent non-benzoquinone ansamycin heat shock protein 90 inhibitors from genetic engineering of *Streptomyces hygroscopicus*, *J. Med. Chem*., 52, 1518, 2009.
86. Cysyk, R.L., Parker, R.J., Barchi, J.J., Steeg, P.S., Hartman, N.R., and Strong, J.M., Reaction of geldanamycin and C17-substituted analogues with glutathione: Product identifications and pharmacological implications, *Chem. Res. Toxicol*., 19, 376, 2006.

87. Zhao, P., Bai, L., Ma, J., Zeng, Y., Li, L., Zhang, Y., Lu, C. et al., Amide *N*-glycosylation by Asm25, an *N*-glycosyltransferase of ansamitocins, *Chem. Biol*., 15, 863, 2008.
88. Höfle, G., Bedorf, N., Steinmetz, H., Schomburg, D., Gerth, K., and Reichenbach, H., Epothilone A and B: Novel 16-membered macrolides with cytotoxic activity: Isolation, crystal structure, and conformation in solution, *Angew. Chem. Int. Ed*., 35, 1567, 1996.
89. Rak Tkaczuk, K.H., Review of the contemporary cytotoxic and biologic combinations available for the treatment of metastatic breast cancer, *Clin. Ther*., 31, 2273, 2009.
90. Bollag, D.M., McQueney, P.A., Zhu, J., Hensens, O., Koupal, L., Liesch, J., Goetz, M., Lazarides, E., and Woods, C.M., Epothilones, a new class of microtubule-stabilizing agents with a taxol-like mechanism of action, *Cancer Res*., 55, 2325, 1995.
91. Molnár, I., Schupp, T., Ono, M., Zirkle, R.E., Milnamow, M., Nowak-Thompson, B., Engel, N. et al., The biosynthetic gene cluster for the microtubule-stabilizing agents epothilones A and B from *Sorangium cellulosum* So ce90, *Chem. Biol.*, 7, 97, 2000.
92. Tang, L., Shah, S., Chung, L., Carney, J., Katz, L., Khosla, C., and Julien, B., Cloning and heterologous expression of the epothilone gene cluster, *Science*, 287, 640, 2000.
93. O'Connor, S.E., Chen, H., and Walsh, C.T., Enzymatic assembly of epothilones: The EpoC subunit and reconstitution of the EpoA-ACP/B/C polyketide and nonribosomal peptide interfaces, *Biochemistry*, 41, 5685, 2002.
94. Arslanian, R.L., Tang, L, Blough, S., Ma, W., Qiu, R.-G., Katz, L., and Carney, J.R., A new cytotoxic epothilone from modified polyketide synthases heterologously expressed in *Myxococcus xanthus*, *J. Nat. Prod*., 65, 1061, 2002.
95. Starks, C.M., Zhou, Y., Liu, F., and Licari, P.J., Isolation and characterization of new epothilone analogues from recombinant *Myxococcus xanthus* fermentations, *J. Nat. Prod*., 66, 1313, 2003.
96. Boddy, C.N., Hotta, K., Lovato Tse, M., Watts, R.E., and Khosla, C., Precursor-directed biosynthesis of epothilone in *Escherichia coli*, *J. Am. Chem. Soc*., 126, 7436, 2004.
97. Mutka, S.C., Carney, J.R., Liu, Y., and Kennedy, J., Heterologous production of epothilone C and D in *Escherichia coli*, *Biochemistry*, 45, 1321, 2006.
98. Tse, M.L., Watts, R.E., and Khosla, C., Substrate tolerance of module 6 of the epothilone synthetase, *Biochemistry*, 46, 3385, 2007.
99. O'Connor, S.E., Walsh, C.T., and Liu, F., Biosynthesis of epothilone intermediates with alternate starter units: Engineering polyketide-nonribosomal interfaces, *Angew. Chem. Int. Ed.*, 42, 3917, 2003.
100. Hara, M., Asano, K., Kawamoto, I., Takiguchi, T., Katsumata, S., Takahashi, K.-I., and Nakano, H., Leinamycin, a new antitumor antibiotic from *Streptomyces*; producing organism, fermentation and isolation, *J. Antibiot*., 42, 1768, 1989.
101. Hara, M., Takahashi, I., Yoshida, M., Asano, K., Kawamoto, I., Morimoto, M., and Nakano, H., DC 107, a novel antitumor antibiotic produced by a *Streptomyces* sp., *J. Antibiot.*, 42, 333, 1989.
102. Nakano, H. and Tamaoki, T., Mechanism based screens for natural product leads as sources for antitumor drugs, in *Harnessing Biotechnology for the 21st Century*, Ladisch, M.R. and Bose, A., Eds., American Chemical Society, Washington, 1992, 72.
103. Hara, M., Saitoh, Y., and Nakano, H., DNA strand scission by the novel antitumor antibiotic leinamycin, *Biochemistry*, 29, 5676, 1990.
104. Zhang, H. and Gates, K.S., Sequence specificity of DNA alkylation by the antitumor natural product leinamycin, *Chem. Res. Toxicol*., 16, 1539, 2003.
105. Nooner, T., Dutta, S., and Gates, K.S., Chemical properties of the leinamycin 2′-deoxyguanosine adduct, *Chem. Res. Toxicol*., 17, 942, 2004.
106. Viswesh, V., Gates, K., and Sun, D., Characterization of DNA damage induced by a natural product antitumor antibiotic leinamycin in human cancer cells, *Chem. Res. Toxicol*., 23, 99, 2010.
107. Chen, Y.-Q., Tang, G.-L., and Shen, B., Identification and localization of the gene cluster encoding biosynthesis of the antitumor macrolactam leinamycin in *Streptomyces atroolivaceus* S-140, *J. Bacteriol.*, 184, 7013, 2002.
108. Tang, G.-L., Cheng, Y.-Q., and Shen, B., Leinamycin biosynthesis revealing unprecedented architectural complexity for a hybrid polyketide synthase and nonribosomal peptide synthetase, *Chem. Biol*., 11, 33, 2004.
109. Cheng, Y.-Q., Tang, G.-L., and Shen, B., Type I polyketide synthase requiring a discrete acyltransferase for polyketide biosynthesis, *Proc. Natl. Acad. Sci. U.S.A*., 100, 3149, 2003.
110. Cheng, Y.-Q., Coughlin, J.M., Lim, S.-K., and Shen, B. Type I polyketide synthases that require discrete acyltransferases, *Methods Enzymol*., 459, 165, 2009.

111. Nguyen, T., Ishida, K., Jenke-Kodama, H., Dittmann, E., Gurgui, C., Hochmuth, T., Taudien, S., Platzer, M., Hertweck, C., and Piel, J., Exploiting the mosaic structure of trans-acyltransferase polyketide synthases for natural product discovery and pathway dissection, *Nat. Biotechnol.*, 26, 225, 2008.
112. Shen, B., Oxidative activation and episulfonium ion-mediated DNA alkylation-based anticancer. U.S. Patent No. 7,345,069 B2, March 18, 2008.
113. Tang, G.-L., Cheng, Y.-Q., and Shen, B., Chain initiation in the leinamycin-producing hybrid nonribosomal peptide/polyketide synthetase from *Streptomtyces atroolivaceus* S-140: Discrete, monofunctional adenylation enzyme and peptidyl carrier protein that directly loads D-alanine, *J. Biol. Chem.*, 282, 20273, 2007.
114. Balibar, C.J., Vaillancourt, F.H., and Walsh, C.T., Generation of D amino acid residues in assembly of arthrofactin by dual condensation/epimerization domains, *Chem. Biol.*, 12, 1189, 2005.
115. Tang, G.-L., Cheng, Y.-Q., and Shen, B., Polyketide chain skipping mechanism in the biosynthesis of the hybrid nonribosomal peptide-polyketide antitumor antibiotic leinamycin in *Streptomyces atroolivaceus* S-140, *J. Nat. Prod.*, 69, 387, 2006.
116. Liu, T., Huang, Y., and Shen, B., Bifunctional acyltransferase/decarboxylase LnmK as the missing link for β-alkylation in polyketide biosynthesis, *J. Am. Chem. Soc.*, 131, 6900, 2009.
117. Xi, Z. and Goldberg, I.H., DNA-damaging enediyne compounds, in *Comprehensive Natural Products Chemistry*, Kool, E.T, Ed., Elsevier, Amsterdam, 1999, 553.
118. Galm, U., Hager, M.H., Van Lanen, S.G., Ju, J., Thorson, J.S., and Shen, B., Antitumor antibiotics: Bleomycins, enediynes, and mitomycin, *Chem. Rev.*, 105, 739, 2005.
119. Shao, R.-G., Pharmacology and therapeutic applications of enediyne antitumor antibiotics, *Curr. Mol. Pharmacol.*, 1, 50, 2008.
120. Van Lanen, S.G. and Shen, B., Biosynthesis of enediyne antitumor antibiotics, *Curr. Top. Med. Chem.*, 8, 448, 2008.
121. Beerman, T.A., Gawron, L.S., Shin, S., Shen, B., and McHugh, M.M., C-1027, a radiomimetic enediyne anticancer drug, preferentially targets hypoxic cells, *Cancer Res.*, 69, 593, 2009.
122. Maeda, H., *Enediyne Antibiotics as Antitumor Agents*, Marcel Dekker, New York, 1995, 363.
123. Larson, R.A., Boogaerts, M., Estey, E., Karanes, C., Stadtmauer, E.A., Sievrs, E.L., Mineur, P. et al., Antibody-targeted chemotherapy of older patients with acute myeloid leukemia in first relapse using Mylotarg (gemtuzumab oxogamicin), *Leukemia*, 16, 1627, 2002.
124. Liu, W., Christenson, S.D., Standage, S., and Shen, B., Biosynthesis of the enediyne antitumor antibiotic C-1027, *Science*, 297, 1170, 2002.
125. Liu, W., Nonaka, K., Nie, L., Zhang, J., Christenson, S.D., Bae, J., Van Lanen, S.G. et al., The neocarzinostatin biosynthetic gene cluster from *Streptomyces carzinostaticus* ATCC 15944 involving two iterative type I polyketide synthases, *Chem. Biol.*, 12, 293, 2005.
126. Van Lanen, S.G., Oh, T.-J., Liu, W., Wendt-Pienkowski, E., and Shen, B., Characterization of the maduropeptin biosynthetic gene cluster from *Actinomadura madurae* ATCC 39144 supporting a unifying paradigm for enediyne biosynthesis, *J. Am. Chem. Soc.*, 129, 13082, 2007.
127. Ahlert, J., Shepard, E., Lomovskaya, N., Zazopoulos, E., Staffa, A., Bachmann, B.O., Huang, K. et al., The calicheamicin gene cluster and its iterative type I enediyne PKS, *Science*, 297, 1173, 2002.
128. Gao, Q. and Thorson, J.S., The biosynthetic genes encoding for the production of the dynemicin enediyne core in *Micromonospora chersina* ATCC 53710, *FEMS Microbiol. Lett.*, 282, 105, 2008.
129. Zazopoulos, E., Huang, K., Staffa, A., Liu, W., Bachmann, B.O., Nonaka, K., Ahlert, J., Thorson, J.S., Shen, B., and Farnet, C.M., A genomics-guided approach for discovering and expressing cryptic metabolic pathways, *Nat. Biotechnol.*, 21, 187, 2003.
130. Liu, W., Ahlert, J., Gao, Q., Wendt-Pienkowski, E., Shen, B., and Thorson, J.S., Rapid PCR amplification of minimal enediyne polyketide synthase cassettes leads to a predictive familial classification, *Proc. Natl. Acad. Sci. U.S.A.*, 100, 11959, 2003.
131. Horsman, G.P., Van Lanen, S.G., and Shen, B., Iterative type I polyketide synthases for enediyne core biosynthesis, *Methods Enzymol.*, 459, 97, 2009.
132. Kennedy, D.R., Gawron, L.S., Ju, J., Liu, W., Shen, B., and Beerman, T.A., Single chemical modifications of the C-1027 enediyne core, a radiomimetic antitumor drug, affect both drug potency and the role of ataxia-telangiectasia mutated in cellular responses to DNA double-strand breaks, *Cancer Res.*, 67, 773, 2007.
133. Kennedy, D.R., Ju, J., Shen, B., and Beerman, T.A., Designer enediynes generate DNA breaks, interstrand cross-links, or both, with concomitant changes in the regulation of DNA damage responses, *Proc. Natl. Acad. Sci. U.S.A.*, 104, 17632, 2007.

134. Murrell, J.M., Liu, W., and Shen, B., Biochemical characterization of the SgcA1 α-D-glucopyranosyl-1-phosphate thymidylyltransferase from the enediyne antitumor antibiotic C-1027 biosynthetic pathway and overexpression of *sgcA1* in *Streptomyces globisporus* to improve C-1027 production, *J. Nat. Prod.*, 67, 206, 2004.
135. Christenson, S.D., Liu, W., Toney, M.D., and Shen, B., A novel 4-methylideneimidazole-5-one-containing tyrosine aminomutase in enediyne antitumor antibiotic C-1027 biosynthesis, *J. Am. Chem. Soc.*, 125, 6062, 2003.
136. Christenson, S.D., Wu, W., Spies, M.A., Shen, B., and Toney, M.D., Kinetic analysis of the 4-methylideneimidazole-5-one-containing tyrosine aminomutase in enediyne antitumor antibiotic C-1027 biosynthesis, *Biochemistry*, 42, 12708, 2003.
137. Van Lanen, S.G., Lin, S., and Shen, B., Biosynthesis of the enediyne antitumor antibiotic C-1027 involves a new branching point in chorismate metabolism, *Proc. Natl. Acad. Sci. U.S.A.*, 105, 494, 2008.
138. Zhang, J., Van Lanen, S.G., Ju, J., Liu, W., Dorrestein, P.C., Li, W., Kelleher, N.L., and Shen, B., A phosphopantetheinylating polyketide synthase producing a linear polyene to initiate enediyne antitumor antibiotic biosynthesis, *Proc. Natl. Acad. Sci. U.S.A.*, 105, 1460, 2008.
139. Lin, S., Horsman, G.P., Chen, Y., Li, W., and Shen, B., Characterization of the SgcF epoxide hydrolase supporting a (R)-vicinal diol intermediate for enediyne antitumor antibiotic C-1027 biosynthesis, *J. Am. Chem. Soc.*, 131, 16410, 2009.
140. Kong, R., Goh, L.P., Liew, C.W., Ho, Q.S., Murugan, E., Li, B., Tang, K., and Liang, Z.-X., Characterization of a carbonyl-conjugated polyene precursor in 10-membered enediyne biosynthesis, *J. Am. Chem. Soc.*, 130, 8142, 2008.
141. Belecki, K., Crawford, J.M., and Townsend, C.A., Production of octaketide polyenes by the calicheamicin polyketide synthase CalE8: Implications for the biosynthesis of enediyne core structures, *J. Am. Chem. Soc.*, 131, 12564, 2009.
142. Sun, H., Kong, R., Zhu, D., Lu, M., Ji, Q., Liew, C.W., Lescar, J., Zhong, G., and Liang, Z.-X., Products of the iterative polyketide synthases in 9- and 10-membered enediyne biosynthesis, *Chem. Commun.*, 7399, 2009.
143. Horsman, G.P., Chen, Y., Thorson, J.S., and Shen, B., Polyketide synthase chemistry does not direct biosynthetic divergence between 9- and 10-membered enediynes, *Proc. Natl. Acad. Sci. U.S.A.*, 107, 11331, 2010.
144. Chen, Y., Yin, M., Horsman, G.P., Huang, S., and Shen, B. Manipulation of pathway regulation in *Streptomyces globisporus* for overproducing the enediyne antitumor antibiotic C-1027, *J. Antibiot.*, 63, 482, 2010.
145. Van Lanen, S.G., Dorrestein, P.C., Christenson, S.D., Liu, W., Ju, J., Kelleher, N.L., and Shen, B., Biosynthesis of the β-amino acid moiety of the enediyne antitumor antibiotic C-1027 featuring β-amino acyl-*S*-carrier protein intermediates, *J. Am. Chem. Soc.*, 129, 12432, 2005.
146. Van Lanen, S.G., Lin, S., Dorrestein, P.C., Kelleher, N.L., and Shen, B., Substrate specificity of the adenylation enzyme SgcC1 involved in the biosynthesis of the enediyne antitumor antibiotic C-1027, *J. Biol. Chem.*, 281, 29633, 2006.
147. Lin, S., Van Lanen, S.G., and Shen, B., Characterization of the two-component, FAD-dependent monooxygenase SgcC that requires carrier protein-tethered substrates for the biosynthesis of the enediyne antitumor antibiotic C-1027, *J. Am. Chem. Soc.*, 130, 6616, 2008.
148. Van Lanen, S.G., Lin, S., Horsman, G.P., and Shen, B., Characterization of SgcE6, the flavin reductase component supporting FAD-dependent halogenations and hydroxylation in the biosynthesis of the enediyne antitumor antibiotic C-1027, *FEMS Microbiol. Lett.*, 300, 237, 2009.
149. Lin, S., Van Lanen, S.G., and Shen, B., Regiospecific chlorination of (*S*)-β-tyrosyl-*S*-carrier protein catalyzed by SgcC3 in the biosynthesis of the enediyne antitumor antibiotic C-1027, *J. Am. Chem. Soc.*, 129, 12432, 2007.
150. Lin, S., Van Lanen, S.G., and Shen, B., A free-standing condensation enzyme catalyzing ester bond formation in C-1027 biosynthesis, *Proc. Natl. Acad. Sci. U.S.A.*, 106, 4183, 2009.
151. Zhang, C., Bitto, E., Goff, R.D., Singh, S. Bingman, C.A., Griffith, B.R., Albermann, C., Phillips, G.N., and Thorson, J.S., Biochemical and structural insights of the early glycosylation steps in calicheamicin biosynthesis, *Chem. Biol.*, 15, 842, 2008.
152. Zheng, C., Griffith, B.R., Fu, Q., Albermann, C., Fu, X., Lee, I.-K., Li, L., and Thorson, J.S., Exploiting the reversibility of natural product glycosyltransferase-catalyzed reactions, *Science*, 313, 1291, 2006.
153. Flatman, R.H., Eustaquio, A., Li, S.-M., Heide, L., and Maxwell, A., Structure-activity relationships of aminocoumarin-type gyrase and topoisomerase IV inhibitors obtained by combinatorial biosynthesis, *Antimicrobiol. Agents Chemother.*, 50, 1136, 2006.

154. Maxwell, A., DNA gyrase as a drug target, *Trends Microbiol*., 5, 102, 1997.
155. Maxwell, A. and Lawson, D.M., The ATP-binding site of type II topoisomerases as a target for antibacterial drugs, *Curr. Top. Med. Chem*., 3, 283, 2003.
156. Rappa, G., Lorico, A., and Sartorelli, A.C., Potentiation by novobiocin of the cytotoxic activity of etoposide (VP-16) and teniposide (VM-26), *Int. J. Cancer*, 52, 903, 1992.
157. Marcu, M.G., Schulte, T.W., and Neckers, L., Novobiocin and related coumarins and depletion of heat shock protein 90-dependent signaling proteins, *J. Natl. Cancer Inst*., 92, 242, 2000.
158. Steffensky, M., Mühlenweg, A., Wang, Z.X., and Li, S.-M., and Heide, L., Identification of the novobiocin biosynthetic gene cluster of *Streptomyces spheroids* NCIB 11891, *Antimicrob*, *Agents Chemother.*, 44, 1214, 2000.
159. Pojer, F., Li, S.-M., and Heide, L., Molecular cloning and sequence analysis of the clorobiocin biosynthetic gene cluster: New insights into the biosynthesis of aminocoumarin antibiotics, *Microbiology*, 148, 3901, 2002.
160. Wang, Z.-X., Li, S.-M., and Heide, L., Identification of the coumermycin A_1 biosynthetic gene cluster of *Streptomyces rishiriensis* DSM 40489, *Antimicrob. Agents Chemother*., 44, 3040, 2000.
161. Trefzer, A., Pelzer, S., Shimana, J., Stockert, S., Bihlmaier, C., Fiedler, H.-P., Welzel, K., Vente, A., and Bechtold, A., Biosynthetic gene cluster of simocyclinone, a natural multihybrid antibiotic, *Antimicrob. Agents Chemother.*, 46, 1174, 2002.
162. Sohng, J.K., Oh, T.J., Lee, J.J., and Kim, C.G., Identification of a gene cluster of biosynthetic genes of rubradirin substructures in *S. achromogenes* var. *rubradiris* NRRL 3061, *Mol. Cells*, 7, 674, 1997.
163. Heide, L., The aminocoumarins: Biosynthesis and biology, *Nat. Prod. Rep*., 26, 1241, 2009.
164. Heide, L., Genetic engineering of antibiotic biosynthesis for the generation of new aminocoumarins, *Biotechnol. Adv*., 27, 1006, 2009.
165. Heide, L., Aminocoumarins: Mutasynthesis, chemoenzymatic synthesis, and metabolic engineering, *Methods Enzymol*., 459, 437, 2009.
166. Flatman, R.H., Eustaquio, A., Li, S.-M., Heide, L., and Maxwell, A., Structure-activity relationships of aminocoumarin-type gyrase topoisomerase IV inhibitors obtained by combinatorial biosynthesis, *Antimicrob. Agents Chemother*., 50, 1136, 2006.
167. Anderle, C., Alt, S., Gulder, T., Bringmann, G., Kammerer, B., Gust, B., and Heide, L., Biosynthesis of clorobiocin: Investigation of the transfer and methylation of the pyrrolyl-2-carboxyl moiety, *Arch. Microbiol*., 187, 227, 2007.
168. Garneau, S., Dorrestein, P.C., Kelleher, N.L., and Walsh, C.T., Characterization of the formation of the pyrrole moiety during clorobiocin and coumermycin A_1 biosynthesis, *Biochemistry*, 44, 2770, 2005.
169. Garneau-Tsodikova, S., Stapon, A., Kahne, D., and Walsh, C.T., Installation of the pyrrolyl-2-carboxyl pharmacophore by CouN1 and CouN7 in the late biosynthetic steps of the aminocoumrain antibiotics clorobiocin and coumermycin A_1, *Biochemistry*, 45, 8568, 2006.
170. Balibar, C.J., Garneau-Tsodikova, S., and Walsh, C.T., Covalent CouN7 enzyme intermediate for acyl group shuttling in aminocoumarin biosynthesis, *Chem. Biol*., 14, 679, 2007.
171. Fridman, M., Balibar, C.J., Lupoli, T., Kahne, D., Walsh, C.T., and Garneau-Tsodikova, S., Chemoenzymatic formation of novel aminocoumarin antibiotics by the enzymes CouN1 and CouN7, *Biochemistry*, 46, 8462, 2007.
172. Williams, G.J., Zhang, C., and Thorson, J.S., Directed evolution of a natural product glycosyltransferase, *Nat. Chem. Biol*., 3, 657, 2007.
173. Komatsu, M., Uchiyama, T., Omura, S., Cane, D.E., and Ikeda, H., Genome-minimized Streptomyces host for the heterologous expression of secondary metabolism, *Proc. Natl. Acad. Sci. U.S.A.*, 107, 2646, 2010.

26 Developments and Future Trends in Anticancer Natural Products Drug Discovery

Gordon M. Cragg and David J. Newman

CONTENTS

26.1 Introduction 699
26.2 Plant Sources 704
26.2.1 Novel Chemotypes 705
26.2.1.1 Englerins 705
26.2.1.2 Schweinfurthins 705
26.2.2 Flavopiridol 705
26.2.3 Olomucine, Roscovotine, and the Purvalanols 706
26.2.4 Benzopyrans and Privileged Structures 708
26.2.5 Microbial Associates and Endophytic Fungi 709
26.2.6 Old Molecules, New Uses 710
26.2.6.1 Bruceantin 710
26.2.6.2 Triterpenoid Acids 710
26.2.6.3 β-Lapachone 711
26.3 Marine Sources 712
26.3.1 Microbial Associates 712
26.3.1.1 Dolastatins 713
26.3.1.2 Ecteinascidins 713
26.3.1.3 Jaspamide/Jasplakinolide 713
26.3.1.4 Geodiamolides and Chondramides 714
26.3.1.5 Pederins, Mycalamides, and Related Structures 714
26.3.2 Independent Microbes 715
26.3.2.1 Salinosporamide 716
26.3.2.2 Largazole 716
26.4 Plant–Microbe–Marine Interface 717
26.4.1 Indigo and the Indirubins 717
26.5 Conclusion 718
References 719

26.1 INTRODUCTION

Important, naturally derived chemotypes currently in clinical use or development as anticancer agents have been discussed in earlier chapters, and the purpose of this chapter is to provide an overview, by no means exhaustive, of developments and future trends in the generation of novel agents from nature. For reference, a list of approved antitumor agents (as of the end of 2010) is shown in Table 26.1, using the data from Newman et al.[1]

TABLE 26.1
All Anticancer Drugs (1940–2010)

Generic Name	Year	Source[a]
Interferon, alfa2a	1986	B
Interleukin-2	1989	B
Celmoleukin	1992	B
Interferon, gamma-1a	1992	B
Teceleukin	1992	B
Pegaspargase	1994	B
Rituximab	1997	B
Trastuzumab	1998	B
Denileukin diftitox	1999	B
Mobenakin	1999	B
Tasonermin	1999	B
Alemtuzumab	2001	B
Ibritumomab	2002	B
Cetuximab	2003	B
Tositumomab	2003	B
Bevacizumab	2004	B
H-101	2005	B
Nimotuzumab	2006	B
Panitumumab	2006	B
Rexin-G®	2007	B
131I-chTNT	2007	B
Catumaxomab	2009	B
Ofatumumab	2009	B
Sipuleucel-T	2010	B
Testosterone	Pre-1970	N
Streptozocin	Pre-1977	N
Leucovorin	1950	N
Carzinophilin	1954	N
Sarkomycin	1954	N
Mitomycin C	1956	N
Chromomycin A3	1961	N
Mithramycin	1961	N
Vincristine	1963	N
Actinomycin D	1964	N
Vinblastine	1965	N
Bleomycin	1966	N
Doxorubicin	1966	N
Daunomycin	1967	N
Asparaginase	1969	N
Neocarzinostatin	1976	N
Aclarubicin	1981	N
Peplomycin	1981	N
Solamargines	1989	N
Masoprocol	1992	N
Pentostatin	1992	N
Paclitaxel	1993	N
Angiotensin II	1994	N
Arglabin	1999	N

TABLE 26.1 (continued)
All Anticancer Drugs (1940–2010)

Generic Name	Year	Source[a]
Paclitaxel nanoparticles	2005	N
Trabectedin	2007	N
Paclitaxel nanoparticles	2007	N
Romidepsin	2010	N
Ethinyl estradiol	Pre-1970	ND
Fluoxymesterone	Pre-1970	ND
Hydroxyprogesterone	Pre-1970	ND
Prednisone	Pre-1970	ND
Fosfestrol	Pre-1977	ND
Norethindrone acetate	Pre-1977	ND
Prednisolone	Pre-1977	ND
Methylprednisolone	1955	ND
Dexamethasone	1958	ND
Medroxyprogesterone acetate	1958	ND
Triamcinolone	1958	ND
Nandrolone phenylpropionate	1959	ND
Dromostanolone	1961	ND
Teniposide	1967	ND
Testolactone	1969	ND
Megesterol acetate	1971	ND
Calusterone	1973	ND
Methyltestosterone	1974	ND
Mitobronitol	1979	ND
Vindesine	1979	ND
Estramustine	1980	ND
Etoposide	1980	ND
Elliptinium acetate	1983	ND
Epirubicin HCI	1984	ND
Triptorelin	1986	ND
Pirarubicin	1988	ND
Vinorelbine	1989	ND
Idarubicin hydrochloride	1990	ND
Cladribine	1993	ND
Cytarabine ocfosfate	1993	ND
Formestane	1993	ND
Miltefosine	1993	ND
Irinotecan hydrochloride	1994	ND
Zinostatin stimalamer	1994	ND
Docetaxel	1995	ND
Etoposide phosphate	1996	ND
Topotecan HCl	1996	ND
Alitretinoin	1999	ND
Exemestane	1999	ND
Valrubicin	1999	ND
Gemtuzumab ozogamicin	2000	ND
Amrubicin HCl	2002	ND
Fulvestrant	2002	ND
Belotecan hydrochloride	2004	ND

continued

TABLE 26.1 (continued)
All Anticancer Drugs (1940–2010)

Generic Name	Year	Source[a]
Hexyl aminolevulinate	2004	ND
Talaporfin sodium	2004	ND
Vapreotide acetate	2004	ND
Temsirolimus	2007	ND
Ixabepilone	2007	ND
Pralatrexate	2009	ND
Mifamurtide	2010	ND
Vinflunine	2010	ND
Cabazitaxel	2010	ND
Eribulin	2010	ND
Diethylstilbestrol	Pre-1970	S
Razoxane	Pre-1977	S
Semustine (MCCNU)	Pre-1977	S
Chlortrianisene	Pre-1981	S
Levamisole	Pre-1981	S
Nimustine hydrochloride	Pre-1981	S
Triethylenemelamine	Pre-1981	S
Busulfan	1954	S
Chlorambucil	1956	S
Cyclophosphamide	1957	S
Mechlorethanamine	1958	S
Thiotepa	1959	S
Melphalan	1961	S
Pipobroman	1966	S
Hydroxyurea	1968	S
Procarbazine	1969	S
Mitotane	1970	S
Dacarbazine	1975	S
Ifosfamide	1976	S
Lomustine (CCNU)	1976	S
Carmustine (BCNU)	1977	S
Cis-diamminedichloroplatinum	1979	S
Hexamethylmelamine	1979	S
Aminoglutethimide	1981	S
Flutamide	1983	S
Carboplatin	1986	S
Amsacrine	1987	S
Lonidamine	1987	S
Nilutamide	1987	S
Ranimustine	1987	S
Fotemustine	1989	S
Bisantrene hydrochloride	1990	S
Porfimer sodium	1993	S
Sobuzoxane	1994	S
Nedaplatin	1995	S
Oxaliplatin	1996	S
Lobaplatin	1998	S
Heptaplatin/SK-2053R	1999	S

TABLE 26.1 (continued)
All Anticancer Drugs (1940–2010)

Generic Name	Year	Source[a]
Arsenic trioxide	2000	S
Zoledronic acid	2000	S
Sorafenib	2005	S
Plerixafor hydrochloride	2009	S
Miriplatin hydrate	2010	S
Nafoxidine	Pre-1977	S/NM
Tamoxifen	1973	S/NM
Camostat mesylate	1985	S/NM
Toremifene	1989	S/NM
Anastrozole	1995	S/NM
Bicalutamide	1995	S/NM
Fadrozole HCl	1995	S/NM
Letrazole	1996	S/NM
Imatinib mesilate	2001	S/NM
Gefitinib	2002	S/NM
Temoporfin	2002	S/NM
Bortezomib	2003	S/NM
Erlotinib hydrochloride	2004	S/NM
Sunitinib malate	2006	S/NM
Dasatinib	2006	S/NM
Lapatinib ditosylate	2007	S/NM
Nilotinib hydrochloride	2007	S/NM
Pazopanib	2009	S/NM
Azacytidine	Pre-1977	S*
Mercaptopurine	1953	S*
Methotrexate	1954	S*
Fluorouracil	1962	S*
Thioguanine	1966	S*
Uracil mustard	1966	S*
Cytosine arabinoside	1969	S*
Floxuridine	1971	S*
Ftorafur	1972	S*
Carmofur	1981	S*
Enocitabine	1983	S*
Mitoxantrone HCl	1984	S*
Doxifluridine	1987	S*
Fludarabine phosphate	1991	S*
Gemcitabine HCl	1995	S*
Capecitabine	1998	S*
Azacytidine	2004	S*
Clofarabine	2005	S*
Nelarabine	2006	S*
Decitabine	2006	S*
Raltitrexed	1996	S*/NM
Temozolomide	1999	S*/NM
Bexarotene	2000	S*/NM
Abarelix	2004	S*/NM
Pemetrexed disodium	2004	S*/NM

continued

TABLE 26.1 (continued)
All Anticancer Drugs (1940–2010)

Generic Name	Year	Source[a]
Tamibarotene	2005	S*/NM
Vorinostat	2006	S*/NM
Degarelix	2009	S*/NM
BCG live	1990	V
Melanoma theraccine	2001	V
Cervarix®	2007	V
Autologous tumor cell-BCG	2008	V
Vitespen	2008	V

[a] Newman et al.[1]

As in the first edition, the organization of the chapter is according to the putative sources of agents where these are known or assumed, and the chapter ends with a discussion, together with examples, of what appears to be an evolving trend about the actual source organisms. As more is learned about the genetics of a "producing organism," frequently it is realized that the actual organism from which the original material was isolated and identified is either a host for microbial biosynthetic machinery or may perform a tailoring function on materials produced by a microbe.

26.2 PLANT SOURCES

As mentioned in the first edition, on the basis of prior experience using the National Cancer Institute (NCI) 60-cell line screen, the potential for the discovery of a new cytotoxic chemotype from plants, comparable to the taxanes or camptothecins, appeared to be relatively low. Our reason for making this statement approximately six years ago was due to the results from NCI's work, covering vascular plants from extensive collections in the tropics over the last 25+ years. In this time frame, only a few novel chemotypes have been reported from these collections, including the englerins and schweinfurthins. These are discussed a little later on in this chapter.

However, in the last five years, other research groups have reported very significant novel biological activities for earlier plant-derived compounds. In the first example, the old compound withacnistin (**1**), first reported in 1969[2] was shown to inhibit Stat-3, a novel mechanism of action,[3] both *in vitro* and *in vivo*, although the compound was identified as cucurbitacin Q in the original publication, with the correct assignment being given three years later.[4] The second example is drawn from work on the rocaglate series of compounds. This basic structural class has been well documented in the literature but, in the early 2000s, workers at the University of Illinois at Chicago (UIC) reported the isolation and identification of two compounds, silvestrol and epi-silvestrol (**2a, b**). Initial *in vitro* and *in vivo* activities were reported by the UIC investigators,[5] with an erratum later the same year when the species identity was changed from *Aglaia silvestris* (M. Roemer) Merrill to *Aglaia foveolata* Pannell, but the names of the compounds were not changed.[6] Work continued at both UIC and Ohio State University (OSU) as a result of one of the UIC investigators (ADK) moving to that institution, and over the last few years, novel mechanisms of action involving inhibition of translation initiation have been described by Pelletier at McGill and his collaborators;[7,8] just as importantly, significant activities in chronic lymphocytic leukemia (CLL) and acute lymphoblastic leukemia both *in vitro* and *in vivo* were reported by the OSU group.[9,10]

During the same time frame, a patent application was made by an Australian group for compounds that were probably very similar if not the same as silvestrol and epi-silvestrol (cf., reference 7 in Ref. 5). This subsequently turned out to be the case, although the patent structures were misassigned as suggested by Hwang et al. This patent was subsequently assigned to the Malaysian

State of Sarawak/Sarawak Biodiversity Council (SBC) as the source plant for these compounds (identified as *A. leptantha*), was collected in conjunction with the SBC. Work is still continuing on these agents and syntheses of the original materials and the derivatives have been recently reported from Australia[11] and the United States.[12]

26.2.1 Novel Chemotypes

26.2.1.1 Englerins

Englerins A (3) and B (4) are two new guaiane sesquiterpenes that were isolated from the Tanzanian plant, *Phyllanthus engleri*. Testing of the extract in the NCI 60-cancer cell line screen showed selective inhibition of growth of the renal cancer cell lines. Bioassay-guided fractionation yielded englerins A (3) and B (4), and englerin A showed 1000-fold selectivity against six of eight renal cancer cell lines with GI(50) values ranging from 1 to 87 nM.[13] These compounds are being developed in collaboration with scientists from the Institute of Traditional Medicine of Muhimbili University of Health and Allied Sciences in Dar es Salaam, Tanzania.

26.2.1.2 Schweinfurthins

The schweinfurthins (e.g., schweinfurthins A, B, and F; **5**, **6**, and **7**, respectively) were isolated from the African plant *Macaranga schweinfurthii* Pax, collected in Cameroon. They display significant selective activity against central nervous system, and renal and breast cancer cell lines in the NCI 60 cell line anticancer assay.[14] The spectrum of anticancer activity does not match that of any currently used agent, indicating that these compounds may be acting at a previously unrecognized target or through a novel mechanism. Thus far, 10 schweinfurthins (A to J) are known. While scale-up recollections and isolations have been undertaken in collaboration with colleagues in Cameroon,[15] the isolation of sufficient quantities of the schweinfurthins from the natural source remain challenging, and synthetic strategies have been developed to provide a reliable source of natural schweinfurthins and synthetic analogs for further biological testing.[16,17] In the case of schweinfurthin F (**7**), total synthesis of the (*R,R,R*)- and (*S,S,S*)-enantiomers and comparisons of spectral data, optical rotations and bioassay data with those reported for the natural product, have resulted in assignment of the natural material as the (*R,R,R*)-isomer.[18] These synthetic efforts are continuing.[19,20]

26.2.2 Flavopiridol

Flavopiridol (**8**) was prepared by the Indian subsidiary of Hoechst (now Sanofi-Aventis) following the isolation and synthesis of the plant-derived natural product, rohitukine (**9**). It was the most active of approximately 100 analogs made when assayed against cyclin-dependent kinases (CDKs) and showed about 100-fold more selectivity compared with its activity versus tyrosine kinases. Although it showed roughly comparable activity (IC_{50}: 100–400 nM) against CDKs, it turned out to be the first compound at NCI identified as a potential antitumor agent that subsequently was proven to be a relatively specific CDK inhibitor.[21] The initial report[22] on its CDK2 inhibitory activity was made in 1994, followed by data demonstrating antitumor activity, provided by Czech et al.,[23] in 1995. Recent (2008) reports indicate that it also acts through as yet undefined mechanism(s), and results from the Aggarwal group at M. D. Anderson Cancer Center suggest that it interferes with the tumor necrosis factor (TNF) cell-signaling pathway, resulting in the suppression of antiapoptotic mechanisms and enhancement of apoptosis.[24] In addition, there have been recent efforts to overcome the low solubility of flavopiridol by generating liposomal flavopiridol and demonstrating that this construct has significantly improved pharmacokinetics (PKs) in relevant animal models.[25]

Flavopiridol is currently (November 2010) in 12 phase I and II clinical trials, both as a single agent and as a modulator in combination with other agents, which are actively recruiting patients, from a total of 57 trials listed in the clinical trials database where nine further trials are in the "active but not

recruiting" category. It has been reported to lead to partial or complete remissions in a number of phase I patients, leading to phase II studies in patients with paclitaxel-resistant tumors. There have been a number of earlier reports of uses of this agent and the various combinations with other drugs and drug candidates, a significant number of which were either natural products or are derived from natural products.[26–28] This pattern of combinations has continued in the more recent trials. A recent review by Romano discusses the agents that are now in clinical trials that have activities similar to flavopiridol with respect to the CDK-9 pathway and should be consulted by the interested reader.[29]

There have been a number of publications covering the results of earlier clinical trials where this agent, usually in combination with other cytotoxins, has shown some antitumor activity in humans. These citations are not meant to be exhaustive, simply representative. Some promise was shown in a phase I study involving the treatment of patients with relapsed and refractory acute leukemias by initial infusion with flavopiridol, followed by sequential administration of 1-β-D-arabinofuranosylcytosine (ara-C) and mitoxantrone.[30] In a phase II study, treatment of patients with relapsed CLL with single-agent flavopiridol, and subsequent addition of dexamethasone to suppress cytokine release syndrome achieved a 53% response rate, including 1 complete response and 30 partial responses out of 64 patients treated.[31] The same group reported on phase I studies of patients with relapsed CLL, including full PK data,[32] and they have also reviewed the use of this agent in the treatment of CLL.[33] For recent progress in the treatment of CLL using a variety of agents, including flavopiridol, readers are referred to reviews by Maddocks and Lin[34] and by Hallek.[35] Initially promising results have been obtained in the treatment of patients with acute myelogenous leukemia (AML) with flavopiridol, followed sequentially by ara-C and mitoxantrone.[36] Progress in the treatment of AML has also been recently reviewed.[37]

In contrast, a phase II study in the treatment of patients with refractory multiple myeloma with single-agent flavopiridol showed disappointing results.[38] Other phase II studies have been reported for the following cancers with observations summarized in parentheses: refractory metastatic pancreatic cancer using flavopiridol in combination with docetaxel (minimal activity and significant toxicity);[39] previously untreated metastatic or locally advanced soft-tissue sarcoma using flavopiridol as a single agent (drug well tolerated, but no objective responses);[40] recurrent or persistent endometrial adenocarcinoma refractory to established treatments using single-agent flavopiridol (minimal activity as a second-line chemotherapy);[41] malignant melanoma (no objective responses);[42] advanced renal cell cancer (overall response rate of 12% and 41% stable disease);[43] and untreated metastatic hormone-refractory prostate cancer (no objective responses).[44]

Results of phase I trials have been reported for treatment of the following cancers: flavopiridol and FOLFOX (folinic acid, 5FU, and oxaliplatin) for advanced solid tumors;[45] flavopiridol, fludarabine, and rituximab for mantle-cell lymphoma, indolent B-cell non-Hodgkin's lymphomas, and CLL;[46] flavopiridol/paclitaxel/carboplatin for advanced-stage non-small-cell lung cancer (NSCLC);[47] docetaxel followed by flavopiridol for advanced solid tumors;[48] docetaxel and flavopiridol for metastatic breast cancer;[49] sequential combination of irinotecan followed by flavopiridol for advanced solid tumors;[50,51] and flavopiridol as a single agent for children with recurrent or refractory solid tumors.[52]

In closing this section, it should be noted that Sanofi-Aventis obtained orphan drug status in the European Union for the treatment of CLL, and according to the current listing in the Thomson-Reuters Integrity® database, phase III trials against CLL are in progress under the aegis of Sanofi-Aventis, although no record is yet shown in the clinical trials database.

26.2.3 Olomucine, Roscovotine, and the Purvalanols

Continuing on the theme of plant-derived products being leads to cell-cycle modulators, Meijer, one of the early researchers in pharmacologic intervention in the cell cycle,[53] demonstrated that, using the simple starfish oocyte model of cell division, substituted purines, particularly 6-dimethylaminopurine and isopentenyladenine (from *Castanea* sp.), were found to inhibit the mitotic histone H1 kinase, which is now better known as CDK1/cyclin B, at the 50- to 100-μM level *in vitro*. On

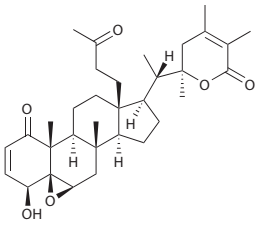

1. Withacnistin

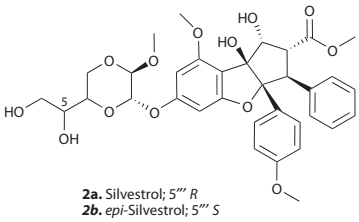

2a. Silvestrol; 5‴ *R*
2b. *epi*-Silvestrol; 5‴ *S*

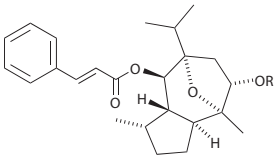

3. Englerin A; R = $COCH_2OH$
4. Englerin B; R = H

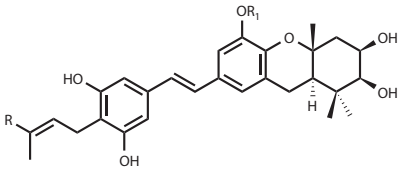

5. Schweinfurthin A; R = $CH_2CH_2CH = CMe_2$, R_1 = H
6. Schweinfurthin B; R = $CH_2CH_2CH = CMe_2$, R_1 = CH_3
7. (*R,R,R*)-Schweinfurthin F; R = R_1 = CH_3,

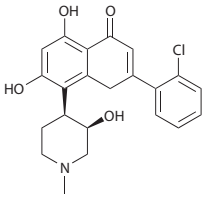

8. Flavopiridol

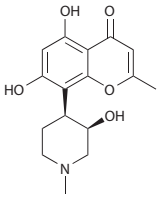

9. Rohitukine

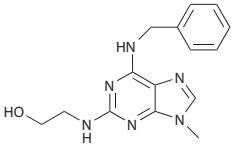

10. Olomucine

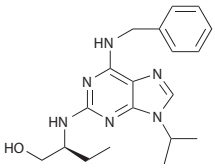

11. (R)-Roscovitine
CYC 202
Seliciclib

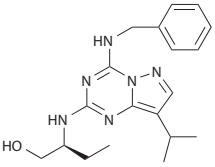

12. N&N1

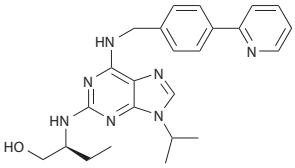

13. CR8

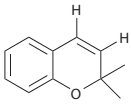

14. 2,2-dimethyl-2H-benzopyran

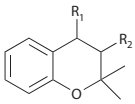

15. Modified double bond structures

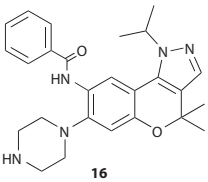

16

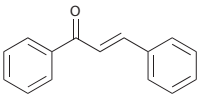

17. Chalcone

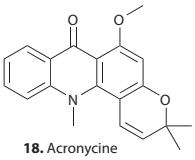

18. Acronycine

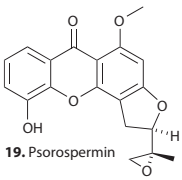

19. Psorospermin

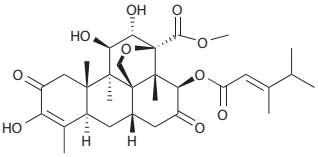

20. Bruceantin

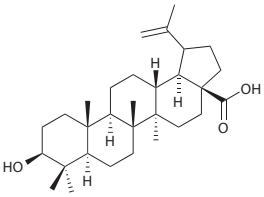

21. Betulinic Acid

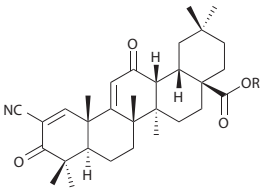

22. CDDO, Bardoxolone; R = H
23. CDDO-Me; R = CH_3

STRUCTURE 26.1 Structures **1** through **23**.

searching for other purine-derived compounds, the group tested a plant secondary metabolite, subsequently named olomucine (**10**), which was originally isolated from the cotyledons of the radish, but had been synthesized in Australia in 1986 by Parker et al.[54] This material disproved the current dogma about adenosine triphosphate-binding sites not having specificity, because it demonstrated an improved efficacy (IC_{50}: 7 μM) and selectivity for CDKs and, to some extent, MAP kinases by direct competition with adenosine triphosphate. Further development of this series led to roscovitine (**11**), and then following synthesis of a very focused library *via* combinatorial chemistry techniques, the purvalanols, which were even more potent, with IC_{50} values in the 4 to 40nM range (compared with 450 nM for roscovitine).[55]

The preclinical development, mechanism of action, and clinical development of the (*R*)-isomer of roscovitine (seliciclib) have recently (2009) been reviewed.[56] It was selected for clinical development under the code CYC202 under license to Cyclacel in Dundee, Scotland. Phase I clinical trials indicated that it was fairly well tolerated with the possibility of efficacy in nasopharyngeal carcinoma and NSCLC. Phase II trials are being conducted in patients with NSCLC who have failed at least two prior therapies, but only modest activity has been observed, with stabilization of disease rather than objective responses being the main effect.[56] A phase II evaluation of seliciclib is also being conducted as a single agent in nasopharyngeal cancer (http://www.cyclacel.com/). As with other signal transduction inhibitors in clinical trials, sequential treatment with cytotoxins may be the best approach to achieving improved efficacy.

Although some beneficial effects are seen with the signal transduction inhibitors, complete or partial responses tend to only be demonstrated when sequential treatments of signal transduction inhibitor/cytotoxin are used. *R*-roscovitine has been shown to downregulate nuclear factor-κB (NF-κB) activation in response to TNFα and IL-1. Treatment of cells with TNFα and *R*-roscovitine causes potentiation of cell death,[57] and it is suggested that *R*-roscovitine could potentially be used as a bitargeted anticancer drug functioning by simultaneously causing p53 activation and NF-κB suppression. *R*-roscovitine has been reported to sensitize cells such as thyroid carcinoma cell lines to TRAIL (TNF-related apoptosis-inducing ligand)-induced apoptosis.[58,59] Thus, the combination of *R*-roscovitine and TRAIL may provide a novel approach to the treatment of anaplastic thyroid carcinomas resistant to conventional chemotherapy.

The Meijer group has synthesized several novel classes of analogs and isosteres of roscovotine that exhibit considerably enhanced selectivity and potency compared with the parent compound. Among these are the biosteres, "N&N" of which N&N1 (**12**), pyrazolo[1,5-a]-1,3,5-triazine, showed significantly higher potency at inhibiting various CDKs and at inducing cell death in a wide variety of human tumor cell lines.[60,61] In another study, extensive medicinal chemistry resulted in the identification of an optimal substitution at the N6 position (compound CR8; **13**). CR8 consistently showed significantly improved apoptotic cell death-inducing activity in 25 different cell lines.[62]

In addition to these primary literature sources, there is a recent (2009) review by Malumbres and Barbacid covering the differences in CDKs and their responses. This is an excellent introduction to the problems involved in targeting these pathways.[63]

26.2.4 Benzopyrans and Privileged Structures

The chemical modification of an existing basic "privileged structure" is documented in the combinatorial chemistry literature, particularly in the case of the formally plant-derived base structure, the benzopyran molecule. The term, "privileged structures," was originally introduced by Evans et al.[64] for benzazepines and benzdiazepines because of their ability to bind to a multitude of unrelated classes of peptide receptors with high affinity. The term was later extended by Mason et al.[65] to other structural classes, such as benzamidines, biphenyltetrazoles, spiropiperidines, indoles, and benzylpiperidines and the concept was reviewed by Patchett and Nargund in 2000.[66] More recent reviews that cover many classes of privileged structures, including purines and flavones discussed above, and the benzopyrans discussed below, have appeared.[67,68]

In a series of elegant papers, Nicolaou et al.[69–71] dramatically extended the concept to include benzopyrans, as a result of the researchers' hypothesis: "We were particularly intrigued by the possibility that using scaffolds of natural origin, which presumably have undergone evolutionary selection over time, might confer favorable bioactivities and bioavailabilities to library members."[69] A search of the literature showed almost 4000 2,2-dimethyl-2H-benzopyran moieties (**14**); a slight structural modification whereby the pyran ring is reduced (**15**) identified another 8000 structures. Examples of the multiplicity of bioactive derivatives of this general structure are given in detail in Figure 2 of the first paper in the series,[69] which should be consulted by the interested reader. Their initial libraries, and subsequent derivatives based on the "active" benzopyrans, were then tested against a variety of pharmacologic screens, and the leads were then reoptimized, using the screening data. By mid-2004, four publications had come from these initial libraries, with activities in the inhibition of NADH:ubiquinone oxidoreductase giving rise to benzopyrans with IC_{50} values in the 18s to 55s nM range and having predominately cytostatic effects on tumor lines, thus indicating a possible potential in chemoprevention. Interested readers should consult Figures 4 and 5 in the relevant publication for more information on the actual structures and activities in both types of assay.[72] This report, relevant to antitumor studies, was then followed by others in different disease states covering antibiotics, energy metabolism, and genetic dissection of a cell pathway.[73–75]

More recent work has been focused on the s-*cis*-enone embedded in the benzopyran skeleton and it was utilized as a key intermediate for the synthesis of four different heterocyclic libraries; these are composed of four novel core skeletons incorporating a benzopyran substructure fused to pyridine, pyrazole, pyrazolopyrimidine, and pyrimidine moieties.[76] An efficient synthesis of benzopyranylpyrazoles (e.g., 16) has been developed *via* regioselective condensation of substituted hydrazines with beta-keto aldehydes.[77]

Chalcone (**17**), considered as a privileged structure, shows antiinflammatory and anticancer activities. Libraries of chalcone-based compounds have been synthesized to study their structure–activity relationships as potential NF-κB inhibitors. It was found that the level of NF-κB inhibitory activities correlated moderately well with the degrees of cytotoxicity, suggesting that suppression of NF-κB activation is probably responsible, at least in part, for some of the cytotoxicities observed.[78] As mentioned above, benzopyran moieties are privileged structures, and to these may be added benzofurans. These moieties are present in many bioactive natural products, and in the field of anticancer drugs, they are best exemplified by the pyranoacridone, acronycine (**18**), and the furanoxanthone, psorospermin (**19**), respectively.[79] Structure–activity studies have been carried out on analogs of both these compounds, and it has been observed that hybrid compounds associating the acridone or benzo[*b*] acridone chromophore of acronycine derivatives with the epoxyfuran alkylating unit present in psorospermin display very potent antiproliferative activities.

26.2.5 Microbial Associates and Endophytic Fungi

As mentioned in the introduction, there is now a realization that materials that were often thought to be from—in this case—plants are actually produced in large part by another organism, and the plant host may only perform some final tailoring of the molecule. Such is the case with maytansine since, as reported by Floss (Chapter 17), the actual source of the base structure is a bacterium, with perhaps the modification leading to maytansine being performed by the plant itself. There are other examples given later in the chapter that continue on this theme.

In addition to the above example of what may be a simple transfer of material to the host from a microbe, there are some extremely interesting examples in the recent review by Strobel et al.[80] of materials that are produced by plant endophytic microbes, predominately from the fungi. Among the organisms reported are a series of fungal endophytes from the well-known genus *Pestalotiopsis* and a report that *Pestalotiopsis micromonospora*, a very common endophytic fungus, produces paclitaxel (Chapter 6) at low levels. This followed on from the initial report, which was greeted with a fair amount of skepticism that the novel fungus *Taxomyces andreanae*, isolated from *Taxus brevifolia*,

produced paclitaxel at very low levels. Since the original report in 1993, many further examples of paclitaxel production at low levels have been reported in the scientific literature, not just from *Taxus* spp., but from trees of many other genera. These findings have led Strobel to suggest that paclitaxel production by endophytic fungi is a protective mechanism for the plant host against plant pathogens, such as *Pythium* spp. and *Phytophora* spp., as paclitaxel is known to be very active as a fungicide against these particular pathogens. A very recent report demonstrated the presence of fungal paclitaxel in *Pestalotiopsis breviseta* isolated and purified from the infected leaves of *Ervatamia divaricata* using ultraviolet, mass spectroscopy, and NMR techniques to confirm identity.[81]

Very recently, there have been two reports, with one being in English, the other in a Russian language reference within an English language review (reference 48 in Miller et al.[82]) that the one essential enzyme in the biosynthesis of the taxanes, taxadiene synthase, has now been definitively identified in the original fungal endophyte from a paclitaxel-producing tree, *Taxomyces andreaneae*.[83] Very recently, Zhou et al.[84] and Kumaran and Hur[85] have reviewed the production levels and the fungi that have been reported to produce paclitaxel through 2008–2009. The figures, in some cases, approach levels within half an order of magnitude of those isolated from the plants themselves.

Further examples of important anticancer agents produced by endophytic fungi isolated from the original source plants include camptothecin (Chapter 2),[86,87] podophyllotoxin, an epimer of the precursor to the anticancer drug etoposide (Chapter 5),[88,89] and the vinca alkaloids, vinblastine,[90] and vincristine (Chapter 7).[91,92] The fact that these compounds have been shown not to be artifacts offers the prospect for their increased production, provided the gene/gene product(s) controlling their production by the relevant endophytes can be identified.

At the present time, effectively nothing is known about the regulation/control of these gene clusters and whether there is some form of chemical communication analogous to the well-described "quorum sensing" known to occur in microbes. Similar discoveries could provide an entry into greatly increased production of other key bioactive natural products.

26.2.6 Old Molecules, New Uses

26.2.6.1 Bruceantin

An example of an "old" drug of the same vintage as Taxol® and camptothecin, and having a possibility of revival, is bruceantin (**20**), which was first isolated from a tree, *Brucea antidysenterica*, used in Ethiopia for the treatment of "cancer." Activity was observed in animal models bearing a range of tumors, but no objective responses were observed in clinical trials, and further development was terminated. Interest has been revived by the observation of significant activity against panels of leukemia, lymphoma, and myeloma cell lines, as well as in animal models bearing early and advanced stages of the same cancers. This activity has been associated with the downregulation of a key oncoprotein (c-*myc*), and these data are being presented as strong evidence supporting the development of bruceantin as an agent for the treatment of hematological malignancies,[93] including multiple myeloma.[93,94] More recently, the potential for the quassinoids and bruceantin in particular has been reviewed by Lucas et al.,[10] and the potential for altering chemosensitivity has been reported by Robert et al. Where it is involved in studies on effects upon translation, as in a genetically modified *in vivo* mouse model, bruceantin and other translation inhibitors were able to synergize with doxorubicin, reestablishing an apoptotic program in tumors harboring PTEN/AKT/mTOR pathway mutations.[95]

26.2.6.2 Triterpenoid Acids

Betulinic acid (**21**) is a lupane-type triterpene that has been isolated from many taxonomically diverse plant genera, and one of the major sources is the birch tree, *Betula* spp., which is also a primary source of its C_{28} alcohol precursor, betulin, whose isolation was first reported in 1788.[96]

Betulinic acid showed cytotoxicity against a range of cancer cell lines, as well as significant *in vivo* activity in animal models bearing human melanoma xenografts. Reduction of ultraviolet-C-induced DNA breakage in congenital melanocytic naeval cells indicated a potential role as a chemopreventive agent,[97] and systemic and topical formulations of the agent have been developed. A 20% betulinic acid ointment is currently being evaluated in the treatment of dysplastic nevi (moderate to severe dysplasia). A recent review by Mullauer et al. implies that one of the major sites of action may well be a direct effect upon the mitochondrion where it induces *Bax*/*Bak*-independent cytochrome c release.[98]

Triterpenoid acids such as oleanolic and ursolic acid, which are common plant constituents, are known to possess weak antiinflammatory and antitumor activities. Attempts to synthesize new analogs having increased potencies have led to the synthesis of 2-cyano-3,12-dioxoolean-1,9-dien-28-oic acid (CDDO; bardoxolone; **22**) and its methyl ester (MeCDDO, bardoxolone methyl; **23**), which have potent *in vitro* and *in vivo* antitumor activity against a wide range of tumors, including breast carcinomas, leukemias, and pancreatic carcinomas. Of particular interest was the significant activity of CDDO against epithelial ovarian carcinoma cell lines, including lines that were resistant to clinically used agents such as cisplatin. Because epithelial ovarian carcinoma is the leading cause of death from gynecologic cancers, further evaluation of CDDO in the treatment of these cancers was being pursued[99] until recently. No current phase I trials appear to be ongoing with the base molecule.

However, evaluation of C-28 derivatives of CDDO, such as CDDO methyl ester (MeCDDO; **23**), CDDO imidazolide (CDDOIm), CDDO ethyl amide (CDDO-EA), CDDO trifluoroethyl amide (CDDO-TFEA), and CDDO diethylamide (CDDO-DE), against pediatric solid tumor cell lines indicate their potential for the treatment of high-risk pediatric solid tumors.[100] The mechanisms of action and molecular targets of these compounds are the focus of ongoing research. Reported effects include blocking of the synthesis of inducible nitric oxide synthase and inducible cyclooxygenase (COX-2), two enzymes involved in inflammation and carcinogenesis, and inhibition of the interleukin-1 (IL-1)-induced expression of the proinflammatory proteins matrix metalloproteinase-1 (MMP-1) and MMP-13. *In vitro* and *in vivo* studies of CDDO-Me have indicated that it has a potent antiangiogenic activity,[101] it also inhibits the expression of interleukin 6 and Stat-3 phosphorylation in drug-resistant ovarian cancer cells,[102] and when combined with the staurosporin derivative PKC412, it synergistically induces apoptosis in AML cells that contain the internal tandem duplication mutation.[103]

What is also of interest is that CDDO-Me, in addition to its antitumor activities, has also demonstrated activity in chronic kidney disease (CKD) and type II diabetes.[104] Inspection of the current clinical trials database shows that of the eight trials listed under RTA 402 (the code number for CDDO-Me), four are at the phase I or II level against solid or lymphoid tumors, with one phase II against melanoma being withdrawn. The other four are trials in diabetes/CKD, and three are either completed or underway, with one being terminated. A search on bardoxolone or RTA-401 brings up only one completed trial at the phase I level. A recent review by Petronelli et al.[105] should also be consulted for further information on the potential of this class of agents.

26.2.6.3 β-Lapachone

The relatively simple naphthoquinone β-lapachol (**24**) is a well-known compound obtained from the bark of the lapacho tree, *Tabebuia avellanedae*, and other species of the same genus native to South America, and it, together with other components of the plant, have extensive usage as an ethnobotanical treatment in the Amazonian region. Although advanced to clinical status by the NCI in the 1970s, this compound showed unacceptable levels of toxicity and was dropped.

Recently, however, a close relative, β-lapachone (**25**), has shown very interesting molecular target activity, with induction of apoptosis in transformed cells being one of the mechanisms of action. What is of prime import, however, is that one of the possible routes of apoptotic induction is *via* the transcription factor E2F1[106] and appears to only function in transformed cells, as no effect was shown in nontransformed cells at comparable concentrations of the agent. Evidence of further involvement in the transcription processes was the demonstration by Choi et al.[107] that this agent induced activation

of caspase-3, inhibition of NF-κB, and subsequent downregulation of bcl-2. Further information on the background of β-lapachone agents is given in the review by Ravelo et al.[108]

Selective killing of human cancer cells by β-lapachone has been associated with the overexpression of NAD(P)H:quinone oxidoreductase-1 (NQO1). NQO1 expression in FSaII fibrosarcoma of C3H mice, human A549 lung cancer cells, and human MDA-MB-231 breast cancer cells has been found to be elevated by mild temperature heat shock, which has been shown to significantly increase the sensitivity of the cells to β-lapachone.[109] This effect has been attributed to increased NQO1 transcription, as well as increased Hsp70-mediated NQO1 stabilization.[110] The combination of β-lapachone with cisplatin increased the sensitivity of NQO1-positive, but not NQO1-negative MDA-MB-231 cells, as well as suppressing the growth of FSaII tumors in the legs of C3H mice in a greater than additive manner.[111] The authors concluded that this increase in sensitivity is due to the upregulation of NQO1 by the cisplatin.

β-lapachone exhibits cytotoxicity in retinoblastoma (RB) cell lines at low micromolar concentrations,[112] and, in combination with paclitaxel, it has been shown to induce potent synergistic apoptotic effects in human RB Y79 cells; this effect is suggested by the authors as being due to the lowering of phospho-Akt.[113] Elevated levels of NQO1 have been observed in tumors from NSCLC patients, and it has been shown that β-lapachone kills A549 NSCLC cells in an NQO1-dependent manner at an LD_{50} of ~4 μM with a minimum two-hour exposure, with cell death being mediated by NQO1 and hyperactivation of poly(ADP-ribose)polymerase-1 (PARP-1).[114] Studies of the inhibition of the progression and metastasis of the human hepatocarcinoma cell lines, HepG2 and Hep3B, by β-lapachone suggest that inhibition of the invasion of the cells may, at least in part, be due to upregulation of the expression of the Egr-1, TSP-1, and E-cadherin.[115]

Despite the therapeutic promise of β-lapachone, its preclinical evaluation and clinical translation have been limited by poor aqueous solubility. β-lapachone-containing poly(ethylene glycol)-block-poly(D,L-lactide) (PEG-PLA) polymer micelles have been developed, which show a marked increase in cytotoxicity in NQO1-positive H596 lung, DU-145 prostate, and MDA-MB-231 breast cancer cells, resembling free drug both in efficacy and mechanism of cell death. These results demonstrate that β-lapachone-containing micelles may have potential as an effective therapeutic strategy against NQO1-overexpressing tumor cells.[116] Likewise, intratumoral delivery of polymer millirods, formed by the incorporation of solid-state inclusion complexes of β-lapachone with hydroxypropyl-beta-cyclodextrin into poly(D,L-lactide-co-glycolide), show significant tumor growth inhibition of three different prostate cancer cell lines in an NQO1-dependent manner; *in vivo* efficacy was shown in PC-3 prostate tumor xenografts in athymic nude mice.[117] In addition, very recently, a version of the PEG-PLA micelle technique has produced materials that have activity against NQO1-overexpressing cells.[118]

To date, β-lapachone (ARQ 501) has been in three phase II clinical trials as a single agent against head and neck, leiomyosarcoma, and pancreatic cancers, as well as three phase I trials, including one in combination with docetaxel, together with one extension trial at the phase I/II level for patients previously treated with ARQ 501.

The synthesis of several 3-arylamino (e.g., **26**) and 3-alkoxy-nor-β-lapachone derivatives has been reported, and some have shown significant cytotoxicity against SF295 (CNS), HCT8 (colon), MDA-MB435 (melanoma), and HL60 (leukemia) cell lines.[119] Recent reports on the metabolism of β-lapachone have also appeared.[120,121]

26.3 MARINE SOURCES

26.3.1 Microbial Associates

Perhaps it is in this area that the interplay of microbes and a host invertebrate/alga is becoming a significant part of the overall equation. For many years, it has been speculated by workers in the field that a number of potent marine-derived molecules, which were active as antitumor agents,

might be the product of interactions between the organism from which the agent was isolated and associated microbes. Recently, there have been some excellent reviews published demonstrating the complexity of the interactions at the genetic levels, and these should be consulted for overviews of the problems and potential solutions.[122–125]

26.3.1.1 Dolastatins

A driving force behind such suppositions was the number of reports in the marine natural product literature over the last 10–15 years, where the structures of compounds isolated from an invertebrate or, in an increasing number of cases, from multiple different invertebrate phyla in distinct geographical areas of the oceans, were similar to each other or to metabolites from terrestrial bacteria. Some relevant examples are the dolastatins from *Dolabella auricularia* and simplostatins, and now dolastatins from the cyanophyte, *Simploca* sp., on which the nudibranch feeds (Chapter 11).

The interplay of derivatives of these agents (auristatins, see Chapter 11) with monoclonal antibodies has been covered in reasonable detail in the clinical update at the end of Chapter 11, and currently brentuximab vedotin has been reported to have demonstrated significant activities in phase II trials against both relapsed or refractory systemic anaplastic large-cell lymphoma, and also in Hodgkin's lymphoma. Seattle Genetics, the sponsor, is in the process of discussing future submission to the EMEA in 2011. In addition, a recent review article should be consulted for up to date information.[126]

26.3.1.2 Ecteinascidins

When the structure of ET743 was established by the groups of Rinehart and Wright in 1990 (Chapter 12), it became obvious that this compound had a base structure[127] that was well known from microbial sources on land, from invertebrates in the ocean, and from a marine bacterium. Thus, ET743 resembled the naphthyridinomycins and saframycins from terrestrial streptomycetes, renieramycins from oceanic sponges, jorumycin from the nudibranch, *Jorunna funebris*,[128] and safracin B from a marine-derived *Pseudomonas fluorescens*. The latter compound, as its cyano-derivative, is the basis for the semisynthesis of ET743 (see Chapter 12 for further information). The ecteinascidins all contain a fourth exocyclic isoquinoline group when compared with their putative siblings, together with a bridging cysteinyl-derived grouping.

At present, there is work ongoing on identifying the endosymbionts of *Ecteinascidia turbinata*, with the ultimate aim of identifying, cloning, and expressing the putative ET743 biosynthetic genes, if the potential producing organism, known currently as *Candidatus* Endoecteinascidia frumentensis, is not amenable to cultivation.[129] Further work demonstrating that similar microbes occur in different geographical areas associated with ET743-containing *E. turbinata* has been covered recently in two publications.[130,131]

Further examples of the potential involvement of microbes in the production of sponge-isolated secondary metabolites with antitumor potential (either directly or as a warhead on a delivery system) include, but are not limited to, the following.

26.3.1.3 Jaspamide/Jasplakinolide

Jaspamide (**27**) is the major metabolite[132] of the Pacific sponge, *Dorypleres splendens* (also identified as a *Jaspis* sp.), and was also reported as jasplakinolide when it was isolated from a Fijian-derived sample of *Jaspis johnstoni*.[133] In addition, modified jaspamides were also reported from the sponge *Jaspis splendens* collected in Vanuatu.[134] Jaspamide was initially reported to be a potent insecticide and antifungal agent,[132,133] but subsequent work by NCI scientists demonstrated that it induces actin polymerization *in vitro*, leading to disruption of the actin skeleton.[135,136]

Over the years since 2004, a number of other derivatives of jaspamide have been isolated and identified,[137–140] plus some more have recently been synthesized.[141,142] However, in spite of many attempts at NCI, no reproducible *in vivo* antitumor activity could be demonstrated because the therapeutic index was very close to unity.[143] In this respect, it is similar to the effects seen with other

actin inhibitors, such as the cucurbitacins, latrunculins, and cytochalasins. However, with a suitable delivery system, these molecules may well be of utility.

26.3.1.4 Geodiamolides and Chondramides

The possible involvement of microbes as a source of these compounds was raised by the reports of the structures of the closely related geodiamolides,[144] from a *Geodia* sp. in 1987 and from other taxonomically distant sponges in following years.[145] The potential for microbial involvement was reinforced by the reports from the Reichenbach group in 1995 of the isolation and purification of similar molecules, the chondramides (**28**), with an 18-membered macrolide ring from a terrestrial myxobacterium.[146] Analogous to the jaspamides, their first reported activities were as antifungal compounds, but subsequent investigation demonstrated their actin-stabilizing activity.[147]

In the last five or six years, a significant amount of work on the genetic analysis of the producing clusters has been reported, all from the group of Müller (originally at the GBF, but now at the University of the Saarland). In 2006, they reported on the presence of a very unusual tyrosine aminomutase that is responsible for the β-tyrosine formation, together with a previously unreported tryptophan-2-halogenase.[148] This was followed in 2009 by two important papers, one on the discovery of additional members of the tyrosine aminomutase family,[149] and the second, a review article on the use of genomics on exploitation of myxobacterial secondary metabolites.[150]

Marine-sourced myxobacteria were reported in the 1960s, and then the Reichenbach group reported on the apicularen group of structures that resembled the salicylihalimides (originally isolated from the marine sponge *Haliclona* sp.),[151] from a myxobacterium, implying that such a microbe could be involved in the production of such metabolites within the sponge. This early paper was followed in 2008 by a report by an Irish group working with *Haliclona simulans* from Atlantic waters, on the presence of keto synthase sequences that were closely associated with myxobacteria.[152] Then in 2010, the König group at Bonn reported on the potential of marine-derived myxobacteria as sources of novel antibiotics produced by polyketide genes. Thus, the possibility that the jaspamides and the geodiamolides have mxyobacterial production in their backgrounds is quite a reasonable assumption.

26.3.1.5 Pederins, Mycalamides, and Related Structures

An early entrant to the potential for microbial involvement was the recognition in the late 1980s that the highly cytotoxic sponge metabolites known as the mycalamides,[153] and subsequently other derivatives of the basic structure, the onnamides, theopederins, and the ring-opened form known as irciniastatin A (also reported later as psymberin),[154,155] all contained the basic ring structure of the toxin from the *Paederus* beetle, pederin (**29**). These molecules (which currently number over 30[155]) are very interesting from the perspective of potential antitumor drug leads, but development has been bedeviled by sourcing problems, even though a formal synthesis of mycalamide A (**30**) was published in 2004 by Trost et al.[156]

In 2002, work by Kellner[157] on the source of pederin from the *Paederus sabaeus* beetle from Turkey demonstrated that the actual source was a putative pseudomonad. This work was extended from a molecular genetics aspect by Piel et al.,[158] demonstrating a symbiosis island in the microbe that indicates the potential for horizontal gene transfer to other organisms and, most importantly, the presence in the microbe of a PKS–PS cluster that formally codes for the biosynthetic pathway for pederin.[159] The link to microbial involvement in production by the Mycale sponge was also implied in the in-sea aquaculture work reported by a New Zealand group where the coproduction of mycalamides and peloruside was determined under various conditions and geographic areas.[160]

In the last two years, Piel has published two excellent reviews on the biosynthetic mechanisms underpinning the production of the pederin-related and other potential microbial products that should be consulted by the interested reader.[124,125] If the clusters can be expressed in another host, then the sourcing problems of this class of molecules may well be on the way to being solved, allowing further investigation of their potential.

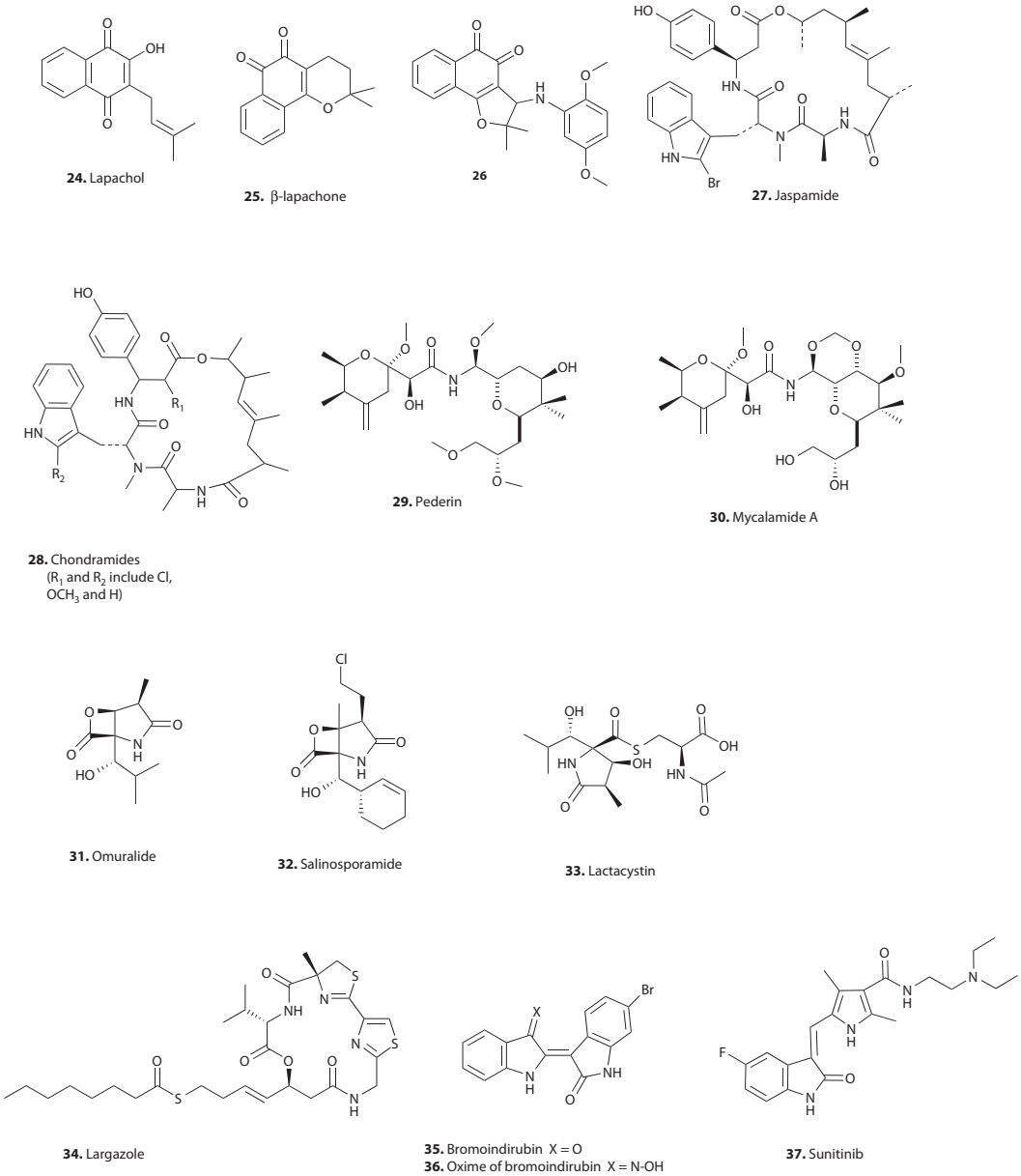

STRUCTURE 26.2 Structures **24** through **37**.

26.3.2 Independent Microbes

Although pioneering work was carried out in the middle of the last century in isolating and culturing marine microbes from a microbiological aspect, it was not until the 1980s that significant time and effort was devoted to the isolation, identification, and fermentation of marine microbes (or microbes from marine sources) in order to evaluate their potential to produce secondary metabolites with antitumor activity. This comment would also apply to free-living cyanophyta, even though, in most cases, a significant number of very active compounds have been obtained from both fermentation of isolated cyanophytes and from freely collected assemblages. The cryptophycins (Chapter 9) are

prime examples of the fermentative process, and later in this section, we will see a very interesting compound from an assemblage that may have potential as an antitumor compound in due course.

26.3.2.1 Salinosporamide

In retrospect, what probably had the most effect on the isolation techniques was the realization that the media used for work with terrestrial microbes was much too rich in carbon for their marine-based cousins. Once a series of suitable media and storage/recovery techniques was established, in large part because of the work of Fenical and Jensen and their colleagues at The Scripps Institute of Oceanography, the field opened up, with reports of active and chemically unique molecules being published at frequent intervals. What is of prime import is that as a result of their systematic searching for marine bacteria, the Fenical group described a totally new genus[161] within the order *Actinomycetales*, for which they proposed the genus name of *Salinospora*.[162]

This bacterium, on fermentation in suitable media in seawater, produced the omuralide (**31**) derivative salinosporamide A (**32**). Omuralide (**31**) is the spontaneous reaction product from the terrestrial Streptomycete metabolite, lactacystin (**33**), first reported in 1991 by Omura et al.[163] and synthesized, together with analogs, by Corey's group.[164] Subsequently, omuralide was found to be a specific inhibitor of the 20*S* proteosome, modifying a subunit-specific threonine.[165] That such an inhibitor had drug potential was demonstrated by the approved antitumor agent, Velcade®, a synthetic peptide boronate, so the search for other molecules with similar activities was worthwhile.

Salinosporamide itself, which differs from lactacystin/omuralide in terms of its substitution pattern around the pyrrolid-2-one ring, is also a potent proteosome inhibitor. The many discoveries from this particular genus, now named systematically as *Salinispora* with currently at least three species, have been discussed at length by Fenical and his coworkers and collaborators at the Scripps Institute of Oceanography and Nereus Pharmaceuticals in a recent series of excellent primary and review papers.[166–170]

The complete annotated genetic sequence of the microbe has been reported, and, to date, over 17 putative biosynthetic clusters have been identified and, in a number of cases, the products have been isolated and identified.[167] Currently the compound is under clinical development by Nereus Pharmaceuticals in San Diego, California, and a search of the clinical trials database (November 2010) indicated four active phase I trials in leukemias or solid tumors, and one in conjunction with the histone deacetylase (HDAC) inhibitor vorinostat directed against a variety of cancers, including pancreatic and non-small-cell lung cancers.

To date, only abstract-based reports of activity in these phase I patients has been reported, together with data suggesting that the drug candidate is well tolerated and achieves proteasome inhibition in a dose-dependent manner in multiple myeloma patients.[171]

26.3.2.2 Largazole

In the first edition, we demonstrated how Novartis had been able to use the structural data from a series of HDAC inhibitors of natural origin to derive the compound known as NVP-LAQ824 from comparison of the structures of psammaplin, trapoxin, and trichostatin A. This compound entered phase I clinical trials but was discontinued in 2005.

In 2008, Taori et al. reported the structure of the very interesting HDAC inhibitor isolated from a wild collection of a Floridian species of the cyanophyte, *Symploca*, that they named largazole (**34**).[172] Later the same year, they followed up with a total synthesis that permitted sufficient material to be obtained for further work and reported on its molecular target.[173] Over the last two years, this molecule has evinced significant interest in the synthetic chemistry community, with a number of different routes to both the base molecule and to modified structures being reported in the primary and review literature.[174–179]

Finally, demonstrating that nature also produces not just combinatorial products, but also synergistic mixtures, recently the Luesch group reported that the largazole-producing cyanophyte also

produced a dolastatin 10/15 hybrid that they named simplostatin 4 (an antimitotic agent), that when combined with largazole, demonstrated higher efficacy in inhibiting cancer cell growth than either agent alone.[180]

26.4 PLANT–MICROBE–MARINE INTERFACE

Finally, there is one class of compounds that, though covered in the first edition, have now been shown to have a wider range of activities that cover a more pharmacologically diverse area than originally thought. These compounds have a very long provenance as chemical entities, in some cases as mixtures and in others as single compounds, and whose listed activities range from dyestuffs, through a traditional Chinese medical treatment for leukemia, to very specific inhibition of an essential cellular enzyme cascade.

26.4.1 Indigo and the Indirubins

The compounds in question are all based on the simple heterocycle, indole. The essential aminoacid tryptophan is formed from the chorismate pathway, *via* cyclization of anthranilate, and indole is formed from tryptophan catabolism. If indole is hydroxylated in the 3 position, presumably by a suitable cytochrome P450, then it is tautomeric with the 3 keto analog, indoxyl. Various levels of oxidation then lead to the mixture of indigo, indirubin, and their isomers that are commonly used as the source of indigo dyestuffs for either clothing or as war paint (the ancient Celtic "woad" being a mixture from the plant *Isatis tinctora*[181]).

Although usually thought of as being plant products, indigo and the indirubins have been reported from four nominally independent sources: a variety of plants,[181] a number of marine mollusks (usually belonging to the *Muricidae* family of gastropods),[182] natural or recombinant bacteria,[183] and human urine.[184] It is highly probable, however, that in all cases, the indirubins and indigo are the terminal oxidation products of tryptophan/indole catabolism—perhaps even a method of removing excess indole from the organism.

However, irrespective of the reason for their production, the indirubins have been identified as the major active ingredient of the traditional Chinese medical recipe known as Danggui Longhui Wan, used to treat chronic myelogenous leukemia[185,186] in China for many years. What is of import from both a natural product and a pharmacological perspective was the recognition by Meijer's group that the indirubins as a class were both inhibitors of several CDKs and also potent inhibitors of glycogen synthase kinase-3 (GSK-3).

Thus, in 2003, Meijer et al.[187] described the early work on this enzyme and then demonstrated that simple indirubins, including a brominated version (**35**) that had never been isolated from natural sources before their work with the mollusk *Hexaplex trunculus*, and its chemically modified oxime derivative (**36**), were potent and selective inhibitors of both the α and β variants of GSK-3, with IC_{50} values of 22 and 5 nM, respectively. There was at least a fivefold specificity versus CDK1/cyclin B or CDK/p25, and significantly more specificity against a wide range of other kinases. A slightly later paper from the same group gave full details of the chemistry involved, and established structure–activity relationships using x-ray crystallography and molecular-modeling techniques.[188]

By using immobilized indirubins, Meijer's group was able to conclusively identify GSK-3 as the target of these molecules in cell lysates, to demonstrate that they had a significant effect *in vivo* on *Xenopus* development, consonant with the suggested mechanism, and to derive x-ray crystallographic evidence for the binding of the agents at the active site (adenosine triphosphate-binding site) of GSK-3. They also demonstrated that the activation of the enzyme *via* phosphorylation by an as-yet-unidentified kinase on two specific tyrosine residues (GSK-3 is a Ser/Thr kinase) is blocked when indirubins are bound, perhaps because of a conformational shift in the bound versus free protein.

These papers were then followed by another from the same group in which they demonstrated that the indirubins actually had yet another, independent action at the cell receptor level. By using the same basic suite of compounds, they demonstrated that they serve as ligands for the "orphan receptor" known as the aryl hydrocarbon receptor (AhR). To date, no natural ligands have been identified for AhR, even though, contrary to earlier beliefs, it has existed for over 450 million years (although there have been proposals that indole-containing compounds are among the natural ligands[189]). From a series of elegant biochemical and biological studies, including the use of cells that were null–null mutants for the AhR, the researchers were able to differentiate between the cytostatic effects of some indirubins following their activation of the AhR from kinase inhibition, which appears to be a main mechanism underlying the cytotoxicity of the molecules.[190]

Since these reports, the chemical modifications of the basic indirubin skeleton have continued. In 2006, the Meijer group reported that 3′-substituted 7-halogeno derivatives induced cell death by means of an unknown mechanism,[191] and later in 2006, demonstrated that one of these compounds, 7-bromoindirubin-3′-oxime, induced caspase-independent cell death.[192]

Recently, Kritsanida et al. demonstrated that replacing the 7-halogeno substituent in indirubin-3′-oximes with a ring-nitrogen, thus giving the 7-aza disostere of the indirubin pharmacophore, led to a lower activity as a kinase inhibitor, but till maintained significant antiproliferative activity at submicromolar levels.[193] A slightly later paper from a Chinese group reported on compounds with the same base ring structure, but lacking the oxime group. These compounds had hydrocarbon substituents on the pyrrolic nitrogen of the aza-indole ring system, being based on the structure of methylisoindigotin.[194] Although these molecules had kinase inhibitory and some antiproliferative activities in DU145 cells, including the diminution of phospho-CDK2 and reduction in cyclin D1 expression, there was an upregulation of the endogenous p27 CDK inhibitor at the same time. Such an effect had been previously linked to activation of the AhR receptor pathway.[190]

Although there are no reports as yet of formal clinical trials, the indirubins have been used in traditional Chinese medicine for centuries as mentioned earlier in this section,[185,186] and inspection of the Thomson-Reuters Integrity® database in late 2010 indicates "clinical status" in the People's Republic of China. Recently, Vine et al. reviewed the literature on the cytotoxic and anticancer activities of isatin and its derivatives, covering data from 2000 to 2008. This review should be read in conjunction with other citations in this section to better appreciate the influence of "indoles and their derivatives" upon drug discovery.[195] It might also be of interest to the reader that the kinase inhibitor, sunitinib (**37**), is based upon a substituted oxindole linked to a pyrrole.

26.5 CONCLUSION

Although one generally thinks of the organism from which a compound is isolated and purified as being the source of the natural product, it is becoming more and more difficult to actually state that this is so. From the information presented in the case of plants and marine invertebrates, it can be seen that in many instances, microbes (perhaps from all three domains) are intimately involved at some stage in the production of those secondary metabolites that are being evaluated for their potential as drug leads or entities.

We deliberately have not given any details of the work now ongoing in studies of the metagenomes[196] of either soils or marine sediments, because, as yet, no compounds have been reported in the open literature that are acting as leads to new antitumor agents. However, the number of novel agents that are now being reported from consortia, not only of microbes but also from interactions across kingdoms and from activation of the so-called "cryptic clusters" in microbes from all three domains of life,[197–199] is indicative that such agents will be forthcoming in due course.

Thus, the future will probably involve much greater attention to the interplay between single-celled organisms and their multicellular compatriots. It is highly probable that the small molecules

known in the microbial world as quorum sensors or in the plant world as elicitors could aid materially in the expression of secondary metabolites.[200]

When information from such studies is linked to the massive explosion of microbial and other organism DNA sequence data, then the potential for the discovery and expression of novel pharmacologically active secondary metabolites is vast.

REFERENCES

1. Cragg, G. M., Grothaus, P. G., and Newman, D. J., Impact of natural products on developing new anticancer agents, *Chem. Rev.*, 109, 3012, 2009.
2. Kupchan, S. M., Anderson, W. K., Bollinger, P., Doskotch, R. W., Smith, R. M., Saenz-Renauld, J. A., Schnoes, H. K., Burlingame, S. L., and Smith, D. H., Tumor inhibitors. XXXIX. Active principles of *Acnistus arborescens*. Isolation and structural and spectral studies of withaferin A and withacnistin, *J. Org. Chem.* 34, 3858, 1969.
3. Sun, J., Blaskovich, M. A., Jove, R., Livingston, S. K., Coppola, D., and Sebti, S. M., Cucurbitacin Q: A selective STAT3 activation inhibitor with potent antitumor activity, *Oncogene* 24, 3236, 2005.
4. Sun, J., Blaskovich, M. A., Jove, R., Livingston, S. K., Coppola, D., and Sebti, S. M., Cucurbitacin Q: A selective STAT3 activation inhibitor with potent antitumor activity (Corrigendum), *Oncogene* 27, 1344, 2008.
5. Hwang, B. Y., Su, B.-N., Chai, H., Mi, Q., Kardono, L. B. S., Afriastini, J. J., Riswan, S. et al., Silvestrol and episilvestrol, potential anticancer rocaglate derivatives from *Aglaia silvestris*, *J. Org. Chem.* 69, 3350, 2004.
6. Hwang, B. Y., Su, B.-N., Chai, H., Mi, Q., Kardono, L. B. S., Afriastini, J. J., Riswan, S. et al., Silvestrol and episilvestrol, potential anticancer rocaglate derivatives from *Aglaia silvestris* (Erratum), *J. Org. Chem.* 69, 6156, 2004.
7. Cencic, R., Carrier, M., Galicia-Vázquez, G., Bordeleau, M.-E., Sukarieh, R., Bourdeau, A., Brem, B. et al., Antitumor activity and mechanism of action of the cyclopenta[b]benzofuran, Silvestrol, *PLoS ONE* 4, e5223, 2009.
8. Lindqvist, L. and Pelletier, J., Inhibitors of translation initiation as cancer therapeutics, *Fut. Med. Chem.* 1, 1709, 2009.
9. Lucas, D. M., Edwards, R. B., Lozanski, G., West, D. A., Shin, J. D., Vargo, M. A., Davis, M. E. et al., The novel plant-derived agent silvestrol has B-cell selective activity in chronic lymphocytic leukemia and acute lymphoblastic leukemia *in vitro* and *in vivo*, *Blood* 113, 4656, 2009.
10. Lucas, D. M., Still, P. C., Bueno Pérez, L., Grever, M. R., and Kinghorn, A. D., Potential of plant-derived natural products in the treatment of leukemia and lymphoma, *Curr. Drug Targets* 11, 812, 2010.
11. El Sous, M., Khoo, M. L., Holloway, G., Owen, D., Scammells, P. J., and Rizzacasa, M. A., Total synthesis of (-)-episilvestrol and (-)-silvestrol, *Angew. Chem. Int. Ed.* 46, 7835, 2007.
12. Gerard, B., Cencic, R., Pelletier, J., and Porco Jr., J. A., Enantioselective synthesis of the complex rocaglate (-)-silvestrol, *Angew. Chem. Int. Ed.* 46, 7831, 2007.
13. Ratnayake, R., Covell, D., Ransom, T. T., Gustafson, K. R., and Beutler, J. A., Englerin A, a selective inhibitor of renal cancer cell growth, from *Phyllanthus engleri*, *Org. Lett.* 11, 57, 2009.
14. Beutler, J. A., Jato, J. G., Cragg, G. M., Wiemer, D. F., Neighbors, J. D., Salnikova, M., Hollingshead, M., Scudiero, D. A., and McCloud, T. G., The Schweinfurthins. Issues in development of a plant-derived anticancer lead, in *Medicinal and Aromatic Plants*, Bogers, J., Craker, L. E., and Langa, D., Eds., Springer, Amsterdam, 2006, 301 pp.
15. Klausmeyer, P., Van, Q. N., Jato, J. G., McCloud, T. G., and Beutler, J. A., Schweinfurthins I and J from *Macaranga schweinfurthii*, *J. Nat. Prod.* 73, 479, 2010.
16. Neighbors, J. D., Beutler, J. A., and Wiemer, D. F., Synthesis of nonracemic 3-deoxyschweinfurthin, *J. Org. Chem.* 70, 925, 2005.
17. Neighbors, J. D., Salnikova, M. S., Beutler, J. A., and Wiemer, D. F., Synthesis and structure-activity studies of schweinfurthin B analogs: Evidence for the importance of a D-ring hydrogen bond donor in expression of differential cytotoxicity, *Bioorg. Med. Chem.* 14, 1771, 2006.
18. Mente, N. R., Wiemer, A. J., Neighbors, J. D., Beutler, J. A., Hohl, R. J., and Wiemer, D. F., Total synthesis of (*R*,*R*,*R*)- and (*S*,*S*,*S*)-schweinfurthin F: Differences of bioactivity in the enantiomeric series, *Bioorg. Med. Chem. Lett.* 17, 911, 2007.
19. Topczewski, J. J., Neighbors, J. D., and Wiemer, D. F., Total synthesis of (+)-schweinfurthins B and E, *J. Org. Chem.* 74, 6965, 2009.

20. Mente, N. R., Neighbors, J. D., and Wiemer, D. F., BF3 x Et_2O-mediated cascade cyclizations: Synthesis of schweinfurthins F and G, *J. Org. Chem.* 73, 7963, 2008.
21. Sielecki, T., Boylan, J. F., Benfield, P. A., and Trainor, G. L., Cyclin-dependent kinase inhibitors: Useful targets in cell cycle regulation, *J. Med. Chem.* 43, 1, 2000.
22. Losiewicz, M. D., Carlson, B. A., Kaur, G., Sausville, E. A., and Worland, P. J., Potent inhibition of CDC2 kinase activity by the flavanoid, L86-8275, *Biochem. Biophys. Res. Comm.* 201, 589, 1994.
23. Czech, J., Hoffman, D., Naik, R., and Sedlacek, H., Anti-tumoral activity of flavone L 86-8275, *Int. J. Oncol.* 6, 31, 1995.
24. Takada, Y., Sethi, G., Sung, B., and Aggarwal, B. B., Flavopiridol suppresses tumor necrosis factor-induced activation of activator protein-1, c-Jun N-terminal kinase, p38 mitogen-activated protein kinase (MAPK), p44/p42 MAPK, and Akt, inhibits expression of antiapoptotic gene products, and enhances apoptosis through cytochrome *c* release and caspase activation in human myeloid cells, *Mol. Pharmacol.* 73, 1549, 2008.
25. Yang, X., Zhao, X., Phelps, M. A., Piao, L., Rozewski, D. M., Liu, Q., Lee, L. J. et al., A novel liposomal formulation of flavopiridol, *Int. J. Pharm.* 365, 170, 2009.
26. Dai, Y. and Grant, S., Cyclin-dependent kinase inhibitors, *Curr. Opin. Pharmacol.* 3, 362, 2003.
27. Dancey, J. and Sausville, E. A., Issues and progress with protein kinase inhibitors for cancer treatment, *Nat. Rev. Drug Discov.* 2, 296, 2003.
28. Senderowicz, A. M., Small-molecule cyclin-dependent kinase modulators, *Oncogene* 22, 6609, 2003.
29. Romano, G., An overview on the cyclin-dependent kinase 9-related pathway, *Drugs Fut.* 35 (1), 59, 2010.
30. Karp, J. E., Passaniti, A., Gojo, I., Kaufmann, S., Bible, K., Garimella, T. S., Greer, J. et al., Phase I and pharmacokinetic study of flavopiridol followed by 1-beta-D-arabino-furanosylcytosine and mitoxantrone in relapsed and refractory adult acute leukemias, *Clin. Cancer Res.* 11, 8403, 2005.
31. Lin, T. S., Ruppert, A. S., Johnson, A. J., Fischer, B., Heerema, N. A., Andritsos, L. A., Blum, K. A. et al., Phase II study of flavopiridol in relapsed chronic lymphocytic leukemia demonstrating high response rates in genetically high-risk disease, *J. Clin. Oncol.* 27, 6012, 2009.
32. Phelps, M. A., Lin, T. S., Johnson, A. J., Hurh, E., Rozewski, D. M., Farley, K. L., Wu, D. et al., Clinical response and pharmacokinetics from a phase 1 study of an active dosing schedule of flavopiridol in relapsed chronic lymphocytic leukemia, *Blood* 113, 2637, 2009.
33. Christian, B. A., Grever, M. R., Byrd, J. C., and Lin, T. S., Flavopiridol in chronic lymphocytic leukemia: A concise review, *Clin. Lymphoma Myeloma* 9(Suppl. 3), S179, 2009.
34. Maddocks, K. J. and Lin, T. S., Update in the management of chronic lymphocytic leukemia, *J. Hematol. Oncol.* 2, 29, 2009.
35. Hallek, M., State-of-the-art treatment of chronic lymphocytic leukemia, *Hematology, Am. Soc. Hematol. Educ. Prog.* 440, 2009.
36. Karp, J. E., Blackford, A., Smith, B. D., Alino, K., Seung, A. H., Bolaños-Meade, J., Greer, J. M. et al., Clinical activity of sequential flavopiridol, cytosine arabinoside, and mitoxantrone for adults with newly diagnosed, poor-risk acute myelogenous leukemia, *Leuk. Res.* 34, 877, 2010.
37. Fathi, A. T. and Karp, J. E., New agents in acute myeloid leukemia: Beyond cytarabine and anthracyclines, *Curr. Oncol. Rep.* 11, 346, 2009.
38. Dispenzieri, A., Gertz, M. A., Lacy, M. Q., Geyer, S. M., Fitch, T. R., Fenton, R. G., Fonseca, R. et al., Flavopiridol in patients with relapsed or refractory multiple myeloma: A phase 2 trial with clinical and pharmacodynamic end-points, *Haematologica* 91, 390, 2006.
39. Carvajal, R. D., Tse, A., Shah, M. A., Lefkowitz, R. A., Gonen, M., Gilman-Rosen, L., Kortmansky, J., Kelsen, D. P., Schwartz, G. K., and O'Reilly, E. M., A phase II study of flavopiridol (Alvocidib) in combination with docetaxel in refractory, metastatic pancreatic cancer, *Pancreatology* 9, 404, 2009.
40. Morris, D. G., Bramwell, V. H., Turcotte, R., Figueredo, A. T., Blackstein, M. E., Verma, S., Matthews, S., and Eisenhauer, E. A., A phase II study of flavopiridol in patients with previously untreated advanced soft tissue sarcoma, *Sarcoma* 2006, Article ID 64374, 2006.
41. Grendys Jr., E. C., Blessing, J. A., Burger, R., and Hoffman, J., A phase II evaluation of flavopiridol as second-line chemotherapy of endometrial carcinoma: A Gynecologic Oncology Group study, *Gynecol. Oncol.* 98, 249, 2005.
42. Burdette-Radoux, S., Tozer, R. G., Lohmann, R. C., Quirt, I., Ernst, D. S., Walsh, W., Wainman, N., Colevas, A. D., and Eisenhauer, E. A., Phase II trial of flavopiridol, a cyclin dependent kinase inhibitor, in untreated metastatic malignant melanoma, *Invest. New Drugs* 22, 315, 2004.
43. Van Veldhuizen, P. J., Faulkner, J. R., Lara Jr., P. N., Gumerlock, P. H., Goodwin, J. W., Dakhil, S. R., Gross, H. M., Flanigan, R. C., and Crawford, E. D., A phase II study of flavopiridol in patients with

advanced renal cell carcinoma: Results of Southwest Oncology Group Trial 0109, *Cancer Chemother. Pharmacol.* 56, 39, 2005.
44. Liu, G., Gandara, D. R., Lara Jr., P. N., Raghavan, D., Doroshow, J. H., Twardowski, P., Kantoff, P., Oh, W., Kim, K., and Wilding, G., A Phase II trial of flavopiridol (NSC #649890) in patients with previously untreated metastatic androgen-independent prostate cancer, *Clin. Cancer Res.* 10, 924, 2004.
45. Rathkopf, D., Dickson, M. A., Feldman, D. R., Carvajal, R. D., Shah, M. A., Wu, N., Lefkowitz, R. et al., Phase I study of flavopiridol with oxaliplatin and fluorouracil/leucovorin in advanced solid tumors, *Clin. Cancer Res.* 15, 7405, 2009.
46. Lin, T. S., Blum, K. A., Fischer, D. B., Mitchell, S. M., Ruppert, A. S., Porcu, P., Kraut, E. H. et al., Flavopiridol, fludarabine, and rituximab in mantle cell lymphoma and indolent B-cell lymphoproliferative disorders, *J. Clin. Oncol.* 28, 418, 2010.
47. Kasimis, G. S., Cogswell, J., Schwarzenberger, P., Shapiro, G. I., Fidias, P., and Bukowski, R. M., Phase I study of flavopiridol in combination with paclitaxel and carboplatin in patients with non-small-cell lung cancer, *Clin. Lung Cancer* 9, 160, 2008.
48. Fornier, M. N., Rathkopf, D., Shah, M., Patil, S., O'Reilly, E., Tse, A. N., Hudis, C., Lefkowitz, R., Kelsen, D. P., and Schwartz, G. K., Phase I dose-finding study of weekly docetaxel followed by flavopiridol for patients with advanced solid tumors, *Clin. Cancer Res.* 13, 5841, 2007.
49. Tan, A. R., Yang, X., Berman, A., Zhai, S., Sparreboom, A., Parr, A. L., Chow, C., Brahim, J. S., Steinberg, S. M., Figg, W. D., and Swain, S. M., Phase I trial of the cyclin-dependent kinase inhibitor flavopiridol in combination with docetaxel in patients with metastatic breast cancer, *Clin. Cancer Res.* 10, 5038, 2004.
50. Shah, M. A., Kortmansky, J., Motwani, M., Drobnjak, M., Gonen, M., Yi, S., Weyerbacher, A. et al., A phase I clinical trial of the sequential combination of irinotecan followed by flavopiridol, *Clin. Cancer Res.* 11, 3836, 2005.
51. Ambrosini, G., Seelman, S. L., Qin, L. X., and Schwartz, G. K., The cyclin-dependent kinase inhibitor flavopiridol potentiates the effects of topoisomerase I poisons by suppressing Rad51 expression in a p53-dependent manner, *Cancer Res.* 68, 2312, 2008.
52. Whitlock, J. A., Krailo, M., Reid, J. M., Ruben, S. L., Ames, M. M., Owen, W., and Reaman, G., Phase I clinical and pharmacokinetic study of flavopiridol in children with refractory solid tumors: A Children's Oncology Group Study, *J. Clin. Oncol.* 23, 9179, 2005.
53. Meijer, L. and Raymond, E., Roscovitine and other purines as kinase inhibitors. From starfish oocytes to clinical trials, *Acc. Chem. Res.* 36, 417, 2003.
54. Parker, C. W., Entsch, B., and Letham, D., Inhibitors of two enzymes which metabolize cytokinins, *Phytochemistry* 25, 303, 1986.
55. Chang, Y. T., Gray, N. G., Rosania, G. R., Sutherlin, D. P., Kwon, S., Norman, T. C., Sarohia, R., Leost, M., Meijer, L., and Schultz, P. G., Synthesis and application of functionally diverse 2,6,9-trisubstituted purine libraries as CDK inhibitors, *Chem. Biol.* 6, 361, 1999.
56. Aldoss, I. T., Tashi, T., and Ganti, A. K., Seliciclib in malignancies, *Expert Opin. Investig. Drugs* 18, 1957, 2009.
57. Dey, A., Wong, E. T., Cheok, C. F., Tergaonkar, V., and Lane, D. P., *R*-Roscovitine simultaneously targets both the p53 and NF-kappaB pathways and causes potentiation of apoptosis: Implications in cancer therapy, *Cell Death Differ.* 15, 263, 2008.
58. Festa, M., Petrella, A., Alfano, S., and Parente, L., *R*-Roscovitine sensitizes anaplastic thyroid carcinoma cells to TRAIL-induced apoptosis via regulation of IKK/NF-kappaB pathway, *Int. J. Cancer* 124, 2728, 2009.
59. MacFarlane, M., TRAIL-induced signalling and apoptosis, *Toxicol. Lett.* 139, 89, 2003.
60. Bettayeb, K., Sallam, H., Ferandin, Y., Popowycz, F., Fournet, G., Hassan, M., Echalier, A. et al., N-&-N, a new class of cell death-inducing kinase inhibitors derived from the purine roscovitine, *Mol. Cancer Ther.* 7 (9), 2713, 2008.
61. Popowycz, F., Fournet, G., Schneider, C., Bettayeb, K., Ferandin, Y., Lamigeon, C., Tirado, O. M. et al., Pyrazolo[1,5-a]-1,3,5-triazine as a purine bioisostere: Access to potent cyclin-dependent kinase inhibitor (R)-roscovitine analogue, *J. Med. Chem.* 52, 655, 2009.
62. Bettayeb, K., Oumata, N., Echalier, A., Ferandin, Y., Endicott, J. A., Galons, H., and Meijer, L., CR8, a potent and selective, roscovitine-derived inhibitor of cyclin-dependent kinases, *Oncogene* 27, 5797, 2008.
63. Malumbres, M. and Barbacid, M., Cell cycle, CDKs and cancer: A changing paradigm, *Nat. Rev. Cancer* 9, 153, 2009.
64. Evans, B. E., Rittle, K. E., Bock, M. G., DiPardo, R. M., Freidinger, R. M., Whitter, W. L., Lundell, G. et al., Methods for drug discovery: Development of potent, selective, orally effective cholecystokinin antagonists, *J. Med. Chem.* 31, 2235, 1988.

65. Mason, J. S., Morize, I., Menard, P. R., Cheney, D. L., Hulme, C., and Labaudiniere, R. F., New 4-point pharmacophore method for molecular similarity and diversity applications: Overview of the method and applications, including a novel approach to the design of combinatorial libraries containing privileged sub-structures, *J. Med. Chem.* 42, 3251, 1999.
66. Patchett, A. A. and Nargund, R. P., Privileged structures—An update, in *Annual Reports in Medicinal Chemistry*, Doherty, A. M., Ed., Academic Press, San Diego, CA, 2000, 289 pp.
67. DeSimone, R. W., Currie, K. S., Mitchell, S. A., Darrow, J. W., and Pippin, D. A., Privileged structures: Applications in drug discovery, *Combi. Chem. HTS* 7, 473, 2004.
68. Costantino, L. and Barloccob, D., Privileged structures as leads in medicinal chemistry, *Curr. Med. Chem.* 13, 65, 2006.
69. Nicolaou, K. C., Pfefferkorn, J. A., Roecker, A. J., Cao, G.-Q., Barluenga, S., and Mitchell, H. J., Natural product-like combinatorial libraries based on privileged structures. 1. General principles and solid-phase synthesis of benzopyrans, *J. Am. Chem. Soc.* 122, 9939, 2000.
70. Nicolaou, K. C., Pfefferkorn, J. A., Mitchell, H. J., Roecker, A. J., Barluenga, S., Cao, G.-Q., Affleck, R. L., and Lillig, J. E., Natural product-like combinatorial libraries based on privileged structures. 2. Construction of a 10,000-membered benzopyran library by directed split-and-pool chemistry using NanoKans and optical encoding, *J. Am. Chem. Soc.* 122, 9954, 2000.
71. Nicolaou, K. C., Pfefferkorn, J. A., Barluenga, S., Mitchell, H. J., Roecker, A. J., and Cao, G.-Q., Natural product-like combinatorial libraries based on privileged structures. 3. The 'Libraries from Libraries' principle for diversity enhancement of benzopyran libraries, *J. Am. Chem. Soc.* 122, 9968, 2000.
72. Nicolaou, K. C., Pfefferkorn, J. A., Schuler, F., Roecker, A. J., Cao, G.-Q., and Casida, J. E., Combinatorial synthesis of novel and potent inhibitors of NADH:ubiquinone oxidoreductase, *Chem. Biol.* 7, 979, 2000.
73. Nicolaou, K. C., Roecker, A. J., Barluenga, S., Pfefferkorn, J. A., and Cao, G.-Q., Discovery of novel antibacterial agents active against methicillin-resistant *Staphylococcus aureus* from combinatorial benzopyran libraries, *ChemBioChem.* 2, 460, 2001.
74. Nicolaou, K. C., Evans, R. M., Roecker, A. J., Hughes, R., Downes, M., and Pfefferkorn, J. A., Discovery and optimization of non-steroidal FXR agonists from natural product-like libraries, *Org. Biomol. Chem.* 1, 908, 2003.
75. Downes, M., Verdecia, M. A., Roecker, A. J., Hughes, R., Hogenesch, J. B., Kast-Woelbern, H. R., Bowman, M. E., et al., A chemical, genetic, and structural analysis of the nucelar bile acid receptor FXR, *Mol. Cell* 11, 1079, 2003.
76. An, H., Eum, S. J., Koh, M., Lee, S. K., and Park, S. B., Diversity-oriented synthesis of privileged benzopyranyl heterocycles from s-cis-enones, *J. Org. Chem.* 73, 1752, 2008.
77. Park, S. O., Kim, J., Koh, M., and Park, S. B., Efficient parallel synthesis of privileged benzopyranylpyrazoles via regioselective condensation of beta-keto aldehydes with hydrazines, *J. Comb. Chem.* 11, 315, 2009.
78. Srinivasan, B., Johnson, T. E., Lad, R., and Xing, C., Structure-activity relationship studies of chalcone leading to 3-hydroxy-4,3′,4′,5′-tetramethoxychalcone and its analogues as potent nuclear factor kappaB inhibitors and their anticancer activities, *J. Med. Chem.* 52, 7228, 2009.
79. Nguyen, H. T., Lallemand, M. C., Boutefnouchet, S., Michel, S., and Tillequin, F., Antitumor Psoropermum xanthones and Sarcomelicope acridones: Privileged structures implied in DNA alkylation, *J. Nat. Prod.* 72, 527, 2009.
80. Strobel, G., Daisy, B., Castillo, U., and Harper, J., Natural products from endophytic microorganisms, *J. Nat. Prod.* 67, 257, 2004.
81. Kathiravan, G. and Raman, V. S., *In vitro* Taxol production, by *Pestalotiopsis brevista*—A first report, *Fitoterapia* 81, 557, 2010.
82. Miller, K., Neilan, B., and Sze, D. M., Development of Taxol and other endophyte produced anti-cancer agents, *Recent Pat. Anti-Cancer Drug Discov.* 3, 14, 2008.
83. Staniek, A., Woerdenbag, H. J., and Kayser, O., *Taxomyces andreanae*: A presumed Paclitaxel producer demystified?, *Planta Med.* 75, 1561, 2009.
84. Zhou, X., Zhu, H., Liu, L., Lin, J., and Tang, K., A review: Recent advances and future prospects of taxol-producing endophytic fungi, *Appl. Microbiol. Biotechnol.* 86, 1707, 2010.
85. Kumaran, R. S. and Hur, B.-K., Screening of species of the endophytic fungus *Phomopsis* for the production of the anticancer drug taxol, *Biotechnol. Appl. Biochem.* 54, 21, 2009.
86. Puri, S. G., Verma, V., Amna, T., Qazi, G. N., and Spiteller, M., An endophytic fungus from *Nothapodytes foetida* that produces camptothecin, *J. Nat. Prod.* 68, 1717, 2005.

87. Amna, T., Puri, S. C., Verma, V., Sharma, J. P., Khajuria, R. K., Musarrat, J., Spiteller, M., and Qazi, G. N., Bioreactor studies on the endophytic fungus *Entrophospora infrequens* for the production of an anticancer alkaloid camptothecin, *Can. J. Microbiol.* 52, 189, 2006.
88. Eyberger, A. L., Dondapati, R., and Porter, J. R., Endophyte fungal isolates from *Podophyllum peltatum* produce podophyllotoxin, *J. Nat. Prod.* 69, 1121, 2006.
89. Puri, S. C., Nazir, A., Chawla, R., Arora, R., Riyaz-Ul-Hasan, S., Amna, T., Ahmed, B. et al., The endophytic fungus *Trametes hirsuta* as a novel alternative source of podophyllotoxin and related aryl tetralin lignans, *J. Biotech.* 122, 494, 2006.
90. Guo, B., Li, H., and Zhang, L., Yunnan Daxue Xuebao, Ziran Kexueban, *J. Yunnan Univ.*, 20, 214, 1998.
91. Zhang, L., Guo, B., Li, H., Zeng, S., Shao, H., Gu, S., and Wei, R., Zhong Cao Yao, *Chin. Trad. Herbal Drugs* 31, 805, 2000.
92. Yang, X., Zhang, L., Guo, B., and Guo, S., Zhong Cao Yao, *Chin. Trad. Herbal Drugs* 35, 79, 2004.
93. Cuendet, M. and Pezzuto, J. M., Antitumor activity of Bruceantin. An old drug with new promise, *J. Nat. Prod.* 67, 269, 2004.
94. Cuendet, M., Christov, K., Lantvit, D. D., Deng, Y., Hedayat, S., Helson, L., McChesney, J. D., and Pezzuto, J. M., Multiple myeloma regression mediated by bruceantin, *Clin. Cancer Res.* 10, 1170, 2004.
95. Robert, F., Carrier, M., Rawe, S., Chen, S., Lowe, S., and Pelletier, J., Altering chemosensitivity by modulating translation elongation, *PLoS ONE* 4, e5428, 2009.
96. Cichewitz, R. H. and Kouzi, S. A., Chemistry, biological activity, and chemotherapeutic potential of betulinic acid for the prevention and treatment of cancer and HIV infection, *Med. Res. Rev.* 24, 90, 2004.
97. Salti, G. I., Kichina, J. V., Das Gupta, T. K., Uddin, S., Bratescu, L., and Pezzuto, J., Betulinic acid reduces ultraviolet-C-induced DNA breakage in congenital melanocytic naeval cells: Evidence for a potential role as a chemopreventive agent, *Melanoma Res.* 11, 99, 2001.
98. Mullauer, F. B., Kessler, J. H., and Medema, J. P., Betulinic acid, a natural compound with potent anticancer effects, *Anticancer Drugs* 21, 215, 2010.
99. Melichar, B., Konopleva, M., Hu, W., Melicherova, K., Andreef, M., and Freedman, R. S., Growth-inhibitory effect of a novel synthetic triterpenoid, 2-cyano-3,12-dioxoalean-1,9-dien-28-oic acid, on ovarian carcinoma cell lines not dependent on peroxisome proliferator-activated receptor-expression, *Gynecol. Oncol.* 93, 149, 2004.
100. Alabran, J. L., Cheuk, A., Liby, K., Sporn, M., Khan, J., Letterio, J., and Leskov, K. S., Human neuroblastoma cells rapidly enter cell cycle arrest and apoptosis following exposure to C-28 derivatives of the synthetic triterpenoid CDDO, *Cancer Biol. Ther.* 7, 709, 2008.
101. Vannini, N., Lorusso, G., Cammarota, R., Barberis, M., Noonan, D. M., Sporn, M. B., and Albini, A., The synthetic oleanane triterpenoid, CDDO-methyl ester, is a potent antiangiogenic agent, *Mol. Cancer Ther.* 12, 3139, 2007.
102. Duan, Z., Ames, R. Y., Ryan, M., Hornicek, F. J., Mankin, H., and Seiden, M. V., CDDO-Me, a synthetic triterpenoid, inhibits expression of IL-6 and Stat3 phosphorylation in multi-drug resistant ovarian cancer cells, *Cancer Chemother. Pharmacol.* 63, 681, 2009.
103. Ahmad, R., Liu, S., Weisberg, E., Nelson, E., Galinsky, I., Meyer, C., Kufe, D., Kharbanda, S., and Stone, R., Combining the FLT3 inhibitor PKC412 and the triterpenoid CDDO-Me synergistically induces apoptosis in acute myeloid leukemia with the internal tandem duplication mutation, *Mol. Cancer Res.* 8, 986, 2010.
104. Schwartz, S. L., Denham, D. S., Hurwitz, C. A., Meyer, C. J., and Pergola, P. E., Bardoxolone methyl shown to improve renal function in patients with chronic kidney disease and type 2 diabetes mellitus, in *69th Annual Meeting of the American Diabetes Association (ADA)*, New Orleans, 2009, Abst 112-OR.
105. Petronelli, A., Pannitteri, G., and Testa, U., Triterpenoids as new promising anticancer drugs, *Anticancer Drugs* 20, 880, 2009.
106. Li, Y., Sun, X., LaMont, J. T., Pardee, A. B., and Li, C. J., Selective killing of cancer cells by beta-lapachone: Direct checkpoint activation as a strategy against cancer, *Proc. Natl. Acad. Sci., U.S.A.* 100, 2674, 2003.
107. Choi, B. T., Cheong, J., and Choi, Y. H., β-Lapachone-induced apoptosis is associated with activation of caspase-3 and inactivation of NF-kB in human colon cancer HCT-116 cells, *Anti-Cancer Drugs* 14, 845, 2003.
108. Ravelo, A. G., Estevez-Braun, A., Chavez-Orellana, H., Perez-Sacau, E., and Mesa-Siverio, D., Recent studies on natural products as anticancer agents, *Curr. Topics Med. Chem.* 4, 241, 2004.
109. Song, C. W., Chae, J. J., Choi, E. K., Hwang, T. S., Kim, C., Lim, B. U., and Park, H. J., Anti-cancer effect of bio-reductive drug β-lapachone is enhanced by activating NQO1 with heat shock, *Int. J. Hyperthermia* 24, 161, 2008.

110. Dong, G. Z., Youn, H., Park, M. T., Oh, E. T., Park, K. H., Song, C. W., Choi, E. K., and Park, H. J., Heat shock increases expression of NAD(P)H:quinone oxidoreductase (NQO1), mediator of β-lapachone cytotoxicity, by increasing NQO1 gene activity and via Hsp70-mediated stabilisation of NQO1 protein, *Int. J. Hyperthermia* 25, 477, 2009.
111. Terai, K., Dong, G. Z., Oh, E. T., Park, M. T., Gu, Y., Song, C. W., and Park, H. J., Cisplatin enhances the anticancer effect of β-lapachone by up-regulating NQO1, *Anticancer Drugs* 20, 901, 2009.
112. Shah, H. R., Conway, R. M., Van Quill, K. R., Madigan, M. C., Howard, S. A., Qi, J., Weinberg, V., and O'Brien, J. M., β-lapachone inhibits proliferation and induces apoptosis in retinoblastoma cell lines, *Eye (Lond.)* 22, 454, 2008.
113. D'Anneo, A., Augello, G., Santulli, A., Giuliano, M., di Fiore, R., Messina, C., Tesoriere, G., and Vento, R., Paclitaxel and β-lapachone synergistically induce apoptosis in human retinoblastoma Y79 cells by downregulating the levels of phospho-Akt, *J. Cell Physiol.* 22, 433, 2010.
114. Bey, E. A., Bentle, M. S., Reinicke, K. E., Dong, Y., Yang, C. R., Girard, L., Minna, J. D., Bornmann, W. G., Gao, J., and Boothman, D. A., An NQO1- and PARP-1-mediated cell death pathway induced in non-small-cell lung cancer cells by β-lapachone, *Proc. Natl. Acad. Sci. U.S.A.* 104, 11832, 2007.
115. Kim, S. O., Kwon, J. I., Jeong, Y. K., Kim, G. Y., Kim, N. D., and Choi, Y. H., Induction of Egr-1 is associated with anti-metastatic and anti-invasive ability of β-lapachone in human hepatocarcinoma cells, *Biosci. Biotechnol. Biochem.* 71, 2169, 2007.
116. Blanco, E., Bey, E. A., Dong, Y., Weinberg, B. D., Sutton, D. M., Boothman, D. A., and Gao, J., β-lapachone-containing PEG-PLA polymer micelles as novel nanotherapeutics against NQO1-overexpressing tumor cells, *J. Control. Release* 122, 365, 2007.
117. Dong, Y., Chin, S. F., Blanco, E., Bey, E. A., Kabbani, W., Xie, X. J., Bornmann, W. G., Boothman, D. A., and Gao, J., Intratumoral delivery of β-lapachone via polymer implants for prostate cancer therapy, *Clin. Cancer Res.* 15, 131, 2009.
118. Blanco, E., Bey, E. A., Khemtong, C., Yang, S. G., Setti-Guthi, J., Chen, H., Kessinger, C. W., Carnevale, K. A., Bornmann, W. G., Boothman, D. A., and Gao, J., β-lapachone micellar nanotherapeutics for non-small cell lung cancer therapy, *Cancer Res.* 70, 3896, 2010.
119. da Silva Jr., E. N., de Deus, C. F., Cavalcanti, B. C., Pessoa, C., Costa-Lotufo, L. V., Montenegro, R. C., de Moraes, M. O. et al., 3-arylamino and 3-alkoxy-*nor*-β-lapachone derivatives: Synthesis and cytotoxicity against cancer cell lines, *J. Med. Chem.* 53, 504, 2010.
120. Savage, R. E., Tyler, A. N., Miao, X. S., and Chan, T. C., Identification of a novel glucosylsulfate conjugate as a metabolite of 3,4-dihydro-2,2-dimethyl-2H-naphtho[1,2-b]pyran-5,6-dione (ARQ 501, β-lapachone) in mammals, *Drug Metab. Dispos.* 36, 753, 2008.
121. Miao, X. S., Song, P., Savage, R. E., Zhong, C., Yang, R. Y., Kizer, D., Wu, H. et al., Identification of the in vitro metabolites of 3,4-dihydro-2,2-dimethyl-2H-naphthol[1,2-b]pyran-5,6-dione (ARQ 501; β-lapachone) in whole blood, *Drug Metab. Dispos.* 36, 641, 2008.
122. Taylor, M. W., Radax, R., Steger, D., and Wagner, M., Sponge-associated microorganisms: Evolution, ecology, and biotechnological potential, *Microbiol. Mol. Biol. Rev.* 71, 295, 2007.
123. Uria, A. and Piel, J., Cultivation-independent approaches to investigate the chemistry of marine symbiotic bacteria, *Phytochem. Rev.* 8, 401, 2009.
124. Piel, J., Metabolites from symbiotic bacteria, *Nat. Prod. Rep.* 26, 338, 2009.
125. Piel, J., Biosynthesis of polyketides by trans-AT polyketide synthases, *Nat. Prod. Rep.* 27, 996, 2010.
126. Copeland, A. and Younes, A., Brentuximab vedotin, *Drugs Fut.* 35, 797, 2010.
127. Scott, J. D. and Williams, R. M., Chemistry and biology of the tetrahydroisoquinoline antitumor antibiotics, *Chem. Rev.* 102, 1669–1730, 2002.
128. Fontana, A., Cavaliere, P., Wahidulla, S., Naik, C. G., and Cimino, G., A new antitumor isoquinoline alkaloid from the marine nudibranch *Jorunna funebris*, *Tetrahedron* 56, 7305, 2000.
129. Moss, C., Green, D. H., Perez, B., Velasco, A., Henriquez, R., and McKenzie, D., Intracellular bacteria associated with the ascidian *Ecteinascidia turbinata*: Phylogenetic and in situ hybridization analysis, *Mar. Biol.* 143, 99, 2003.
130. Perez-Matos, A. E., Rosado, W., and Govind, N. S., Bacterial diversity associated with the Caribbean tunicate *Ecteinascidia turbinata*, *Antonie van Leeuwen. J. Gen. Mol. Microbiol.* 92, 155, 2007.
131. Newman, D. J. and Cragg, G. M., Microbial antitumor drugs: Natural products of microbial origin as anticancer agents, *Curr. Opin. Investig. Drugs* 10, 1280, 2009.
132. Zabriskie, T. M., Klocke, J. A., Ireland, C. M., Marcus, A. H., Molinski, T. F., Faulkner, D. J., Xu, C., and Clardy, J., Jaspamide, a modified peptide from a Jaspis sponge, with insecticidal and antifungal activity., *J. Am. Chem. Soc.* 108, 3123, 1986.

133. Crews, P., Manes, L. V., and Boehler, M., Jasplakinolide, A cyclodepsipeptide from the marine sponge, *Jaspis* sp., *Tetrahedron Lett.* 27, 2797, 1986.
134. Zampella, A., Giannini, C., Debitus, C., Roussakis, C., and D'Auria, M. V., New jaspamide derivatives from the marine sponge *Jaspis splendans* collected in Vanuatu, *J. Nat. Prod.* 62, 332, 1999.
135. Bubb, M. R., Senderowicz, A. M., Sausville, E. A., Duncan, K. L., and Korn, E. D., Jasplakinolide, a cytotoxic natural product, induces actin polymerization and competitively inhibits the binding of phalloidin to F-actin, *J. Biol. Chem.* 269, 14869, 1994.
136. Senderowicz, A. M., Kaur, G., Sainz, E., Laing, C., Inman, W. D., Rodriguez, J., Crews, P., Malspeis, L., and Grever, M. R., Jasplakinolide's inhibition of the growth of prostate carcinoma cells *in vitro* with disruption of the actin cytoskeleton, *J. Nat. Can. Inst.* 87, 46, 1995.
137. Gala, F., D'Auria, M. V., De Marino, S., Sepe, V., Zollo, F., Smith, C. D., Copper, J. E., and Zampella, A., Jaspamides H-L, new actin-targeting depsipeptides from the sponge *Jaspis splendans*, *Tetrahedron* 64, 7127, 2008.
138. Gala, F., D'Auria, M. V., De Marino, S., Sepe, V., Zollo, F., Smith, C. D., Keller, S. N., and Zampella, A., Jaspamides M-P: New tryptophan modified jaspamide derivatives from the sponge *Jaspis splendans*, *Tetrahedron* 65, 51, 2009.
139. Ebada, S. S., Wray, V., De Voogd, N. J., Deng, Z., Lin, W., and Proksch, P., Two new jaspamide derivatives from the marine sponge *Jaspis splendens*, *Mar. Drugs* 7, 435, 2009.
140. Robinson, S. J., Morinaka, B. I., Amagata, T., Tenney, K., Bray, W. M., Gassner, N. C., Scott Lokey, R., and Crews, P., New structures and bioactivity properties of jasplakinolide (jaspamide) analogues from marine sponges, *J. Med. Chem.* 53, 1651, 2010.
141. Terracciano, S., Bruno, I., D'Amico, E., Bifulco, G., Zampella, A., Sepe, V., Smith, C. D., and Riccio, R., Synthetic and pharmacological studies on new simplified analogues of the potent actin-targeting jaspamide, *Bioorg. Med. Chem.* 16, 6580, 2008.
142. Tannert, R., Milroy, L.-G., Ellinger, B., Hu, T.-S., Arndt, H.-D., and Waldmann, H., Synthesis and structure-activity correlation of natural-product inspired cyclodepsipeptides stabilizing F-actin, *J. Am. Chem. Soc.* 132, 3063, 2010.
143. Andavan, G. S. B. and Lemmens-Gruber, R., Cyclodepsipeptides from marine sponges: Natural agents for drug research, *Mar. Drugs* 8, 810, 2010.
144. Chan, W. R., Tinto, W. F., Manchand, P. S., and Todaro, L. J., Stereostructures of geodiamolides A and B, novel cyclodepsipeptides from the marines *Geodia* sp., *J. Org. Chem.* 52, 3091, 1987.
145. Coleman, J. E., Van Soest, R. W. M., and Andersen, R. J., New geodiamolides from the sponge *Cymbastela* sp. collected in Papua New Guinea, *J. Nat. Prod.* 62, 1137, 1999.
146. Kunze, B., Jansen, R., Sasse, F., Höfle, G., and Reichenbach, H., A-D, new antifungal and cytostatic depsipeptides from *Chondromyces crocatus* (myxobacteria). Production, physico-chemical and biological properties, *J. Antibiot.* 48, 1262, 1995.
147. Sasse, F., Kunze, B., Gronewold, T. M. A., and Reichenbach, H., The chondramides: Cytostatic agents from myxobacteria acting on the actin cytoskeleton, *J. Nat. Can. Inst.* 90, 1559, 1998.
148. Rachid, S., Krug, D., Kunze, B., Kochems, I., Scharfe, M., Zabriskie, T. M., Blöcker, H., and Müller, R., Molecular and biochemical studies of chondramide formation-highly cytotoxic natural products from *Chondromyces crocatus Cm c5*, *Chem. Biol.* 13, 667, 2006.
149. Krug, D. and Müller, R., Discovery of additional members of the tyrosine aminomutase enzyme family and the mutational analysis of CmdF, *ChemBioChem.* 10, 741, 2009.
150. Wenzel, S. C. and Müller, R., The impact of genomics on the exploitation of the myxobacterial secondary metabolome, *Nat. Prod. Rep.* 26, 1385, 2009.
151. Kunze, B., Jansen, R., Sasse, F., Höfle, G., and Reichenbach, H., Apicularens A and B, new cytostatic macrolides from *Chondromyces* species (Myxobacteria): Production, physico-chemical and biological properties, *J. Antibiot.* 51, 1075, 1998.
152. Kennedy, J., Codling, C. E., Jones, B. V., Dobson, A. D. W., and Marchesi, J. R., Diversity of microbes associated with the marine sponge, *Haliclona simulans*, isolated from Irish waters and identification of polyketide synthase genes from the sponge metagenome, *Environ. Microbiol.* 10, 1888, 2008.
153. Perry, N. B., Blunt, J. W., Munro, M. H. G., and Pannell, L. K., Mycalamide A, an antiviral compound from a New Zealand sponge of the genus Mycale, *J. Am. Chem. Soc.* 110, 4850, 1988.
154. Pettit, G. R., Xu, J.-P., Chapuis, J.-C., Pettit, R. K., Tackett, L. P., Doubek, D. L., Hooper, J. N. A., and Schmidt, J. M., Antineoplastic agents. 520. Isolation and structure of irciniastatins A and B from the Indo-Pacific marine sponge *Ircinia ramosa*, *J. Med. Chem.* 47, 1149, 2004.
155. Cichewicz, R. H., Valeriote, F. A., and Crews, P., Psymberin, a potent sponge-derived cytotoxin from *Psammocinia* distantly related to the pederin family, *Org. Lett.* 6, 1951, 2004.

156. Trost, B. M., Yang, H., and Probst, G. D., A formal synthesis of (-)-Mycalamide A, *J. Am. Chem. Soc.* 126, 48, 2004.
157. Kellner, R. L., Molecular identification of an endosymbiotic bacterium associated with pederin biosynthesis in *Paederus sabaeus* (Coleoptera: Staphylinidae), *Insect Biochem. Mol. Biol.* 32, 389, 2002.
158. Piel, J., Hofer, I., and Hui, D., Evidence for a symbiosis island involved in horizontal acquisition of pederin biosynthetic capabilities by the bacterial symbiont of *Paederus fuscipes* beetles, *J. Bacteriol.* 186, 1280, 2004.
159. Piel, J., A polyketide synthase-peptide synthase gene cluster from an uncultured bacterial symbiont of *Paederus* beetles, *Proc. Natl. Acad. Sci. U.S.A.* 99, 14002, 2002.
160. Page, M. J., Northcote, P. T., Webb, V. L., Mackey, S., and Handley, S. J., Aquaculture trials for the production of biologically active metabolites in the New Zealand sponge *Mycale hentscheli* (Demospongiae: Poecilosclerida), *Aquaculture* 250, 256, 2005.
161. Mincer, T. J., Jensen, P. R., Kauffman, C. A., and Fenical, W., Widespread and persistent populations of a major new marine actinomycete taxon in ocean sediments, *Appl. Environ. Microbiol.* 68, 5005, 2002.
162. Feling, R. H., Buchanan, G. O., Mincer, T. J., Kauffman, C. A., Jensen, P. R., and Fenical, W., Salinosporamide A: A highly cytotoxic proteosome inhibitor from a novel microbial source, a marine bacterium of the new genus *Salinospora*, *Angew. Chem. Int. Ed.* 42, 355, 2003.
163. Omura, S., Fujimoto, K., Otoguro, K., Matsuzaki, K., Moriguchi, R., Yanaka, H., and Sasaki, Y., Lactacystin, a novel microbial metabolite, induces neuritogenesis of neuroblastoma cells, *J. Antibiot.* 44, 113, 1991.
164. Corey, E. J. and Li, W. D., Total synthesis and biological activity of lactacystin, omuralide and analogs, *Chem. Pharm. Bull.* 47, 1, 1999.
165. Fenteany, G., Standaert, R. F., Lane, W. S., Choi, S., Corey, E. J., and Schreiber, S. L., Inhibition of proteosome activities and subunit-specific amino-terminal threonine modification by lactacystin, *Science* 268, 726, 1995.
166. Fenical, W., Jensen, P. R., Palladino, M. A., Lam, K. S., Lloyd, G. K., and Potts, B. C., Discovery and development of the anticancer agent salinosporamide A (NPI-0052), *Bioorg. Med. Chem.* 17, 2175, 2009.
167. Gulder, T. A. and Moore, B. S., Chasing the treasures of the sea—Bacterial marine natural products, *Curr. Opin. Microbiol.* 12, 252, 2009.
168. Groll, M., McArthur, K. A., Macherla, V. R., Manam, R. R., and Potts, B. C., Snapshots of the fluorosalinosporamide/20S complex offer mechanistic insights for fine tuning proteasome inhibition, *J. Med. Chem.* 52, 5420, 2009.
169. Jensen, P. R., Linking species concepts to natural product discovery in the post-genomic era, *J. Ind. Microbiol. Biotechol.* 37, 219, 2010.
170. Potts, B. C. and Lam, K. S., Generating a generation of proteasome inhibitors: From microbial fermentation to total synthesis of salinosporamide A (marizomib) and other salinosporamides, *Mar. Drugs* 8, 835, 2010.
171. Richardson, P., Hofmeister, C., Jakubowiak, A., Zimmerman, T. M., Spear, M. A., Palladino, M. A., Longenecker, A. M. et al., Phase 1 clinical trial of the novel structure proteasome inhibitor NPI-0052 in patients with relapsed and relapsed/refractory multiple myeloma (MM), *Blood* 114, 179 (abst. 431), 2009.
172. Taori, K., Paul, V. J., and Luesch, H., Structure and activity of largazole, a potent antiproliferative agent from the Floridian marine cyanobacterium *Symploca* sp, *J. Am. Chem. Soc.* 130, 1806, 2008.
173. Ying, Y., Taori, K., Kim, H., Hong, J., and Luesch, H., Total synthesis and molecular target of largazole, a histone deacetylase inhibitor, *J. Am. Chem. Soc.* 130, 8455, 2008.
174. Bowers, A. A., Greshook, T. J., West, N., Estiu, G., Schreiber, S. L., Wiest, O., Williams, R. M., and Bradner, J. E., Synthesis and conformation-activity relationships of the peptide isosteres of FK228 and largazole, *J. Am. Chem. Soc.* 131, 2900, 2009.
175. Bowers, A. A., West, N., Newkirk, T. L., Troutman-Youngman, A. E., Schreiber, S. L., Wiest, O., Bradner, J. E., and Williams, R. M., Synthesis and histone deacetylase inhibitory activity of largazole analogs: Alteration of the zinc-binding domain and macrocyclic scaffold, *Org. Lett.* 11, 1301, 2009.
176. Morris, J. C. and Phillips, A. J., Marine natural products: Synthetic aspects, *Nat. Prod. Rep.* 27, 1186, 2010.
177. Li, W., Schlecker, A., and Ma, D., Total synthesis of antimicrobial and antitumor cyclic depsipeptides, *Chem. Comm.* 46, 5403, 2010.
178. Mwakwari, S. C., Patil, V., Guerrant, W., and Oyelere, A. K., Macrocyclic histone deacetylase inhibitors, *Curr. Topics Med. Chem.* 10, 1423, 2010.
179. Souto, J. A., Vaz, E., Lepore, I., Pöppler, A.-C., Franci, G., Álvarez, R., Altucci, L., and De Lera, A. R., Synthesis and biological characterization of the histone deacetylase inhibitor largazole and C7-modified analogues, *J. Med. Chem.* 53, 4654, 2010.

180. Taori, K., Liu, Y., Paul, V. J., and Luesch, H., Combinatorial strategies by marine cyanobacteria: Symplostatin 4, an antimitotic natural dolastatin 10/15 hybrid that synergizes with the coproduced HDAC inhibitor largazole, *ChemBioChem.* 10, 1634, 2009.
181. Maugard, T., Enaud, E., Choisy, P., and Legoy, M. D., Identification of an indigo precursor from leaves of *Isatis tinctoria* (Woad), *Phytochemistry* 58, 897, 2001.
182. Cooksey, C. J., Tyrian purple: 6,6′-dibromoindigo and related compounds, *Molecules* 6 (9), 736, 2001.
183. MacNeil, I. A., Tiong, C. L., Minor, C., August, P. R., Grossman, T. H., Loiacono, K. A., Lynch, B. A. et al., Expression and isolation of antimicrobial small molecules from soil DNA libraries, *J. Mol. Microbiol. Biotechnol.* 3, 301, 2001.
184. Adachi, J., Mori, Y., Matsui, S., Takigam, H., Fujino, J., Kitagawa, H. C. A., Miller III, C. H., Kato, T., Saeki, K., and Matsuda, T., Indirubin and indigo are potent aryl hydrocarbon receptor ligands present in human urine, *J. Biol. Chem.* 276, 31475, 2001.
185. Chen, D. and Xie, J., Chemical constituents of a traditional Chinese medicine Qing Dai, *Zhongcaoyao* 15, 534, 1984.
186. Xiao, Z., Hao, Y., Liu, B., and Qian, L., Indirubin and mesoindigo in the treatment of chronic myelogenous leukemia in China, *Leuk. Lymphoma* 43, 1763, 2002.
187. Meijer, L., Skaltsounis, A.-L., Magiatis, P., Polychronopoulos, P., Knockaert, M., Leost, M., Ryan, X. P. et al., GSK-3-selective inhibitors derived from Tyrian purple indirubins, *Chem. Biol.* 10, 1255, 2003.
188. Polychronopoulos, P., Magiatis, P., Skaltsounis, A.-L., Myrianthopoulos, V., Mikros, E., Tarricone, A., Musacchio, A. et al., Structural basis for the synthesis of indirubins as potent and selective inhibitors of glycogen synthase kinase-3 and cyclin-dependent kinases, *J. Med. Chem.* 47, 935, 2004.
189. Denison, M. S. and Nagy, S. R., Activation of the aryl hydrocarbon receptor by structurally diverse exogenous and endogenous chemicals, *Annu. Rev. Pharmacol. Toxicol.* 43, 309, 2003.
190. Knockaert, M., Blondel, M., Bach, S., Leost, M., Elbi, C., Hager, G. L., Nagy, S. R. et al., Independent actions on cyclin-dependent kinases and aryl hydrocarbon receptor mediates the antiproliferative effects of indirubins, *Oncogene* 23, 4400, 2004.
191. Ferandin, Y., Bettayeb, K., Kritsanida, M., Lozach, O., Polychronopoulos, P., Magiatis, P., Skaltsounis, A.-L., and Meijer, L., 3′-substituted 7-halogenoindirubins, a new class of cell death inducing agents, *J. Med. Chem.* 49, 4638, 2006.
192. Ribas, J., Bettayeb, K., Ferandin, Y., Knockaert, M., Garrofé-Ochoa, X., Totzke, F., Schächtele, C. et al., 7-Bromoindirubin-3′-oxime induces caspase-independent cell death, *Oncogene* 25, 6304, 2006.
193. Kritsanida, M., Magiatis, P., Skaltsounis, A.-L., Peng, Y., Li, P., and Wennogle, L. P., Synthesis and antiproliferative activity of 7-azaindirubin-3′-oxime, a 7-aza isostere of the natural indirubin pharmacophore, *J. Nat. Prod.* 72, 2199, 2009.
194. Wang, Z.-H., Wang, T., Yao, S.-N., Chen, J.-C., Hua, W.-Y., and Yao, Q.-Z., Synthesis and biological evaluation of 7-azaisoindigo derivatives, *Archiv. Pharm.* 343, 160, 2010.
195. Vine, K. L., Matesic, L., Locke, J. M., Ranson, M., and Skropeta, D., Cytotoxic and anticancer activities of isatin and its derivatives: A comprehensive review from 2000–2008, *Anti-Cancer Agents Med. Chem.* 9, 397, 2009.
196. Schloss, P. D. and Handelsman, J., Biotechnological prospects from metagenomics, *Curr. Opin. Biotechnol.* 14, 303, 2003.
197. Cichewicz, R. H., Epigenome manipulation as a pathway to new natural product scaffolds and their congeners, *Nat. Prod. Rep.* 27, 11, 2010.
198. Osbourn, A., Secondary metabolic gene clusters: Evolutionary toolkits for chemical innovation, *Trends Genet.* 26, 449, 2010.
199. Palmer, J. M. and Keller, N. P., Secondary metabolism in fungi: Does chromosomal location matter?, *Curr. Opin. Microbiol.* 13 431, 2010.
200. Choudhary, S. and Schmidt-Dannert, C., Applications of quorum sensing in biotechnology, *Appl. Microbiol. Biotechnol.* 86, 1267, 2010.

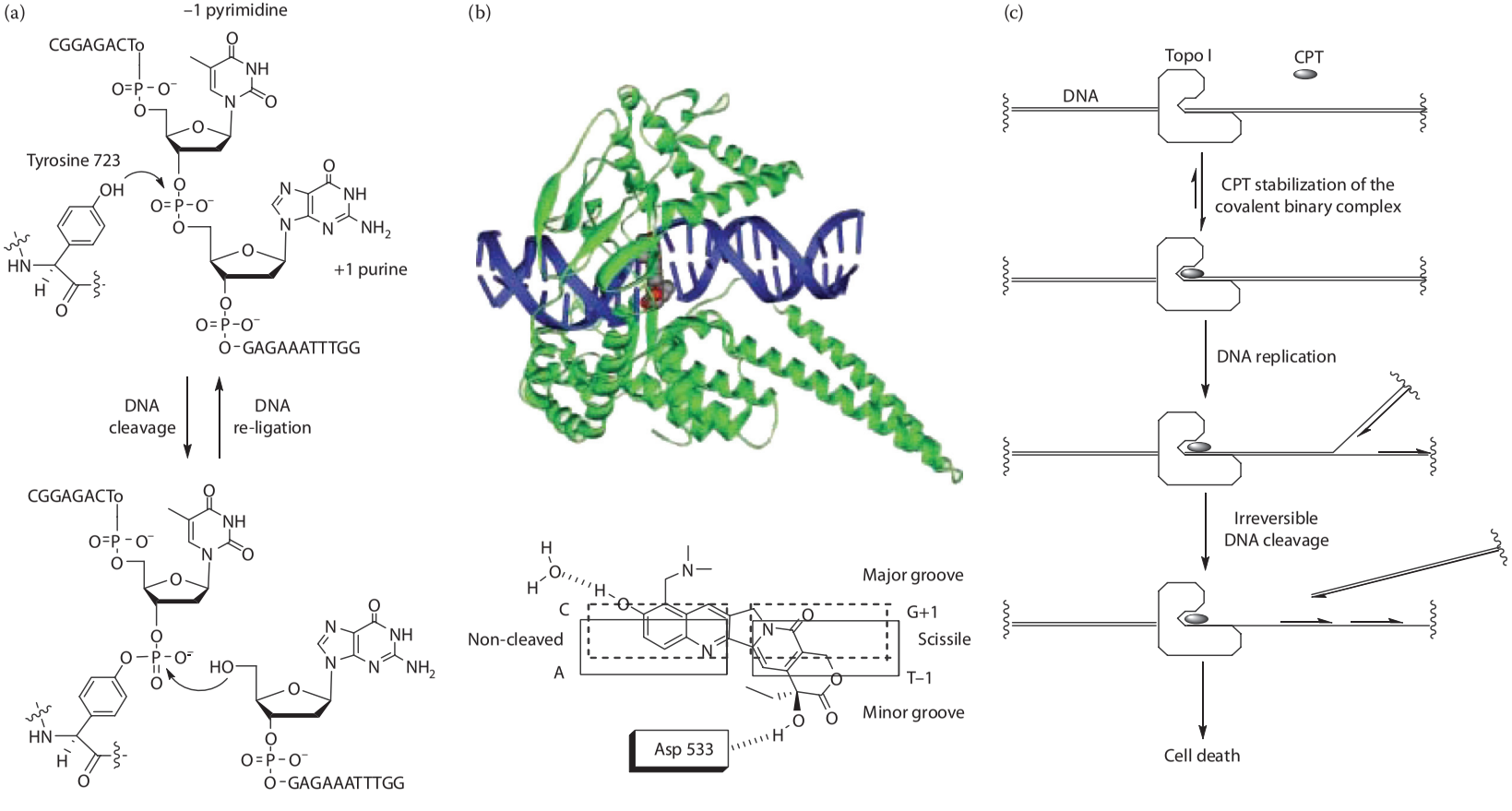

FIGURE 2.2 (a) Mechanism of DNA relaxation by topo I. (b) X-ray crystal structure of the DNA–topo I covalent complex in the presence of topotecan and a two-dimensional representation of the position of topotecan and key interactions with the covalent complex. (c) S-phase-specific cytotoxic mechanism of CPT.

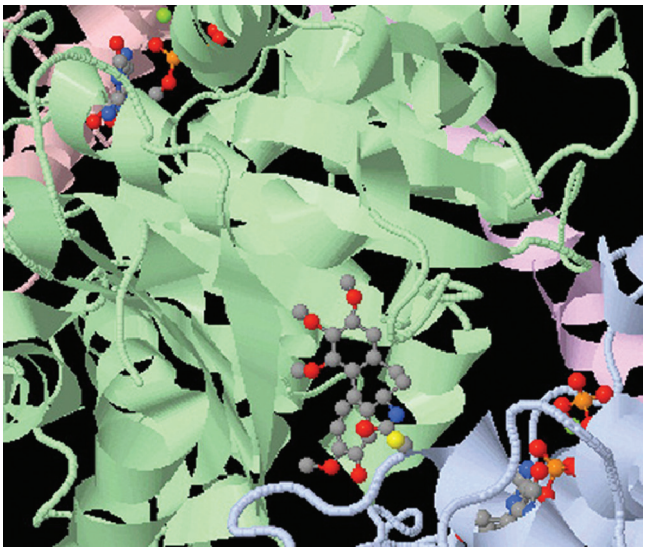

FIGURE 3.3 Colchicine analog (C, gray; O, red; N, blue; S, yellow) bound to the β-subunit (green) of a tubulin complex with the SLD of regulatory protein RB3 (pink). A small region of the α-subunit (blue) binding GTP is shown (C, gray; O, red; N, blue; P, orange). PDB ID: 1SA0.

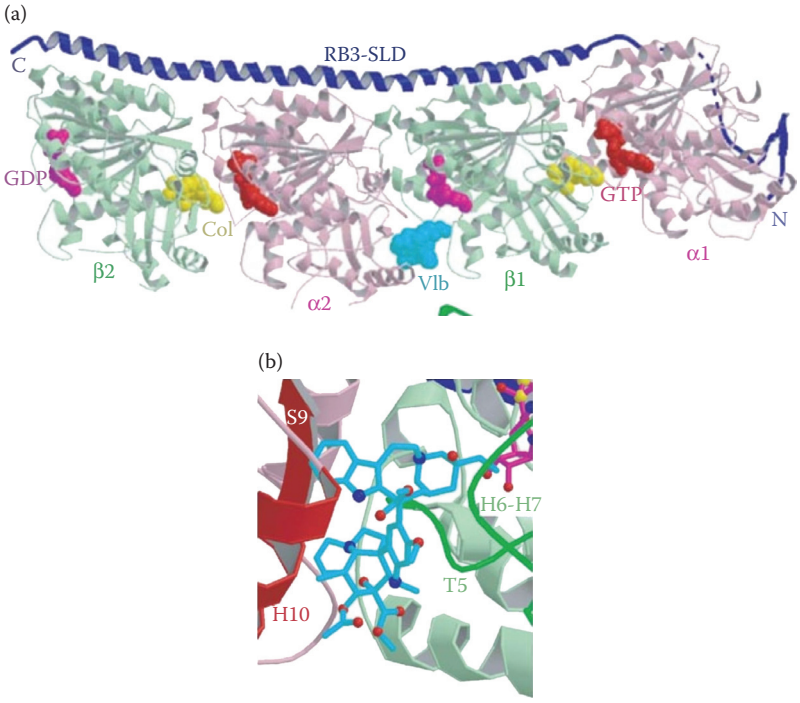

FIGURE 7.3 Vinblastine (Vlb, cyan)-binding site: (a) location of vinblastine in $(Tc)_2R$; (b) precise location of the vinblastine-binding site at the interface between two tubulin heterodimers (α2–β1).

The effects of 355703 on HeLa cell mitotic spindle structure

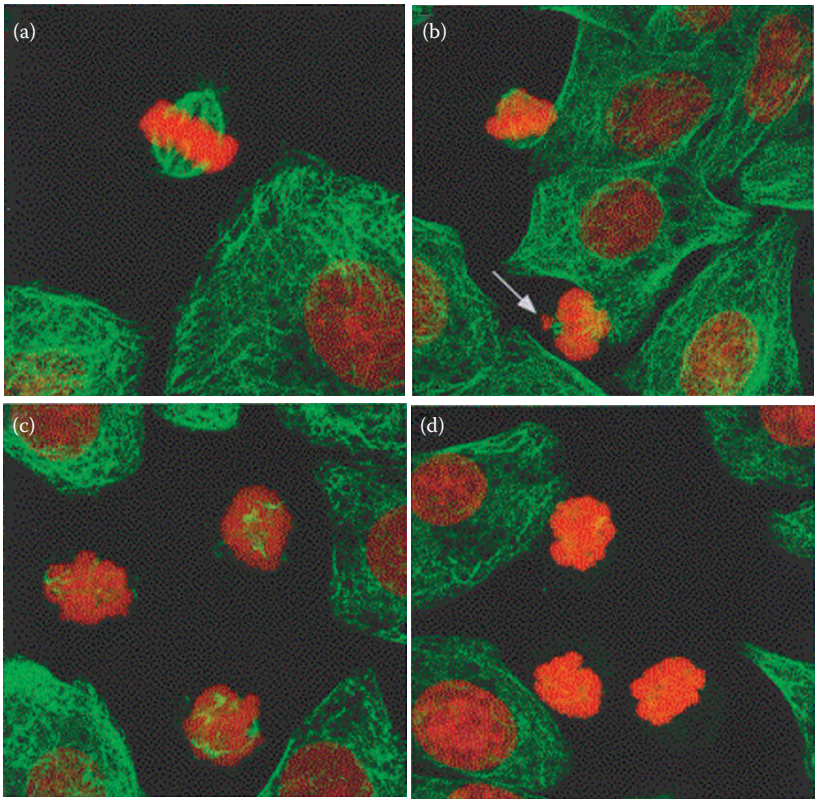

FIGURE 9.2 Fluorescence confocal micrographs of HeLa cells: (a) shows a metaphase mitotic spindle in an untreated control cell. The metaphase spindle is bipolar, with the chromosomes located in a compact metaphase plate at the midpoint between the spindle poles; (b) shows cells treated with 30 pM of LY355703 (approximately IC_{50}) for 8–10 h. The mitotic spindles look relatively normal. The most obvious abnormality involves the displacement of chromosomes from the compact metaphase plate. In the lower spindle, a chromosome (red) can be seen near the spindle pole (arrow); (c) (8–10 h; 100 pM of LY355703), and (d) (8–10 h; 300 pM of LY355703) show increased fragmentation of the spindle microtubules and disorganization of the chromosome mass into ball-like clusters.

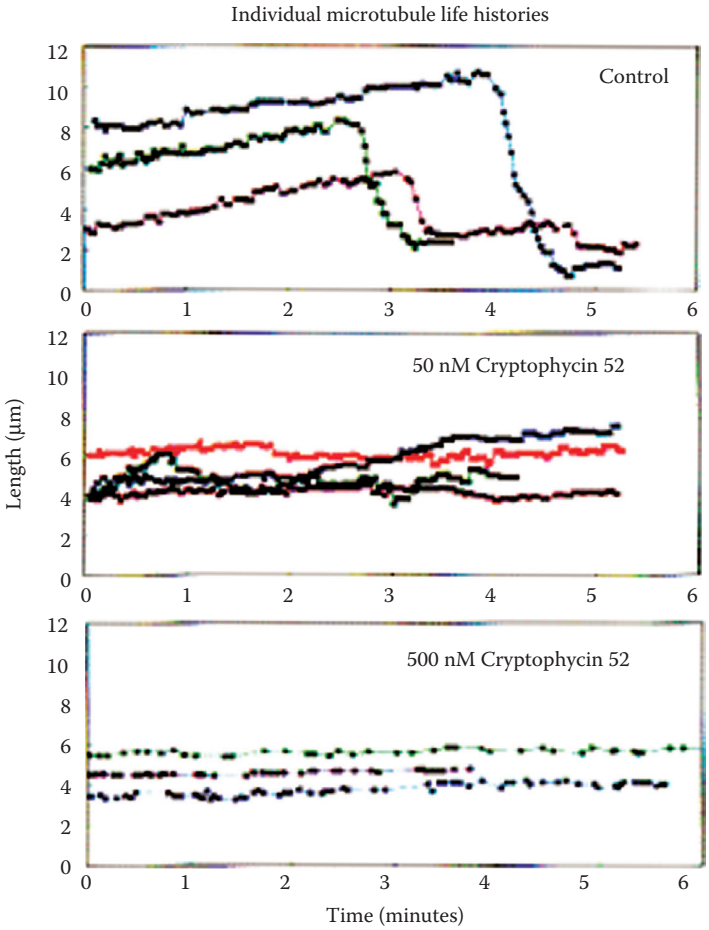

FIGURE 9.3 Microtubule life histories.

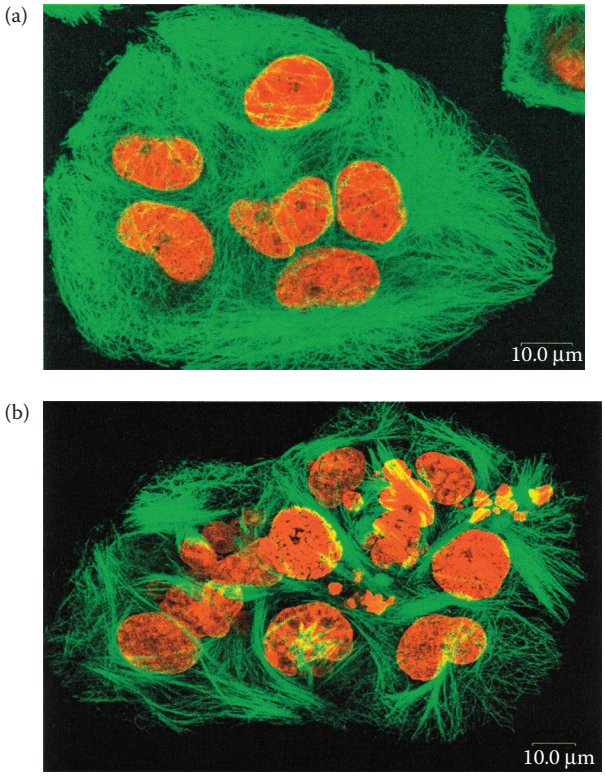

FIGURE 10.1 Immunofluorescence images of A549 cells stained with anti-α-tubulin (green) and propidium iodide (red) and observed by confocal microscopy. Cells were exposed to (a) 0.05% ethanol (vehicle control), or (b) (+)-discodermolide at a concentration of 100 nM.

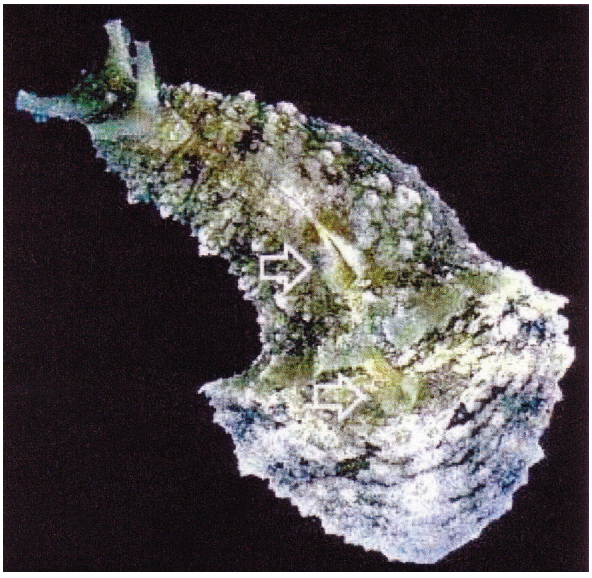

FIGURE 11.1 *Dollabella auricularia.*

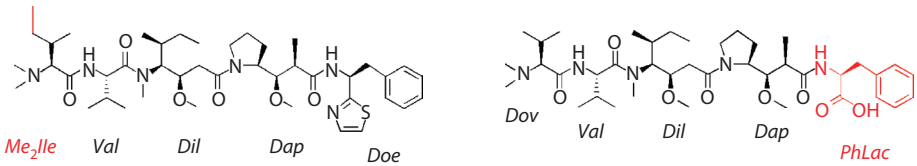

Symplostatin 1 (**35**)

$IC_{50} = 3.0 \times 10^{-4}$ mg/mL
KB cells (epidemoid carcinoma)

Symplostatin 3 (**36**)

$IC_{50} = 3.9 \times 10^{-3}$ mg/mL
KB cells (epidemoid carcinoma)

FIGURE 11.6 Naturally occurring derivatives of dolastatin 10.

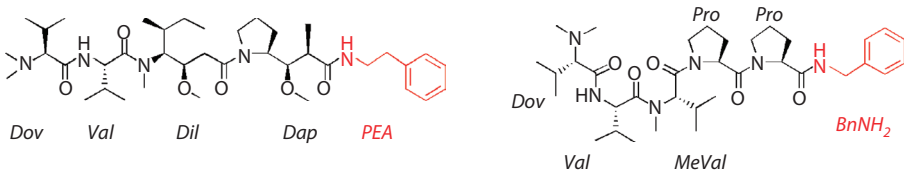

Soblidotin (**37**)
(TZ-1027, Auristatin PE)

$GI_{50} = 3.0 \times 10^{-6}$ mg/mL
NCI-H460 (Lung-NSC)

Cemadotin (**38**)
(LU103793)

$IC_{50} = 7.0 \times 10^{-4}$ mg/mL
HeLa-S_3 (cervical carcinoma)

FIGURE 11.7 Synthetic derivatives of dolastatin 10 (soblidotin) and dolastatin 15 (cematodin) in phase II clinical trials.

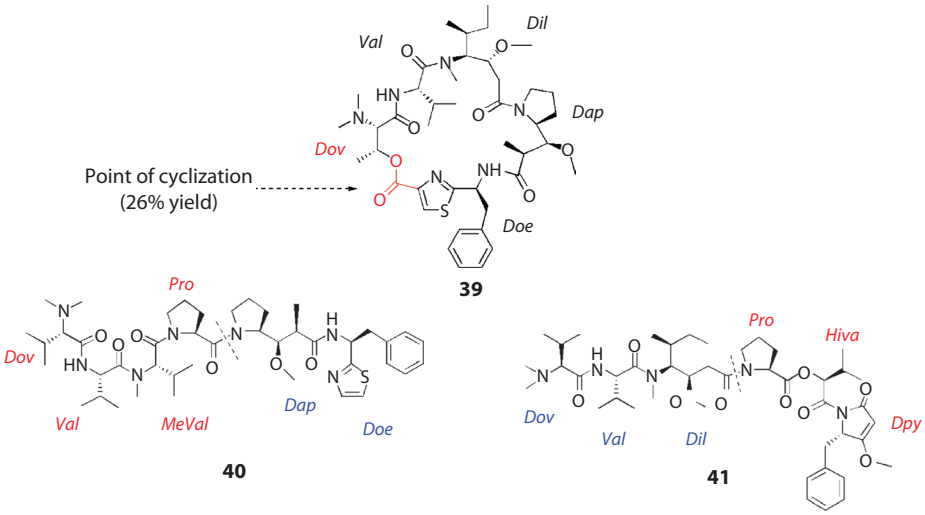

FIGURE 11.9 Dolastatin 10 cyclic derivative and D-10/D-15 hybrid compounds.

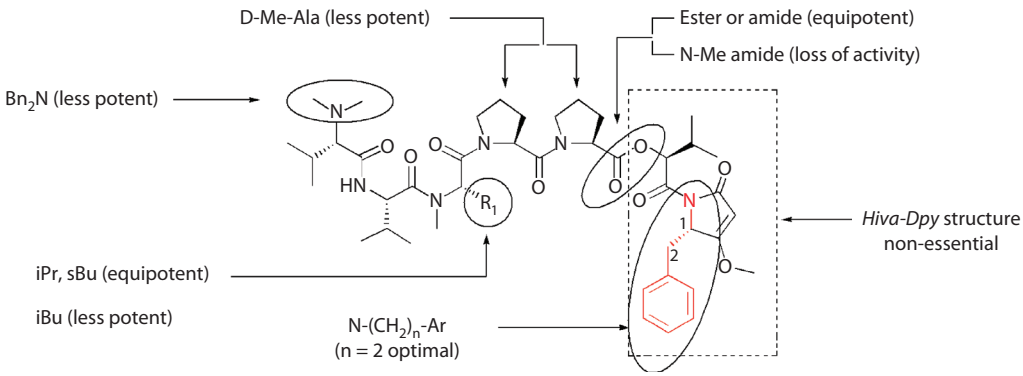

FIGURE 11.10 Effects of structural modifications on dolastatin 15 activity.

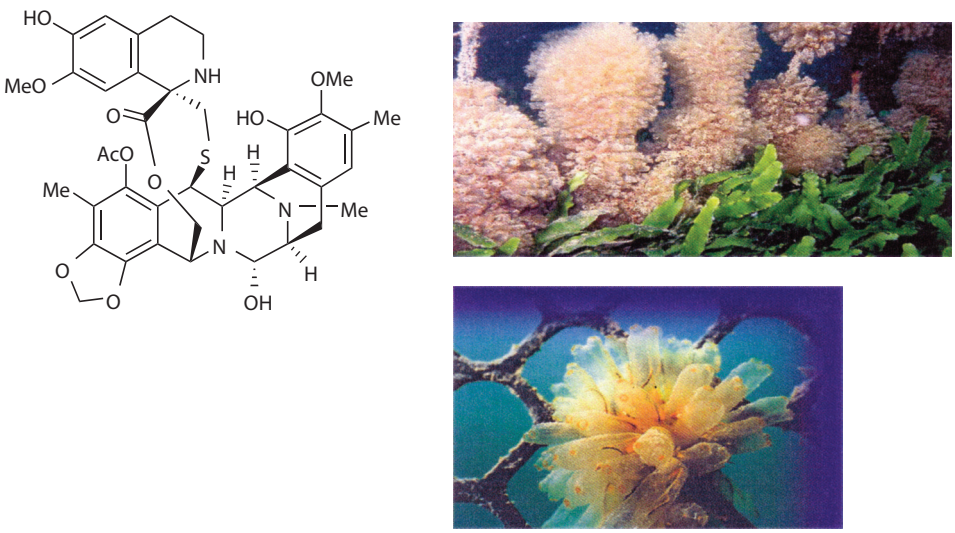

FIGURE 12.1 Structure of ET-743 (Yondelis) and source organism, *Ecteinascidia turbinata*.

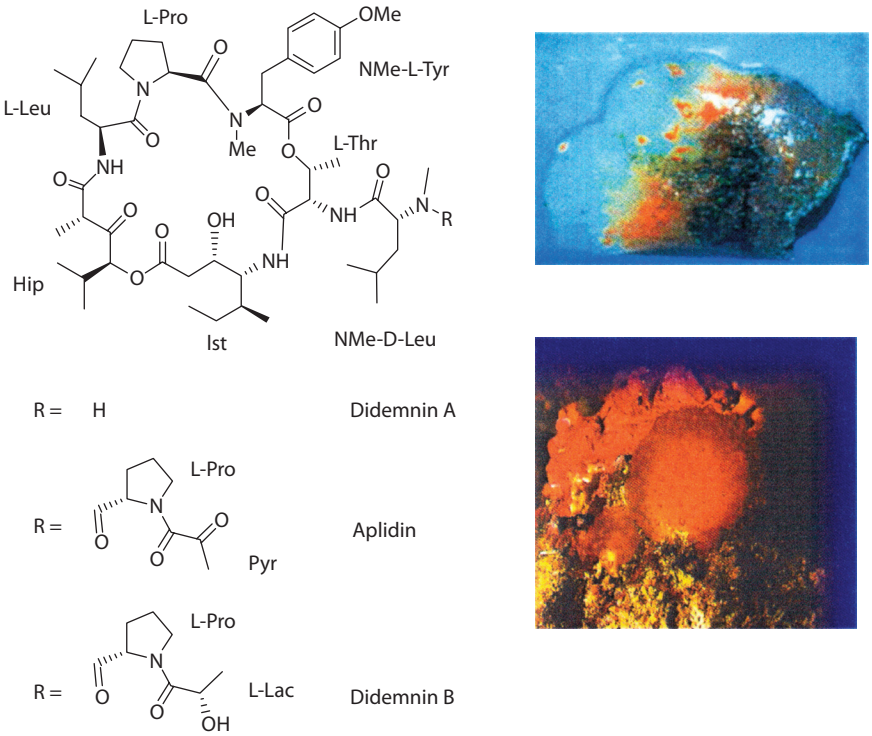

FIGURE 12.2 Structure and source organism of Aplidin.

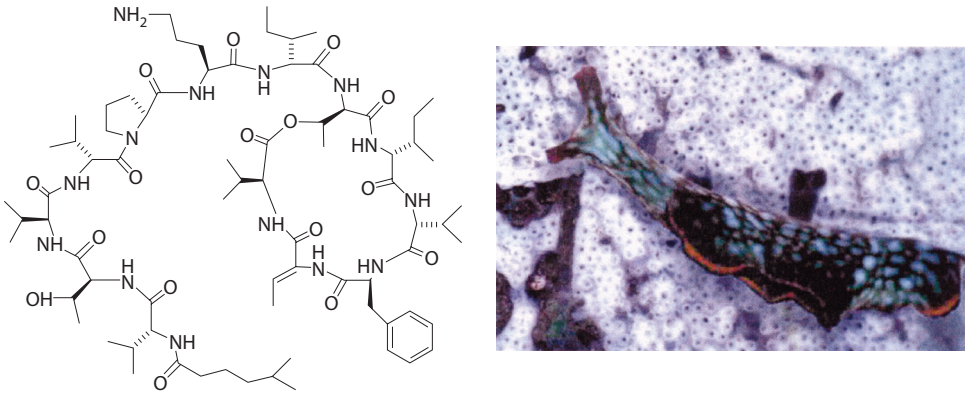

FIGURE 12.4 Structure and source organism of Irvalec.

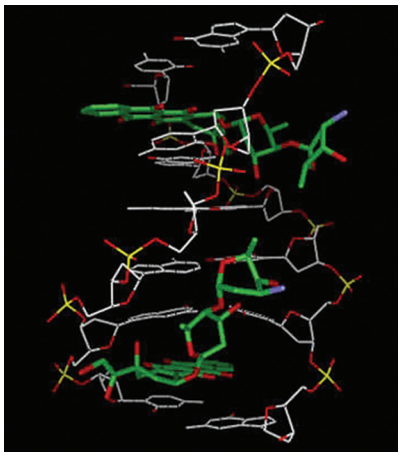

FIGURE 16.1 Representation of the sabarubicin intercalation complex with d(CGATCG)2 according to an x-ray crystal diffraction study. (Drawing courtesy of Dr. Giovanni Ughetto, Laboratorio del CNR di Montelibretti, Rome.)

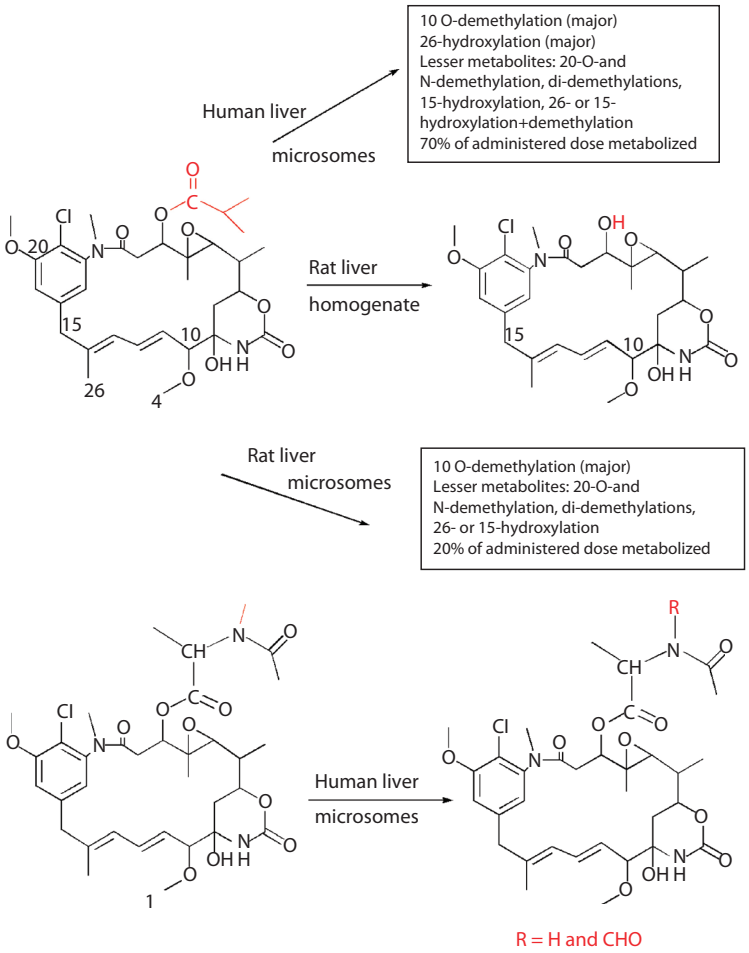

FIGURE 17.6 Results on the mammalian metabolism of ansamitocin P-3 and maytansine.

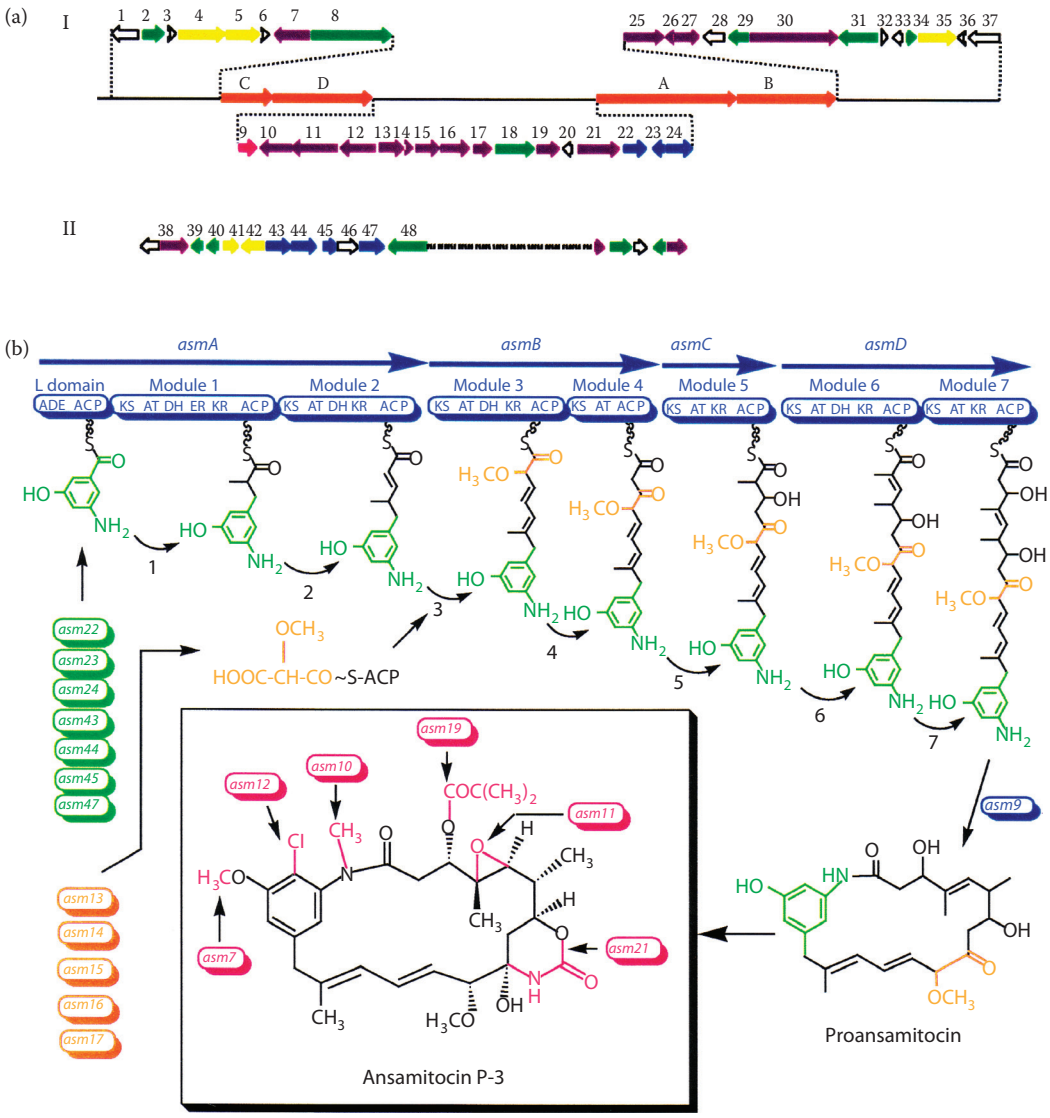

FIGURE 17.8 Biosynthesis of ansamitocin P-3: (a) the ansamitocin biosynthetic gene cluster from *Actinosynnema pretiosum*; (b) assembly of proansamitocin on a type I PKS and post-PKS modification to ansamitocin.

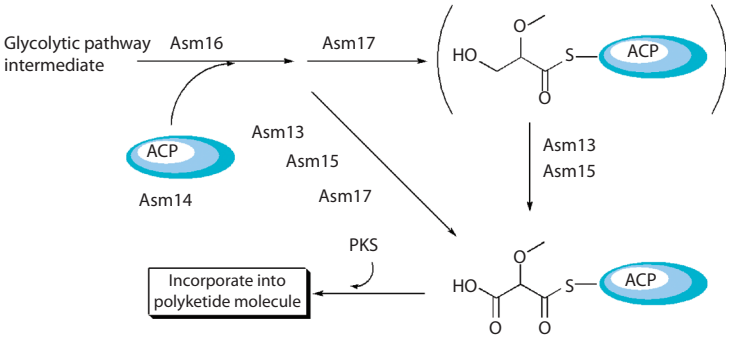

FIGURE 17.9 Formation of 2-methoxymalonyl-ACP, the substrate for the incorporation of the "glycolate" chain extension unit into ansamitocin.

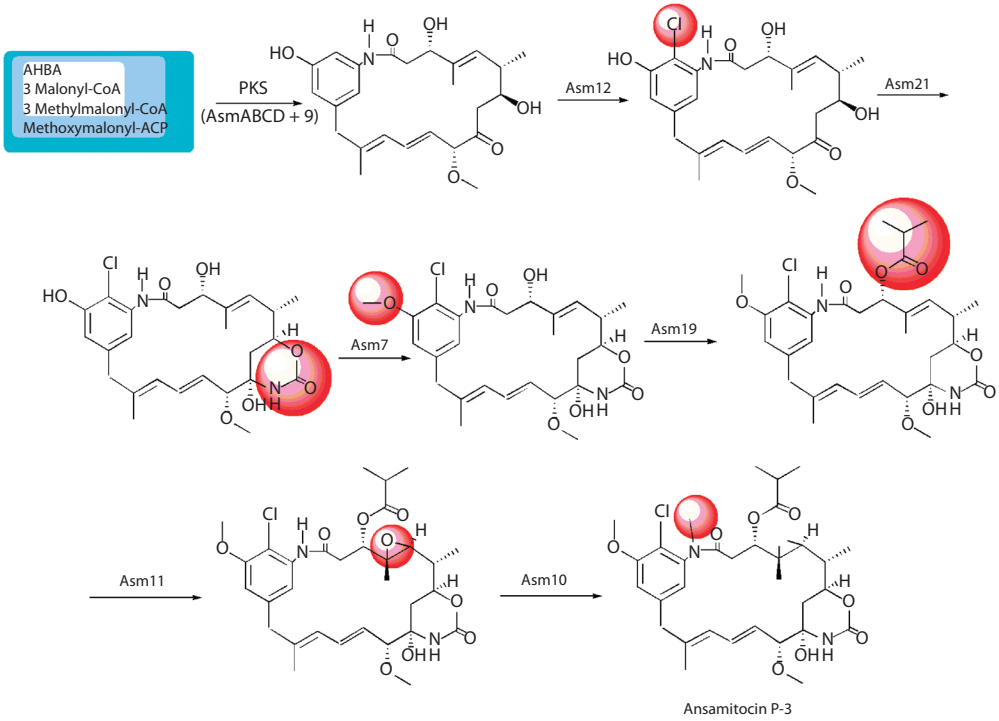

FIGURE 17.10 The sequence of post-PKS modification reactions converting proansamitocin into ansamitocin P-3.

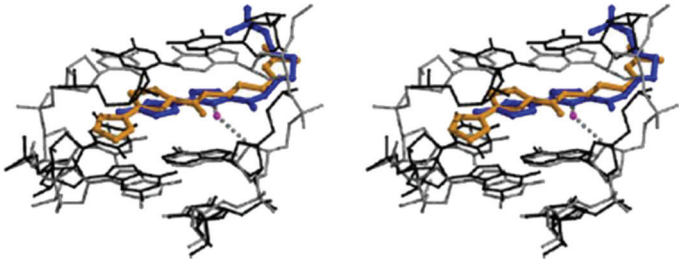

FIGURE19.3 Stereodiagramofsuperimposed5-GTTsitesinDNAoligonucleotidesd(ATTAGTTATAACTAAT)$_2$ (gray, with BLM in blue) and d(ATTTAGTTAACTAAAT)$_2$ (black, with BLM in orange) with associated BLM bithiazole moieties and C-terminal substituents.

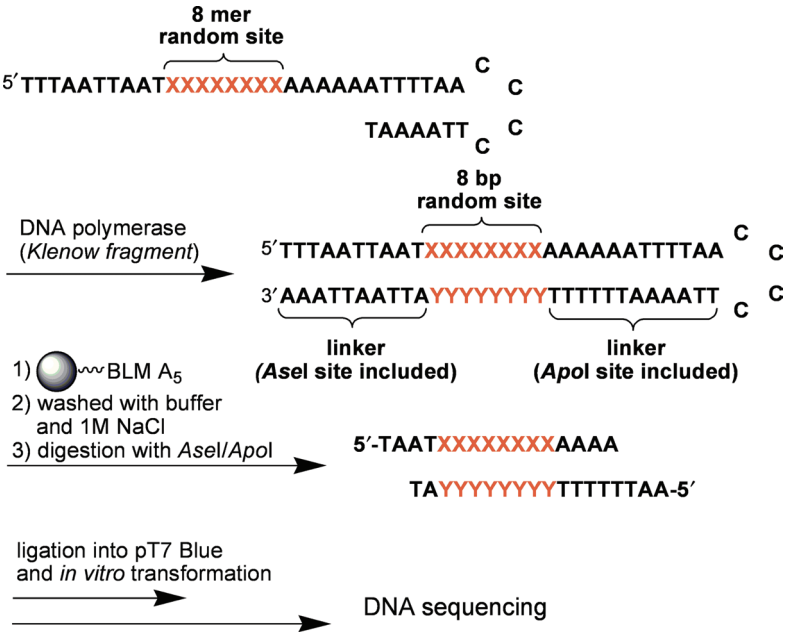

FIGURE 19.4 Scheme used for the selection of hairpin DNAs that bind tightly to BLM.

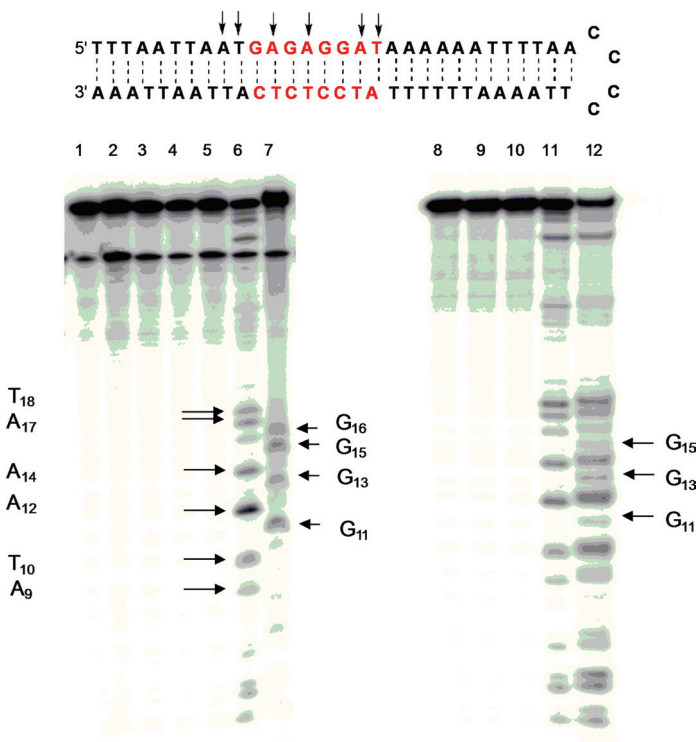

FIGURE 19.5 Sequence-selective cleavage of [5′-^{32}P]-end labeled 64-nt hairpin DNA 4 by BLM A_5. Lane 1, radiolabeled 4 alone; lane 2, 20 μM Fe^{2+}; lane 3, 5 μM BLM A_5; lane 4, 5 μM Fe(II)·BLM A_5; lane 5, 20 μM BLM A_5; lane 6, 20 μM Fe(II)·BLM A_5; lane 7, G lane; Lane 8, radiolabeled 4 alone; lane 9, 20 μM Fe^{2+}; lane 10, 20 μM BLM A_5; lane 11, 20 μM Fe(II)·BLM A_5; lane 12, 20 μM Fe(II)·BLM A_5, followed treatment with 0.2 M *n*-butylamine.

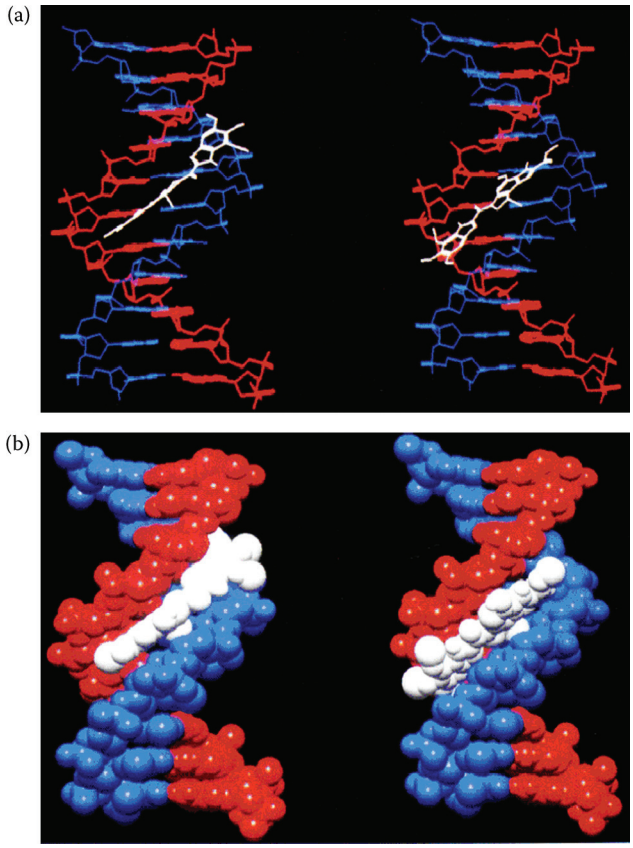

FIGURE 20.2 Comparison stick and space-filling models of the (+)-duocarmycin SA (left) and ent-()-duocarmycin SA (right) alkylation at the same site within w794DNA: duplex 5-d(GACTAATTTTT). The natural enantiomer binding extends in the 3 → 5 direction from the adenine N3 alkylation site 5-CTAA. The unnatural enantiomer binding extends in the 5 → 3 direction across the site 5-AATT.

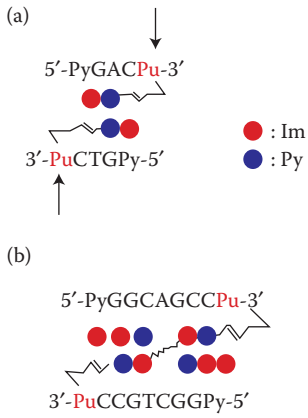

FIGURE 20.5 (a) The chemical structure of ImPyLDu86 83 and a schematic representation of the recognition of the 5-PyGACPu-3 sequence by the homodimer of 83. The arrows indicate the site where alkylation takes place. (b) A putative binding mode of the 1:2 complex of covalent dimer of 83, 84, with ImImPy to 5-PyGGCAGCCPu-3 sequence.

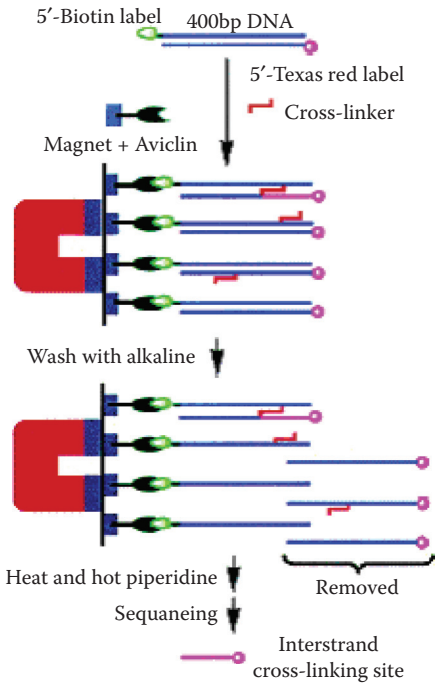

FIGURE 20.6 Determination of interstrand cross-linking sites.

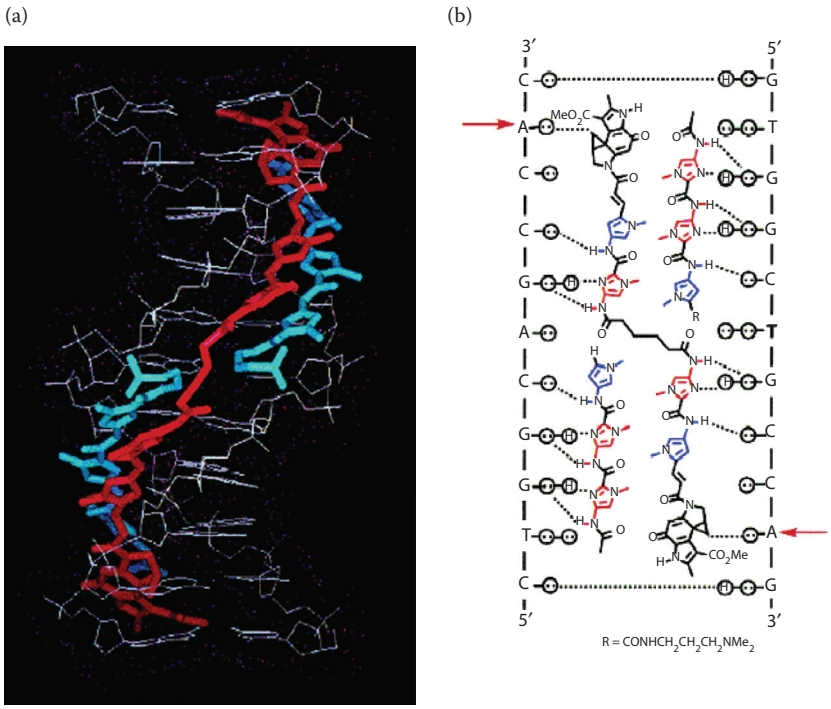

FIGURE 20.7 (a) Energy-minimized structure of 84-ImImPy$_2$-d(CTGGCTGCCAC)/d(GTGGCAGCCAG) interstrand cross-linked complex. DNA is drawn in white. Py and Im residues of 84 and ImImPy are drawn in blue and red, respectively. (b) A DNA interstrand cross-linking mode of the 1:2 complex of 84 with ImImPy.

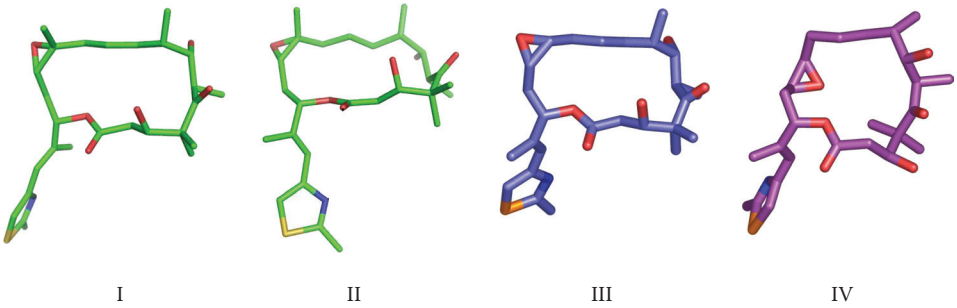

FIGURE 21.14 Crystal structure of epothilone B from dichloromethane/petroleum ether (I), methanol/water (II), and the tubulin-bound structures of epothilone A from NMR (III), and electron crystallography (IV). (Modeling by W.-D. Schubert.)

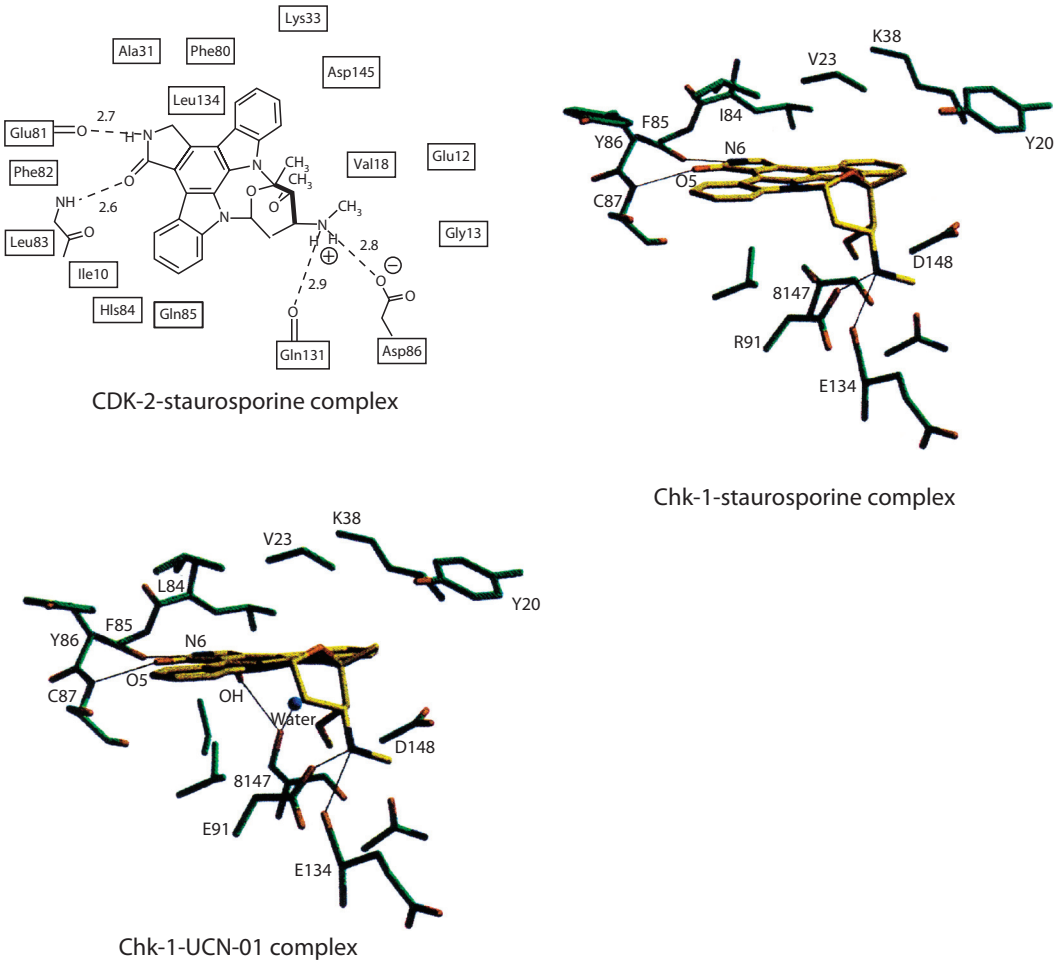

FIGURE 24.2 Crystal structures of staurosporine and UCN-01 complexes with kinases.

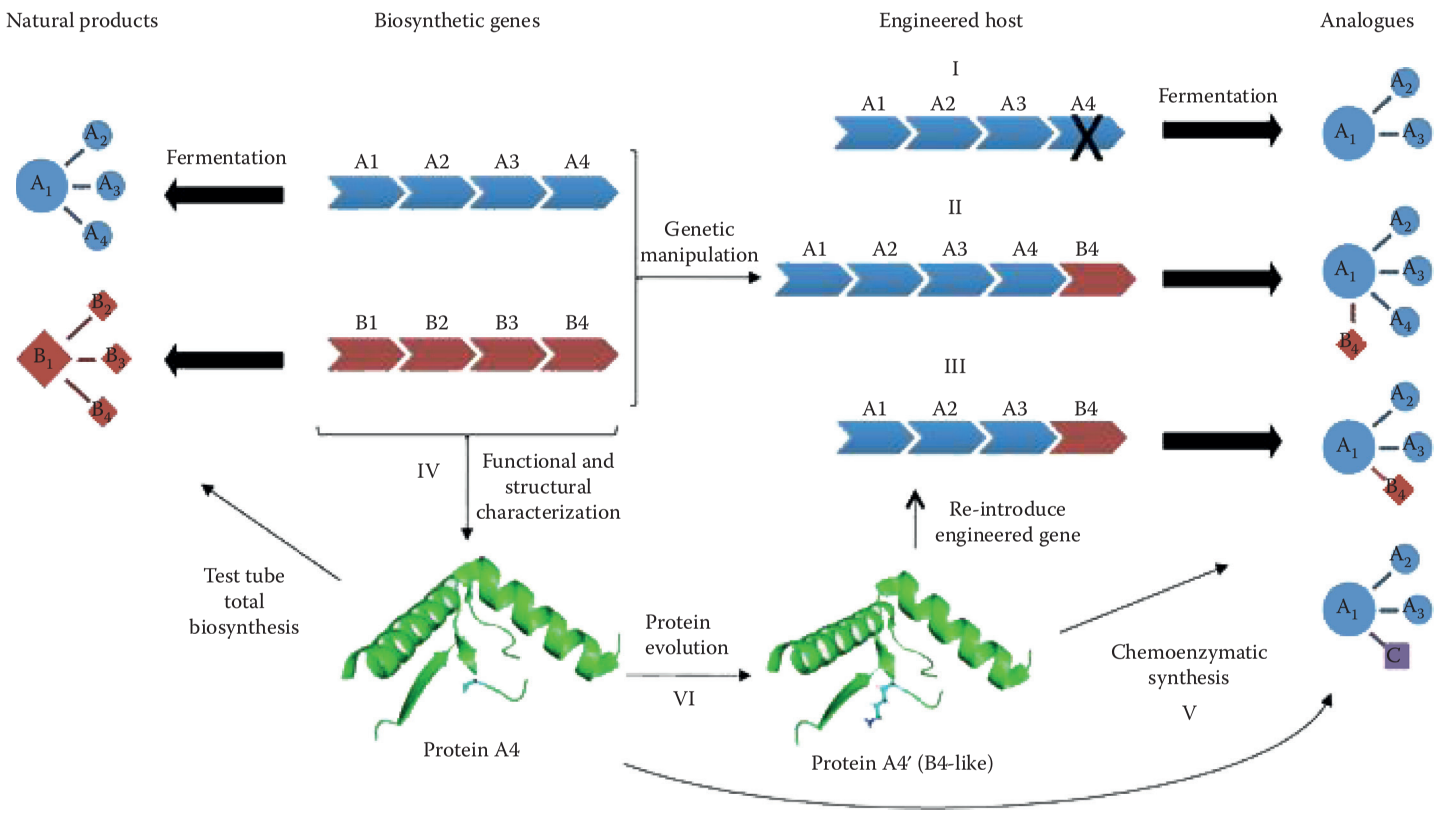

FIGURE 25.1 Potential combinatorial biosynthetic strategies for producing natural products and analogs: I, gene inactivation; II, gene expression; III, cross-complementation; IV, functional and structural characterization of key biosynthetic enzymes; V, chemoenzymatic synthesis; and VI, enzyme engineering by mutagenesis or directed evolution.

General Chemistry

ANTICANCER AGENTS from NATURAL PRODUCTS

Praise for the First Edition

"The book brings home to us not only the amazing chemical complexity of the natural world but also the vast reservoir of potential new healing agents that yet remain to be tapped. This impressive work, which maintains a uniformly high standard throughout, will be of major benefit to a wide readership."

—**Chemistry World**

"An ideal foundation for scientists engaged in developing new and improved drugs based on natural sources."

—**Memoriile Sectiilor Stiintifice**

The approach to drug discovery from natural sources has yielded many important new pharmaceuticals inaccessible by other routes. In many cases the isolated natural product may not be an effective drug for any of several reasons, but it nevertheless may become a drug through chemical modification or have a novel pharmacophore for future drug design. In summarizing the status of natural products as cancer chemotherapeutics, **Anticancer Agents from Natural Products, Second Edition** covers the:

- History of each covered drug—a discussion of its mechanism on action, medicinal chemistry, synthesis, and clinical applications
- Potential for novel drug discovery through the use of genome mining as well as future developments in anticancer drug discovery
- Important biosynthetic approaches to "unnatural" natural products

Anticancer Agents from Natural Products, Second Edition discusses how complex target-oriented synthesis—enabled by historic advances in methodology—has enormously expanded the scope of the possible. This book covers the current clinically used anticancer agents that are either natural products or are clearly derived from natural product leads. It also reviews drug candidates currently in clinical development since many of these will be clinically used drugs in the future.

K10713

CRC Press
Taylor & Francis Group
Boca Raton London New York

CRC Press is an imprint of the Taylor & Francis Group, an **informa** business

6000 Broken Sound Parkway, NW
Suite 300, Boca Raton, FL 33487
711 Third Avenue
New York, NY 10017
2 Park Square, Milton Park
Abingdon, Oxon OX14 4RN, UK

ISBN: 978-1-4398-1382-9
90000
9 781439 813829

WWW.CRC PRESS.COM